NUREG/CP-0024
Vol. 1

Proceedings of the U.S. Nuclear Regulatory Commission

Ninth Water Reactor Safety Research Information Meeting

Held at
National Bureau of Standards
Gaithersburg, Maryland
October 26-30, 1981

U.S. Nuclear Regulatory Commission

Office of Nuclear Regulatory Research

Available from

GPO Sales Program
Division of Technical Information and Document Control
U.S. Nuclear Regulatory Commission
Washington, DC 20555

Printed copy price: $18.00

and

National Technical Information Service
Springfield, VA 22161

NUREG/CP-0024
Vol. 1

Proceedings of the U.S. Nuclear Regulatory Commission

Ninth Water Reactor Safety Research Information Meeting

Held at
National Bureau of Standards
Gaithersburg, Maryland
October 26-30, 1981

Date Published: March 1982

Office of Nuclear Regulatory Research
U.S. Nuclear Regulatory Commission
Washington, D.C. 20555

FINAL AGENDA

NINTH WATER REACTOR SAFETY RESEARCH
INFORMATION MEETING

AT THE

NATIONAL BUREAU OF STANDARDS
ADMINISTRATION BUILDING 101
GAITHERSBURG, MARYLAND

October 26-30, 1981

TABLE OF CONTENTS

MONDAY, OCTOBER 26, 1981

INTEGRAL SYSTEMS EXPERIMENTS

LOFT Experimental Results

Chairman: G. D. McPherson, NRC

10:30 am -	Introduction	G. D. McPherson, NRC
10:35 am -	Pumps Off (L3-5) and Pumps On (L3-6) Results and Implications	J. H. Linebarger, INEL
11:05 am -	Multiple Failure Loss-of-Feedwater Transient Results and Implications (LOFT Experiment L9-1/L3-3)	C. W. Solbrig, INEL
11:30 am -	Results from LOFT Experiment L6-7/L9-2	J. P. Adams, INEL
11:50 am -	Preliminary Results of Intermediate Break Experiments L5-1 and L8-2	W. H. Grush, INEL
12:05 pm -	A Summary of LOFT Conclusions Relevant to Licensing	R. R. Landry, NRC
12:35 pm -	Blowdown Quench Characteristics of Nuclear and Electric Rods - Influence of Cladding Surface Thermocouples	E. L. Tolman, INEL

Co-Chairmen: G. D. McPherson, W. C. Lyon, NRC

2:00 pm -	Results of Semiscale MOD-2A Upper Head Injection Test Series	A. G. Stephens, INEL

2:35 pm -	Semiscale MOD-2A Natural Circulation Test Series - Preliminary Results	D. J. Shimeck, INEL
3:30 pm -	Break Area Parameter Test Series of ROSA-III for BWR LOCA/ECCS Tests	M. Shiba, JAERI
3:50 pm -	ROSA IV Program at JAERI for PWR Small-Break LOCA Experiments	M. Shiba, JAERI
4:10 pm -	Large Break Integral Test with TBL-1 (Hitachi BWR Integral Facility)	M. Naitoh, Hitachi
4:30 pm -	LOBI* - Influence of PWR Primary Loops on Blowdown - First Results	W. L. Riebold, JRC Ispra
5:00 pm -	PKL-I Findings - PKL-II Plans	D. Hein, KWU, FRG

MECHANICAL/STRUCTURAL ENGINEERING

Load Combinations

Chairman: J. A. O'Brien, NRC

10:30 am -	LOCA-SSE Combination and Asymmetric Blowdown Probability Assessment	C. K. Chou, LLNL
11:10 am -	Piping Reliability Model Validation Based on PWR Feedwater Line Cracking Data	H. Woo, LLNL
11:40 am -	Reliability Approach and Load Combination Criteria	C. A. Cornell, MIT
12:15 pm -	Design Criteria for Shipping Containers Used for Transporting Irradiated Fuel	R. Langland, LLNL

Seismic Safety Margins Research

Chairman: C. W. Burger, NRC

2:00 pm -	Overview	M. Bohn, LLNL
2:30 pm -	Structural Responses (SMACS Code)	J. Johnson, SMA
3:30 pm -	Building and Piping Sensitivity Studies	S. Shukla, LLNL
4:00 pm -	Probability and Risk (SEISIM Code)	J. Wells, LLNL
4:30 pm -	Application of SSMRP to San Onofre Plant	T. Chuang, LLNL

*Loop Blowdown Investigations

5:00 pm -	Ongoing Development	M. Bohn, LLNL

TUESDAY, OCTOBER 27, 1981

SEPARATE EFFECTS

Co-Chairmen: W. B. Beckner, M. W. Young, NRC

9:15 am -	Overview of NRC's BWR Safety Research	W. D. Beckner, NRC
9:25 am -	BWR Blowdown/Emergency Core Cooling Integral Test Program - Final Results from the Two Loop Test Apparatus (TLTA)	G. L. Sozzi, GE
9:40 am -	BWR Refill/Reflood Test Results	J. A. Findlay, GE
9:55 am -	BWR TRAC Model Development and Assessment	J. G. M. Andersen, GE
10:25 am -	TRAC-BWR Heat Transfer	R. E. Phillips and R. W. Shumway, INEL
10:40 am -	Precursory Cooling Effect on the Reflooding of a Hot Vertical Rod	Y. W. Lee, KAERI
11:00 am -	Rod Bundle Heat Transfer Research at ORNL	W. G. Craddick, ORNL
11:20 am -	FLECHT-SEASET Program	L. E. Hochreiter, W
12:00 pm -	Phenomenological Modeling of Two Phase Flow in a Water Reactor at ANL	M. Ishii, ANL
12:20 pm -	Parallel Channel Effects During the Emergency Core Cooling of a BWR	R. T. Lahey, Jr., RPI
12:40 pm -	Countercurrent Flow of Steam and Cold Water in an Inclined Rectangular Channel	S. G. Bankoff, NWU

ADVANCED INSTRUMENTATION

Co-Chairmen: Y. Y. Hsu, A. L. Hon, NRC

2:00 pm -	Introduction	Y. Y. Hsu, NRC
2:10 pm -	Improved Measurements of Cladding Temperature and Fluid Velocity for LOFT	D. J. Hanson, INEL
2:45 pm -	Determining Non-Condensible Gas Concentrations Using Wet Bulb and Dry Bulb Temperature Measurements	P. Griffith, MIT
3:00 pm -	Two-Phase Flow Measurements by Pulsed Neutron Activation Techniques	P. Kehler, ANL

3:30 pm -	Development and Evaluation of Liquid Level Sensors for Use in PWRs	J. E. Hardy, ORNL
4:20 pm -	A Concept for a Fast Neutron, Non-Invasive, Liquid Level and Density Gauge for Nuclear Power Reactors	W. A. Jester, Penn State Univ.
4:35 pm -	Water Spray Studies	R. S. Tankin, NWU
4:50 pm -	Two-Phase Performance Characteristics of of the LOBI Pump	L. Piplies, JRC, Ispra
5:05 pm -	Containment Emergency Sump Studies to Investigate Unresolved Safety Issue A-43	G. G. Weigand, SNL

STRUCTURAL ENGINEERING

Chairman: J. F. Costello, NRC

9:15 am -	Introduction	W. F. Anderson, NRC
9:30 am -	Structural Safety Margins of Containments	W. A. Von Riesemann, SNL
10:30 am -	Design Recommendations Based on Large Scale Testing of Containment Elements	H. G. Russell, PCA
11:00 am -	Safety Margin in Shear Design Criteria for Reinforced Concrete Containments	R. N. White, Cornell U.
11:30 am -	Hydrogen Detonation Loading on Reinforced Concrete Containments	M. N. Fardis, MIT
12:00 pm -	Category I Structures Program	E. G. Endebrock, LANL
12:30 pm -	Containment Buckling Program	C. A. Anderson, LANL
2:00 pm -	Load Combinations for Design of Category I Structures	M. Shinozuka, Columbia U./BNL
2:25 pm -	Errors Resulting from Dynamic Reduction	C. A. Miller, CUNY/BNL
2:50 pm -	Evaluation of Dynamic Testing of Nuclear Power Plant Structures	B. J. Hsieh, ANL
3:30 pm -	Experimental and Analytical Results of Coupled Fluid-Structure Interactions During Blowdown of the HDR Vessel	L. Wolf, KFK, FRG

HUMAN FACTORS RESEARCH

Chairman: R. DiSalvo, NRC

9:15 am -	Welcome and Introductory Remarks	R. DiSalvo, NRC
9:30 am -	A Validated Task Analysis for Reactor Operators	S. Eckel, General Physics
10:30 am -	Time Response Data on Safety-Related Operator Actions	E. Kozinsky, General Physics
11:15 am -	Sandia Human Factors Projects in Nuclear Power	A. D. Swain, SNL
11:45 am -	Results of Graphic Display Evaluation During Transients at the Loss-of-Fluid Test Facility (LOFT)	O. R. Meyer, INEL
2:00 pm -	Results of Control Room Annunciator Systems Evaluations	W. W. Banks, INEL
2:30 pm -	Training Simulator Requirements - A Comparison Among Several Industries	P. M. Haas, ORNL
4:15 pm -	Preliminary Findings of the Human Factors Society Study of Nuclear Reactor Safety Research	H. L. Snyder, VPI

WEDNESDAY, OCTOBER 28, 1981

ANALYSIS DEVELOPMENT

Chairman: S. Fabic, NRC

9:15 am -	RELAP5; Status and Application Experience	V. H. Ransom, INEL
9:45 am -	TRAC-BWR - Transient Reactor Analysis Codes for Boiling Water Reactors	W. L. Weaver III, INEL
10:30 am -	TRAC-PF1 Methods and Models	D. R. Liles, LANL
11:10 am -	Modeling of H_2 Migration in LWR Containments	J. R. Travis, LANL
11:30 am -	Status and Application of COBRA/TRAC and COBRA-TF Codes	M. J. Thurgood, PNL
12:30 pm -	Stability Criteria for PWR Fuel Assemblies in a Baffle Jet Flow	H. Lee, KAERI
2:00 pm -	Status of Code Assessment	F. Odar, NRC

2D/3D PROGRAM

Chairman: L. H. Sullivan, NRC

3:30 pm -	Introduction	L. S. Tong, NRC
3:40 pm -	SCTF Core-I Test Results (System Pressure Effects on Reflooding Phenomena)	H. Adachi, JAERI
4:20 pm -	CCTF Core I Test Results	Y. Murao, JAERI
5:00 pm -	TRAC Analysis Support for the SCTF and CCTF Tests	K. A. Williams, LANL

MECHANICAL ENGINEERING

Chairman: J. A. O'Brien, NRC

9:15 am -	Introduction	J. Richardson, NRC
9:30 am -	Thermal Shock Tests on a Nozzle Corner Performed Within the HDR-Safety Program	W. Muller-Dietsche KFK, FRG
10:30 am -	HDR Analyses (German Standard Problem 4a)	G. E. Howard, ANCO
11:30 am -	Seismic Investigation of HDR Piping	G. L. Thinnes, INEL
12:15 pm -	Computer Code Verification - Mechanical Piping Benchmark Problems	P. Bezler, M. Subudhi, and M. Reich, BNL

Chairman: D. J. Guzy, NRC

2:00 pm -	WIPS: Computer Code for Pipe Whip and Impact Analysis	G. Powell, UCB
2:30 pm -	Two-Phase Jet Loads	S. L. Thompson, SNL
3:30 pm -	Pipe-to-Pipe Impact Tests	M.C.C. Bampton, PNL
4:00 pm -	Characterization of Pressurized Water Reactor Response During Small Break LOCAs	J. A. Hunter, INEL
4:30 pm -	Qualification, Application and Testing of Snubbers	A. T. Onesto, ETEC

INSTRUMENTATION AND CONTROL RESEARCH

Chairman: G. S. Lewis, Jr., NRC

9:15 am -	Instrumentation and Control Program - An Overview	E. C. Wenzinger, NRC

9:40 am -	Demonstration of an On-line Reactor Noise Surveillance System at a PWR	N. E. Clapp, Jr., C. M. Smith, ORNL
10:20 am -	Summary of Studies on Methods for Detecting, Locating and Characterizing Metallic Loose Parts in Nuclear Reactor Coolant Systems	R. C. Kryter, ORNL F. Shahrokhi, U. of Tennessee
10:45 am -	BWR Stability Monitoring Using Neutron Noise	B. R. Upadhyaya, J. March-Leuba, U. of Tennessee
11:10 am -	Feasibility of Detecting and Quantifying PWR Fuel Assembly Vibrations Using Ex-Core Neutron Detectors	F. J. Sweeney, J. A. Reiner, ORNL
11:35 am -	BWR Subcritical Reactivity Monitoring Using the ^{252}Cf Source Driven Neutron Noise Method	J. T. Mihalczo, W. T. King, J. A. Reiner, ORNL
12:00 pm -	Base Neutron Noise in PWRs	G. Kosaly, R. W. Albrecht, D. J. Dailey, U. of Wash. D. N. Fry, ORNL

SELECTED R&D AT EPRI

Chairman: W. B. Loewenstein, EPRI

2:00 pm -	EPRI Safety Program Highlights	W. B. Loewenstein and A. G. Adamantiades, EPRI
2:35 pm -	EPRI Pressurized Thermal Shock Program	T. Marston and K. H. Sun, EPRI
3:30 pm -	Modular Modeling System Code: Review and Qualification	A. B. Long and J. P. Sursock, EPRI
4:00 pm -	Status of EPRI's Dynamic Piping Test Program	H. T. Tang, EPRI
4:30 pm -	Mechanistic Modeling of Two-Phase Flow in Vertical Geometry	G. Lellouche and B. Zolotar, EPRI
5:00 pm -	Early Results of EPRI Research on Hydrogen Combustion and Management	L. Thompson, EPRI

THURSDAY, OCTOBER 29, 1981

FUEL BEHAVIOR RESEARCH

DBA/LOCA - Recent Progress and Status

Chairman: M. Silberberg, NRC
Session Secretary: G. P. Marino, NRC

9:15 am -	Trends in Thermal Calculations for Light Water Reactor Fuel (1971 - 1981)	D. D. Lanning, PNL
9:45 am -	Independent Assessment of FRAPCON-2 and FRAP-T6	E. T. Laats, INEL
10:30 am -	Fuel Rod Bundle Ballooning Test Results from FRG-REBEKA	F. Erbacher, KFK, FRG
11:00 am -	Preliminary Results of MRBT Bundle B-5 (8x8) Test	R. Chapman, ORNL
11:30 am -	LOCA Simulation in NRU	C. Mohr, PNL
12:10 pm -	Results of PBF Appendix K Tests	P. E. MacDonald, INEL

2:00 pm - Panel Discussion: DBA/LOCA: What Remains to be Done in Fuel Behavior Research

Panel Chairman: R. Van Houten, NRC
Panel Secretary: G. P. Marino, NRC
Panel Members: R. Meyer, NRC
S. Schultz, Yankee Atomic
P. Rotundo, CE
P. E. MacDonald, INEL

2D/3D Program Workshop

Chairman: L. M. Shotkin, NRC

9:15 am -	Introduction	L. M. Shotkin, NRC
10:30 am -	Flow Reversal Studies During Hot Leg Injection	P. H. Rothe, Creare
11:00 am -	Jet Disintegration in Upper Plenum	J. B. Colson, INEL
11:30 am -	Measurement of Two-Phase Flow at the Core-Upper Plenum Interface Under Simulated Reflood Conditions	D. G. Thomas, ORNL

SEVERE ACCIDENT ASSESSMENT

Co-Chairmen: T. J. Walker, J. T. Larkins, NRC

2:10 pm -	The Large-Scale Melt Facility	T. Y. Chu, SNL

2:25 pm -	Core/Concrete Experiments at Sandia National Laboratories	W. W. Tarbell, Ktech Corp.
3:00 pm -	Core Retention Assessment Program at Sandia National Laboratories	J. D. Fish, SNL
3:30 pm -	CORCON Molten Fuel-Concrete Interactions Code	R. K. Cole, SNL
3:45 pm -	Development of CONTAIN for LWR Containment Analysis	M. J. Clauser, SNL
4:00 pm -	Hydrogen Behavior and Control in Light Water Reactor Accidents	M. Berman, SNL
4:40 pm -	Core-Melt/Coolant Interactions	M. Corradini, SNL
5:10 pm -	SNL Program in Support of LWR Degraded Core Accident Analysis	G. A. Greene, BNL

MATERIALS ENGINEERING

9:15 am -	Introduction, MEB 5-Year Plans, RES & SD	C. Z. Serpan, Jr., NRC

Pressure Vessel Integrity

Chairman: M. Vagins, NRC

9:35 am -	Integrity of Reactor Pressure Vessels During Overcooling Accidents	R. D. Cheverton, ORNL
10:30 am -	Pressurized-Thermal-Shock Tests	G. D. Whitman, ORNL
10:50 am -	Small Specimen Fracture Toughness	R. K. Nanstad, ORNL
11:30 am -	Low Ductile Shelf Intermediate Vessel Test V-8A	R. H. Bryan, ORNL
11:50 am -	Crack Arrest Status	G. R. Irwin, U. of Maryland

Irradiation Effects and Dosimetry

Chairman: M. Vagins, NRC

12:20 pm -	J-R Curve Characterization of Irradiated, Low-Upper Shelf Welds	F. J. Loss, NRL
2:00 pm -	Charpy Toughness of Irradiated High Copper Welds	R. G. Berggren, ORNL
2:20 pm -	IARAR Program	R. Hawthorne, NRL
2:40 pm -	Surveillance Dosimetry of Operating Power Plants	W. N. McElroy, HEDL

3:20 pm -	NRC-EPRI Studies of Pressure-Vessel-Cavity Neutron Fields	J. Grundl, NBS

MATERIALS ENGINEERING

Piping and Crack Growth

Chairman: J. Strosnider, NRC

3:40 pm -	Environmental Effects on Crack Growth	W. Cullen, ENSA-Buffalo
4:05 pm -	J-R Curve Characteristics of Piping Material and Welds	J. Gudas, NSRDC
4:25 pm -	Degraded Pipe Experimental Program	M. Vassilaros, NSRDC
4:45 pm -	Probabilistic Fracture Mechanics for Piping	D. O. Harris, SAI

FRIDAY, OCTOBER 30, 1981

MATERIALS ENGINEERING

Steam Generator Integrity and Corrosion

Chairman: J. Muscara, NRC

9:15 am -	Leak Rate and Burst Strength of Laboratory SCC Steam Generator Tubes	R. A. Clark, PNL
10:30 am -	Environmentally Assisted Cracking in LWRs	W. J. Shack, ANL

Non-Destructive Examination

Chairman: J. Muscara, NRC

11:10 am -	AE Monitoring of Test and Operating Pressure Vessels	P. H. Hutton, PNL
12:25 pm -	ISI Application of SAFT-UT	J. L. Jackson, SWRI
2:00 pm -	Reliability of UT Flaw Detection	F. L. Becker, PNL
2:25 pm -	Improved Eddy-Current Inspection of Power Reactor Steam Generator Tubing	C. V. Dodd, ORNL
2:50 pm -	Possibilities for NDE Round Robin on a Retired-from-Service Steam Generator	R. A. Clark, PNL

RISK ANALYSIS RESEARCH

Chairman: C. E. Johnson, NRC

10:30 am -	Reactor Safety Study - Methodology Applications Program (RSSMAP)	J. J. Curry, NRC
11:00 am -	IREP/NREP Results	J. A. Murphy, NRC
11:30 am -	Reactor Siting Criteria	W. R. Ott, NRC
12:00 pm -	Consequence Analysis Results	R. M. Blond, NRC
2:00 pm -	CORRAL Code Upgrading	P. Baybutt, BCL
2:30 pm -	Overview of Research on Risk Methodology and Data	W. E. Vesely, NRC
3:30 pm -	Reliability Data Analysis	R. L. Dennig, NRC

Severe Accident Sequence Analysis

Chairman: R. T. Curtis, NRC

9:30 am -	Strategies for Managing Potentially Severe Accidents at Large Four-Loop PWRs	N. S. DeMuth, LANL
10:00 am -	BWR Station Blackout Studies - Accident Sequence Analysis	S. A. Hodge, ORNL
10:30 am -	Station Blackout at Browns Ferry Unit 1	R. P. Wichner, ORNL
11:15 am -	Post Meltdown Analyses for PWRs	F. E. Haskin and J. L. Darby, SNL
11:45 am -	Severe Accident Mitigation Studies	H. J. Reilly, INEL
12:00 pm -	Assessment of the MARCH Computer Code	J. B. Rivard, SNL
12:30 pm -	NUREG-0772, Results and Plans in Perspective	R. R. Sherry, NRC

UNITED STATES
NUCLEAR REGULATORY COMMISSION
Office of Public Affairs
Washington, D.C. 20555

No. S-4-81
Tel. 301/492-7715

FOR IMMEDIATE RELEASE

Remarks by Nunzio J. Palladino, Chairman
U.S. Nuclear Regulatory Commission
at the
Ninth Water Reactor Safety Research
Information Meeting, October 26, 1981

Good morning ladies and gentlemen.

I want to add my words of welcome to those of you already received to this safety research conference.

I would especially like to welcome our guests from overseas. Your attendance indicates to me that the information shared at previous meetings of this type was of sufficient value to cause your home organizations to send you back.

Also, I would like to thank the National Bureau of Standards for allowing us to use these fine facilities.

I feel very much at home in this type of gathering. A good portion of my life has been spent in efforts that relate to reactor research and development. I appreciate the contribution that many of you have made to the storehouse of safety information which allows us to regulate with confidence. I am looking forward to the valuable research information that many of you will be providing to help us deal with regulatory issues in the coming years.

To set the stage for my remarks, let me give you a little background.

When I first came to the NRC in July, I knew that I would want to look back after several months, after a couple of years, and at the end of my full 5-year term, to see what of significance had been done. To give myself a way of charting accomplishments, I decided first to define the areas of major importance to nuclear regulation and to the proper functioning of the NRC. In each of these areas I could then begin to establish benchmarks and, with the passing of time, measure actual achievements against them.

Of course, my first thoughts and projections have changed somewhat as I broaden my contacts within the agency and among members of Congress and the Executive Branch. No doubt I will be altering my expectations further from time to time in the future. Nevertheless, five themes consistently emerge that call for action.

What I want to say this morning relates to these five themes.

First, I will describe the themes for action.

Second, I will highlight those themes in which research could prove particularly useful.

I should emphasize at the outset, however, that in whatever actions my fellow Commissioners and I--as well as the entire NRC staff--decide to take, protecting the health and safety of the public shall be of overriding importance. I recognize that this fundamental goal is easily stated. Sorting out and taking those actions that will most effectively and efficiently achieve it is quite another matter.

Here in summary fashion are the five themes.

The first is that we must avoid a potential near-term reactor licensing logjam. We are planning to process license applications at an unprecedented pace in the next two years.

Second, we must promptly make sense--in terms of establishing priorities and realistic schedules--out of the deluge of requirements imposed on the nuclear industry or backlogged in the aftermath of the Three Mile Island accident. We also must make sure that future regulatory requirements are worth doing in terms of safety.

The third theme is that we must take near-term steps to pave the way for long-term streamlining of the nuclear reactor licensing process. To borrow the well used phrase, I do not want to reinvent the wheel. I simply want the wheel to roll forward by implementing some of the streamlining features already well studied and known to many of us.

Fourth, while maintaining the basic independence of nuclear regulation mandated by the Congress, we must support initiatives of the Executive Branch--as well as the Congress--to solve the long-term problems of nuclear waste and to expedite the cleanup of Three Mile Island.

And finally, we must steadily forge ahead in a number of important management and technical areas to improve the efficiency and effectiveness of nuclear regulation. Both

near-term and long-term steps are contemplated. Specifically, we need to formulate an overall safety goal, to expand the use of probabilistic risk assessment, to reexamine the pace of developing a new siting rule, and to improve our ability to learn from operating experience.

As I see it, these five action themes characterize the major current challenges facing the NRC. Successfully meeting several of these challenges will depend on the ability of the research community to provide valid and useful results.

In a sense much of NRC's program stands on a foundation that is made of information from research. In the early 1970s, for example, the AEC held a series of hearings lasting over a year on the adequacy of emergency core cooling systems. One of the outcomes of that set of hearings was the realization that the reactor regulations did not have an adequate underpinning of safety test and analysis information. The research that produced the needed information was essential for the design of effective emergency core cooling systems.

Let me highlight those themes in which research could prove particularly useful today.

I would welcome any research breakthrough that might miraculously remove the threat of a licensing logjam or help us streamline the legal complexities of our licensing process, but that would be an unrealistic expectation. However, the second, fourth, and fifth themes that I spoke of--namely getting control of requirements, solving the nuclear waste and Three Mile Island cleanup problems, and forging ahead in areas such as safety goal and risk assessment--each have information needs which should be fulfilled from the research program.

With respect to the theme that involves getting control of requirements, I have no doubt that nuclear power plants are safer now than they were before the TMI accident. NRC requirements and inspections as well as industry initiatives have a great deal to do with that. But I also believe that our safety priorities have not been made clear, that our demands on licensee resources have sometimes been excessive, and that these demands have not always been well coordinated.

This situation is intolerable. It is vital that we get a firm hold on the flow of regulatory requirements.

Just the week before last I announced that Mr. Dircks, our Executive Director for Operations, would be implementing a top level NRC reorganization that has the main objective of centralizing the review and approval of all requirements that we put on our licensees.

I believe that the research program will benefit this initiative in that it can provide an improved basis on which to evaluate NRC requirements, both for effective treatment of safety questions and the conservatisms or uncertainties involved. Research that can help us to better understand safety and cost trade-offs will also be of much assistance.

The theme that addresses waste management and the cleanup of three mile island relies on research efforts already under way or soon to be launched. I am particularly encouraged by the President's support of Federal participation in TMI-2 cleanup on the basis of the opportunity it presents for fundamental research into reactor fuel behavior under accident conditions. While many of us here this morning may not be directly involved in this effort, its results could have a strong bearing on what regulatory actions we might take in the future.

I want to focus now on the role of research in the theme that involves safety goal, risk assessment, siting, and operating experience.

Formulation of an overall safety goal for nuclear operations has been under way for some time. It is an ambitious undertaking. The final enunciation of a safety goal will reflect a painstaking examination of the views of a great many individuals and organizations. That takes time--first to elicit, then to analyze, and finally to evaluate these many contributions. It is an arduous process, but we are bound to carry through with it. The benefit to us and to our licensees--as well as to the general public--could be considerable.

The probabilistic risk assessment research effort is contributing toward the establishment of a basis for the development of the safety goal. I am told that an up-to-date comparison of nuclear risks with other risks has been developed. Studies are underway to develop a methodology for applying a safety goal to regulatory decision making. This is a several-faceted research effort which should be of significant help to my fellow Commissioners and to me in formulating an overall safety goal.

In addition, it appears that the use of probabilistic risk assessment techniques will provide a basis for making our safety priorities clearer. It is a developing area, but one full of potential usefulness both for judging risks against one another and for defining achieved safety levels. I believe a rigorous application of this methodology can do a great deal to dispel the murkiness that surrounds so many regulatory decisions.

Also, I would encourage all of you to use this methodology to set priorities on your research. It cannot be the only criterion for program selection, but it can help significantly. After all, in an era of increasingly tight research budgets, we can only afford the type of research expected to produce the most useful results.

Consistent with the emphasis on a safety goal and risk assessment, I believe we must review the pace of development of a new siting rule. Without going into a lot of detail about it now, I believe we are proceeding in an order that is the reverse of what logic seems to dictate.

I am willing to acknowledge that some improvement in reactor siting practices may be needed in the near-term. However, rather than rush to develop a comprehensive new siting rule for reactors, I think we ought first to develop a safety goal. Second, through our research efforts we should gain a better understanding of the source term, that is, the types and amounts of radioactivity that might be dispersed in various nuclear accident scenarios. This understanding is important because recent preliminary studies suggest that less radioactivity may be dispersed than was once generally believed.

Only after we have a safety goal and understand the true potential for radioactive dispersion should we attempt to develop a new siting rule. Such a rule must also take account of the engineered safety features designed into the nuclear power plants.

A final aspect of this theme is learning from operating experience. Over the last several years operating experience has indicated new areas in which research efforts can help. The large break LOCA issue has received a lot of research and regulatory attention. But we need more knowledge both on lesser, more probable accidents and on accidents that could lead to degraded core conditions. We want to understand what really happens in such accidents and to tailor our requirements to fit the realities involved. We also

want licensees to be highly aware of what is happening during all phases of plant operations--normal and off-normal--and to tailor their procedures accordingly.

You have an important role in this. You must help regulators and licensees understand what may take place when something breaks or shorts out, or when an operator makes a mistake. In that way requirements and procedures that don't help can be eliminated and new ones can be developed where needed in line with what we know.

In conclusion, let me underscore the ideas I wanted to offer you this morning.

I have described five themes for action. This should give you a sense of where I believe NRC ought to be headed.

I have highlighted three of those themes as areas in which research could help us get where we are headed. In summary, research can help us get control of requirements. Research can help us progress in waste management and in expediting the cleanup of Three Mile Island. And research is highly relevant to formulating a safety goal, making practical use of risk assessment, reexamining the pace of a siting rule, and learning from operating experience.

More often than not, research that you conduct in these areas will be done under various pressures--the pressure of budgets being squeezed, the pressure of needing valid results tomorrow rather than next month or next year, and the pressure of trying to make others understand the true significance of what you are doing. As a technical person at heart, I understand pressures such as these. There are no simple answers; we simply have to accept these pressures as part of our job.

Finally, you should know that I am eager to make changes in the way we regulate when I am convinced changes are needed to make better sense out of what we do. I look to those of you who conduct research for the development of information on which to base such changes, or information with which to confirm that no changes are needed in order to protect the public health and safety.

Thank you. I would now be happy to answer questions that some of you might have.

NINTH WATER REACTOR SAFETY RESEARCH
INFORMATION MEETING

INTRODUCTION TO SESSION ON:

INTEGRAL SYSTEMS EXPERIMENTS

CHAIRMAN: DR. G. DONALD MCPHERSON

It is generally recognized that full accreditation and acceptance of our system thermal hydraulic codes can only be expected if they are shown to describe the behavior of several different Light Water Reactor system simulators. Due to the competing demands of other reactor safety research on available financial and technical resources, and the high cost of integral system facilities, there are only a few such facilities in the world. Thus, to achieve accreditation and acceptance of our system thermal hydraulic codes, it is essential that the countries which operate these facilities cooperate closely.

To me, there appears to be four important elements in this cooperation:

1. Coordination of test objectives and test programs,

2. Assistance by the host organizations to enable others to accurately model their system facility(s),

3. Rapid exchange of test data, and

4. Regular and periodic meetings at the technical level to discuss test results and progress in code predictive capabilities.

Just last month, the NRC and Gesellschaft Fuer Reaktorsicherheit, in cooperation with the Bundesminister Fuer Forschung and Technologie had their first official meeting to discuss the coordination of the LOFT, Semiscale, LOBI and PKL test programs. We plan to continue these discussions, and next, to formalize discussions of program coordination with the Japanese.

Modeling of foreign facilities has increased significantly over the past year and this is helping to achieve closer cooperation and more rapid exchange of test data.

Regarding the fourth element, as an initial effort in establishing regular meetings, we have altered the content of today's presentations. Instead of the usual coverage of LOFT and Semiscale, the program has been augmented to include reports from all principal integral system facilities. Thus, you will note that in addition to LOFT and Semiscale, today's agenda will cover ROSA III and IV, Hitachi's BWR Facility, the Europeon Community's LOBI Facility and Germany's PKL I and II.

The NRC is pleased to welcome these presentations within today's session of Integral Systems Experiments.

PUMPS OFF (L3-5) AND PUMPS ON (L3-6)
RESULTS AND IMPLICATIONS

J. H. Linebarger

Presented at
The Ninth Water Reactor Safety Research
Information Meeting

October 26 - 30, 1981
Gaithersburg, Maryland

Idaho National Engineering Laboratory
Idaho Falls, Idaho 83415

EG&G Idaho
Idaho Falls, Idaho 83415

PUMPS OFF (L3-5) AND PUMPS ON (L3-6) RESULTS AND IMPLICATIONS

J. H. Linebarger
EG&G Idaho, Inc.

The question of primary coolant pump (PCP) operation during a small break loss-of-coolant accident (SBLOCA) arose following the Three Mile Island (TMI) incident. The Nuclear Regulatory Commission (NRC) required the utilities to manually trip the pumps when the reactor tripped and the high pressure injection system (HPIS) was initiated.[1] This decision was based on:

1. Vendor and audit calculations showing greater system mass loss during delayed versus early pump trip.[2]

2. The desire to ensure pump integrity and availability later in the accident scenario, if needed.[3]

The NRC requested integral system data from both the Loss-of-Fluid-Test (LOFT) and Semiscale programs at the Idaho National Engineering Laboratory (INEL). They desired data to address a number of specific issues related to the pump operation question. This paper summarizes the findings from the LOFT Program which relate to the following issues:

1. Does delayed pump trip lead to greater system mass inventory loss than an early pump trip during a SBLOCA? Vendor evaluation model calculations showed this mass loss led to unacceptable fuel cladding temperatures for a limited range of break diameters, that is, 0.05 m (2 in.) to 0.10 m (4 in.) or 0.17 m (6.8 in.) for Westinghouse/CE and B&W respectively.[2]

2. What procedures or criteria will minimize pump tripping during non-LOCA events and optimize the trip time during LOCA events? The NRC staff favored not tripping the pumps during non-LOCA events and during SBLOCAs which do not pose a depleted mass inventory problem.[2]

3. What problems are encountered when measuring reactor vessel liquid level with pumps off and pumps running? Reactor vessel liquid level measurements are being required in commercial PWRs.[4]

On September 29 and December 10, 1980, LOFT Experiments L3-5 and L3-6/8-1, early and delayed pump trip transient respectively, were conducted. These experiments simulated a 0.102-m (4-in.) break in a commercial PWR. The communicative break branched from the midplane of the intact loop cold leg between the pump outlet and the reactor vessel.

The 8-1 designation following L3-6 refers to a tandem experiment. To initiate L8-1, the pumps were tripped and the break closed following L3-6.

The LOFT data principally from L3-5 and L3-6/L8-1, but also from L6-7 (which will be reported in a subsequent paper), suggest the following conclusions and recommendations:

1. On an integral basis, more coolant was lost from the LOFT system when the pumps were running than when the pumps were off. However, early in the transients more coolant left the system when the pumps were off. This trend reversed once the break uncovered during the pumps-off transient. After break uncovery, less mass exited the system during the pumps-off transient than when the pumps were on. The optimum pump trip procedure would keep the pumps on until insufficient coolant inventory remains to cover the break, and then trip the pumps. That procedure is not operationally feasible.

However, the phenomena which affect the time-dependent relative mass inventory, as well as the integral mass loss effects, should be considered when proposing the long term resolution of the pumps on-off issue. This is particularly important when specifying the pump trip criteria which determines the time of pump trip.

2. Pump current is directly proportional to the fluid density in the loop piping. Concurrence of a pump current criterion, such as 90% of the steady-state value, and the present criteria is recommended. The addition of pump current would minimize unnecessary pump tripping and optimize the time of trip.

3. Pump current versus cold leg coolant temperature is recommended as a display to aid the operator in deciding whether to trip the pumps and when to trip them. This display allows the operator to unambiguously differentiate between a cooldown transient and a loss-of-coolant transient.

4. Reactor vessel liquid level cannot be measured with the pumps running because a distinct liquid level does not exist. System void fraction, however, can be measured with gamma densitometers or inferred from pump current when the pumps are running. If the liquid level measurement requirement for PWRs remains in Regulatory Guide 1.97, we recommend the requirement be limited to pumps-off operation.

REFERENCES

1. IE Bulletin Nos. 79-05C and 79-06C, July 26, 1979.

2. Brian Sheron, Generic Assessment of Delayed Reactor Coolant Pump Trip During Small Break Loss-of-Coolant Accidents in Pressurized Water Reactors, NUREG-0623, November 1979.

3. Transcript of ACRS, ECCS Subcommittee, Idaho Falls, Idaho, October 22-23, 1980.

4. U.S. Nuclear Regulatory Commission, Instrumentation for Light-Water Cooled Nuclear Power Plants to Assess Plant and Environs Conditions During and Following an Accident, Regulatory Guide 1.97, Revision 2, December 1980.

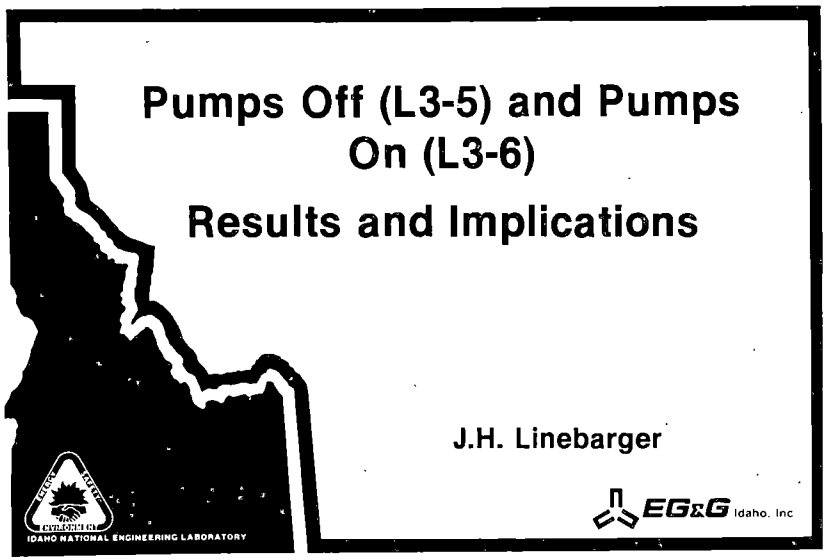

Outline

- Background
- Experiments
- Results vs Issues
- Summary

Background

- Pumps - Off or On (SBLOCA)?

Background

- Pumps - Off or On (SBLOCA)?
- Trip Criteria - Optimized?

Background

- Pumps - Off or On (SBLOCA)?
- Trip criteria - Optimized?
- Reactor vessel liquid level measurement
  - Linked with pump operation?

INEL-S-34 256

Experiments

INEL-S-34 257

Severe Consequenses Break Size Window

Vendors	Break diameters
B&W	0.05 m (2 in.) — 0.17 m (6.7 in.)
CE	0.10 m (4 in.)
W	LOFT L3-5/L3-6 Scaled Break Diameter

INEL-S-34 258

LOFT Primary System

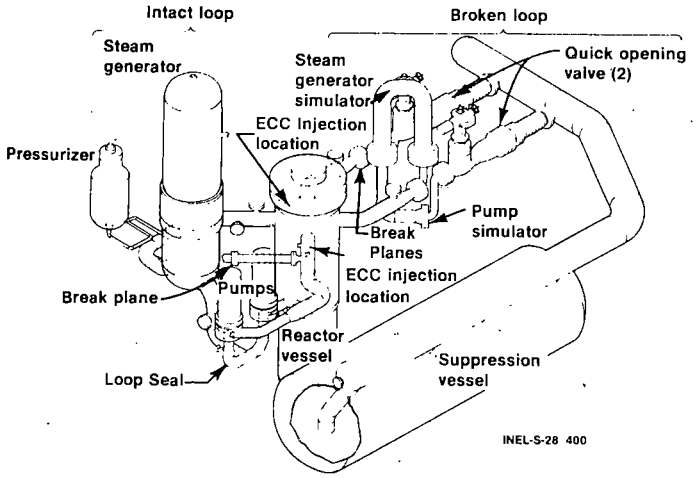

INEL-S-28 400

JHL-6

Results vs Issues

INEL-S-34 259

L3-5 (Pumps off) and L3-6 (Pumps on) System Pressure and Fuel Clad Temperature

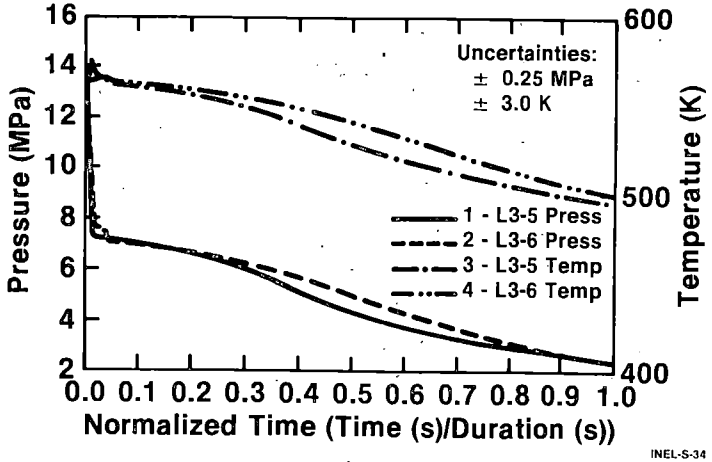

INEL-S-34 260

JHL-7

Issue

Pumps ON or OFF (SBLOCA)?

INEL-S-34 261

LOFT System Mass Inventory for Pumps On and Pumps Off Experiments

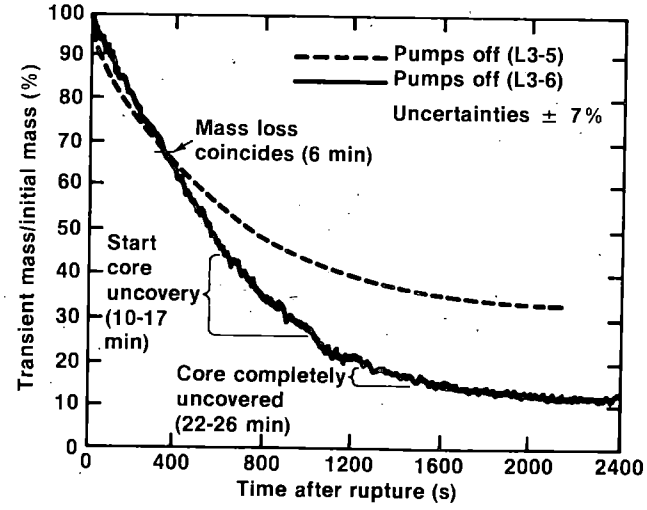

INEL-S-33 546

Pumps - ON or OFF?

Conclusion:

- Pumps off during SBLOCA

Reasons:

- Mass inventory (Integral basis)
- Pump availability later in event
- RV liquid level measurement

But:

- Reconsider pump trip criteria

INEL-S-34 262

Issue

Pump Trip Criteria

INEL-S-34 263

Pump Current and System Coolant Inventory During L3-6 (Pumps on)

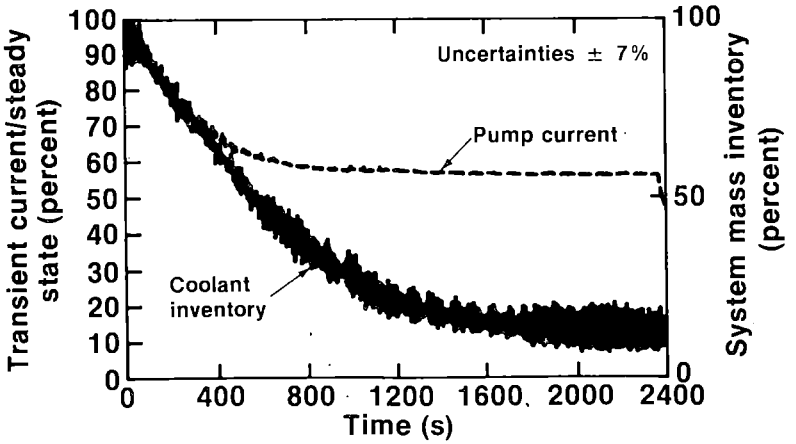

Pump Current and Densitometer Void Fraction During LOFT L3-6

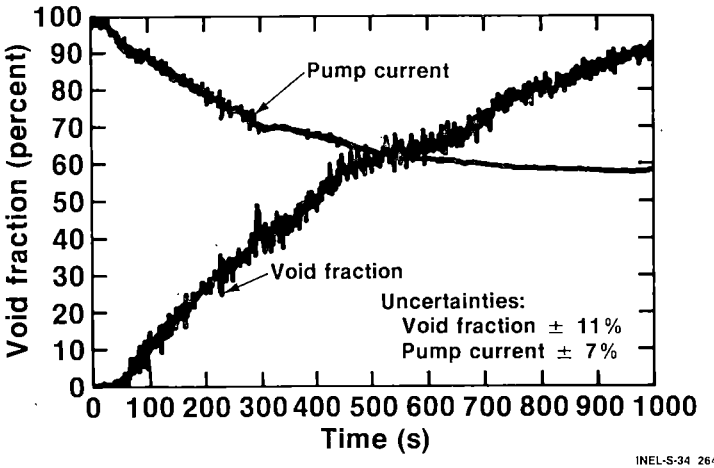

INEL-S-34 264

JHL-8

90% Pump Current Criterion

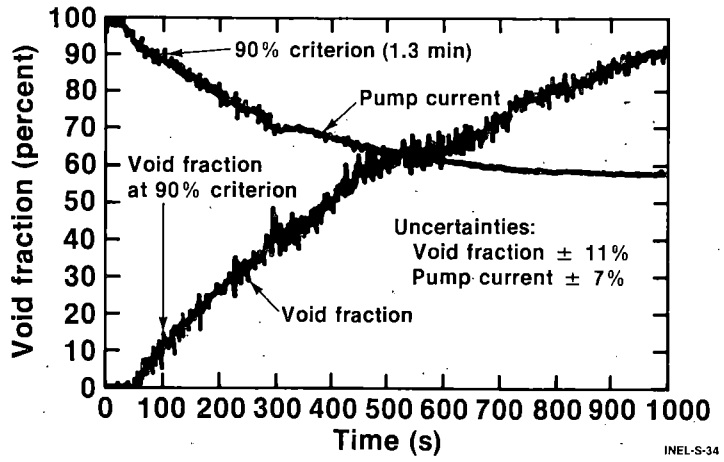

Pump Current vs Cold Leg Coolant Temperature for Cooldown Transient (L6-7)

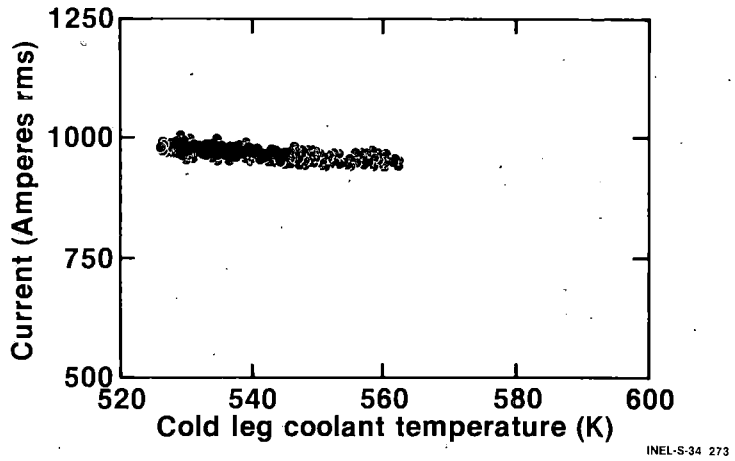

Pump Current vs Cold Leg Coolant Temperature for Heatup Transient (L9-1)

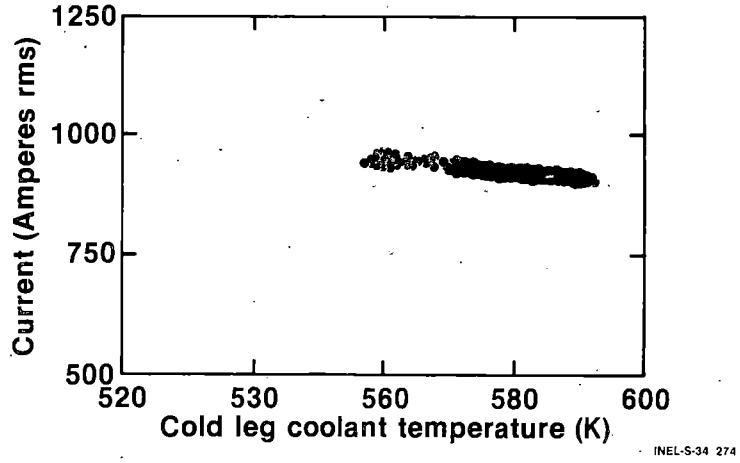

Pump Current vs. Cold Leg Coolant Temperature for Small Break Transient (L3-6)

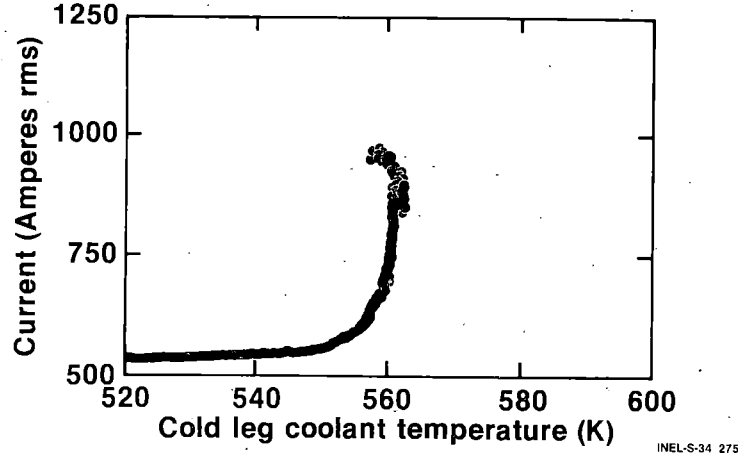

Pump Current vs. Cold Leg Coolant Temperatures Proposed Display

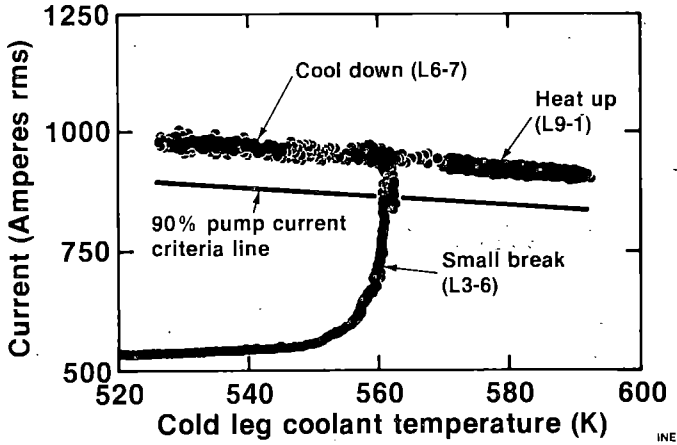

INEL-S-34 276

Issue

Reactor Vessel Liquid Level Measurement

INEL-S-34 270

Pump Trip Criteria

Recommendations:

- Concurrent addition of pump current
- Pump current vs. cold leg coolant temperature display

Reason:

- Trip criteria related to system mass inventory, i.e. system state
  - — Optimizes trip time
  - — Minimizes unnecessary trips
    - Non LOCA
    - Small LOCA

INEL-S-34 266

Reactor Vessel Liquid Level Measurement

Recommendation:

- Require reactor vessel liquid level measurement when pumps off (Reg. Guide 1.97)

Reason:

- No liquid level to measure when pumps on

INEL-S-34 271

JHL-10

Summary

- Support pumps off procedure during SBLOCA
- Include pump current in trip criteria
- Consider pump current vs cold leg coolant temperature display
- Reg. Guide 1.97 require reactor vessel liquid level measurement when pumps off

INEL-S-34 272

JHL-11

MULTIPLE FAILURE LOSS-OF-FEEDWATER TRANSIENT RESULTS AND IMPLICATIONS (LOFT EXPERIMENT L9-1/L3-3)

C. W. Solbrig

Presented at

The Ninth Water Reactor Safety Research Information Meeting

October 26 - 30, 1981

Gaithersburg, Maryland

Idaho National Engineering Laboratory

Idaho Falls, Idaho 83415

MULTIPLE FAILURE LOSS-OF-FEEDWATER TRANSIENT RESULTS AND IMPLICATIONS (LOFT EXPERIMENT L9-1/L3-3)

C. W. Solbrig
EG&G Idaho, Inc.

The purpose of performing the L9-1/L3-3[1,2,3] experiment, conducted at the LOFT facility at the Idaho National Engineering Laboratory, was to investigate a loss-of-all-feedwater transient and the operator actions recommended to arrest this transient. The first part of this exeriment, L9-1, was a simulation of an accident with multiple failures in which loss of all feedwater was assumed and the first scram signal, that would normally occur in a PWR due to low water level in the steam generators' secondary, was assumed to fail. The second portion of this experiment, L3-3, investigated methods of arresting or mitigating the accident simulated in the L9-1 portion of the transient. A third portion of the experiment was planned which was to be a slow core uncovery similar to the core uncovery experienced in Three Mile Island. This phase of the experiment was not initiated because much less water was lost from the primary system than predicted in the first two phases. The RELAP5 computer code was used to calculate the simulated transient. The change in plant behavior as a result of operator action can be assessed, and with the computer codes, can be used in licensing evaluations to determine how effective similar actions would be in a large PWR.

A comparison of the Three Mile Island (TMI) accident to the L9-2/L3-3 experiment is useful. In TMI all feedwater was lost to the secondary side of the PWR. This caused interruption of the heat transfer from the primary to the secondary and a pressure increase on the primary side. The decrease in the water level on the secondary side caused a shutdown signal to scram the reactor. In the LOFT experiment the reactor was not allowed to shut down (scram) on this signal. Instead, the reactor was scrammed somewhat later from the primary side pressure increase signal. In TMI, the primary side pressure increased due to the decrease in the heat removal capability from the secondary and caused the power operated relief valve (PORV) to

open. This valve stuck open in TMI and a large water loss was experienced, partly because the primary pumps were still operating. The pumps were finally turned off one hour and forty minutes after the initiation of the transient. In the LOFT experiment, the power operated relief valve was allowed to cycle open and close while the pumps were running. The recovery action from this simulated accident in LOFT was to simultaneously lock open the PORV and shut off the primary pumps before the system reached a saturation temperature corresponding to the open pressure of the PORV. The time at which the PORV was locked open signaled the time of transition between the two parts of the experiment. Due to the late time at which the PORV was locked open in the LOFT experiment compared to TMI, less mass was predicted to be lost from the LOFT system. In fact, even less mass was lost from the system than was predicted, resulting in no core uncovery during the experiment, thus, although the initiating event in the LOFT experiment and TMI were very similar, the results were much different.

Since less mass was lost in the experiment than in the RELAP5 prediction, this could be interpreted to mean that there is a large conservatism in the calculational techniques. However, it is important for computer codes such as RELAP5 to be able to predict accurately what actually occurs in the transient because these computer codes are needed in several critical areas of reactor operation. For example, the NRC Action Plan as a result of Three Mile Island specified that considerably more operator training should be done than was done previously. This operator training involves realistic training for incidents which include multiple failures and which are not expected to occur in a power plant. Since knowledge of plant behavior will not be forthcoming from plant data, the training information must come from predictive computer codes.

The two most obvious discrepancies between the experiment and the prediction were in the secondary side steam generator pressure, where the experimental pressure was lower than the prediction, and in the fluid heatup rate in the primary system, where the data showed a low heatup rate than the prediction. Both of these facts indicate that more heat was lost from the primary system than was predicted. The steady state heat

loss calibrations were immediately checked after the experiment and determined to be correct. In fact, heat loss calibrations were performed again as a check and shown to be in agreement with the previous data and input to the computer predictions. However, a simple heat balance showed that the primary temperature increase could be matched by taking out an additional 300 kW of heat from the primary system for the time period of 60 s to 1300 s in the transient. A RELAP5 computer run then showed that this heat transfer could account for the differences in the water loss from the system.

Examination of the input computer model showed that this additional amount of heat transfer from the primary fluid could be accounted for in two places. The first was an additional flow path in the reactor vessel that had been negligible in previous experiments. This flow path was used to cool the core filler blocks in the LOFT vessel. The second area was the metal mass on the secondary side that could store heat. In previous experiments the accurate representation of the heat storage in the secondary had been insignificant, and it was assumed that it would be insignificant for this transient also. However, this transient was different in one very important aspect than the previous LOFT experiments. This was the first experiment in which the pressure on the secondary increased during the transient. In depressurization transients, the pressure and hence the saturation temperature decreases. For these transients, heat stored in the metal retards heat loss from the fluid. In a pressurization transient such as this, the pressure and saturation temperature in the secondary increased, which allowed additional heat to be stored in the metal. This additional heat storage mechanism acts as a natural brake on the maximum temperature and pressure which can occur in a primary system. A computer run showed that these two effects can account for the differences between the experiment and the prediction.

In conclusion, analysis has shown that the differences between the prediction and the experiment are understood so that an accurate calculation of the experiment can be made. The results have shown that small simplifications can make large differences in the results,

particularly for transients which occur over a long period of time. With these details included in the model, it is apparent that a core uncovery experiment cannot be run with only the PORV locked open. Finally, it appears that knowledge of how to represent systems is increasing, but improvements are still being made based upon new experimental information.

REFERENCES

1. J. P. Adams, Quick-Look Report on LOFT Nuclear Experiment L9-1/L3-3, EGG-LOFT-5430, April 1981.

2. G. A. Taylor, R. J. Beelamn, and S. R. Behling, Best Estimate Prediction for LOFT Nuclear Experiment L9-1/L3-3, EGG-LOFT-5413, April 1981.

3. R. J. Beelman, LOFT Anticipated Transients with Multiple Failures, Test Series L9, Nuclear Test L9-1/L3-3/L8-1A, EGG-LOFT-5362, April 13, 1981.

Multiple Failure Loss-of-Feedwater Results and Implications

(LOFT L9-1/L3-3 Experiments)

Charles W. Solbrig

EG&G Idaho Inc

IDAHO NATIONAL ENGINEERING LABORATORY

USNRC Reactor Safety Research Test Facilities Compared to PWR

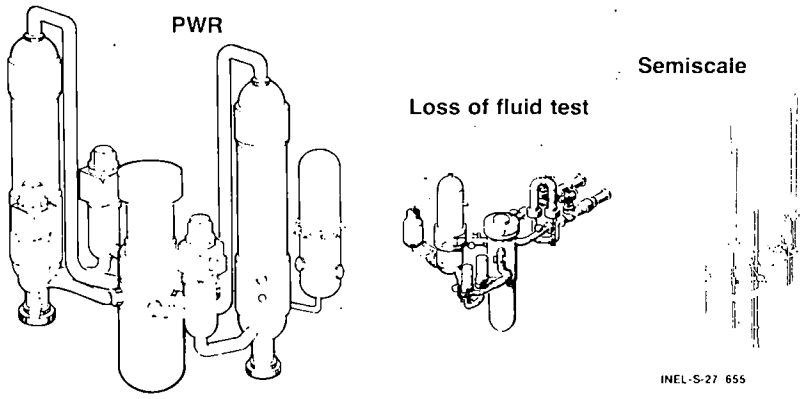

INEL-S-27 655

What Happened at Three Mile Island?

- Loss of water supply to secondary
- SG water level caused shut down
- Relief valve opened - stuck open
- Large water loss - pumps were running
- Pumps turned off very late

INEL-S-32 906

What Happened in LOFT

- Loss of water supply to secondary
- Pressure increase caused shut down
- Relief valve cycled - opened and closed
- Relief valve was locked open - pumps shut off
- Little mass was lost from the system
- No core uncovery

INEL-S-32 898

CWS-5

Primary System Mass

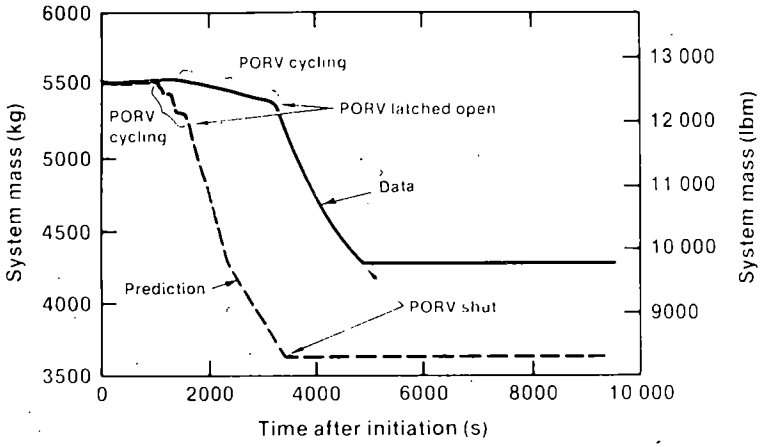

Ability to Predict is Important

- Operator training
- Operating procedures
- Technical specifications
- Development of simulators

Steam Generator Pressure

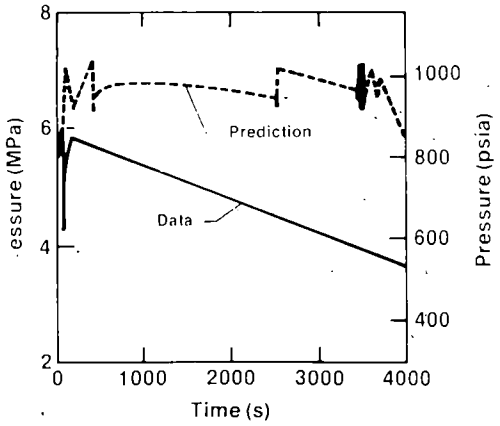

Hot Leg Temperature

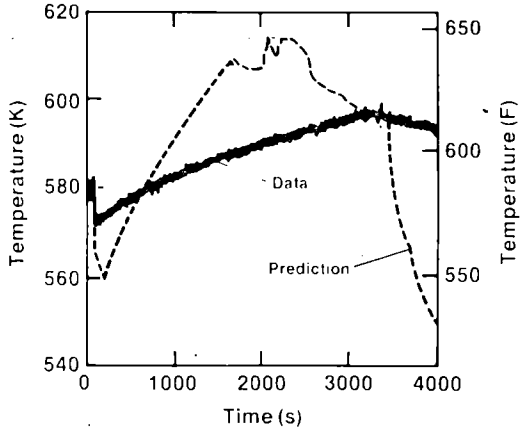

Why Were the Predictions So Far Off?

- Heat transferred from the fluid was underpredicted (300 kw)
- Steady state heat loss calibrations are available and were modeled correctly in the code (250 kw)
- Small heat transfer effects cause large differences in loss of water from the system
- Accurate distribution of heat sinks is necessary

Small Heat Transfer Effects Cause Large Differences in Loss of Water from the System

Hot Leg Temperature with Increased Heat Loss

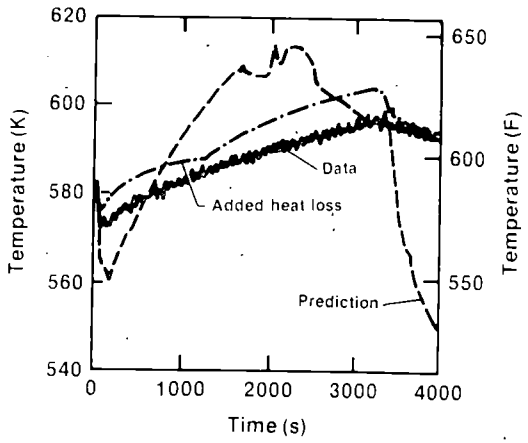

Primary System Pressure with Added Heat Loss

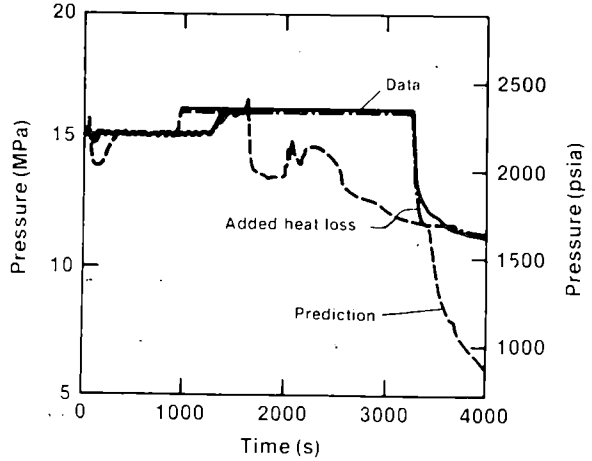

Integrated Mass Loss

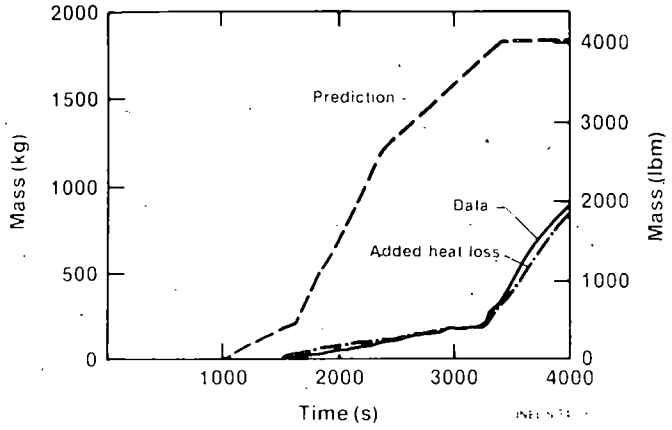

Major Areas of Heat Storage Unaccounted for in Predictions (~ 300 kw)

- Filler blocks and LOFT reactor vessel 65%
- Secondary side of steam generator 35%

Accurate Distribution of Heat Sinks is Necessary

Heat transferred to or from fluid

- Energy storage in metal
- Heat loss to the surroundings

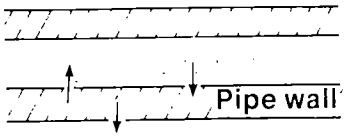

Pressure increase, these add
Pressure decrease, these subtract

Hot Leg Temperature with Flow Path and Conductors

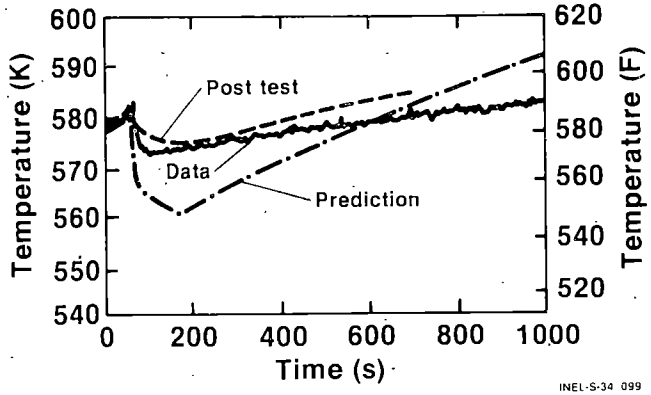

INEL-S-34 099

Why Didn't We Model These Before?

- It was not possible
- It is very expensive
- Simplifications are necessary

RELAP-LOFT Model Evolution

Code	Analysis	Number Volumes	Number Junctions	Number Heat Slabs
R4	L3-1, L3-2 EP	37	44	16
R5	L3-2 EP	84	100	33
R5	R5 base deck	113	122	43
R5	L3-7, L3-5 EP L3-6, L9-1 EP	115	120	65
R5	L3-1, L3-5 Post L3-6 Post L9-1 EP	118	125	120
R5	L9-1 Post	162	170	131

Conclusions

- We think we understand the differences
- Small simplifications can make large differences
- L8-1A could not be run in this geometry
- We continue to learn

RESULTS FROM LOFT EXPERIMENT L6-7/L9-2

J. P. Adams

Presented at

The Ninth Water Reactor Safety Research

Information Meeting

October 26 - 30, 1981

Gaithersburg, Maryland

Idaho National Engineering Laboratory

Idaho Falls, Idaho 83415

RESULTS FROM LOFT EXPERIMENT L6-7/L9-2

J. P. Adams
EG&G Idaho, Inc.

Loss-of-Fluid Test (LOFT) Experiment L6-7/L9-2[1] was successfully completed on July 31, 1981. The results from the preliminary analysis of this experiment are presented in this summary including comparison of L6-7/L9-2 data with the pre-experiment prediction and with data obtained during a turbine trip test[2] conducted in the Arkansas Nuclear One--Unit Two (ANO-2) commercial pressurized water reactor (PWR).

The LOFT facility[3] is a 50-MW(t), volumetrically scaled PWR designed to reproduce, both in time and approximate magnitude, the significant thermal and hydraulic events expected in a commercial PWR during a postulated loss-of-coolant accident (LOCA). Although the LOFT design was based specifically on and was intended to reproduce LOCA phenomena, ongoing analysis of LOFT scaling with respect to commercial PWRs indicates that anticipated transients such as L6-7/L9-2 can also be simulated in the LOFT facility, that is, similar phenomena will occur in LOFT as are expected to occur in a commercial PWR.

Experiment L6-7/L9-2 consisted of two parts which were completed sequentially. The first part, L6-7, simulated a loss of load accident compounded by an uncontrolled secondary steam leakage which produced a rapid (300 K/h) cooldown of the primary coolant system. This part was based on and was intended to simulate an unplanned secondary induced cooldown that occurred during a turbine trip transient test conducted at ANO-2 in January 1980.[2] These two data sets (L6-7 and ANO-2) will be used to conduct a typicality study of LOFT and a commercial PWR as part of the ongoing qualification of computer codes to license reactors. The

second part of the experiment, L9-2, was initiated by turning off the primary coolant pumps at the end of L6-7 and simulating a continued rapid cooldown. L9-2 was conducted to provide data on the effects of voids and thermal stratification on natural circulation during a cooldown transient without forced flow.

Experiment L6-7/L9-2 was initiated from conditions generally representative of a commercial PWR. Differences between the LOFT initial conditions and those of ANO-2 resulted from differences in the scaled pressurizer volumes and LOFT experiment safety considerations and include (comparing L6-7 to ANO-2) larger scaled pressurizer liquid mass, smaller scaled reactor power, and smaller core fluid temperature rise. Consideration of these differences will be included in the L6-7/ANO-2 comparison analysis.

Experiment L6-7/L9-2 was initiated by manually establishing a steam flow rate which was calculated by the HYBRID[4] code to produce a primary coolant system cooldown similar to ANO-2. This controlled steam flow transient continued until the pressurizer emptied at 278 s (4.6 min). The primary coolant pumps were turned off 46 s later, terminating L6-7 and initiating L9-2. Natural circulation initiated at 341 s and the cooldown was continued. After the pressure had decreased to approximately 6.0 MPa (870 psia), flashing of hot stagnant fluid in the primary system outside the pressurizer decreased the depressurization rate by almost a factor of 10, from 2.0×10^{-2} MPa/s (2.9 psi/sec) to 2.5×10^{-3} MPa/s (0.36 psi/sec), and the system slowly depressurized until the accumulator injection pressure of 4.3 MPa (625 psia) was reached at 1832 s (30.5 min) which terminated the experiment.

Comparison of L6-7 and ANO-2 indicates that similar phenomena occurred in both transients. Subsequent to 100 s the cold and hot leg cooldown rates for L6-7 and ANO-2 matched closely. After 50 s and prior to pressurizer emptying, the primary system depressurization rates matched closely. Differences between ANO-2 and L6-7 during other times are

currently being evaluated and, at this time, are considered to result from scaling and initial condition differences.

The L6-7 primary coolant pumps data support the conclusion previously drawn from LOFT Experiment L3-6 data,[5] that pump current can be used to differentiate between transients that result in fluid density decreases (such as loss-of-coolant accidents) and those which result in fluid density increases (such as cooldown transients). This phenomena has potential application to licensing in that (a) additional information on primary coolant mass inventory would be available to operators which would be useful in determining the nature of a depressurization transient, and (b) leaving the pumps on during a cooldown transient would result in a more rapid recovery since more complete thermal mixing would occur.

Natural circulation, which initiated after cessation of pump forced flow, was not significantly affected by coolant flashing in the reactor vessel upper plenum or by the presence of steam from the pressurizer in the reactor vessel outlet piping. These data will be used in the resolution of safety issues involving natural circulation cooldown in the presence of reactor vessel and loop voiding.[6]

The best estimate experiment prediction[7] was calculated by RELAP5,[8] an advanced one-dimensional system analysis code based on a nonhomogeneous, nonequilibrium, hydrodynamic model. RELAP5 calculations predicted the L6-7 transient very well. The L9-2 transient was not as well predicted. However, differences between the boundary conditions in the L9-2 transient and the boundary conditions assumed for the RELAP5 prediction are considered to be the principal cause of the differences between the actual and predicted L9-2 transient.

In summary, preliminary analysis of the LOFT Experiment L6-7/L9-2 data indicates that these data will be useful in addressing several current licensing issues including: qualification of best estimate codes, natural circulation cooldown with loop voiding, and the effect of tripping primary coolant pumps during cooldown transients.

REFERENCES

1. J. P. Adams, Quick Look Report on LOFT Nuclear Experiment L6-7/L9-2, EGG-LOFT-5526, August 1980.

2. D. P. Siska, NSSS Transient Tests at ANO-2, EPRI NP-1708, May 1981.

3. D. L. Reeder, LOFT System and Test Description (5.5-ft Nuclear Core 1 LOCES), NUREG/CR-0247, TREE-1208, July 1978.

4. F. K. Hyer and C. D. Clayton, Hybrid Computer Simulation at the LOFT Plant, LOFT Technical Report 10-2, Rev. C, December 1980.

5. P. D. Bayless, J. M. Carpenter, Experiment Data Report for LOFT Nuclear Small Break Experiment L3-6 and Severe Core Transient Experiment L8-1, NUREG/CR-1868, EGG-2075, January 1981.

6. D. F. Ross (NRC) Memorandum to D. G. Eisenhut Followup Action on Natural Circulation Cooldown, November 20, 1980.

7. W. H. Grush, Best Estimate Prediction for LOFT Nuclear Experiment L6-7/L9-2, EGG-LOFT-5506, July 1981.

8. V. H. Ransom, et al., RELAP5/MOD1 Code Manual, NUREG/CR-1826, EGG-2070, November 1980.

Results from LOFT Experiment L6-7/L9-2

James P. Adams

EG&G Idaho, Inc.

Contents

- Experiment Description
- Event Sequence
- Phenomena
- Conclusions

INEL-S-41 019

LOFT System Configuration

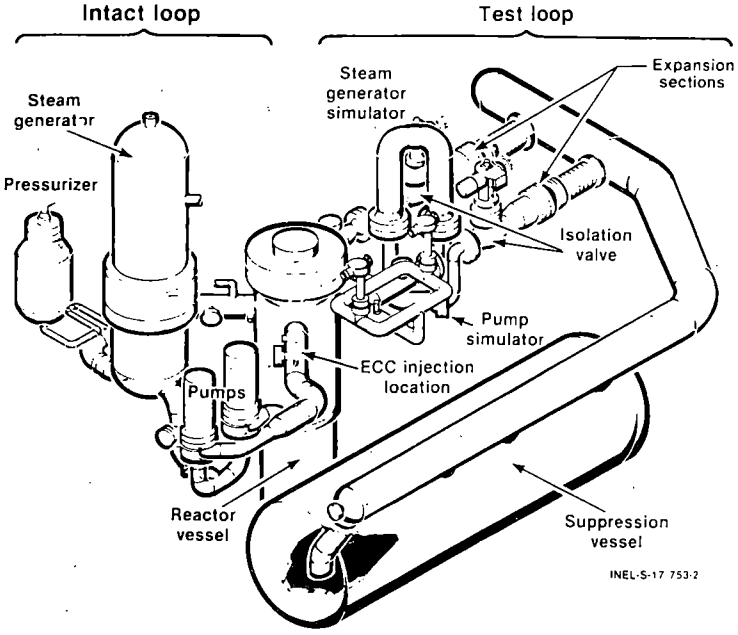

Experiment Description

L6-7

- Rapid cooldown (270 K/h)
- Simulated ANO-2 Turbine trip

L9-2

- Continued rapid cooldown
- Effect of voids on natural circulation

INEL-S-41 020

Initial Conditions

Parameter	LOFT	ANO-2
Core Power / System Volume $\left(\frac{MW}{m^3}\right)$	7.2	10.4
Primary Pressure (MPa)	14.8	15.6
Cold Leg Temperature (K)	557	561
Core Δ T (K)	20	32
Primary Flow / System Volume $\left(\frac{kg}{s.m^3}\right)$	67.5	63.1
∘ Pressurizer Liquid Volume / Effective System Volume	0.09	0.06

∘ LOFT Effective System Volume=Volume affected by the cooldown

INEL-S-41 018

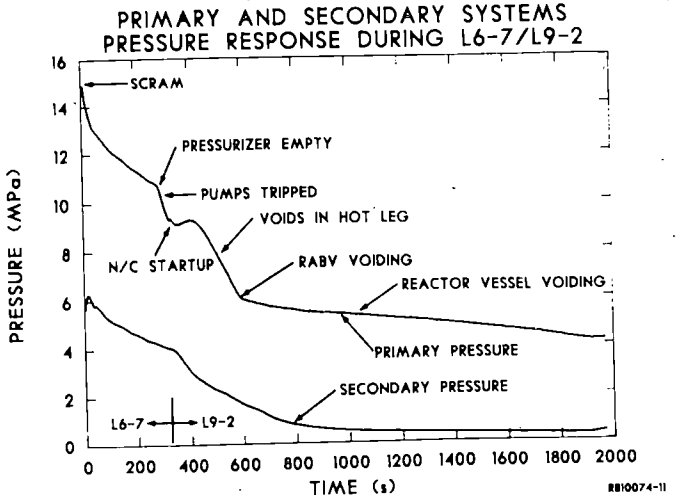

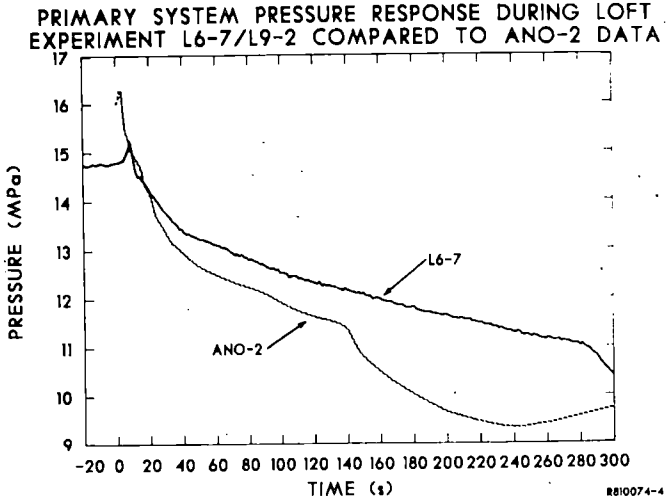

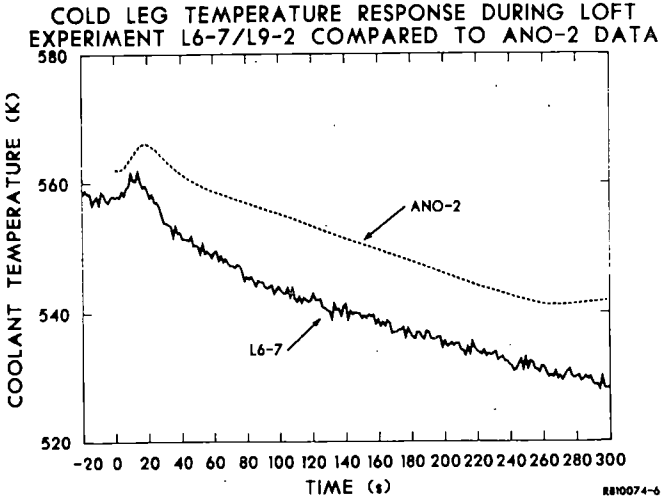

HOT LEG TEMPERATURE RESPONSE DURING LOFT EXPERIMENT L6-7/L9-2 COMPARED TO ANO-2 DATA

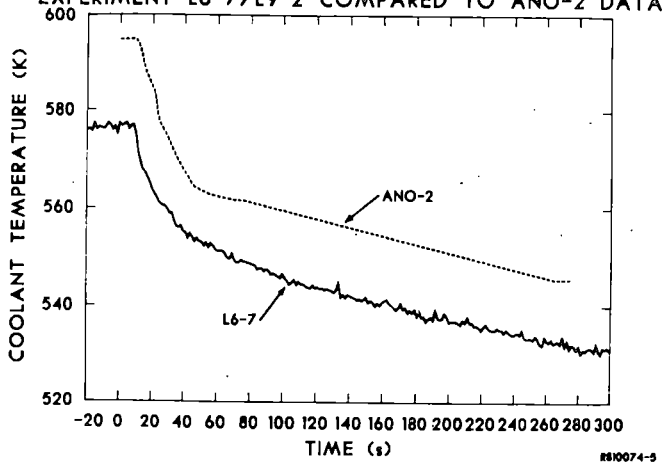

COOLANT PUMP CURRENT VS COOLANT DENSITY FOR L3-6 AND L6-7

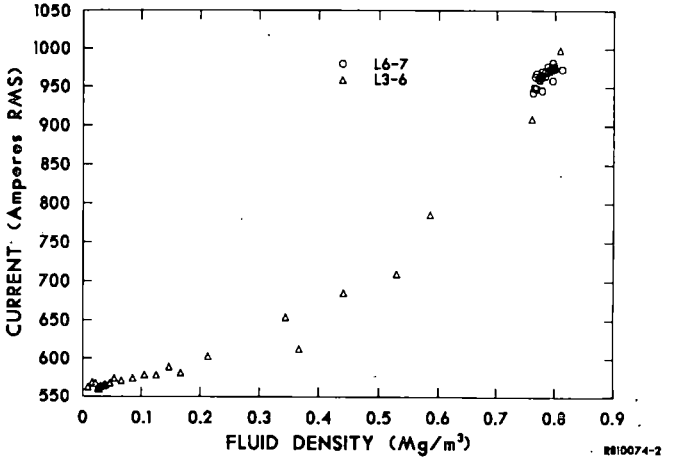

COMPARISON OF PRIMARY COOLANT PUMP CURRENT HISTORIES FOR L6-7 AND L3-6

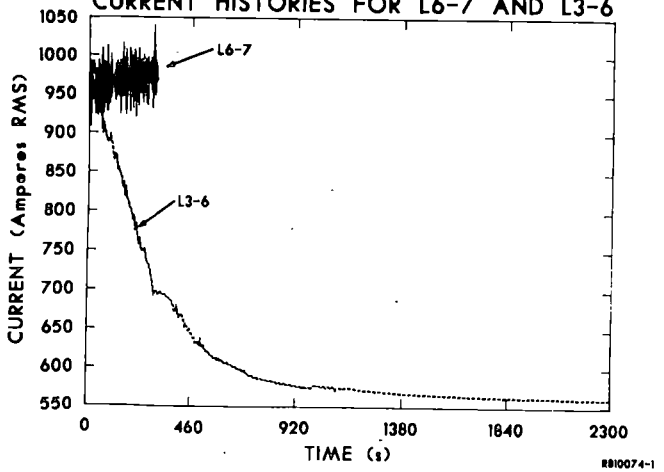

NATURAL CIRCULATION FLOW MEASUREMENTS USING TWO METHODS FOR EXPERIMENT L9-2

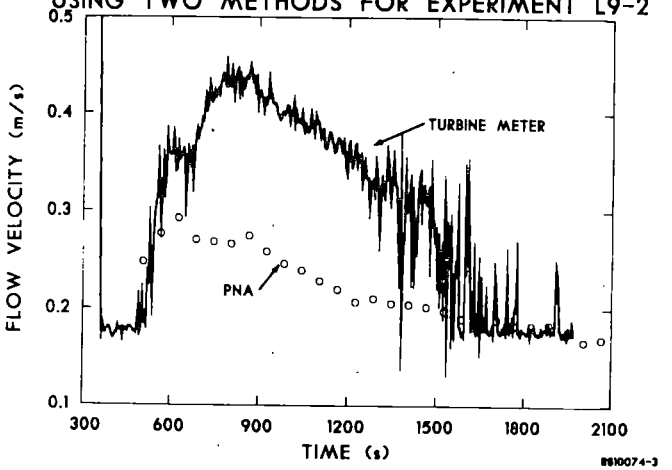

LIQUID LEVEL IN THE INTACT LOOP HOT LEG
0.0 = PIPE BOTTOM

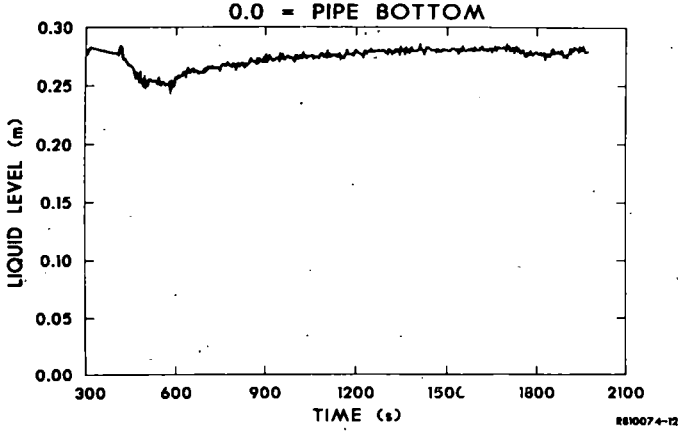

LIQUID LEVEL IN THE
REACTOR VESSEL UPPER PLENUM

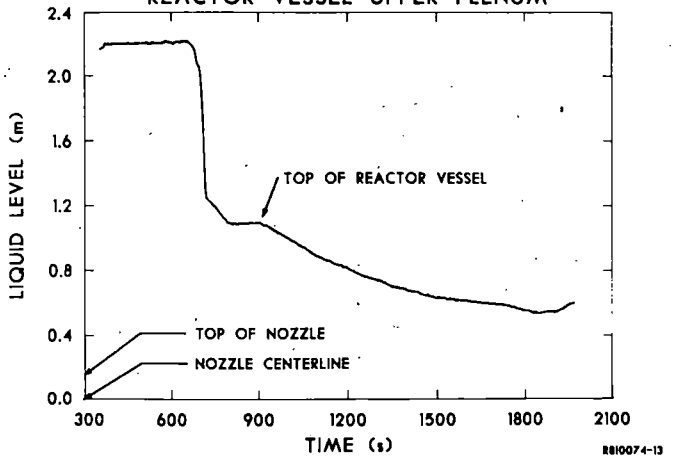

FLUID TEMPERATURE COMPARISONS IN UPPER PLENUM, HOT AND COLD LEGS, AND SATURATION PRESSURE

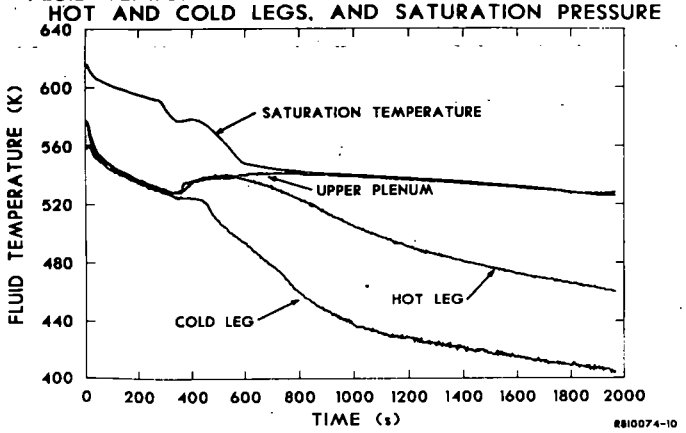

COMPARISON OF L6-7/L9-2 TO MIXED AND UNMIXED PREDICTIONS OF PRIMARY SYSTEM PRESSURE

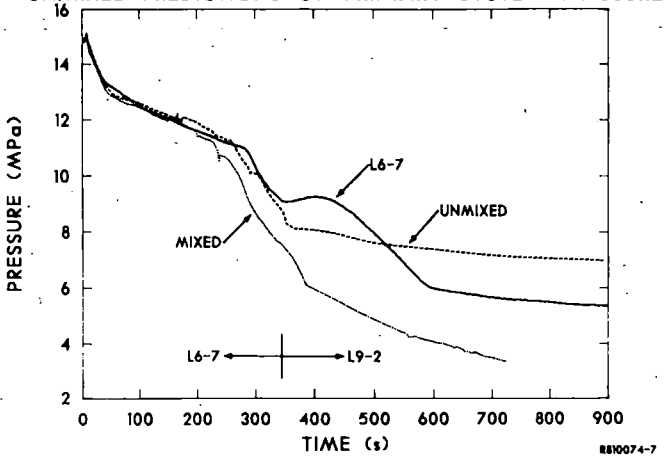

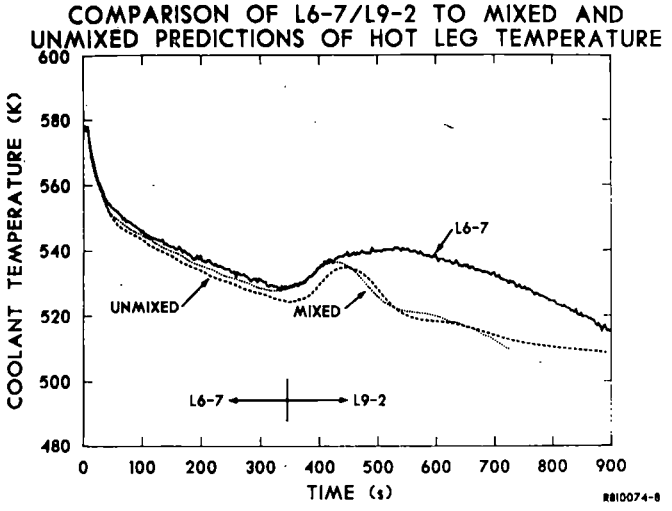

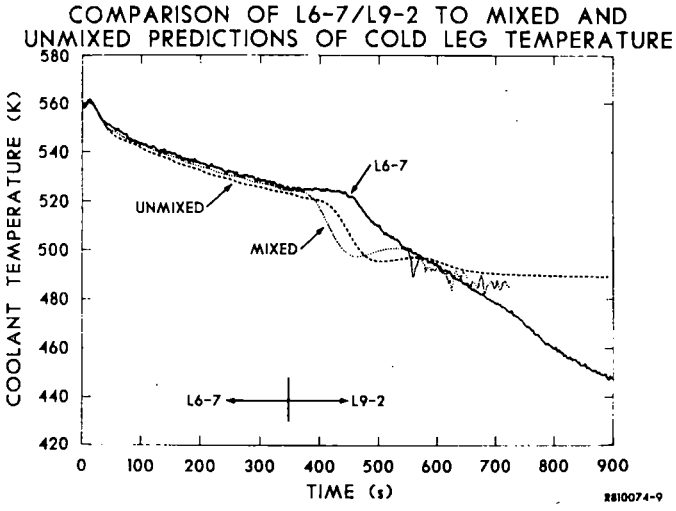

Conclusions

L6-7

- ANO-2 Turbine trip transient adequately simulated
- PCP Current may be useful to differentiate between LOCAs and cooldown transients
- RELAP5 Pre-experiment predictions closely matched the data

L9-2

- Natural circulation started up following pump trip and was not affected by voids in the loop or reactor vessel
- Differences exist between ep and data caused differences in boundary conditions

INEL-S-41 024

PRELIMINARY RESULTS OF INTERMEDIATE BREAK EXPERIMENTS L5-1 AND L8-2

W. H. Grush

Presented at

The Ninth Water Reactor Safety Research Information Meeting

October 26 - 30, 1981

Gaithersburg, Maryland

Idaho National Engineering Laboratory

Idaho Falls, Idaho 83415

EG&G Idaho

Idaho Falls, Idaho 83415

Preliminary Results of Intermediate Break Experiments L5-1 and L8-2

W. H. Grush
EG&G Idaho, Inc.

Intermediate break loss-of-coolant experiments (LOCEs) L5-1 and L8-2 were completed at the Loss-of-Fluid Test (LOFT) facility at the Idaho National Engineering Laboratory on September 24 and October 12, 1981, respectively. Each 15% break experiment simulated the rupture of a 14-inch schedule 160 emergency core cooling (ECC) pipe in a commercial pressurized water reactor (PWR). Prior to the initiation of each experiment, the reactor system was operating at approximately nominal PWR operating conditions with the power at 46 MWth with the primary coolant system (PCS) pressure at about 15 MPa (2170 psia). The PCS flow was 310 kg/s (2.45×10^6 lbm/hr) which gives a reactor vessel temperature rise of 27.4 K (49.3°F). The cold leg temperature was 551 K (532°F).

For experiment L5-1 the ECC was scaled to represent three of the four ECC systems in a PWR. The accumulator pressure was reduced from the normal 4.22 MPa (612 psia) to 1.66 MPa (240 psia) to depict the most limiting of commercial PWR ECC system designs. Thus, L5-1 addressed the licensing issue of ECC effectiveness for intermediate break loss-of-coolant accidents (LOCAs).

Immediately following the initiation of experiment L5-1, flow through the pressurizer surge line choked allowing the remainder of the PCS to depressurize very rapidly. Reactor scram occurred at 0.17 s. At 2.5 s, the PCS pressure reached the saturation pressure of the upper plenum fluid. High pressure injection started at 2.9 s followed by manual tripping of the primary coolant pumps (PCPs) at 4 s. The depressuration rate slowed significantly when the fluid upstream of the break became saturated at 10.5 s. The pressurizer emptied at 15.5 s. At 19.3 s, the PCPs were decoupled from the motor generator (MG) sets, indicating that the

pump coastdown was nearly completed. During the next 90 s, a well defined, radially uniform liquid interface was dropping through the upper plenum of the reactor vessel. At 108.4 s, the liquid interface passed the highest cladding thermocouple in the core and the thermal excursion (cladding temperature rise) began. The level continued to fall through the core at a rate of approximately 0.019 m/s (0.76 in./s). Accumulator injection began at 185.8 s when the level was less than 0.13 m (5 in.) above the bottom of the core. Within 3 s the fuel cladding temperatures began dropping to the system saturation temperature (quench) from the bottom up. The maximum cladding temperature of 715 K (828°F) was reached at a thermocouple located 1.0 m (39 in.) above the core bottom at 198 s. Low pressure injection started at 201 s and the highest cladding thermocouple quenched at 213 s. The average reflood rate was 0.058 m/s (2.3 in./s). A gradual PCS repressurization began during the reflood which caused the accumulator injection to stop temporarily at 225 s.

Experiment L8-2 was planned to duplicate the initial portion of L5-1 except that the accumulator and low pressure injection system (LPIS) were inhibited. Preliminary evaluation of the data confirmed that results from the two tests were very similar until the time of accumulator injection in L5-1. In experiment L8-2, the entire core was uncovered and the cladding temperatures exceeded those observed during L5-1.

When a fuel cladding temperature of 811 K (1000°F) was reached, the PCPs were restarted to test the core cooling effectiveness of pump restart at high system void conditions. As expected, a slight cooling effect was observed in the lower half of the core while the heatup continued with no significant change in the rest of the core. When the cladding temperature reached 950 K (1250°F), the accumulator, which had been inhibited, was allowed to inject. Less than 10 s later when a cladding temperature of 978 K (1300°F) was reached, the plant protection system activated a second accumulator. Reflood of the core was completed by 307 s.

The RELAP5/MOD1 experiment prediction for each test consisted of a nominal calculation and a sensitivity calculation. The sensitivity calculation used a nozzle coefficient of 0.84 for the break compared to the nominal calculation value of 1.0. (These values represent the range of uncertainty in the break flow behavior.) Comparisons of the sensitivity calculations to the measured data for both tests show that the hydraulic behavior was very well predicted with the actual nozzle coefficient being close to 0.84. The core thermal response during the heatup was also well predicted; however, several low amplitude, short-duration thermal excursions prior to the principal dryout were calculated. The cause of these excursions will be investigated in the posttest analysis.

In summary, the experiments were highly successful. The high degree of reproducibility observed in these tests gives added confidence both in the LOFT experimental data and in the code assessment efforts based on that data. RELAP5/MOD1 predicted the phenomena very well. Experiment L5-1 demonstrated the effectiveness of the LOFT ECC systems at mitigating the consequences of an intermediate break loss-of-coolant accident. This result implies that PWR ECC systems which were designed primarily for large break LOCAs can successfully terminate an intermediate break LOCA transient.

As predicted, experiment L8-2 demonstrated the ineffective core cooling afforded by PCP restart at high void conditions. Therefore, while PCP restart may be effective during a small break LOCA in a PWR when the system mass inventory is higher, it would probably not be effective for intermediate break LOCAs.

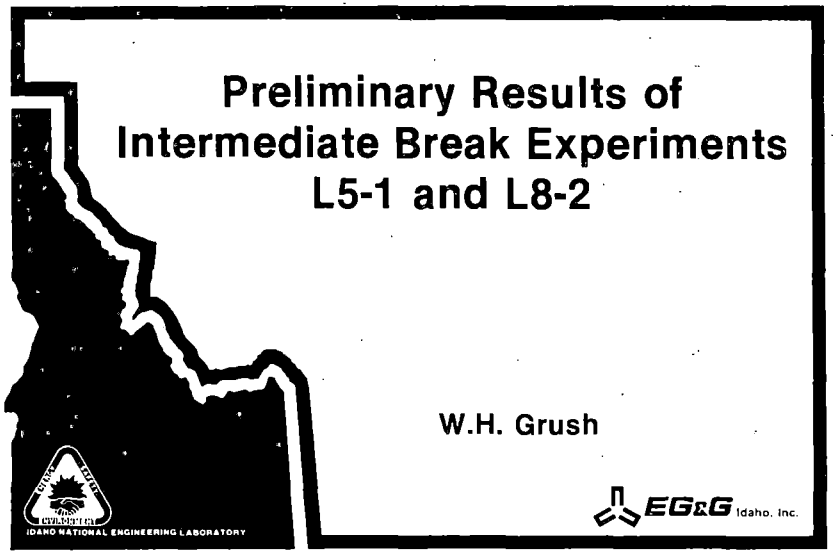

L5-1 / L8-2

- Experiment L5-1 completed 9-24-81
- Experiment L8-2 completed 10-12-81
- Simulated rupture of a 14 inch (ECC) pipe in a commercial PWR

INEL-S-40 020

Overview

L5-1

- ECC scaled to 3 of 4 PWR ECC systems
- Accumulator at low pressure-1.66MPa (240 psia)

L8-2

- Same as L5-1 until accumulator injection
- Accumulator and LPIS inhibited
- PC pumps restarted at 811K (1000°F)

INEL-S-40 021

Initial Conditions

Parameter	Units	L5-1	L8-2	Uncertainty
Reactor power	MWth	45.9	46.0	±1.2
PCS pressure	MPa psia	15.0 2176.	14.9 2161.	±0.2 ±30.
PCS flow	kg/s 10^6lbm/hr	309. 2.45	311. 2.45	±4.0 ±0.02
Reactor vessel ΔT	K F	27.0 48.6	27.8 50.0	±1.6 ±2.9
Cold leg temperature	K F	551.3 532.7	551.6 533.2	±0.8 ±1.4
Accumulator pressure	MPa psia	1.66 240.8	---- ----	±0.06 ±8.7

INEL-S-40 022

WHG-4

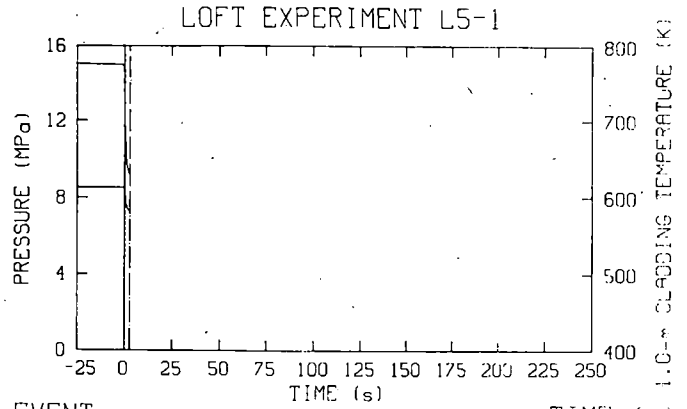

EVENT	TIME (s)
EXPERIMENT INITIATION	0.000
REACTOR SCRAM	0.166
HPIS INJECTION STARTS	2.88

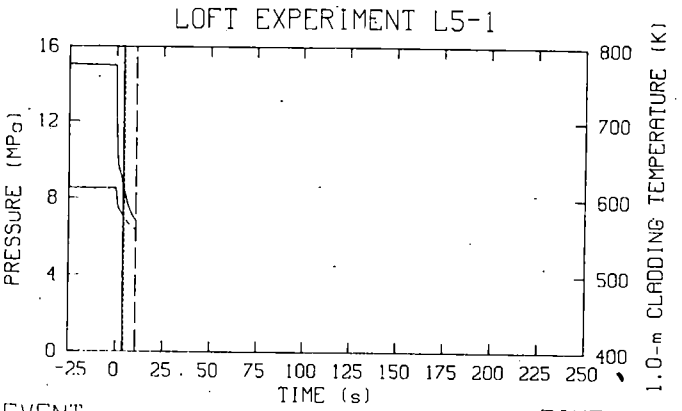

EVENT	TIME (s)
MAIN FEED OFF	4.0
PRIMARY COOLANT PUMPS TRIPPED	4.0
SUBCOOLED BREAK FLOW ENDS	10.5

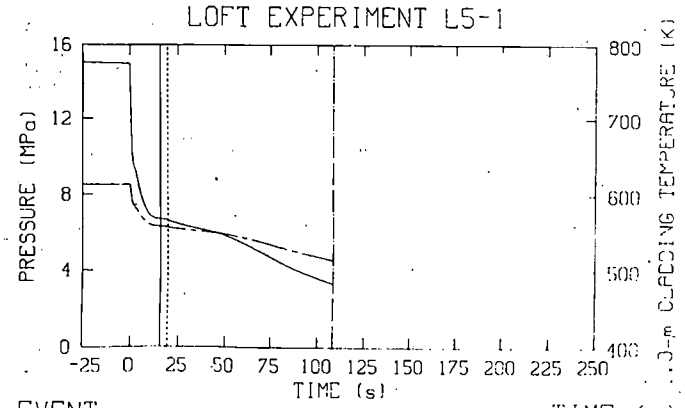

EVENT	TIME (s)
PRESSURIZER EMPTIES	15.5
PCP DECOUPLED FROM MG SET	19.3
FUEL CLADDING EXCURSION BEGINS	108.4

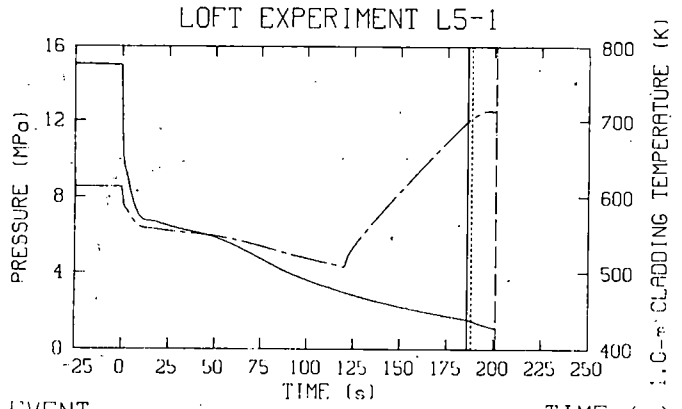

EVENT	TIME (s)
ACCUMULATOR INJECTION STARTS	185.8
FIRST FUEL CLADDING TEMPERATURE QUENCH	188.1
LPIS INJECTION STARTS	201.0

WHG-5

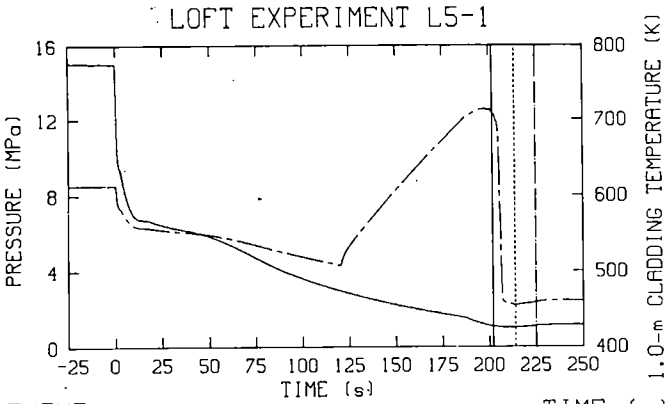

EVENT	TIME (s)
FUEL CLADDING QUENCHED AT .66-m ELEV.	202.0
REFLOOD COMPLETED	214.0
ACCUMULATOR INJECTION STOPS	225.0

L5-1 Hot Leg Pressure

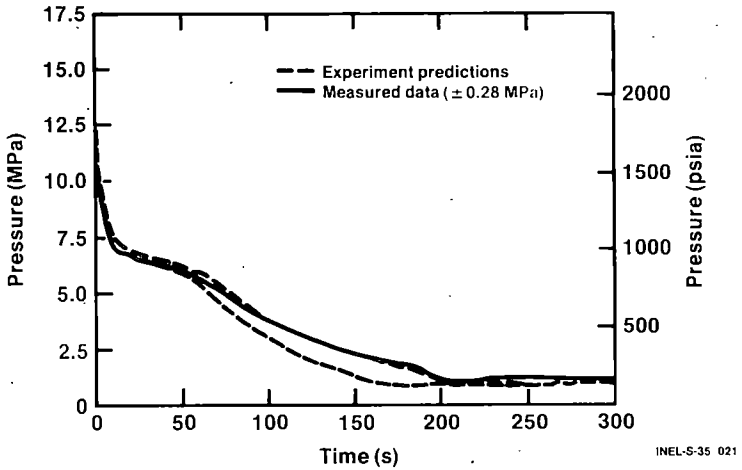

INEL-S-35 021

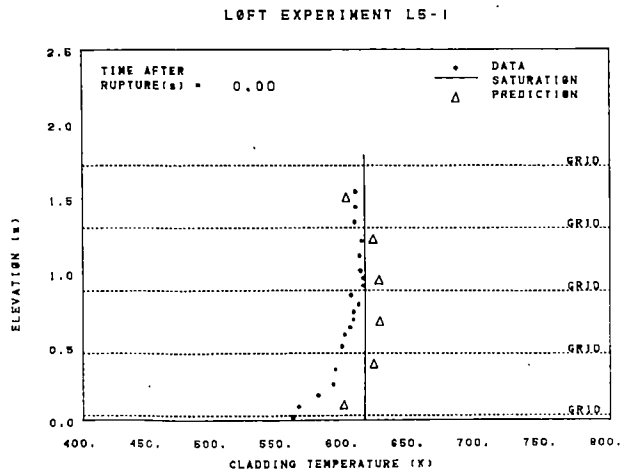

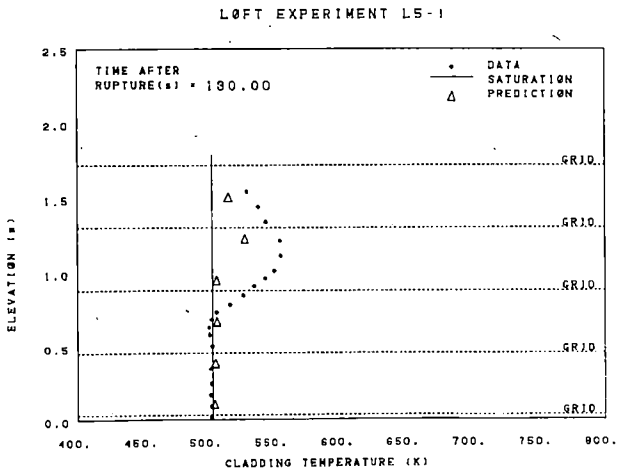

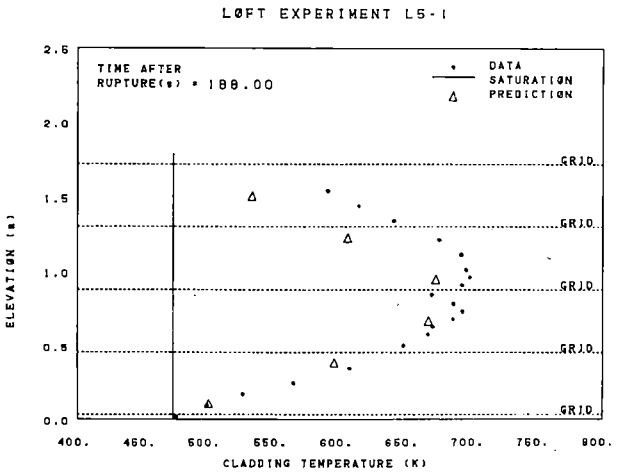
LØFT EXPERIMENT L5-1
TIME AFTER
RUPTURE(s) = 188.00
DATA
SATURATION
PREDICTION
GRID
ELEVATION (m)
CLADDING TEMPERATURE (K)

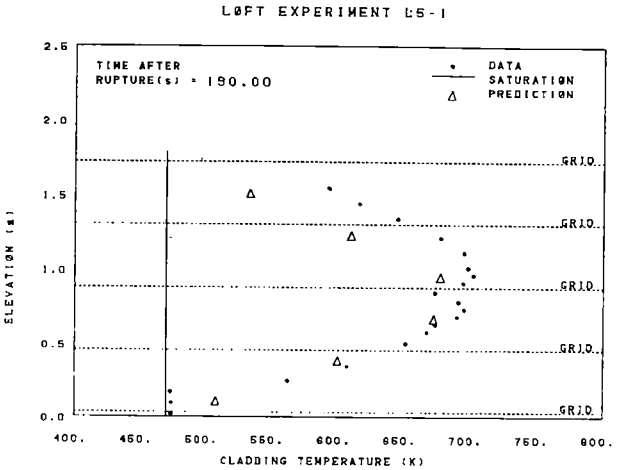
LØFT EXPERIMENT L5-1
TIME AFTER
RUPTURE(s) = 190.00
DATA
SATURATION
PREDICTION
GRID
ELEVATION (m)
CLADDING TEMPERATURE (K)

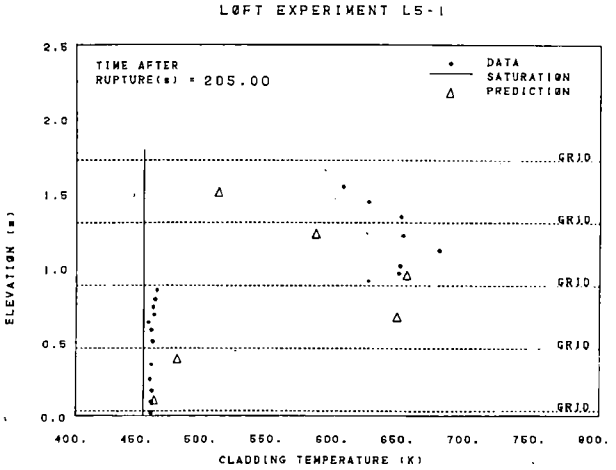
LØFT EXPERIMENT L5-1
TIME AFTER
RUPTURE(s) = 205.00
DATA
SATURATION
PREDICTION
GRID
ELEVATION (m)
CLADDING TEMPERATURE (K)

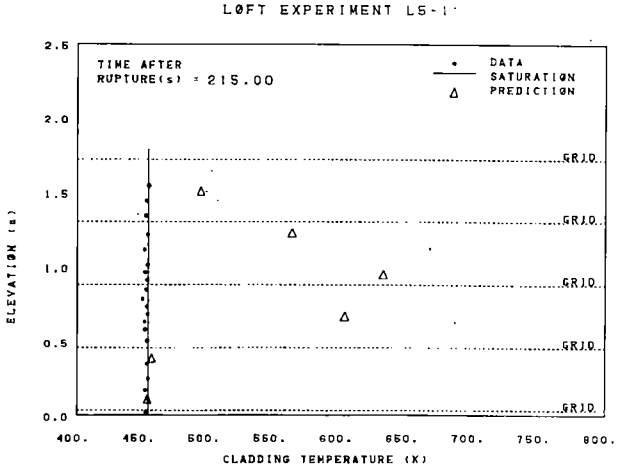
LØFT EXPERIMENT L5-1
TIME AFTER
RUPTURE(s) = 215.00
DATA
SATURATION
PREDICTION
GRID
ELEVATION (m)
CLADDING TEMPERATURE (K)

L5-1/L8-2 Pressure Comparison

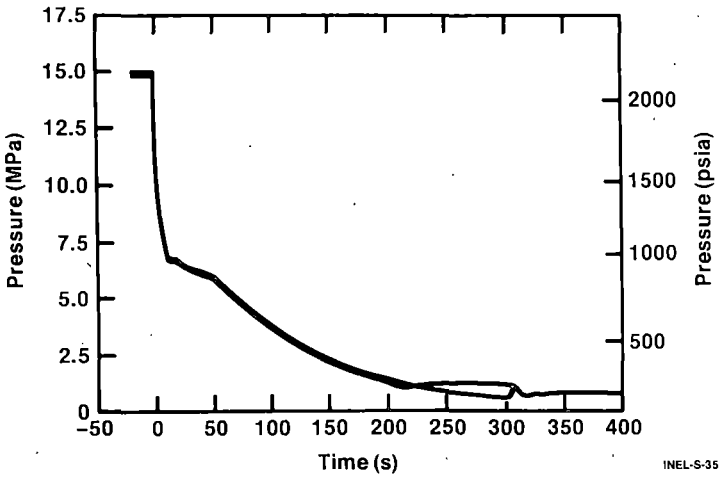

INEL-S-35 022

L8-2 Hot Leg Pressure

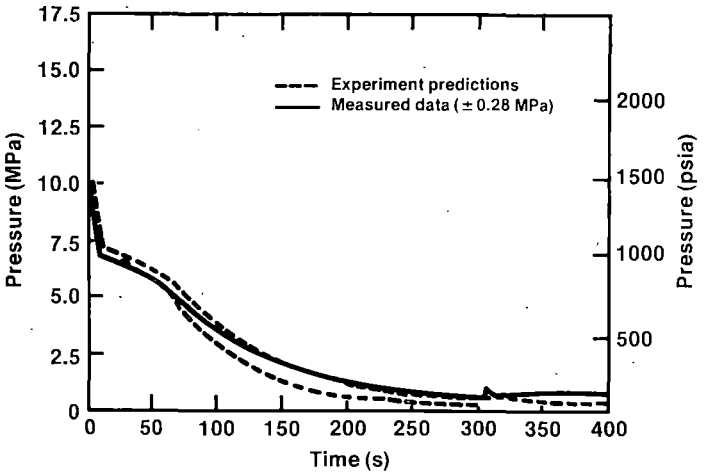

INEL-S-35 032

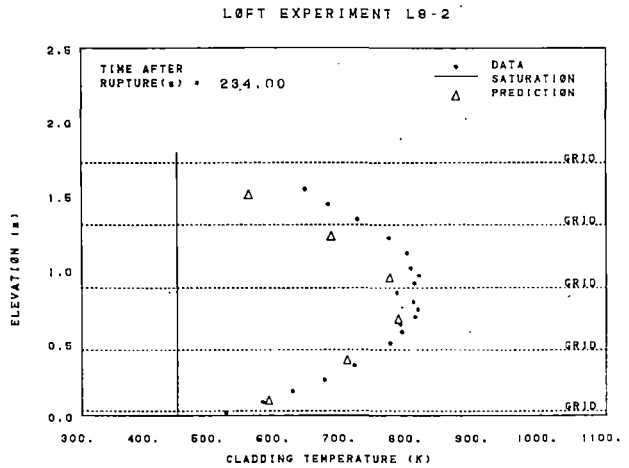

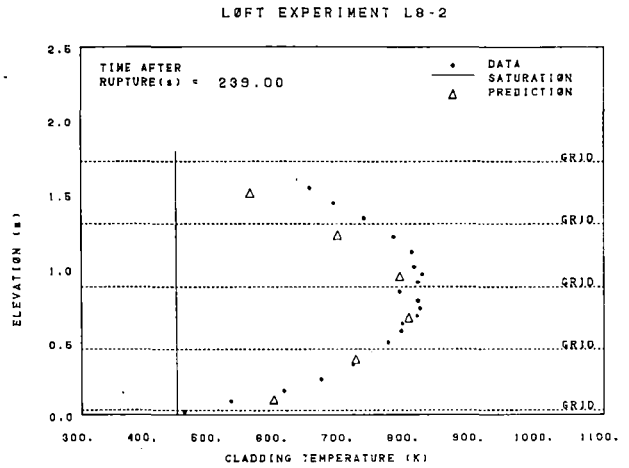

WHG-8

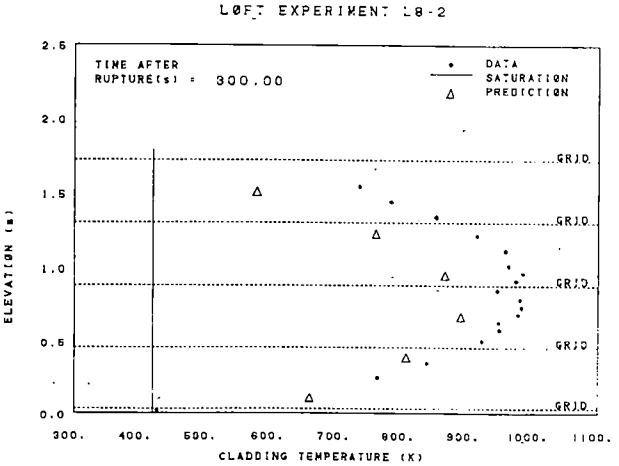

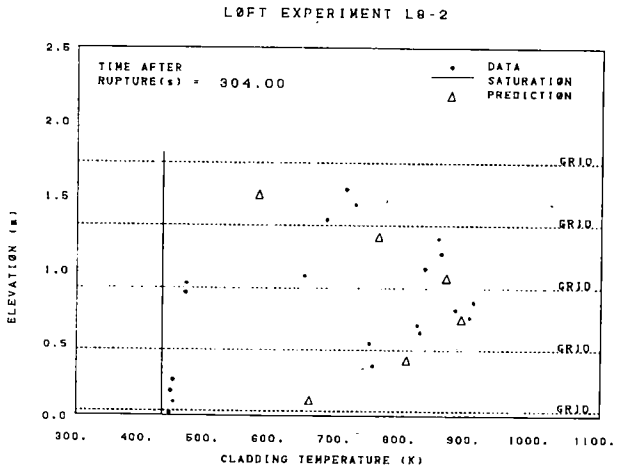

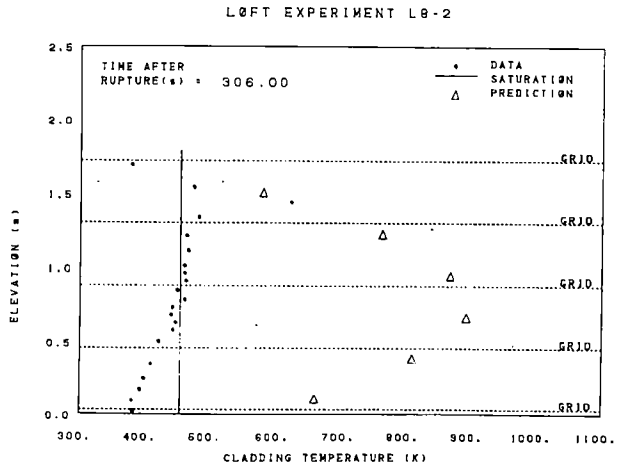

Conclusions

- Experiments were successful
- RELAP5/MOD1 predicted phenomena very well
- L5-1 demonstrated effectivness of ECC systems for intermediate break
- L8-2 demonstrated ineffective core cooling afforded by primary coolant pump restart at high void conditions

INEL-S-40 023

SUMMARY OF LOFT CONCLUSIONS RELEVANT TO LICENSING

Water Reactor Safety Research

Information Meeting

October 26, 1981

Gaithersburg, MD

LOFT RESEARCH INFORMATION LETTERS IN PROCESS

1. ANTICIPATED TRANSIENT L6-1, L6-2, L6-3 AND L6-5 PHENOMENA EVALUATION
2. SMALL BREAK LOCE'S L3-0, L3-1, L3-2 AND L3-7 PHENOMENA EVALUATION
3. SMALL BREAK PREDICTION CAPABILITIES
4. LOFT LOCE'S L3-5 AND L3-6 PUMPS OFF/ON RESULTS
5. COMPARISON OF NUCLEAR AND ELECTRICAL ROD RESPONSE FOR LARGE BREAK PWR LOCA CONDITIONS
6. RESULTS OF THE AUGMENTED OPERATOR CAPABILITY PROGRAM
7. LOFT TECHNICAL SUPPORT CENTER DEVELOPMENT
8. LOFT INSTRUMENT EVALUATION

ANTICIPATED TRANSIENT EXPERIMENTS

- THE FOUR AT SIMULATIONS AT LOFT WERE:
  1. LOSS-OF-STEAM LOAD IN ALL STEAM GENERATORS (L6-1)
  2. LOSS OF ALL FORCED PRIMARY COOLANT SYSTEM (PCS) FLOW (L6-2)
  3. EXCESSIVE LOAD INCREASE (L6-3)
  4. LOSS OF FEEDWATER TO ALL STEAM GENERATORS (L6-5)

LPL4-19

ANTICIPATED TRANSIENT EXPERIMENTS (cont'd)

- EXPERIMENT RESULTS SHOWED
  1. NONE OF THE TRANSIENTS PRESENTED A HAZARD TO THE LOFT REACTOR SYSTEM
  2. IMPROVEMENTS ARE NEEDED IN CALCULATIONAL ABILITY

LPL4-19A

SMALL BREAK EXPERIMENT L3-0, L3-1, L3-2, L3-7

- NATURAL CIRCULATION READILY OCCURS IN BOTH SINGLE AND TWO-PHASE MODES
- REFLUX FLOW MODE DOES NOT OCCUR FOR SMALL BREAKS IN THE COLD LEG
- OPERATOR AUGMENTATION POSSIBILITIES EXISTED IN AREAS OF ACCIDENT RECOGNITION
- PHENOMENA ASSOCIATED WITH SMALL BREAK EVENTS ARE WELL UNDERSTOOD

LPL4-15

SMALL BREAK PREDICTION CAPABILITY

- EACH EXPERIMENT REVEALED AREAS WHERE DEVELOPMENT WAS CLEARLY IDENTIFIED IN ONE OR MORE OF THREE ASPECTS OF PWR TRANSIENT:
  1. CALCULATION - THE COMPUTER CODE
  2. THE PWR SYSTEM MODEL
  3. OPTION SELECTION

LPL4-10

SMALL BREAK PREDICTION CAPABILITY (cont'd)

- SPECIFIC RECOMMENDATIONS DEALING WITH
  - CRITICAL FLOW
  - PRESSURIZER BEHAVIOR
  - HEAT SOURCES & SINKS
  - SG HEAT TRANSFER
  - ACC GAS EXPANSION
  - LOOP SEAL BEHAVIOR

LPL4-11

PUMP ON-OFF

- PUMPS ON COMPARED TO PUMPS OFF EXHIBITED:
  1. HIGHER BREAK MASS FLOW RATE THROUGH TRANSIENT
  2. MORE HOMOGENEOUS COOLANT MASS DISTRIBUTION IN THE SYSTEM
  3. SUBSTANTIALLY LESS COOLANT MASS IN THE CORE

LPL4-18

PUMP ON-OFF (cont'd)

- PUMPS ON COMPARED TO PUMPS OFF EXHIBITED:

  4. SLIGHTLY LOWER DEPRESSURIZATION RATE

  5. VESSEL LIQUID LEVEL RATE LESS DISTINCT AND LESS EASILY MEASURABLE

- RESULTS SUPPORT TRIPPING PUMPS EARLY IN SMALL BREAK TRANSIENT

LPL4-18A

NUCLEAR AND ELECTRICAL ROD RESPONSE FOR LARGE BREAK PWR LOCA

- SIGNIFICANT DIFFERENCES BETWEEN NUCLEAR & ELECTRIC ROD THERMAL RESPONSE EXPERIMENTALLY OBSERVED

- SMALL SCALE ELECTRIC EXPERIMENTS ADEQUATE FOR SEPARATE EFFECT STUDIES BUT CAN NOT PRODUCE ALL DATA REQUIRED TO ASSESS NUCLEAR CORE T/H

LPL4-12

AUGMENTED OPERATOR CAPABILITY PROGRAM

- AOC SYSTEM USED IN 8 LOFT TESTS PRODUCING PROMISING RESULTS IN MAXIMIZING OPERATOR COMPREHENSION
- DEMONSTRATED COMPUTER-BASED DIAGNOSTIC COLOR GRAPHICS FEASIBLE & USEFUL ADDITION TO MCR & TSC
- FURTHER STANDARDS & GUIDES FOR HUMAN ENGINEERING FACTORS NEEDED

LPL4-17

TECHNICAL SUPPORT CENTER

- TSC STAFF TRAINING REQUIREMENTS WERE FOUND TO BE SIGNIFICANT
- INFORMATION REQUIREMENTS ARE DIFFERENT FOR TSC AND PLANT OPERATORS
- VERIFIED IMMEDIATE TECHNICAL ASSISTANCE IS VALUABLE TO PLANT OPERATORS

LPL4-16

LOFT INSTRUMENT EVALUATION

- LOFT PROCESS INSTRUMENTS REPRESENTATIVE OF PWR PLANT INSTRUMENTATION
- REQUIRED INSTRUMENT RANGES NOT EXCEEDED IN LOFT SIMULATIONS
- RESPONSE TIME ADEQUATE IN TRACKING SYSTEM BEHAVIOR

LPL4-13

LOFT INSTRUMENT EVALUATION (cont'd)

- ADDITION TO PWR INSTRUMENTS RECOMMENDED ARE:
  1. FUEL ROD CLADDING TEMPERATURE MEASUREMENTS
  2. DENSITY MEASUREMENTS IN PIPING
  3. DENSITY COMPENSATION OF LIQUID LEVEL MEASUREMENTS

LPL4-13A

BLOWDOWN QUENCH CHARACTERISTICS OF NUCLEAR AND ELECTRIC RODS - INFLUENCE OF CLADDING SURFACE THERMOCOUPLES

E. L. Tolman

Presented at
The Ninth Water Reactor Safety Research Information Meeting

October 26 - 30, 1981
Gaithersburg, Maryland

Idaho National Engineering Laboratory
Idaho Falls, Idaho 83415

EG&G Idaho
Idaho Falls, Idaho 83415

BLOWDOWN QUENCH CHARACTERISTICS OF NUCLEAR AND ELECTRIC RODS - INFLUENCE OF CLADDING SURFACE THERMOCOUPLES

E. L. Tolman
EG&G Idaho, Inc.

The large break loss-of-coolant experiments (LOCE) conducted in the Loss-of-Fluid Facility[1,2] (LOFT) have shown that early cladding rewet occurs during the first 15 s of the transient. Because the measured cladding quenches during these experiments generally were not predicted well and because several experimenters had previously observed significant cooling perturbations as a result of using cladding surface thermocouples during slower low pressure reflood experiments, the influence on the cladding behavior and the accuracy of the LOFT surface thermocouples during this early cooling period was questioned.

To evaluate the perturbation effect and accuracy of cladding surface thermocouples for hydraulic conditions similar to those experienced during the LOFT quenches, two major test programs have been conducted at the Idaho National Engineering Laboratory. Quench experiments have been conducted in the LOFT Test Support Facility (LTSF) on solid, internal heater rods, and cartridge-type heater rods. Additional quench experiments have also been conducted in the Power Burst Facility (PBF) reactor using LOFT-type nuclear rods. Both programs simulated the coolant conditions which resulted in the LOFT quenches--an inlet quality range of 0 to 20%, flow velocities ranging from 1 to 2 m/s, and a system pressure range of 6 to 7 MPa. These experiments have (a) provided an understanding of the influence of external cladding thermocouples during the LOFT experiments, (b) clearly shown that very rapid cooling of the cladding is possible with nuclear fuel rods, and (c) have provided an important data base to assess the capability of best-estimate computer models and to establish licensing model conservatism related to the rapid cooling of nuclear fuel rods from temperatures as high as 1200 K.

Quench experiments have been conducted in the LTSF using a single-rod and a nine-rod bundle configuration. The initial single-rod experiments[3] utilized a solid heater rod (one without an internal gap) and were scoping experiments. The nine-rod bundle experiments utilized German-supplied heater rods of the FEBA (solid) and REBEKA (cartridge) designs. The REBEKA rods, which more closely simulate the thermal response and fuel-cladding gap, were modified to include small embedded thermocouples on the inside cladding surface. In these experiments the rods were heated to a desired initial temperature in a nitrogen environment and then reflooded rapidly with low quality coolant while maintaining a high system pressure. Rods with and without surface thermocouples were tested under identical quench conditions. The results show (a) the REBEKA rod cools four to five times more rapidly than solid heater rods, (b) surface thermocouples accurately measure the cladding temperature and provide a negligible thermal perturbation on the cartridge type REBEKA heaters, and (c) on the solid FEBA heater rods, surface thermocouples provide significant thermal perturbation and do not accurately measure cladding temperature.

RELAP4/MOD6 calculations were performed to evaluate best-estimate code capability to predict the single-rod LTSF quench behavior. The initial cooling rates in general were well predicted, and the final quench was predicted within 2 s. The code also showed that the rod thermal properties and gap conductance had significant effects on the rod cooling behavior under hydraulic conditions experienced during the LTSF experiments.

The PBF quench experiments (designated TC series) have recently been completed on rods with and without surface thermocouples.[4] Two of the PBF rods were instrumented with small embedded thermocouples on the cladding inside surface similar to those to be used in future LOFT experiments. The PBF LOCA system was operated to produce cladding quench response (as measured by cladding surface thermocouples) similar to LOFT cladding temperatures during LOFT tests. The results show that the nuclear rod cladding can be cooled at rates as high as 200 to 300 K/s, similar to the REBEKA cooling rates measured in the LTSF experiments, and that the surface thermocouples do not significantly affect the cooling

characteristics during such cooling transients. The nuclear rod response was consistent with similar rapid cooling of the REBEKA heater rods in the LTSF experiment and with the calculated trends produced by RELAP4/MOD6.

The LTSF and PBF quench experiments support the LOFT measurements showing a cladding quench during the first 10 s of the large break experiments. However, because of differences in hydraulic conditions between the LTSF, PBF, and LOFT experiments, it is not possible to quantify exactly the LOFT cladding temperatures. The separate effects experiments have proved that small embedded cladding thermocouples can be used in future LOFT experiments to measure cladding temperature accurately. In addition, the LTSF and PBF data demonstrate the inability of solid heater rods to simulate rapid nuclear rod cooling characteristics and provide an important data base to assess the conservatism in current licensing regulations limiting cladding rewet and quench during the blowdown phase of a loss-of-coolant accident.

REFERENCES

1. M. L. McCormick-Barger, Experiment Data Report for LOFT Power Ascension Test L2-2, NUREG/CR-0492, February 1979.

2. P. G. Prassinios et al., Experiment Data Report for LOFT Power Ascension Experiment L2-3, NUREG/CR-0792, July 1979.

3. R. C. Gottula, J. A. Good, The Effect of Cladding Surface Thermocouples on the Quench Behavior of an Electrical Heater Rod, EG&G Idaho Report LO-00-80-115, March 1980.

4. R. W. Garner, PBF, Thermocouple Effects Tests - Test Series TC-4 Quick Look Report, EGG-TFBP-5465, August 1981.

Blowdown Quench Characteristics of Nuclear and Electric Rods - Influence of Cladding Surface Thermocouples

E. Tolman

EG&G Idaho, Inc.

IDAHO NATIONAL ENGINEERING LABORATORY

Cladding Temperature Response

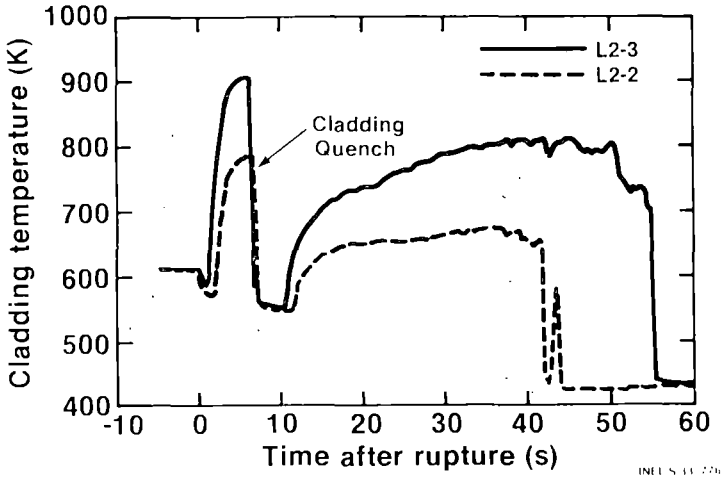

LOFT L2-3 Predictions

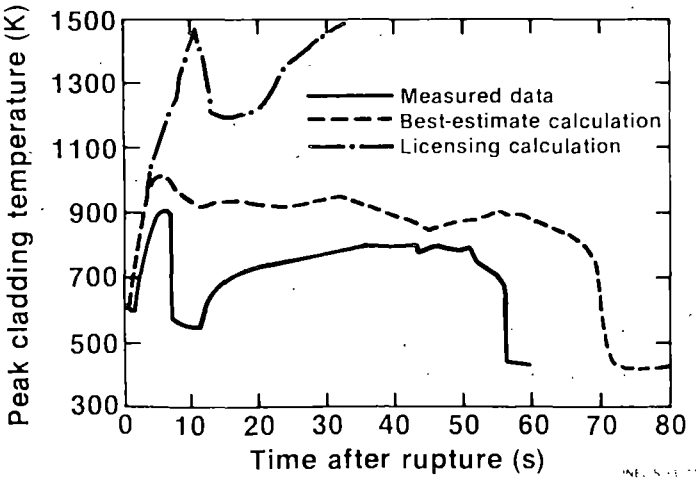

L2-3 Quench Simulation Experiments

- LOFT Test Support Facility (LTSF)
  - Single rod (semiscale heater rod)
  - Nine rod bundle (REBEKA, FEBA heater rods)
- Power Burst Facility (PBF)
  - TC-1, LOFT nuclear rods
  - TC-3, LOFT nuclear rods
  - TC-4, LOFT nuclear rods with embedded cladding thermocouples

LTSF Cladding Quench Test 11A

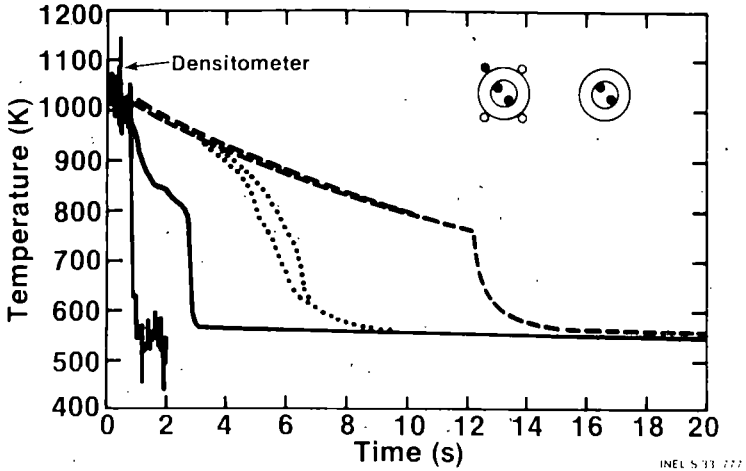

LTSF Cladding Quench - REBEKA Rod and Nearby FEBA Rod Data

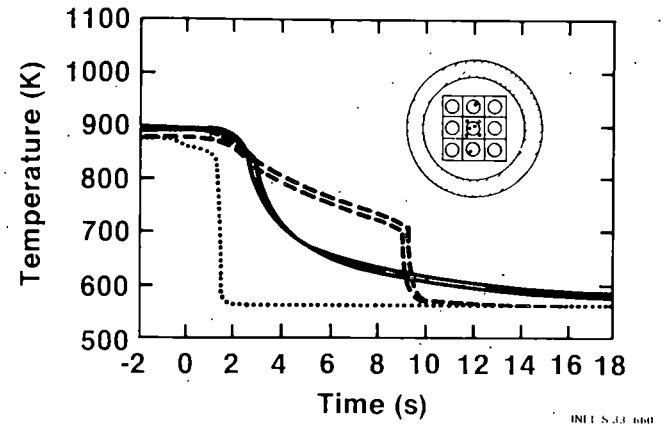

Embedded Zircaloy-Sheated Thermocouple on Inner Fuel Rod Cladding Surface

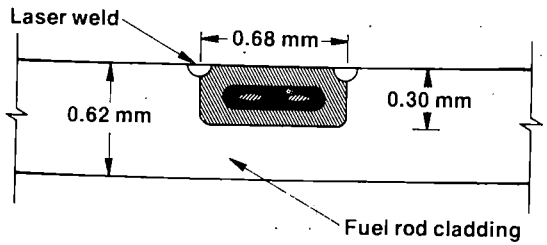

INEL-S-34 994

Calculated Nuclear and Electrical Rod Response for LTSF Quench Tests

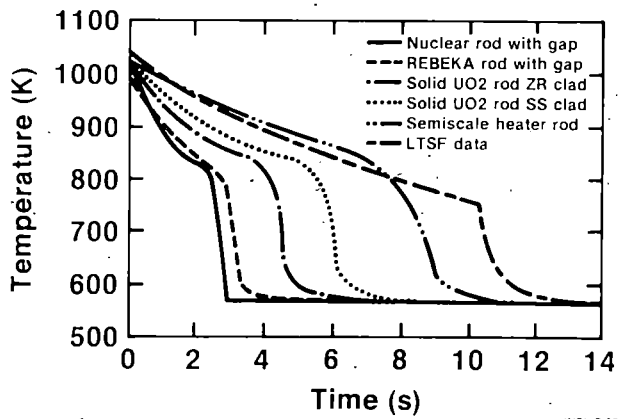

INEL-S-33 658

PBF Cladding Quench - Effects of LOFT Surface Thermocouples

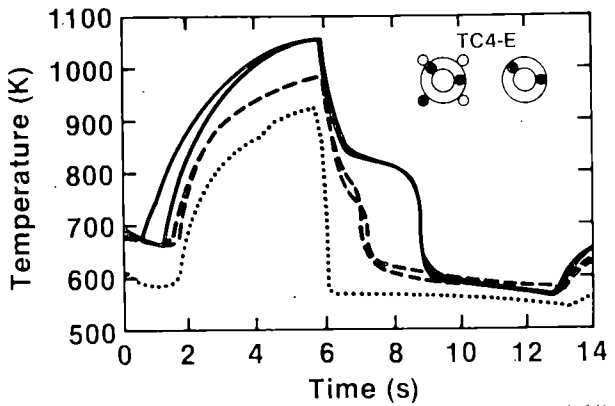

INEL-S-33-662

PBF Cladding Quench - Effects of LOFT Surface Thermocouples

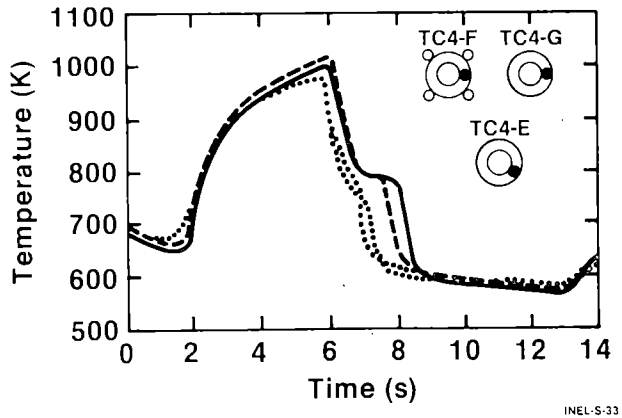

INEL-S-33-664

Summary

1. Thermocouples not a significant effect on clad cooling during early quenches in L2-2 and L2-3
2. L2-2 and L2-3 experienced dominant cooling during first 12 s of transient
3. Blowdown quench characteristics can be significantly different for nuclear and electric heater rods
4. Embedded thermocouples are capable of measuring accurate cladding temperatures for future LOFT experiments

INEL-S-33-774

RESULTS OF SEMISCALE MOD-2A
UPPER HEAD INJECTION TEST SERIES

A. G. Stephens

Presented at

The Ninth Water Reactor Safety Research

Information Meeting

October 26 - 30, 1981

Gaithersburg, Maryland

Idaho National Engineering Laboratory

Idaho Falls, Idaho 83415

RESULTS OF SEMISCALE MOD-2A UPPER HEAD INJECTION TEST SERIES

A. G. Stephens
EG&G Idaho, Inc.

A series of small break loss-of-coolant experiments designed to evaluate the effectiveness of an upper head injection (UHI) emergency core cooling system (ECCS) has recently been completed in the Semiscale Mod-2A system. The series simulated full-scale communicative cold leg breaks of 11, 15.6, and 22.1 cm diameters, corresponding to 2.5, 5, and 10% of the cold leg flow area. For each break size, an experiment was first conducted that did not employ UHI, but did use the normal ECCS loop accumulators pressurized to 2.86 MPa (as nominally specified for UHI-equipped plants) in order to establish baseline response data. These were followed by similar experiments that used UHI in addition to loop accumulator injection. Data from these experiments may be found useful in evaluating ECC systems in licensing applications.

Preliminary analyses of the experimental results have been conducted to evaluate the influence of UHI and also break spectrum behavior. No significant core heatup was observed in any of the six tests. Overall, UHI was found to have little impact on transient behavior other than to provide increased core liquid inventory over that observed in the baseline tests. A relative maximum severity in core uncovery was predicted and observed for a scaled break size of 15.6 cm as compared with either the smaller (11 cm) or larger (22.1 cm) breaks.

System pressures for the experiments and pressure setpoints of various emergency core coolant systems are shown in the figure titles "Comparison of System Pressures for Baseline and UHI Tests. As noted above, in the baseline tests, the loop accumulators were pressurized to the same value as used in the UHI tests (2.86 MPa). This is lower than the nominal value for most non-UHI plant accumulators (4.3 MPa). Relative to the baseline pressure responses, a more rapid depressurization occurred during the period of upper head accumulator injection. However, in all cases there was

a gradual convergence in pressure between the UHI and baseline experiments. This convergence was found to exist for most system parameters, including system residual mass inventories and distributions. Each experiment was run until low pressure injection occurred, to verify that conditions remained stable with sufficient core cooling.

The differences between UHI and baseline experiments are most distinctly seen in the figure titled "MOD-2A Upper Head Liquid Levels." During the 22.1-cm-break experiment, the injection rate was high enough to keep the upper head nearly full. Once injection terminated, the drain was nearly identical to that during the baseline test. For the 11-cm break, the injection rate was slow enough that, while draining was delayed compared to baseline results, the upper head emptied well before UHI was terminated. The residual coolant inventories shown in the figure titled "System Mass Inventories (UHI Tests)" are based in part on data obtained by condensing and collecting the break flow and are therefore considered very accurate.

The figure titled "Core Liquid Levels" shows the core and downcomer collapsed liquid levels. The liquid level behavior is generally characterized by three periods: an initial large depression and refill resulting from loop (liquid) seal formation and blowout, a boiloff of fluid in the core and downcomer resulting in falling levels, and a slow refilling following loop accumulator injection. The contribution of UHI to increasing core liquid inventories is apparent from the UHI/baseline differences in minimum levels at the end of the boiloff period.

In no experiment was there any significant heatup of the core. The figure "Representative Upper Core Heater Temperatures from MOD-2A UHI Tests" presents representative heater rod cladding temperatures from the UHI tests. The behaviors were similar in the baseline tests, with only slightly increased temperatures. There was no heatup at all during the 11-cm break experiments. The 15.6 and 22.1-cm-break experiments both exhibited brief dryout temperature excursions, but no temperatures exceeded those at initial conditions.

The most significant comparisons of the data set can be seen by examining the minimum collapsed levels at the end of boiloff. Plotting them against break size, one may compare these to the collapsed levels that have been observed to initiate core dryout in numerous Semiscale Mod-2A and Mod-3 experiments. These curves are shown in the figure "Comparison of Minimum Core Collapsed Liquid Levels" and Dryout Levels for the UHI experiments and as estimated for a non-UHI plant configuration with 4.3 MPa loop accumulators.[a] The liquid levels are a direct indication of total system coolant inventories since, at these times, essentially all the remaining coolant is in the vessel. The results indicate a large variation over a relatively narrow break size range. Also of interest are the occurrence of a minimum in the UHI curve and the general similarity of the UHI and non-UHI cases. The lower minimum in the UHI tests is a direct result of the 2.86-MPa loop accumulator setpoint and the resulting longer boiloff period. This occurred in spite of the increase in core liquid inventories from upper head accumulator water. However, the break size range that would lead to core dryout appears to be rather narrow, and the tests conducted within this range produced no severe core heater rod temperatures.

In summary, none of the transients conducted in the series exhibited any severe core temperature excursions. The dominant effect of UHI is caused by lower setpoint loop accumulators relative to those of a non-UHI configuration. This leads to greater coolant depletion. Finally, the extent of coolant depletion was observed to be very sensitive to break size.

---

a. Many Semiscale small break experiments have shown that upon initiation of loop accumulator injection, a continuous refill of the core begins. Minimum levels for the non-UHI case were therefore inferred from the baseline tests at the time the system had depressurized to 4.3 MPa.

Semiscale MOD-2A Upper Head Injection Test Series

A.G. Stephens

EG&G Idaho, Inc.

IDAHO NATIONAL ENGINEERING LABORATORY

Small Break/UHI Experiment Series

Issues:

- UHI performance
- Break spectrum
- Code performance

Experiments:

Equivalent break size	Baseline	UHI
4.3''	S-UT-4	S-UT-5
6.1''	S-UT-6	S-UT-7
8.7''	S-UT-1	S-UT-2

INEL-S-34 087

Comparison of System Pressures for Baseline and UHI Tests

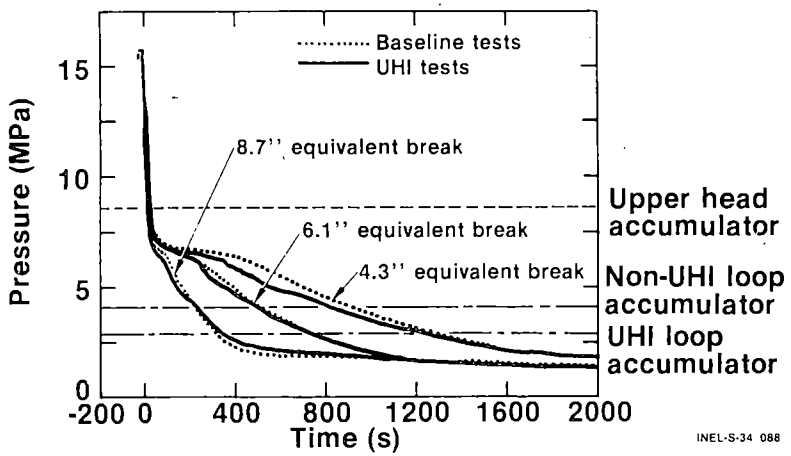

INEL-S-34 088

MOD-2A Upper Head Liquid Levels

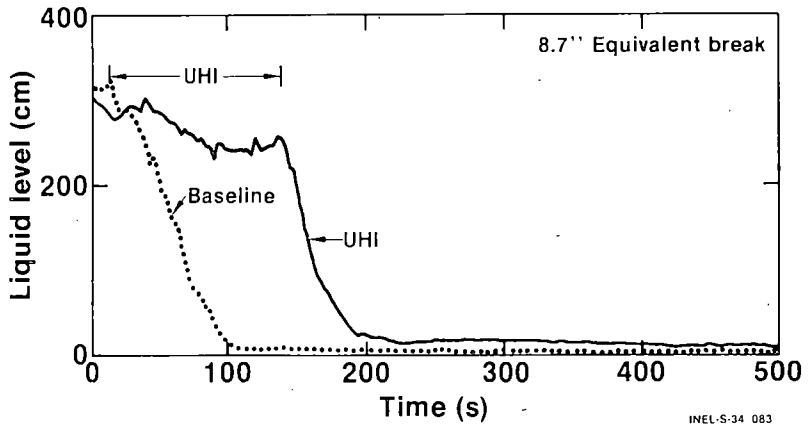

INEL-S-34 083

MOD-2A Upper Head Liquid Levels

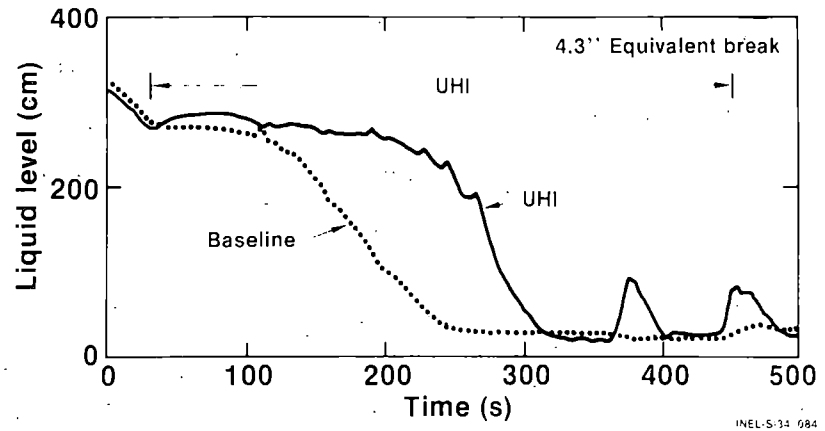

Core Liquid Levels

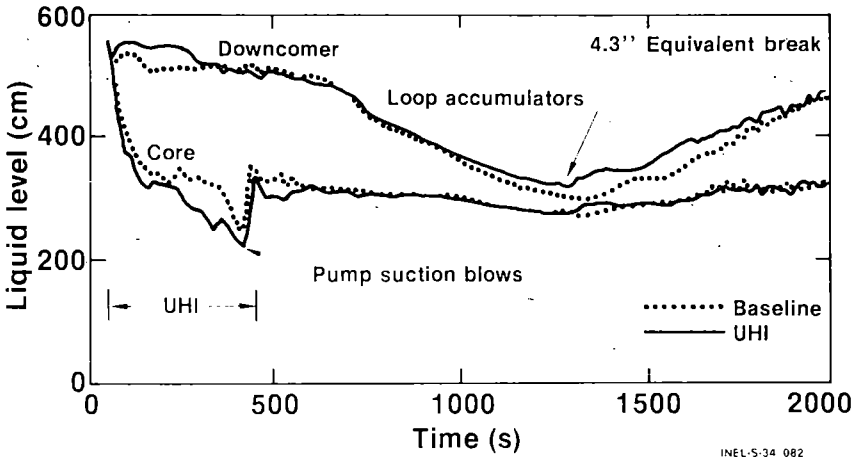

Core Liquid Levels

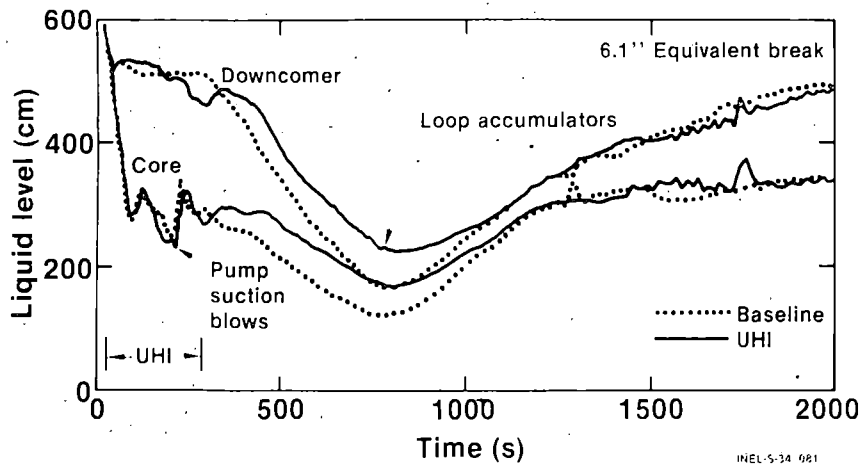

System Mass Inventories (UHI Tests)

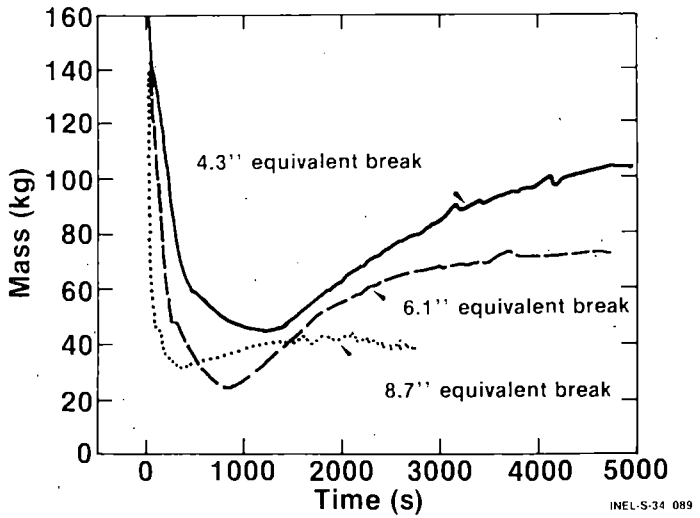

Comparison of Integrated Break Flows and UHI Masses

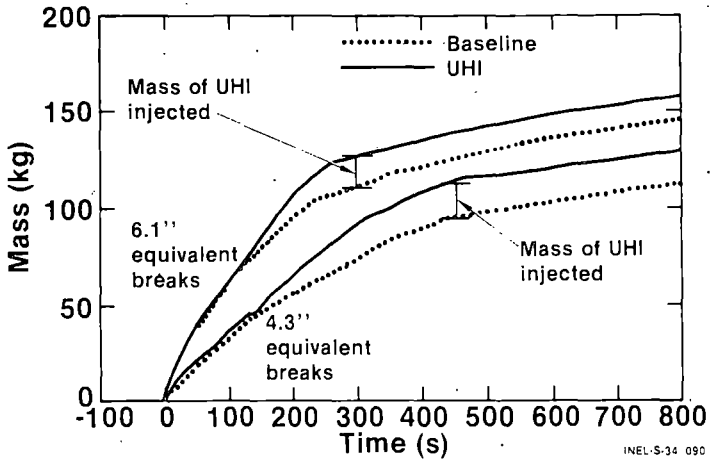

Representative Upper Core Heater Temperatures from MOD-2A UHI Tests

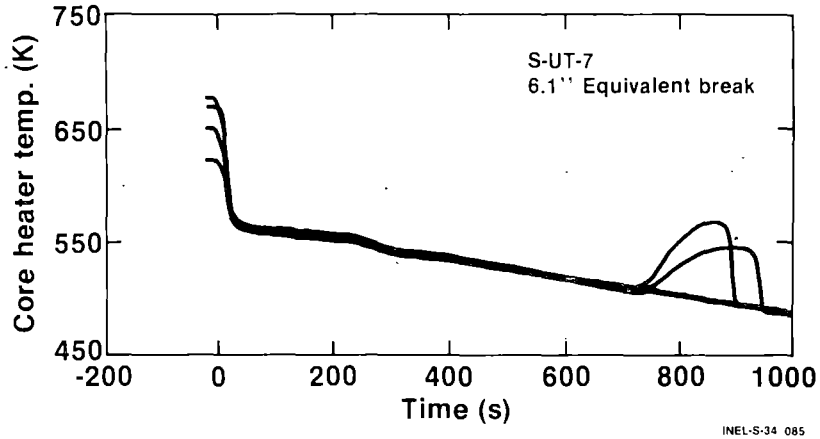

Representative Upper Core Heater Temperatures from MOD-2A UHI Tests

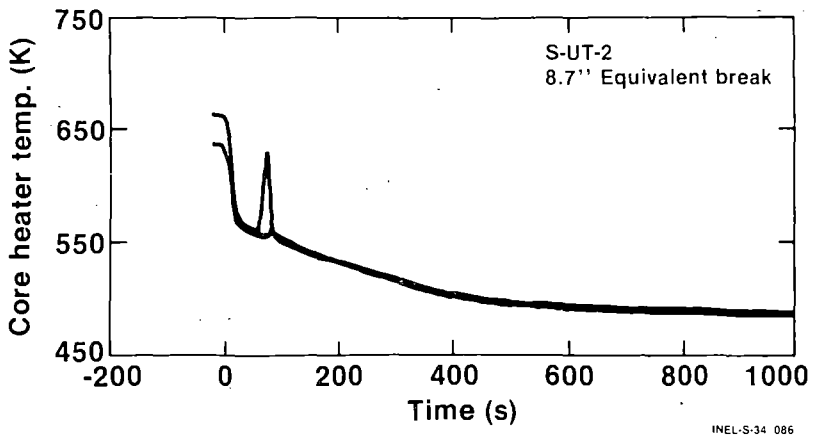

Comparison of Minimum Core Collapsed Liquid Levels and Dryout Levels

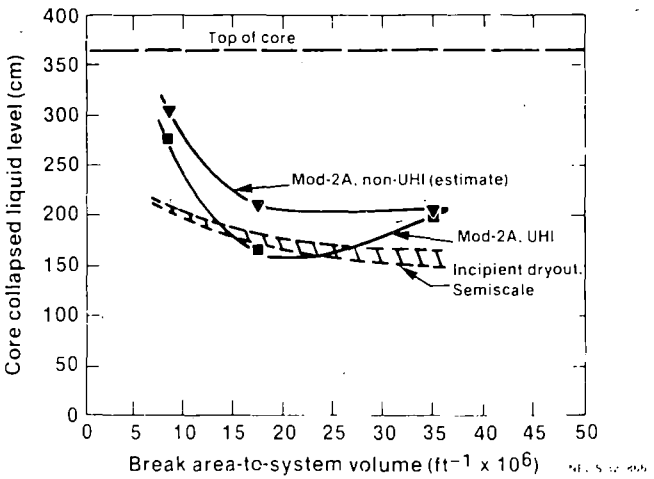

UT Series Conclusions

- No significant core heatup for any test
- Most severe size near 6'' equivalent diameter (UHI, non-UHI)
- UHI influence on transients:
  - Injection has small effect on transient
  - 400 psi loop accumulators provide less margin against core uncovery

SEMISCALE MOD-2A NATURAL CIRCULATION TEST SERIES PRELIMINARY RESULTS

D. J. Shimeck

Presented at

The Ninth Water Reactor Safety Research Information Meeting

October 26 - 30, 1981

Gaithersburg, Maryland

Idaho National Engineering Laboratory

Idaho Falls, Idaho 83415

EG&G Idaho

Idaho Falls, Idaho 83415

SEMISCALE MOD-2A NATURAL CIRCULATION TEST SERIES
PRELIMINARY RESULTS

D. J. Shimeck
EG&G Idaho, Inc.

A series of experiments is being conducted in the Semiscale Mod-2A facility at the Idaho National Engineering Laboratory (INEL) to investigate the charactistics of natural circulation cooling. Natural circulation is an important heat rejection mechanism during certain accidents or transients in a pressurized water reactor (PWR) such as small break loss-of-coolant accidents or operational transients involving loss of primary pumping. The objectives of the experiments were to examine the thermal-hydraulic phenomena associated with various modes of natural circulation, to identify the transitions between modes, and to quantify the sensitivity to varied primary and secondary conditions. Safety analysis codes used in licensing applications can be tested against the data from this test series.

The controlled variables are: core power (30, 60, and 100kW), primary inventory (48 to 100%), secondary inventory (0 to 100%), secondary pressure (atmospheric to 6.0 MPa), and noncondensible gas concentration. The dependent parameters of particular interest are the mass flow rates, system pressure and temperature distribution, and the transition points between natural circulation modes. Testing was predominantly performed in the system with only one loop connected to the vessel/downcomer. This allowed for improved control and greater measurement accuracy. An experiment was performed with a two-loop system to examine loop imbalance effects with varied secondary conditions. The test series also includes two ultra-small-break (0.4%) loss-of-coolant experiments which are designed to provide information on the adequacy of natural circulation for core cooling under transient conditions.

Single-phase natural circulation data were taken to benchmark the data and code predictions. Results showed that flow rates and system conditions behaved as predicted. The two-phase data base consists of over 150 steady-state data points. General results of system behavior are described below.

Effect of Primary Inventory. Little effect is observed until the vessel upper plenum is drained to the approximate hot leg elevation. The mass flow rate then rapidly increases to a peak at approximately 88% inventory (one-loop configuration). Further draining results in a continuously decreasing flow with reflux conditions being established at approximately 70% inventory. Measurements show that the reflux flow rate is approximately one-half of the core boiloff rate, with the remainder condensed on the steam generator downflow side. Primary system pressure remained fairly constant, while mass flow rates increased with increasing core power. Core cooling was adequate for inventories above approximately 50%.

Effect of Secondary Conditions. Little effect was observed at collapsed secondary levels above 50%. Below 50%, the two-phase natural circulation flow decreased with secondary level and large oscillations occurred. Adequate core cooling was provided for levels as low as 8%. Reducing the level below 50% for reflux conditions caused the primary pressure to rise, but had little effect on the reflux behavior or core coolability.

Effect of Noncondensibles. The initial injection (approximately 10% steam generator tube volume) of noncondensible gas (N_2) had significant effects on both two-phase and reflux flows. The two-phase test flow rate dropped to about half while the reflux rate increased to near 100% with corresponding reduction in carryover. Further injections, however, resulted in only an increase in system pressure with little influence on flow and core cooling.

Natural circulation results to date have included a characterization of transitions between modes, quantification of natural circulation flows including reflux, and examination of the influence of noncondensibles. An extensive data base has been accumulated which will support much further analysis and computer code modeling evaluation.

Semiscale MOD-2A Natural Circulation Test Series Preliminary Results

D.J. Shimeck

EG&G Idaho, Inc.

IDAHO NATIONAL ENGINEERING LABORATORY

Natural Circulation Series

Objectives:

- Examine T-H phenomena associated with various modes of natural circulation
- Identify transitions between modes and transition behaviors
- Provide data for code assessment
- Develop measurement techniques

INEL-S-34 913

Semiscale MOD-2A Single Loop Configuration

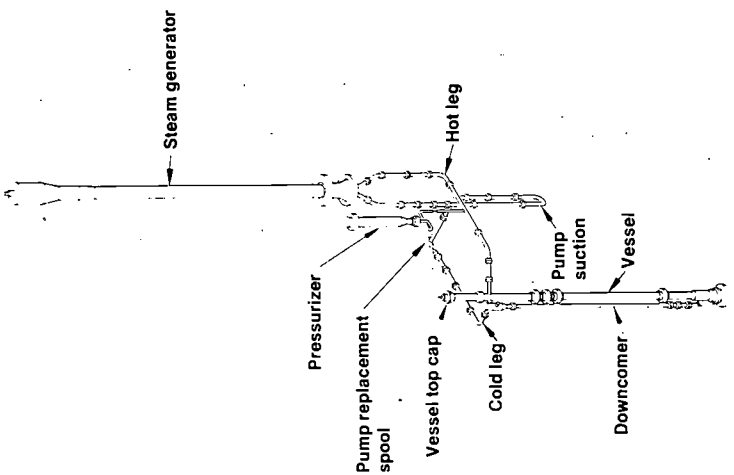

INEL-S-34 916

Steam Generator Inlet/Outlet Instrumentation

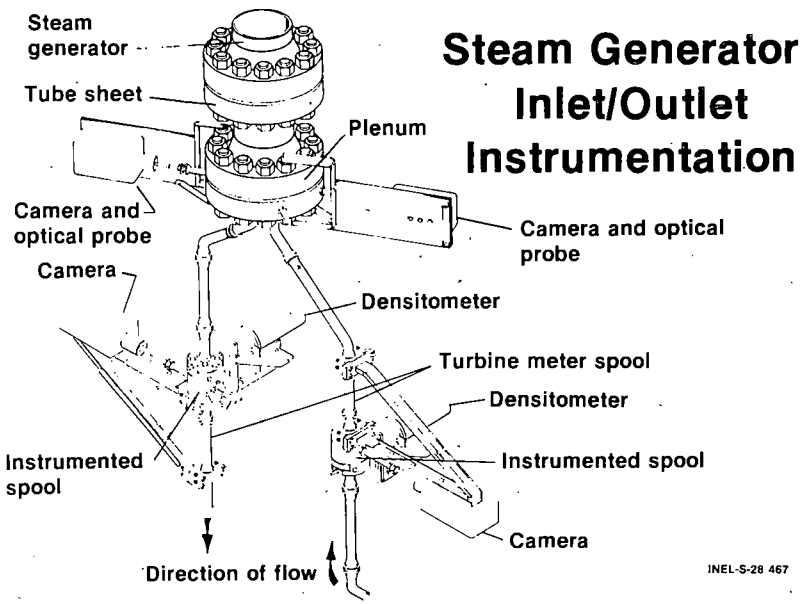

INEL-S-28 467

Semiscale MOD-2A Natural Circulation Series

- Controlled variables
  1. Core power
  2. Primary inventory
  3. Secondary inventory
  4. Secondary pressure
  5. Noncondensible gas volume
- Dependent parameters
  1. Mass flow
  2. Primary pressure
  3. Primary ΔT
  4. Mass distribution

INEL-S-34 912

Semiscale MOD-2A Natural Circulation Experiments

Test	Configuration	Natural Circulation Mode			Noncondensibles	Secondary Conditions	
		1Ø	2Ø	Reflux		Constant	Varied
1	1-loop	X				X	
2		X	X	X		X	
3			X				X
4				X			X
5			X		X	X	
6				X	X	X	
10			X				X
7	2-loop	X	X				X
8		Ultra-SBLOCA w/o ECCS				Isolated	
9		Ultra-SBLOCA w/ECCS				Feed & Bleed	

INEL-S-34 917

Cold Leg Mass Flow Rates

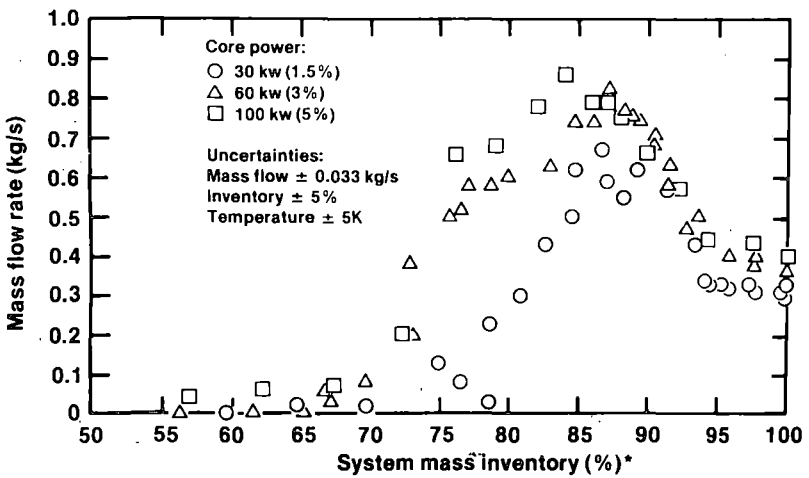

* Single loop configuration excluding pressurizer

INEL-S-34 916

Cold Leg Mass Flow Rates and Core Temperature Differentials

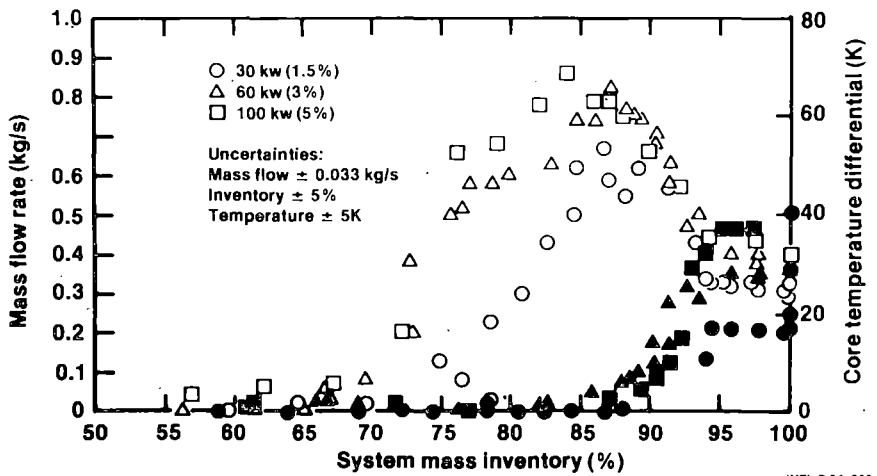

INEL-S-34 908

Two-Phase Natural Circulation Cold Leg Mass Flow Rates vs. Steam Generator Inventory

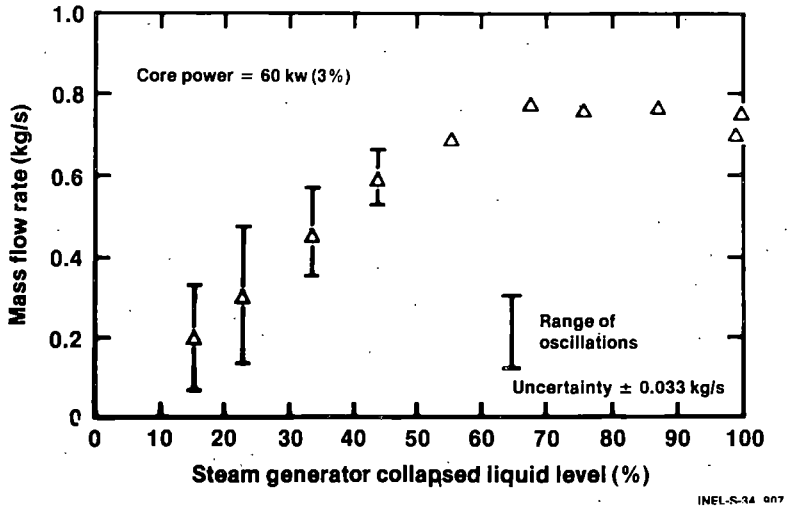

Reflux Meter Configuration

(Not to scale)

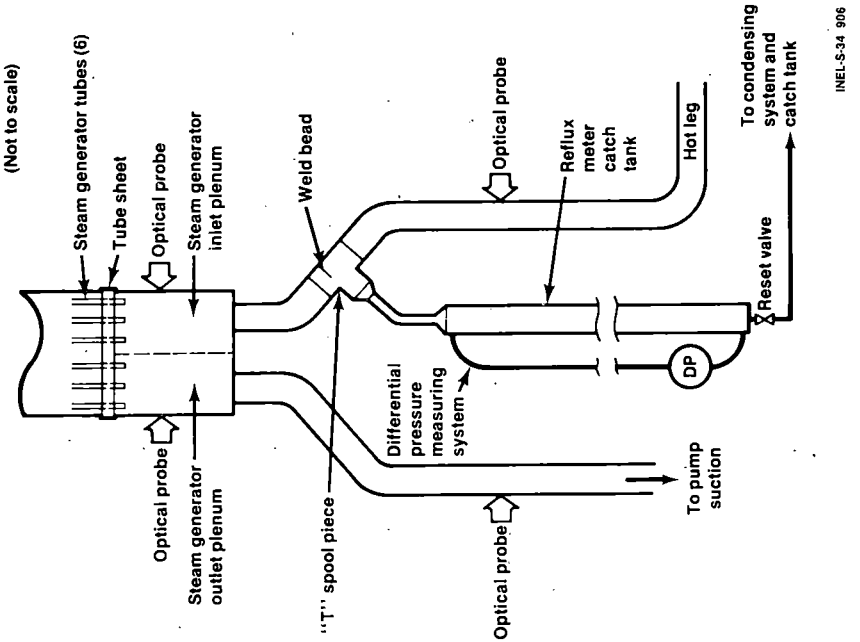

Reflux Mode Mass Flow Rates

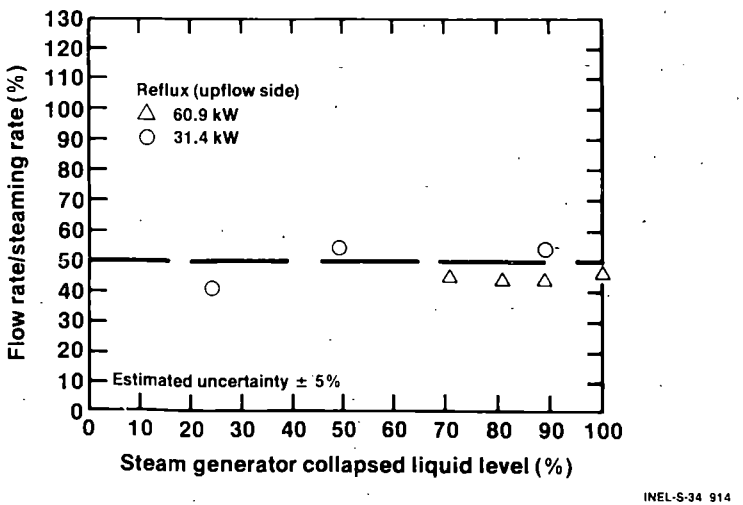

Influence of Noncondensible Gas on Reflux

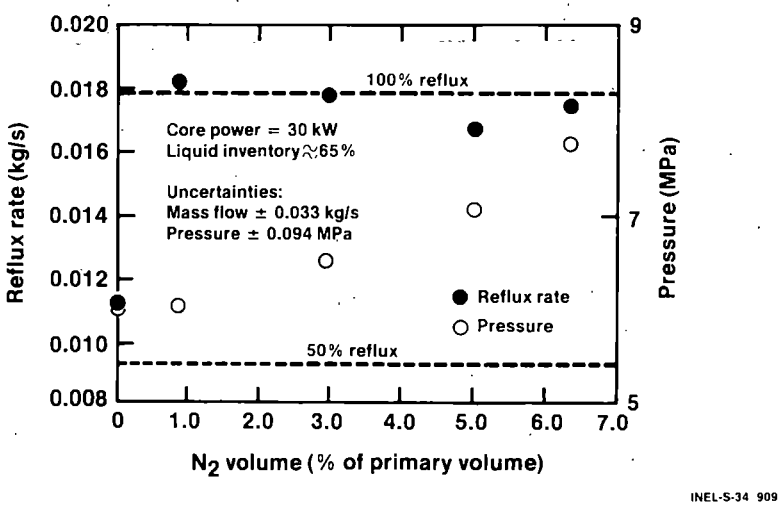

DJS-6

Influence of Noncondensible Gas on Two-Phase Natural Circulation

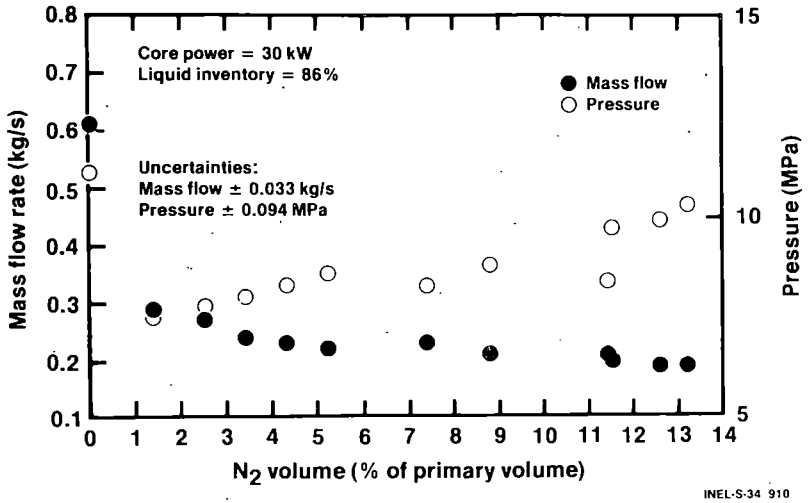

Natural Circulation Experiments Results to Date

(Single Loop Configuration)

- Adequate decay heat rejection demonstrated down to
  - 50% primary inventory
  - 8% secondary inventory
- Mode transitions quantified
  - Single-phase 100% to 95% inventory
  - Two-phase 95% to 70% inventory
  - Reflux<70% inventory
- 1:1 reflux/carryover ratio measured
- Noncondensible gas effect minimal, adequate heat rejection at acceptable pressures
  - Two-phase inventory up to 50% accumulator and rod gas content
  - Reflux inventory up to 24% accumulator and rod gas content

Break Area Parameter Test Series of ROSA-III for BWR LOCA/ECCS Tests

Presented at

The Ninth Water Reactor Safety Research Information Meeting

October 26 - 30 , 1981

Gaithersburg, Maryland

M. Shiba

Japan Atomic Energy Research Institute

Tokai-Mura, Ibaraki-Ken, 319-11, Japan

Break Area Parameter Test Series of
ROSA-III for BWR LOCA/ECCS Tests

The ROSA-III facility is shown in Figs. 1a and 1b. It is a volumetrically scaled (1/424) BWR system with an electrically heated core to study the response of BWR and the effectiveness of the ECCS during a LOCA. The core is consisted of four half-length simulated fuel assemblies. Each fuel assembly contains 62 fuel rods and two water rods which are spaced in a square 8x8 array. The coolant recirculation system consists of two loops, intact and broken loops, provided with a recirculation pump and two jet pumps in each loop. Jet pumps are installed outside the pressure vessel to simulate the height and the volume satisfactorily.

Five experiments have been conducted now in the break area parameter test series. They are Run 912 (5% Break), Run 913 (15%), Run 914 (100%), Run 915 (2%) and Run 916 (50%). The break location is at the recirculation pump inlet line and the break type is communicative split break. The high pressure core spray system (HPCS) was assumed to be inactive as a single failure assumption. Pressure control system was also assumed in failure after initiation of the blowdown.

Fig.2 shows the system pressure transients in the various tests. The system pressure decreases after break until the main steam isolation valve (MSIV) is closed. The MSIV is closed by the low L2 level signal (1.9 m below the operating liquid level in the downcomer of a BWR) with the time delay of 3 s. The system pressure recovers after the closure of MSIV and the safety relief valve opens in the 5% break test at the system pressure greater than 8.2 MPa.

In large and medium breaks greater than 5% the system pressure starts to decrease rapidly when the recirculation line outlet uncovers in the downcomer following the

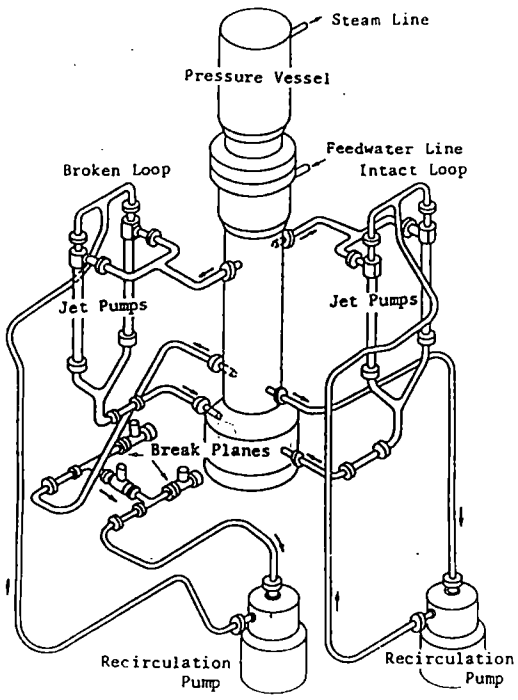

Fig. 1a ROSA-III Test Facility

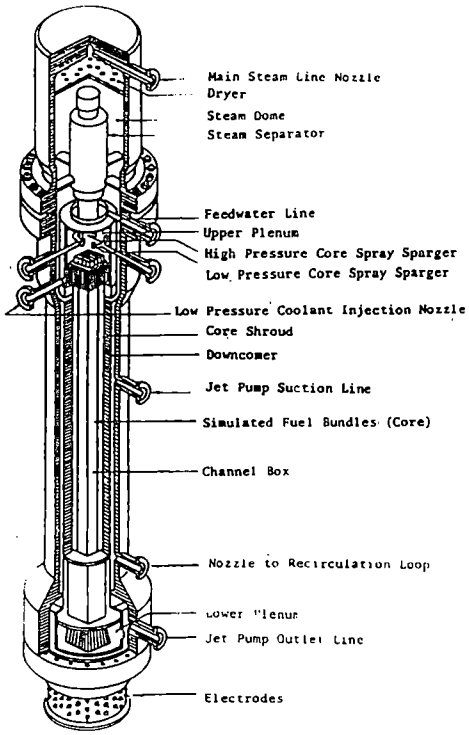

Fig. 1b ROSA-III Pressure Vessel

liquid level fall and the steam in the pressure vessel is discharged through the break. In a small break less than 5%, the system pressure starts to decrease rapidly when the automatic depressurization system (ADS) is actuated 120 s after the low L1 liquid level signal (4.7 m below the operating liquid level in the downcomer).

The lower plenum initiates flashing when the system pressure decreases to 6.4 MPa following the rapid decrease in the system pressure after the uncovery of the recirculation line or the actuation of ADS. The mixture level in the core recovers by the lower plenum flashing and improves the core cooling below the mixture level.

Fig.3 shows the two-phase level in the core and the surface temperature of model fuel rod. The whole core is uncovered to the steam environment by the mixture level decrease in the core after the lower plenum flashing and the fuel rod surface temperature starts to rise from the top following the level fall. The low pressure core spray system (LPCS) and the low pressure coolant injection system (LPCI) are actuated at system pressure of 2.2 and 1.6 MPa, respectively, due to continuous decrease of the system pressure. The LPCS sprays water from the top of the core and improves core cooling, rewetting the low power region at the top and the bottom of the core by the falling water from the upper plenum.

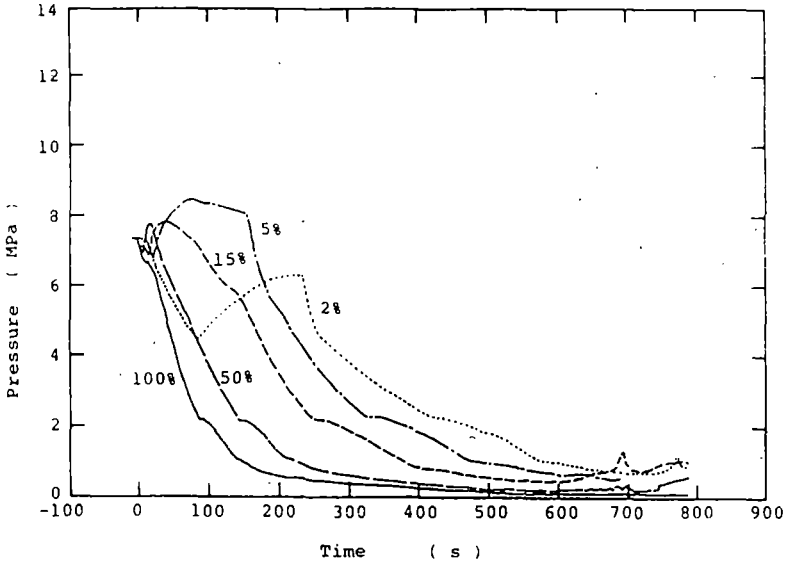

Fig. 2 Pressure Transients

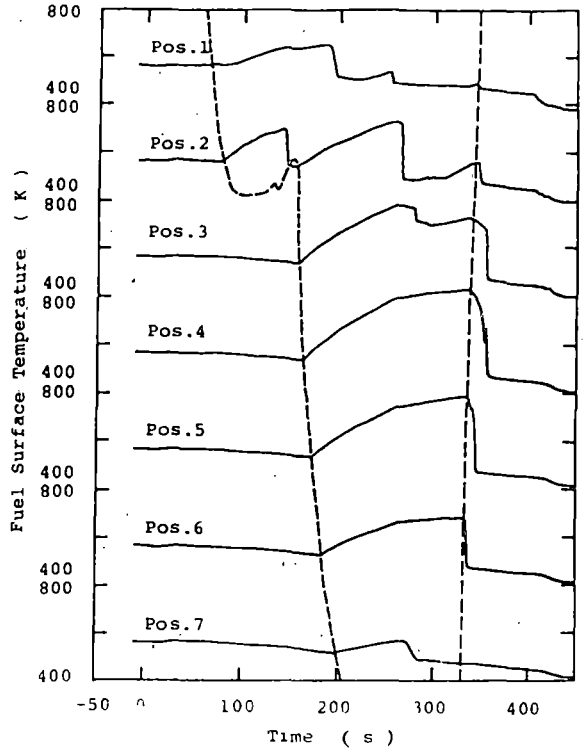

Fig. 3 Fuel Surface Temperatures of Peak Power Rod All (15% Break)

Objectives

1. To study the BWR LOCA scenario comprehensively varying the break area as a test parameter.

2. To identity any problem area or unexpected phenomena in a BWR LOCA.

3. To provide experimental data for the computer code assessment.

ROSA-III Flow Diagram

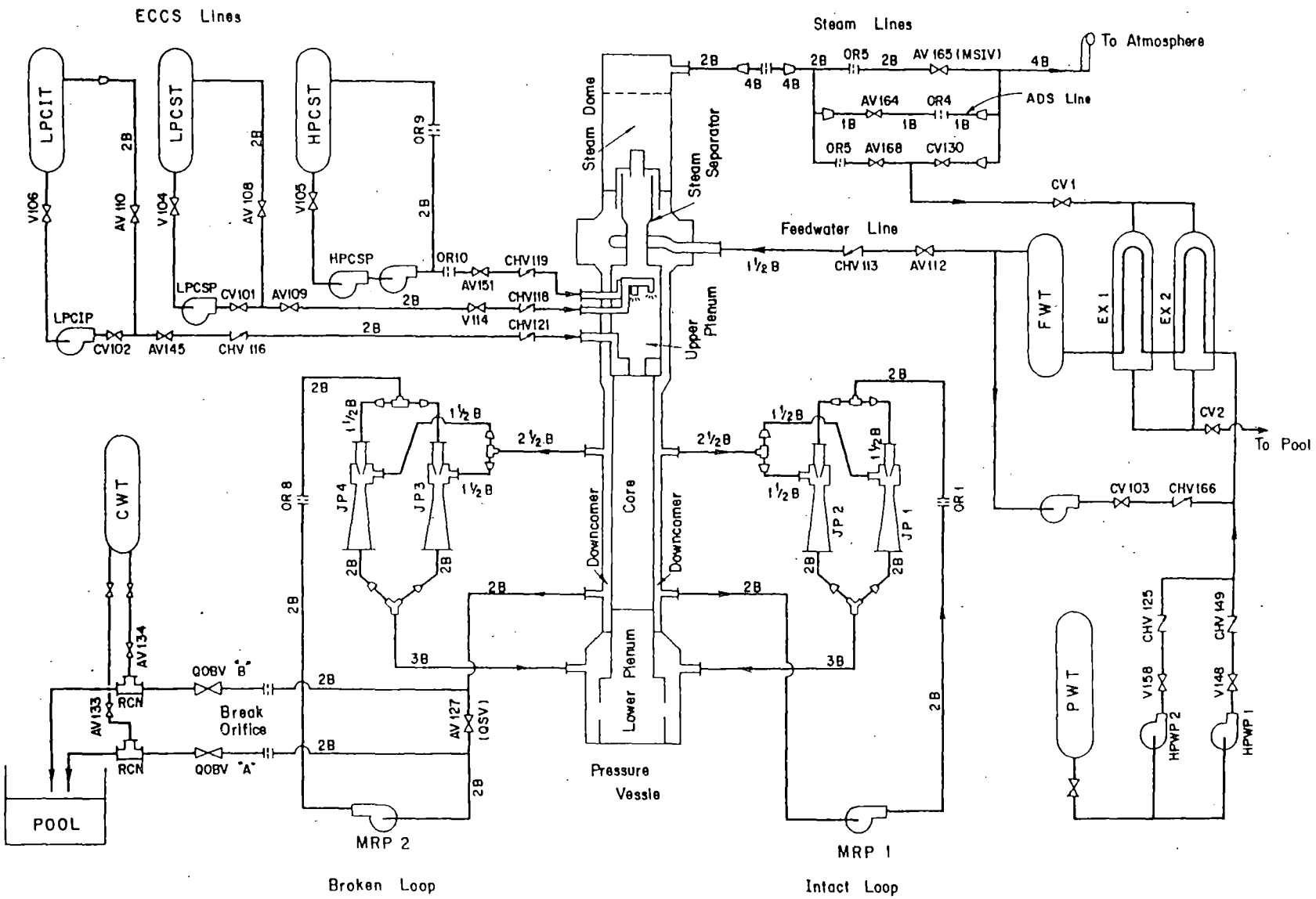

ROSA-III Test Facility

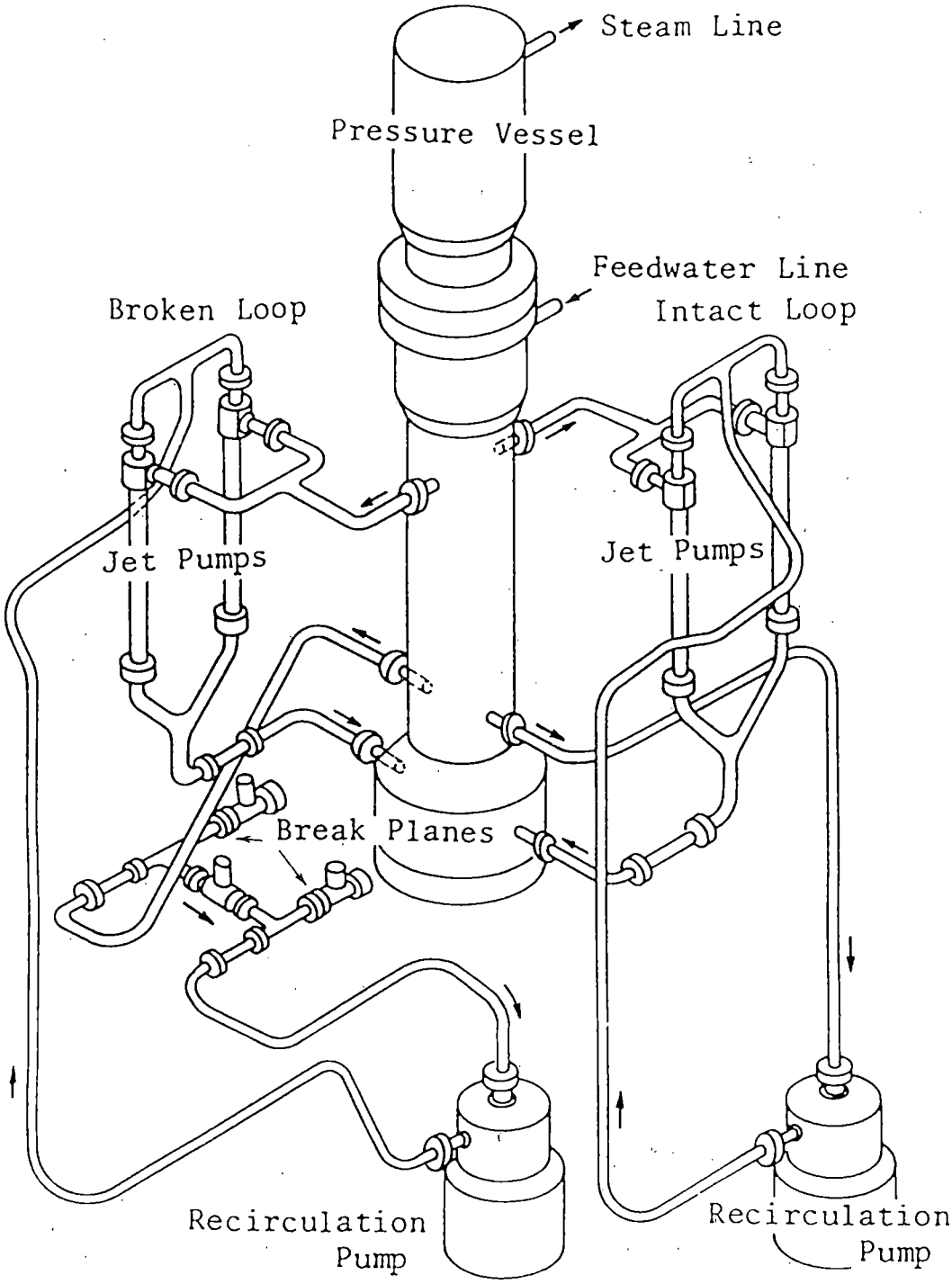

ROSA-III Pressure Vessel

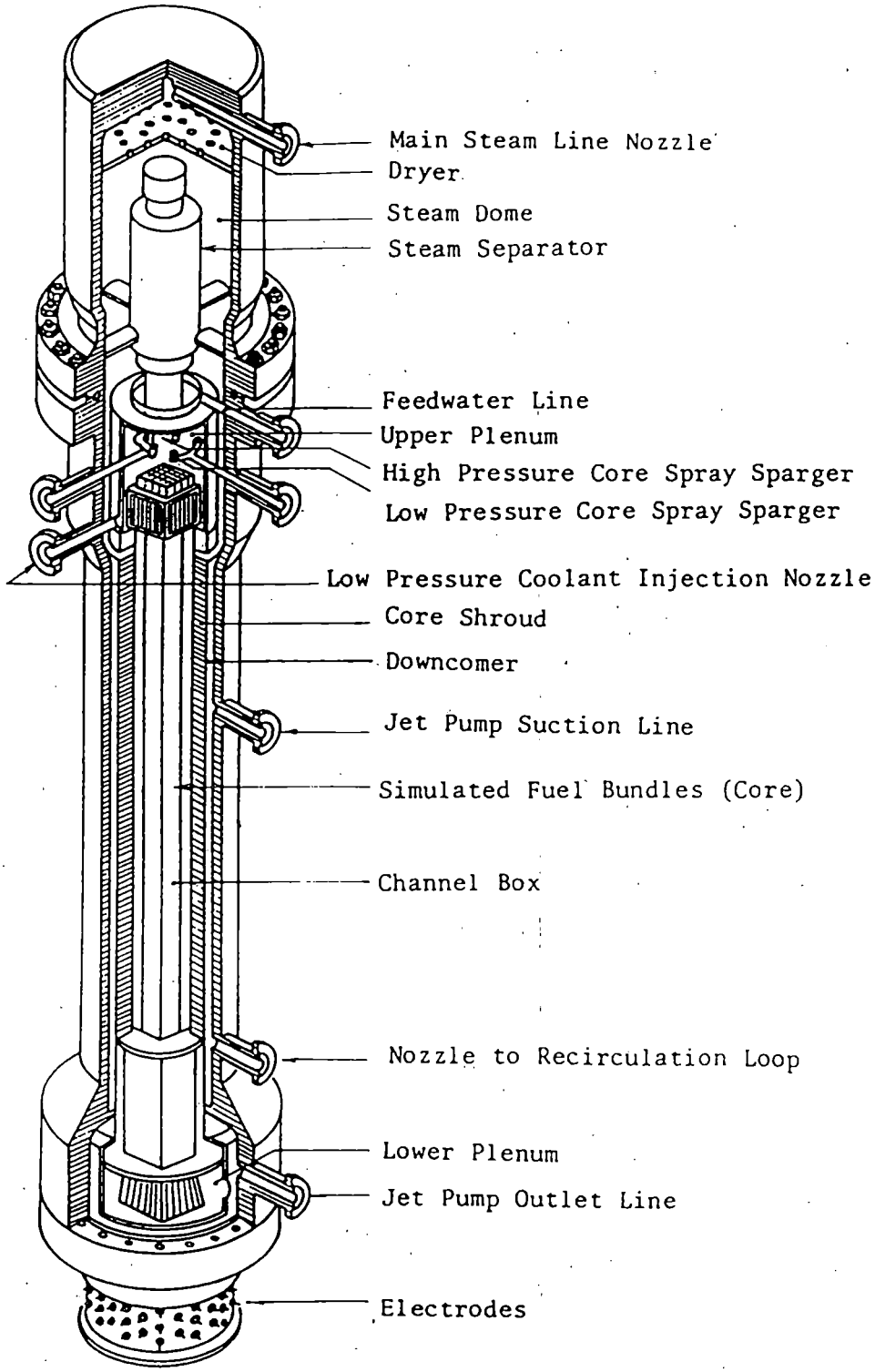

RADIAL POWER DISTRIBUTION

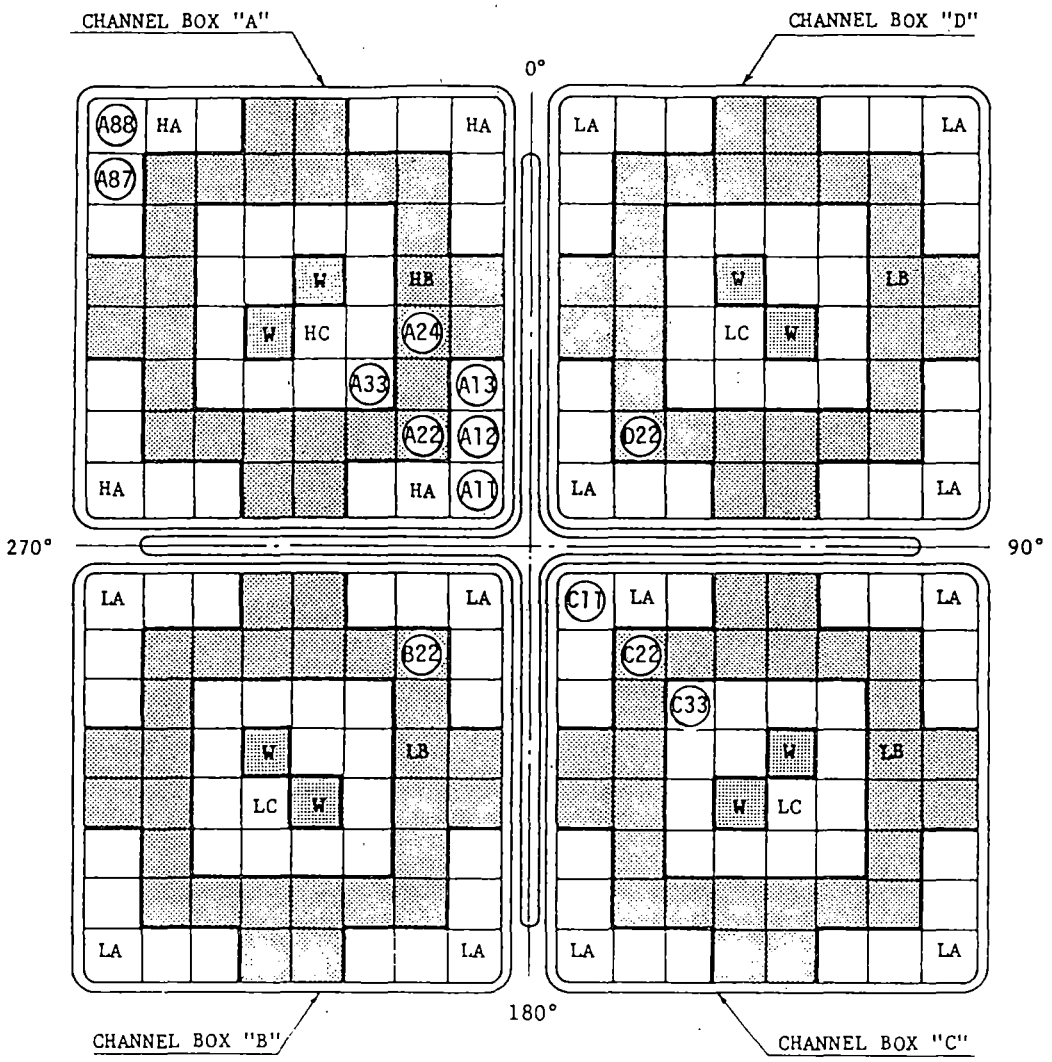

Region	HA	HB	HC	LA	LB	LC	W
Lenear Heat Rate (kW/m)	18.5	16.81	14.41	13.21	12.01	10.29	0.0
Local peaking factor	1.1	1.0	0.875	1.1	1.0	0.875	0.0
No. of Rods	20	28	14	60	84	42	8

Test Conditions

Break Position : Recirculation Pump Inlet

Break Type : Split Break

Failure Assumptions : HPCS and
Pressure Control System

Test Parameter : Break Area

Run	Break Area
912	5 %
913	15 %
914	100 %
915	2 %
916	50 %

POWER TRANSIENT

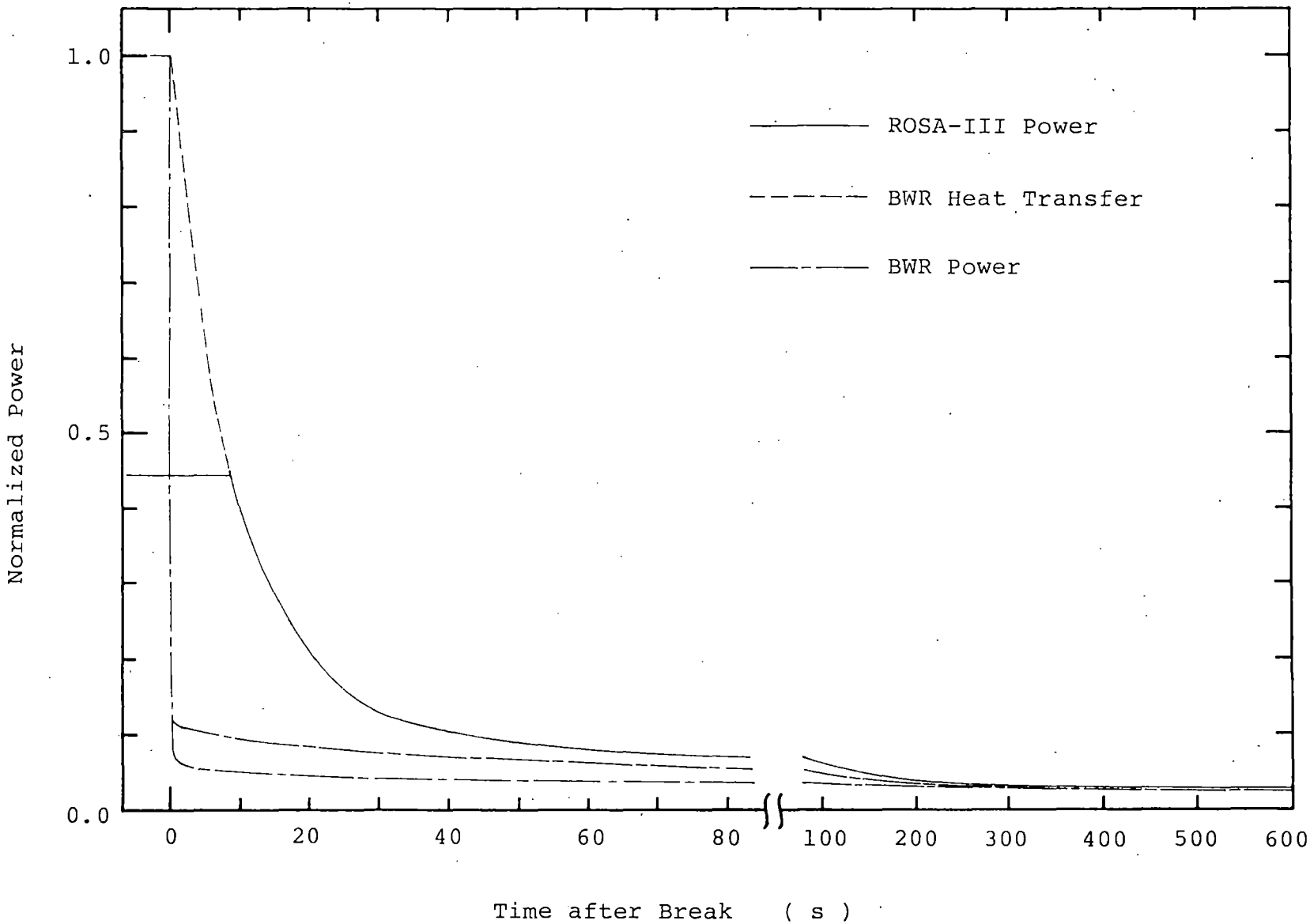

PRESSURE TRANSIENT (15% BREAK)

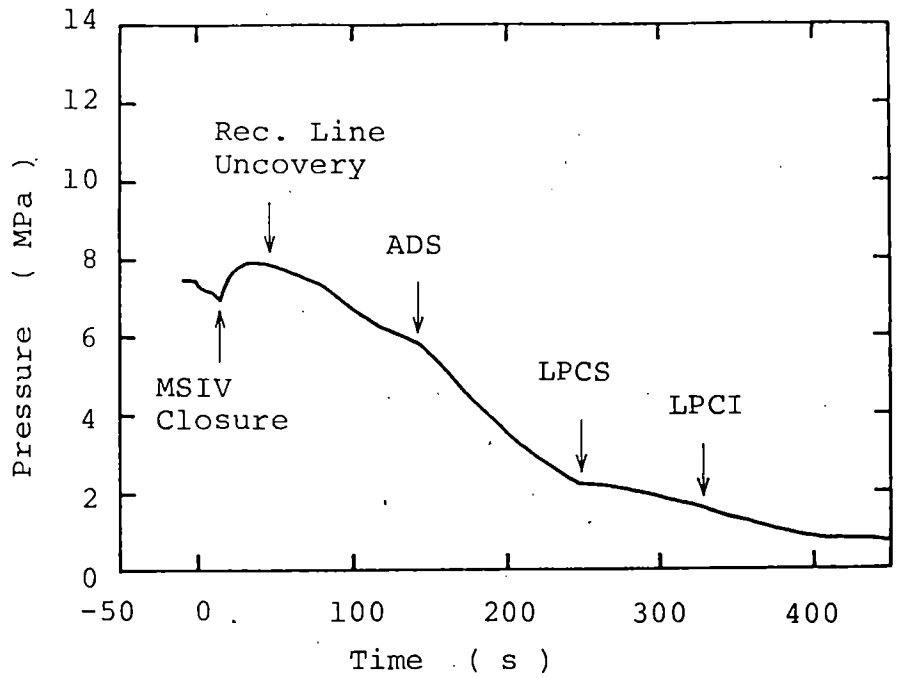

Liquid Level (15% Break)

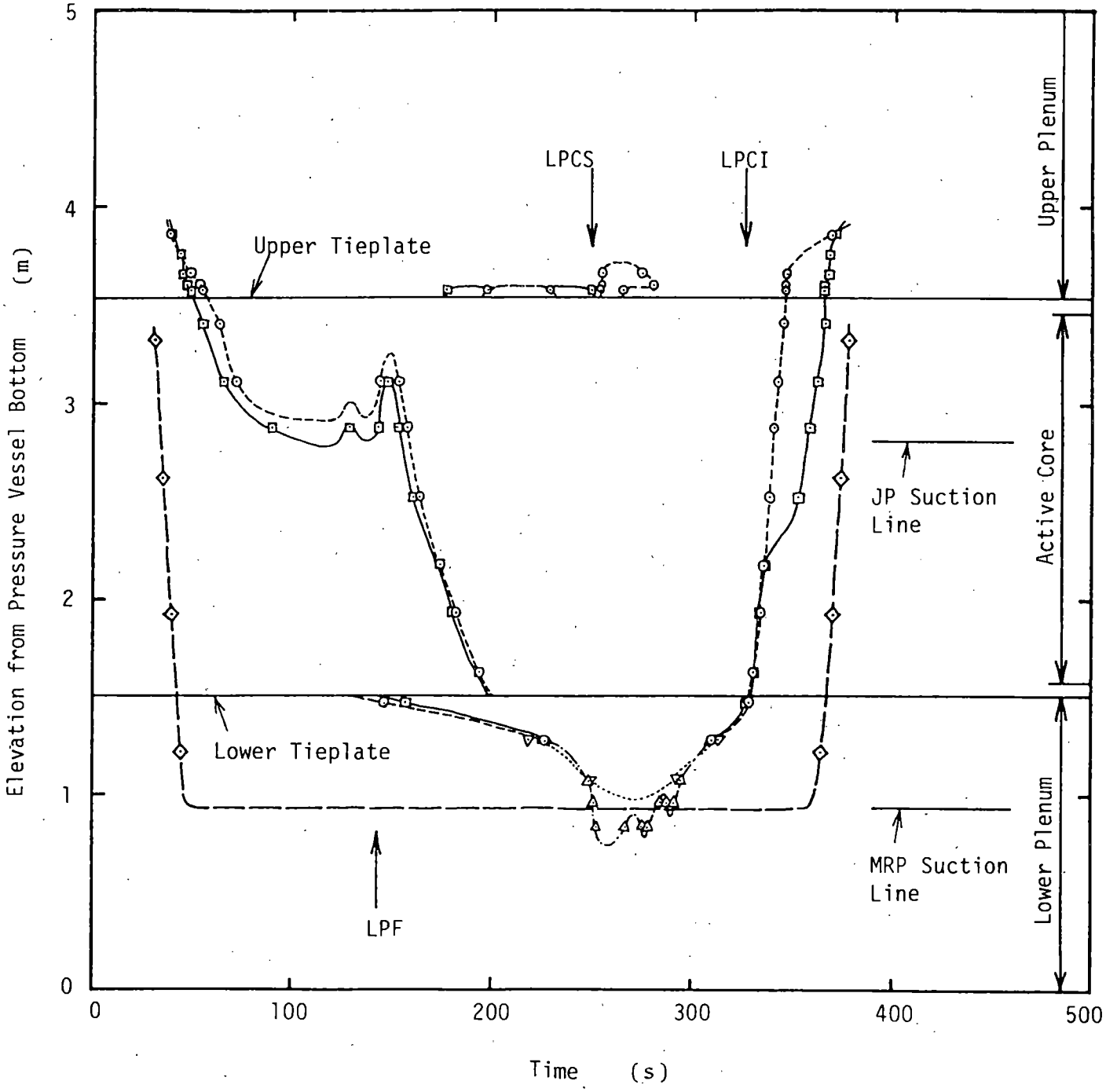

FUEL SURFACE TEMPERATURES OF

PEAK POWER ROD A11 (15% BREAK)

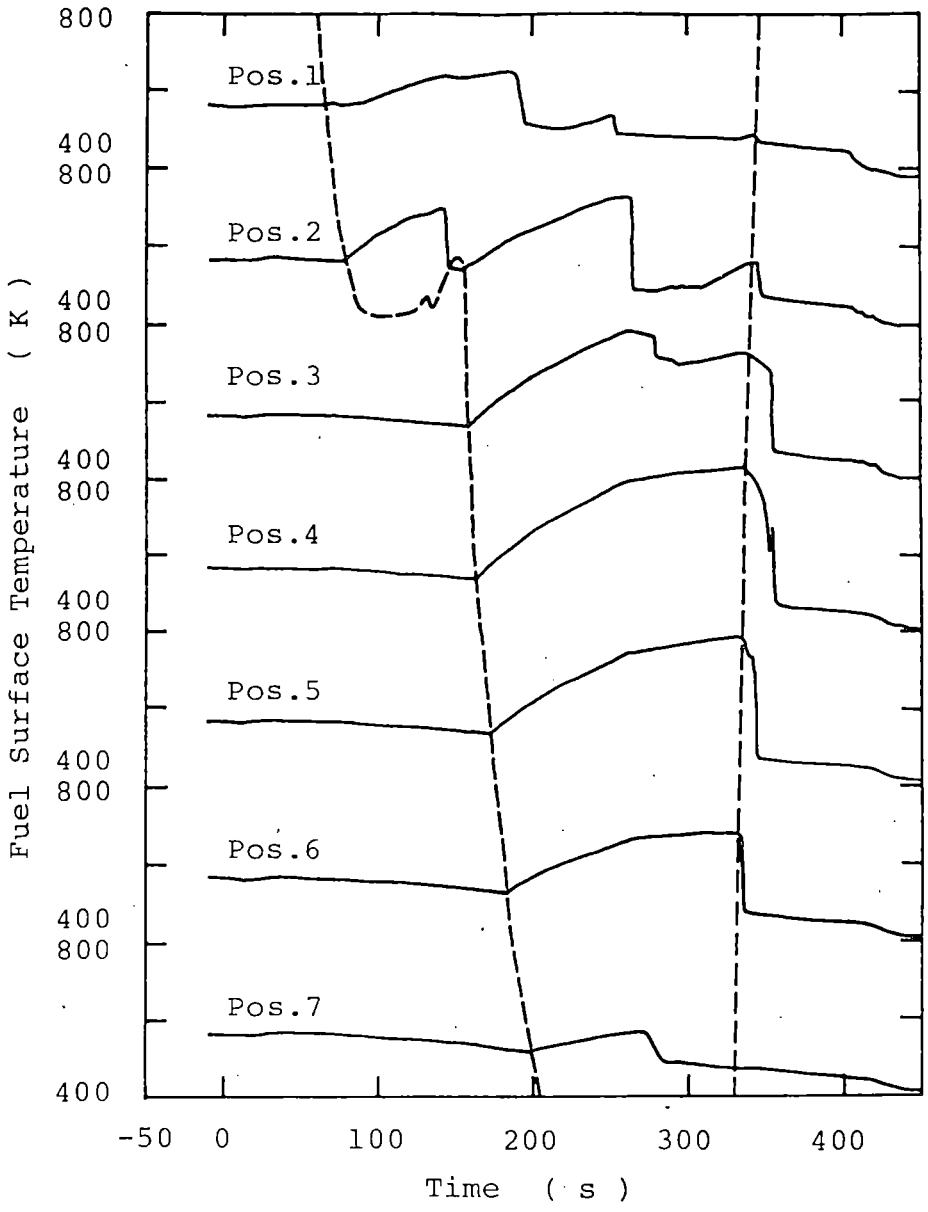

Pressure Transients

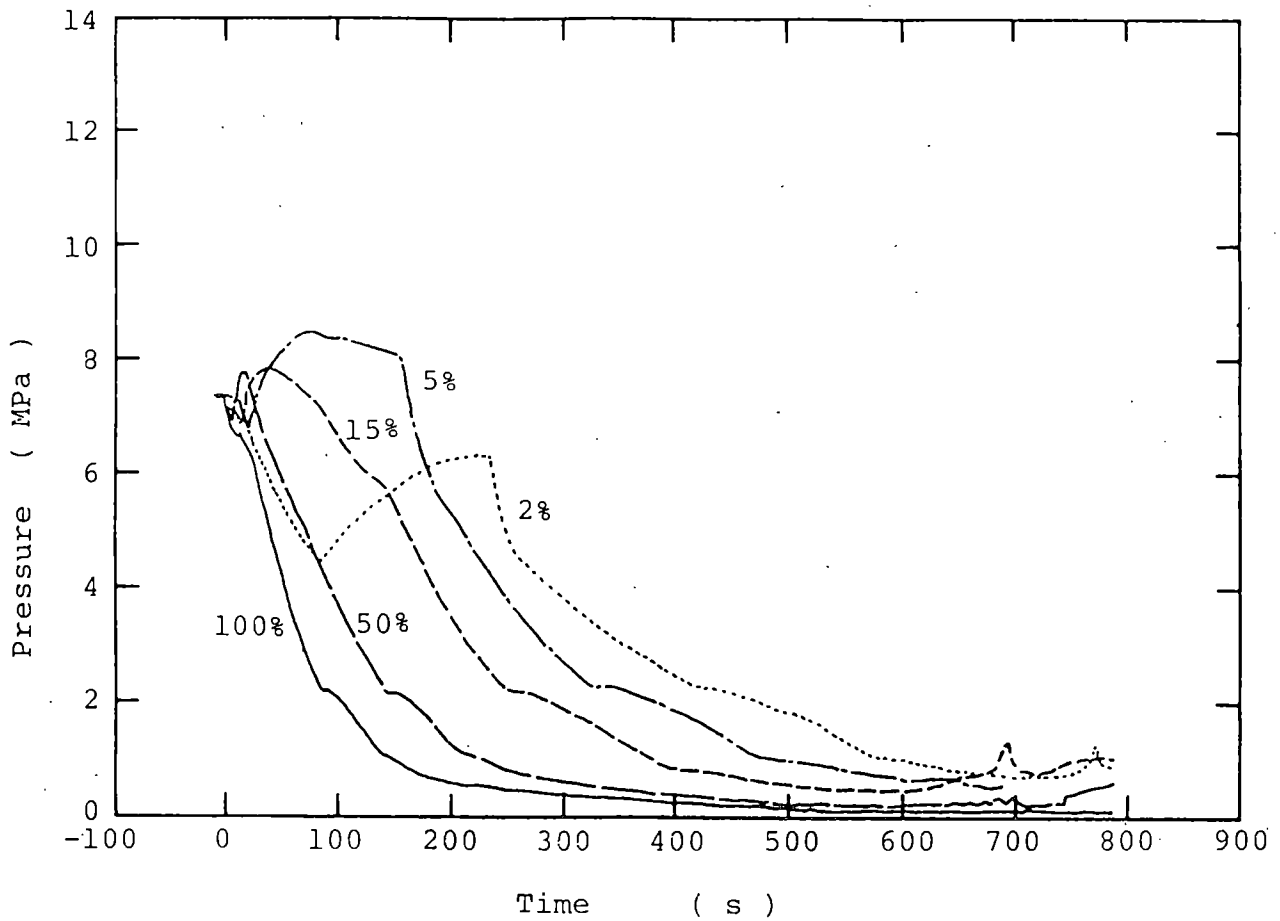

Liquid Level Transients

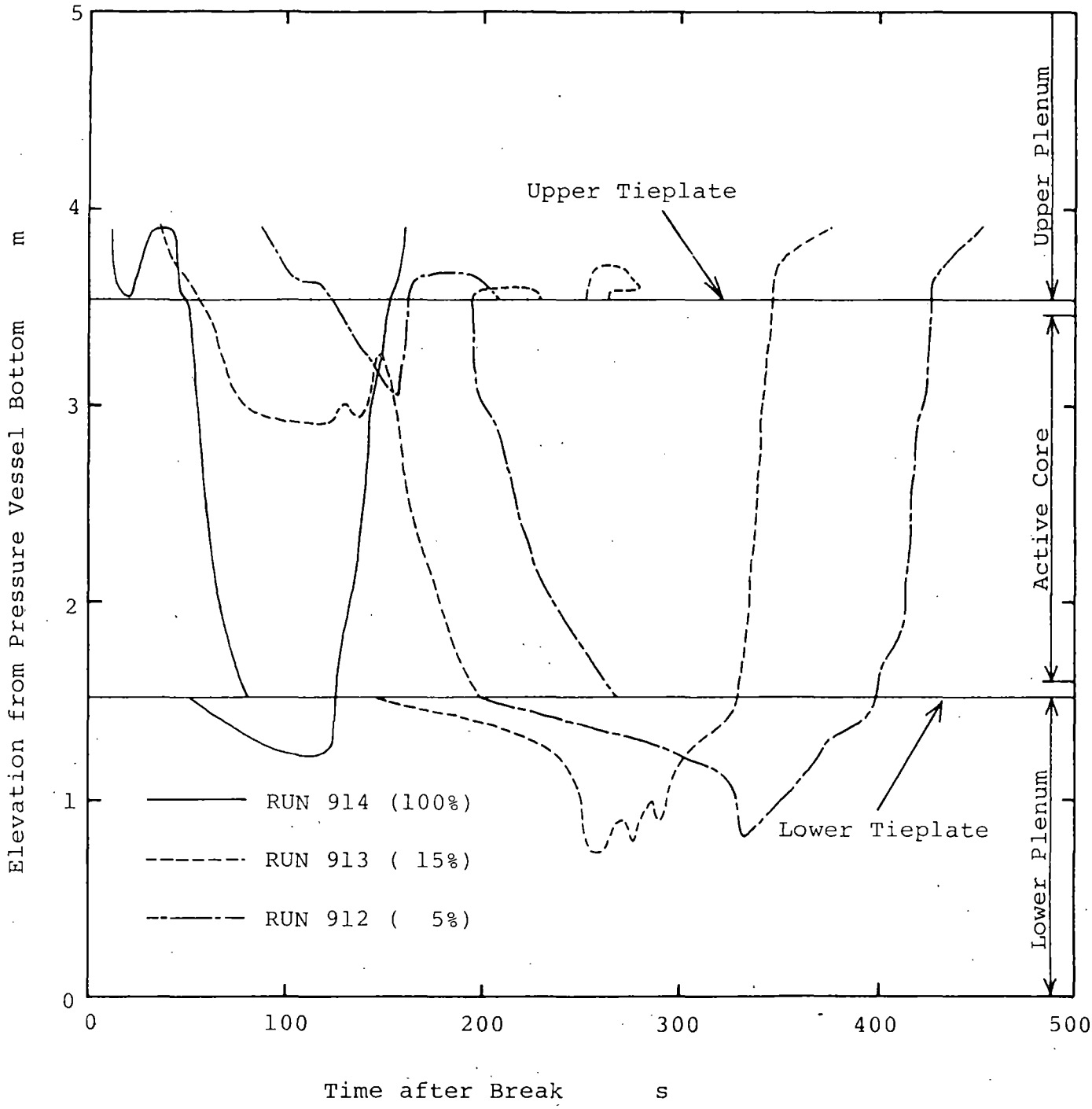

CORE UNCOVERY TIMES

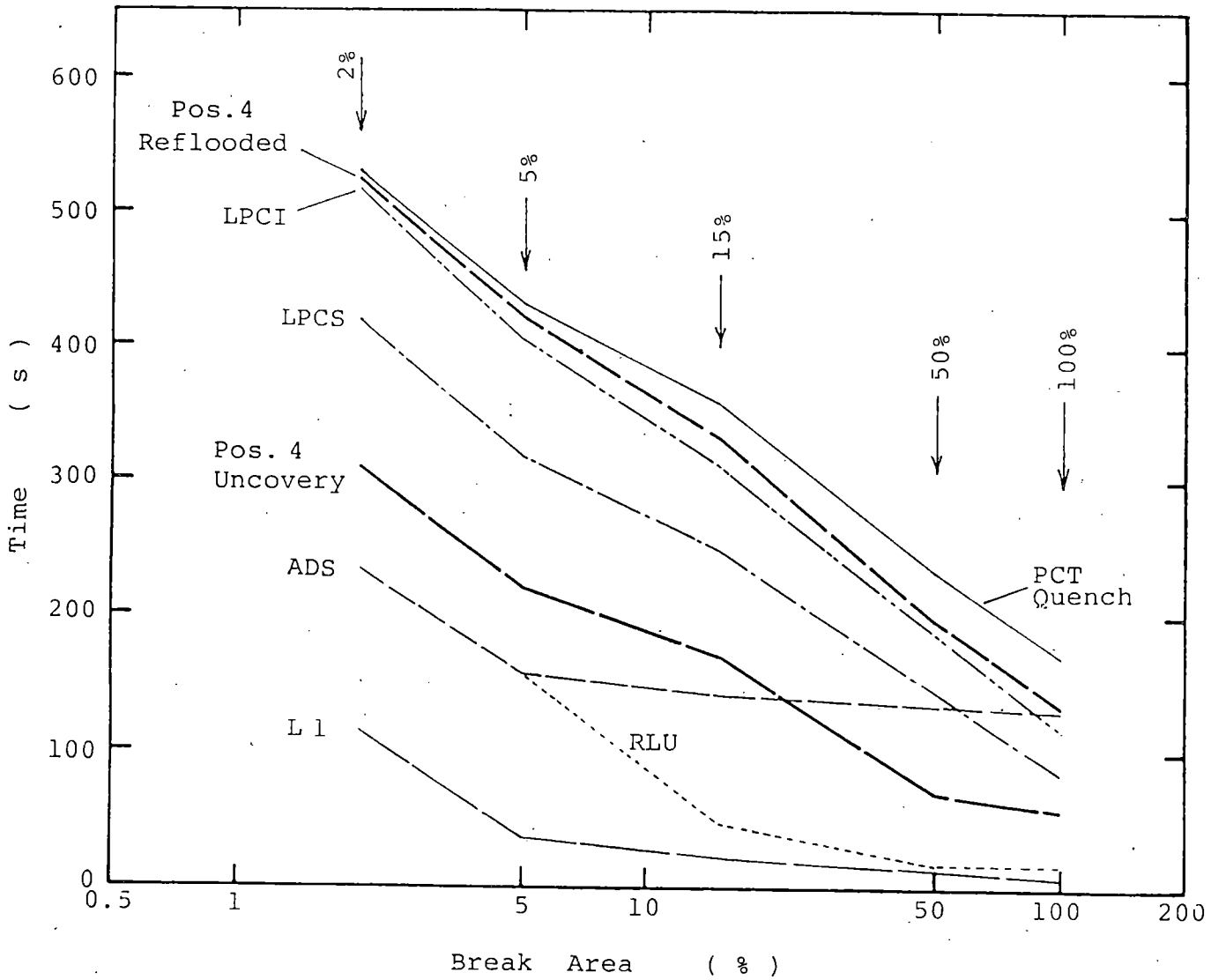

COMPARISON OF PCT

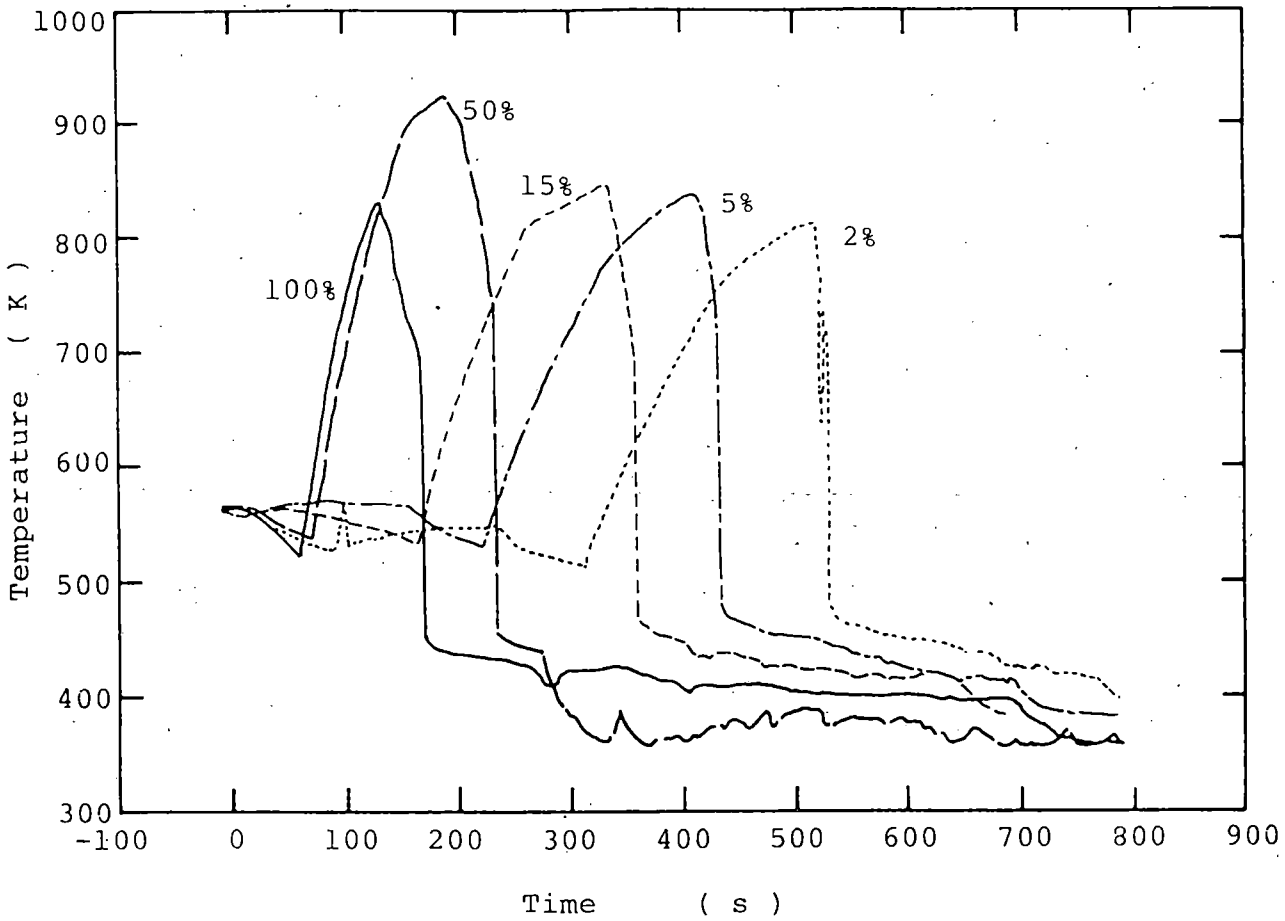

PCT vs. Break Area

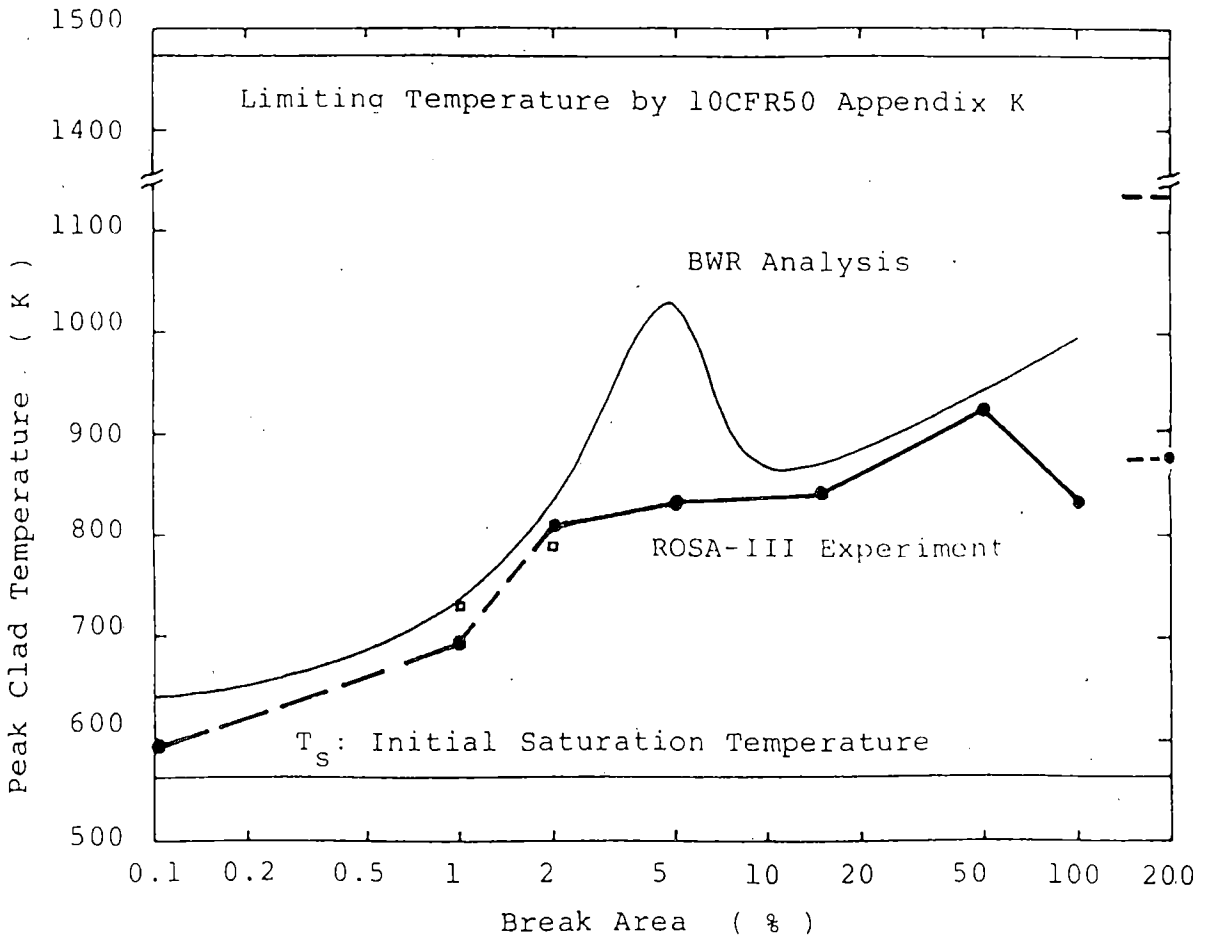

PCT vs. Break Area

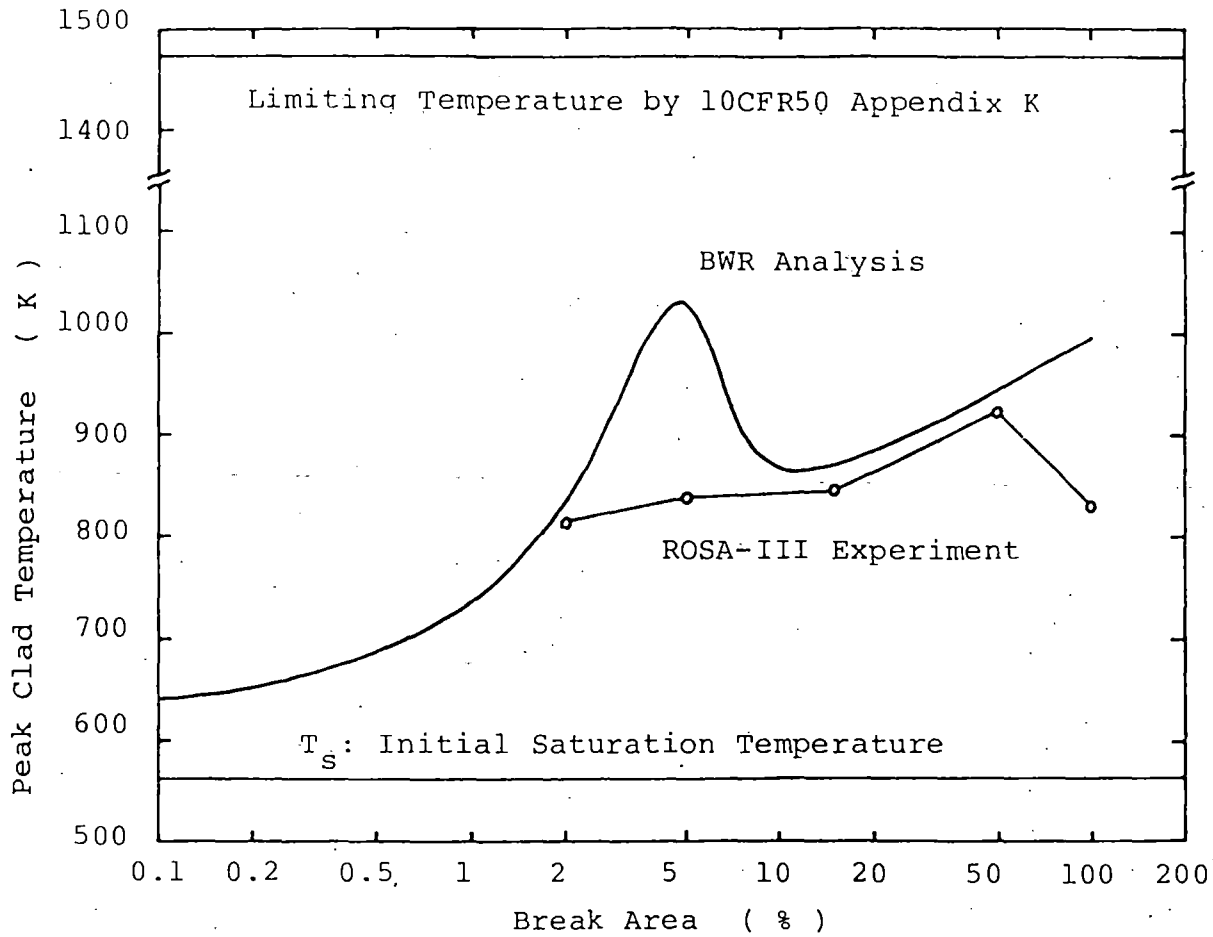

Conclusions

1. System pressure decreases rapidly by the fall of downcomer liquid level after uncovery of recirculation line for $S \geq 15$ % and after ADS actuation at (L1 + 120 s) for $S \leq 5$ %.

2. Lower plenum flashing initiates at 6.4 MPa resulting in core liquid level recovery and improved core cooling.

3. The whole core is uncovered after mitigation of LPF and fuel surface temperature initiates increasing.

4. LPCI initiates at 1.5 MPa resulting in reflooding and quenching of the whole core.

5. PCT observed is between 812 and 922 K for break area between 2 and 100 % and well below the present safety criteria of 1473 K.

ROSA-IV PROGRAM AT JAERI FOR PWR SMALL-BREAK LOCA EXPERIMENTS

Presented by
Masayoshi SHIBA

JAPAN ATOMIC ENERGY RESEARCH INSTITUTE

ROSA-IV Program at JAERI for PWR Small-Break LOCA Experiments

Masayoshi SHIBA

Japan Atomic Energy Research Institute

Introduction

There has been an extensive reorientation of the light-water-reactor (LWR) safety research program since the TMI-2 accident and the emphasis is now on small break loss-of-coolant accidents (SBLOCAs) and related transients. The Japan Atomic Energy Research Institute (JAERI) has instituted the Rig of Safety Assessment Number 4 (ROSA-IV) Program for the purpose of studying SBLOCAs and related transients. JAERI is constructing the Two-Phase Test Facility (TPTF) for separate effect tests and planning construction of the Large Scale Test Facility (LSTF) for system effect tests.

The schedule for ROSA-IV is shown in Table 1.

Objectives

The technical subject for the LSTF system effect tests are : (1) PWR Small Break LOCAs and Related Transients, (2) Reflux Cool-

Table 1 Time Schedule of ROSA-IV Program

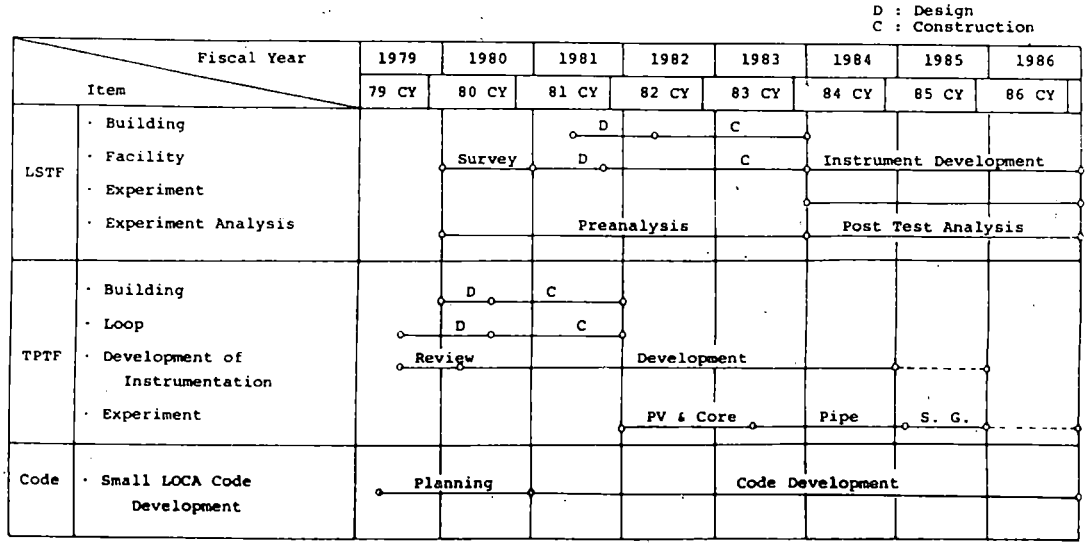

ing, (3) Natural Circulation in the Primary Loop, (4) Alternate ECCS, (5) Plant Recovery Technique. Technical subject for the TPTF separate effect tests are : (1) Heat Transfer in Uncovered Core, (2) 2ϕ Flow Patterns in a Horizontal Pipe, (3) Heat Transfer in the Steam Generator.

Design Concept of LSTF

The LSTF simulates a 3423MWt PWR with 17x17 fuel bundles. The volumetric scale ratio of the LSTF to the PWR is 1/48 and elevation scaling of each component is 1/1. The maximum core power is 10MW which provides the same power input per unit volume as the decay heat core power of the PWR below approximately 14% of full power. LSTF has two equal volume loops, each 2/48 volumetric scaled. Break size to be investigated will be restricted to those less than the 10% break.

The general view of LSTF is shown in Fig. 1.

Present Status of ROSA-IV Program

TPTF is now under construction and is to be completed at the end of FY 1981 as shown in Table 1.

LSTF is being designed and construction will start in this year. Preanalyses with the RELAP5 code are also being carried out to help in designing LSTF and determining the test matrix.

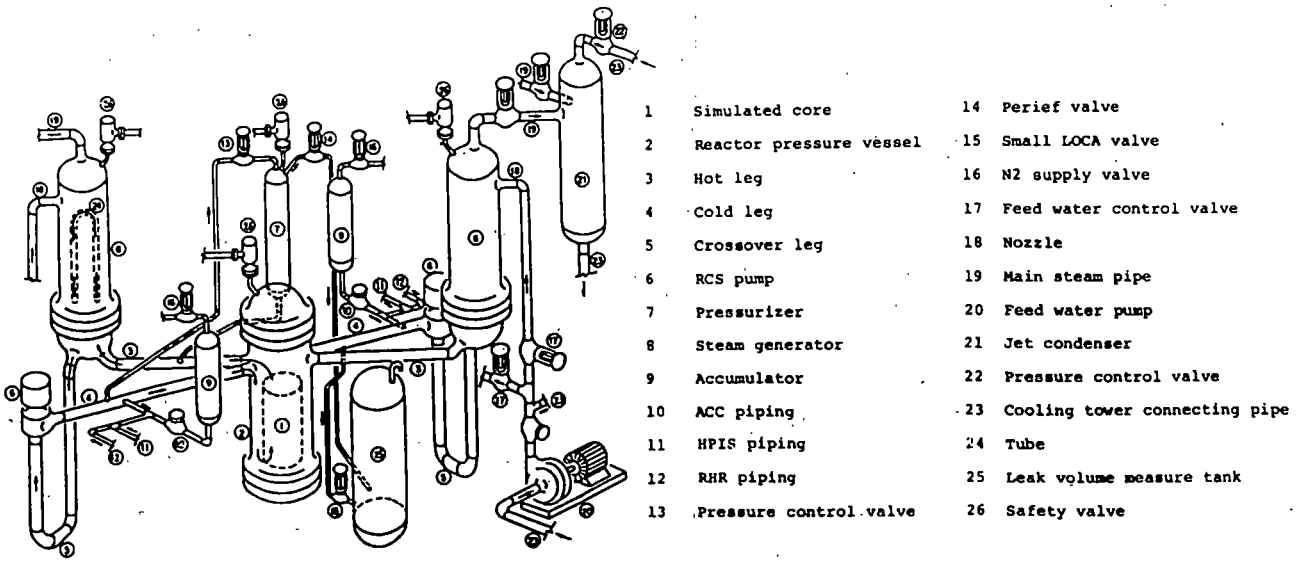

Fig. 1 General View of LSTF

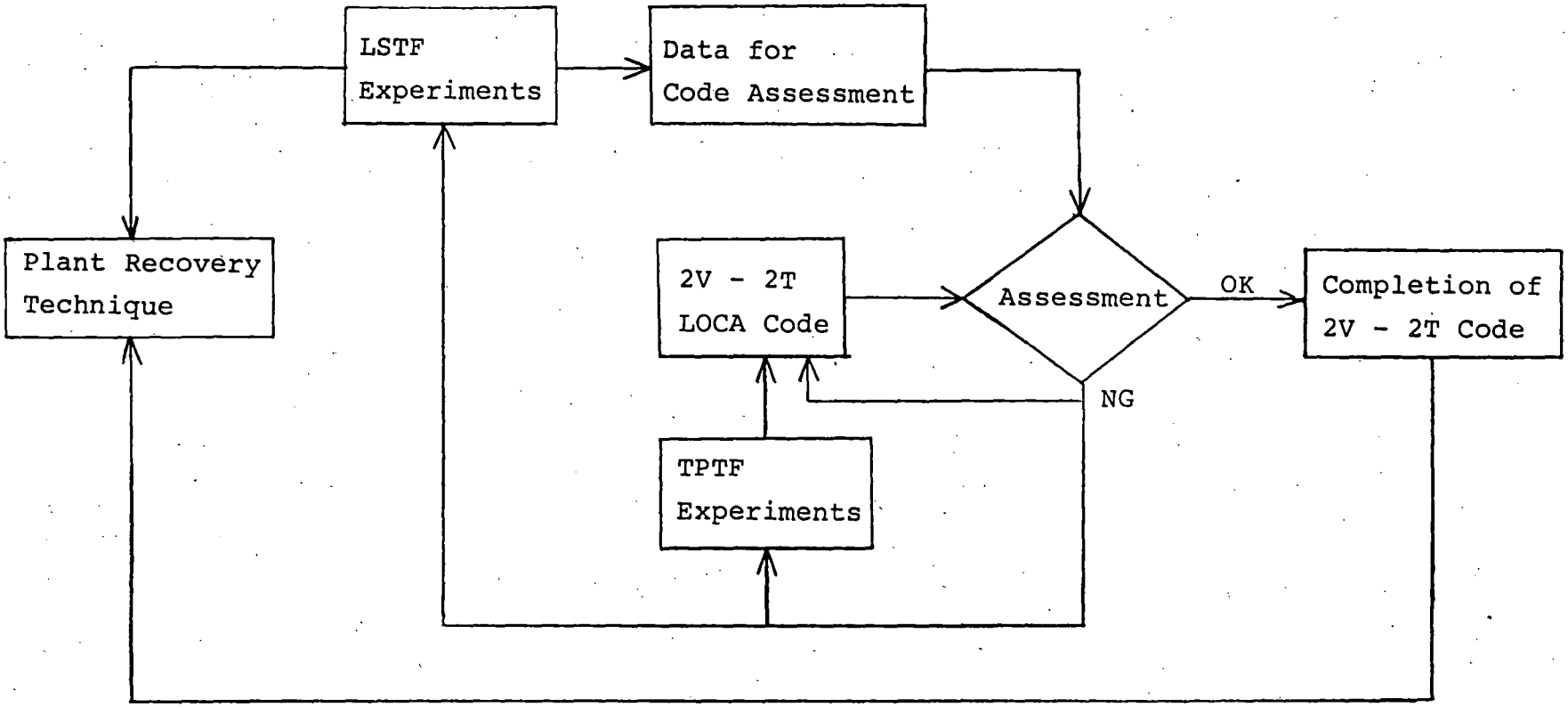

Schematic of ROSA-IV Program

Time Schedule of ROSA-IV Program

D : Design
C : Construction

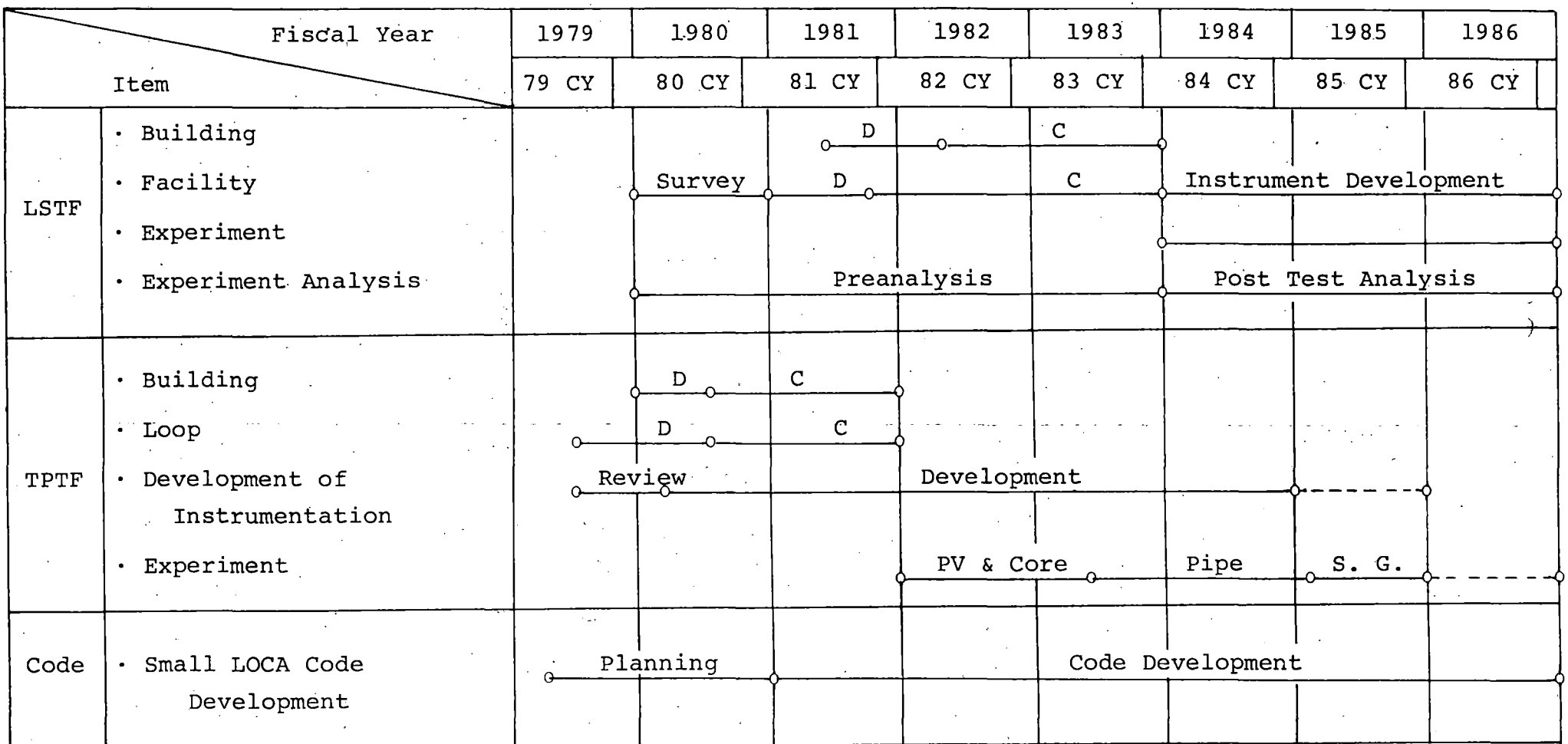

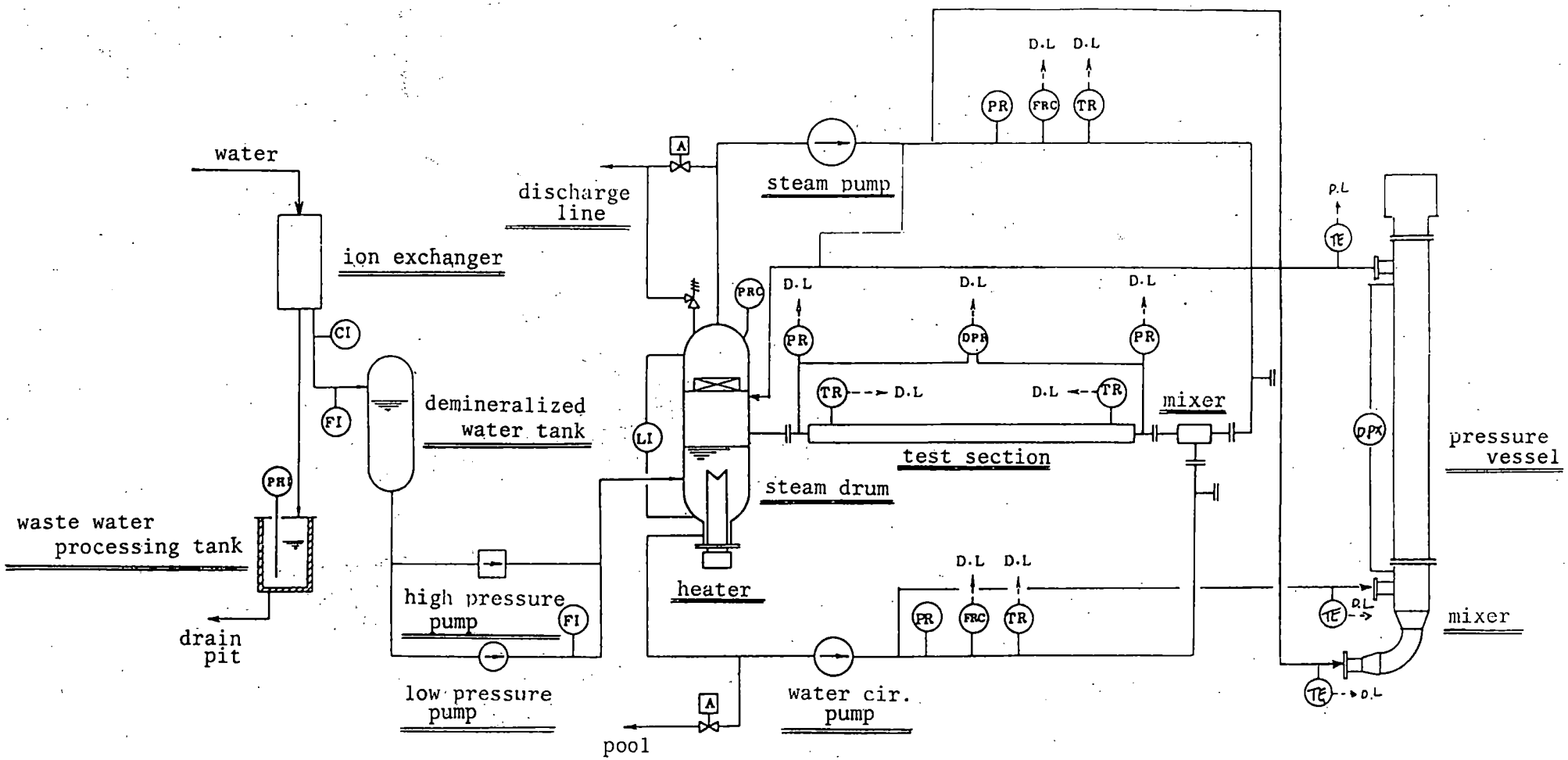

D.L data logger

Flow Diagram of TPTF

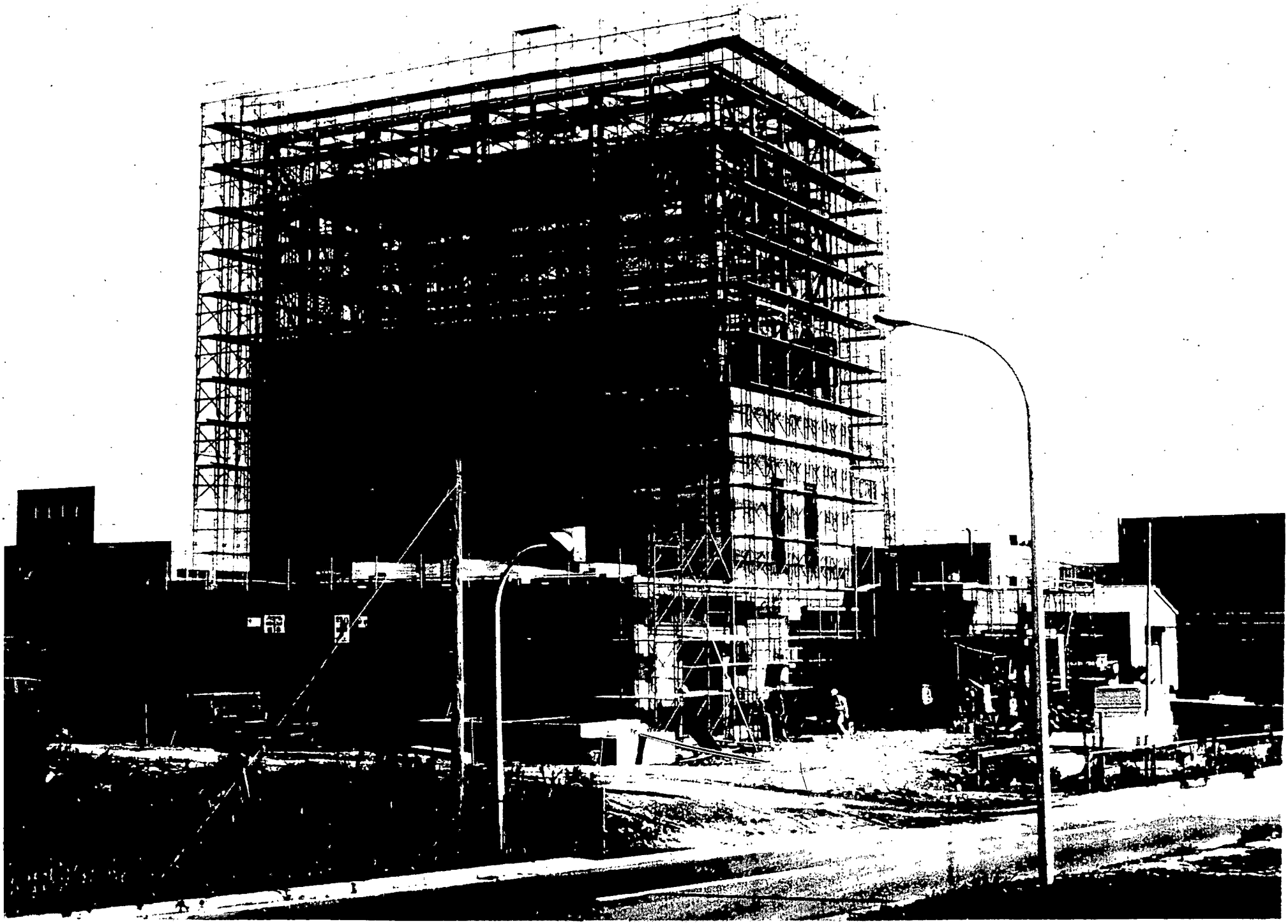

Major Dimensions of LSTF

		LSTF	PWR	PWR/LSTF
Pressure	(MPa)	16	16	1
Temperature	(K)	598	598	1
No. of fuel pins		1080	50952	48
Core height	(m)	3.66	3.66	1
Fluid volume V	(m^3)	7.23	347	48
Core power P	(MW)	10	3840	384
P/V	(MW/m^3)	1.4	11.1	8
Core inlet flow	(ton/s)	1.4	66.8	48
Downcomer gap	(mm)	60	260	4.3
Hot leg D	(mm)	207	737	3.6
L	(m)	3.53	3.94	1.8
$L/\sqrt{D}$	($mm^{1/2}$)	245	145	0.94
$\frac{\pi}{4}D^2 L$	(m^3)	0.119	1.68	24
No. of loops		2	4	2

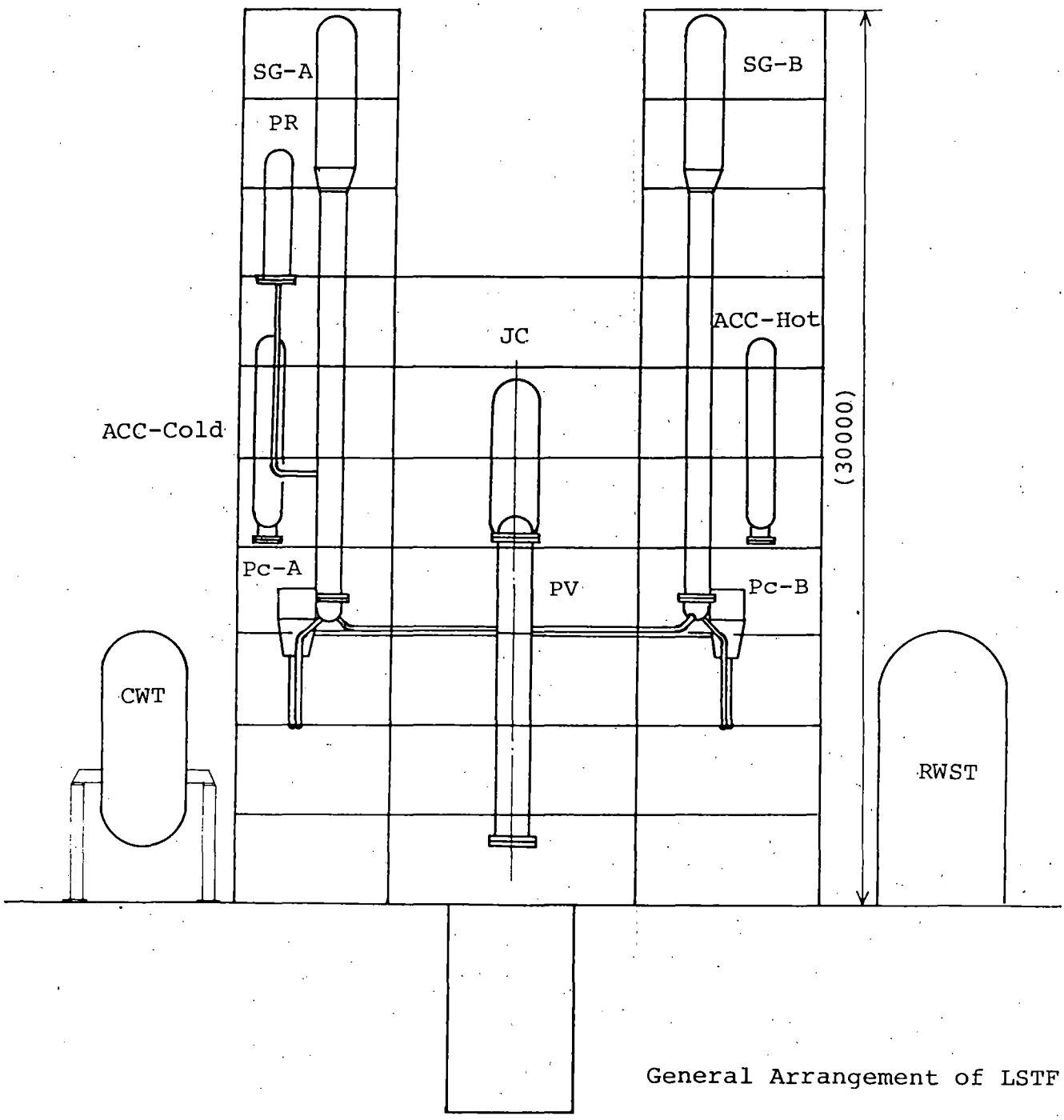

General Arrangement of LSTF

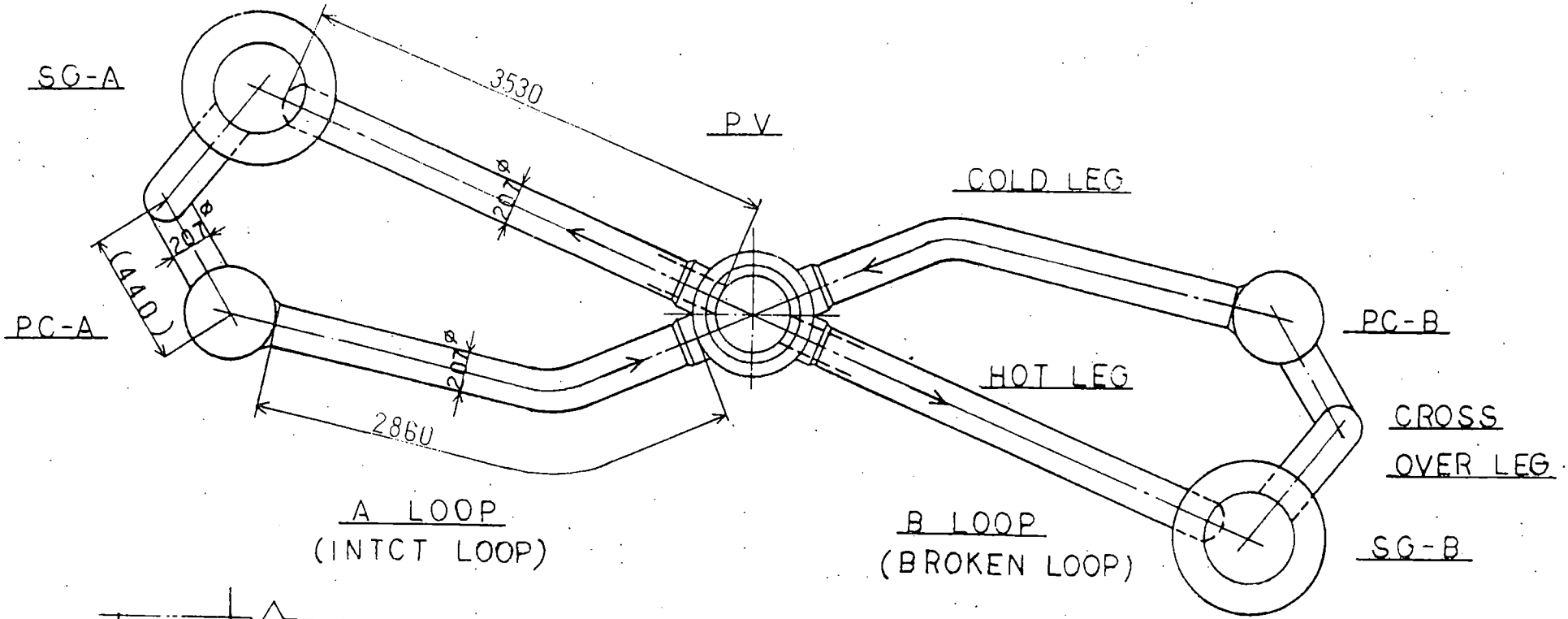

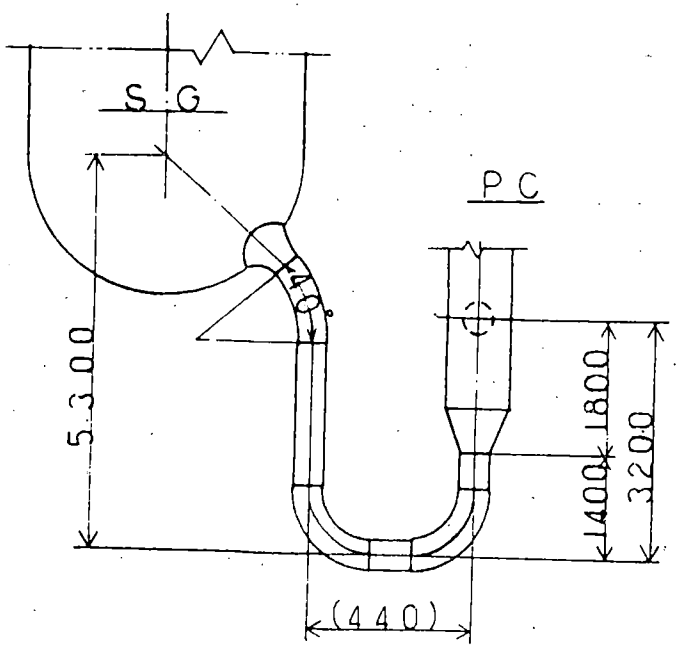

CROSS OVER LEG

Primary Coolant Piping of LSTF

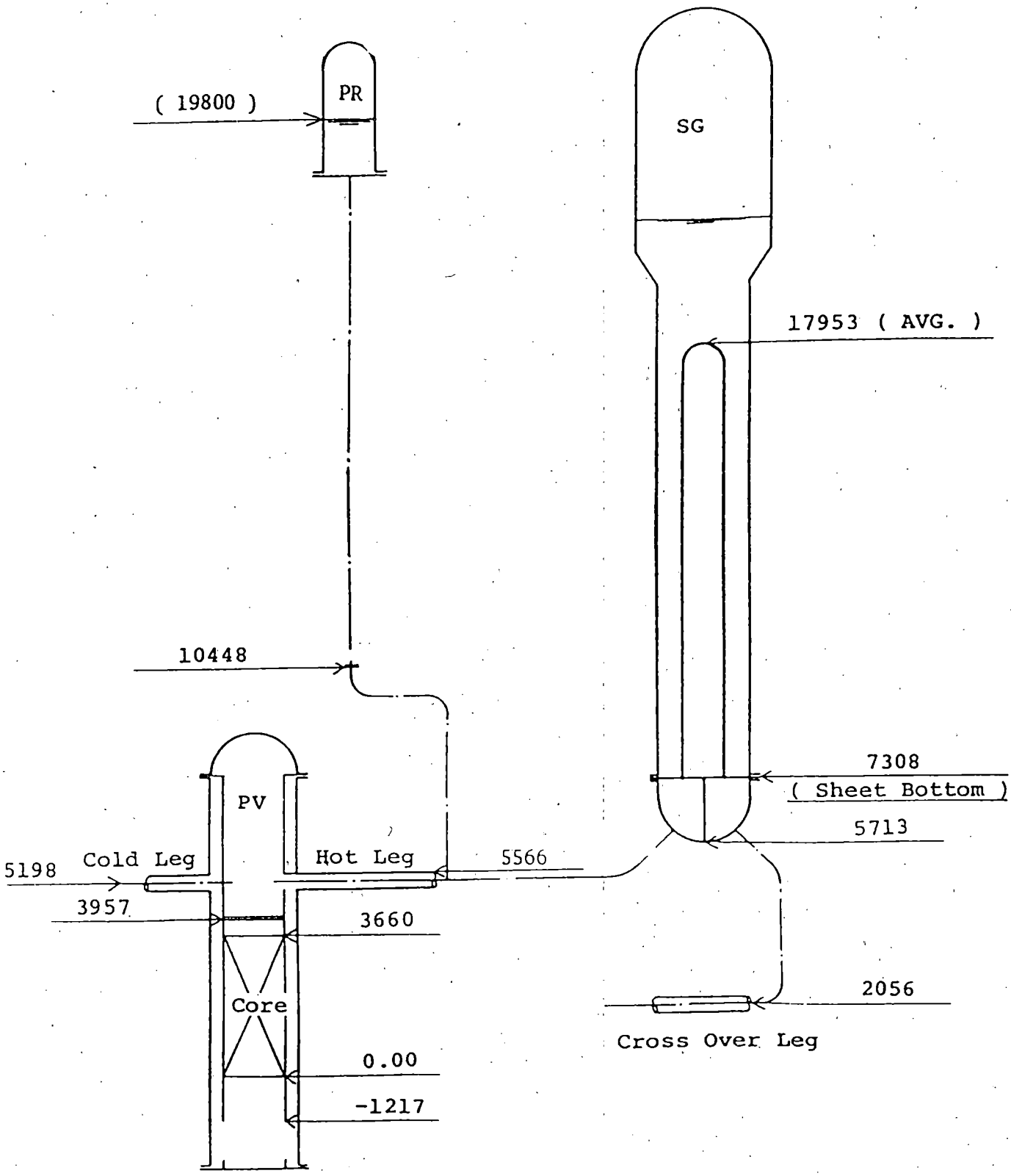

Primary Coolant System Elevation of LSTF

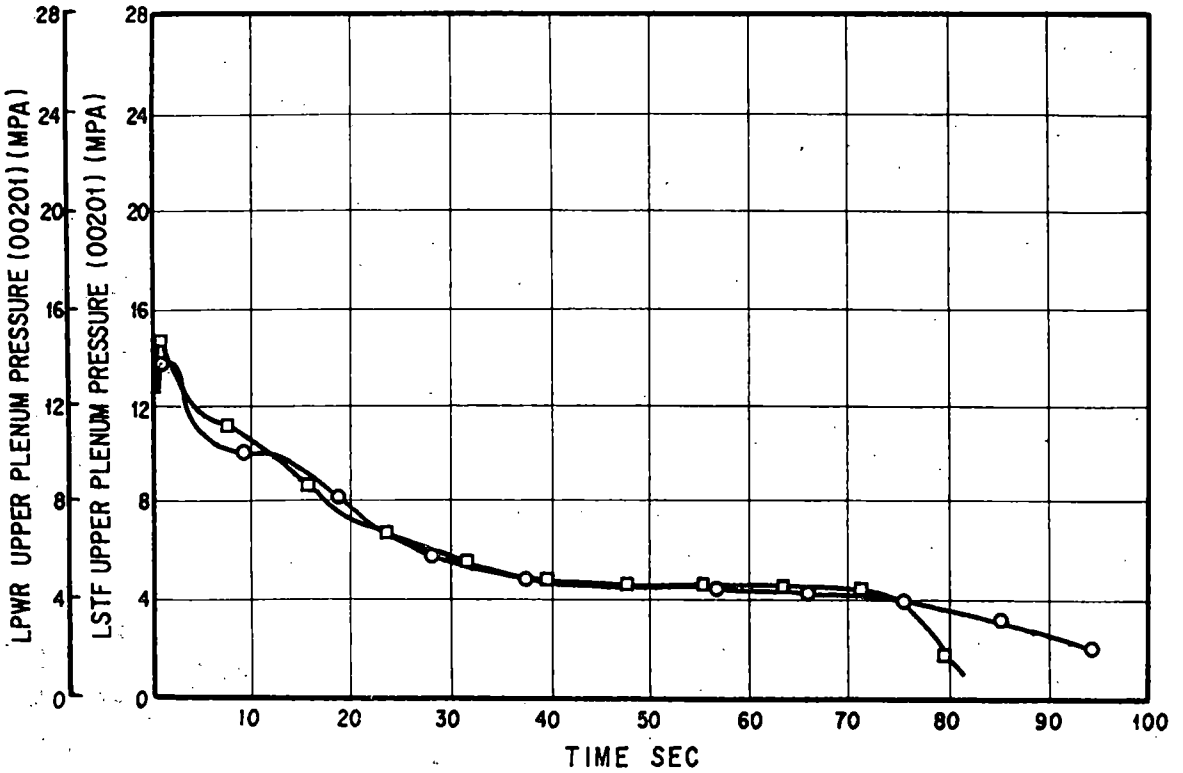

Preanalysis of ROSA-IV LSTF with RELAP5 Code

Comparison of Upper Plenum Pressure between PWR and LSTF

(10% cold-leg break LOCA with HPI failure, with RELAP5/MOD0)

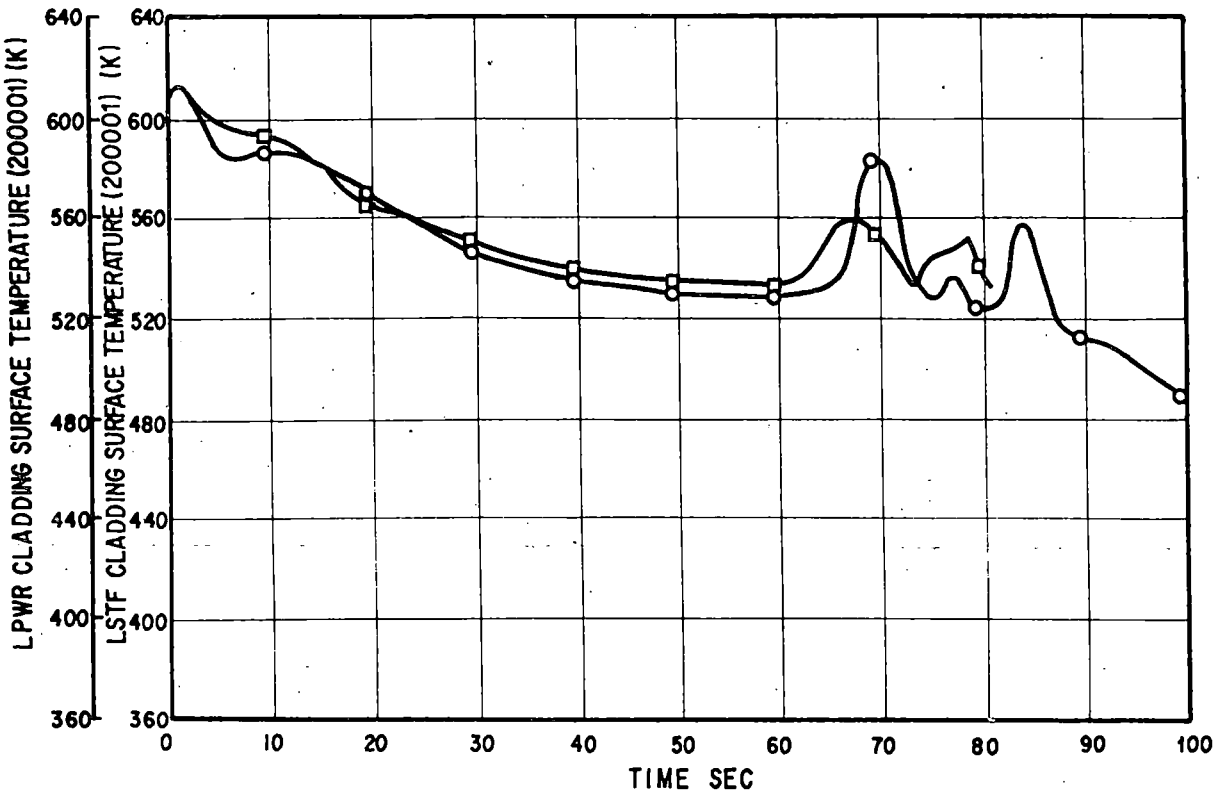

Preanalysis of ROSA-IV LSTF with RELAP5 Code

Comparison of Cladding Surface Temperature between PWR and LSTF

(10% cold-leg break LOCA with HPI Failure,
with RELAP5/MOD0)

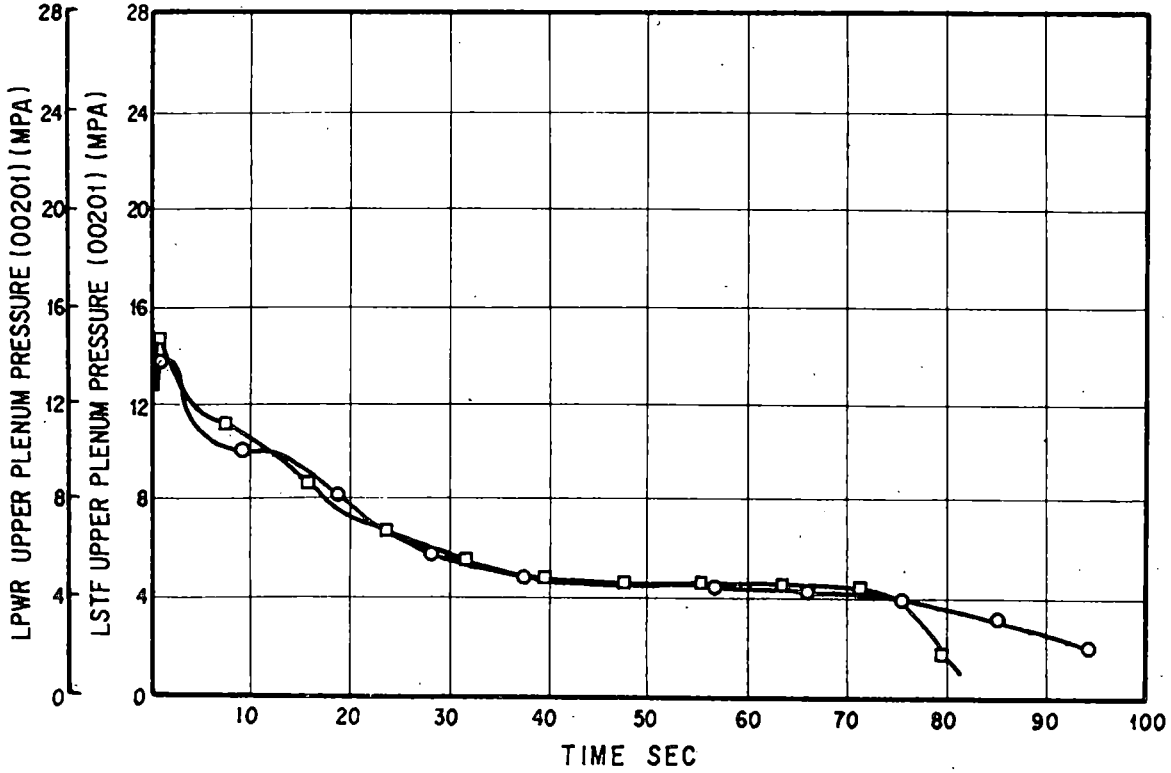

Preanalysis of ROSA-IV LSTF with RELAP5 Code

Comparison of Upper Plenum Pressure between PWR and LSTF

(10% cold-leg break LOCA with HPI failure, with RELAP5/MOD0)

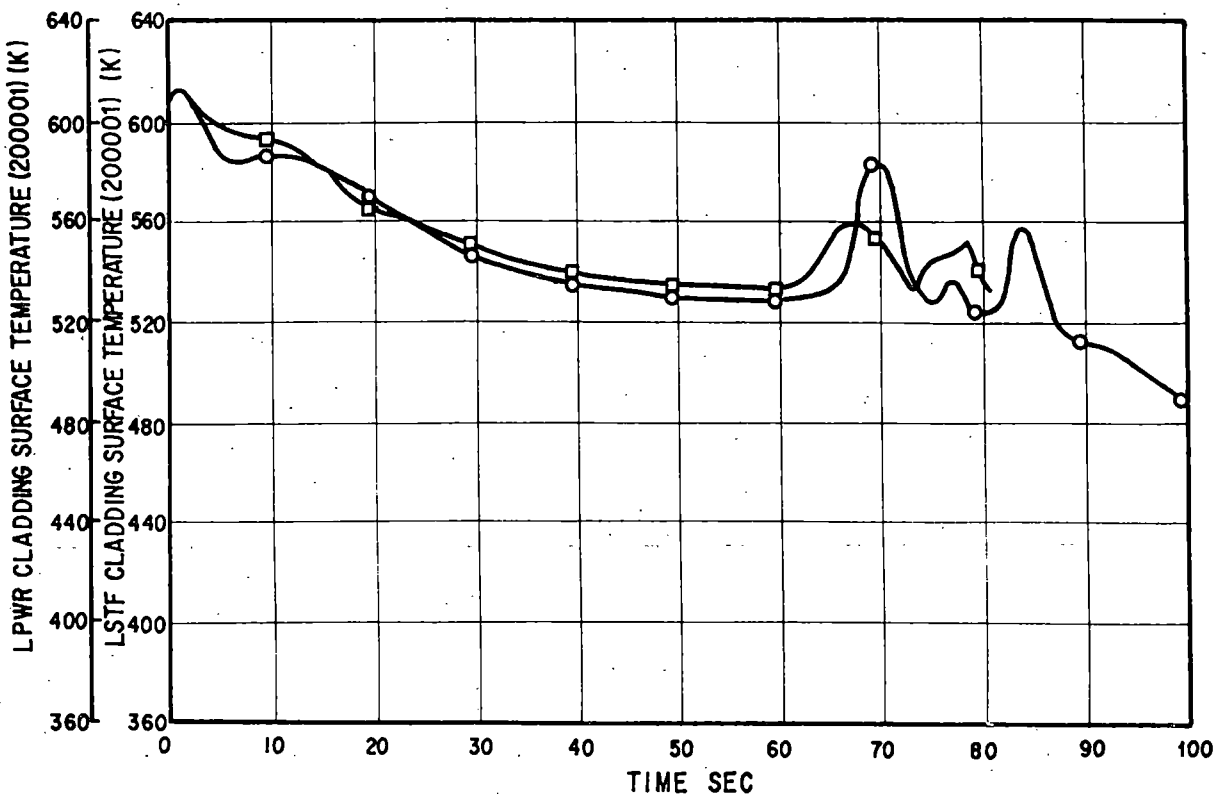

Preanalysis of ROSA-IV LSTF with RELAP5 Code

Comparison of Cladding Surface Temperature between PWR and LSTF

(10% cold-leg break LOCA with HPI Failure, with RELAP5/MOD0)

Present Status of ROSA-IV Program

- TPTF is now under construction and is to be completed at the end of FY 1981.
- LSTF is being designed and construction will start in this year.
- Preanalyses of LSTF tests with the RELAP5 code are being carried out to help in designing LSTF and determining the test matrix.

LARGE BREAK INTEGRAL TEST WITH TBL-1
(HITACHI BWR INTEGRAL FACILITY)

Masanori NAITOH, Michio MURASE

Energy Research Laboratory,
Hitachi Co. Ltd.
Moriyama-cho, Hitachi, Ibaraki 316
JAPAN

and
Ryoosuke TSUTSUMI

The Tokyo Electric Power Co., Inc.
Uchisaiwai-cho, Chiyodaku, Tokyo 100
JAPAN

FOR PRESENTATION AT:

The 9th Water Reactor Safety Research Information Meeting

October 26, 1981

National Bureau of Standards
Gaithersburg, Maryland

JOINT STUDY OF JAPAN BWR UTILITIES,
HITACHI CO. LTD., AND TOSHIBA CORPORATION

LARGE BREAK INTEGRAL TEST WITH TBL-1
(HITACHI BWR INTEGRAL FACILITY)

Masanori NAITOH, Michio MURASE, and Ryoosuke TSUTSUMI

BWR simulation tests are being conducted to obtain an integral system response at loss of coolant conditions with the Hitachi BWR Integral Facility. The first series of the tests are focused on the simulation of a recirculation line break. The facility for this purpose is called a Two Bundle Loop which consists of two full size electrically heated bundles (TBL-1). This is a joint study program of Japan BWR utilities, Hitachi Co. Ltd., and Toshiba Corporation.

the objective of this test program is to obtain physical understanding of an entire transient response which appears in a multi-channel core during a period from an initiation of a recirculation line break to cool down of the core by reflooding, and to provide data for evaluation of the best estimate and the licensing codes.

The Two Bundle Loop is scaled to a reference BWR/5-251 plant with 764 fuel bundles. The TBL consists of a feed water line, a main steam line, two recirculation lines, a emergency core cooling system, and core internals. A power supply system has the maximum capacity of 10 MW for two electrically heated bundles. Each bundle consists of 63 heater rods and a water rod with an 8x8 array. The actual upper tie plate from a production line are installed in the heater bundles for good simulation of counter-current flow phenomenon at the top. A configulation of the bundle inlet is slightly different from an actual one, because rods penetrate a lower plenum and a lower flange of a pressure vessel. The height from the bottom of two jet pumps to a separator in the TBL is the same as the actual height. The scale ratio of regional volumes, masses,and flow rates in the pressure vessel is 2/764 which is the same as the bundle ratio of the TBL to the BWR. To obtain this scale ratio, filler blocks are inserted in an annulus, a downcomer, and the lower plenum. The height of a steam dome and the lower plenum is shorter than actual ones, however the volume is scaled down to 2/764.

The TBL has capability to maintain the rated steady state condition with 10 MW power for 45 minutes, however, at a blowdown test, a pipe break is simulsted by a quick open valve after the steady state condition for 15 minutes. Data acquisition starts from the 35 seconds before the break for the maximum 15 minutes. Four hundred signuls from sensors are recorded on a magnetic tape every 0.1 seconds : 39 differential pressures to measure water heads, 2 absolute pressures in the vessel, 20 coolant temperatures, 256 rod surface temperatures, 10 signals from conductivity type void sensors, 2 bundle powers, system flow rates, and signals from 2-phase-flow measurement devices which consist of 2-beam gamma densitometers, turbine meters, drag discs, pressure transducers, and thermocouples.

The TBL-1 test parameters were a break diameter, a bundle power combination, and an ECCS operation mode. A bundle power combination was mainly 4 MW + 6 MW for the two bundles, and several tests with 4 MW + 4 MW and 5 MW + 5 MW combinations were performed for a comparison.

From large break tests, or simulation of the design basis accident, the results are summarized as follows;

(1) There was little difference of thermal hydraulic characteristics between the two bundles during the blowdown period for about 30 seconds after the break, or before HPCS initiation.

(2) Initiation of rod heat up was later in the higher power bundle than in the lower power bundle. This was caused by the following phenomenon : At the blowdown period, some water stayed in bundles due to the counter-current flow limitation at the bundle inlets, and ascending steam flow entrained the water resulting in the higher heat transfer coefficient. This restricted a bundle heat up. This sequential phenomenon was considered to appear more conspicuously in the higher power bundle with more ascending steam flow than in the lower power bundle.

(3) The increasing rate of rod surface temperature was proportional to a bundle power, however, from the above cooling effect, the higher peak cladding temperature did not always appear in the higher power bundle.

(4) Since heat capacity of the core internals and the pressure vessel per coolant volume in the TBL is about 5 times of the reference BWR's, and steam generation rate during depressurization period is larger, decreasing rate of pressure was smaller than expected. This makes delay of initiation of low pressure ECC systems, LPCS and LPCI, than expected.

(5) In the TBL-1 tests with ECCS single failure modes, the lowest peak cladding temperature, 315 C, appeared in the case of HPCS+ 2LPCI and the highest 588 C in the case of LPCS + 3LPCI.

The second series of tests (TBL-2) will follow the present TBL-1 under the joint utility study. In the second series, tests will simulate other breaks of a feed water line, core spray line, and a drain line than a recirculation line. The TBL-2 will be completed at September 1983.

Table 1 Scaling of the facility

ITEM	BWR5/251	FACILITY	SCALING
RECIRC. LOOP	2	2	1
NO. OF JET-PUMP	20	2	1/10
M. S. LINE	4	1	1/4
VESSEL VOLUME	596 M^3	1.55 M^3	2/764
VESSEL HEIGHT	22.3 M	12.9 M	1/1.7
VESSEL I.D.	6.38 M	0.41 M	1/16
FUEL BUNDLE	764	2	2/764
THERMAL POWER	3323 MW	10 MW	23/764
RODS NUMBER	63	63	1
WATER ROD	1	1	1
ACTIVE FUEL LENGTH	3.708 M	3.708 M	1
ROD O.D.	12.52 MM	12.52 MM	1
AXIAL POWER DISTRIBUTION		COSINE	
VESSEL PRESS.	7.2 MPA	7.2 MPA (9.0MPA)	1
COOLANT TEMP. (SAT.)	285 °C	285°C (303°C)*	1

* DESIGN VALUE

Table 2 Typical Test Conditions

Run No.	Break Dia.	Initial Power		ECCS Operation Mode
		Bundle A	Bundle B	
104	28 mm*	4.1 MW	3.9 MW	HPCS + 2LPCI
105	28 mm*	3.9 MW	5.8 MW	HPCS + 2LPCI
107	28 mm*	4.0 MW	5.9 MW	HPCS + LPCS + LPCI
108	28 mm*	4.1 MW	5.9 MW	LPCS + 3LPCI
112	28 mm*	5.1 MW	4.9 MW	HPCS + 2LPCI
119	28 mm*	4.9 MW	4.9 MW	LPCS + 3LPCI

* Simulation of Design Basis Accident

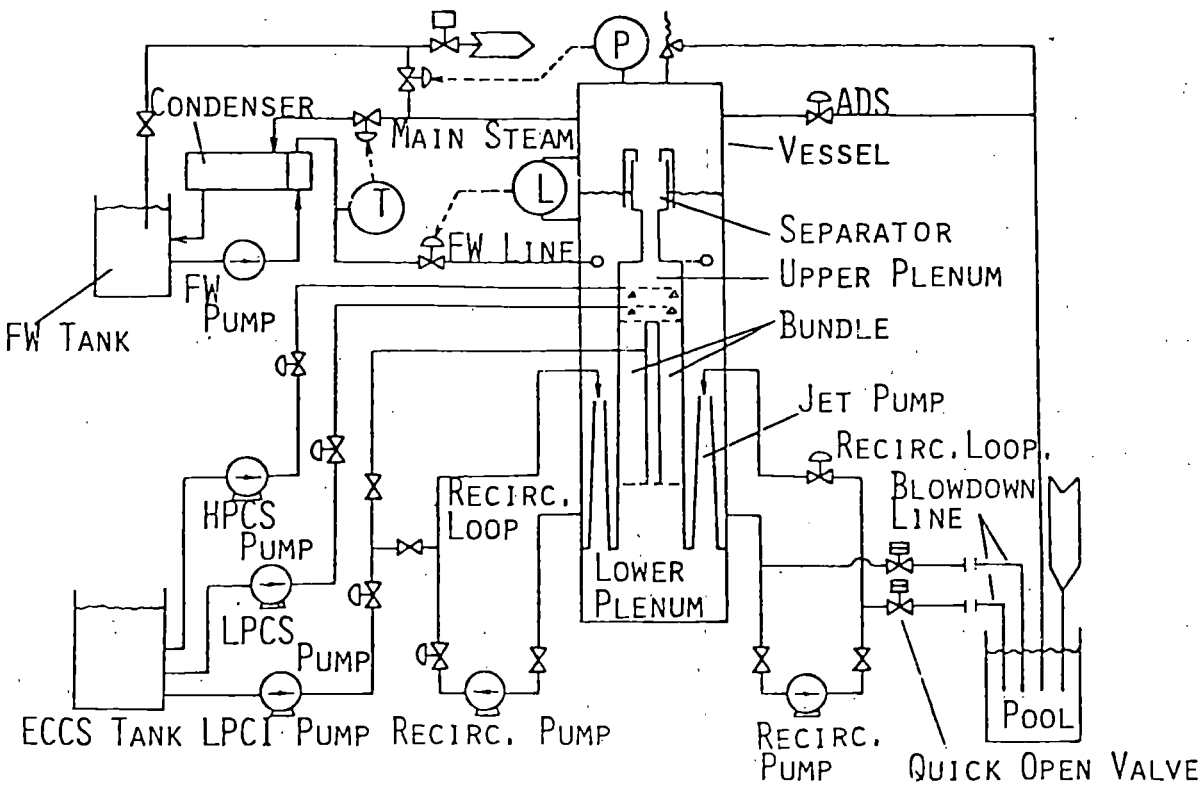

FIG. 1 FACILITY OVERVIEW

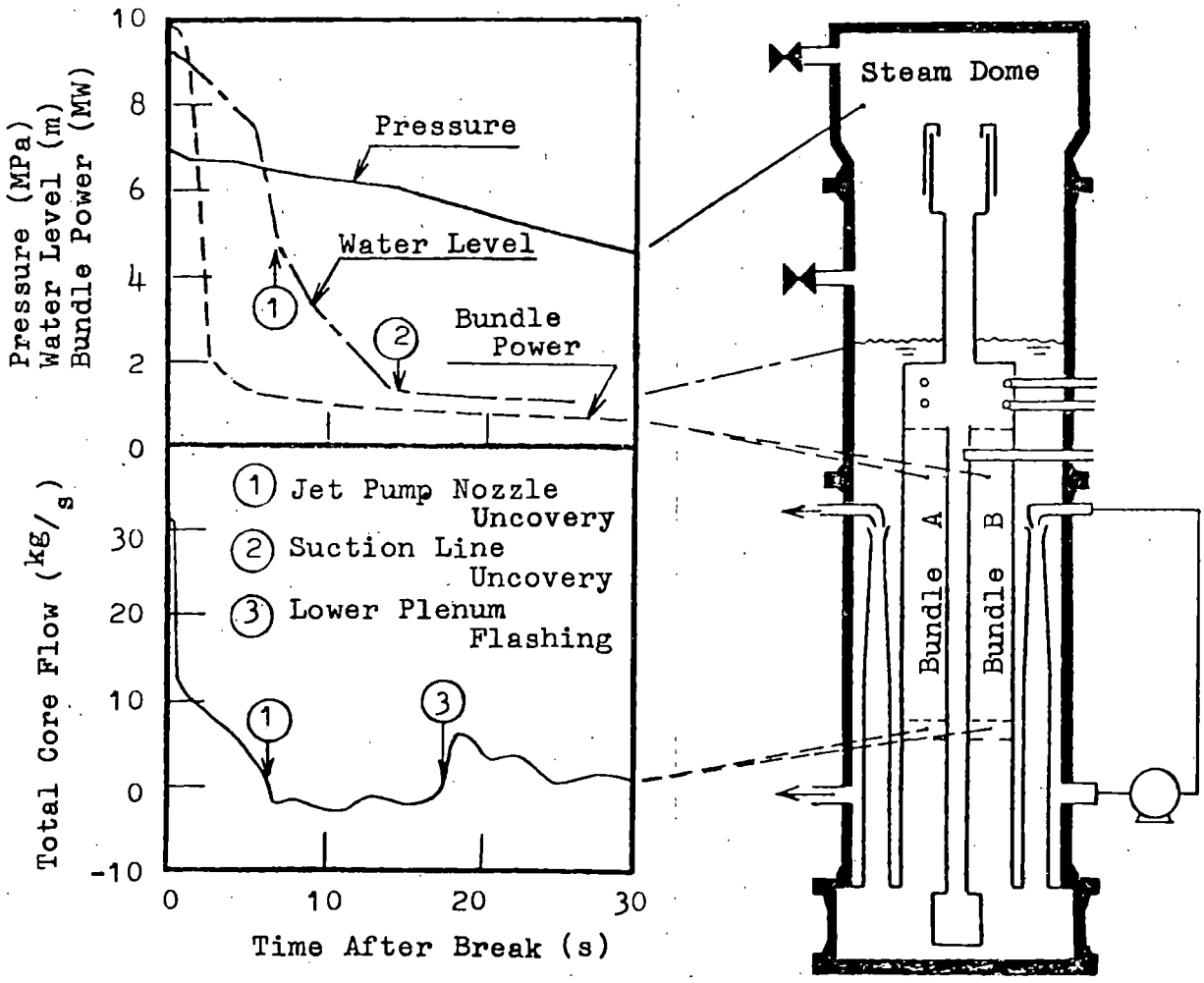

Fig 2 Blowdown Characteristics (Run 107)

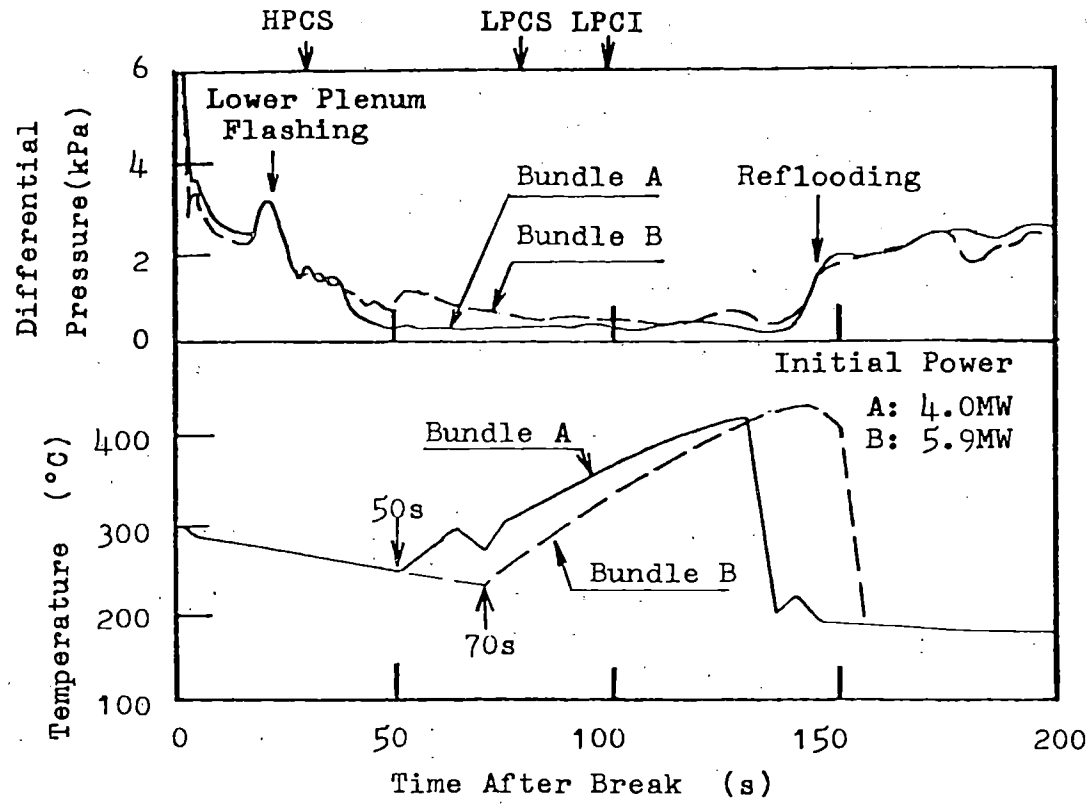

Fig 3 Differential Pressure and Temperature at Midplane of Bundles (Run 107)

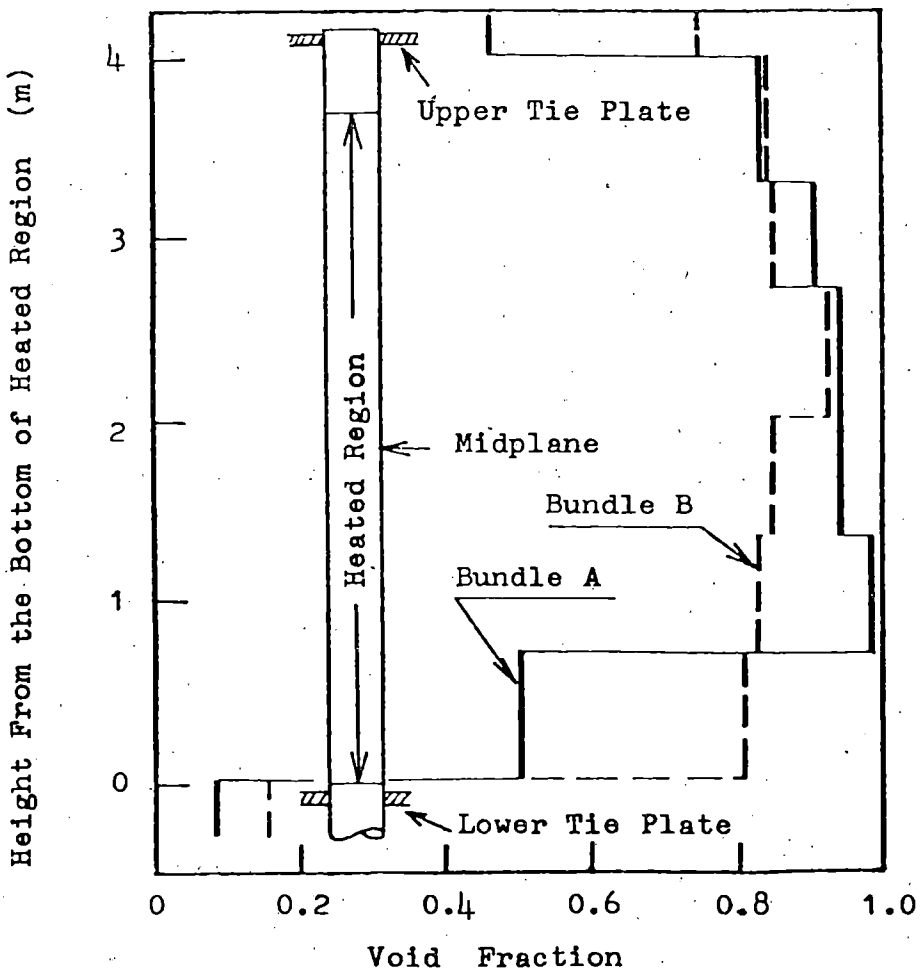

Fig 4 Void Fraction in Bundles at 50s

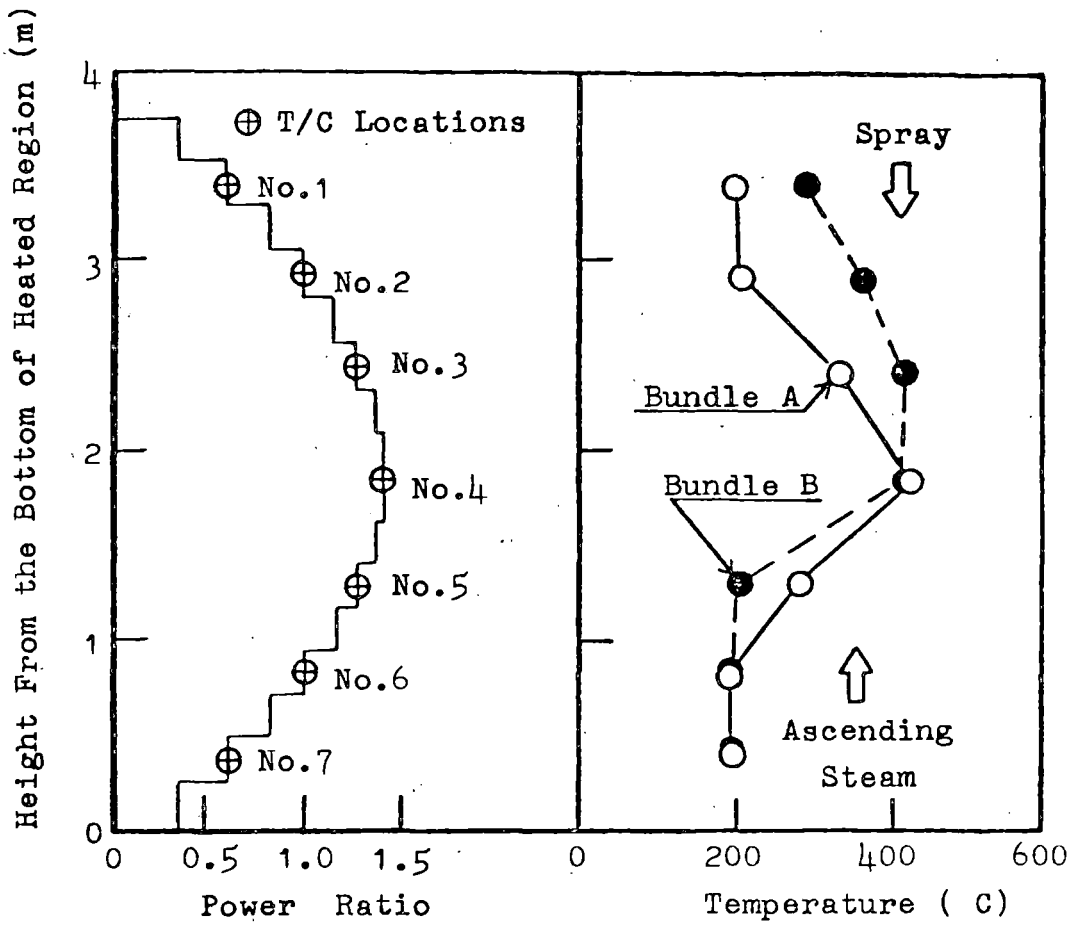

Fig 5 Temperature Distribution at 130s

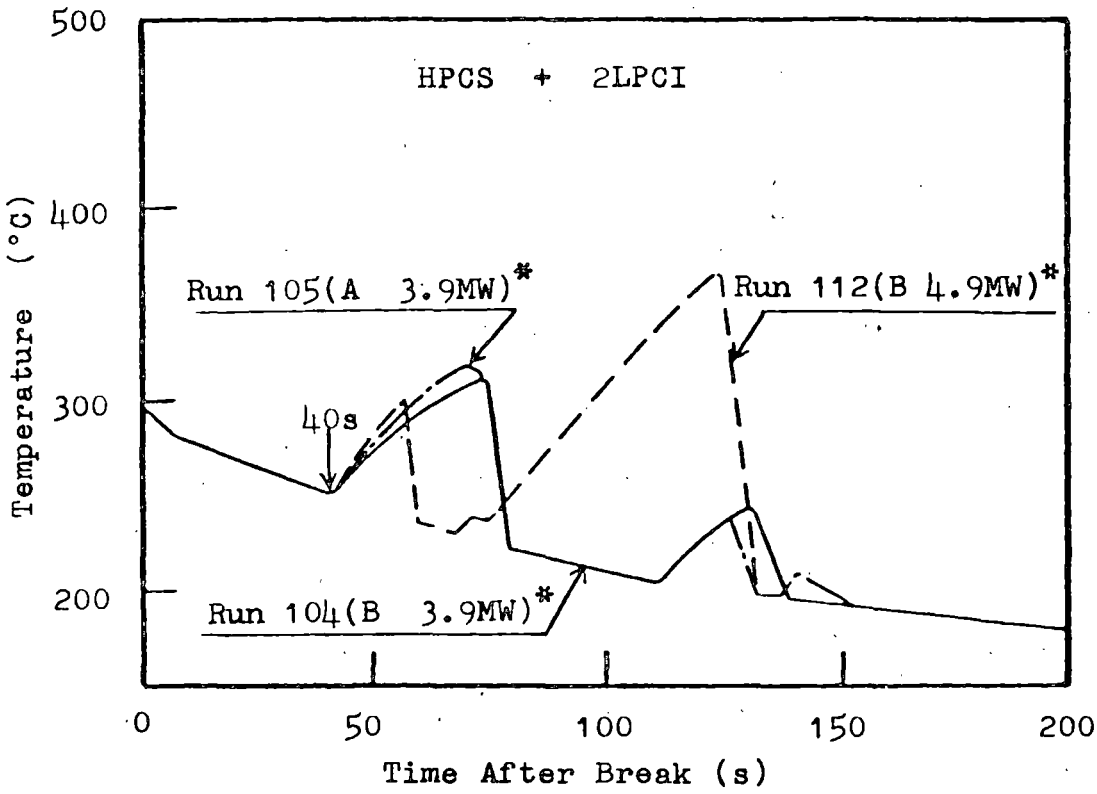

Fig 6 Effect of Bundle Power (Low Power Bundle)

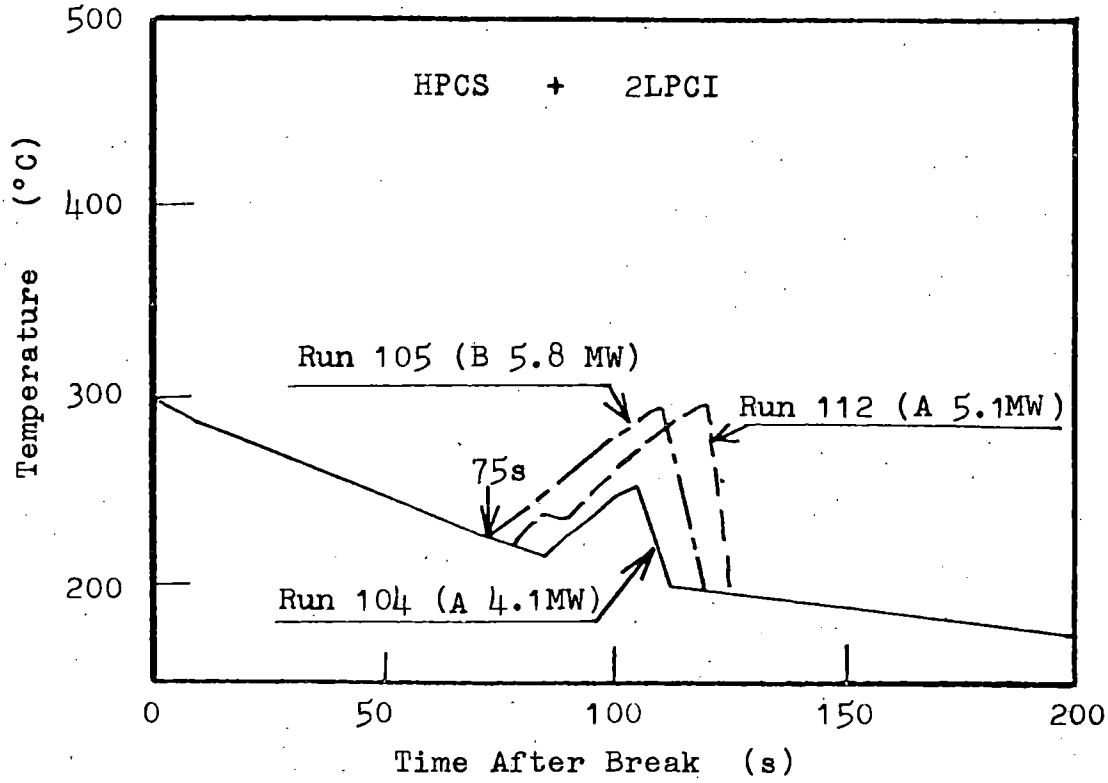

Fig 7 Effect of Bundle Power (High Power Bundle)

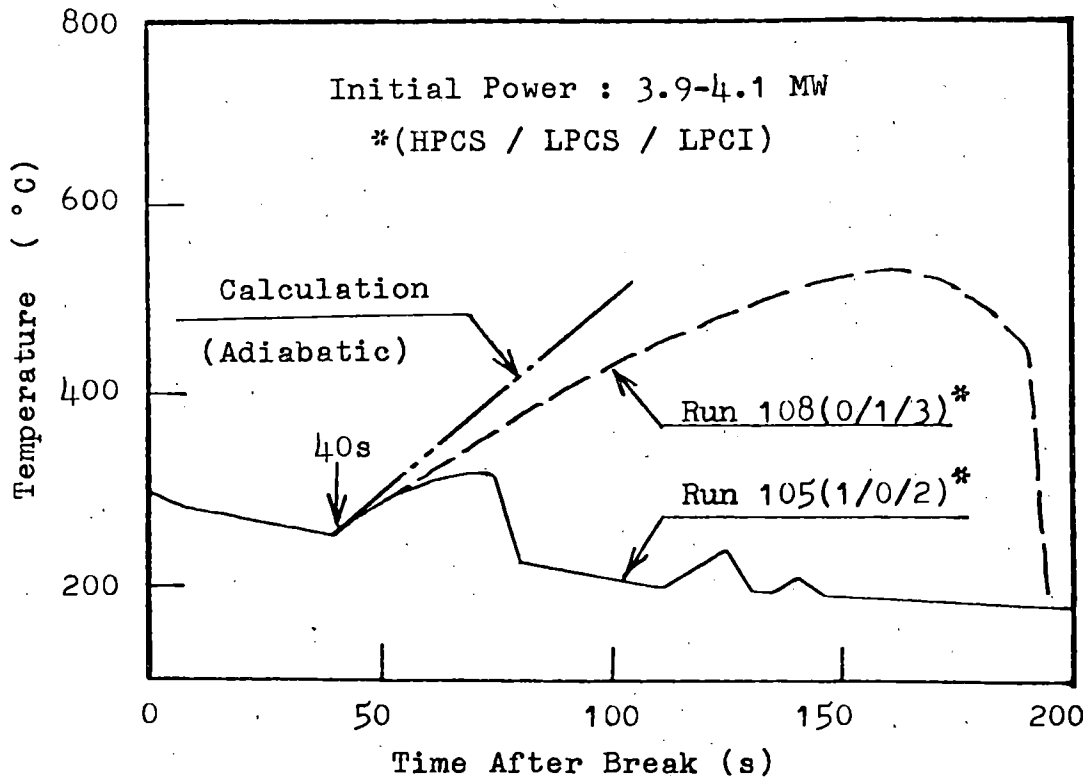

Fig 8 Cooling Effect of ECCS

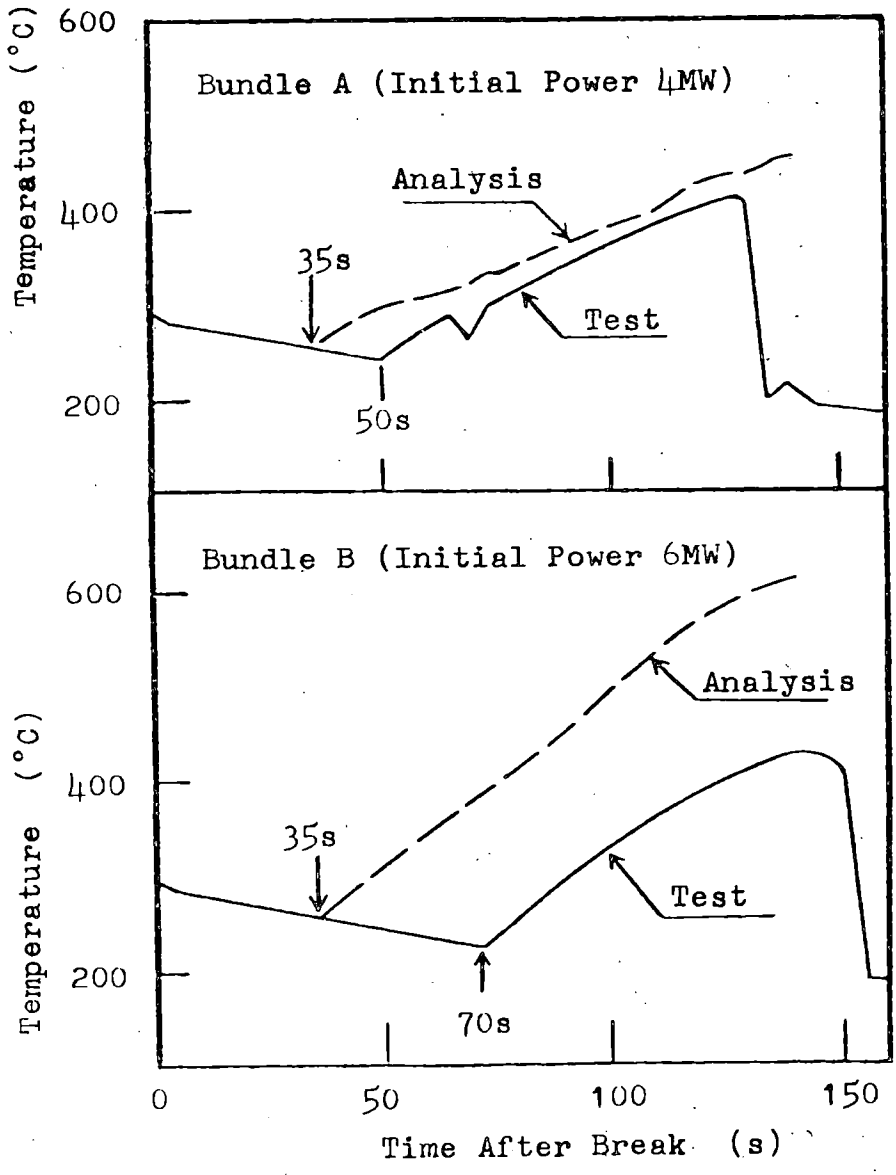

Fig 9 Comparison of Relap-5 Mod 0 Analysis with Test Result Run 107

LOBI* - INFLUENCE OF PWR PRIMARY LOOPS ON BLOWDOWN. FIRST RESULTS

W. L. Riebold, H. Städtke

Commission of the European Communities
EURATOM Joint Research Centre - Ispra Establishment
LOBI Project, Heat Transfer Division
I-21020 ISPRA/Varese (I)

Abstract

The LOBI test facility and the experimental programme are described with particular emphasis on the test facility design rationals and the programme objectives. The future small break test programme and the test facility modifications required for these tests are briefly referred to.

The present status of the LOBI project is outlined by summarizing the four test series performed so far which were concerned with large break A1-tests, with small break scoping tests, and with large break A2- and B-tests in the framework of an interim test programme; all these tests were executed with the large downcomer. The fourth series presently being performed is concerned with large break A1-tests with the small downcomer.

Analysis results are presented of the comparison between prediction and experimental data of the very first LOBI test A1-04 which was used for a special, blind post-test prediction exercise with international participation (LOBI PREX).

The present paper is an updated version of the invited paper of the same title, given at the ANS 27th Annual Meeting, June 7 - 11, 1981, Bal Harbour, Florida/USA.

Paper presented at the 9th Water Reactor Safety Research Information Meeting, October 26 - 30, 1981, Gaithersburg MD/USA.

---

* LOOP BLOWDOWN INVESTIGATIONS

1. Introduction

The general purpose of research and development programmes related to the hypothesized loss-of-coolant accident (LOCA) in light-water nuclear reactors (LWR) is to provide descriptive analysis techniques verified by experimental data, for assessing the behaviour of the primary cooling system (PCS) and the performance of the emergency core cooling system (ECCS) under LOCA conditions. In view of this general aim, in several countries all over the world separate effects and integral system effects tests are conducted in scaled models of components and of complete reactor cooling systems to provide the experimental data base required.

The LOBI programme represents a significant contribution to this research effort by supplying experimental data on simulated LWR primary cooling system response during the initial or high pressure or blowdown time period of a LOCA. These data will provide information on transient thermohydraulic phenomena involved in a LOCA, on the effects of component simulation as they relate to these phenomena, and on coupling effects with the aim to check the capabilities of analytical models to properly describe the coupling of components' response during a LOCA transient.

The LOBI test facility is designed as a scaled-down version, and is hence - due to its reduced size - a nearly one-dimensional representation of the primary cooling system of a pressurized water reactor (PWR). However, the use of a nearly one-dimensional experiment to investigate large systems' response is, on one hand, physically reasonable as far as the high pressure time period of a LOCA is concerned where acceleration forces are the prevailing driving forces for the fluid flow; it is, on the other hand, consistent with the capability of present analytical models which mostly use still a one-dimensional physical representation of the various components.

The LOBI Project is being executed in the Ispra Establishment of the EURATOM Joint Research Centre (J.R.C.) of the

Commission of the European Communities (C.E.C.) in the framework of an R&D-contract (RS-109/143-73 PIHOD) between the Bundesminister für Forschung und Technologie (BMFT), Bonn, Federal Republic of Germany, and the Commission of the E.C.. This project represents an important effort in the Reactor Safety Research Programme of both contract partners. In fact, the LOBI test facility is the only high pressure integral system test facility within the European Community, available for the experimental investigation of LWR loss-of-coolant accidents.

The experimental programme, which at present comprises a total of about 90 tests, is being executed since December 1978. A total of 21 tests have been performed so far starting with 4 shake-down tests. The LOBI large break test programme is running since December 1979. Three small break scoping tests were performed during 1980. The final LOBI small break test programme will be started after the completion of a number of test facility modifications presently scheduled for mid 1982.

Till now, the data of only a part of the tests performed have been evaluated and documented.

In the present report, the results of the very first main test, A1-04, are described in greater detail. Of all the other tests, only the main trends of the results are mentioned.

2. Project Objectives

The particular objectives of the LOBI Project may be summarized as follows:

- design, construction and operation of a large-scale 2-loop blowdown test facility for performing loss-of-coolant experiments (LOCE) by simulating pipe ruptures of different sizes and at various locations within the primary cooling system of pressurized water reactors (PWR).

- experimental investigation of the transient thermohydraulic behaviour of a simulated PWR primary cooling system (PCS) during the blowdown period of a loss-of-coolant accident (LOCA), and in particular of the influence of the individual PCS components on the course of the blowdown transient, by measuring all significant thermohydraulic quantities relevant for the core cooling.

- application of the experimental results to check and improve blowdown computer codes and associated analytical models used for the safety analysis of LWRs.

Several complementary research activities conducted in the framework of separate research contracts are aimed at providing further technical and scientific support and contributions required to ensure the achievement of the LOBI Programme objectives.

3. Research Programme

According to the LOBI R&D-contract, two experimental programmes, called A and B, comprising a total of 90 tests have been agreed upon between the BMFT-Bonn and the Commission of the E.C., see Table 1. They were preceded by the execution of a preliminary tests programme.

Four preliminary or shake-down test (SD-01 ... -04), conducted during 1979 were aimed at determining the mechanical and thermohydraulic characteristics of the LOBI test facility, to check the appropriate performance of the measurement instrumentation, data acquisition and process control system, and to check the measured results on physical consistency and reproducibility.

The Experimental Programme A defined so far consists of 60 tests in total aiming at the investigation of the influence of seven important parameters on the blowdown: (1) rupture location and size, (2) downcomer gap width, (3) pump operation conditions, (4) heating power input, (5) steam generator secondary side conditions (heat sink strength), (6) pressurizer connection (to broken or intact loop), (7) ECC water injection (location, rate).

These 60 tests are subdivided into two parts, A1 and A2, of 30 tests each / 1 /:

- part A1 tests (no. 1 - 30) are defined by the BMFT-Bonn exclusively, and the test results will be exclusively available to the BMFT-Bonn as well. The first test, A1-04, was used for a blind post-test prediction exercise (LOBI PREX) with international participation

Table 1 :

LOBI EXPERIMENTAL PROGRAMME A&B (Preliminary) :

RUPTURE LOCATION & BREAK SIZE SPECTRUM

(Comparison before - after TMI)

Number of Tests	Status	A1 (=30 Tests)				A2 (=30 Tests)				B (=30 Tests)						Total
		C.L.	H.L.	P.S.	Total	C.L.	H.L.	P.S.	Total	C.L.	H.L.	P.S.	L.PL.	S.G.	Total	
Large Breaks	March 79	8	7	2	17	13	2	2	17	5	2	3		2	12	46
	Sept. 79	8	7	2	17	13	2	2	17	5	2	3		2	12	46
Intermediate Breaks	March 79	1			1	11	1		12	5	3		1		9	22
	Sept. 79	1			1	11	1		12	7	2				9	22
Small Breaks	March 79	8	4	1	13	4	1		5	6	1				7	25
	Sept. 79	8	4	1	13	4	1		5	12	5		1		18	36
Total	March 79	17	11	3	31	28	4	2	34	16	6	3	1	2	28	93
	Sept. 79	17	11	3	31	28	4	2	34	24	9	3	1	2	39	104

Recommendation for final test matrix A2 and B :

- total of 60 tests (instead of 73)
- ~30% large break tests (instead of 40%)
- ~70% small and intermediate break tests (instead of 60%)

P.S. = pump suction

L.PL = lower plenum

S.G. = steam generator U-tube

- part A2 tests (no. 31 - 60) are again defined by the BMFT-Bonn, however taking into account suggestions from the Member Countries of the E.C.; the test results will be freely available to all Member Countries of the E.C..

The Experimental Programme B is defined jointly by all Member Countries of the E.C. and comprises 30 tests (no. 61 90); the test results will be freely available to all Member Countries of the E.C.. These tests are aiming at the investigation of the influence of the geometrical shape and the elevation of some individual components on the blowdown.

An important and integrated part of the LOBI research programme is represented by the analytical work directly connected with the execution of the experimental programme. An essential part of the test preparation consists in the execution of pre-test prediction calculations. The results of these calculations form at the same time the basis for a first and quick validation of a test. Overlay plots produced for the individual calculated and experimental parameters allow a more detailed analysis by comparison. Post-test prediction calculations required in most cases for the final analysis of a test represent at the same time an essential part of the code validation and improvement work.

For all A1-tests, those pre-test and post-test prediction calculations are performed by the LOBI project staff with RELAP4/MOD6 and in the near future with RELAP5/MOD1, and by the GRS*-Munich/FRG with the DRUFAN code.

For A2- and B-tests, also organisations of the other Member Countries of the E.C. are participating in these calculations and analysis work.

Since 1974, several parallel R&D contracts have been sponsored by the BMFT-Bonn with the aim to develop and qualify transient two-phase mass flow measurement methods and devices to be used in the LOBI experiments / 2 /; those are (1) the radionuclid tracer techniques, (2) special dragbody devices for fluid momentum measurements, (3) the temperature signal correlation techniques, (4) the nuclear magnetic resonance (NMR) techniques.

Special study contracts in support to the LOBI Project have been concluded also by the Commission of the E.C. covering

---

* GRS = Gesellschaft für Reaktorsicherheit

(1) the experimental investigation of the LOBI pump characteristics in two-phase flow conditions, (2) the calibration of the LOBI discharge nozzles under two-phase flow conditions, (3) the development of statistical analysis methods, applied to turbine flow meter, dragbody and pressure transducer signals, (4) the analytical establishment of the heat exchanger operation characteristics of the LOBI inverted U-tube steam generators under steady-state and transient, single- and two-phase flow conditions.

4. The LOBI Experimental Facility

4.1 General Description

The objectives of the LOBI Programme demand a test facility with thermohydraulic operation characteristics during the blowdown period of a LOCA which should be as close as possible reactor-typical.

The LOBI test facility is designed as an approximately 1/700 scale model of a 4-loop 1300 MWe PWR primary cooling system (PCS). It consists of two primary cooling loops connected to the reactor model. See Fig. 1. Both experimental loops are active loops each containing a circulation pump and a steam generator. One loop (intact loop) has three times the capacity (water volume and mass flow) of the other (single or broken loop), both representing so the four loops of a PWR primary cooling system. The whole test facility is designed for 160 bar and 325 °C operation pressure and temperature respectively. Tube ruptures of various sizes, ranging from double-ended large breaks to single-ended small leaks, may be simulated at three different locations within the single or broken loop (hot leg, cold leg, loop seal). Other possible rupture locations are in the lower plenum of the reactor pressure vessel model, and in steam generator U-tubes. Heat is removed from the steam generators of the primary loops by an active secondary cooling circuit containing two condensers and a cooler (simulating the heat sink represented by the turbines and condensers in the real plant), and a feedwater circulation pump. The nominal operation conditions of the secondary circuit are 54 bar and 270 °C pressure and temperature respectively, and may be extended to about 80 bar and the corresponding saturation temperature of 295 °C. See Fig. 2.

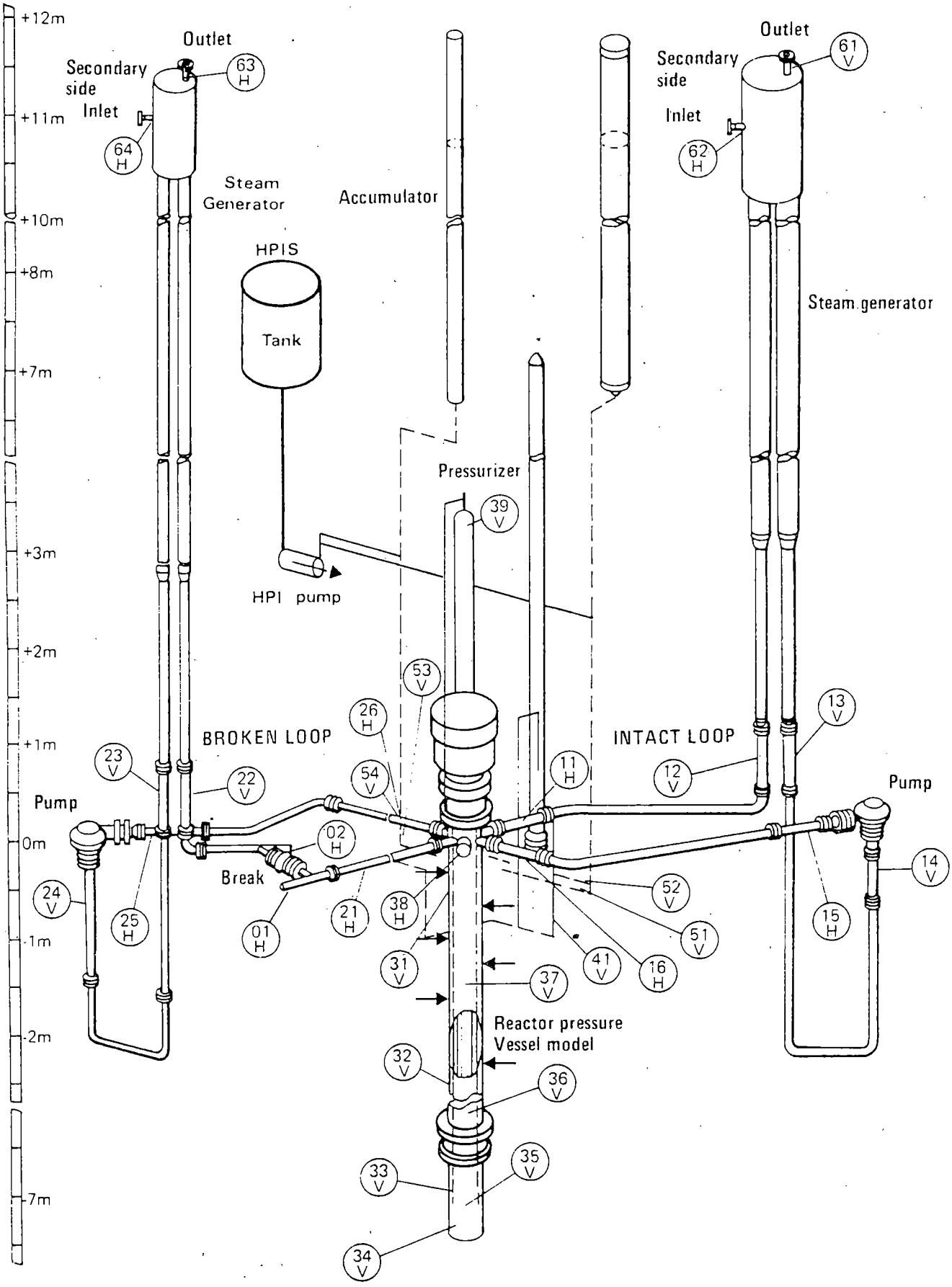

FIG. 1 : LOBI Test Facility

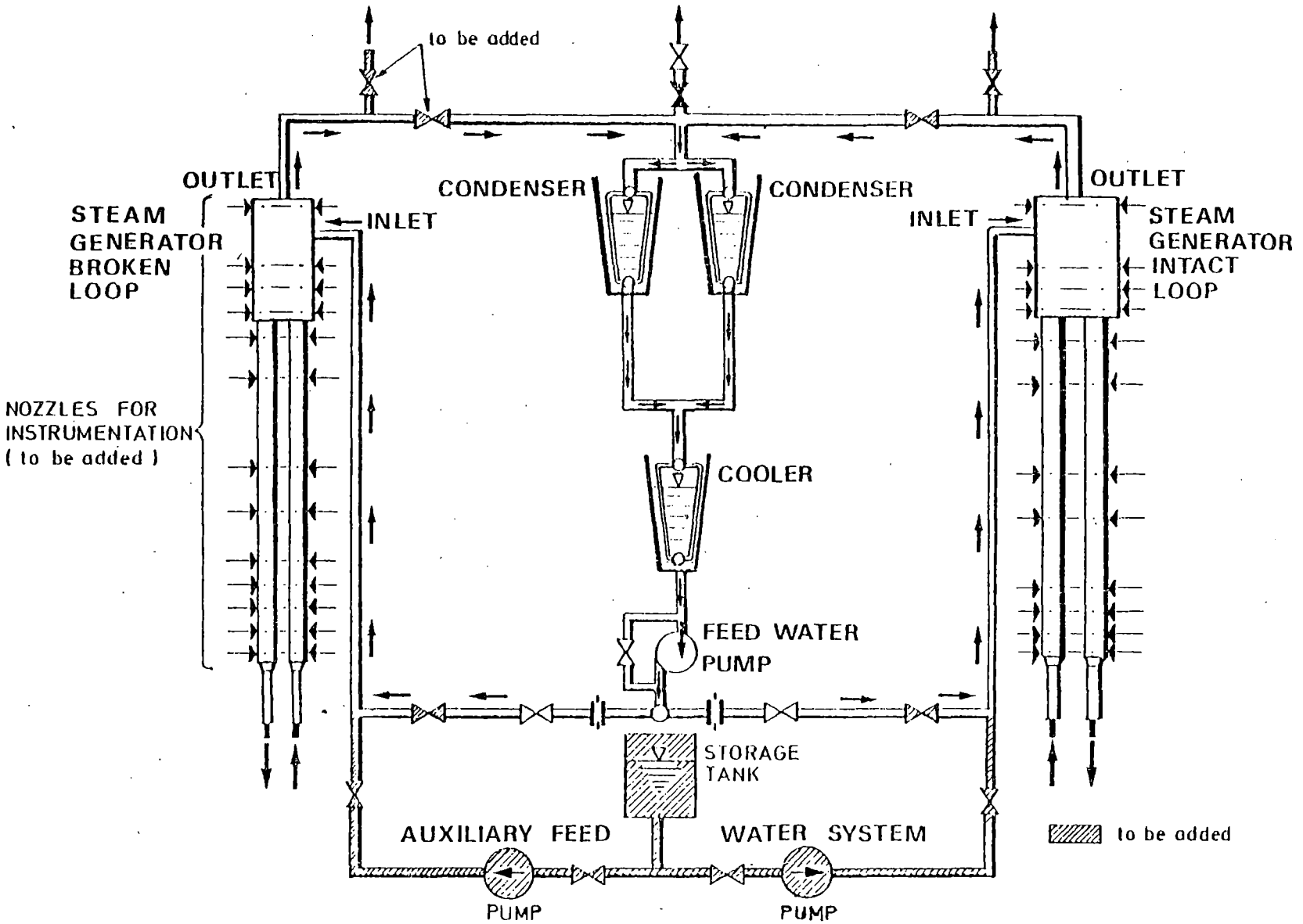

Fig. 2: LOBI Secondary Loop System

From the emergency core cooling system for the time being only the intermediate pressure (up to 60 bars) or accumulator system is represented, providing ECC water for both cold leg and combined cold and hot leg injection into both test loops.

The measurement instrumentation system installed at the test facility comprises a total of about 400 measurement channels. It allows the measurement of all relevant thermohydraulic quantities (pressure, temperature, velocity, flow momentum and fluid density) under LOCA typical transient conditions at the boundaries (inlet and outlet) of each individual loop component and within the reactor model.

The measurement signals are recorded by a specially tailored data acquisition system using three different signal scanning rates (5000, 400 and 100 Hz), PCM (pulse coded modulation) techniques and analogue magnetic tapes.

The process control system allows the simulation of both, (1) the reactor pump hydraulic behaviour by appropriate speed control of the experimental pumps, and (2) the fuel decay heat and stored heat by controlling the power input to the heater rod bundle during the blowdown transient.

4.2 Design Rationals

The design of the mechanical parts of the test facility, of the measurement instrumentation system and of the data acquisition system as they stand till now reflect clearly the simulation requirements resulting from the original objective of the experimental programme which was predominantly oriented versus large break tests.

For the lay-out of the LOBI test facility, a scaling factor of 712 has been applied to the thermal power, coolant mass flow and coolant volume of the primary cooling system of the reference plant. This led to the following values for the experimental plant:

(1) 5,3 MW electrical heating power supplied to the 64 (8 x 8) heater rod bundle of a 1 : 1 PWR design

(2) 21 kg/s and 7 kg/s coolant mass flow for the intact and broken loop respectively, resulting in 28 kg/s core mass flow

(3) 0.82 m^3 coolant volume within the primary loop system, the pressurizer included; this value holds for the not at all scaled 50 mm downcomer gap width.

The design of the experimental primary loops and the individual components was performed such that (1) the ratio of power to volume, (2) the ratio of the volumes of various components and pipework sections to each other and (3) the ratio of rupture size to PCS volume, as well as (4) the (single-phase steady-state) pressure drop and temperature distribution along the flow paths was maintained as close as possible equal to the value of the reference plant.

With respect to the pipework within each loop, the application of these criteria led to a reduced length and a relatively too large diameter. As a consequence, the steady-state single-phase coolant velocity and, hence, mass flux is by about a factor 2 reduced with regard to that in the reference plant.

The height, and relative heigths (elevation) of components are scaled 1 : 1, thus preserving gravitational heads. The heat transfer surfaces (core rod bundle, steam generators) are full length.

A thorough review of the small break experimental programme performed in the second half of 1979 after the TMI-2 reactor accident, revealed the need of several modifications of the test facility in order to make it cope at best with special requirements of small break experiments.

Those modifications are (1) the addition of a high pressure injection system (HPIS), (2) new steam generators with a still more rigorous volume and height scaling and a very intensive measurement instrumentation, (3) a new reactor pressure vessel model with an increased number of measurement nozzles, (4) the addition of an auxiliary feedwater system (AFS) to the secondary cooling circuit, (5) the replacement of several of the existing measurement devices (absolute and differential pressure transducers, turbine flow meters) by those with specification performances which are better suited for small break transients, e.g. less fast response, higher accuracy and resolution, (6) the extension of the data recording system allowing a software controlled lower scanning rate and a

much longer signal recording time (2 - 4 hours instead of 30 minutes so far).

All these modifiactions are under preparation, and their installation is scheduled to be completed at about mid 1982.

4.3 Mechanical Components

The main mechanical components of the primary LOBI loops shall be briefly described more in detail as follows:

The reactor model, Fig. 3, comprises the pressure vessel, the core barrel tube and the 64 heater rod bundle, simulating thus the internal, annular downcomer, the core and the lower and upper plenum.

A new reactor pressure vessel model will contain 11 additional nozzles within the heated length and upper plenum region for differential pressure measurements in both the bundle and the downcomer region. Besides the individual collapsed levels and the overall collapsed level, also the void fraction distribution and possibly the bubble rise velocity within the bundle region are expected to be obtained from these measurements.

Two core barrel tubes of different wall thickness are available allowing the variation of the downcomer gap width and, hence, the investigation of its effect on the course of the blowdown transient particularly on the core mass flow behaviour and on the ECC bypass.

With the present core barrel tube of 7 mm wall thickness the downcomer gap width amounts to 50 mm and is out-of-scale with respect to both the volume and the pressure drop of the downcomer. It results in a too large total volume, by about 40 %, of the primary cooling system. A second core barrel tube with 45 mm wall thickness (in a honey-comb design) leads to a 12 mm downcomer gap width which yields a nearly 1 : 1 scaled pressure drop, but a still too large downcomer volume (by about 48 %). However, the total volume of the primary cooling system is now scaled nearly exactly (less than 5 % too large).

The average channel fuel rods with an average linear power of 206 W/cm are simulated 1 : 1 with respect to outer diameter (10.75 mm) and heated length (3.9 m) by electrically

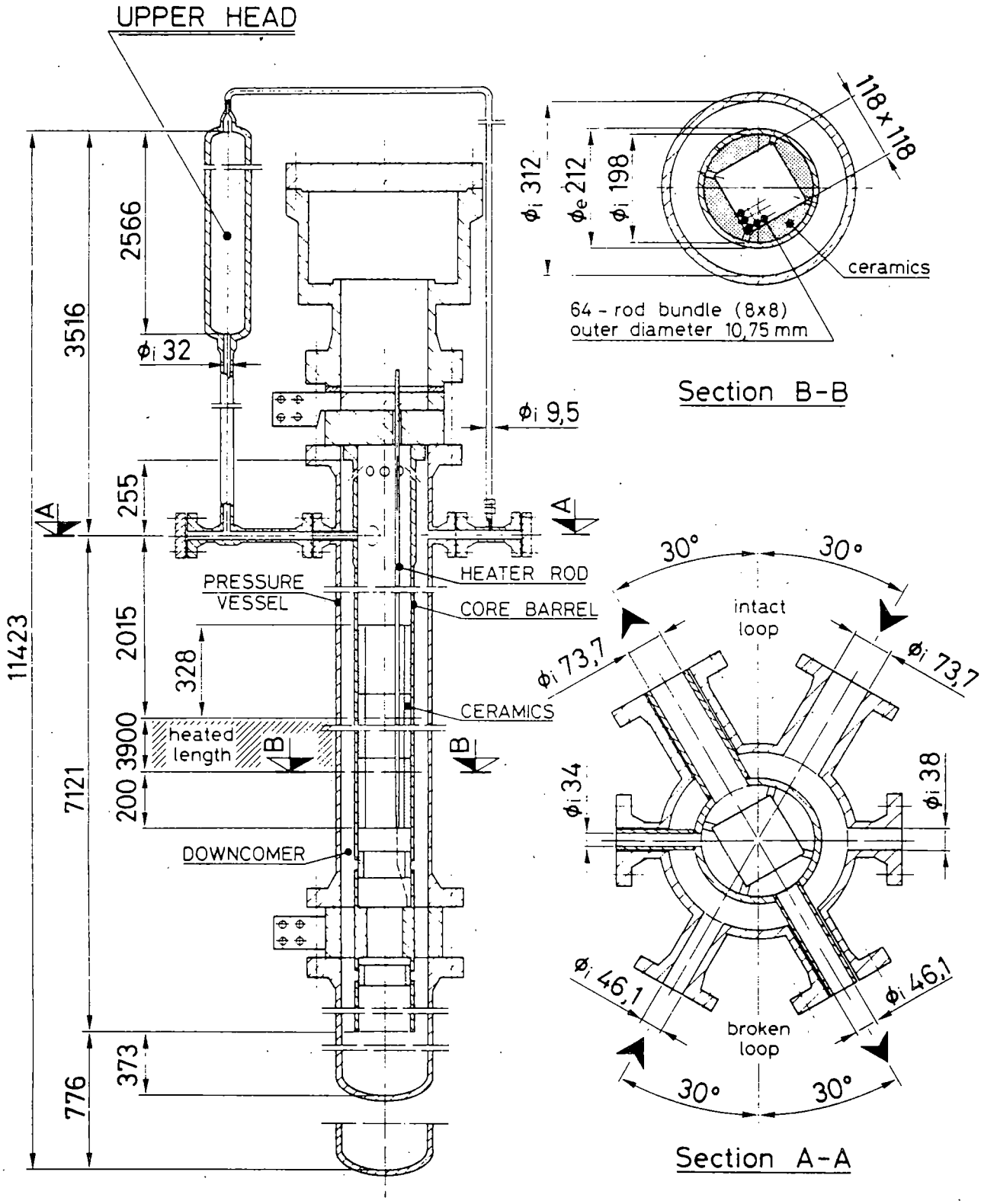

Fig. 3 : Schematic Drawing of the Reactor Pressure Vessel Model with Heated Section.

directly heated hollow tubes. The stepwise varying wall thickness yields a chopped, cosine shaped axial power distribution. Each heater rod tube is supplied with three sheathed thermocouples of 0.8 mm outer diameter, embedded into the outer surface of the tube wall at different locations such as to lead to a total of 188 surface temperature measurements at 12 different elevations within the heated length, Fig. 4.

As in the reactor core of the reference plant, grid spacers of original design are equidistantly placed over the heated length; five further spacers are arranged in the upper "unheated" part of the heater rod bundle.

The existing two U-tube steam generators are different in volume (3 : 1) and U-tube number (18 and 6) for the intact and broken loop, but equal in height. Their design is geometrically similar to that of the reference plant steam generator with an annular downcomer for the secondary water. The primary and secondary water volumes are only globally scaled, their total ratio is maintained 1 : 1.

The new steam generators will exhibit a much more detailed and rigorous (to within 6 %) volume scaling within the various regions of both the primary and secondary side, a 1 : 1 scaling of the various volume ratios within and between both sides, and a 1 : 1 scaling of all heights between the horizontal centre line of the main coolant piping and the lowest U-tube bend. The height preservation above the highest U-tube bend and within the steam dome was not considered necessary since gravitational heads are not relevant within this region. A throttle device installed in the downcomer will allow the adjustment of the internal recirculation ratio. The very intensive instrumentation with 47 and 44 measurement channels on the primary and secondary side respectively is expected to allow a local determination of fluid flow and heat transfer conditions.

The main coolant pumps for the two loops are equal in size and type. They are operated at different speeds in order to obtain the two different steady-state mass flows of 21 kg/s and 7 kg/s for the intact and broken loop respectively at the same pressure head. A specially designed drive system allows the pump speed control during the blowdown transient in both directions over the range $\pm$ 8500 rpm which corresponds to about 200 % nominal speed.

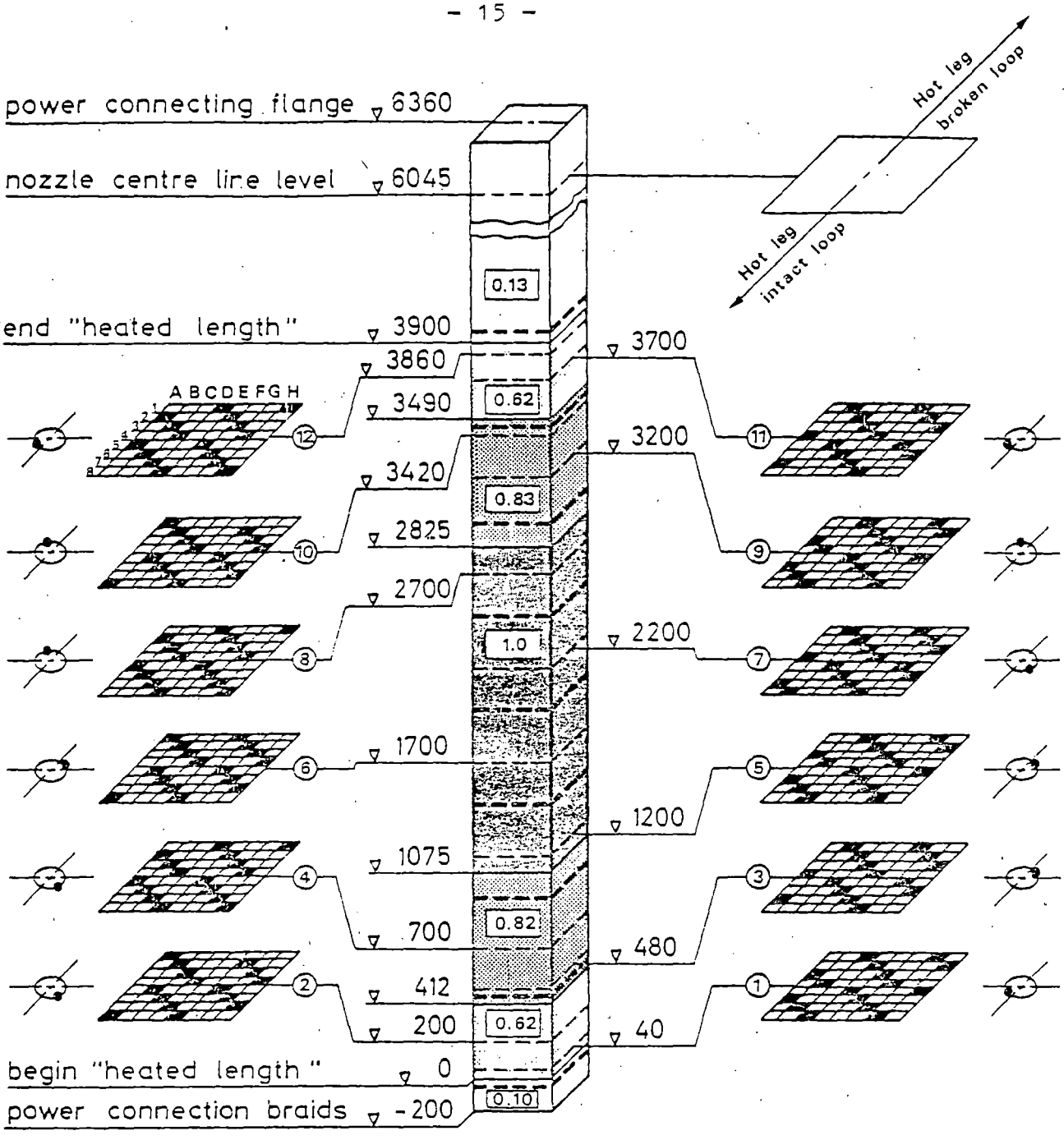

heater rod TC in use

TC - orientation in the rods at each level

① TC - Location level in the bundle (last number in TH-identifier)

0.82 relative heater power $\dot{q}/\dot{q}_{max}$

bundle spacer grids

Fig. 4 LOCATION OF HEATER ROD THERMOCOUPLES

The geometrical configuration of the main coolant pipework connecting the individual components of the PCS to each other is similar to that of the reference plant. The pipe inner diameter is 46.1 and 73.7 mm for the broken and intact loop respectively.

Special rupture devices for simulating single- and double-ended pipe ruptures are inserted in the broken loop piping at the three different rupture locations. Ruptures are simulated by quick-opening flap valves with an opening time of about 20 ms which are mounted at the straight pipe outlets of the rupture devices. These devices are situated within a concrete bunker and supported against the hydraulic reaction forces during blowdown by shock arrestors fixed at the bunker walls. The bunker is vented to the open atmosphere through two open steel pipes of 400 mm I.D..

The LOBI pressurizer is scaled down in both the total and the water volume; height and elevation are executed 1 : 1. A 20 kW heat source is installed to generate the system pressure; 5 cooling tubes placed in the vapour region form a heat sink to regulate the system pressure.

The surge line is connecting the pressurizer to either the intact loop or the broken loop hot leg pipe.

Two accumulators, one for each loop, are installed for ECC water injection, the accumulator for the intact loop having three times the volume and water capacity of that for the broken loop. Their total volume is scaled down from that of the reference plant accumulators, their height and elevation are executed 1 : 1. ECC water injection is started automatically by differential pressure controlled quick-opening ball valves as soon as the system pressure has decreased below the accumulator pressure, which may be set to preselected values ranging up to 60 bars. Injection lines are connecting each accumulator to both cold and hot leg piping of its loop for allowing both cold leg and combined cold and hot leg injection.

The high pressure injection system (HPIS) to be added to the primary cooling system as part of the emergency core cooling system will consist of a positive displacement pump with a special speed control device for an appropriate head and delivery variation, a flooding tank and

injection lines connected to the already existing ones for the accumulators. Appropriately designed and calibrated throttling devices will be installed in the injection lines to provide a 1 : 3 subdivision of the injection rate between the broken and intact loop respectively.

The secondary cooling circuit will be modified by the installation of shut-off valves in the steam lines and feedwater lines, and of pressure relief valves in the steam lines to allow the isolation and blowdown of the steam generator secondary side respectively.

The auxiliary feedwater system (AFS) to be added to the secondary cooling circuit will consist of a storage tank, two positive displacement pumps, one for each steam generator, again with special speed control devices as mentioned before, and the corresponding injection lines. See Fig. 2.

5. The LOBI Project Status

The experimental programme executed during the period from December 1979 to July 1981 may be subdivided into three parts:

(1) the six large break A1-tests with the large downcomer of 50 mm gap width

(2) the three small break scoping tests with the large downcomer

(3) the five large break interim tests of the A2- and B-programme with the large downcomer

(4) the first three large break A1-tests with the samll downcomer of 12 mm gap width

5.1 Large Break A1-tests with the Large Downcomer

All six large break A1-tests were simulating double-ended, 2 x 100 % cold leg breaks. Since they were performed with the large downcomer of 50 mm gap width and, hence, a too large primary cooling system volume, the real volume related rupture size was only 2 x 75 %.

These first tests were aiming at essentially two different objectives, (1) to establish the final nominal heating power time function which appropriately simulated both the reactor decay heat and the fuel stored heat, and (2) to investigate the effect of different ECC injection modes on the course of the blowdown transient, namely cold leg injection and combined cold and hot leg injection.

In addition, a particular objective was assigned to the very first main LOBI test, A1-04, which was chosen to be used for a special type of a "blind" standard problem calculation exercise, the LOBI pre-prediction exercise (LOBI PREX). The particular aspect of this exercise was that the transient behaviour characteristics of the LOBI test facility was completely unknown to everybody outside of the LOBI project staff and, hence, to all participants in this exercise. Therefore, the blowdown codes could not at all be adapted to the test facility before performing the test prediction ("virginity" aspect). A more detailed description of the special procedures and conditions to be followed as well as the results of this important exercise is given in chapter 8 of this paper.

The PREX test A1-04 was followed by the power ascension test series A1-01 through A1-04R:

- the tests A1-01 to A1-03 were performed with combined injection
- test A1-04R was a repetition of the PREX test and therefore performed with cold leg injection only, but with the meanwhile established nominal heating power input which amounted to a total of 10.2 full power seconds (fps).

Test A1-05 was essentially the counterpart test to A1-04R with respect to the ECC injection mode; it was again a combined cold and hot leg injection with an increased injection rate.

A summary of these six tests is given in Table 2. More detailed results of these tests, with the exception of the PREX test A1-04, cannot be reported as yet due to proprietary aspects. Exception is made, again, with respect to the effect of the by far too large downcomer gap width which led to an untypical positive core mass flow during the time period between about 10 and 40 seconds into the transient. This behaviour may significantly effect the core conditions at the end of blowdown and, hence, the ECC efficiency.

5.2 Small Break Scoping Tests with the Large Downcomer

A thorough review of the objectives of the small break test programme of March 1979 resulted in essentially two conclusions: (1) that several modifications would have to be applied to the test facility in order to make it

TABLE 2
LOBI Tests Summary, Programme A1

Test Nr / Date	Initial Conditions: Po bar	To /T °C	Mo kg/s	Po MW	Boundary Conditions: Rupture Position	Rupture Size	Core Power P = f (t)	Pump I, II	ECCS	Results/Commentary
A1-04C 12-12-79	153	330/291.	25.8	5.38	cold leg	2x1A	off at t= 1.8s 1.8 full power seconds	I:ramp to 70% in 5s II:ramp to 0 O in 3s	Accu (26 bar) intact loop cold leg	- PREX test - 2x1A double-ended, cold leg break - 1.8s full power - cold leg Accu injection
A1-01B 29-01-80	152.4	323.3 | 289 327.7	26.2	5.11	cold leg	2x1A	t≤2.6s : 100% t≤ 15s : 20% t≤ 30s : 10% t > 30s : 0 6.58 full power seconds	I:ramp to 70% in 5s II:ramp to 0 O in 2s	Accu (27 bar, 30 °C): IL:h. +c. leg BL:h.leg	- Power ascension series - 2x1A d.e. - c.l. break - combined, hot & cold leg injection - core power:3.9 full power seconds only, due to control error - B.L. Accu injection delayed - oscillations during injection period
A1-02B 14-02-80	153	322 | 290 326.5	28	5.33	cold leg	2x1A	t ≤ 3s : 100% t≤15s : 25% t≤30s : 10% t≤50s : 5% >50s : 0 8,5 f.p.s.	I:ramp to 70% in 5s II:ramp to 0 O in 2s	Accu (27 bar, 30 °C): IL:h. +c. leg BL:h.leg	- Power ascension series - 2x1A d.e. - c.l. break - combined, h. & c. leg inject. - core power:8.5 full power seconds - oscillations during injection period

TABLE 2 (continued)

Test Nr. / Date	Initial Conditions: Po bar	T_o / T_i °C	M_o kg/s	P MW	Boundary Conditions: Rupture Position	Rupture Size	Core Power P = f (t)	Pump I, II	ECCS	Results/Commentary
A1 - 03 19-03-80	153	320 / 289 325.6	28	5.22	cold leg	2x1A	t ≤3.2s : 100% ≤15s : 30% ≤20s : 15% ≤30s : 10% ≤50s : 5% >50s : 0% 9.49 full power seconds	I : ramp to 70% in 5s II : ramp to 0 in 2s	Accu (27 bar, 30 °C) : IL . h. +c. leg BL : h. leg	- Power ascension series - 2x1A d.e. - c.l. break - combined, h.&c. leg inject. - 9.04 full power seconds due to temporary power shut-off - oscillations during injection period
A1-04R 17-04-80	153	328 / 298 332	28	5.12	cold leg	2x1A	t ≤3.2s : 100% ≤15s : 36% ≤20s : 15% ≤30s : 10% ≤50s : 5% >50s : 0 10.2 full power seconds	I : ramp to 70% in 5s II : ramp to 0 in 2s	Accu (27 bar, 30 °C) : IL : c. leg BL : ·	- Power ascension series (last test) - Repeat of PREX test - 2x1A d.e. - c.l. break - only cold leg injection - 10.2 full power seconds - increased Accu injection rate due to piping modification
A1-05A 06-05-80	153	324 / 291 328	28	5.26	cold leg	2x1A	t ≤3.2s : 100% ≤15s : 36% ≤20s : 15% ≤30s : 10% ≤50s : 5% >50s : 0 10.2 full power seconds	I : ramp to 70% in 5s II : ramp to 0 in 2s	Accu (27 bar, 30 °C) : IL : h. +c. leg BL : h. leg	- 8 Accu plant ref. test - 2x1A d.e. - c.l. break - combined h.&c. leg inject. - 10.2 full power seconds - Accu injection rate into I.L. not high enough for simulating 8 Accu plant

better satisfy specific requirements from small break tests, and (2) that some small break scoping tests should be performed in advance of the main small break test programme.

The small break scoping tests proposed should be performed with the test facility as it stood and without having applied any modification.

The objective of these scoping tests was to possibly establish further specification criteria for the before mentioned modifications of both the test facility mechanical components and the measurement instrumentation system.

The three scoping tests to be executed during 1980 were all single-ended cold leg break tests with only cold leg injection from the accumulators; the break sizes were 10 %, 1 % and 0.4 %.

All tests were started from nominal initial conditions; the heating power curves were appropriately established and led to a total power input of about 16, 90 and 120 full power seconds; the pumps were run down according to an exponential speed time function with a half-value-time of about 10 s, and set to zero after about 70 and 90 seconds.

The secondary loop system was to be operated such that a depressurization was obtained with a temperature gradient of about 100 K/h.

Table 3 gives a short summary of the scoping tests.

Although only the 0.4 % break test has been evaluated so far in sufficient detail and to the extent to which it was possible with data obtained from a not typical instrumentation system / 3 /, the overall results may be considered to be quite satisfactory. They can be summarized as follows:

(1) the measurement instrumentation system has supplied much more useful data than was to be expected due

TABLE 3
LOBI Tests Summary:Small Break Scoping Tests

Test No: / Date	Initial Conditions	Boundary Conditions: Rupture Location	Rupture Size	Core Power	Pumps (intact and broken loop)	ECCS Accumulator	Remarks
SD-SL-01 04-06-80	Nominal : p = 155 bar T_i = 290 °C T_o = 323 °C M_o = 28 kg/s P_o = 5.3 MW	cold leg between RPVM and MCP	1 x 10%	3.2 - 50s: decrease to 3% > 250s:0% 16.2 fps	exponential coast-down with 9.6s half value time (hvt): t ⩾ 3.2s O for t>70s	cold leg injection into intact loop p_{ACCU}=27 bar T_{ACCU}=30 °C	- p_{PCS} < 10bar: ≈ 540s - pressurizer empty: ≈10s - Accu inject. start: ≈ 240s -p_{PCS}<p_{SCS} for t > 110s
SD-SL-02 18-06-80			1 x 1%	3.2 - 50s: decrease to 5%; < 250s:3% <3960s:2% 90.4 fps	exp. coast-d. 9.6 s hvt: t ⩾3.2s O for t>70s		-p_{PCS} < 10bar: ≈ 4000s - pressurizer empty: ≈ 25s - Accu inject. start: ≈ 2760s - p_{PCS} > p_{SCS} for all the time - $T_{F\,SCS}$ ≈100K/h
SD-SL-03 24-09-80			1 x 0.4%	20-65s: decrease to 5%; 65-265s: 3% 265-4380s: 2% 120.6 fps	exp. coast-d. 9.6s hvt: t ⩾20s O for t>87s		- p_{PCS} < 15 bar: 4800s - pressurizer empty: ≈100s - Accu inject. start: 2900s - p_{PCS} > p_{SCS} for all the time - $T_{F\,SCS}$ ≈100K/h

the inappropriate resolution power and measuring range of most of the devices installed. Therefore, the modifications envisaged are appropriate and should result in providing all essential information to be expected from small break tests

(2) the secondary loop system could be controlled such as to achieve the desired operation behaviour during small break transients. The modifications foreseen will certainly ease the required operation.

(3) the improvement of the thermal insulation especially of the broken loop piping work has revealed to be indispensable.

5.3 The Interim Tests with the Large Downcomer

After completion of the small break scoping tests, the A1-test programme could not be continued since the second core barrel tube leading to the smaller, pressure drop scaled downcomer gap width of 12 mm was not available. Therefore, an interim test programme was defined to cover the delay period until the availability of the new core barrel tube.

The 6 interim tests, all to be executed with the large 50 mm downcomer, were three A2- und three B-tests, see Table 4; in this case, the pre-test prediction calculations were performed by organisations of the Member Countries of the E.C.. Two of the defined tests were finally not executed: (1) test B-101M was different from test B-101 only by a modified pump operation mode; since pre-test prediction calculations did not show any significant difference between the results to be expected from these two experiments, test B-101M was cancelled for the time being and will possibly be performed later with the small downcomer; (2) test B-102, a hot leg break test, was cancelled since there was a potential risk for some damage to the LOBI heater rod bundle due to lifting forces caused by the strong differential pressure increase over the core region during the initial phase of such a break. These two tests have finally been substituted by test B-R1M, a single-ended 1 x 25 % cold leg break test, see Table 4.

The objectives of these interim tests are presented in Table 5. Since two tests were cancelled, two effects could not be investigated: (1) the break location and (2) the

Table 4:

LOBI Interim Test Matrix

Period : Oct. 1980 - April 1981

Test No / Date	Break Size	Break Locat.	ECCS Accu	Remarks
A2 - 59 / 27-10-80	1x100%	C.L.	cold leg inject.	- specification : LOBI - prediction : GRS - Munich - successfully run
B - 101 / 26-11-80	2x 50%	C.L.		- specification / prediction : C.E.A.- France
B - 101M * / Dec. 80/Jan.81	2x 50%	C.L.		- modified pump operat. mode - specification / prediction : C.E.A.- France
A2 - 55 / 19-01-81	1x 50%	C.L.		- specification / prediction : Univ. Pisa
A2 - 59R / 11-02-81	1x100%	C.L.		- repetition of A2 - 59 - specification / prediction : see A2 -59
B - 102 * / March/April 81	2x 50%	H.L.		- specification / prediction : Univ. Pisa
B - R1M / 17-03-81	1x 25%	C.L.		- specification / prediction : GRS - Munich

* Cancelled and replaced by B - R1M

Table 5:

LOBI Interim Test Programme Objectives

Effect	Tests	Break		Remarks
		Size	Location	
- Reproducibility	A2 - 59 A2 - 59R	1x100%	C.L.	- reliability
- Break Geometry	A2 - 59 B - 101	1x100% 2x 50%	C.L.	- harmonization of A - and B - matrix
- Break Size	A2 - 55 A2 - 59 B - R1M	1x 50% 1x100% 1x 25%	C.L.	- importance of 1x50% break size for B- matrix - smallest large break test
- Break Location	B - 101 B - 102 *	2x 50%	C.L. H.L.	- reference tests of B - matrix
- Pump Operation mode	B - 101 B - 101M *	2x 50%	C.L.	- simulation of different pump characteristics - harmonization of A - and B - matrix

* Cancelled and replaced by B - R1M

pump operation mode; therefore, only three effects remained to be investigated: (1) reproducibility, (2) break geometry and (3) break size.

With respect to the influence of break size in cold leg break conditions and with only cold leg ECC injection, the large break spectrum is now covered by tests ranging from single-ended 1 x 25 % as the smallest large break, through 1 x 50 % and 1 x 100 % breaks up to the double-ended 2 x 75 % breaks (referred to the ratio of break area to PCS volume). This spectrum will be completed during the future experimental programme by double-ended 2 x 100 % break tests (referred to both ratios the break area to PCS volume and the break area to main coolant pipe cross section area in the reference plant).

The experimental data of all interim tests have not yet been evaluated.

5.4 Large Break A1-Tests with the Small Downcomer

After the installation of a new core barrel tube leading to the small downcomer of 12 mm gap width, the large break A1-tests programme has been continued in May 1981. This programme comprises about 12 tests and will be completed by April 1982.

So far, three double-ended 2 x 100 % cold leg break tests have been performed, see Table 6: one test (A1-66) with cold leg ECC injection, one test (A1-07) with no ECC injection at all, and one test (A1-06) with combined cold and hot leg injection. The results of these tests are still under evaluation; a first analysis has shown a more reactor-typical thermohydraulic core behaviour during the blowdown period than in case of previous tests with the 50 mm downcomer gap width.

6. Future Programme

The test facility modifications required for the small break test programme will be performed during summer time 1982.

The start of the small break test programme is presently scheduled for October 1982 after completion of the before mentioned modifications and several shake-down tests to be performed with the partially new test facility.

The small break A1-test programme will comprise about 15 tests and is expected to be terminated during the first half of 1984.

The A2-test programme and the B-test programme will be executed thereafter.

TABLE 6:
LOBI Tests Summary: Programme A1, small downcomer

Test n° / Date	Initial Conditions (*) Po bar	To/Ti °C	Mo kg/s	Po MW	Boundary Conditions: Rupture Position	Rupture Size	Core Power P= f (t)	Pump I, II	ECCS	Results/Commentary
A1-66 03-07-81	155	323/290	28	5,28	cold leg	2x1A	t ≤ 2,5s: 100% t ≤ 8,5s: 33% t ≤ 10 s: 24% t ≤ 12 s: 16% t ≤ 16 s: 10% t ≤ 20 s: 5% t ≤ 30 s: 4% t > 30 s: 0% 6,16 full power seconds	I: ramp to 70% in 5s II: ramp to 0% in 2s	Accu (27 bar, 30 °C): IL: cold leg BL: no	— 2x1A, double-ended — cold leg break — cold leg ECC injection only — core temperature level for t > 10 s higher than with 50 mm downcomer; no core quenching except in uppermost core region
A1-07 09-07-81	155	323/290	28	5,28	cold leg	2x1A	same as A1-66	same as A1-66	no	— 2x1A d.e. — c.l. break — no ECC injection — core temperature behaviour for t < 30 s: similar to A1-66 t > 30 s: more gradual temperature decrease than observed in A1-66
A1-06 21-07-81	155	323/290	28	5,28	cold leg	2x1A	same as A1-66	same as A1-66	Accu (27 bar, 30 °C) IL: hot and cold leg BL: hot leg	— 2x1A d.e. — c.l. break — combined, cold and hot leg ECC injection — core temperature behaviour for t < 30 s similar to A1-66; between 30 and 70 s complete core quenching occurred

(*) Specified values

7. LOBI Test A1-04

7.1 Test Conditions

The test A1-04 was the first test in a power ascension test series, where the electrical power input to the heater rod bundle was successively increased. The test was a simulation of a large double-ended offset-shear break in the cold leg pipe between the pump and the pressure vessel of a PWR. The used break nozzles were designed to simulate full size (100 %) breaks of a reactor coolant pipe in case of a completely volume scaled test facility. However, due to the large not volume scaled downcomer in the present design of the LOBI facility, the break area-to-primary-volume-ratio of this test was equivalent to a 2 x 75 % break for the reactor.

The main objective of test A1-04 was to study the DNB behaviour of the LOBI heater rod bundle under large break LOCA conditions. The electrical power input to the bundle was kept constant over 1.8 s into the transient to ensure that critical heat flux conditions occurred at least in the high-powered middle section of the heater rods. After 1.8 s the power was set to zero and kept at zero for the remainder of the transient.

The initial conditions prior to the blowdown transient were close to the specified nominal values, see Table 2.

The blowdown was initiated by the unlocking of the two CISE quick-opening flap valves. The complete opening of the valves was measured to occur within 15 ms. The opening of the pump side flap valve was delayed by 55 ms. An unexpected behaviour was measured for the break isolation valve. This ball valve started closing 200 ms too early. By the time the vessel side flap began to open the closure angle of the isolation valve was already 65°. The valve remained at this partially closed position for 1.1 s and afterwards closed completely within 15 ms. Code calculations have shown that the non-synchronization of the two break valves, and of the isolation valve between the two break branches has only a minor effect on the subsequent blowdown transient.

Both, the intact and broken loop pumps were controlled using specified speed-time curves. The pump speed of the intact loop pump was reduced to 70 % of the initial value within 5 s and the pump speed of the broken loop pump was reduced to zero within 2 s after initiation of the blowdown.

The feedwater mass flows to the secondary sides of the steam generators were reduced to zero within 25 s as specified prior to the test. The steam outlets of the steam generators were kept open during the whole transient. The resulting pressure in the steam lines is determined by the characteristics of the secondary system.

The LOBI model containment was connected to the atmosphere. Therefore, the containment pressure did not greatly exceed the atmospheric pressure.

7.2 Test Results

A complete documentation of test A1-04 including the initial and boundary condiditions, the actual instrumentation and all the measured quantities with error bands are given in the Quick Look Report / 4 / and in the Experimental Data Report / 5 /. In the following only some of the measured parameters are selected to characterize the system behaviour of test A1-04. These measured parameters are shown in Fig. 5 to Fig. 19 together with the corresponding calculated values from pre-test and post-test predictions which were performed in Ispra using the RELAP4/MOD6 computer code. A detailed description of the test predictions including a complete RELAP4 input listing is given in a pre-test prediction / 6 / and in a post-test analysis report / 7 /.

After initiation of the blowdown the system pressure falls very rapidly within 50 ms to the saturation pressure corresponding to the fluid temperature in the hot leg pipes as shown for the intact loop hot leg in Fig. 5. The start of the evaporation of the fluid in the hot leg pipes, upper plenum and core region results in a more moderate depressurization of the primary system. Between 2.5 s and 3.0 s the system pressure has reached the saturation pressure corresponding to the fluid temperature in the cold leg pipes, downcomer and lower plenum. The evaporation of the fluid begins now also in the 'cooler' parts of the system which leads again to a decrease of the depressurization rate.

The behaviour of the system pressure is mainly governed by the two break mass flows, which are shown in Fig. 6 and 7. During most of the blowdown transient critical flow conditions exist at the throat of the discharge nozzles, which means that the break mass flows are determined only by the upstream flow conditions given by the stagnation pressure and degree of subcooling or by the stagnation pressure and the vapor quality.

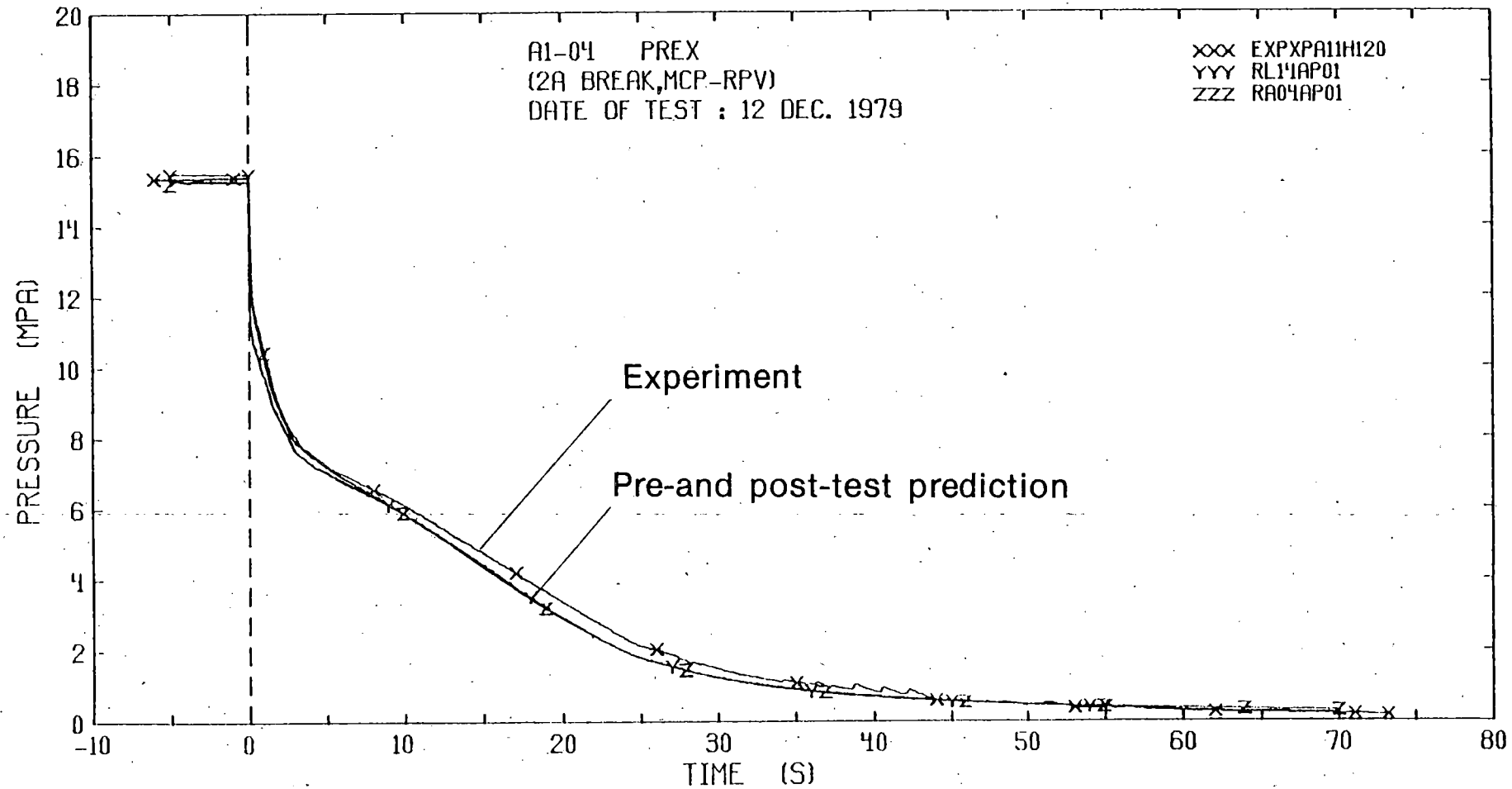

FIGURE 5: PRESSURE IN INTACT LOOP HOT LEG, VESSEL OUTLET

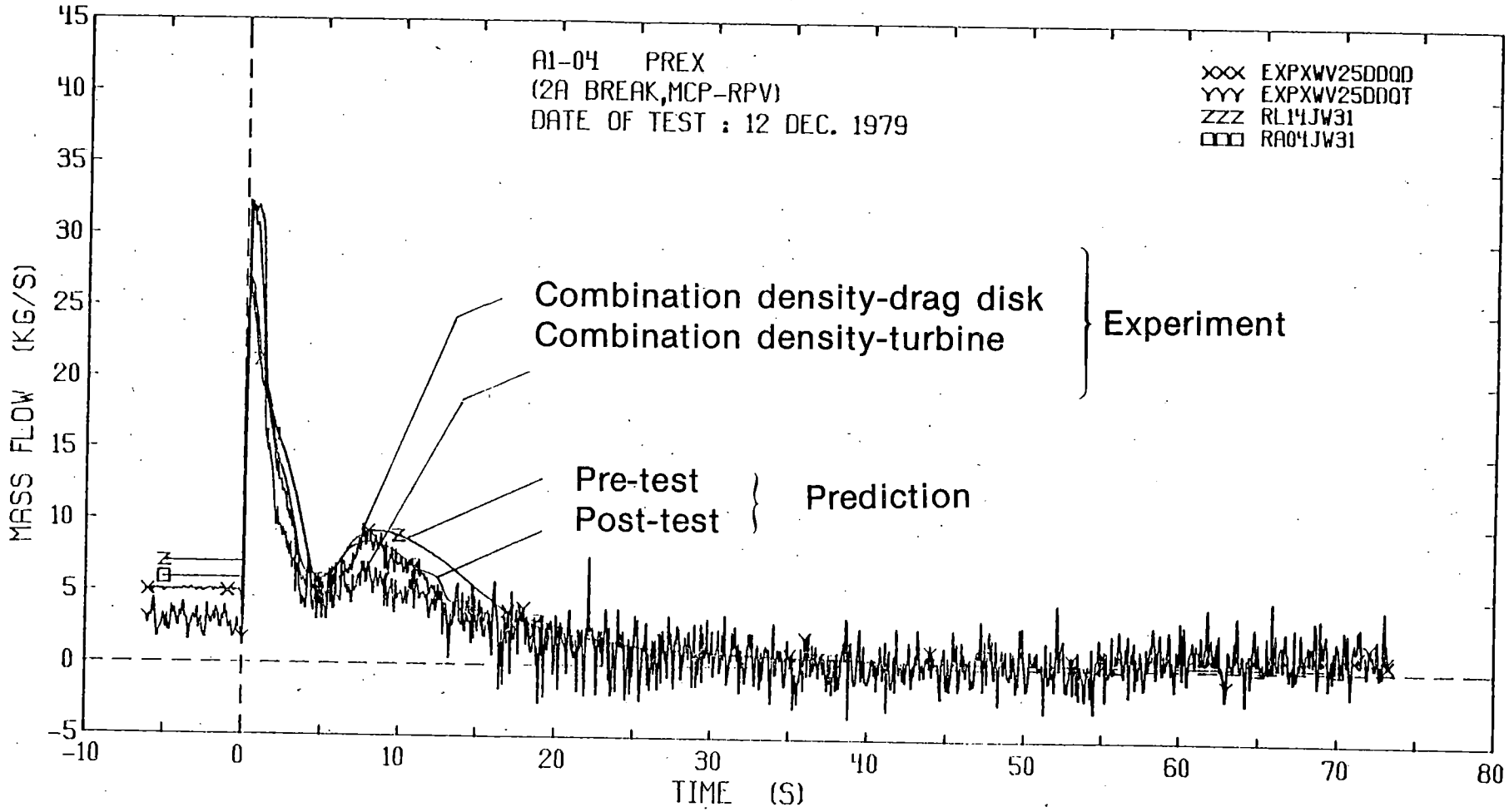

FIGURE 6 : MASS FLOW IN BROKEN LOOP COLD LEG, PUMP OUTLET NEAR PUMP SIDE BREAK

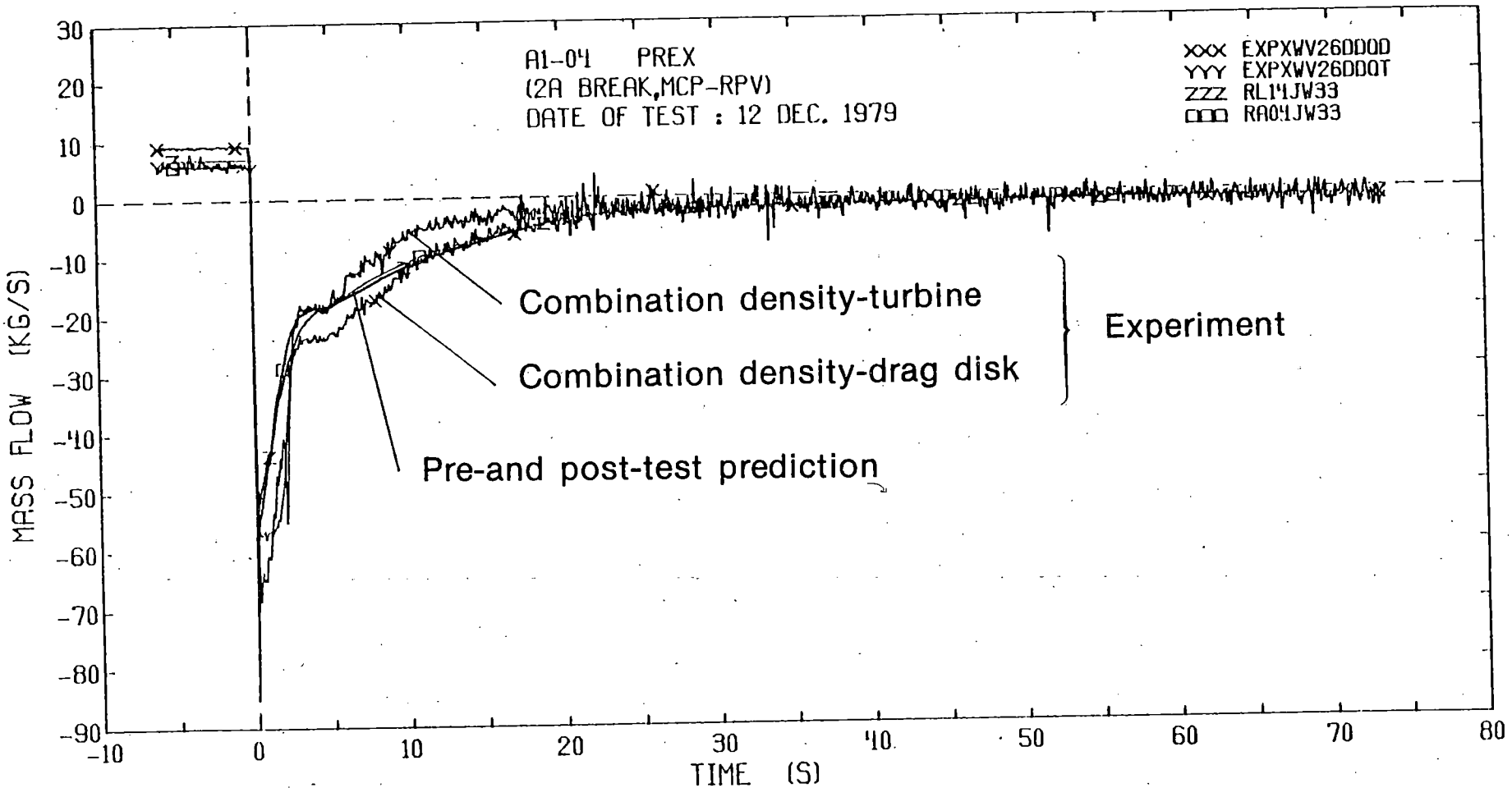

FIGURE 7 : MASS FLOW IN BROKEN LOOP COLD LEG, VESSEL INLET NEAR VESSEL SIDE BREAK

Due to the relatively large flow resistance of the pump, pipe and steam generator upstream of the pump side break, the pump side break mass flow is limited to values below 30 kg/s. To the vessel side break, however, subcooled water is supplied directly from the large downcomer region which leads to prolonged subcooled conditions upstream of the vessel side break. As a consequence large break mass flows occurred during the first 2 s of the transient for the vessel side break with values up to 70 kg/s.

The unbalance of the two break mass flows leads to a reversal of the core mass flow within the first period of the blowdown transient, when the evaporation process is restricted to the hot leg pipes, upper plenum an core region. This is indicated by the negative values for the differential pressure over the 'heated length' of the core region during this time period as shown in Fig. 8. After the evaporation has started in the downcomer region a positive core mass flow is re-established again as shown by the relatively large positive differential pressure values over the core between 3 s and 10 s. The relatively large positive core mass flow, which remains up to the end of the blowdown has been found as a typical system behaviour for the present design of the LOBI test facility with the large not volume scaled downcomer. Planned tests with a reduced downcomer gap width from 50.0 mm to 12.0 mm will give more information on the influence of the downcomer volume and gap width.

After the local pressure has fallen to the saturation pressure the fluid temperatures follow closely the saturation temperature as shown for axample for the fluid in the broken loop hot leg in Fig. 9.

The relatively low differential pressure for the intact loop steam generator in Fig. 10 indicates low flow velocities and some stagnation conditions for the intact loop during the blowdown transient. This explains the occurrence of inhomogeneous two-phase flow conditions as shown in Fig. 11 by the differences between the density signals from diametral and peripheral beam of the γ-densitometer in the intact loop pump suction pipe.

Large positive flow velocities exist in the broken loop during the whole blowdown transient as shown by the differential pressure values for the broken loop steam generator, Fig. 12. Therefore, homogeneous flow conditions exist

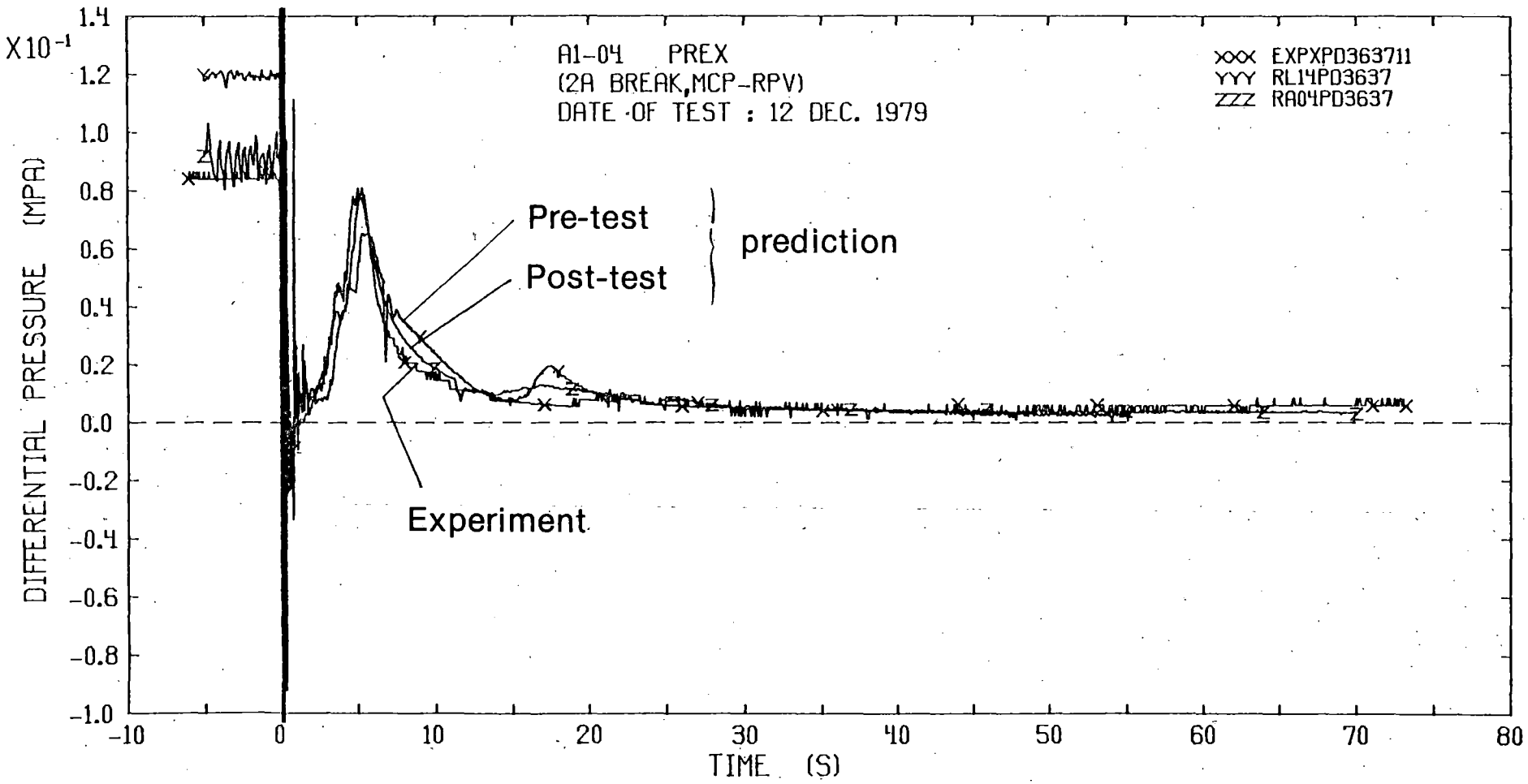

FIGURE 8 : DIFFERENTIAL PRESSURE OVER CORE

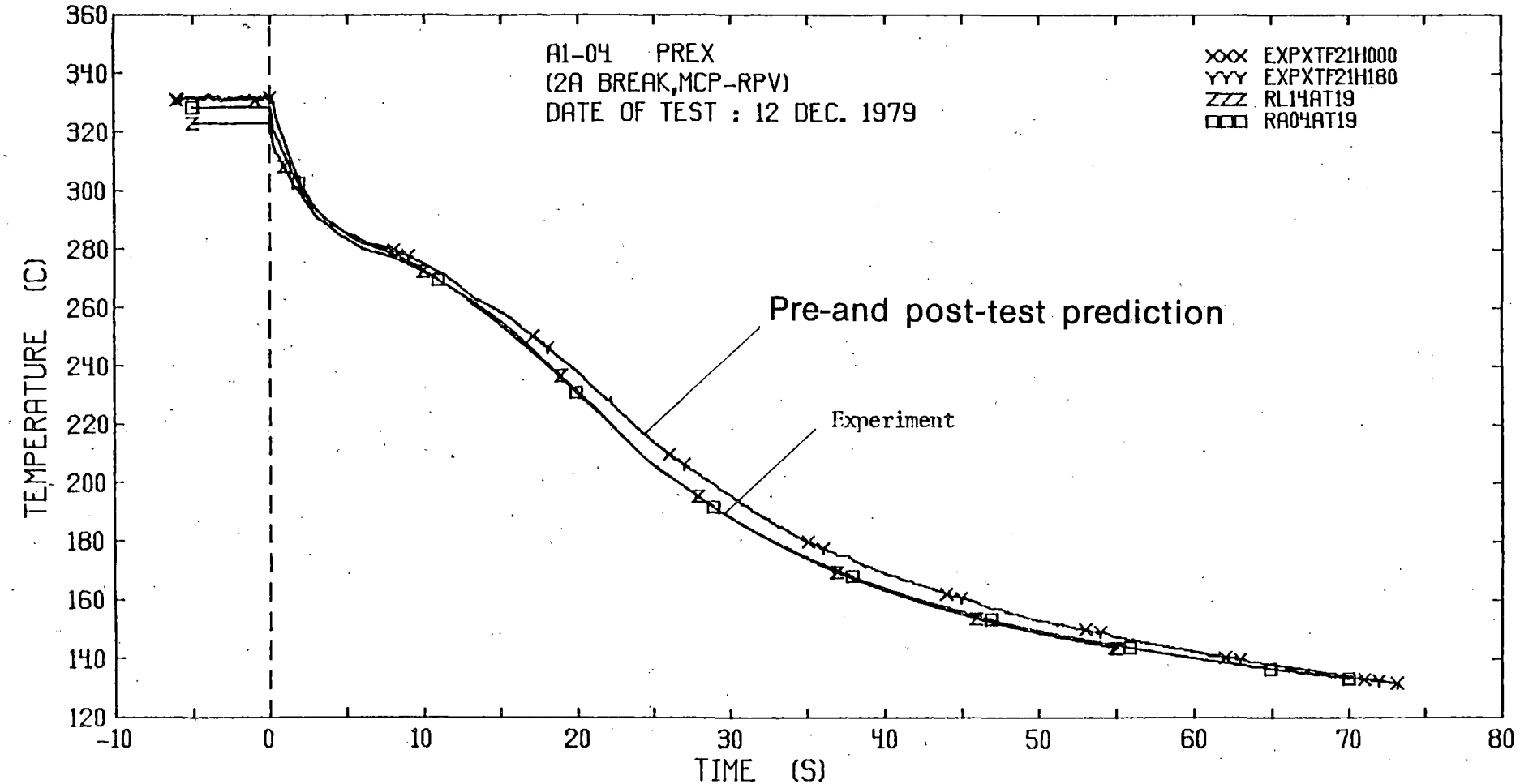

FIGURE 9 : FLUID TEMPERATURE IN BROKEN LOOP HOT LEG, VESSEL OUTLET

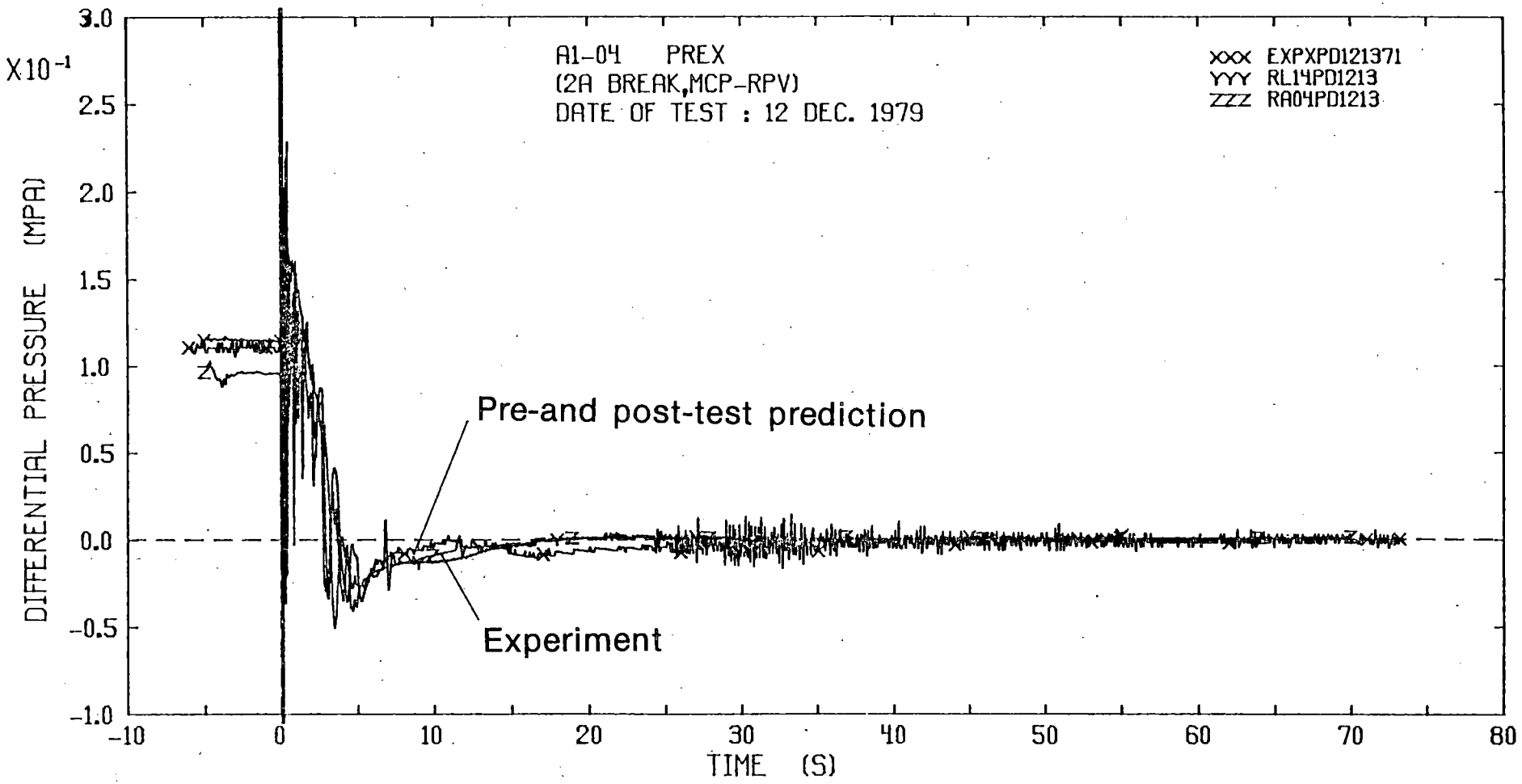

FIGURE 10 : DIFFERENTIAL PRESSURE OVER INTACT LOOP STEAM GENERATOR

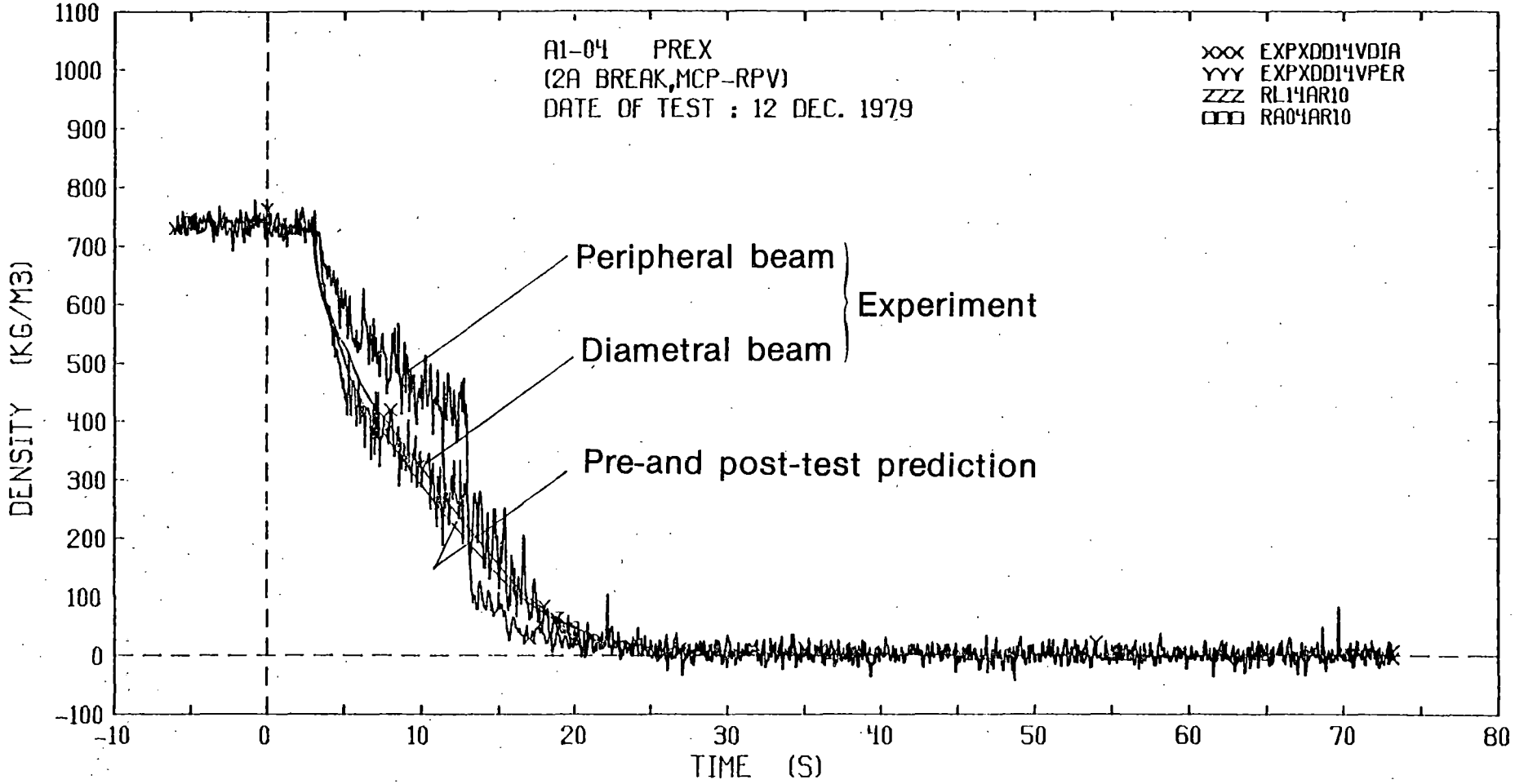

FIGURE 11 : FLUID DENSITY IN INTACT LOOP SUCTION LEG, PUMP INLET

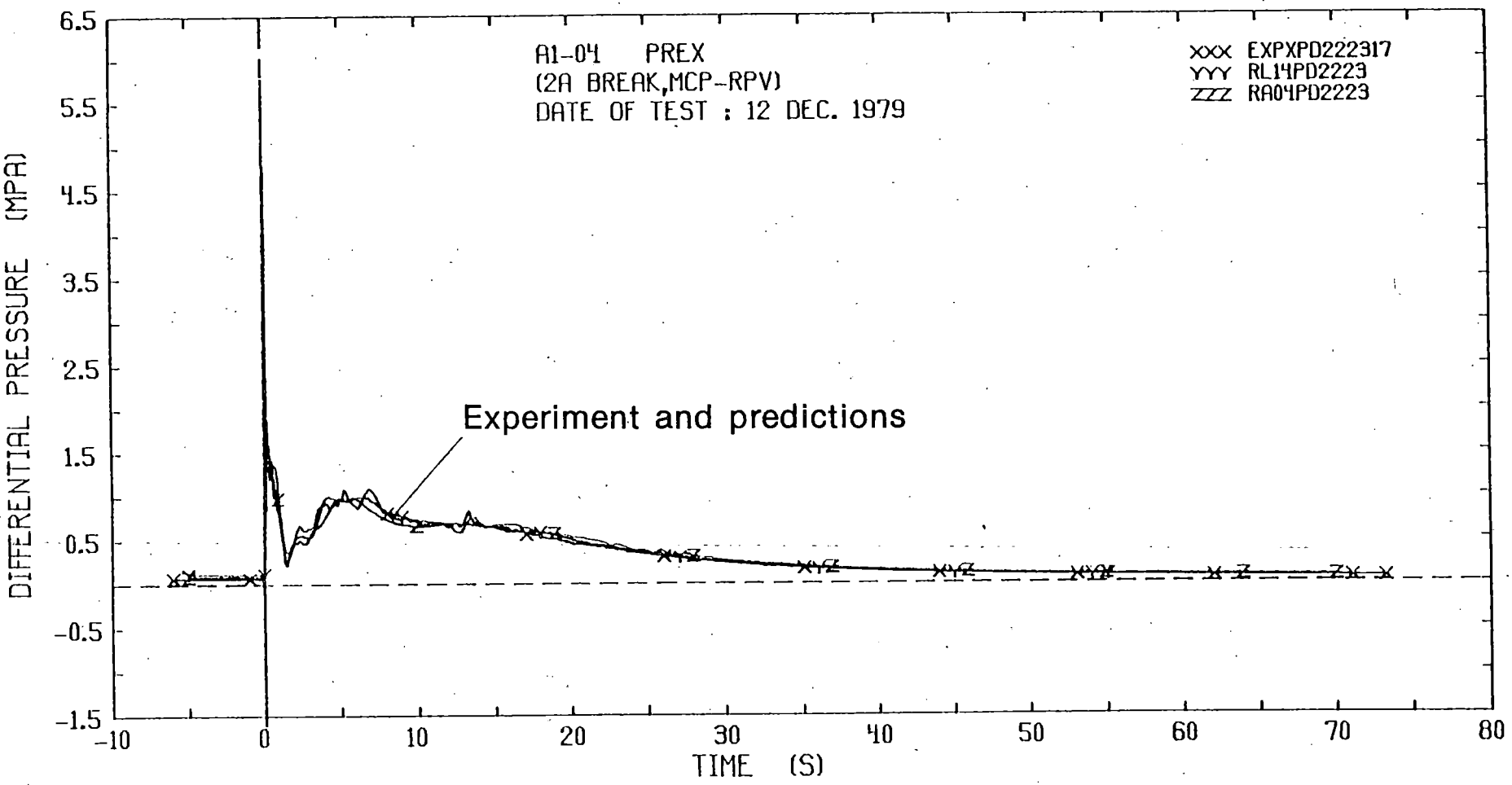

FIGURE 12 : DIFFERENTIAL PRESSURE OVER BROKEN LOOP STEAM GENERATOR

in the broken loop as indicated by the equal density signals from the two beams of the γ-densitometer in the broken loop hot leg pipe in Fig. 13. The increased fluid density in the broken loop between 5 s and 10 s corresponds with the large positive differential pressure over the core and with the increased mass flow upstream of the pump side break. This behaviour is related to the evaporation in the downcomer region which drives fluid with relatively high density from the lower part of the downcomer through the core, upper plenum and broken loop towards the pump side break.

The injection of ECC water from the intact loop accumulator was initiated when the pressure in the intact loop cold leg had fallen below the accumulator activation pressure of 2.7 MPa. This occurred at 22.5 s after blowdown initiation as shown in Fig. 14. About 2 s after the injection has started the cold leg pipe between the injection point and the pressure vessel is completely filled with subcooled water as indicated by the steep increase of the fluid density during this time period in Fig. 15. That most of the injected ECC water is discharged through the vessel side break during the blowdown period (ECC bypass) can be concluded from the relatively constant fluid density in the lower plenum as shown in Fig. 16.

Arithmetic mean values of measured heater temperatures (excluding the thermocouple signals from the outer, peripheral bundle zone) are shown for three different measurement elevations in Fig. 17 to 19. A DNB (critical heat flux at low or intermediate vapor quality) was measured for the whole 'heated length' of the bundle between 0.9 s and 1.1 s after blowdown initiation. The maximum heater rod temperature of 420 °C was measured for the high powered middle section of the bundle at 1.8 s, when the power input to the bundle was reduced to zero. Both, the shut-down of the power and the improved cooling conditions beginning at 3.0 s with the flashing in the downcomer region, caused the early rewetting of the rods between 3 s and 5 s. A dry-out (second critical heat flux at high quality) was measured to occur only for the upper part of the bundle in the later blowdown period between 35 s and 40 s.

A comparison of the measured and calculated parameters in Fig. 5 to 19 indicate that the general system behaviour was well predicted by the RELAP4/MOD6 computer code. However, the good agreement between the experiment and the

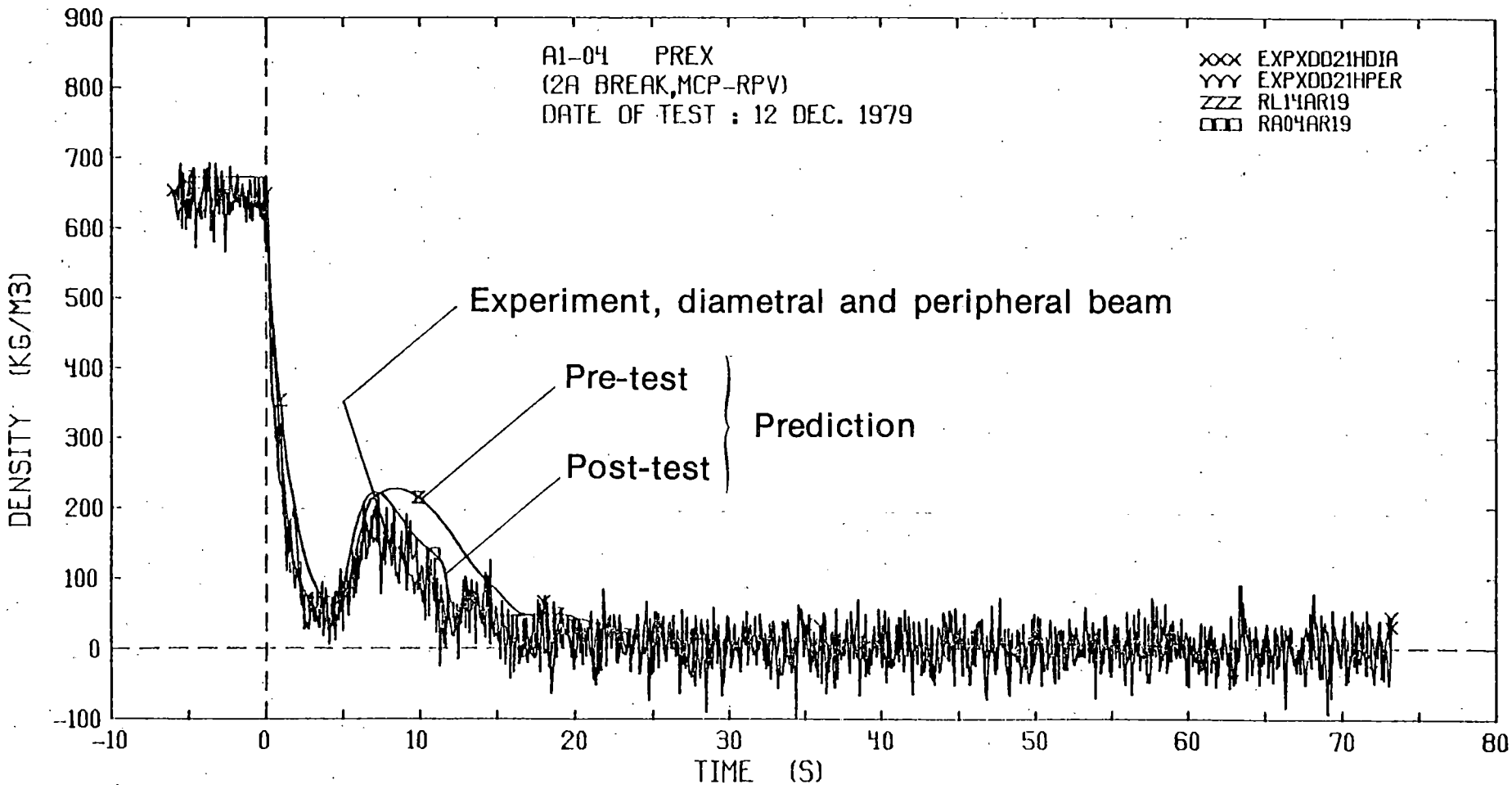

FIGURE 13 : FLUID DENSITY IN BROKEN LOOP HOT LEG, VESSEL OUTLET

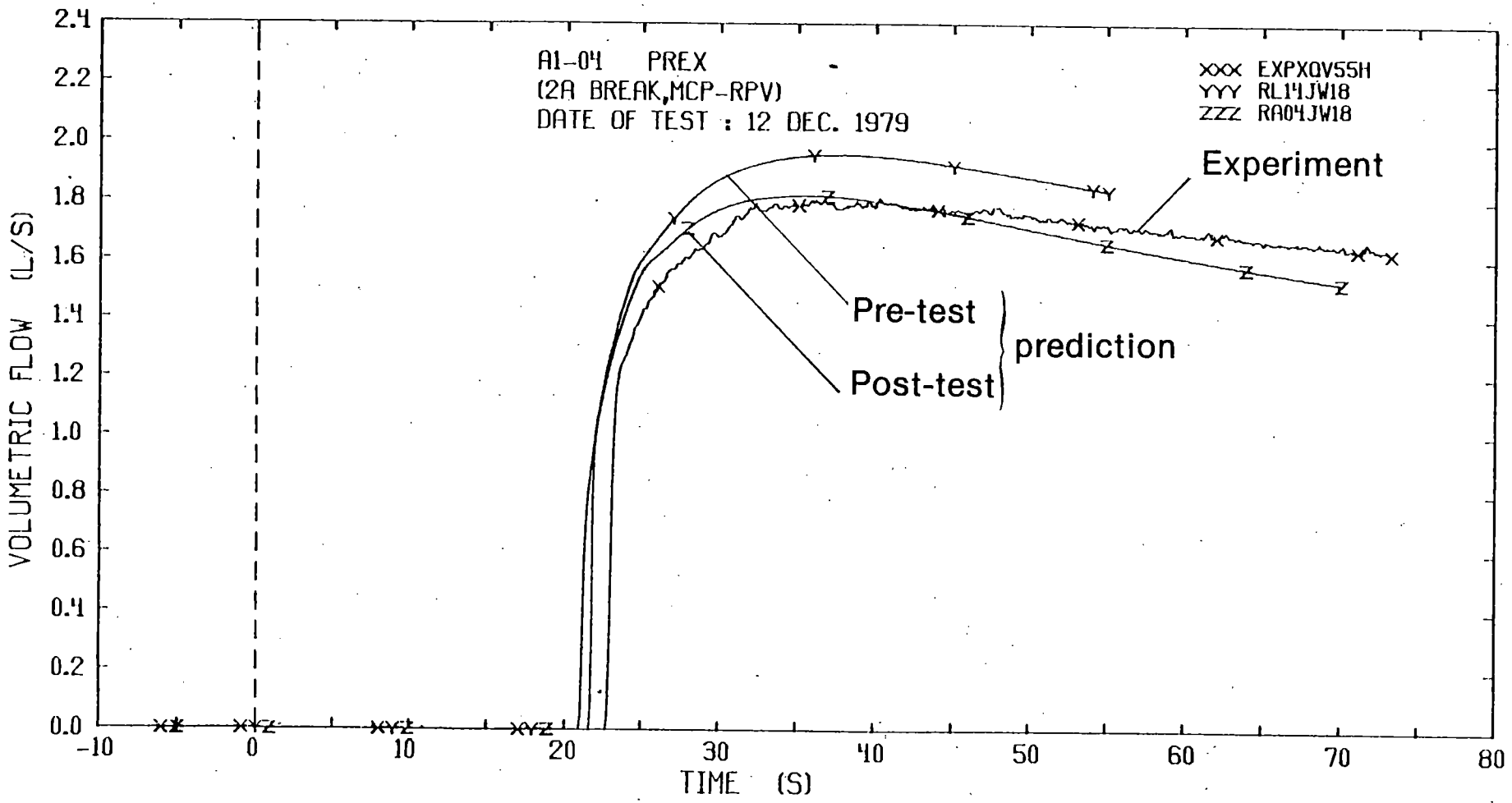

FIGURE 14 : VOLUMETRIC FLOW FROM ACCUMULATOR

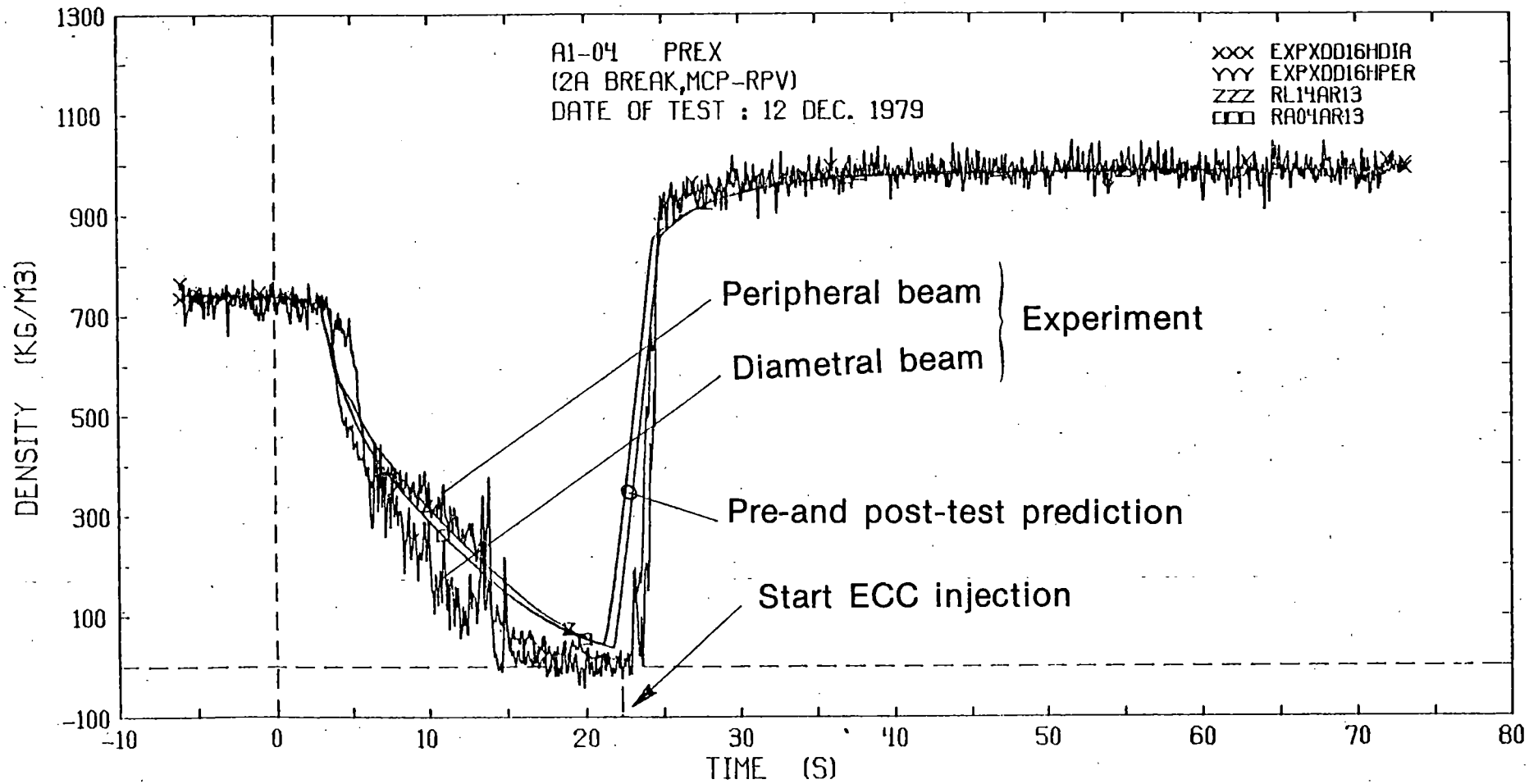

FIGURE 15 : FLUID DENSITY IN INTACT LOOP COLD LEG, VESSEL INLET NEAR ECC INJECTION POINT

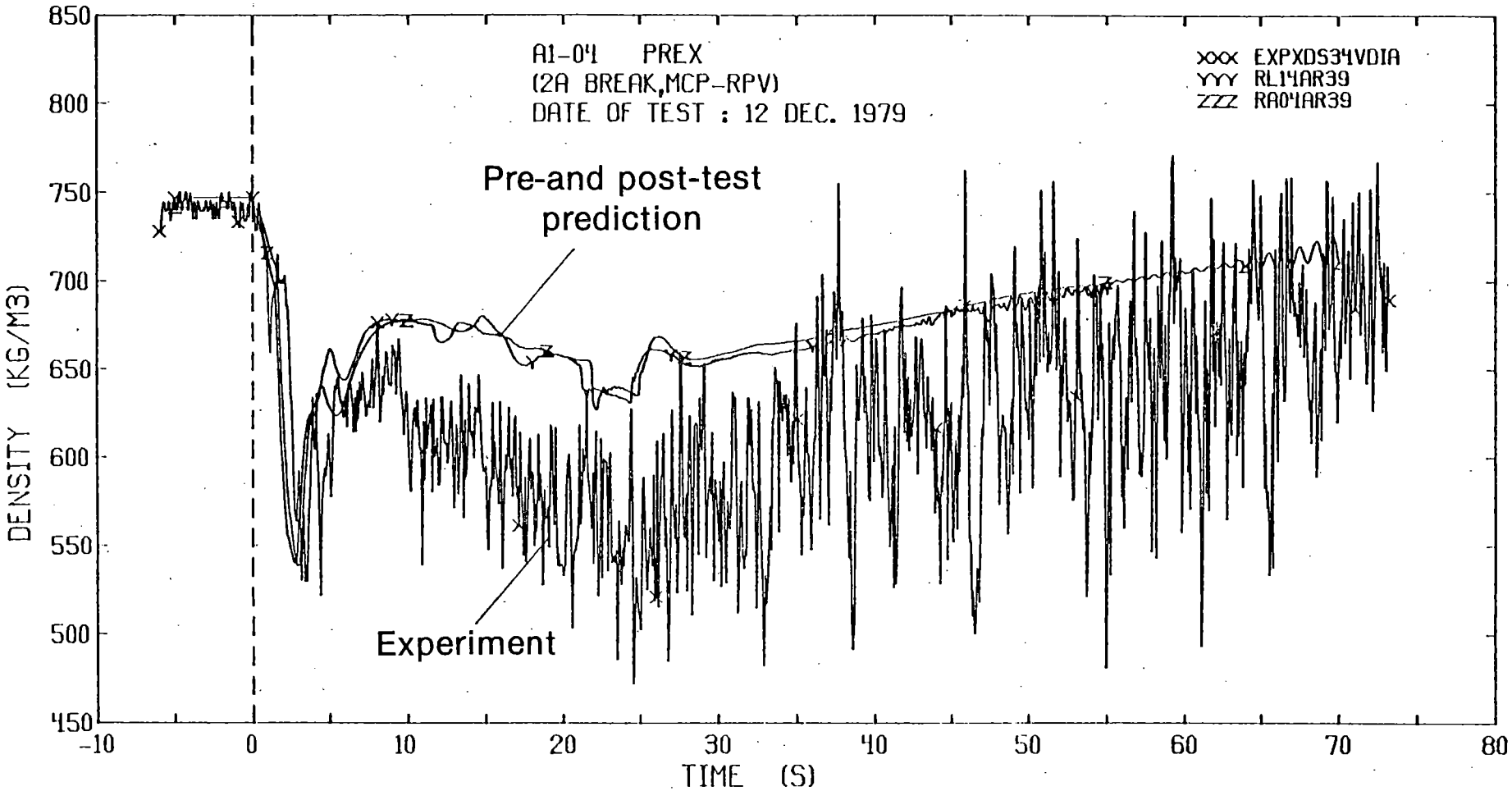

FIGURE 16 : FLUID DENSITY IN LOWER PLENUM

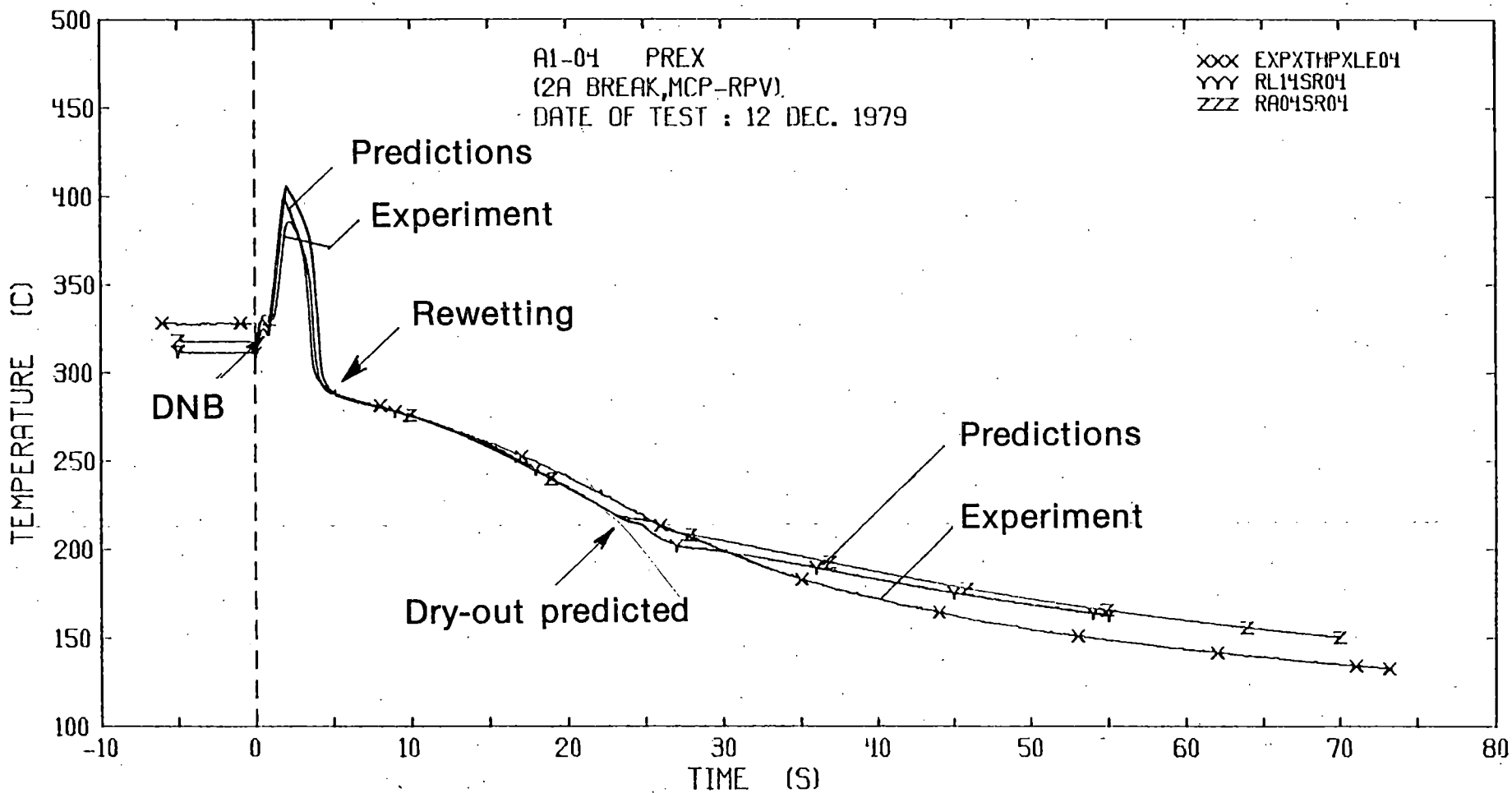

FIGURE 17 : HEATER ROD TEMPERATURE, LEVEL 4

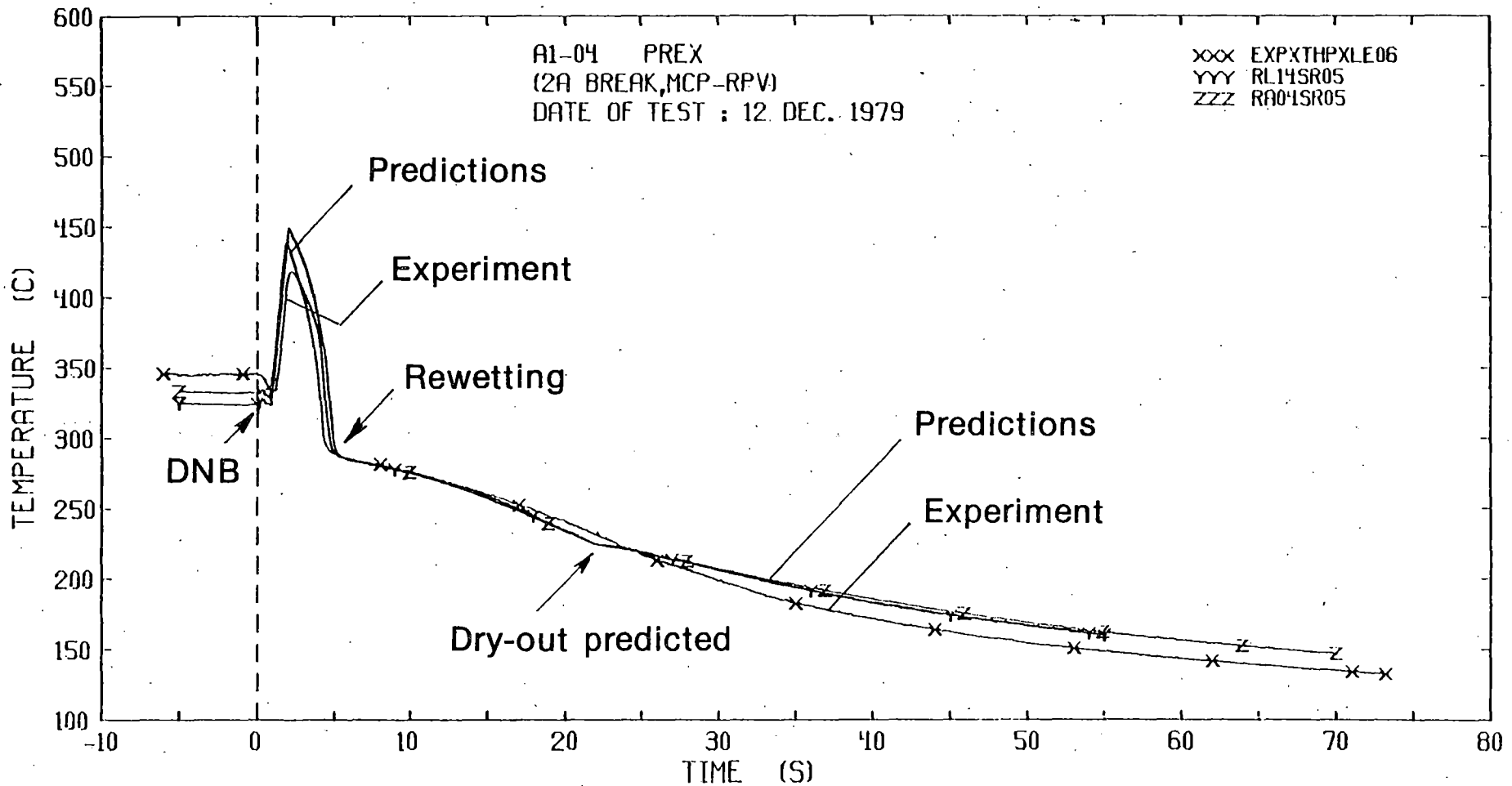

FIGURE 18 : HEATER ROD TEMPERATURE, LEVEL 6

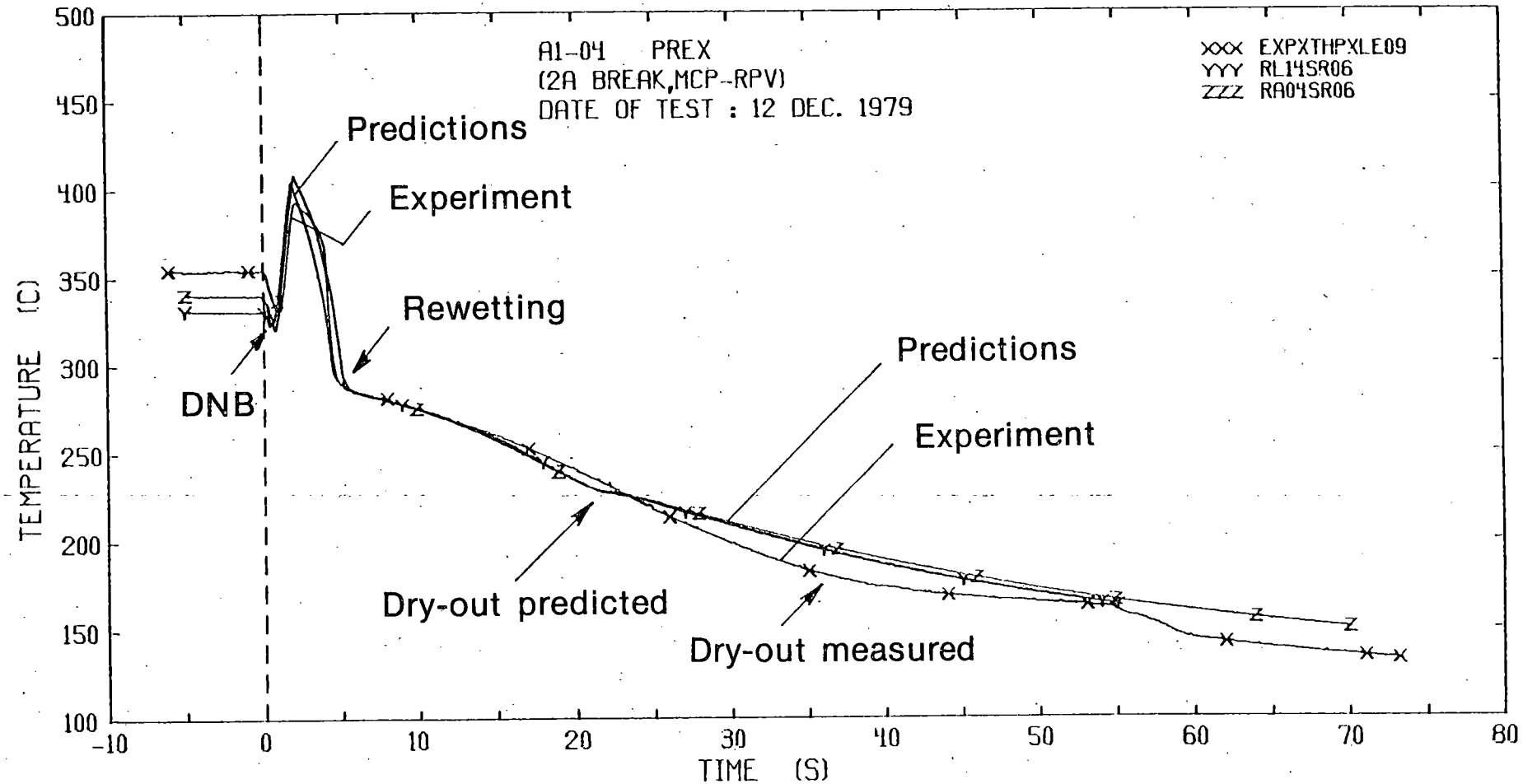

FIGURE 19 : HEATER ROD TEMPERATURE, LEVEL 9

prediction is related to the simplified boundary conditions for the first LOBI test. Larger discrepancies between measured and calculated data have been found in the following LOBI test programme for tests with increased power input to the heater rod bundle, for tests with larger ECC injection rates and for tests with combined hot and cold leg ECC injection.

8. LOBI Pre-Prediction Exercise (PREX)

8.1 PREX Procedure

The special features of the PREX test A1-04 are already described in chapter 7. The initial and boundary conditions are listed in Table 2.

After the PREX test A1-04 had been performed in December 1979, only the measured initial and boundary conditions were communicated to the participants of this prediction exercise. In the following time period all further information of the test results were locked up until the last mailing date for the predicted results on May 2, 1980.

After the predicted results had been received at Ispra, overlay plots were produced by the LOBI analysis group with the predicted results of each participant and the measured data / 8 /, and with the predicted results of all participants and the measured data / 9 /. These documents were sent to all participants before the second and final PREX Workshop was held in Ispra in January 1981. During this workshop, the comparisions of the predicted and measured data were presented and the discrepancies were discussed in detail.

8.2 PREX Participants

Sixteen different organisations participated in the prediction calculation. The results from two participants were sent to Ispra much later than the final mailing date. Their results are not included in the overlay plots showing all predicted data together with the measurements. The predicted results from one participant show very strong non-physical oscillations. Also this prediction was not presented in the overlay plots. A complete list of the participants and the codes used is given in Table 7.

Table 7: List of PREX Participants

Participant	Code	LOBI Data Base Descriptor
GKSS, Forschungszentrum Geesthacht G.m.b.H., Geesthacht, Germany	RELAP3	GKSS
IKE, Institut für Kern-energetik und Energie-systeme, Stuttgart, Germany	RELAP4/Mod5	IKE
Nuclear Installation Inspectorate, London, United Kingdom	RELAP4/Mod5	NII
TÜV-Rheinland Köln, Germany	RELAP4/Mod5	TRHL**
Rheinisch-Westfälischer TÜV, Essen, Germany	RELAP4/Mod5	TRW
Université Catholique de Louvain Louvain, Belgique	RELAP4/Mod5	USLB*
Babcock-Brown-Boveri Reaktorbau m.b.H., Mannheim, Germany	RELAP4/Mod6	BBR
C.E.A., Centre d'Etudes Nucléaires, Fontenay-aux-Roses, France	RELAP4/Mod6	CEA
EG&G Idaho Inc., Idaho National Engineering Laboratory, Idaho Falls, USA	RELAP4/Mod6	INEL
TÜV-Baden, Mannheim, Germany	RELAP4/Mod6	TBAD
TÜV-Hannover, Hannover, Germany	RELAP4/Mod6	THAN
United Kingdom Atomic Energy Authority, Culcheth, United Kindgom	RELAPUK	UKEA*
TÜV-Bayern, München, Germany	LECKMOD	TBAY

Table 7 (cont'd)

Participant	Code	LOBI Data Base Descriptor
Los Alamos Scientific Laboratory, Los Alamos, USA	TRAC-P1A	LASL
Risø National Laboratory, Roskilde, Denmark	TRAC-P1A	RISO
GRS, Gesellschaft für Reaktorsicherheit m.b.H., Garching, Germany	DRUFAN01/Mod2	GRSM

* not included in the overlay-plots due to delayed mailing of predicted results

** not included in the overlay-plots due to strong oscillations in the predicted results

8.3 General Trends of the Predicted Results

Although the transient characteristics of the LOBI test facility were completely unknown, the challenge for the prediction exercise participants was fairly reduced due to the above mentioned simplified conditions for this first LOBI blowdown test. However, the predicted results from the 16 PREX participants show a widespread band of data with partially large deviations from the measured values.

The behaviour of the primary system is mainly characterized by the system pressure. Most of the predictions indicate a too fast pressure drop as shown for the pressure in the lower plenum in Fig. 20. A first group of predicted results start to deviate from the measured values at about 3 s into the transient. This is caused by an overprediction of the break mass flow during this time period as shown for the vessel side break in Fig. 21. Different reasons might have contributed to the incorrect prediction of the break mass flow including errors in the specification of the break geometry, the selection of the critical flow model for subcooled and low quality conditions in the RELAP4 code, and in case of the TRAC and DRUFAN code the use of not verified equations for interfacial exchange processes for the flow in the break nozzle with the large pressure gradient.

A second group of predicted results begins to deviate from the measured data at about 12 s after blowdown initiation. All the predictions in this group are based on homogeneous flow assumptions and, therefore, do not predict the phase separation process in the large downcomer region. The neglection of the phase separation in the downcomer leads to an overprediction of the fluid density in the broken loop cold leg upstream of the vessel side break. This results in too large break mass flows and, as a consequence, in an increased depressurization of the system.

A third time period where the predicted pressure values begin to deviate from the measured data, exists between 20 and 25 s. This seems to be related to the start of the injection of subcooled water from the accumulator into the primary coolant loop. The assumption of thermal equilibrium leads to an overprediction of the condensation rate which results in an unrealistically high pressure drop.

In the later blowdown period only two participants have predicted pressure values close to the measured data. Both predictions were performed with the RELAP4/MOD6 code using

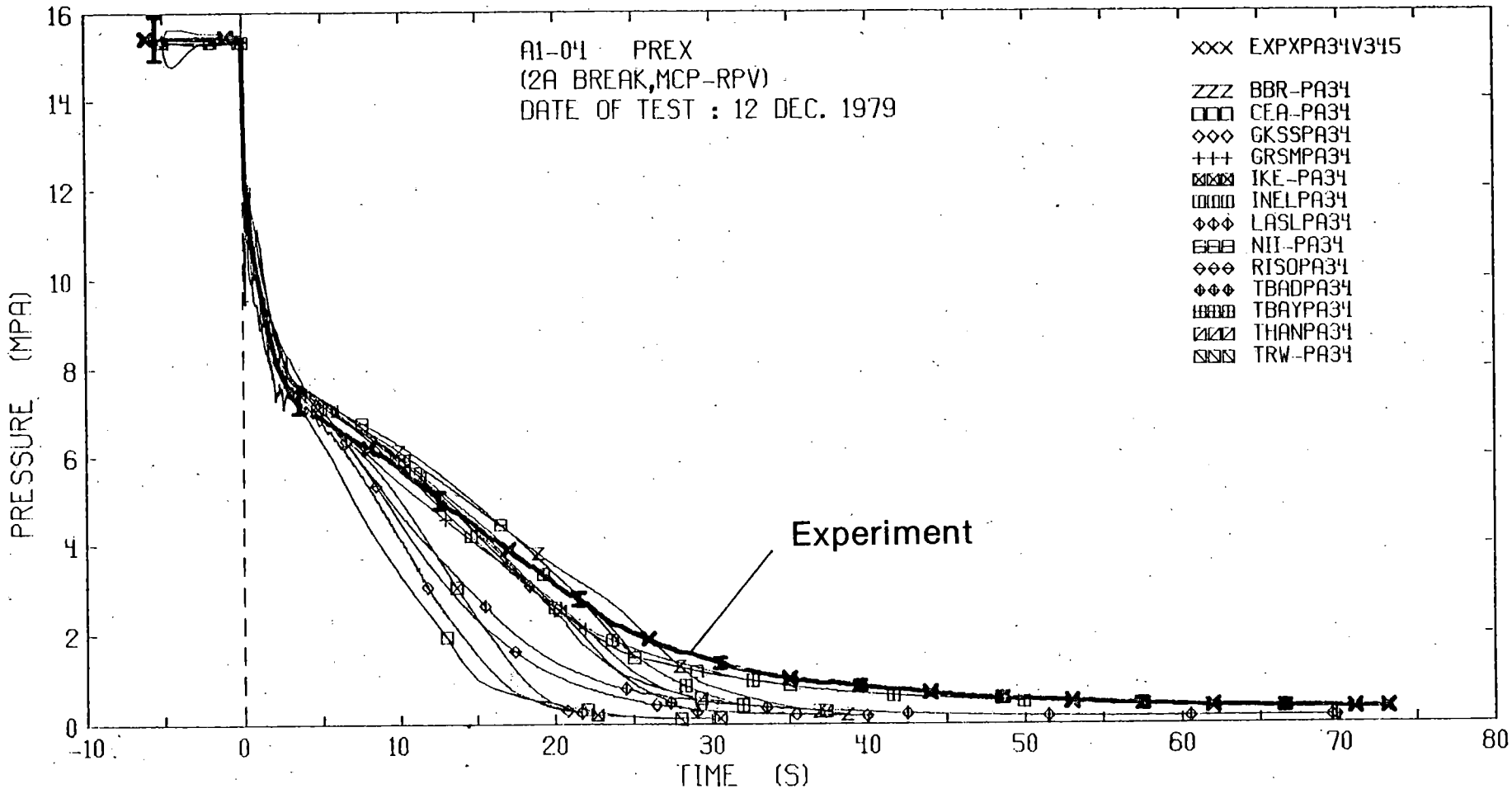

FIGURE 20 : PRESSURE IN LOWER PLENUM

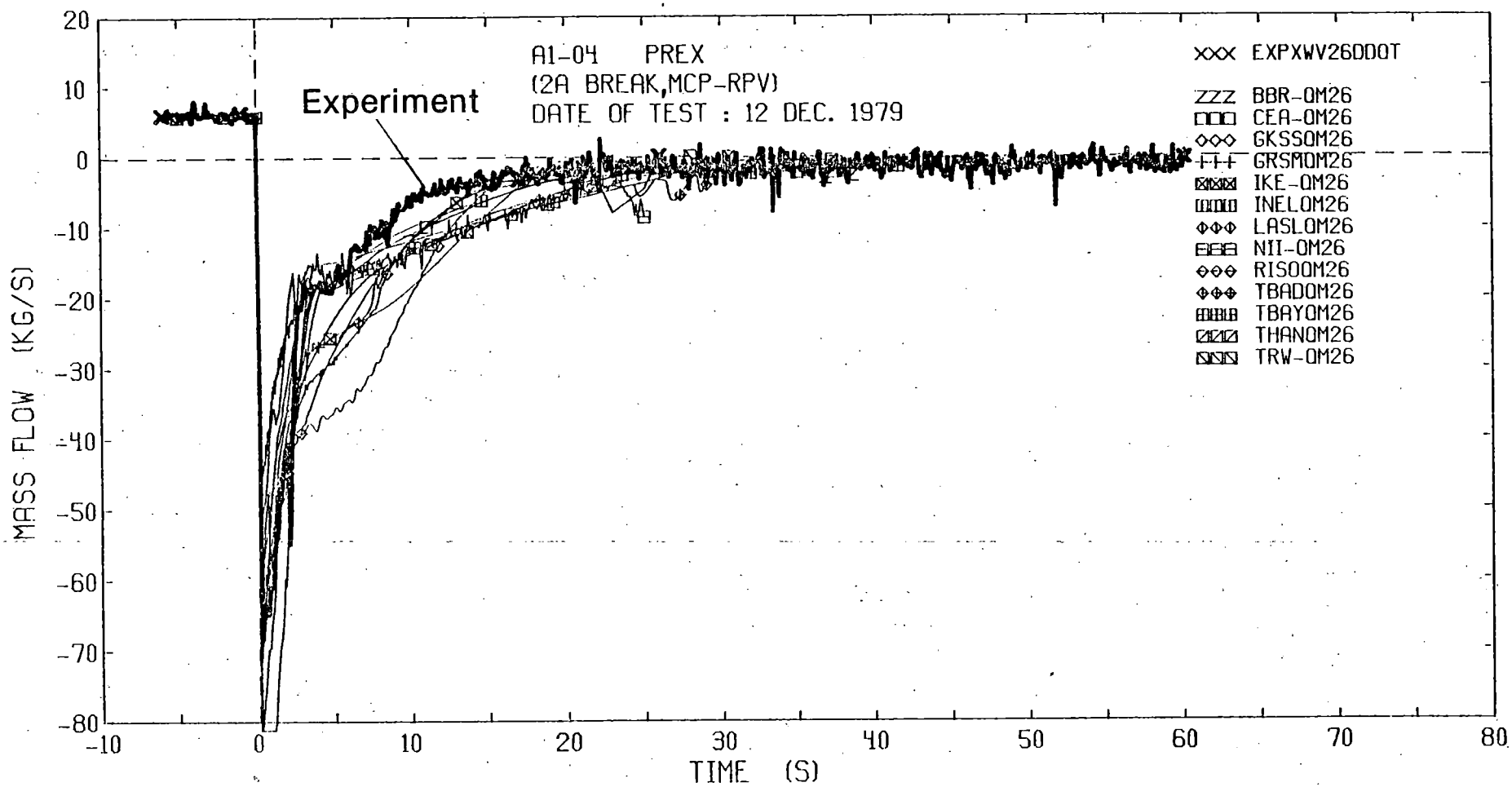

FIGURE 21 : MASS FLOW AT RPV INLET - BROKEN LOOP
MASS FLOW COMPUTED FROM DENSITY (DD) AND
FLUID VELOCITY (QT)

the vertical slip option for the calculation of the phase separation in the downcomer region.

The fluid temperature, shown for the intact loop hot leg and for the lower plenum in Fig. 22 and 23, follow the saturation temperature after the local pressure has fallen to the corresponding saturation pressure value. Due to the overpredicted depressurization of the system all predicted fluid temperatures are considerably lower than the measured temperature.

The occurrence of superheated steam as measured for example for the intact loop hot leg between 25 s and 50 s was not predicted with the exception of the results from one participant. Only in this prediction a large number of structural heat slabs was used to model the energy release of the loop piping material.

The incorrect description of the mass distribution in most of the predicted results is indicated in Fig. 24 and 25 where the fluid density is shown in the broken loop cold leg (upstream of the vessel side break) and in the lower plenum. The codes which are based on homogeneous flow models could not predict the phase separation in the downcomer and in the plena of the pressure vessel which resulted in a too large fluid density in the broken loop cold leg, and in an underprediction of the mass inventory in the lower plenum. The density distribution was well predicted only by the RELAP4/MOD6 code in case where the vertical slip option was used in the downcomer region and in the lower plenum.

Measured and calculated differential pressure values are shown for the broken loop pump and for the "heated length" of the core region in Fig. 26 and 27. In most predictions the optional two-phase pump model in the code was used together with pump input data based on the two-phase flow performance of the Semiscale pump. The generally large deviations of the predicted values from the measured data indicate, that the two-phase flow characteristics of the Semiscale pump can not directly be applied to the LOBI pump.

The differential pressure over the core region, which gives a qualitative picture for the core mass flow is fairly well predicted by most of the participants. After a short period of flow reversal (negative differential pressure values)

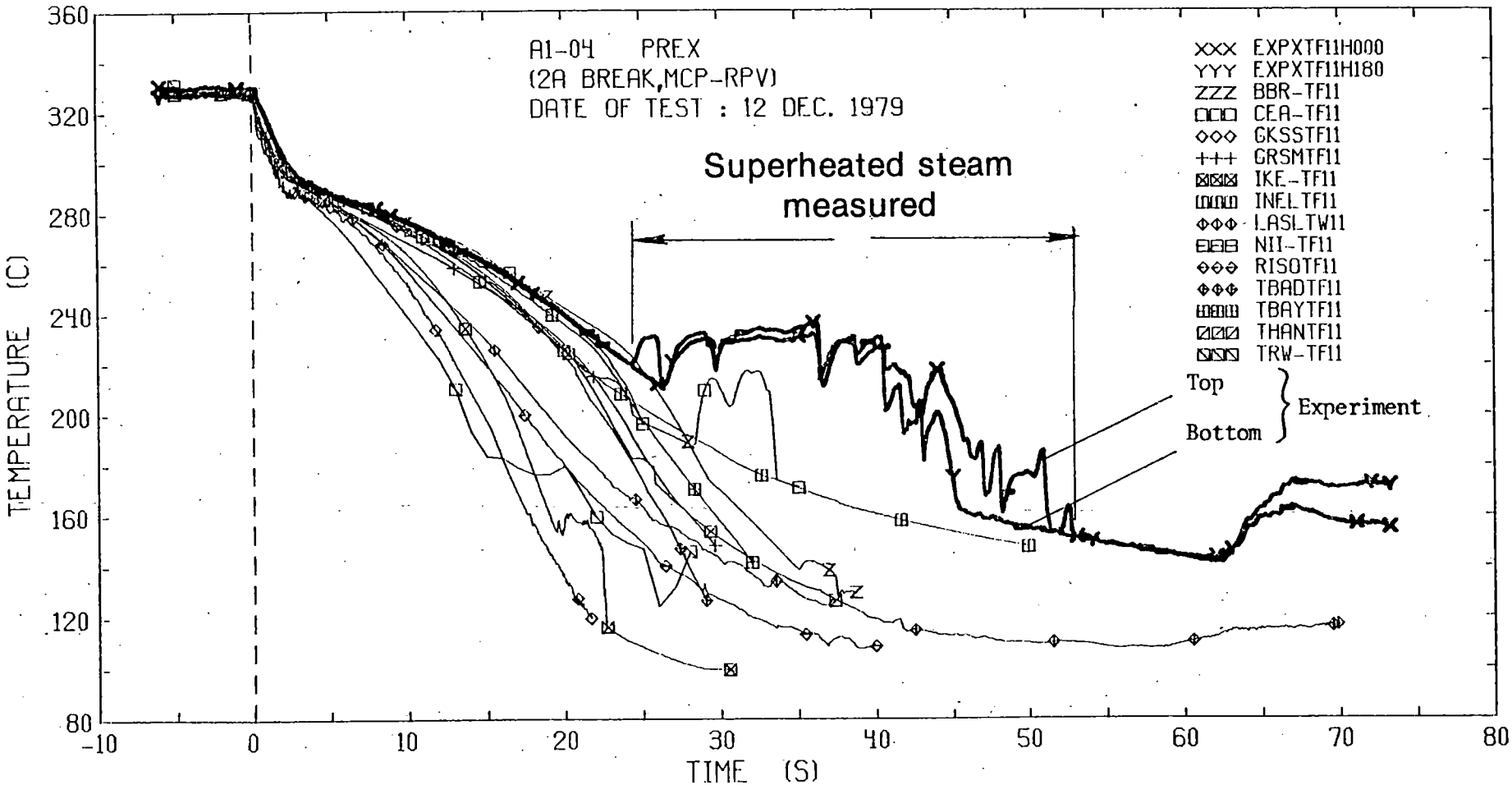

FIGURE 22 : FLUID TEMPERATURE AT RPV OUTLET - INTACT LOOP

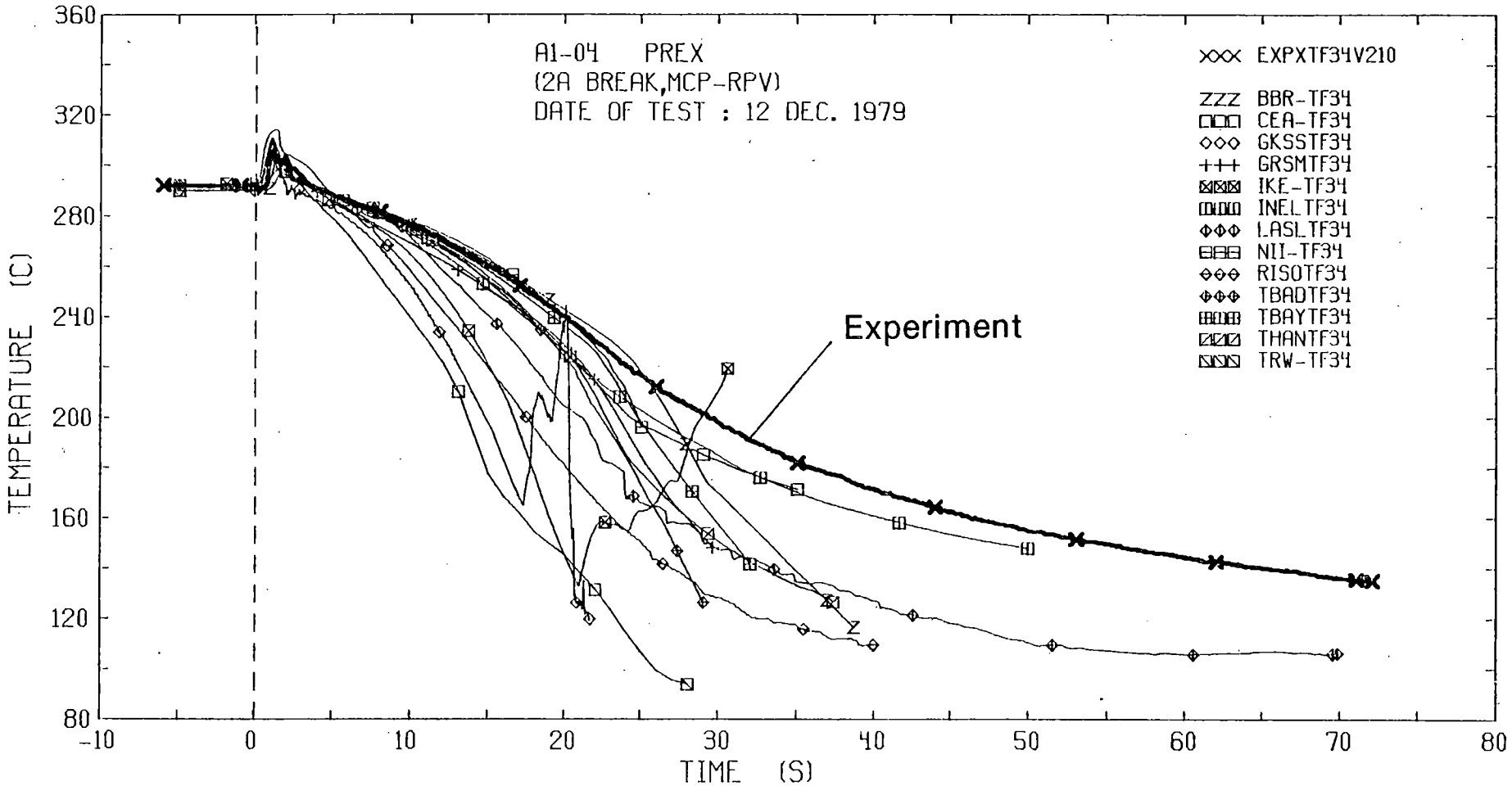

FIGURE 23 : FLUID TEMPERATURE IN LOWER PLENUM

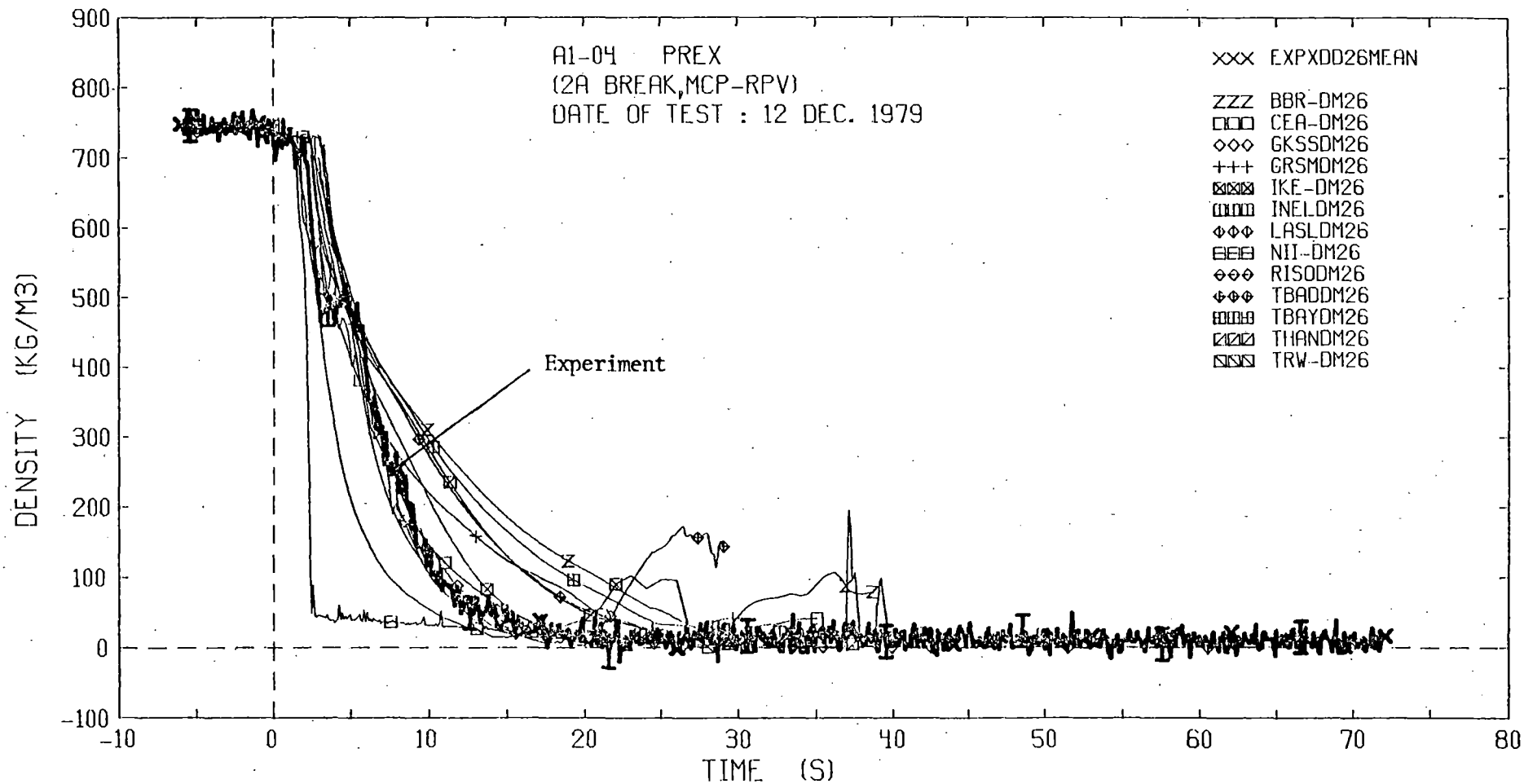

FIGURE 24 : DENSITY AT RPV INLET - BROKEN LOOP

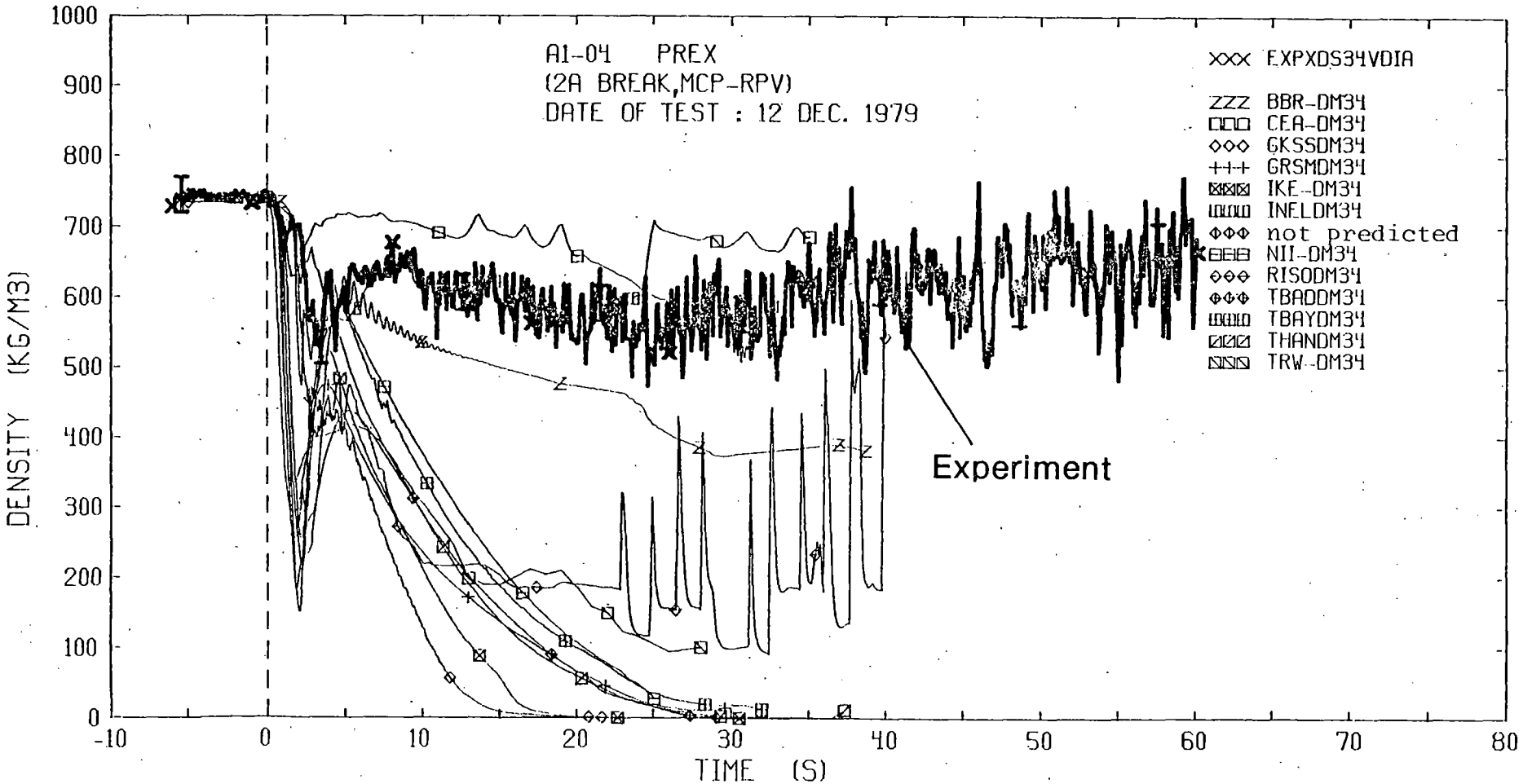

FIGURE 25 : DENSITY IN LOWER PLENUM

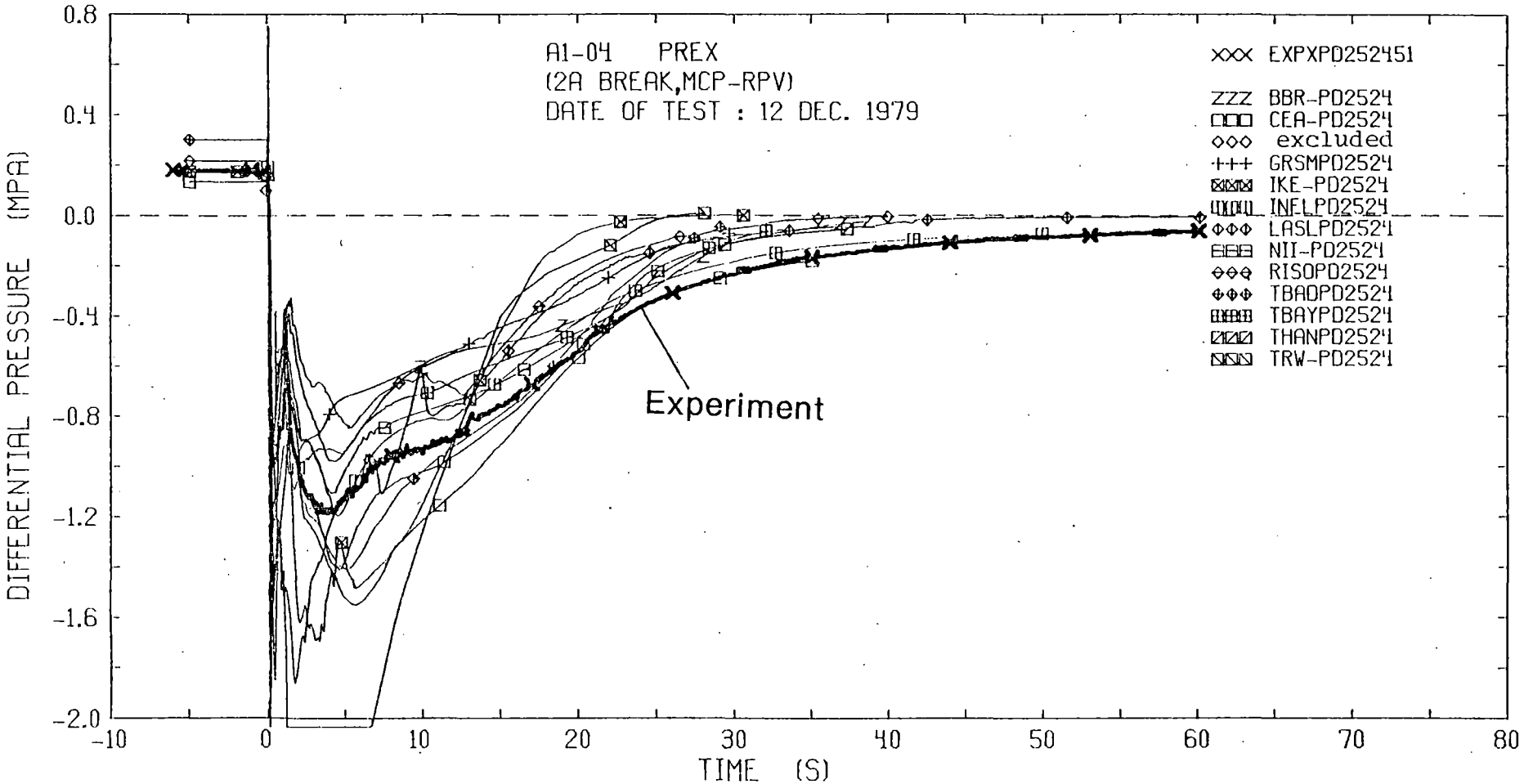

FIGURE 26 : DIFFERENTIAL PRESSURE OVER PUMP - BROKEN LOOP

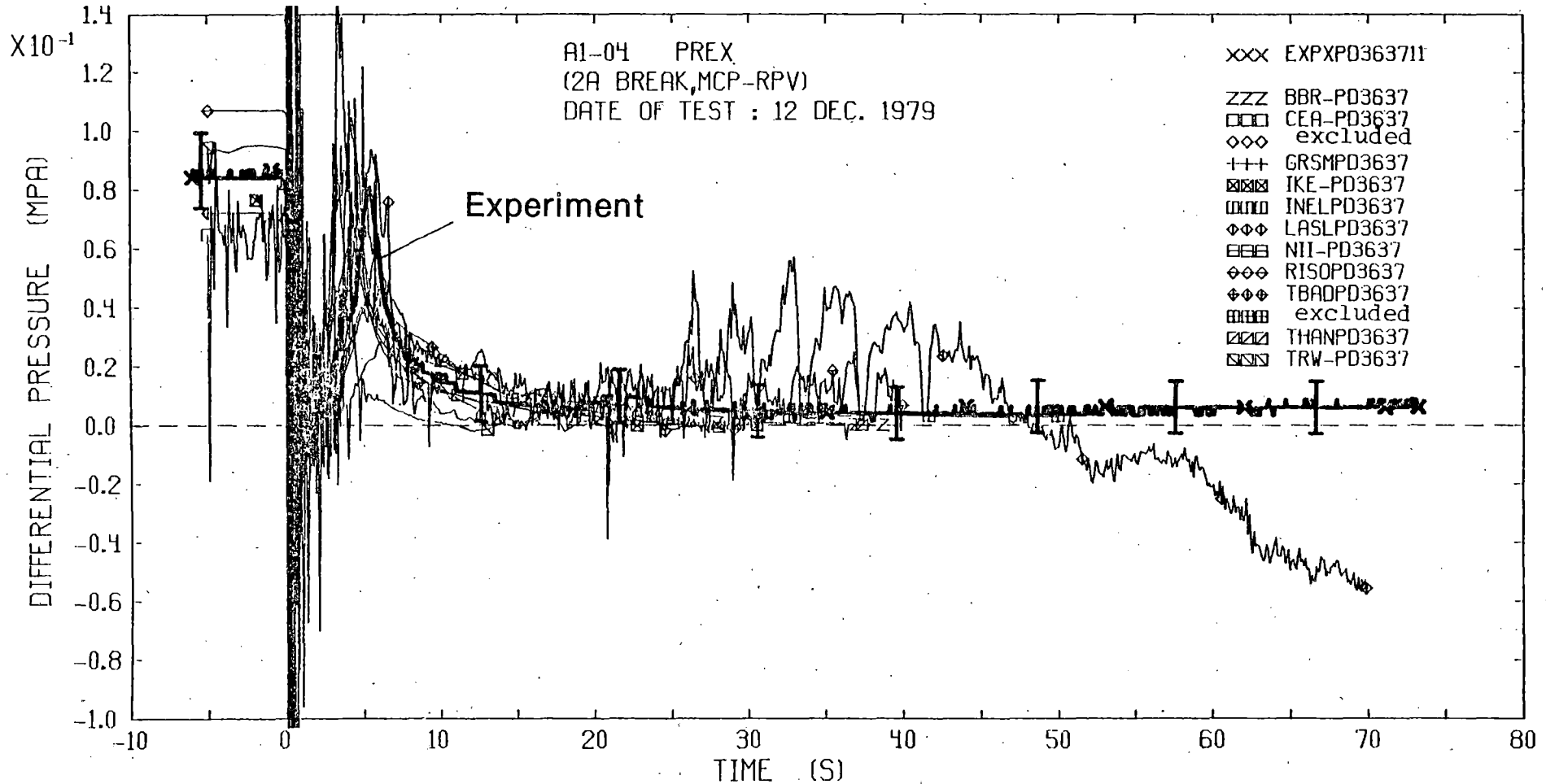

FIGURE 27 : DIFFERENTIAL PRESSURE CORE

all the predicted differential pressures indicate a relatively large positive core mass flow. This behaviour has been found to be typical for the present design of the test facility with the large not volume scaled downcomer. Oscillations in some of the calculated data prior to the blowdown and in the early transient are obviously caused by insufficient stable initial conditions in the input data. No explanation could be given for the large deviation from the measurement and for the osciallatory character beginning at 25 s for one of the TRAC results.

The injection of subcooled water from the accumulator started in the experiment at 22.5 s, after the pressure in the intact loop cold leg has fallen below the accumulator activation pressure of 27 bar. This was calculated to occur much earlier in most cases due to a too fast predicted depressurization of the primary system. The injection rate is generally overpredicted as shown in Fig. 28 where measured and predicted volume flows in the accumulator injection line are compared. Different reasons might have contributed to this discrepancy including a not correctly specified flow resistance in the injection line, the overprediction of the depressurization of the primary system and an unrealistic pressure drop in the receiver volume as a result of the thermal equilibrium assumptions in the code.

The too early predicted start of the ECC injection is shown also by the predicted fluid density in the intact loop cold leg pipe between the injection point and the pressure vessel, given in Fig. 29. The measured steep density increase after the initiation of the ECC injection is, with only one exception, well predicted by all participants. No explanation can be given for the strong non-physical density fluctuations predicted by the TRAC code. These fluctuations begin at about 20 s when the pipe section was predicted to be completely filled with subcooled water. At nearly the same instant, problems occurred also in the DRUFAN calculations which led to a termination of the prediction.

Measured and calculated heater rod temperatures for the middle section of the "heated length" are shown in Fig. 30. The calculated heater rod surface temperature is compared with the arithmetic mean value of the measurements in the measurement elevation 6; excluded are the thermocouple signals of the outer (peripheral) zones of the bundle.

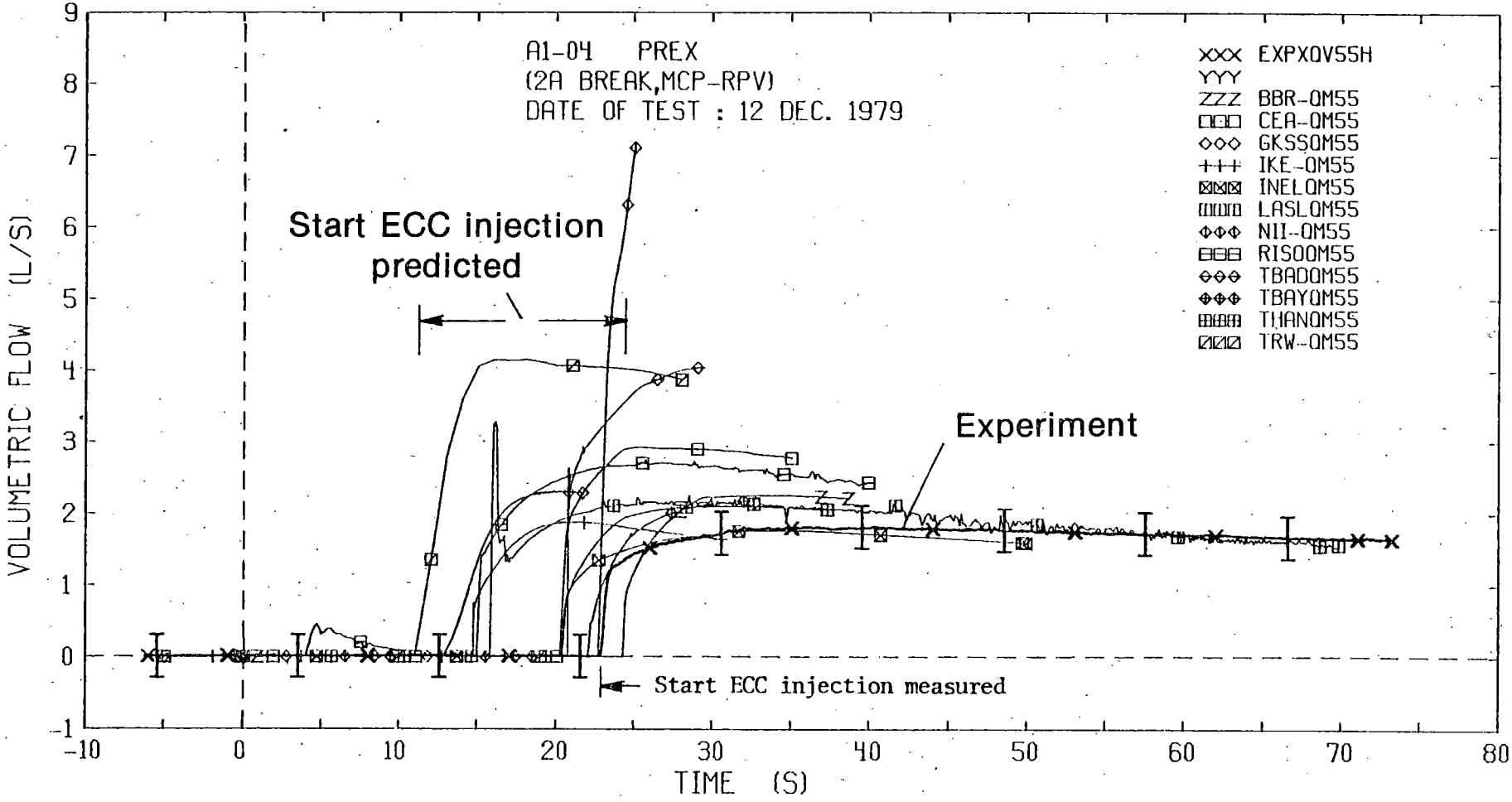

FIGURE 28 : VOLUMETRIC FLOW FROM ACCUMULATOR INTACT LOOP

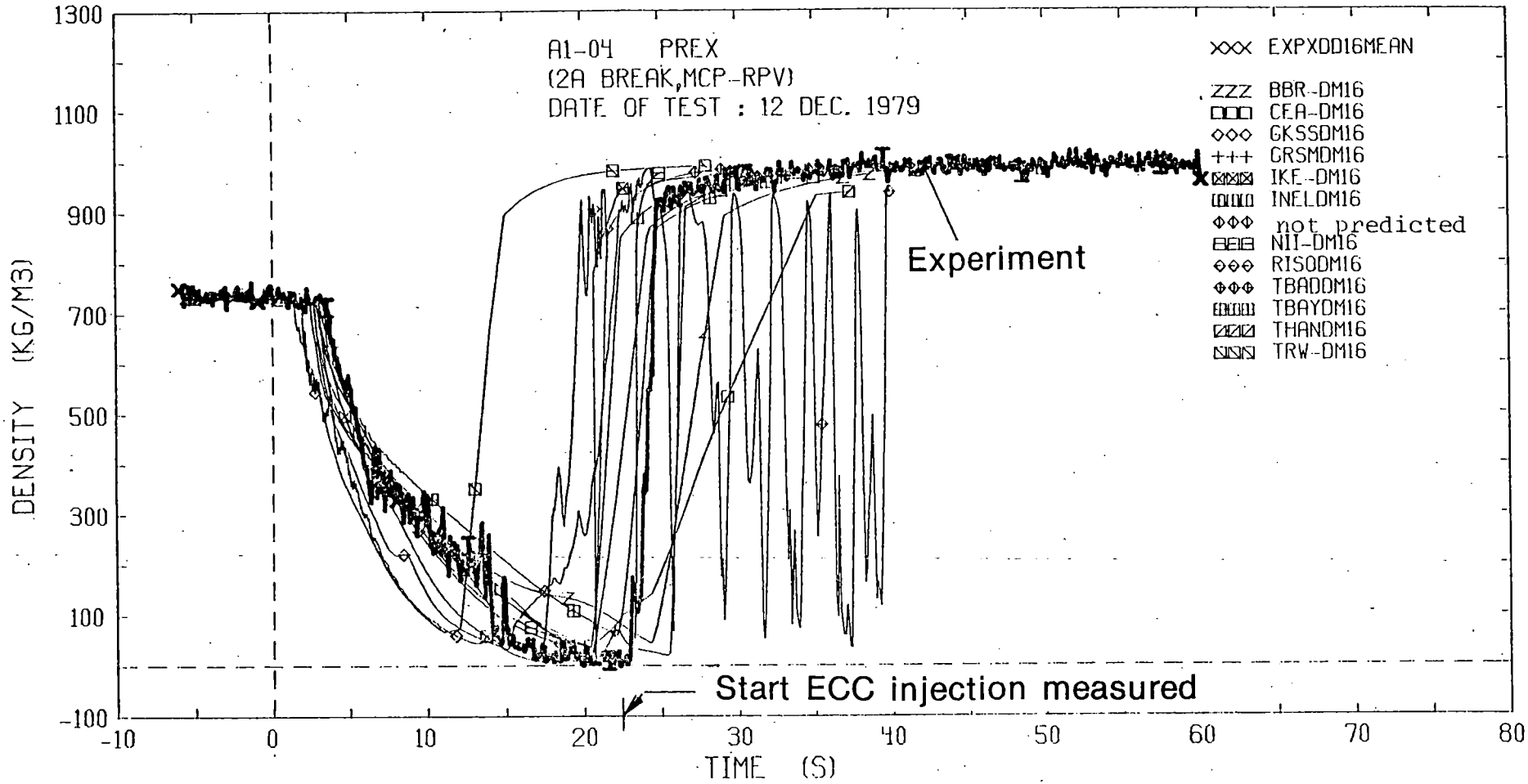

FIGURE 29 : DENSITY AT RPV INLET - INTACT LOOP

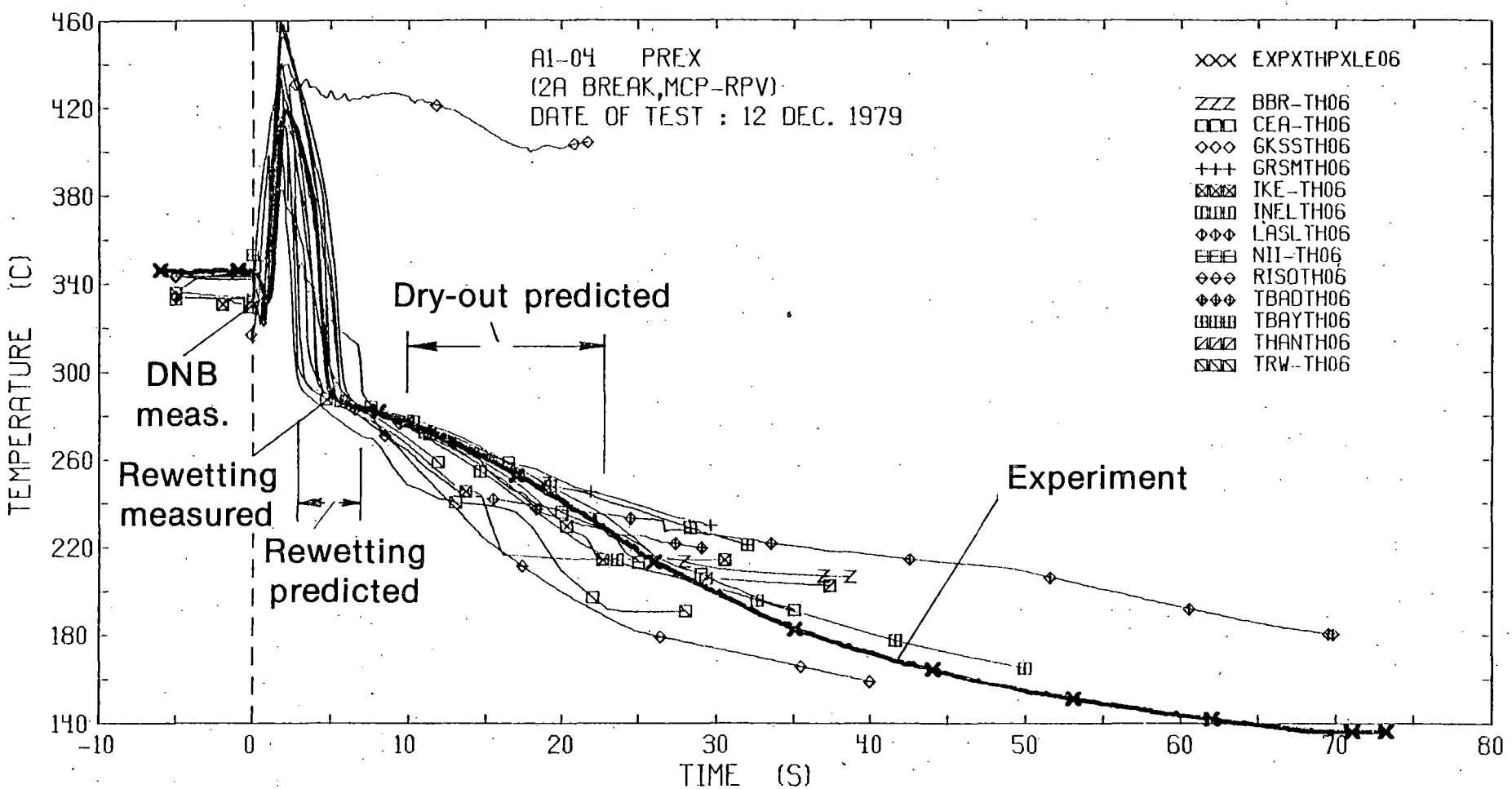

FIGURE 30 : MEAN HEATER ROD TEMPERATURE LEVEL 6

The response of the heater rod bundle is at least qualitatively well predicted within the first 10 s of the transient, except the results from the RELAP3 calculation. The good agreement holds for the time for DNB (first occurrence of critical heat flux conditions), the time for the temperature maximum and the rewetting behaviour.

Differences between measured and predicted temperatures prior to the DNB are a result of the radial temperature profile in the heater tube walls for the high surface heat fluxes during the forced convection and nucleate boiling period. The thermocouples which are located 0.4 to 0.5 mm beneath the outer rod surface indicate during this time period up to 15 °C higher temperatures compared with the calculated surface temperatures.

After the rewetting of the rods has occurred the heater rod temperatures follow closely the continuously decreasing fluid saturation temperatures. As a consequence of the overpredicted depressurization rate most of the calculated heater rod temperatures are below the measured values during the rewetting time period.

In all the predictions a dry-out (second critical heat flux at large vapor quality) was calculated to occur between 10 s and 22 s which is not shown by the measured data. The predicted dry-out is indicated by a considerable deviation of the heater rod temperature from the fluid saturation temperature. However, the not correctly predicted heat transfer conditions for the heater rod bundle in the later blowdown transient had no large influence on the heater rod temperatures because there was no electrical power input during this time period.

8.4 Conclusions from the LOBI Prediction Exercise

The limited capability of the codes to describe the complex thermo-hydraulic phenomena which occur during a large break LOCA, as well as a not optimal application of the code have been identified as main reasons for the deviation of the predicted results from the measured data. In this context it is of interest, that the (new) advanced codes TRAC and DRUFAN not a priori give better results than the simpler lumped parameter codes like RELAP4.

The following problem areas have been found where further effort is needed to improve the presently existing blowdown codes:

(1) critical mass flows for subcooled and saturated conditions with low vapor qualities upstream of the break area

(2) phase separation in vertical channels for low mean flow velocities due to gravitational forces

(3) release of stored energy in the pressure vessel and loop structures

(4) pump behaviour for two-phase flow conditions

(5) injection of subcooled water into volumes with saturated conditions (condensation phenomena)

(6) dryout behaviour and film boiling heat transfer for bundle geometries with presence of spacer grids

The large differences between the results of different participants using the same code version RELAP4/MOD6 (5 participants) and TRAC P1A (2 participants) indicate the importance of the user experience in the application of the code. The quality of the predicted results depends strongly on the code input data including the nodalization of the system, the selection of the code options and the establishing of the initial and boundary conditions. This requires an experienced code user who is aware of the capabilities and the limitations of the code. The intention of the LOBI prediction exercise was to contribute to the transfer of knowledge in this area.

9. Summary

The LOBI Programme represents a significant contribution to the international research efforts in the field on LWR Safety: it aims at the experimental investigation of the primary cooling system behaviour and the emergency core cooling system performance under loss-of-coolant accident conditions.

The LOBI test facility is designed for high pressure integral system tests; it is the only such facility within the European Community which is available for the experimental investigation of loss-of-coolant accidents in PWRs. The project is being executed in the Ispra establishment of the EURATOM Joint Research Centre of the Commission of the European Communities.

The experimental programme for the time being comprises a total of 90 tests; it is subdivided into three parts of

30 tests each, and is being executed since December 1979. Apart from three small break scoping tests, all other tests performed so far have been large cold leg break tests. The main objective of these tests was to establish the nominal heating power input curve (power ascension test series) and to investigate the effect of the ECC injection mode (cold leg and combined cold and hot leg injection), of the break size ranging from single-ended 1 x 25 % up to double-ended 2 x 100 % breaks, of the pump operation mode, and of the downcomer gap width (50 and 12 mm). The major part of the results are either proprietary or not yet evaluated.

The very first LOBI test, A1-04, of the main experimental programme was used for a special blind post-test prediction exercise with international participation (LOBI PREX).

The main results of pre- and post-test prediction calculations performed by the LOBI staff, and of their comparison with the experimental data of this test A1-04 have been analysed, particularly with respect to the discrepancies observerd. The same analysis was applied also to the prediction results of the PREX participants. From both analyses, several problem areas have been identified which require further research effort in order to improve the presently existing blowdown computer codes.

The future experimental LOBI programme is briefly outlined especially with respect to the small break test programme for which several test facility modifications are envisaged.

References:

/ 1 / W. L. Riebold:
LOBI-Experimental Programme A.
Testmatrix Part A1 and A2
Technical Note No. I.06.01.111.79
Nov. 1979

/ 2 / W. L. Riebold et al.:
Summary of German Instrumentation Research
Paper presented to 5th Water Reactor Safety Research Information Meeting of USNRC, Gaithersburg/MD, USA
November 7-11, 1977
EUR-5951 E (1977)

/ 3 / W. L. Riebold, L. Piplies:
The LOBI Project Small break Experimental Programme.
Paper to be presented to "Specialists Conference on Small Breaks in LWRs",
August 25-27, 1981, Monterey/California, USA

/ 4 / L. Piplies:
Quick Look Report on LOBI Test A1-04
EUR-6969 EN (1980)

/ 5 / E. Ohlmer, T. Fortescue, W. Kolar, J. Eder:
Experimental Data Report on LOBI Test A1-04
EUR-6970 EN (1980)

/ 6 / H. Städtke:
Pre-Test Prediction for LOBI Test A1-04 (PREX Test)
EUR-6993 EN (1980)

/ 7 / H. Städtke:
Post-Test Analysis for LOBI Test A1-04 (PREX TEST)
EUR-6972 EN (1981)

/ 8 / W. Kolar, L. Piplies, W. Brewka:
Comparison of PREX Calculations with the Experimental Results
Commission of the European Communities, J.R.C.-Ispra
Technical Note No. I.06.01.80.92

/ 9 / W. Kolar, W. Brewka, L. Piplies:
Overlays Combining PREX Calculations of all Participants with the Experiment
Commission of the European Communities, J.R.C.-Ispra
Technical Note No. I.06.01.80.104.

PKL I FINDINGS - PKL II PLANS

B. Brand, D. Hein, P. Weiss
Kraftwerk Union AG, Erlangen

9th Water Reactor Safety Research Information Meeting
Oct. 26 to 30, 1981 - Gaithersburg, U.S.A.

1. Introduction

System effect tests are an important step towards the verification of ECCS efficiency: the general aim of these projects is to simulate the system behaviour during a LOCA in order

- to identify and appraise the system response to off-design operating conditions and
- to verify the efficiency of ECC systems and of particular countermeasures.

The importance of these issues led to the construction of test facilities, partly in international cooperation, where the tests with the above mentioned scope are carried out.
These are to mention but a few:

in the United States:	LOFT /1/, FLECHT /2/, SEMISCALE /3/
in Japan:	ROSA /4/, CCTF /5/
in Europe:	LOBI /6/, PKL /7/

With this large number of facilities already in existence one has to ask where does PKL differ from, or go beyond, the capabilities of others to justify the existence of yet another test facility.

The PKL capabilities of special interest are:

1) testing of KWU's ECCS with combined injection that is coolant injection into the hot as well as cold legs
2) special design of the facility such that
   - the end-of-blowdown phase which preceeds the refill and reflood phases of a large break LOCA can also be investigated
   - the system behaviour of three independent loops can be studied (e.g. the influence of pressurizer on loop flow)
   - the rod bundle simulating the core is large enough so that radial effects become visible and above all the facility heat losses do not decisively influence the system behaviour
   - during small break tests the important phase up to the point where low pressure injection is initiated can be covered.

The diagram in Fig. 1 shows those areas where PKL can contribute.

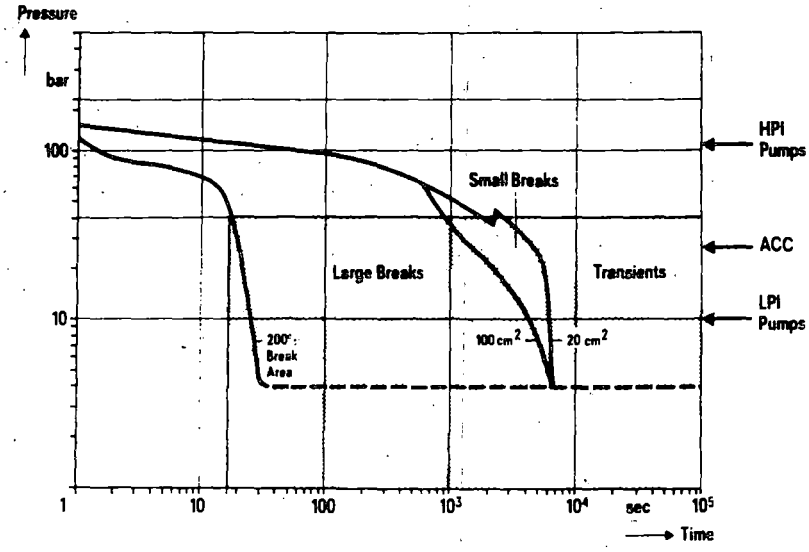

Pressure Transients During LOCA
Scope of Investigation in PKL Test Facility

Fig. 1

2. Findings from Test Series PKL I

The main objectives of the test performed by PKL I are shown in Fig. 2.

Test Series	Break Size	Main Objectives	No of Run
IA	Large Break Tests	– Loop Resistance – Injection Rate – Injection Mode	16
IB	Large Break Tests	– Break Size – Containment Back Pressure – Upper Plenum Internals – Combined Injection	15
IC	Small Break Tests	– Shake-Down Test Series for Small Breaks	–
ID	Small Break Tests	– Steady State Tests – Transient Tests	75 12
IE	Large Break Tests	– End of Blowdown (Preliminary Test)	1

PKL I – Test Series

Fig. 2

It also has to be pointed out that PKL together with the LOBI facility has to cover the area "Loss of Coolant" within the German reactor safety research program and the LOCA-phases which can be simulated over a wide range.

The PKL test facility - the program is supported by the German Minister of Research and Technology - represents a typical KWU 1300 MWe 4-Loop PWR on a scale of 1:134. In view of the importance of the driving gravity forces during reflood as well as for natural circulation, all elevations correspond to actual reactor dimensions. The test facility is designed for a maximum pressure of 40 bar. The test bundle simulating the core consists of 340 electrically heated rods. The three loops - one of double capacity simulating two loops - contain active steam generators whose secondary sides can be cooled down.

Especially, the maximum design pressure of 40 bar and careful simulation of all primary loop components with respect to their thermohydraulic behaviour makes it possible to employ the PKL facility for a variety of tasks:

1) - for Large and Intermediate Size Break LOCAs
   - end-of-blowdown
   - refill
   - reflood
   - long term cooling

   that is, the course of a LOCA from initiating the accumulators onwards.

2) - for Small Break LOCA phases with different energy transport mechanisms and at different water inventories on the primary or secondary side i.e.
   - natural circulation (single and two-phase)
   - reflux condenser mode
   - reflux condenser mode with core uncovery

3) - for transients with and without break and injection, and shutdown of the plant.

After completing the PKL facility in 1976, the system response to refill and reflood phase of large break LOCAs was examined in test series IA and IB. In these tests the main interest was focused on the effects of loop restistance and injection mode. In autumn 1979 the facility was modified for small break tests.

Series ID consisting of both transient and steady state tests was carried out in 1980. The aim here was to investigate the energy transport from the core to the steam generators as well as the effictivness of steam generator secondary side cooldown as a countermeasure to attain a fast pressure reduction on the primary side and the subsequent fast switch to low pressure ECC injection.

As a preparation for series PKL II - which will have more extensive instrumentation - a scoping test, IE, was carried out which included the end-of-blowdown phase. The results of this test were encouraging and contributed to the shift of interest towards 40 bar tests.

Summarizing the findings of PKL I it can be asserted that the efficiency of KWU's ECCS with combined injection has been confirmed and it has shown advantages to alternate ECCS.

Conclusion for large breaks:

- Condensation of steam in upper plenum and top of core reduces steam binding
- Early rewetting also from the top of core was observed
- Significant heater rod cooling already in the refill phase reduces duration in high temperature region
- ECC process is mainly concentrated to the RPV itself, so that loop influences as pump resistance and energy input from SG are of less importance than with cold leg injection only

Conclusions for small breaks:

- The decay heat and the stored heat in the system can be removed via the steam generator secondary side by natural circulation and even better by heat transfer in the reflux condenser mode with reduced inventory.
- The transient tests proved that the primary side follows closely the secondary side cooldown and therefore confirmed the effectivness of this measure.
- There are no dangerous situations in terms of core temperatures to be expected as long as the core is covered with a two phase coolant mixture.

2.1 Large Breaks: Series IA and IB

The kind of understanding that system effects tests enhance can be pointed out by mass and energy transport maps shown in Fig. 3 and 4 for a large break LOCA and in Fig. 5 for a small break LOCA.

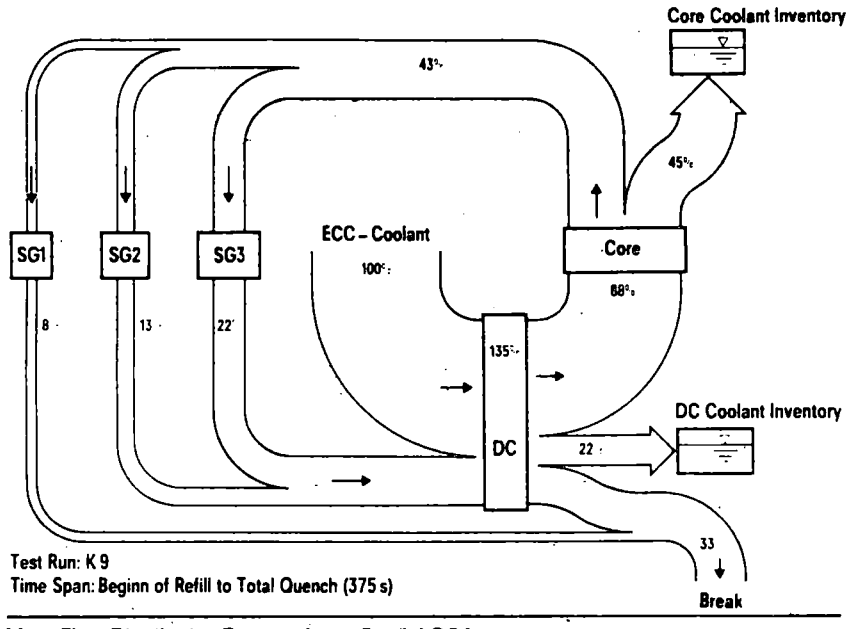

Mass Flow Distribution During a Large Break LOCA

Fig. 3

Fig. 3 shows the cumulative mass flow distribution during a double ended guillotine break test with cold leg injection only. It covers the time span from test initiation i.e. beginning of refill up to total quench - alltogether 375 seconds. Taking the total injected coolant from accumulators and low pressure pumps as being 100 %, there flows 88 % towards the core of which about half (i.e. 43 %) is entrained into the steam generators. 45 % of the injected mass fills the core up to about a third of its volume. In this test 33 % of injected coolant flowed via the break into the containment, most of it as steam.

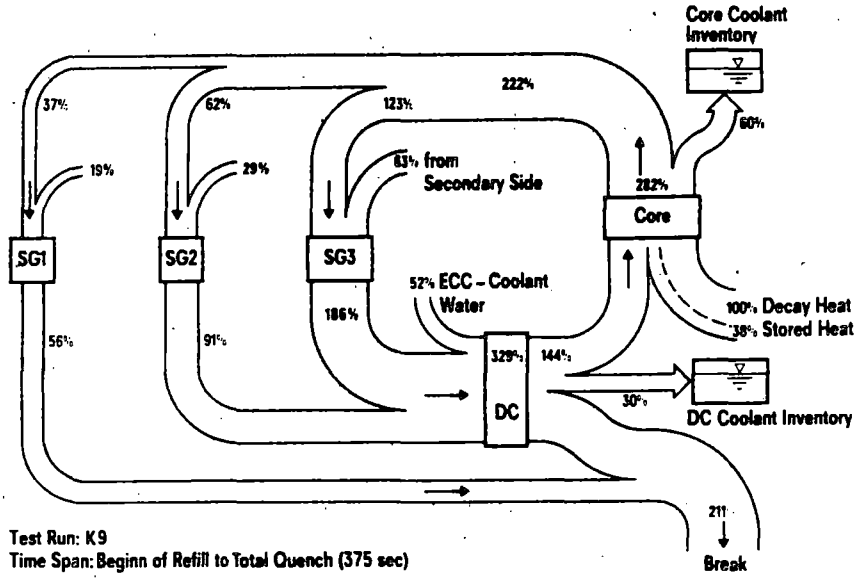

Energy Flow Distribution During a Large Break LOCA

Fig. 4

Fig. 4 shows the cumulative energy distribution during the same time period. Here, the total decay heat is taken as 100 %. The 43 % mass flowing through the steam generators cause additional 111 % heat transferred from the secondary to the primary side. The energy removing capacity out of the system is however not impeded - 211 %, leaves the system via the break. This way of looking at it suggests to judge the ECC systems by their ability to limit the flow through the steam generators: in other words, trying to prevent water entrainment from the upper plenum. This can be achieved by injecting the emergency core coolant simulataniously via the hot legs into the upper plenum. The energy transfer from the secondary to the primary side of the steam generator is in such a case reduced drastically /8/.

2.2 Small Breaks: Series IC and ID

For a small break LOCA the energy removed from the primary system by the break flow is only small and an additional heat sink - the secondary side - may be needed. Therefore in a KWU-PWR the secondary side is cooled down automatically at a rate of 100 K/h, to assure that in such cases the steam generators act as a heat sink.

When we consider the energy transport during a small break LOCA, we find that the important question is how much energy has to be removed in order to reach 180 °C on the primary side - this being the saturation temperature at 10 bar which is the pressure at which the low pressure injection pumps comes into operation.

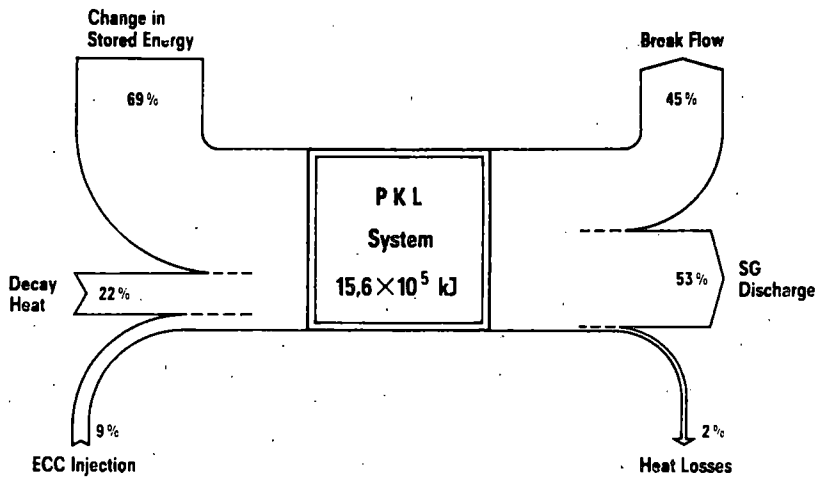

Energy-Transport during a Small Break LOCA

Fig. 5

The cumulative flow of energy is shown in Fig. 5. This diagram shows where the energy to be removed comes from and where it is goint to. One recognizes immediately that the largest share of energy to be removed is the energy stored initially within the system, namely 69 %. This number includes the energy stored within the fluid - primary as well as secondary side - and within the structural materials.

In contrast to the above the decay heat contributes only about 22 %. In this particular test 45 % of the energy left the system via the break and 53 % via the steam generators secondary sides. The system heat losses amounted to only 2 % and thus did not at all influence the course of the test.

2.3 End of Blowdown: Scoping Test IE

The final test for core I was carried out in order to learn how to include the end of blowdown phase in test series PKL II. The intention of this scoping test, which was started at 30 bar, covered three areas:

- how to run these tests
- wether core instruments will withstand the dynamic forces
- how the core will behave.

The results gained from this test, IE, are encouraging so that it was decided to include the end of blowdown phase within the tests of series PKL II.

3. Plans for PKL II Test Series

The inclusion of the end-of-blowdown phase (EoB) is considered important because by injecting ECC coolant into the hot legs (combined injection) early rewetting at pressures 26 to 4,5 bar is expected. The energy removed from the core during this period assists reflood and refill considerably. In addition, tests that span the end-of-blowdown and reflood phases will enable the quantification of safety margins regarding conservative assumptions on rewetting during EoB, residual water within the primary system and the heat transfer during the refill phase. It is expected that with combined injection no pronounced second temperature peak will occur and as a consequence the possibility of damage caused to the rods will be considerably reduced.

The inclusion of EoB requires modifications to the facility. It is especially important to strictly adhere to the scaling of volumes which were not of first order importance in refill and reflood tests e.g. upper dome, core bypass etc. This requirement made it necessary to install a new pressure vessel.

As opposed to Core I (340 heated rods), Core II consists of 315 heated rods and 25 unheated positions simulating control rods. These positions have been used for installing extensive two-phase flow advanced instrumentation provided by USNRC.

The test matrix provides for 4 refill and reflood tests which will show the influence (if any) of the changes made - e.g. unheated rods in core. In addition in this test series IIA the advanced instrumentation will be tested.

There are 10 tests to follow - these will have break sizes 200 and 25 %, starting from 40 bar. The next ca. 10 tests will be speefied at a later date, taking into account the results obtained up till then.

3.1 Test Procedure

The difficulties here stem from the necessity to slip into the blowdown at 40 bar in such a manner that at the time the accumulators begin to inject, the flow conditions and water distribution are correctly established. This will be achieved by releasing water from special reservoirs into the steam filled system immediately after opening the break valve at 40 bar. This mass of water equals the calculated water inventory of the system at 40 bar going through a transient initiated at full pressure. The rapid flow towards the break will be utilized to achieve the desired water distribution. Therefore tne phase from 40 to 26 bar is to be considered as a purely "conditioning" phase. The actual test covers the range from start of accumulator injection at 26 bar to the end of reflood i.e. coolant covered core.

4. Conclusions

The PKL facility makes by virtue of its size and the ability to simulate the end-of-blowdown phase, an important contribution towards examining and understanding Loss of Coolant Accidents and towards developing computer programs simulating such accidents.

References

/1/ D.L. Reeder
LOFT System and Test Description
Tree/NUREG - 120', EG+G Idaho, Sept. 80

/2/ L.E. Hochreiter et. al.
PWR FLECHT SEASET Unblocked Bundle, Forced
and Gravity Reflood Task: Task Plan Report
NRC/EPRI/Westinghouse-3, March 1978

/3/ P. North
System Design Description of the MOD-3 SEMISCALE System
EG+G, Idaho, Dec. 1980

/4/ M. Shiba et. al.
Experiment on Performance of Upper Head Injection
System with ROSA II
JAERI-M-6707 (2976)

/5/ Y. Murao, K. Hirano, M. Nozawa
Results of CCTF Core I Tests
8th Water Reactor Safety Research Information Meeting, 1980

/6/ W.L. Riebold, H. Städke
LOBI - Influence of PWR Primary Loops on Blowdown:
First Results
Transactions of ANS, TANSAO 38 1-776 (1981)

/7/ H. Schmidt et. al.
Wiederauffüllversuche mit Berücksichtigung der
Primärkreisläufe - PKL
Beschreibung der Versuchsanlage
KWU RE 23/011/79, Oct. 1979

/8/ D. Hein, H. Watzinger
Energy Transport to EC Coolant with in the Primary
System - PKL Test Results
Transactions of ASME, HTD-Vol. 7

LOCA - SSE Combination and Asymmetric Blowdown Probability Assessment

Dr. C. K. Chou

Lawrence Livermore National Laboratory
University of California
P. O. Box 808, L-90
Livermore, California 94550, U.S.A.

SUMMARY

A double-ended guillotine break of primary coolant loop in a pressurized water reactor (PWR) nuclear power plant can introduce large forcing functions on the piping system itself. In addition, it can generate huge impingement force and pressure onto adjacent components and component supports which can lead to some degrees of difficulty on the design of components, component supports, and component protection systems. The situation can be much worse when the break occurs inside the reactor cavity wall and introduce asymmetric pressurization between compartments surrounding the reactor pressure vessel.

The U.S. Nuclear Regulatory Commission (USNRC) in its role of making licensing regulation is seeking a technical judgement in the determination of the necessity for postulating asymmetric blowdown events and the combination of large loss-of-coolant accident (LOCA) with safety shutdown earthquake load (SSE) in the PWR nuclear power reactor design. Various research has been conducted by the nuclear industry and the NRC in the area of material behavior and fracture mechanics evaluations on the reactor coolant pipes. Most of the work is in deterministic form. Results of the studies tend to conclude that a double-ended guillotine break for the PWR primary system is an inconceivable event. However, a deterministic approach cannot properly estimate the margin of safety due to the limitation of the approach and the variations of piping fragility and applied loads. The technical community generally agrees that such an accident is an extremely rare event; but whenever it happens the consequence can be great, and the risk level may not be acceptable.

In order to assess the consequence and risk associated with different requirements, a probabilistic assessment is inevitable. The existing knowledge on material behavior and material defect rate, as well as uncertainty of other variables, introduces great difficulty for a probabilistic assessment. However, the determination of the distribution of many of the variables can still be achieved by incorporating the available data with experts' judgements. With the assistance of sensitivity studies and proper handling of uncertainty to each random variable, a range of failure probability can be obtained to bound the actual probability.

This research program, undertaken by the Lawrence Livermore National Laboratory for the United States Nuclear Regulatory Commission, is intended to provide a sound technical basis to enable the NRC to establish a regulatory position. The probabilistic fracture mechanics approach is used. Initial crack size, crack length and depth aspect ratio, material properties, operating transient and seismic stress histories, pre-service and in-service inspections, as well as leak detections are considered as random variables. Best estimate models are used in the computation. Fatigue crack growth is simulated through time for the various transients and earthquakes. The degraded pipe section is compared with elastic-plastic failure criteria to determine the leak and break probabilities. Probability results indicate that a double-ended guillotine break is an inconceivable event with the probability of it occurring smaller than 10^{-10} with or without earthquakes. A leak is found to be several orders of magnitude greater than that of a double-ended guillotine break.

In view of the extremely low probabilities results, it can be concluded that the primary coolant loop break as a result of fatigue crack growth subjected to all plant transients including seismic is extremely unlikely. Current design requirements of postulating asymmetric blowdown events and the combination of large LOCA with SSE are not necessary for the plants having similar system design as Zion Unit 1 (plant used in the analysis). Please note that the pipe break caused by external loading such as falling crane, failure of pressure vessel, steam generator, and reactor coolant pump supports and internal loading such as water hammer are not included in the analysis. These indirect causes and gross construction and design error may substantially change the conclusion. However, most of these potential problems can be prevented by different ways, such as: to reinforce support structures to avoid support failure, to develop improved system operation procedures to avoid water hammer, to upgrade quality assurrance program to avoid gross construction and design errors, etc. Detailed descriptions of all the work presented here can be found in the Load Combination Program Project I final report, NUREG/CR-2189, UCID-18967, "Probability of Pipe Fracture in the Primary Coolant Loop of a PWR Plant", (9 volumes), August, 1981.

NSSP
NUCLEAR SYSTEMS SAFETY PROGRAM

3

LOCA - SSE COMBINATION AND ASYMMETRIC BLOWDOWN PROBABILITY ASSESSMENT

PRESENTED BY

C. K. CHOU

PRESENTATION TO

9TH WATER REACTOR SAFETY RESEARCH INFORMATION MEETING

GAITHERSBURG, MARYLAND

OCTOBER 26, 1981

NSSP
NUCLEAR SYSTEMS SAFETY PROGRAM

4

OUTLINE OF PRESENTATION

- BACKGROUND INFORMATION
- TECHNICAL APPROACH
- RESULTS
- SENSITIVITY STUDIES
- CONCLUSIONS
- DISCUSSIONS
- REPORTS

BACKGROUND INFORMATION

- WE HAVE ESTIMATED THE PROBABILITY OF A DOUBLE-ENDED GUILLOTINE BREAK IN THE PRIMARY SYSTEM OF ZION NUCLEAR POWER PLANT UNIT #1.

- THE WORK WAS FUNDED BY THE U. S. NUCLEAR REGULATORY COMMISSION, OFFICE OF NUCLEAR REGULATORY RESEARCH.

- THE OBJECTIVES OF THIS ACTIVITY ARE:
  - TO ASSESS WHETHER LARGE LOCA AND SSE EARTHQUAKE LOADS NEED TO BE COMBINED IN THE NUCLEAR POWER PLANT DESIGN.
  - TO ASSESS WHETHER ASYMMETRIC BLOWDOWN LOCA LOAD NEEDS TO BE POSTULATED.

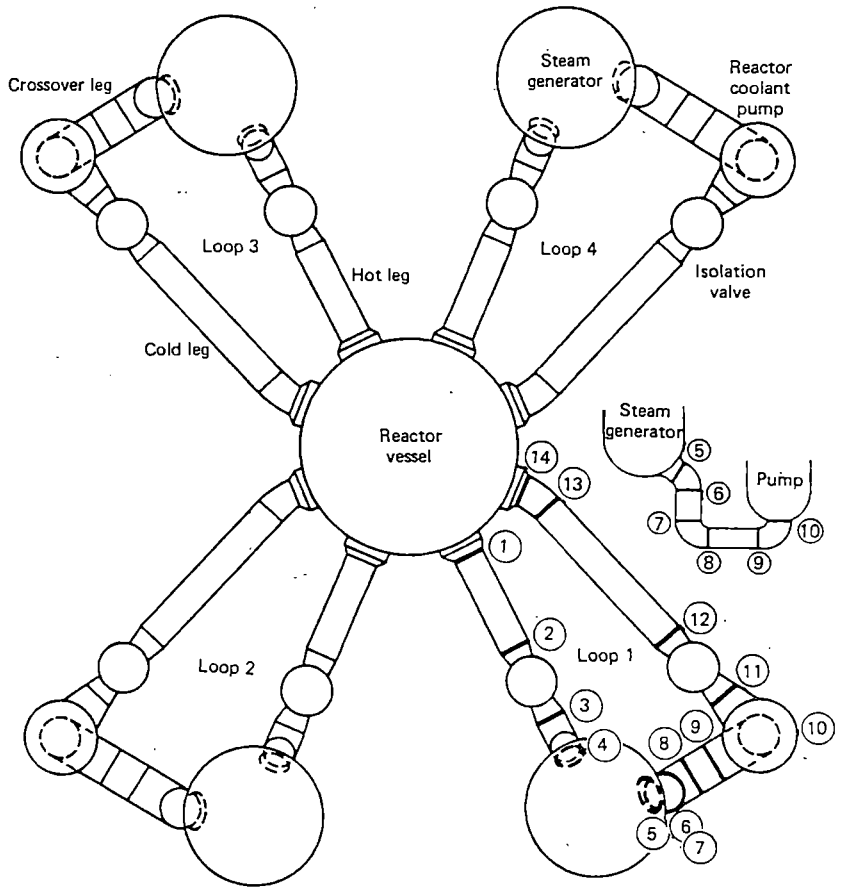

Schematic of the four-loop PWR nuclear steam supply system at Zion Unit 1. Shown in Loop 1 are the 14 circumferential girth-welded butt joints common to each loop that were analyzed in the fracture mechanics model.

ANALYTICAL APPROACH FOR DIRECT FAILURE (FAILURE CAUSED BY FATIGUE CRACK GROWTH)

- PROBABILISTIC FRACTURE MECHANICS MODEL
  - RANDOM VARIABLES:
    - 2-DIMENSIONAL (DEPTH, LENGTH) INITIAL CRACK SIZE DISTRIBUTION
    - PRE-SERVICE AND IN-SERVICE INSPECTION DISTRIBUTION
    - PROOF TEST DISTRIBUTION
    - LEAK DETECTION DISTRIBUTION
    - SEISMIC HAZARD
    - MATERIAL PROPERTIES
  - BEST ESTIMATE ON
    - OPERATING TRANSIENTS AND SEISMIC EXCITATION STRESS CALCULATIONS.
  - SIMULATE PIPE DEGRATION THROUGH TIME AS A FUNCTION OF FATIGUE CRACK GROWTH.
- ELASTIC-PLASTIC FAILURE CRITERIA
  - $J > J_{IC}$ OR
  - $\sigma_{LC} \geqslant \sigma_{FLOW} = 1/2\ (\sigma_{YIELD} + \sigma_{ULT.})$ GOVERNS FOR A316 S.S.
- SYSTEM EVALUATION
  - INTEGRATE ALL JOINTS IN THE SYSTEM
  - INTEGRATE THROUGH SEISMIC HAZARD CURVE

8

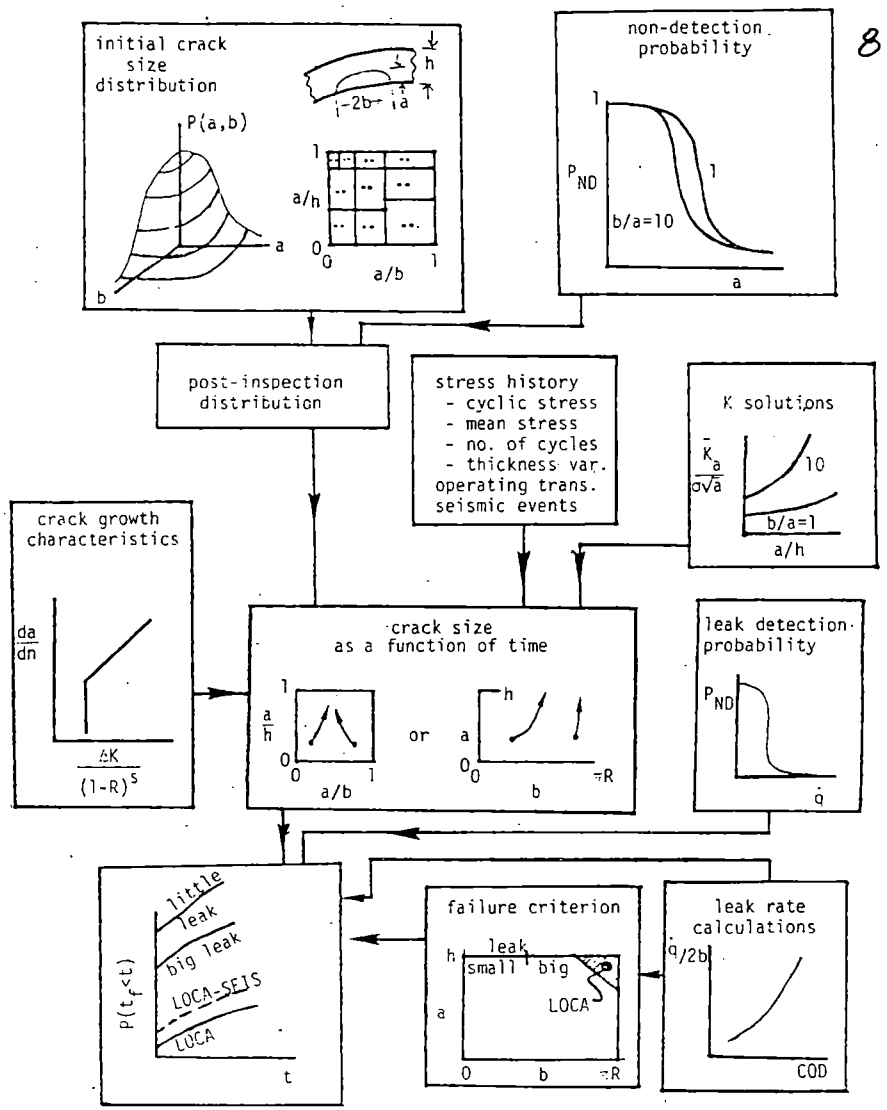

Schematic Diagram of Steps in Analysis of Reliability of a Given Weld Location.

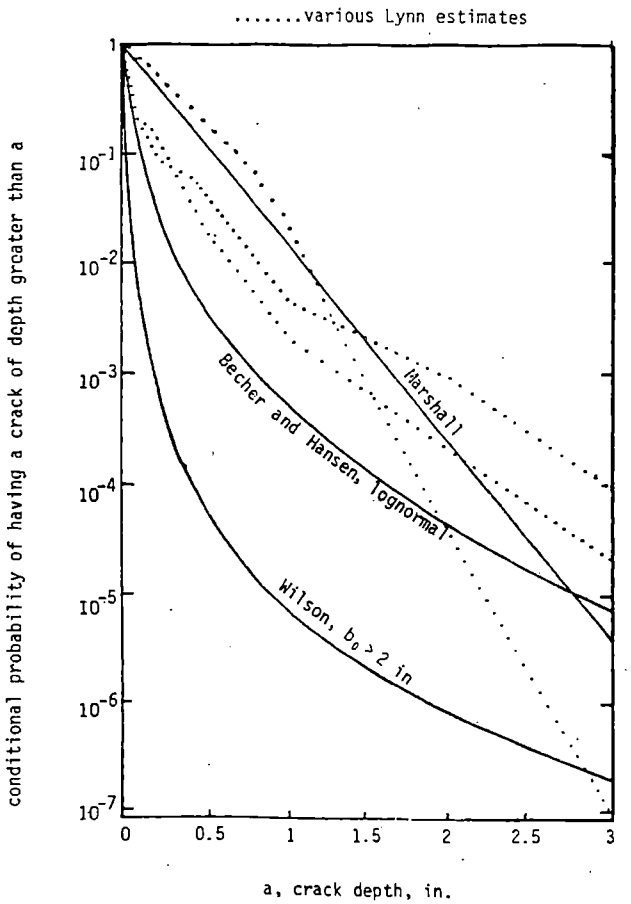

Various Complementary Cumulative Marginal Crack Depth Distributions.

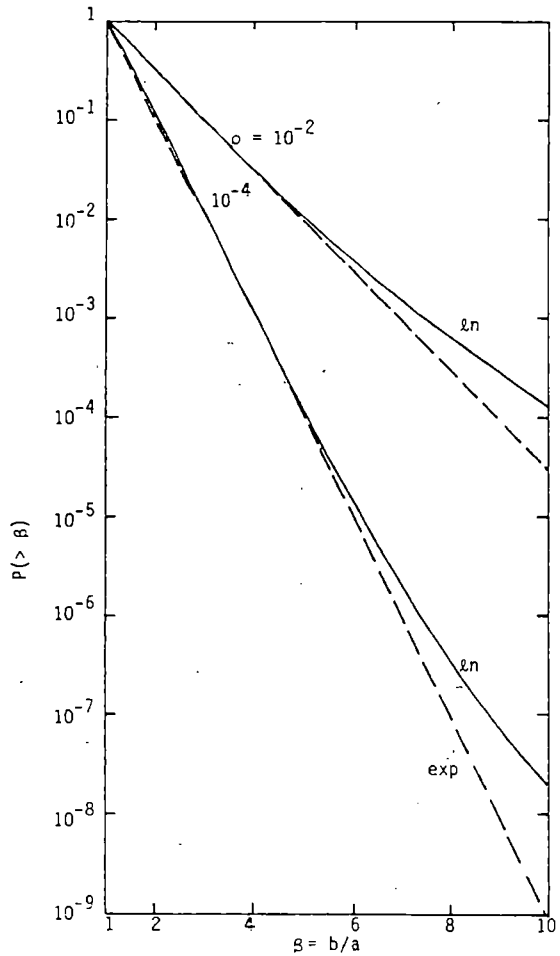

Various Complementary Cumulative Marginal Distributions of Crack Aspect Ratio.

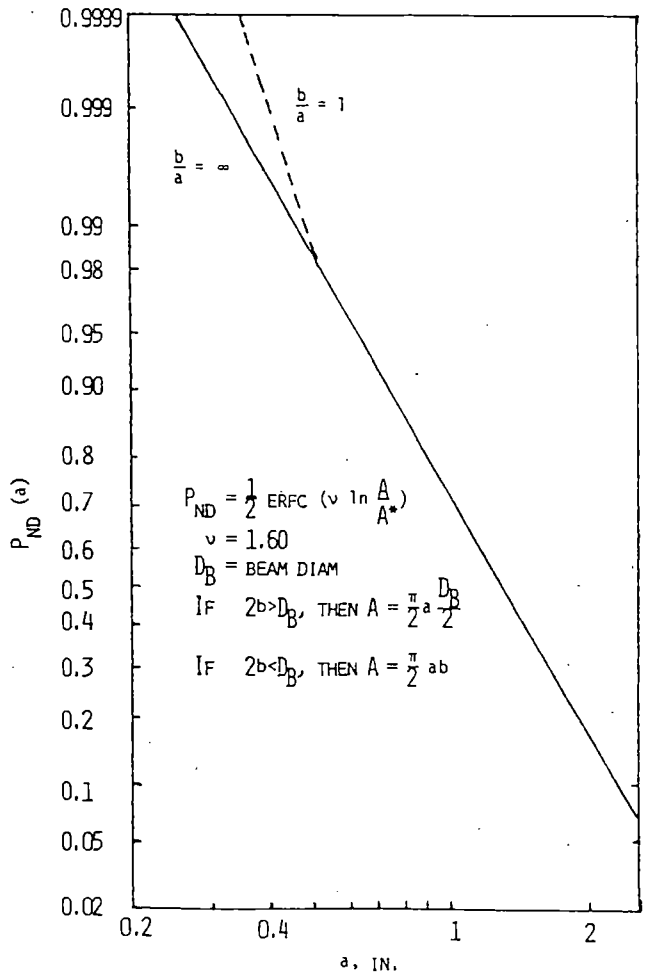

Two Dimensional Lognormal Model for Probability of Non-Detection of a Crack in Cast Austenitic Material.

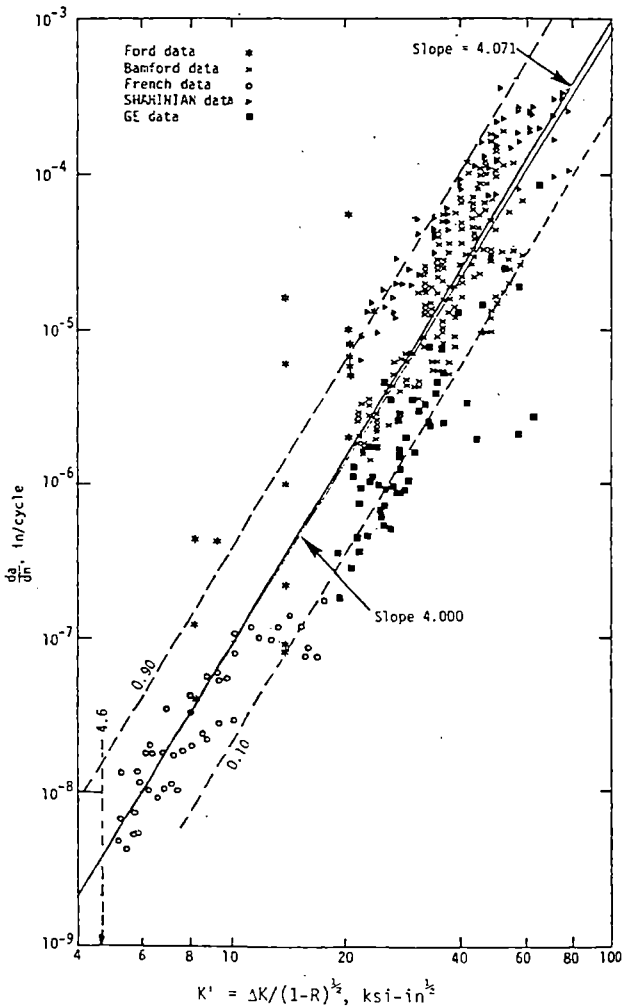

Fatigue Crack Growth Rate Data as a Function of Effective Stress Intensity Shown Along with the Least Square Curve-Fit.

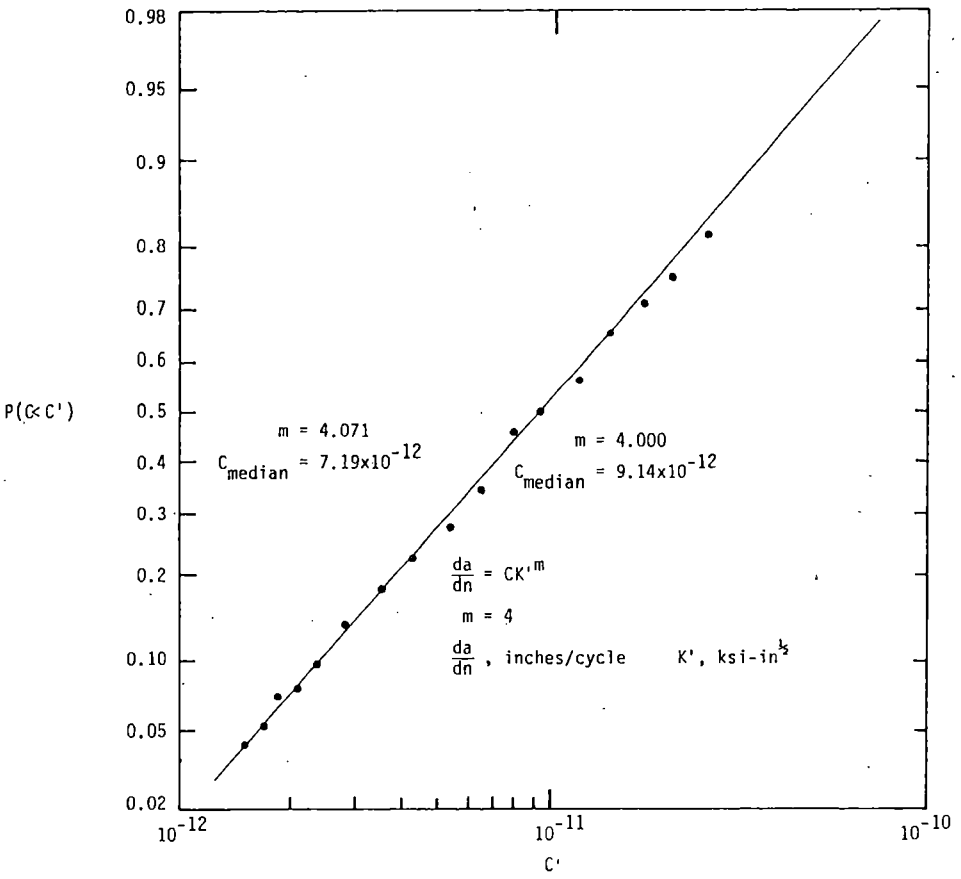

Cumulative Distribution of C Plotted on a Lognormal Probability Paper.

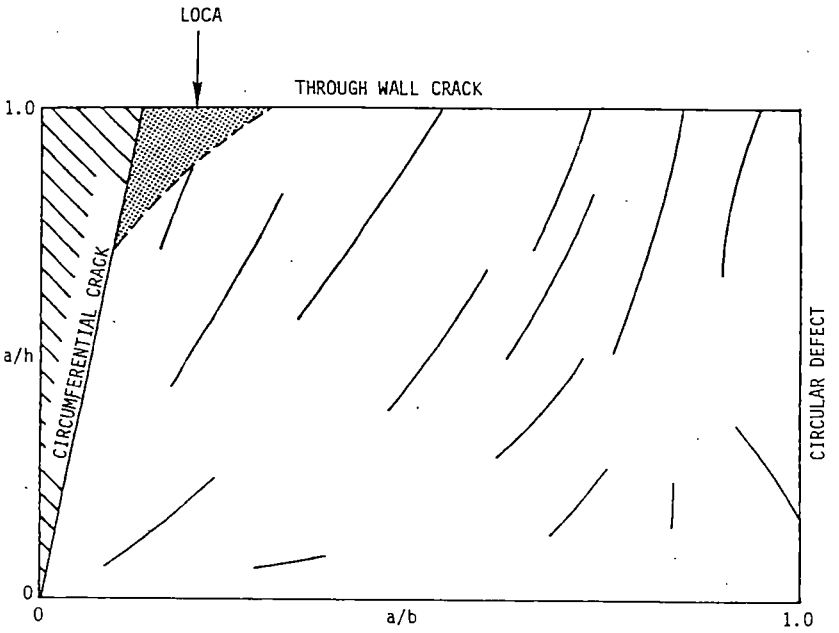

Sample Space for PRAISE Code.

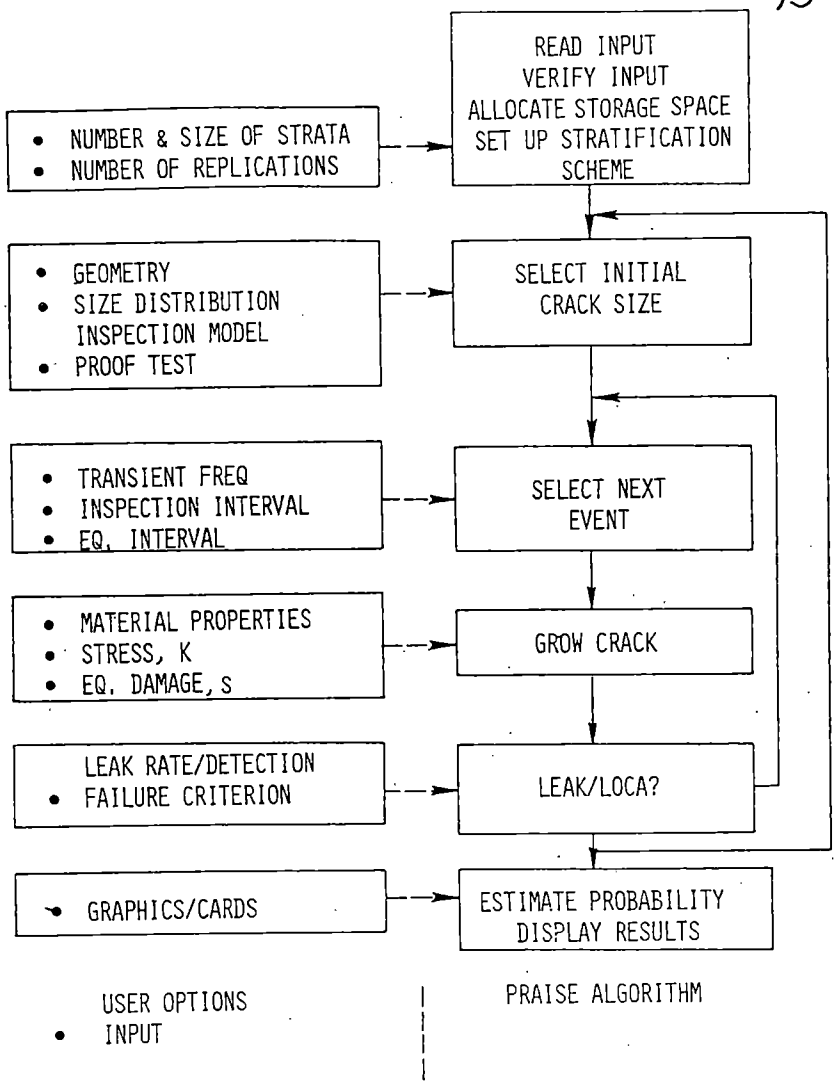

Simplified Praise Flowchart.

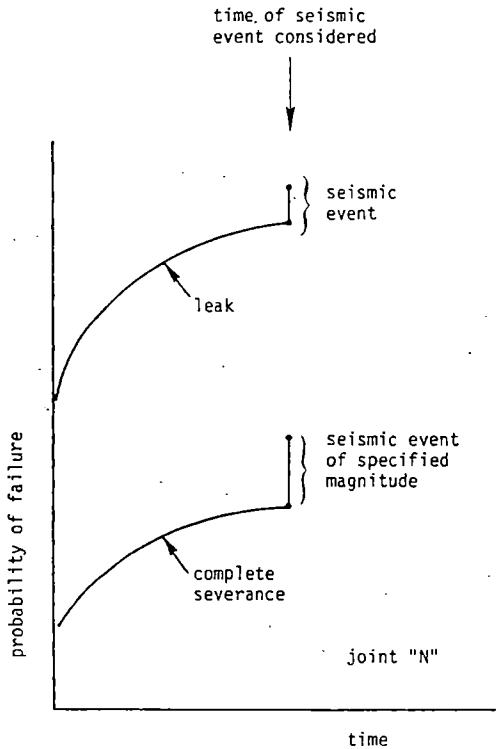

Schematic Representation of Type of Basic Results Generated to Ascertain Influence of Seismic Events on Piping Weld Joint Reliability.

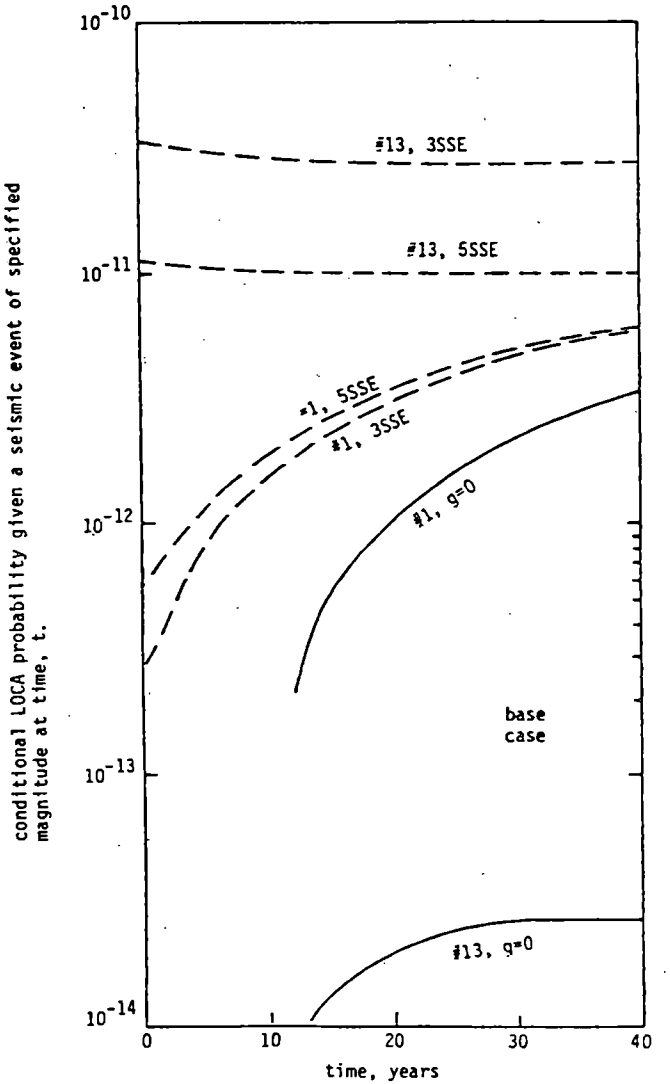

Conditional LOCA Probability as a Function of Time for Two Representative Weld Locations Showing Influence of Seismic Events.

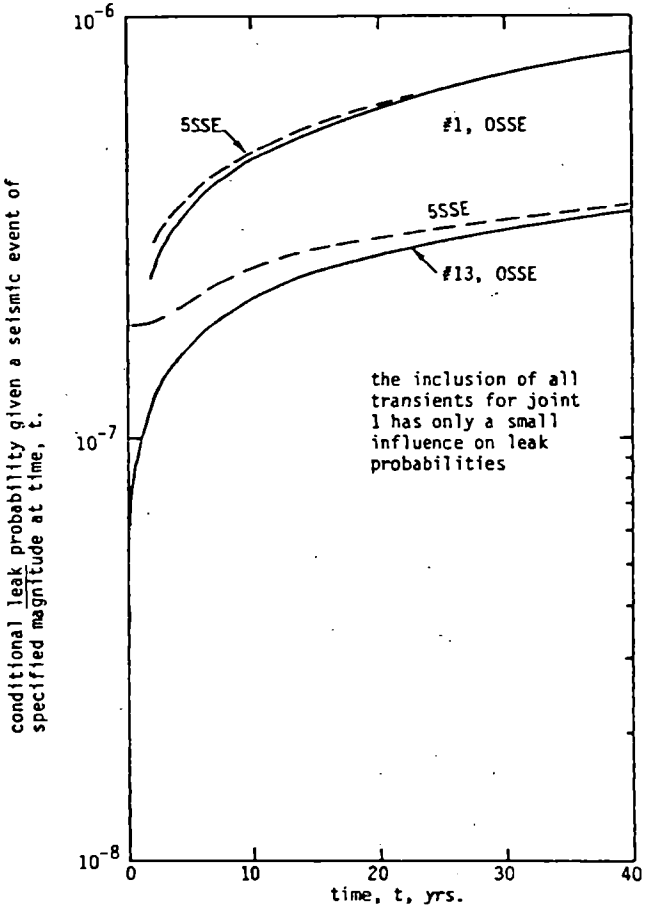

Conditional Leak Probabilities as a Function of Time for Two Representative Weld Locations Showing Influence of Seismic Events.

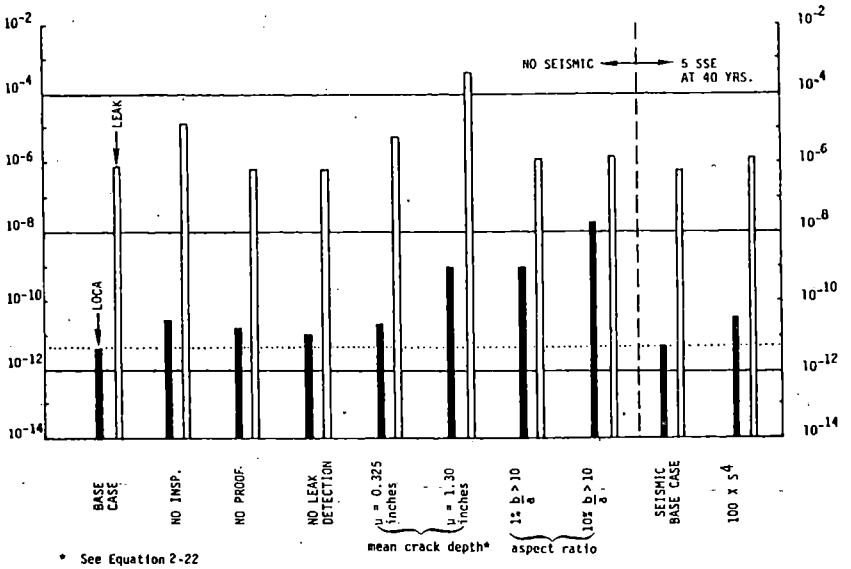

* See Equation 2-22

Cumulative Probability of Failure at Hot Leg to Pressure Vessel Weld Within 40 Years, Given That a Crack is Initially Present.

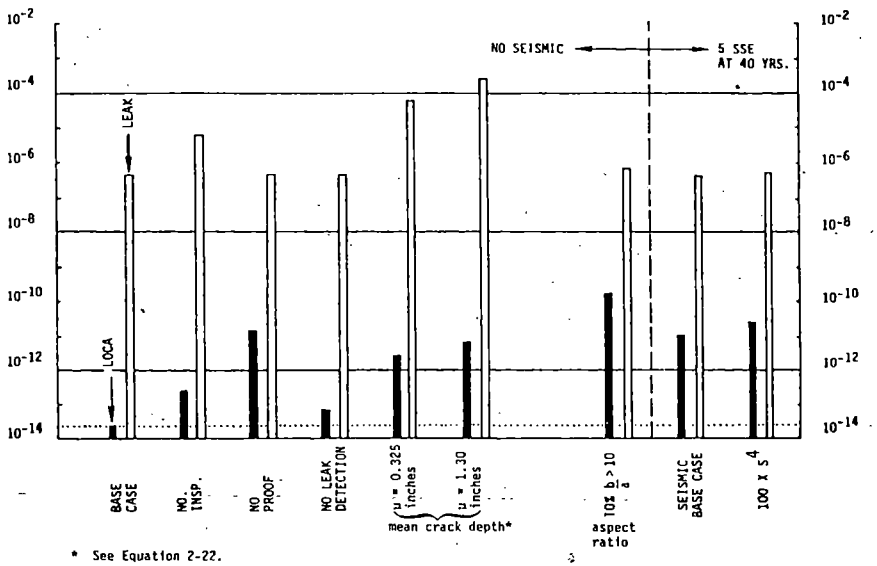

* See Equation 2-22.

Cumulative Probability of Failure at Cold Leg Elbow Weld Within 40 Years, Given that a Crack is Initially Present.

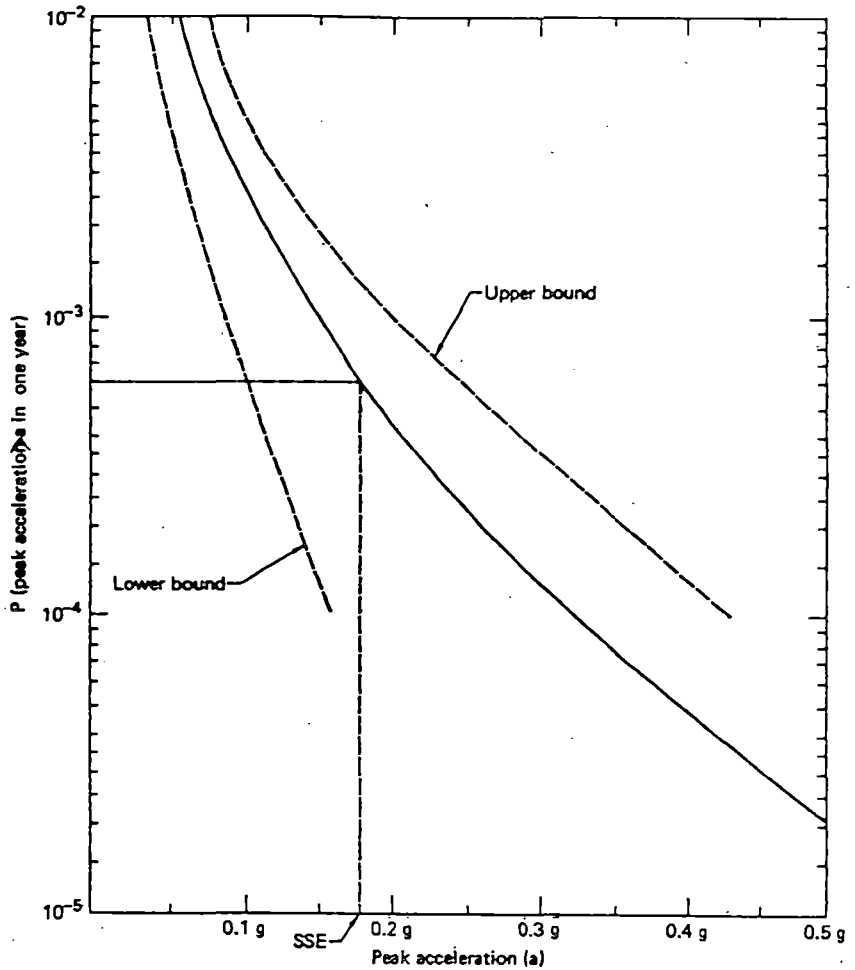

Seismic hazard curve at Zion-1.

DIRECT FAILURE RESULTS
(FAILURE CAUSED BY FATIGUE CRACK GROWTH)

- THE PROBABILITY OF A DOUBLE-ENDED GUILLOTINE BREAK INDUCED BY PLANT TRANSIENTS GIVEN THE CONDITION THAT NO EARTHQUAKE OCCURS DURING THE 40-YEAR PLANT LIFE IS ESTIMATED TO BE 1.6×10^{-12}.
- THE PROBABILITY OF A DOUBLE-ENDED GUILLOTINE BREAK INDUCED BY PLANT TRANSIENTS AND EARTHQUAKES IS ESTIMATED TO BE 1.8×10^{-12}.
- THE PROBABILITY OF AN EARTHQUAKE AND AN EARTHQUAKE-INDUCED DOUBLE-ENDED GUILLOTINE BREAK OCCURING SIMULTANEOUSLY DURING THE PLANT'S LIFE IS ABOUT 4×10^{-13}.
- THE PROBABILITY OF LEAK IS ESTIMATED TO BE 8×10^{-7} DURING THE PLANT'S LIFE.

CONCLUSIONS

- PRIMARY COOLANT LOOP BREAK AS A RESULT OF FATIGUE CRACK GROWTH SUBJECTED TO ALL PLANT TRANSIENTS INCLUDING SEISMIC IS EXTREMELY UNLIKELY.

- CURRENT DESIGN REQUIREMENTS OF POSTULATING ASYMMETRIC BLOWDOWN EVENTS AND THE COMBINATION OF LARGE LOCA WITH SSE ARE NOT NECESSARY FOR THE PLANTS HAVING SIMILAR SYSTEM DESIGN AS ZION UNIT I.

- IN MAKING ABOVE LICENSING DECISION SPECIAL EFFORTS NEED TO BE MADE:
  - TO AVOID INDIRECT PIPE FRACTURE
  - TO AVOID WATER HAMMER
  - TO AVOID CONSTRUCTION AND DESIGN ERRORS

DISCUSSIONS

- ASSUMPTIONS
- VALIDATIONS
- UNCERTAINTIES
- RESULT GENERALIZATION
- INDIRECT CAUSED LOCA
- CONSTRUCTION AND DESIGN ERRORS

TECHNICAL DETAILS ARE PROVIDED IN THE FOLLOWING REPORTS

PROBABILITY OF PIPE FRACTURE IN THE PRIMARY COOLANT LOOP OF A PWR PLANT, NUREG/CR-2189

- VOLUME 1: SUMMARY
- VOLUME 2: PRIMARY COOLANT LOOP MODEL
- VOLUME 3: NON-SEISMIC STRESS ANALYSIS
- VOLUME 4: SEISMIC RESPONSE ANALYSIS
- VOLUME 5: PROBABILISTIC FRACTURE MECHANICS ANALYSIS
- VOLUME 6: FAILURE MODE ANALYSIS
- VOLUME 7: PIPING SYSTEM FRACTURE PROBABILITY ESTIMATION
- VOLUME 8: PIPE FRACTURE INDIRECTLY INDUCED BY EARTHQUAKES
- VOLUME 9: PRIASE COMPUTER CODE USER'S MANUAL

PIPING RELIABILITY MODEL VALIDATION BASED ON PWR FEEDWATER LINE CRACKING DATA

Dr. H. H. Woo

Lawrence Livermore National Laboratory
University of California
P. O. Box 808, L-90
Livermore, California 94550, U.S.A.

SUMMARY

One of the objectives for the Load Combination Program [1] at the Lawrence Livermore National Laboratory was to determine the probability of a large loss-of-coolant accident (LOCA)in the primary piping system induced directly by an earthquake. As a result of this work, a computer code PRAISE (Piping Reliability Analysis Including Seismic Event) was developed [2]. The PRAISE code assumes that piping failures occur as a result of crack-like defects introduced during fabrication, with the initial crack size being randomly distributed. The linear elastic fracture mechanics technique is used to calculate crack growth during service transients. In addition to initial crack size distribution, other mechanisms that affect crack growth are fatigue crack growth, vibratory stresses, and residual stresses, stress corrosion cracking. The piping model has been applied to the primary coolant loop at Unit 1 of the Zion plant. The results showed that the probability of the simultaneous occurrence of an earthquake and a large LOCA is about 4×10^{-13} per plant life and the probability of leaking during plant life is estimated to be 1.26×10^{-9} [3]. This very low probability result can not be verified through actual data base because there is no operating failure reported.

Instead PWR feedwater line cracking incidents were chosen. to validate the piping reliability model developed in PRAISE. The first incident was reported by Indiana & Michigan Power Company to the Nuclear Regulatory Commission (NRC),on May 20, 1979 for the leaking of two feedwater lines of D.C. Cook Unit 2. Circumferential leaking cracks were identified in the 16-in.(406-cm) lines in the immediate vicinity of the steam generator nozzles. Subsequent volumetric examination (radiography) revealed crack indications at similar locations in all feedwater lines of both Units 1 and 2. As a result of this finding NRC issued Bulletin 79-13 [4] which requires inspection of all PWR feedwater lines. Inspections through March 1980 have revealed piping cracks or fabrication defects that requires repair in the vicinity of the feedwater nozzles at 16 of 35 PWR plants [5]. In an effort to identify the mechanisms of cracking at PWR feedwater lines, an Owner's Group, with the technical support from Westinghouse Corporation, was formed. Extensive studies concluded that the primary cause of cracking is thermal fatigue [6].

With the help from the information contained in Reference 6, the PRAISE code was validated by evaluating the feedwater lines of five plants--D.C. Cook 2, H.B. Robinson, Salem 1, R.E. Ginna, and Millstone 2. The time up to the inspection of feedwater line cracking since the first day of commerical service for these plants ranges from 11 months (D.C. Cook 2) to 10 years (R. E. Ginna). Furthermore, the metallurigical investigation [7] revealed that the cracks varied from through-wall cracking at D.C. Cook 2 to 13% partial wall penetration at R. E. Ginna. All cracks were initiated from pipe inner surfaces. Comparison of failure probabilities estimated by PRAISE and failure data in five PWR plants showed that the piping reliability model used in PRAISE can provide a reasonable estimate of the reliability of PWR feedwater lines.

REFERENCES

[1] S. Lu, R. D. Streit, and C. K. Chou, "Probability of Pipe Fracture in the Primary Coolant Loop of a PWR Plant, Vol. 1: Summary," NUREG/CR--2189, Vol. 1, Aug. 1981.

[2] E. Y. Lim, "Probability of Pipe Fracture in the Primary Coolant Loop of a PWR Plant, Vol. 9: PRAISE Computer Code User's Manual," NUREG/CR-2189, Vol. 9, Aug. 1981.

[3] L. George and R. Mensing, "Probability of Pipe Fracture in the Primary Coolant Loop of a PWR Plant, Vol. 7: System Failure Probability Analysis," NUREG/CR-2189, Vol. 7, 1981.

[4] U.S. Nuclear Regulatory Commission, Office of Inspection and Enforcement Bulletin No. 79-13, "Cracking in Feedwater System Pipe," June 25, 1979.

[5] U.S. Nuclear Regulatory Commission, "Investigation and Evaluation of Cracking Incidents in Piping in Pressurized Water Reactors," NUREG-0691, Sept. 1980.

[6] Westinghouse Electric Corporation, "Investigation of Feedwater Line Cracking in Pressurized Water Reactor," WCAP-9693, June, 1980.

[7] A. Goldberg, R. D. Streit, and R. G. Scott, "Evaluation of Cracking in Feedwater Piping Adjacient to the Steam Generators in Nine Pressurized Water Reactor Plants," NUREG/CR-1603, Oct. 1980.

PIPING RELIABILITY MODEL VALIDATION BASED ON PWR FEEDWATER LINE CRACKING DATA

PRESENTED BY

DR. H. H. WOO

PRESENTATION TO

9TH WATER REACTOR SAFETY RESEARCH INFORMATION MEETING

GAITHERSBURG, MARYLAND

OCTOBER 26, 1981

OUTLINE OF PRESENTATION

- REVIEW OF PIPING RELIABILITY MODEL
- PWR FEEDWATER LINE CRACKING EXPERIENCE
- RESULTS FOR PIPING RELIABILITY MODEL VALIDATION WORK
- CONCLUSIONS
- RECOMMENDATIONS
- PROPOSED FUTURE WORK
- LLNL LOAD COMBINATION PROGRAM POSITION

REVIEW OF PIPING RELIABILITY MODEL (PRAISE)

- o PROBABILISTIC ELASTIC FRACTION MECHANICS
- o MONTE CARLO SIMULATION & STRATIFIED SAMPLING
- o STATISTICAL DISTRIBUTIONS FOR VARIOUS PARAMETERS
  - INITIAL CRACK SIZE
  - NONDETECTION PROBABILITY
  - PRESERVICE & INSERVICE INSPECTION
  - MATERIAL PROPERTIES
  - LEAK DETECTION PROBABILITY
- o LOADINGS
  - PRESSURE
  - PIPING LOADS
  - SERVICE TRANSIENTS
  - VIBRATORY STRESSES
  - RESIDUAL STRESSES
  - STRESS CORROSION CRACKING
- o LEAK AND LOCA

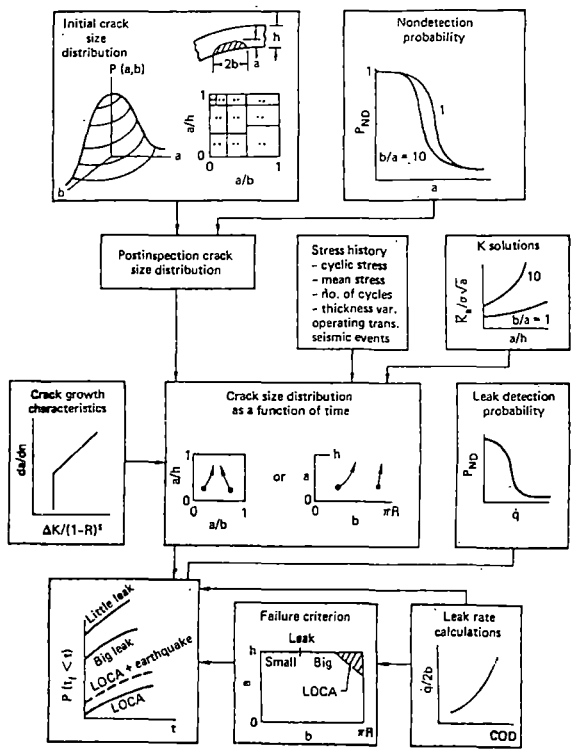

SCHEMATIC REPRESENTATION OF THE VARIOUS STEPS IN THE ANALYSIS SHOWS THEIR INTERRLATIONSHIPS

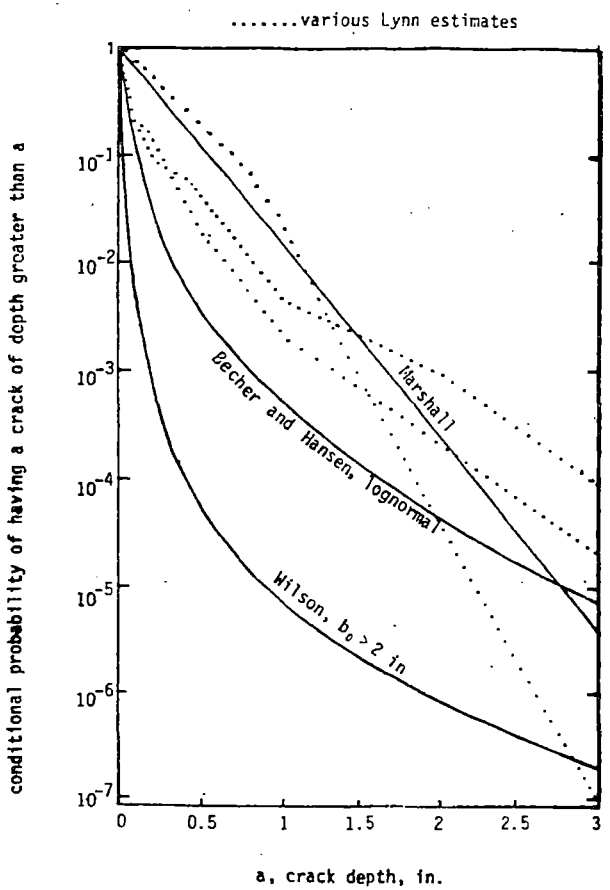

VARIOUS COMPLEMENTARY CUMULATIVE MARGINAL CRACK DEPTH DISTRIBUTIONS

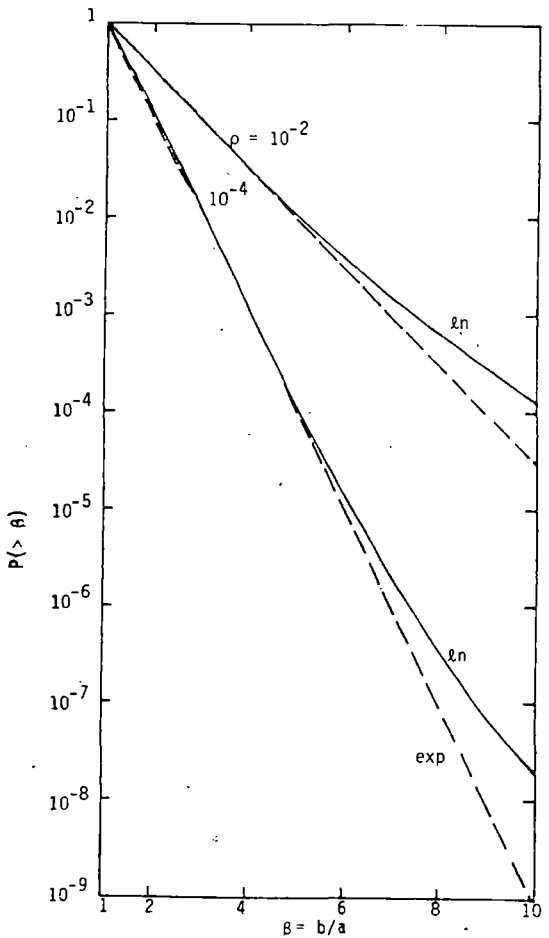

VARIOUS COMPLEMENTARY CUMULATIVE MARGINAL DISTRIBUTIONS OF CRACK ASPECT RATIO

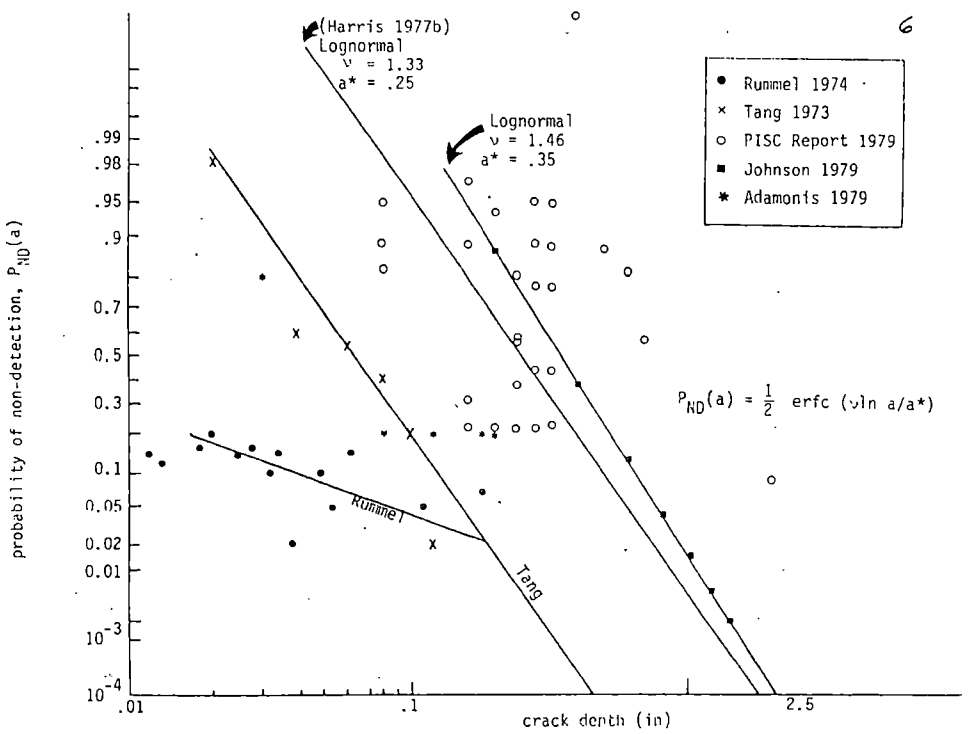

PROBABILITY OF NON-DETECTION OF A CRACK AS A FUNCTION OF ITS DEPTH FOR AN ULTRASONIC INSPECTION--DATA FROM LITERATURE

PWR FEEDWATER LINE CRACKING EXPERIENCE

- BACKGROUND
  - LEAKING IN D. C. COOK 2 MAY 1979
- NRC ACTIONS
  - BULLETIN 79-23, JUNE 1979
  - INSPECTION OF ALL PWR FEEDWATER LINES MARCH 1980
- RESULTS REPORTED FROM UTILITIES
  - MARCH 1980
  - CRACKS FOUND IN 16 OF 35 PWRs

PWR FEEDWATER LINE CRACKING EXPERIENCE (cont)

- PWR PLANTS WITH FEEDWATER LINE CRACKING

- D. C. COOK 1 & 2	SURRY 1 & 2
- H.B. ROBINSON 2	PT. BEACH 1 & 2
- BEAVER VALLEY 1	KEWAUNEE
- SALEM 1	YANKEE ROWE
- R. E. GINNA	PALISADES*
- SAN ONOFRE	MILLSTONE 2*

- COOPERATIVE INDUSTRY PROGRAM
  - OWNERS'S GROUP : 11 UTILITIES
  - TECHNICAL AGENT: WESTINGHOUSE

- CONCLUSION OF INVESTIGATIONS (REFERENCE 6)
  - THERMAL FATIGUE: THERMAL STRATIFICATION
    THERMAL STRIPING

* COMBUSTION ENGINEERING PLANTS

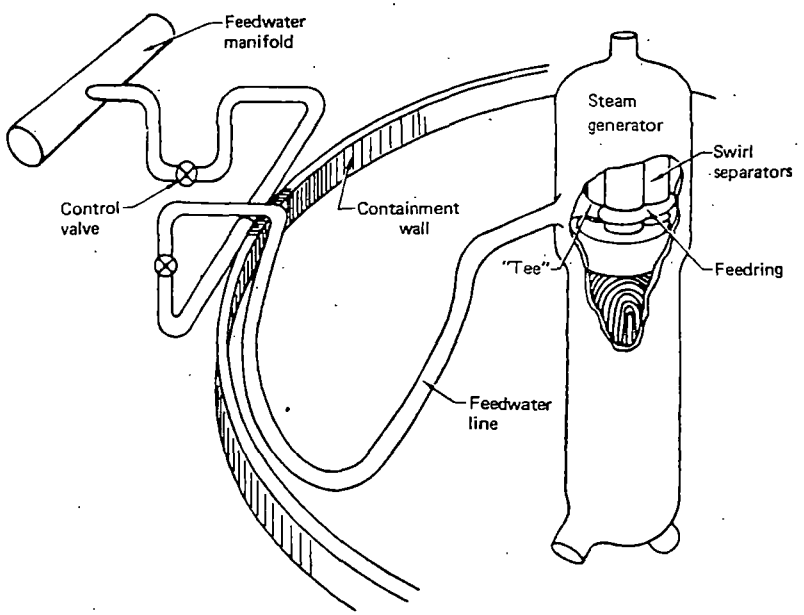

LAYOUT FOR PWR FEEDWATER LINE

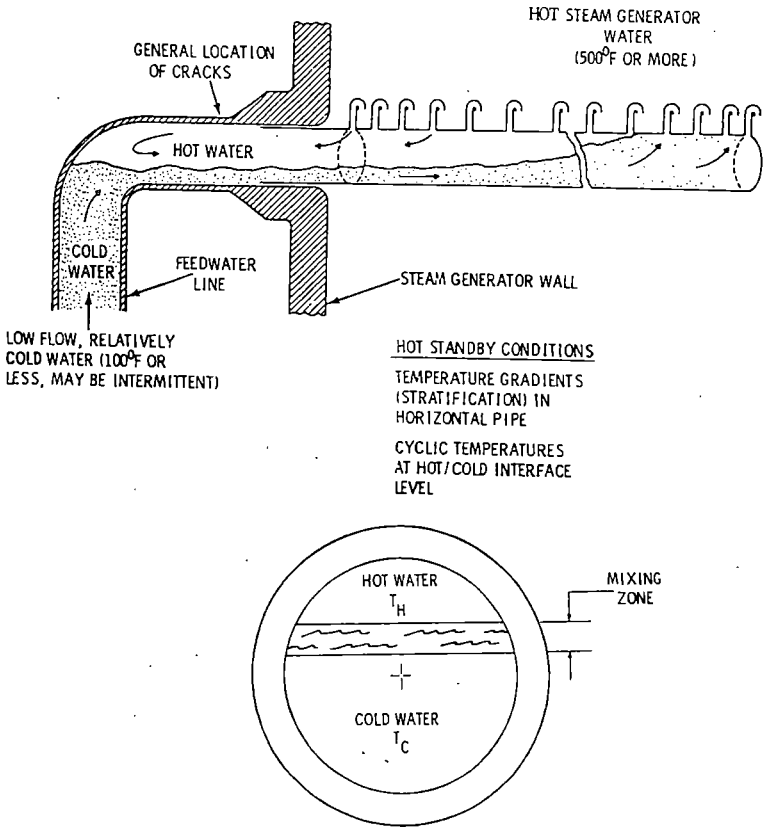

THERMAL STRATIFICATION AND STRIPING PHENOMENON

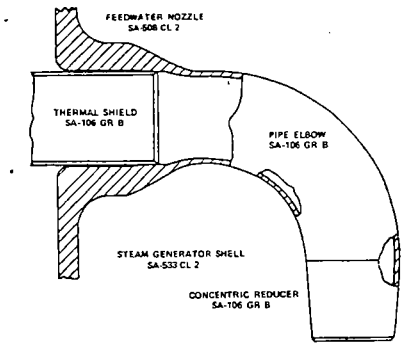

FEEDWATER NOZZLE AND CONNECTION ELBOW

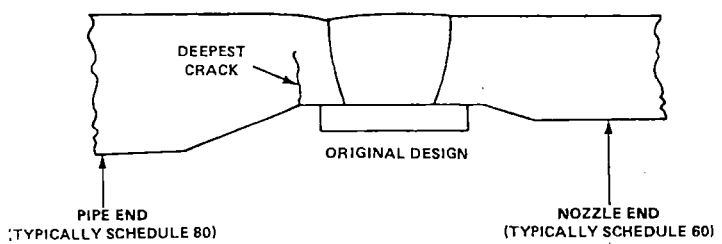

CRACK LOCATION IN FEEDWATER PIPE ELBOW

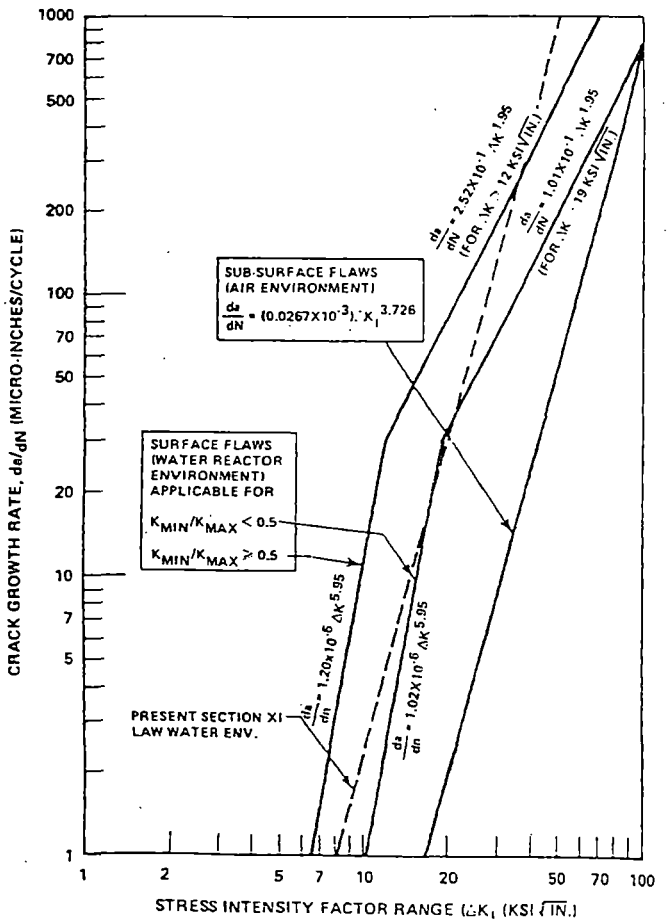

FATIGUE CRACK GROWTH DATA FOR CARBON AND LOW ALLOY FERRITIC STEELS

DESIGN TRANSIENTS (TYPICAL FEEDWATER LINE) AND THERMAL STRATIFICATION TRANSIENTS'

DESIGN[2] TRANSIENT	NUMBER OF OCCURRENCES IN 40 YEARS
SECONDARY SIDE HYDROTEST	5
HOT STANDBY	18,300
UNIT LOAD - UNLOAD 5% PER MINUTE	18,300
SMALL STEP LOAD DECREASE	2,000
LARGE STEP LOAD DECREASE	200
LOSS OF POWER	40
PARTIAL LOSS OF FLOW	30
LOSS OF LOAD	400

NOTES: (1) STRESSES AND NO. OF CYCLES FOR THERMAL STRATIFICATION TRANSIENT ARE CONTAINED IN REFERENCE 6

(2) STRESSES FOR DESIGN TRANSIENTS ARE CONTAINED IN REFERENCE 6

SUMMARY OF OBSERVED CRACKS AND ESTIMATED LEAK PROBABILITY

PLANT	TIME UP TO INSPECTION SINCE SERVICE T'(YR)	MAX CRACK DEPTH A (IN.)	COUNTER BORE THICKNESS T(IN.)	A/T	LEAK PROBABILITY AT T' [2] WITH ISI, PSI	WITHOUT ISI, PSI
A	11 MO	0.57	0.57	1.	0.68	0.9
B	2 YR. 9 MO	0.235	0.875	0.27	0.32	0.63
C	4 YR. 3 MO	0.028	0.75	0.04	0.0022	0.074
D	9 YR.	0.75	1.21	0.62	0.08	0.29
E	10 YR.	0.107	0.843	0.13	0.55	0.92

NOTES: (1) LEAKING WAS DISCOVERED AT PLANT A 5/79, AND THE BALANCE WAS REPORTED IN 3/80 (REF. 5)

(2) ISI = INSERVICE INSPECTION, PSI = PRESERVICE INSPECTION
ISI WAS BASED ON ASME XI INSPECTION PROGRAM A, 1980.

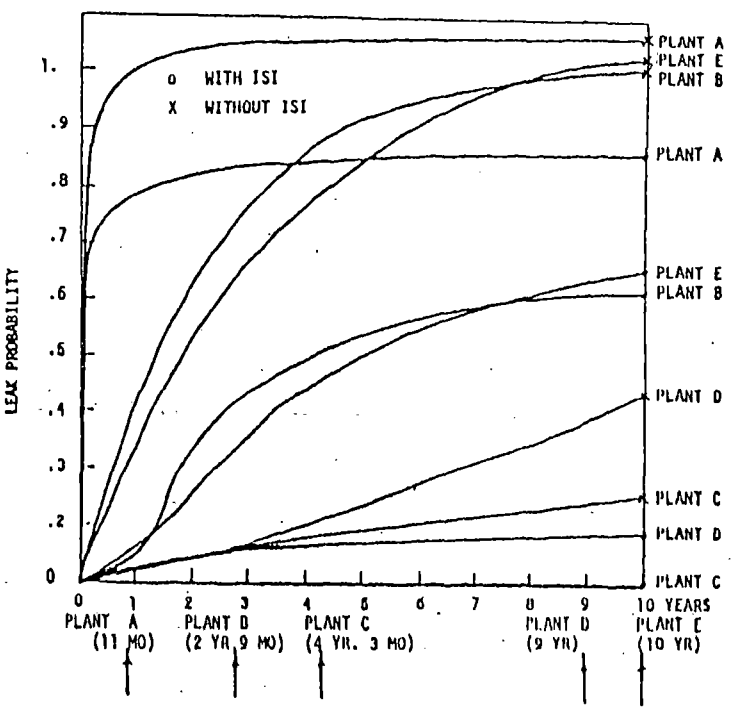

LEAK PROBABILITIES OF FEEDWATER LINES FOR FIVE PWR PLANTS

CONCLUSIONS

- LLNL PIPING RELIABILITY MODEL CAN PROVIDE A GOOD ESTIMATE OF PWR FEEDWATER LINE RELIABILITY
- PRESERVICE AND INSERVICE INSPECTIONS WILL DEFINITELY INCREASE PWR FEEDWATER LINE RELIABILITY

RECOMMENDATIONS

- AUGMENTED INSPECTION PLAN FOR PWR FEEDWATER LINE IS REQUIRED.
- DEVELOPMENTS OF IMPROVED CRACK DETECTION METHODS ARE NECESSARY.
- IMPROVED OPERATION PROCEDURE TO AVOID THERMAL STRATIFICATION PHENOMENON FOR PWR FEEDWATER LINES IS RECOMMENDED.

PROPOSED FUTURE WORK

- CONTINUE ON VALIDATION WORK
- PROVIDE SUGGESTIONS TO IMPROVE PLANT OPERATIONS
- PROPOSE NEW DESIGN CRITERIA FOR FUTURE PLANTS
- MODIFY PIPING RELIABILITY MODEL AND APPLY IT TO PRESSURE VESSELS

LLNL LOAD COMBINATION PROGRAM POSITION

- ARE WILLING TO OFFER HELP TO NUCLEAR INDUSTRY
- REQUIRE COOPERATION FROM UTILITIES, VENDERS AND CONSULTING FIRMS
- NEED ASSISTANCE FROM NRC

Ninth Light Water Reactor Safety Research Information Meeting
October, 1981, Gaithersburg, Maryland

LOAD COMBINATIONS: RELIABILITY APPROACH AND LOAD COMBINATION CRITERIA

Dr. C. Allin Cornell
P.O. Box 9260
Stanford, CA 94305-2179

In an environment of rapidly growing application of probabilistic risk analysis (PRA) in nuclear power plants (NPP), it is important to address its place in the structural/mechanical field. This presentation considers first some of the implications of possessing a capability of evaluating quantitatively the reliability of mechanical components. These include improved "deterministic" design criteria for load combinations. Secondly, the presentation discusses recent developments towards achieving, demonstrating, and excercising that capability. In particular, these are the results of the Lawrence Livermore National Laboratory's (LLNL's) Load Combination Methodology Development Project*, sponsored by NRC. In order to evaluate component reliability it is essential, of course, to be able to consider probabilistically the multiple static and dynamic load history over the life of the component, i.e., to analyze stochastic load combinations.

Given the ability to analyze mechanical component reliability under multiple stochastic loads, the profession could use it for several purposes. First, we could use it to study a particular existing (or planned, designed) component, a pipe run, for example. Analogous to plant PRA's, this component reliability could be compared with quantitative safety goals (QSG) for such components to assess the adequacy of the element. Such goals are being prepared for NPP's in the U.S. It remains, however, to allocate those plant goals to specific system (e.g., AFWS) and specific component goals, a necessity if PRA is to be applied in this way at the component level. Second, with PRA for individual mechanical/structural components under combined loads, we have the input needed for thorough plant PRA's. For example, the probabilities of

*Project II, Load Combination Methodology, of the Load Combination Program, See Project II Final Report, NUREG/CR-2087, UCRL-53025, September, 1981.

certain initiating events and of certain failures in system fault trees depend on structural/mechanical behavior, e.g., under normal plus seismic plus accident load conditions. To date, probabilistic multiple load analysis has not been used as explicitly as one would like in these plant PRA's.

We could have a second primary use for component analysis capability. We could evaluate a conventional set of design criteria or of (existing plant) review criteria. Because the item-by-item probabilistic evaluation above would be expensive and initially impractical, criteria in conventional (deterministic) formats such as the ASME code (together with NRC/client load cases) will remain necessary indefinitely. But in establishing such criteria for, for example, new PWR's or all GE Mark II BWR's, the profession could use component analysis repeatedly on a sample of representative components that have been deemed adequate by the proposed set of criteria to provide the information to evaluate the criteria set in general. A sample is necessary because no set of deterministic criteria can be expected to produce uniform reliability results. There are two implications. First, a representative sample is necessary. Second, the results are a family of failure probabilities, which can be best represented by a histogram. Different criteria sets (e.g., different choices of design load levels, design combinations, and service level choices) will produce histograms of different kinds. We would therefore have to establish QSG for criteria reliability (or "failure probability") histograms. For example, the mean must be less than 10^{-4} and the 90% percentile less than 10^{-3}. For the advantage of design efficiency, the system must tolerate components of somewhat uncertain reliability.

A third use of the structural/mechanical reliability calculation is suggested immediately by the second. If one can evaluate a criteria set, he can compare two or more sets and choose the best. For example, if two criteria sets are identical except that they suggest different rules for combining dynamic responses (e.g., SRSS vs. absolute sum), then evaluating samples of designs to each criteria set will yield two histograms of failure probabilities. It may or may not be an easy task to determine the preferred criteria set: is it better to have a low mean and high dispersion than the opposite? Presumably system studies would be necessary to resolve such conflicts. The fourth use is a simple next step. It is to use this criteria set comparison capability systematically to develop an "optimal" criteria set. At least within a parametric class of criteria sets, one adjusts parameters (e.g., design load return periods) to find the "best" set of criteria. To do this systematically, one might choose to minimize some objective function such as the sum of average squared deviations from a "target" (i.e., QSG) failure probability.

A fifth use of the component safety analysis under combined stochastic loads can be envisioned: as a building block in an algorithm for determining "optimal" (i.e., good) allocation of plant QSG among components. This might be done (a) for an individual plant or for a set of plants, and (b) for individual components or for, again, criteria sets.

From 1979 through 1980 a team working through LLNL set out to address some of the technical aspects of these problems. (Initially, of course, the "load combination" problem was not viewed in the terms stated above; this point of view itself represents a product of the project.) We have developed, first, a viable robust approach to analyzing the reliability of mechanical components under combined stochastic histories of loads of several types. Second, we have made initial attempts at applying the capability to the criteria set evaluation, comparison, and even (in a narrow sense) optimization. The development process and the attempt to apply it to a sample of essential service water (ESW) pipes both led to several insights, further developments, and further development needs. In addition it can now be specified what the preferred data for a realistic application would be. Something can be done with less data, of course; it would always represent at least as much information as is used in current criteria set decisions. Some details are given in the attached transparencies. The final report of the project contains further details and is referenced above. A project at the Center of Brookhaven National Lab with somewhat parallel aims has begun to attack the same problem for structural elements. Much more effort is needed to complete the process begun.

DESIGN CRITERIA FOR SHIPPING CONTAINERS USED FOR TRANSPORTING IRRADIATED FUEL

DR. M. W. SCHWARTZ

Lawrence Livermore National Laboratory
University of California
P. O. Box 808, L-90
Livermore, California 94550, U.S.A.

SUMMARY

This presentation summarizes the results of Phase I of a project to develop design criteria for shipping containers used for transporting irradiated fuel. The project is concerned with two materials for shipping containers; nodular or ductile cast iron and thick wall (greater than 4") steel forgings. The effort under Phase I which covers the period from July to September of 1981 was devoted to gathering and reviewing materials data, deriving design criteria for one candidate ductile cast iron in accordance with the format of USNRC Regulatory Guide 7.6 and revising the proposal for FY 82 based upon the results of Phase I. The ductile cast iron chosen for study was a ferritic type which appears to be the most likely candidate for shipping containers. Based on data provided by the literature search the design stress intensity for membrane stress was derived in accordance with position 1 of RG 7.6. Available fatigue data were compared with the fatigue curves in Appendix I of Section III of the ASME Boiler and Pressure Vessel Code as required by regulatory position 3b. Fracture toughness properties of the candidate ductile cast iron in terms of Charpy, valid K_{IC} and J_{IC} data were used to approximate a lower bound curve for K_{IC} vs. temperature. Since the lowest operating temperature is in the vicinity of the nil ductility transition temperature the methods of linear elastic fracture mechanics were used to identify the largest allowable flaw size that would not propagate under conditions of general yielding.

DESIGN CRITERIA FOR SHIPPING CONTAINERS USED FOR TRANSPORTING IRRADIATED FUEL

PRESENTED BY

M. W. SCHWARTZ

PRESENTATION TO

9TH WATER REACTOR SAFETY RESEARCH INFORMATION MEETING

GAITHERSBURG, MARYLAND

OCTOBER 26, 1981

LAWRENCE LIVERMORE LABORATORY
University of California

SCOPE OF WORK FOR ESTABLISHING DESIGN CRITERIA FOR SHIPPING CONTAINERS USED FOR TRANSPORTING IRRADIATED FUEL

DUCTILE CAST IRON CONTAINERS

- DESIGN CRITERIA FOR STRUCTURAL ANALYSIS (BASED ON RG 7.6)
- ACCEPTANCE CRITERIA FOR FRACTURE TOUGHNESS
- MATERIAL SENSITIVITIES TO FABRICATION PROCESSES

THICK WALL FORCED STEEL CONTAINERS (> 4")

- ACCEPTANCE CRITERIA FOR FRACTURE TOUGHNESS
- MATERIAL SENSITIVITIES TO FABRICATION PROCESSES

PHASE I EFFORT COVERS PERIOD FROM JULY TO SEPTEMBER 1981

- GATHER AND REVIEW MATERIALS PROPERTY DATA.
- DETERMINE DESIGN CRITERIA FOR ONE CANDIDATE DUCTILE CASE IRON IN ACCORDANCE WITH FORMAT OF RG 7.6
- REVISE INITIAL PROPOSAL WHERE REQUIRED BASED UPON INFORMATION DEVELOPED DURING PHASE I

ULTIMATE TENSILE STRENGTH OF FERRITIC NODULAR CAST IRON VERSUS TEMPERATURE

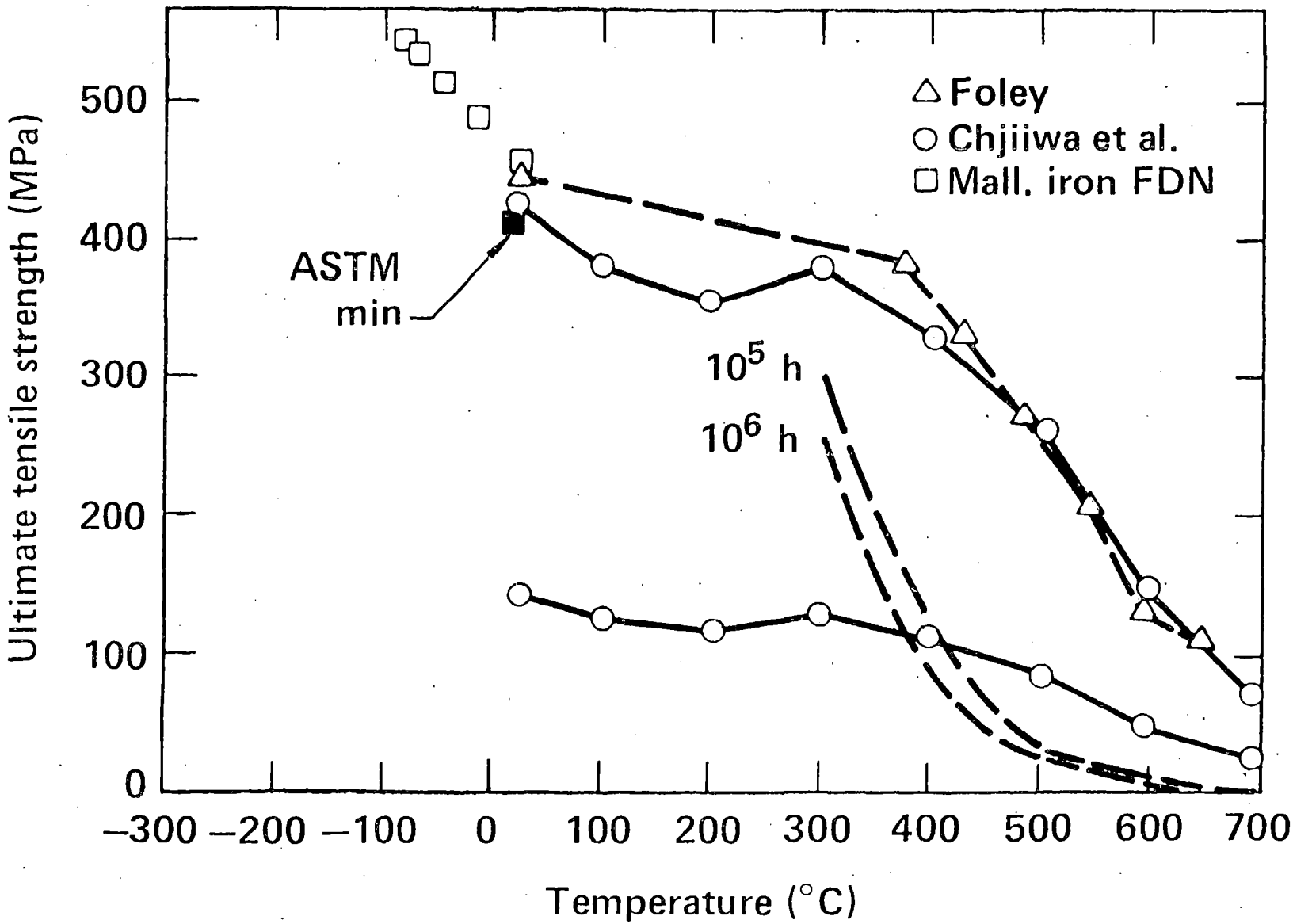

YIELD STRENGTH OF FERRITIC NODULAR CAST IRON VS TEMPERATURE

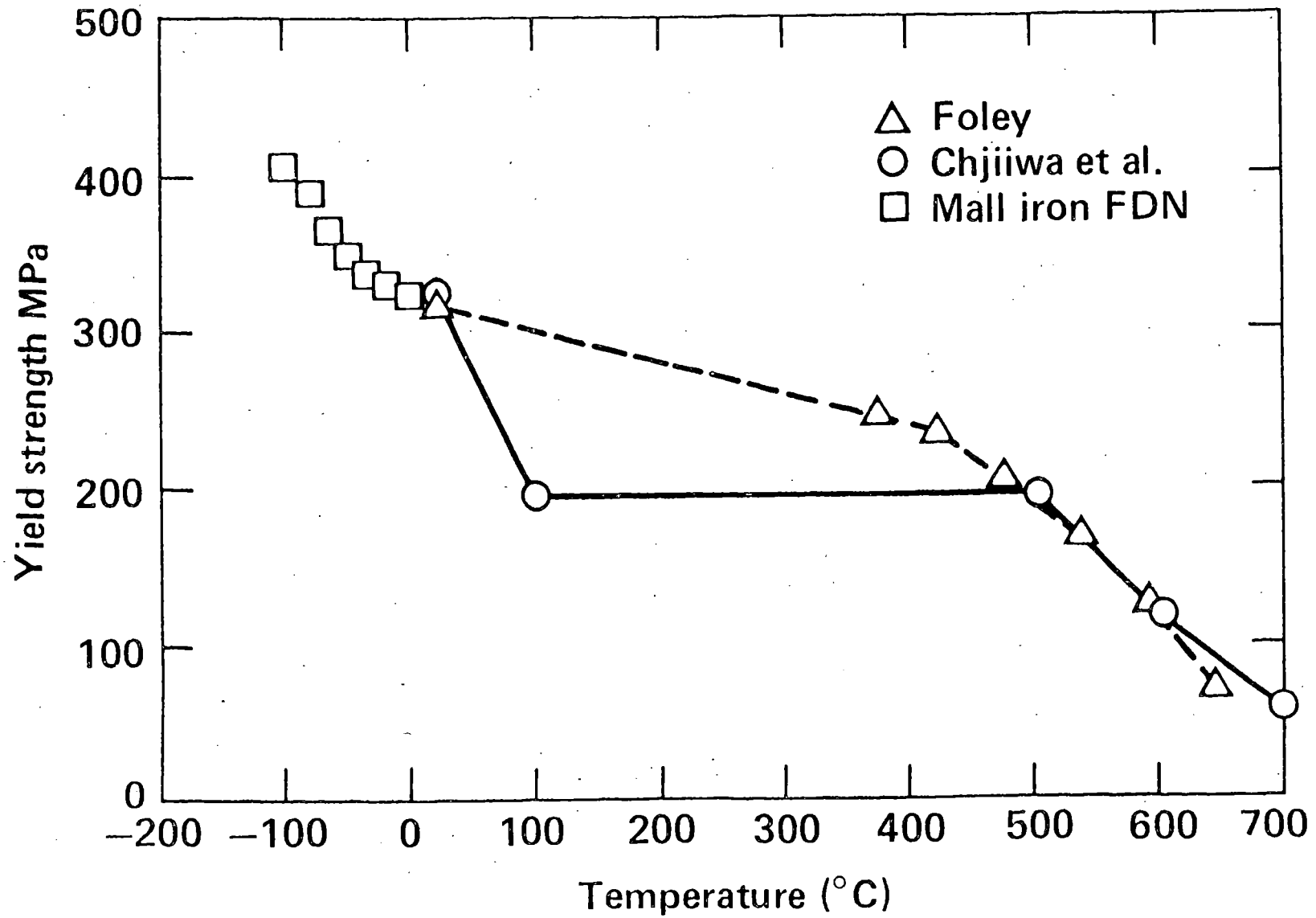

FATIGUE PROPERTIES of DUCTILE CAST IRON

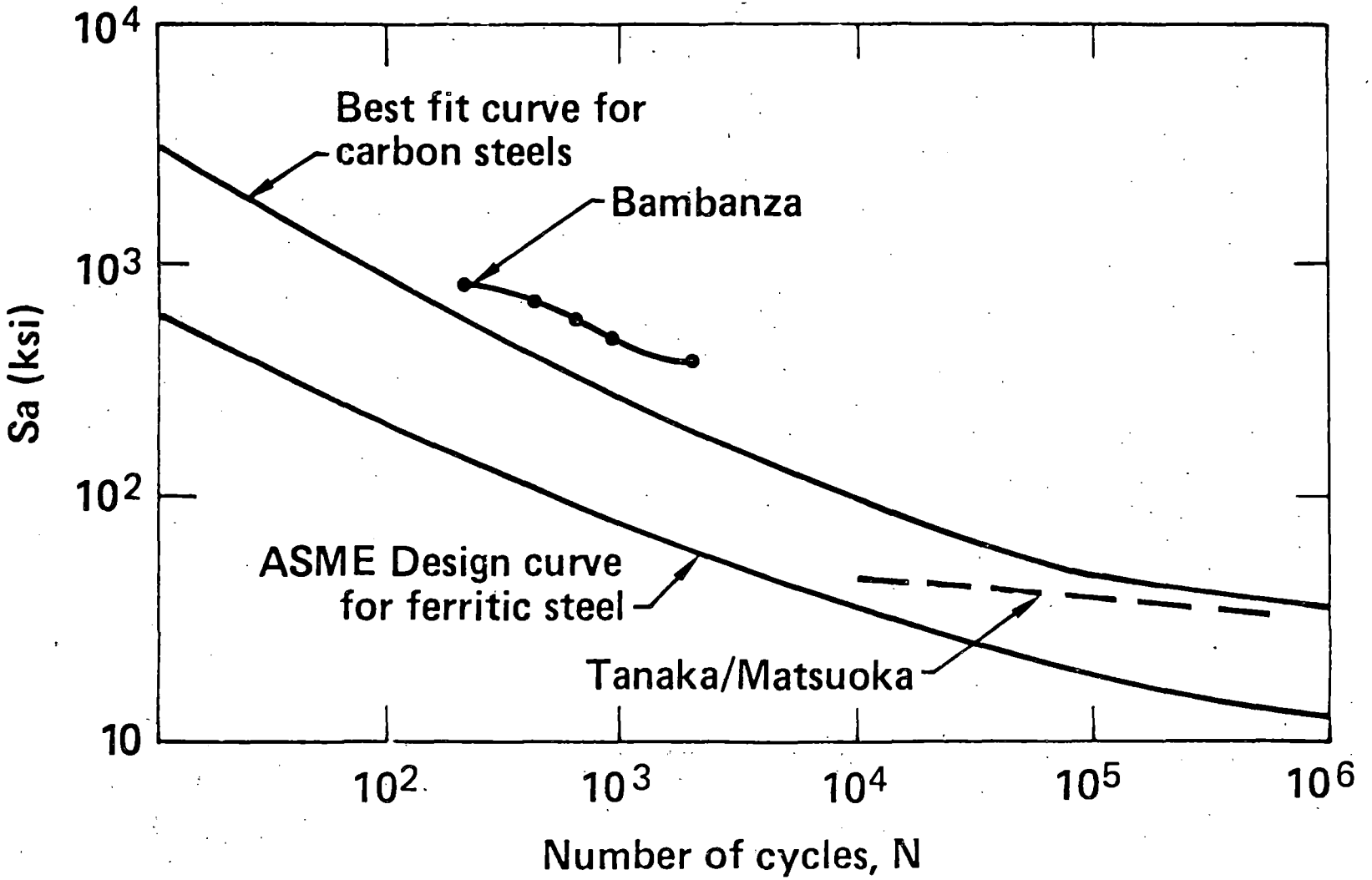

ENVELOPE OF CONSERVATIVE VALUES FOR FATIGUE LIFE REDUCTION FACTOR K_e

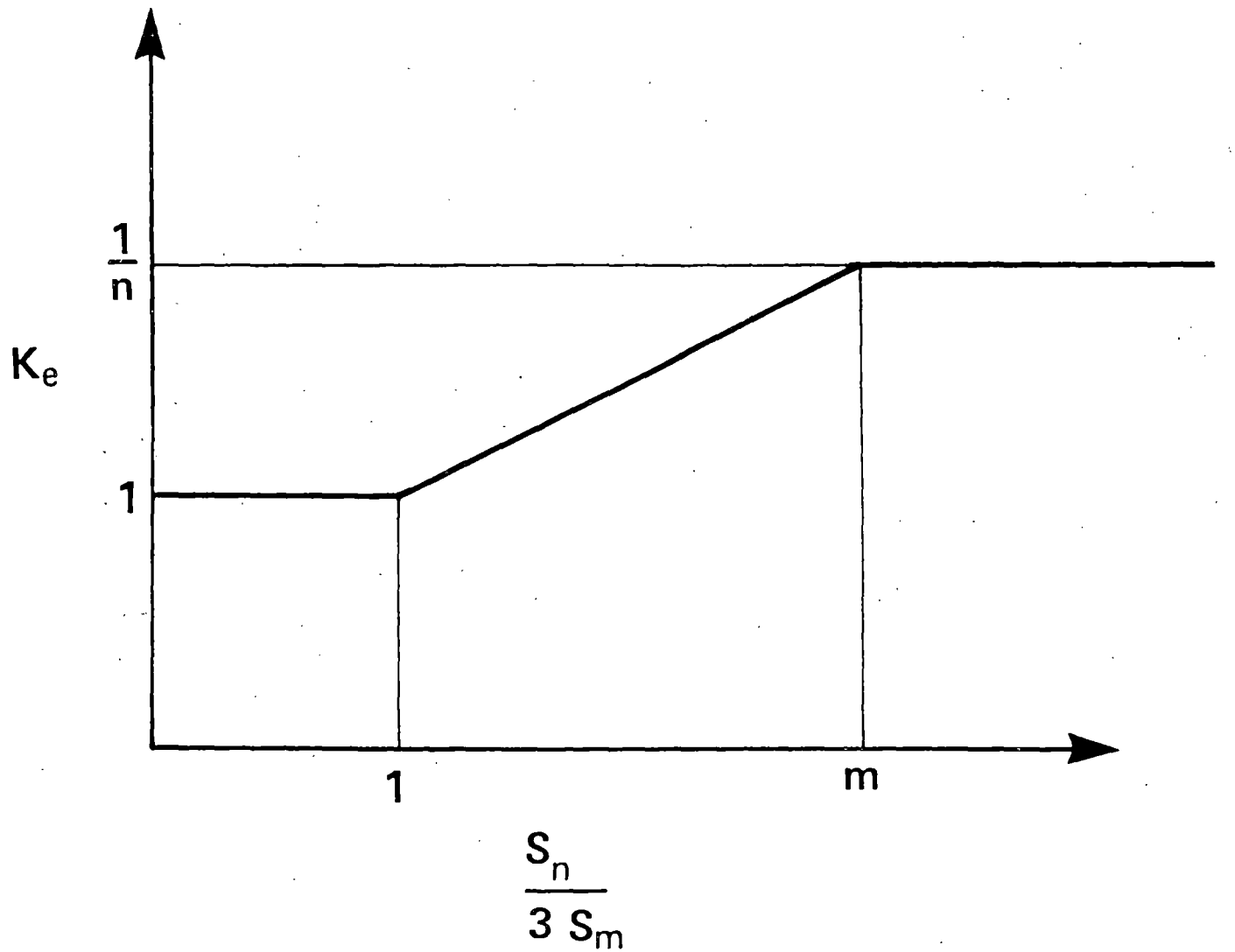

THERMAL STRESS BEYOND WHICH RATCHETING OCCURS

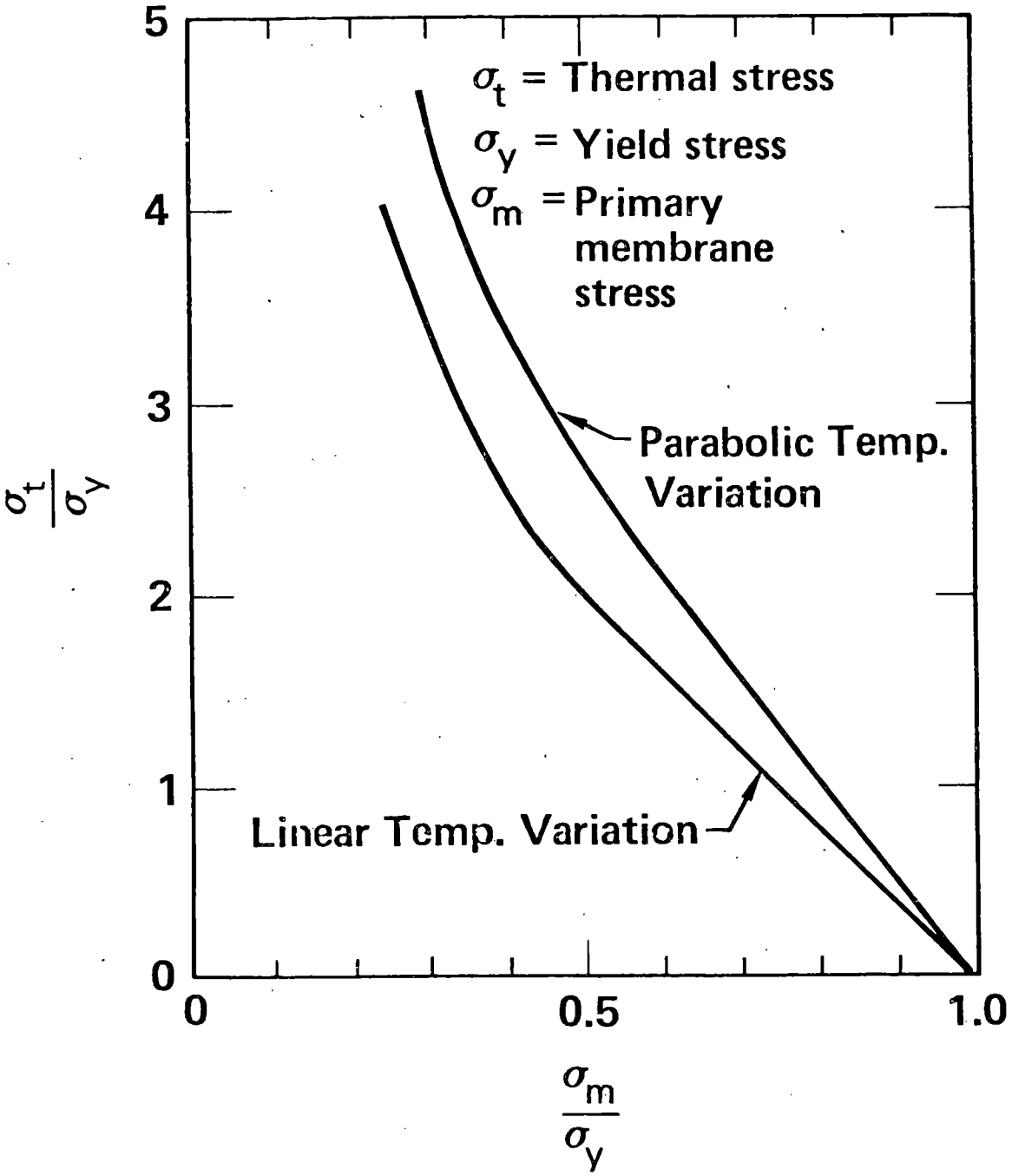

CHARPY "V" NOTCH ENERGY TRANSITIONS FOR DUCTILE IRON, CAST STEEL AND ROLLED STEEL

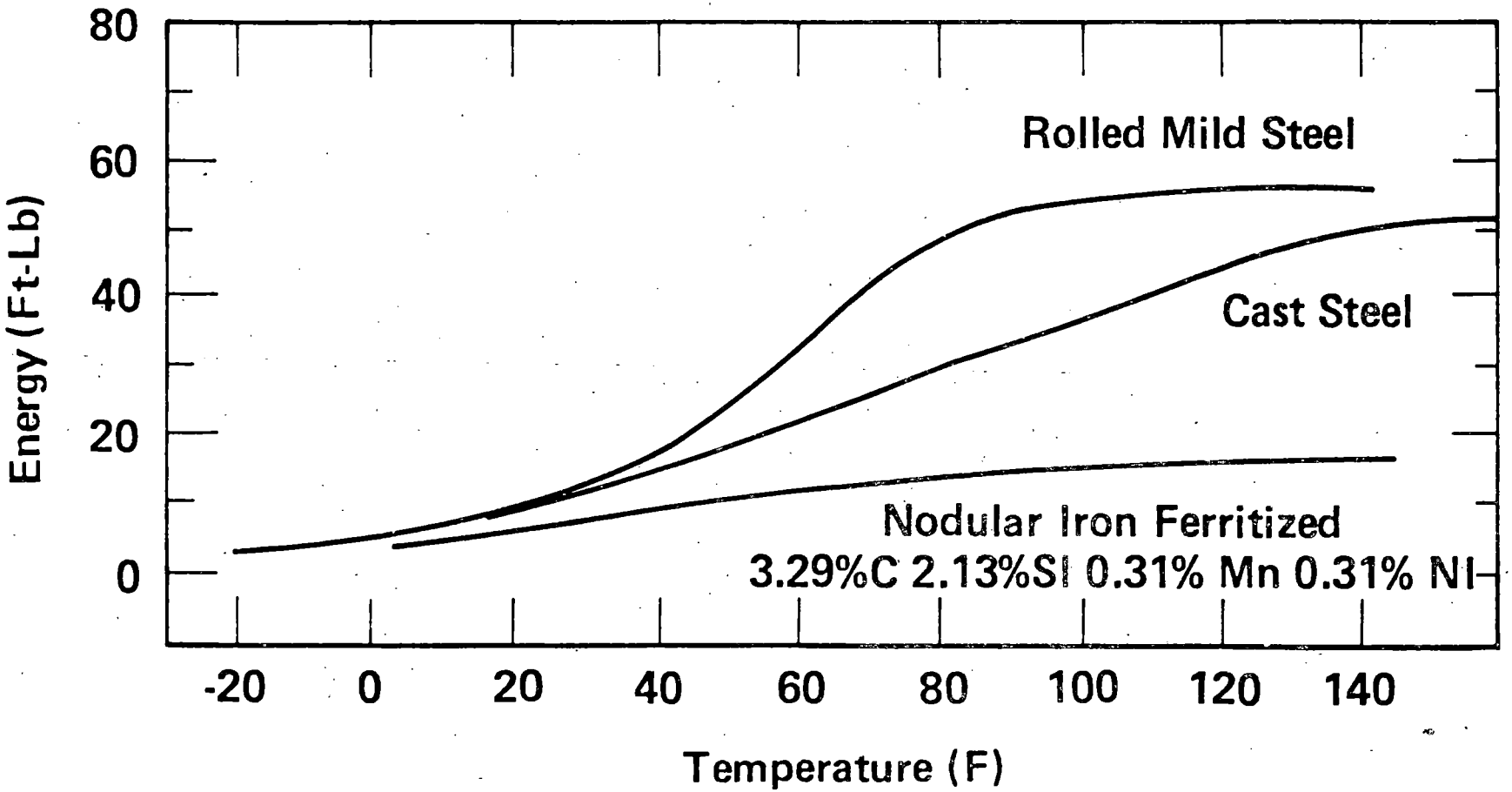

FRACTURE TOUGHNESS OF DUCTILE CAST IRON VERSUS TEMPERATURE

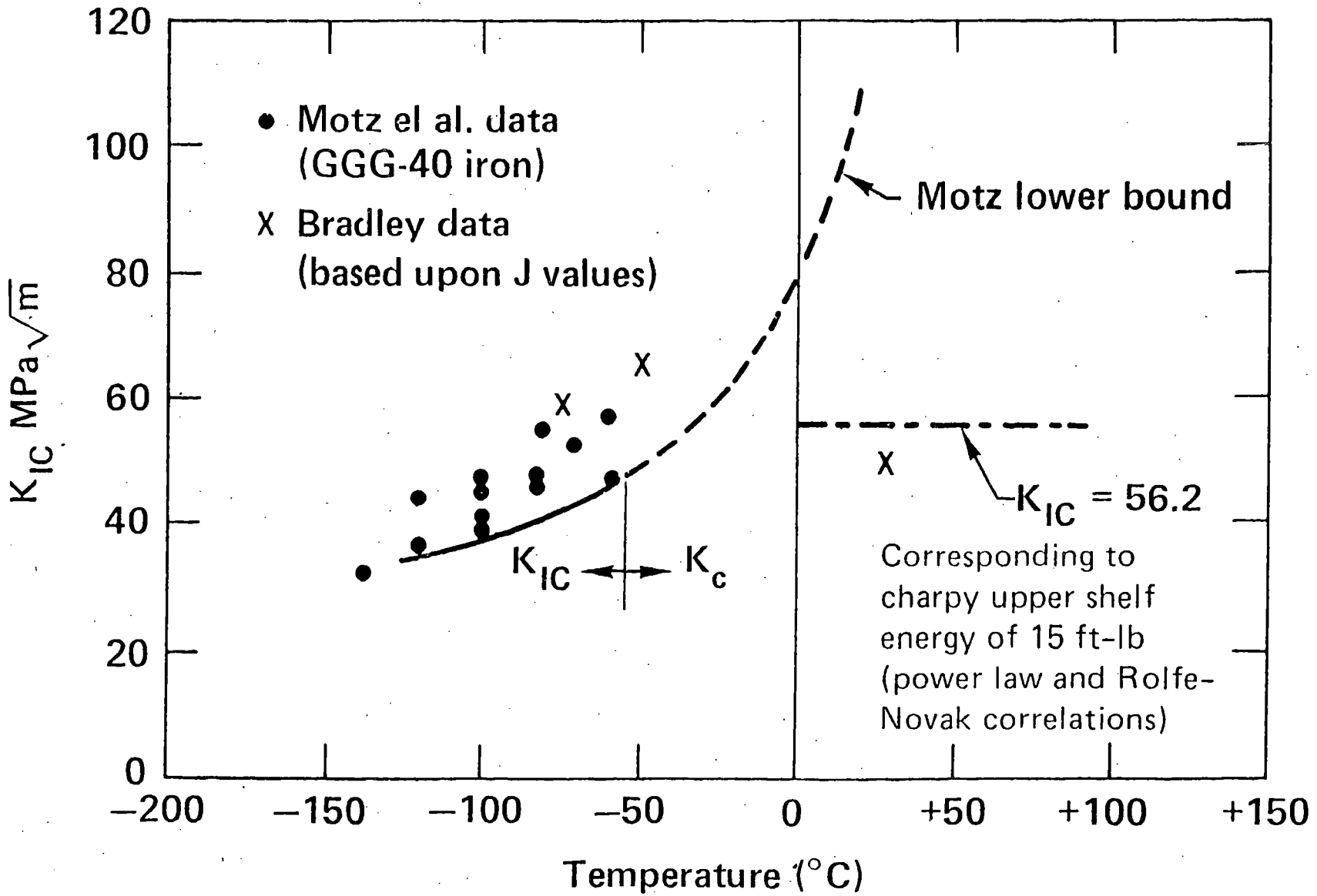

CRITICAL FLAW SIZE VERSUS STRESS FOR FERRITIC NODULAR CAST IRON AT −40°C (−40°F)

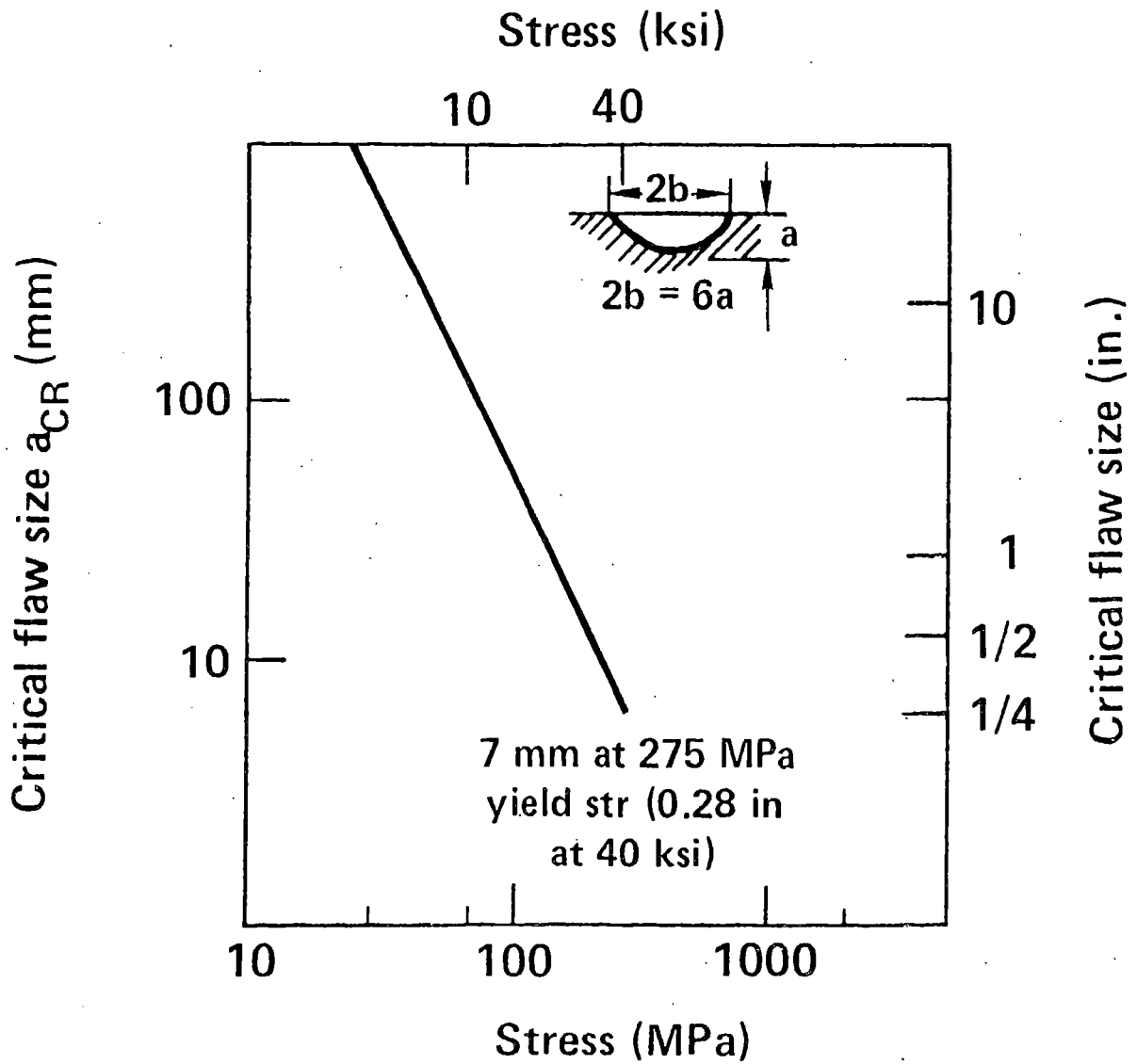

SEISMIC SAFETY MARGINS RESEARCH PROGRAM

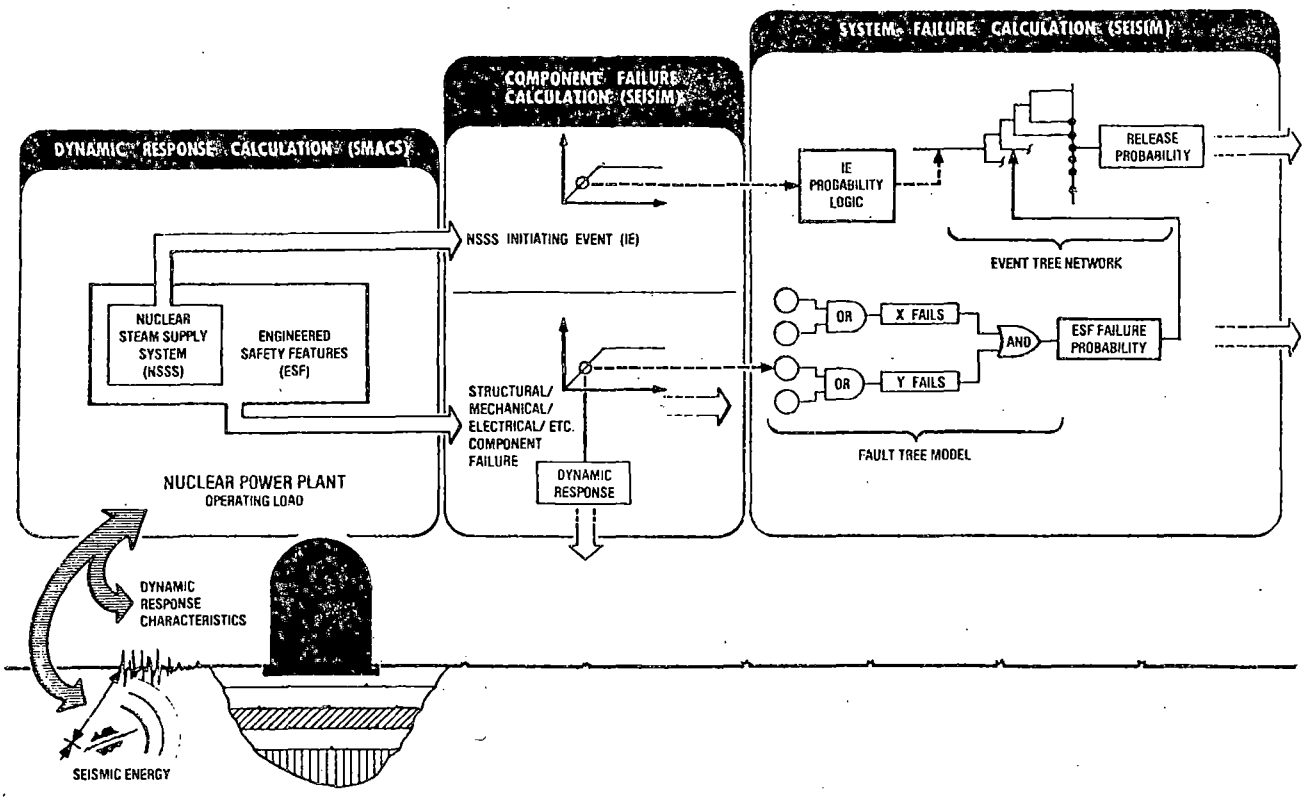

Presented at
9th Water Reactor Safety Research
Information Meeting

October 26, 1981

NSSP
NUCLEAR SYSTEMS SAFETY PROGRAM

LAWRENCE LIVERMORE NATIONAL LABORATORY

Prepared for U.S. Nuclear
Regulatory Commission

ABSTRACT

The Seismic Safety Margins Research Program (SSMRP) is an NRC-funded multiyear program directed towards estimating the conservatism in the Standard Review Plan seismic safety requirements with the ultimate goal of developing improved seismic requirements. As part of this program, calculations of the seismic risk for a typical commercial nuclear reactor are being made. The SSMRP was planned in several phases. In Phase I, which was successfully completed in January 1981, the tools (computer codes), data bases and methodology were developed and demonstrated. Demonstration calculations were performed for the Zion nuclear power plant (Unit 1) north of Chicago, Illinois. In Phase II, sensitivity studies will be run on the Zion calculations and improved data and models will be used to complete the Zion risk analysis. The six presentations included herein will present the highlights of the results obtained during Phase I of the SSMRP, and planned ongoing activity in Phase II. In addition, the SSMRP methodology is being applied for the first time to a current licensing issue on auxiliary feedwater systems. For this task, the methodology is being used to analyze the auxiliary feedwater system for Unit 1 of the the San Onofre Nuclear Generating Station. A description of this technical assistance task is given in the presentation by T. Y. Chuang.

The major steps in the seismic risk analysis procedure are:

- Definition of earthquake hazard (hazard curve and time histories).
- Calculation of plant response, including soil-structure interaction, responses of major buildings and responses for critical piping and components.
- Evaluation of failure and radioactive release probabilities. This includes development of event and fault trees to model the reactor systems functional interactions and hypothesized accident scenarios, definition of probabilistic failure criteria (fragilities) for all critical buildings, piping and components, and performing statistical risk calculations.

An overview of the SSMRP methodology and Phase I results is given in the first presentation.

Development of the hazard curve for the Zion site and associated time histories was reported at the 8th Water Reactor Safety Information Meeting, and hence is not reported this year.

Calculations of structural response and soil-structure interaction are described in the presentation by J. J. Johnson. Uncertainties were input by specifying uncertainties on soil shear modulus and damping, and on the natural frequencies and damping of both buildings and piping systems. These input uncertainties led to considerable uncertainties in computed accelerations and piping moments. A side study revealed that embedment had a significant effect on structural response. In another side study, building modeling techniques were shown to be a larger contributor to response uncertainties than expected.

The presentation by S. N. Shukla describes an extensive sensitivity study performed to evaluate the relative contributions to uncertainties in piping response due to seismic input (time histories), soil structure interaction, major structural modeling, and piping modeling. This study revealed that computed uncertainties in piping responses were not dominated by the inherent uncertainties in the time histories but in fact were most affected by piping modeling uncertainties.

The presentation by J. E. Wells provides a description of the SEISIM code which performs the probabilistic risk and failure computations. Preliminary failure and risk results for the Zion plant are presented, as well as some very recent results indicating which components and safety systems failures dominated the overall risk calculations.

Finally, a description of the ongoing FY 82 workscope is presented. This describes the scope and depth of sensitivity studies to be performed in the coming year. Sensitivity and modeling studies are planned in each of the areas of the seismic risk calculational methodology. These studies will form the basis for any additional modeling requirements as well as planned simplifications of the methodology.

OVERVIEW

THE SEISMIC SAFETY MARGINS RESEARCH PROGRAM

Presented by:
Michael P. Bohn
Lawrence Livermore National Laboratory

Presented at:
9th Water Reactor Safety Research
Information Meeting

Sponsored by:
U.S. Nuclear Regulatory Commission
Office of Nuclear Regulatory Research
Division of Reactor Safety Research
Gaithersburg, Maryland
October 26, 1981

THE SSMRP IS A MULTI-YEAR, MULTI-MILLION DOLLAR RESEARCH PROGRAM INVOLVING DIVERSE DISCIPLINES

- 1978-1984 timespan
- Total estimated cost $18 million
- Program requires personnel from
  - Civil engineering
  - Systems analysis
  - Computer science
  - Earth sciences
  - Statistics
- Extensive use is made of internationally known experts in risk and seismic analysis

UNIQUE ASPECTS OF SEISMIC DESIGN

- Maximum earthquake possible unknown
- Strengthening may result in increased risk
- Little experimental verification
- Earthquake ground shaking compromises redundancy

Picking parameters to assure a conservative design is difficult because of the complex interactions between site, structures and safety systems

NSSP
NUCLEAR SYSTEMS SAFETY PROGRAM

GOALS OF THE SSMRP

- Develop and apply a methodology for computing probability of radioactive release due to earthquakes including all common-mode failures.
- Determine conservatism in current NRC licensing criteria for seismic design
- Determine major contributors to probability of radioactive release
- Rank R&D areas for validation of risk results

UNCERTAINTY

- Current design analyses are deterministic, and based on design codes with built-in safety factors
- The SSMRP explicitly considers uncertainties in:
  - Earthquake hazard (occurrence rate, magnitude)
  - Soil properties which can affect reactor system response (layering, shear modulus, damping)
  - Structure geometry, material, strength
  - Failure levels for components, piping, electrical equipment
- The effect of these uncertainties on risk is being ascertained

EXAMPLE OF DEPENDENT FAILURES

Consider a system consisting of two identical pumps. Assume each pump alone has failure probability of 0.1

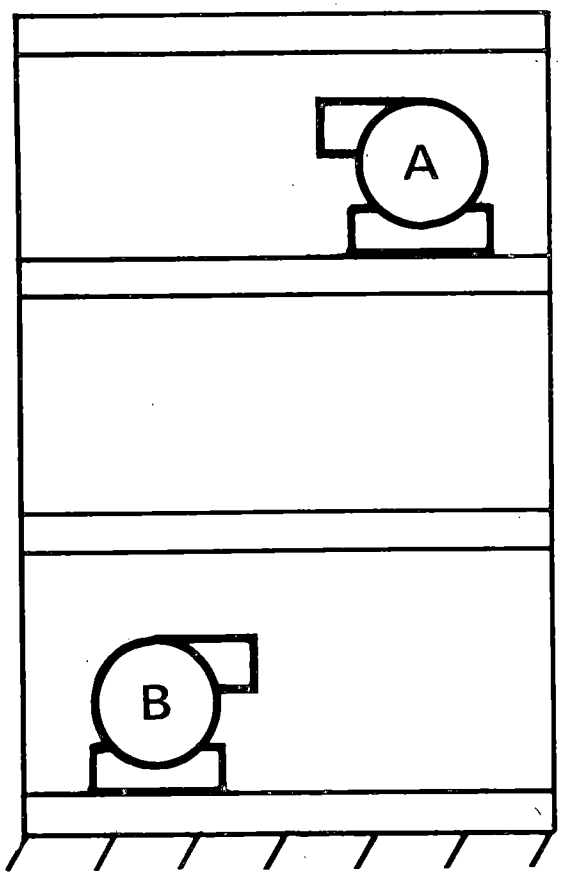

Probability of failure of both components

$P_{together} = MIN\ (P_A,\ P_B) = 0.10$

$P_{separated} = P_A\ P_B = 0.01$

NSSP
NUCLEAR SYSTEMS SAFETY PROGRAM

PHASE I OF THE SSMRP COMPLETED IN JANUARY 1981

- Preliminary methodology assembled and computer codes developed
- Seismic and failure data bases developed
- Demonstration calculations completed using Zion Unit 1 plant as example

NSSP

A SEISMIC RISK ANALYSIS METHODOLOGY REQUIRES CONSIDERING EVERYTHING FROM SOURCE TERM TO RELEASE PATHS

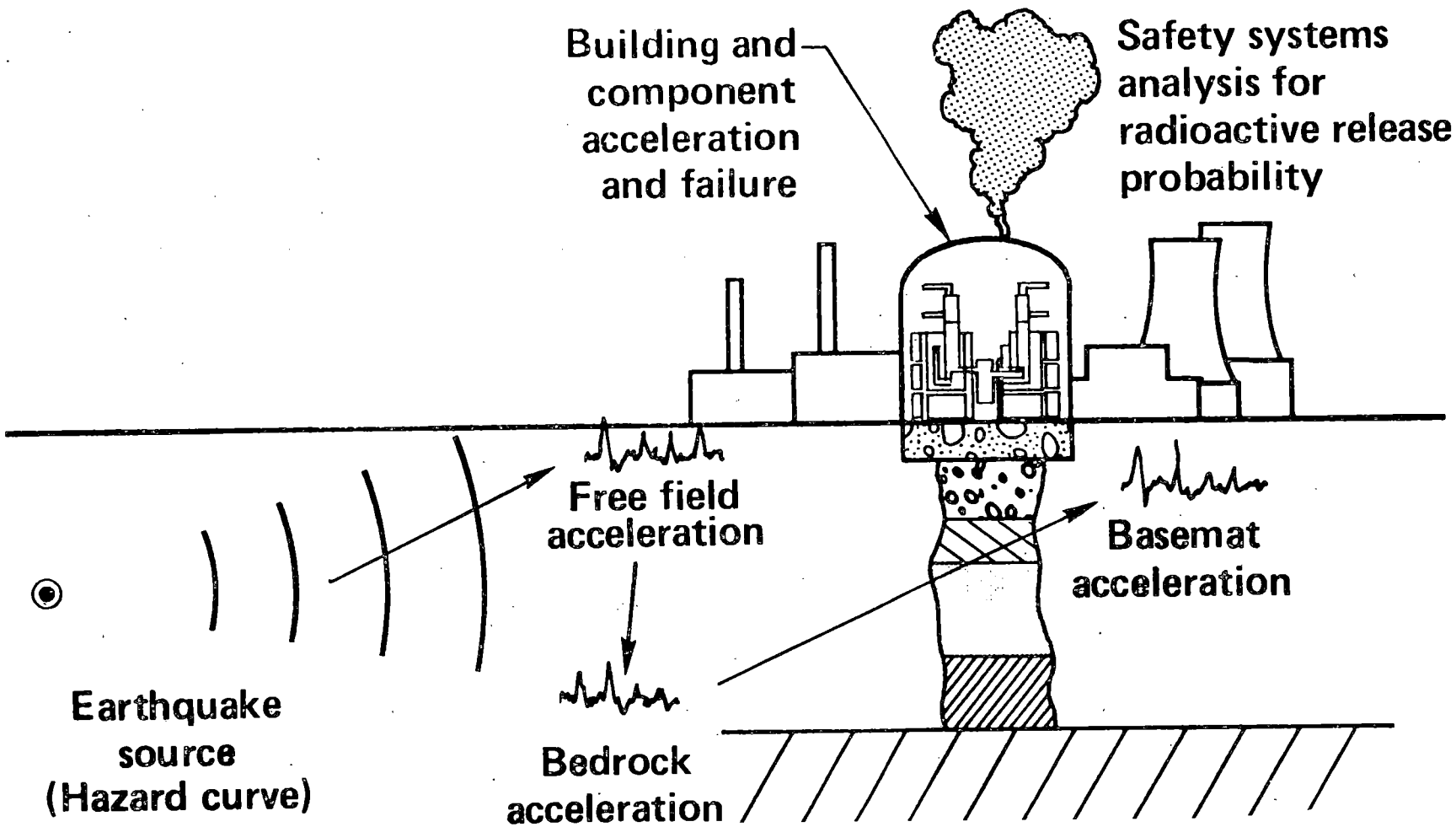

NSSP

OUR METHODOLOGY REQUIRED DEVELOPMENT OF THREE COMPUTER CODES

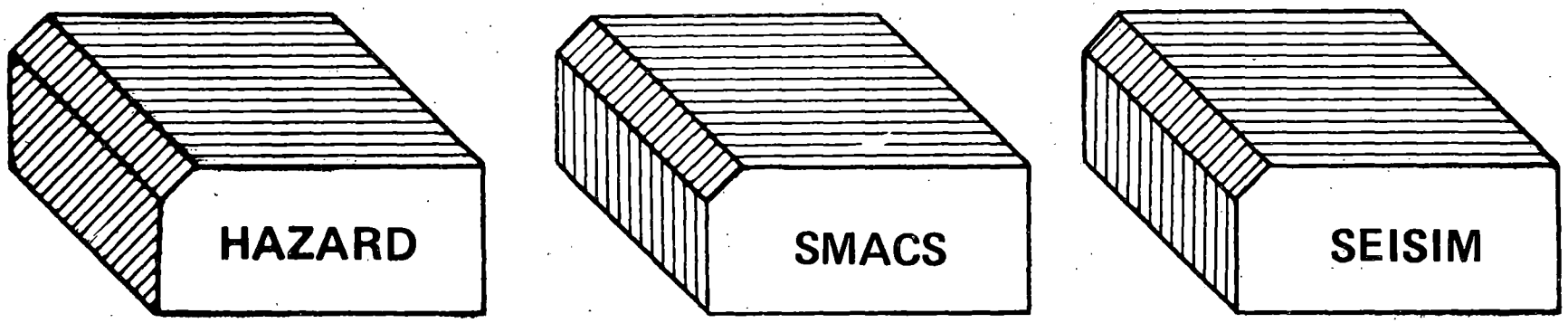

HAZARD	SMACS	SEISIM
Hazard curve and time histories	Soil, building and piping response	Risk and failure calculations

NSSP
NUCLEAR SYSTEMS SAFETY PROGRAM

THE HAZARD CODE COMPUTES THE HAZARD CURVE AND CORRESPONDING TIME HISTORIES

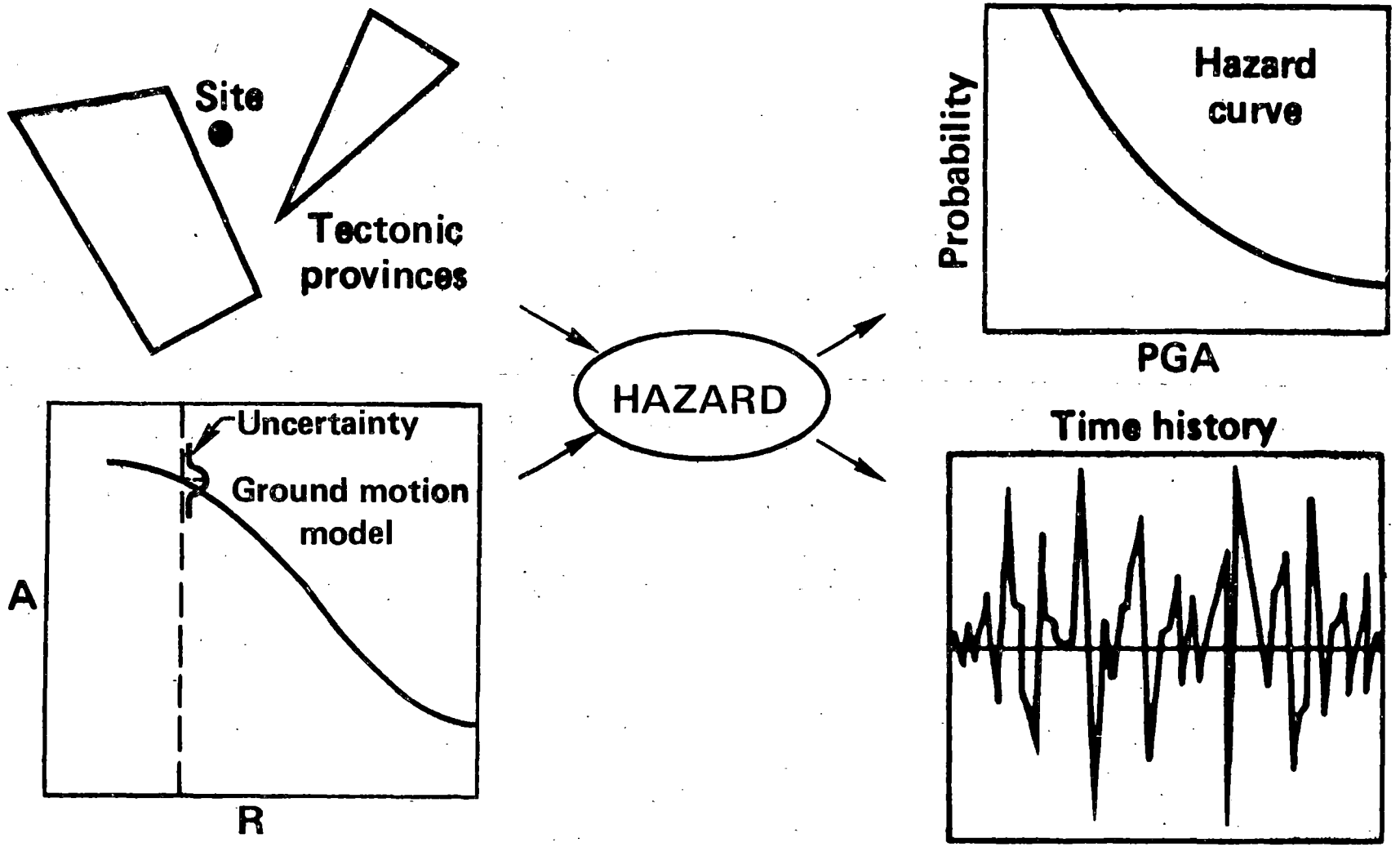

NSSP

RESULTS FROM ZION DEMONSTRATE THE HAZARD CODE OUTPUTS

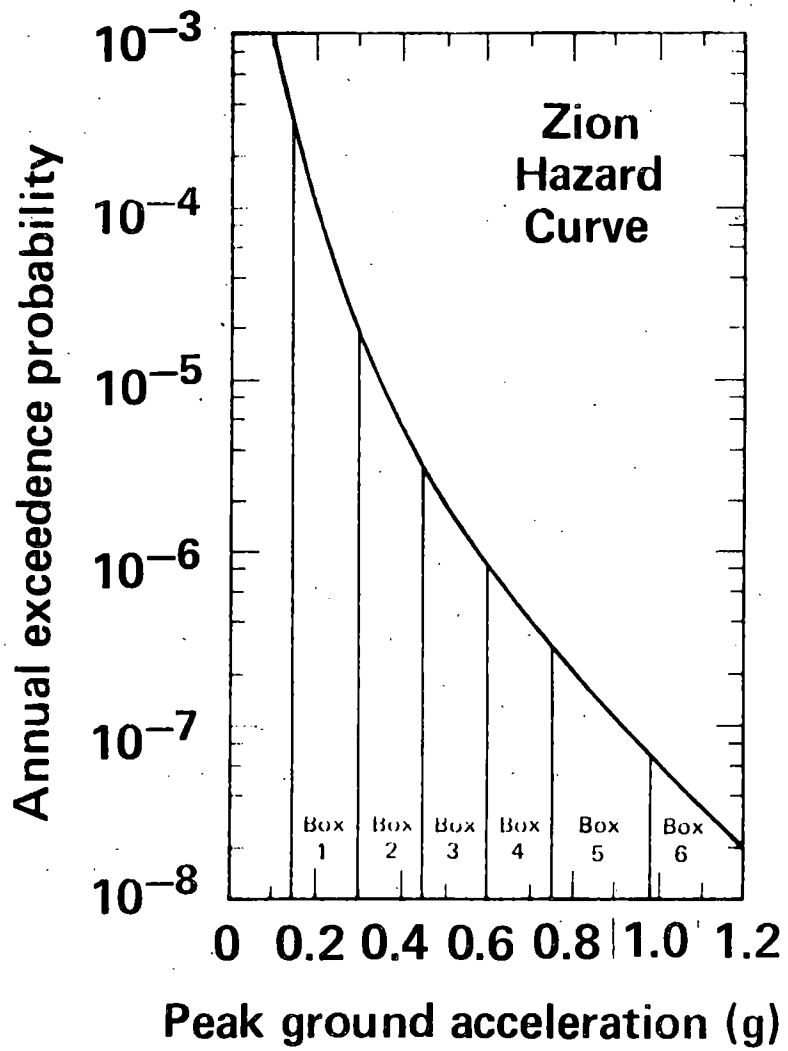

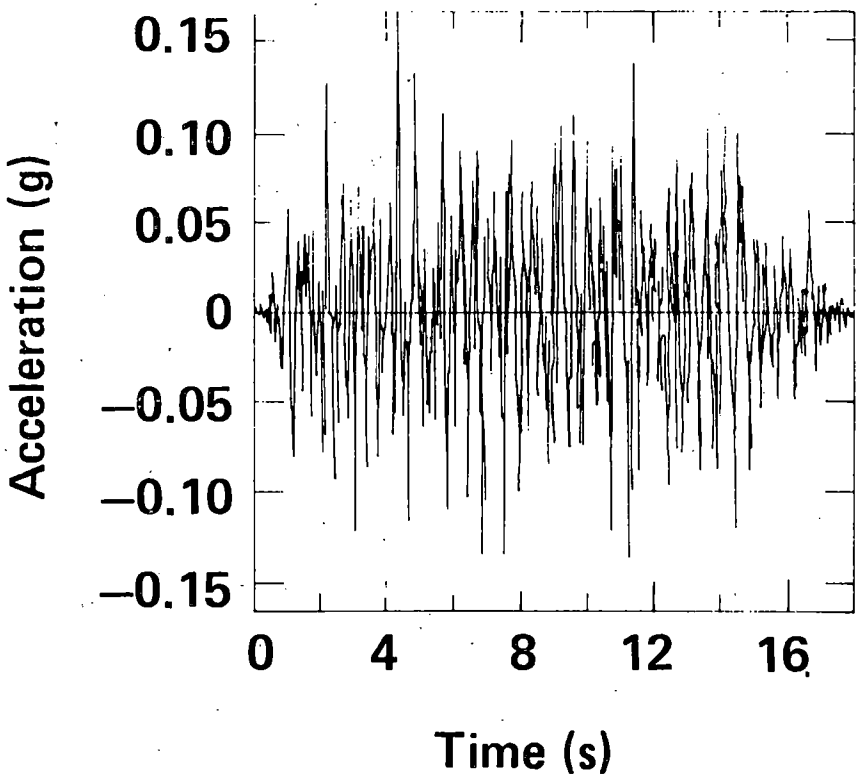

NSSP

THE SMACS CODE GENERATES RESPONSES AND UNCERTAINTY IN RESPONSES

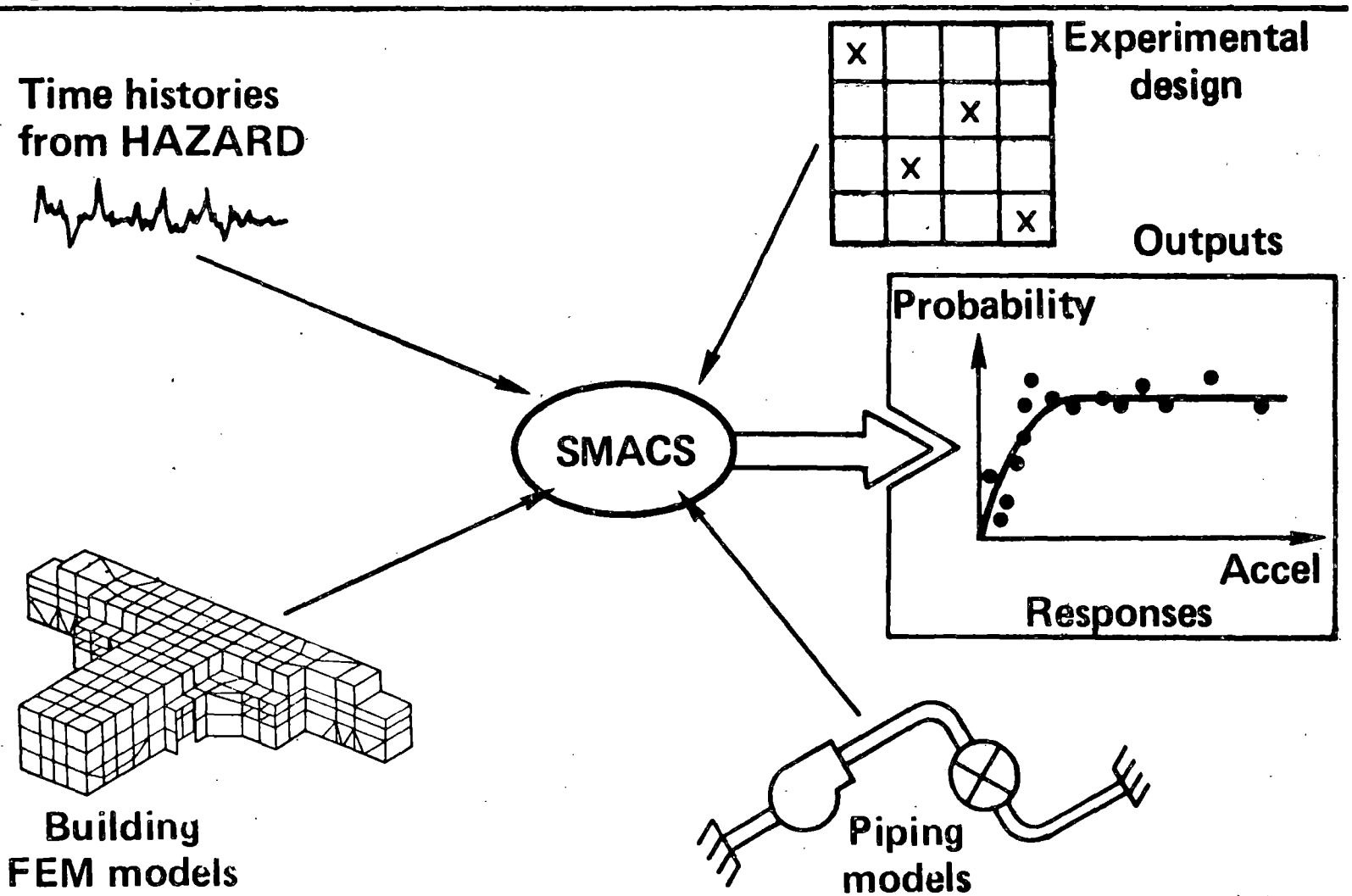

nssp
NUCLEAR SYSTEMS SAFETY PROGRAM

OUR SMACS CODE RESPONSE CALCULATIONS WERE COMPREHENSIVE

30 – 90 Time histories

3 Soil layers

3 Building models

4000 mesh points

Up to 120 natural modes

13 Piping runs

1000 responses

Up to 130 natural modes

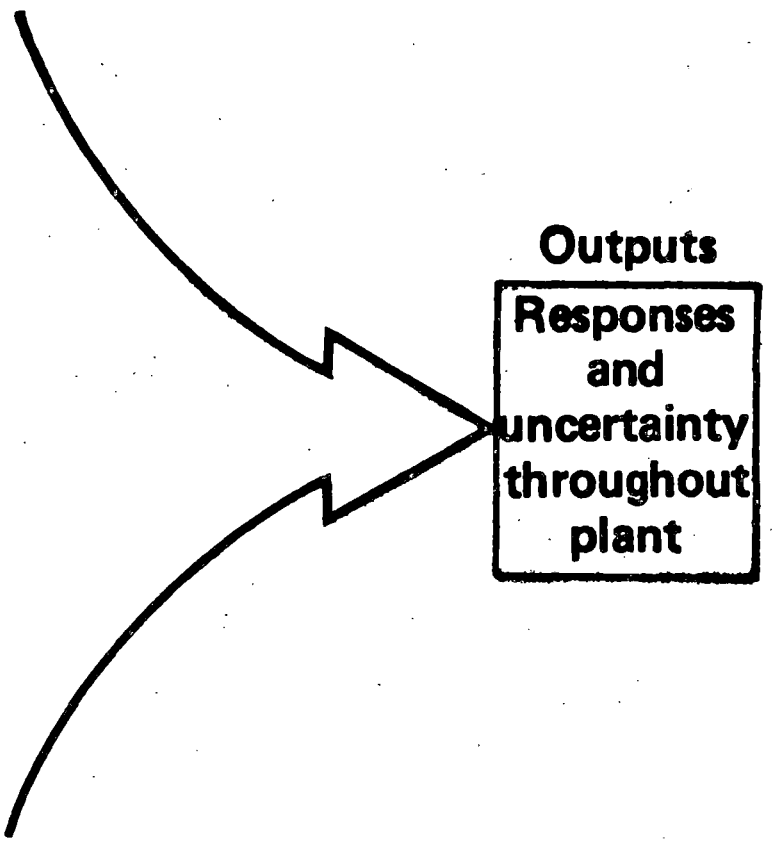

THE UNCERTAINTY THAT COMES OUT OF OUR RESPONSE CALCULATIONS IS A RESULT OF THE UNCERTAINTY WE PUT IN

- Seismic input
  - 30 sets of three components of free-field motion. ZPA from 0.15G to 1.8G
- Soil-structure interaction
  - Soil shear modulus
    - Cov = 0.7
  - Soil damping
    - Cov = 1.0
- Structural response
  - Frequency
    - Cov = 0.5
  - Damping
    - Cov = 0.7
- Subsystem (piping) response
  - Frequency
    - Cov = 0.5
  - Damping
    - Cov = 0.7

nssp
NUCLEAR SYSTEMS SAFETY PROGRAM

SMACS CALCULATIONS REVEAL SIGNIFICANT UNCERTAINTIES ON RESPONSE

Example: Peak moment in auxiliary feedwater nozzle

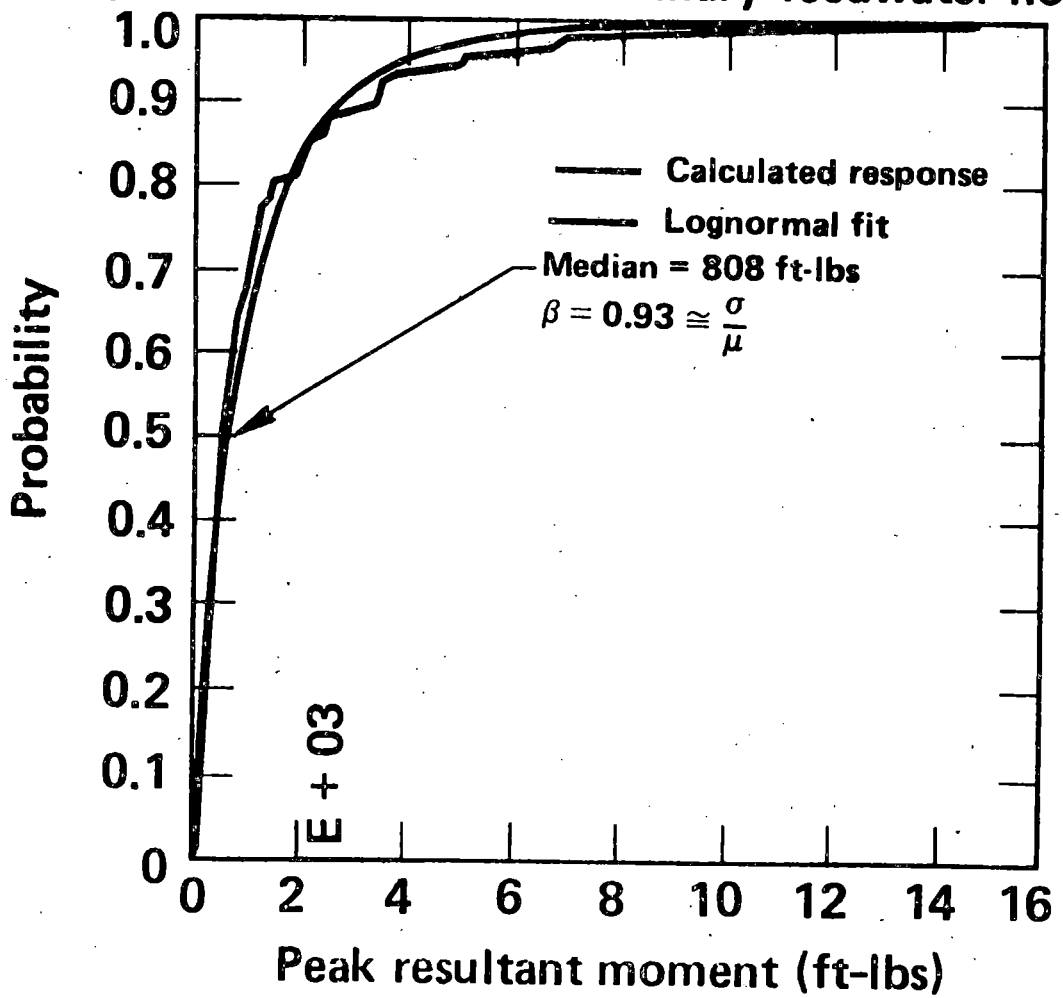

NSSP

CONTRARY TO EXPECTATION, INHERENT VARIATION IN TIME HISTORIES DID NOT DOMINATE RESPONSE UNCERTAINTIES

Example: Peak moment in auxiliary feedwater nozzle

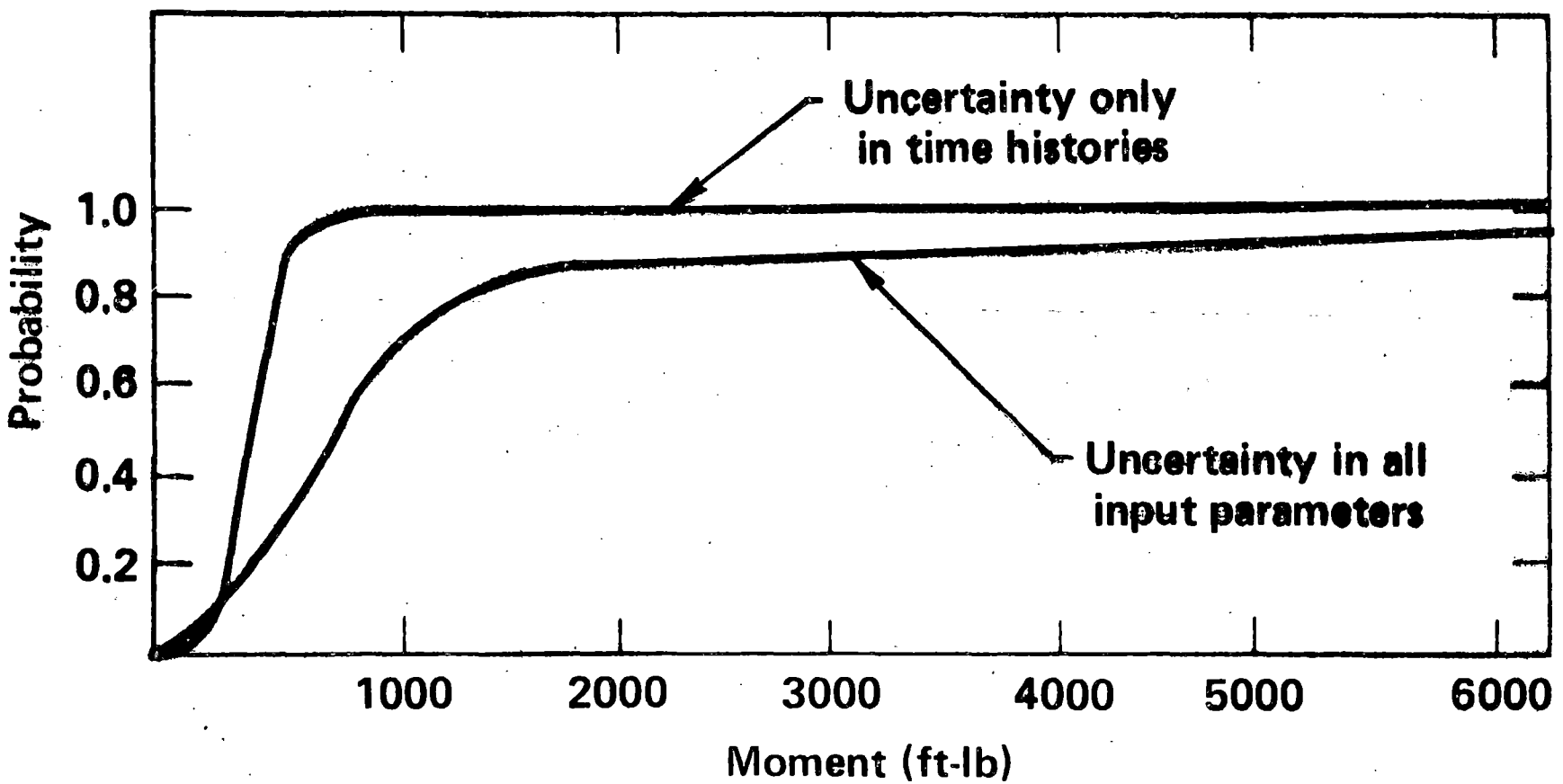

nssp

IN SPITE OF UNCERTAINTIES, THERE APPEARS TO BE CONSERVATISM IN THE ZION DESIGN

Example: Seismic stress of loop 1 hot leg RPV nozzle

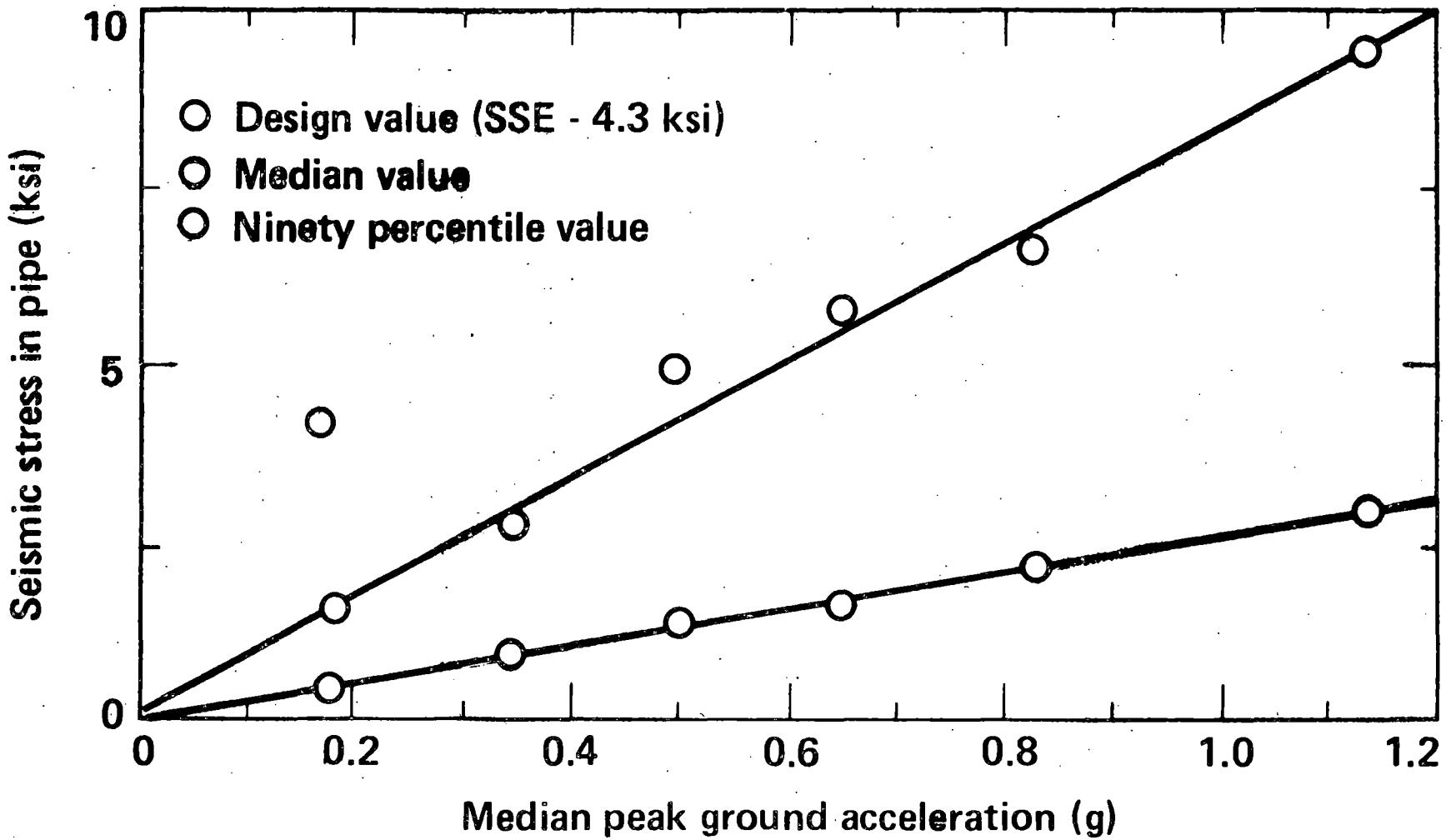

NSSP

BOTH PARAMETER AND MODEL UNCERTAINTIES CONSIDERED

Example: Modeling technique uncertainty found significant

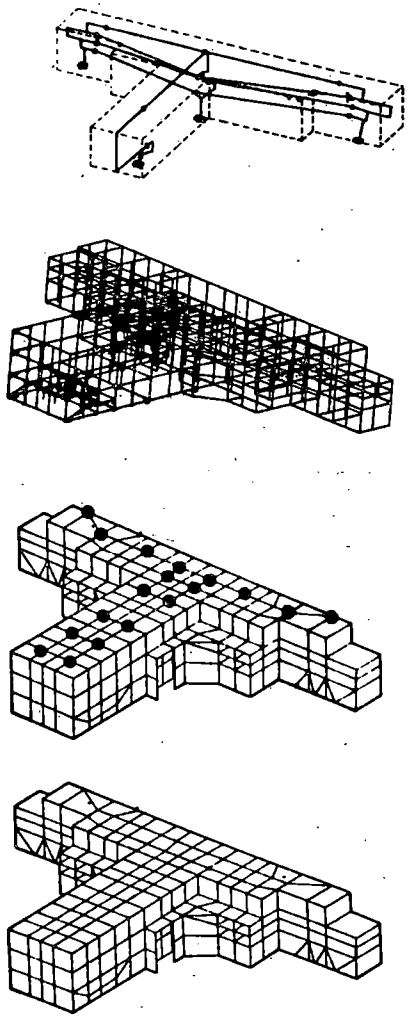

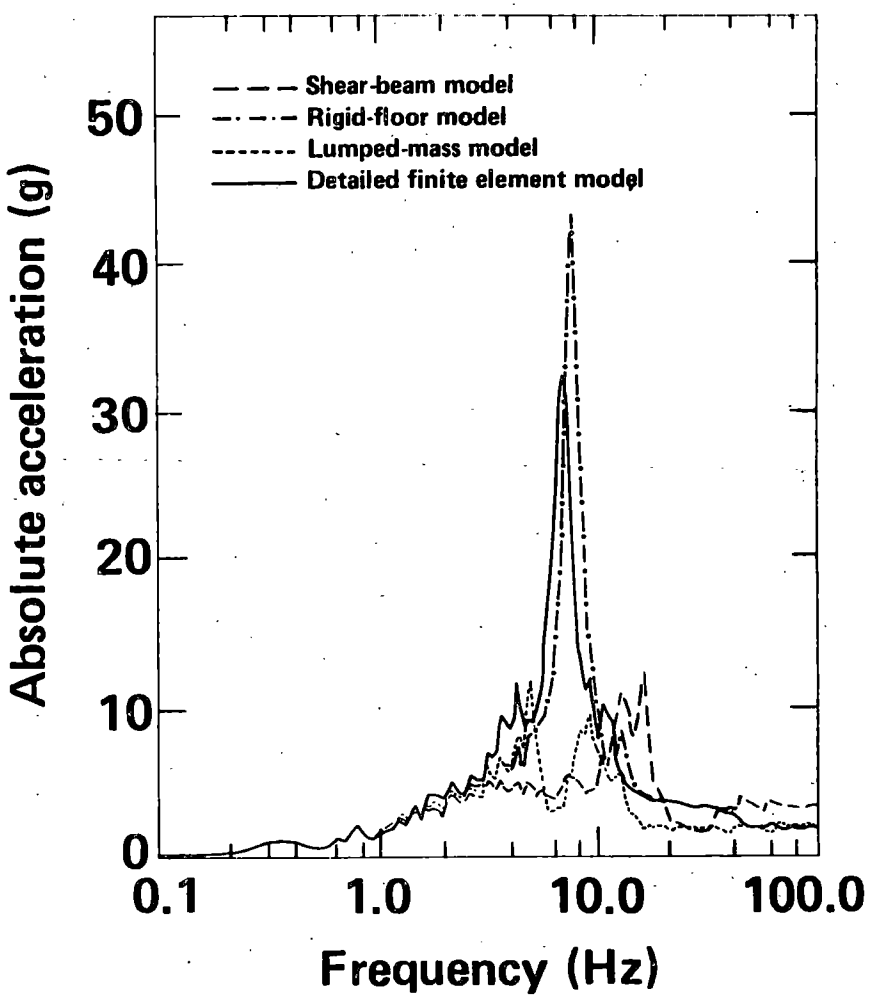

NSSP
NUCLEAR SYSTEMS SAFETY PROGRAM

THE SEISIM CODE COMPUTES PROBABILITY OF RADIOACTIVE RELEASE OF ENTIRE REACTOR SYSTEMS AND HAS UNIQUE COMMON MODE FEATURES

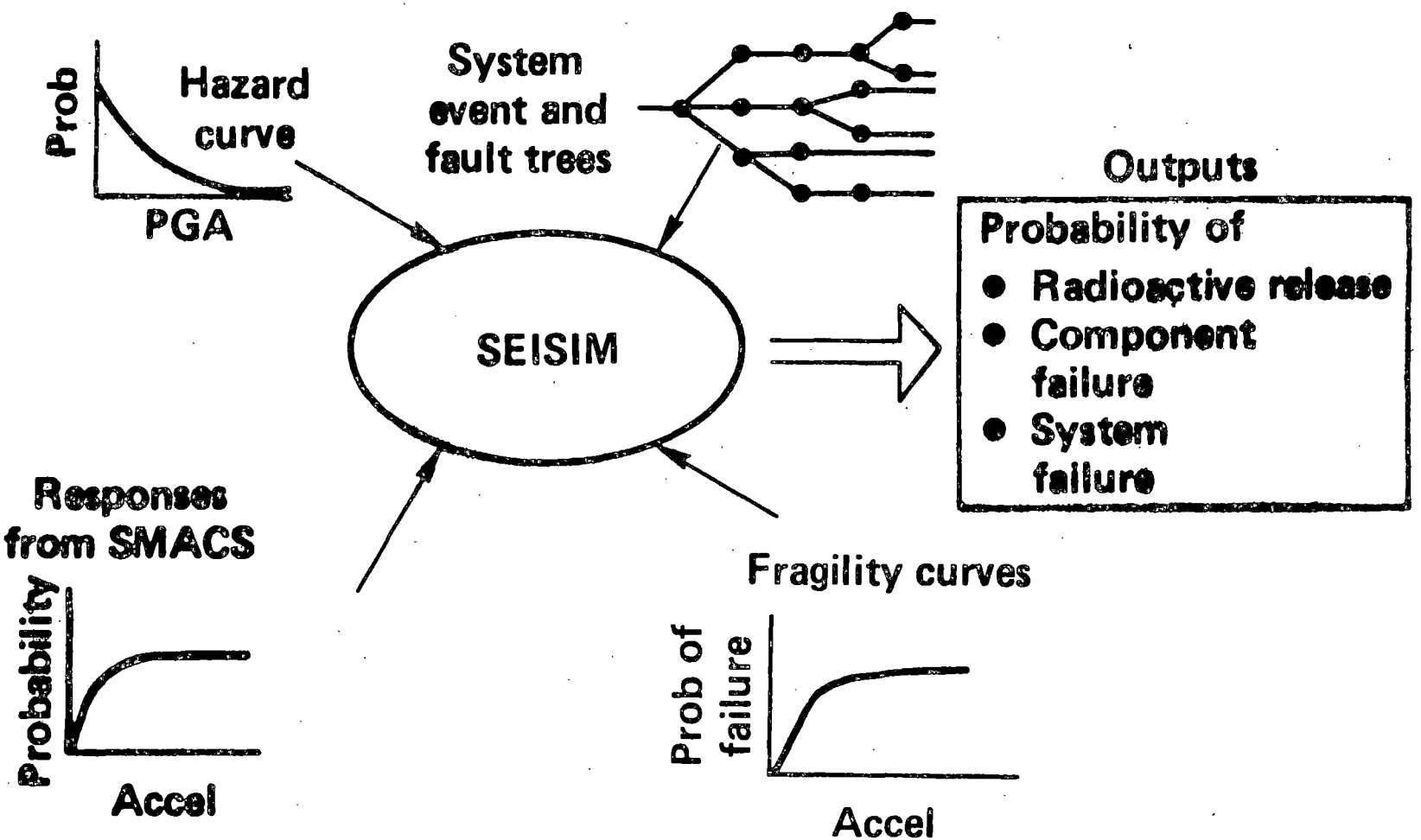

NSSP

A UNIQUE FRAGILITIES DATA BASE WAS DEVELOPED

- For all components identified on the fault trees, probability of failure as a function of acceleration or force was developed from data or analysis
- Data was formulated into normal or log normal distributions for calculations

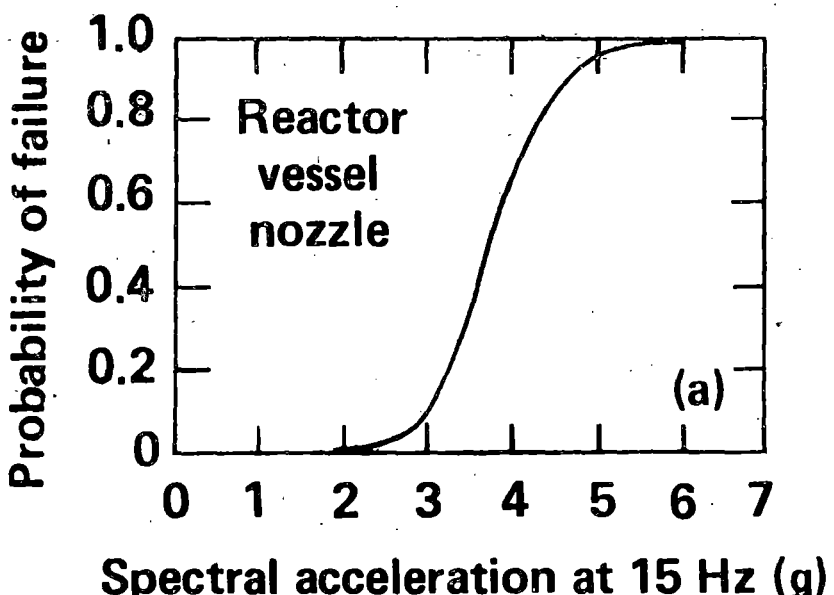

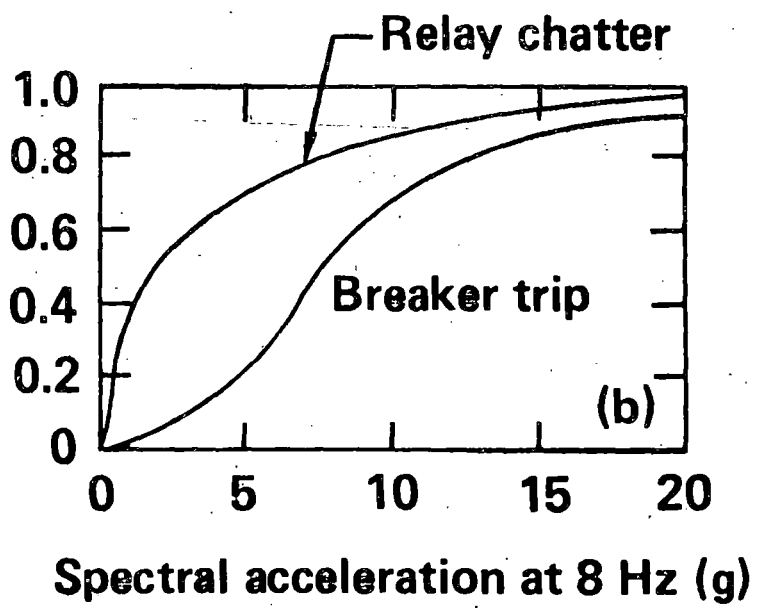

NSSP
NUCLEAR SYSTEMS SAFETY PROGRAM

SEISIM HANDLES MANY COMPLEX SYSTEM INTERACTIONS

Up to 100 vectors from SMACS

7 initiating events

8 event trees

148 core melt accident sequences

5000 cut sets per sequence

817 random failure events

2300 seismic component failure events

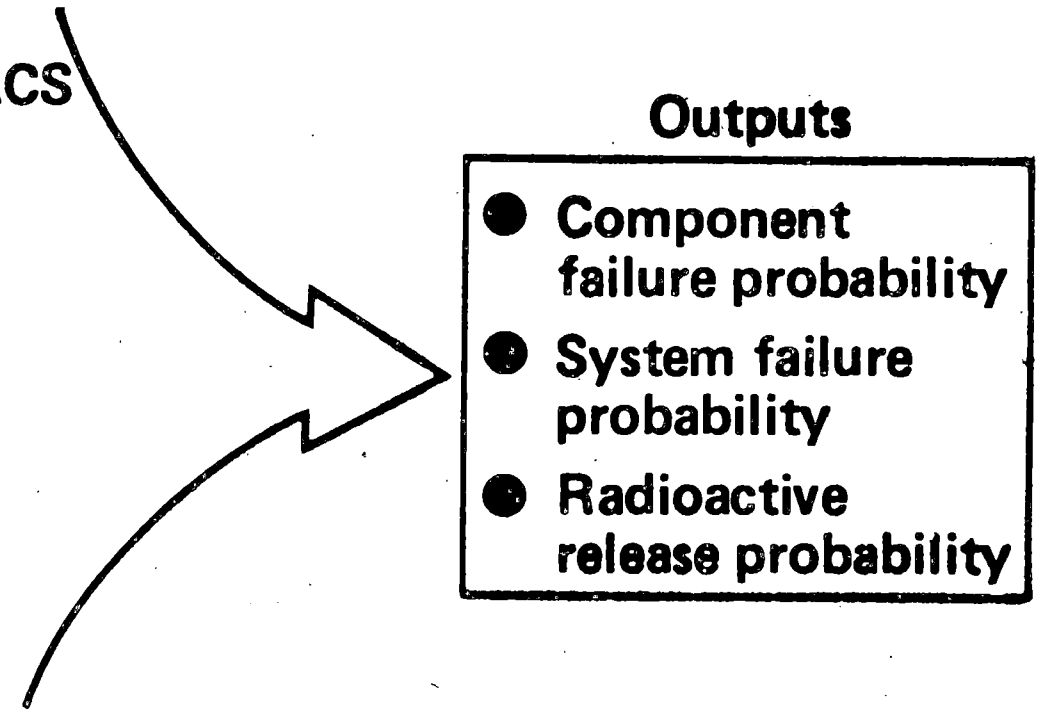

NSSP
NUCLEAR SYSTEMS SAFETY PROGRAM

SEISIM SHOWED FAILURE OF COMPONENTS TO BE DOMINATED BY UNCERTAINTIES RATHER THAN MEDIAN RESPONSES

- SMACS response calculations showed large uncertainties (β values > 1.0)
- SEISIM showed:
  - Doubling median response changed component failure probability by only a factor of 2 or 3
  - Doubling the uncertainties made orders of magnitude difference

NSSP
NUCLEAR SYSTEMS SAFETY PROGRAM

SEISIM OUTPUT PROVIDES RELATIVE HARDNESS OF REACTOR SAFETY SYSTEMS

	Annual failure probability
Residual heat removal system	1×10^{-4}
Charging system	5×10^{-5}
Safety injection system	2×10^{-5}
Auxiliary feedwater system	8×10^{-6}
Accumulators	3×10^{-7}
Service water system	2×10^{-7}

nssp
NUCLEAR SYSTEMS SAFETY PROGRAM

PRELIMINARY SEISIM CALCULATIONS LEAD TO ZION CORE MELT PROBABILITIES ON THE ORDER OF WASH-1400

Mode of release	Annual probability due to earthquake	Random failure Wash-1400
Containment rupture (UO_2/steam explosion)	2×10^{-8}	9×10^{-7}
Containment rupture overpressure	2×10^{-7}	4×10^{-6}
Containment fails to isolate	2×10^{-6}	7×10^{-7}
Melt thru bottom of containment	1×10^{-5}	4×10^{-5}

NSSP
NUCLEAR SYSTEMS SAFETY PROGRAM

SUMMARY

We have completed Phase I and demonstrated our technique on Zion. Some preliminary conclusions are:

- Earthquake induced radioactive release risk can be equally as important as that due to random failure even for Eastern plants
- Uncertainties in responses tend to dominate component failure probabilities rather than median responses
- Inherent uncertainty due to random time history input does not dominate response uncertainty

PRODUCTS OF THE SSMRP

- A demonstrated methodology for comprehensive and systematic assessment of seismic risk in nuclear plants
- New computer codes to perform the assessment (HAZARD, SMACS, SEISIM)
- Improvements in state-of-the-art in:
  - Soil structure interaction
  - Failure of dependent systems
  - Characterization of earthquake hazard
  - Characterization of uncertainty
- Data base of probabilistic component failure relations
- Results of support studies on specific immediate concerns of the NRC

SEISMIC SAFETY MARGINS RESEARCH PROGRAM (SSMRP)

Seismic Response Using the SMACS Computer Program

Presented by:

Dr. James J. Johnson
Structural Mechanics Associates
for
Lawrence Livermore National Laboratory

Presented at:

9th Water Reactor Safety Research
Information Meeting

Sponsored by:

U.S. Nuclear Regulatory Commission
Office of Nuclear Regulatory Research
Division of Reactor Safety Research

October 26, 1981

THERE ARE THREE OBJECTIVES OF THIS PRESENTATION

- Role of SMACS in the SSMRP and elements of the SMACS methodology
- Description of the SMACS analysis of the Zion NPP – SSMRP Phase I
- Phase I results

SMACS IS THE FIRST STAGE OF THE SSMRP SYSTEMS ANALYSIS

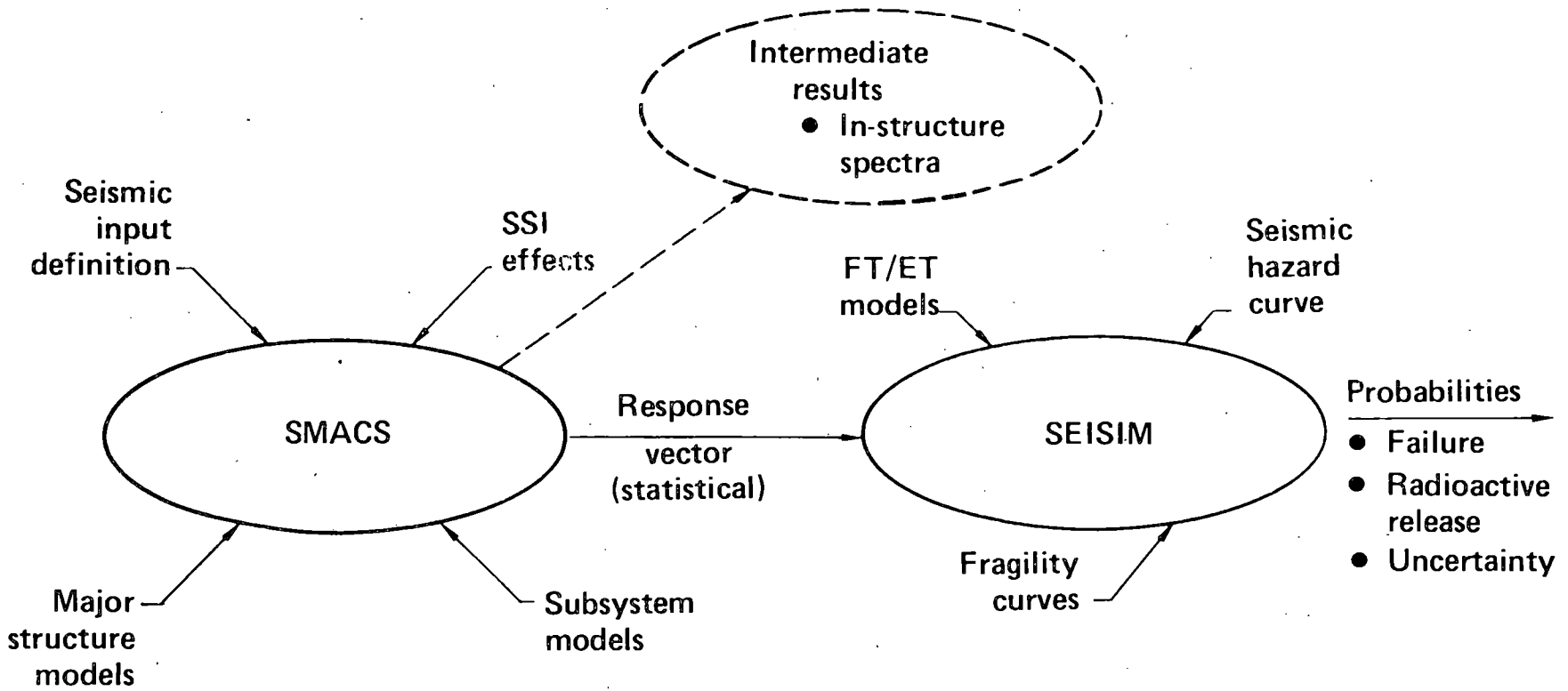

THE RESPONSES CALCULATED BY SMACS CORRESPOND TO BASIC EVENTS DEFINED BY SYSTEM FAULT TREES

- Pump fails
- Valve fails to open
- Pipe ruptures
- Structure collapses

RESPONSE PARAMETERS CORRESPOND TO THOSE REQUIRED FOR FRAGILITY DESCRIPTIONS

- Spectral acceleration
- Peak moment in pipe
- Relative displacement
- Peak force in structural element
- Etc.

SMACS LINKS SEISMIC INPUT, SSI, MAJOR STRUCTURES, AND SUBSYSTEMS FOR 3-D RESPONSE CALCULATIONS

- Performs time history analysis from free-field through response
- Seismic input defined by ensemble of earthquake time histories
  — 3 components on surface of soil
- SSI and major structure response are calculated by the sub-structure approach (CLASSI)
- Subsystem response is calculated by multi-support time history analysis
- Uncertainties in seismic input, SSI, structures, and subsystems are included
- The SMACS procedure is to perform repeated deterministic analyses--each analysis is for a unique earthquake and input parameters selected according to a Latin hypercube experimental design
- SMACS is computationally efficient - vectorized
- NUREG/CR-2015 Vol 9

SSI AND MAJOR STRUCTURES WERE ANALYZED BY THE SUBSTRUCTURE APPROACH (CLASSI)

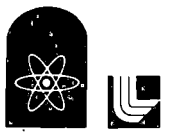

- Soil is modeled as a linear visco-elastic material
- Primary nonlinear behavior of soil is treated by equivalent linear techniques
- Layered half-space
- Foundations for the demonstration case are assumed rigid and embedded
- Detailed finite element structure models are used
- Structure dynamic characteristics defined by eigensystem and modal damping
- Response of structures serves two main purposes
  - Structural fragility
  - Input excitation for subsystems

A LIMITED NUMBER OF PARAMETERS WERE THE MECHANISMS TO INCORPORATE UNCERTAINTY IN THE SMACS CALCULATIONS

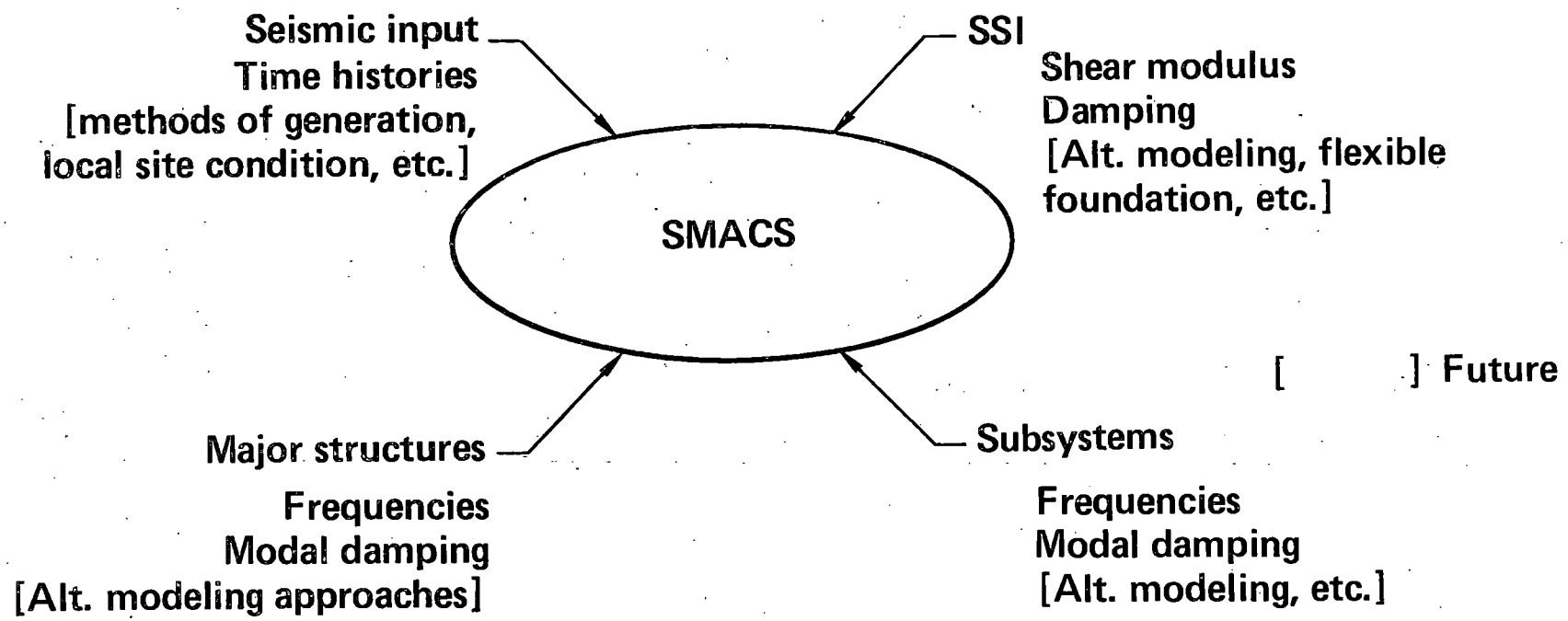

THE UNCERTAINTY PARAMETERS WERE INTENDED TO REPRESENT ALL SOURCES OF UNCERTAINTY

- SSI – soil shear modulus and material damping
  - Soil properties
  - SSI analysis techniques
  - Model idealizations – foundations, embedment, structure-to-structure interaction, etc.
  - Nonlinearities
  - etc.
- Structures – frequencies and damping
  - Material properties
  - Nonlinear behavior
  - Model idealization
  - etc.
- Subsystems – frequencies and damping
  - Material properties
  - Supports
  - Model idealization
  - etc.

FOR OUR PHASE 1 DEMONSTRATION CALCULATIONS LOG NORMAL DISTRIBUTIONS WERE ASSUMED ON THE INPUT PARAMETERS

	COV	10%	50%	90%
Soil shear modulus	0.7	0.45	1.0	2.24
Soil damping	1.0	0.34	1.0	2.91
Structure frequency	0.5	0.55	1.0	1.90
Structure damping	0.7	0.45	1.0	2.24
Subsystem (piping) frequency	0.5	0.55	1.0	1.90
Subsystem (piping) damping	0.7	0.45	1.0	2.24

ONCE PROBABILITY DISTRIBUTIONS ARE ASSUMED FOR THE UNCERTAINTY PARAMETERS, THEIR VALUES ARE SELECTED ACCORDING TO A LATIN HYPERCUBE EXPERIMENTAL DESIGN FOR EACH EARTHQUAKE SIMULATION

For only two parameters . . . .

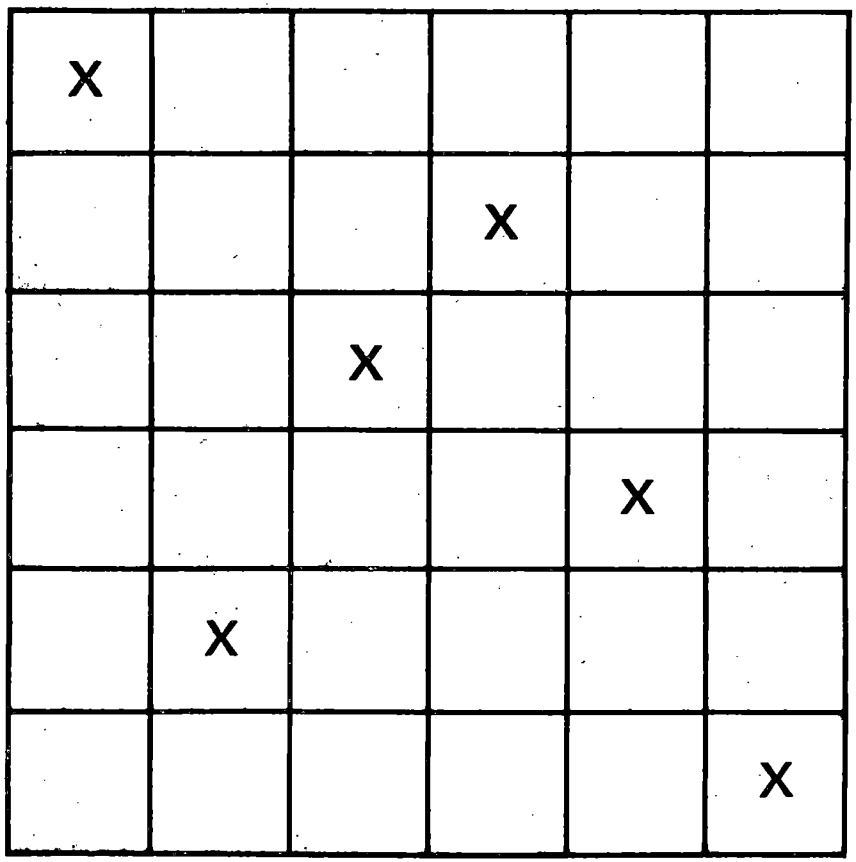

THREE ZION NUCLEAR POWER PLANT BUILDINGS ARE IMPORTANT FOR OUR ANALYSIS

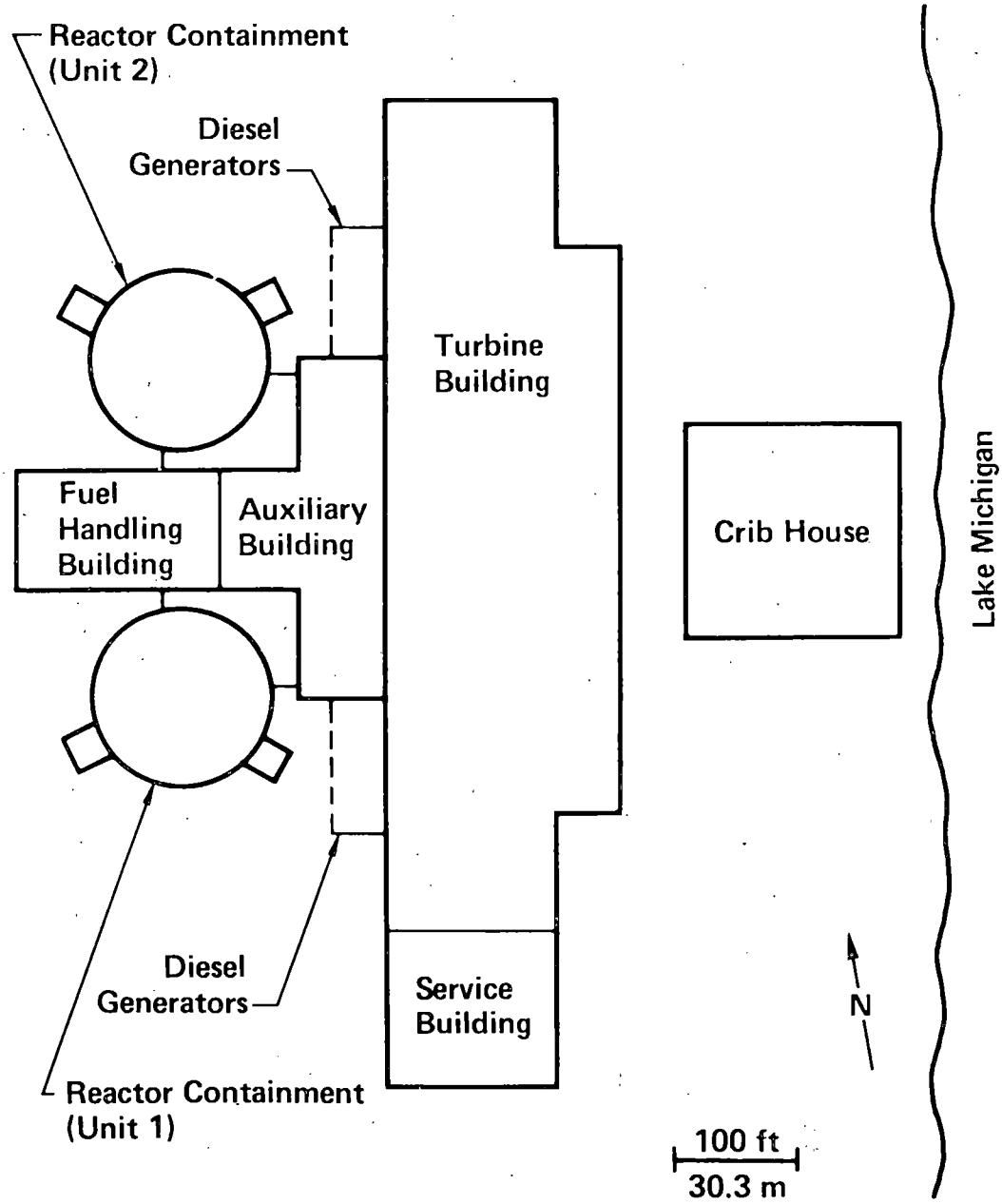

THE ZION SITE IS CHARACTERIZED BY THREE DISTINCT LAYERS OVER BEDROCK

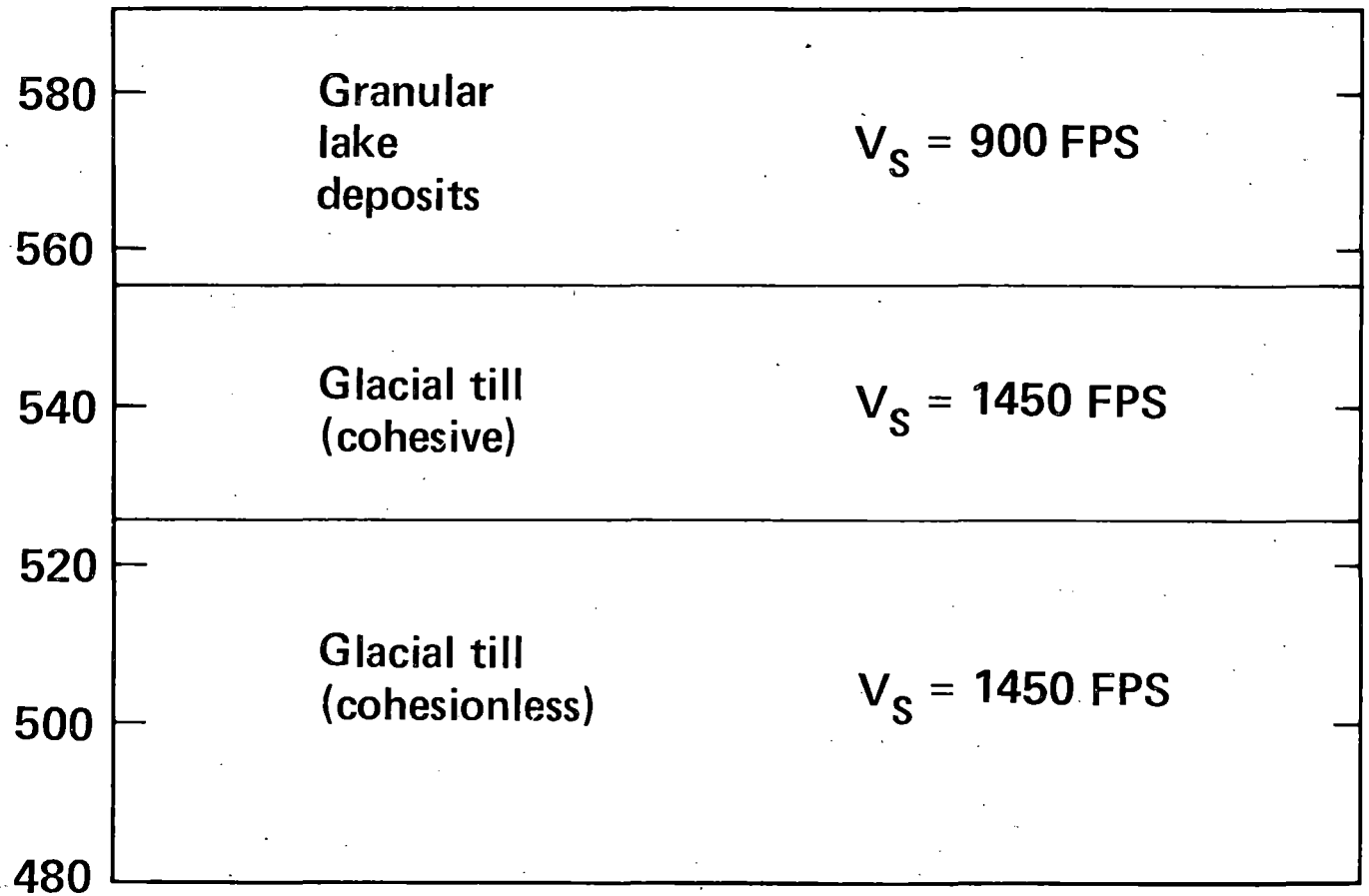

THE REACTOR BUILDING SEISMIC ANALYSIS MODEL CONSISTS OF THREE MAJOR PARTS

- Containment shell
  - 13 modes
  - 28 responses
- Internal structure
- NSS system

- 60 modes
- 184 responses

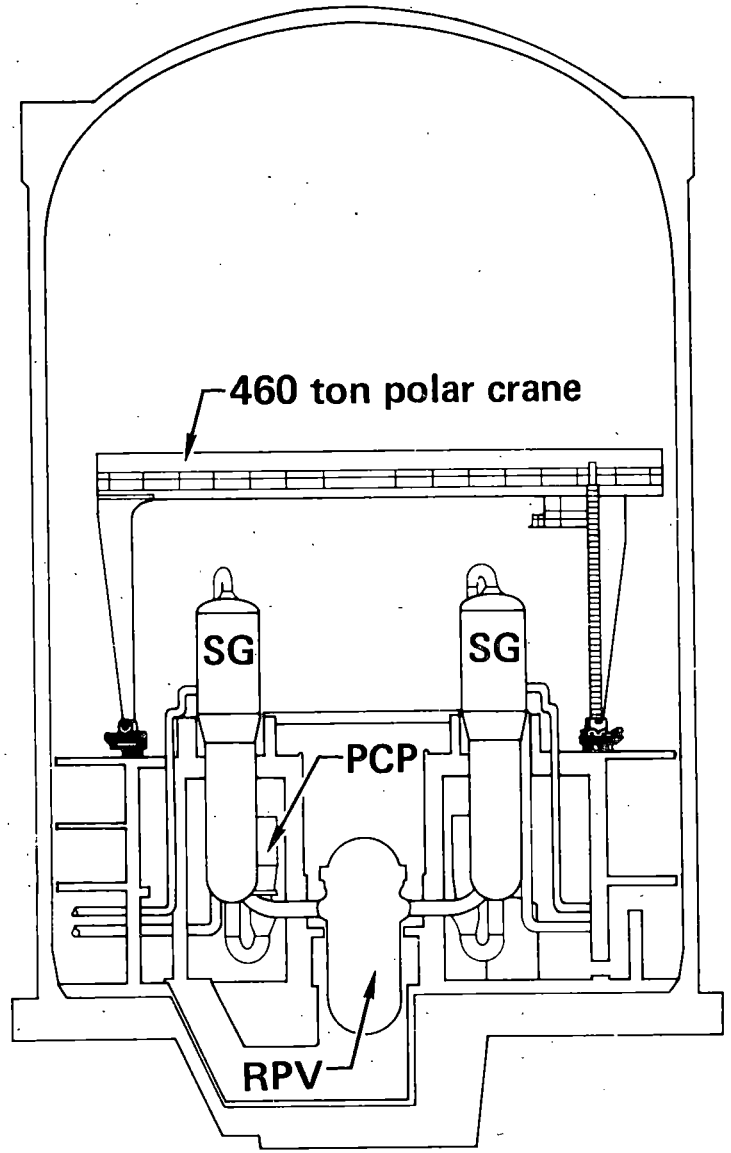

A SINGLE DYNAMIC ANALYSIS MODEL IS NEEDED FOR THE THREE FUNCTIONAL BUILDINGS

- Auxiliary bldg
- Fuel handling bldg
- Turbine bldg

} they are connected

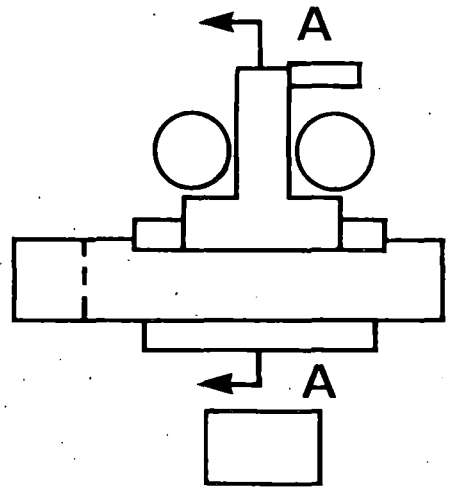

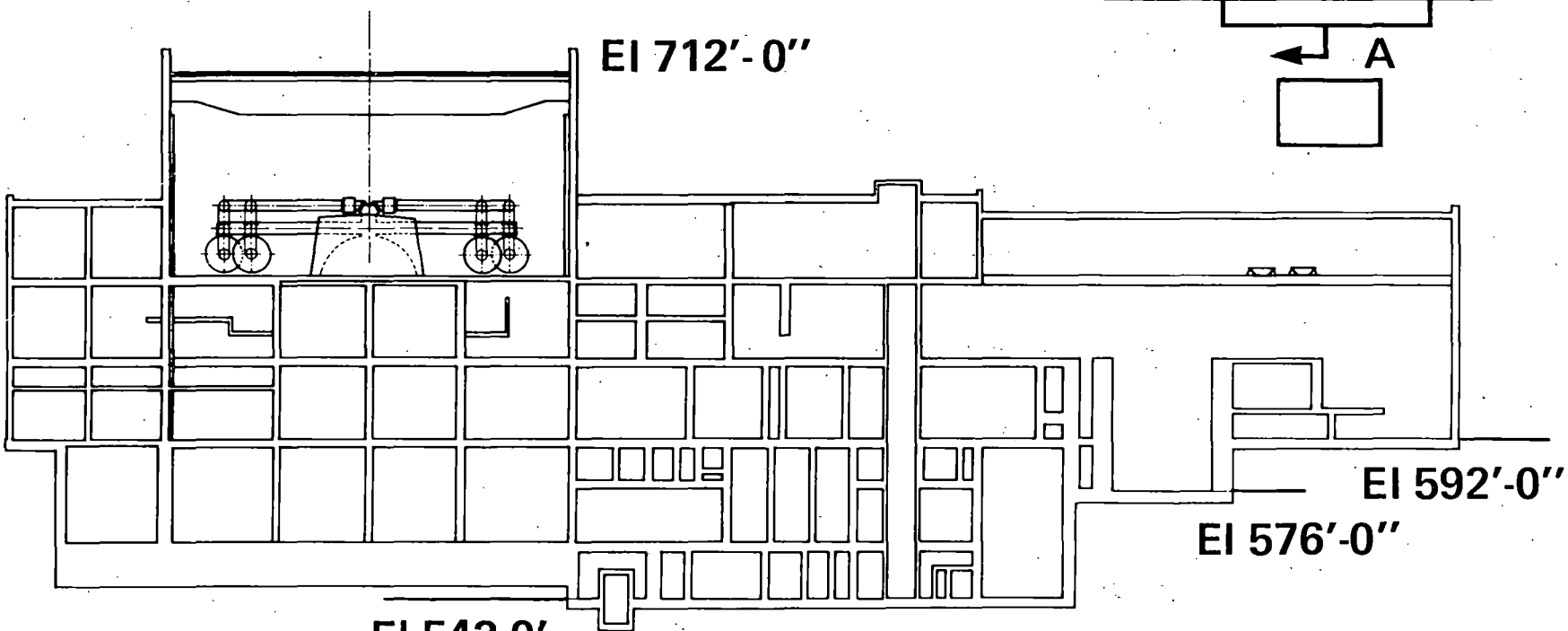

"A-A"

- 113 modes
- 124 responses

ZION HAZARD CURVE

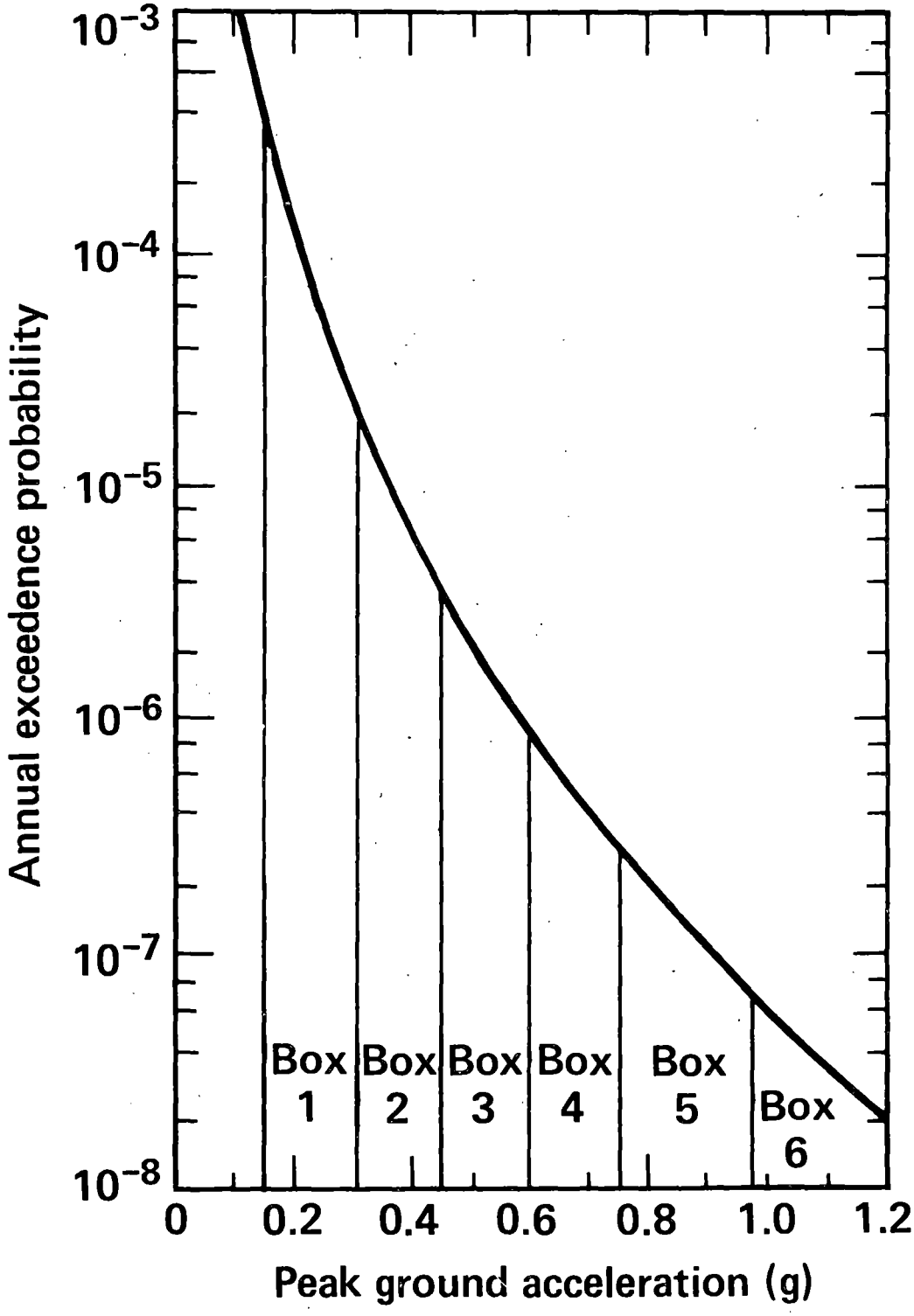

Note: Design earthquakes do not play a direct role

IT IS OF INTEREST TO EXAMINE SOME RESULTS AT THE RESPONSE LEVEL AS WELL AS THE RISK LEVEL

- 30 earthquakes
- Variations in all elements of the seismic methodology chain

VARIATION OF PEAK FREE-FIELD ACCELERATION X-DIRECTION

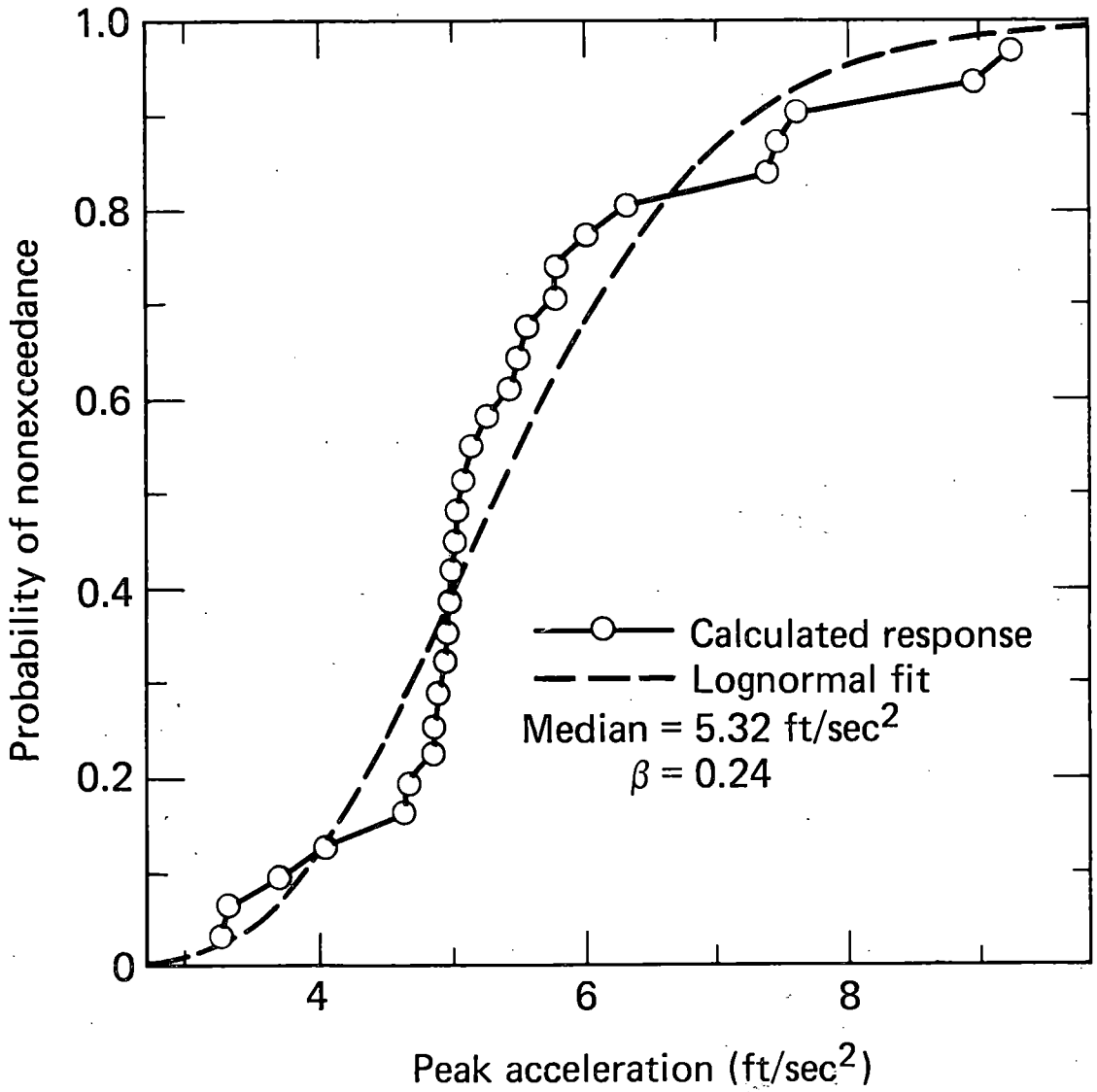

MEAN AND MEAN-PLUS-ONE-STANDARD-DEVIATION RESPONSE SPECTRA – FREE-FIELD, X-DIRECTION

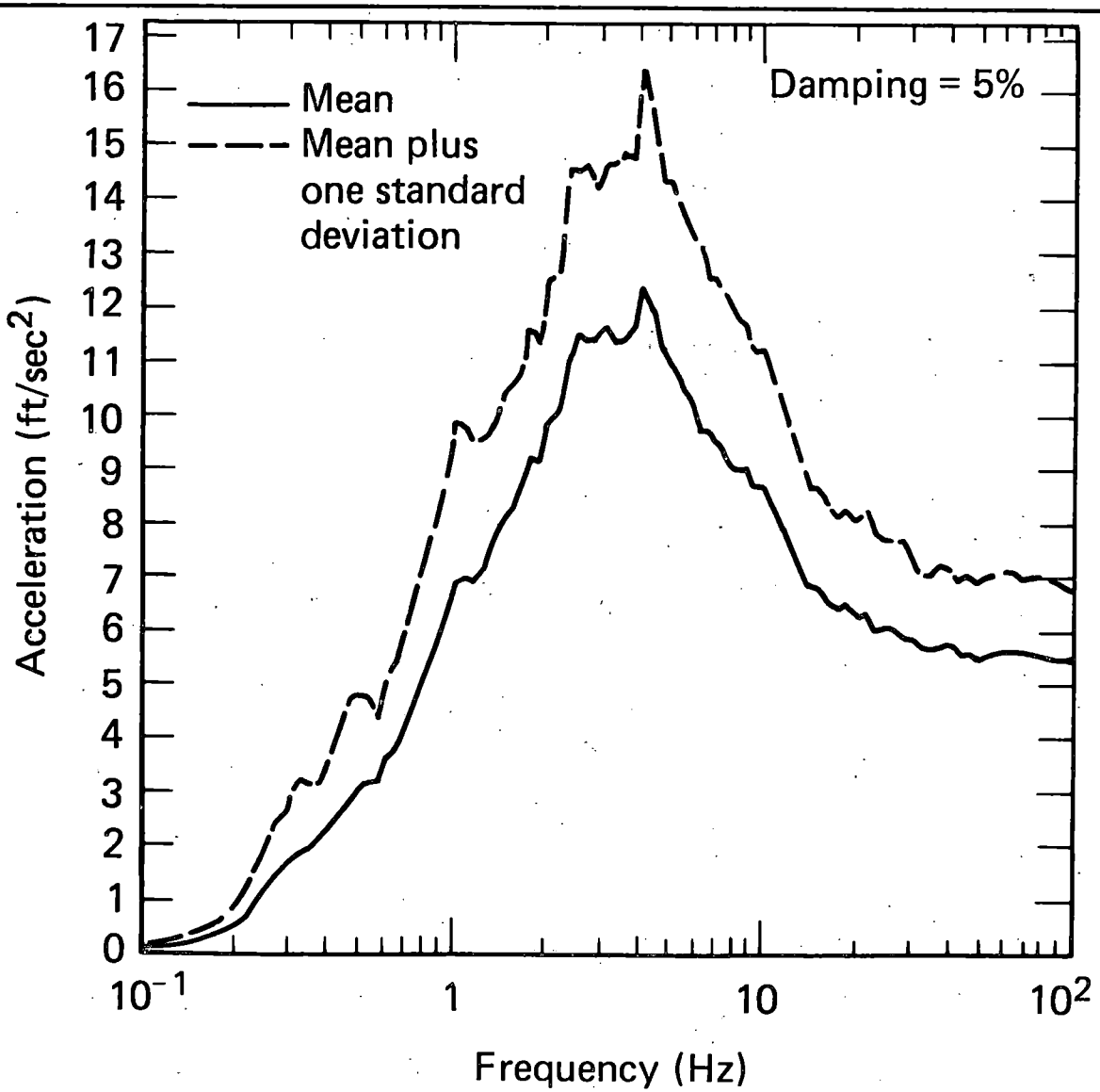

VARIATION OF FOUNDATION PEAK ACCELERATION X-DIRECTION

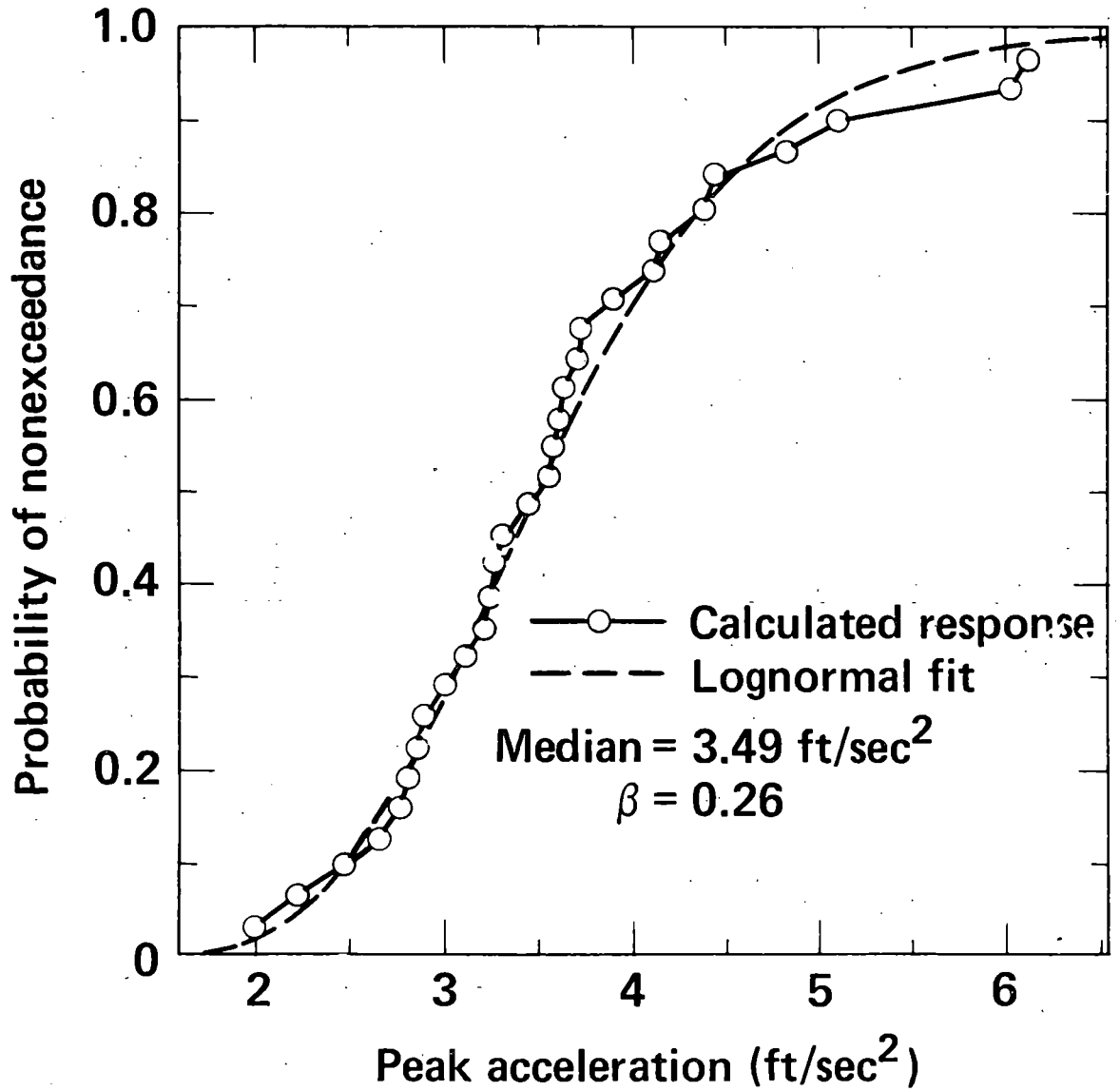

MEAN AND MEAN-PLUS-ONE-STANDARD-DEVIATION RESPONSE SPECTRA--CONTAINMENT BUILDING FOUNDATION, X-DIRECTION

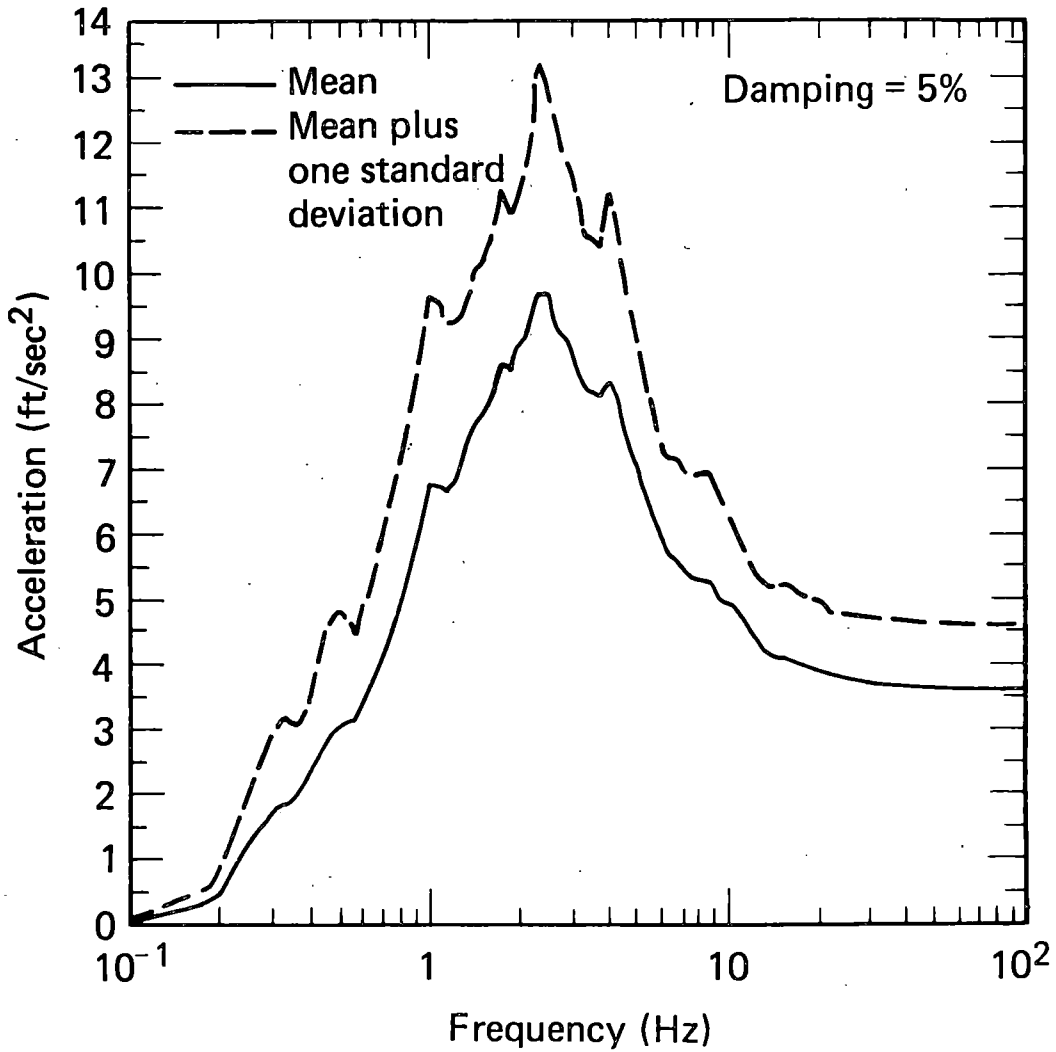

VARIATION OF PEAK ACCELERATION – TOP OF INTERNAL STRUCTURE, X-DIRECTION

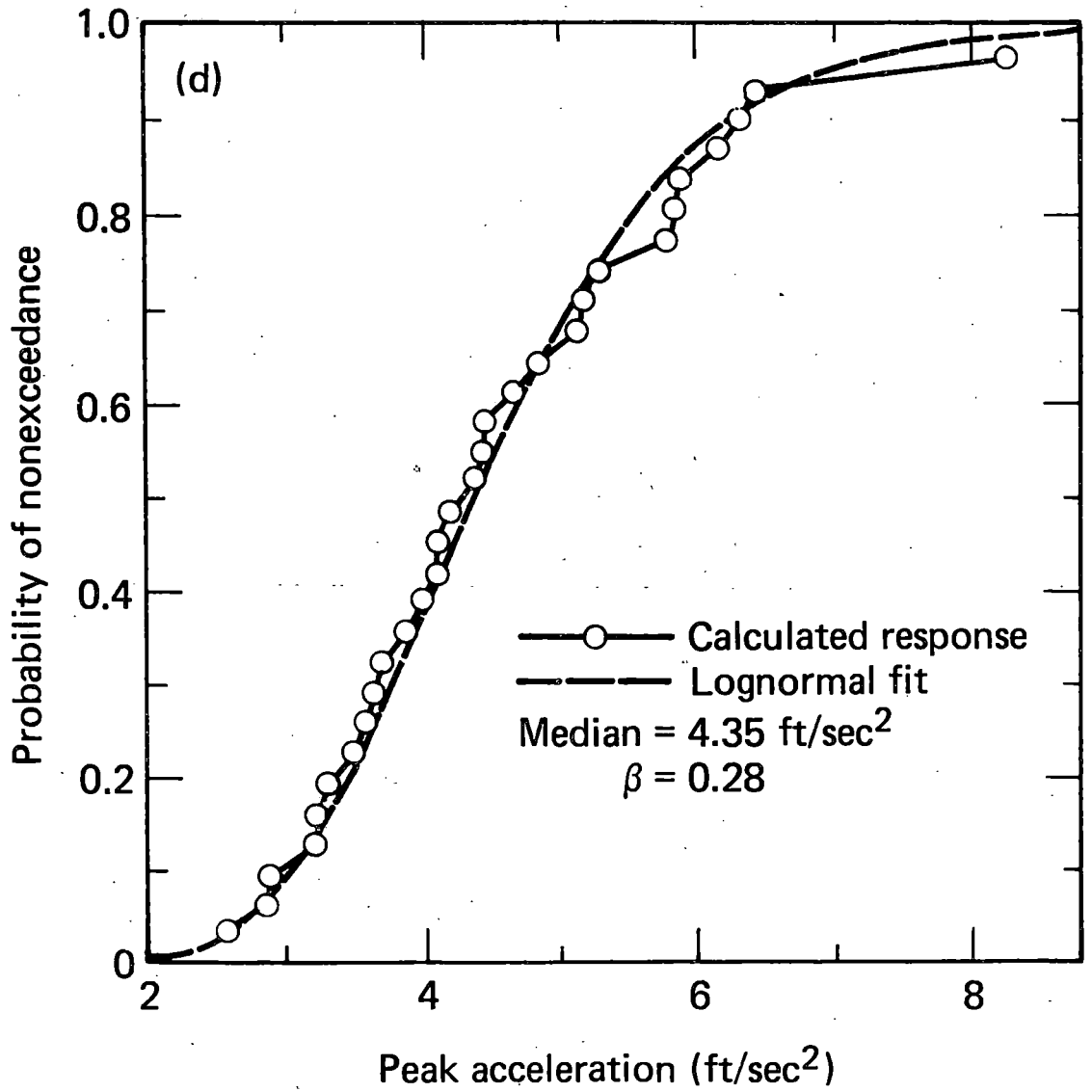

MEAN AND MEAN-PLUS-ONE-STANDARD-DEVIATION RESPONSE SPECTRA--TOP OF CONTAINMENT SHELL, X-DIRECTION

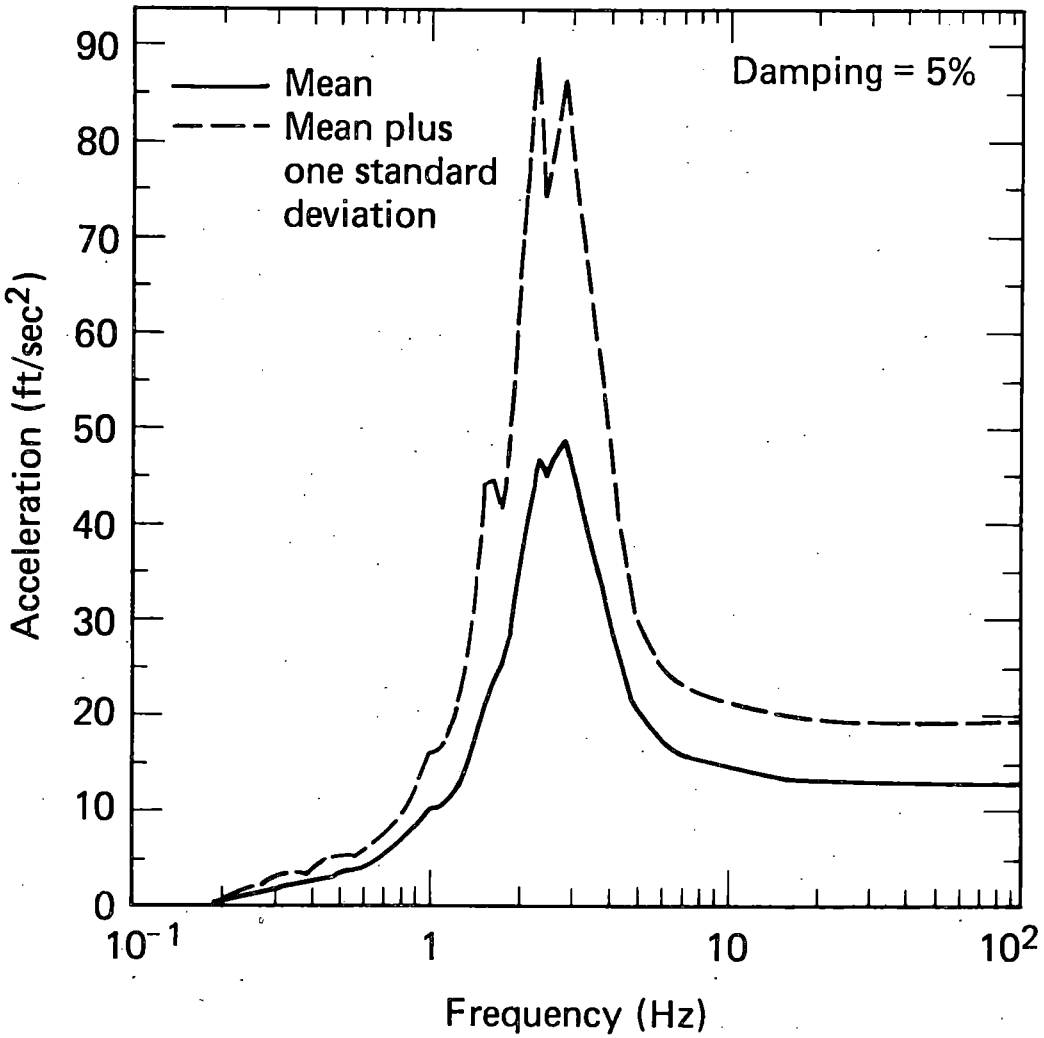

VARIATION OF PEAK ACCELERATION – TOP OF CONTAINMENT, X-DIRECTION

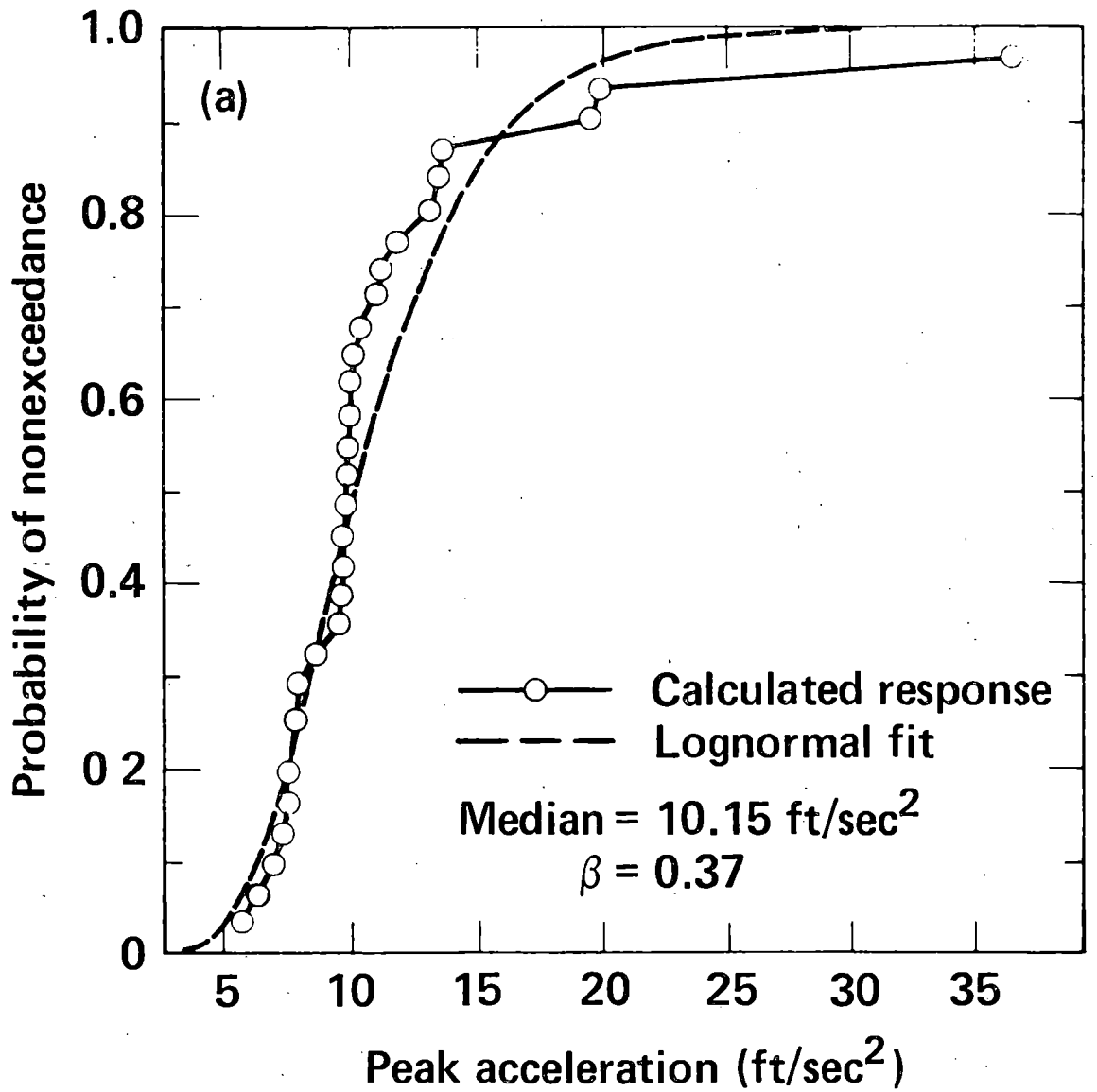

VARIATION OF PEAK ACCELERATION – CONTROL ROOM AFT COMPLEX, X-DIRECTION

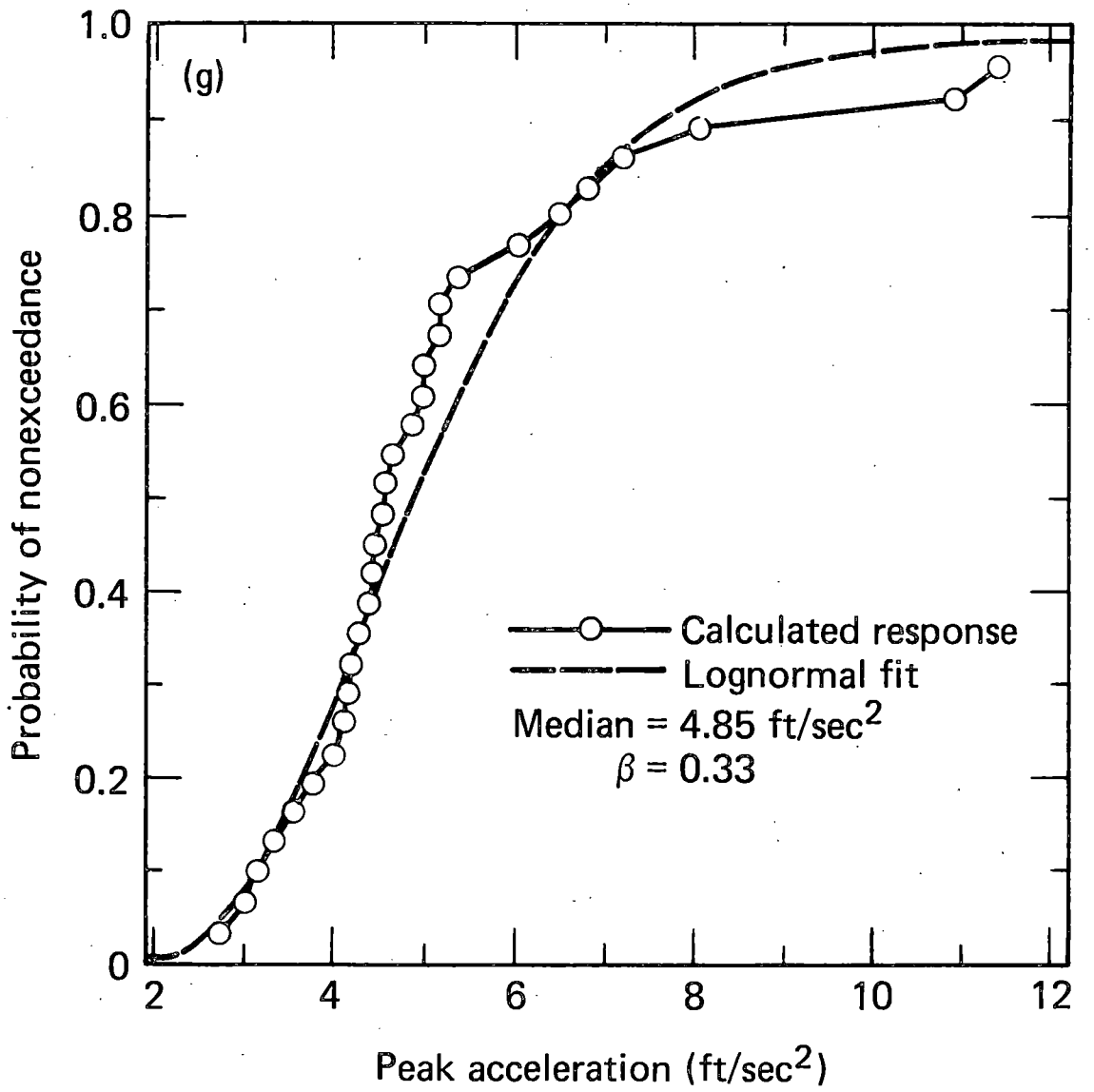

VARIATION OF PEAK ACCELERATION AT CHECK VALVE IN AFW LINE

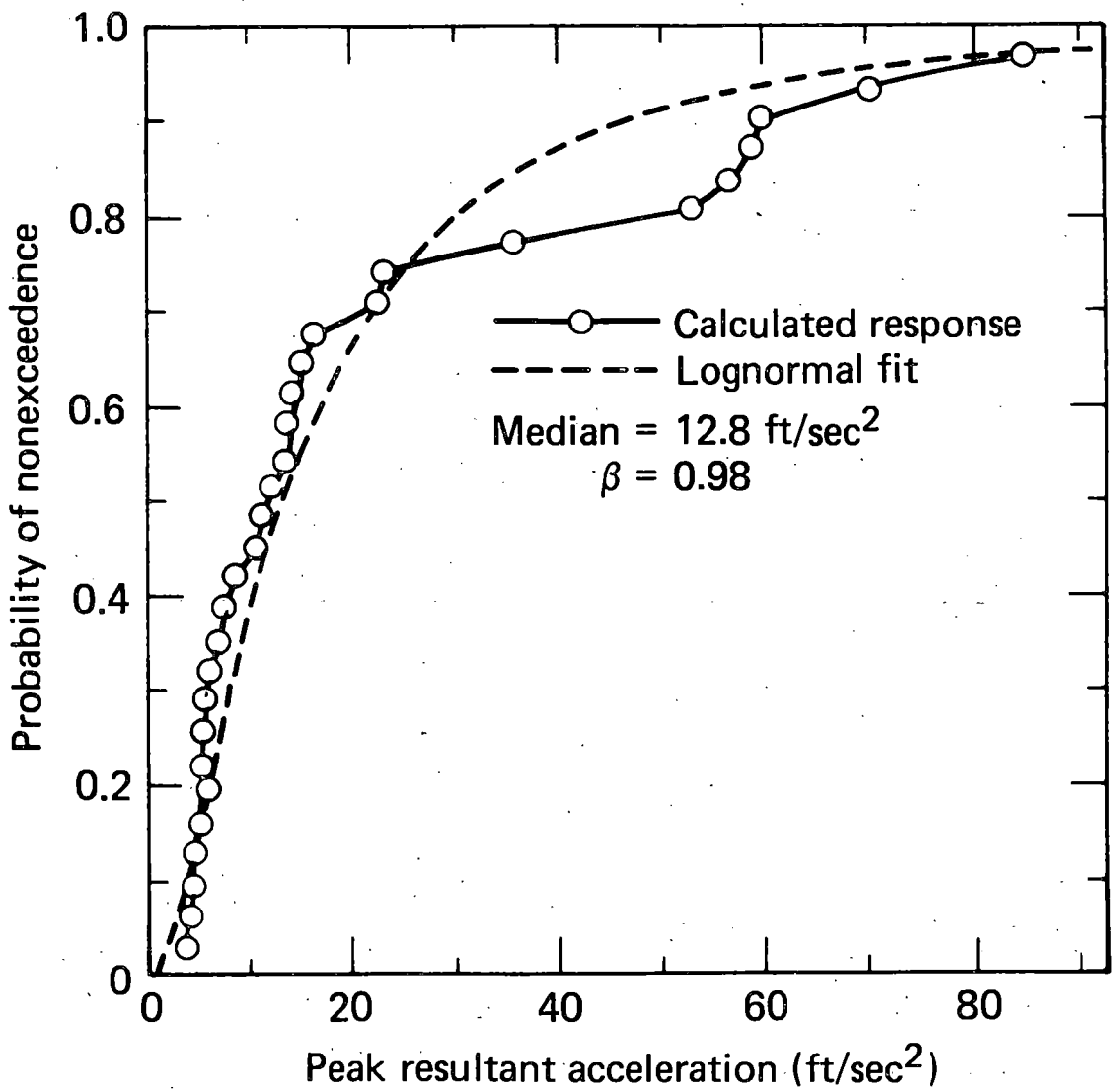

VARIATION IN MOMENT OF THE RCL

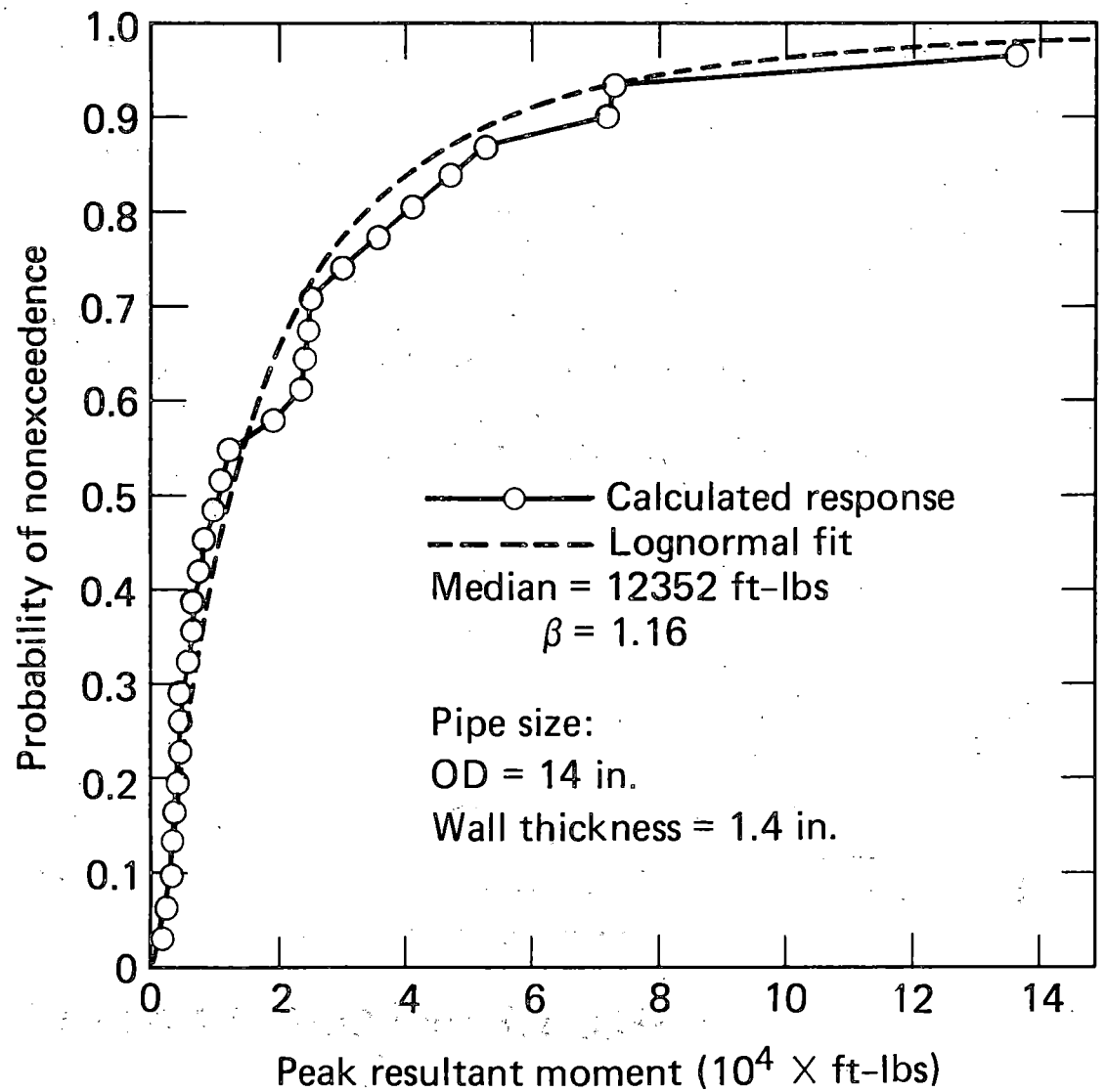

VARIATION IN CRITICAL MOMENT OF THE AFW LINE

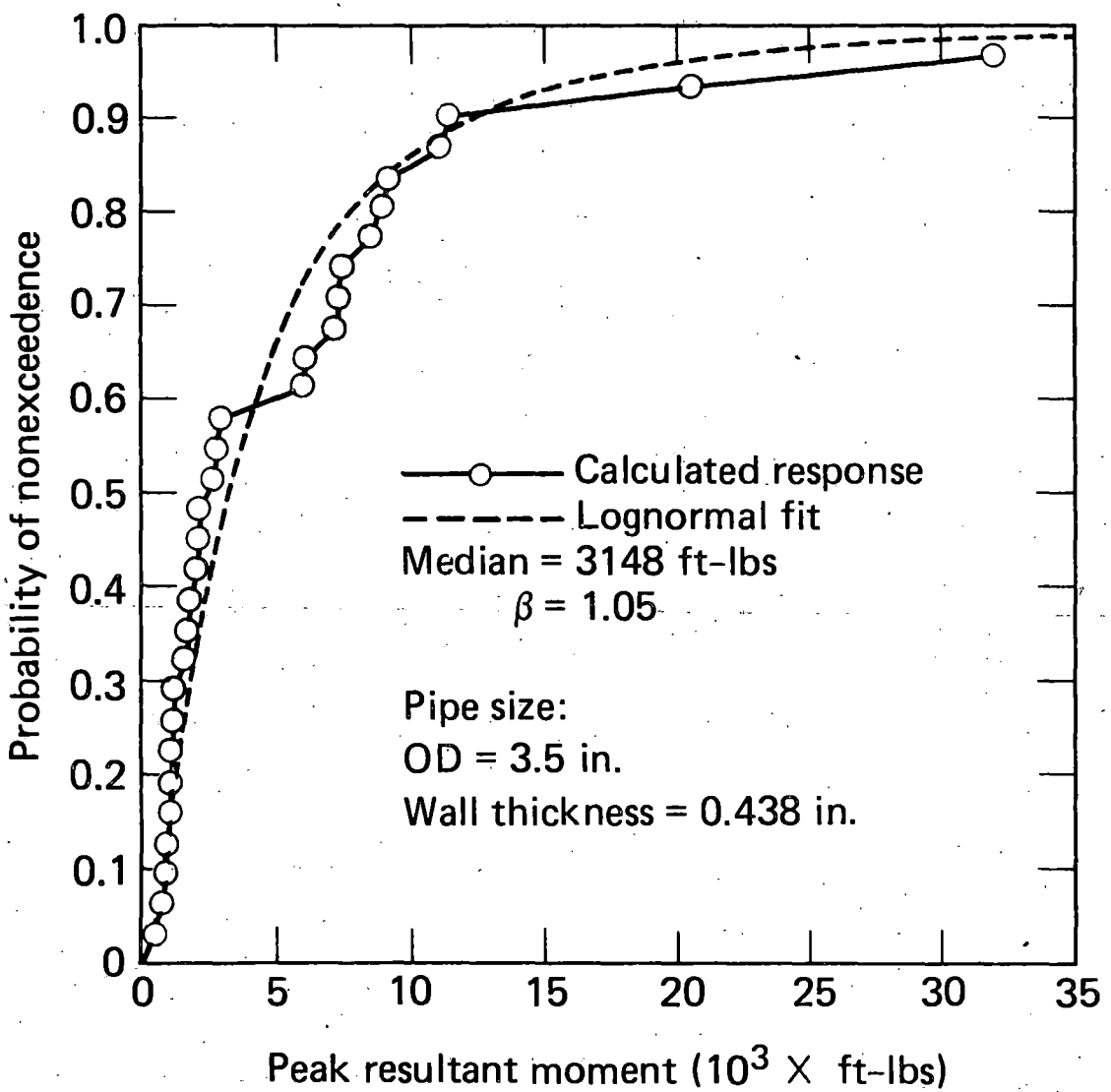

VARIATION IN MOMENT OF THE AFW NOZZLE OF MAIN FW LINE

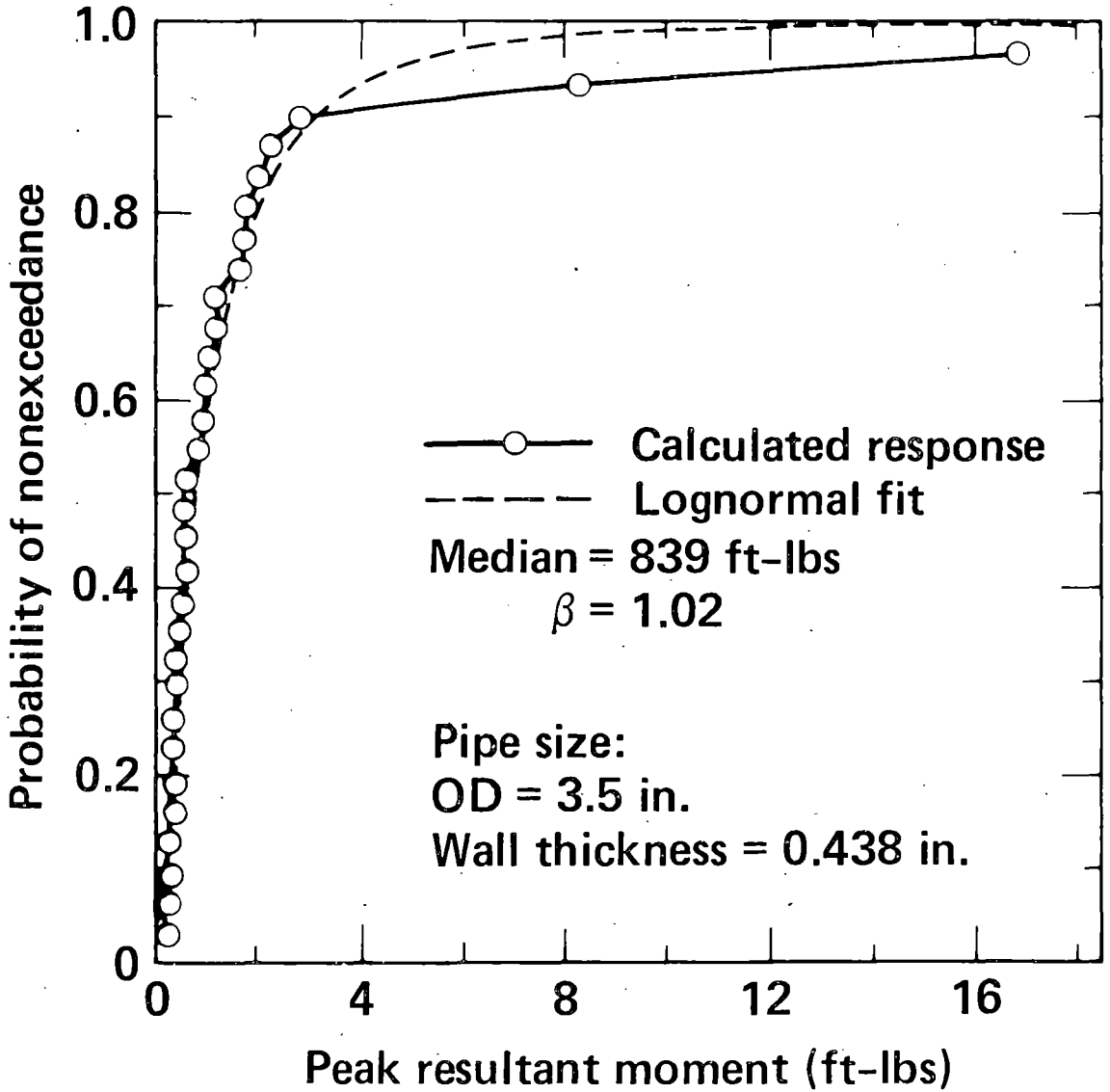

VARIATION IN CRITICAL MOMENT FOR RHR AND SWS

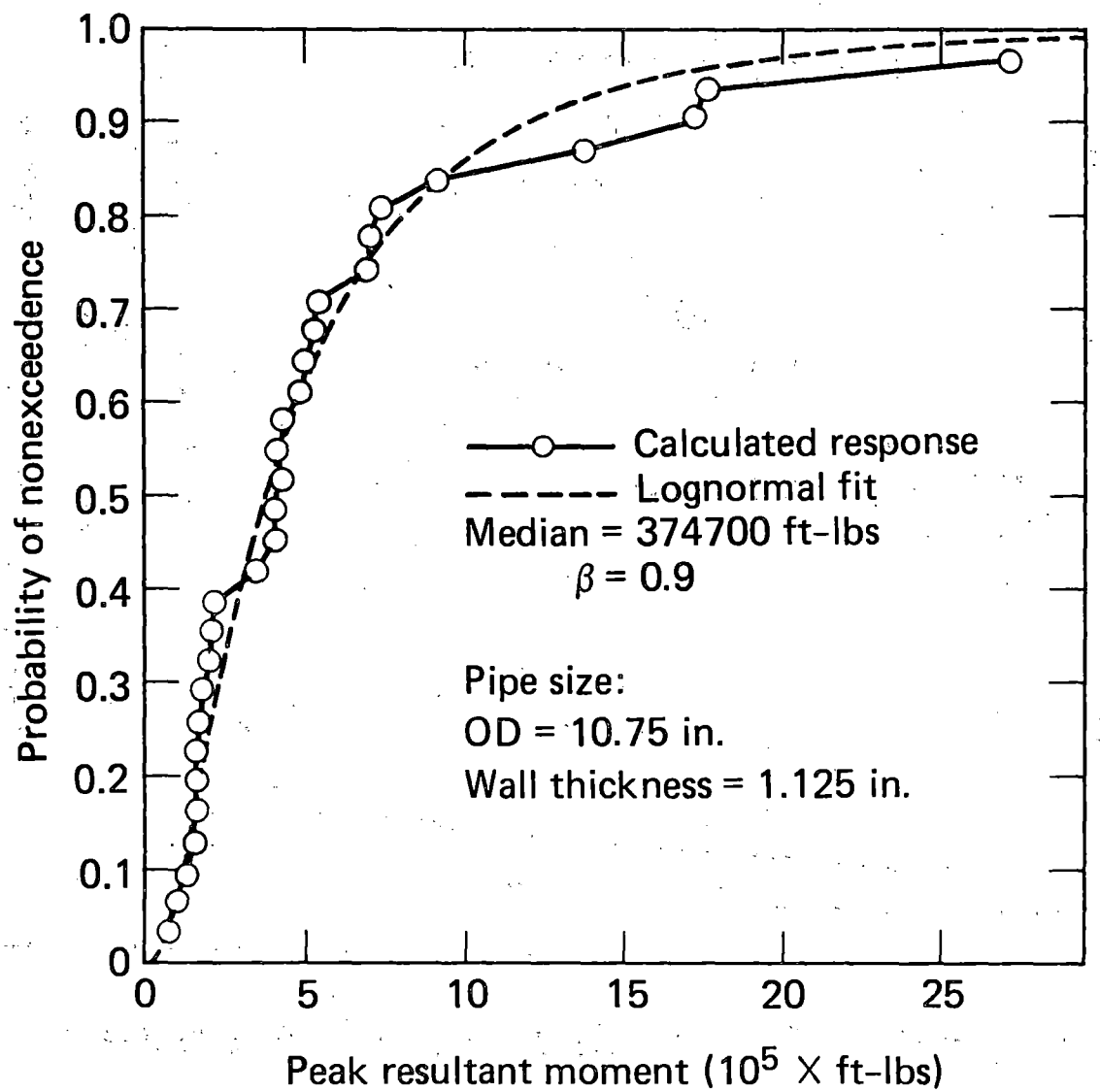

VARIATION OF PEAK ACCELERATION AT SERVICE WATER SYSTEM CRITICAL VALVE

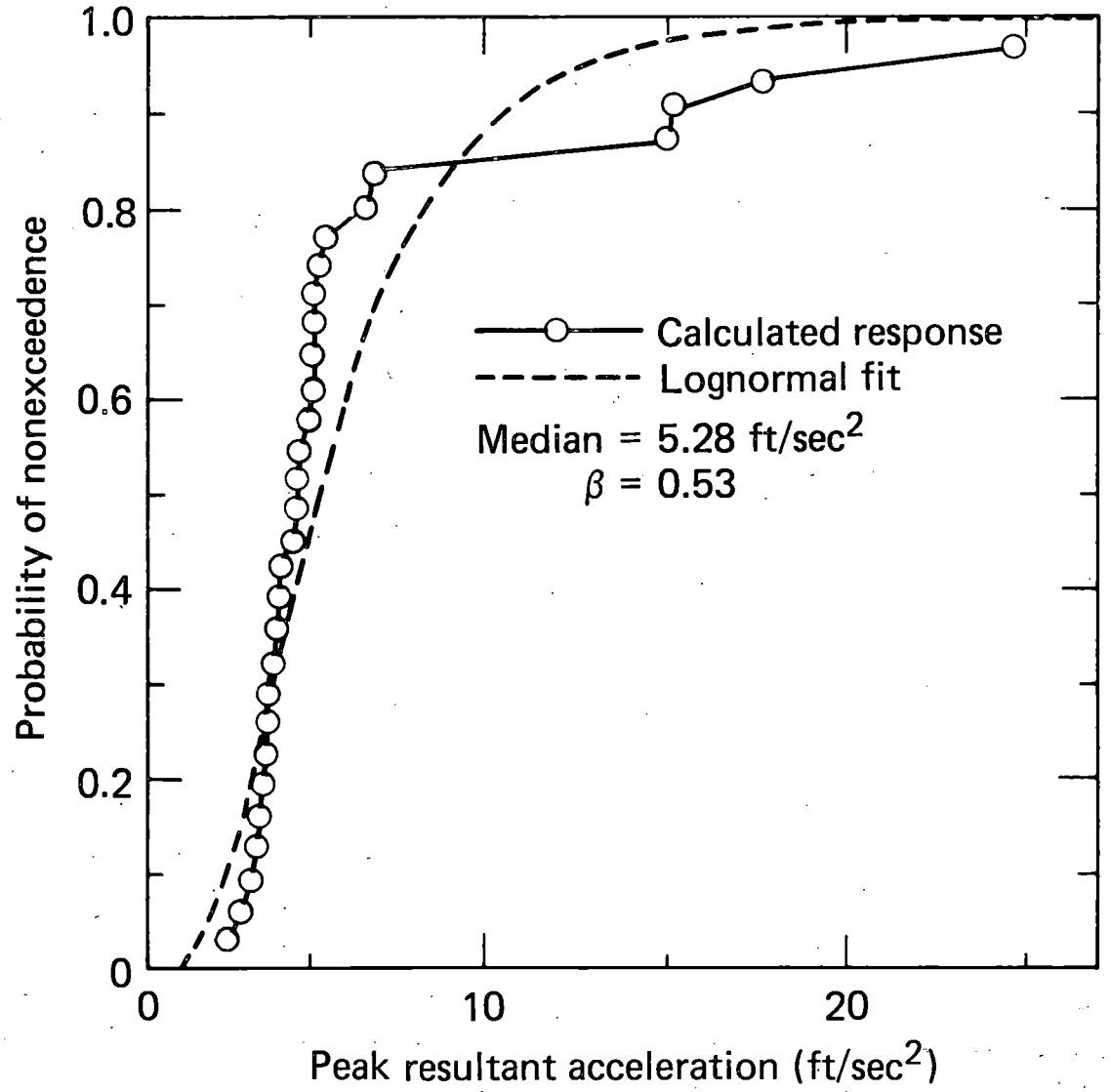

BETA VALUES FOR THE RESPONSES (ACCELERATION RANGE 1)

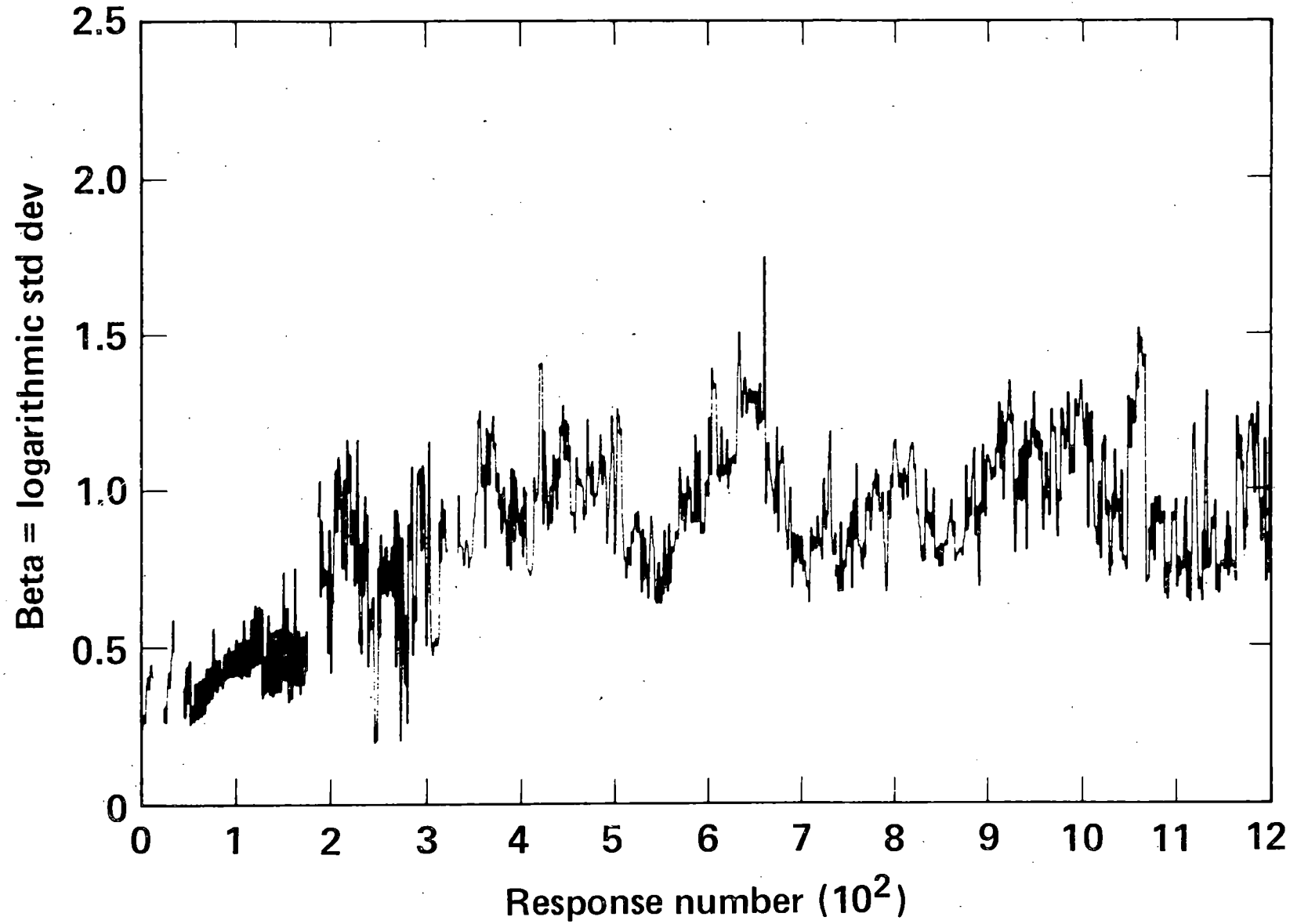

BETA VALUES FOR THE RESPONSES (ACCELERATION RANGE 6)

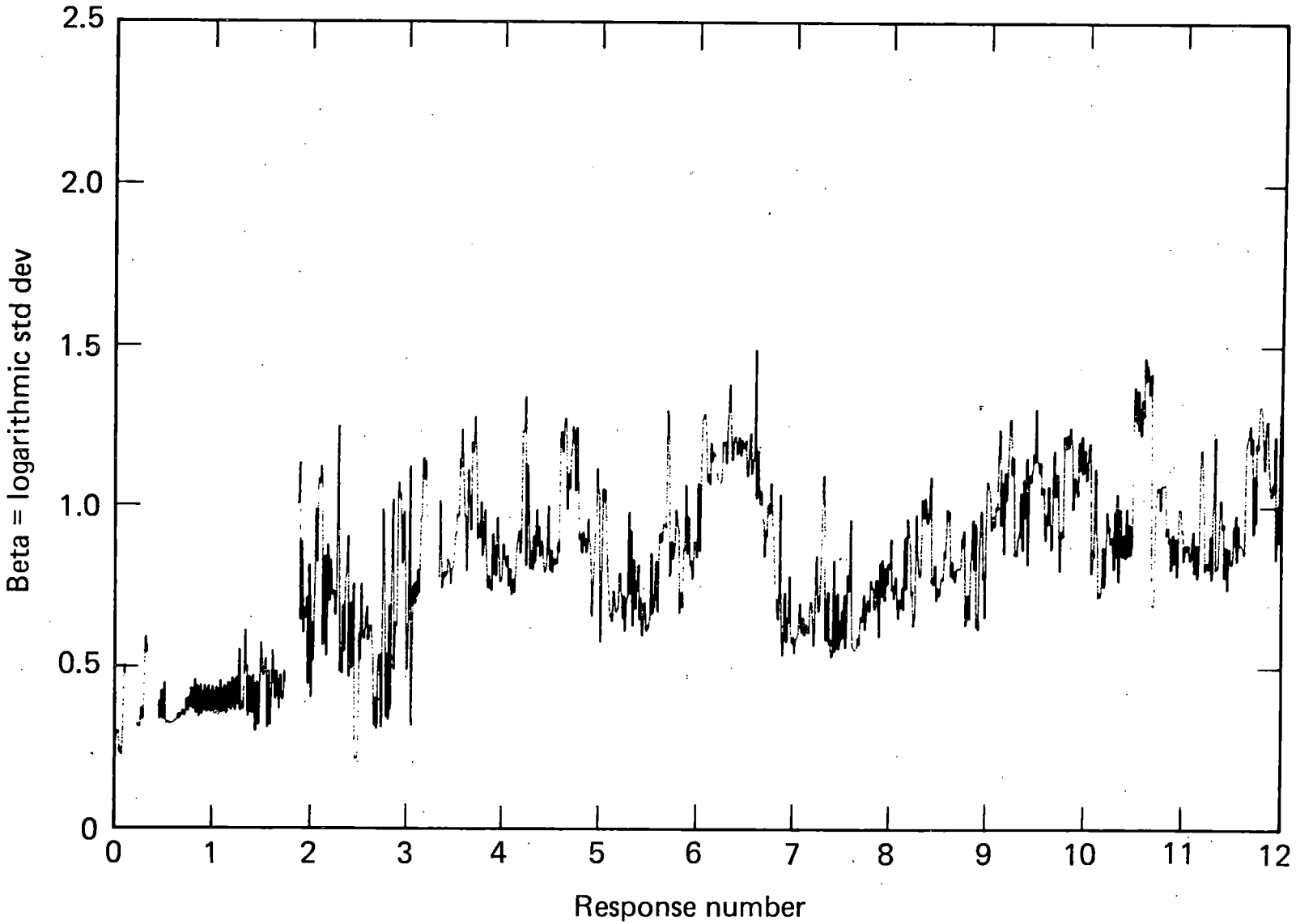

COMPARISON OF MEDIAN RESPONSE VALUES FOR 30 VS 90 EARTHQUAKE SIMULATIONS

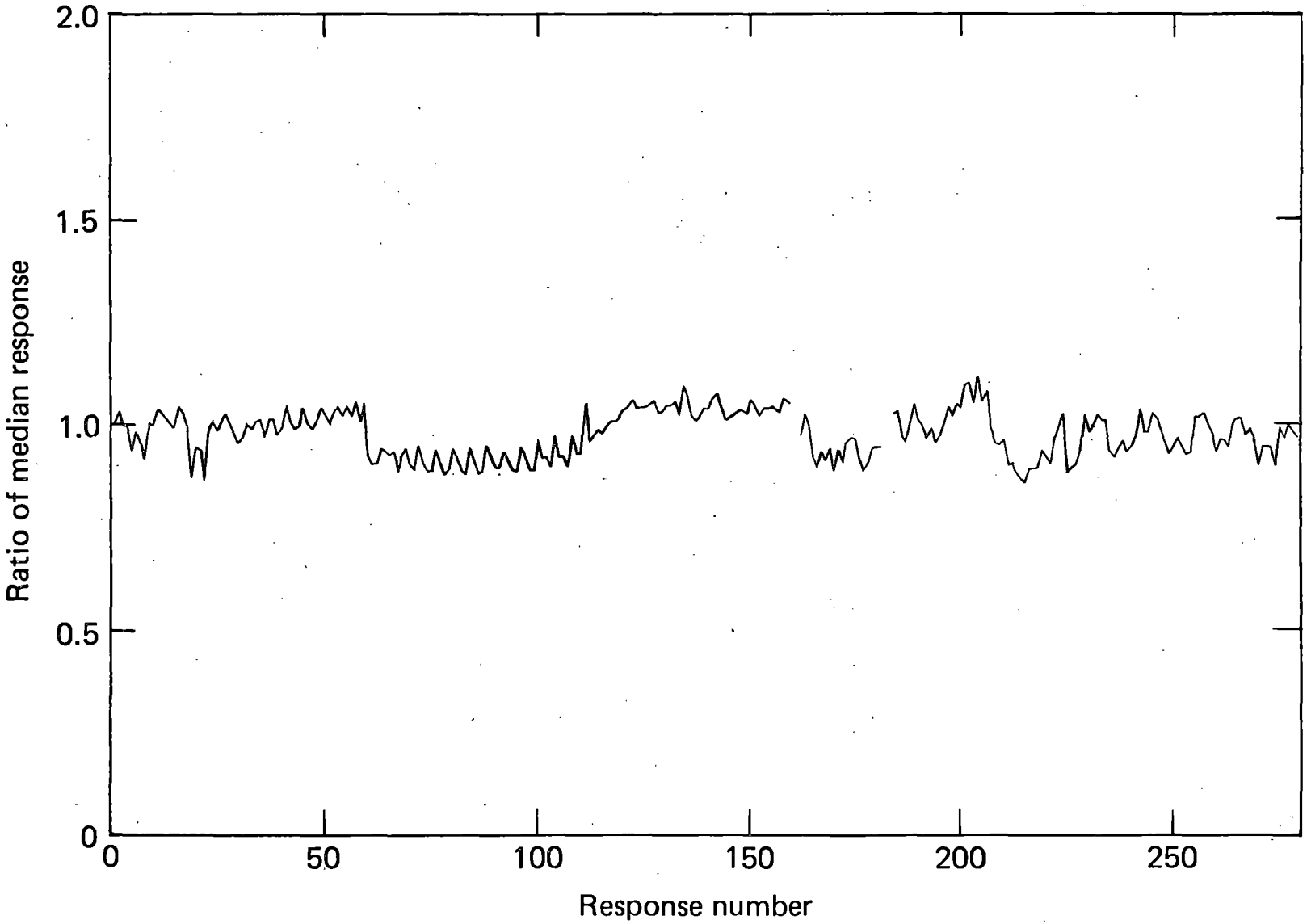

COMPARISON OF BETA VALUES FOR 30 vs 90 EARTHQUAKE SIMULATIONS

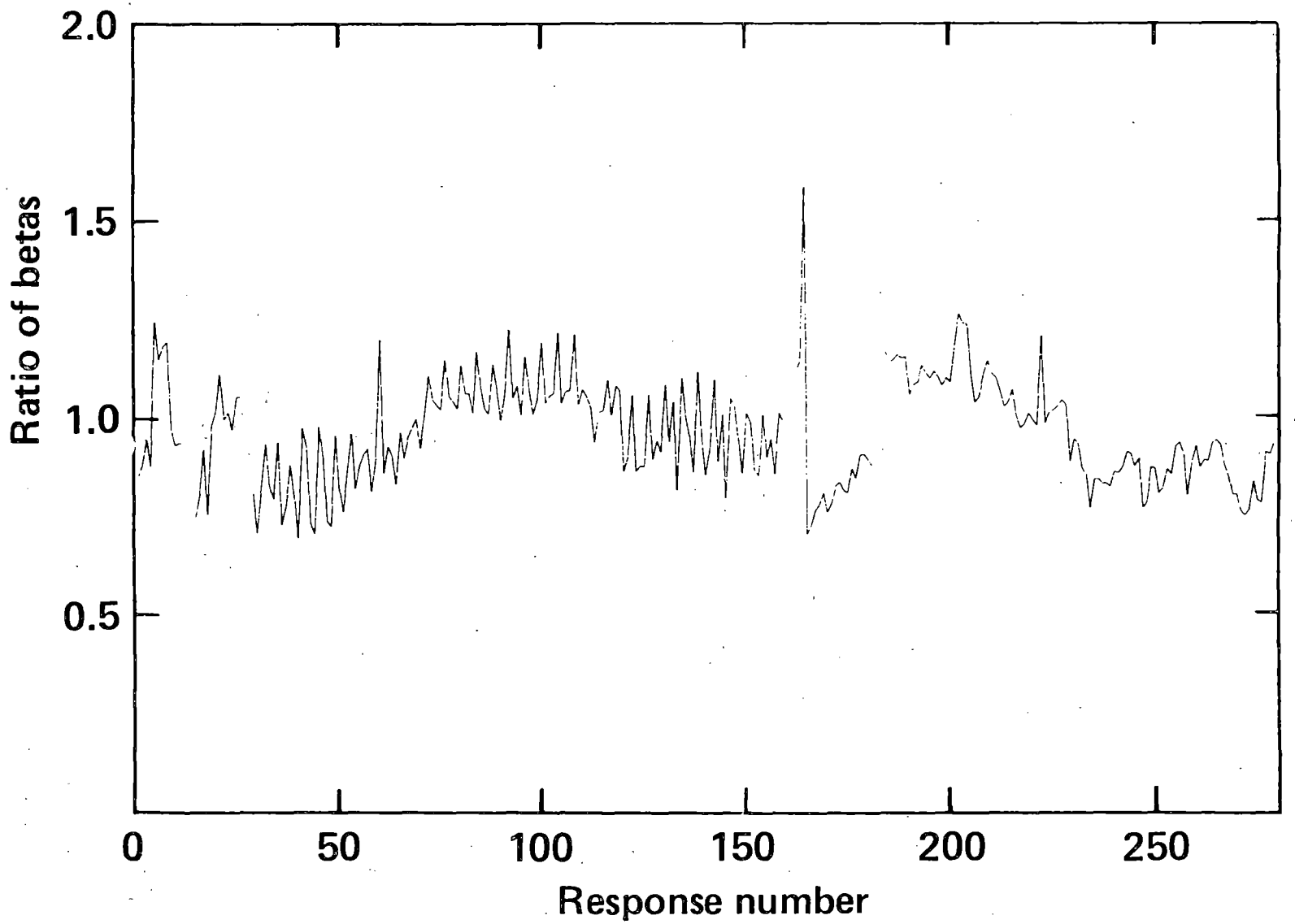

TO ASSESS THE OVERALL EFFECT OF INPUT PARAMETER DISTRIBUTIONS ON RESPONSE, THE FOLLOWING LOG NORMAL DISTRIBUTIONS WERE CONSIDERED

	COV	10%	50%	90%
Soil shear modulus	0.35	0.65	1.0	1.55
Soil damping	0.50	0.55	1.0	1.90
Structure frequency	0.25	0.73	1.0	1.37
Structure damping	0.35	0.65	1.0	1.55
Subsystem (piping) frequency	0.25	0.73	1.0	1.37
Subsystem (piping) damping	0.35	0.65	1.0	1.55

COMPARISON OF MEDIAN RESPONSE VALUES FOR HALF VARIABILITY VS FULL VARIABILITY

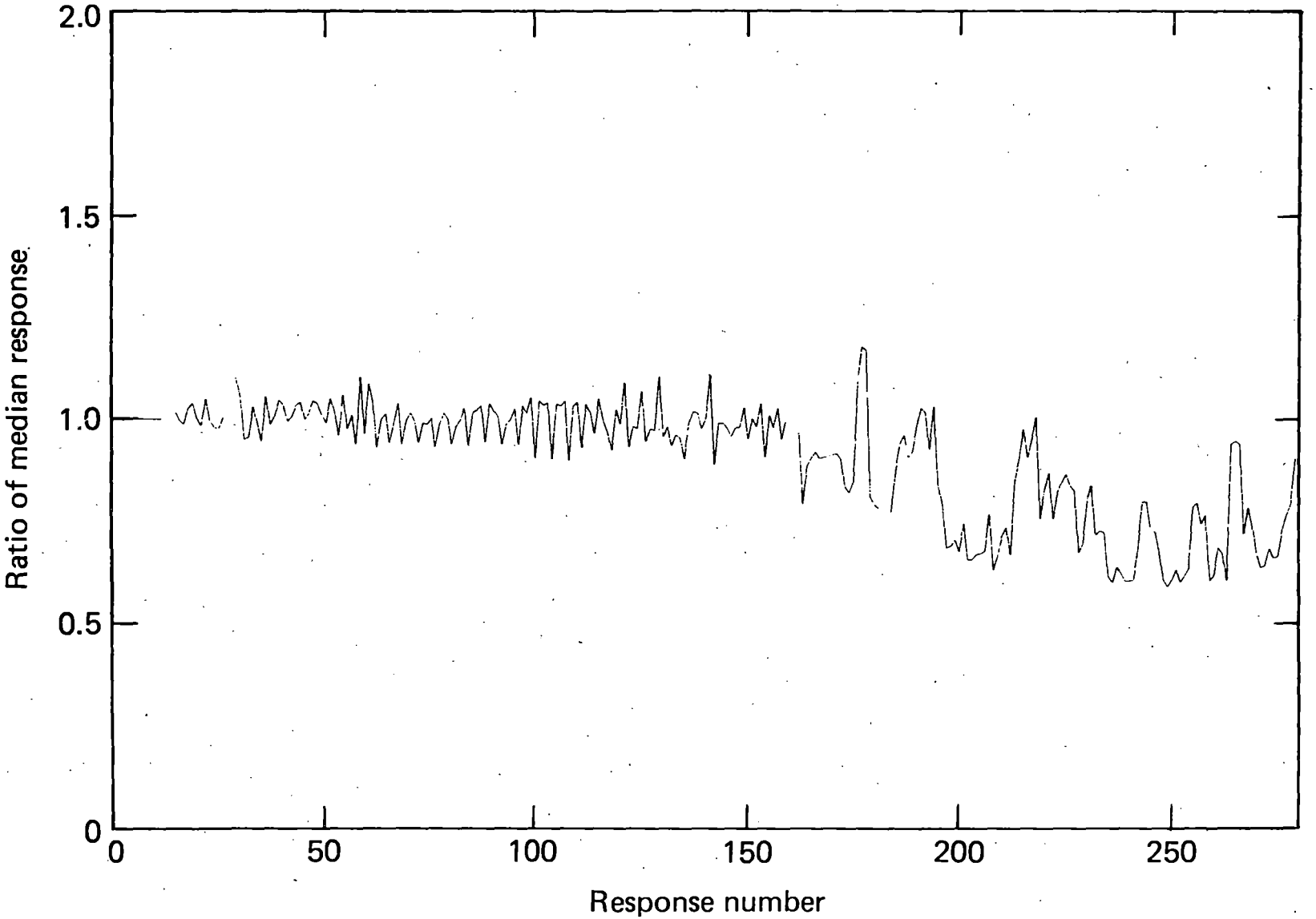

COMPARISON OF BETA VALUES FOR HALF VARIABILITY vs FULL VARIABILITY

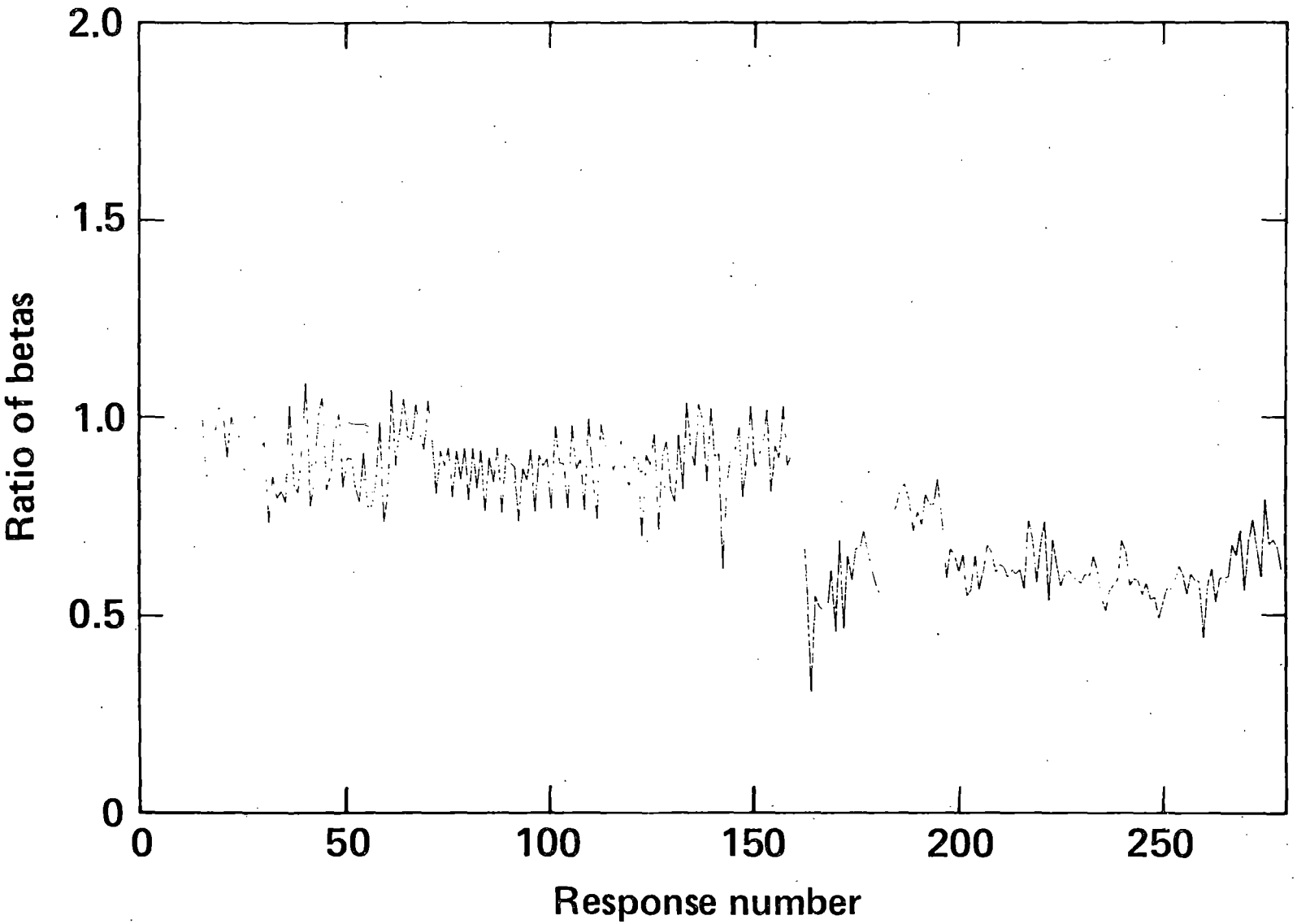

SEISMIC SAFETY MARGINS RESEARCH PROGRAM (SSMRP)

BUILDING AND PIPING SENSITIVITY STUDIES

Presented by:
Shyam N. Shukla

Lawrence Livermore National Laboratory

Presented at:
9th Water Reactor Safety Research
Information Meeting

Sponsored by:
U.S. Nuclear Regulatory Commission
Office of Nuclear Regulatory Research
Division of Reactor Safety Research
Gaithersburg, Maryland
October 26 1981

OUTLINE

- Objectives
- Structural dynamics models
- Modeling of uncertainty
- Results
- Conclusions

OBJECTIVES

- To study the sensitivity of structural and subsystem response due to input variations
- To rank the sources of uncertainty contributing to response uncertainty

THE STEPS IN THE SEISMIC METHODOLOGY CHAIN, COMPUTE DYNAMIC RESPONSES OF STRUCTURES AND EQUIPMENT

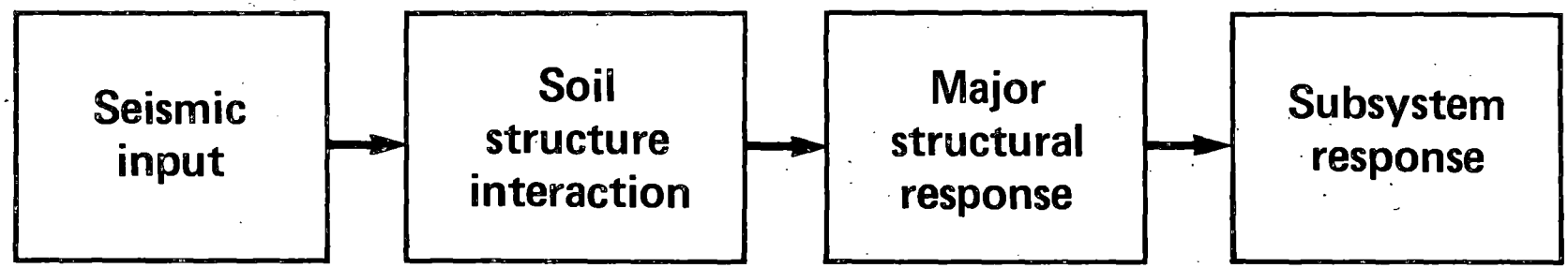

Seismic Methodology Chain (SMC)

THE ZION-1 PLANT WAS MODELED AS A REPRESENTATIVE EXAMPLE

- Structures
  - Reactor building (containment shell and internal structure)
  - Auxiliary-fuel-turbine building complex
- Subsystems
  - Reactor coolant loop (RCL)
  - Auxiliary feedwater (AFW) piping inside containment
  - RHR-SI piping in auxiliary building

CROSS SECTION OF THE CONTAINMENT BUILDING AT ZION, SHOWING THE APPROXIMATE EXTENT OF EMBEDMENT

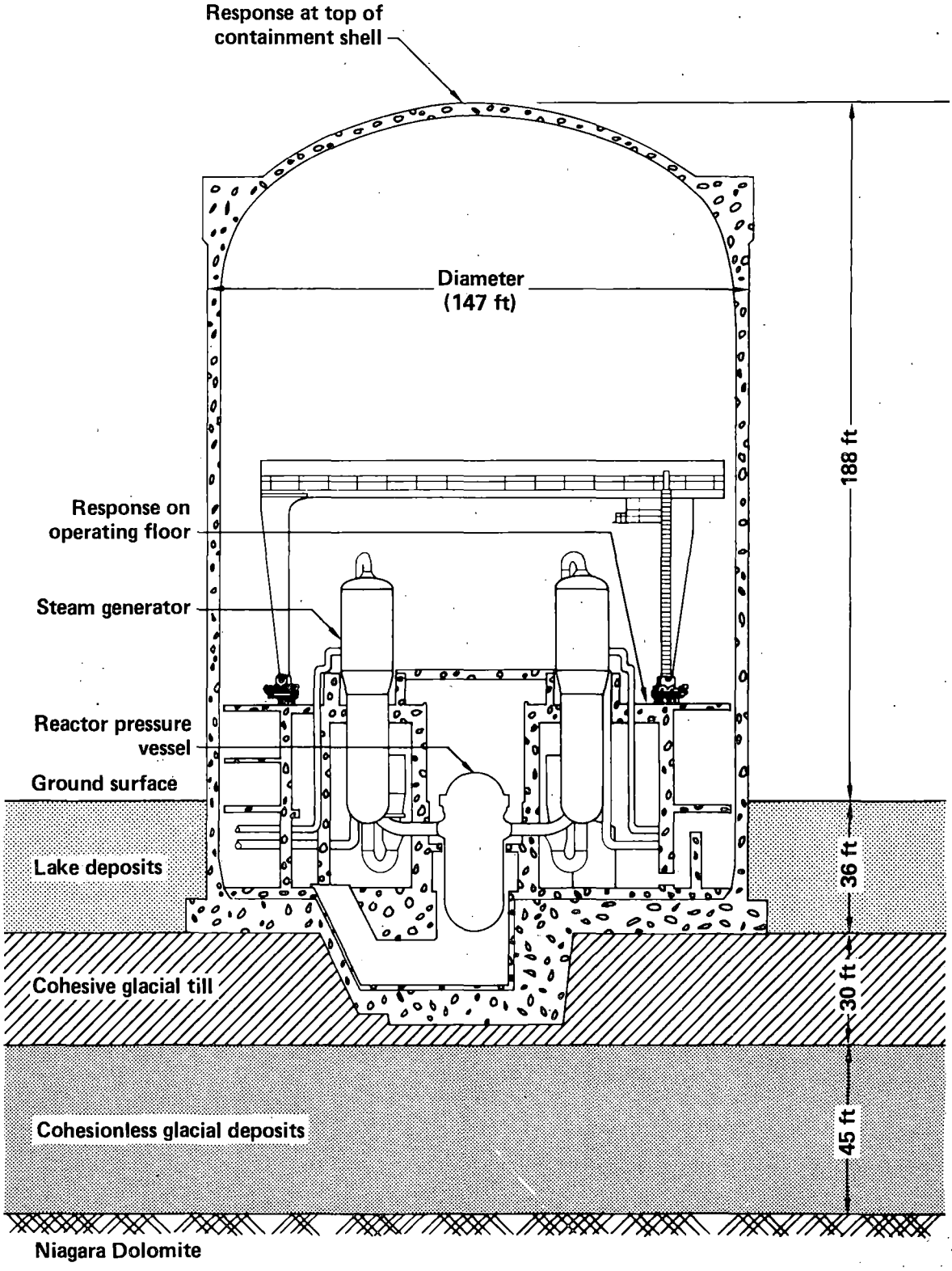

FINITE ELEMENT MODEL OF A PORTION OF THE AUXILIARY BUILDING

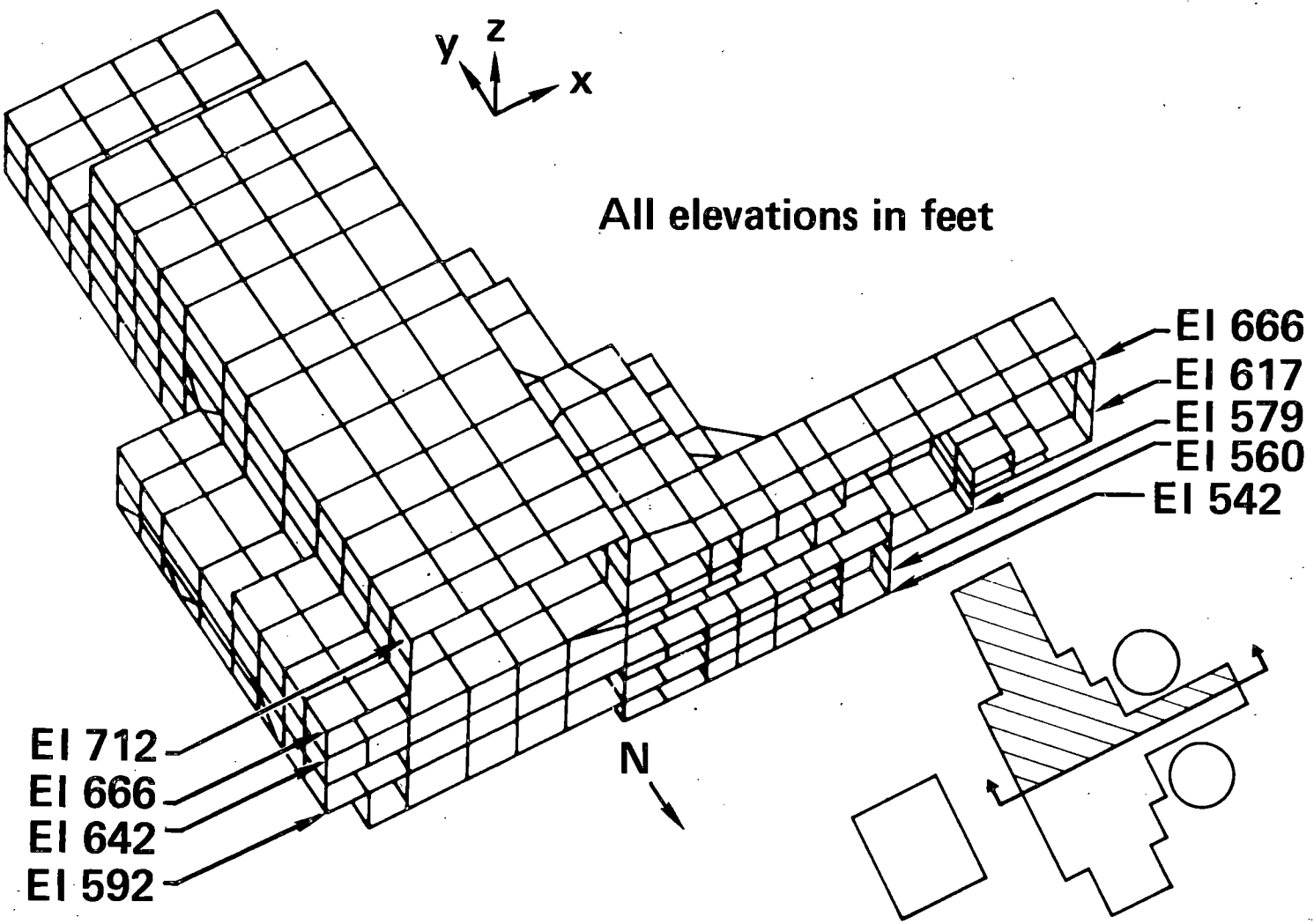

MODELING OF UNCERTAINTY

- Key parameters
- Uncertainty estimates
- Response sample using latin hypercube sampling

LOGNORMAL DISTRIBUTION IS ASSUMED FOR THE KEY PARAMETERS IN SEISMIC METHODOLOGY CHAIN (SMC)

SMC	Key parameter	CV
Seismic Input (SI)	Time histories	N/A
Soil	Shear modulus	0.5
	Damping	1.0
Structure (STR)	Frequency	0.5
	Damping	0.7
Subsystem (SUB)	Frequency	0.5
	Damping	0.7

LATIN HYPERCUBE SAMPLING IS USED TO EVALUATE THE PROBABILISTIC MODEL

- Variations in material properties
- Variations in construction details
- Modeling uncertainty
- Analysis uncertainty

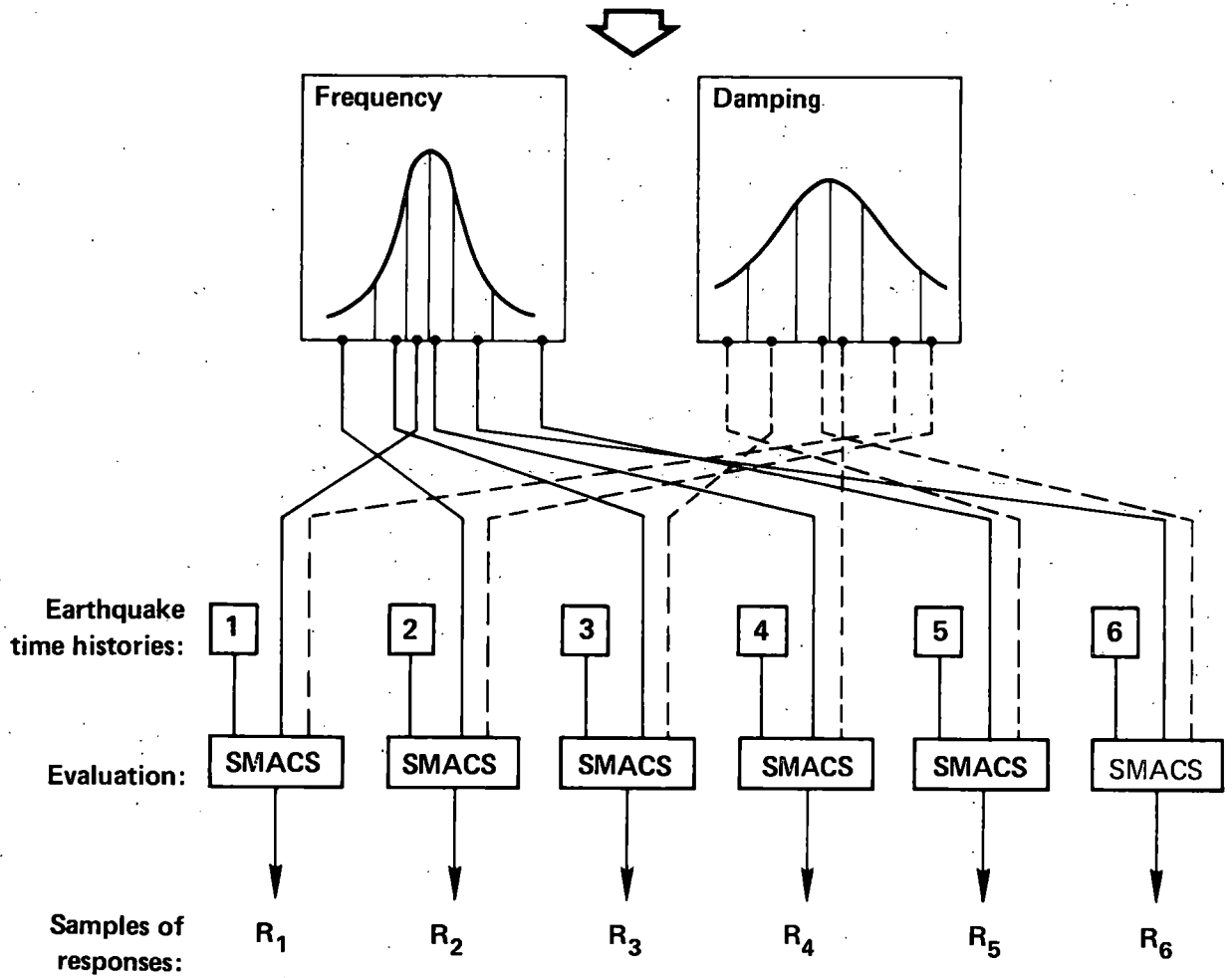

NUMERICAL EXPERIMENTS SEPARATE THE EFFECTS OF UNCERTAINTY IN THE DIFFERENT SMC AREAS

Expt. No.	SI	Soil	STR	SUB
1	V	V	V	V
2	V	V	V	F
3	V	V	F	F
4	V	F	F	F
5	V	F	V	V
6	V	F	F	V
7	V	V	F	V
8	V	F	V	F
9	F	V	V	V

Notes

V: key parameters varied

F: key parameters fixed

CUMULATIVE DISTRIBUTION FUNCTION OF PEAK RESULTANT MOMENTS SHOWS A LOGNORMAL DISTRIBUTION

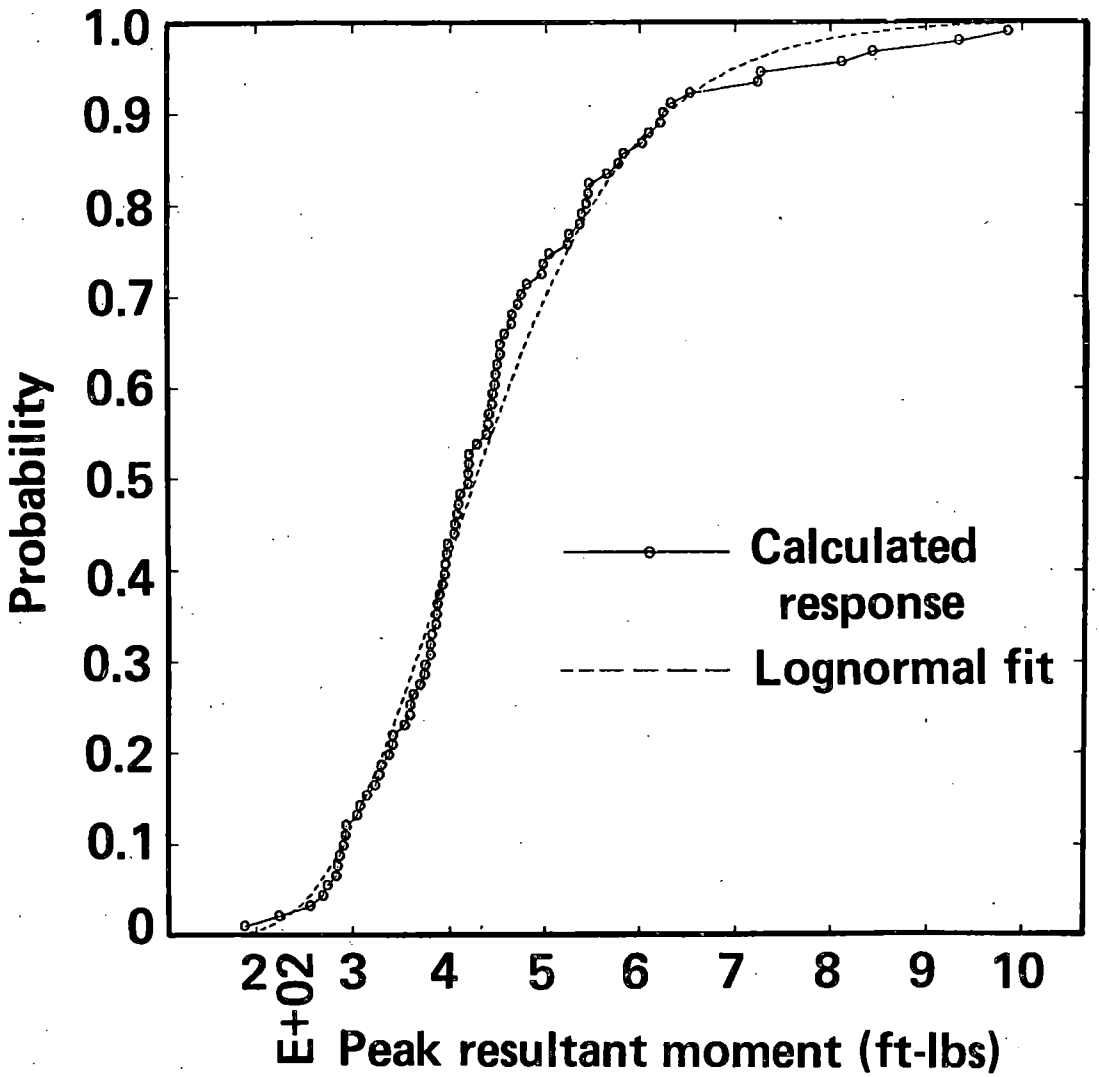

FOR LOG NORMAL DISTRIBUTION
β IS A MEASURE OF UNCERTAINTY

- β = standard deviation of the log of the variables
- $\beta \approx \sigma/\mu \approx$ cov for $\beta \ll 1$

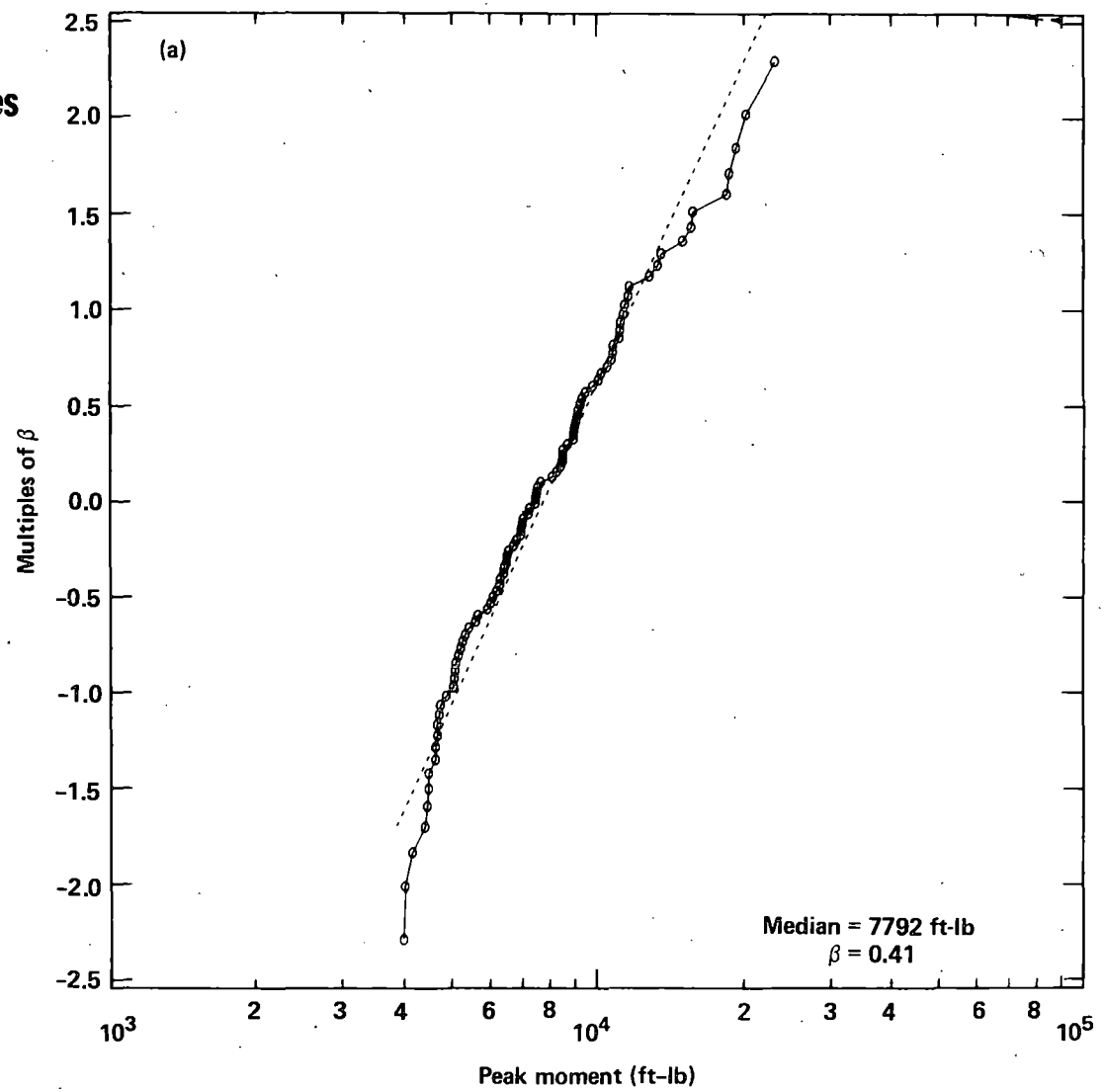

THE RESPONSE UNCERTAINTIES ARE LARGEST IN THE SUBSYSTEMS, EXPERIMENT 1

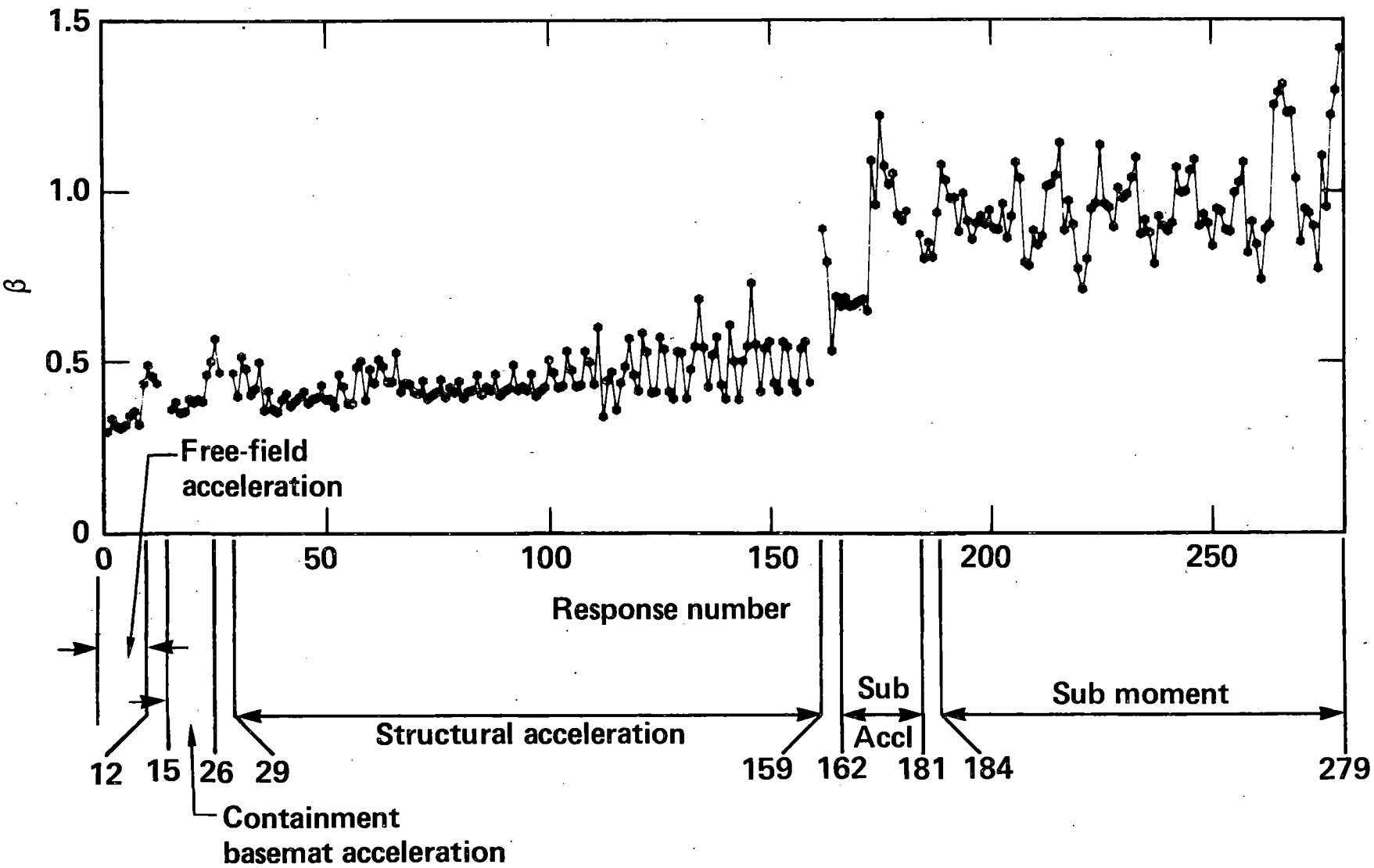

KEY PARAMETERS REPRESENTING UNCERTAINTY IN SMC

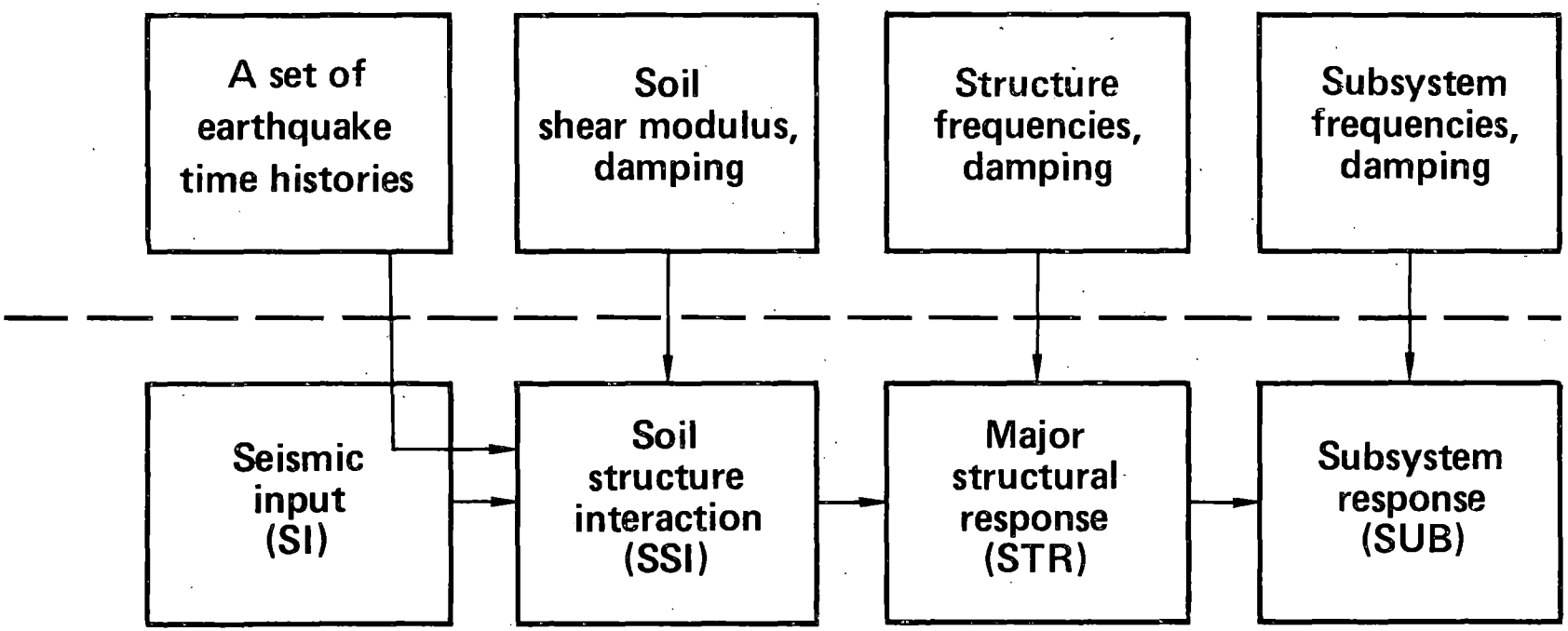

WHEN ONLY SEISMIC INPUT IS VARYING RESPONSES IN ALL AREAS HAVE SIMILAR UNCERTAINTIES, EXPT 4

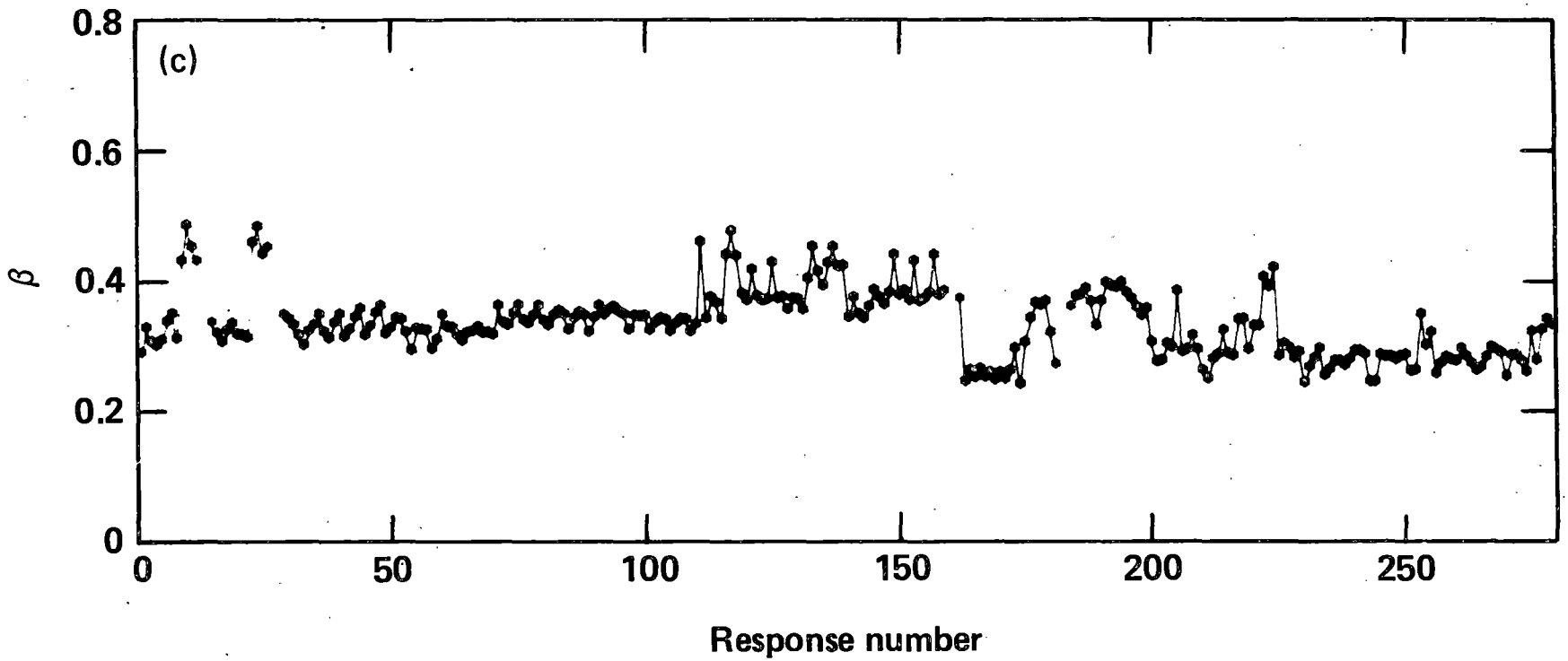

NUMERICAL EXPERIMENTS SEPARATE THE EFFECTS OF UNCERTAINTY IN THE DIFFERENT SMC AREAS

Expt No.	SI	Soil	STR	SUB	Variables
1	V	V	V	V	
2	V	V	V	F	
3	V	V	F	F	SI + SSI
4	V	F	F	F	SI
5	V	F	V	V	
6	V	F	F	V	SI + SUB
7	V	V	F	V	
8	V	F	V	F	SI + STR
9	F	V	V	V	

Notes

V: key parameters varied

F: key parameters fixed

$$\sigma^2(\text{SI}) = \sigma^2(4)$$
$$\sigma^2(\text{SSI}) = \sigma^2(3) - \sigma^2(4)$$
$$\sigma^2(\text{STR}) = \sigma^2(8) - \sigma^2(4)$$
$$\sigma^2(\text{SUB}) = \sigma^2(6) - \sigma^2(4)$$

THE CONTRIBUTION TO RESPONSE β^2 FROM STR AND SUB ARE LARGE

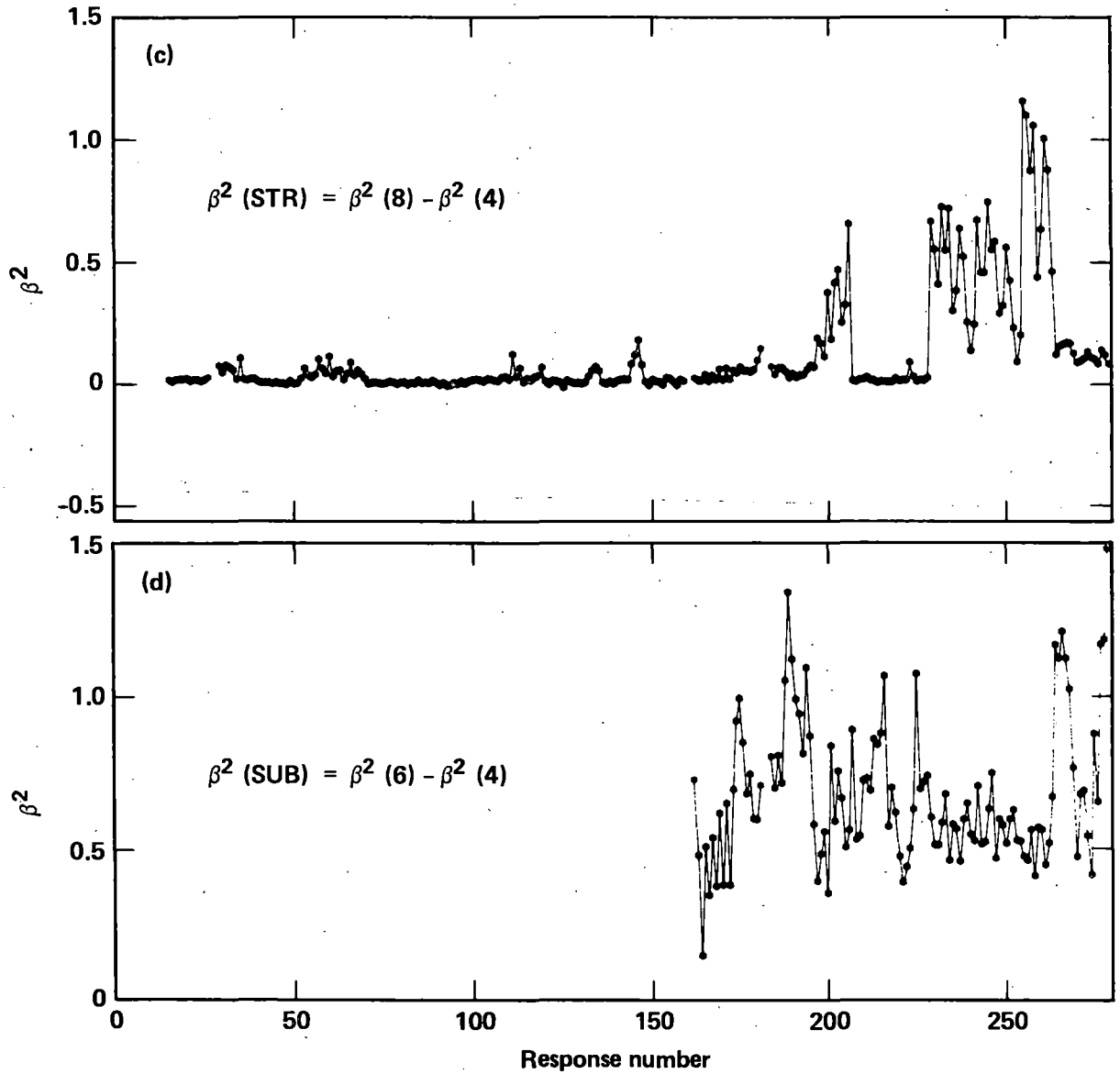

THE SEPARATE CONTRIBUTIONS TO RESPONSE β^2 FROM SI AND SSI ARE SMALL

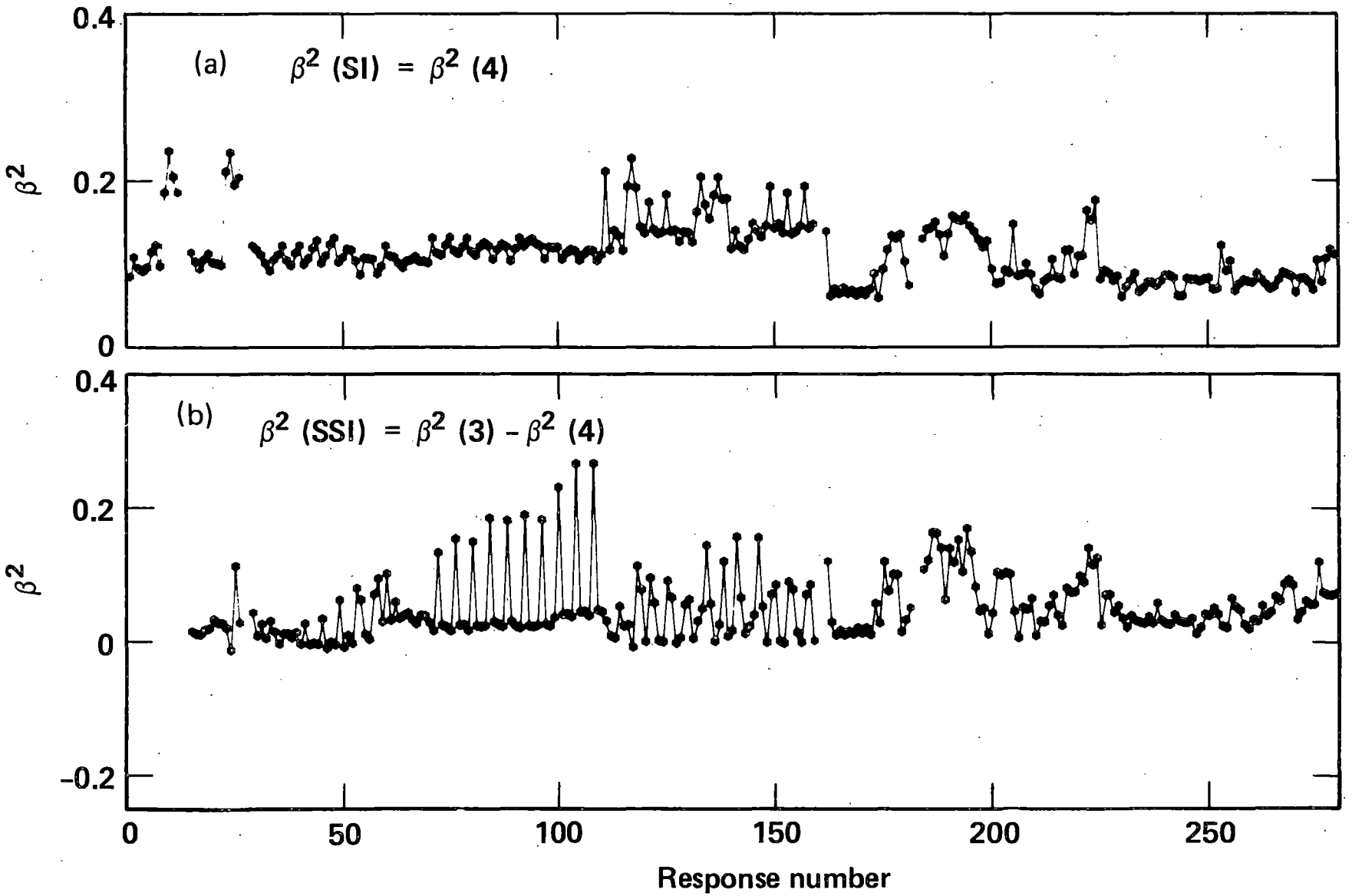

CONCLUSIONS

- Subsystem area of SMC is very important
- Structure area is important
- Seismic input — for given peak acceleration — is of modest importance
- Soil properties — at this site — are of modest importance

Seismic Safety Margins Research Program
Lawrence Livermore National Laboratory

PROBABILITY AND RISK:
Importance Measures

by
J. E. WELLS

Presented to:

Ninth WRSRIM
Gaithersburg, Maryland
October 26, 1981

PRESENTATION OUTLINE

- Role of systems analysis in the computational procedure
- Systems modeling: event and fault tree development
- Analytical capabilities developed – SEISIM importance analysis
- Importance analysis results

OVERVIEW OF SSMRP METHODOLOGY ILLUSTRATING THE USE OF EVENT AND FAULT TREE LOGIC

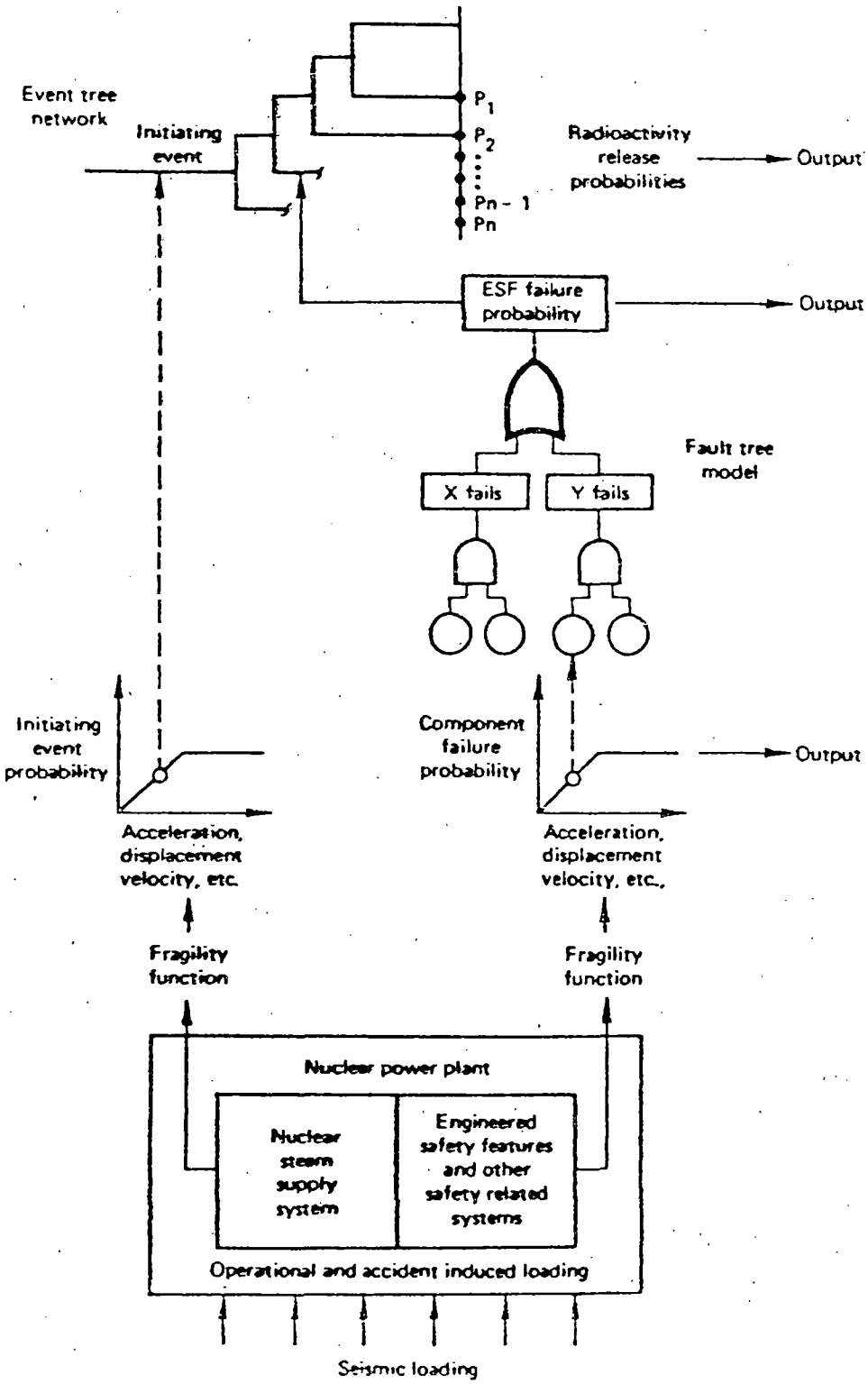

APPROACH TO EVENT-TREE/FAULT-TREE DEVELOPMENT IN SSMRP

- Initiating events have been selected and event trees developed for Zion I
- These event trees and studies of the Zion systems were used to prioritize fault tree development
- Fault trees for some systems have been constructed
- Logical descriptions of the event trees and fault trees were input to the computational procedure – SEISIM

EIGHT EVENT TREES WERE DEVELOPED FOR SSMRP

- Reactor vessel rupture
- Large LOCA (>6 in)
- Medium LOCA (3-6 in)
- Small LOCA (1.5-3 in)
- Small-small LOCA (0.5-1.5 in)
- Transient with PCS
- Transient without PCS
- Containment failure

— 148 core melt accident sequences result from these event trees

— Release categories were assigned based on Wash-1400 results

FAULT TREES WERE DEVELOPED ON A PRIORITY BASIS

Listed in event trees

* Auxiliary feed system
  Cont fan cooler system
  Cont spray system
  Chem volume and control system
* Emergency core cooling system
  - Charging pumps
  - Safety injection system
  - Residual heat removal system
  - Accumulators

  Power conversion system
  Reactor protection system

Supporting systems

* Electric power
* Service water
  Heating and ventilating system
  Component cooling water system
  Instrumentation and control system

* Phase I Fault Trees

PROBABILISTIC COMPUTATIONAL PROCEDURE

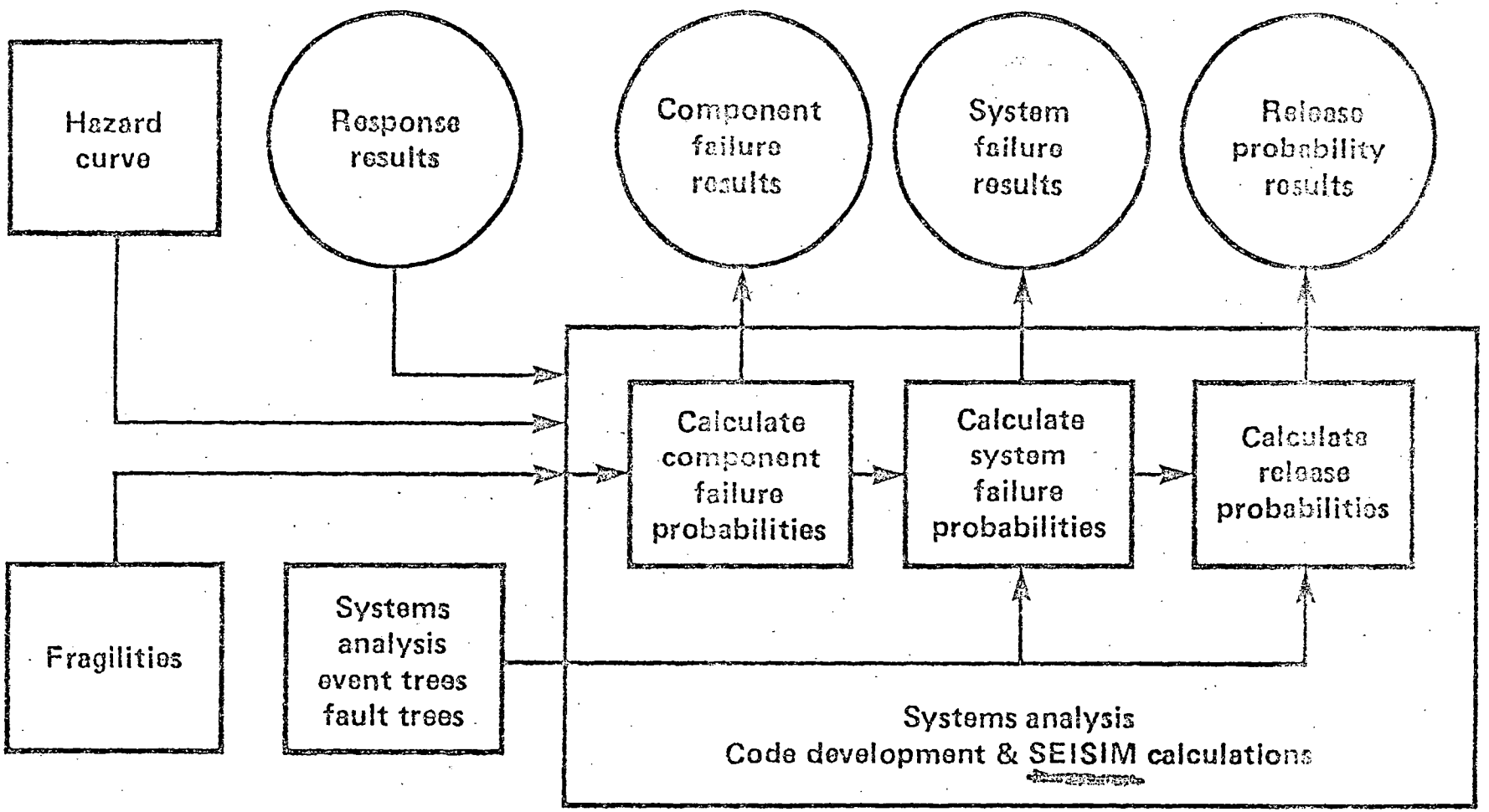

SEISIM HAS SEVERAL UNIQUE FEATURES

- Initiating event, system, and accident sequence probabilities are calculated with correlated responses and strengths
- Accident sequence failure probabilities are generated taking into account common components but individual system probabilities can be calculated also
- Dominance rankings for release sequences, components, systems and component types are calculated

DEMONSTRATION CALCULATIONS HAVE BEEN COMPLETED USING SEISIM

- Purpose of these calculations was to demonstrate code operation
- Further calculations are necessary to refine results and establish uncertainties

SEISIM Importance Measures

- Terminal Event Sequences
- Components (2 measures)
- Input Variables
- Primary Input Variables

Terminal Event Sequence Importance Measure

The measure of importance of a terminal event sequence is its probability.

Note: P(TES) contains the probabilities of the earthquake, initiating event, accident sequences, and containment failure.

Important Terminal Event Sequences for Earthquake Level 1

Release category	Top four sequences 1	2	3	4
1	3e-10 s1-7,a			
3	2e-8 t2-4,a	8e-9 s1-7,d	3e-11 t1-7,a	8e-12 a-2,a
5	2e-7 t2-4,g	8e-8 t2-4,d	2e-9 t2-4,b	4e-10 t1-7,g
7	2e-6 t2-4,e	2e-9 t1-7,e	8e-10 a-2,e	3e-23 s2-29,e

Importance Measures of Components

- Probability that at least one cut set containing the component fails conditioned on release category (Vesely–Fussel).

- Derivative of release category probability with respect to component failure probability (Birnbaum).

Important Components for Earthquake Level 1

Release category 1	Top four components 2	3	4
1 rca1383-mc	rec1383bmj	lofp-------	rec1383amj
2 rca1383-mc	rec1383bmj	Ozz1roofmg	lofp-------
5 Ozz1roofmg	mvd10019md	-vy1-----ma	-vy1-----mb
7 Ozz1roofmg	mvd10019md	-vy1-----ma	-vy1-----mb

Important Systems for Earthquake Level 1

Release category	Top three systems 1	2	3
1	afws	sis	chg
3	afws	sis	chg
5	afws	chg	sis
7	afws	chg	sis

SEISMIC SAFETY MARGINS RESEARCH PROGRAM (SSMRP)

Application to San Onofre Nuclear Steam Generating Station (SONGS)

Presented by:
Dr. Tien-yuh Chuang
Lawrence Livermore National Laboratory

Presented at:
9th Water Reactor Safety Research Information Meeting

Sponsored by:
U.S. Nuclear Regulatory Commission
Office of Nuclear Regulatory Research
Division of Reactor Safety Research
Gaithersburg, Maryland
October 26, 1981

PRESENTATION OUTLINE

- General plant description and seismic design criteria
- Objectives
- Approach
- AFW system and its related system
- Structure and soil description
- Piping models
- Progress to date
- Future work
- Schedule

SONGS-1 IS A WESTINGHOUSE THREE LOOP PWR

- Located in San Onofre, California
  - About halfway between Los Angeles and San Diego
- Rated output is 450 MWe
- Owned by Southern California Edison Company (SCEC) and San Diego Gas and Electric Company
- Designed and constructed by Bechtel Power Corporation in 1960's

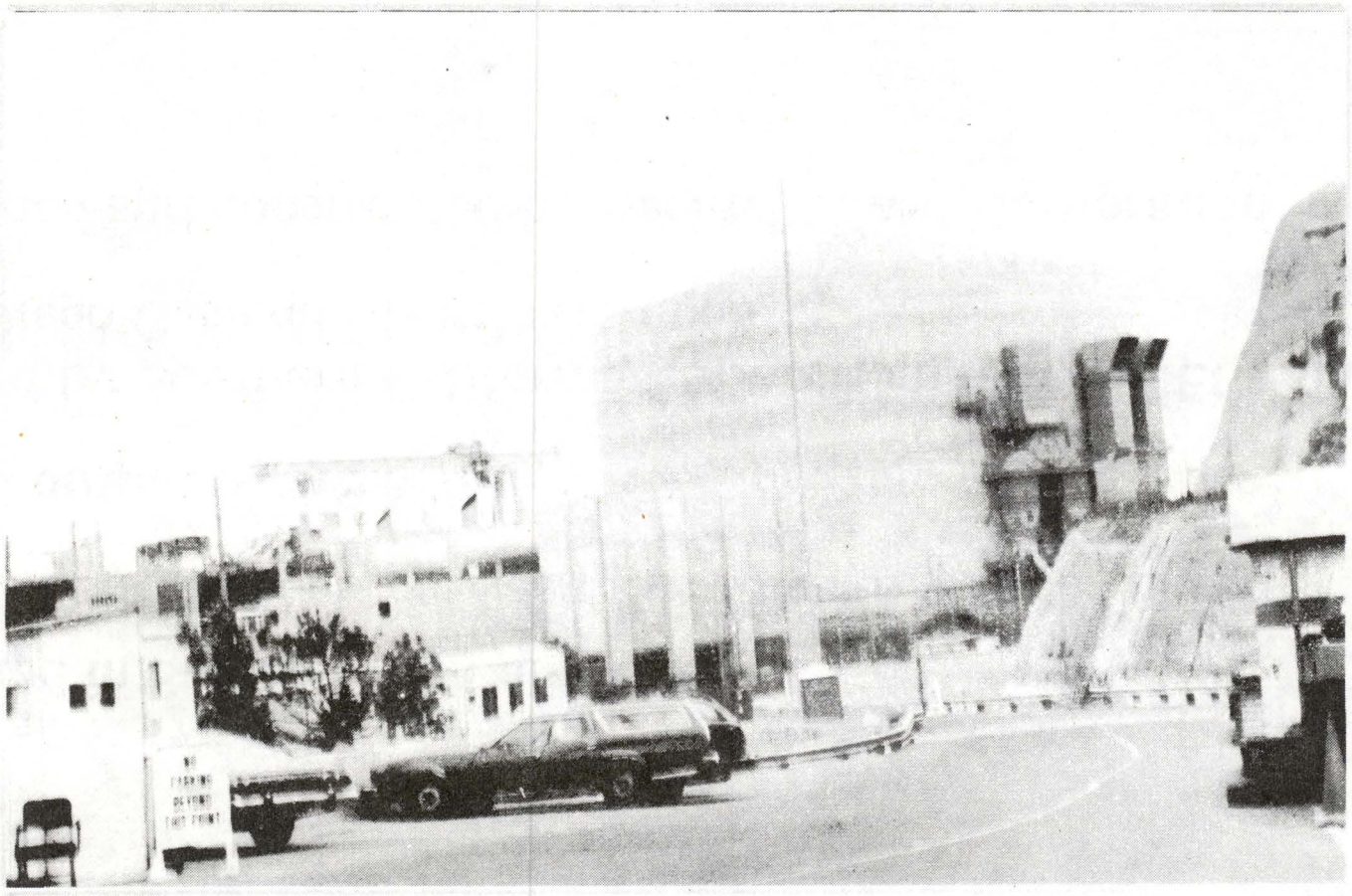

THE SEISMIC DESIGN CRITERIA OF SONGS HAS CHANGED

- SONGS-1 was originally designed to 0.5 g Housner spectra (DBE)
- SONGS-1 is using 0.67 g Housner spectra for seismic reevaluation
- SONGS-2 & 3 SSE is 0.67 g modified Newmark and Hall spectra

FIRE HOSE CONNECTION AT AFW PUMP

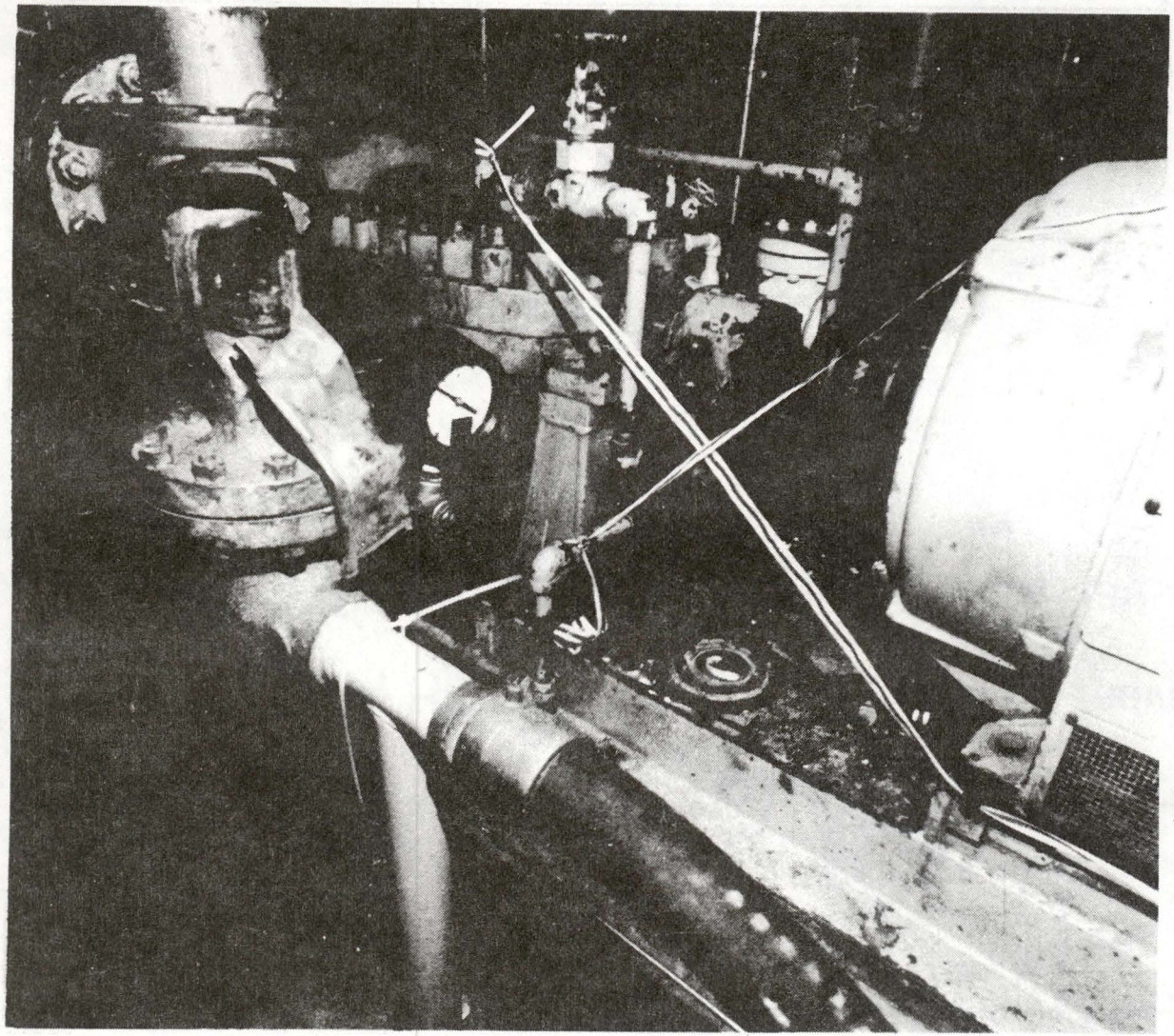

AFW PUMP TURBINE

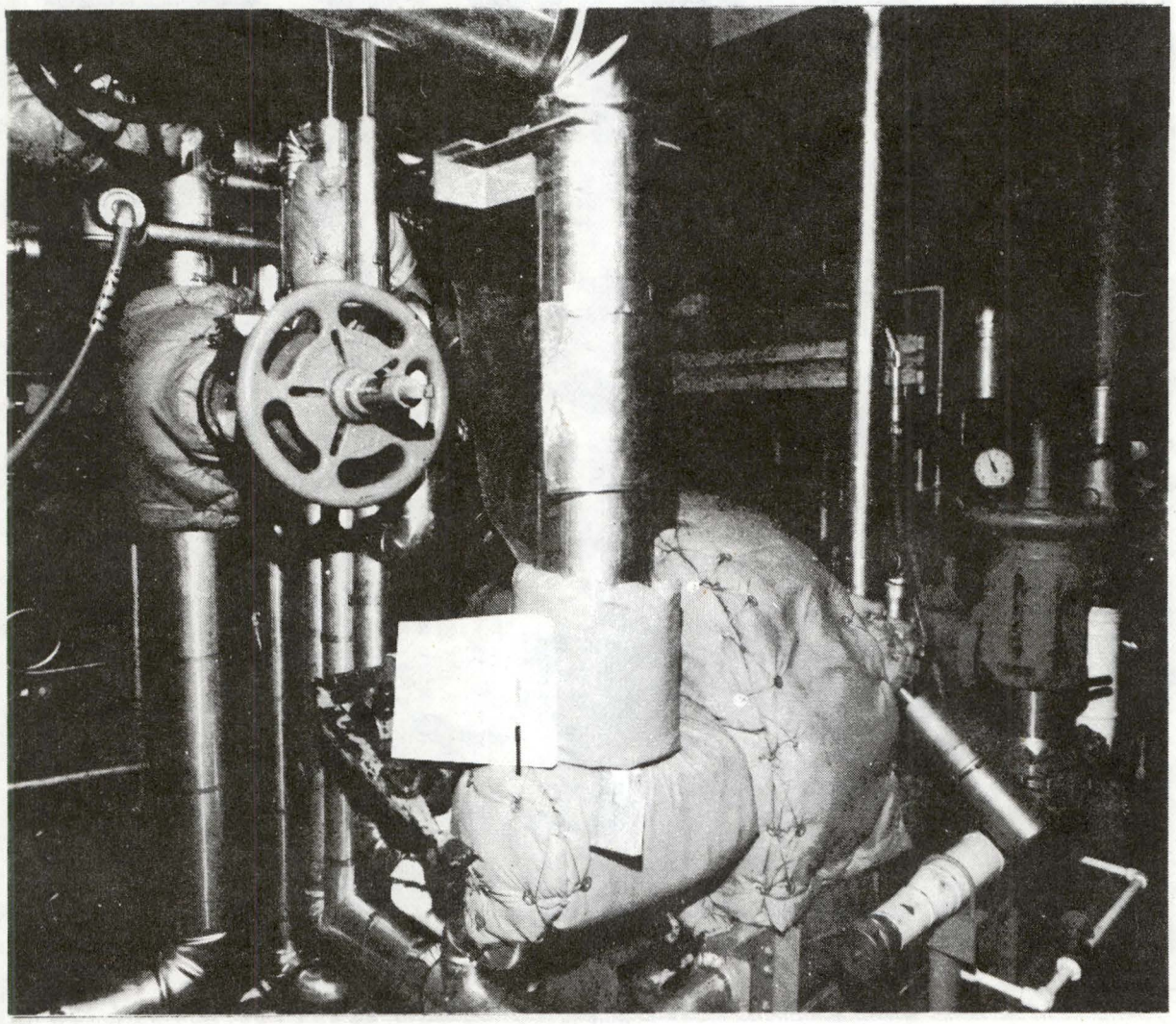

AFW PUMP-MOTOR DRIVEN

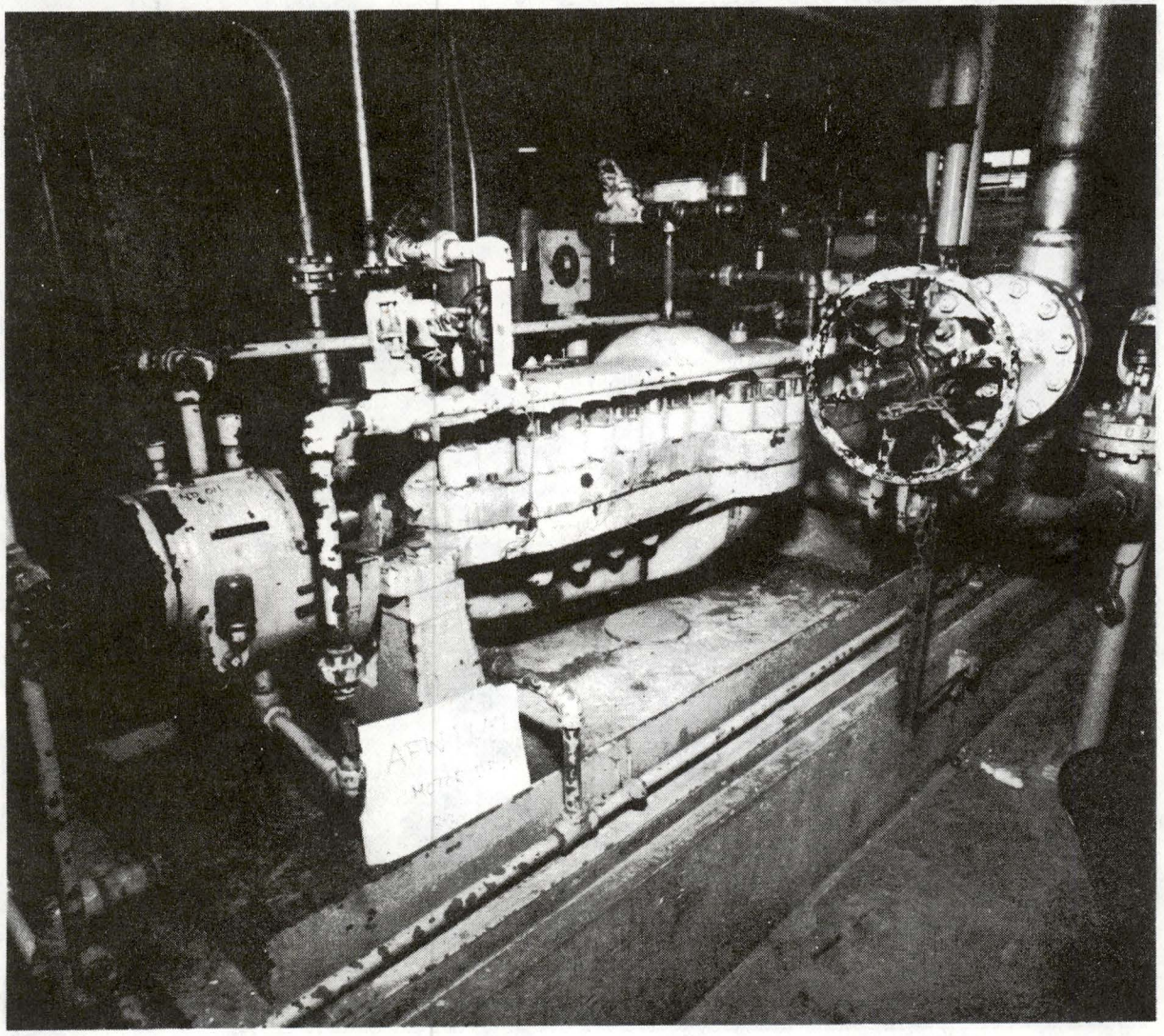

CONDENSATE STORAGE TANK

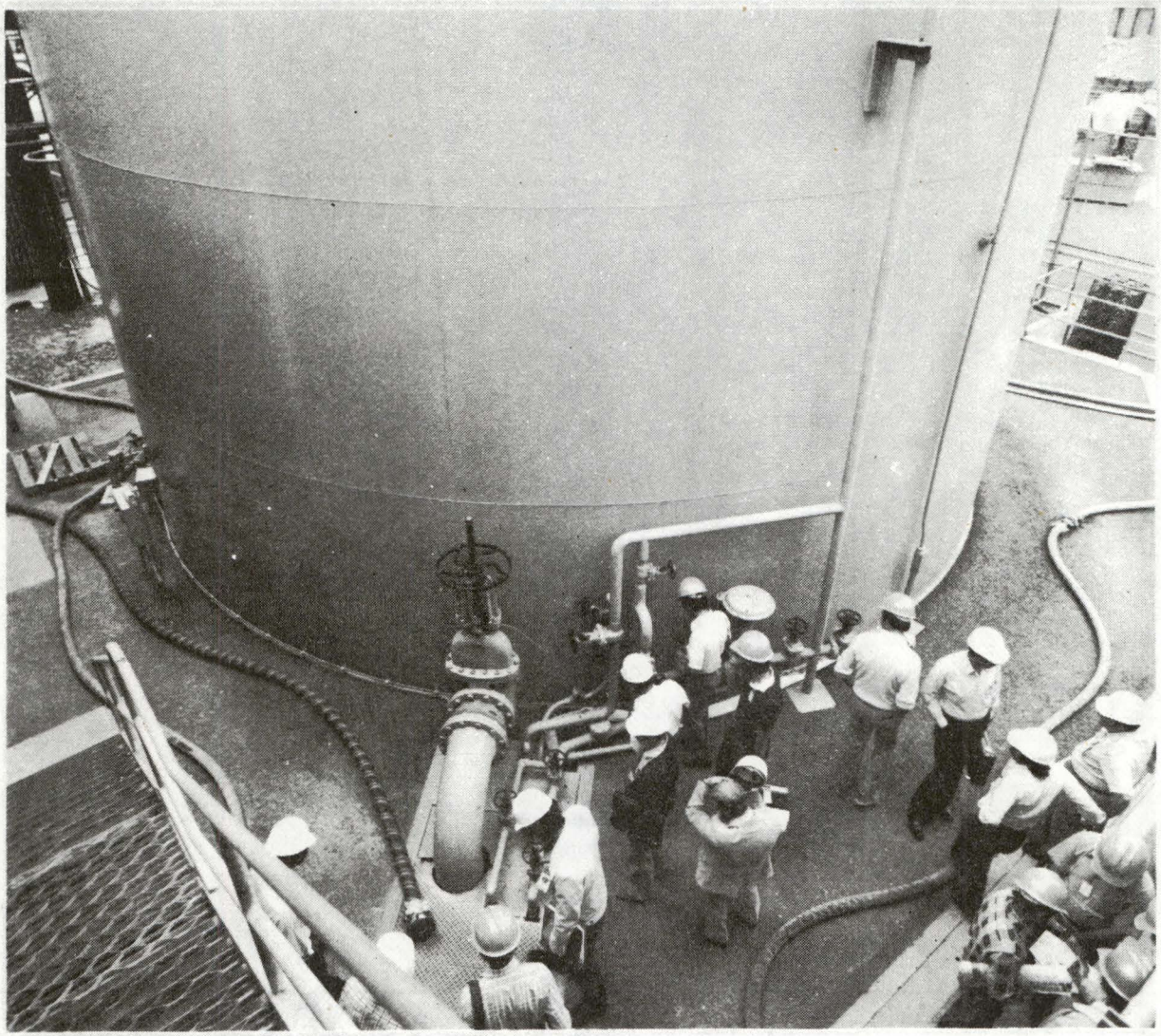

CONDENSATE STORAGE TANK

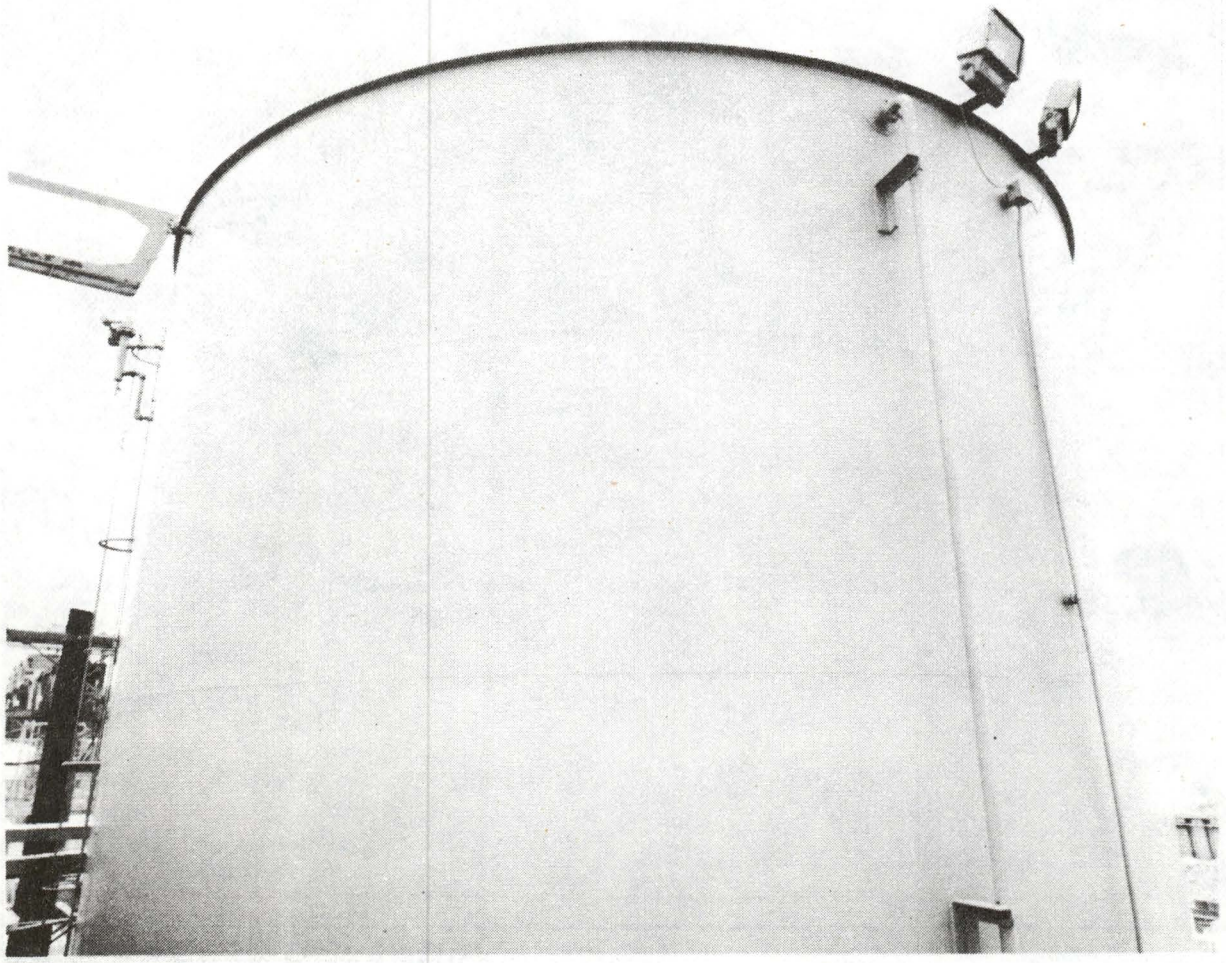

THE DESIGN SPECTRA FOR UNITS 2 AND 3 ARE HIGHER THAN UNIT 1

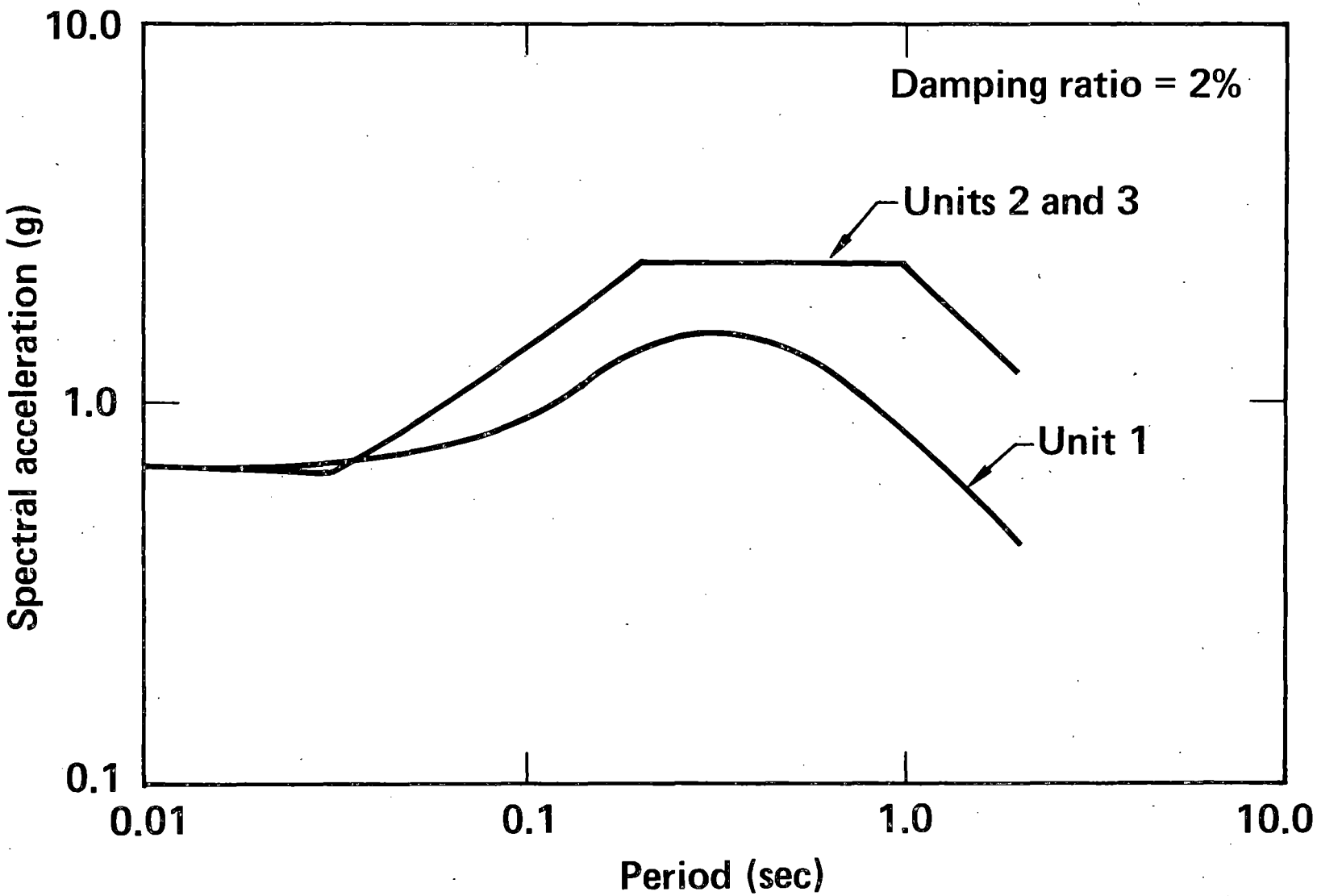

THE MAJOR OBJECTIVES OF THE SONGS-1 AFWS PROJECT ARE TO:

- Compare the seismic responses of SONGS-1 structures and piping systems as computed by:
  - SSMRP best estimate results
  - Design results
- Calculate seismic failure probability of SONGS-1 AFWS and identify significant contributors
- Compare AFWS seismic failure probabilities for Zion-1 and SONGS-1

FOR SONGS-1 WE WILL USE THE SSMRP PHASE I APPROACH USING SMACS & SEISIM CODES

- Seismic hazard and time histories
- SSI, structure and subsystem models
- SMACS calculations
- Mechanical, electrical and building fragilities
- AFWS fault tree
  - No event tree
- SEISIM calculations

THE AFW PIPING DELIVERS WATER FROM CONDENSATE STORAGE TANK TO STEAM GENERATORS

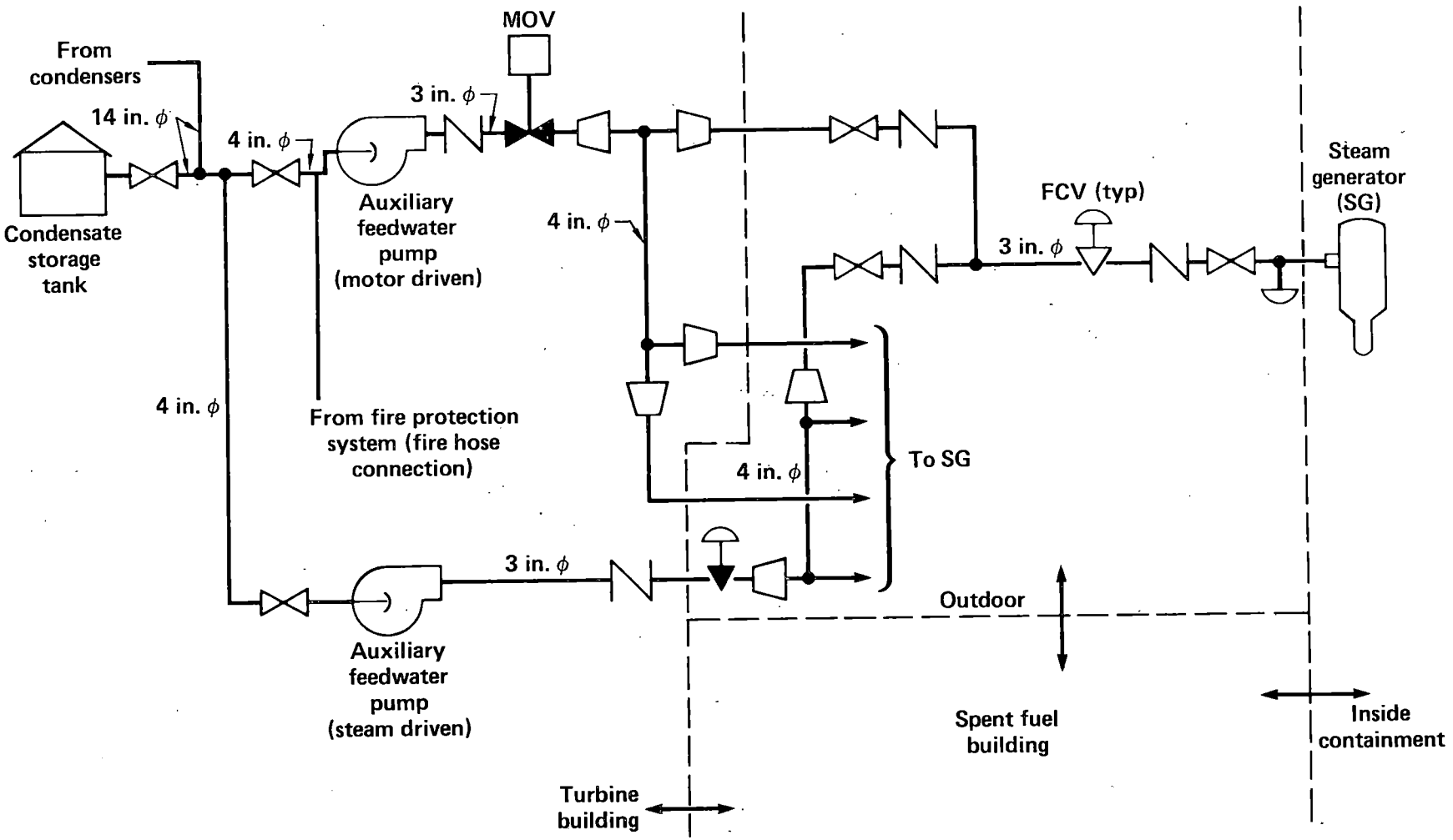

THE FAULT TREES HAVE BEEN DEVELOPED FOR THE AFW SYSTEM AND ITS RELATED SYSTEMS

- Steam supply to AFW pump turbine
- Electric power supply
- Fire protection system
  - Backup supply to AFW pump

THE SONGS-1 AFWS PROJECT MUST CONSIDER ALL STRUCTURES HOUSING THE AFW SYSTEM AND RELATED SYSTEMS SPECIFIED BY AFW FAULT TREE AND DYNAMIC RESPONSE CONSIDERATIONS

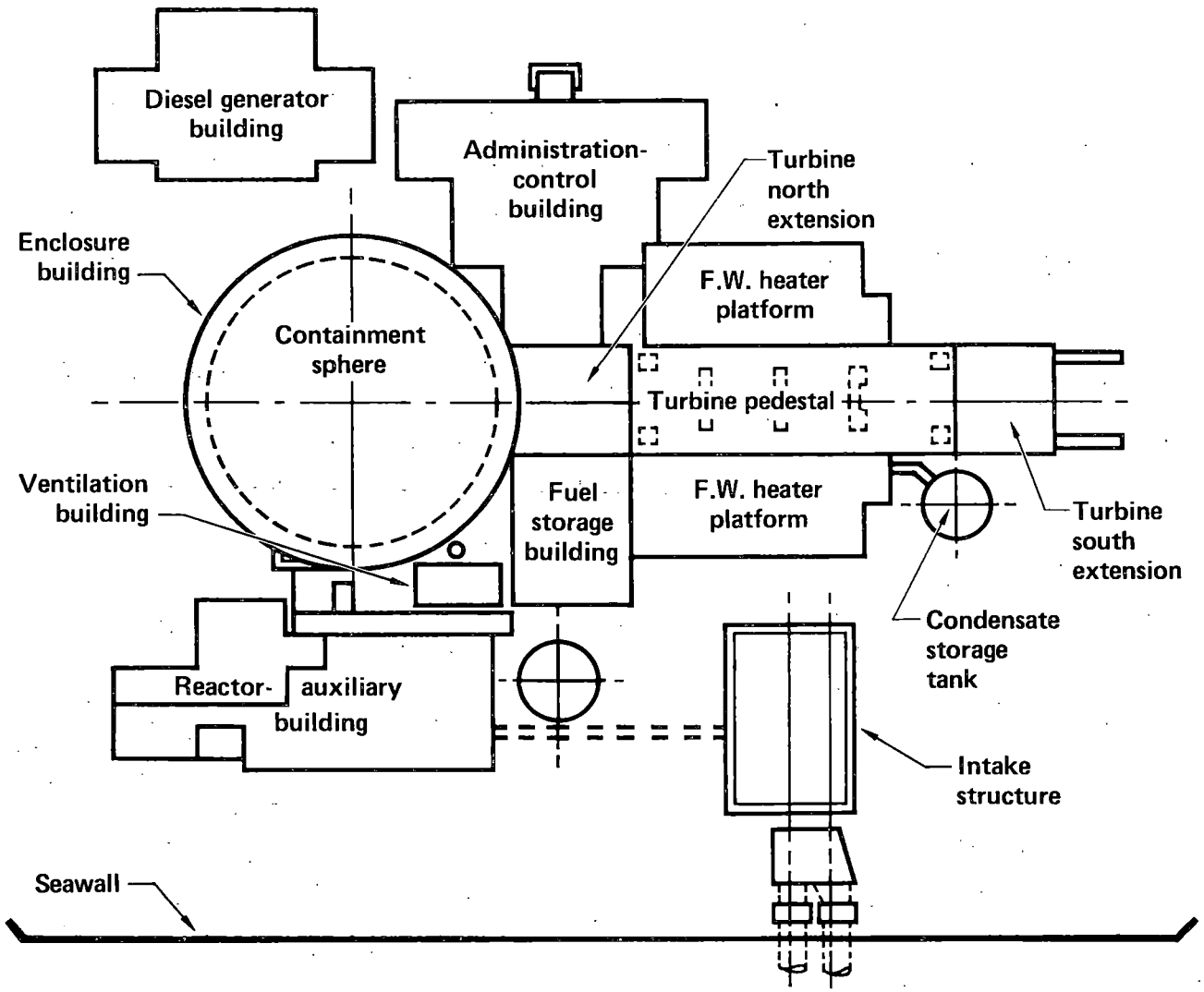

THE SOIL STRATIFICATION AT THE SAN ONOFRE SITE CONSISTS OF

- About 40 feet of sand and gravel terrace deposits overlying about 900 feet of fine to coarse San Mateo sand
  - — Average low strain shear wave velocity of ~ 2000 ft/sec

SSI AND MAJOR STRUCTURE RESPONSE ARE CALCULATED BY THE SUBSTRUCTURE APPROACH

- Soil is modeled by viscoelastic layered half-space
- SSI requires impedances and scattering matrices
- Structures are represented by modal coordinates of fixed base models
  - Detailed 3-D models are used

THE REACTOR BUILDING/CONTAINMENT SPHERE ARE SUPPORTED ON A PARTIAL SPHERICAL FOUNDATION

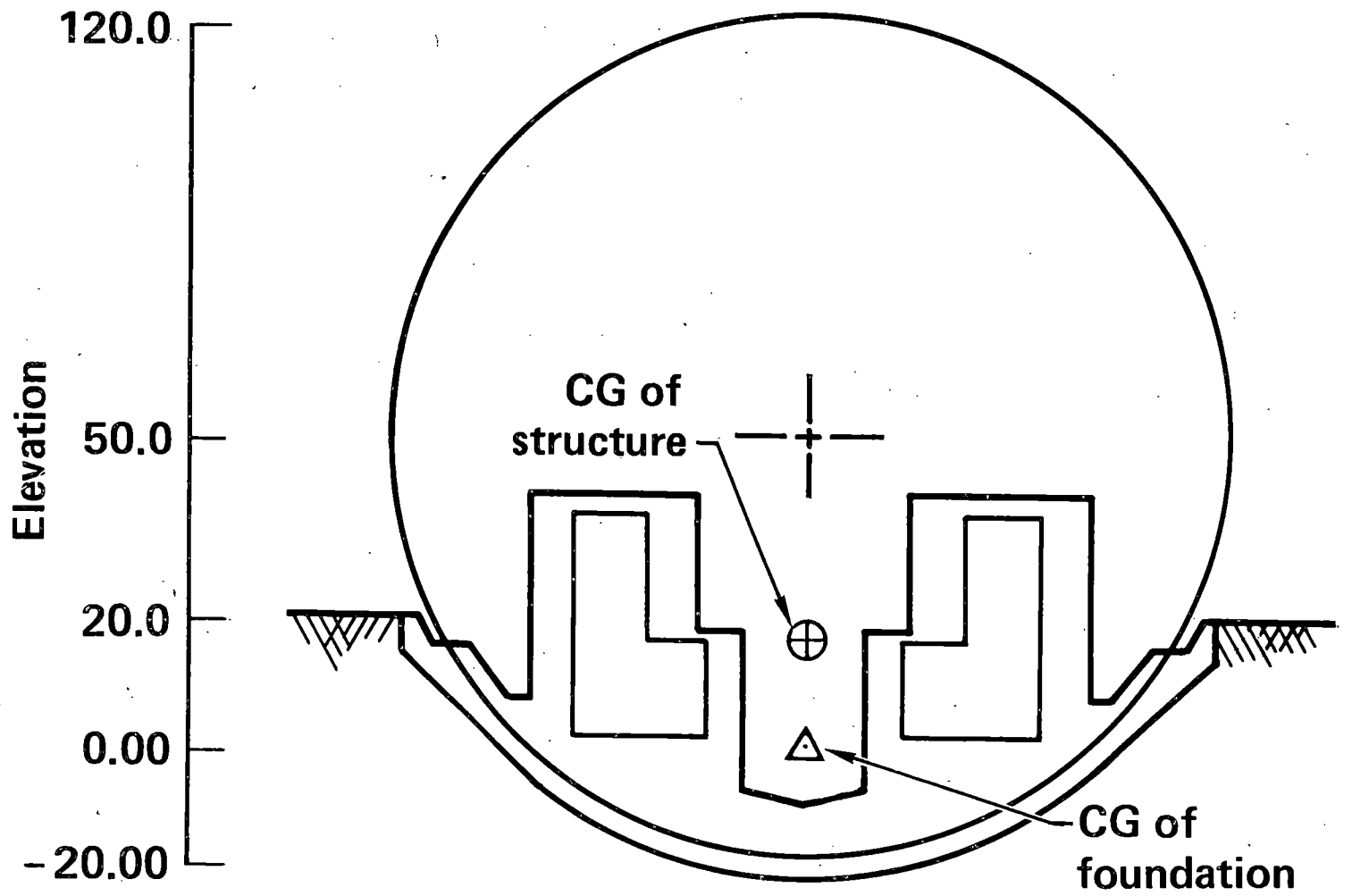

- The effects of embedment are treated in our SSI analysis

THE SPHERE ENCLOSURE BUILDING IS A REINFORCED CONCRETE CYLINDRICAL SHELL WHICH SURROUNDS THE REACTOR BUILDING/CONTAINMENT SPHERE

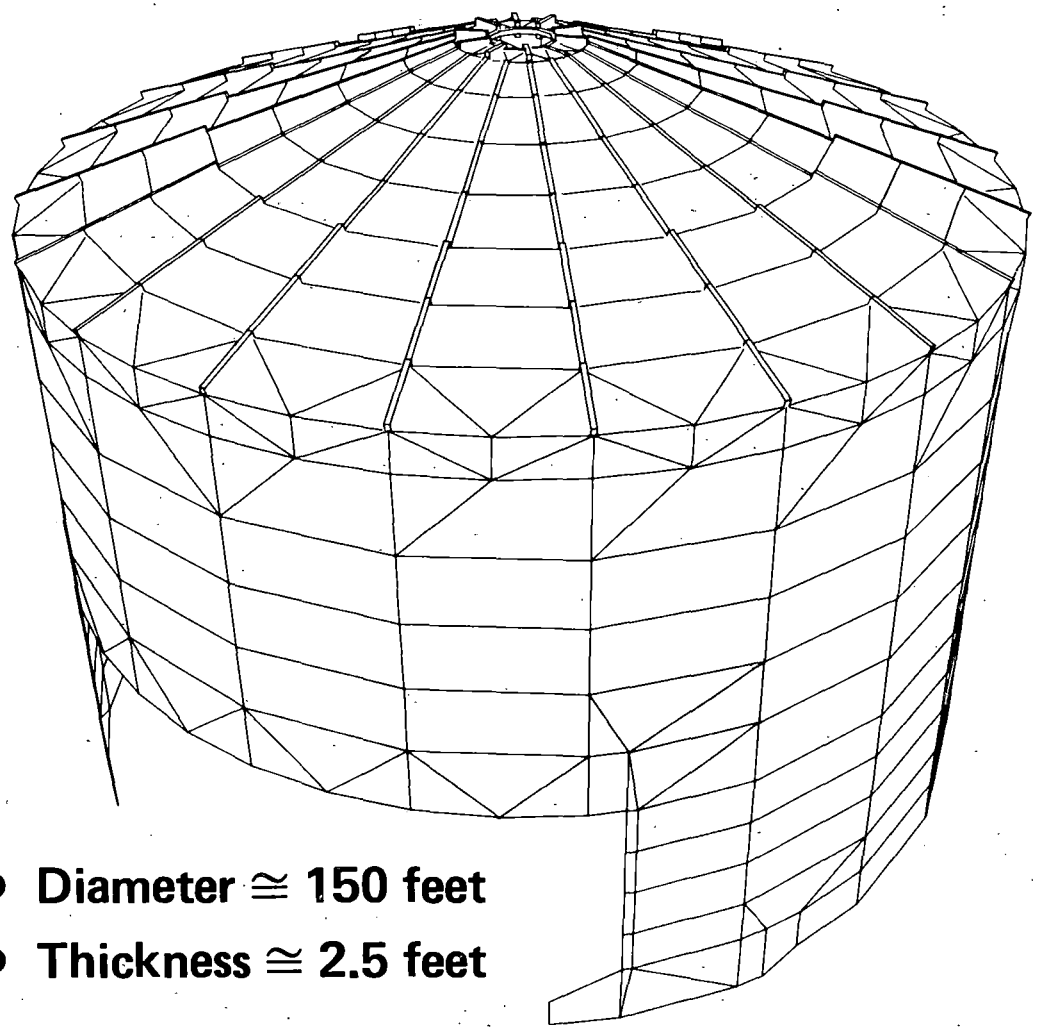

- Diameter ≅ 150 feet
- Thickness ≅ 2.5 feet

THE CONTAINMENT SPHERE IS A SPHERICAL STEEL SHELL WHICH IS MODELED WITH ISOPARAMETRIC SHELL OF REVOLUTION FINITE ELEMENTS

- Thickness = 1 inch
- Diameter = 140 feet
- Fourier harmonic representation N = 0, 1

THE REACTOR BUILDING IS COMPOSED OF A CONCRETE INTERNAL STRUCTURE WHICH SUPPORTS NSSS AND RELATED EQUIPMENT

- Modeled by 3-D finite elements
- NSSS is modeled by reduced mass and stiffness matrices

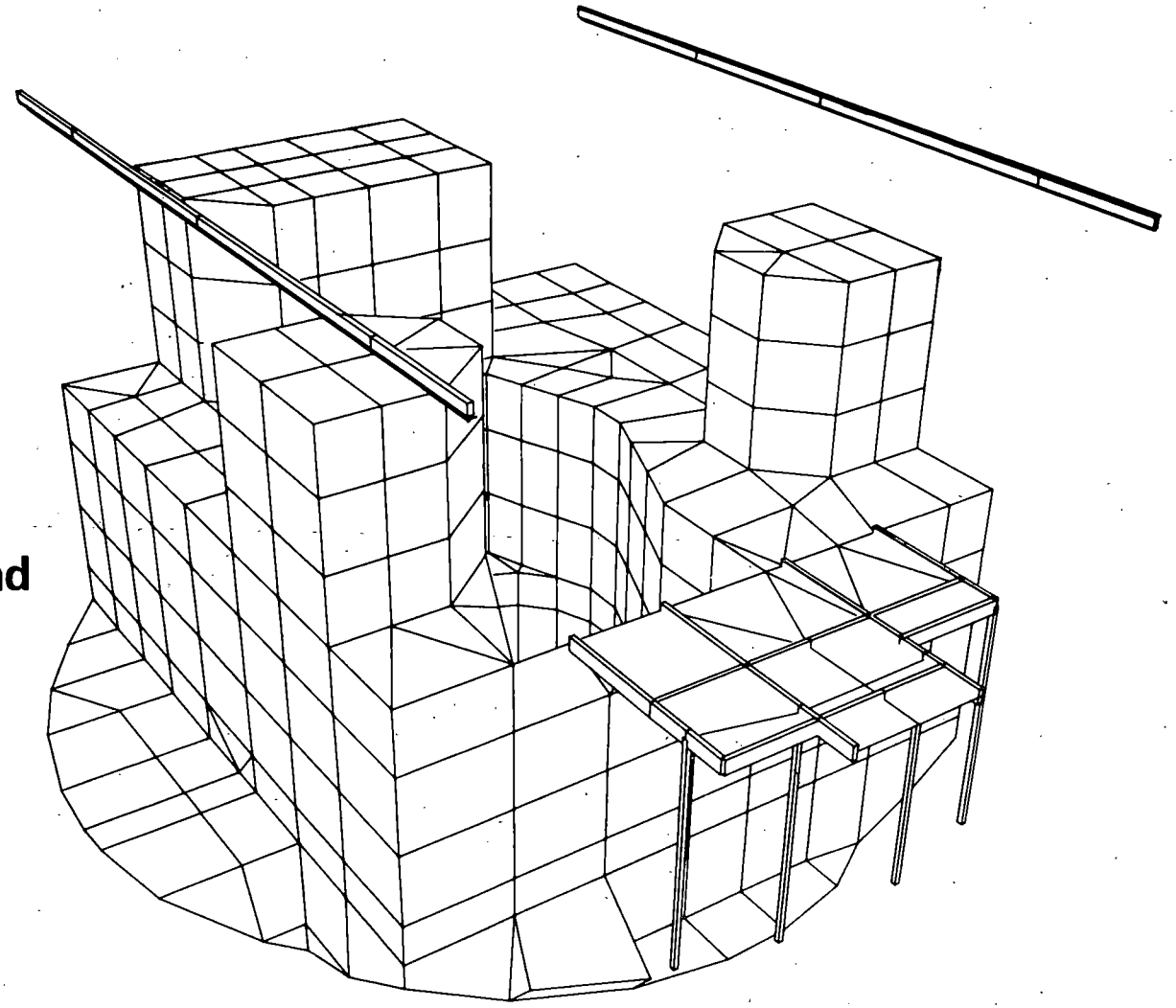

THE FUEL STORAGE BUILDING IS COMPOSED OF A CONCRETE FUEL STORAGE POOL WITH A STEEL FRAME SUPERSTRUCTURE

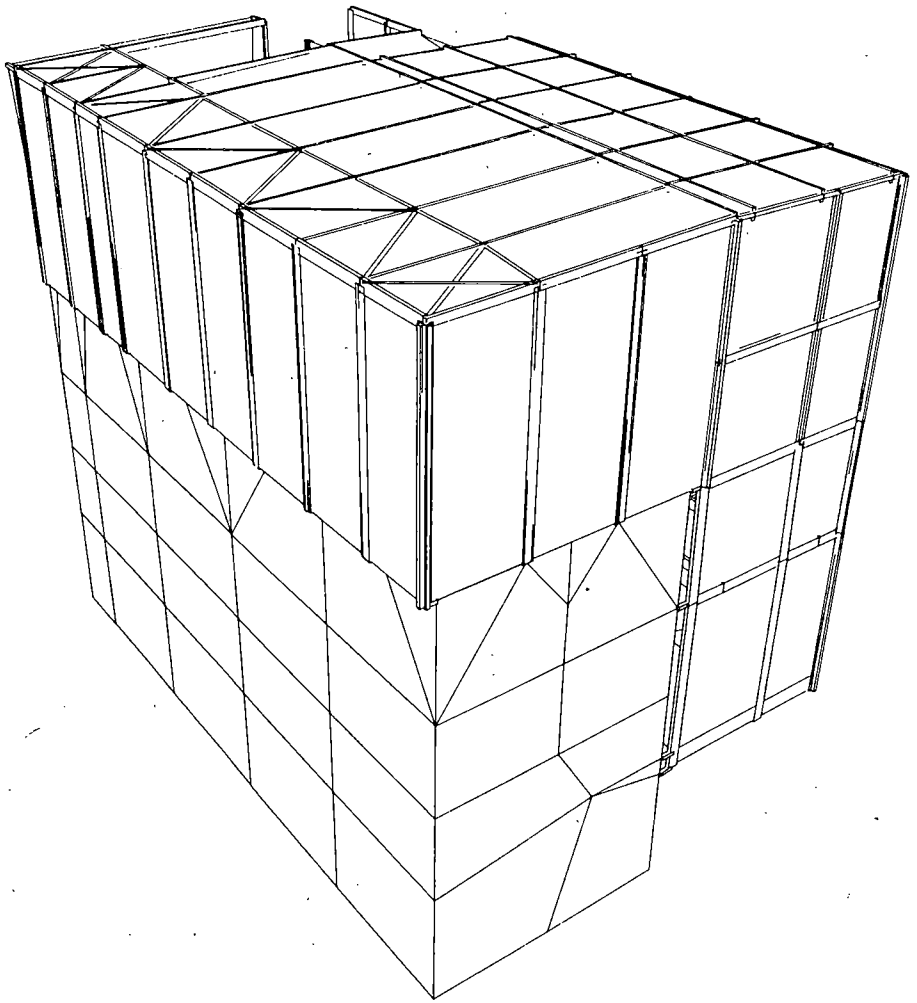

- AFW piping is supported on outside of fuel storage building

THE TURBINE BUILDING IS COMPOSED OF FIVE SEPARATE STRUCTURES WHICH INTERACT THROUGH THE BASE

- Turbine pedestal
- East and west feedwater platforms
- North and south turbine extensions

14 PIPING MODELS WILL BE GENERATED

Description	No. of models
AFW pump discharge	9
AFW pump suction	1
Steam supply to AFW pump turbine	3
Secondary water and supply path	1

PROGRESS TO DATE

- Fault tree
- Structure models
  - Reactor building/containment sphere/enclosure building
  - Administration-control building
- SSI
  - Impedance and scattering matrices for reactor building
- Time histories of three spectra for design result comparison (first objective)

THIRTY SETS OF SYNTHETIC TIME HISTORIES ARE GENERATED FOR SONGS-1 SPECTRA

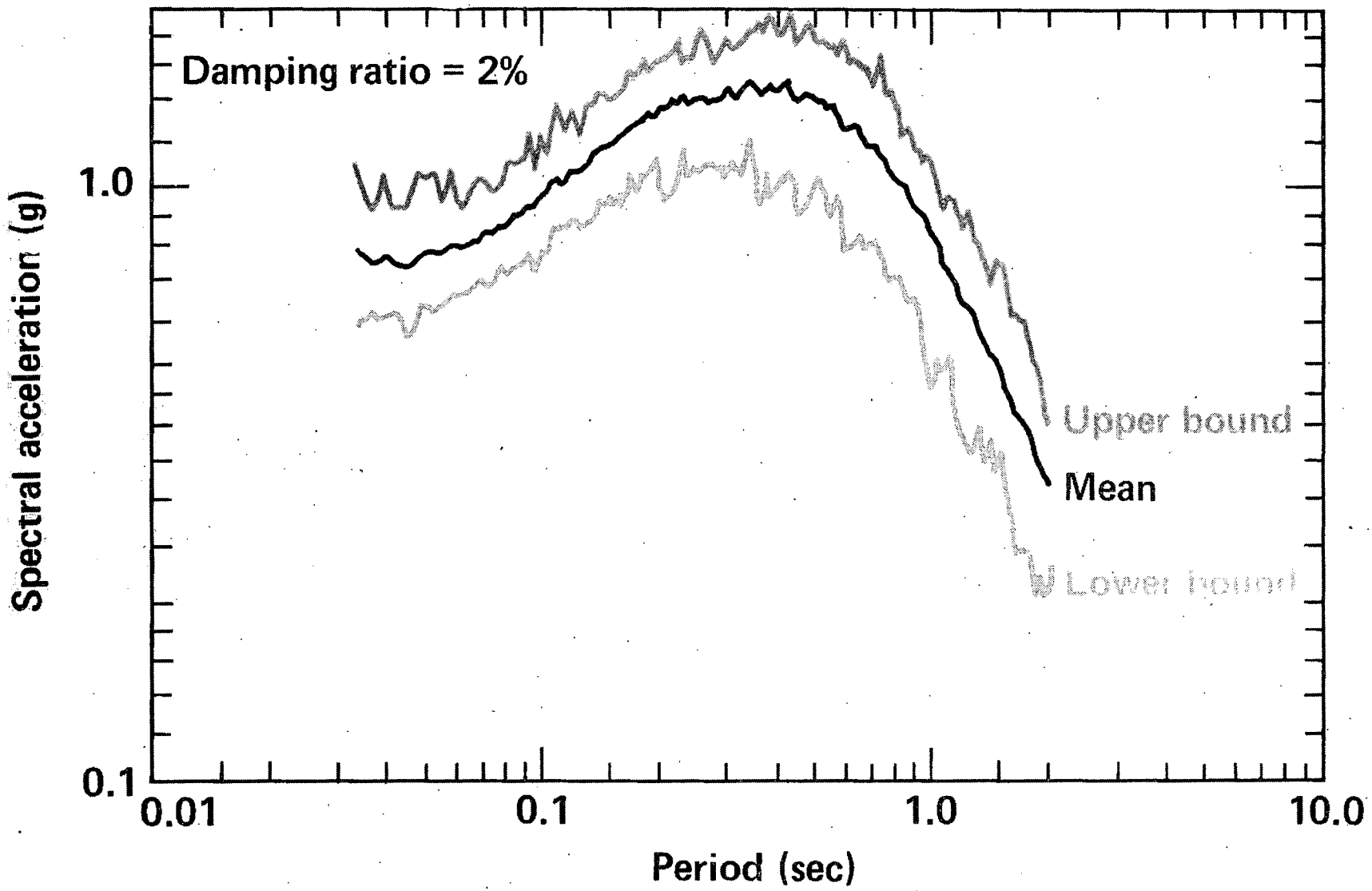

REMAINDER OF WORK

- Develop hazard curve and time histories for SONGS
- Complete structure models
- Complete piping models
- Complete structure fragility curves
- Calculate responses and failure probabilities
- Perform comparisons

ALL MAJOR COMPUTER PROGRAMS DEVELOPED IN THE SSMRP PHASE I WILL BE EMPLOYED

- HAZARD — Time history and hazard curve generation
- SMACS — Responses computation
- SEISIM — Failure probabilities calculation

FRAGILITY CURVES MUST BE DEVELOPED FOR THE STRUCTURES HOUSING AFW SYSTEM AND ITS RELATED SYSTEMS

- Reactor building/containment sphere and sphere enclosure building
- Turbine building
- Administration-control building
- Fuel storage building
- Diesel generator building

THE BEST ESTIMATE RESPONSES GENERATED BY SSMRP METHODOLOGY WILL BE COMPARED WITH THE RESPONSES RESULTING FROM SEISMIC REEVALUATION BY THE SCEC

- Structures
  - In-structure spectra
  - Forces, moments in structure members
- Piping systems
  - Resultant moments in pipes
  - Resultant acceleration of values

THE GENERIC FRAGILITY DATA BANK DEVELOPED IN THE SSMRP PHASE I WILL BE USED TO THE MAXIMUM POSSIBLE EXTENT

- Mechanical components
- Electrical components
- Piping components

COMPARISONS WITH DESIGN RESULTS WILL BE MADE FOR EACH OF THREE TARGET SPECTRA

- SONGS-1 seismic reevaluation spectra
  - 0.67 g Housner curve
- SONGS-2 and 3 design spectra
  - 0.67 g modified Newmark and Hall curve
- The average spectra of the above two spectra

SONGS-1 AFWS PROJECT SCHEDULE

- Complete the SMACS computation by February, 1982
- Complete the seismic design results comparison final report by March, 1982
- Complete the failure probability comparison final report by May, 1982

ONGOING DEVELOPMENT IN THE SEISMIC SAFETY MARGINS RESEARCH PROGRAM

Presented by:

Michael P. Bohn

Lawrence Livermore National Laboratory

Presented at:

9th Water Reactor Safety Research
Information Meeting

Sponsored by:

U.S. Nuclear Regulatory Commission
Office of Nuclear Regulatory Research
Division of Reactor Safety Research
Gaithersburg, Maryland
October 26, 1981

COMPLETE SONGS AUXILIARY FEEDWATER SYSTEM ANALYSIS

- Mechanical responses by Feb 1982
- Fault trees by Nov 1981
- System failure analysis by Feb 1982
- Final documentation by May 1982

MAJOR STEPS TO COMPLETION OF THE SSMRP

- Develop methodology (phase I, completed Jan 1981)
- Perform sensitivity studies
- Complete Zion PWR risk analysis
- Apply methodology to BWR
- Develop simplified models/methods
- Validation
- Recommendations

PERFORM SENSITIVITY STUDIES

- Preliminary versions of the codes HAZARD, SMACS, and SEISIM, and the preliminary fragility data base, will be used to make an initial determination of the relative importance of the various aspects of the seismic problem, using sensitivity studies

- Sensitivity studies scheduled for completion in June, 1982

PLANNED SENSITIVITY STUDIES

- Systems analysis
  - Un-modeled safety systems effect on risk
  - Dominance ranking, component failure on risk
  - Shift in risk due to shift in response and fragility means, variances
  - Effect of variation of primary input variables on responses
  - Level of fault tree development
  - Initiating event hierarchy effects
  - Variation of risk with correlation

PLANNED SENSITIVITY STUDIES (Cont)

- Seismic input
  - Effect of GM model on hazard curve
  - Alternate seismic zonation
  - Method of treating M_{max}
  - Variations in eq occurrence model parameters
- Soil–structure interaction
  - Effects of embedment, str-to-str interaction, method of varying soil properties, and wave passage effects
  - SSI at Zion by FLUSH and CLASSI
  - Comparison of CLASSI with direct linear and non-linear SSI analyses

PLANNED SENSITIVITY STUDIES (Cont)

- Building response
  - Sensitivity to variations in eigensystem and damping
  - Alternative modeling techniques for Zion
- Fragilities
  - Variation in risk and component failure due to shift in fragility levels

COMPLETE ZION PWR RISK ANALYSIS

Having run sensitivity studies and improved our codes and data (to the minimum extent required), we can now evaluate the risk at Zion. This will include uncertainty bands.

Products

- Hazard curve with uncertainty finalized
- Fault trees finalized
- Fragilities with modeling and random uncertainties finalized
- A model to handle small pipe failures completed (preliminary model)
- Uncertainty in structural response separated into random and modeling components

COMPLETE ZION SEISMIC RISK STUDY

- Initial work done in FY'82
- Based on sensitivity studies additional work may be required
- Study completed in FY'83

BWR RISK ANALYSIS

PURPOSE OF BWR RISK ANALYSIS

- Carry out study of BWR equivalent to Zion PWR analysis to demonstrate applicability of methodology or required modifications
- To compare risk characteristics between BWR and PWR
- To provide a benchmark against which simplifications of methodology can be compared

SCOPE OF BWR ANALYSIS IN FY'82

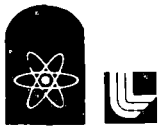

- Develop event trees and fault trees for BWR to same level as Zion
- Using estimated responses, perform sensitivity studies on the fault trees to identify any essential differences and serve as basis for developing simplified models applicable to BWR
- Study BWR structural characteristics to see if additional structural considerations are required (e.g., steam relief valve loads, etc.)
- Decision in December FY'82 on further BWR effort and level of analysis required

SIMPLIFIED MODELS AND METHODOLOGY

GOALS OF DEVELOPING SIMPLIFIED MODELS AND METHODOLOGY

- To simplify and improve the computational efficiency of the phase I SSMRP methodology
- To develop simplified versions of the SSMRP models and methods which can be used in a timely fashion to perform seismic PRA

WORK ON SIMPLIFIED MODELS IN FY'82

- Work will begin in the last three months of FY'82 (following the sensitivity studies)
- Review previous or existing simplified modeling methods
- Begin to develop simplified models for:
  - Soil-structure interaction
  - Structures
  - Piping

VALIDATION

Having gotten Zion risk numbers, it is imperative that we devote considerable effort to "verifying" these numbers to the extent possible. Clearly the overall risk cannot be "verified" but we perform studies, compare with other codes, compare with data at the project level

Possible products/steps

- Compare SEISIM with other codes in their overlapping capabilities
- Benchmark fragility curves against data not used in development
- Independently check structural response uncertainties against other codes or measured building response

RECOMMEND CHANGES

Based on all the above, we will be able to recommend changes or improvements to the licensing standard review plan which make explicit use of risk as a licensing criteria. The major task will be to define cost effective implementation

Possible products

- Standardization of design response output format for use with SMACS

or

- A recommended set of uncertainty factors to be used with design response results in SEISIM
- Standardize level and detail of fault trees, with requirement that both seismic and non-seismic failures be simultaneously considered
- Recommendations for further seismic safety research, both experimental and analytical

U.S.GPO:1981/587-067/1039

BWR BLOWDOWN/EMERGENCY CORE COOLING INTEGRAL TEST PROGRAM FINAL RESULTS FROM THE TWO LOOP TEST APPARATUS (TLTA)

G. L. Sozzi, L. S. Lee

General Electric Company
Nuclear Fuels and Services Engineering Department
San Jose, California

Program Sponsored by: U.S. Nuclear Regulatory Commission, Electric Power Research Institute, and General Electric Company

For Presentation at 9th Water Reactor Safety Research Information Meeting
October 26, 1981
National Bureau of Standards
Gaithersburg, Maryland

INTRODUCTION

The principal objective of the BD/ECC Program is to obtain and evaluate basic Blowdown and Emergency Core Cooling (BD/ECC) data from test system configurations which have performance characteristics similar to a BWR during a hypothetical LOCA. Other objectives include the determination of the degree to which current LOCA models describe the observed phenomena and, where necessary, development of improved physical interpretation of the governing phenomena. The program is jointly funded by NRC, EPRI and GE.

The Two Loop Test Apparatus (TLTA) shown in Figure 1 was the BWR system simulator used to provide the thermal hydraulic response of a BWR. Main features of this system simulator include: a full size, electrically heated bundle

that is capable of duplicating the power output of a fuel bundle from full operating power to the decay heat power. Also included is a coolant injection system to supply the ECC flows.

The TLTA configuration has evolved over many years and has been modified to meet the primary objective of each testing phase with the overall objective of maintaining a real-time, thermal-hydraulic system response.

Under the BD/ECC Program, 14 tests were conducted in TLTA: eleven tests simulated a large break (DBA) LOCA; two tests simulated a small break LOCA; and one separate-effects test series simulated low-flow, core uncovery heat transfer. Some of the test results have been presented at previous Water Reactor Safety Research Meetings. Complete results are contained in three separate reports[1][2][3] that are being issued. Key results were also presented at technical conferences[4][5].

TLTA TESTS COMPLETED:

The objective of the program has been met: test data from the BWR system simulator, TLTA, have been obtained and evaluated. The data are being used to compare with predictions from a best estimates code, TRAC-BWR. In addition, the data are used for designing an upgraded facility - Full Integral Simulation Test (FIST) facility.

FINAL TLTA RESULTS:

Significant findings from this program are:

- The phenomenon of counter current flow limitation at the bundle inlet was important in maintaining liquid in the bundle, and, thus, in removing the stored energy.

- The subcooled ECC injection was sufficient to condense all the steam generated in the core region and led to CCFL breakdown at the top of the core.

- The maximum bundle temperature of <1000°F was well below the licensing limit of 2200°F.

- The small break tests showed the same governing phenomena throughout the system as those observed in large break tests.

The counter current flow limiting (CCFL) conditions at the inlet and outlet of the bundle are shown in Figure 2. The CCFL condition at the inlet is seen to be more restrictive than at the outlet. Consequently, conditions exist whereby the vapor flow from the lower plenum due to flashing is large enough to shut off the liquid drain from the inlet. At the top of bundle, however, the steam updraft due to bundle vaporization and flashing might be insufficient to stop the liquid (supplied by ECC injection) from draining into the bundle.

During the early part of the large break transient, the CCFL condition at the bundle inlet maintained the bundle inventory for approximately 40 seconds. Consequently, the stored energy in the rods was almost completely removed before the bundle inventory was lost and bundle uncovery occurred. Later in the transient, the CCFL condition at the bundle inlet enhanced bundle reflooding.

The two-phase mixture level response along the bundle path for the reference BWR simulation DBA is shown in Figure 3. The CCFL conditions at the bundle inlet and outlet can be seen: the lower plenum level is below the bundle inlet while the bundle level is maintained. At the top of the bundle, the breakdown of CCFL leads to draining of the upper plenum. This occurs after the subcooled ECC injection

has reached the rate sufficient to condense all the steam.

The peak cladding temperature (PCT) response for this reference test is shown in Figure 4. The maximum cladding temperature due to heat-up is less than 700°F (370°C). The peak cladding temperature response for the peak power test (also shown in Figure 4) exhibits a similar trend but higher temperatures as expected. These temperatures approach the saturation temperature at ∿130 seconds as the bundle refloods in both tests. The early temperature increase is attributable to the short jet pump in TLTA [6]. The early boiling transition is nonetheless rewetted by subsequent fluid re-distribution following lower plenum flashing. The PCT's are seen to have reached a plateau or to be on the decline before the bundle quenches as it refloods. This mitigation of PCT results from draining of the ECC fluid into the bundle.

The maximum cladding temperature due to sustained heat-up is ∿810°F (432°C) for the peak bundle power. This temperature is significantly smaller than the 2200°F (1204°C) licensing limit. The reason for this difference is the inherently high heat transfer in the bundle that persisted throughout the test. The high bundle heat transfer can be seen from the comparison of heat transfer coefficients (HTC's) in Figure 5. The HTC's obtained from data are compared with that determined from the current BWR evaluation methods. The test data show much higher bundle heat transfer after the boiling transition.

The controlling phenomena in the small break tests were found to be similar to those in the large break tests, as shown in Figures 6 and 7. The system pressure responses, Figure 6, show that following the activation of the auto-

matic depressurization system (ADS) the system blowdown response is similar to that of the large break test. The event in the small break test is, of course, stretched out in time. The two-phase level response, Figure 7, shows the existence of CCFL at bundle inlet for both the small and large break tests. Because of CCFL at bundle inlet in the small break test, the bundle was never uncovered and, therefore, no heat up occurred. For the large break test, as was discussed before, the CCFL condition at bundle inlet delayed dryout in the bundle early in the transient and contributed to advancing the reflooding of the bundle later in the transient.

CONCLUSIONS - (From the BD/ECC Program):

The BD/ECC Program has come to a successful conclusion. Test data were obtained; evaluation of these data has led to the following improved understanding of the BWR LOCA phenomena:

- Delay of bundle dryout, by CCFL at the inlet, enabled the bundle stored heat to be removed before sustained heat-up began.

- CCFL at the top of the bundle broke down as the ECC injection reached a sufficient rate to condense the vapor at the bundle outlet.

- The bundle reflooded rapidly as CCFL at the bundle outlet broke down while a CCFL condition at the inlet restricted liquid from draining from the bundle.

- The controlling phenomena of a small break were found similar to those of a large break LOCA.

FUTURE PROGRAM DIRECTION

The BD/ECC Program is complemented by the BWR Refill/Reflood Program[7]. The BD/ECC Program has also been extended for additional testing in an upgraded facility called Full Integral Simulation Test (FIST). This facility will replace the TLTA.

Under the complementary Refill/Reflood Program, a best estimate code, TRAC-BWR is to be developed and qualified. In addition, large scale, multichannel experiments are being conducted to investigate the BWR refill/reflood response.

The TLTA data are being compared to TRAC-BWR predictions as part of the code qualification effort. These comparisons will result in identifying code improvements and will contribute to the final qualification and independent assessment of the code. Final qualification of TRAC-BWR will be completed with data from the FIST facility.

The FIST facility is intended for non-LOCA as well as small break LOCA transients. The FIST facility features a full size bundle together with a full height simulation of the key reactor components. A comparison of the axial height for the FIST facility, its predecessor the TLTA, and a BWR plant is shown in Figure 8. For the FIST facility, full scale length of lower plenum, upper plenum, separator, dryer, steam dome, jet pumps, as well as the bundle will be preserved. Also preserved will be the BWR/FIST regional volume ratio which is the same as the BWR/FIST bundle ratio.

The schedule for the new test program is given in Figure 8. Testing is scheduled to begin near the end of 1982 and to be completed by mid 1983. The model comparisons and final report will be issued at the end of 1983.

REFERENCES

(1) L. S. Lee, G. L. Sozzi, and S. A. Allison, "BWR Large Break Simulation Tests - BWR Blowdown/Emergency Core Cooling Program," General Electric Company, March 1981, (GEAP-24962, NUREG/CR-2229, EPRI-NP-1783).

(2) W. S. Hwang, "BWR Small Break Simulation Tests with and without Degraded ECC Systems - BWR Blowdown/Emergency Core Cooling Program", General Electric Company, February 1981, (GEAP-24963, NUREG/CR-2230, EPRI-NP-1782).

(3) D. S. Seely and R. Muralidharan, "BWR Low Flow Bundle Uncovery Tests and Analysis - BWR Blowdown/Emergency Core Cooling Program", General Electric Company, February 1981, (GEAP-24964, NUREG/CR-2231, EPRI-NP-1782).

(4) L. S. Lee and G. L. Sozzi, "Thermal-Hydraulic Response in the Scaled BWR System Simulator During a Design Basis Accident Simulation Test", Thermal-Hydraulics in Nuclear Power, The American Society of Mechanical Engineers, 1981 (HTD-Vol. 15). (Paper presented at 20th National Heat Transfer Conference, August 2-5, 1981, Milwaukee, Wisconsin).

(5) W. S. Hwang and S. P. Kalra, "Results of BWR Small Break Simulation Test", ANS Specialists Meeting on Small Break Loss of Coolant Accident Analyses in LWRS, August 25-27, 1981, Monterey, California.

(6) W. S. Hwang and B. S. Schneidman, "BWR Blowdown/Emergency Core Cooling Program - 64 - Rod Bundle Blowdown Heat Transfer (8x8 BDHT) Final Report", General Electric Company, September 1978, (GEAP-23977).

(7) D. G. Schumacher, "BWR Refill-Reflood Program Task 4.4 - CCFL/Refill System Effects Tests (30^{o} Sector) Experimental Task Plan", General Electric Company, April 1981, (NUREG/CR-1846, EPRI-NP-1525, GEAP-24893).

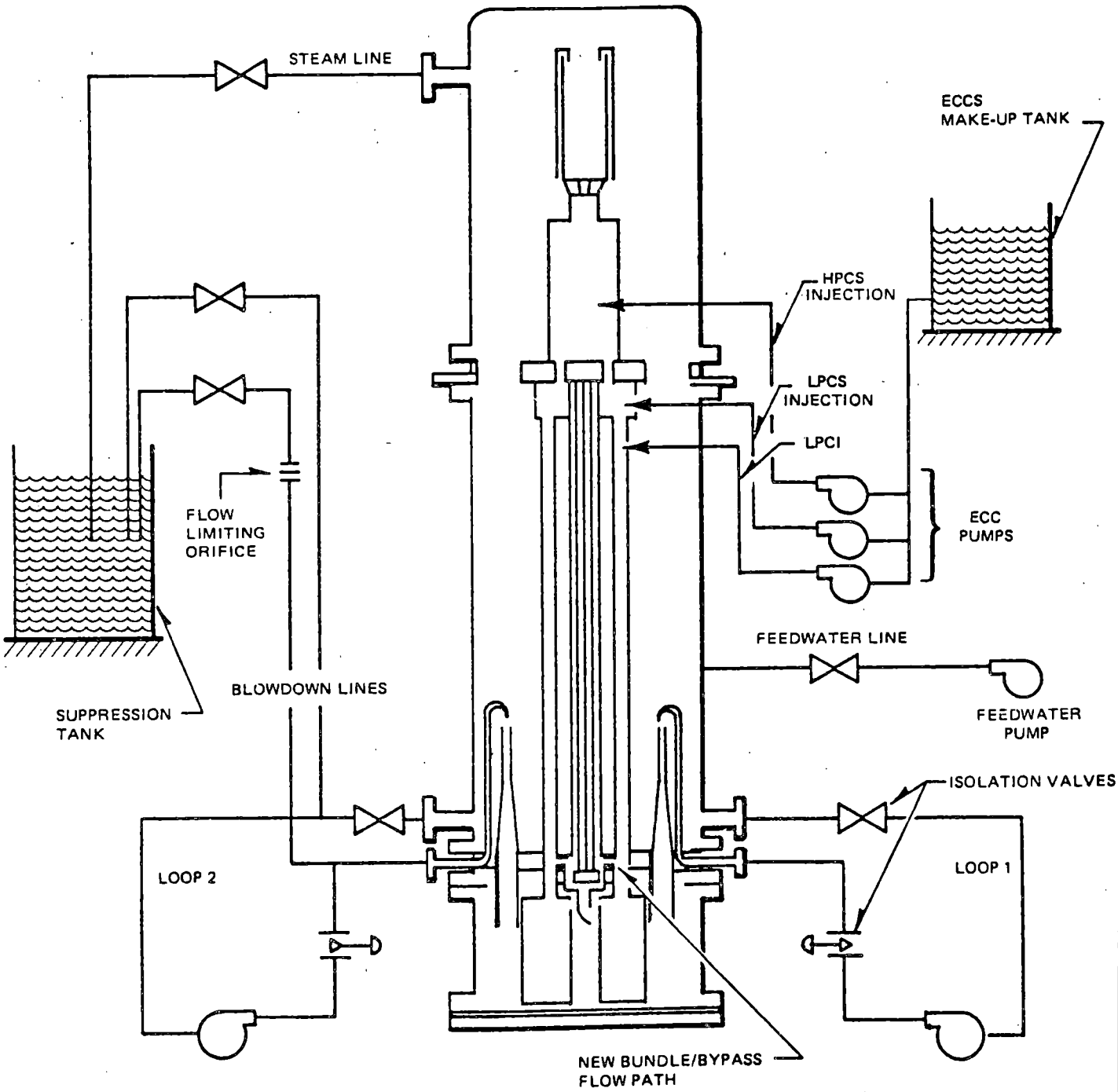

Figure 1 Two-Loop Test Apparatus

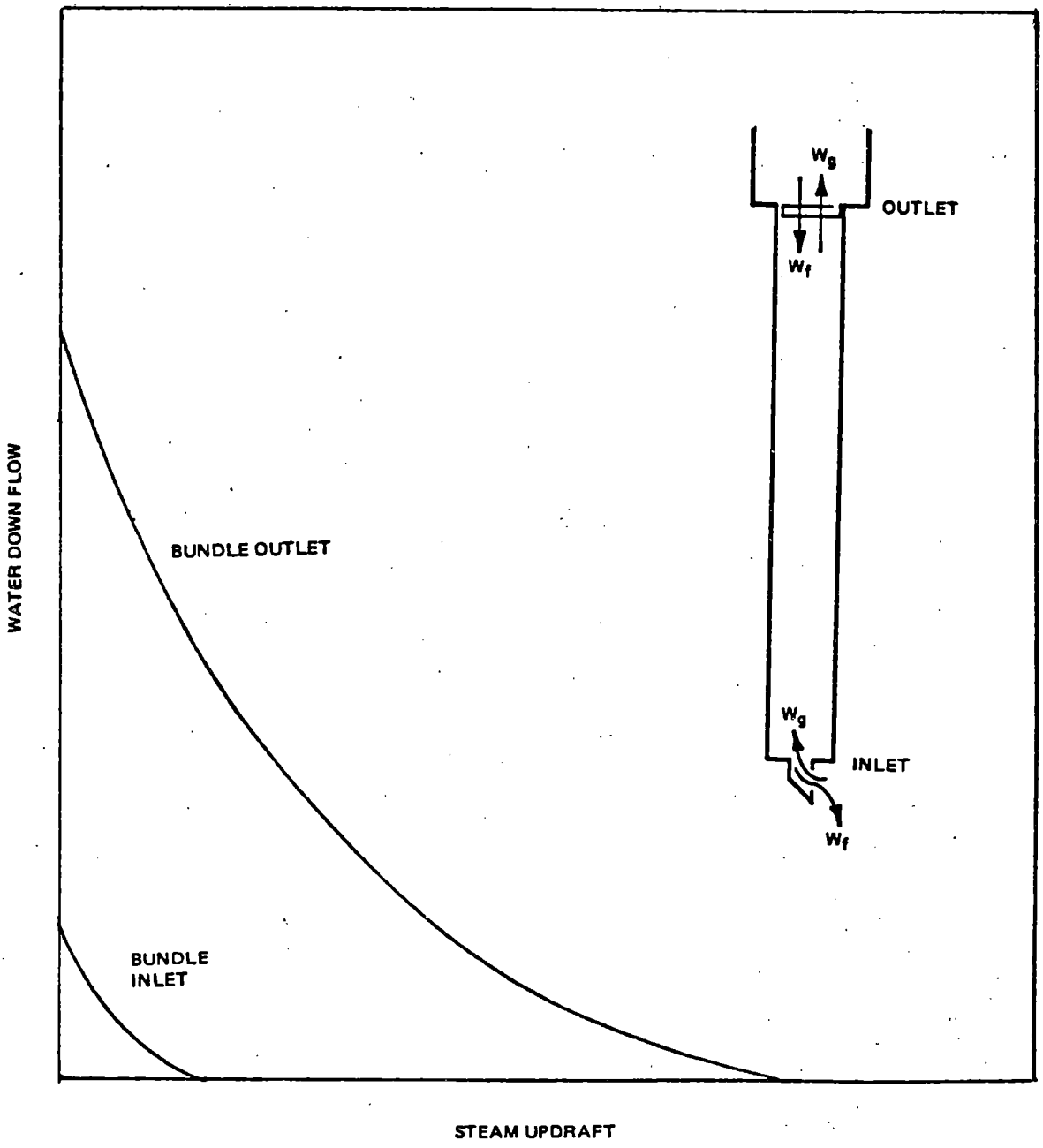

Figure 2 Core Region Counter Current Flow Limiting (CCFL) Conditions

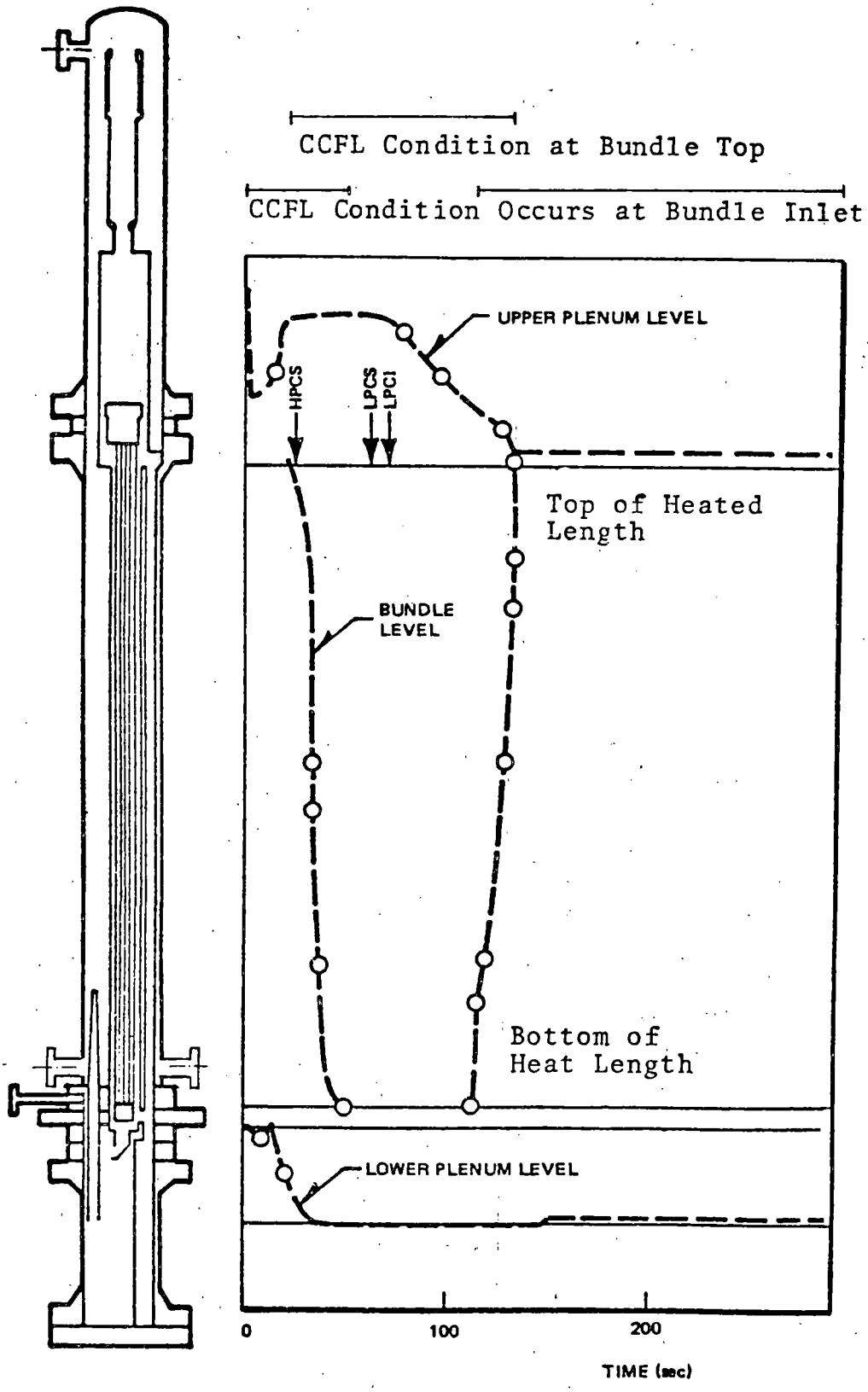

Figure 3 Two-phase Mixture Level Response

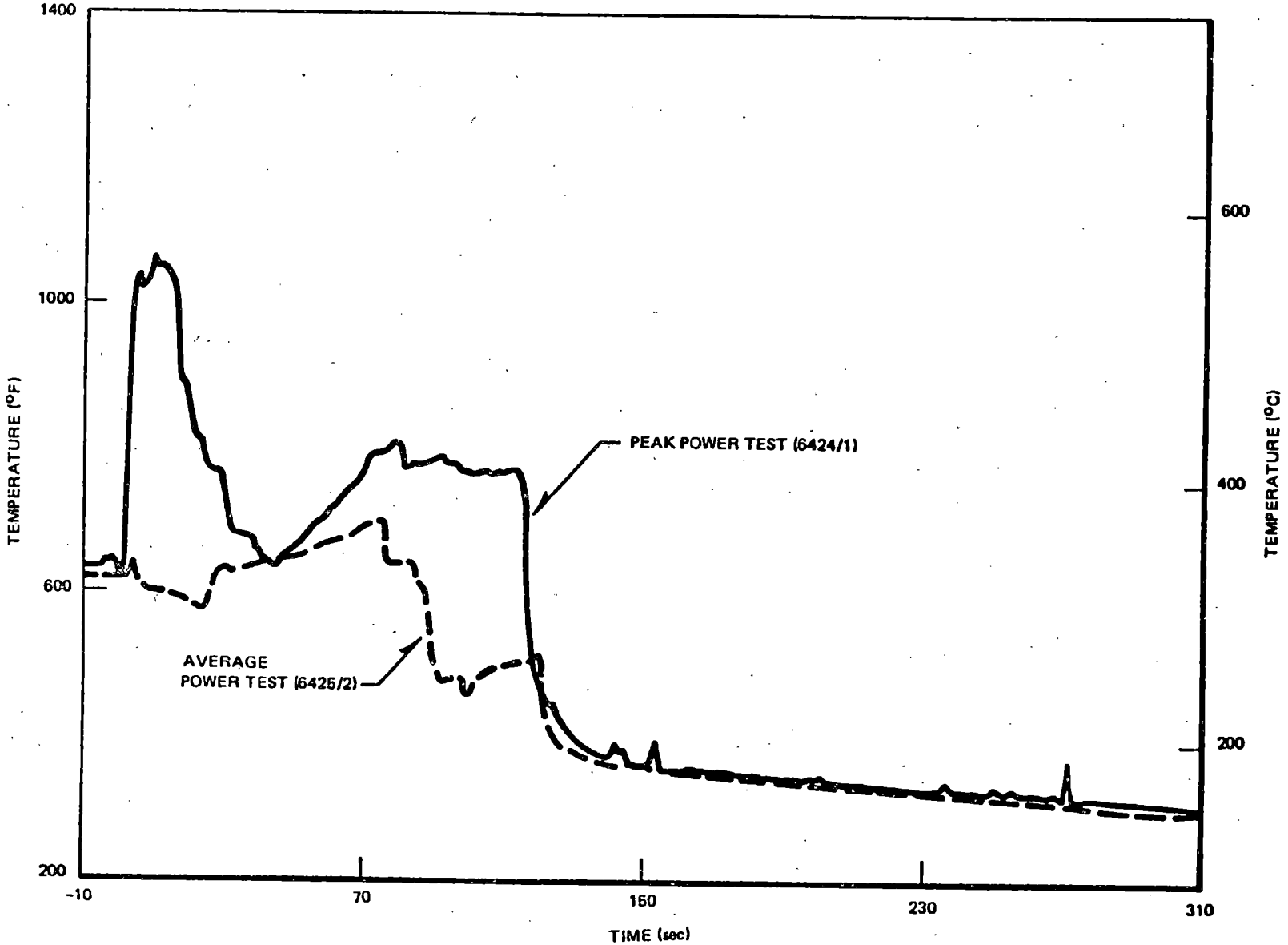

FIGURE 4 Peak Cladding Temperature Responses for Reference ECCS Injection Tests

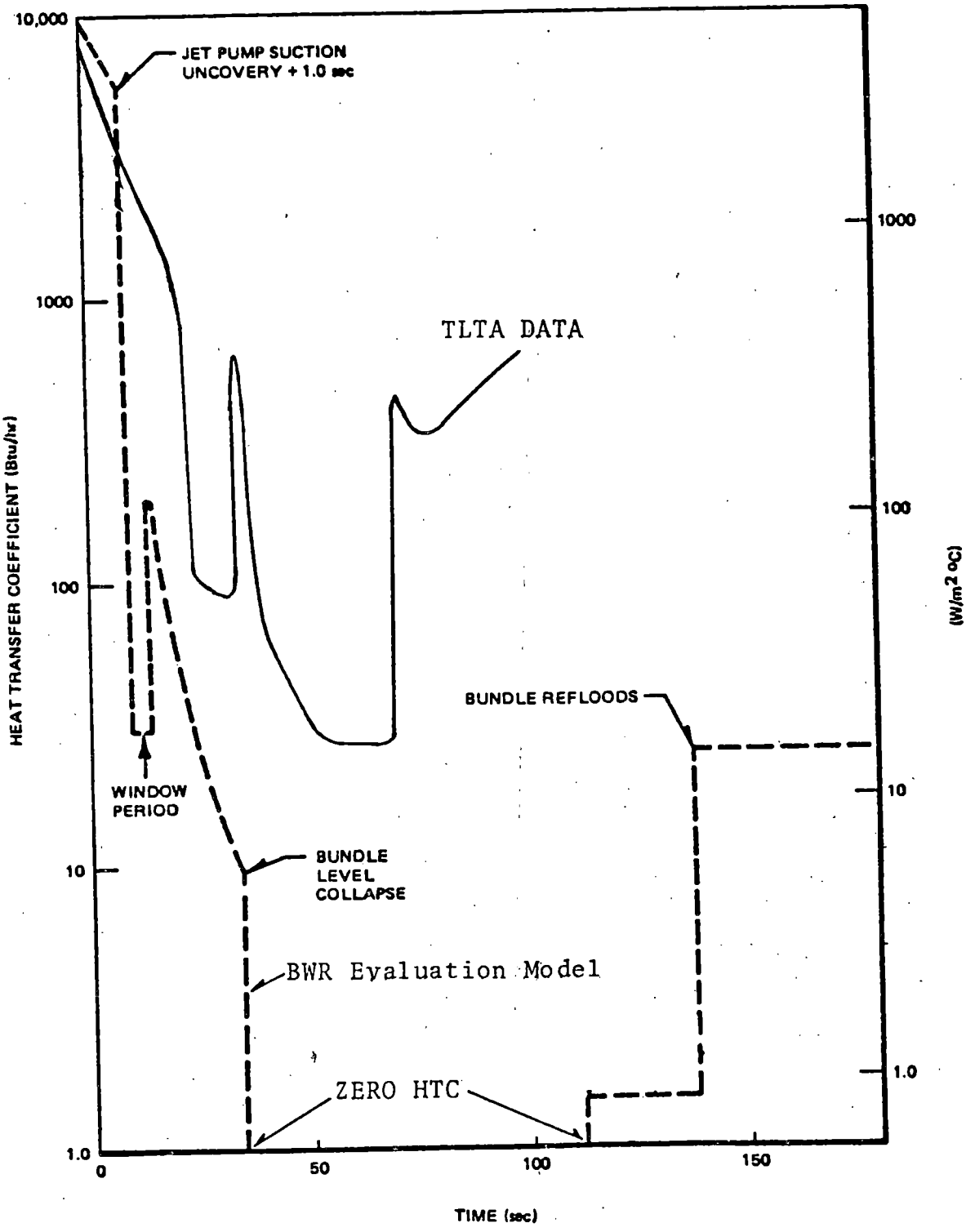

Figure 5 Bundle Heat Transfer Comparison

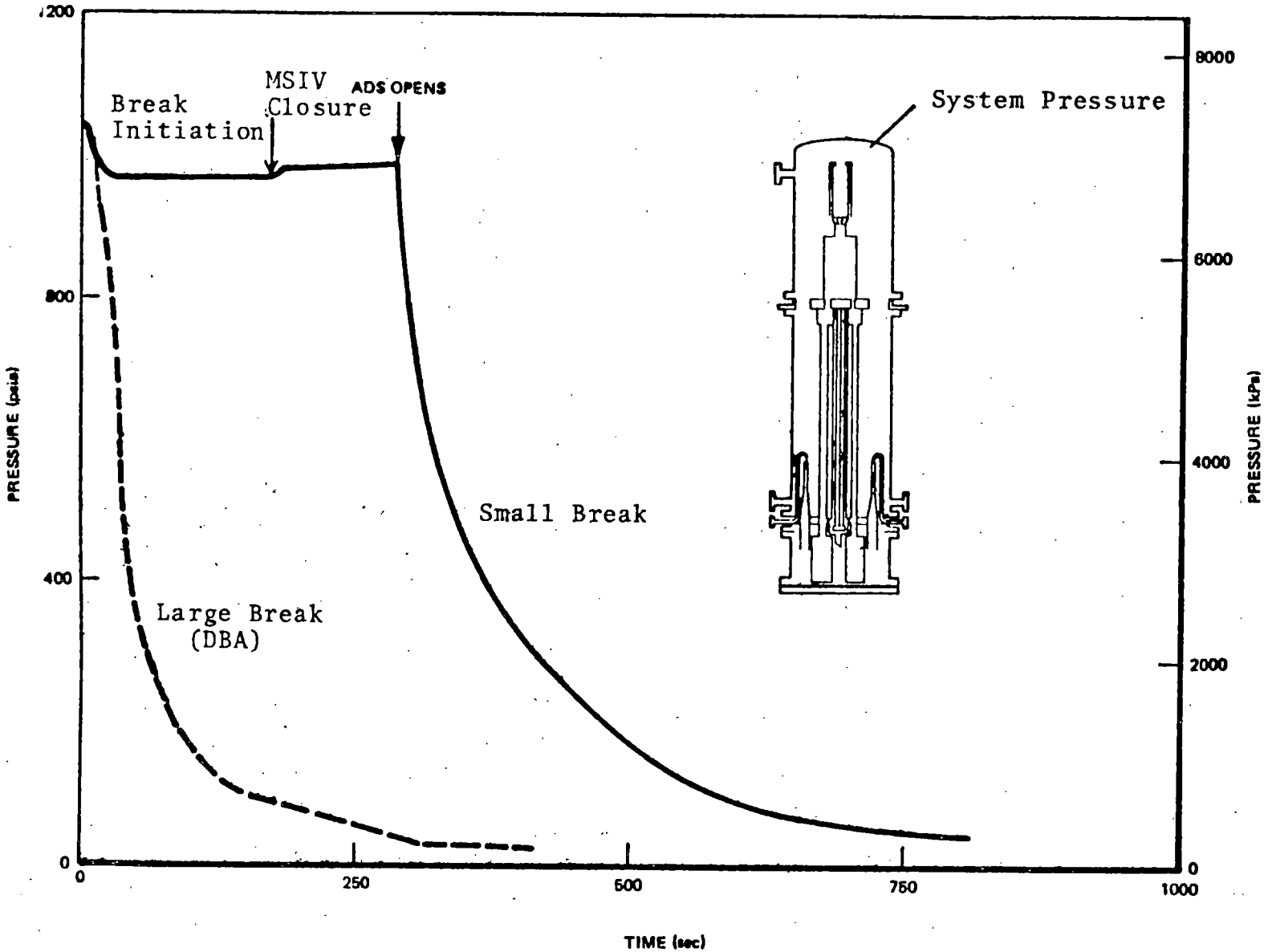

Figure 6 System Pressure Responses for Large and Small Break Simulation Tests

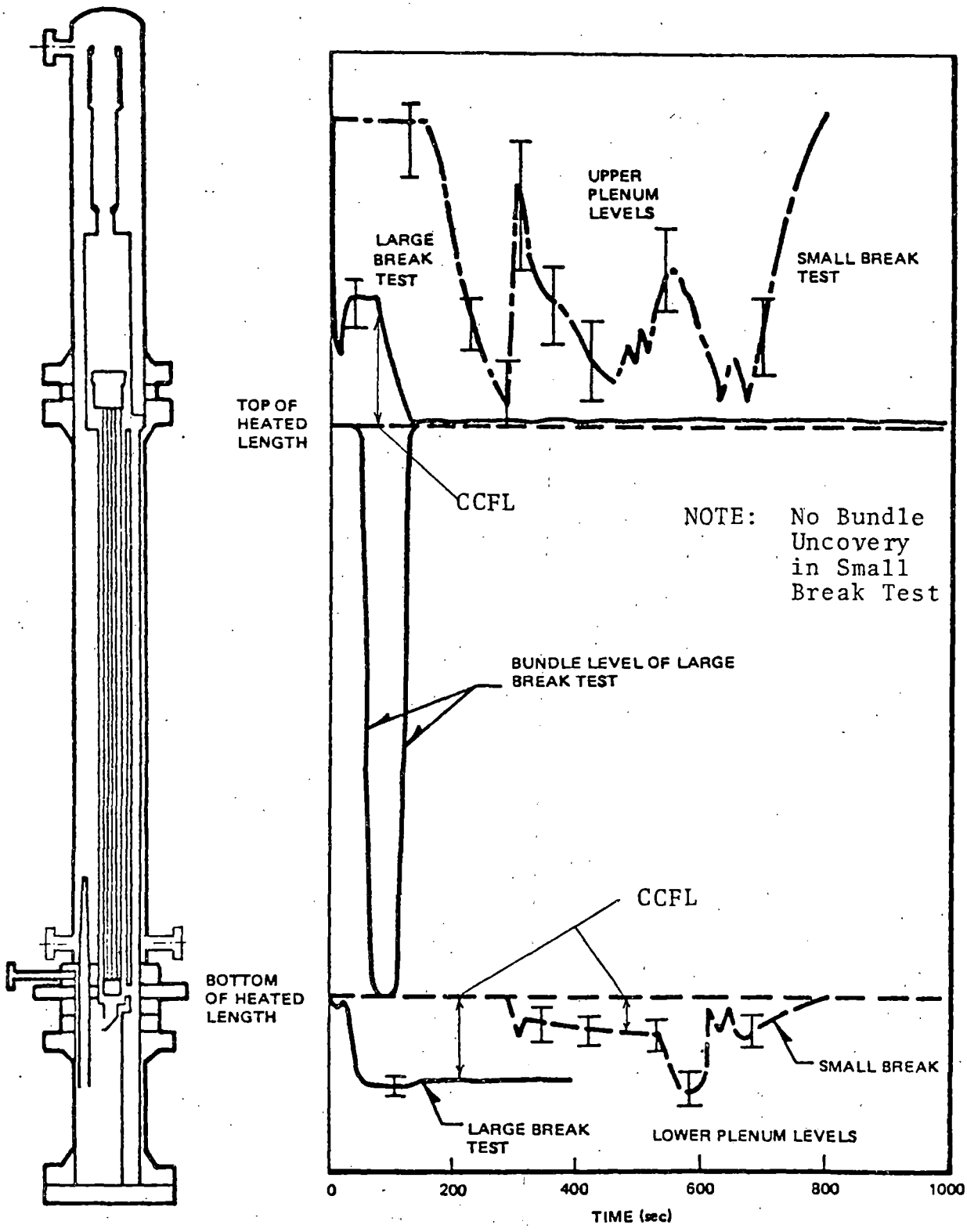

Figure 7 Comparison of Two-phase Levels for Large and Small Break LOCA Simulation Tests

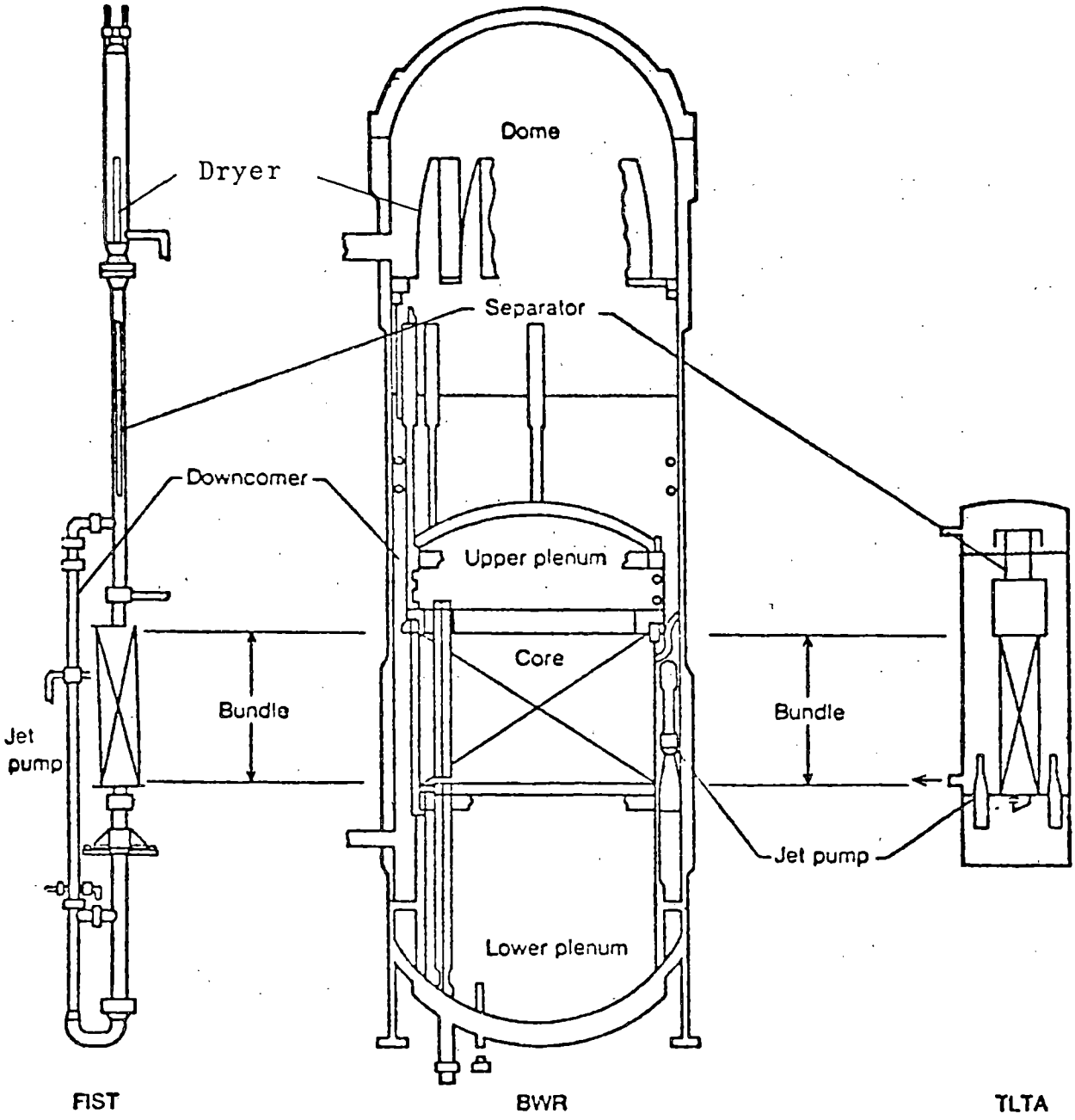

Figure 8 Comparison of BWR, TLTA, and FIST Facility

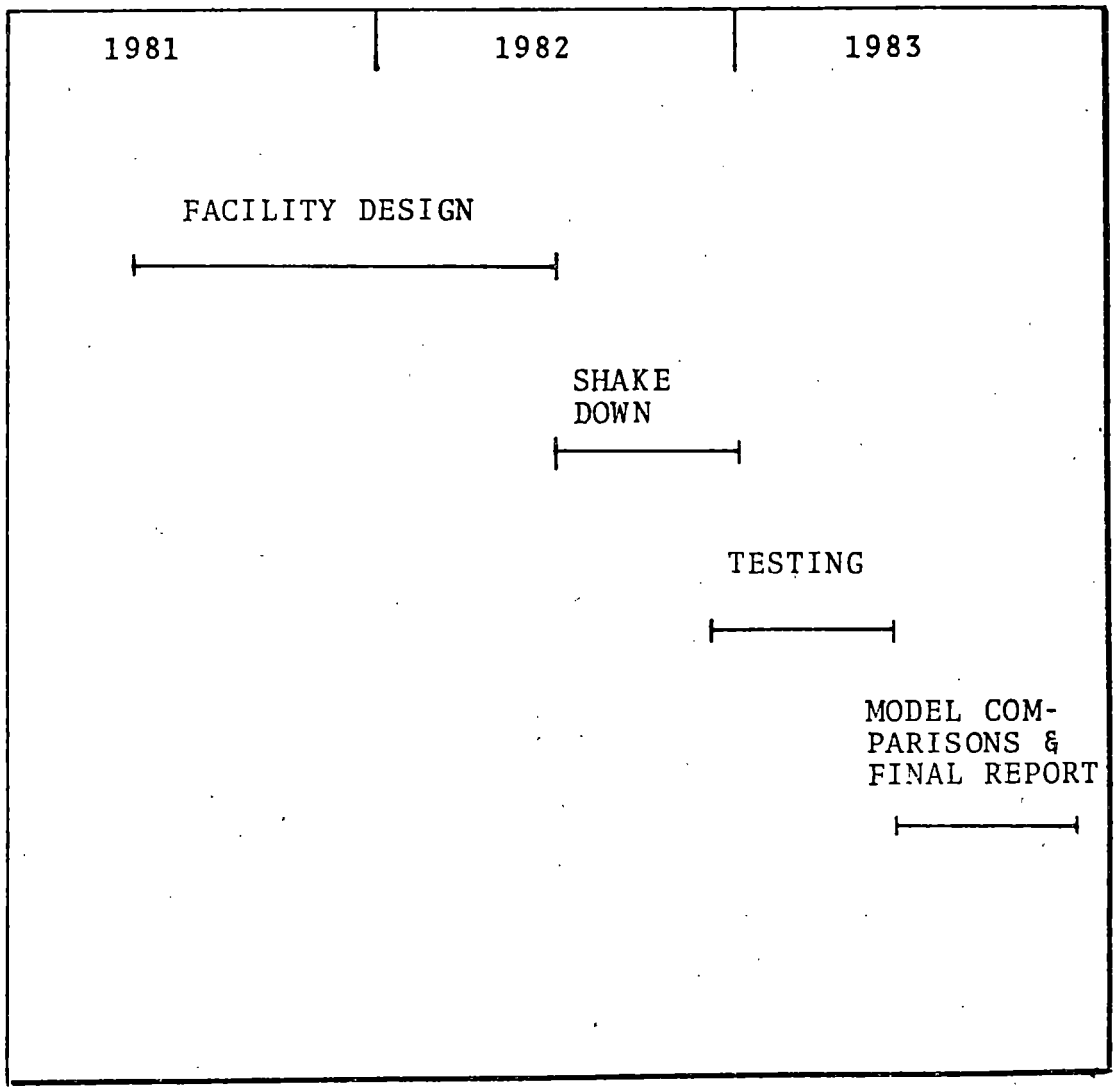

FIGURE 9 FIST Program Schedule

BWR REFILL/REFLOOD TEST RESULTS

J. A. Findlay

General Electric Company
Nuclear Fuels and Services Engineering Department
San Jose, California

For Presentation at the

Ninth Water Reactor Safety Research Information Meeting
October 26-30, 1981
National Bureau of Standards
Gaithersburg, Maryland

BWR REFILL-REFLOOD PROGRAM SPONSORS:

U.S. NUCLEAR REGULATORY COMMISSION
ELECTRIC POWER RESEARCH INSTITUTE
GENERAL ELECTRIC COMPANY

This program is obtaining BWR LOCA Refill/Reflood performance data to identify and evaluate the controlling phenomena, and for developing and assessing best estimate analysis methods. The tests are performed in the 30° Sector Steam Test Facility (SSTF), which mocks up in full scale a sector of the BWR. The principal components of the system are a) the upper plenum region, with core spray spargers and seperator stand pipes, b) the core region, with individual fuel channels and bundle hardware, c) the bypass region, with control blades and LPCI injection, d) the control rod guide tube region, e) the lower plenum region, and f) the downcomer region, with jet pumps and recirculation line, (i.e. break location). There are two categories of tests carried out with this facility. The first group, separate effects experiments, investigate refill/reflood phenomena under quasi steady state conditions. The second group, LOCA system response tests, investigate the refill-reflood performance during a blowdown transient. This paper sumerizes the results from these investigations.

SEPERATE EFFECT TESTS

The CCFL drainage characteristics of the bundle upper tie plates is measured over a range of core steam upflows. The flow path through the bypass is blocked by flooding this region with the LPCI. As shown in Figure 1, it is found that total upper tie plate CCFL drainage followed a prediction made from single channel characteristics when the channels were isolated at the inlet by a high plenum water level. With the inlet orifices uncovered, allowing steam redistribution through the lower plenum, the drainage was greater.

The CCFL drainage characteristic of the bundle inlet orifices is measured over a range of lower plenum steam

up flows. The liquid flow path into the bundles is from the bypass region through the lower tie plate leakage holes, and, in some cases, spilling over the top of the channels. The onset of inlet orifice CCFL is predicted from the single channel characteristics. However, the resultant steady drain rate is higher due to parallel channel effects. As shown in Figure 2, most of the channels are observed to be in counter-current flow, while a small number, usually near the apex of the sector, are in co-current upflow. Because the channels at the periphery are more tightly orificed, they are in a liquid downflow flow regime. These flow regimes allow steam redistribution in the lower plenum, and greater drainage than the single channel prediction.

The CCFL drainage characteristic of the top of the bypass is measured over a range of guide tube steam upflows. The flow path through the core region is limited by CCFL from the core steam. As shown in Figure 3, the byapss drainage is much higher than predicted by single channel CCFL characteristics due to the open communication in the bypass region allowing redistribtuion of the steam.

The upper plenum mixing characteristic is measured over a range of system pressure and ECC temperature. A two-phase mixture is established in the upper plenum with saturated water injected through the recirculation path, and the injection then quickly changed to subcooled water through the core spray sparger(s). Since the subcooled spray is concentrated near the periphery, the peripheral channels quickly experienced subcooling at the upper tie plate. As shown in Figure 4, the subcooling induces CCFL breakdown, which drains all of the upper plenum spray injection.

Bypass mixing and channel wall heat transfer is measured by injecting steam into the bottom of the region from the guide tubes, establishing a two-phase mixture in

the bypass, and then injecting subcooled water through the LPCI. Although the subcooling is concentrated near the periphery, the condensation zone stretches across the region to condense all the steam entering from the guide tubes. The channel wall heat transfer is evaluated by injecting steam into the channels and cold water into the bypass. No guide tube/bypass steam is used. Approximately 95% of the water subcooling is used consensing steam. About half is steam condensing on the cold channel walls, and the other half is steam condensing on the leakage flow of subcooled bypass water into the channels.

SYSTEM RESPONSE TESTS

The system response tests investigate the refill/reflood performance during a blowdown transient from 150 psi. To initialize the refill-reflood transients, steam is injected into the core, lower plenum, and guide tube regions at steady pressure to simulate flashing. Water is recirculated from the lower plenum to the upper plenum to set initial mass distribution. However, because of the high drainage rates that result from parallel channel effects, very little water inventory is held up in the upper plenum. When the initial mass distribution is set, the blowdown transient is initiated by closing the steam vent, opening the blowdown line, and closing of the steam injection simulating flashing.

Due to CCFL at the inlet orifice, the channels start filling as soon as the ECCS come on, as shown in Figure 6. The peripheral channels show rapid CCFL breakdown at the upper tie plates, and there is flow of bypass water into the channels through the lower tie plate holes. The test with all ECC systems operating (HPCS + LPCS + 3 LPCI) filled the quickest, and also depressurized the fastest. The reference test (HPCS + LPCS + 1 LPCI), which represents one

ECC division off, depressurized more slowly, but refilled and reflooded the system adequately. A bounding case without ECC systems depressurized slowest since there is no condensing taking place. Variation of the ECCS temperature or initial water mass does not significantly affect the channel reflooding response.

The effect of LPCI injection into the bypass is shown in Figure 7. Tests run with ECCS combinations of (a) HPCS + 2 LPCI, (b) LPCS + 2 LPCI, and (c) 2 LPCI are compared with HPCS + LPCS + 3 LPCI and HPCS + LPCS + 1 LPCI. As the number of LPCI systems injecting cold water into the bypass increases, subcooling occurs sooner at the channel inlet orifices and lower plenum condensing steam in the lower plenum region, and making the refill-reflood process more effective.

As shown in Figure 8, decreasing break size to 45% of the reference case causes the system to depressurize slower, as expected. The refill-reflood performance is faster than in the reference case, but otherwise similar.

The observations from these tests demonstrate rapid refill-reflood performance, and have identified the controlling phenomena. The results provide insight into parallel channel effects for modeling system performance, and a data base for assessing best estimate analysis methods.

U. S. NUCLEAR REGULATORY COMMISSION
PREVIOUS REPORTS IN BWR REFILL-REFLOOD PROGRAM SERIES

BWR Refill-Reflood Program Task 4.1 - Program Plan, G.W. Burnette, General Electric Company, NUREG/CR-1972, January 1981.

BWR Refill-Reflood Program Task 4.2 - Core Spray Distribution Experimental Task Plan, T. Eckert, General Electric Company, NUREG/CR-1558, August 1980.

BWR Refill-Reflood Program Task 4.2 - Core Spray Distribution Final Report, T. Eckert, General Electric Company, NUREG/CR-1707, September 1980.

BWR Refill-Reflood Program Task 4.3 - Single Heated Bundle Experimental Task Plan, D.D. Jones, L.L. Myers, J.A. Findlay, General Electric Company, NUREG/CR-1788, January 1980.

BWR Refill-Reflood Program Task 4.3 - Single Heated Bundle Experimental Task Plan, Addendum I, Stage 3 - Seperate Effects Bundle, D.D. Jones, General Electric Company, NUREG/CR-1708 - Add. I, July 1980.

BWR Refill-Reflood Program Task 4.4 - CCFL Refill System Effects Tests (30 Sector) Experimental Task Plan, D.G. Schumacher, General Electric Company, NUREG/CR-1846, December 1980.

BWR Refill-Reflood Program Task 4.4 - CCFL Refill System Effects Tests (30 Sector) Experimental Task Plan, Addendum A, SSTF CCFL/Refill Shakedown Plan, D.G. Schumacher, General Electric Company, NUREG/CR-1846, April 1981.

BWR Refill-Reflood Program Task 4.4 - CCFL Refill System Effects Tests (30 Sector) Experimental Task Plan, Addundum B, 30° SSTF CCFL/Refill Separate Effects Test Plan, D. G. Schumacher, General Electric Company, NUREG/CR-1846, April 1981.

BWR Refill-Reflood Program Task 4.4 - CCFL Refill System Effects Tests (30 Sector) Experimental Task Plan, Addendum C, BWR/6 System Response Test Plan, D.G. Schumacher, General Electric Company, NUREG/CR-1846, October 1981.

BWR Refill-Reflood Program Task 4.7 - Model Development Task Plan, J.G.M. Andersen, General Electric Company, NUREG/CR-2057, March 1981.

BWR Refill-Reflood Program Task 4.8 - Model Qualification Task Plan, J.A. Findlay, General Electric Company, NUREG/CR-1899, January 1981.

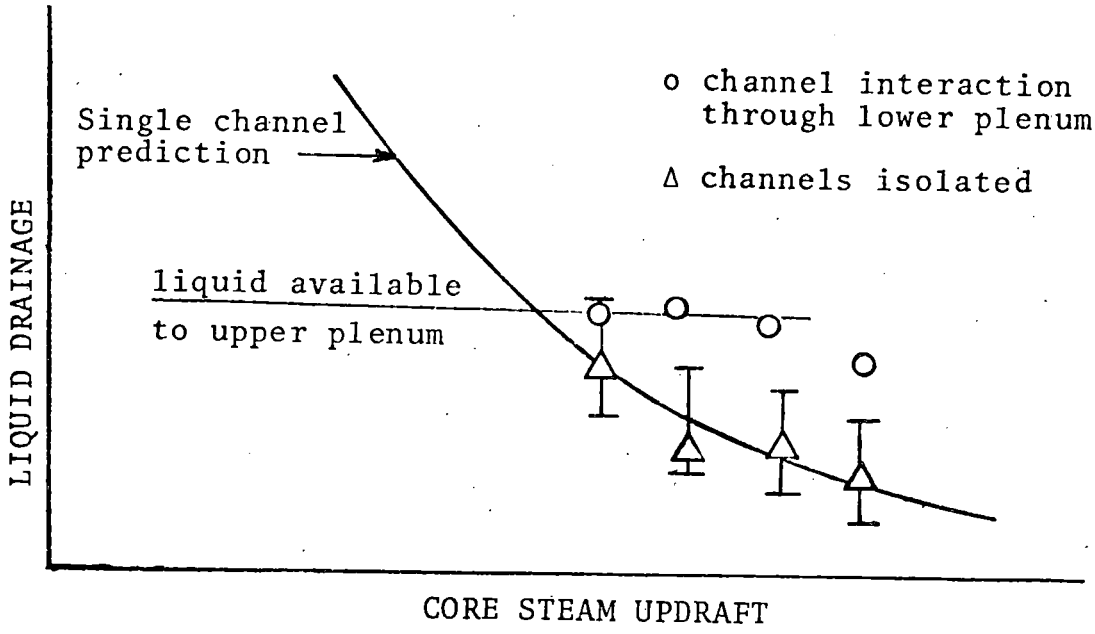

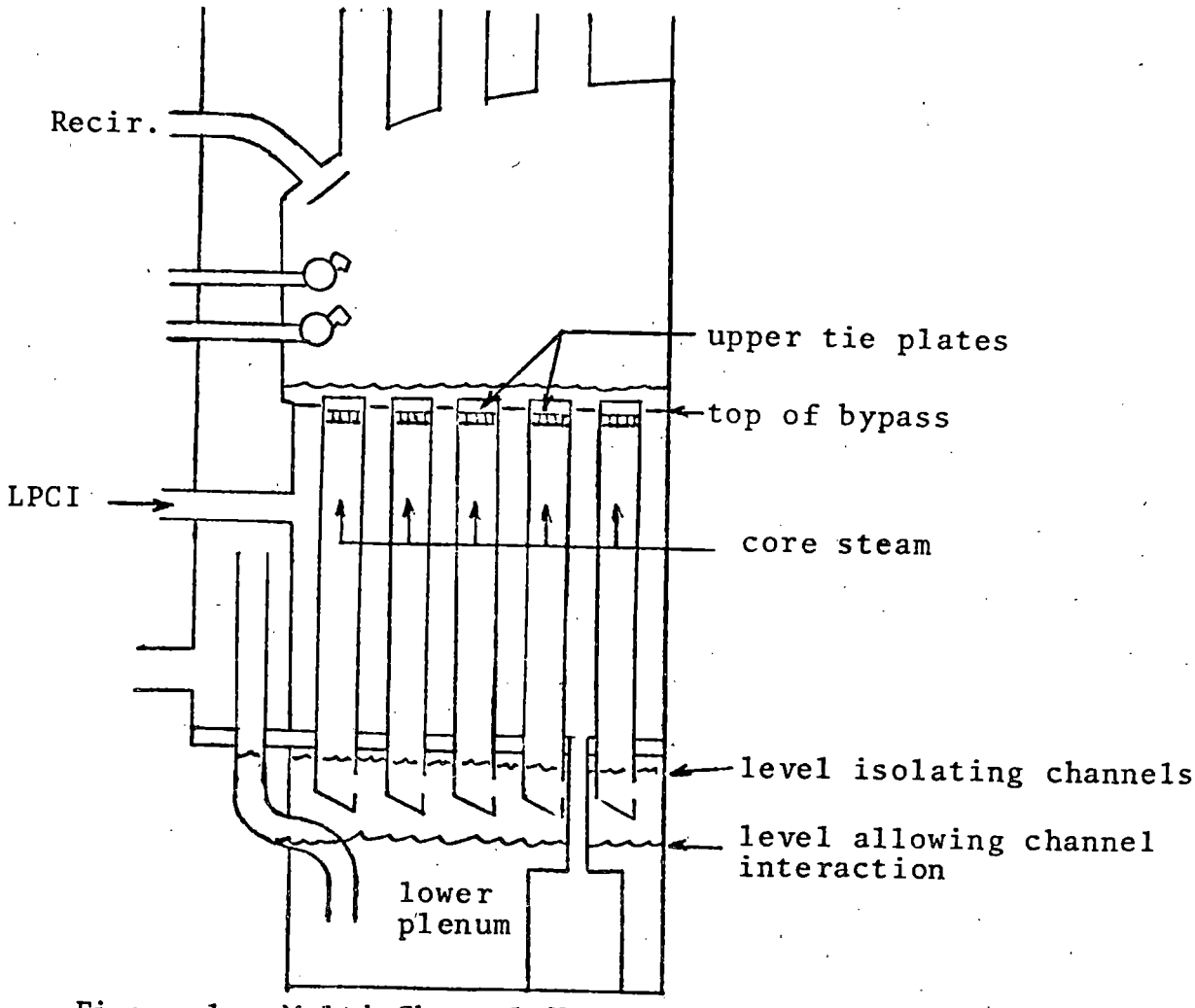

Figure 1 - Multi-Channel Upper Tie Plate CCFL

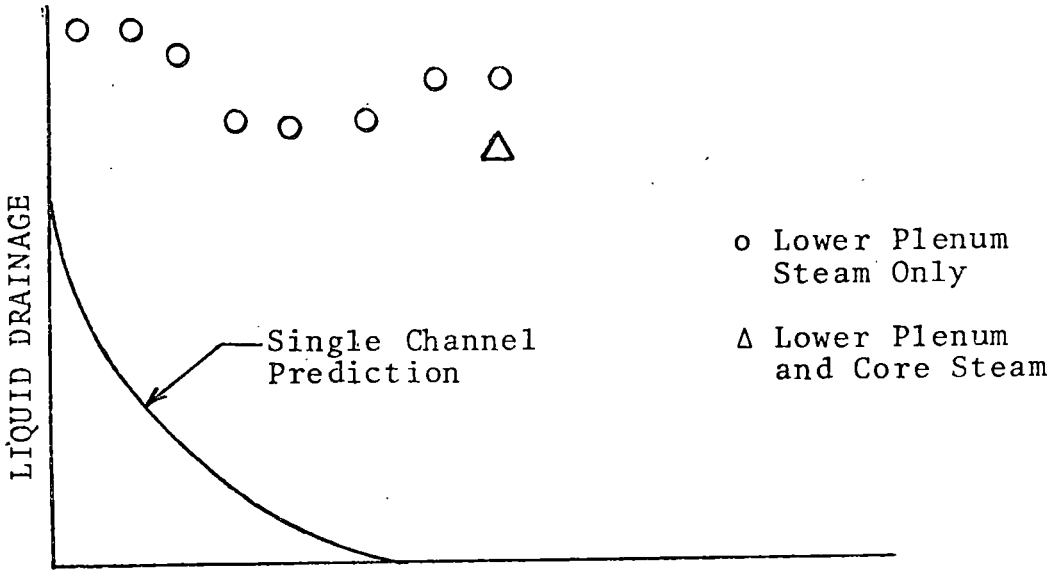

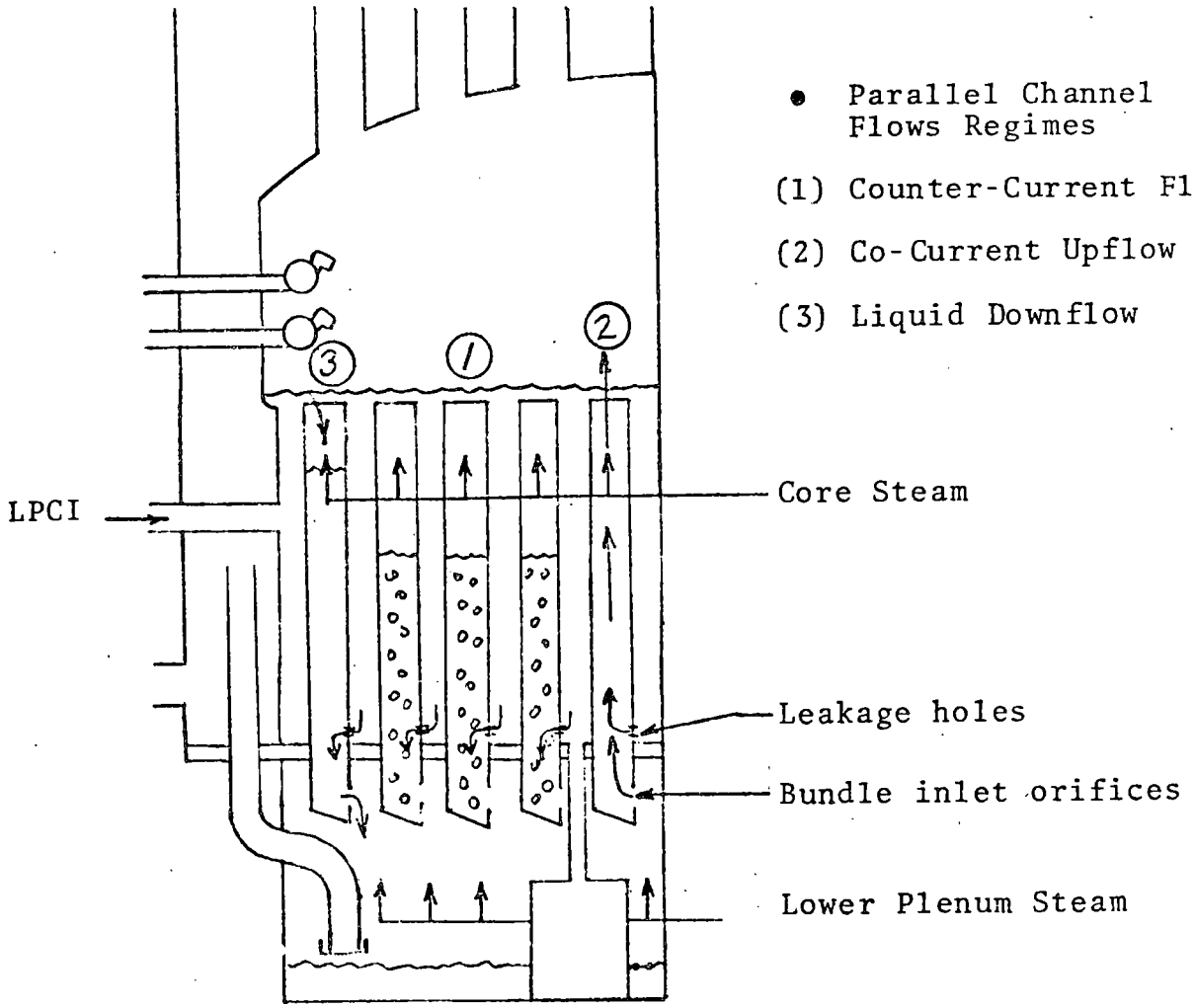

Figure 2 - Multi-Channel Bundle Inlet CCFL

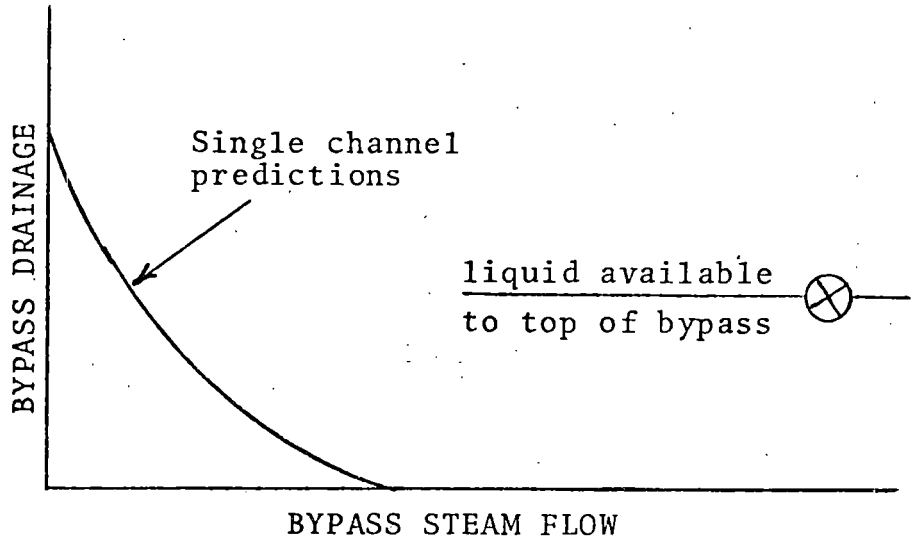

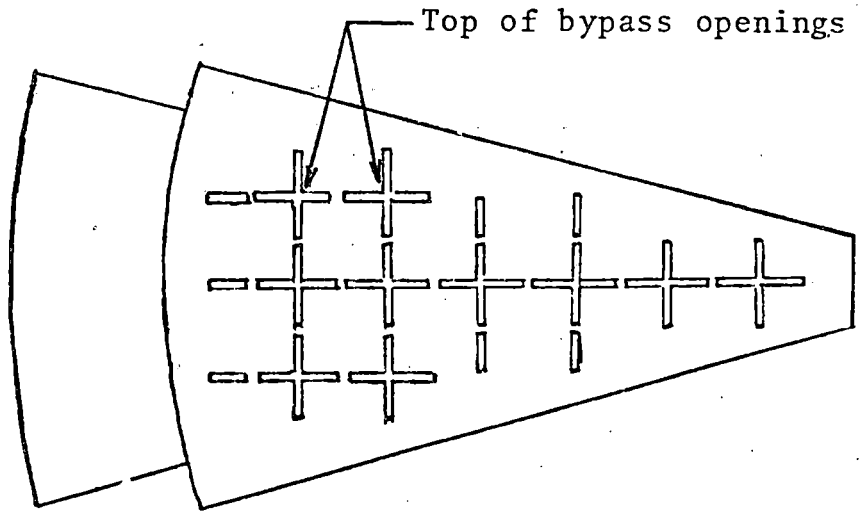

- Bypass Flow Paths
- Flow Communication
- Distributed Flow Area
- No CCFL

Figure 3 - Multi-Channel Top of Bypass CCFL

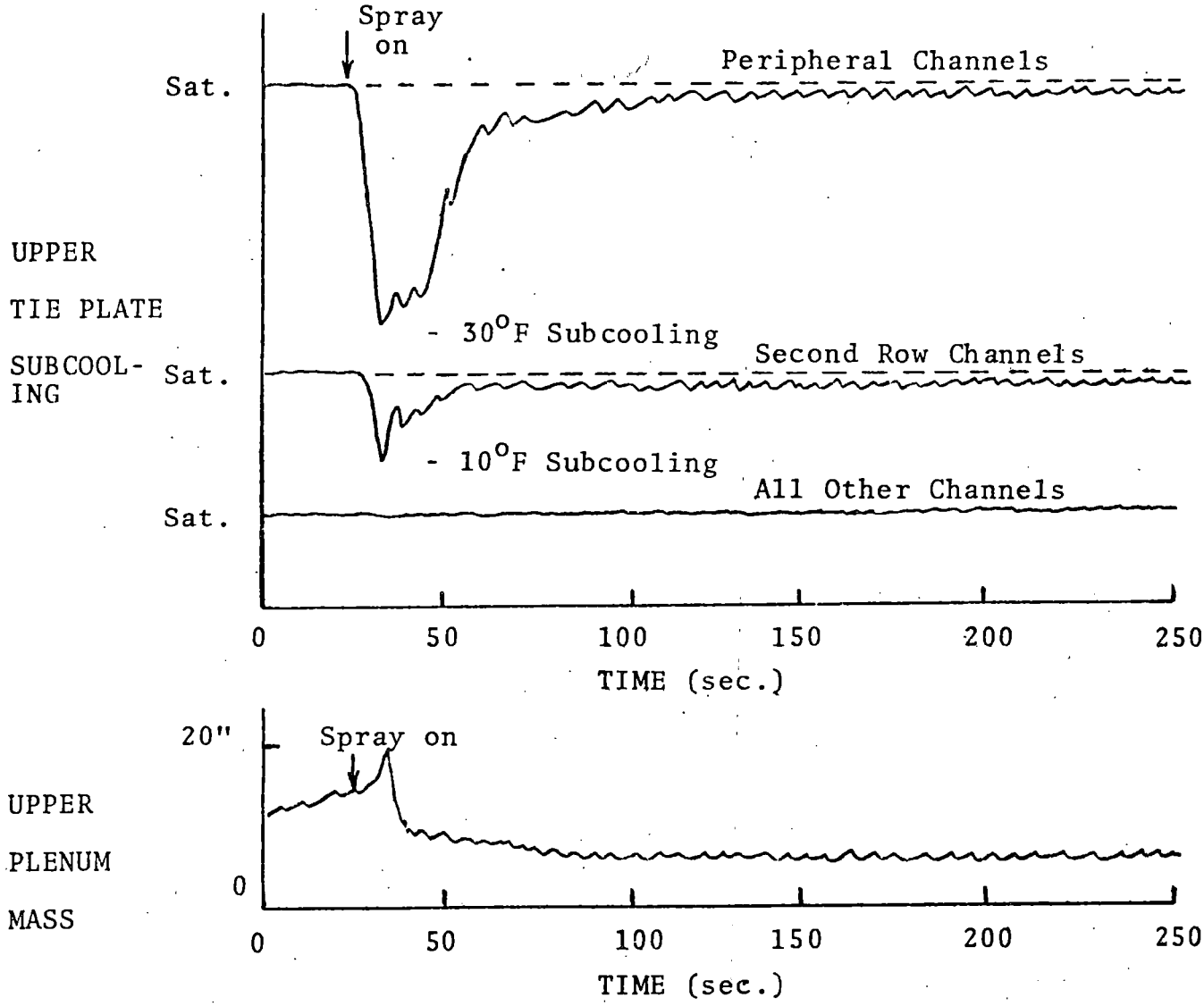

- Upper Plenum Mixing
  - Subcooling Concentrated Near Periphery
  - Rapid CCFL Breakdown in Peripheral Channels
  - Drains all of Upper Plenum Spray Injection

Figure 4 - Upper Plenum Mixing and Subcooled CCFL Breakdown

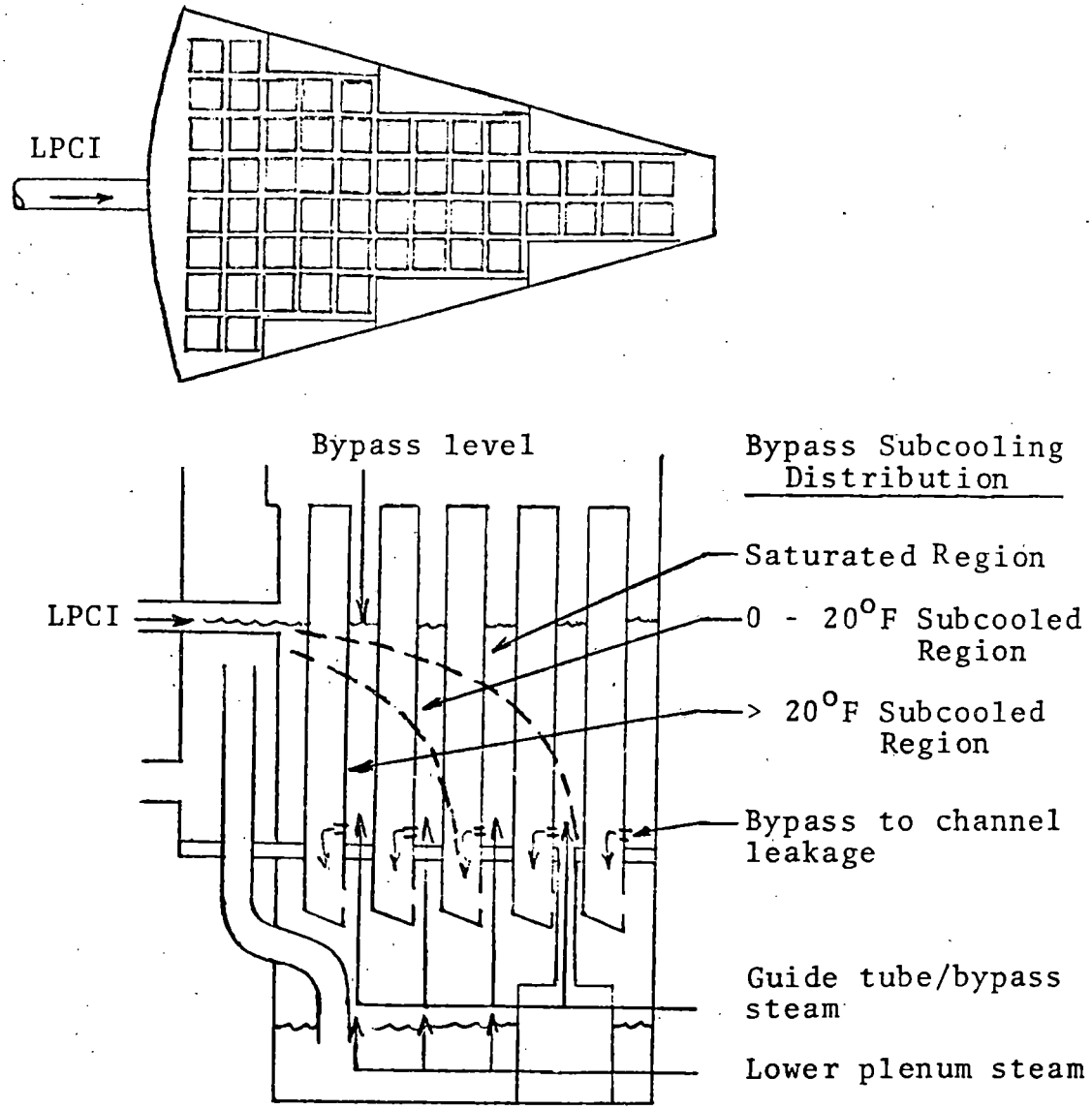

- Bypass Mixing
  - All Guide Tube/Bypass Steam Condensed
  - Channel Wall Heat Transfer from Core Region

Figure 5 - Bypass Mixing and Heat Transfer

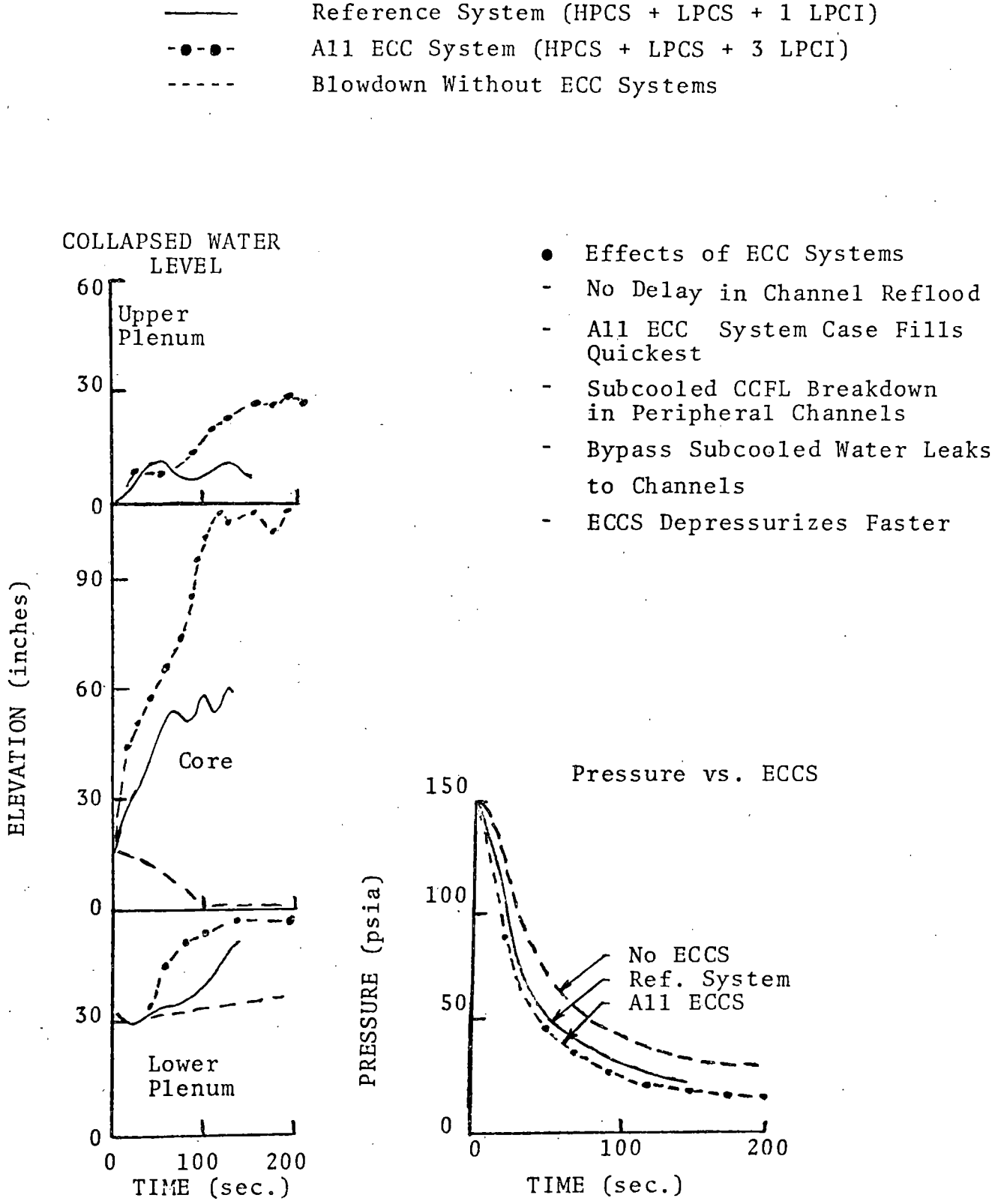

Figure 6 - System Response-ECC Systems

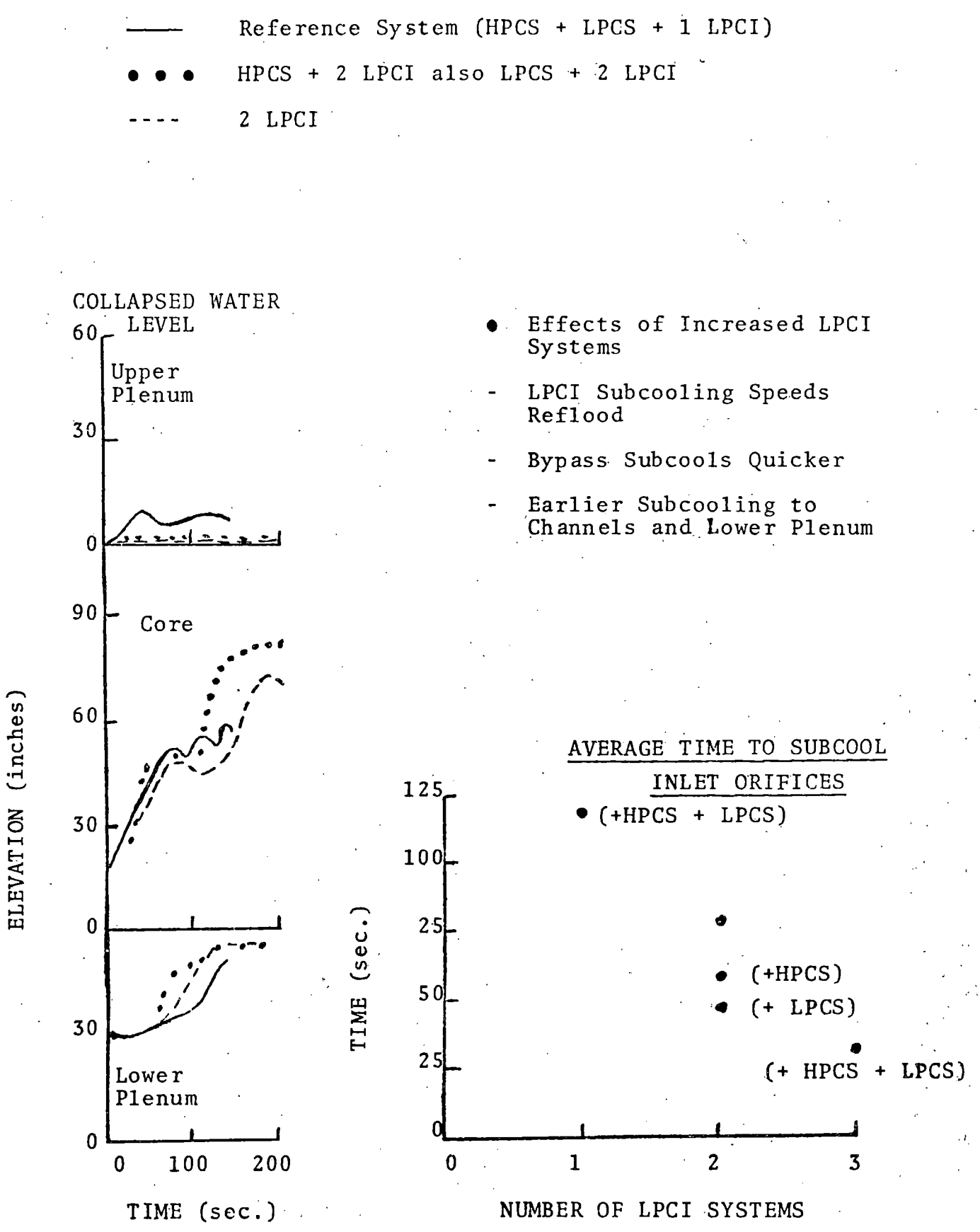

Figure 7 - System Response - LPCI Effectiveness

——— Reference System (100% Break)

----- 45% Break (HPCS + LPCS + 1 LPCI)

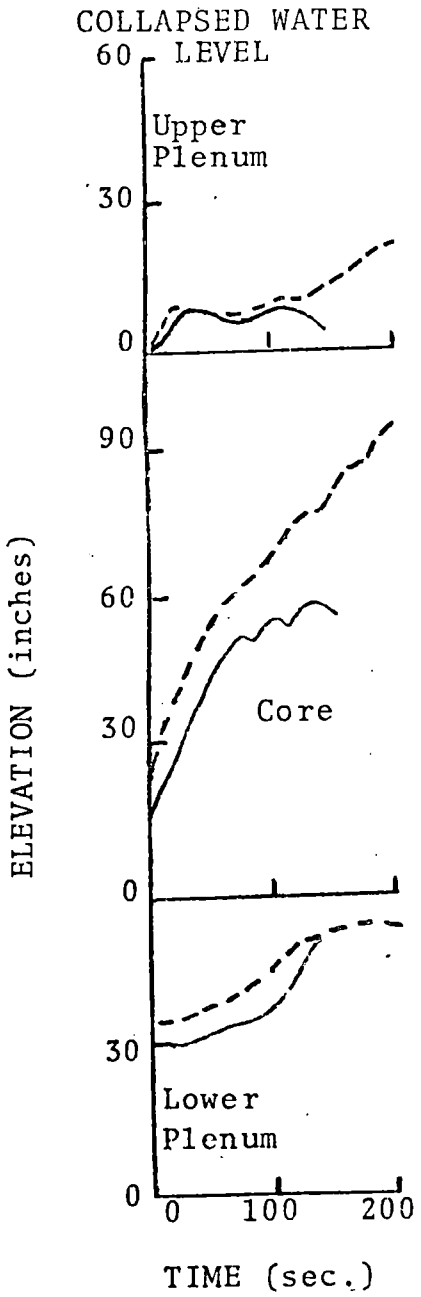

- Effects of Break Size
  - Similar Refill - Reflood
  - Large Break Depressurizes Faster

PRESSURE vs. BREAK SIZE

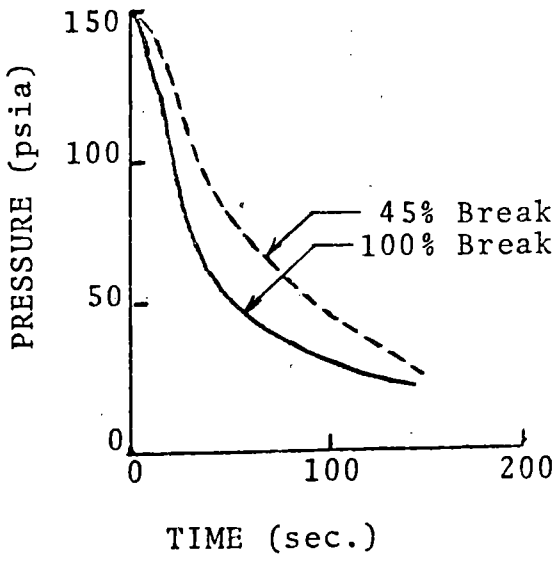

Figure 8 - System Response-Break Size

BWR REFILL-REFLOOD PROGRAM

BWR TRAC MODEL DEVELOPMENT AND ASSESSMENT

J. G. M. Andersen
Md. Alamgir

General Electric Company
Nuclear Fuel & Services Engineering Department
San Jose, California

For Presentation At:

The 9th Water Reactor Safety Research Information Meeting
October 27, 1981
National Bureau of Standards
Gaithersburg, Maryland

Program Sponsors:

U.S. Nuclear Regulatory Commission
Electric Power Research Institute
General Electric Company

BWR REFILL REFLOOD PROGRAM

BWR TRAC MODEL DEVELOPMENT AND ASSESSMENT

The overall Refill/Reflood Program seeks to develop a better understanding of phenomena controlling the refill and reflood phases of boiling water reactor loss-of-coolant accidents (BWR-LOCAs) and to provide a basis for assessing assumptions used in establishing BWR LOCA safety margins. A key objective is to provide a basis for and support to the development and assessment of best estimate BWR system thermal hydraulic codes. This task is especially important because full-scale experiments are impractical, and the systems code will be utilized to synthesize the information from various smaller scale tests. The vehicle chosen for this purpose is the TRAC (1) code developed at Los Alamos National Laboratory. At the present time, however, Idaho National Engineering Laboratory (INEL) has assumed primary responisbility for the development of the BWR series of TRAC codes, and the development and assessment of models for the BWR version of TRAC is consequently conducted in close cooperation with INEL.

The major tasks under the Refill/Reflood program consist of the development of models for the BWR version of TRAC and of the assessment of these models as an integrated part of the TRAC program.

The model development consists of the development of models for the specific BWR components and of models for basic phenomena of particular relevance for BWR's. The BWR component models are the jet pumps, steam separators, dryers, fuel bundles*, and the upper plenum. A jet pump model. based on the conservation of

---

* This task has been done by INEL.

momentum for the mixing process and appropriate models for irreversible losses has been developed, and has been tested for both small and full scale experiments covering all six flow combinations as well as single phase and two-phase flow conditions. Simple models for the separators and dryers giving 100% separation and the correct pressure drop, has been implemented. The upper plenum phenomena have been accounted for using a simple model for the ECC distribution. The basic models and correlations in TRAC for the wall and interface shear and heat transfer and for entrainment and deposition have been reviewed with emphasis on phenomena of particular importance for the BWR. A new model for the interface shear accounting for the effect of phase and velocity distribution has been developed and tested against both tube and bundle void fraction data. Major improvements have been made to the heat transfer. A boiling length model has replaced the CHF correlation and new models have been developed for subcooled boiling and radiation heat transfer.

Future improvements to the BWR version of TRAC will include a mechanistic model for the upper plenum phenomena, improved separator and dryer modeling, and further improvements to the constitutive correlations primarily for the wall and interface heat transfer.

The model assessment is proceeding independent of the model development, and experimental data which have not been used in the development of the models are being utilized. Both separate effects tests and integral system effects tests have been used in the assessment. The separate effects tests include vessel blowdown tests and single channel tests for evaluating critical flow, void distribution, and bundle heat transfer phenomena. The integral system effects tests include the Single Heated Bundle, Two Loop Test Apparatus (TLTA), and the 30° Steam Sector Test Facility (SSTF), for evaluating integral system response, refill-reflood phenomena, and multi-dimensional effects. Good agreement has generally been obtained, and it has been demonstrated that the majority of the controlling phenomena in a BWR are adequately predicted.

BWR REFILL-REFLOOD PROGRAM

BWR-TRAC MODELS

GENERAL ELECTRIC

PROGRAM SPONSORS:

U.S. NUCLEAR REGULATORY COMMISSION

ELECTRIC POWER RESEARCH INSTITUTE

GENERAL ELECTRIC COMPANY

JGM ANDERSEN

OCTOBER 1981

Finally, an assessment has been made of the consequences of a design basis accident for a BWR/6. TRAC predictions show that the peak cladding temperature for a BWR is less than 1000°F.

REFERENCES

1. R.J. Pryor, et al., TRAC-P1A, An Advanced Best Estimate Computer Program for PWR LOCA Analysis, NUREG/CRA-0665, LA, May, 1979.

2. J.G.M. Andersen and B.S. Shiralkar, BWR Refill-Reflood Program, Task 4.7 - Model Development Task Plan, NUREG/CR-2057, March, 1981.

3. J.A. Findlay and G.L. Sozzi, BWR Refill-Reflood Program, Task 4.8 - Model Qualification Task Plan, NUREG/CR-1889, January, 1981.

DEVEOPMENT TEAM:

JGM ANDERSEN
YH CHEUNG
KH CHU
V. PARAMESWARAN
JC SHAUG
BS SHIRALKAR
MM ABUROMIA
RF KIMBRELL

ASSESSMENT TEAM:

MD ALAMGIR
SC CARUSO
SA ALLISON
WS HWANG
JE SHIMON
GL SOZZI
WL WOLFE

JGM ANDERSEN

OCTOBER 1981

PROGRAM OBJECTIVES:

- BETTER UNDERSTANDING OF THE CONTROLLING PHENOMENA IN A BWR LOCA.
- BEST ESTIMATE SIMULATION OF BWR LOCA TRANSIENT
- DEMONSTRATE BWR LOCA SAFETY MARGINS.

TASKS:

- DEVELOPMENT OF MODELS FOR BWR COMPONENTS AND PHENOMENA.
- EXTENSIVE ASSESSMENT AGAINST SEPARATE EFFECTS AND SYSTEM EFFECTS TESTS.

DEVELOPMENT AND ASSESSMENT ARE DONE IN CLOSE COORDINATION WITH IDAHO NATIONAL ENGINEERING LABORATORY.

JGM ANDERSEN

OCTOBER 1981

SCHEDULE

Development of First Version	1980
Assessment of First Version	1981
Development of Final Version	1982
Assessment of Final Version	1982

JGM Andersen

October 1981

BWR TRAC MODEL DEVELOPMENT

BWR COMPONENT MODELS:

- JET PUMP
  - MIXING
  - LOSSES
  - MOMENTUM EQUATION
- STEAM SEPARATOR
  - PRESSURE DROP
  - CARRYOVER AND CARRYUNDER
- STEAM DRYER
  - PRESSURE DROP
  - EFFICIENCY
- UPPER PLENUM
  - MIXING
  - VOID AND ENTHALPY DISTRIBUTION
  - SUBCOOLED CCFL BREAKDOWN
- FUEL CHANNEL (INEL)

JGM ANDERSEN

OCTOBER 1981

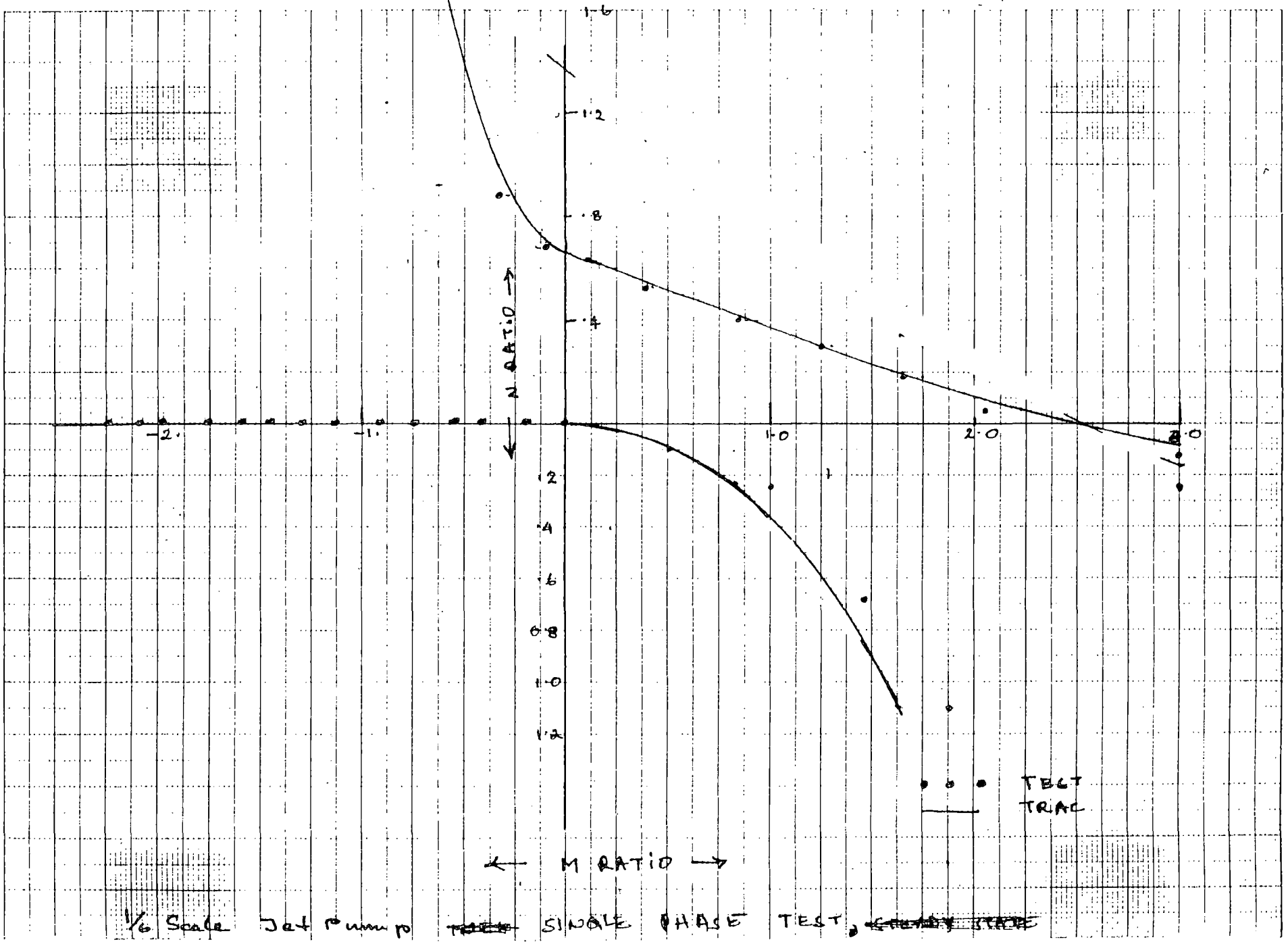

1/6 Scale Jet Pump ~~TEST~~ SINGLE PHASE TEST, ~~STEADY STATE~~

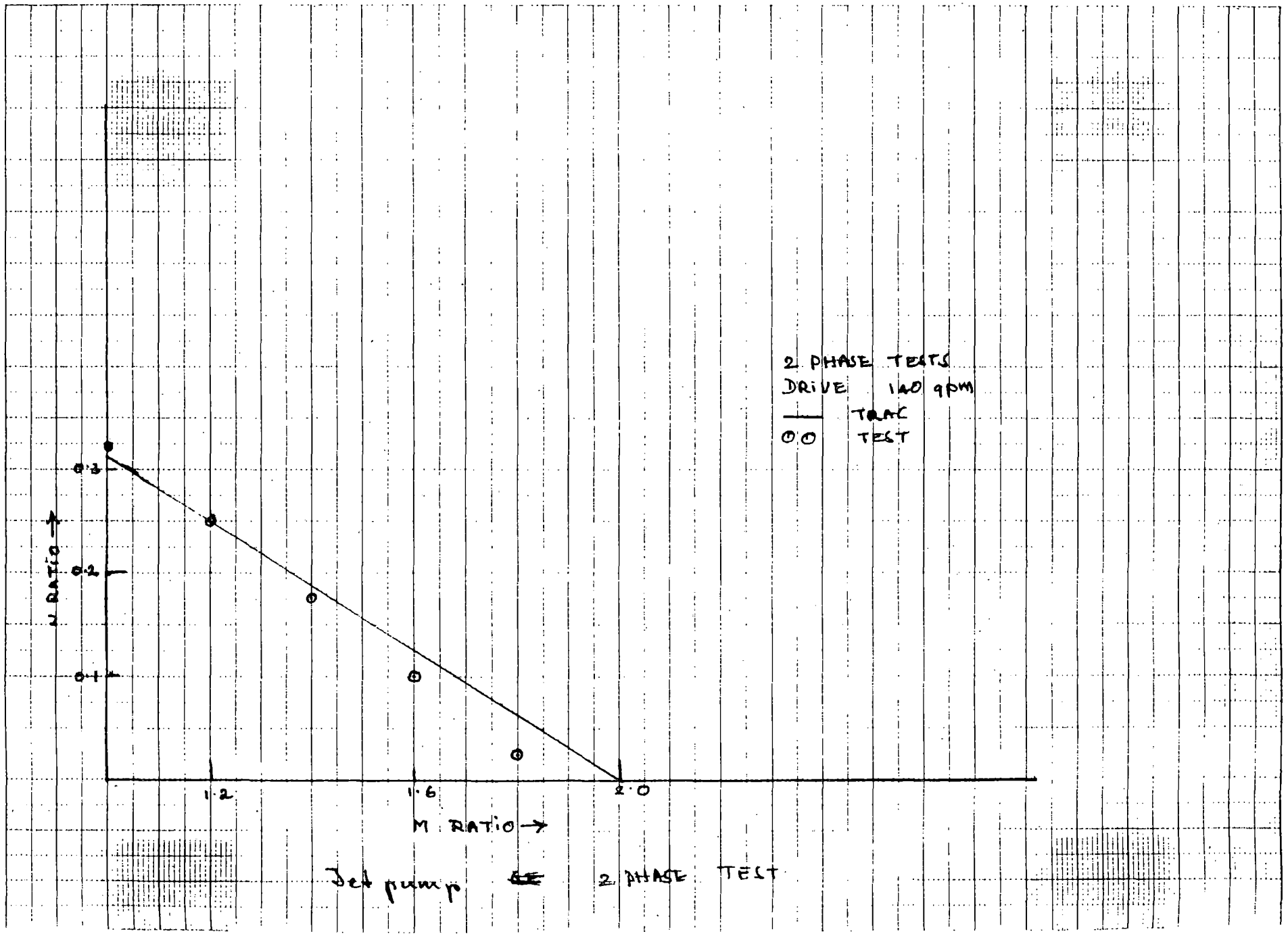
2 PHASE TESTS
DRIVE 1120 rpm
TRAC
TEST
0·3
0·2
0·1
ν RATIO →
1·2
1·6
2·0
M RATIO →
Jet pump
2 PHASE TEST

BWR TRAC MODEL DEVELOPMENT

BASIC MODELS AND CORRELATIONS:

- BASIC EQUATIONS
- WALL AND INTERFACE HEAT TRANSFER
- WALL AND INTERFACE SHEAR
- ENTRAINMENT AND DEPOSITION.

MAJOR RESULTS:

- VOID FRACTION
- CCFL
- THERMAL RADIATION
- SUBCOOLED BOILING
- BOILING TRANSITION.

JGM ANDERSEN

OCTOBER 1981

FRIGG 61124

P = 30.3 MPa

Q = 4.495 MW

G = 472 kg/m²s

ΔTi = 5.9°C

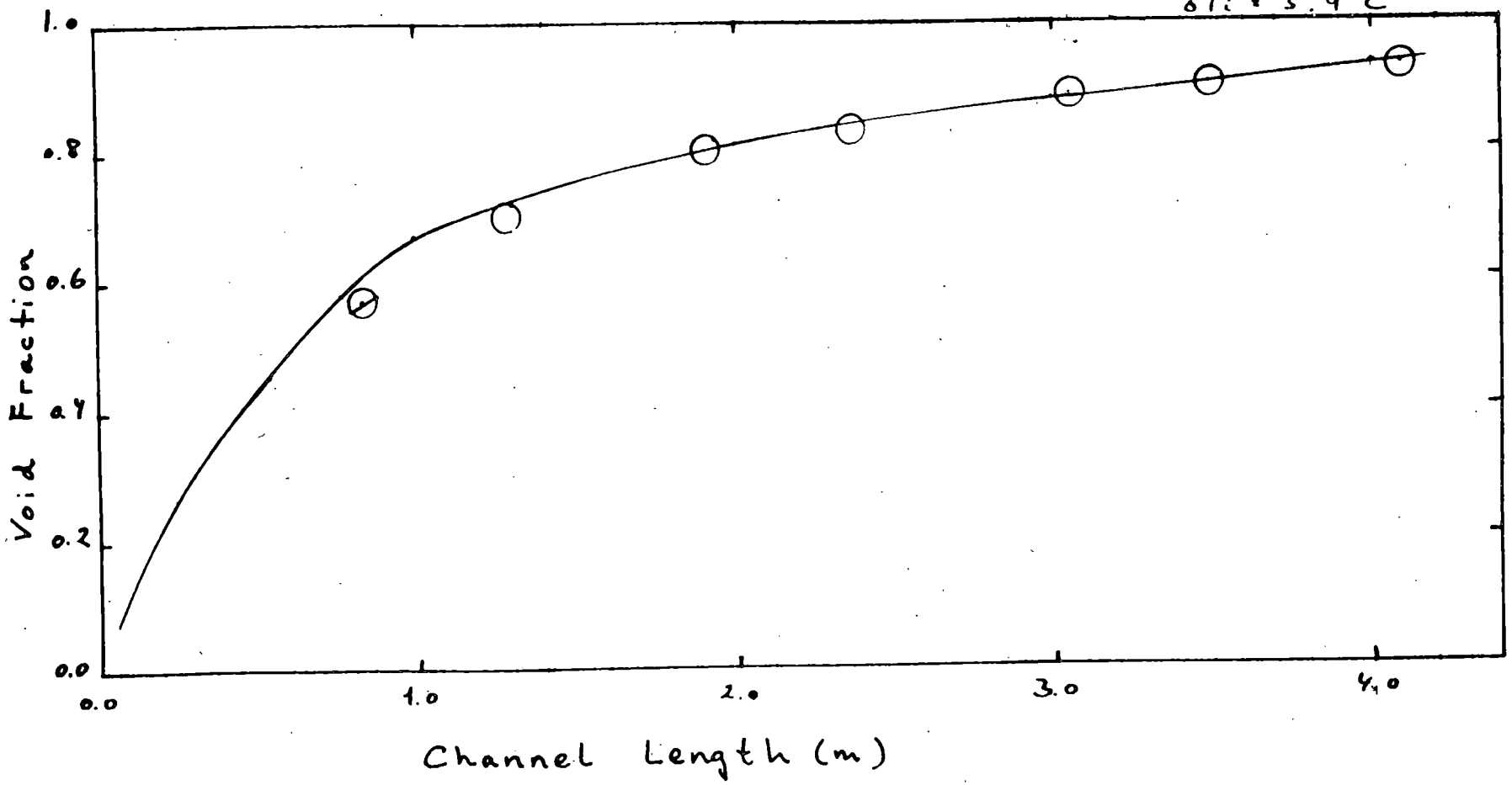

FRIGG 613005

P = 4.82 MPa

Q = 3.51 MW

G = 1022 kg/m²s

ΔT_i = 1.5 °C

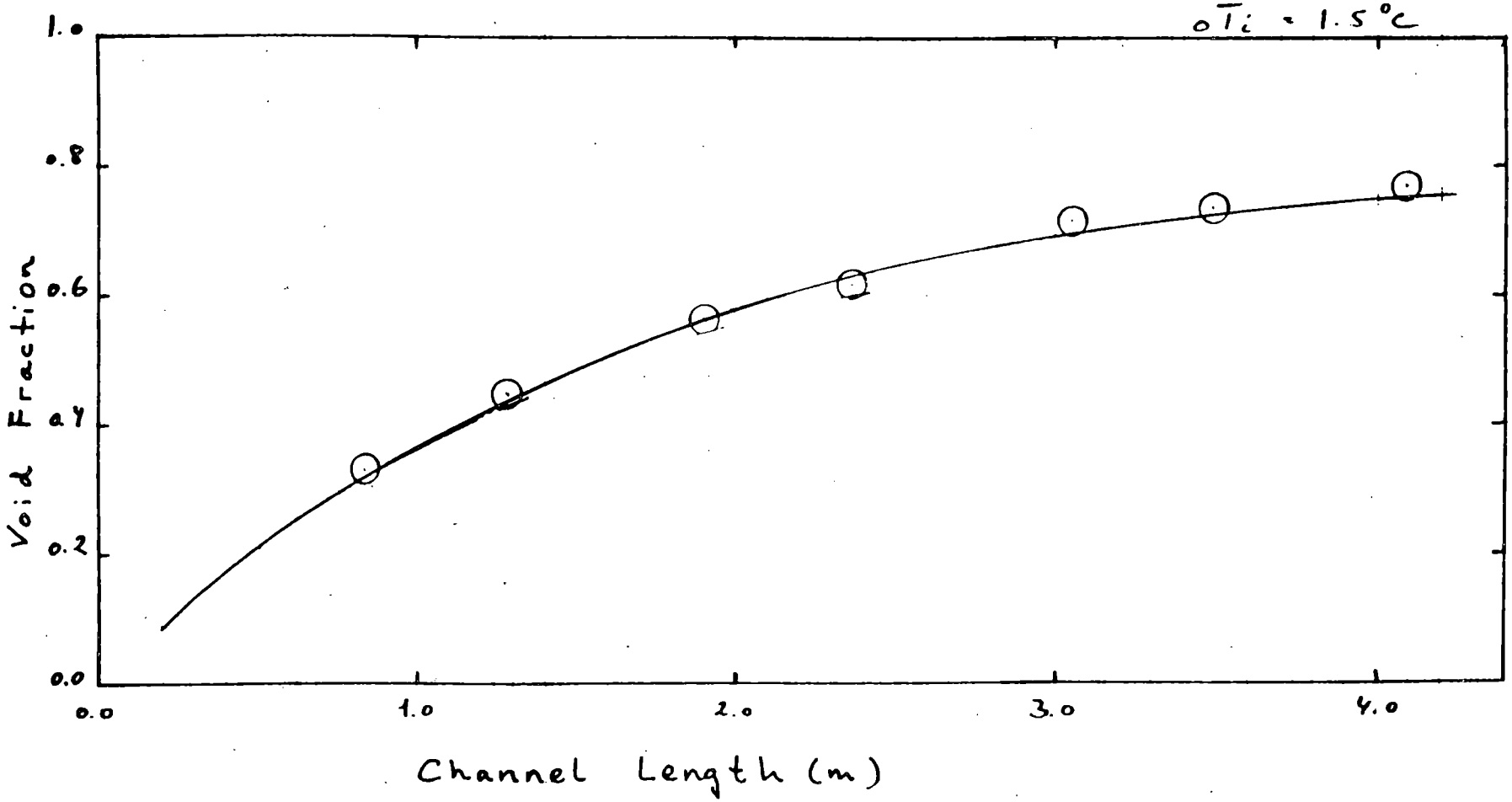

FRIGG 613006

P = 4.82 MPa

Q = 3.51 MW

G = 2146 kg/m²s

$\overline{\Delta T}$ = 1.2 °C

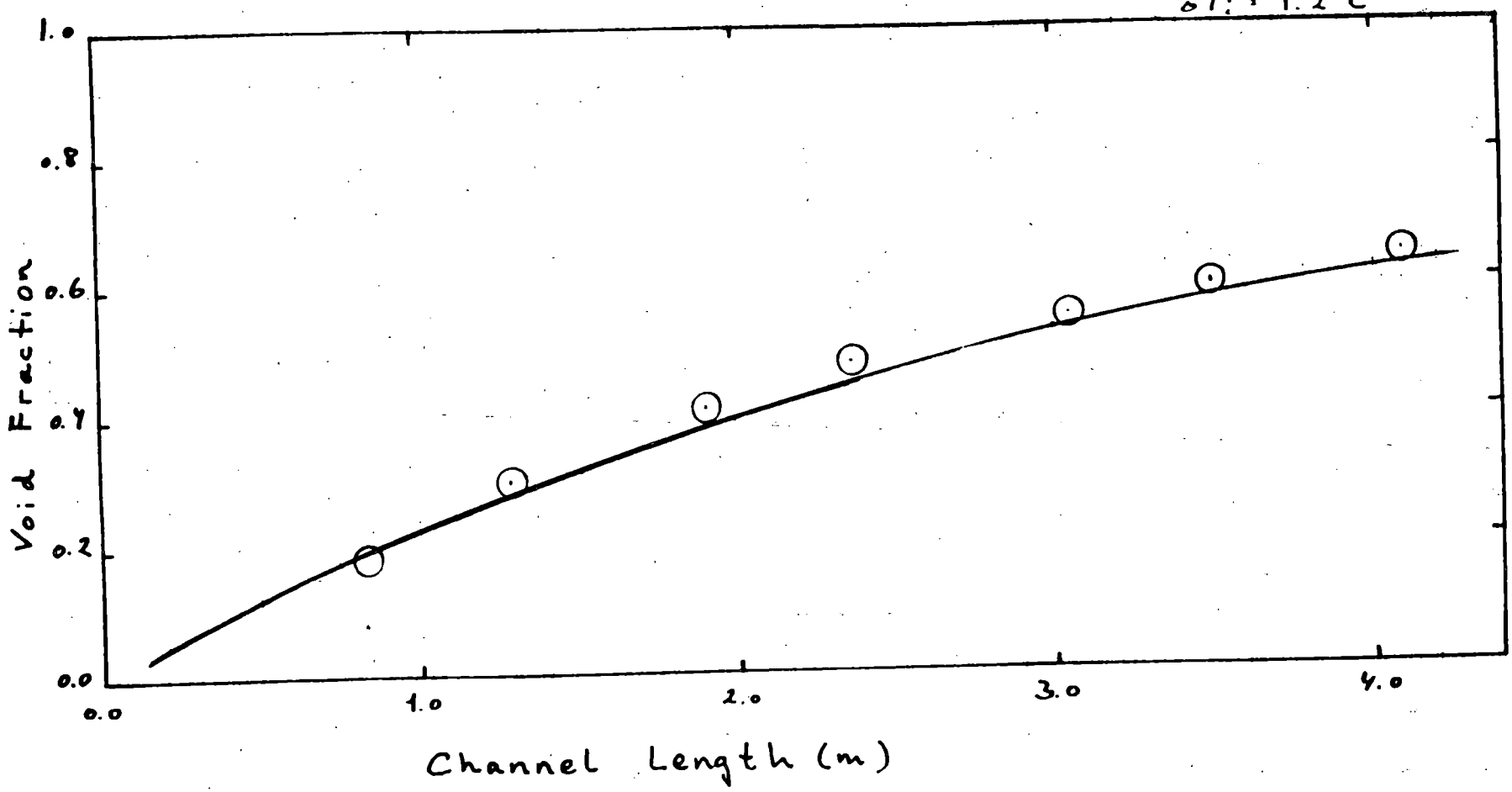

FRIGG 613118

P = 5.00 MPa

Q = 4.516 MW

G = 1018 kg/m²s

$\overline{oT_i}$ = 26.6°C

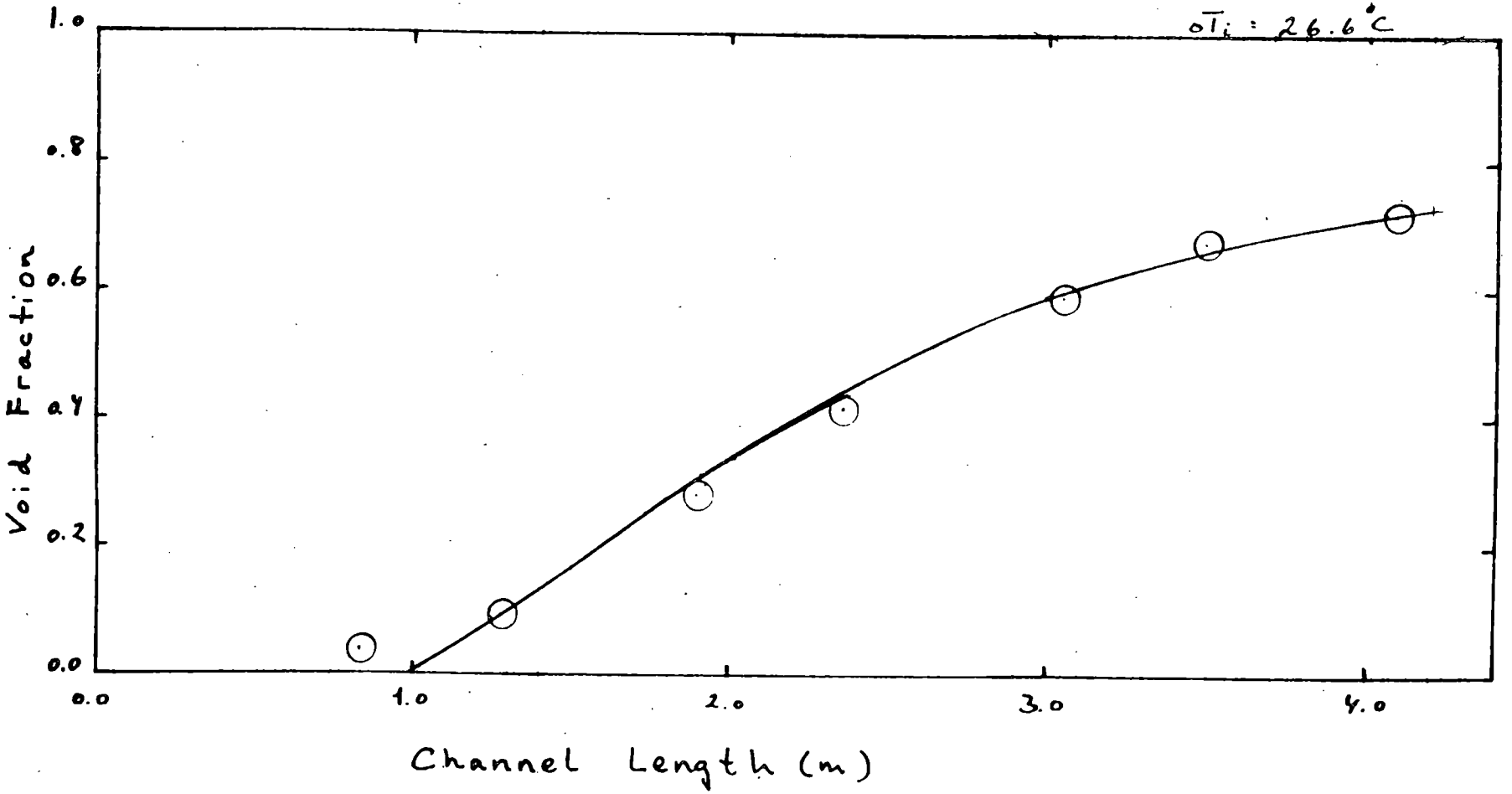

BWR TRAC PRELIMINARY ASSESSMENT

OBJECTIVES:

- Provide Broad Basis Challenge Models
- Provide Timely Feedback to Final Version

SEPARATE EFFECTS TEST:

- Vessel Blowdown
- Single Heated Bundle Tests
- ORNL Single Channel Test
- Two Loop Test Apparatus (TLTA) Separate Effects Tests
- ATLAS Transient CHF

INTEGRAL SYSTEM EFFECTS TESTS:

- Single Heated Bundle System Effects
- TLTA Integral System
- ROSA-III
- 30° - Steam Sector Test Facility (SSTF).

JGM Andersen
October 1981

I. FACILITY DESCRIPTION

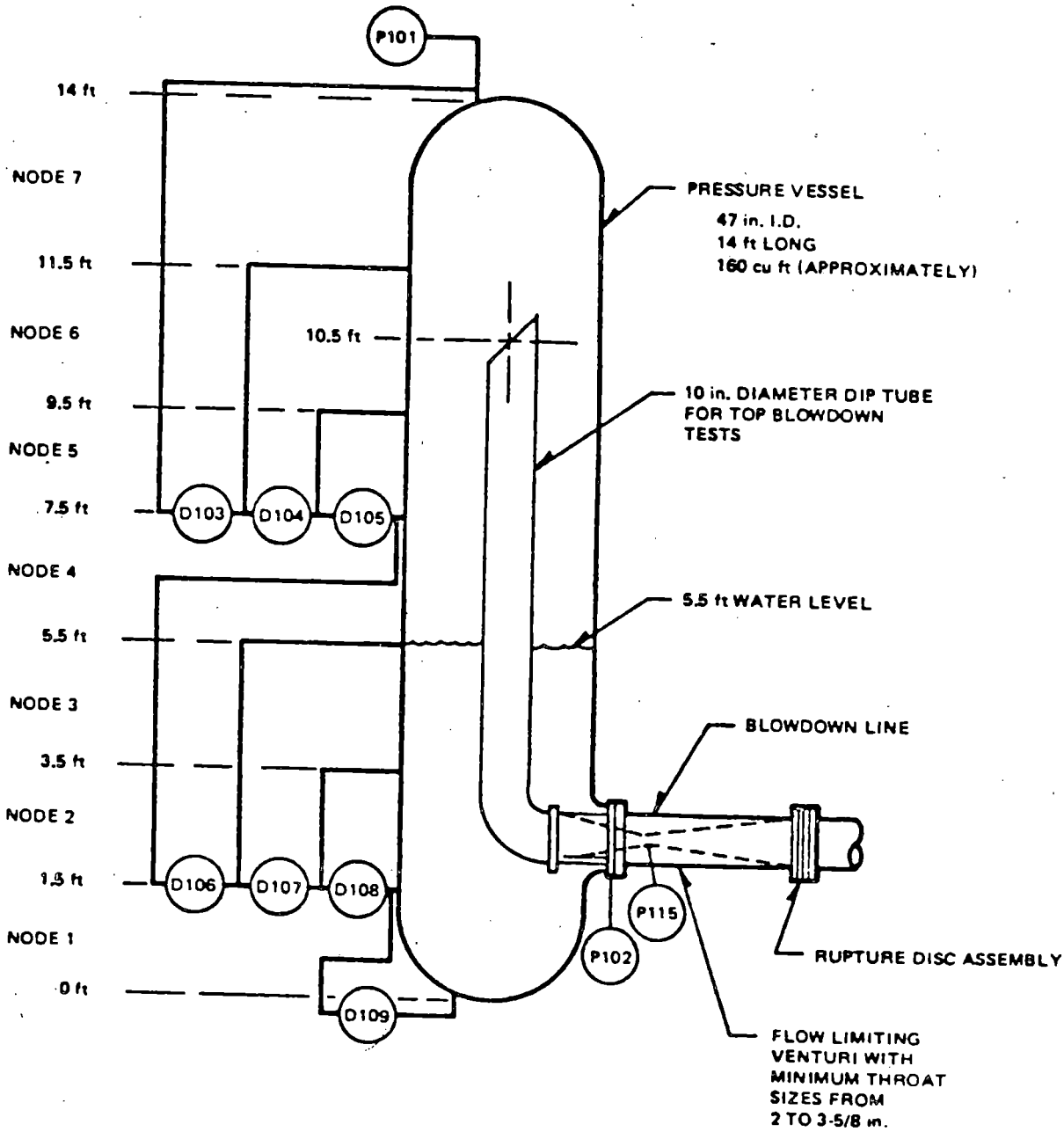

LARGE BLOWDOWN VESSEL
(PSTF)

JES-1
8-28-81

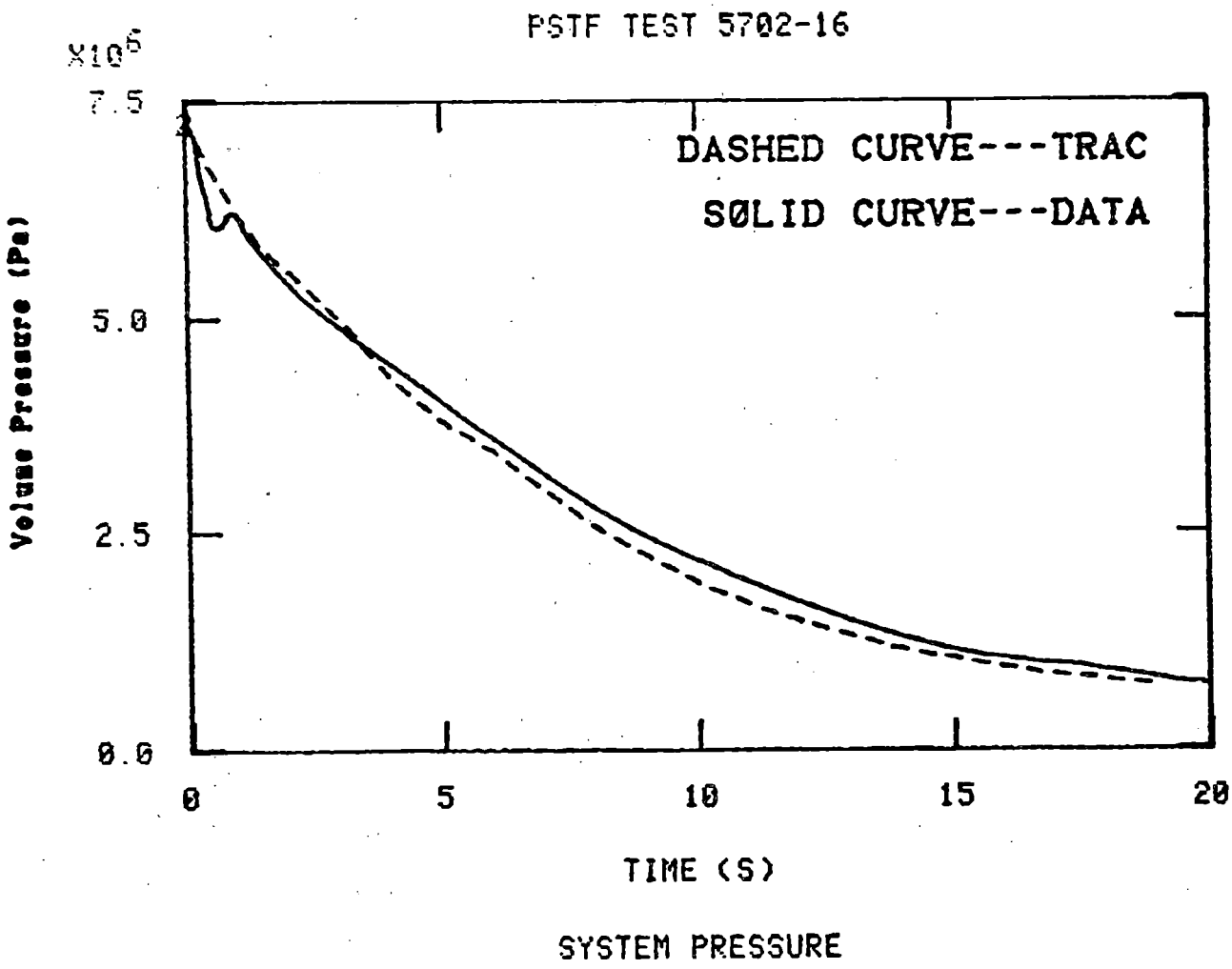
PSTF TEST 5702-16
X10^6
7.5
5.0
2.5
0.0
Volume Pressure (Pa)
DASHED CURVE---TRAC
SØLID CURVE---DATA
0
5
10
15
20
TIME (S)
SYSTEM PRESSURE

JES-12
8/28/81

PSTF TEST 5702-16

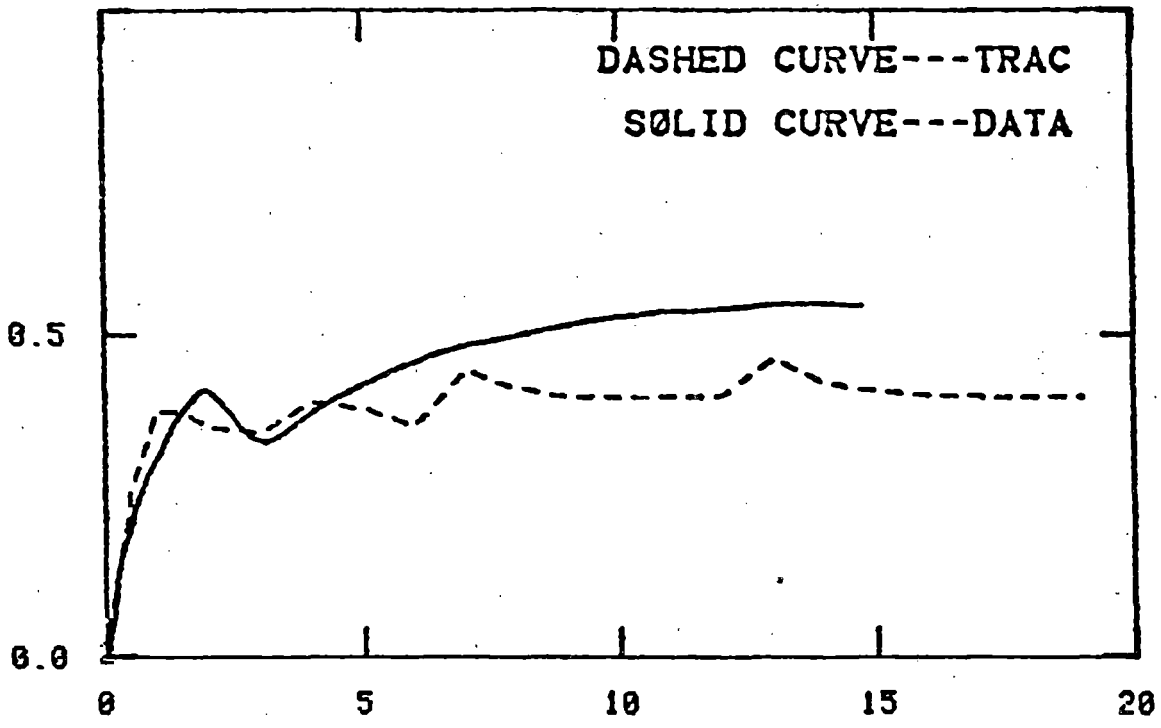

VOID FRACTION
ALPHA 1

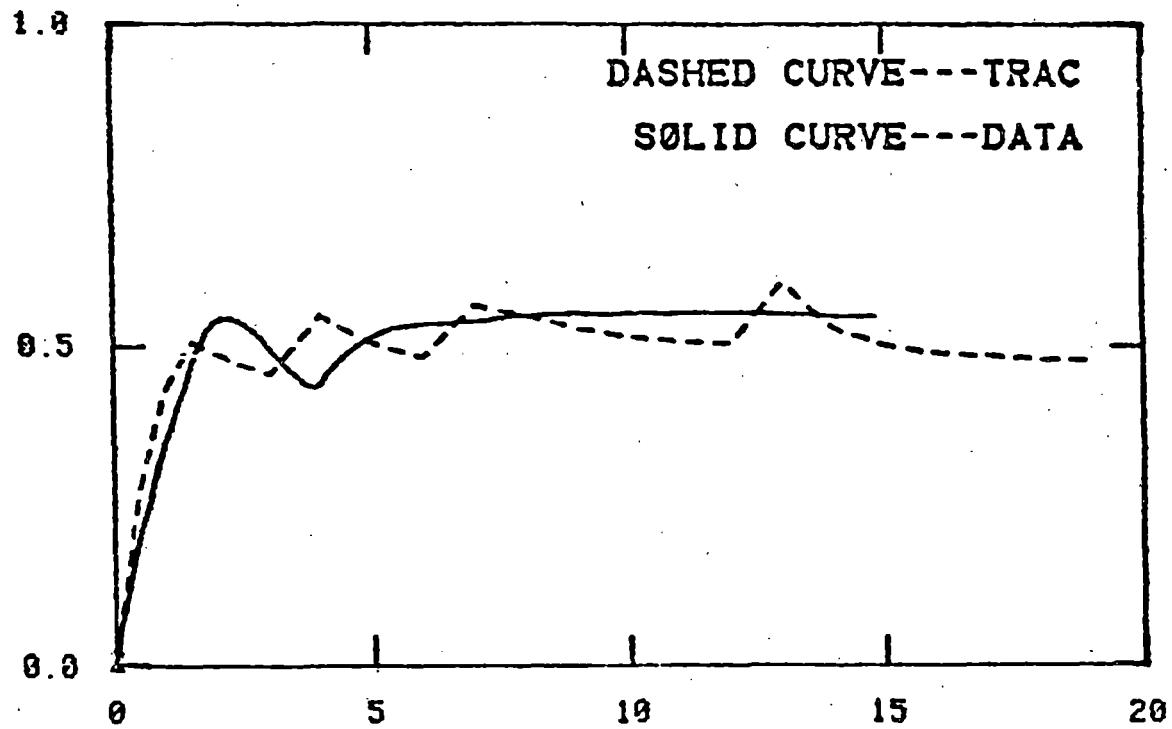

JES-13
8-28-81

VOID FRACTION
ALPHA 2

PSTF TEST 5702-16

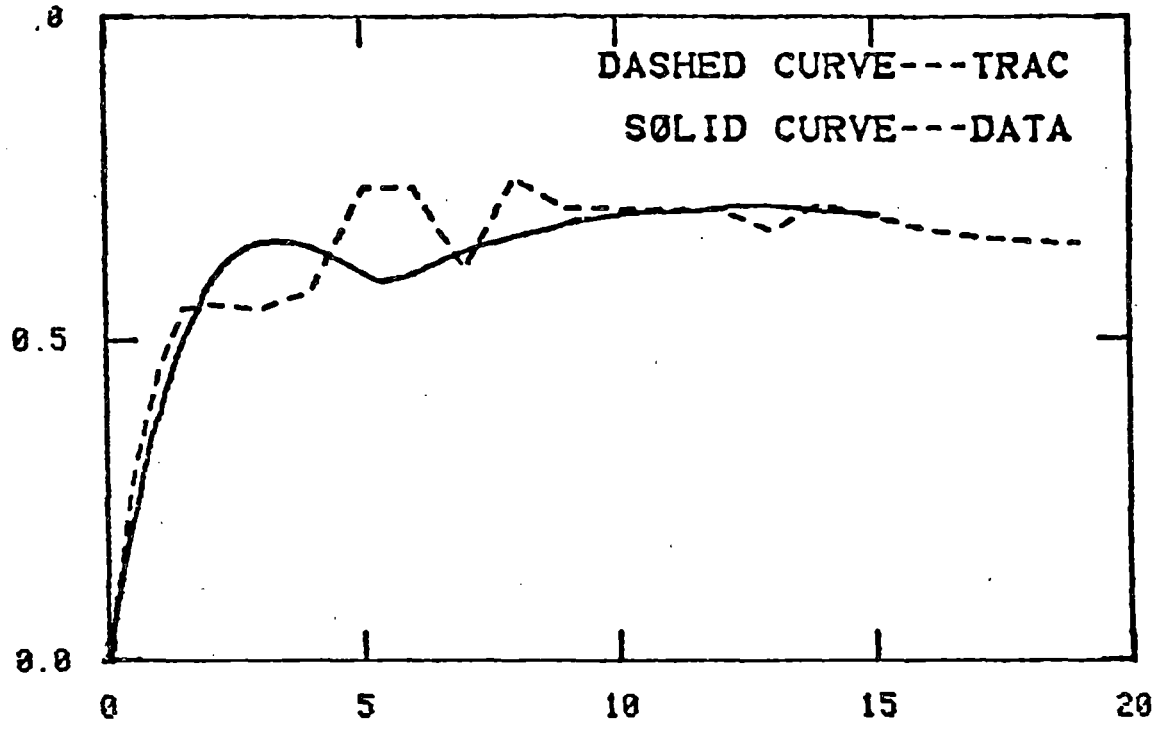

VOID FRACTION
ALPHA 3

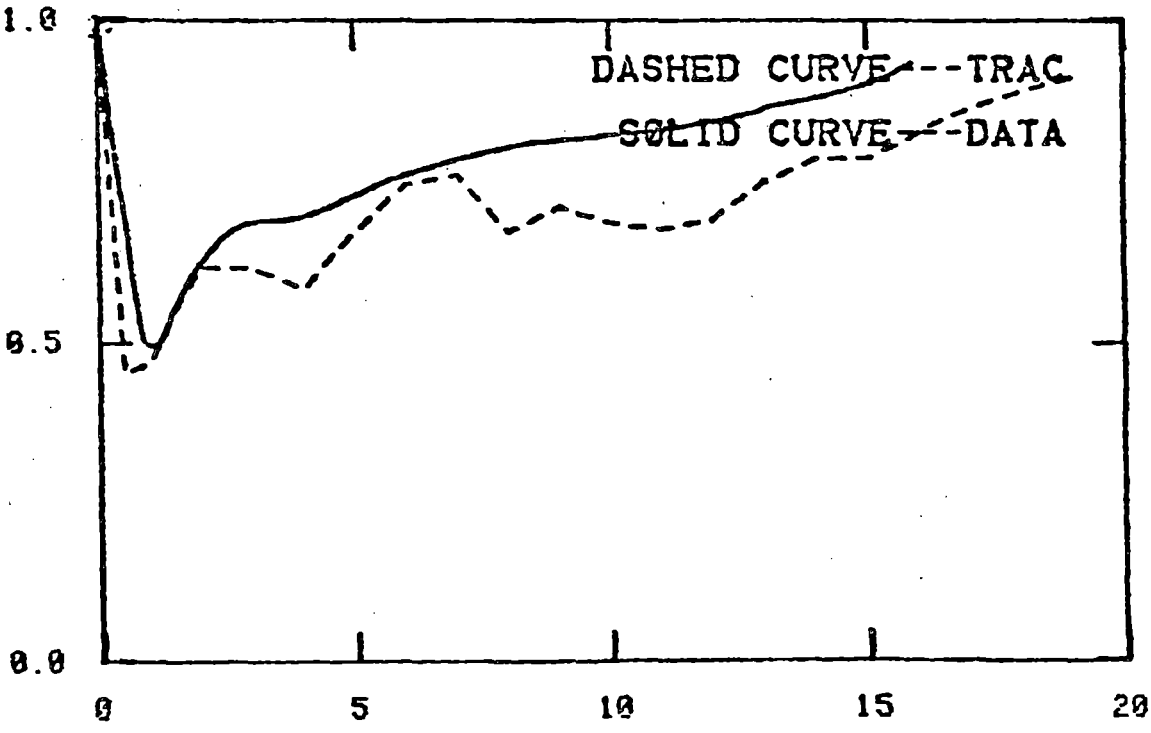

JES-14
8-28-81

VOID FRACTION

PSTF TEST 5702-16

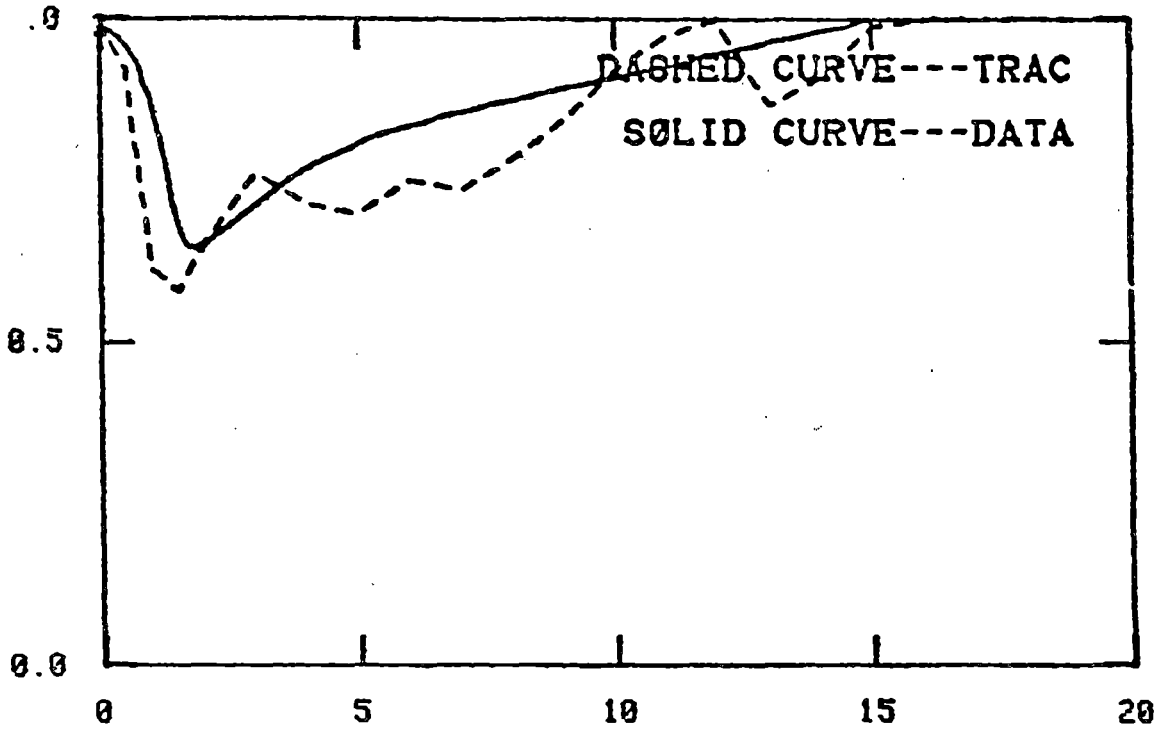

TIME (S)

VOID FRACTION
ALPHA 5

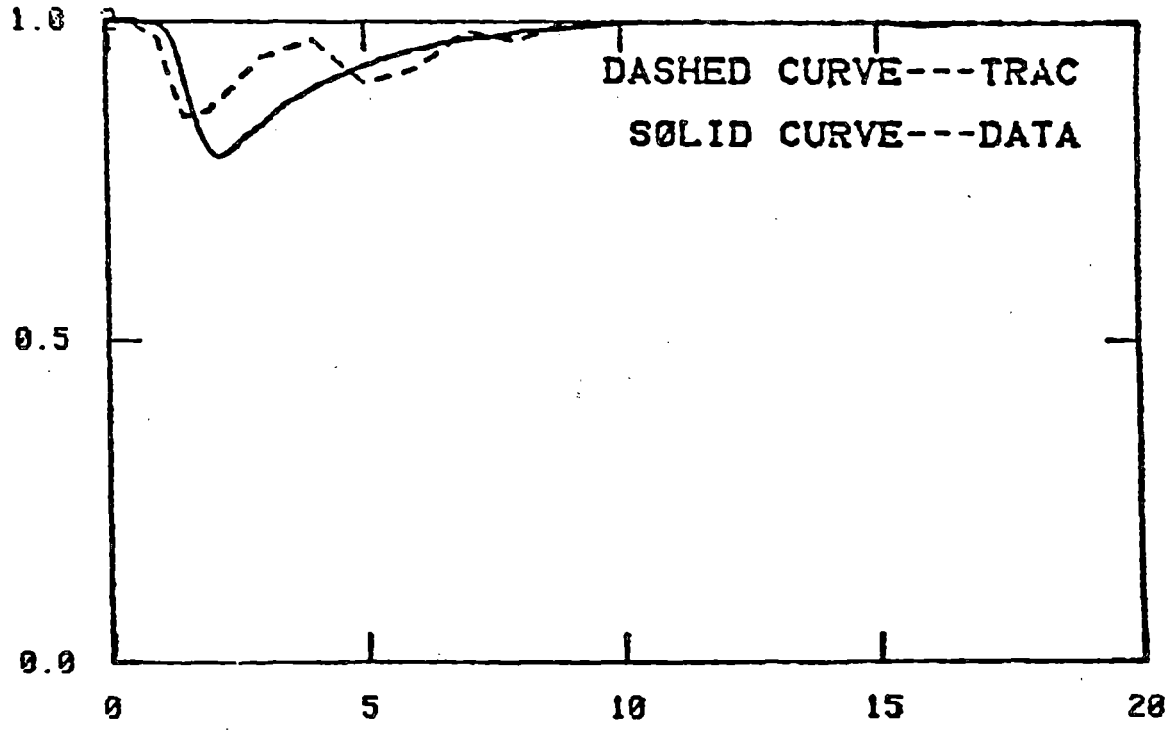

TIME (S)

JES-15
8-28-81

VOID FRACTION
ALPHA 6

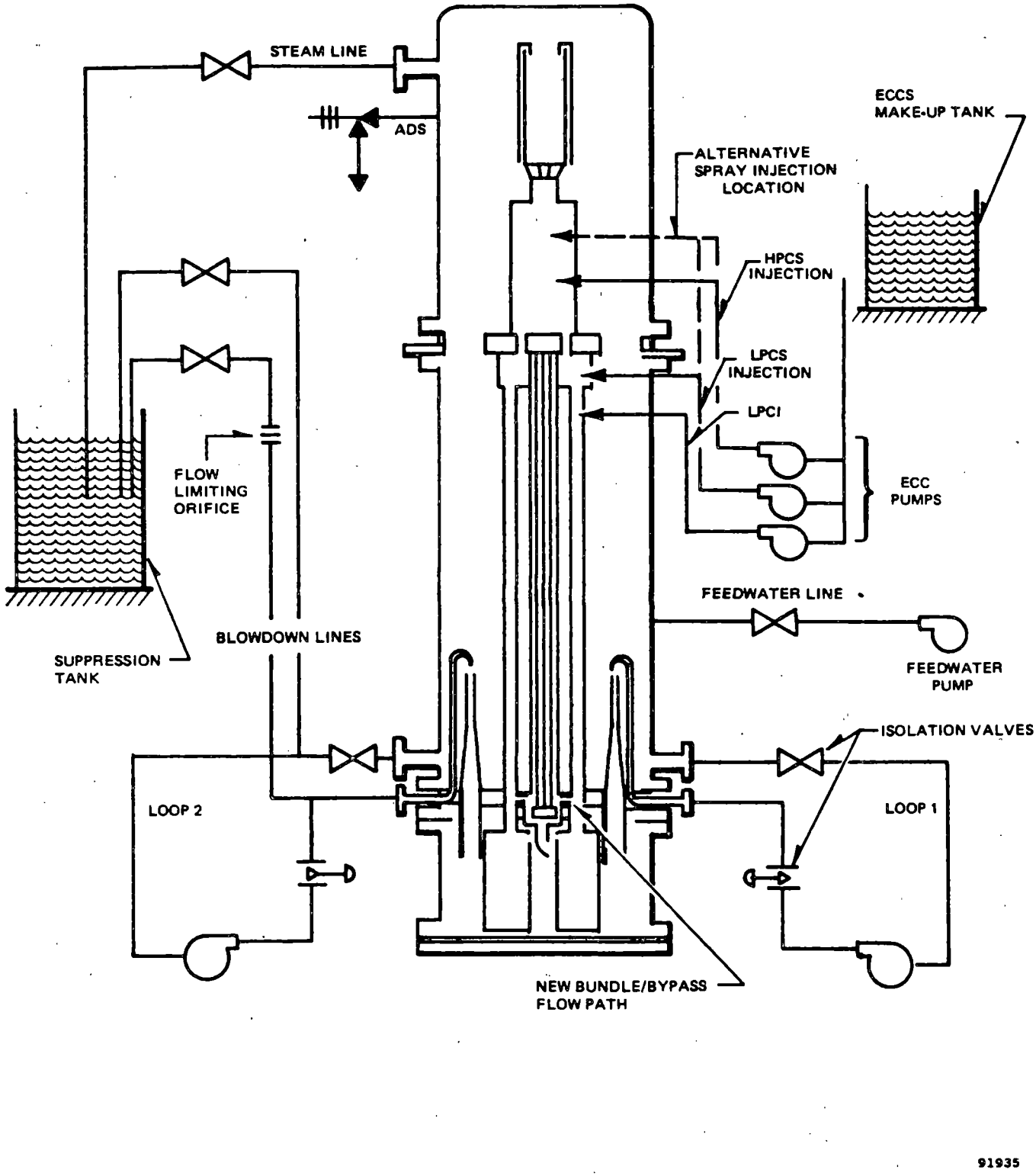

Figure C-1. Two-Loop Test Apparatus Configuration 5A (TLTA-5A) with Emergency Core Cooling Systems

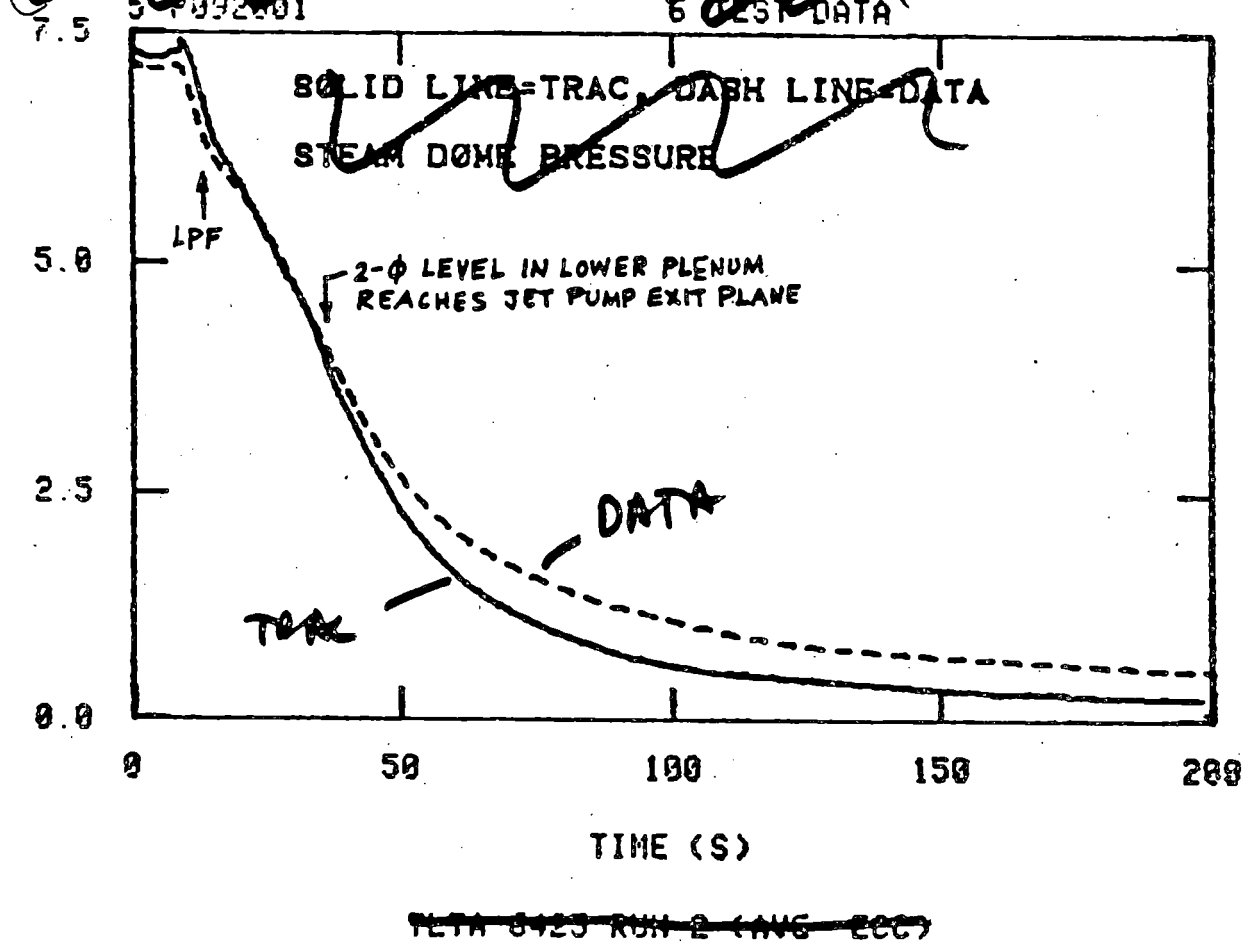
7.5
5.0
2.5
0.0
0
50
100
150
200
SOLID LINE-TRAC, DASH LINE-DATA
STEAM DOME PRESSURE
LPF
2-φ LEVEL IN LOWER PLENUM
REACHES JET PUMP EXIT PLANE
DATA
TRAC
TIME (S)

MDA-2
8/28/81

BYPASS RESPONSE

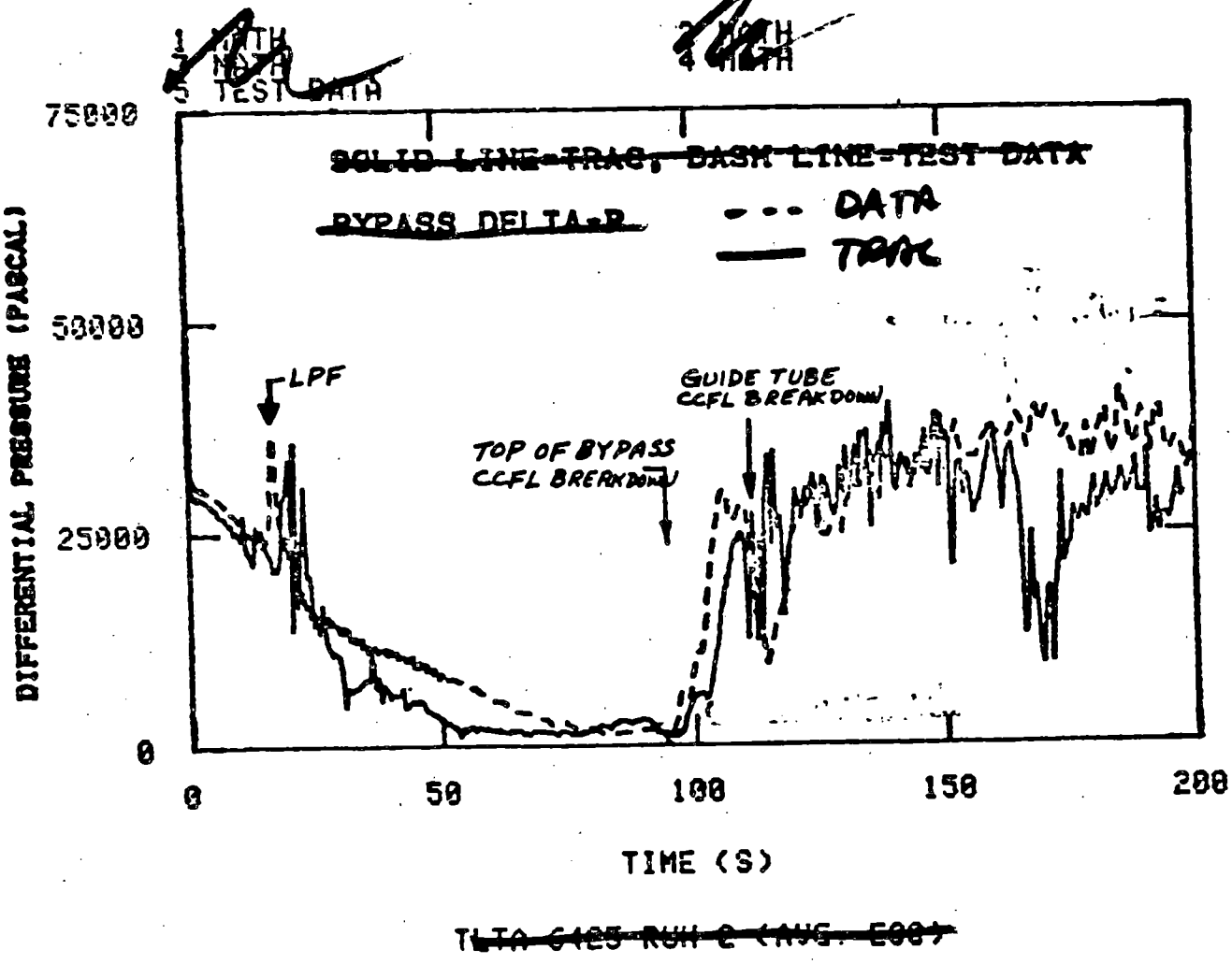

TLTA 6405 RUN 2 (AVG. E00)

MDA-6
8/28/81

CORE RESPONSE

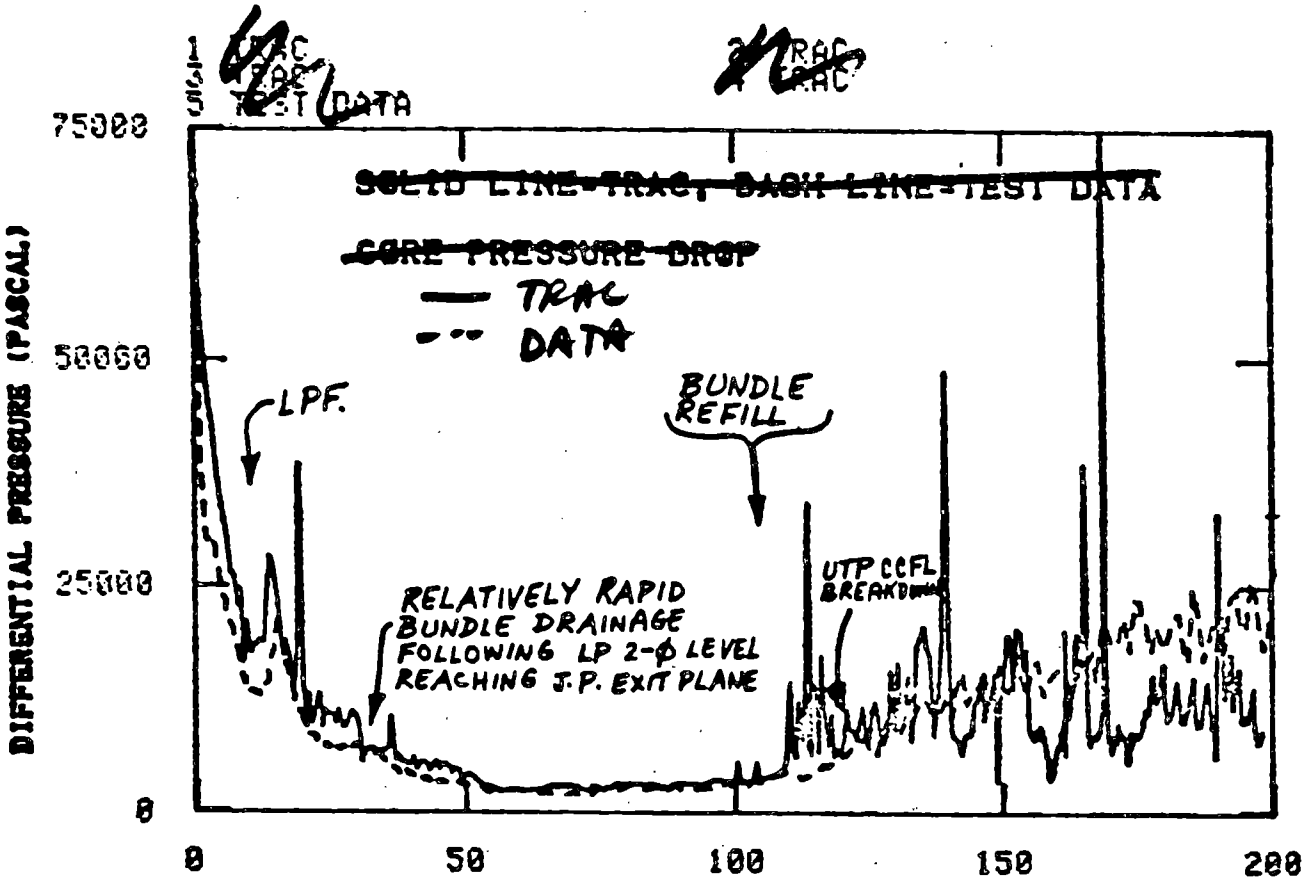

TLTA 6425 RUN 2 (AVG. ECC)

MDA-5
8/28/81

BD/ECC1A 5.05MW TLTA5A

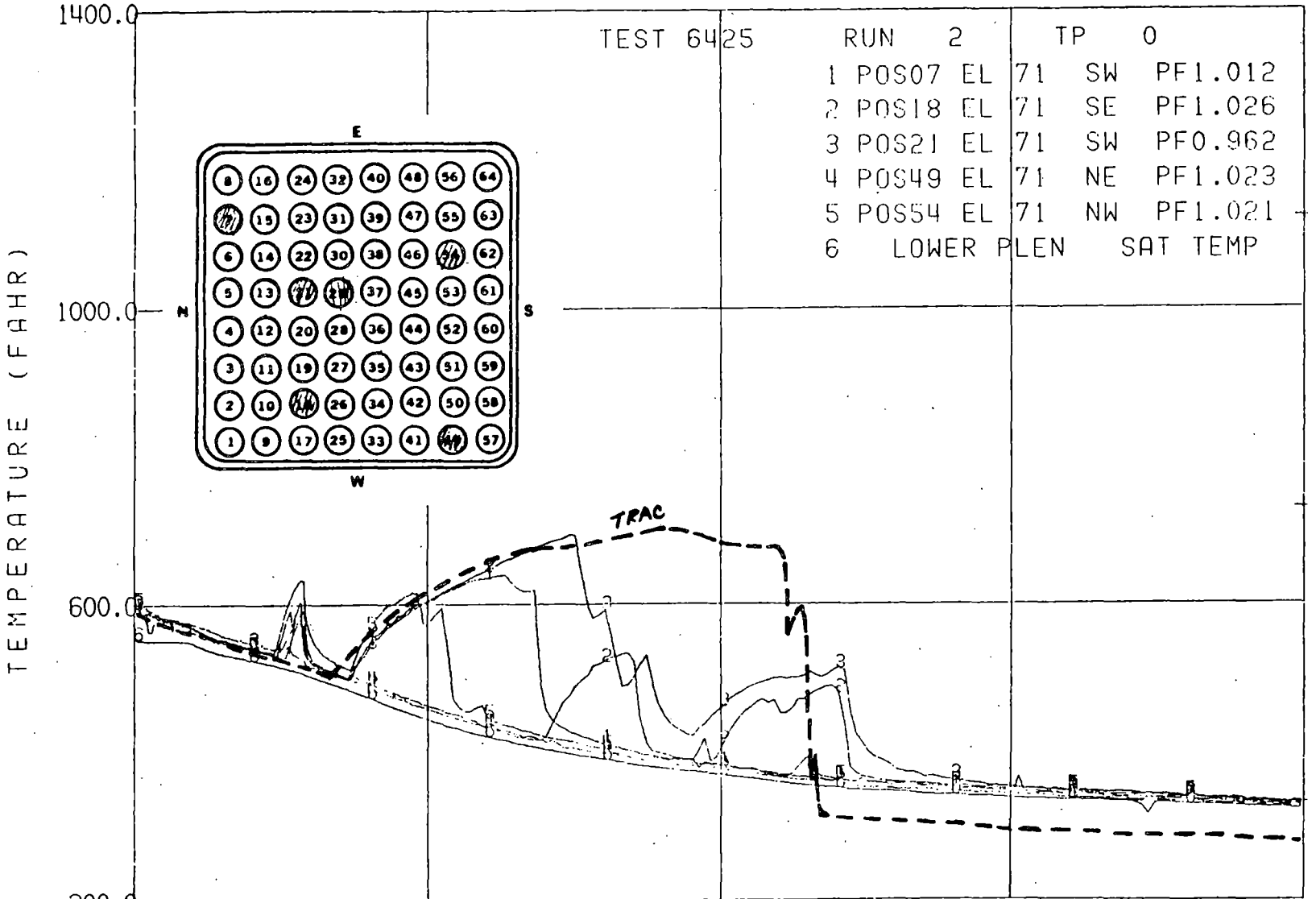

GRID 14 CL

SER: ECC-TI
DATE: 04/29/81
TIME: 12:06Z

TRAC BWR SIMULATION

OBJECTIVE:

DEMONSTRATE THE TRAC CAPABILITY

TRANSIENT:

BWR/6 218 PLANT DBA

NODALIZATION:

VESSEL	10 AXIAL LEVELS
	4 RADIAL RINGS
	2 θ SECTORS

TOTAL NUMBER OF COMPONENTS = 52

JGM ANDERSEN

OCTOBER 1981

BWR NODALIZATION

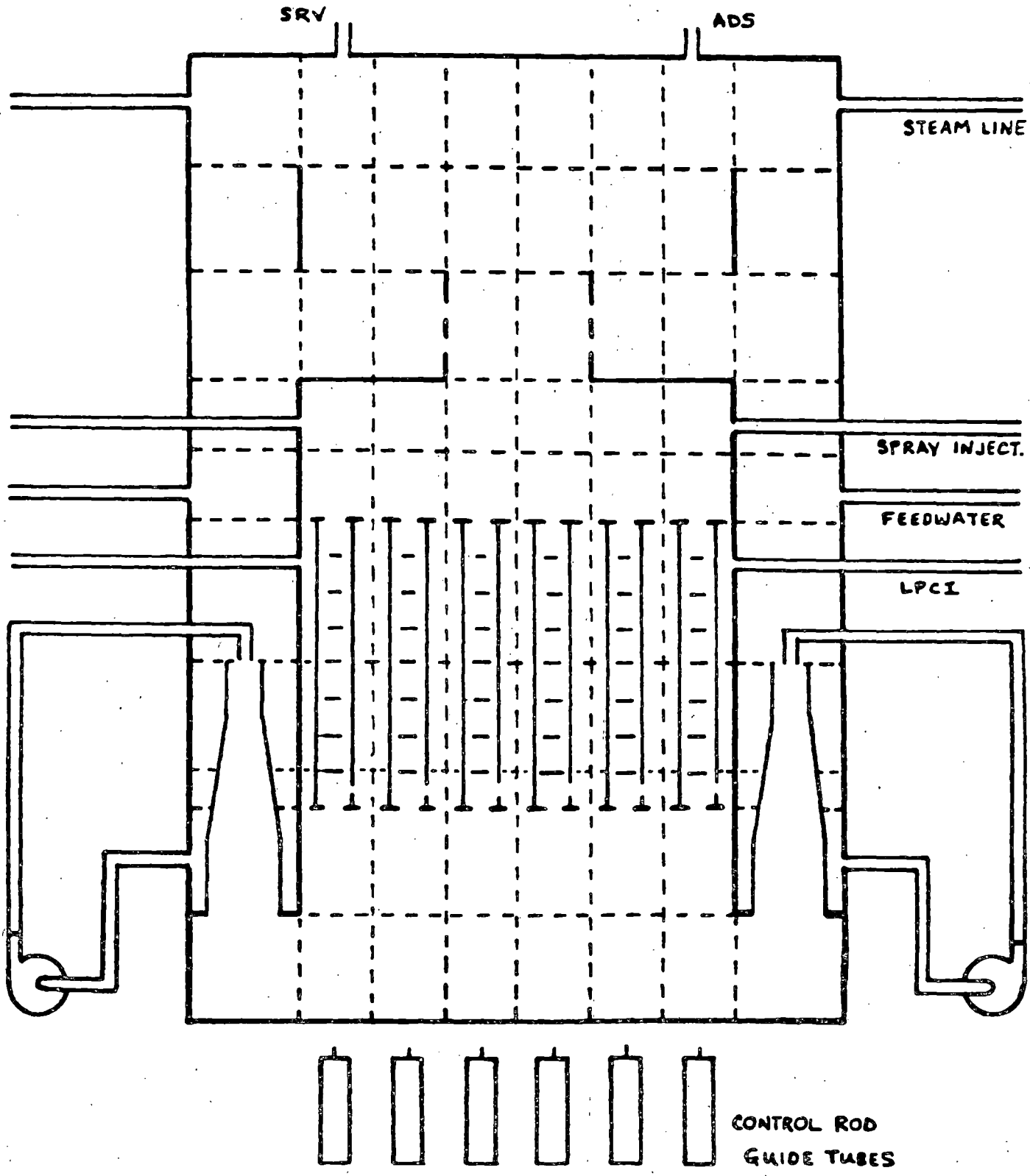

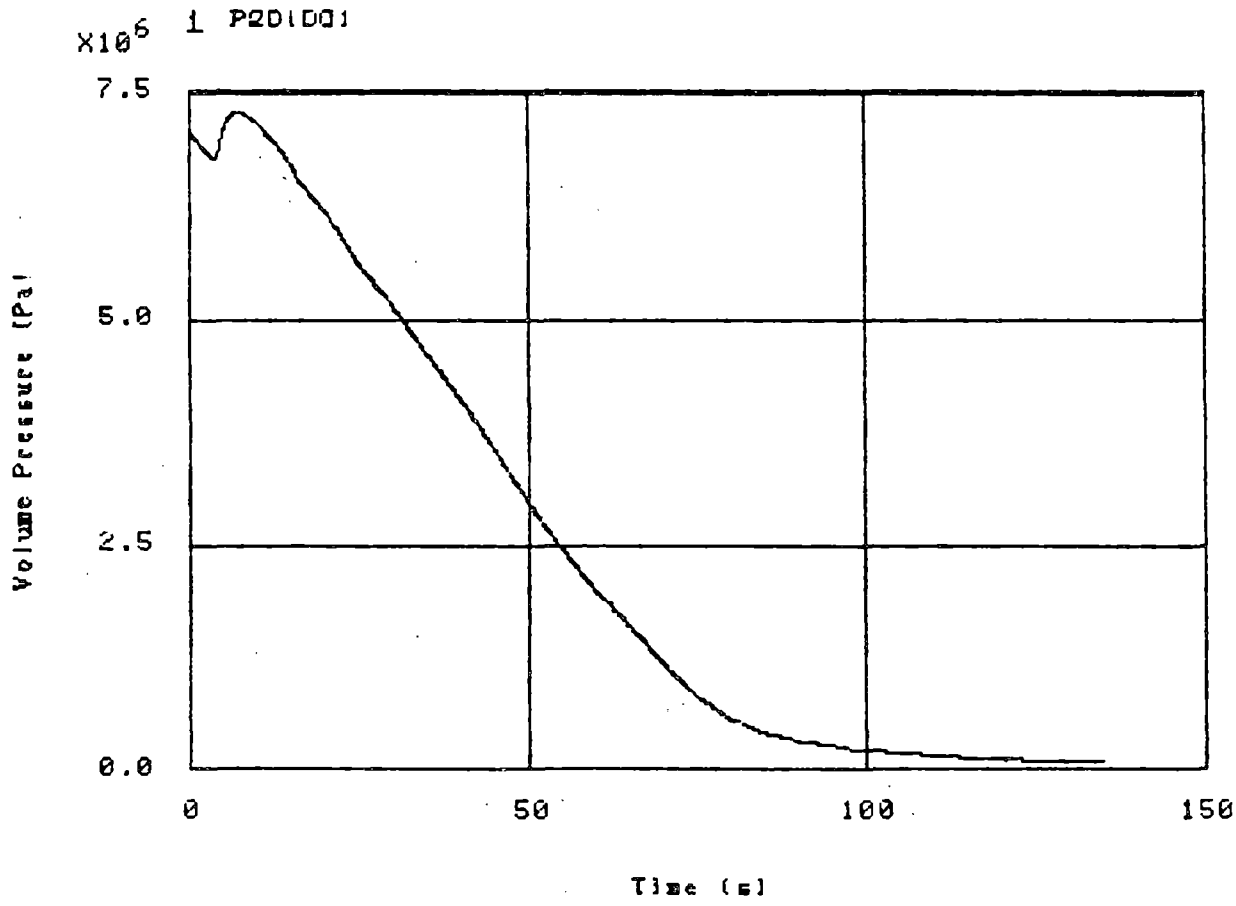
1 P2D1D01
X10^6
7.5
5.0
2.5
0.0
Volume Pressure (Pa)
0
50
100
150
Time (s)

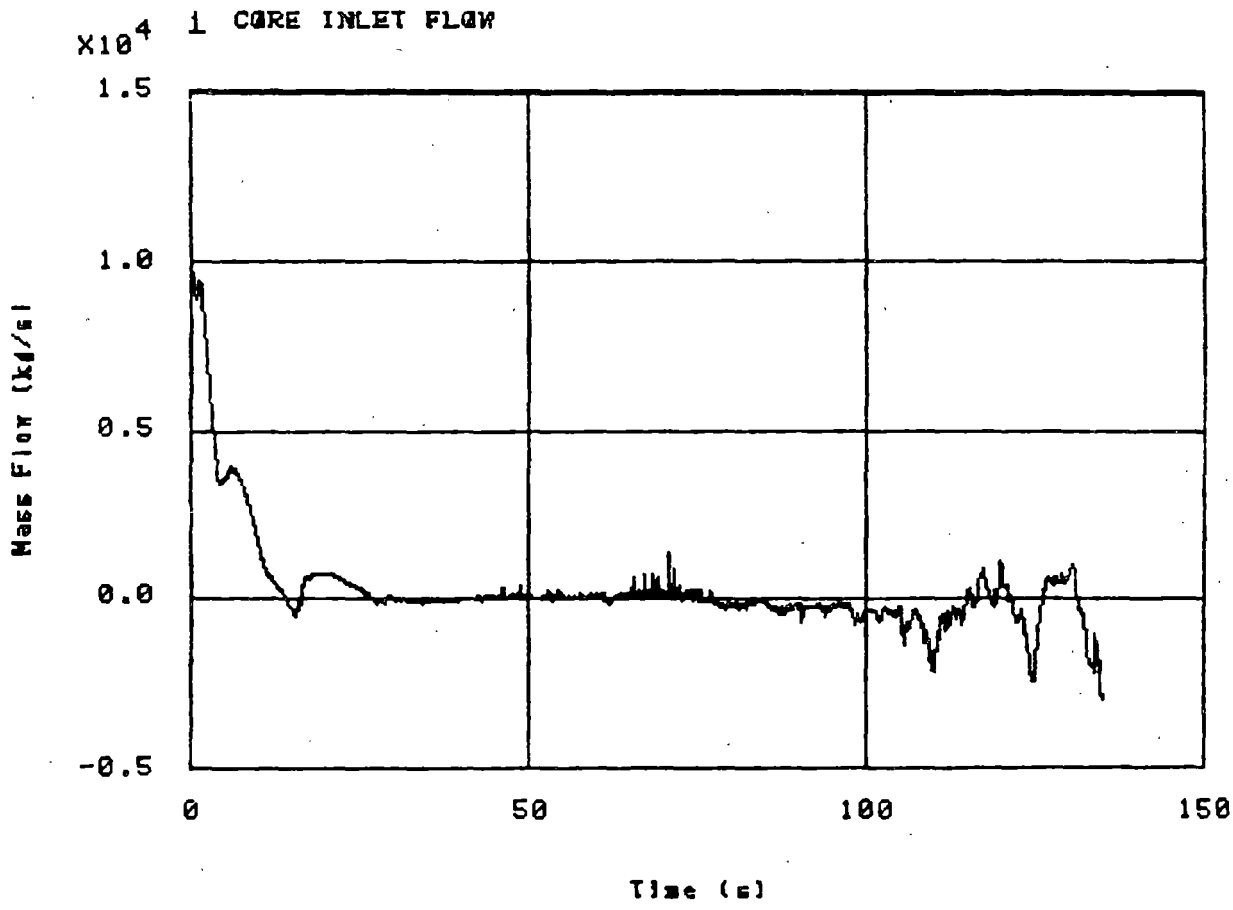
1 CORE INLET FLOW
X10^4
1.5
1.0
0.5
0.0
-0.5
Mass Flow (kg/s)
0
50
100
150
Time (s)

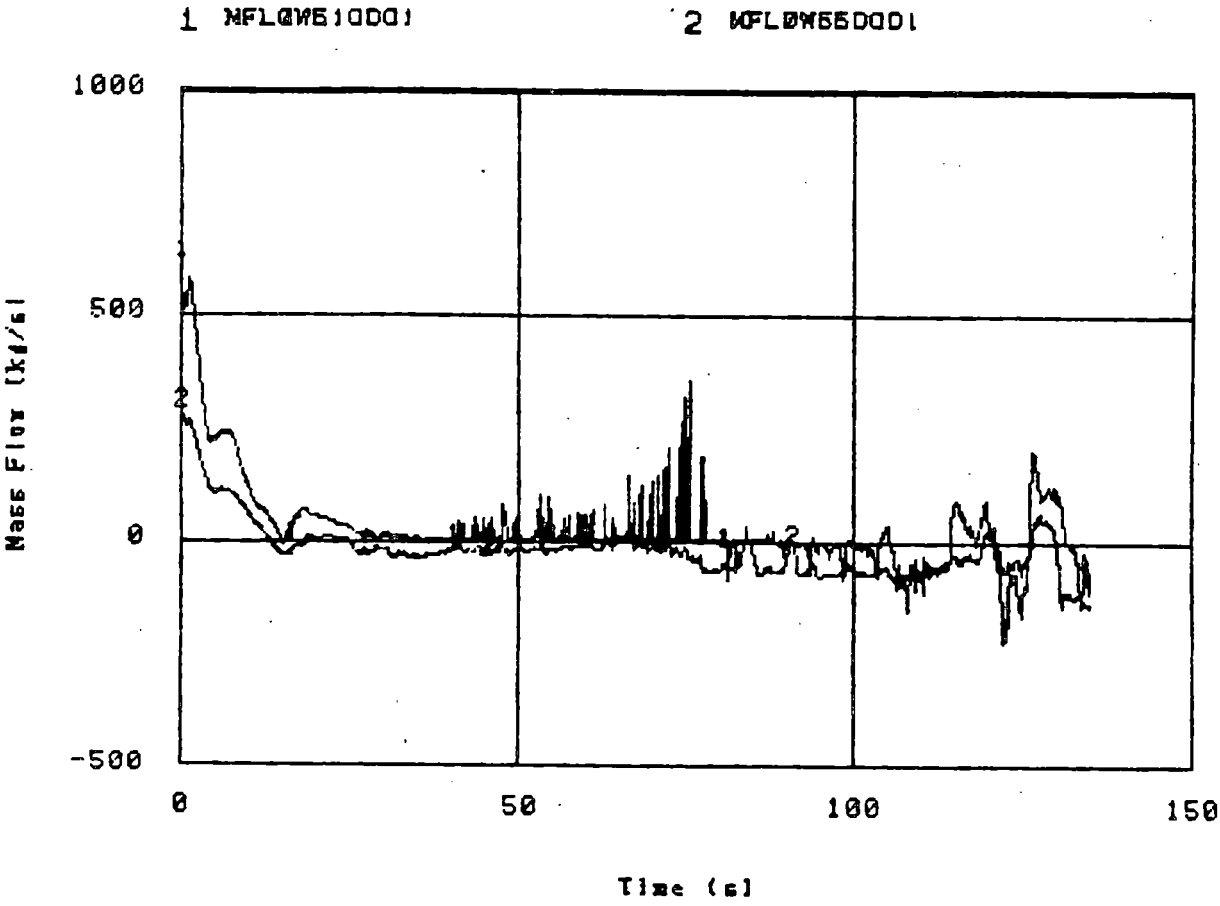
1 MFLOW610001
2 MFLOW650001
1000
500
0
-500
0
50
100
150
Mass Flow (kg/s)
Time (s)

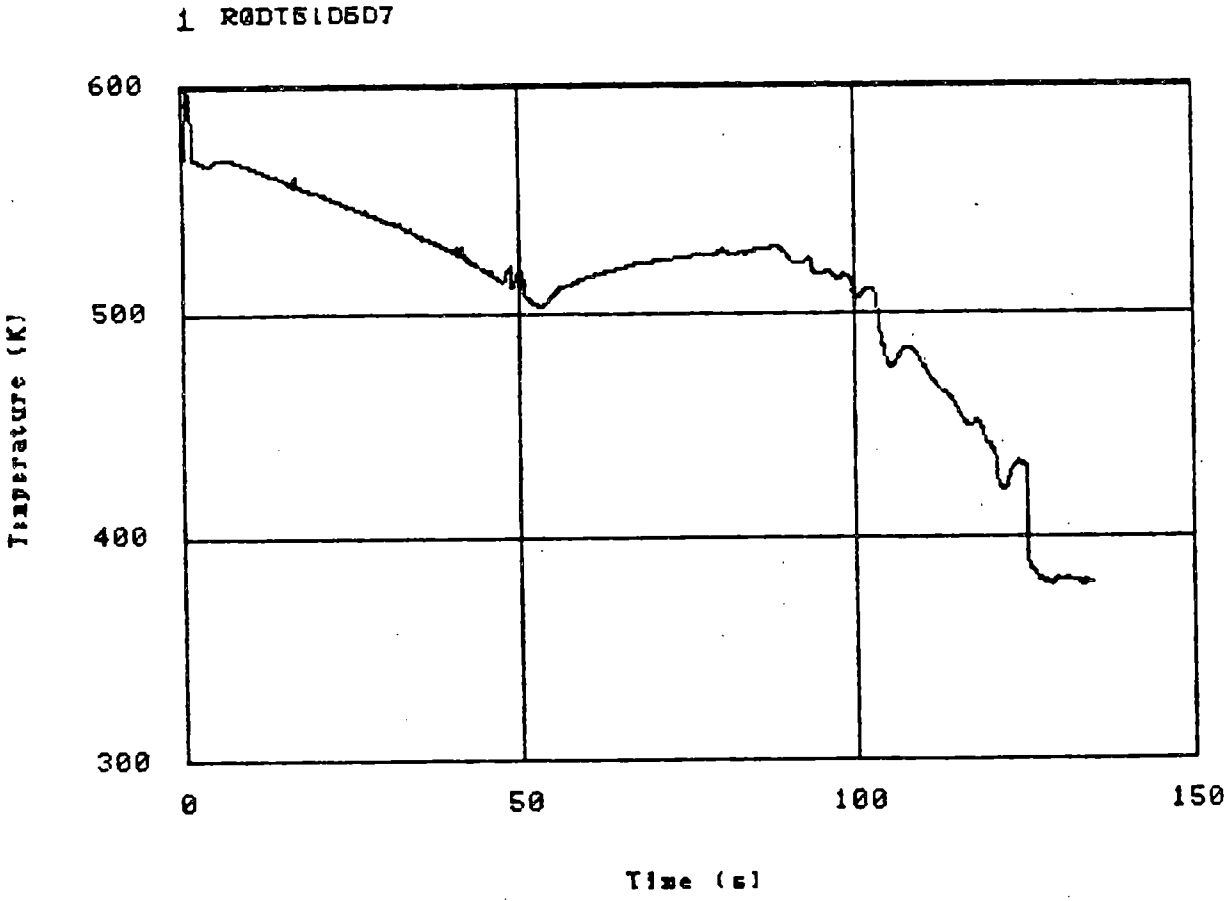
1 R0DT51D5D7
600
500
400
300
0
50
100
150
Temperature (K)
Time (s)

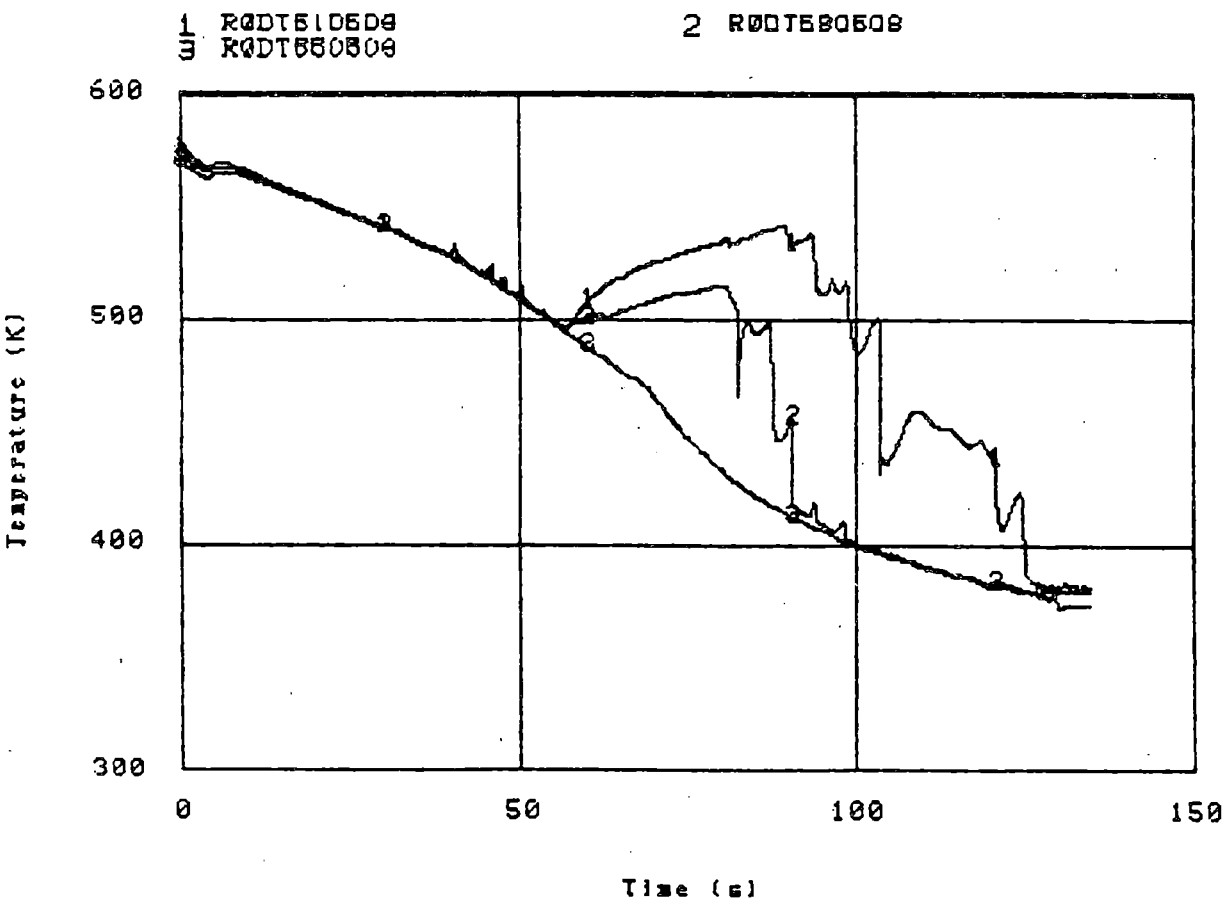
1 R0DT61D6D0
3 R0DT660B08
2 R0DT680B08
600
500
400
300
0
50
100
150
Temperature (K)
Time (s)

CONCLUSION

- ALL MAJOR BWR PHENOMENA CAPTURED.

- A BWR LOCA HAS A PCT LESS THAN 1000°F.

TRAC-BWR HEAT TRANSFER

R. E. Phillips and R. W. Shumway

Presented at

The Ninth Water Reactor Safety Research

Information Meeting

October 26 - 30, 1981

Gaithersburg, Maryland

Idaho National Engineering Laboratory

Idaho Falls, Idaho 83415

EG&G Idaho

Idaho Falls, Idaho 83415

TRAC-BWR HEAT TRANSFER

R. E. Phillips and R. W. Shumway
EG&G Idaho, Inc.

In an effort to understand the consequences of nonstandard operating events which may possibly occur in a boiling water reactor (BWR), the Idaho National Engineering Laboratory is developing the best estimate BWR system analysis program, TRAC-BWR.[1] The general aspects of this development are reported in a companion paper presented at this meeting.[2] One of the most important aspects of this best estimate capability is the prediction of heat transfer between the nuclear fuel rods and the reactor coolant. Several authors[3,4,5] have reviewed heat transfer packages used for the analysis of transients in pressurized water reactors (PWR). The purpose of the TRAC-BWR heat transfer projects is to develop a best estimate heat transfer package for use in the TRAC-BD1 code and to assess the applicability of the package for the prediction of BWR transients. The heat transfer package will be developed within the framework of TRAC-BWR; the specific product will be coding and subroutines containing best estimate correlations for the TRAC-BWR code, which may be used in evaluating operating procedures in license applications and will supply information needed for accident management.

Model Development and Implementation. The TRAC-PD2[6] heat transfer correlation package was used as the starting point for developing the TRAC-BWR heat transfer package. Modifications to the TRAC-PD2 heat transfer package to make it applicable for BWR analysis were the addition of a radiation heat transfer model,[7] inclusion of a critical quality-boiling length correlation for the departure from nucleate boiling,[8] addition of a subcooled boiling model, and the reintroduction of the modified Zuber critical heat flux correlation for low flow conditions.[9] In addition to these changes, the film boiling correlation[10] was simplified and smoothed.

Results of analyses using these improvements are demonstrated both in this paper and in the respective references. As the assessment of the current heat transfer package proceeds, additional modifications will be made as necessary.

Developmental Assessment. The assessment of the heat transfer package is an important second step in the development process that serves two fundamental purposes: to provide insight into model development needs in ranges of interest to BWR transient analysis and to quantify the model's quality of prediction. The assessment methodology consists of the two phases described below.

Quantitative Assessment. The first phase of assessment consists of comparing TRAC-BD1 calculations with existing steady state[11-14] and transient experiments[15-21] for tubes, square channels, annuli, and rod bundles. This phase serves two fundamental purposes. The first is to assess the quality of predictions with respect to these separate effects experiments.

The second and perhaps most important phase deals with the general accuracy of the total heat transfer package. In this phase, the results of comparisons with the transient experimental results will be used. In this case, however, the parameters to be compared will represent areas of concern in reactor safety analysis. Some examples are: time to CHF, time to rewet, clad temperature rise, time at temperature, and time to temperature turnaround. Accurate prediction of these types of parameters do not rely solely on one heat transfer regime's accuracy but rather the ability of the integrated results from many regimes as well as the transition between regimes.

Qualitative Assessment. The second phase of assessment is provided by sensitivity studies on typical BWR full-scale transients.

The focus of the sensitivity studies is limited exclusively to the effects of heat transfer uncertainty on full-scale BWR transient predictive capability. To test the general package, typical full-scale transient calculations will be performed applying the uncertainty bands developed in the quantitative assessment. For BWR/6 large and small break LOCAs and MSIV closure ATWS transients, the following acceptance criteria will be applied to the results: heat transfer uncertainties must not change (a) predicted peak clad temperature more than 10%, (b) predicted time-to-peak clad temperature more than 20%, and (c) predicted ZrO_2 thickness more than 20%. These criteria, although empirically derived, will provide a simple, yet quantitative measure of the estimation capability of the heat transfer package.

Summary and Conclusions. The TRAC-BWR heat transfer task is aimed at providing best estimate heat transfer capability for BWR transient analysis. The first phase is developmental improvement of the existing package. The results described in this presentation demonstrate the dramatic improvements provided to date. The second phase is assessment of the package. The outline provided here gives an overview of the approach which has been derived. The combination of these steps will provide a best estimate heat transfer package to which meaningful quantitative assessment criteria have been applied.

REFERENCES

1. J. W. Spore et al., TRAC-BD1 User's Manual, NUREG/CR-2178, 1981.
2. W. L. Weaver et al., "TRAC-BWR Transient Reactor Analysis Codes for Boiling Water Reactors, Ninth Water Reactor Safety Research Information Meeting, Gaithersburg, Maryland, October 26-30, 1981.
3. L. S. Tong, "Heat Transfer in Reactor Safety," Sixth International Heat Transfer Conference, Vol. 6, Toronto, Canada, 1978, pp. 285-309.
4. Y. Y. Hsu and L. H. Sullivan, "1981 Updating of Best Estimate Heat Transfer Package for Transient CHF and Post-CHF Regimes During Blowdown and Reflood Phases," Third CSNI Specialists Meeting on Transient Two-Phase Flow, Pasadena, California, March 23-25, 1981.

5. T. A. Bjornard and P. Griffith, "PWR Blowdown Heat Transfer," Thermal and Hydraulic Aspects of Nuclear Reactor Safety, Vol. 1, New York: American Society of Mechanical Engineers, 1977, pp 17-41.

6. Reactor Safety Analysis Group, TRAC-PD2: A Best Estimate Computer Code for Pressurized Water Reactor Analysis.

7. J. W. Spore, M. M. Giles, R. W. Shumway, "A Best Estimate Radiation Heat Transfer Model Developed for TRAC-BD1," 20th ASME/AIChE National Heat Transfer Conference, Milwaukee, Wisconsin, August 2-5, 1981.

8. R. E. Phillips, R. W. Shumway, K. H. Chu, "Improvements to the Prediction of Boiling Transition in BWR Transient Calculations, 20th ASME/AIChE National Heat Transfer Conference, Milwaukee, Wisconsin, August 2-5, 1981.

9. R. W. Shumway and R. E. Phillips, "TRAC-BWR Heat Transfer," NRC Heat Transfer Workshop, February 1981.

10. J. W. Spore et al., TRAC-BD1 User's Manual, Volume 4 - Developmental Assessment, NUREG/CR-2178, 1981.

11. A. W. Bennett et al., Heat Transfer to Steam-Water Mixtures Flowing in Uniformly Heated Tubes, AERE-R5373, AERE Harwell, 1967.

12. S. Z. Rouhani, Void Measurements in the Region of Subcooled and Low Quality Boiling, Part 2, AE-239, 1966.

13. H. Christensen, Power-to-Void Transfer Function, ANL-6385, 1961.

14. O. Nylund et al., Measurements of Hydrodynamic Characteristics, Instability Thresholds and Burnout Limits for 6-Rod Clusters in Natural and Forced Convection, ASEA Report, 1967.

15. F. F. Cadek et al., PWR FLECHT Final Report, WCAP-7665, Westinghouse Electric Corporation, 1971.

16. S. Wang and L. E. Hochreiter, Analysis of the FLECHT-SEASET Unblocked Bundle Steam Cooling and Boiloff Tests, NUREG/CR-1533, 1981.

17. D. G. Morris et al., A Preliminary Evaluation of Rod Bundle Post-CHF Heat Transfer to High Pressure Water in Transient Upflow, ORNL Interim Report, 1980.

18. D. G. Morris et al., Dispersed Flow Film Boiling of High Pressure Water in a Rod Bundle, ORNL Interim Report, 1981.

19. R. J. Dallman, private communication, EG&G Idaho, Inc., 1981.

20. D. S. Seely and R. Mulralidhran, BWR Low Flow Bundle Uncovery Test, NUREG/CR-2009 (Draft Report, 1981).

21. B. S. Shiralkar et al., Transient Critical Heat Flux Experimental Results, GEAP-13295, General Electric Company Report, 1972.

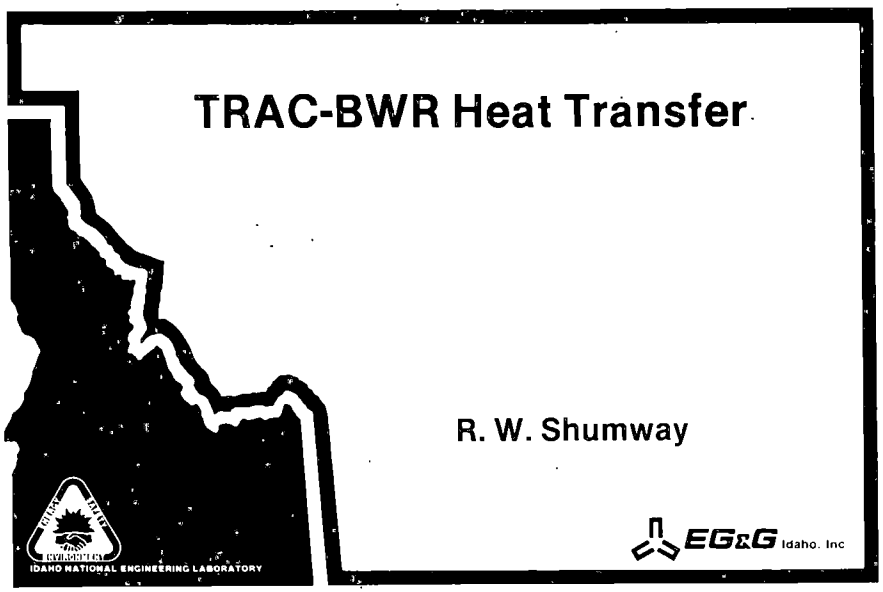

Purpose

- Heat transfer model development and enhancement for use in TRAC-BDI/MOD1 relative to BWR analysis requirements
- Assessment of the TRAC-BD1/MOD1 heat transfer package "Best Estimate" predictive capability during BWR transient analysis

INEL-S-34 602

Assumptions

- Examine only the surface convective heat transfer correlations
- The hydrodynamic solution will not be modified
- The interfacial heat transfer will be modified only relative to improvements in the convective heat transfer package

INEL-S-34 997

Hydraulic Ranges

- Physical parameter ranges of interest to BWR analysis must be identified

INEL-S-34 604

REP-6

BWR6 10% Break Quality vs. Mass Flux

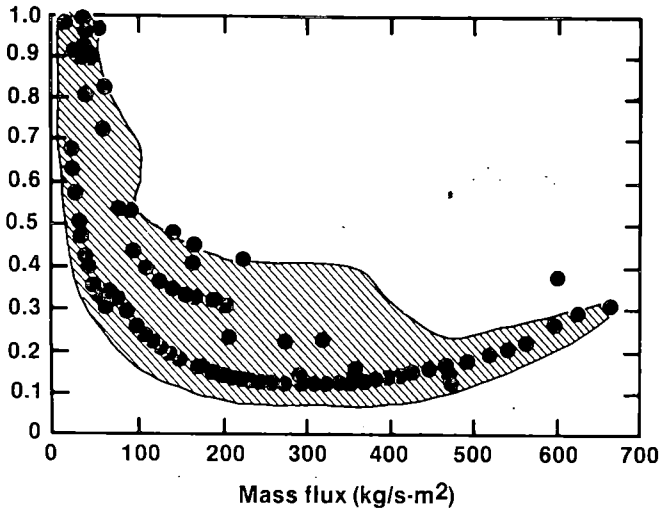

INEL-S-34 601

Developmental Assessment

Assessment methodology

- Quantitative assessment - separate effects
  - Steady state comparisons with experiments
  - Transient comparisons with experiments
- Qualitative assessment
  - System studies using BWR/6 transient predictions
- Develop criteria for acceptance as "Best Estimate"

INEL-S-34 603

Model Development and Enhancement

- Subcooled boiling, improved interfacial condensation model
- Critical quality correlation
- Film boiling, interfacial heat transfer

INEL-S-34 996

Subcooled Boiling

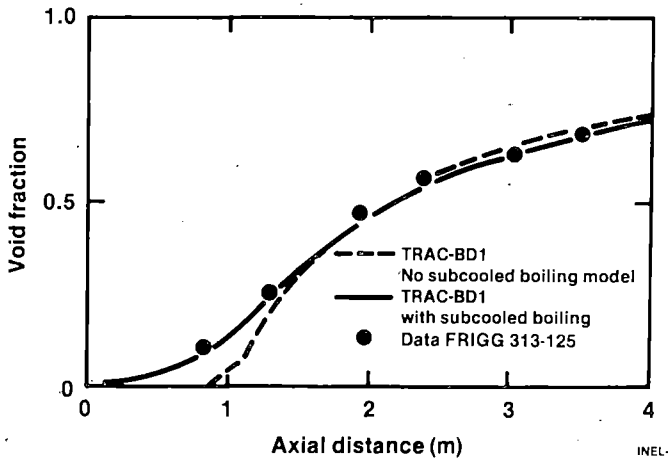

INEL-S-34 600

REP-7

Departure from Nucleate Boiling

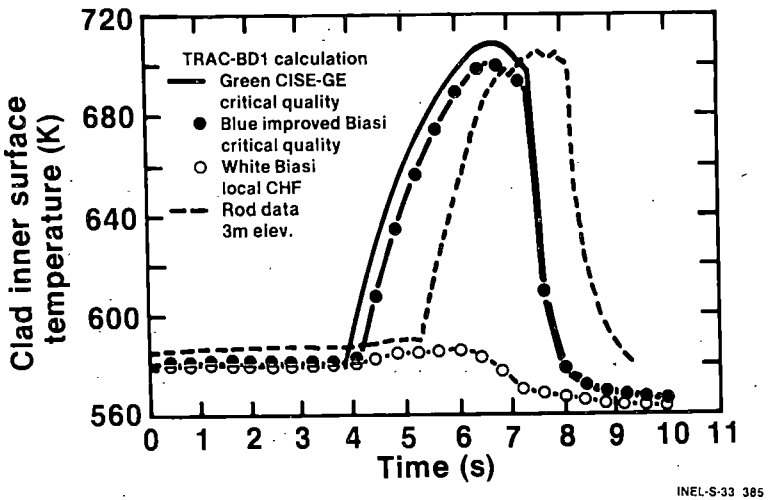

INEL-S-33 385

Quality at DNB

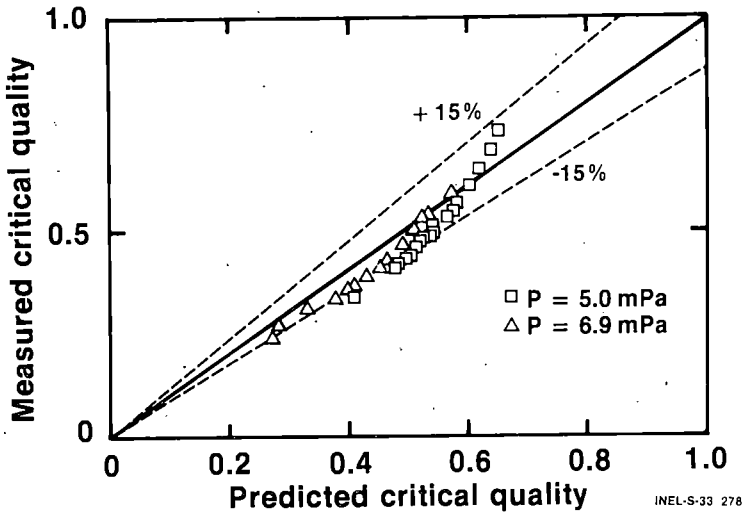

INEL-S-33 278

Film Boiling

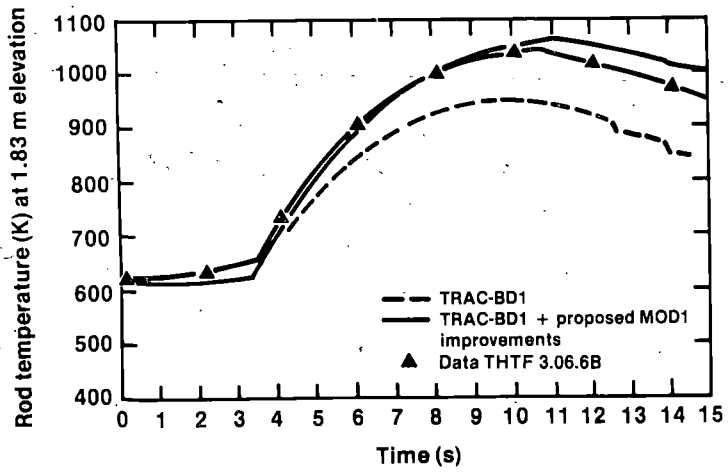

INEL-S-34 998

Acceptance Criteria

- For BWR/6 large and small break LOCA and MSIV closure ATWS transients, heat transfer uncertainties must not change:
  - Predicted peak clad temperature more than 10%
  - Predicted time to peak clad temperature more than 20%
  - Predicted ZrO_2 thickness more than 20%

INEL-S-34 999

Precursory Cooling Effect on the Reflooding of a Hot Vertical Rod

Presented at
The Ninth Water Reactor Safety Research Information Meeting
October 27, 1981
Gaithersburg, Maryland

Y. W. Lee

Korea Advanced Energy Research Institute
P.O. Box 7, Cheong Ryang
Seoul, Korea

Precursory Cooling Effect on the Reflooding of a Hot Vertical Rod

Y. W. Lee
KAERI

Thermal Hydraulic Division in KAERI carried out some basical reflood tests with various test sections since 1978. The objectives of KAERI reflood test activities area

1. Modification and development of a reflood code.
2. To investigate the thermal-hydraulic phenomena during reflood.
3. To obtain basic data for the preparation of 5 x 5 bundle refill/reflood test.

KAERI's reflood test activities are summarized in Fig. 1. KAERI has two reflood test loops; one is 5 rods bundle test loop with which the reflood phenomena for both vertical and horizontal channels were investigated. In horizontal rods bundle test the rods experience the different quench time one another at the same distance from the inlet of the channel due to flow stratification as shown in Fig. 2. This flow stratification causes different thermal stress in each rod, so that it might lead to bowing of the rods under some reflood conditions.

The other is a rod in annulus test loop for visual observations. The flow schematic and test conditions are shown in Fig. 3 and 4. Heater rods are made from double stainless steel tubes as shown in Fig. 5, and flow patterns observed during bottom flooding are shown in Fig. 6 with schematic temperature trace. Fig. 7 represents the measured temperature curves during reflooding with different flooding rate, and the corresponding, calculated heat transfer coefficients and heat fluxes are shown in Fig. 8 and 9. The calculated average heat transfer coefficients in precursory cooling region

are distributed in the range of between 170 and 230 $w/m^{2o}C$ and increase slightly with flooding rate as in Fig. 10.

It is confirmed that the precursory cooling length increases rapidly at the initial stage of each test, but is soon fully developed and reaches almost constant value. Some experiments with low flooding rate were carried out to investigate the precursory cooling length with varying flooding rate. Fig. 11 shows the measured precursory cooling length as a function of the rod elevation with the parameter of the flooding rate, and the comparison of the measured values with the calculated results are represented in Fig. 12. Rewetting temperature increases slightly as flooding rate increases as shown in Fig. 13. Conclusion of the experiments are summarized in Fig. 14.

The author is much indebted to Mr. S. H. Lee, Mr. S.H. Kim, Mr. J.J. Kim Mr. J.S. Park, Mr. M.H. Yu, Mr. S.B. Kim and Mr. S.Y. Won who cooperate or assist in carrying out the reflood experiments as the members of thermal-hydraulic division in KAERI.

Reference

1. Y.W. Lee et al, "Experimental Study of Rewetting Phenomena", J. Korean Nuc. Soc., 12, 9 - 18, May 1980
2. Y.W. Lee et al, "Reflood Experiments with Horizontal and Vertical Flow Channels", 12, 156 - 162, Sep. 1980
3. M. MIRANO and Y. ASAHI, "Analysis of Precursory Cooling in Quenching Phenomena", J. of Nuc. Sci and Tech. 17 (5) pp. 339 - 350, May 1980
4. M.H. Chun and W.Y. Cheon, "Analysis of Rewetting in Water Reactor Emergency Core Cooling Inclusive of Heat Transfer in the Unwetted Region", ASME, Paper No. 75 - WA/HT - 32, 1975

ACTIVITIES
PAST WORK [1),2)] 5-ROD BUNDLE REFLOOD TEST [HORIZONTAL & VERTICAL] SINGLE ROD VISUAL TEST
PRESENT WORK CODE MODIFICATION CONSTRUCTION OF 3X3 TEST LOOP CONCEPTUAL DESIGN OF 5X5 BUNDLE TEST LOOP
FUTURE WORK DEVELOPMENT OF REFLOOD CODE CARRYING OUT 3X3 BUNDLE TEST CONSTRUCTION OF 5X5 TEST LOOP & CARRYING OUT THE TEST

FIG. 1 KAERI REFLOOD TEST ACTIVITIES

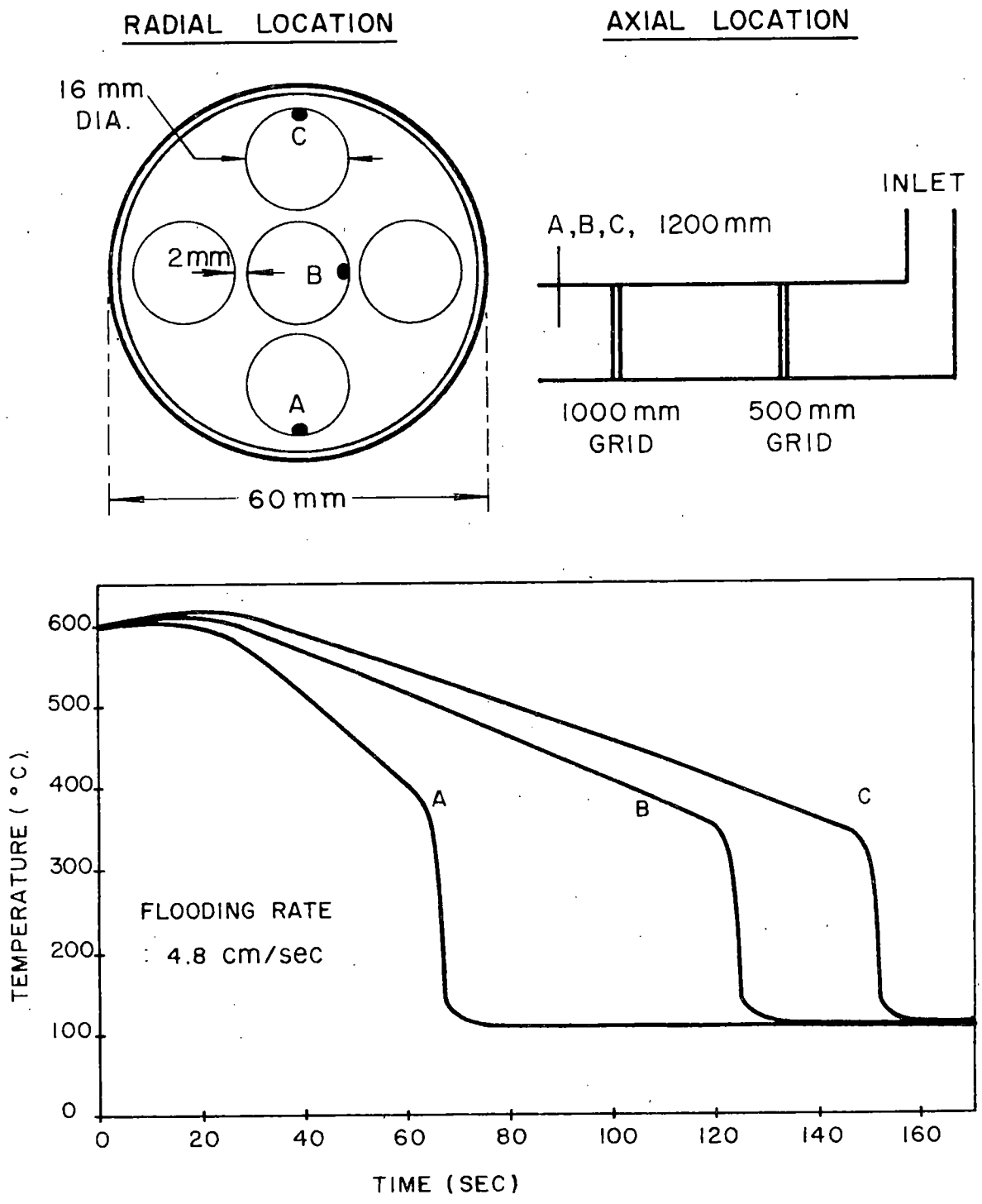

FIG. 2 FLOW STRATIFICATION EFFECT IN HORIZONTAL BUNDLE FLOODING

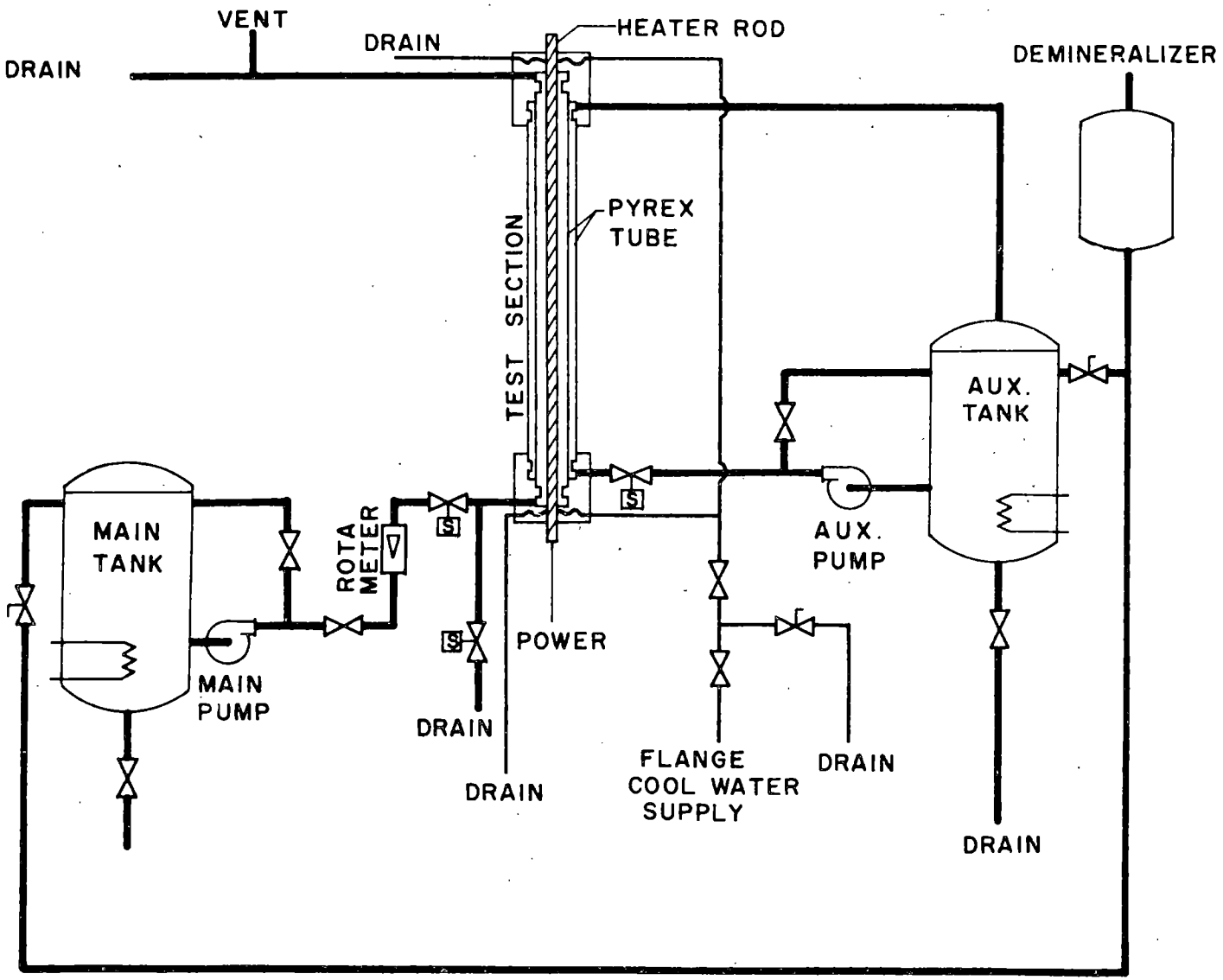

FIG.3 FLOW DIAGRAM OF TEST LOOP FOR VISUAL OBSERVATION

TEST CONDITIONS		
PRESSURE	:	1-6 BAR
WALL TEMPERATURE	:	500-850 °C
INLET SUBCOOLING	:	20-90 °C
FLOODING RATE	:	1-25 cm/sec
POWER DENSITY	:	1.5-2 kw/m
HYDRAULIC DIAMETER	:	1-1.5 cm

FIG. 4 TEST CONDITIONS OF A ROD IN ANNULUS REFLOOD TEST

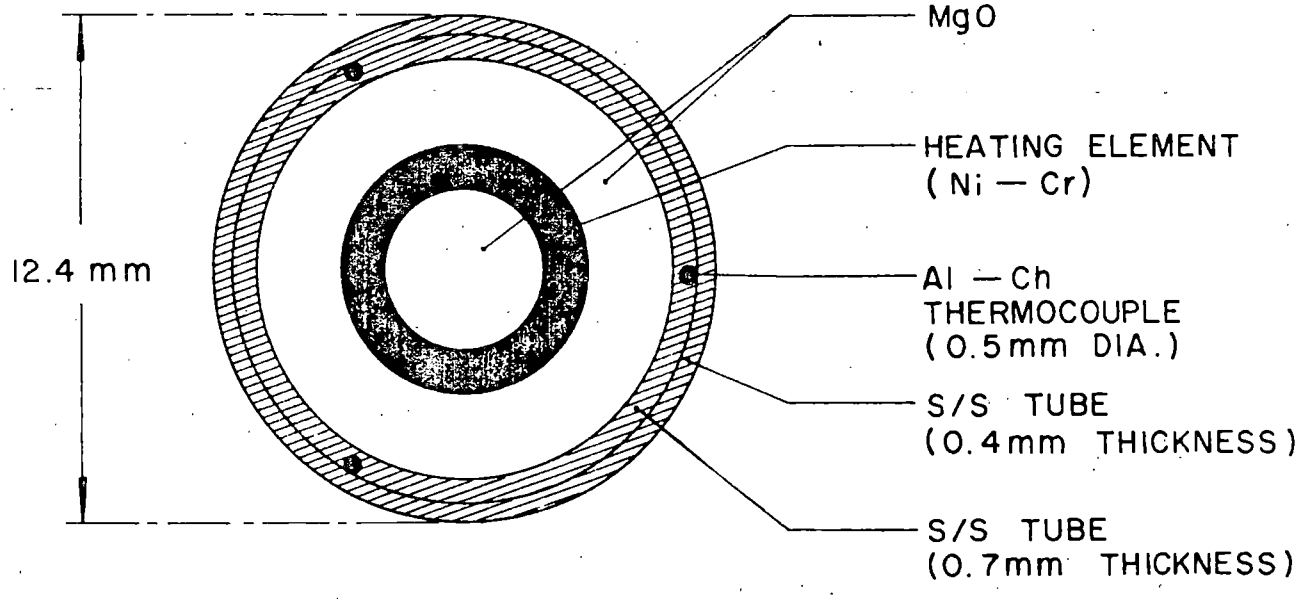

FIG. 5 CROSS SECTION OF HEATER ROD

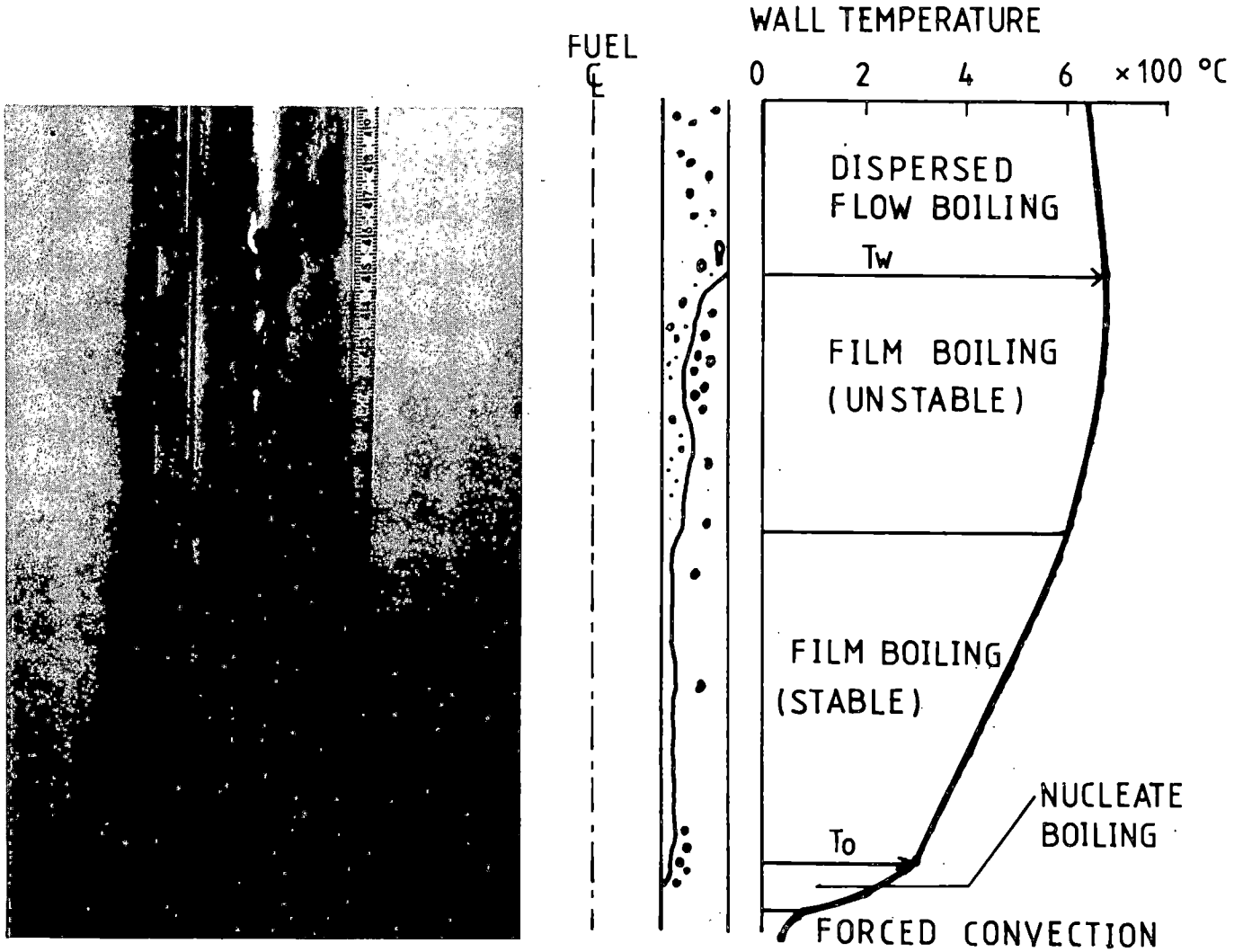

FIG. 6 FLOW PATTERN IN BOTTOM FLOODING

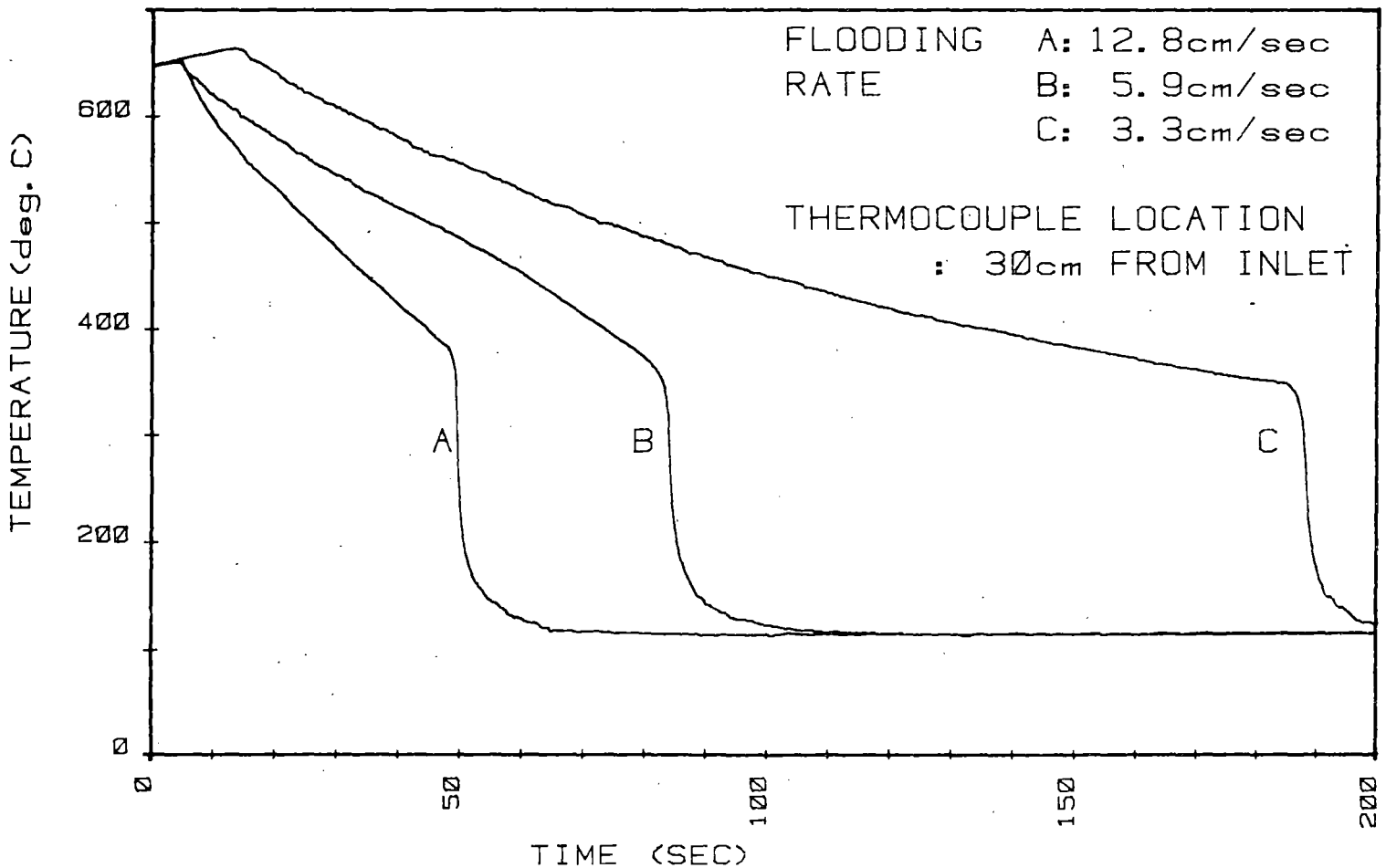

FIG. 7 DEPENDENCE OF TEMPERATURE TRACES ON FLOODING RATE

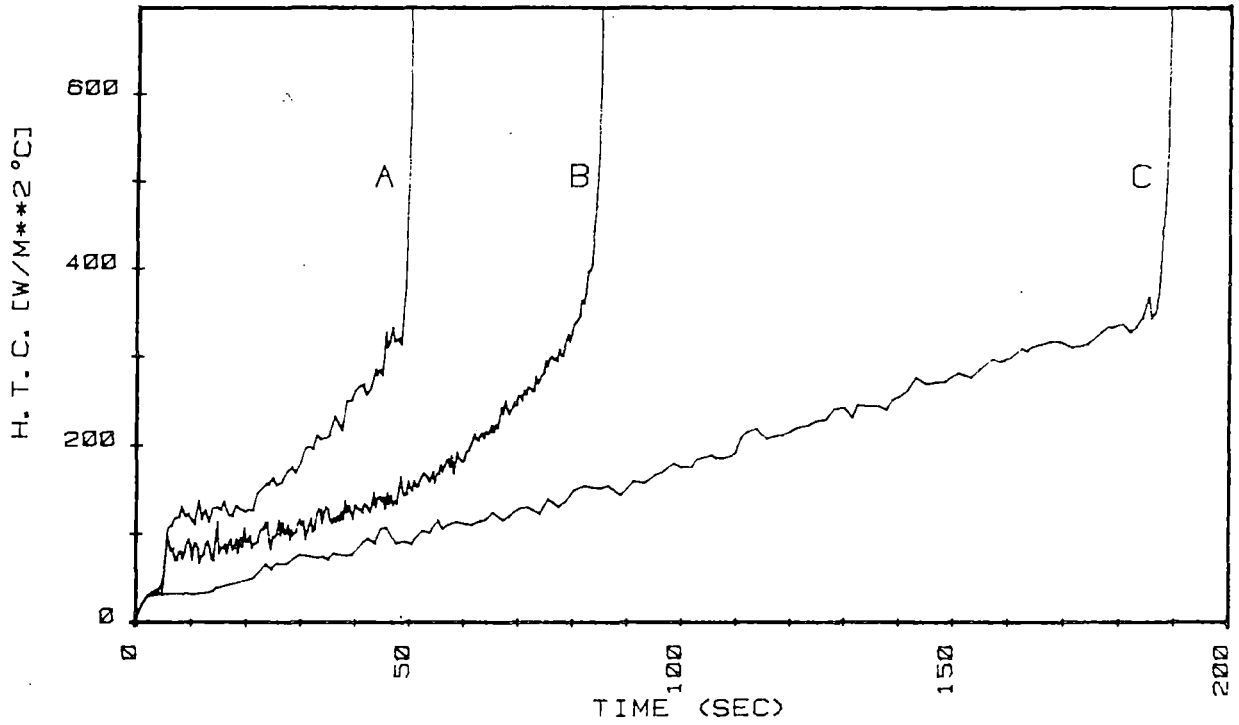

FIG. 8 HEAT TRANSFER COEFFICIENT CORRESPONDING TO FIG. 7

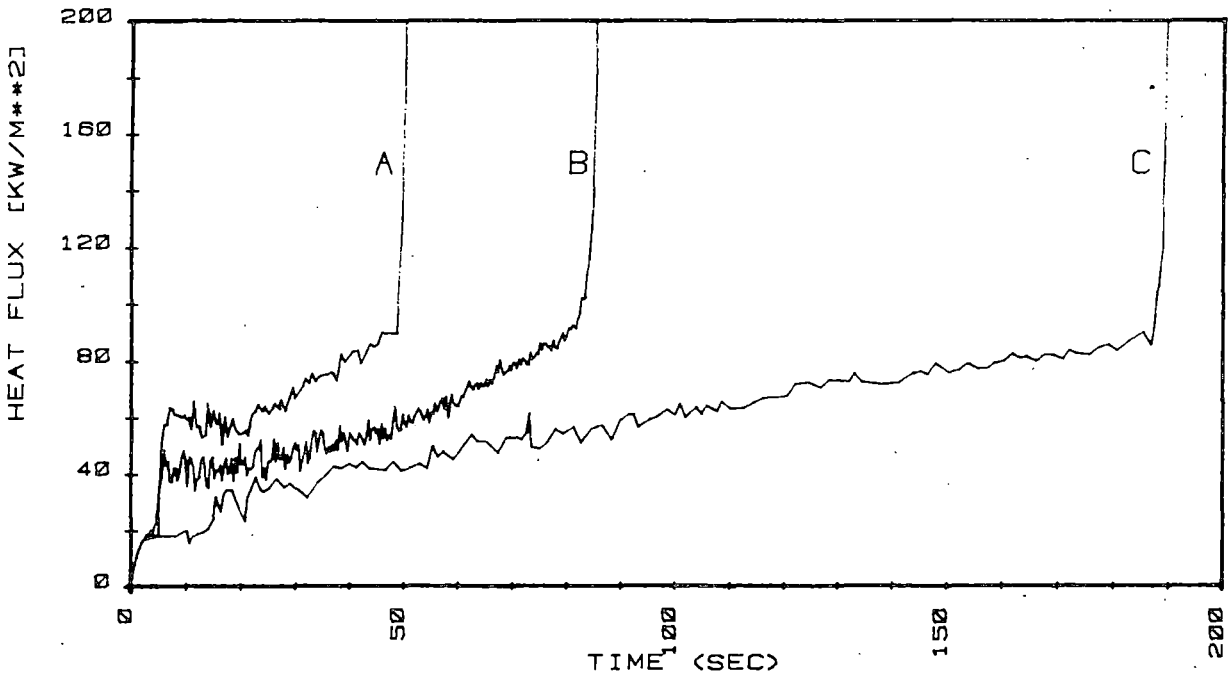

FIG. 9 HEAT FLUX CORRESPONDING TO FIG. 7

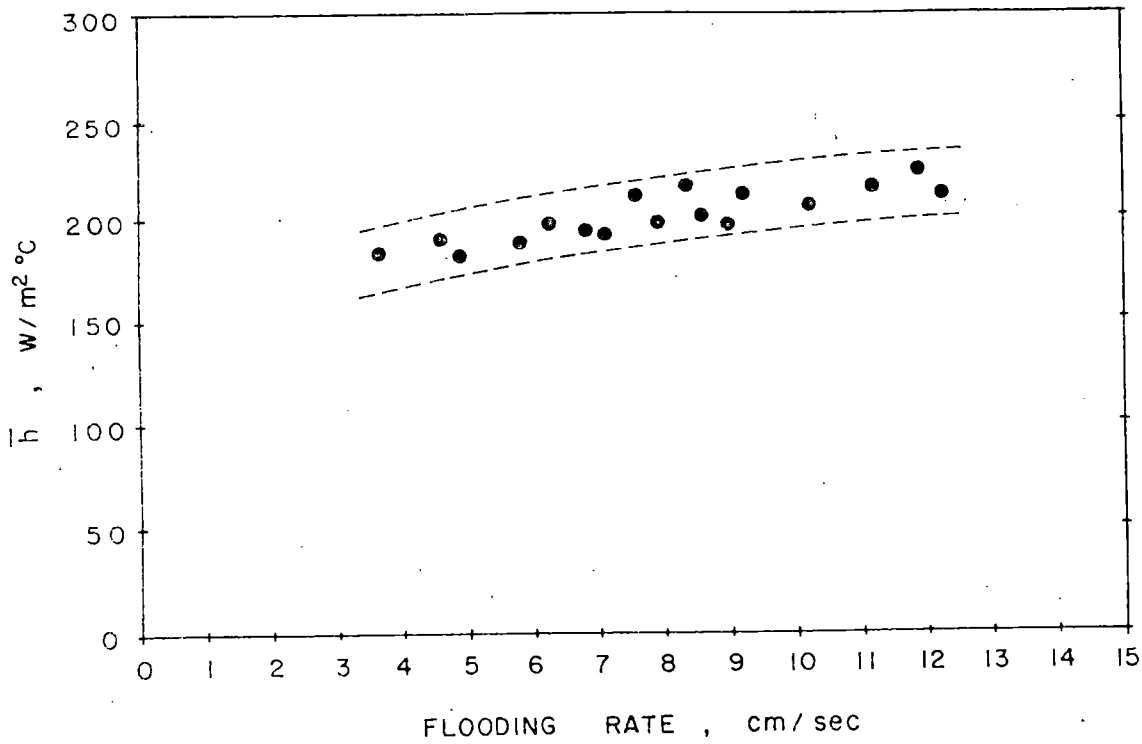

FIG. 10 AVERAGE HEAT TRANSFER COEFFICIENT IN PRECURSORY REGION

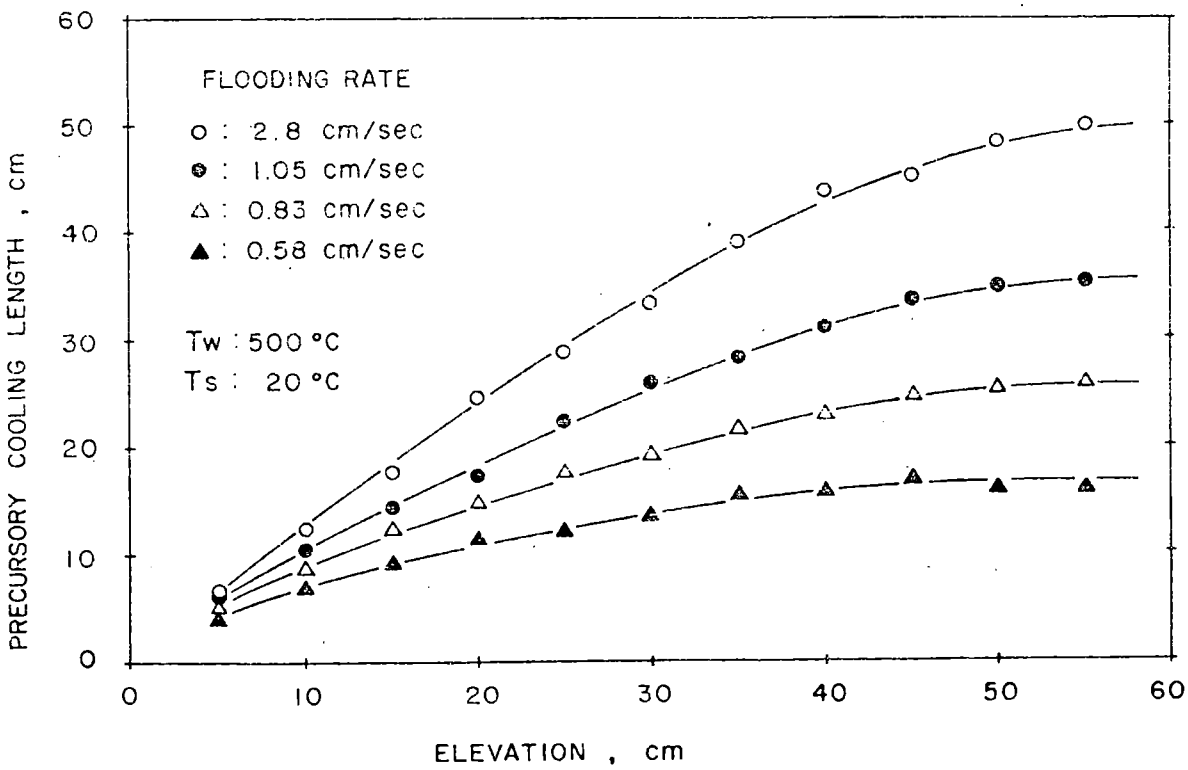

FIG. 11 PARAMETRIC EFFECT OF FLOODING RATE ON PRECURSORY COOLING LENGTH

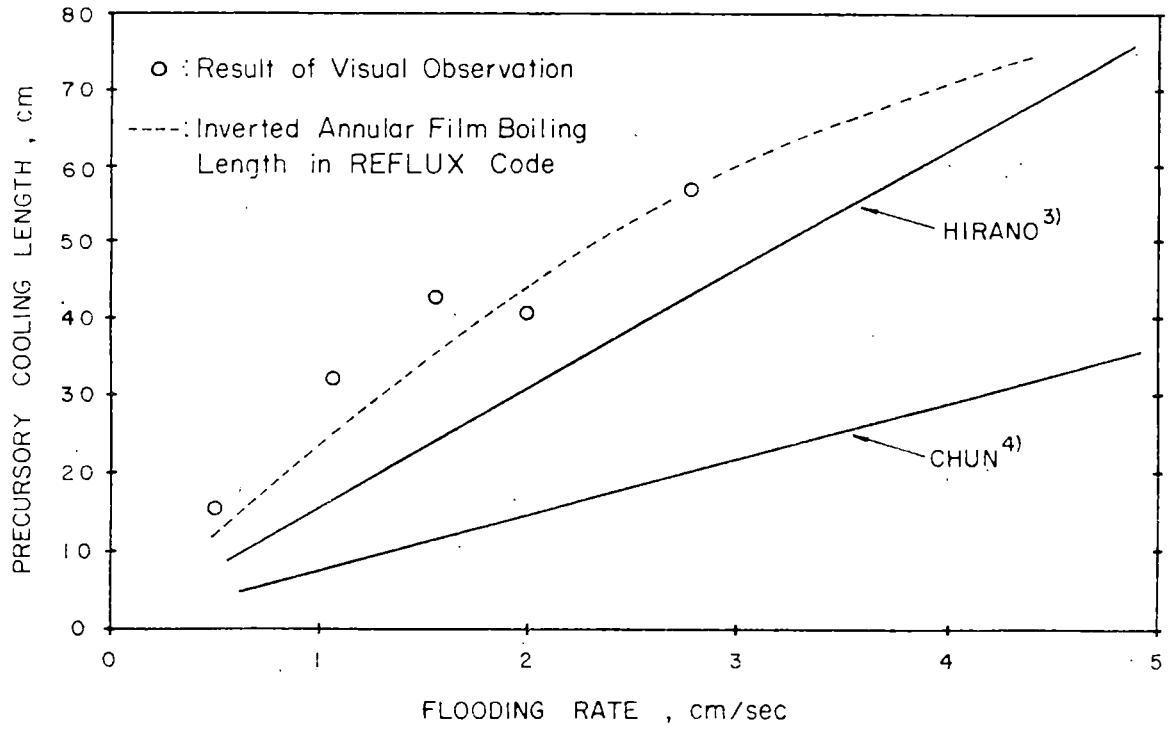

FIG.12 EFFECT OF FLOODING RATE ON PRECURSORY COOLING LENGTH

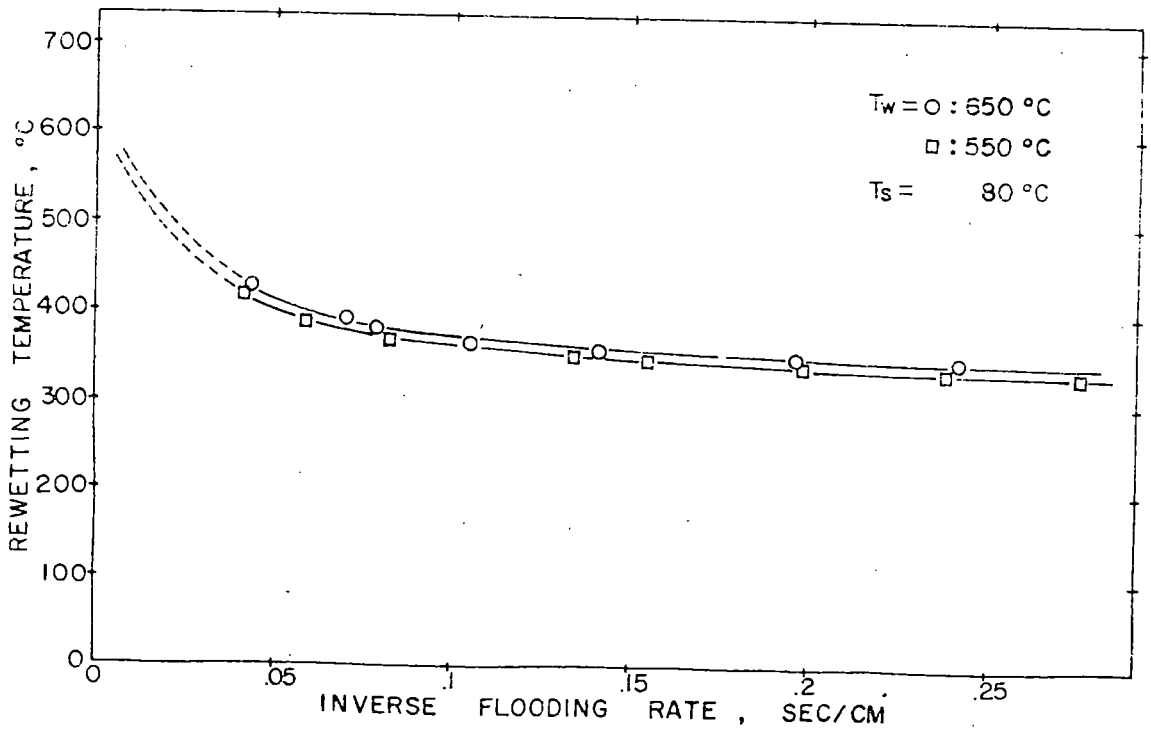

FIG.13 EFFECT OF FLOODING RATE ON REWETTING TEMPERATURE

CONCLUSIONS

1. IN THE CASE OF HORIZONTAL FLOODING FLOW STRATIFICATION PLAYS A SENSITIVE ROLE FOR DEFORMATION OF RODS DUE TO THERMAL STRESS

2. FIVE DIFFERENT FLOW REGIMES WERE VISUALLY OBSERVED THROUGH THE VERTICAL SINGLE ROD TEST

3. INCREASE IN FLOODING RATE INCREASES
   (A) QUENCH TEMPERATURE,
   (B) QUENCH VELOCITY
   (C) PRECURSORY COOLING AND
   (D) MEAN HEAT TRANSFER COEFFICIENT SLIGHTLY IN PRECURSORY REGION.

FIG. 14 CONCLUSIONS IN KAERI REFLOOD TEST

ROD BUNDLE HEAT TRANSFER RESEARCH AT ORNL*

Presented by William G. Craddick
Oak Ridge National Laboratory

Introduction

The Nuclear Regulatory Commission (NRC) has funded experimental studies of heat transfer in rod bundles at Oak Ridge National Laboratory (ORNL). This paper briefly describes the experiments that have been conducted and provides examples of the results of the analysis of the experimental data.

These studies have been conducted in the Thermal Hydraulic Test Facility (THTF), a pressurized water loop containing a 64-rod bundle of 12-ft (3.66-m) long, electrically heated fuel rod simulators (FRS) arranged in an 8 x 8 array. The FRS diameter and pitch and the location of unheated rods match those of 17 x 17 PWR fuel assemblies. The THTF can achieve fluid conditions representative of reactor accident situations. The following sections describe several of the experiments that have been conducted.

High Pressure, Low Flow and Low Power Experiments

(Principal Investigator: T. M. Anklam)

Various accident scenarios can be postulated during which a reactor experiences a net loss of water at a relatively slow rate after having undergone a reactivity scram. Such scenarios (e.g., the accident at Three Mile Island Unit 2) may include the slow boiling off of the core coolant, leading to the uncovering of the fuel rods and eventually to a reflooding of the core. Both boiloff and reflood experiments were conducted under these high pressure, low power conditions. Among the results is the observation that early quenching occurred near the spacer grids during reflood. This phenomenon was observed only at or downstream of the grids, suggesting that it was caused by the grids' perturbation of the fluid flow. Prior to reflood the reactor core would be uncovered and flow and power would be low. The extent of core degradation will depend in part on the heat transfer from the uncovered fuel to the superheated steam and on the void fraction distribution below the fuel dryout elevation. This latter quantity is important because the presence of voids (due to bulk boiling of the coolant) below the dryout elevation displaces the dryout elevation upwards, thus reducing the length of fuel exposed to potentially damaging temperatures and lowering the peak fuel clad temperature. To obtain data on these quantities, a series of steady-state experiments were conducted. It was determined that the convective correlation proposed by Anklam combined with the Hottel empirical radiation model did the best job of predicting heat transfer coefficients for modified wall Reynolds numbers (Re_{mw}) between 2000 and 10,000. Anklam's correlation evaluates all properties at the wall temperature and uses a

*Research sponsored by Division of Reactor Safety Research, U.S. Nuclear Regulatory Commission under Interagency Agreements DOE 40-551-75 and 40-552-75 with the U.S. Department of Energy under contract W-7405-eng-26 with the Union Carbide Corporation.

modified wall Reynold's number, defined as $Re_{mw} = (GD/\mu_w)(\rho_w/\rho_v)$, where the subscripts denote evaluation at the wall temperature (w) or the bulk vapor temperature (v). The correlation is a modification of McEligot's correlation stemming from theoretical considerations, and is not the result of fitting the correlation to the present data. It was found that the Yeh correlation performed best in predicting the void fraction distribution. Other models evaluated include the Wilson bubble-rise model, a drift flux model for churn turbulent flow, and two models proposed by Gardner.

Film Boiling Experiments

(Principal Investigators: C. B. Mullins, D. G. Morris, G. L. Yoder)

Both transient and steady-state experiments were conducted to obtain dispersed flow film boiling data. This regime is expected to occur during loss of coolant accidents of various break sizes. In both transient and steady-state experiments, flow was upwards through the rod bundle and the bundle inlet was supplied with subcooled liquid. This permitted calculation of bundle fluid conditions without reliance on measurements of two-phase flow. The transient tests were conducted in such a manner that flow reversals were avoided, and thus flow remained high enough to measure accurately. Bundle fluid conditions were calculated for the steady-state tests by the application of mass and energy conservation and for the transient tests by the use of a locally modified version of RELAP4 Mod 5 Update 2 that replaces the code's heat transfer logic and correlations with experimentally determined heat fluxes. Both steady-state and transient calculations were made assuming thermodynamic equilibrium between the vapor and liquid phases, as do many of the codes used for reactor licensing and other accident calculations.

The calculated bundle fluid conditions and the rod surface temperatures and surface heat fluxes obtained from FRS data were used to calculate experimental heat transfer coefficients and assess correlations. Among the correlations assessed were the Dougall-Rohsenow correlation, which often substantially overpredicted the heat transfer coefficient, and the Groeneveld 5.7 correlation, which performed much better. Reactor codes which assume thermodynamic equilibrium often switch from a film boiling correlation to a single-phase correlation, such as Dittus-Boelter, when equilibrium quality (X_{eq}) exceeds 1. However, in situations where $X_{eq} > 1$ but liquid droplets remain entrained in the flow, our data indicates that Dittus-Boelter also substantially overpredicts the heat transfer.

UNION CARBIDE
ORNL

WILLIAM G. CRADDICK

ROD BUNDLE HEAT TRANSFER RESEARCH AT ORNL

PRESENTED TO THE
NINTH WATER REACTOR SAFETY RESEARCH
INFORMATION MEETING

OCTOBER 27, 1981

GAITHERSBURG, MARYLAND

UNION CARBIDE
ORNL

SEVERAL TYPES OF HEAT TRANSFER DATA HAVE BEEN ACQUIRED

- HIGH PRESSURE, LOW FLOW AND POWER
  - STEADY STATE STEAM COOLING
  - STEADY STATE VOID DISTRIBUTION
  - TRANSIENT BOILOFF
  - REFLOOD
- HIGH PRESSURE, HIGH FLOW AND POWER
  - STEADY STATE FILM BOILING
  - TRANSIENT FILM BOILING

UNION CARBIDE
ORNL

DATA WAS ACQUIRED IN THE THERMAL HYDRAULIC TEST FACILITY

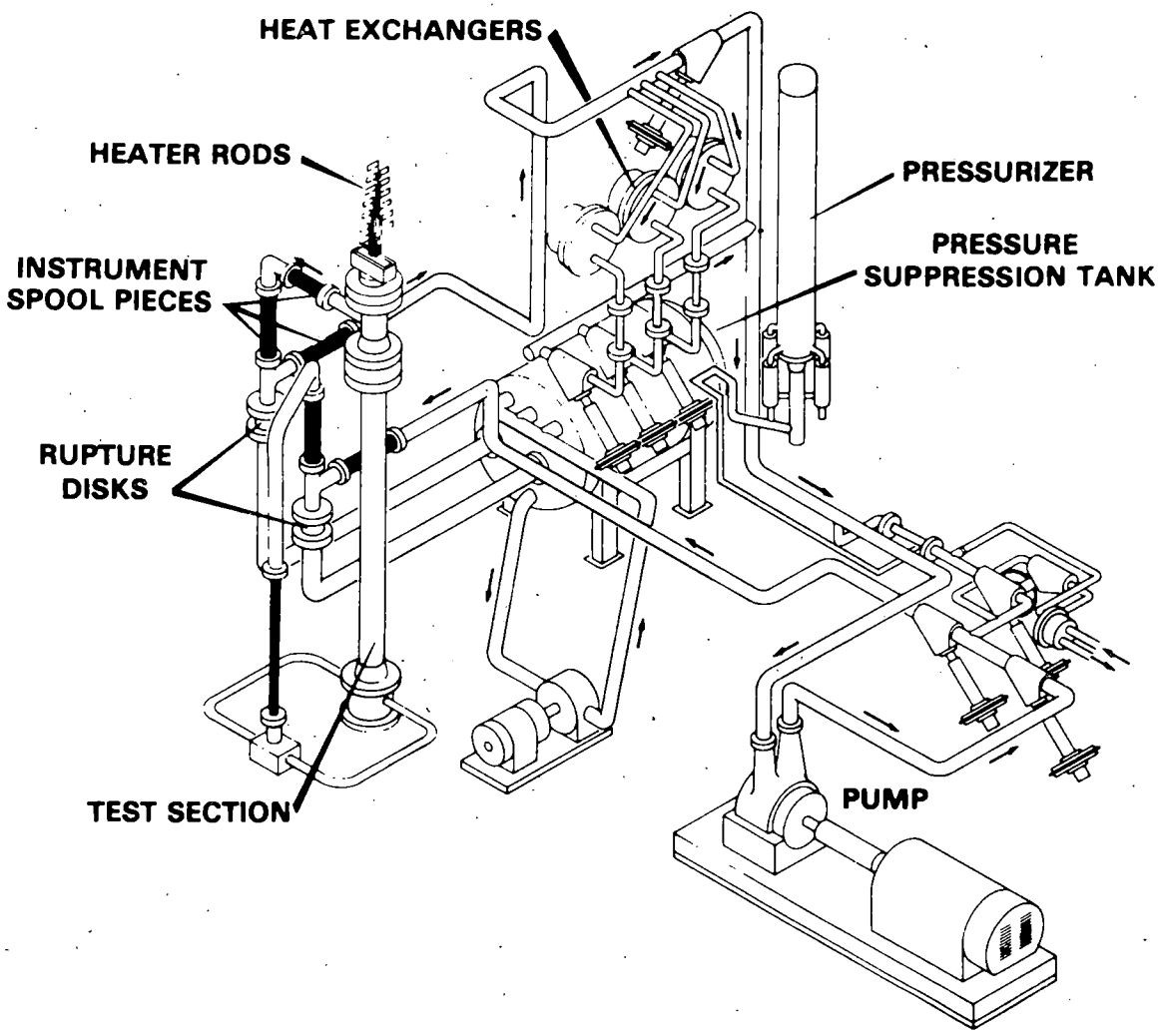

UNION CARBIDE
ORNL

ROD BUNDLE HAS FEATURES OF 17 X 17 PWR FUEL ASSEMBLY

- 64 RODS (8 X 8 ARRAY) WITH 4 UNHEATED RODS IN POSITIONS OF CONTROL RODS
- ROD DIAMETER (0.374 in., 0.95 cm) AND PITCH (0.501 in., 1.27 cm)

  (PITCH/DIAMETER) = 1.34
- 12 FOOT (3.66 m) HEATED LENGTH

UNION CARBIDE

ORNL

TESTS WERE CONDUCTED TO FACILITATE ACCURATE CALCULATION OF BUNDLE FLUID CONDITIONS

- INSTRUMENTATION AND PIPING WERE OPTIMALLY SIZED FOR EACH TEST

- ALL TESTS HAD UNIDIRECTIONAL UPFLOW

  ↓

  NO PERIODS OF FLOW TOO LOW TO MEASURE ACCURATELY

- ALL TESTS HAD INLET FLOW OF SUBCOOLED LIQUID ONLY

  ↓

  NO CALCULATIONS DEPENDED ON MEASUREMENT OF TWO-PHASE FLOW

UNION CARBIDE
ORNL

STEAM COOLING AND VOID DISTRIBUTION AFFECT EXTENT OF FUEL DAMAGE WHEN REACTOR CORE UNCOVERS

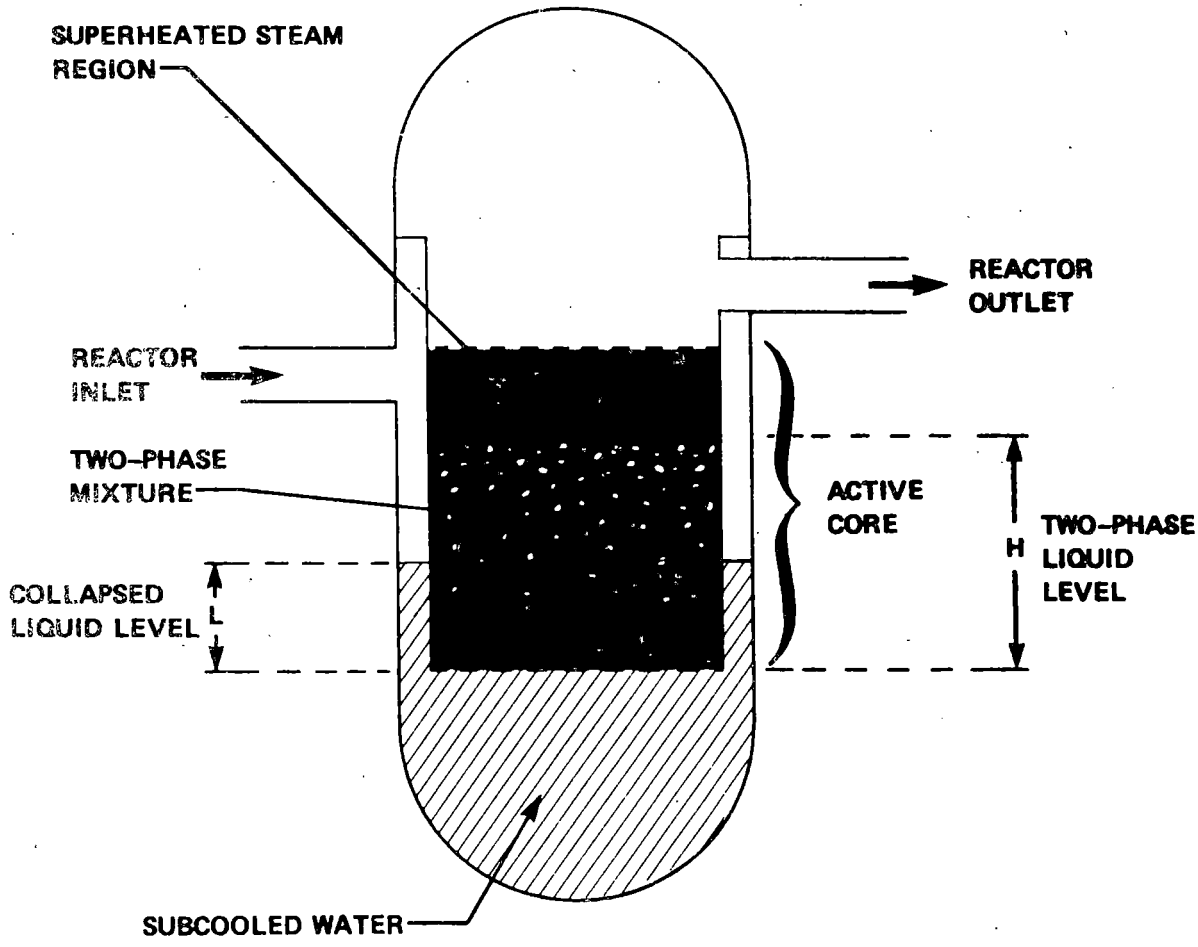

UNION CARBIDE

ORNL

STEAM COOLING DATA WAS OBTAINED FOR HIGH PRESSURES AND LOW FLOWS

PRESSURE:	377 TO 1088 psia 2.6 TO 7.5 MPa
LINEAR POWER:	0.10 TO 0.68 kW/ft 0.33 TO 2.23 kW/m
REYNOLD'S NO.:	1100 TO 17,700
ROD TO VAPOR TEMPERATURE RATIO:	1.10 TO 1.63

UNION CARBIDE
ORNL

CONVECTIVE CORRELATION PROPOSED BY ANKLAM WITH HOTTEL RADIATION MODEL ARE RECOMMENDED

- $2000 \leqslant Re_{mw} \leqslant 10{,}000$
- REFERENCE TEMPERATURE CONVECTIVE CORRELATION

$$Nu_w = 0.021 \left[\frac{G\ D_H}{\mu_w} \left(\frac{\rho_w}{\rho_v} \right) \right]^{0.8} Pr_w^{0.4}$$

THEORETICAL MODIFICATION OF McELIGOT CORRELATION

- HOTTEL EMPIRICAL RADIATION MODEL

$$h_{RAD} = \left[\frac{1}{\epsilon_w} + \frac{1}{\alpha_v\ (T_w)} - 1 \right]^{-1} \left[\frac{(T_w^4 - T_v^4)}{(T_w - T_v)} \right]$$

SIMPLE MODEL IS EFFECTIVE UNDER THESE CONDITIONS

UNION CARBIDE
ORNL

ANKLAM'S CONVECTIVE CORRELATION PERFORMS WELL FOR MODIFIED WALL REYNOLDS NUMBERS ABOVE 2000

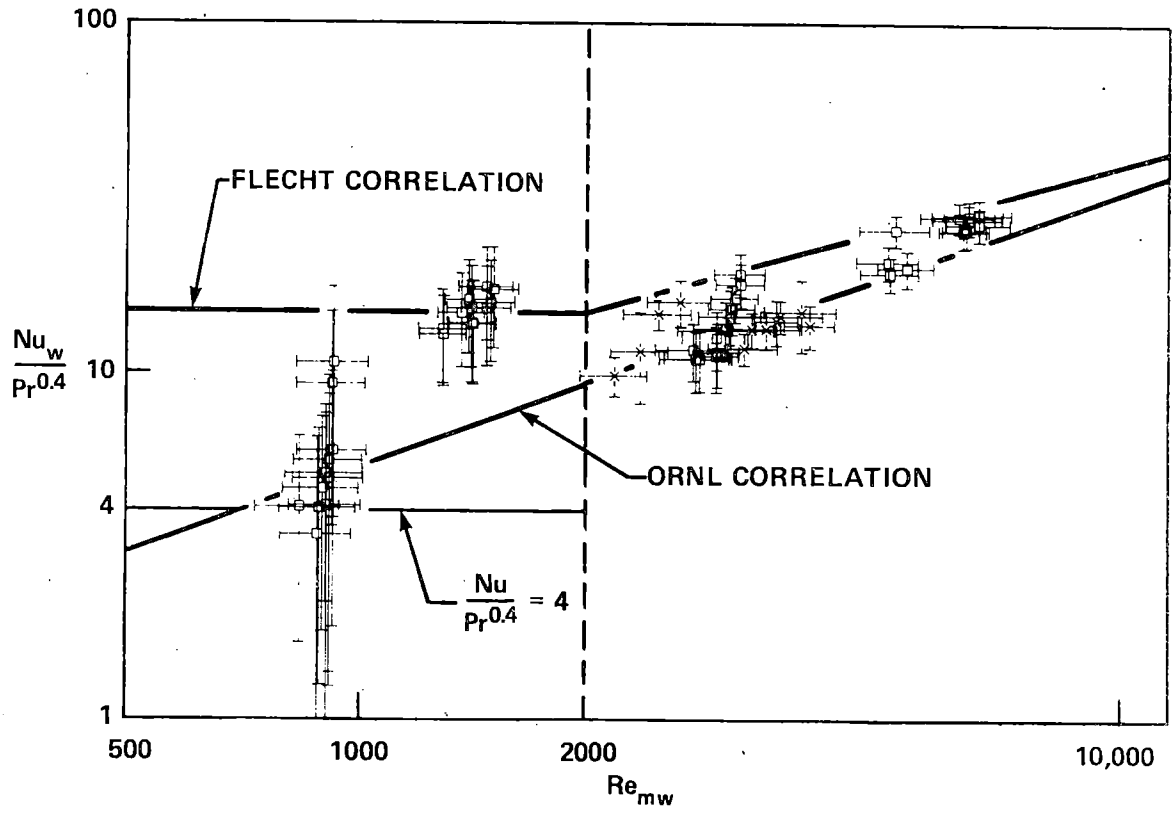

UNION CARBIDE
ORNL

VOID FRACTION DATA WAS ALSO OBTAINED

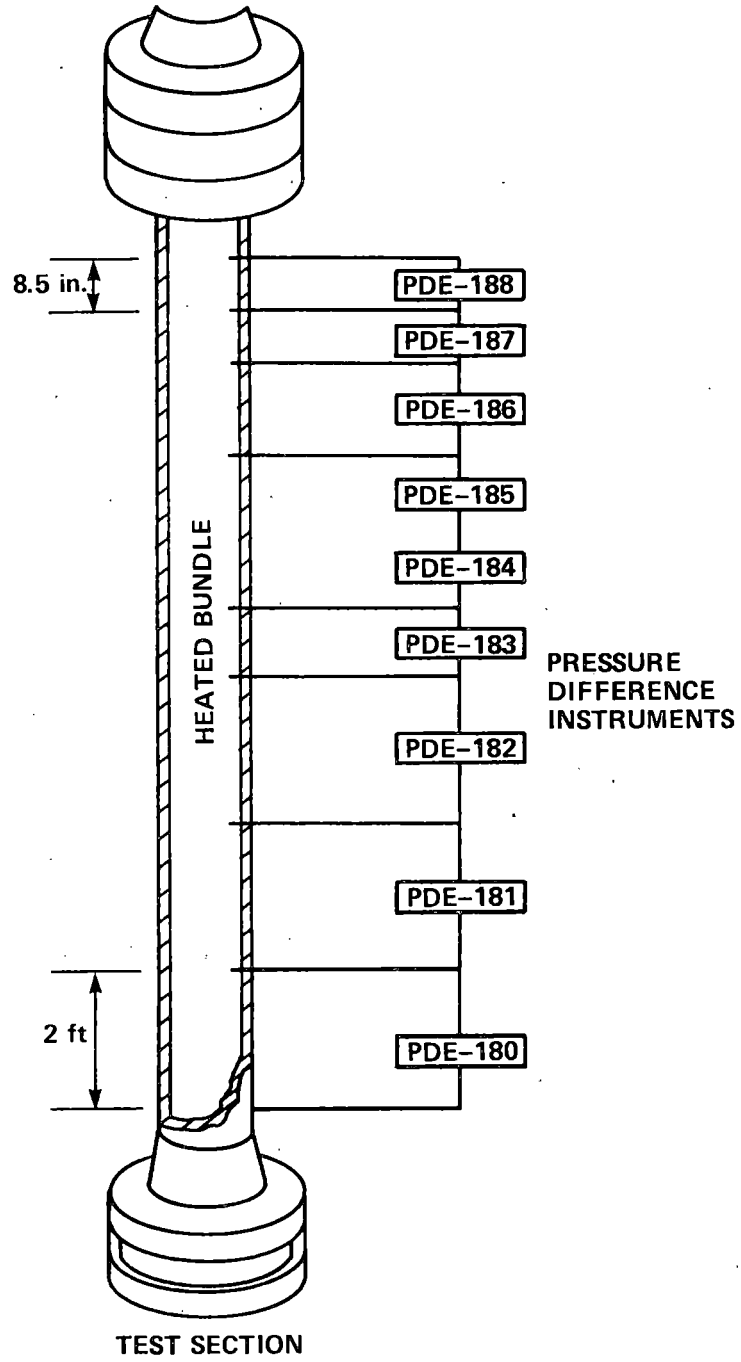

UNION CARBIDE
ORNL

YEH'S CORRELATION PRODUCED BEST PREDICTIONS OF VOID FRACTION PROFILES

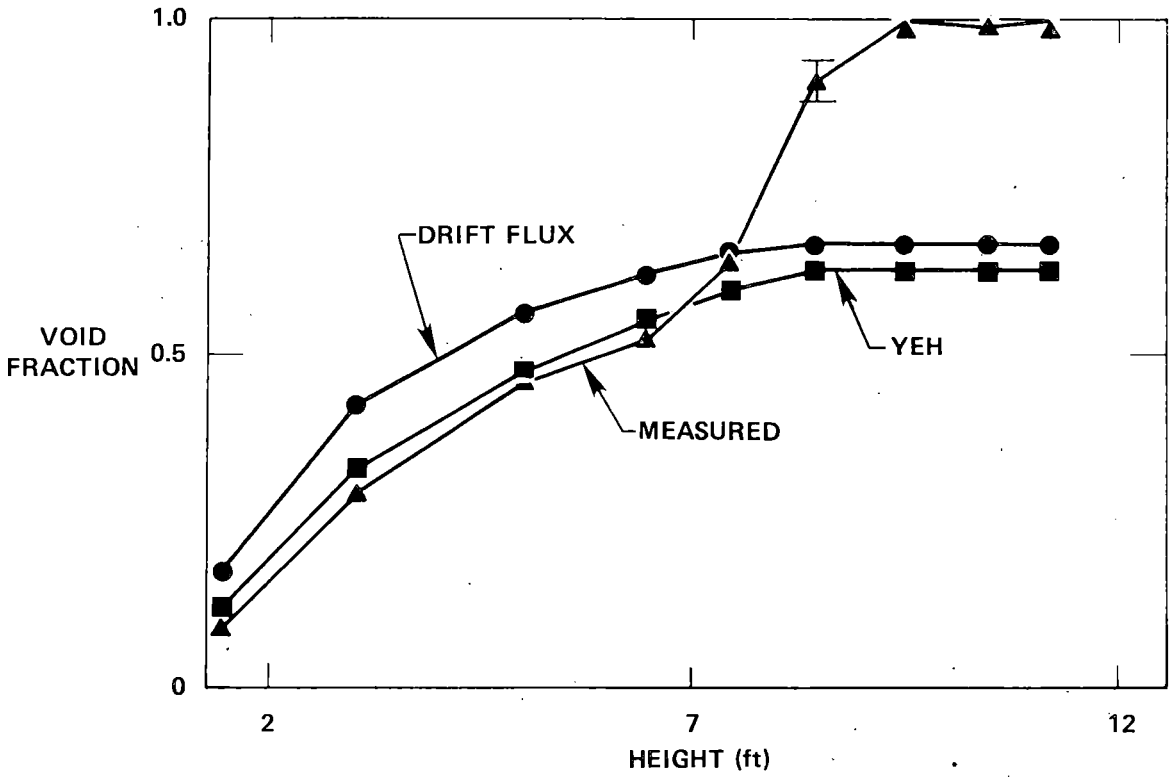

UNION CARBIDE
ORNL

SPACER GRIDS ENHANCED ROD QUENCHING DURING HIGH PRESSURE REFLOODS

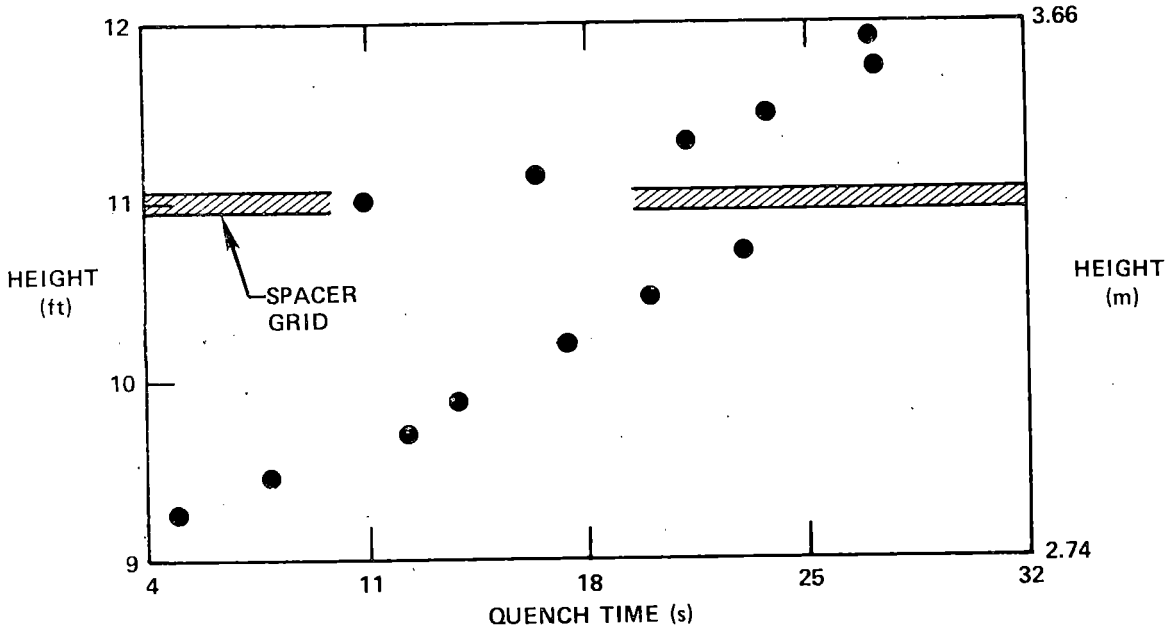

UNION CARBIDE
ORNL

DISPERSED FLOW FILM BOILING DATA WAS OBTAINED AT HIGH PRESSURES AND FLOWS

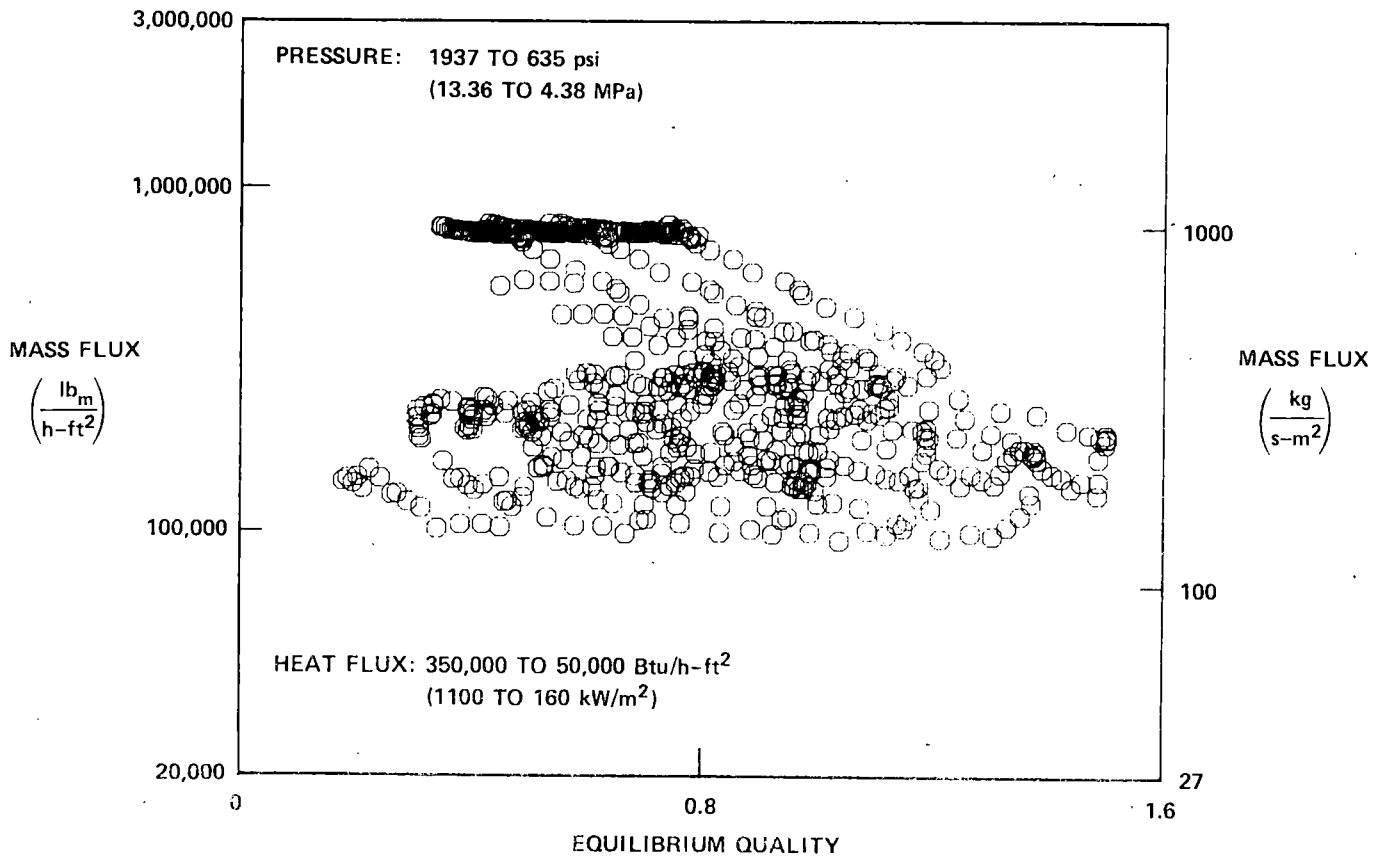

UNION CARBIDE
ORNL

DISPERSED FLOW FILM BOILING DATA WAS OBTAINED AT HIGH PRESSURES AND FLOWS

PRESSURE:	1937 TO 635 psi 13.36 TO 4.38 MPa
MASS FLUX:	8.0 TO 1.0 X 10^5 lbm/h-ft^2 1090 TO 129 kg/s-m^2
EQUILIBRIUM QUALITY:	15 TO 150 PERCENT
HEAT FLUX:	3.5 TO 0.5 X 10^5 Btu/h-ft^2 1100 TO 160 kW/m^2

UNION CARBIDE
ORNL

CORRELATION COMPARISONS WILL SHOW BOTH STEADY STATE AND TRANSIENT DATA

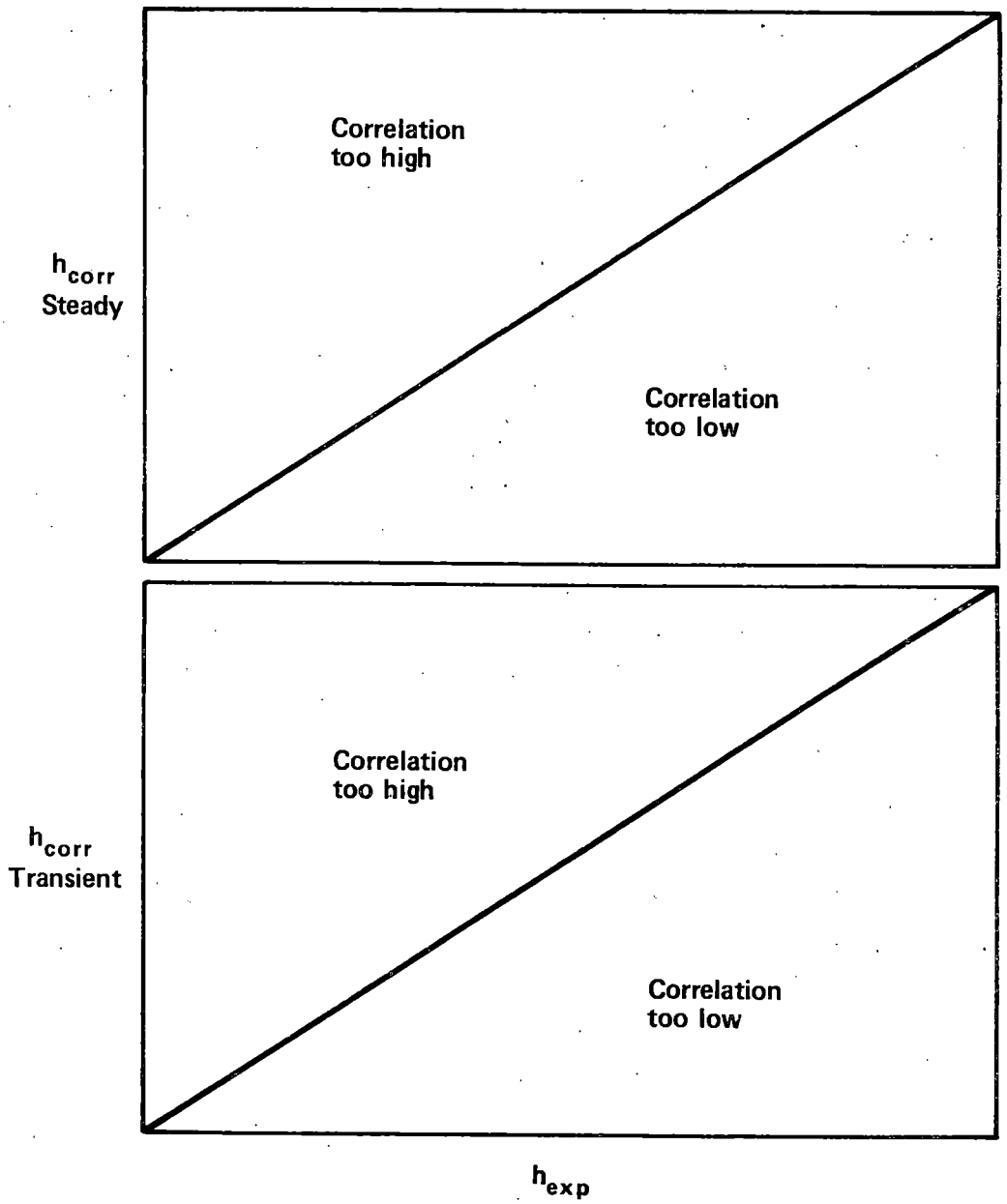

UNION CARBIDE
ORNL

DOUGALL-ROHSENOW CORRELATION OFTEN PREDICTS EXCESSIVELY HIGH HEAT TRANSFER COEFFICIENTS

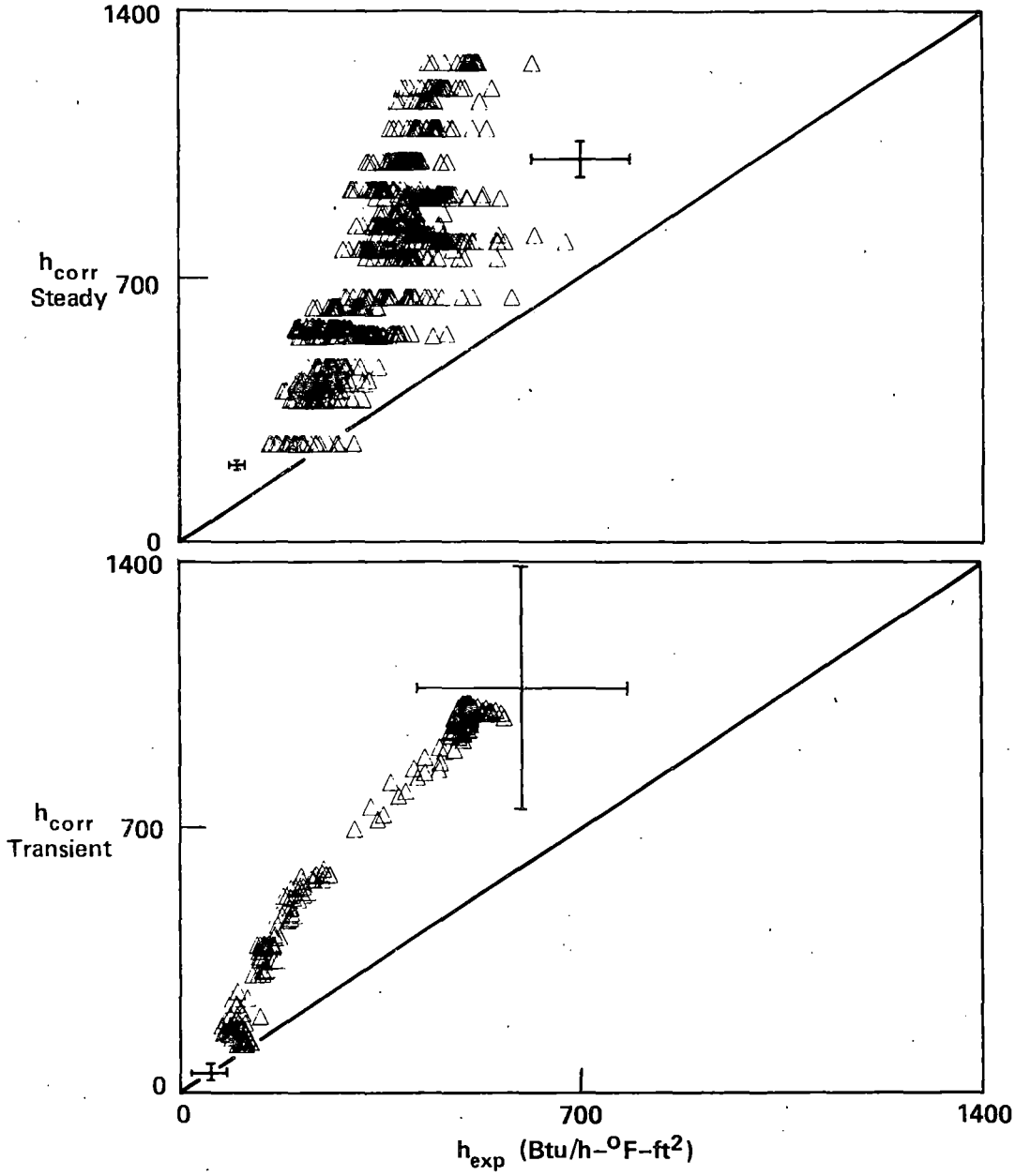

UNION CARBIDE
ORNL

GROENEVELD 5.7 CORRELATION PREDICTS THE DATA WELL

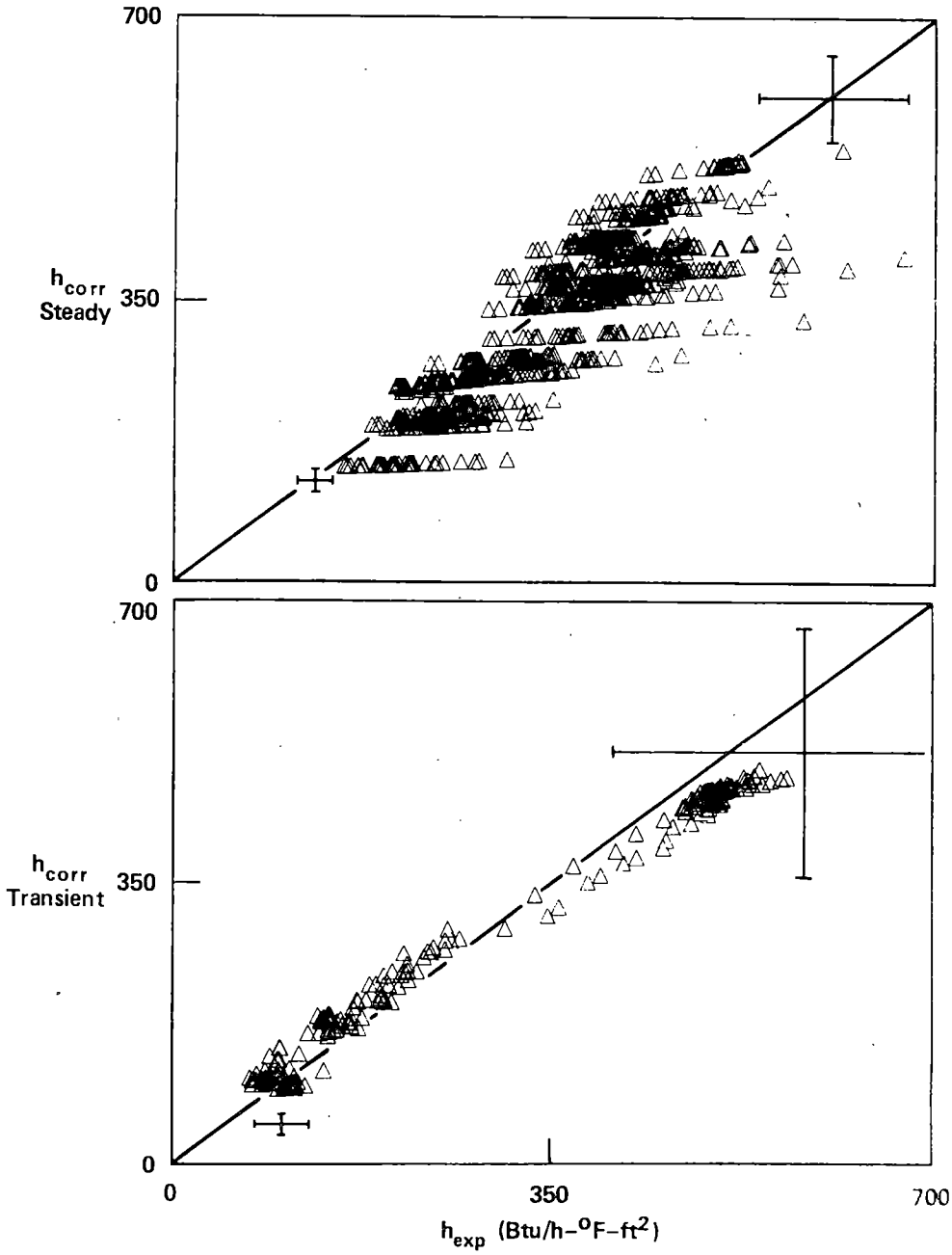

UNION CARBIDE
ORNL

DITTUS–BOELTER CORRELATION OVERPREDICTS HEAT TRANSFER FOR EQUILIBRIUM QUALITIES GREATER THAN ONE

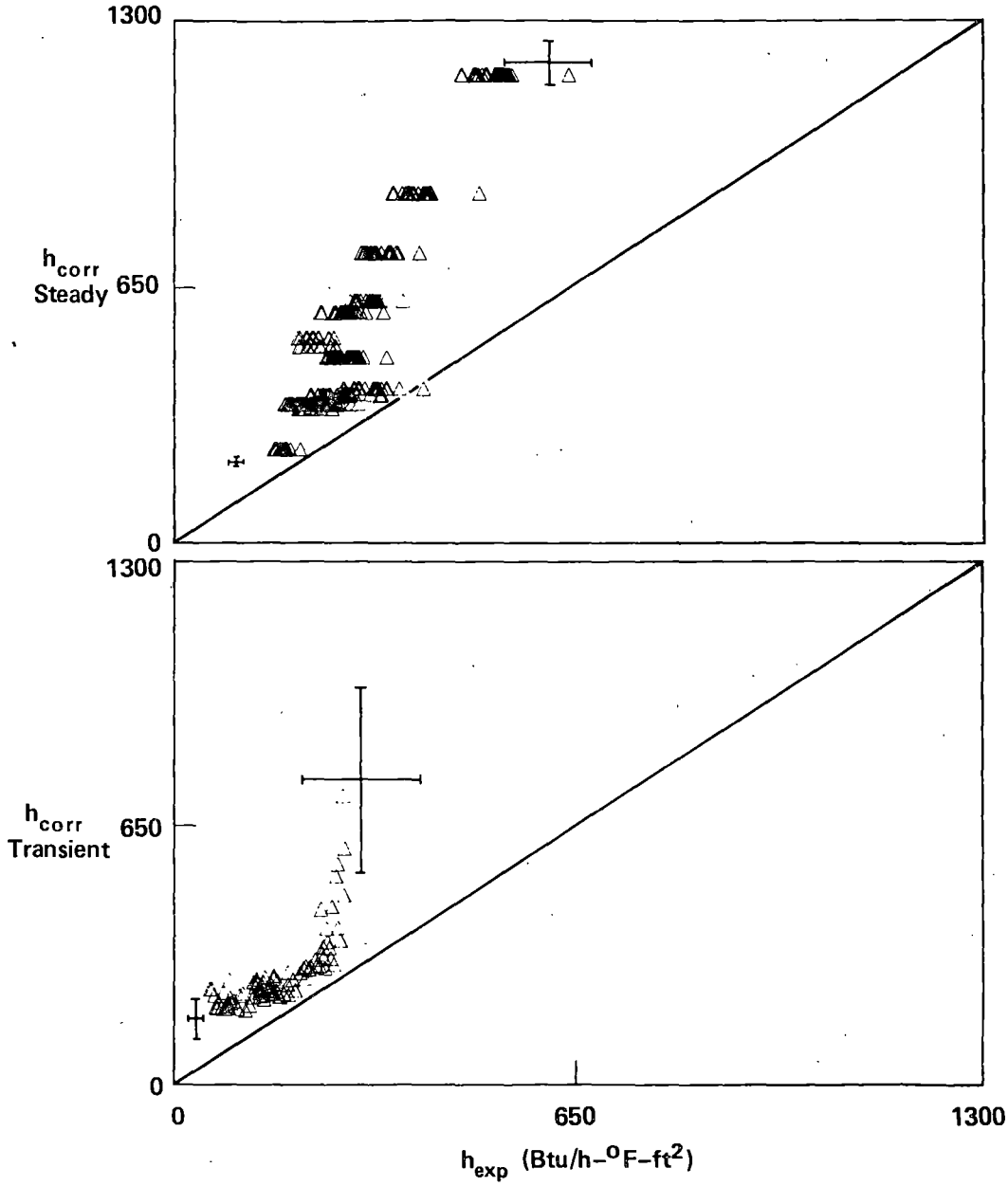

UNION CARBIDE
ORNL

USEFUL HEAT TRANSFER DATA HAS BEEN GENERATED IN ROD BUNDLE GEOMETRY

- HIGH PRESSURE, LOW FLOW, LOW HEAT FLUX
  - STEAM COOLING
  - VOID FRACTION DISTRIBUTIONS
  - REFLOOD AND BOILOFF
- HIGH PRESSURE, HIGH FLOW, HIGH HEAT FLUX
  - STEADY STATE FILM BOILING
  - TRANSIENT FILM BOILING
- INSTRUMENT RESPONSES ARE IN INEL DATA BANK
- ANALYSIS RESULTS WILL BE PUBLISHED IN NEXT FEW MONTHS

NRC/EPRI/WESTINGHOUSE
FULL LENGTH EMERGENCY CORE HEAT TRANSFER
SEPARATE EFFECTS AND SYSTEMS EFFECTS TESTS
(FLECHT-SEASET):

- SYSTEMS EFFECTS NATURAL CIRCULATION TEST PLAN
- 21-ROD BUNDLE FLOW BLOCKAGE RESULTS

Presented by
L. E. Hochreiter
Westinghouse Nulcear Safety Department
Nuclear Technology Division

At
Ninth Water Reactor Safety Information Meeting
October 26, 1981

The FLECHT-SEASET program is a NRC/Electrical Power Research Institute (EPRI)/ Westinghouse cooperative research and development effort who's goal is to improve our understanding of large break LOCA reflood phenomena as well as the different natural circulation cooling modes typical of small break LOCA. The detailed objectives of the program as given in Figure 1. The FLECHT-SEASET program can be subdivided into two major subtasks each of which addresses current PWR licensing and research needs. Those subtasks are, rod bundle flow blockage; and system response during reflood and natural circulation.

The rod bundle flow blockage program utilizes three separate experimental programs as shown in Figure 2. The goal of flow blockage portions of the FLECHT-SEASET program is to provide experimental data and analysis which can be used to address the current Appendix K steam cooling-flow blockage rule at low flooding rates. This particular portion of the program has received more attention due to the concerns raised in NUREG-0630 on LOCA burst strain and blockage models used by the vendors and NRC staff.

The systems effects test portion of the FLECHT-SEASET program also utilizes three separate experiments as shown in Figure 3. The steam generator separate effects tests results were discussed at previous information meetings. The upper plenum flooding tests have been conducted at INEL to obtain the flooding behavior of the FLECHT-SEASET upper plenum and hardware. The systems effects test facility is presently under shakedown and testing will be initiated during the fourth quarter of 1981. Natural circulation cooling modes will be investigated in this scaled facility which utilizes two, full height, well instrumented multitube steam generators. Single phase, two-phase, and reflux condensation cooling modes will be investigated. The effects of different secondary side heat sinks, non-condensible gas injection and ECC injection will be investigated on the stable cooling modes for the primary system.

In this presentation, the test plan for natural circulations systems test as well as the 21-rod bundle flow blockage test results will be discussed in detail. For those interested, a listing of all the published FLECHT-SEASET reports is given in Table 1.

A.) NATURAL CIRCULATION SYSTEMS EFFECTS TASK

The objectives of this task are given in Figure 4. This test series is specifically designed to address post TMI-Accident and accident recovery concerns. The experiements will investigate the different natural circulation cooling modes as well as the transition between modes. A schematic of test facility is given in Figure 5. The test facility was originally designed for reflood heat transfer systems effects tests, however, nearly all the scaling requirements for natural circulation are the same as those for reflood with the exception of system pressure. The test facility is full height, has PWR resistances and preserves the proper power-to-volume ratio. An active secondary side has been added to the two full height steam generators such that a forced flow or boiling secondary side in the steam generators can be used. The one parameter which is not modeled is the system pressure. The desired pressure for small break situations is 600 - 1200 psia, whereas the original design pressure for the FLECHT-SEASET systems effects facility was 60 psia. The concern about the lower pressure in the test was that flow regime transitions could occur at different mass fluxes in the test relative to the PWR because of the lower density resulting in different natural circulation cooling modes. Two changes in the facility design were encorporated to compensate for the lower pressure design. The test facility design was increased from 60 to 150 psia. This was the highest pressure we could go to without a major redesign effort. The hot legs which were normally 3-inch (unbroken loop) and 1 1/2-inch (broken loop) were enlarged to 6-inch and 3-inch respectively. Enlarging the cold legs permitted operation at prototypical decay powers and steam generation rates such that stratified flow would exist at the lower pressures in the hot legs ratherthan a dispersed flow. The concern was that two-phase and reflux condensation cooling modes could be very difficult to obtain with the smaller hot legs.

There are a total of 576 channels of instrumentation in the test with 284 channels in the two steam generators.

One of the unique features of the FLECHT-SEASET natural circulation tests are the detailed steam generator instrumentation. Tube wall, secondary fluid, and

primary fluid temperatures can be measured as well as the tube ΔP at the 0 - 4 foot elevation, over all ΔP, and secondary side level. The steam generator wall, primary fluid, and secondary fluid thermocouples can be connected as a delta or absolute fashion in the smaller generator to measure the small driving ΔT during reflux condensation. Shakedown tests will determine whether the delta or absolute T/C hook-up is preferred.

Very low flow rotameters are used to measure the condensate run back in the hot legs and cold legs during the reflux condensation mode as shown in Figure 6. In this fashion, a system mass and energy balance can be performed.

Several tests will be conducted with helium gas injection to investigate the non-condensible gas effect. The gas will be injected in the hot legs and will be allowed to migrate into the steam generators. A gas analyzer system will be used to detect the presence of the non-condensible gases and to give a rough estimate of the gas concentration. The steam generator steam probe which fits inside the primary steam generator tube will be used as a sampling probe to suck out the gas/water/steam/mixture. A schematic of the gas analyzing system is shown in Figure 7.

The preliminary test matrix for the natural circulation tests is shown in Figures 8, 9, 10 and 11. After each natural circulation cooling mode is investigated, system pertubation on a stable cooling mode will be examined with the objective of examining the system response. Cold leg and UHI (upper head injection) injections will examine if natural circulation can be stalled and if it will recover; non-condensible gas will be injected to stall natural circulation and perhaps force a cooling mode change. We hope to be able to determine from the data how much the steam generator heat transfer is degraded. Transients induced from the secondary side will also be investigated such as steam generator dryout and recovery, excessive cooldown, and limited cooldown. The objective will be to investigate the primary system response, recovery of the primary system, and whether the secondary side induced transient causes a primary side cooling mode transition.

We feel that the natural circulation data developed from the FLECHT-SEASET program will compliment the Semiscale and PKL data as well as provide additional information for model development and system code verification.

B.) 21-ROD BUNDLE FLOW BLOCKAGE PROGRAM.

The objectives of the 21-rod bundle flow blockage program are given in Figure 12. A loop schematic for the 21-rod bundle test facility is shown in Figure 13 and a cross section of the test section is shown in Figure 14. A total of six blockage configurations were examined in the 21-rod bundle program as given in Figure 15. The FLECHT-SEASET flow blockage program which includes the 163-rod bundle to be tested in 1982 was designed to compliment both the Karlsruhe FEBA program and the international 2D/3D slab core flow blockage program in Japan. Two basic sleeve shapes were used to simulate the ballooned and burst fuel rods as shown in Figure 16. These sleeves are slipped over heater rods which had detailed thermocouple measurements downstream of the blockage. Vapor superheat measurements were made in the bundle by specially built subchannel steam probes and bare fluid thermocouples, which were attached to the grids in both the upflow and downflow directions.

Coplanar and non-coplanar blockage distributions were examined in the 21-rod bundle. Our definition of coplanar blockage is one in which all the maximum strain points are at the same elevation. Non-coplanar blockage is when all the maximum strain pounts do not align at the same elevation. Whether this alignment occurs or not can significantly affect the flow area in the bundle. Figure 17 shows the flow area for the short concentric sleeve for coplanar and non-coplanar distributions. As this figure indicates, a factor of three difference in flow area will result depending on the choice of coplanar versus non-coplanar. Examples of the sleeves configuration for different bundles are shown in Figure 18 and 19.

The heat transfer enhancement downstream of the blockage zone has been calculated for each blockage configuration. The enhancement is defined as shown in Figure 20 where the single phase heat transfer effects due to flow redistribution are accounted for using COBRA-IV. The resulting enhancement effect is the local heat transfer behavior due to two phase effects; (droplet breakup, vapor desuperheating, improved droplet/vapor heat transfer due to vapor acceleration) and single enhancement effects such as possible separation, increased turbulence and mixing. Plots of the enhancement for the highest power-to-flow test are shown in Figure 21 for the different sleeve shapes.

Examination of the non-coplanar blockage indicates that one blockage sleeve can induce additional cooling to adjacent rods and sleeves. The flow through the non-coplanar region "snakes" its way through the blockage zone being diverted from one subchannel to another depending on the local hydraulic resistance. Detailed instrumentation locations are shown in Figure 22 for the non-coplanar blockage distribution. The heater rod temperature and resulting heat transfer for an unblocked bundle and the blocked bundle at different elevations is shown in Figures 23 and 24. As the flow is diverted between blockage sleeves, a heat transfer improvement occurs. At the present time the percentage of heat transfer improvement due to convection, droplet breakup, vapor desuperheating and radiation effects are not known. The separation and quantification of these heat transfer mechanisms will be the continuing effort in the next year.

Its felt that the flow blockage program sponsored by the NRC/EPRI/W will address the Appendix K steam cooling flow blockage rule.

TABLE 1

FLECHT-SEASET

REPORTS ISSUED TO DATE

(CONTRACT NO. NRC-04-77-127)

REPORT NO.	TITLE	AUTHOR
1	PWR FLECHT Separate Effects and System Effects Tests (SEASET) Program Plan	C. E. Conway L. E. Hochreiter M. C. Krepinevich H. W. Massie, Jr. E. R. Rosal R. C. Howard
2	PWR FLECHT-SEASET Steam Generator Separate Effects Task Task Plan Report	L. E. Hochreiter R. C. Howard M. J. Loftus W. Kavalkovich H. W. Massie, Jr. M. C. Krepinevich M. C. McGuire A. E. Tome
3	PWR FLECHT-SEASET Unblocked Bundle, Forced and Gravity Reflood Task Task Plan Report	L. E. Hochreiter C. E. Wonway C. E. Dodge M. C. Krepinevich H. W. Massie, Jr. E. R. Rosal T. E. Sobek M. M. Valkovic
4 NUREG/CR-1366	PWR FLECHT-SEASET Steam Generator Separate Effects Task Data Report	R. C. Howard M. F. McGuire L. E. Hochreiter

5 NUREG/CR-1370	PWR FLECHT-SEASET 21-Rod Bundle Flow Blockage Task Task Plan Report	L. E. Hochreiter R. A. Basel R. J. Dennis N. Lee H. W. Massie, Jr. M. J. Loftus E. R. Rosal M. M. Valkovic
6 NUREG/CR-1531	PWR FLECHT-SEASET 161-Rod Bundle Flow Blockage Task Task Plan Report	L. E. Hochreiter N. Lee M. F. McGuire H. W. Massie, Jr. M. J. Loftus M. M. Valkovic
7	PWR FLECHT-SEASET Unblocked Bundle, Forced and Gravity Reflood Task Data Report	M. J. Loftus L. E. Hochreiter C. E. Conway C. E. Dodge A. Tong E. R. Rosal M. M. Valkovic S. Wong
8	Analysis Of The FLECHT-SEASET Unblocked Bundle Steam Cooling And Boiloff Tests	S. Wong L. E. Hochreiter

9

PWR FLECHT-SEASET
Unblocked Bundle, Forced And
Gravity Reflood Task:
Data Evaluation And Analysis

N. Lee
S. Wong
H. C. Yeh
L. E. Hochreiter

W/NRC/EPRI FLECHT-SEASET PROGRAM

THE GOALS OF THE PROGRAM ARE TO:

- ENHANCE THE UNDERSTANDING OF THE PHYSICS OF REFLOOD PHENOMENA IN PWRS.

- AID IN THE IMPROVEMENT OR FURTHER DEVELOPMENT OF THERMAL-HYDRAULIC MODELS AND/OR COMPUTER CODES FOR THE REFLOOD PHASE IN PWRS.

- AID IN THE VALIDATION OF BEST ESTIMATED THERMAL-HYDRAULIC MODELS AND/OR COMPUTER CODES FOR THE REFLOOD PHASE IN PWRS AND AID IN IMPROVING THE UNDERSTANDING OF SAFETY MARGINS ASSOCIATED WITH CURRENT LICENSING EVALUATION MODELS AND CRITERIA.

- BROADEN THE DATA BASE FOR PWR LOCA-ECCS SAFETY EVALUATIONS TO PERMIT A COORDINATED REAPPRAISAL OF EXISTING LICENSING CRITERIA.

- PROVIDE POST TMI DATA AND ANALYSIS ON REFLUX COOLING AND NATURAL CIRCULATION.

FIGURE 1

FLECHT-SEASET TASKS

17 X 17 UNBLOCKED FLECHT TESTS

- GEOMETRY EFFECTS, DATA BASE FOR BLOCKAGE
- PROVIDE DATA FOR REFLOOD CODE DEVELOPMENT/VERIFICATION (TRAC, RELAP MOD-6)

21 - ROD BUNDLE TESTS

- ASSESS BLOCKAGE GEOMETRY AND CONFIGURATION EFFECTS
- PROVIDE DATA FOR BLOCKAGE ANALYSIS METHOD

17 X 17 BLOCKED BUNDLE FLECHT TESTS

- BLOCKAGE AND BYPASS EFFECTS
- ADDRESS CURRENT LICENSING CRITERIA
- ASSESS BLOCKAGE ANALYSIS METHOD

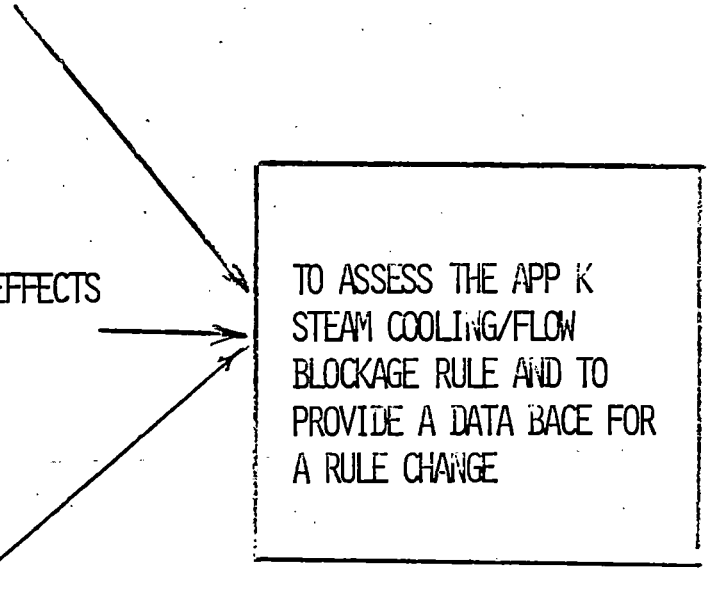

FIGURE 2

FLECHT-SEASET TASKS

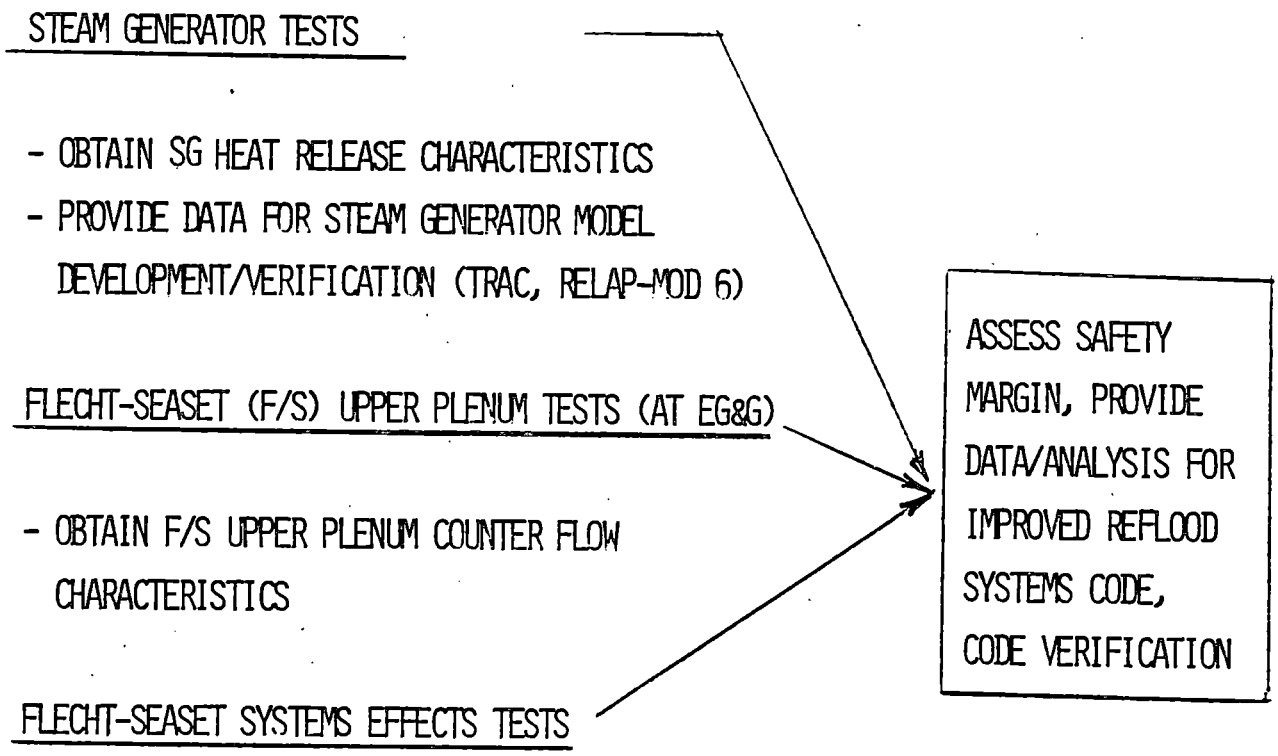

FIGURE 3

SYSTEM EFFECTS NATURAL CIRCULATION TASK:

OBJECTIVES

1. PROVIDE A SINGLE-PHASE AND TWO-PHASE NATURAL CIRCULATION DATA BASE OVER A RANGE OF ROD BUNDLE POWERS SUCH THAT NATURAL CIRCULATION CALCULATIONS CAN BE VERIFIED

2. EXAMINE CORE COOLING TRANSITIONS BETWEEN SINGLE-PHASE, TWO-PHASE, AND REFLUX CONDENSATION

3. EXAMINE SYSTEM REPONSE AND STABILITY WHEN IN A TWO-PHASE OR REFLUX CONDENSATION MODE, AND IN PARTICULAR, CHARACTERIZE THE STEAM GENERATOR BEHAVIOR IN THESE COOLING MODES.

FIGURE 4

FIGURE 5 FLECHT-SEASET SYSTEM EFFECT
NATURAL CIRCULATION AND REFLUX
CONDENSATION TEST FACILITY

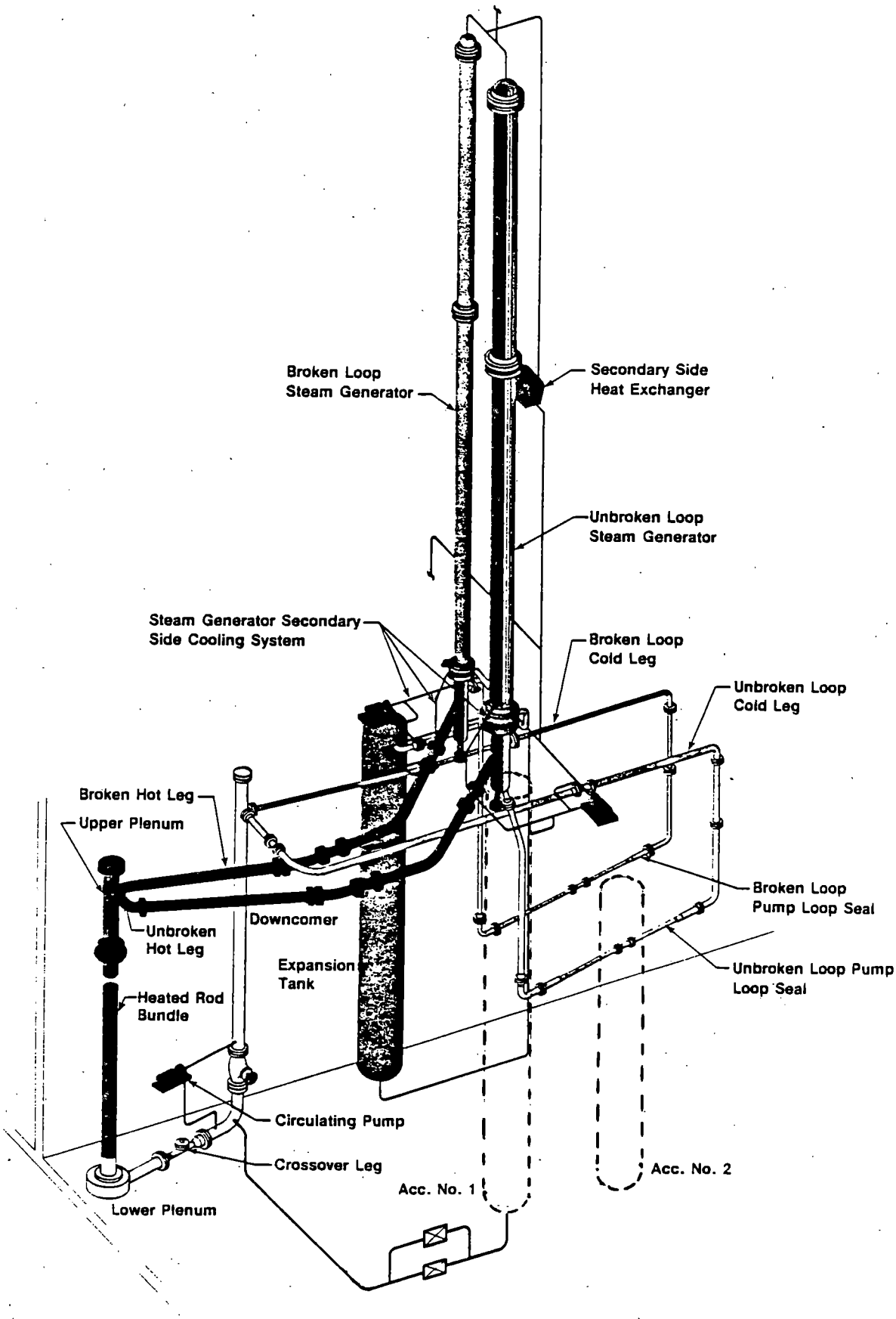

FIGURE 6
FLECHT-SEASET
NATURAL CIRCULATION AND REFLUX CONDENSATION
CONDENSATE FLOW MEASUREMENT SYSTEM

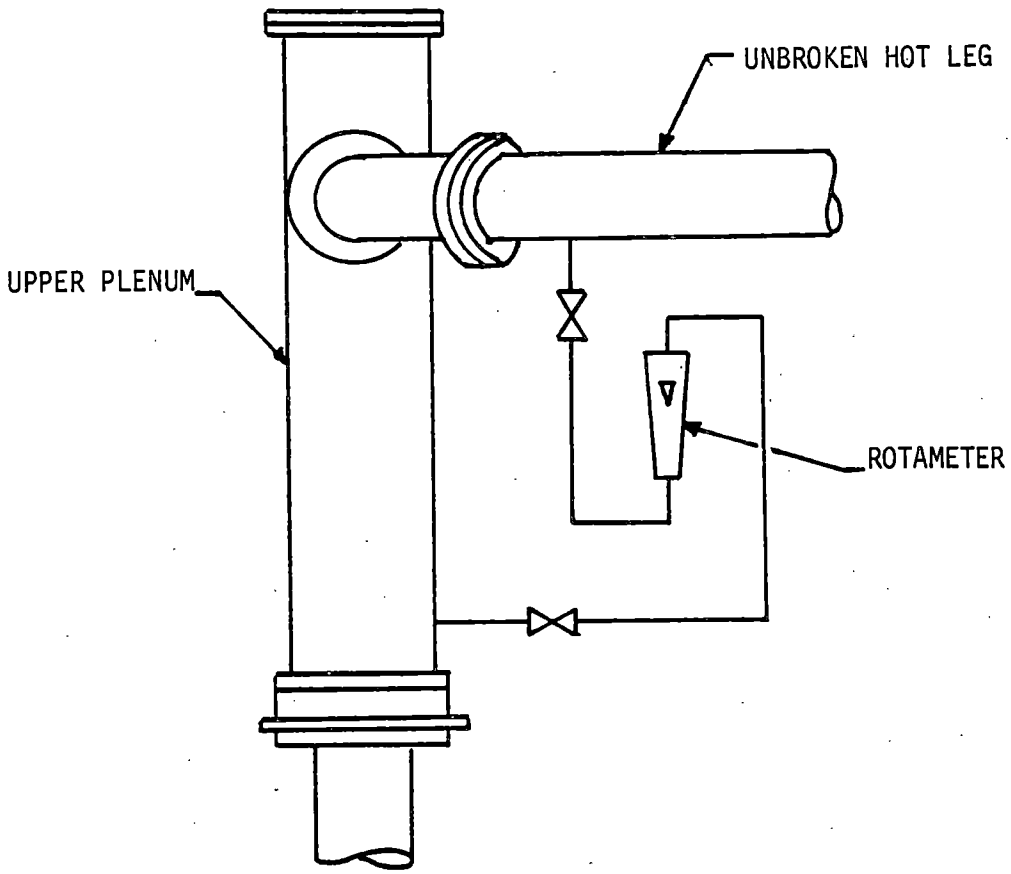

FIGURE 7
FLECHT-SEASET
NATURAL CIRCULATION
NON-CONDENSIBLE GAS SAMPLING SYSTEM

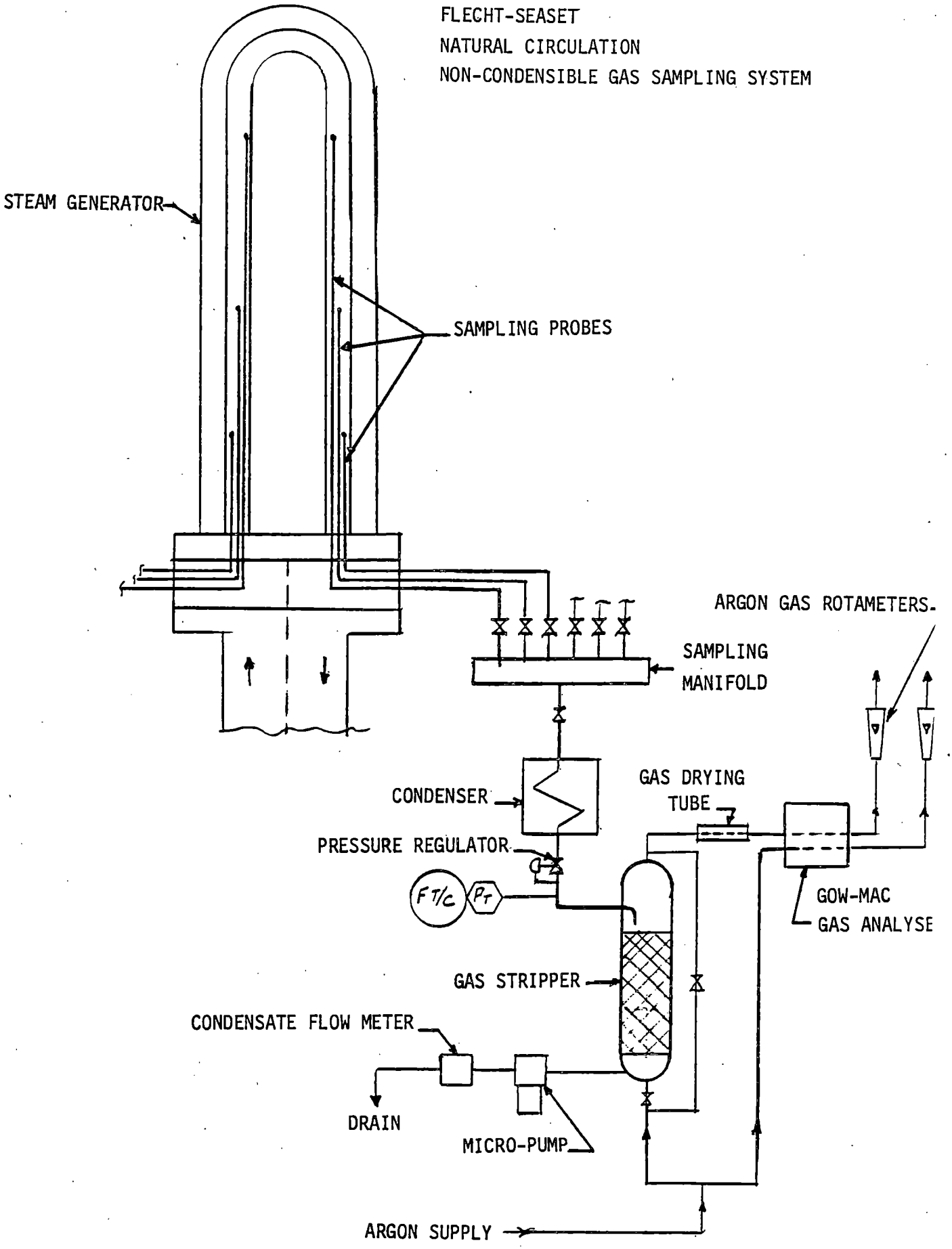

FIGURE 8

Rev. 7/29/81
Rev. 7/2/81
Rev. 1/16/81

FLECHT-SEASET NATURAL CIRCULATION AND REFLUX CONDENSATION TEST

Test Matrix

	Primary Side			Steam Gen. Sec. Side				Water Injection					
Test Number	Pressure	Bundle Power	Fluid Initial Temp.	Pressure	Fluid Temp.	Temp Rise(1)	Flow Condition Rate(1)	Liquid Level	Location	Subcooling	Rate(1)	Non-condensible Gas Injection Rate(1)	Test Description
	MPA (Psia)	Kw	$C^{o}(^{o}F)$	MAP (Psia)	$C^{o}(^{o}F)$	$C^{o}(^{o}F)$	M3/S (GPM)			$C^{o}(^{o}F)$	KG/Sec (lb/sec)	CC/MIN.	
1	0.69 (100)	22.2→66.9→ 111.2→222.4	125.6 (258)	0.14 (20)	Ambient	38.9 (70)	8.3E-3→8.5E-2 (2.2→22.5) Circulating	Full	-	-	-	-	Single Phase Reference Test
2	0.69 (100)	222.4→22.2	125.6 (258)	0.14 (20)	Ambient	38.9 (70)	8.5E-2 (22.5) Circulating	Full	-	-	-	-	Single Phase, power decay and constant heat sink effect
3	0.69 (100)	222.4	125.6 (258)	0.14 (20)	Ambient	38.9→25.5 (70→46)	8.5E-2→1.3E-1 (22.5→33.8) Circulating	Full	-	-	-	-	Single Phase, Increasing Heat Sink Capacity Effect
4	0.69 (100)	222.4	125.6 (258)	0.14 (20)	Ambient	38.9→76.1 (70→137)	8.5E-2→4.23E-2 (22.5→11.2) Circulating	Full	-	-	-	-	Single Phase, Decreasing Heat Sink Capacity Effect
5	0.69 (100)	222.4	125.6 (258)	0.14 (20)	Ambient	38.9 (70)	8.5E-2 (22.5) Circulating	Full	Cold Leg	77.8(140)	0.76 (1.67)	-	Single Phase, Cold Leg Injection Effect
6	0.69 (100)	222.4	125.6 (258)	0.14 (20)	Ambient	38.9 (70)	8.5E-2 (22.5) Circulating	Full	-	-	-	4107 For 5 Min.	Single Phase, Non-condensible Gas Injection Effect Into Both Hot Legs

Note: (1) Nominal Values

FIGURE 9

FLECHT-SEASET NATURAL CIRCULATION AND REFLUX CONDENSATION TEST

Rev. 7/29/81
Rev. 7/2/81
Rev. 1/16/81

Test Matrix

	Primary Side			Steam Gen. Sec. Side					Water Injection				
Test Number	Pressure	Bundle Power	Fluid Initial Temp.	Pressure	Fluid Temp.	Temp. Rise(1)	Flow Condition Rate(1)	Liquid Level	Location	Subcooling	Rate(1)	Non-condensible Gas Injection Rate(1)	Test Description
	MPA (Psia)	Kw	C^{o} (^{o}F)	MAP (Psia)	C^{o} (^{o}F)	C^{o} (^{o}F)	M3/S (GPM)			C^{o} (^{o}F)	KG/Sec (lb/sec)	CC/MIN.	
7	0.69 (100)	222.4	125.6 (258)	0.14 (20)	Ambient	38.9 (70)	8.5E-2 (22.5) Circulating	Full	-	-	-	1020 For 5 Min.	Single Phase, Non-condensible Gas Injection Effect Into Broken Leg only
8	0.69 (100)	222.4	125.6 (258)	0.69 (100)	Ambient → 170.6 (319)	38.9→5.6 (70→10)	8.5E-2→6.06E-1 (22.5→160.0) Circulating	Full	-	-	-	-	Single Phase to Two-Phase To Reflux Condensation Transient Test
9	0.69 (100)	222.4	125.6 (258)	0.103 (15)	Ambient →98.9 (210)	77.8 (140)	Boiling to Dryout and Refill	10.7 0 M (35 → 0 FT) AND 0→10.7M (0 → 35 FT)	-	-	-	-	Single Phase to Two-Phase to Reflux Condensation Transient Test, Secondary Side Effects
10	0.69 (100)	222.4	125.6 (258)	0.103 (15)	Ambient →98.9 (210)	77.8 (140)	Boiling at Const. Level	3/4	Upper Plenum	77.8 (140)	0.42 (0.94) for 347 sec.	-	Single Phase, Two Phase, and Reflux Cond. Transient with UHI Simulation

Note: (1) Nominal Values

FIGURE 10

Rev. 7/29/81
Rev. 7/2/81
Rev. 1/16/81

FLECHT-SEASET NATURAL CIRCULATION AND REFLUX CONDENSATION TEST

Test Matrix

	Primary Side			Steam Gen. Sec. Side				Water Injection					
Test Number	Pressure	Bundle Power	Fluid Initial Temp.	Pressure	Fluid Temp.	Temp. Rise(1)	Flow Condition Rate(1)	Liquid Level	Location	Subcooling	Rate(1)	Non-condensible Gas Injection Rate(1)	Test Description
	MPA (Psia)	Kw	$C^{O}(^{O}F)$	MAP (Psia)	$C^{O}(^{O}F)$	$C^{O}(^{O}F)$	M3/S (GPM)			C^{O}(F)	KG/Sec (lb/sec)	CC/MIN.	
11	0.69 (100)	222.4	125.6 (258)	0.103 (15)	Ambient 98.9 210	77.8 (140)	Boiling at Const. Level	3/4	Cold Leg	77.8 (140)	0.76 (1.67)	-	Two Phase, Cold Leg Injection Effect
12	0.69 (100)	222.4	125.6 (258)	0.14 (20)	Ambient	38.9 (70)	8.5E-2 (22.5) Circulating	Full	Cold Leg	77.8 (140)	0.76 (1.67)	-	Reflux Mode, Cold Leg Injection Effect to Recovery of Single-Phase Mode
13	0.69 (100)	222.4	125.6 (258)	0.14 (20)	Ambient	38.9 (70)	8.5E-2 (22.5) Circulating	Full	-	-	-	4107 For 5 Min.	Two-Phase Mode, Non-Condensible Gas Injection Injection
14	0.69 (100)	222.4	125.6 (258)	0.103 (15)	Ambient →98.9 (210)	77.8 (140)	Boiling	10.7M→MIN. (35 FT→MIN)	-	-	-	-	Single Phase Mode, Minimum Secondary Heat Sink Effect
15	0.69 (100)	222.4	125.6 (258)	0.14 (20)	Ambient	38.9 (70)	8.5E-2 (22.5) Circulating	Full	-	-	-	4107 For 5 Min.	Reflux Mode, Non-Condensible Gas Injection Effects

Note: (1) Nominal Values

FIGURE 11

Rev. 7/29/81
Rev. 7/2/81
Rev. 1/16/81

FLECHT-SEASET NATURAL CIRCULATION AND REFLUX CONDENSATION TEST

Test Matrix

	Primary Side			Steam Gen. Sec. Side				Water Injection					
Test Number	Pressure	Bundle Power	Fluid Initial Temp.	Pressure	Fluid Temp.	Temp. Rise(1)	Flow Condition Rate(1)	Liquid Level	Location	Subcooling	Rate(1)	Non-condensible Gas Injection Rate(1)	Test Description
	MPA (Psia)	Kw	C^{O} (^{O}F)	MAP (Psia)	C^{O}(^{O}F)	C^{O}(^{O}F)	M3/S (GPM)			C^{O}(F)	KG/Sec (lb/sec)	CC/MIN.	
16	0.69 (100)	222.4	125.6 (258)	0.14 (20)	Ambient	38.9→75.5 (70→46)	8.5E-2→12.8E-2 (22.5→33.8) Circulating	Full	-	-	-	-	Two-Phase Mode, Increased Heat Sink Effect
17	0.69 (100)	222.4	125.6 (258)	0.103 (15)	Ambient →98.9 (210)	77.8 (140)	Boiling Brok. St. Gen. To Dry and Refill	BR. ST. GEN. 10.7 → 0 m (35→0 FT) AND 0→10.7M (0 → 35 FT)		-	-	-	Two-Phase Mode, Reduced Heat Sink Effect
18	0.69 (100)	222.4	125.6 (258)	0.14 (20)	93.3 (200)	5.6→8.3 (10→15)	Circulating 6.1E-1 (160)	Full	-	-	-	-	Reflux Mode, Increased Heat Sink Effect
19	0.69 (100)	222.4	125.6 (258)	0.103 (15)	Ambient →98.9 (210)	77.8 (140)	Boiling Brok St. Gen. To Dry and Refill	BR. ST. GEN. 10.7 → 0 M (35 → 0 FT) AND 0→10.7M (0 → 35 FT)		-	-	-	Reflux Mode, Decreased Heat Sink Effect
20	To be Determined												

21-ROD BUNDLE TASK OBJECTIVES

- TO OBTAIN, EVALUATE, AND ANALYZE THERMAL HYDRAULIC DATE USING 21-ROD BUNDLES TO DETERMINE THE EFFECTS OF FLOW BLOCKAGE GEOMETRY VARIATION ON THE REFLOOD HEAT TRANSFER.

- TO GUIDE THE SELECTION OF A BLOCKAGE SHAPE FOR USE IN THE LARGE BLOCKED BUNDLE TASK. (1)

- TO DEVELOP AN ANALYTICAL OR EMPIRICAL METHOD FOR USE IN ANALYZING THE BLOCKED BUNDLE HEAT TRANSFER DATA.

FIGURE 12

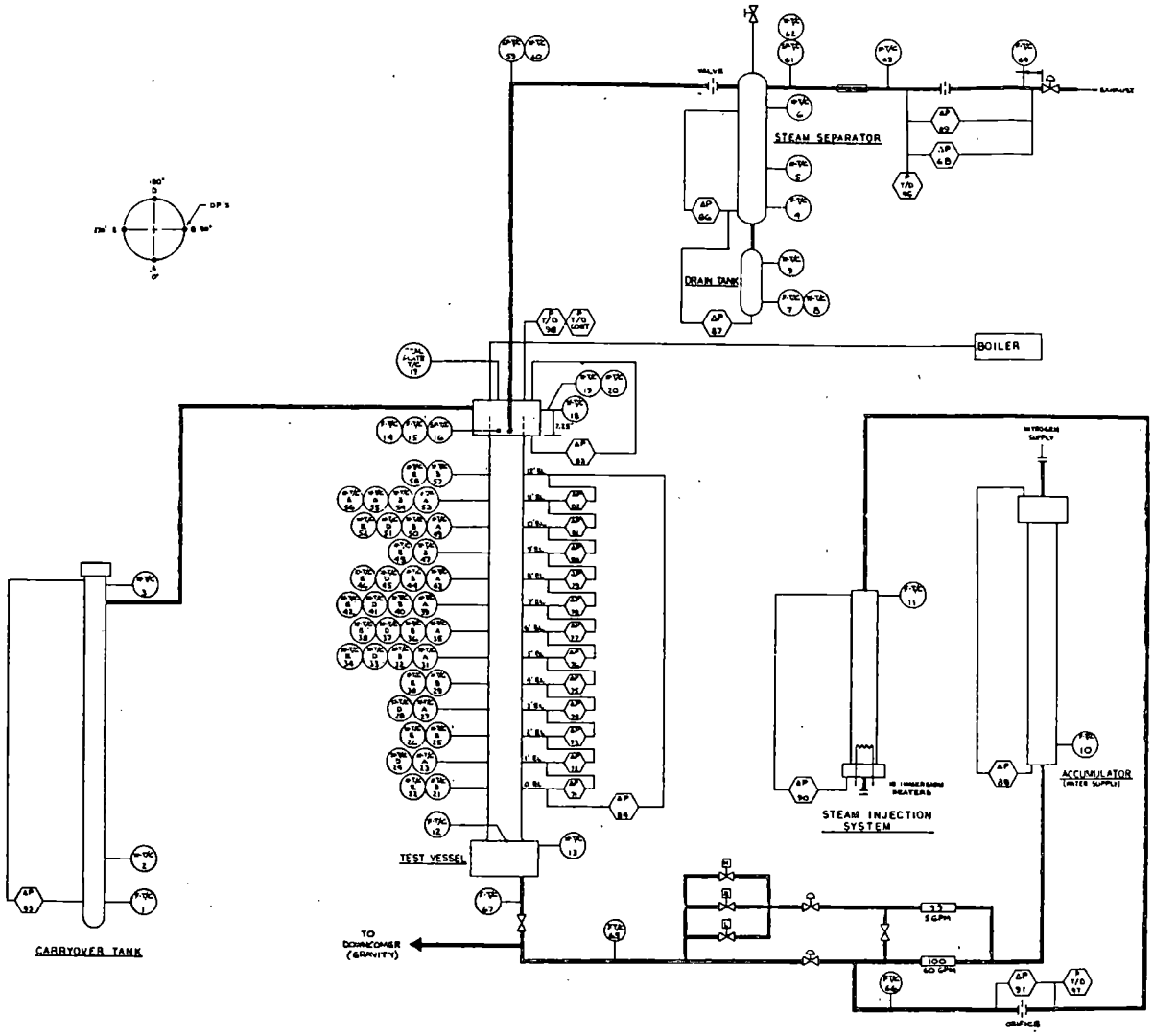

21-Rod Bundle Flow Blockage Task
Instrumentation Schematic Diagram
(sheet 1 of 2) (Drawing No. 1460E40)

FIGURE 13

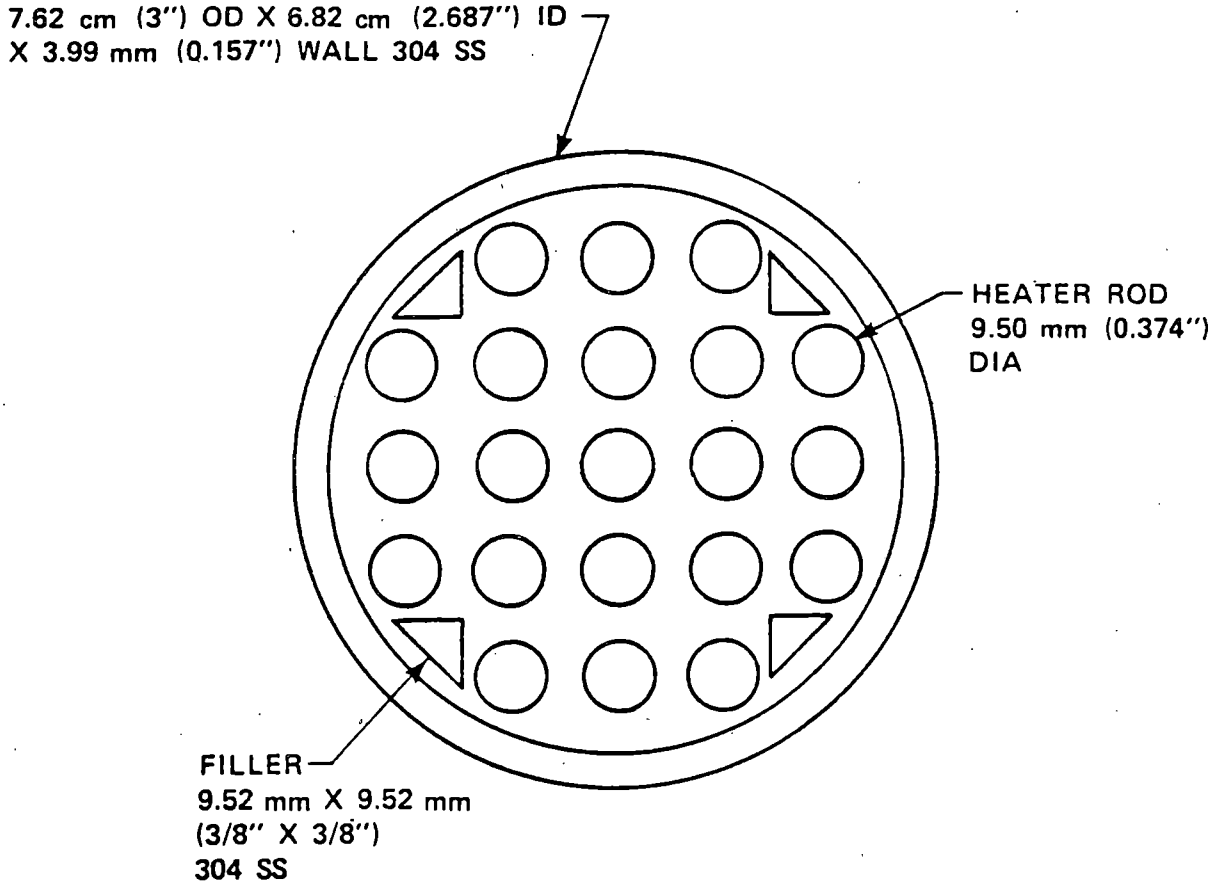

Figure 14 21-Rod Bundle Test Section Cross Section

- 21-ROD BUNDLE PROGRAM WILL TEST:

A - UNBLOCKED REFERENCE

B - 9 RODS BLOCKED COPLANAR, 62%, SHORT CONCENTRIC SLEEVE (SLEEVES JUST TOUCHING)

C - 21 RODS BLOCKED COPLANAR, 62%, SHORT CONCENTRIC SLEEVE

D - 21 RODS BLOCKED NON COPLANAR, SHORT CONCENTRIC SLEEVE

E - 21 RODS BLOCKED NON COPLANAR, LONG NON CONCENTRIC SLEEVE (36% MAX STRAIN)

F - 21 RODS BLOCKED NON-COPLANAR, LONG NON-CONCENTRIC SLEEVE (44% MAX STRAIN)

- 163 ROD BUNDLE WILL BLOCK TWO 21 ROD BUNDLE ISLAND WITH WORST STRAIN .

FIGURE 15

FIGURE 16

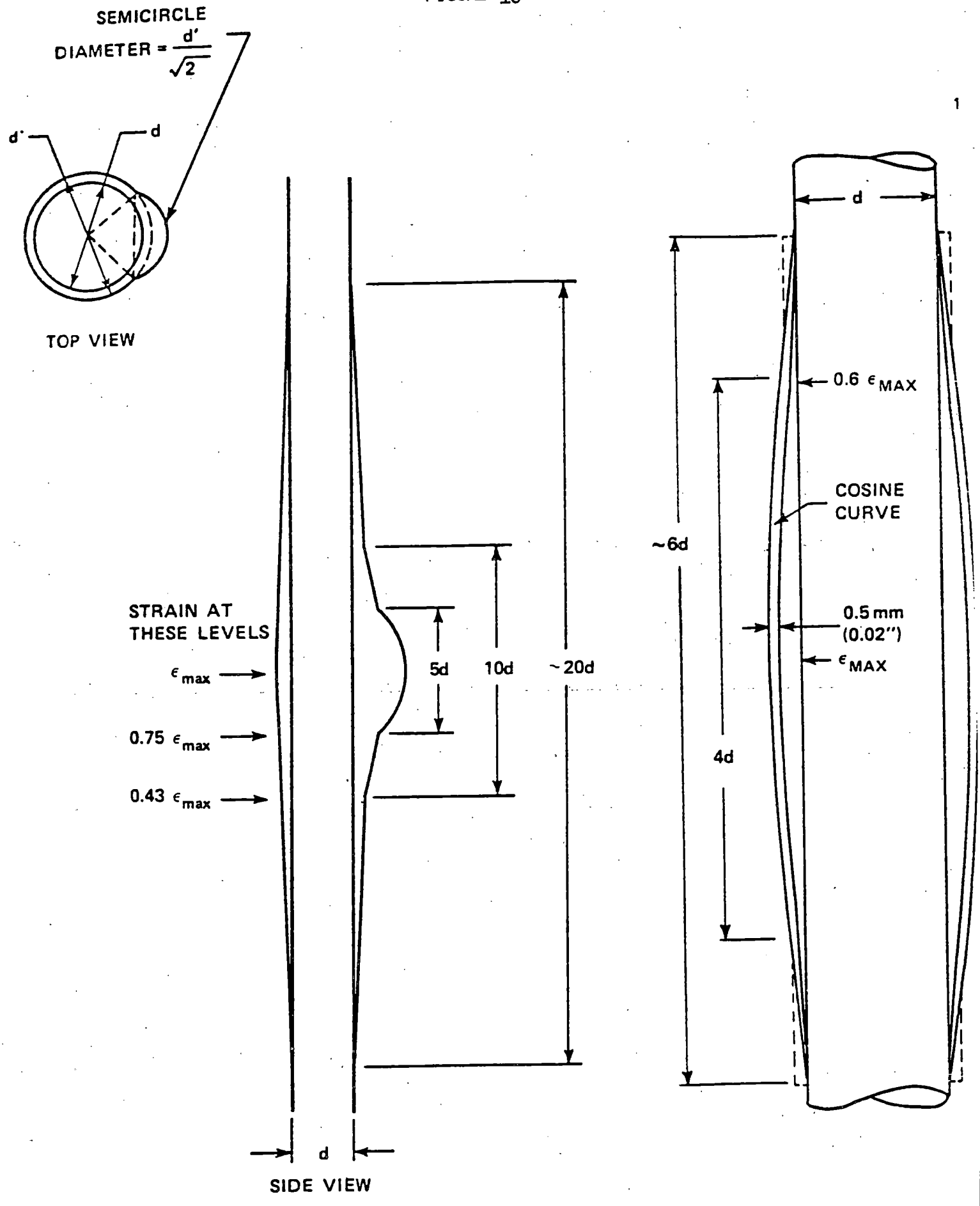
SEMICIRCLE
DIAMETER = d'/√2
d'
d
TOP VIEW
STRAIN AT
THESE LEVELS
ϵ max
0.75 ϵ max
0.43 ϵ max
5d
10d
~20d
d
SIDE VIEW
d
0.6 ϵ MAX
COSINE
CURVE
~6d
0.5 mm
(0.02")
ϵ MAX
4d

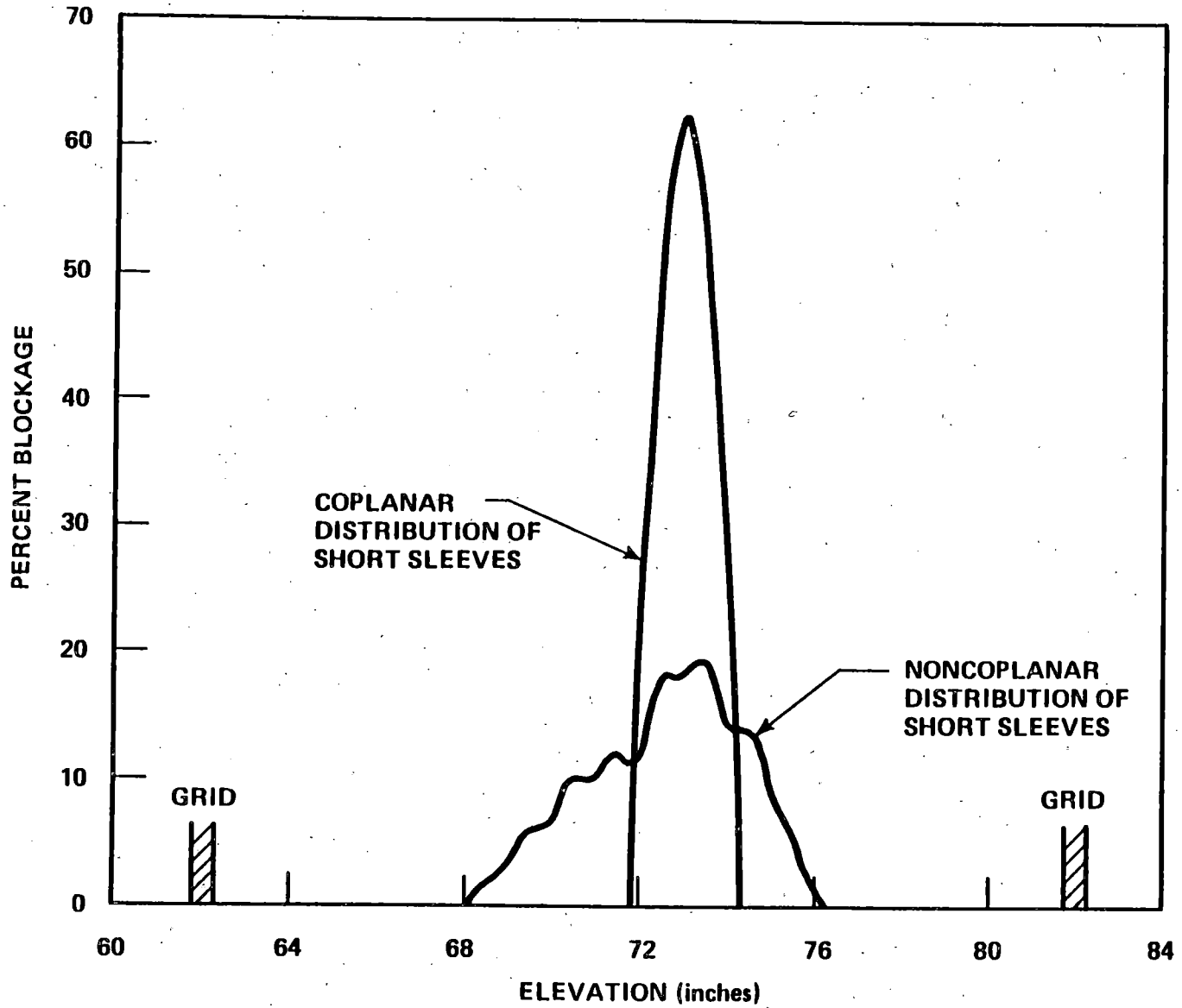

Figure 17 Bundle Blockage Distribution of 21 Rod Bundle

19851-2

PHOTOGRAPH OF 21-ROD BUNDLE D WITH SHORT SLEEVES

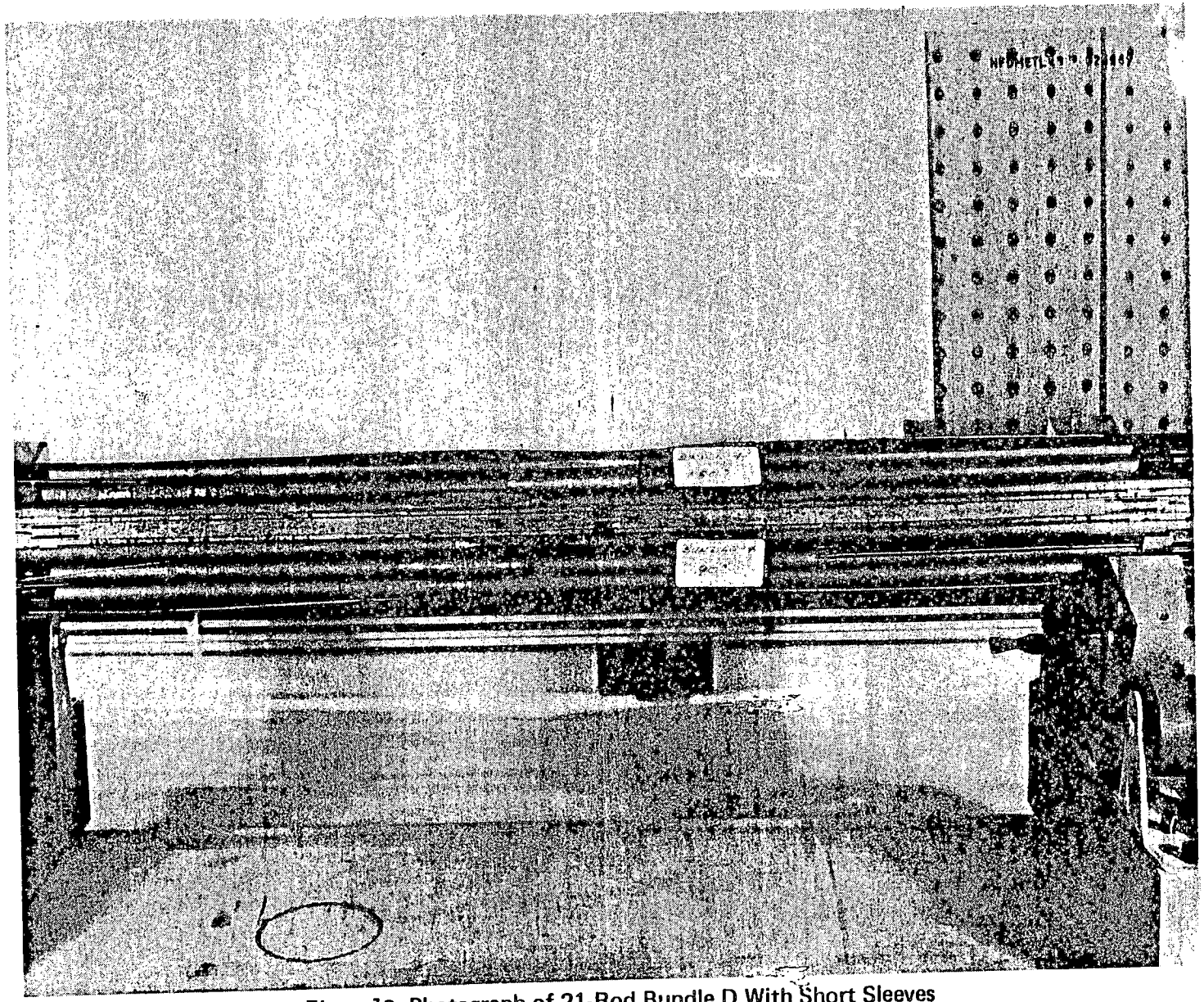

Figure 18 Photograph of 21-Rod Bundle D With Short Sleeves

PHOTOGRAPH OF 21-ROD BUNDLE E WITH LONG SLEEVES

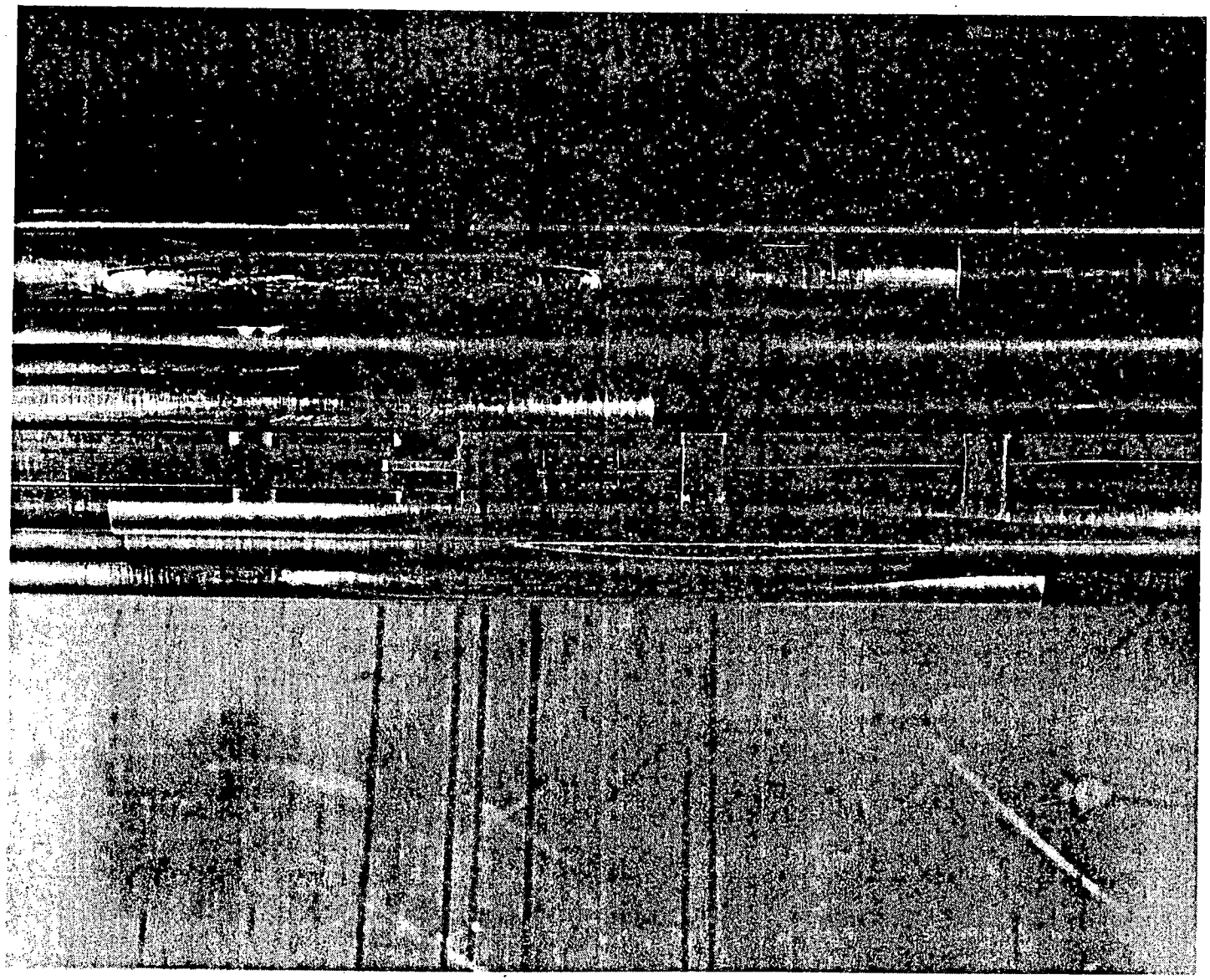

Figure 19 Photograph of 21-Rod Bundle E With Long Sleeves

HEAT TRANSFER ENHANCEMENT

$$\frac{H_B}{H_O} = N_E \left[\frac{\rho U)_B}{\rho U)_O} \right]^M$$

OR

$$N_E = \frac{H_B}{H_O} \Big/ \left[\frac{\rho U)_B}{\rho U)_O} \right]^M$$

FIGURE 20

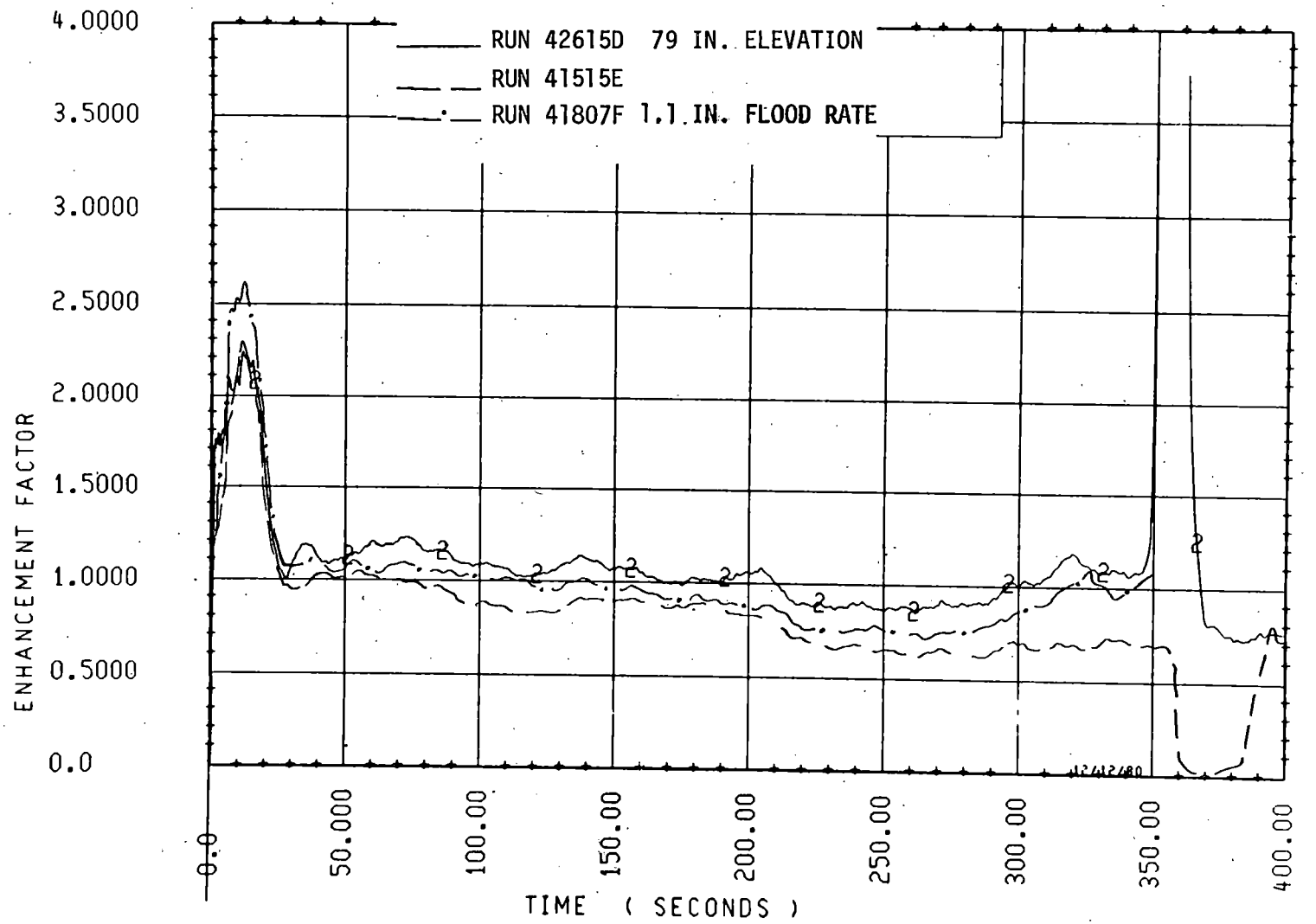
RUN 42615D 79 IN. ELEVATION
RUN 41515E
RUN 41807F 1.1 IN. FLOOD RATE
ENHANCEMENT FACTOR
4.0000
3.5000
3.0000
2.5000
2.0000
1.5000
1.0000
0.5000
0.0
0.0
50.000
100.00
150.00
200.00
250.00
300.00
350.00
400.00
TIME (SECONDS)

FIGURE 21

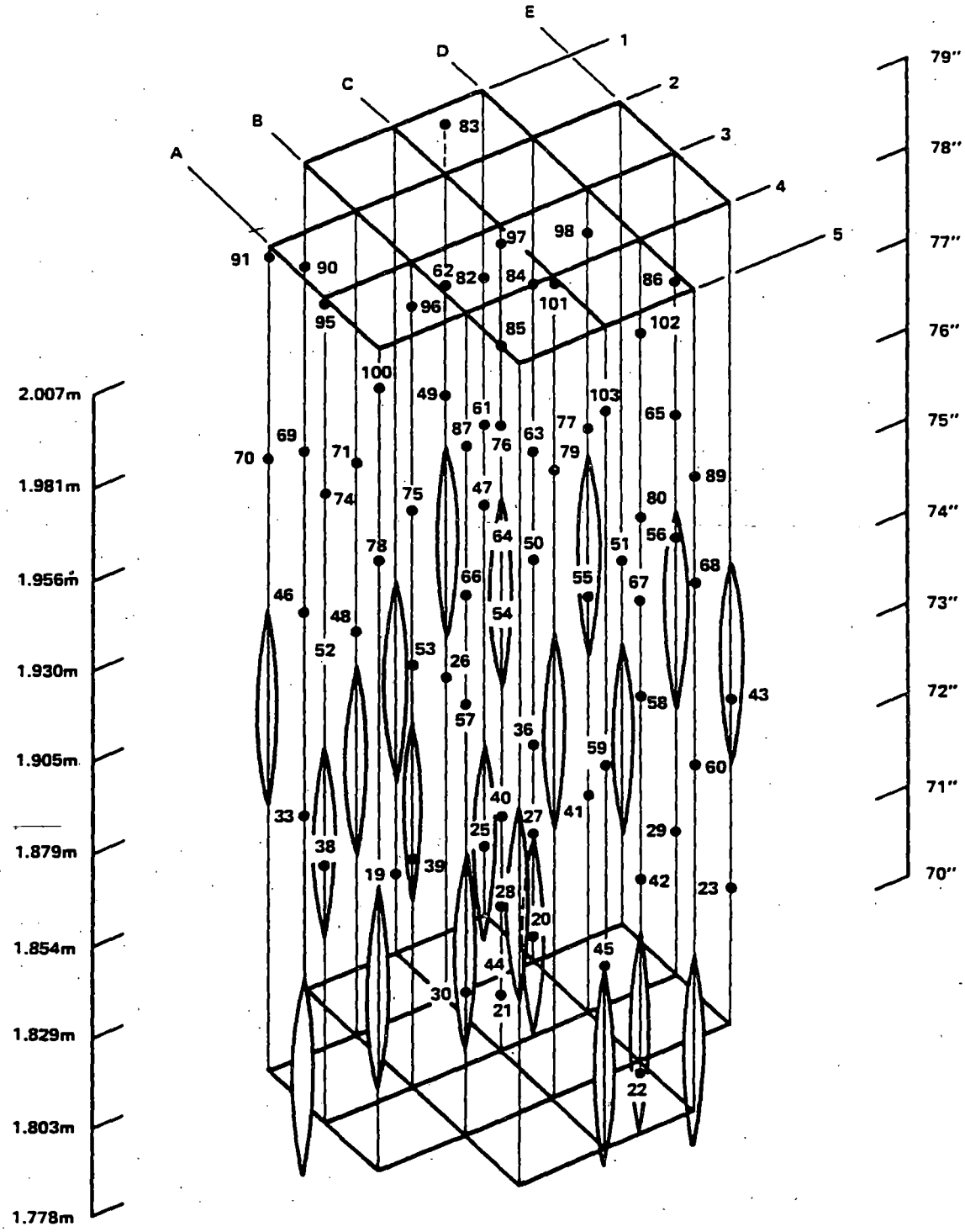

Figure 22 Bundle D Blockage Distribution

FUEL ROD SIMULATION TEMPE ATURE DATA FOR BUNDLES D AN) A

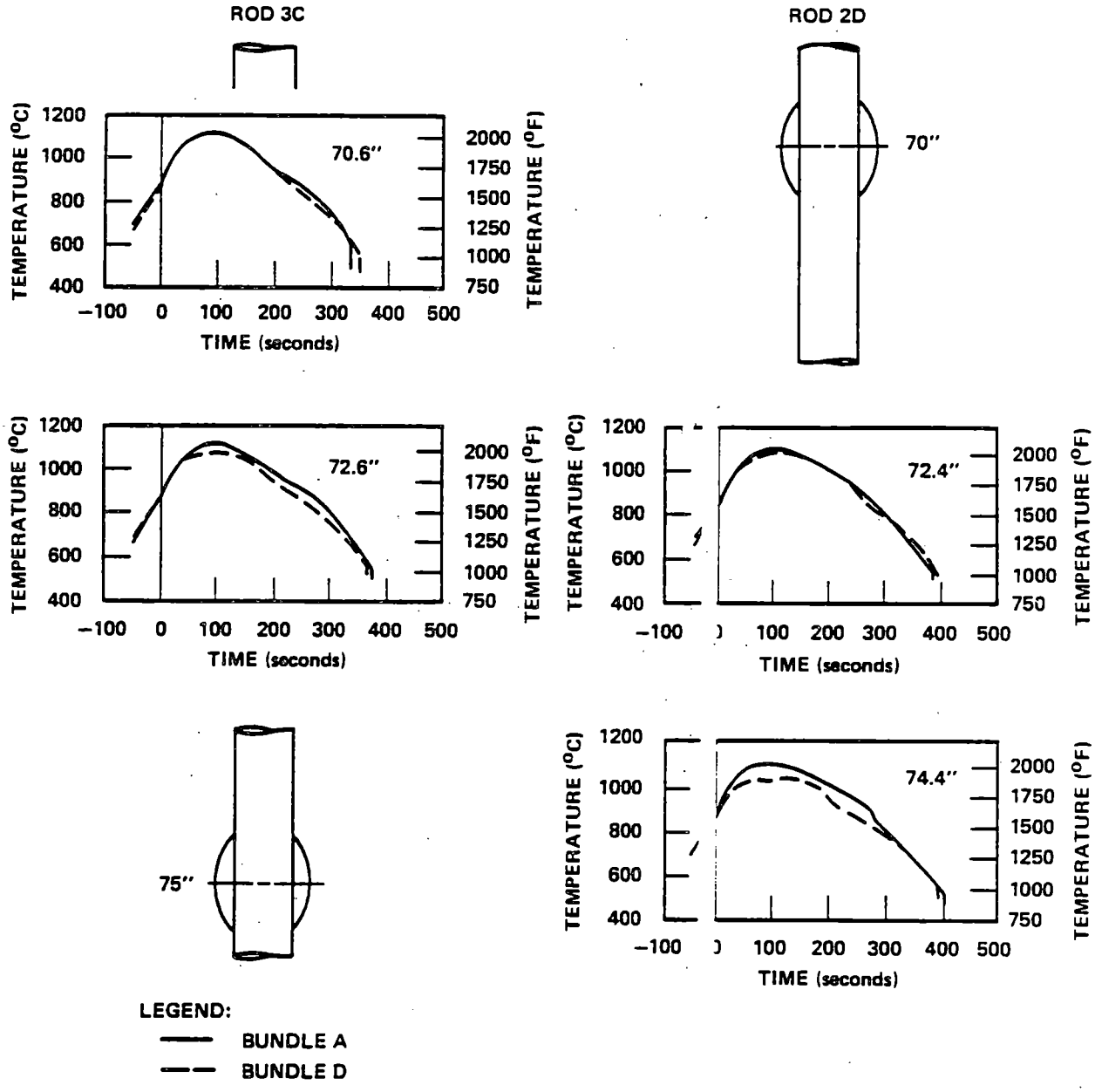

Figure 23 Fuel Rod Simulator Temperature Dat for Bundles D and A

FUEL ROD SIMULATOR TEMPERATURE DATA FOR BUNDLES D AND A (CONTINUED)

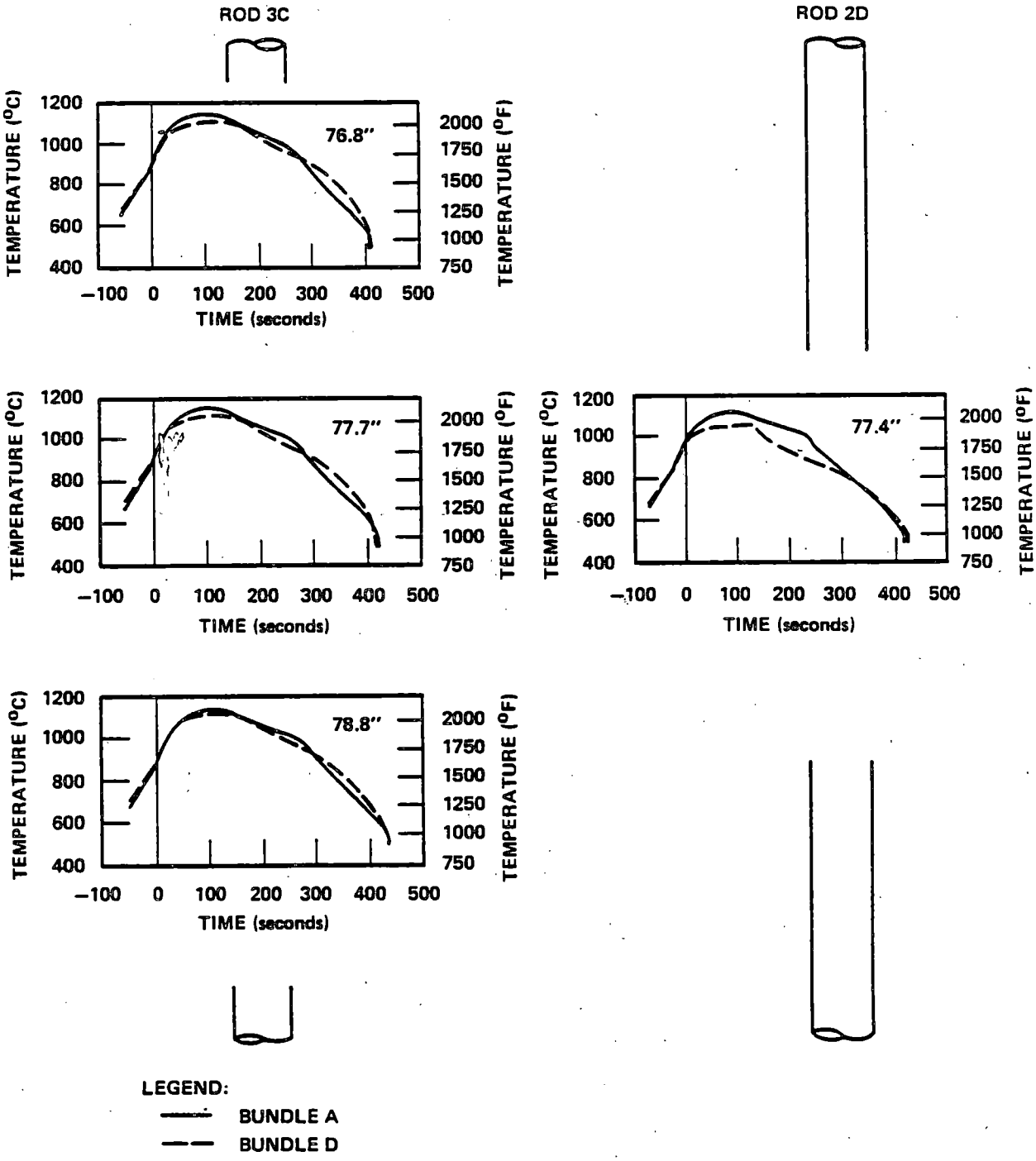

Figure 24 Fuel Rod Simulator Temperature Data for Bundles D and A

Phenomenological Modeling of Two-phase Flow in Water Reactor at ANL

(Two-fluid Model, Interfacial Area, Droplet Entrainment and Droplet Size)

by

M. Ishii
I. Kataoka
G. Kocamastafaogullari*

Reactor Analysis and Safety Division
Argonne National Laboratory

Presented at the NRC 9th Water Reactor Safety Research Information Meeting, Oct. 26-30, 1981, Gaithersburg

*University of Wisconsin at Milwaukee.

Abstract

This is a summary of the research progress on the phenomenological modeling of two-phase flow during 1981 at Argonne National Laboratory. The purpose of this NRC sponsored research is to develop rigorous two-phase flow models and correlations which are the foundation of the reliable and accurate LWR codes. Particular emphasis is on the establishment of the two-fluid model, derivation of interfacial transfer terms and prediction of hydrodynamic transients.

The interfacial transfer terms are the weakest link in a two-fluid model formulation because of considerable difficulties in terms of experimentation as well as modeling. However, these terms are of supreme importance for a two-fluid model in determining phase interactions between liquid and vapor. In view of these, the interfacial transfer terms have been studied in detail and new constitutive relations have been developed. The interfacial terms are proportional to the interfacial area and driving force, therefore, these two effects are modeled separately.

Particular accomplishments under this program are listed below:

1. Completed a framework for interfacial area correlations in bubbly, churn, annular and droplet annular flow.

2. Developed a correlation for the amount of droplet entrainment in annular two-phase flow.

3. Developed a correlation for a droplet size distribution in annular two-phase flow.

4. Developed a correlation for a bubble number density based on a wall nucleation model.

I. Introduction

In predicting two-phase flow transients in nuclear reactors under various accident conditions, the interfacial transfer terms are among the most essential factors in the modeling. These interfacial transfer terms in a two-fluid model specify the rate of phase change, momentum exchange and heat transfer at the interface between phases.

A two-fluid model [1-8] is formulated in terms of two sets of conservation equations governing the balance of mass, momentum and energy of each phase. Since the macroscopic fields of one phase are not independent of those of the other phase, the interaction terms which couple the transport of mass, momentum and energy of each phase across the interfaces appear in the field equation [1]. In the two-fluid model formulation, the transport processes of each phase are expressed by their own balance equations, therefore, it is expected that the model can predict more detailed changes and phase interactions than a mixture model such as the drift flux model [9-10]. In particular, for two-phase flow problems involving a sudden acceleration of one phase, inertia terms of each phase should be considered separately by use of a two-fluid model.

Previous studies have indicated that unless phase interaction terms are accurately modeled in a two-fluid model, complications in the modeling does not necessarily warrant accurate solutions. For example, physically improper solutions and numerical instabilities are frequently encountered in the numerical solution of two-fluid models. A recent study by Lahey et al. [11] has demonstrated that virtual mass originating from momentum interaction between the two phases had a considerable effect on improving numerical stability and efficiency. It has also been suggested [12] that the interaction terms should include first-order time and spatial derivatives. Zuber [13] and others

[14-16] indicated that the momentum interaction term should have time and spatial derivatives and an integral term which expresses short time memory of the fluid. Another approach to achieving numerical stability is the inclusion of "artificial viscosity" in the numerical algorithm to damp out high frequency oscillations occurring possibly due to imprecise modeling. This approach is currently being followed by Amsden and Harlow [7] in their two-fluid digital computer codes. In spite of these shortcomings of a two-fluid model, there is, however, no substitute available for modeling accurately two-phase phenomena where two phases are not strongly coupled as in an entrance flow or suddenly accelerating flow.

The weakest link in the two-fluid model formulation is the constitutive equations for the interfacial interaction terms. The difficulties arise due to the complicated motion and geometry of interfaces in a general two-phase flow. Furthermore, these constitutive equations should be expressed by the macroscopic variables based on proper averaging. As has been shown in detail [1, 17], the interfacial transfer terms in a two-fluid model appear as averaging of local instant transfers of mass, momentum and energy. Because these terms appear as source terms in the field equations, proper averaging alone is not sufficient to develop these constitutive equations. It is essential, therefore, to clarify different physical mechanisms controlling these interfacial transfers as well as to identify important parameters which govern them.

The interfacial transfer terms are strongly related to the interfacial area concentration and to the local transfer mechanisms such as the degree of turbulence near interfaces [1]. Basically, the interfacial transport of mass, momentum and energy is proportional to the interfacial area concentration, a_i, and to a driving force. This parameter, a_i, having the dimension of the

reciprocal of length, characterizes the geometrical effects on the interfacial transfers. On the other hand, the driving forces for the interfacial transports depend on the local turbulence, transport properties, driving potentials and some length scale at the interfaces. This length scale may be related to a transient time such as the particle residence time or to the interfacial area concentration and void fraction α.

The primary objective of the present research is to develop constitutive relations for interfacial transfer terms for a two-fluid model. In particular, the interfacial area concentration has been studied in detail here. An extensive literature survey on the existing experimental data has been completed, and a preliminary analysis on the modeling of the interfacial area concentration has been carried out. It has been shown that the existence and size of small fluid particles is very important in determining the interfacial area for all flow regimes. In view of these, the amount of droplet entrainment and droplet size distribution in annular two-phase flow have been correlated using a simple model based on a force balance at the wave interface. For a bubbly flow the bubble number density is expressed in terms of the wall nucleation sites and heterogeneous bulk nucleation sites.

II. Interfacial Area

A number of experimental studies on interfacial area have been published in chemical engineering fields in the past 15 years. These, and some of the existing correlations for interfacial area, have been reviewed in detail [18]. It indicates that the ranges of available data are very limited. For example, there are no data at higher liquid flow rates beyond j_f = 0.5 m/s. Data for the bubbly to slug flow transition range are missing. Most of the data covers the slug to churn and churn to annular flow transitions. Data at very low

liquid flow and high gas flux are quite inadequate. Apparently there are no data on interfacial areas in counter-current and cocurrent down flows which are important in terms of reactor applications.

There are some interfacial area correlations. These are correlated in terms of a frictional pressure drop and certain velocity scale. Generally, a power relation between the interfacial area a_i and these parameters are assumed. However, it was found that the results strongly depend on system geometries and possibly on the void fraction. Both the power and proportionality constants changed considerably with system geometries. There are no models available to calculate these constants without data for that particular system. In other words, these existing correlations may be useful to rearrange data into a practical empirical correlation, however, the use of it cannot be extended to other systems.

From a physical point of view, there is no doubt that there exists some relation between the fractional pressure drop and the interfacial area. Furthermore, there is a practical advantage for a chemical engineer to use the above correlation methods because in most cases a simple prototypic experiment can be carried out to establish a necessary data base. However, for general two-phase flow systems, the above mentioned methods may not be suitable. Since the interfacial area concentration is a parameter which characterizes the structure of a flow, its mechanistic modeling should have been based on geometrical factors, void fraction and flow. It may be noted that the frictional pressure drop also depends on similar parameters, however, this does not justify the use of a direct relation between a_i and $[\partial p/\partial z]_{fr}$. This mechanistic approach was first suggested by Ishii [1] and subsequently used by Saha [19] in his estimate of interfacial areas. In this study, a preliminary correlation for interfacial area are developed based on the mechanistic approach [18].

Basically four flow regimes, namely, dispersed (bubbly or droplet), slug, churn-turbulent and annular flows have been modeled separately and general characteristics of the prediction have been discussed. The model shows the importance of the existence and size of small fluid particles for all flow regimes. These correlations for interfacial area require the knowledge of fluid particle sizes and number density, therefore, a detailed analysis in this area has been made [20-22]. These are summarized below.

III. Amount of Entrainment

A correlation for the amount of entrained liquid in annular two-phase flow has been developed from a simple model and experimental data. The fraction of liquid flux flowing as droplets, E, is correlated in terms of three dimensionless groups given by

Dimensionless Gas Flux

$$j_g^* = \frac{j_g}{\left[\frac{\sigma g \Delta\rho}{\rho_g^2}\left(\frac{\rho_g}{\Delta\rho}\right)^{2/3}\right]^{1/4}}$$

Total Liquid Reynolds Number

$$Re_f = \frac{\rho_f j_f D}{\mu_f}$$

Dimensionless Diameter

$$D^* = D\sqrt{\frac{g\Delta\rho}{\sigma}} \quad .$$

The entrained fraction reaches a quasi-equilibrium value, E_∞, at points far removed from the tube entrance where the entrainment and deposition processes attain an equilibrium condition. The distance necessary to reach this condition is given approximately by

$$z \simeq 600\ D\sqrt{\frac{j_g^*}{Re_f}}$$

for cases with smooth liquid injection. At this entrance length the entrainment has reached within about 2% of its ultimate value. Then for the region $z \gtrsim 600\ D \sqrt{j_g^*/Re_f}$ the correlation becomes

$$E \simeq E_\infty = \tanh\ (7.25 \times 10^{-7}\ j_g^{*2.5}\ D^{*1.25}\ Re_f^{0.25}) \quad .$$

This correlation has been compared to many experimental data for air-water systems in the ranges of $1 < p < 4$ atm, $0.95 < D < 3.2$ cm, $370 < Re_f < 6400$, and $j_g < 100$ m/sec, and the result has shown to be satisfactory. The various parametric dependencies have been explained in terms of physical mechanisms and information obtained from the onset of entrainment criterion developed previously.

Some experimental data indicated the strong entrance effect as well as the gas expansion effect due to the axial pressure drop in a low pressure system. For the correlation development it was essential to use a local gas velocity or volumetric flux based on a local pressure in evaluating data. By separating these two effects, an additional correlation for the entrance effect on entrainment have been developed. As mentioned above, the entrance region is given by $0 < z < 600\ D \sqrt{j_g^*/Re_f}$. The correlation takes a typical form of an exponential relaxation, and it essentially reaches the quasi-equilibrium value given by E_∞ for large values of z, thus

$$E = (1 - e^{-10^{-5}\zeta^2})E_\infty \quad .$$

Here ζ is the dimensionless distance given by

$$\zeta = \frac{z}{D}\sqrt{\frac{Re_f}{j_g^*}} \quad .$$

Because of the nature of the above equation this correlation is not limited to the entrance region, but it can be used as a general correlation everywhere. A number of data from the entrance region have been successfully correlated by this expression. This inclusion of entrance effect in the correlation is a significant improvement over the conventional correlations.

In the present study, the entrainment model is obtained by considering the mechanism of shearing-off of roll wave crests by streaming gas flow. By starting from the force balance for the onset of entrainment and considering the effect of deposition, basic dimensionless parameters have been identified. For this purpose the theoretical limit of entrainment E_{th}, which can be calculated from the onset of entrainment criterion, has been introduced.

After establishing these basic parameters from a simple model, the above semi-empirical correlation has been developed in colaboration with a large number of data. In addition to being accurate, this correlation also indicates basic mechanisms of entrainment processes and parametric dependencies. These are significant improvements over existing correlations. The correlations for entrainment in the entrance region and for the necessary distance for the development of entrainment are new. These supply very valuable information which has not been available previously.

IV. Droplet Size and Size Distribution

The mean droplet size and size distribution are important for detailed mechanistic modeling of annular two-phase flow. A large number of experimental data indicate that the standard Weber number criterion based on the relative velocity between droplets and gas flow predicts far too large droplet sizes. Therefore, it was postulated that the majority of the droplets were generated at the time of entrainment and the size distribution was the

direct reflection of the droplet entrainment mechanism based on roll-wave shearing off. A detailed model of the droplet size in annular flow was then developed based on the above assumption. The correlations for the volume mean diameter as well as the size distribution were obtained in collaboration with a large number of experimental data. A comparison with experimental data indicated that indeed the postulated mechanism has been the dominant factor in determining the drop size. Furthermore, a large number of data can be successfully correlated by the present model. These correlations can supply accurate information on droplet size in annular flow which has not been available previously.

In terms of the volume median diameter, the correlation is given by

$$D_{vm} = 0.0099 \frac{\sigma}{\rho_g j_g^2} Re_f^{2/3} \left(\frac{\rho_g}{\rho_f}\right)^{-1/3} \left(\frac{\rho_g}{\rho_f}\right)^{2/3} .$$

Hence the average maximum droplet size is

$$D_{max} = 0.031 \frac{\sigma}{\rho_g j_g^2} Re_g^{2/3} \left(\frac{\rho_g}{\rho_f}\right)^{-1/3} \left(\frac{\rho_g}{\rho_f}\right)^{2/3} .$$

The distribution is given in terms of the volume fraction over size Δ and the upper limit log-normal distribution function as

$$\frac{d\Delta}{dy} = - \frac{0.884}{\sqrt{\pi}} e^{-0.781y^2}$$

where $y = \ln [2.13\ D/(D_{max}-D)]$.

V. Bubble Number Density

For a bubbly flow regime a research program was conduced with the purpose of developing a reliable and simple predictive method for the number density

in a nucleate boiling. The bubble number density was formulated in terms of the number density differential balance equation given by

$$\frac{\partial N_b}{\partial t} + \frac{1}{A}\frac{\partial}{\partial z}(AN_b v_b) = \Phi_w + \Phi_{hn} - \Phi_{cond}$$

where N_b, A and v_b are the number density, cross sectional area and bubble velocity, respectively. The right hand sides are the source and sink terms due to the wall nucleation, bulk heterogeneous nucleation and bubble collapse. It is expected that Φ_w is a function of the wall superheat, $T_w - T_{sat}$, whereas Φ_{hn} and Φ_{cond} are functions of the bulk superheat or subcooling, $T_f - T_{sat}$. The initial effort has been concentrated on the development of the correlation for Φ_w.

The wall source term Φ_w can be expressed as

$$\Phi_w = \frac{N_A f \xi_h}{A}$$

where N_A, f and ξ_h are the nucleation site density, frequency of bubble departure and heated perimeter, respectively. An empirical correlation for the active nucleation site density was developed from the following analysis.

The pool boiling heat transfer data from various sources were fitted with the equation

$$Nu = \text{Const.}\ Re^a\ Pr^b\ (D_d/s)^c \quad .$$

The Nusselt number is defined as

$$Nu = h\ s/k_f$$

where s is the average bubble spacing, and it is directly related to the active nucleation site density by $s = N_A^{-1/2}$. The departing bubble diameter, D_d, is calculated by the classical Fritz's equation. The Reynolds number is defined as

$$Re = \frac{sv\rho_f}{\mu_f}$$

where the characteristic velocity, v, is chosen as the mean radial liquid velocity due to the source flow of the liquid associated with a growing bubble, which is given by Zuber [22] as follows

$$v \sim \left(\frac{\Delta T C_{pf}}{i_{fg}}\right)^2 (a_f \sqrt{N_A}) \quad .$$

Fitting the experimental data with the proposed equation, resulted in the following correlation

$$\frac{h}{\sqrt{N_A} k_f} = 14.0 \left[\left(\frac{C_{pf}\Delta T}{i_{fg}}\right)\left(\frac{\rho_f}{\rho_g}\right)\right]^{0.5} \left(\frac{\nu_f}{a_f}\right)^{-0.39} (D_d \sqrt{N_A})^{-0.25} \quad .$$

The number N_A of nucleation site density can be calculated by this equation from experimental values of h and ΔT and from the thermodynamic properties of the boiling liquid. N_A obtained in this way is indirectly correlated in terms of the dimensionless groups characterizing the critical cavity radius, fluid properties and of the pressure level of the system. The correlation developed in this way is a global one because it does not take into account the surface effects in detail. However, since it is based on a large number of experimental data points from a variety of sources, it takes into account the surface effects in an averaged sense.

In general, the bubble actually grows through a liquid film region adjacent to the wall where a high temperature gradient exists, and so in reality it experiences a somewhat lower mean superheat. In the case of pool boiling, the difference is small, and the superheat based on the wall temperature can be taken as the effective mean superheat. However, in the case of forced

convection nucleate boiling the temperature gradient depends on the flow rate and would generally be much steeper than in the corresponding pool boiling case with the same wall superheat. Therefore, the effective wall superheat for bubble growth in the forced convection boiling will be less than the actual wall superheat. Considering this fact, it is postulated that the active nucleation site density correlation obtained for the pool boiling could be used to determine the active nucleation site density in the forced convection nucleate boiling with an effective superheat rather than the actual wall superheat. The effective superheat is determined from Chen's suppression factor [23], which has been proved to be reliable in the subcooled as well as the saturated nucleate boiling regions. The method offered here permits a simple and rapid evaluation of the active nucleation site density in terms of the basic fluid and flow parameters in the subcooled and saturated boiling regions in a heated channel.

The method predicting the active nucleation site density in nucleate boiling was tested against Gunther's data [24], which appears to be the only subcooled nucleate boiling experimental data available in the literature. The good qualitative and quantitative agreement between experimentally measured active nucleation site density and those calculated by the method offered here appears to verify the basic principles involved in the development.

V. Summary

An accurate knowledge of the interfacial transfer terms is required in a two-fluid model formulation of a two-phase flow system. These interfacial transfer terms specify the rate of mass, momentum and energy transports at the interface between phases. They are directly proportional to the interfacial area concentration and to a driving force. The interfacial area

concentration, defined as the interfacial area per unit volume of the mixture, characterizes the kinematic effects, therefore, it must be related to the structure of the two-phase flow field.

In view of the above, the interfacial area is studied in detail. The interfacial area correlations for four basic flow regimes, namely, dispersed (bubbly or droplet), slug, churn-turbulent and annular flow have been developed. For annular flow, correlations for droplet entrainment and droplet size distribution have been obtained. These supply very valuable information which has not been available previously. For bubbly flow the bubble number density is a key parameter in determining the interfacial area. Therefore, a detailed modeling of the number density has been carried out.

Acknowledgments

This work was performed under the auspices of the U. S. Nuclear Regulatory Commission.

References

1. Ishii, M., Thermo-fluid Dynamic Theory of Two-phase Flow, Eyrolles, Paris (1975).

2. Delhaye, J. M., "Equations fondamentales des écoulements diphasiques, Parts 1 and 2," CEA-R-3429, France (1968).

3. Vernier, P. and Delhaye, J. M., "General Two-phase Flow Equations Applied to the Thermohydrodynamics of Boiling Nuclear Reactor," Energ. Prim. 4(1) (1968).

4. Bouré, J. and Réocruex, M., "General Equations of Two-phase Flows," 4th All Union Heat and Mass Transfer Conference, Minsk, USSR (1972).

5. Kocamustafaogullari, G., "Thermo-fluid Dynamics of Separated Two-phase Flow," Ph.D. Thesis, School of Mechanical Engineering, Georgia Institute of Technology, Georgia (1971).

6. Chawla, T. C. and Ishii, M., "Two-fluid Model of Two-phase Flow in a Pin Bundle of a Nuclear Reactor," ANL/RAS/LWR 79-5 (1979).

7. Amsden, A. A. and Harlow, F. H., "K-TIF: A Two-fluid Computer Program for Downcomer Flow Dynamics," LA-6994, NRC-4 (1978).

8. Thurgood, M. J. et al., "Core Thermal Model Development," PNL-2653-2, NUREG/CR0341, p. 101 (1978).

9. Zuber, N., "Flow Excursions and Oscillations in Boiling, Two-phase Flow Systems with Heat Addition," in Proceedings of EURATOM Symposium on Two-phase Flow Dynamics, Commission of European Communities, Brussels, 1, p. 1070-1089 (1967).

10. Ishii, M., "One-dimensional Drift-flux Model and Constitutive Equations for Relative Motion between Phases in Various Two-phase Flow Regimes," Argonne National Laboratory Report, ANL-77-47 (1977).

11. Lahey, Jr., R. T., Cheng, L. Y., Drew, D. A. and Flaherty, J. E., "The Effect of Virtual Mass on the Numerical Stability of Accelerating Two-phase Flows," Presented at AIChE 7th Annual Meeting at Miami Beach, Florida (1978).

12. Réocreux, M., "Contribution á l'étudedes debits critiques en écoulement diphasique eau vapeur," Ph.D. Thesis, University of Grenoble, France (1974), also NUREG-tr-0002, Vol. 1.

13. Zuber, N., "On the Dispersed Two-phase Flow in the Laminar Flow Regime," Chem. Eng. Sci., 19, p. 897 (1964).

14. Ishii, M. and Zuber, N., "Drag Coefficient and Relative Velocity in Bubbly, Droplet or Particulate Flow," AIChE J., 25, p. 843 (1979).

15. Ishii, M. and Zuber, N., "Relative Motion and Interfacial Drag Coefficient in Dispersed Two-phase Flow of Bubbles, Drops or Particles," 71st Am. Inst. of Chem. Engrs. Annual Meeting, Miami (1978).

16. Ishii, M. and Chawla, T. C., "Local Drag Laws in Dispersed Two-phase Flow," ANL-79-105, NUREG/CR-1230 (1979).

17. Ishii, M. and Chawla, T. C., "Two-fluid Model and Momentum Interaction between Phases," NRC 7th Water Reactor Safety Research Information Meeting, Gaithersburg (Nov., 1979).

18. Ishii, M. and Mishima, K., "Two-fluid Model and Analysis of Interfacial Area," NUREG/CR-1873, ANL-80-111 (1980).

19. Saha, P., "Light Water Reactor Thermal/Hydraulic Development Program, 1.1 Development of Constitutive Relations," BNL-NUREG-50683, p. 145 (1977).

20. Ishii, M. and Mishima, K., "Correlation for Liquid Entrainment in Annular Two-phase Flow of Low Viscous Fluid," ANL/RAS/LWR 81-2 (1981).

21. Kataoka, I., Ishii, M. and Mishima, K., "Generation and Size Distribution of Droplet in Gas-liquid Annular Two-phase Flow," ANL/RAS/LWR 81-3 (1981).

22. Zuber, N., "Nucleate Boiling. The Region of Isolated Bubbles and the Similarity with Natural Convection," Int. J. Heat Mass Trans., 6, p. 53 (1963).

23. Chen, J. C., "Correlation for Boiling Heat Transfer to Saturated Fluids in Convective Flows," Ind. Eng. Chem. Process Design and Developments, 5, p. 322 (1966).

24. Gunther, F. C., "Photographic Study of Surface Boiling Heat Transfer to Water with Forced Convections," Trans. ASME, 73-2, p. 115 (1951).

Summary

Two-fluid Model Formulation

Interfacial Transfer Terms

Interfacial Area Correlation

- Data Evaluation of Interfacial Area
- Interfacial Area Model
- Amount of Entrainment Correlation
- Droplet Size and Size Distribution
- Bubble Number Density

Phenomenological Modeling of Two-phase Flow

by

M. Ishii
I. Kataoka
G. Kocamustafaogullari

Reactor Analysis and Safety Division
Argonne National Laboratory

- Objective of the Program

  Develop Rigorous { Two-phase Flow Model; Constitituve Relations } ⟶ LWR Safety Code

- Particular Emphasis

  - Interfacial Interaction Terms
  - Interfacial Area Correlation
    - Model
    - Particle Size (Droplet and Bubble) and Size Distribution
    - Entrainment Amount
    - Bubble Number Density
  - Prediction of Hydrodynamic Transients

Two-Fluid Model

Characteristic

Structured Flow ⟶ Two Coexisting Continua

3 Field Eqs. for Each Phase

Transfer Mechanisms

- Mean Fluid Transfer — Turbulent
- Interfacial Transfer — Interface Motion

Importance

Dynamic Interaction

- Transient
- Entrance
- Flow Regime Change

Non-equilibrium

Γ ⟷ Interfacial Energy Tr.

Location of Phases

Development (Completed)

Fully 3-D Model

1-D Model

Subchannel Model

FORMULATION OF TWO-FLUID MODEL

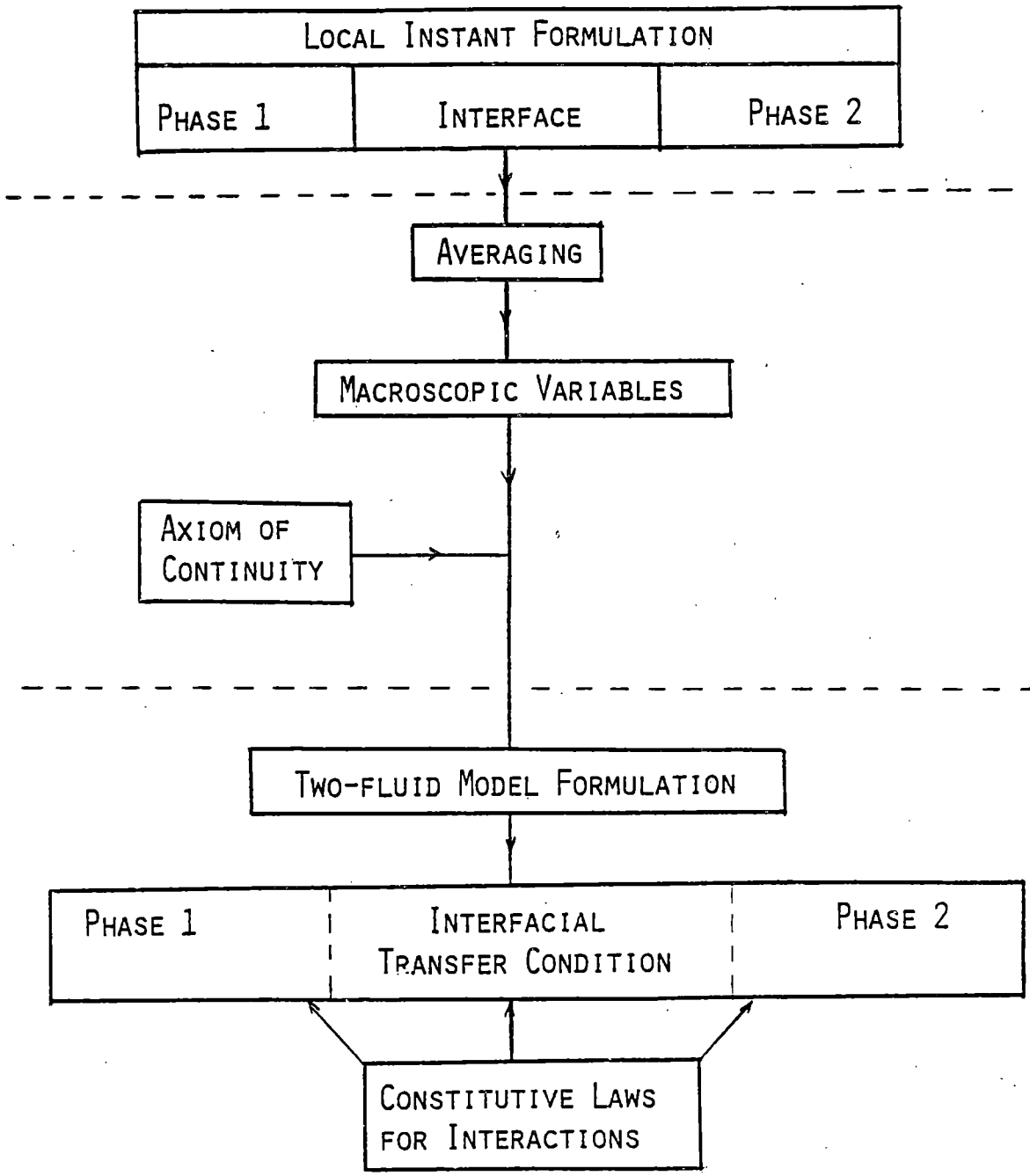

Cocurrent Up Flow Data (Interfacial Area)

- Data ; Slug, Churn, Annular Flows

Ranges (P ≐ 1 atm)
Air - Water

$$\begin{cases} 1.5 < j_f < 50 \text{ cm/s} \\ 0.3 < j_g < 30 \text{ m/s} \end{cases}$$

D = 0.6, 1, 1.5, 2, 2.5 (7 ~ 40) cm

- General Trend

1) $j_g, (j_f) \uparrow$ $\quad a_i \uparrow$

2) Local Maxima — Bubbly* / Slug

3) D ; Mixed

- $1 < a_i < 10$ $\quad cm^2/cm^3$

(Reference: Bubbly Flow α = 0.3, r = 0.1 cm)

IMPORTANCE OF INTERFACIAL AREA CONCENTRATION

MASS $$A\Gamma_K = A\overline{m}_K \, a_I$$

MOMENTUM $$A(M_K^d + \Gamma_K V_{KI}) = A a_I (\tau_K^d + \overline{m}_K V_{KI})$$

ENERGY $$A(Q''_{IK} \xi_I + \Gamma_K H_{KI}) = A a_I (Q''_{IK} + \overline{m}_K H_{KI})$$

a_I ⟶ INTERFACIAL AREA CONCENTRATION (IMPORTANT)

τ_K^d ⟶ CONSTITUTIVE EQUATIONS

Q''_{IK} ⟶ CONSTITUTIVE EQUATIONS

} STANDARD MODELING

$\overline{m}_K$ ⟶ EQUIVALENT TO Q''_{I1} AND Q''_{I2}

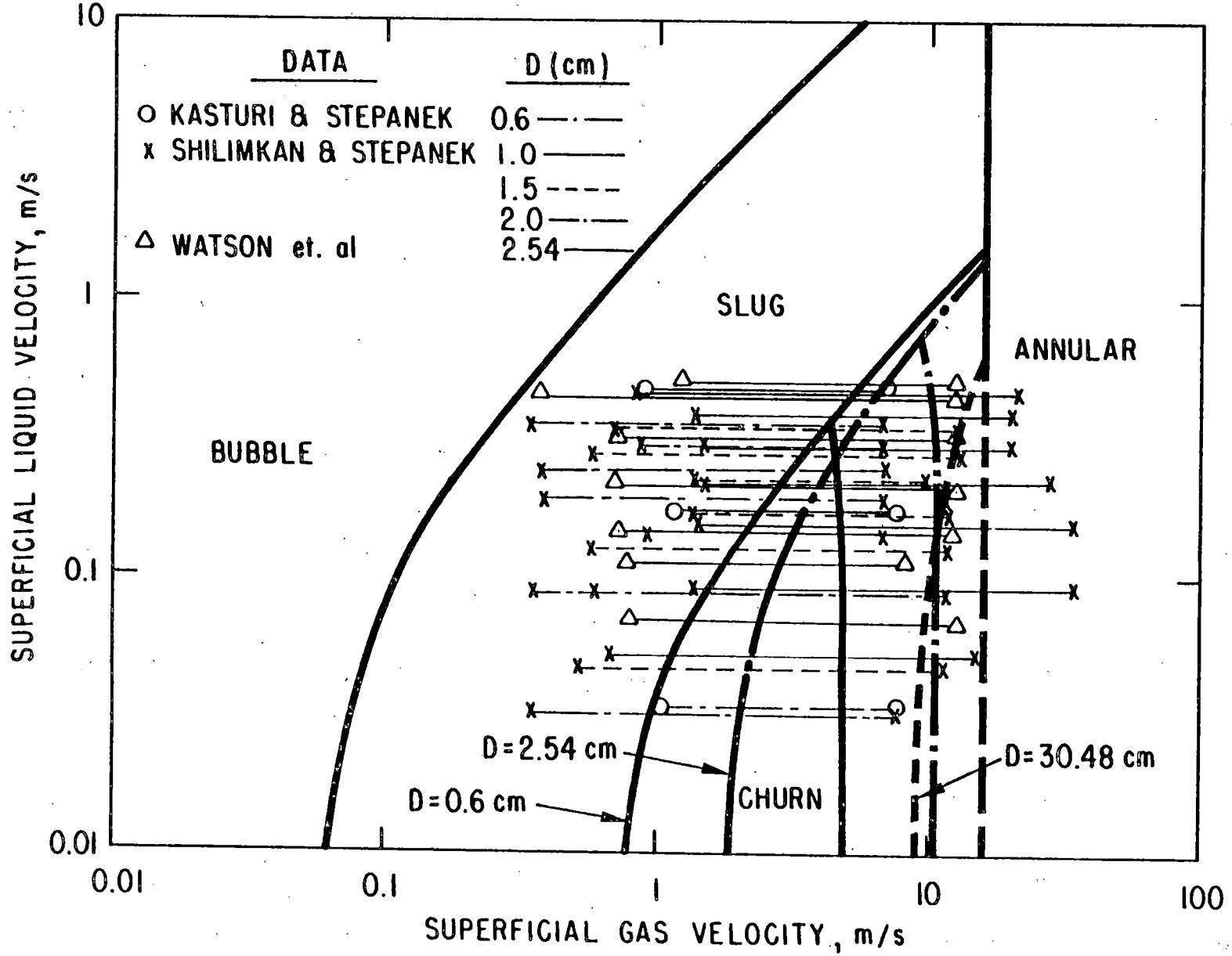

RANGES OF EXPERIMENTS FOR INTERFACIAL AREA

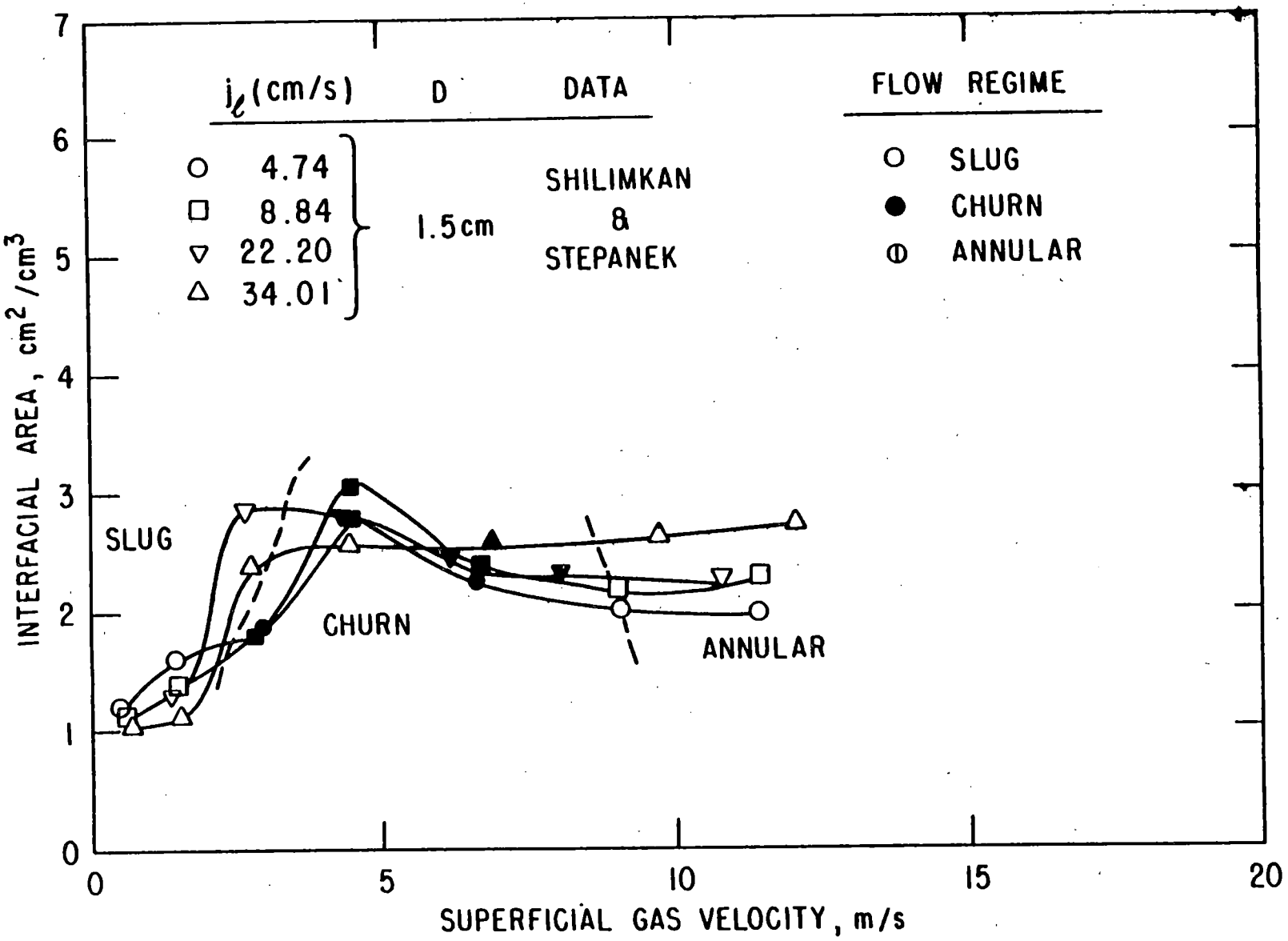

INTERFACIAL AREA IN VERTICAL UP FLOW SYSTEM

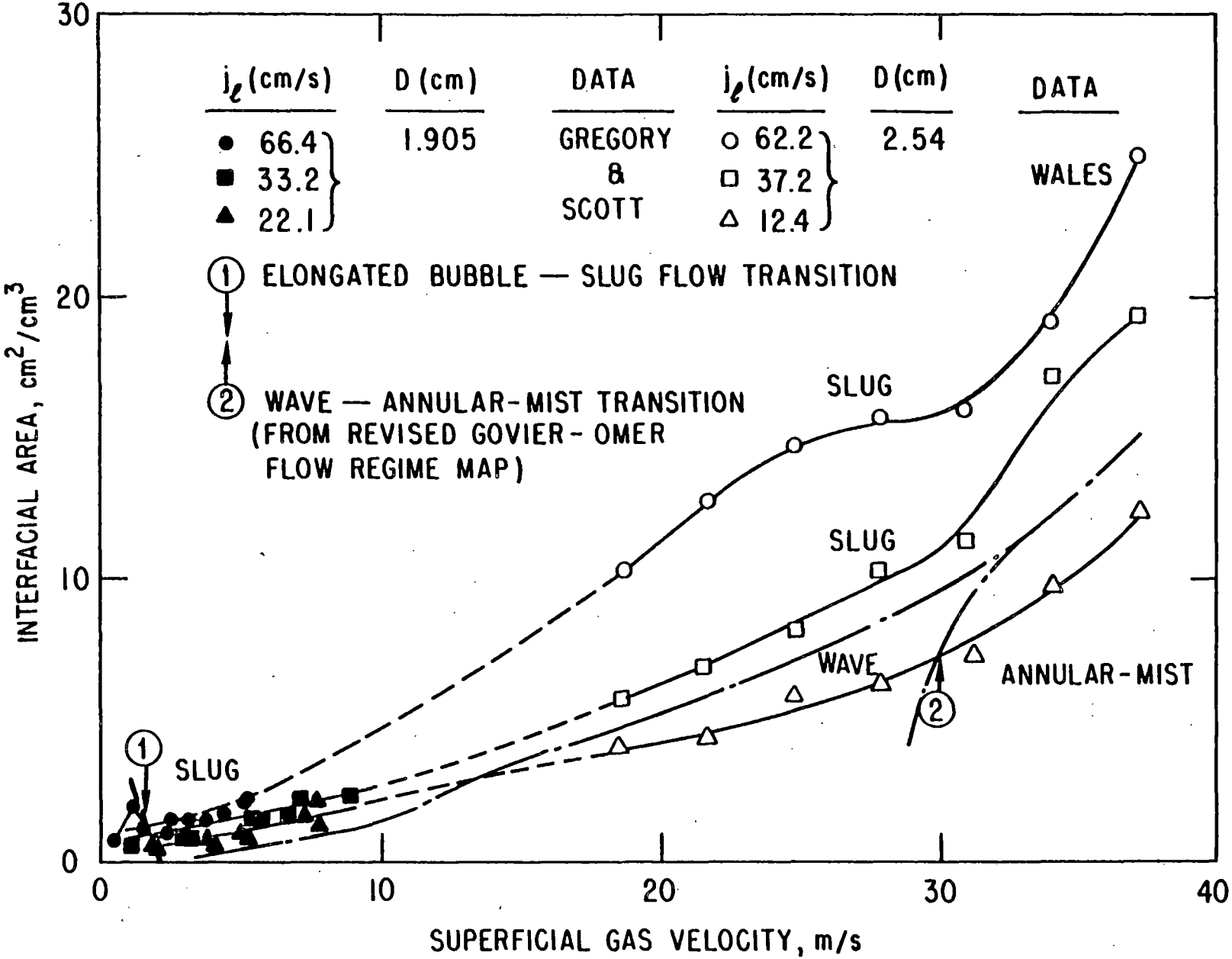

INTERFACIAL AREA IN HORIZONTAL FLOW SYSTEM

Evaluation of Experiments

Sufficient

- Flow Regimes ; Slug, Churn, Annular
- Gas Flux ; Intermediate to High
- Liquid Flux ; Low
- Low Pressure
- Fully Developed
- Adiabatic Measurements
  - Chemical
  - Light Attenuation (α small)
  - Photo (α small)

Insufficient

- Flow Regimes ; Bubbly → Slug
- High Liquid Flux (> 50 cm/s)
- Effects of
  - Pressure
  - Viscosity
  - Surface tension
- Entrance Effect
- Combination ; Flow Regime — Interfacial Area
- Measurement
  - Phase Change
  - High Temperature
  - (Transient)

Correlation for Interfacia Area

- Previous Work : Jepsen
  Banerjee
  Kasturi

$$a_i = f\left(\left[\frac{\partial p}{\partial z}\right]_{fr}, v\right) \dashrightarrow C\left(\left[\frac{\partial p}{\partial z}\right]_{EX} v\right)^n$$

Advantage $a_i \longleftrightarrow$ Dissipation
Prototypic Exp. (Chem Eng.)
a_i , $a_i k_L$ Measurements Similar

Shortcomings $a_i \longleftrightarrow$ Structure of Flow
Nonmechanistic Modeling
n, c ; System Dependent
ΔP_{EX} Dependent

- Present Work

$$a_i = f_1(\alpha, r_v, \text{ shape factor})$$

Mechanistic Modeling

$a_i \longleftrightarrow$ Flow Geometry

Interfacial Area Correlation

- Slug Flow

$$a_i = \frac{4.5}{D}\left(\frac{\alpha - \alpha_{gs}}{1 - \alpha_{gs}}\right) + \frac{3\alpha g_s}{r_{SM}}\left(\frac{1-\alpha}{1-\alpha_{gs}}\right)$$

- Churn Flow

$$a_i = \frac{4.5C_{CI}}{D}\left(\frac{\alpha - \alpha_{gs}}{\alpha - \alpha_{gs}}\right) + \frac{3\alpha g_s}{r_{SM}}\left(\frac{1-\alpha}{1-\alpha_{gs}}\right)$$

$$\begin{cases} C_{CT} > 1 \\ \alpha_{gs}\big)_{SLUG} > \alpha_{gs}\big)_{CT} \end{cases}$$

- Annular Flow

$$a_i = \frac{4C_{AN}}{D}\sqrt{\frac{\alpha}{1-\alpha_{fd}}} + \frac{\alpha}{1-\alpha_{fd}}\left(\frac{3\alpha_{fd}}{r_{SM}}\right)$$

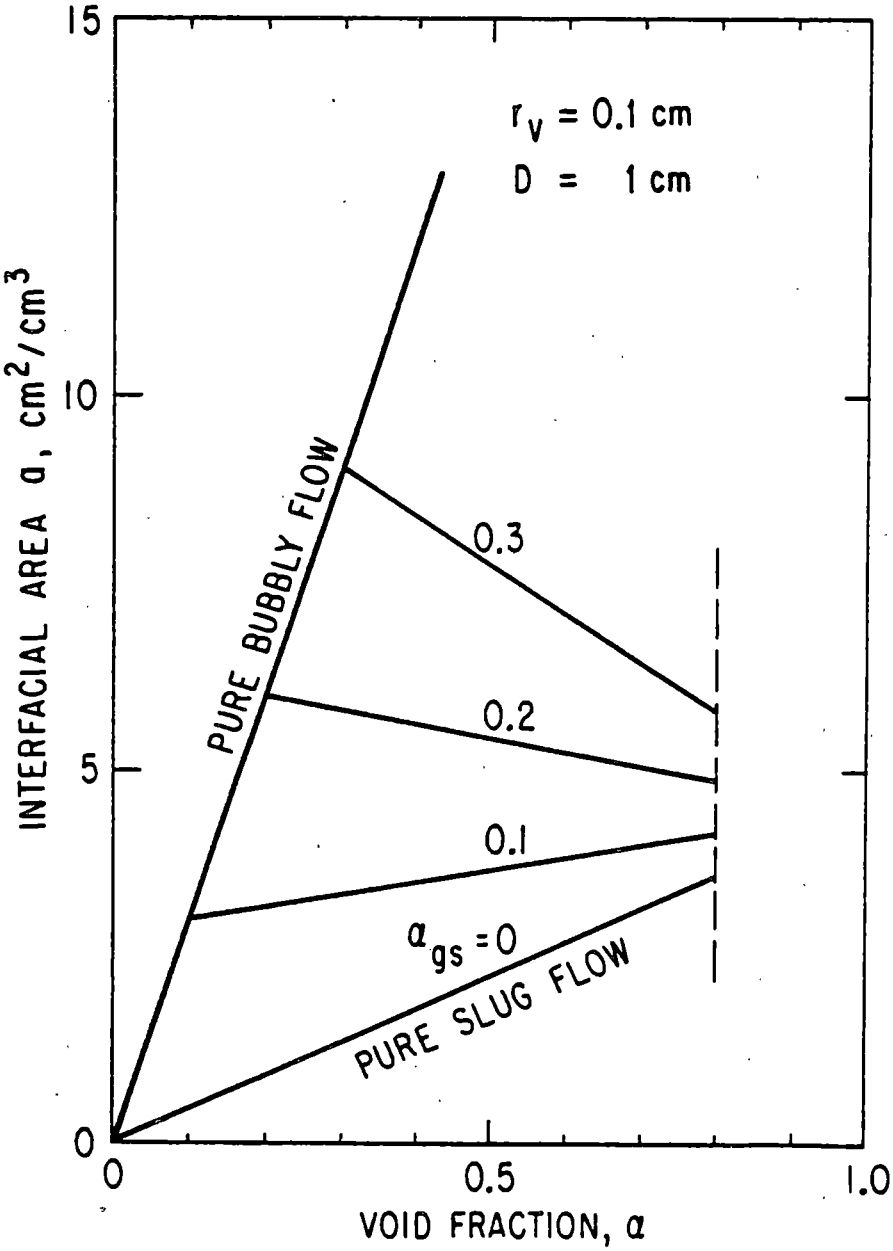
15
10
5
0
0
0.5
1.0
r_v = 0.1 cm
D = 1 cm
PURE BUBBLY FLOW
0.3
0.2
0.1
α_{gs} = 0
PURE SLUG FLOW
INTERFACIAL AREA a, cm^2/cm^3
VOID FRACTION, α

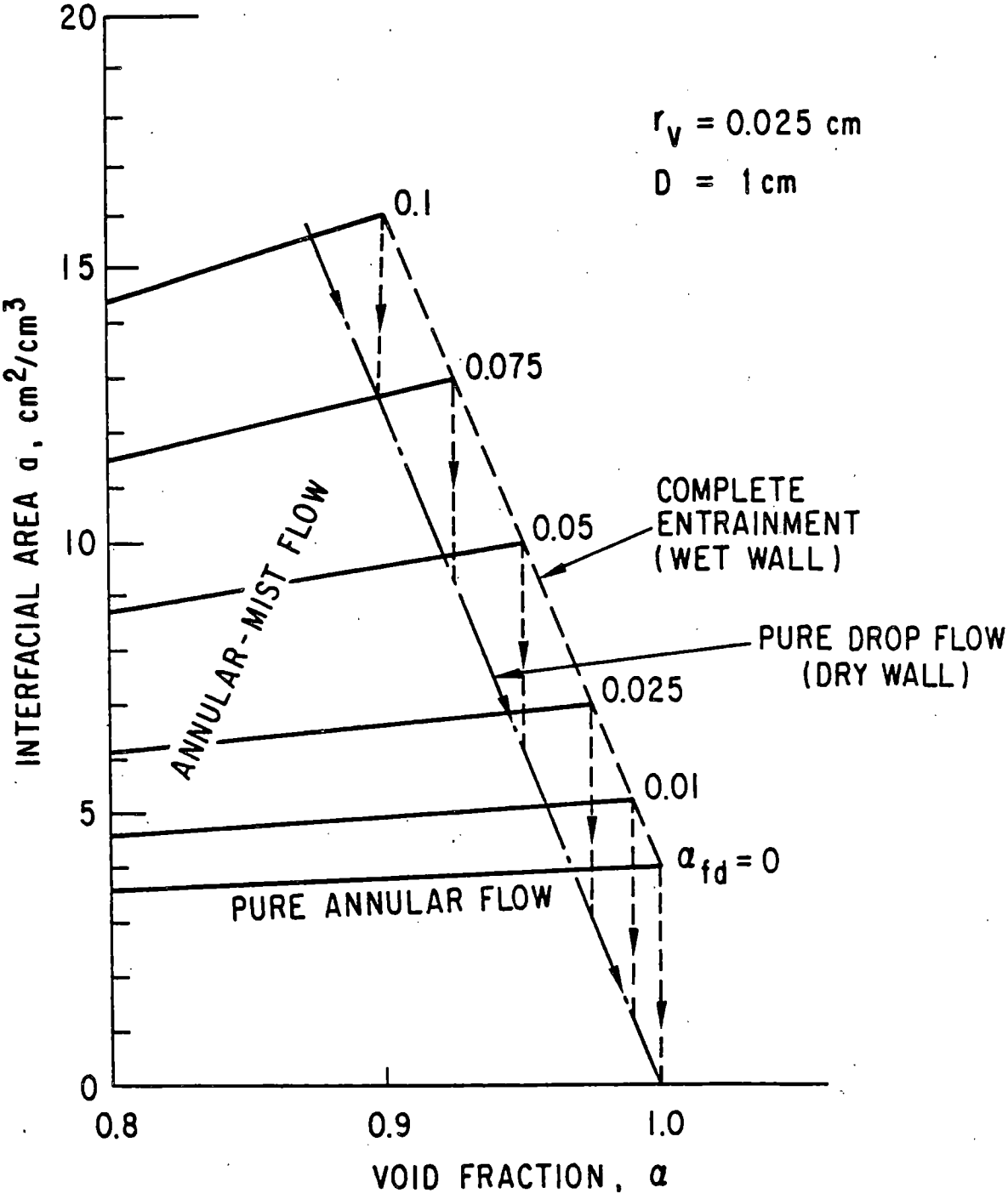
20
15
10
5
0
0.8
0.9
1.0
INTERFACIAL AREA a, cm²/cm³
VOID FRACTION, α
r_v = 0.025 cm
D = 1 cm
0.1
0.075
0.05
0.025
0.01
α_fd = 0
ANNULAR-MIST FLOW
PURE ANNULAR FLOW
COMPLETE ENTRAINMENT (WET WALL)
PURE DROP FLOW (DRY WALL)

Entrainment Model Development

1) Onset of Entrainment

   Theoretical Limit

   Dimensionless Groups

2) Density Effect (of Entrained Drops)

3) Fully Developed Flow

   Effect of $\begin{cases} J_G \\ Re_F \\ D \end{cases}$

4) Entrance Effect

   $\begin{cases} \text{Residence Time} \\ \text{Amount} \longleftrightarrow \text{Rate} \longrightarrow Re_F \text{ Effect} \end{cases}$

5) Combined Overall Correlation

$$E = (1 - e^{-10^{-5}\xi^2}) \tanh(4.5 \times 10^{-7}\eta)$$

$$\begin{cases} \xi = \dfrac{Z}{D}\sqrt{\dfrac{Re_F}{J_G^*}} \\ \eta = J_G^{*\,2.5}\, D^{*\,1.5}\, Re_F^{0.25} \end{cases}$$

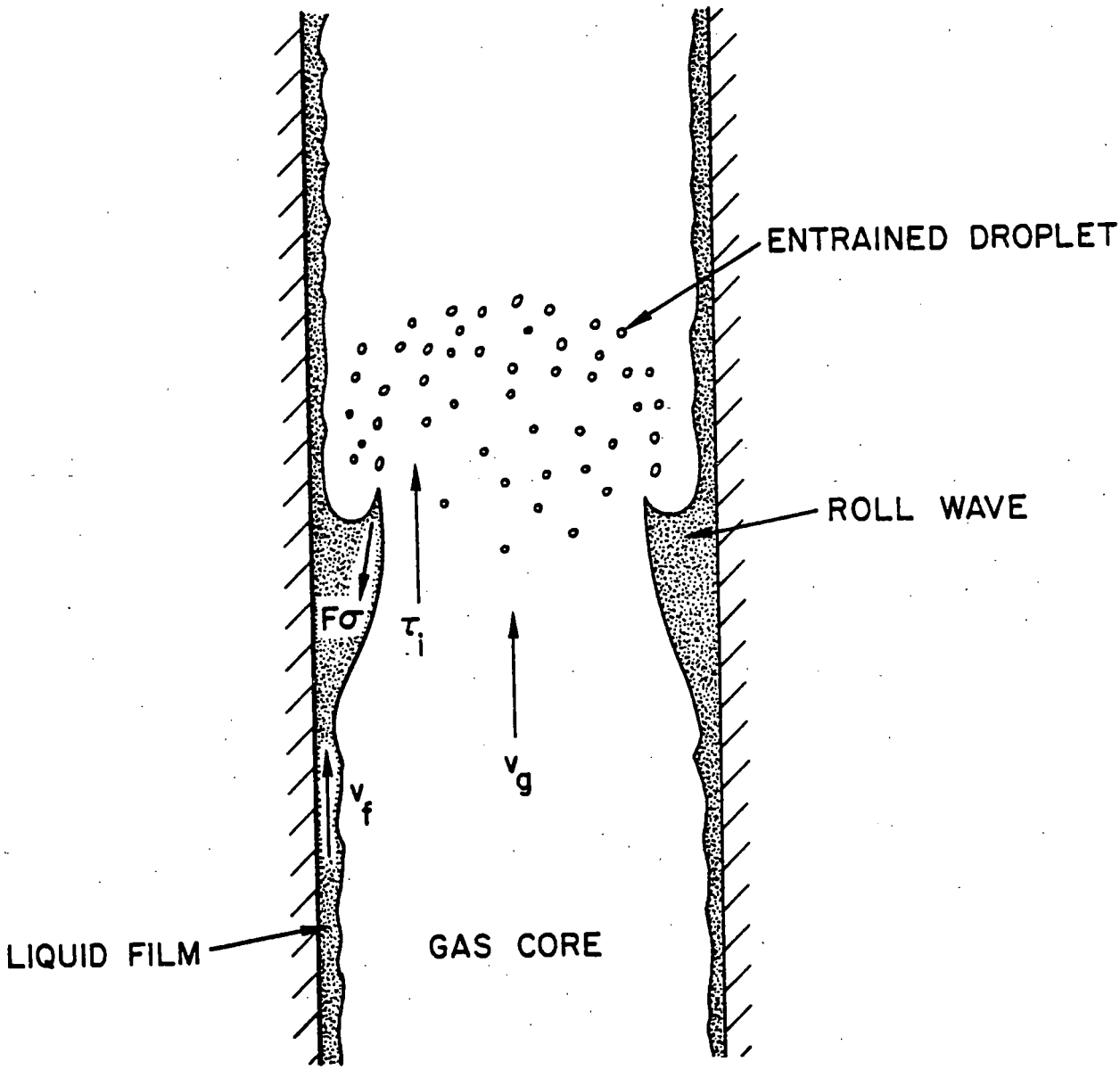
ENTRAINED DROPLET
ROLL WAVE
Fσ
τ_i
v_g
v_f
LIQUID FILM
GAS CORE

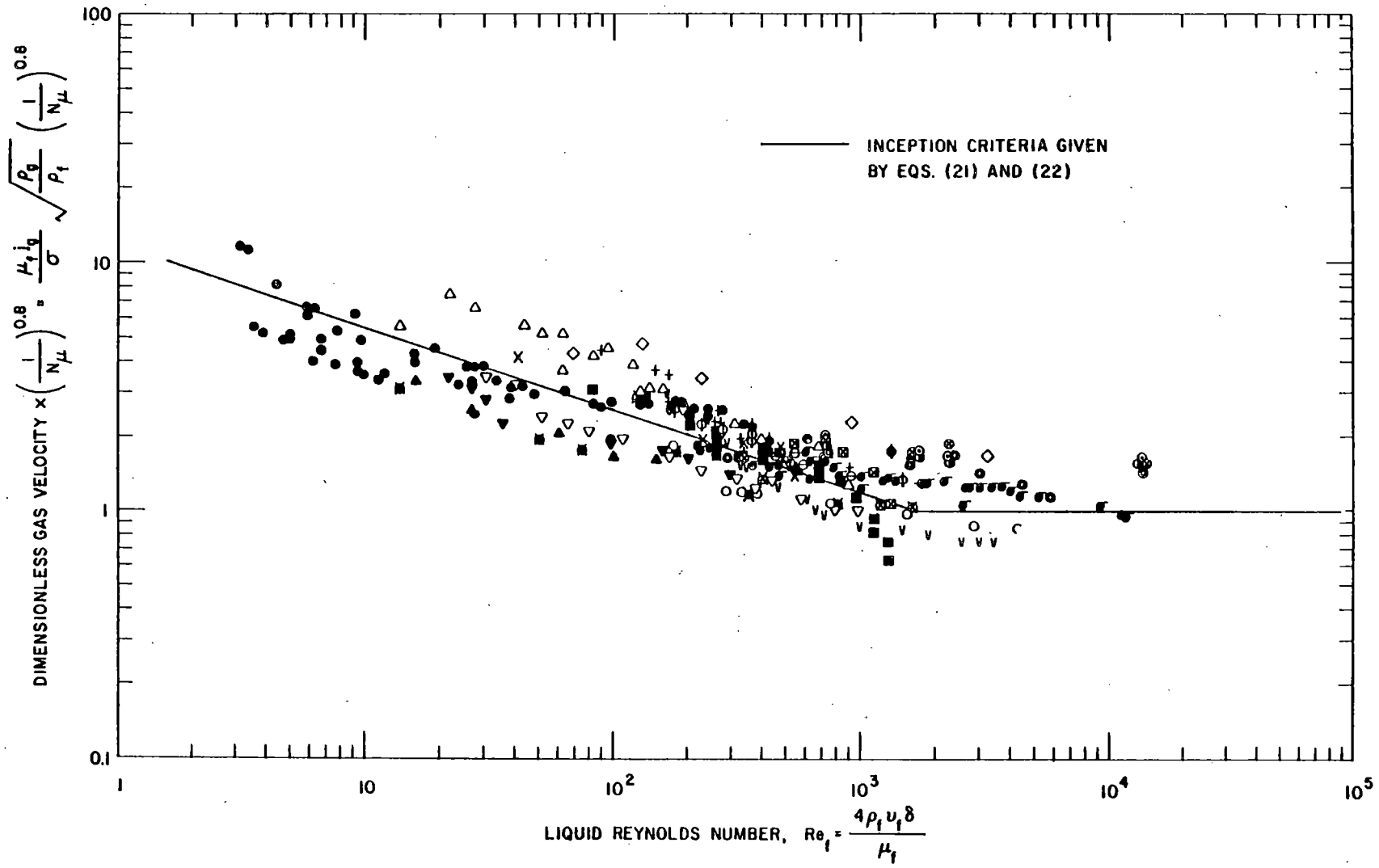
INCEPTION CRITERIA GIVEN
BY EQS. (21) AND (22)
100
10
1
0.1
1
10
10^2
10^3
10^4
10^5
DIMENSIONLESS GAS VELOCITY $\times \left(\frac{1}{N_\mu}\right)^{0.8} = \frac{\mu_f j_g}{\sigma} \sqrt{\frac{\rho_g}{\rho_f}} \left(\frac{1}{N_\mu}\right)^{0.8}$
LIQUID REYNOLDS NUMBER, $Re_f = \frac{4\rho_f v_f \delta}{\mu_f}$

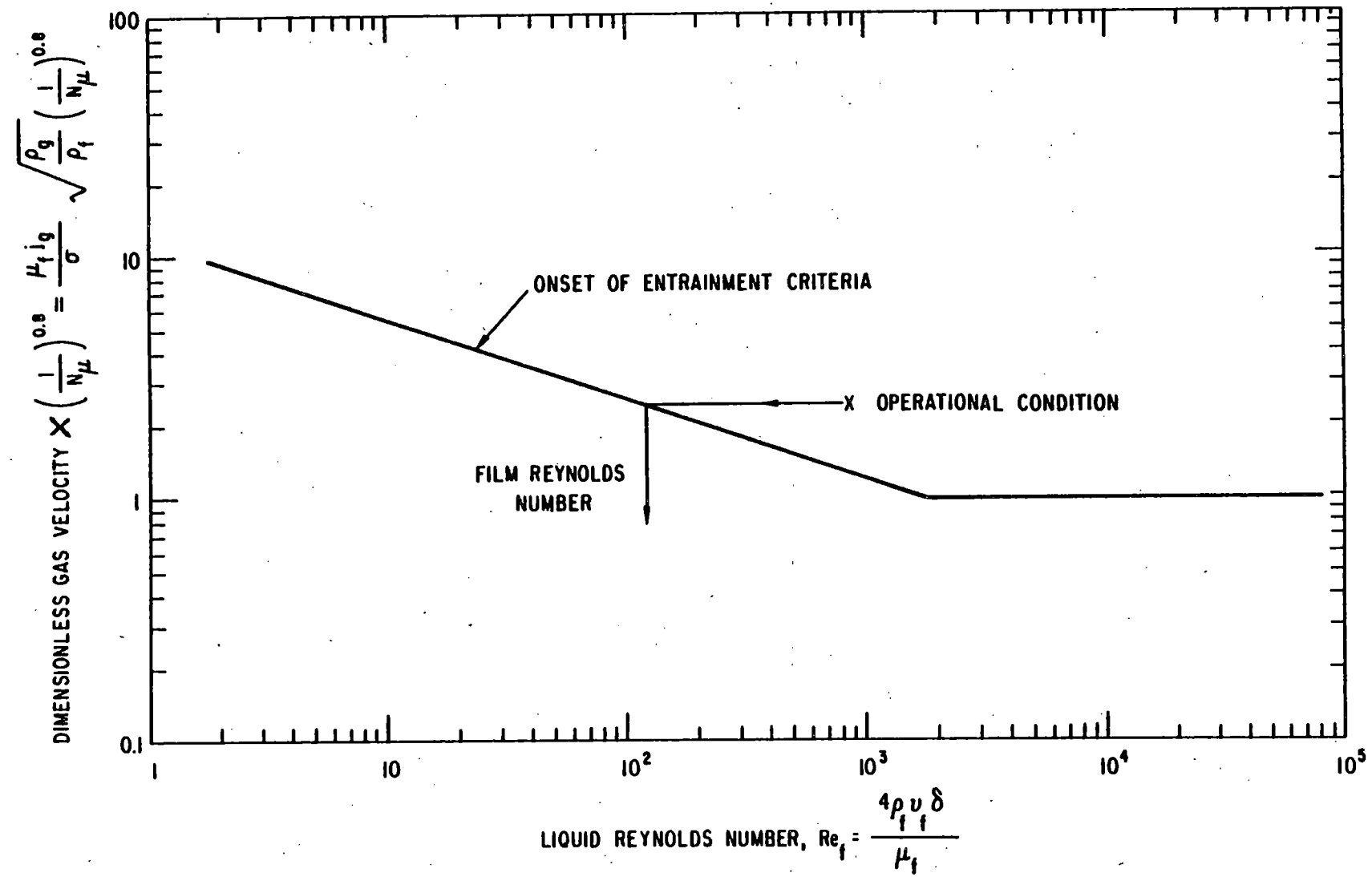
100
10
1
0.1
1
10
10^2
10^3
10^4
10^5
DIMENSIONLESS GAS VELOCITY $\times \left(\frac{1}{N_\mu}\right)^{0.8} = \frac{\mu_f i_g}{\sigma} \sqrt{\frac{\rho_g}{\rho_f}} \left(\frac{1}{N_\mu}\right)^{0.8}$
ONSET OF ENTRAINMENT CRITERIA
X OPERATIONAL CONDITION
FILM REYNOLDS NUMBER
LIQUID REYNOLDS NUMBER, $Re_f = \frac{4\rho_f v_f \delta}{\mu_f}$

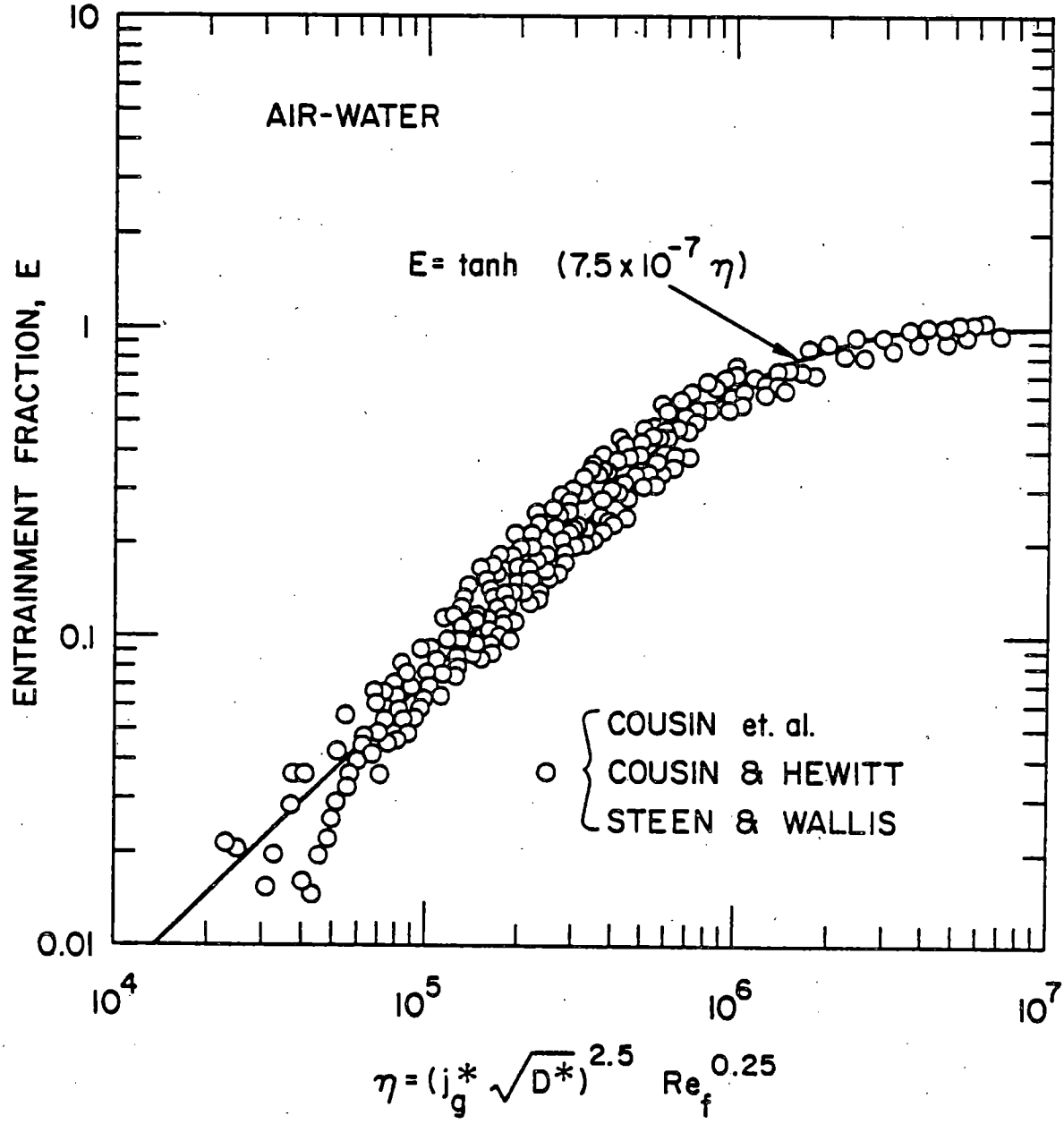

ENTRAINMENT CORRELATION FOR EQUILIBRIUM FLOW

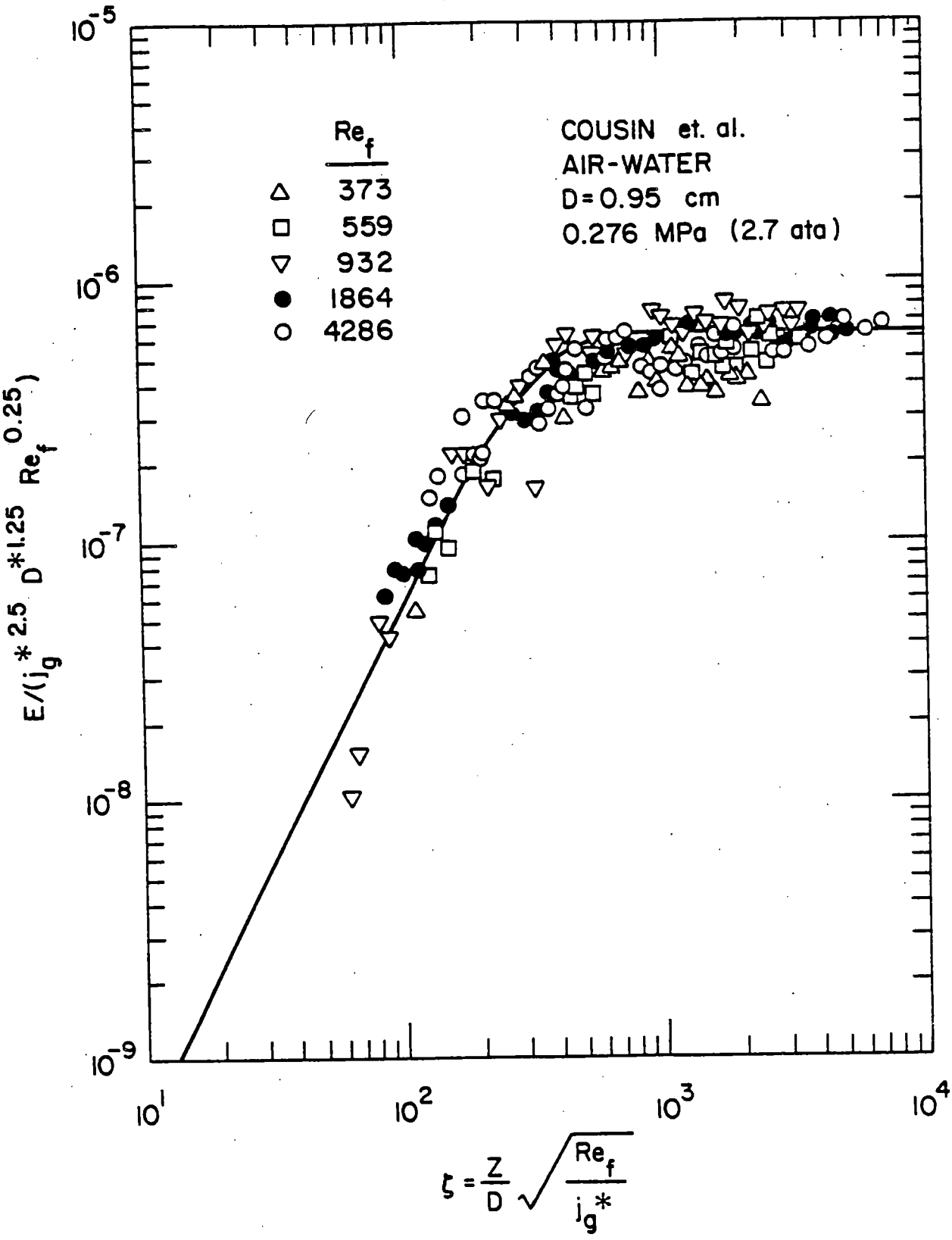

ENTRAINMENT CORRELATION FOR ENTRANCE REGIME

Droplet Size in Annular Flow

Entrainment ⟶ Size of Droplets
(Not the Disintegration of Drops in Gas Core)

- Force Balance at Interface

$$\pi D\sigma = \frac{\pi}{4} D^2 C_D \frac{1}{2} \rho_G J_G^2$$

$$\downarrow$$

$$We = \frac{8}{C_D}$$

- Drag on Wave Crest ~ Interfacial Shear

$$\downarrow \quad \left\{ \begin{array}{l} \text{Wallis Correlation} \\ \text{Ishii \& Grolmes Amplitude Correlation} \end{array} \right.$$

C_D; Re_F, Re_G and $\left(\frac{A_I}{A_{IW}}\right)$

A_I; Interfacial Area of Wave Crest (⟶ Drops)

A_{IW}; Interfacial Area of Waves

- $We = f(Re_F, Re_G)$
  Coefficient Determined from Data

- $We \longrightarrow D_{VM}$ (Volume Median Diameter)

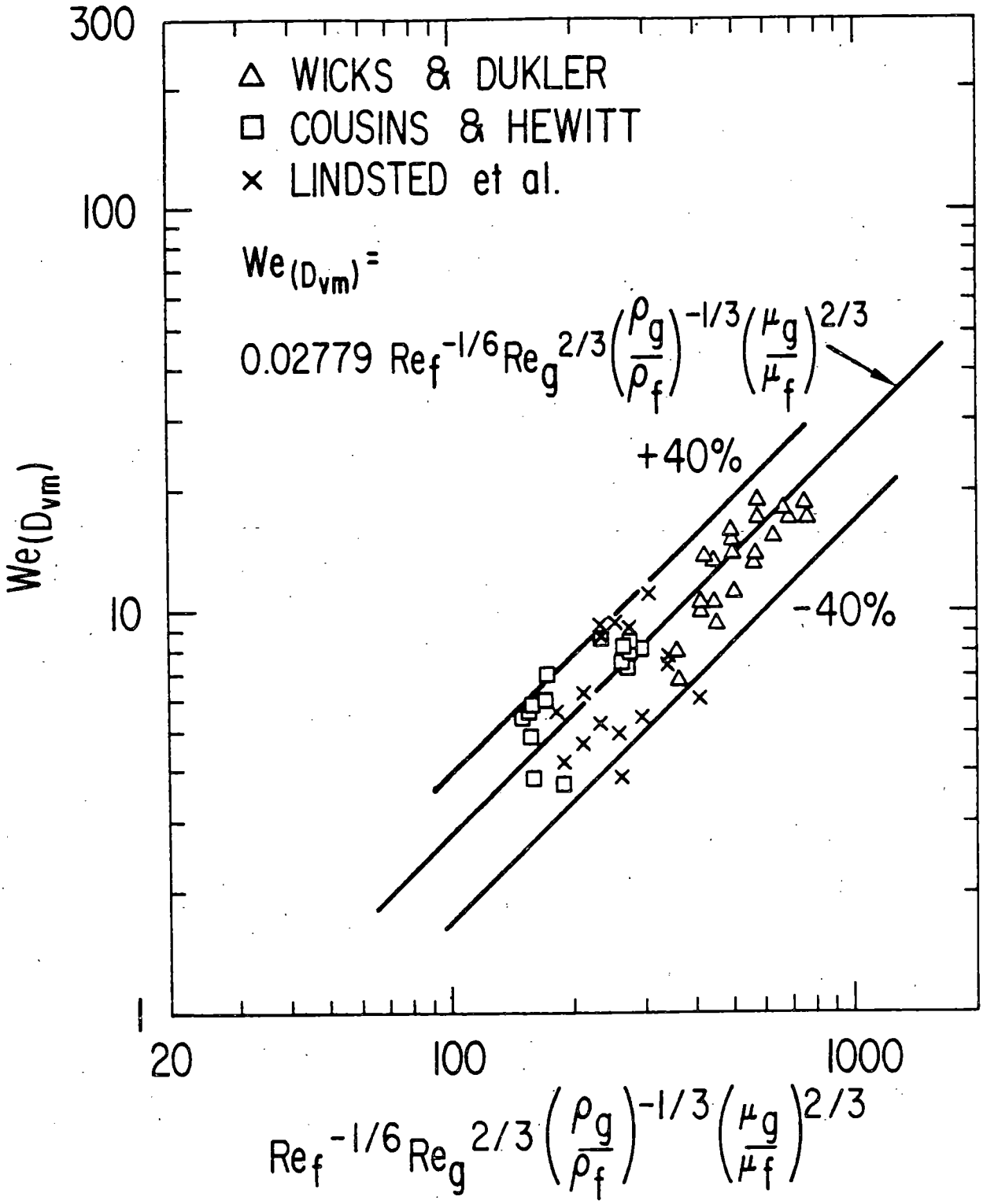

Fig. 3. Comparison of Volume Median Diameter Correlation to Various Data

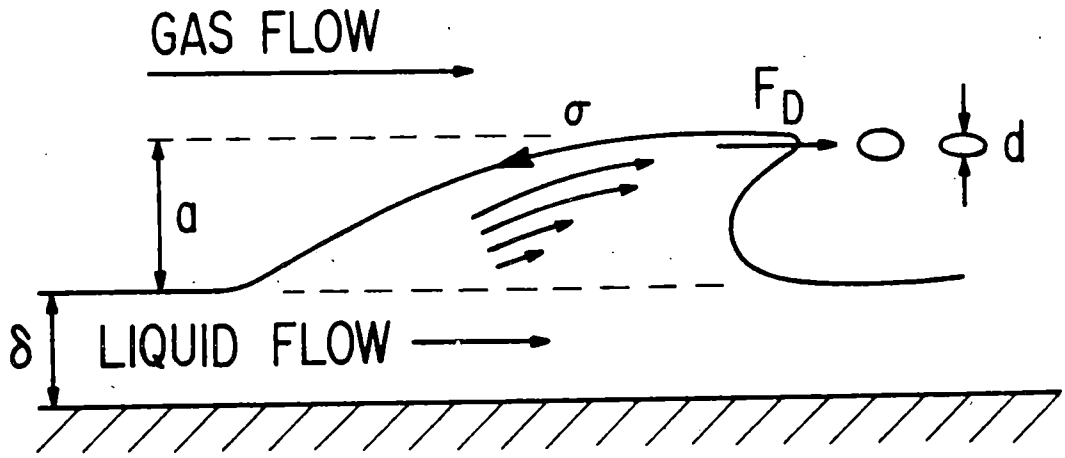

Mechanism of the Shearing off of Roll-Wave

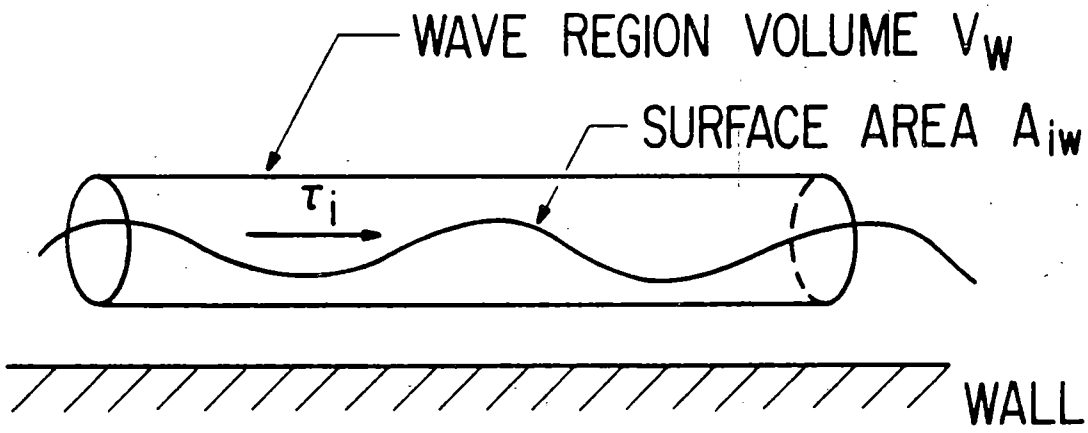

Illustrative Figure of a Neighborhood of a Wave Region

Volume Median Diameter

$$D_{VM} \doteq 0.01 \frac{\sigma}{\rho_G J_G^2} Re_G^{2/3} \left(\frac{\rho_G}{\rho_F}\right)^{-1/3} \left(\frac{\mu_G}{\mu_F}\right)^{2/3}$$

Maximum Droplet Size

$$D_{MAX} = 3.13\, D_{VM}$$

NOTE: (1) $D_{VM} \sim J_G^{-4/3}$

$\Updownarrow$

Standard We_C Criteria

$D_{VM} \sim J_G^{-2}$

(2) Present Model $\longrightarrow$ Much Smaller D_{VM}

Standard $We_C \longrightarrow$ Too Large D_{VM}

Droplet Size Distribution in Annular Flow

- Upper Limit Log-Normal Distribution Function (Mugele and Evance)

$$\frac{D\Delta}{DY} = -\frac{\xi}{\sqrt{\pi}} E^{-\xi Y^2}$$

ξ; Distribution Parameter

Δ; Volume Fraction Oversize

$$Y = \ell N \frac{KD}{D_{MAX}-D} \quad , \quad K = \frac{D_{MAX}-D}{D_{VM}}$$

- Data and Correlation for D_{VM}

$$\begin{cases} \xi = 0.884 \\ K = 2.13 \end{cases}$$

$$\frac{D\Delta}{DY} = -\frac{0.884}{\sqrt{\pi}} E^{-0.781 Y^2}$$

- Generally Well Correlated

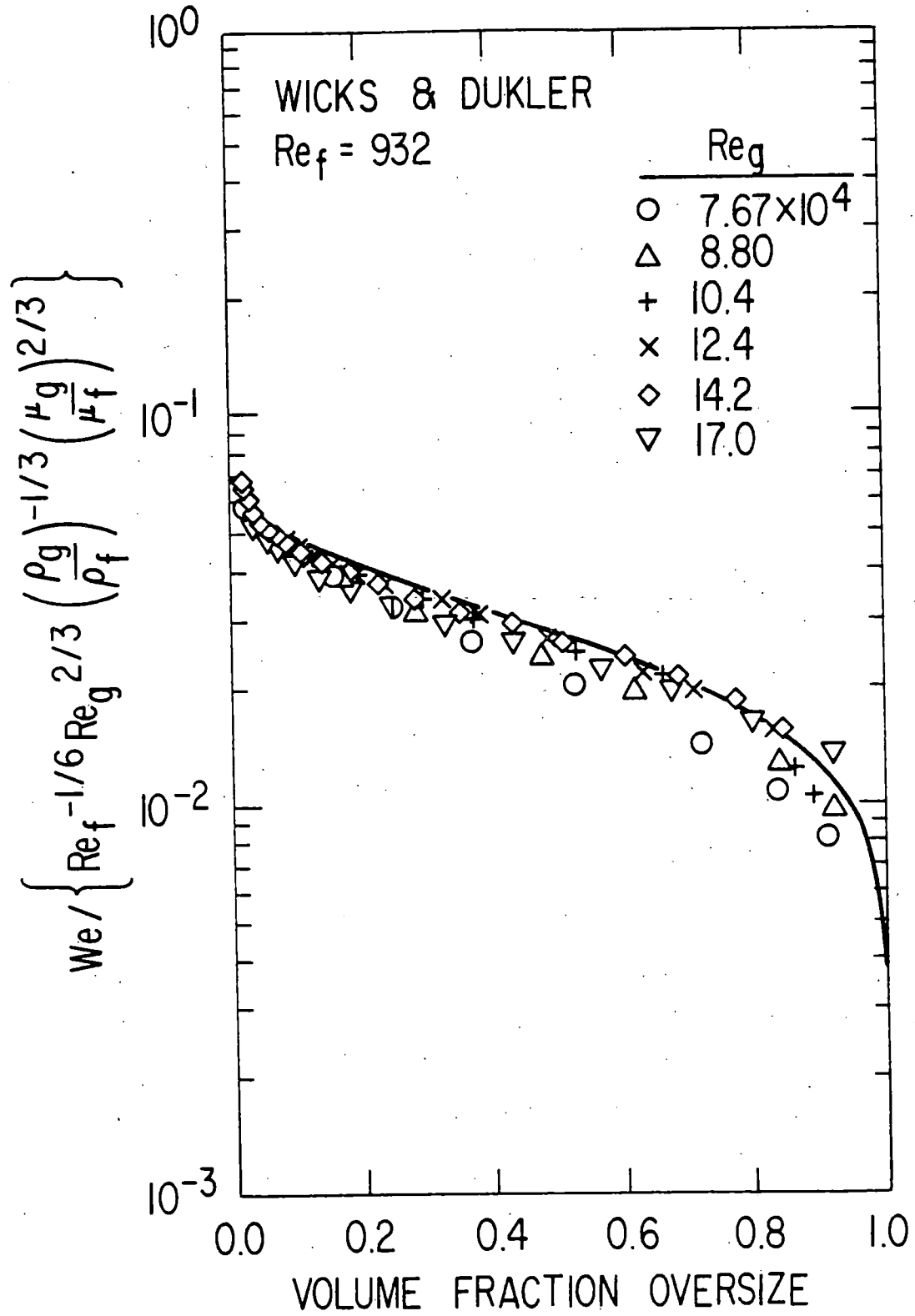

Droplet Size Distributions at Re_f = 932 for Data of Wicks and Dukler

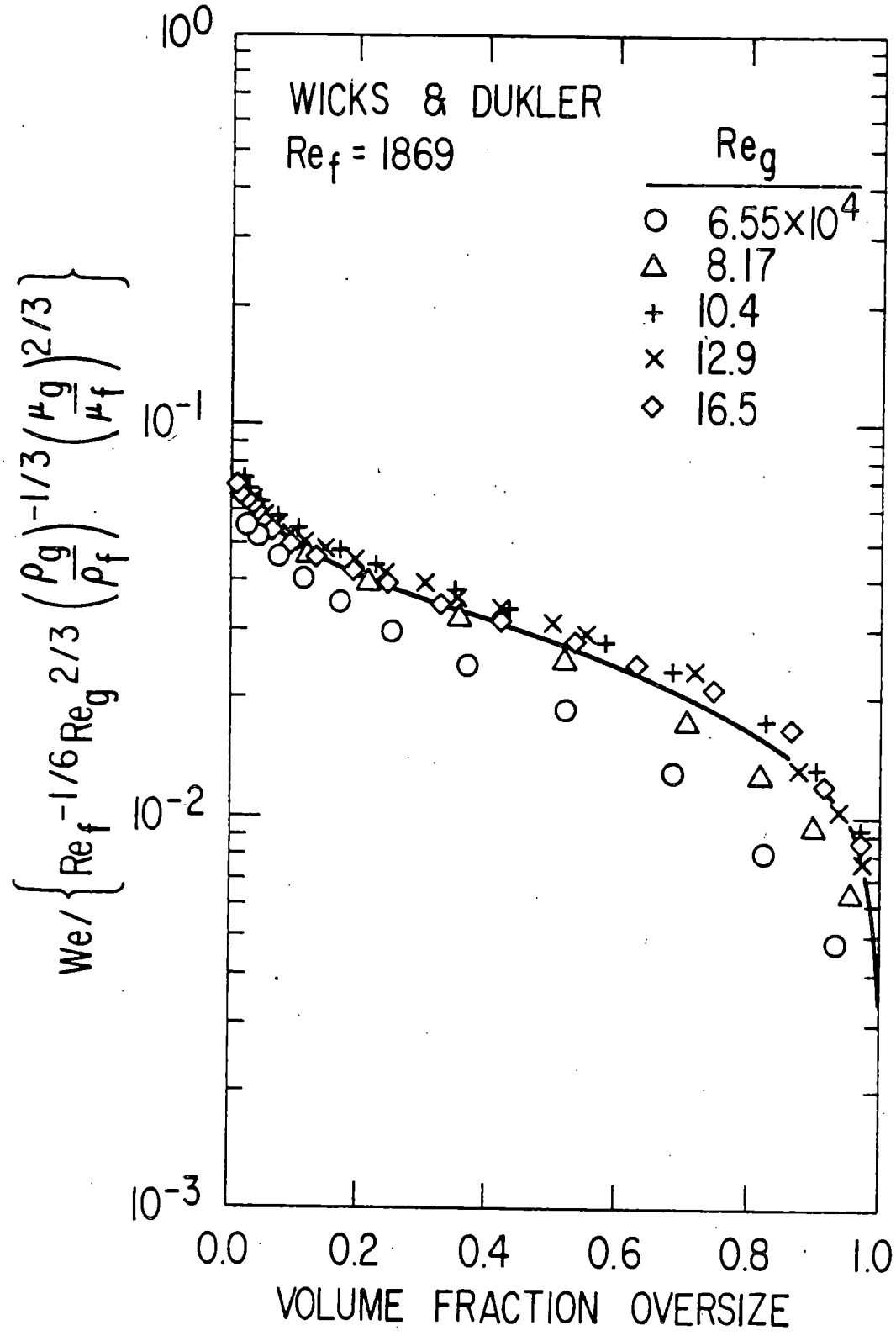

Droplet Size Distributions at Re_f = 1869 for Data of Wicks and Dukler

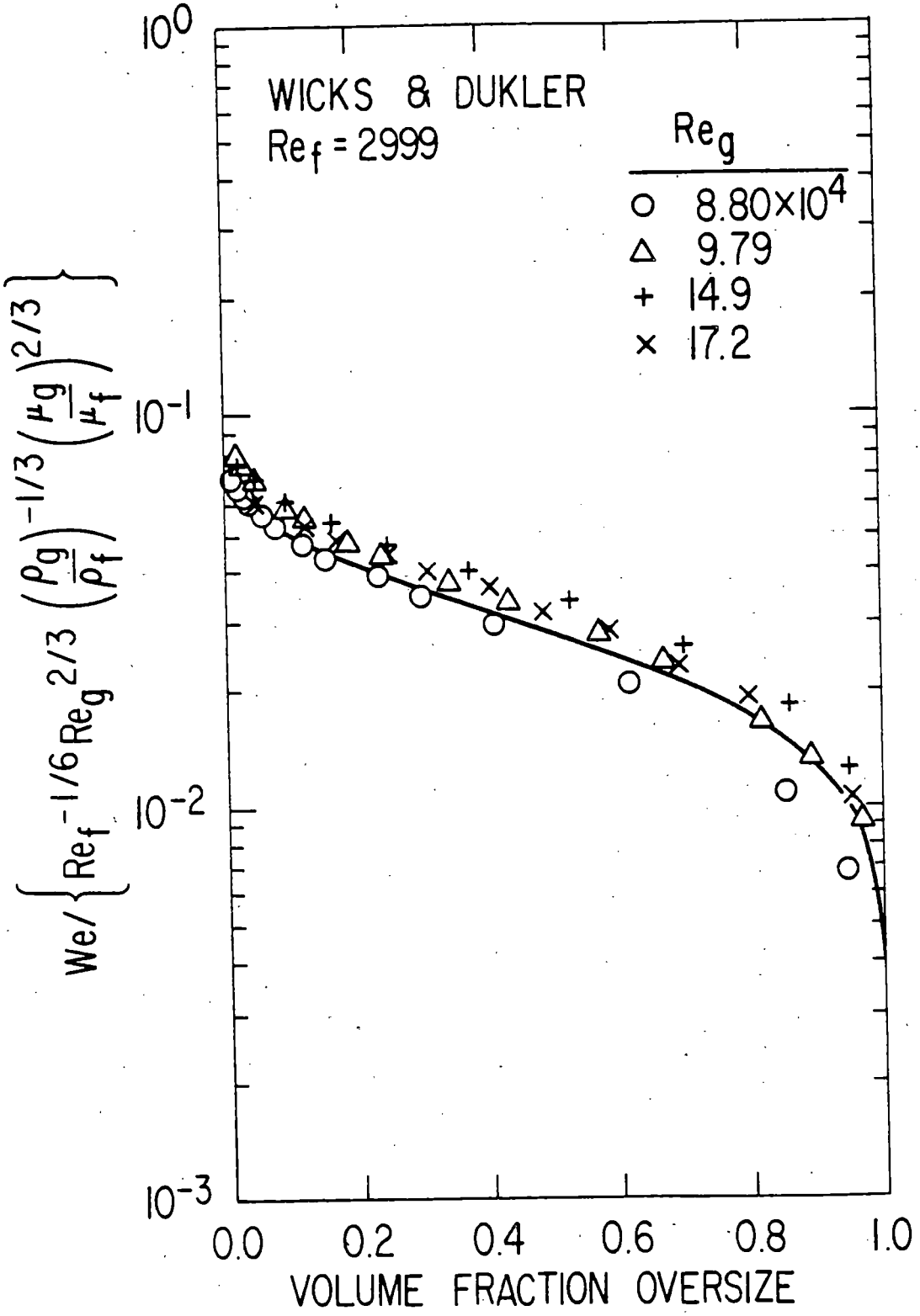

Droplet Size Distributions at Re_f = 2999 for Data of Wicks and Dukler

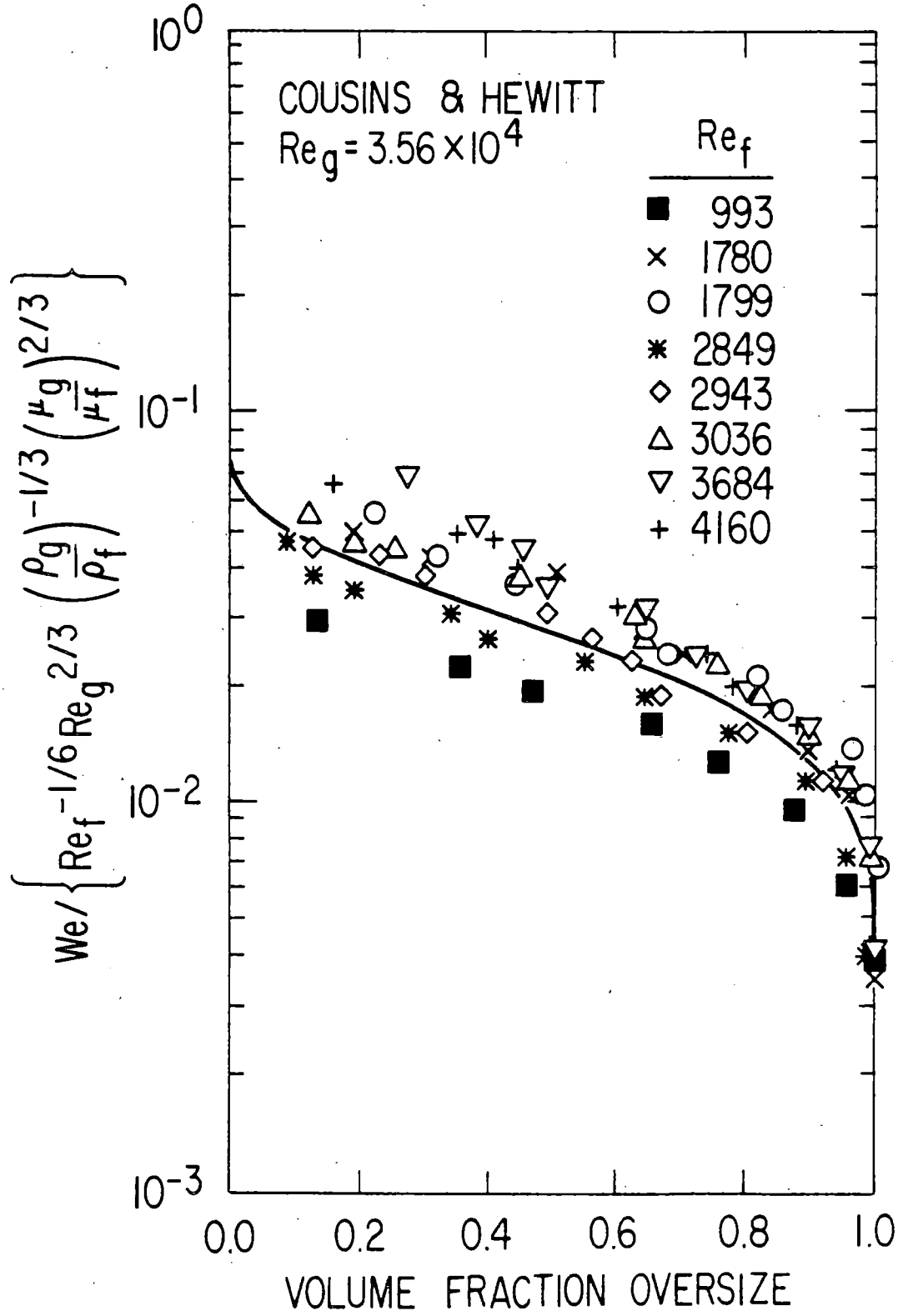

Droplet Size Distributions at $Re_g = 3.56 \times 10^4$ for Data of Cousins and Hewitt

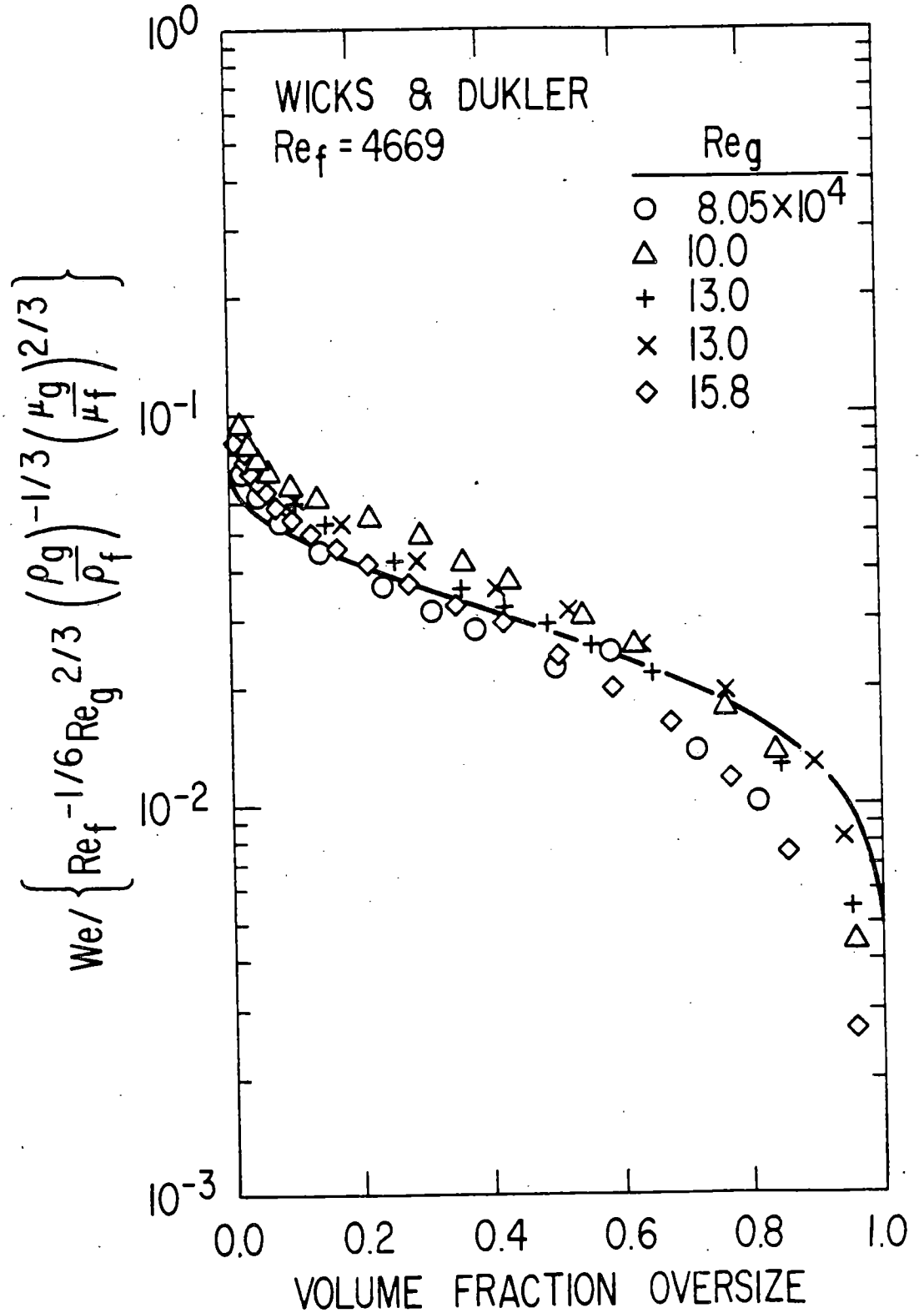

Droplet Size Distributions at Re_f = 4669 for Data of Wicks and Dukler

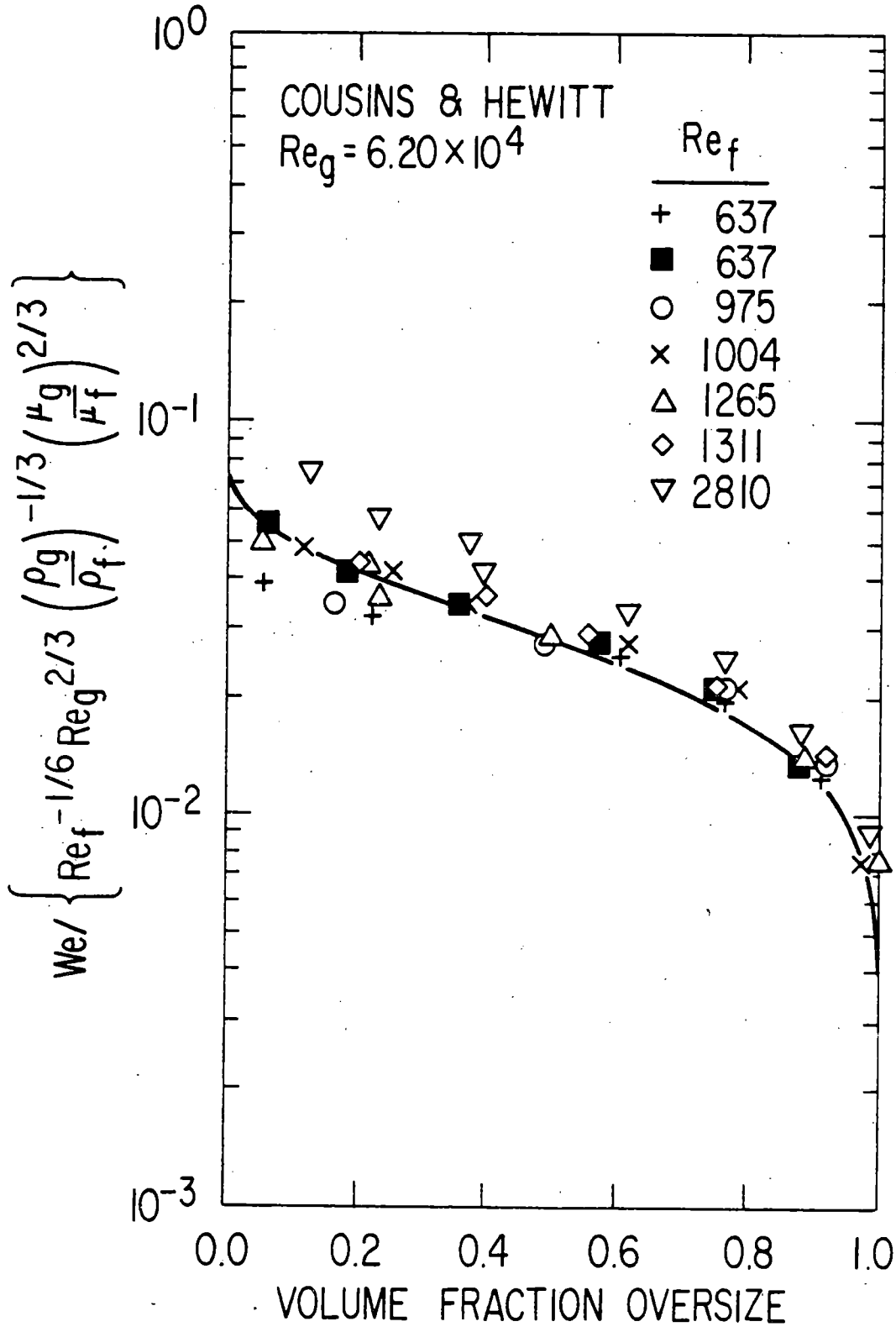

Droplet Size Distributions at $Re_g = 6.20 \times 10^4$ for Data of Cousins and Hewitt

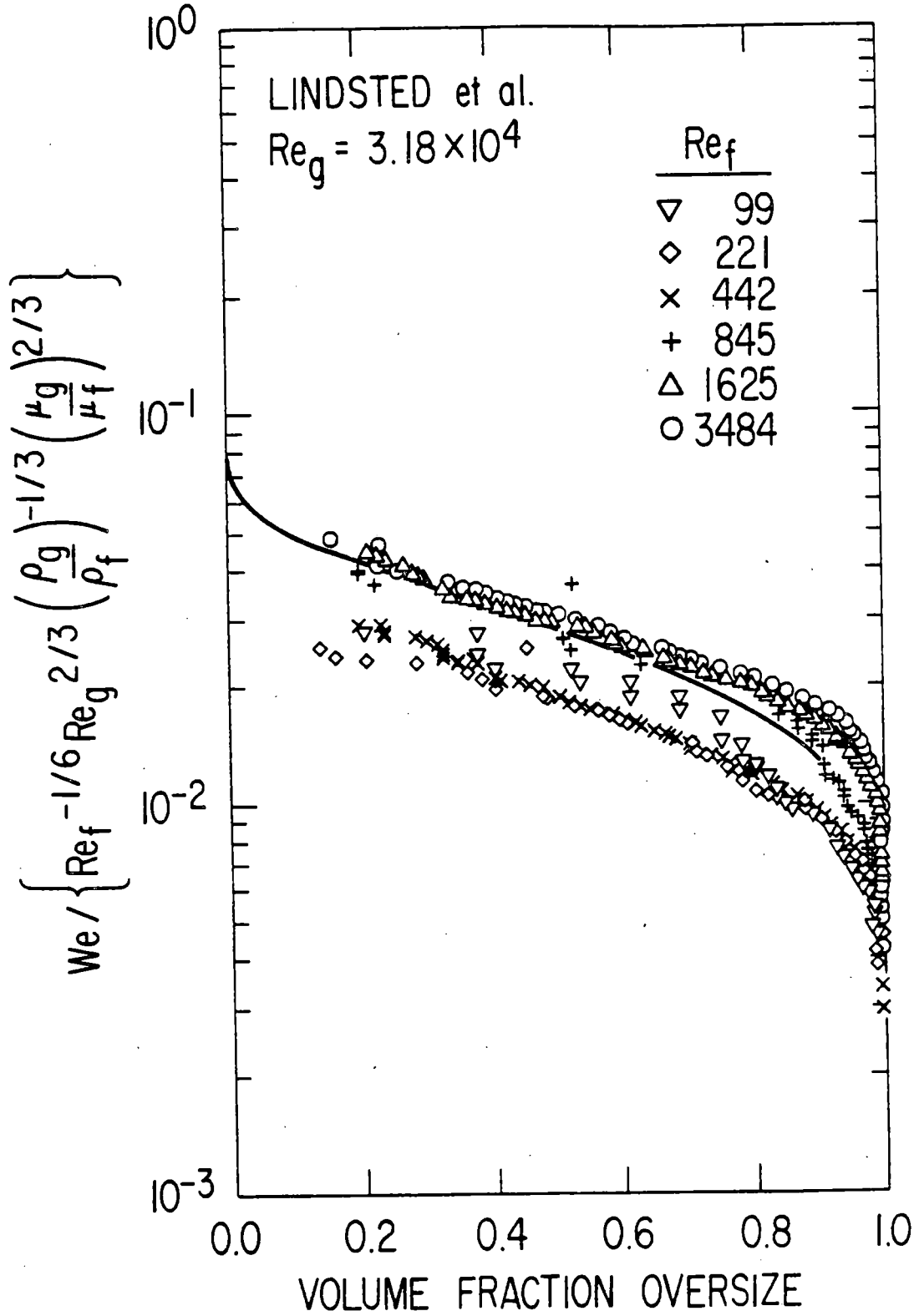

Droplet Size Distributions at $Re_g = 3.18 \times 10^4$ for Data of Lindsted et al.

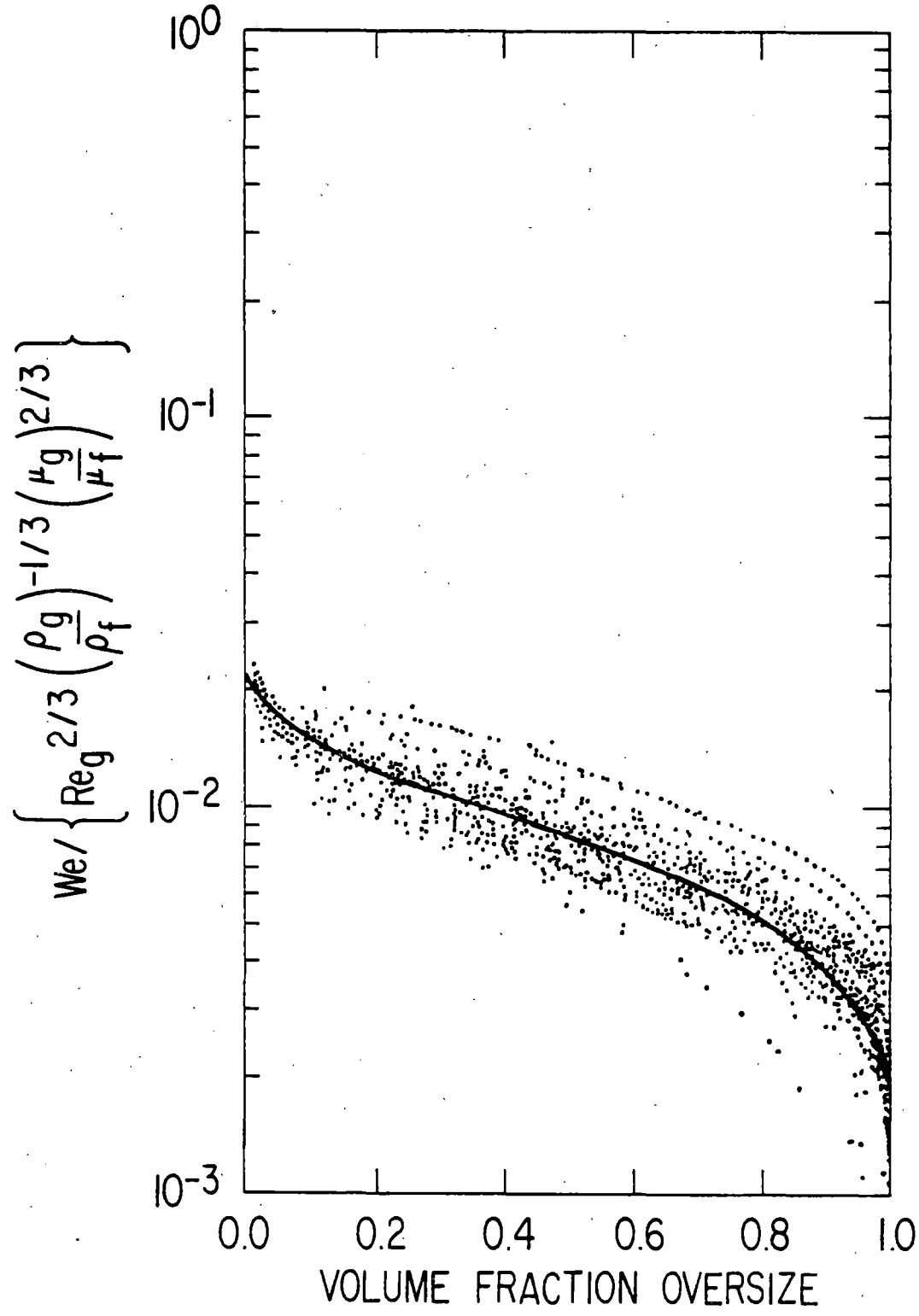

Droplet Size Distributions in $We\Big/\left[Re_g^{2/3}\left(\frac{\rho_g}{\rho_f}\right)^{-1/3}\left(\frac{\mu_g}{\mu_f}\right)^{2/3}\right]$ vs. Volume Fraction Oversize Plot for Data of Wicks and Dukler, Cousins and Hewitt and Lindsted et al.

Table I Various Mean Diameters*

Ratio of diameter A and diameter B

B \ A	$\bar{D}_{10}$	$\bar{D}_{20}$	$\bar{D}_{21}$	$\bar{D}_{30}$	$\bar{D}_{31}$	$\bar{D}_{32}$	$\bar{D}_{43}$	D_{vm}	D_{max}
D_{vm}	0.313	0.409	0.533	0.510	0.650	0.796	1.064	1.0	3.129
D_{max}	0.100	0.131	0.170	0.163	0.208	0.254	0.340	0.320	1.0

*$\bar{D}_{10}$; Linear mean diameter

$\bar{D}_{20}$; Surface mean diameter

$\bar{D}_{21}$; Surface diameter mean diameter

$\bar{D}_{30}$; Volume mean diameter

$\bar{D}_{31}$; Volume diameter mean diameter

$\bar{D}_{32}$; Sauter Mean diameter

$\bar{D}_{43}$; De Brouckere mean diameter

Bubble Number Density; N_B

- $$\frac{\partial N_B}{\partial T} + \frac{1}{A}\frac{\partial}{\partial Z}(AN_B V_B) = \Phi_W + \Phi_{HN} - \Phi_{COND}$$

Φ_W; Wall Nucleation Source

Φ_{HN}; Bulk Heterogeneous Nucleation Source (Flushing)

Φ_{COND}; Sink Due to Collapse

- $$\begin{cases} \Phi_W \sim F_W(T_W - T_{SAT}) & ; T_W > T_{SAT} \\ \Phi_{HN} \sim F_{HN}(T_F - T_{SAT}) & ; T_F > T_{SAT} \\ \Phi_{COND} \sim F_{COND}(T_{SAT} - T_F) & ; T_{SAT} > T_F \ , \ N_B > 0 \end{cases}$$

Modeling of Wall Nucleation Source Φ_W

$$\Phi_W = \frac{N_A \, F \, \xi_K}{A}$$

N_A; Wall Nucleation Sites Density

F; Frequency of Bubble Nucleation

ξ_K; Heated Perimeter

A; Cross Sectional Area

(1) Pool Boiling

$$Nu \sim Re^A \, Pr^B \left(\frac{D_D}{S}\right)^C \quad ; \quad Nu \equiv \frac{HS}{K_F}$$

- D_D; Bubble Departure Size ← Fritz $\left(D_D = 0.85\theta\sqrt{\frac{2\sigma}{\Delta\rho G}}\right)$
- $S \equiv N_A^{-1/2}$
- $V \sim \left(\frac{\Delta T C_{PF}}{I_{FG}}\right)^2 (A_F\sqrt{N_A})$ ← Zuber

↓

- $H = H\,(\Delta T, N_A, \text{Properties})$
- Data for H, ΔT

→ N_A

Correlation for Wall Nucleation Sites N_A

$$N_A^* = 1.36 \times 10^{-8} \Delta T^{*4.5} P^{*1.33} (1 + 5 \times 10^5 \rho^{*3.16})$$

$$N_A^* = N_A D_D^2$$

$$\Delta T^* = \frac{\rho_G I_{FG} D_D}{2\sigma} \frac{\Delta T}{T_S} \left(= \frac{1}{R_C^*} \right)$$

$$P^* = \frac{\sigma}{\rho_G C_{PF} T_S D_D}$$

$$\rho^* = \rho_G / \rho_F$$

Forced Convection

$\Delta T \longrightarrow \Delta T$ Effective

Use Chen's Suppression Factor

9th USNRC WATER REACTOR SAFETY MEETING

Parallel Channel Effects During the Emergency Core Cooling of a BWR

R.T. Lahey, Jr.
W. Conlon
M. Fakory
Rensselaer Polytechnic Institute
Troy, New York - USA

Several years ago a USNRC funded investigation was initiated at RPI to study the potential for "steam binding" in Boiling Water Nuclear Reactors (BWRs). This phenomena is shown schematically in Figure-1. It can be seen that, due to a countercurrent flow limitation (CCFL) at the upper tie plate, the ECCS liquid injected into the upper plenum is postulated to be carried out the top of the steam separators, and/or, be forced out the jet pumps. If this situation occurs, BWR core cooling will be less effective than if core reflood occurred.

In BWRs parallel channel effects can be expected to play an important role in CCFL breakdown and the effectiveness of core cooling. Figure-2 shows a schematic of how CCFL breakdown in the cold bundles might be expected to alter the scenario.

In order to investigate the parallel channel effects which actually occur, a parallel channel effects (PCE) loop was designed and constructed at RPI. As can be seen in Figure-3, this test loop consists of a scaled PCE test section consisting of:

- a core region having a simulated hot, average and cold fuel assembly
- an upper plenum region, which includes a representative ECC spray system
- a vapor separation (i.e., riser) region
- a downcomer region
- a jet pump assembly
- a lower plenum region, including provisions for vapor injection

It can be noted that Freon-22 is used as the heat sink and Freon-114 as the test fluid.

The scaling basis (Freon-114/water) used is summarized in Figure-4. It can be seen that the system has been scaled for representative real-time response.

Figure-5 shows a picture of the lower level of the PCE loop. It can be seen that pyrex glass has been used to allow visualization. Also note that cal-rod

heaters are employed in the three annuli which simulate the hot, average and cold fuel rod bundles. The upper level of the PCE loop is shown in Figure-6. A close-up view of the upper region of the PCE test section is shown in Figure-7. It can be seen that the entire region is constructed from pyrex glass. Finally, Figure-8 shows the upper plenum region (with the head removed). The radio frequency (RF) excited impedance (Z) probes, which are an integral part of the upper tie plate, and are used to detect CCFL breakdown, can be seen.

A number of experiments have been performed in the PCE test facility. The initial and boundary conditions for several representative tests are tabulated in Figure-9. Schematics of the salient experimental phenomena are shown in the following figures.

Figure 10a - 10h show the observed behavior for test C.001,a low L.P. vapor flow simulation. It can be seen in Figure-10b that CCFL breakdown occurred in all the heated channels; however, as can be noted in Figure-10c, when the jet pumped sealed, the liquid was blown out of the hot channel. As can be seen in Figure-10f, when the liquid level reached the level of the (side entry) lower orifice, liquid was injested into the hot channel by the L.P. vapor flow. It should be stressed that the hot channel never reflooded during this experiment and thus the cooling mode was quite different than in the other channels. Note also that in this experiment ECC liquid did spill over from the jet pump but did not fill up the "steam separator" stand pipe.

The C.003 is shown schematically in Figures-11a - 11h. It can be seen for higher L.P. vapor flow rates, CCFL breakdown does not occur in the heated channels, but occurs immediately in the bypass region. Moreover, it can be seen that Figure-11g does duplicate the classical "steam binding" scenario quite well.

The experiment just discussed, run C.003, did not simulate the expected leakage between the (liquid filled) bypass region and the inlet of the heated assemblies. To understand the effect of this leakage on the scenario, test C.006 was performed. It is the same as C.003 in all respect except for spray subcooling. However, extensive testing at RPI has shown that, for the degree of subcooling achievable in the PCE test rig , this parameter has a small effect on the test results. The salient results are shown schematically in Figures 12a - 12d. It can be seen that for high L.P. vapor flow rates, the (subcooled) liquid injected

to simulate the leakage has a pronounced effect on the scenario. In particular, Figures 12b & 12c show that when the jet pump seals the liquid in the bypass is blown out, and CCFL breakdown occurs in the cold channel. The equilibrium situation is shown in Figure-12d; note that the L.P. liquid level never reduces the level of the inlet orifices. It is seen to be very much different than the situation shown in Figure 11g.

It should be apparent to the reader that many scenarios are possible, depending on the initial and boundary conditions. Test C.008 was performed to investigate one of the most important of these parameters; the L.P. vapor flow rate. The scenario is shown in Figures 13a - 13f. This test was exactly like C.003, except that the L.P. vapor flow rate was decayed when the L.P. liquid level reached the orifices ($t \simeq 2$ mins). It can be seen in Figure-13f, that the hot and average channels would not reflood even though there was virtually no L.P. vapor flow. This is apparently due to the fact that the vapor superheat and liquid vaporization in these channels is sufficient to maintain a CCFL condition at the upper tie plates, and the core Δp was high enough to prevent reflood.

Test C.011 was run at intermediate L.P. vapor flow rates to further appraise this parameter. For this test, the effect of leakage was simulated. It can be seen in Figure 14a - 14f, that the effect of the simulated leakage was less for this test, than for the high L.P. vapor flow case, C.006. That is, in C.011 the L.P. liquid level reached the inlet orfices, however, as shown in Figures 14c - 14d,when the jet pump was sealed the liquid in the average channel was blownout, thus the equilibrium situation (Figure 14e) is similar to that in test C.006 (Figure-12d), in that the hot and average channels do not reflood.

Test C.013 was performed to appraise the effect of simulated injection on the core cooling scenario. It was a repeat of test C.011, except there was no liquid injection and no spray subcooling. It can be seen in Figure 15a - 15e, that the thermal-hydraulic scenario is similar, and the equilibrium configuration is the same (i.e., compare Figures 14e & 15e).

These, and many other, PCE experiments performed at RPI have led to the conclusion that parallel channel effects are quite significant. Specifically:

- "Steam binding", of at least the hot channels, was always observed (i.e., complete core reflood never occurred).
- CCFL breakdown of the bypass region occurs immediately after the commencement of the core spray.
- The lower plenum vapor flow rate (a calculated quantity) is an important parameter in the observed thermal-hydraulic scenario.
- Rod Power (i.e., vapor superheat) is an important parameter in the observed thermal-hydraulic scenario.

It is hoped that these results will stimulate more work in this important area of BWR safety technology. Indeed they strongly support the need for a sophisticated systems analysis tool, such as BWR-TRAC.

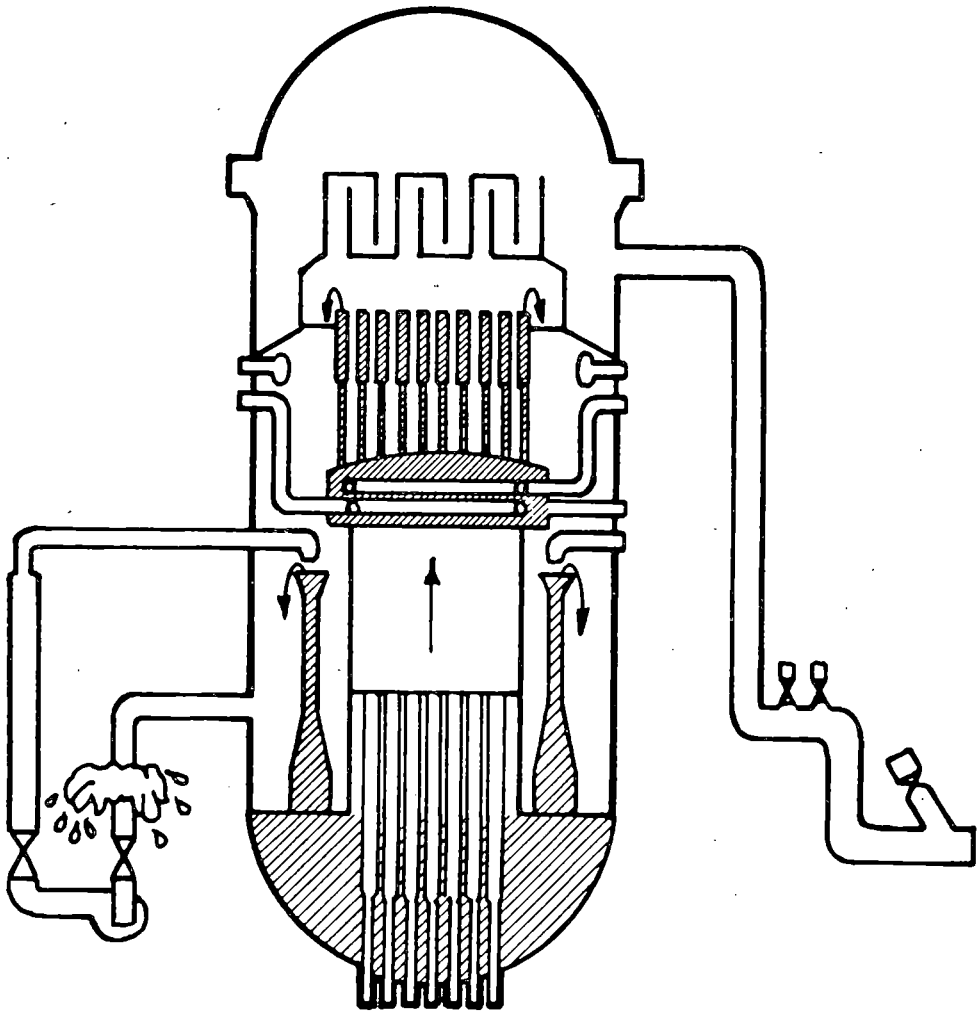

Figure 1. Hypothetical BWR LOCA Event - BWR Steam Binding

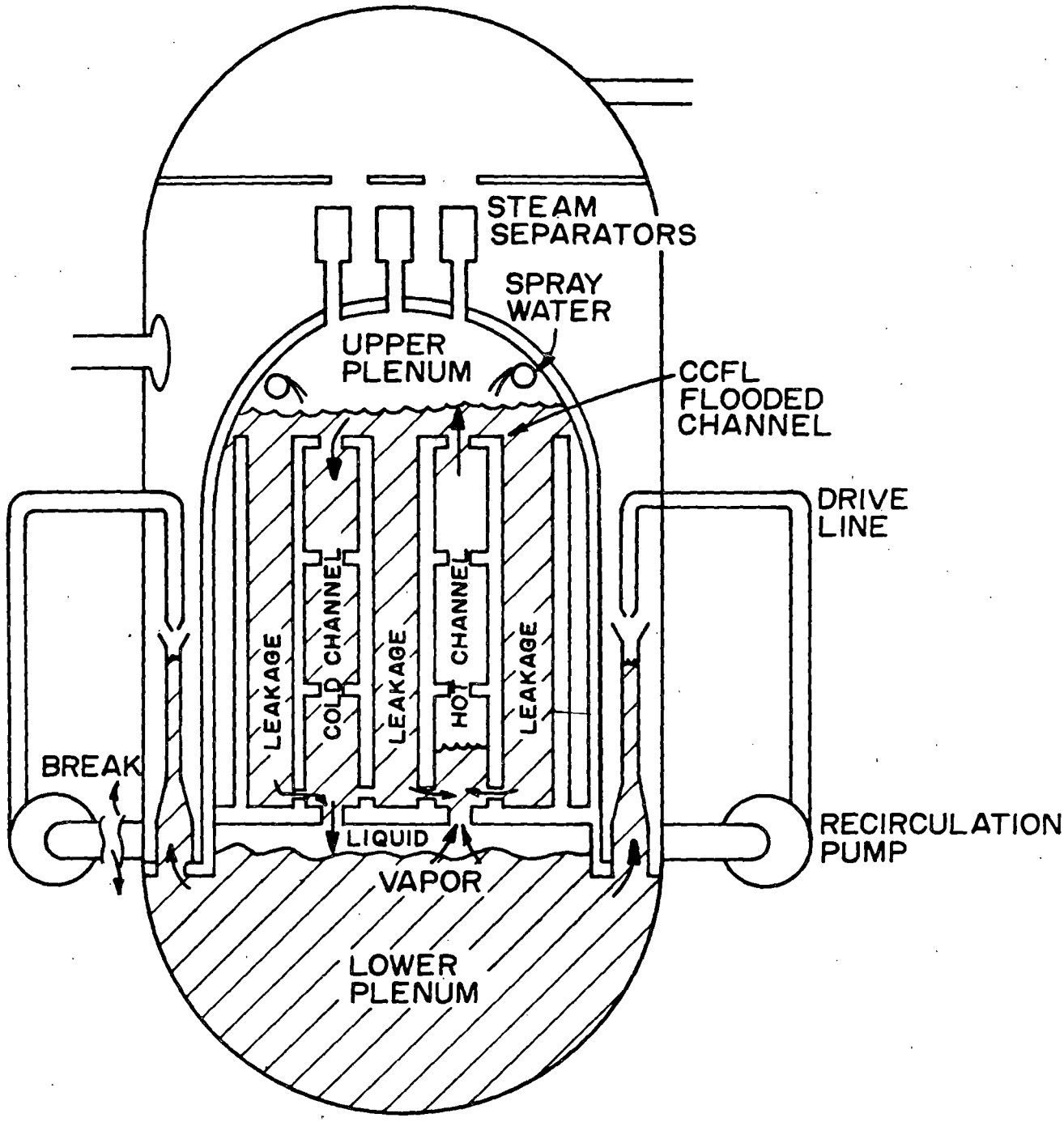

FIGURE 2. CCFL BREAK-DOWN DUE TO PARALLEL CHANNEL EFFECTS

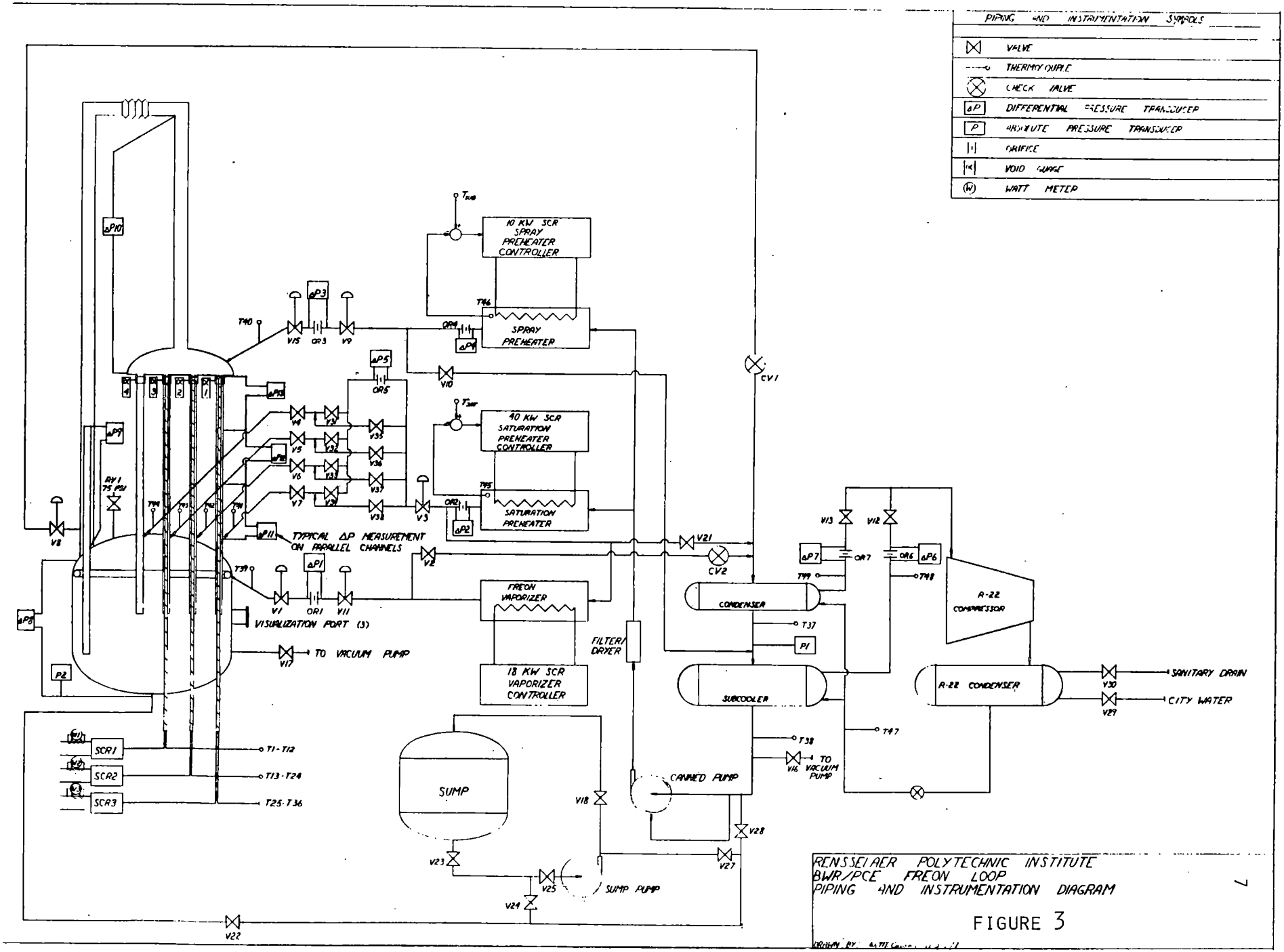

RENSSELAER POLYTECHNIC INSTITUTE
BWR/PCE FREON LOOP
PIPING AND INSTRUMENTATION DIAGRAM

FIGURE 3

7

(1) Pressure

$$\hat{\rho}_f/\hat{\rho}_g = \rho_f/\rho_g$$

(2) Hydrostatic Head

$$\hat{L}_i = 1/2\ L_i$$

(3) Volumetric

$$\hat{V}_i/\hat{V}_{core} = V_i/V_{core}$$

(4) Spray Rate

$$\frac{\hat{Q}_{spray}}{\hat{V}_{core}} = \frac{Q_{spray}}{V_{core}}$$

(5) Core Hydraulics

$$\hat{D}_{rod} = D_{rod}$$

$$\hat{D}_H = D_H$$

(6) Parallel Channels (CCFL Assumed)

$$\hat{K}_v = K_v$$

where,

$$K_v \triangleq \frac{j_v \rho_v^{1/2}}{[\sigma g g_c(\rho_f-\rho_v)]^{1/4}}$$

This scaling implies,

$$\hat{G}_v/G_v = C(p)$$

(7) Jet Pump(s)

$$\frac{\hat{w}_{g,J.P.}}{\hat{w}_{g,L.P.(total)}} = \frac{w_{g,J.P.(s)}}{w_{g,L.P.(total)}}$$

(8) Power Scaling (1st Law)

$$(\hat{h}_v/\hat{h}_{fg})_{exit} = (h_v/h_{fg})_{exit}$$

thus,

$$\hat{\bar{q}}'' = A\,\bar{q}'' + B$$

(9) Spray Subcooling

$$\hat{N}_{sub} = N_{sub}$$

where,

$$N_{sub} = \frac{v_{fg}(h_f-h_{IN})}{v_f h_{fg}}$$

Figure 4

PCE Scaling Basis

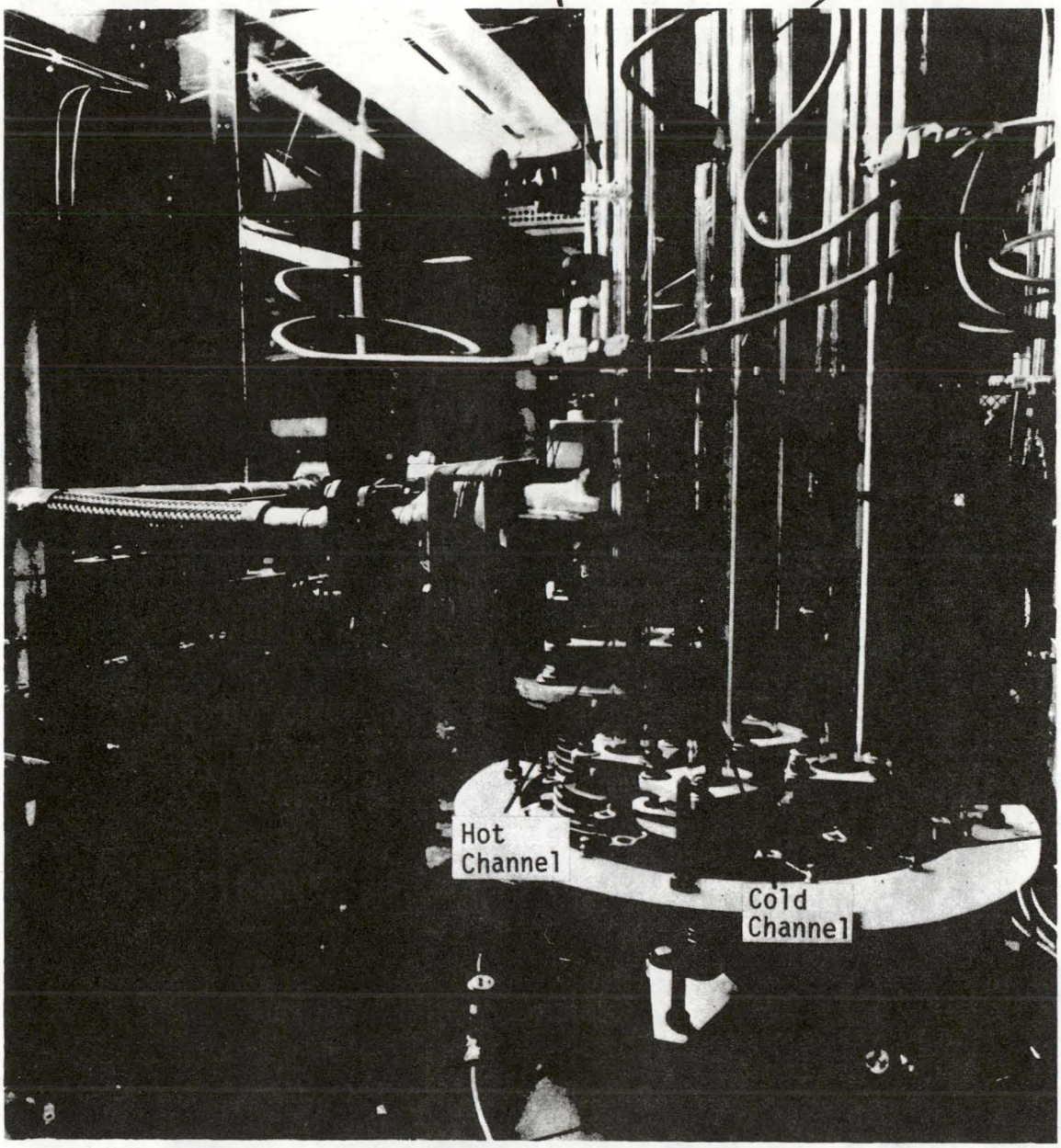

Figure-5
PCE Loop
(Lower Level)

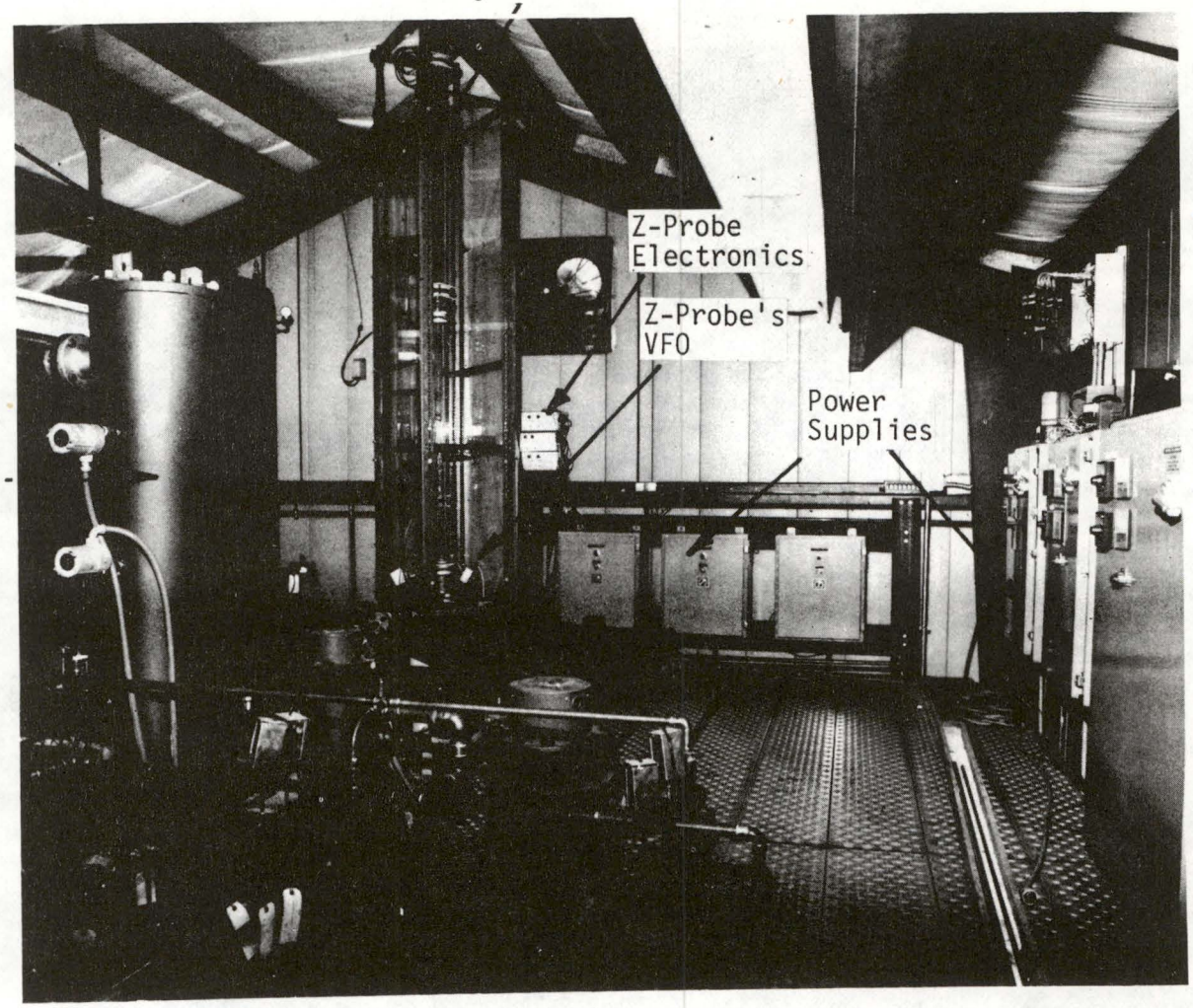

Figure-6
PCE Loop
(Upper Level)

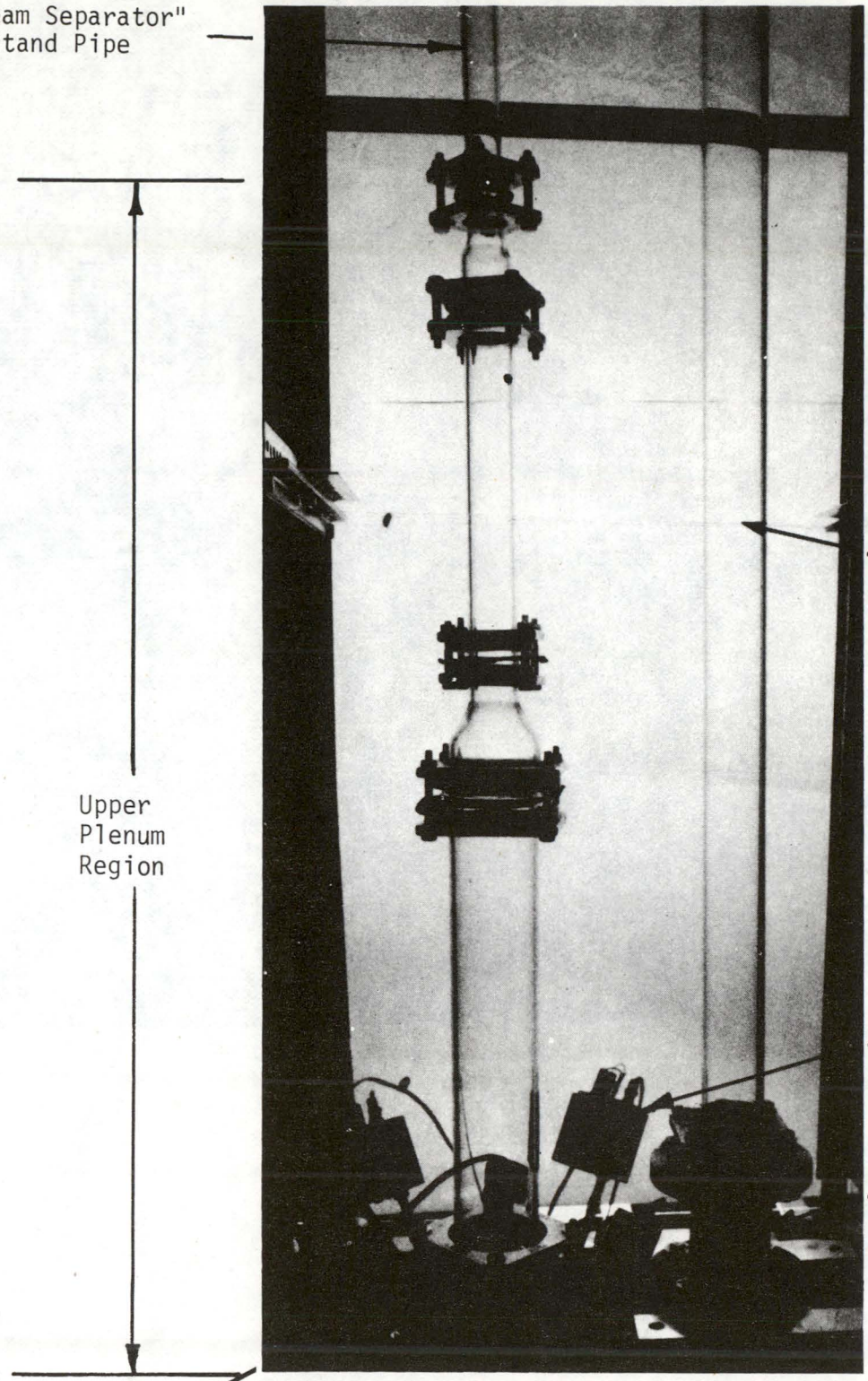

Figure-7
PCE Test Section
(Upper Region)

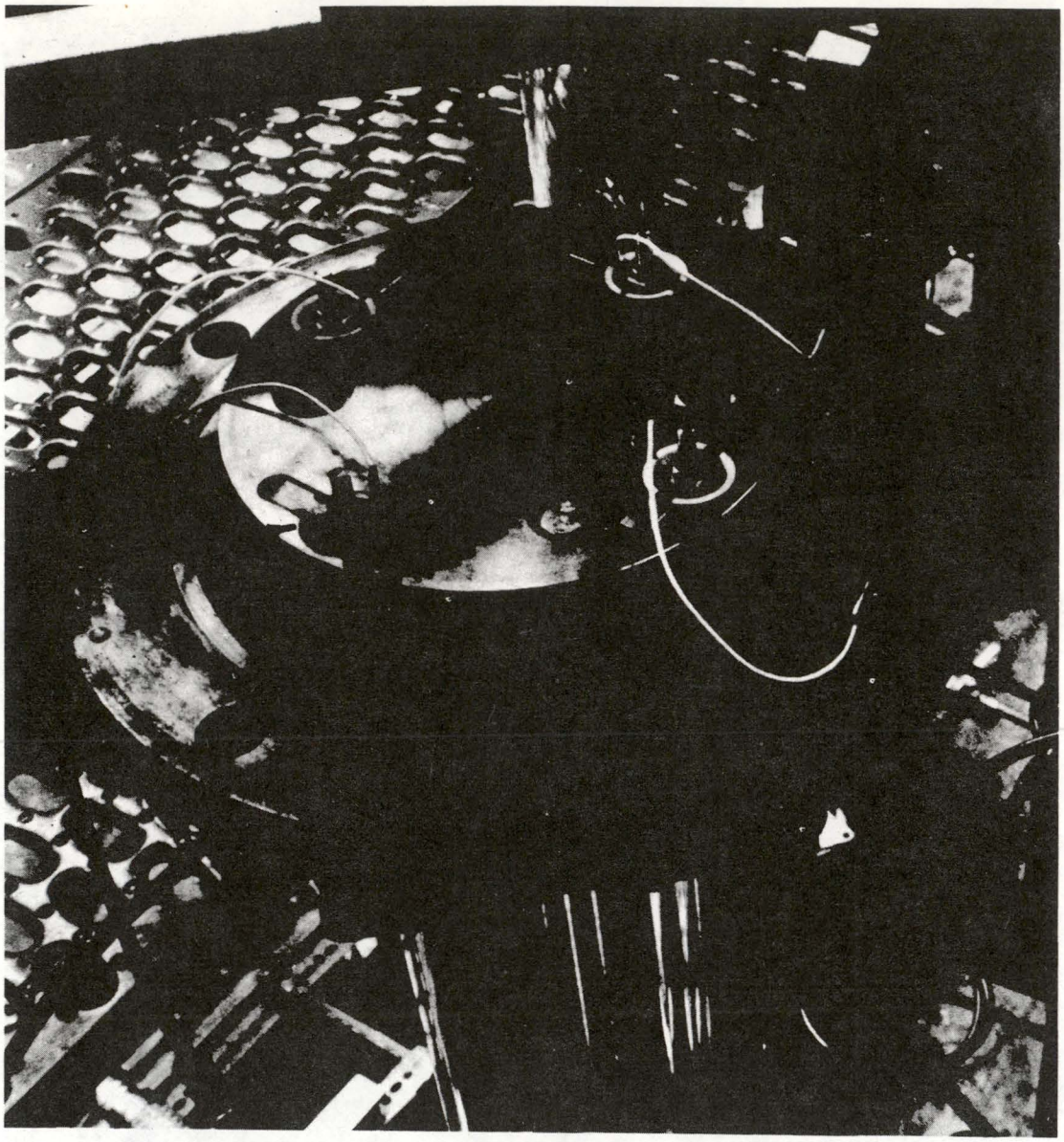

Figure-8

PCE Test Section

(Upper Plenum Region,
with Head Removed)

Run	Pressure (PSIA)		T_{ROD}(0)	L.P. Vapor (lb/hr)		W_{spray}		Subcooling (BTU/hr)		Scaled Power	Comments
	PCE	BWR/4		PCE	BWR/4 (Ave/Cold)	PCE	BWR/4	PCE	BWR/4		
* C.001	25	200	$>T_{CRIT}$	Low	382/185	High	2 Headers	1.4	21	5%	None
* C.003	25	200	$>T_{CRIT}$	High	3700/1800	High	2 Headers	1.4	21	2%	None
C.006	25	200	$>T_{CRIT}$	High	3700/1800	High	2 Headers	0	0	2%	Simulated Leakage
C.008	25	200	$>T_{CRIT}$	High	3700/1800	High	2 Headers	1.4	21	2%	L.P. Vapor Decay
C.011	25	200	$>T_{CRIT}$	Inter-mediate	925/450	High	2 Headers	1.4	21	2%	Simulated Leakage
C.013	25	200	$>T_{CRIT}$	Inter-mediate	925/450	High	2 Headers	0	0	2%	None

Figure-9

Test Conditions for Several PCE Tests

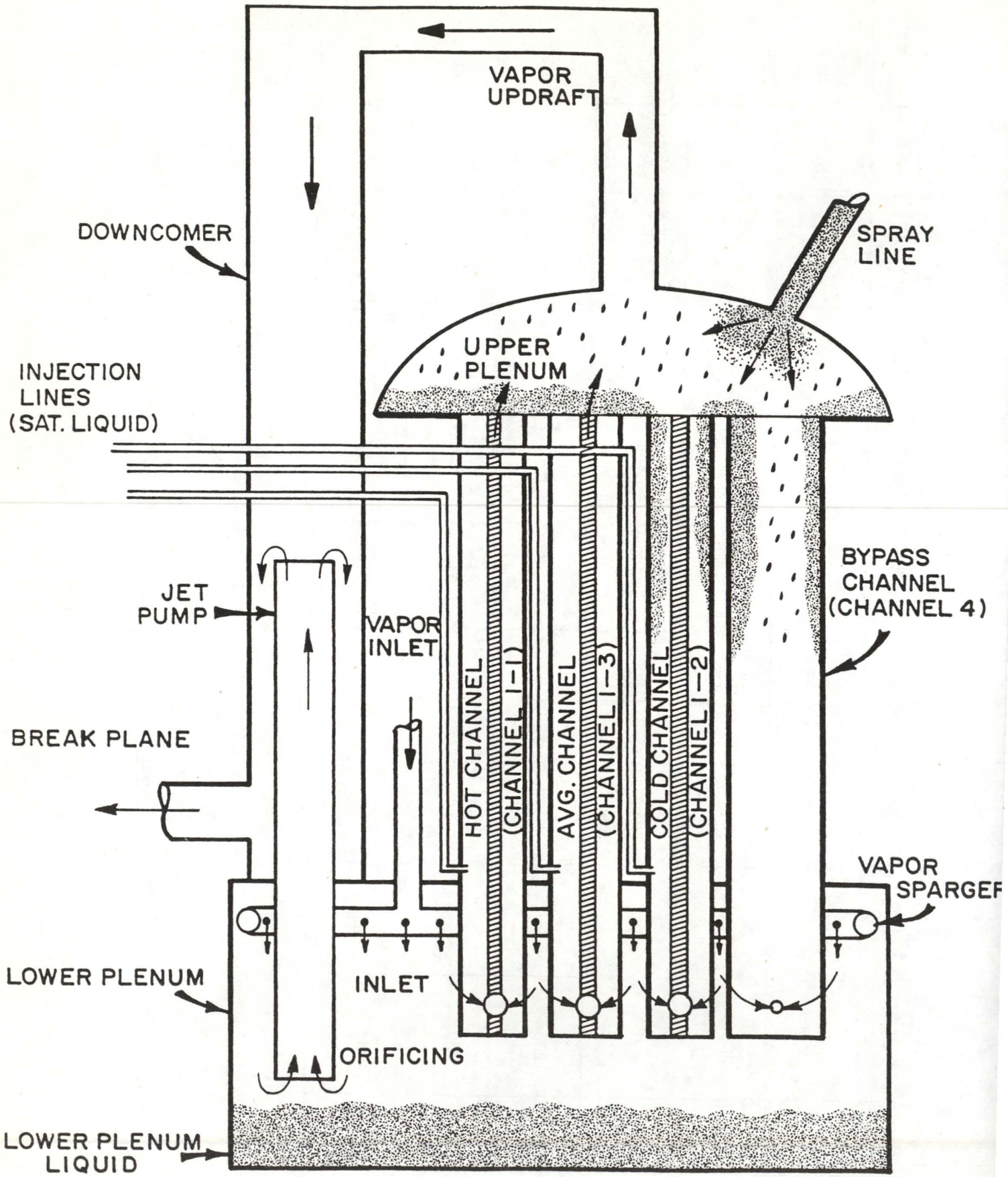

Figure 10a. Test C.001 (t≈5 sec)

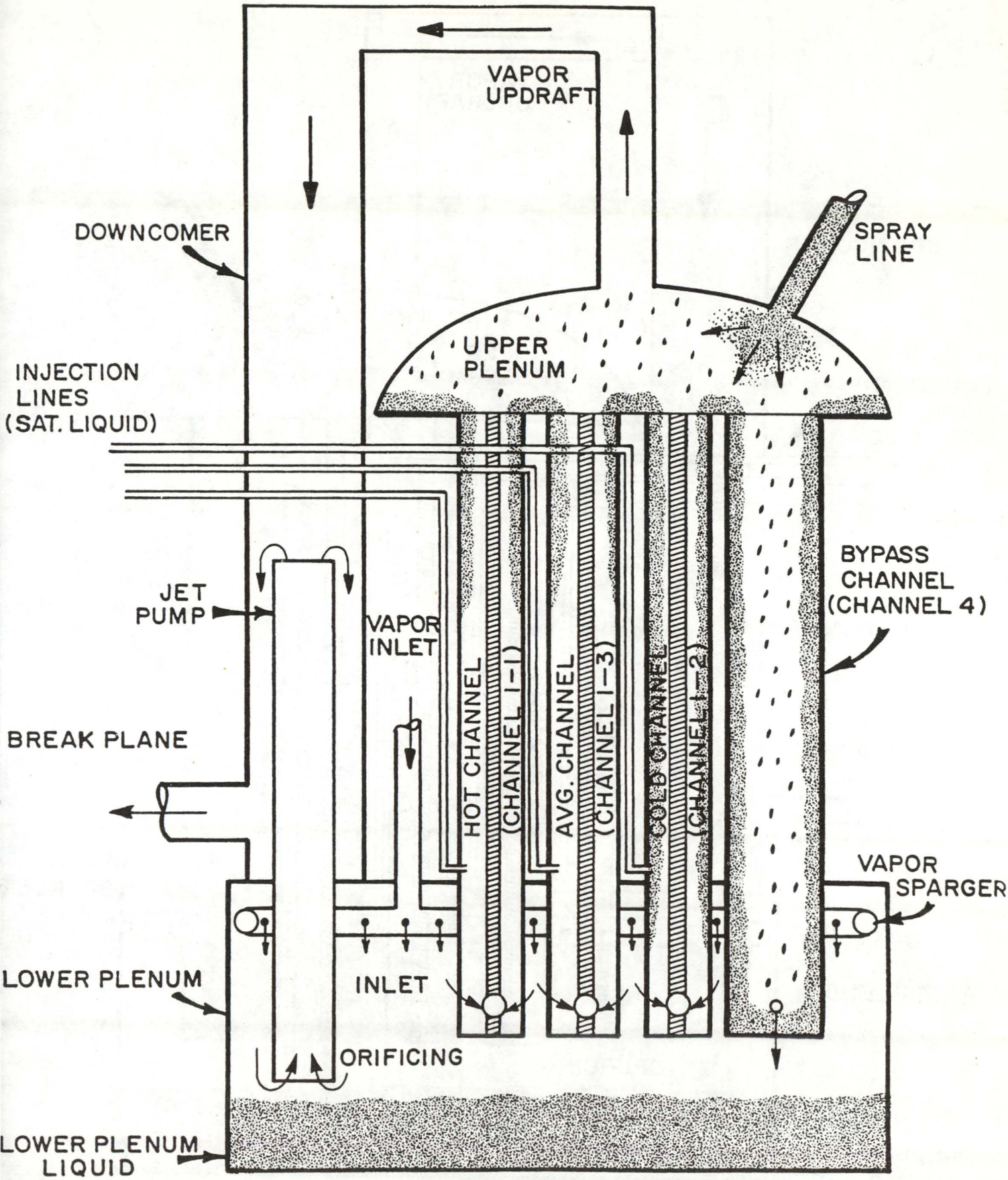

Figure 10b. Test C.001 (t≃20 sec)

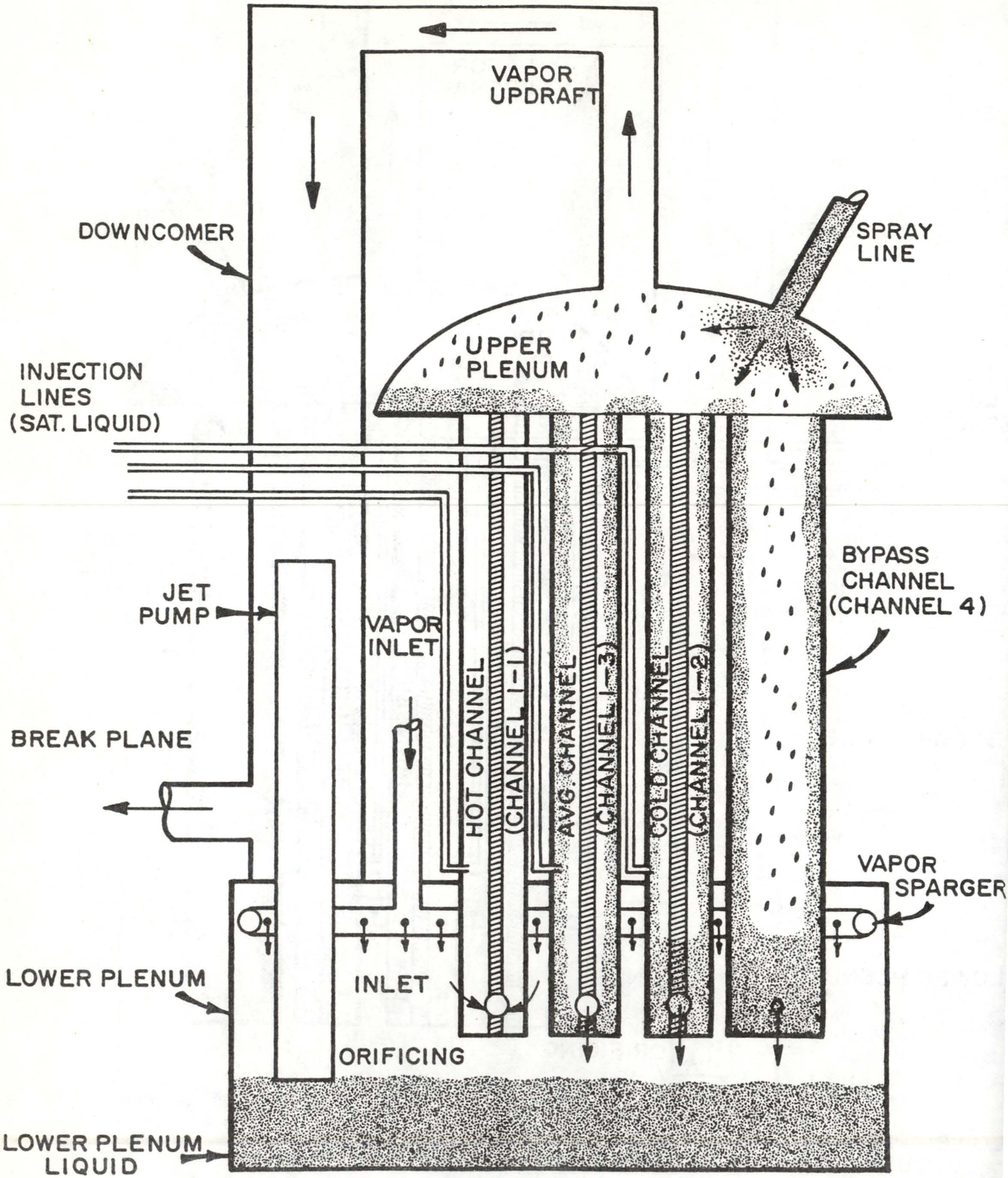

Figure 10c. Test C.001 (t≈2 min)

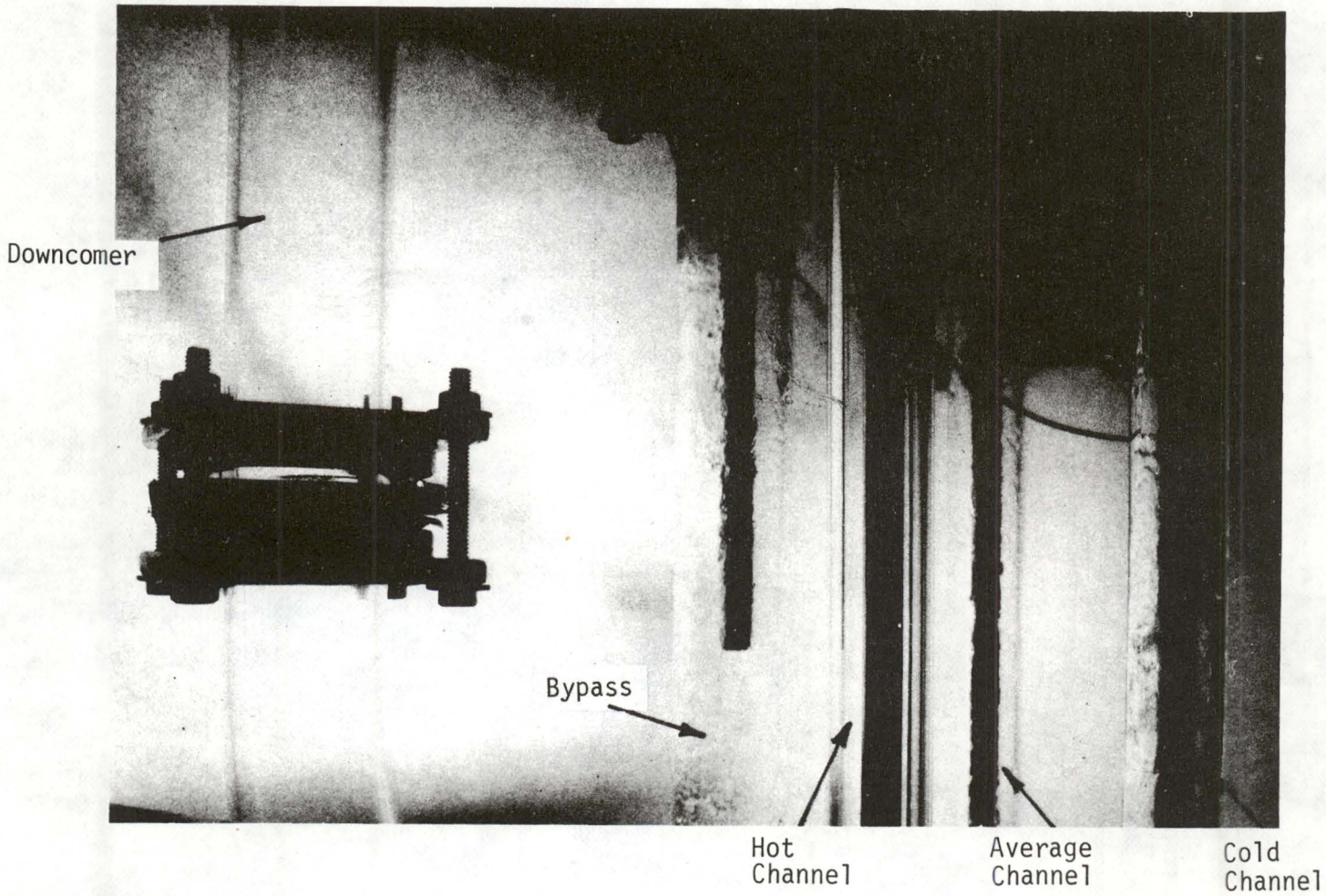

Figure-10d

CCFL Breakdown in

Heated Channels (Top of Core)

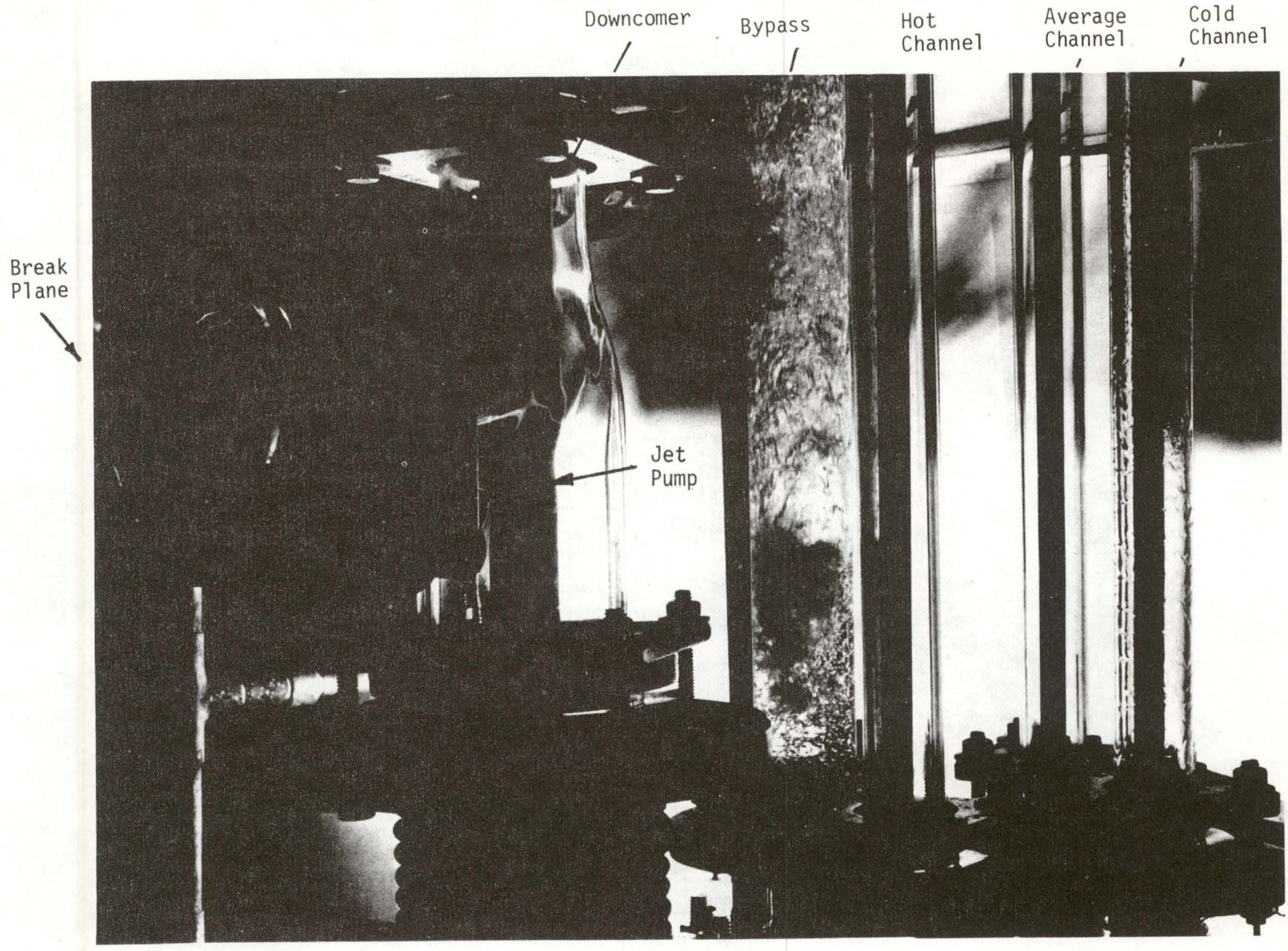

Figure-10e
CCFL Breakdown in
Heated Channels (Bottom of Core)

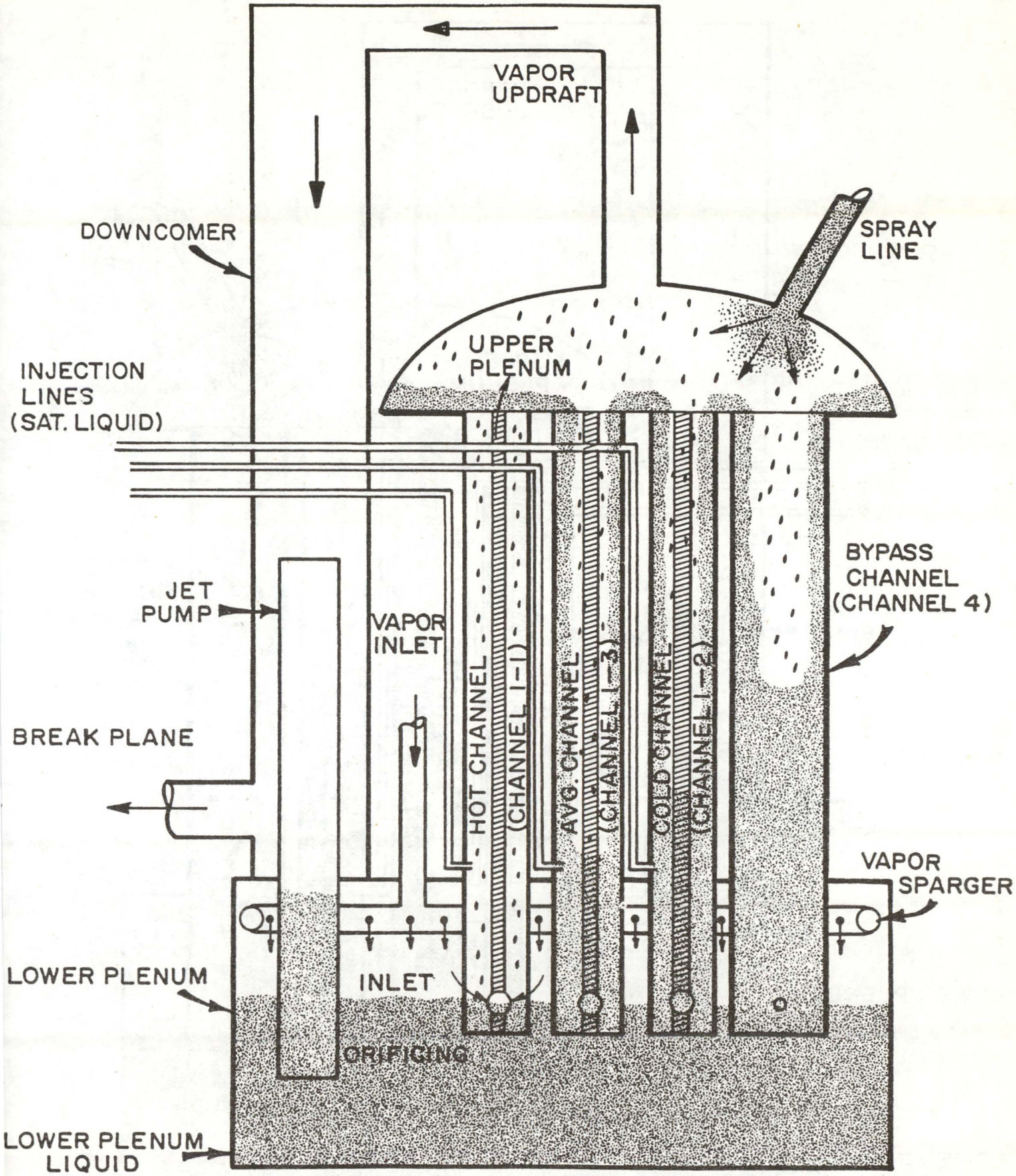

Figure 10f. Test C.001 (t≈5 min)

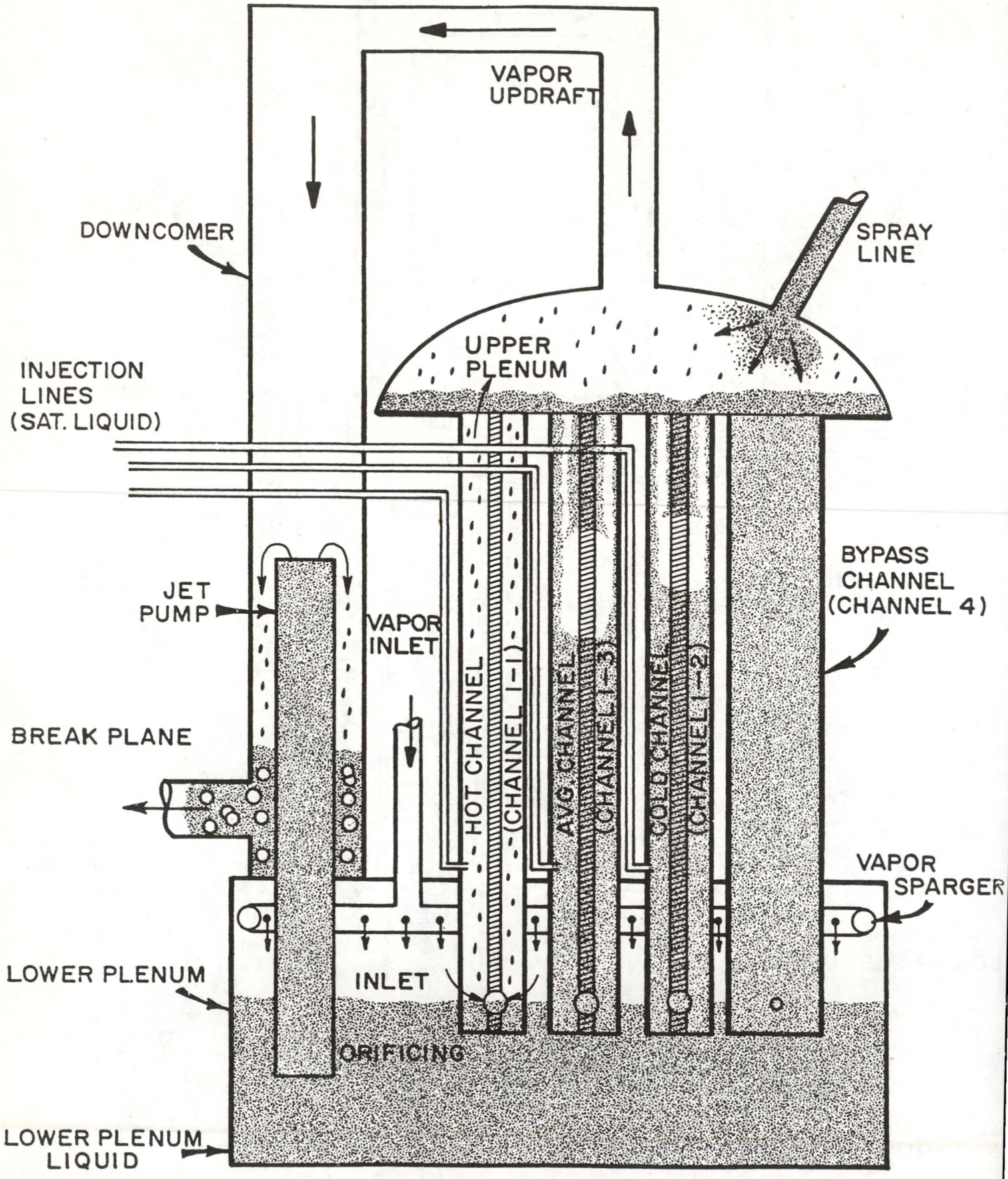

Figure 10g. Test C.001 (t≃8 min)

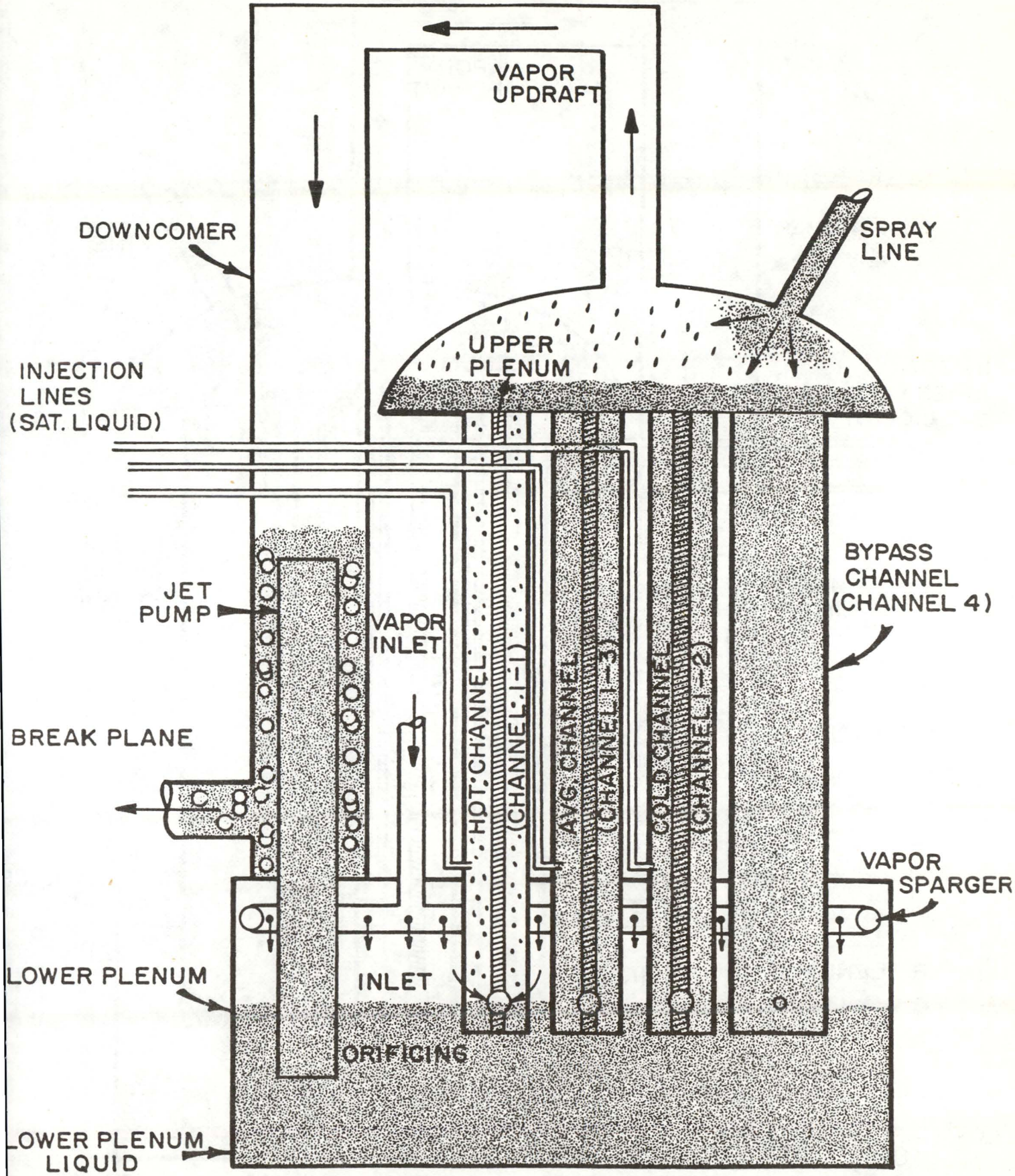

Figure 10h. Test C.001 (t ≈ 10 min)

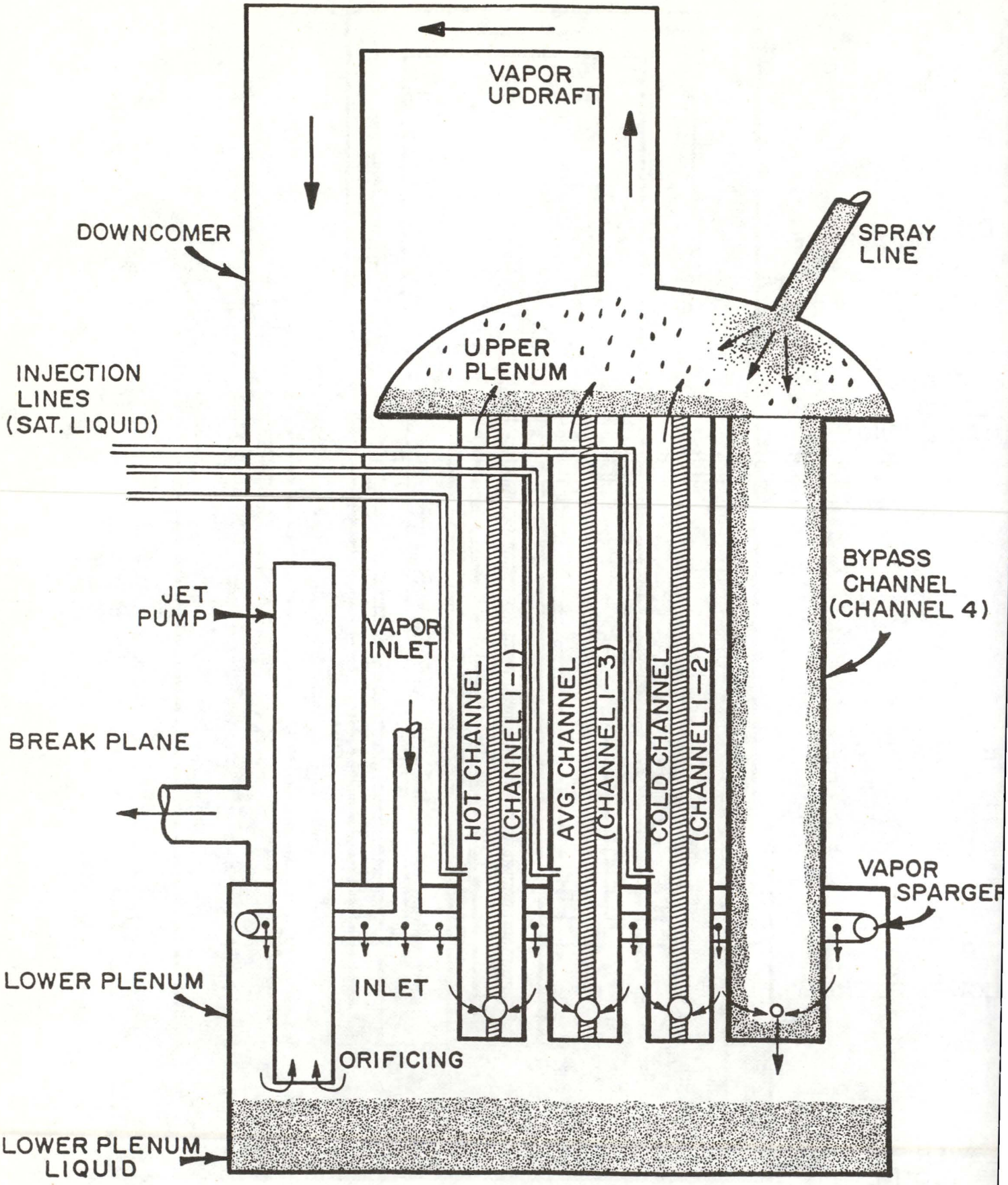

Figure 11a. Test C.003 (t≃20 sec)

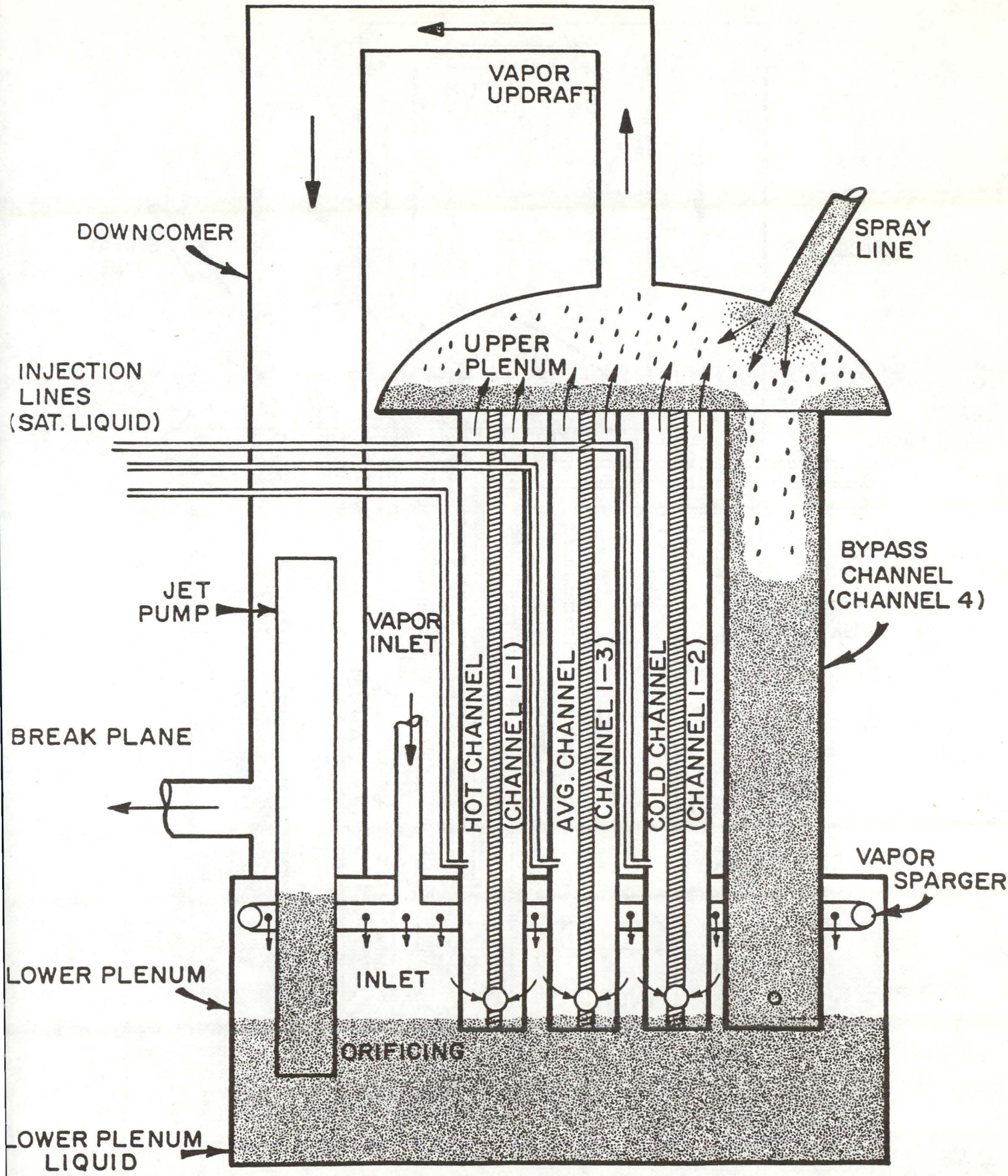

Figure 11b. Test C.003 (t≈60 sec)

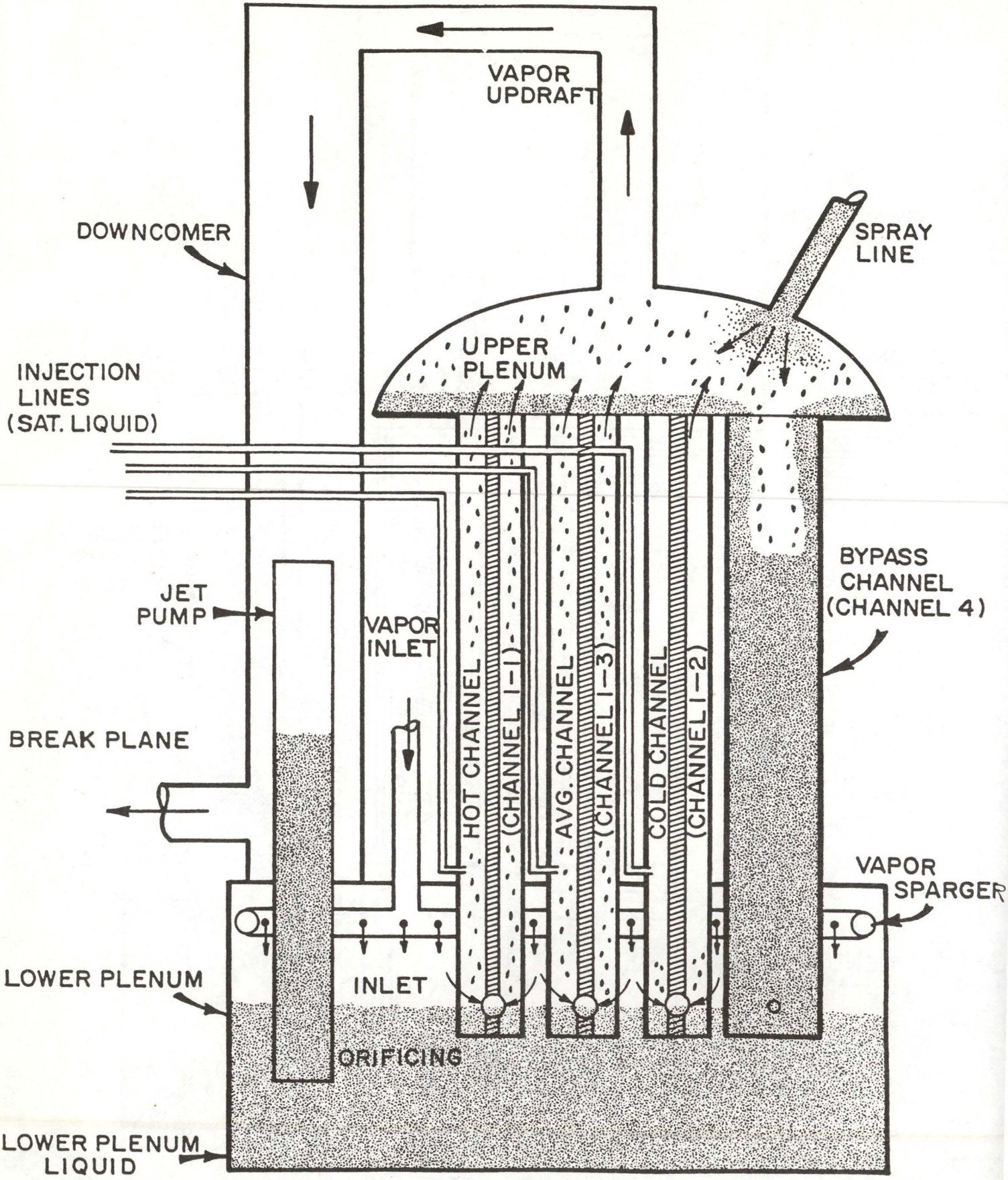

Figure 11c. Test C.003 (t≈75 sec)

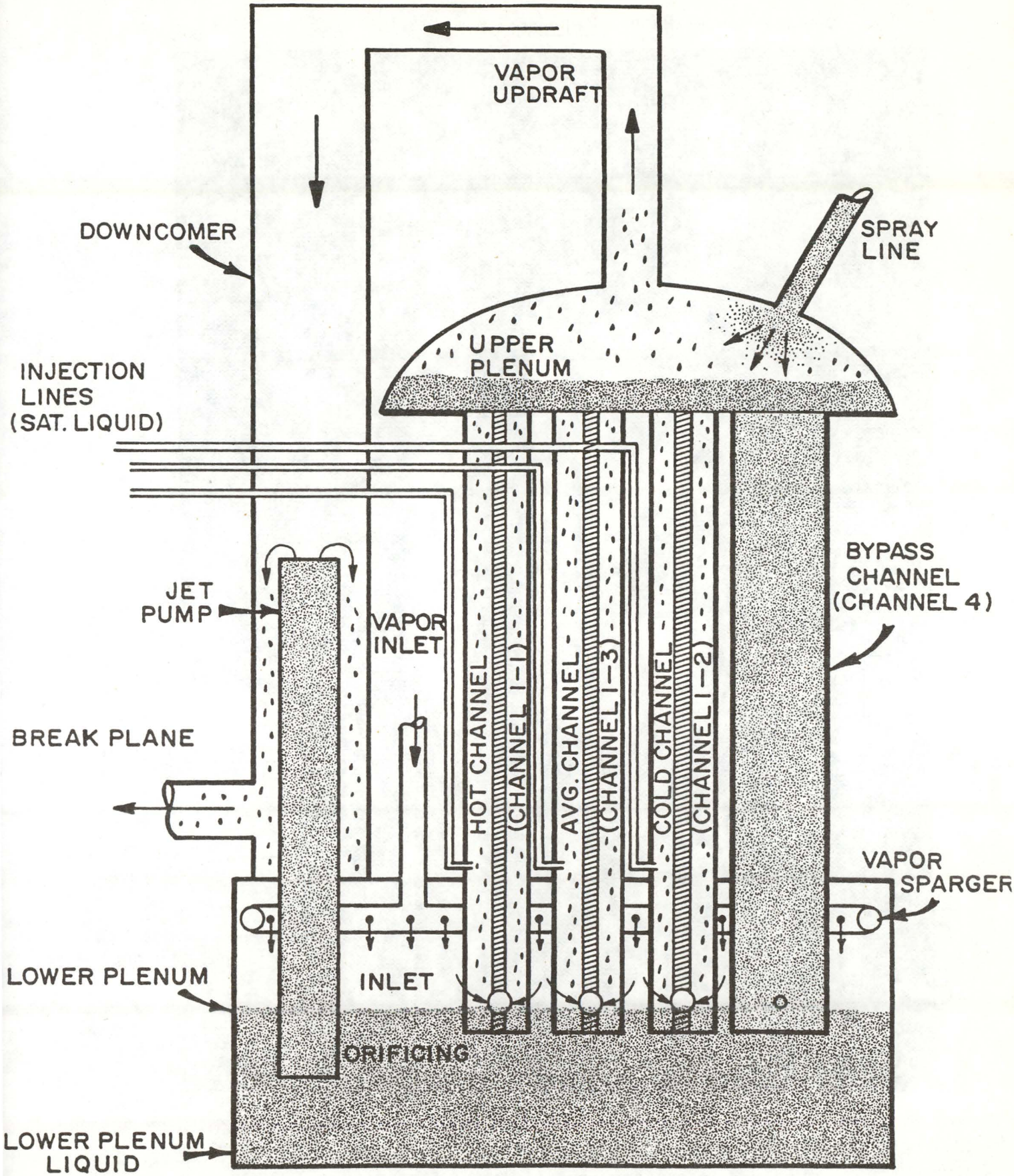

Figure 11d. Test C.003 (t≈2 min)

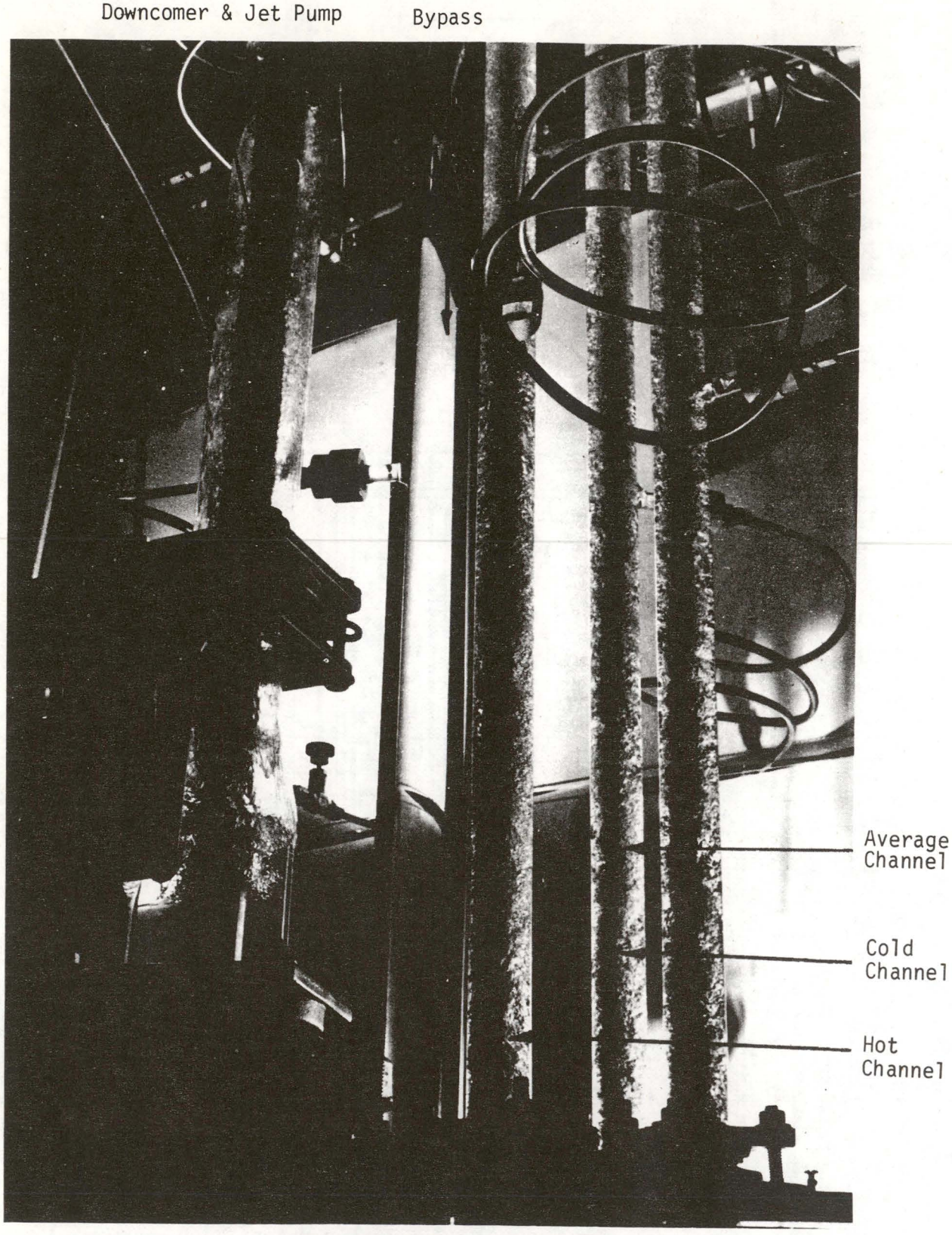

Figure-11e

Liquid Ingestion into all Heated Channels

(Bypass Filled, Jet Pump Spilling Over)

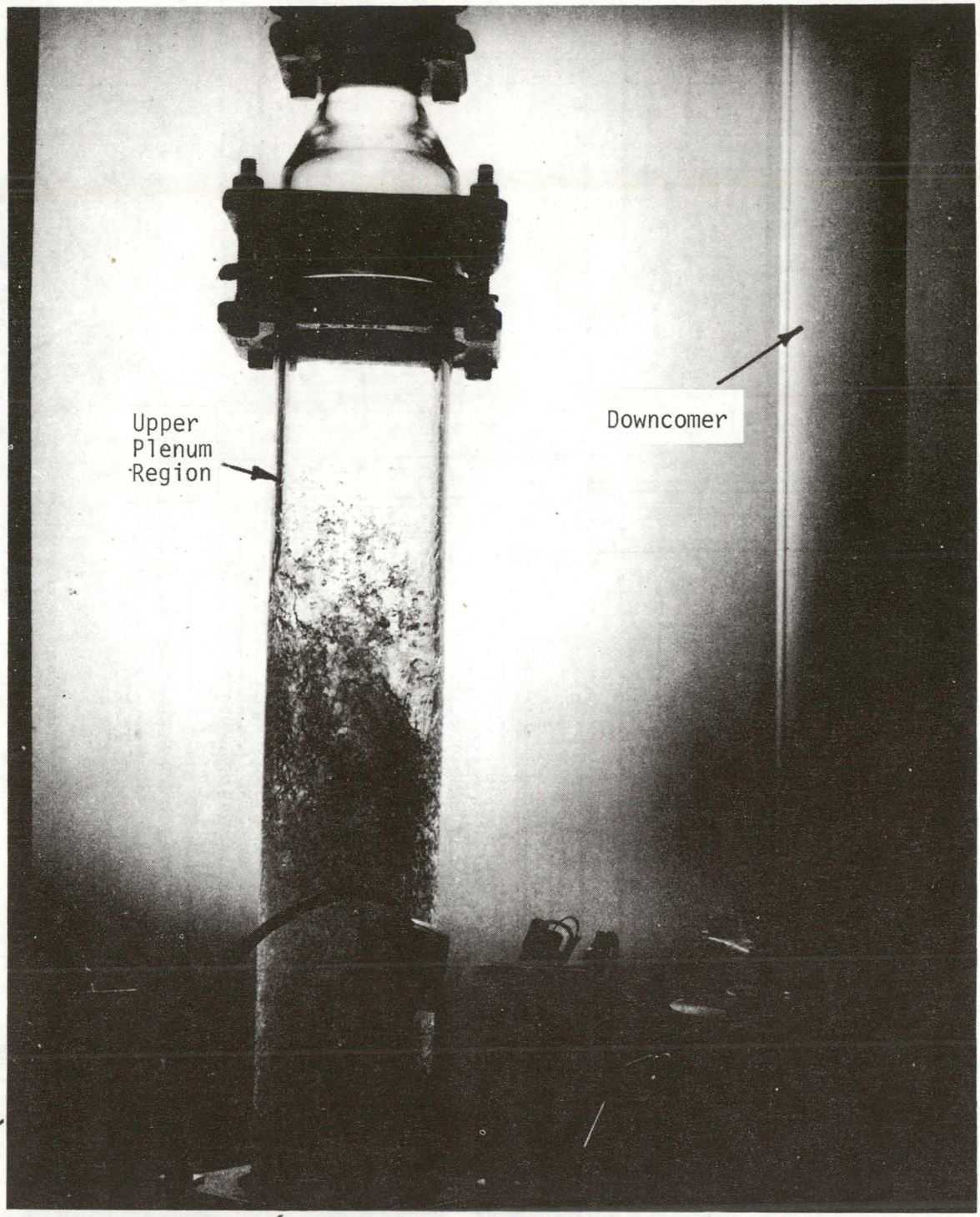

Figure-11f

Two-Phase Mixture in Upper Plenum of PCE Test Section

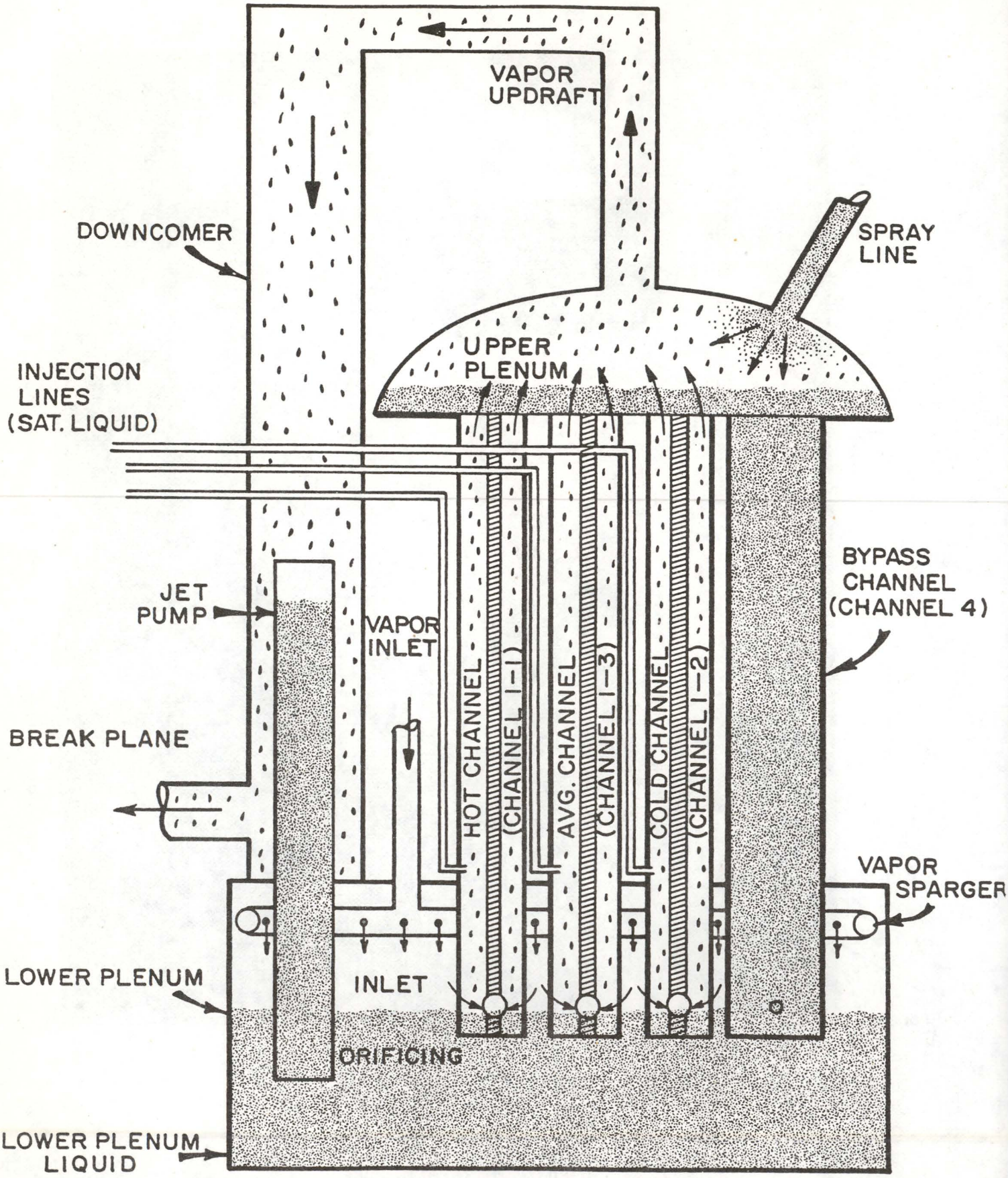

Figure 11g. Test C.003 ($t \geq 3$ min)

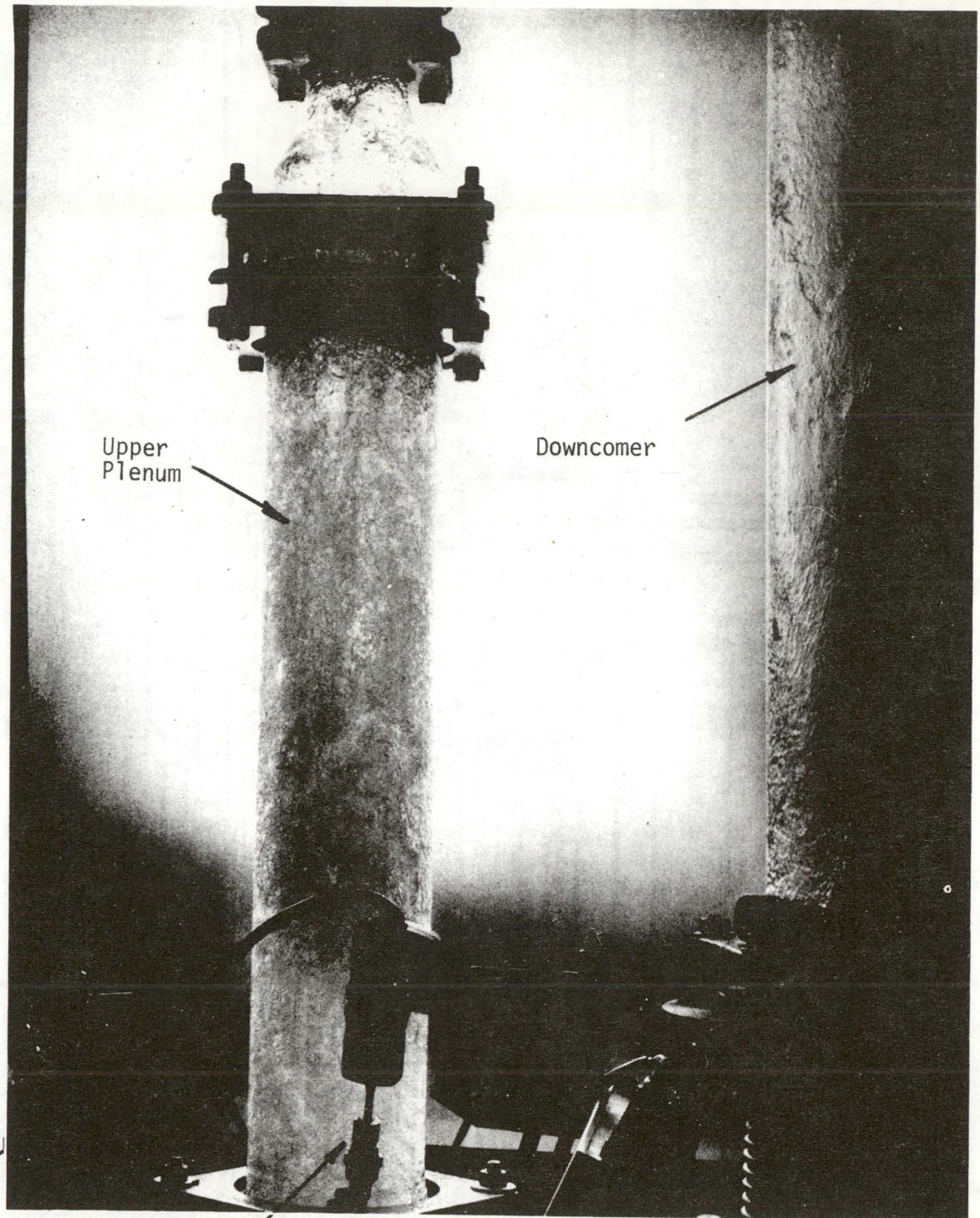

Figure-11h
Liquid Carryover
in PCE Test Section

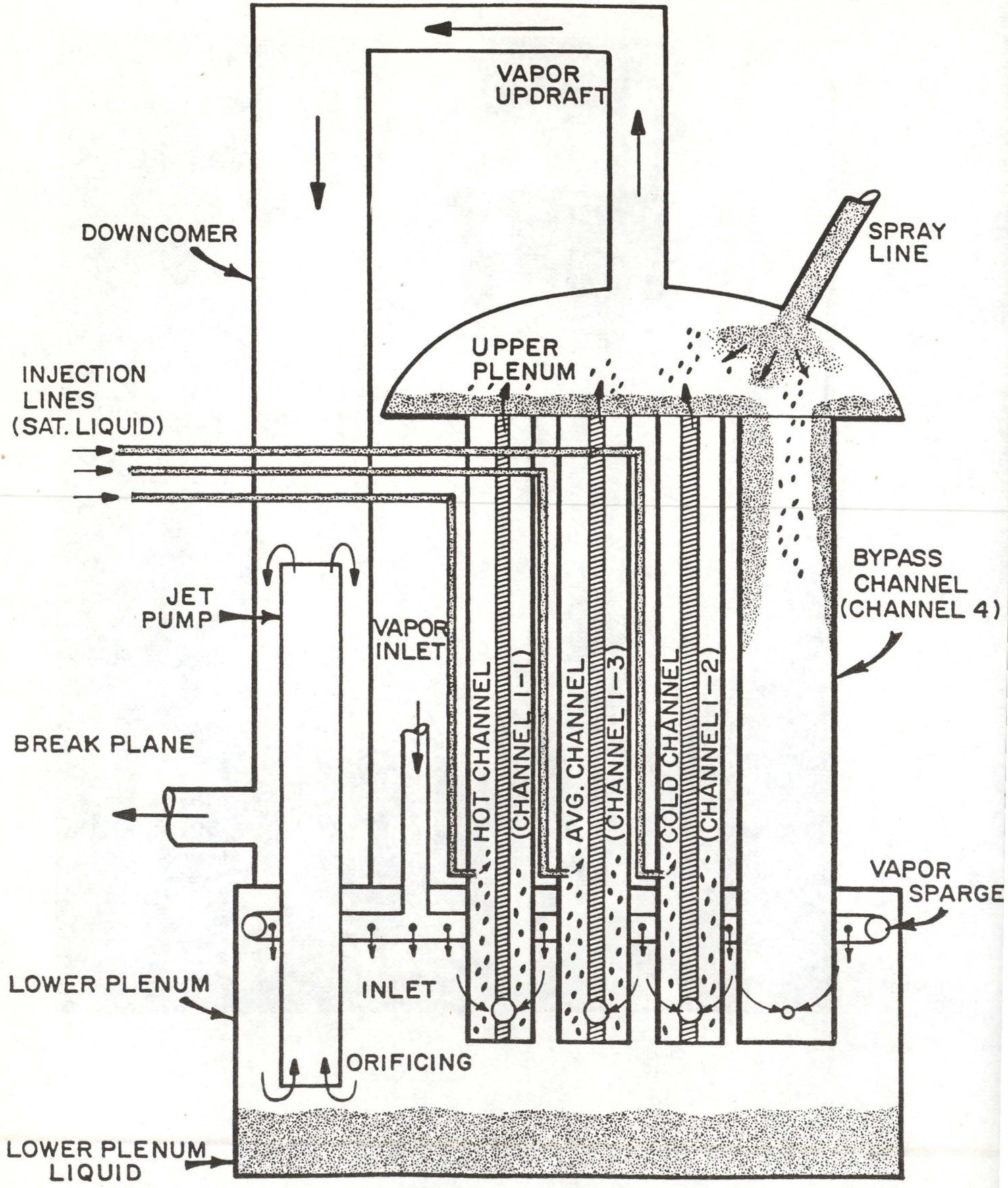

Figure 12a. Test C.006 (t≈5 sec)

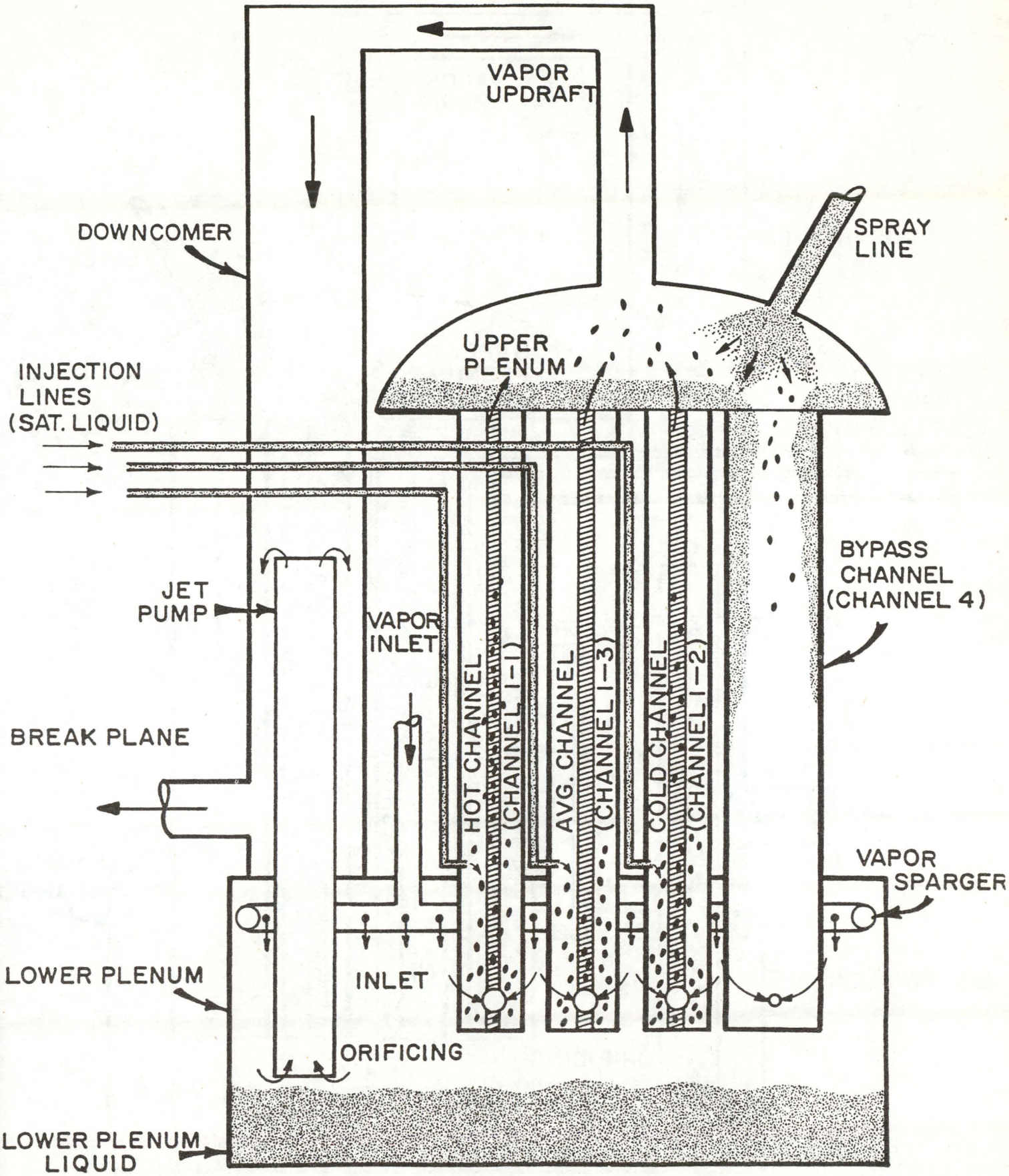

Figure 12b. Test C.006 (t≈20 sec)

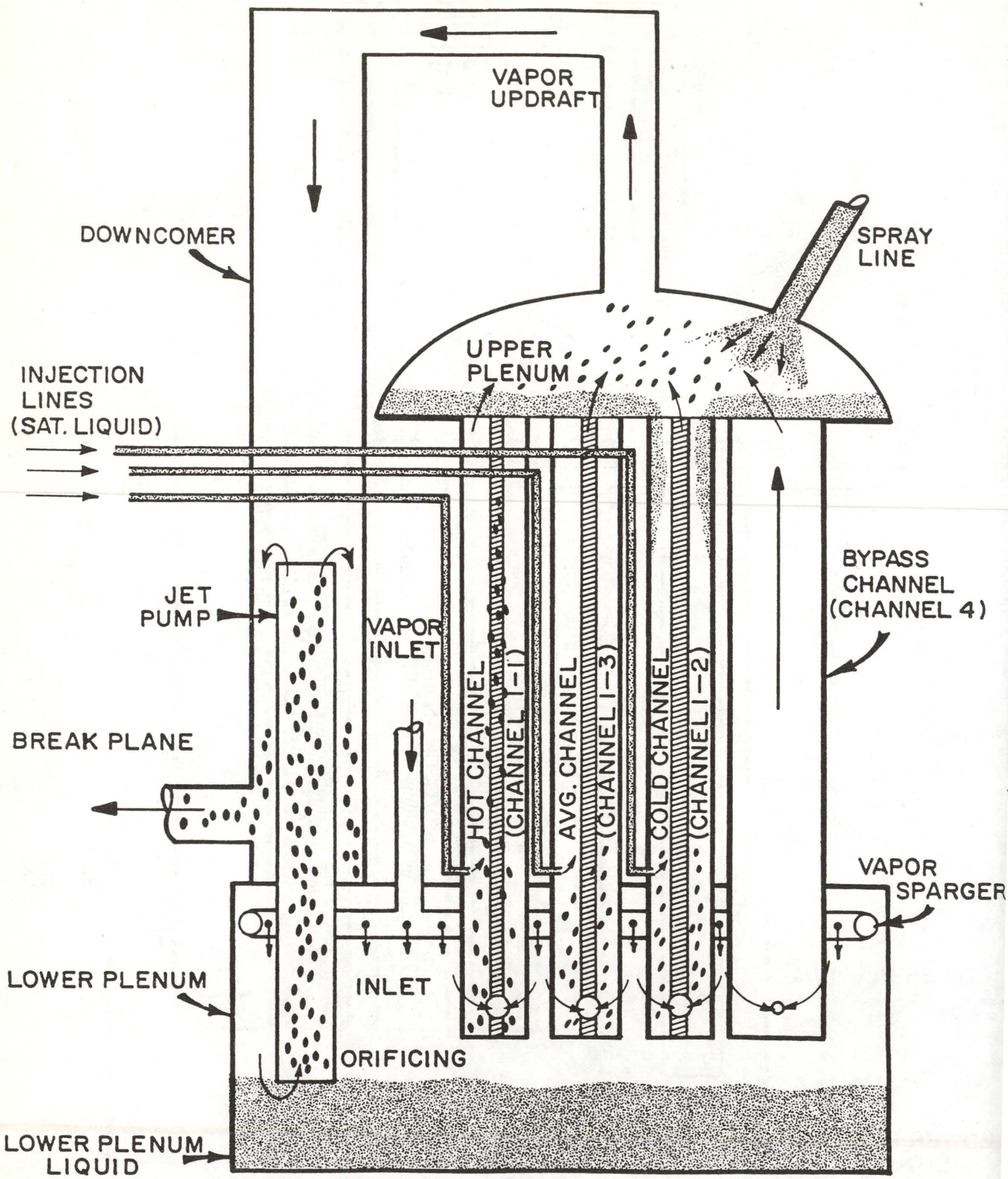

Figure 12c. Test C.006 (t≃1 min)

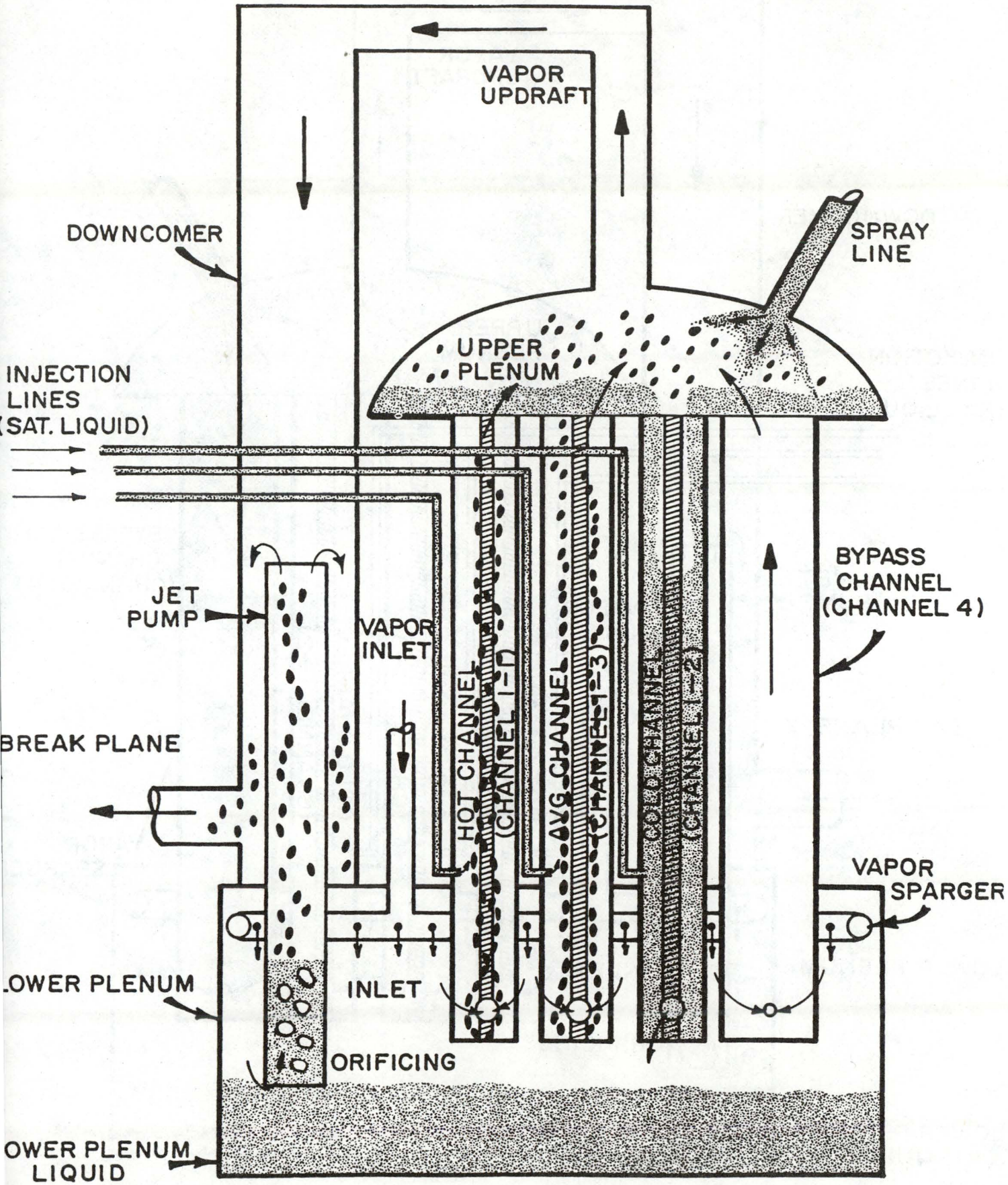

Figure 12d. Test C.006 ($t \geq 7$ min)

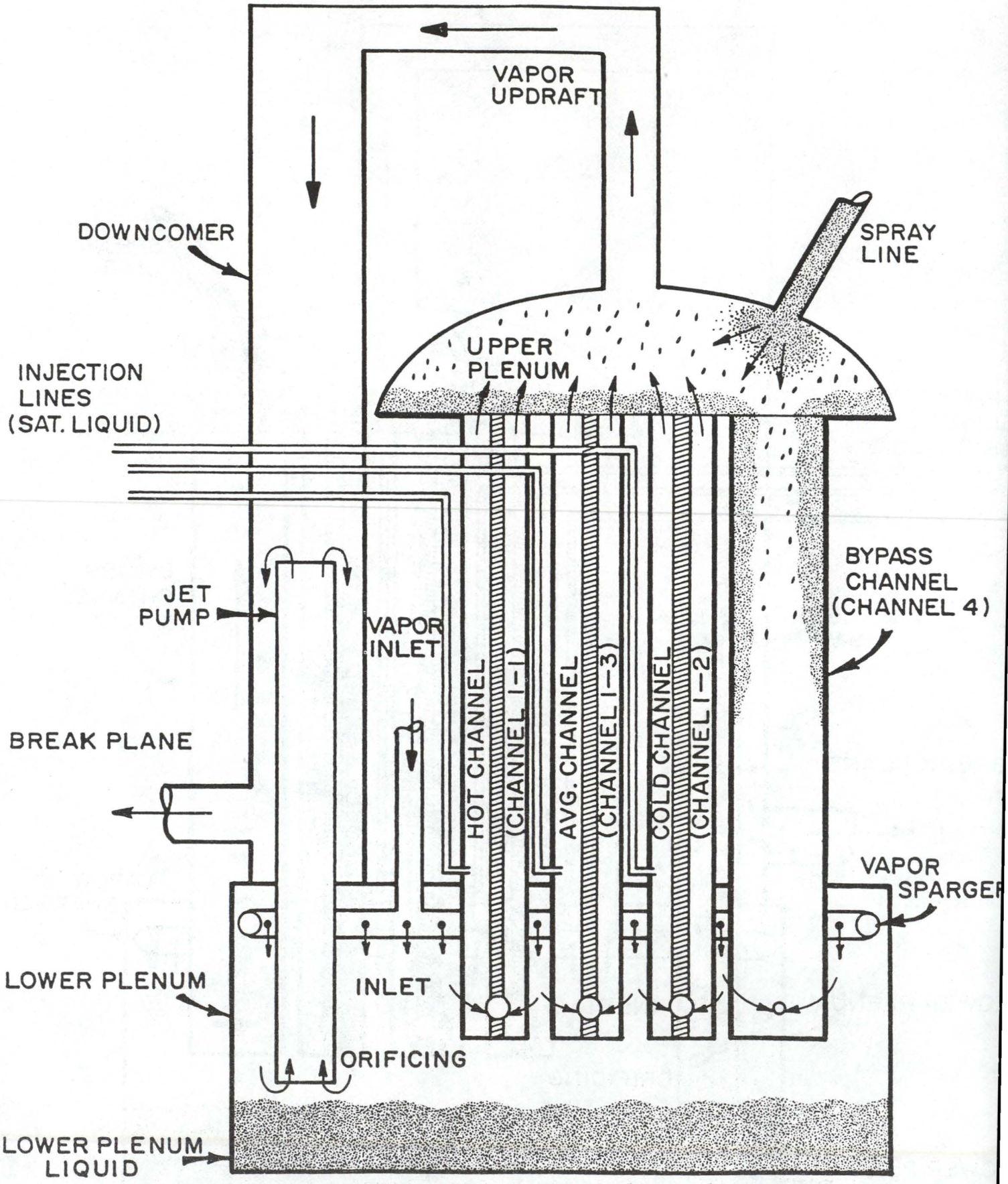

Figure 13a. Test C.008 (t≈5 sec)

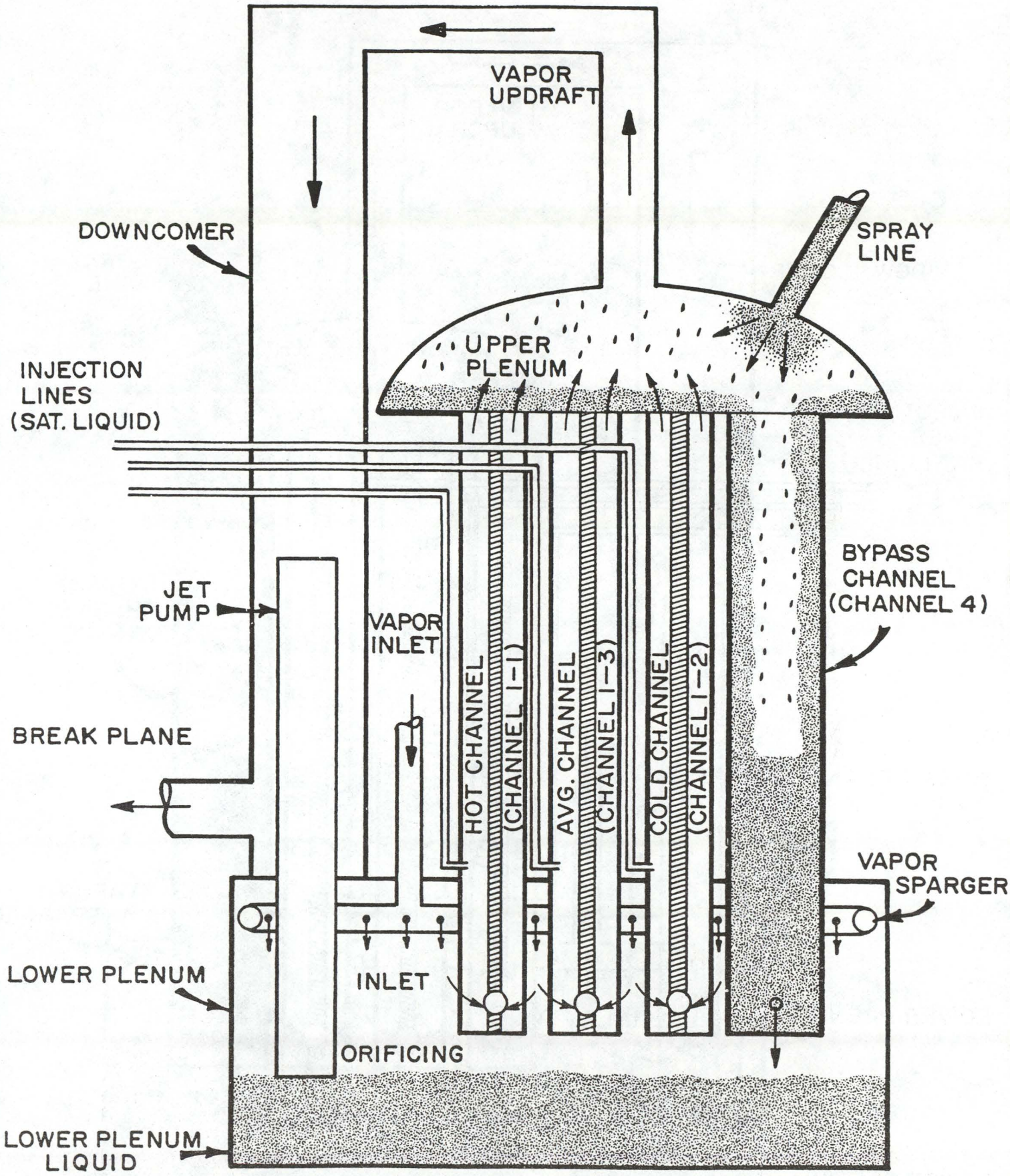

Figure 13b. Test C.008 (t≈1 min)

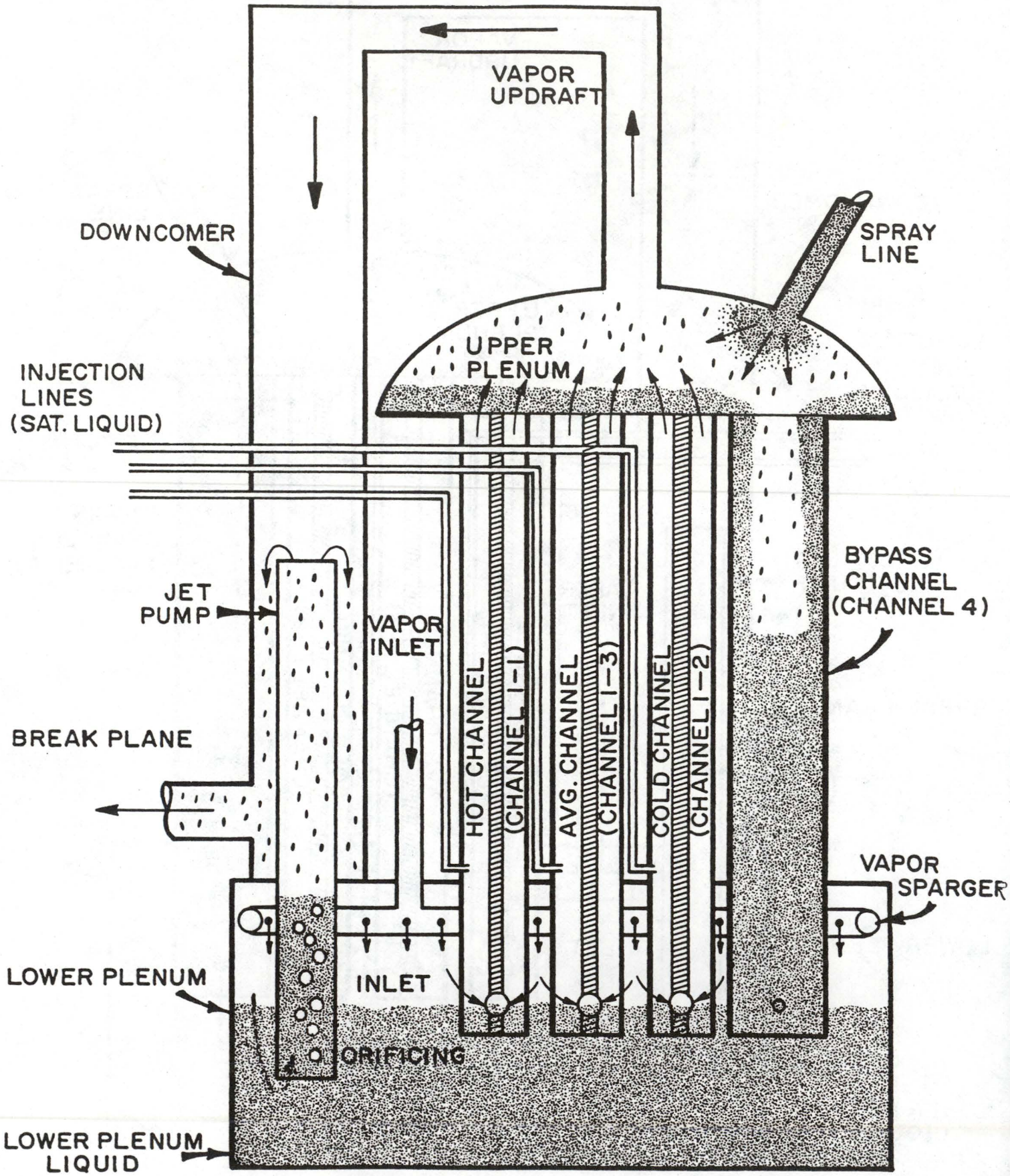

Figure 13c. Test C.008 (t≃2 min)

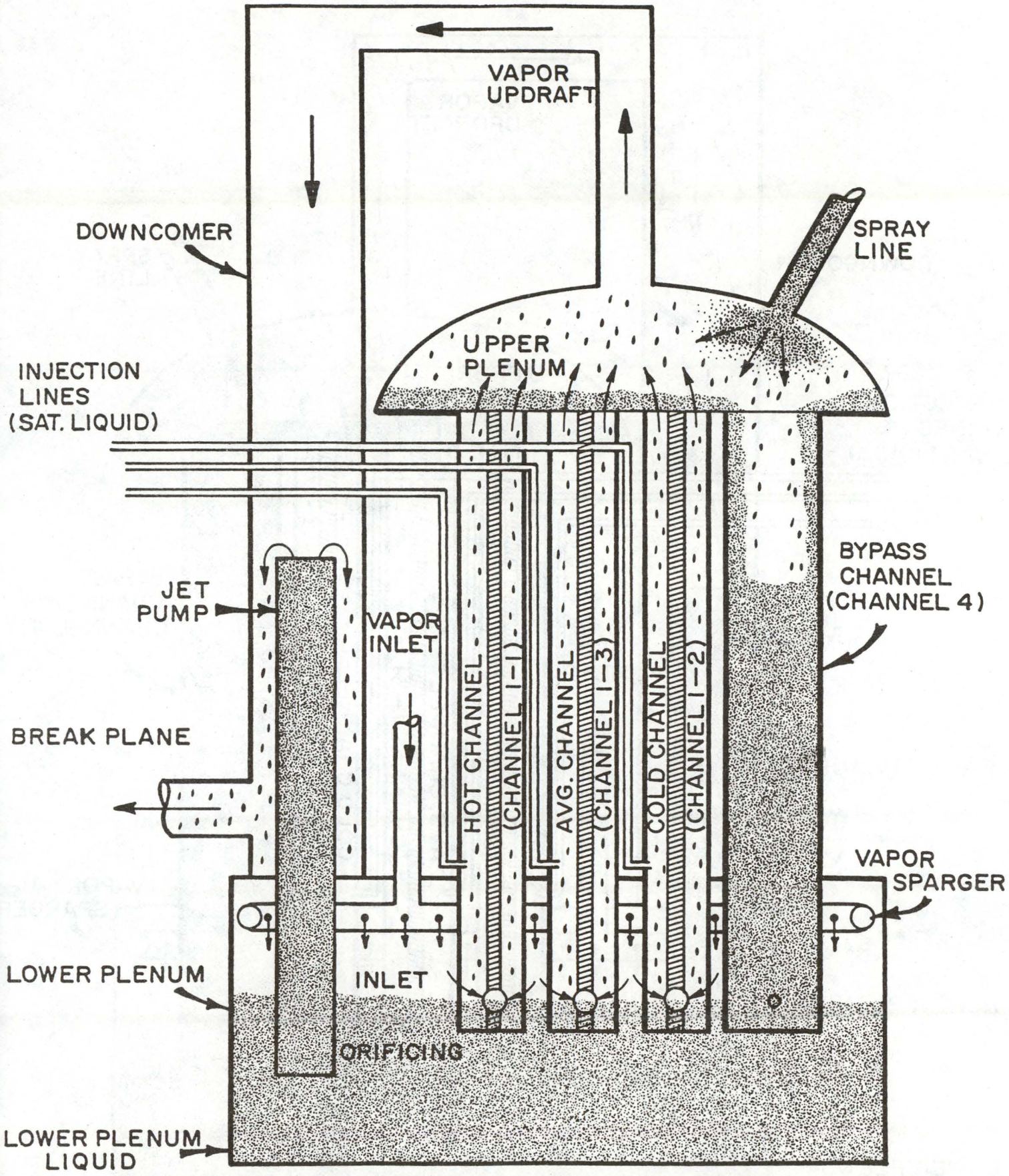

Figure 13d. Test C.008 (t≈3.5 min)

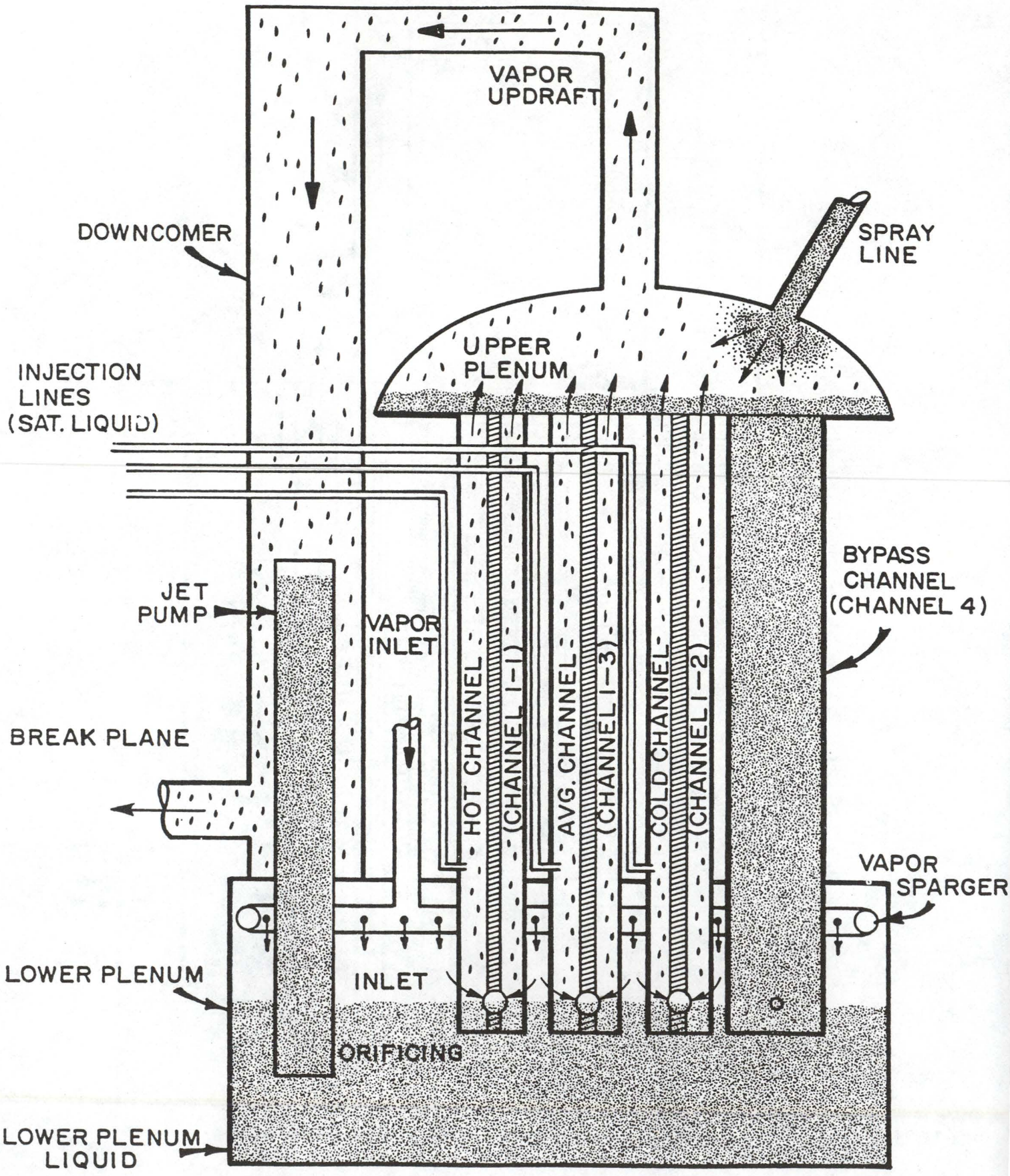

Figure 13e. Test C.008 (t≈4 min)

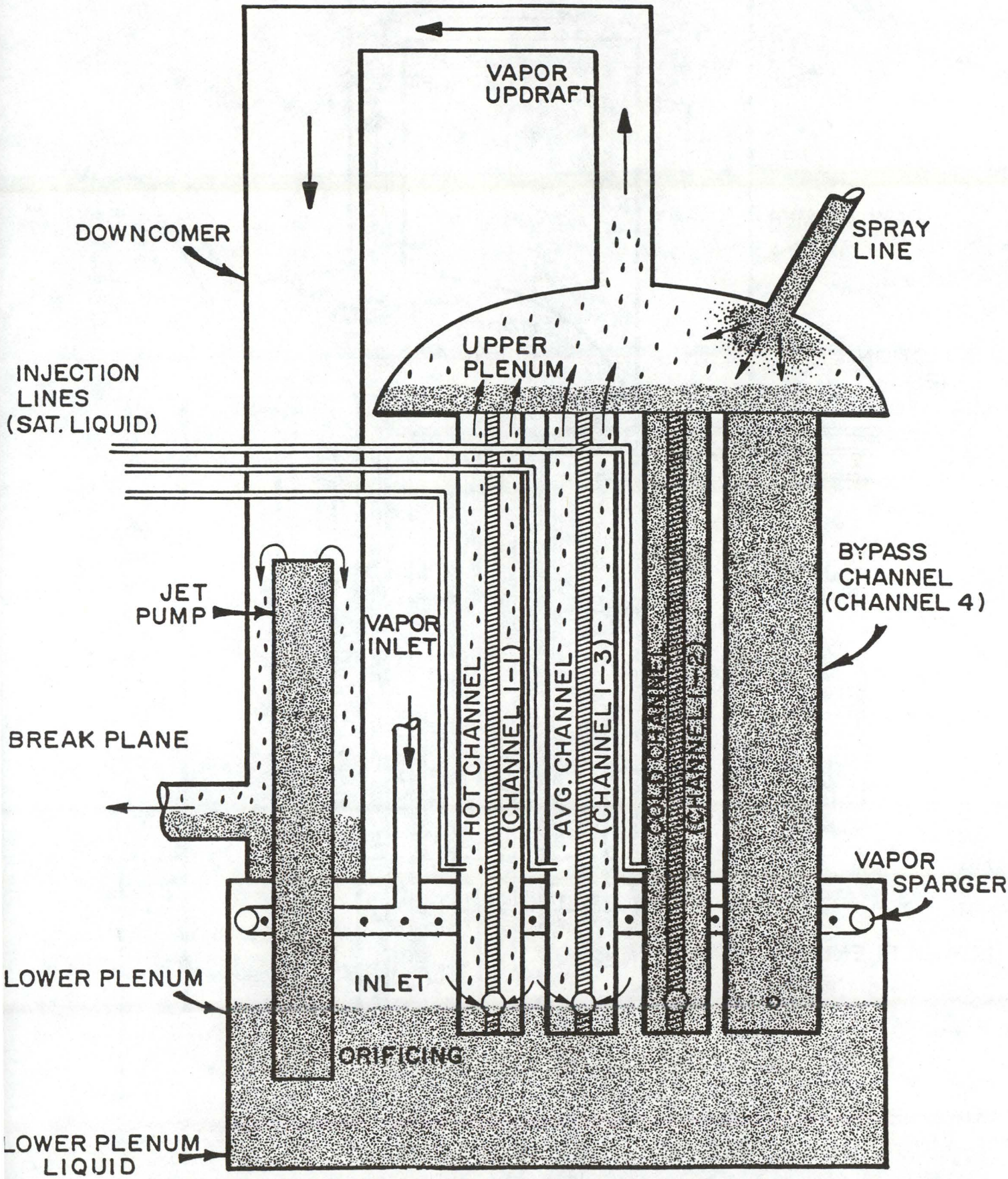

Figure 13f. Test C.008 (t≈9.5 min)

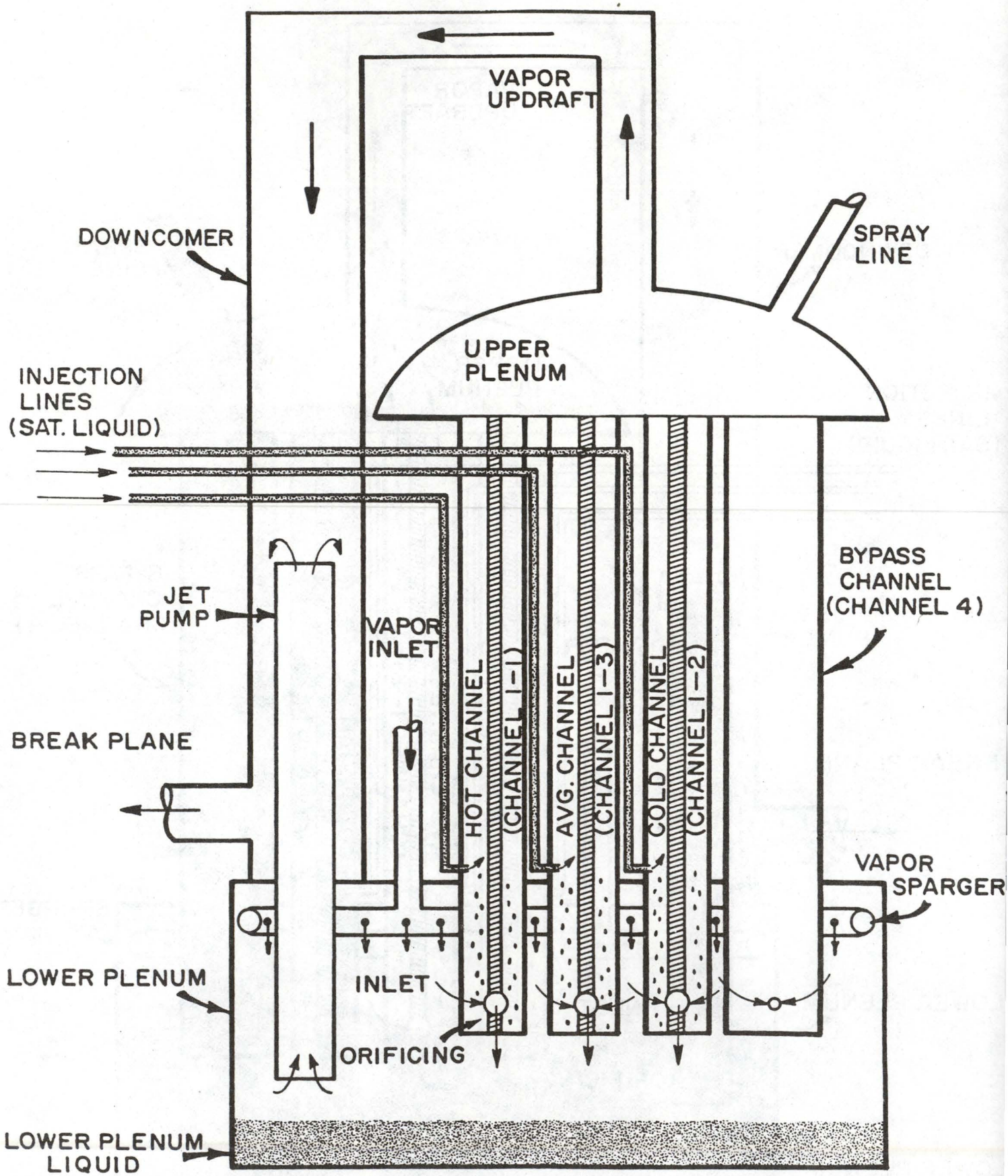

Figure 14a. Test C.011 (t=0)

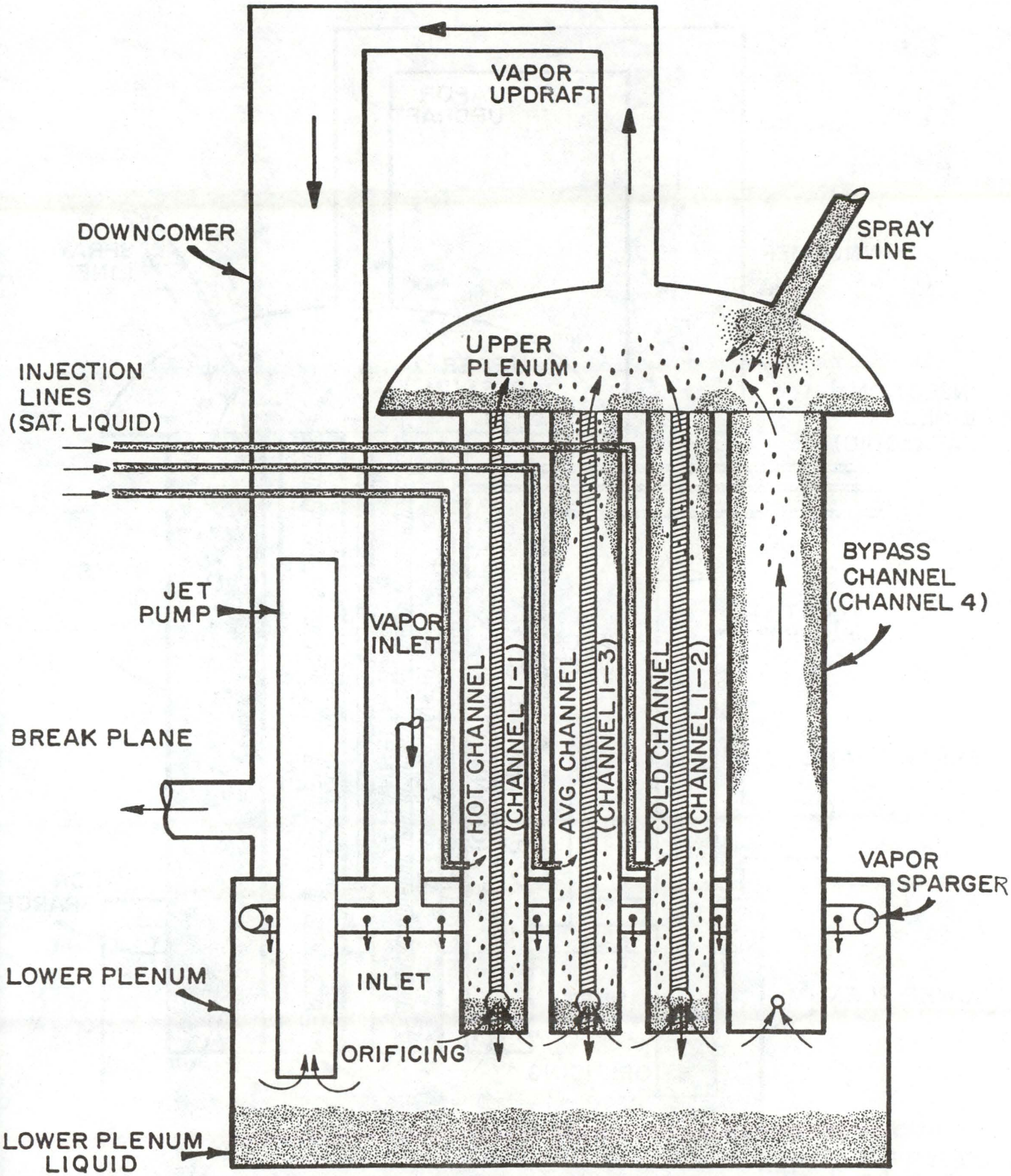

Figure 14b. Test C.011 (t≃20 sec)

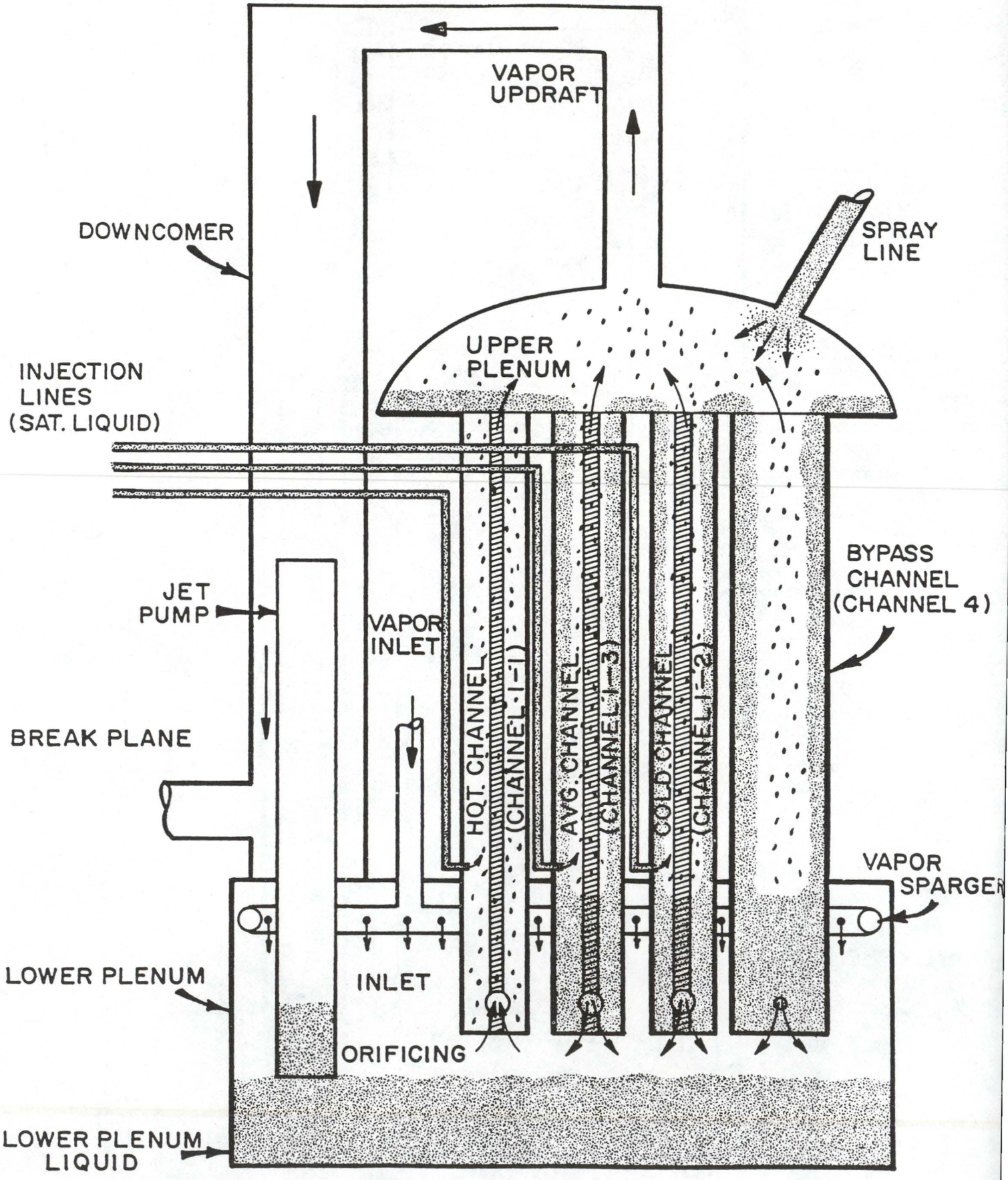

Figure 14c. Test C.011 (t≃1 min)

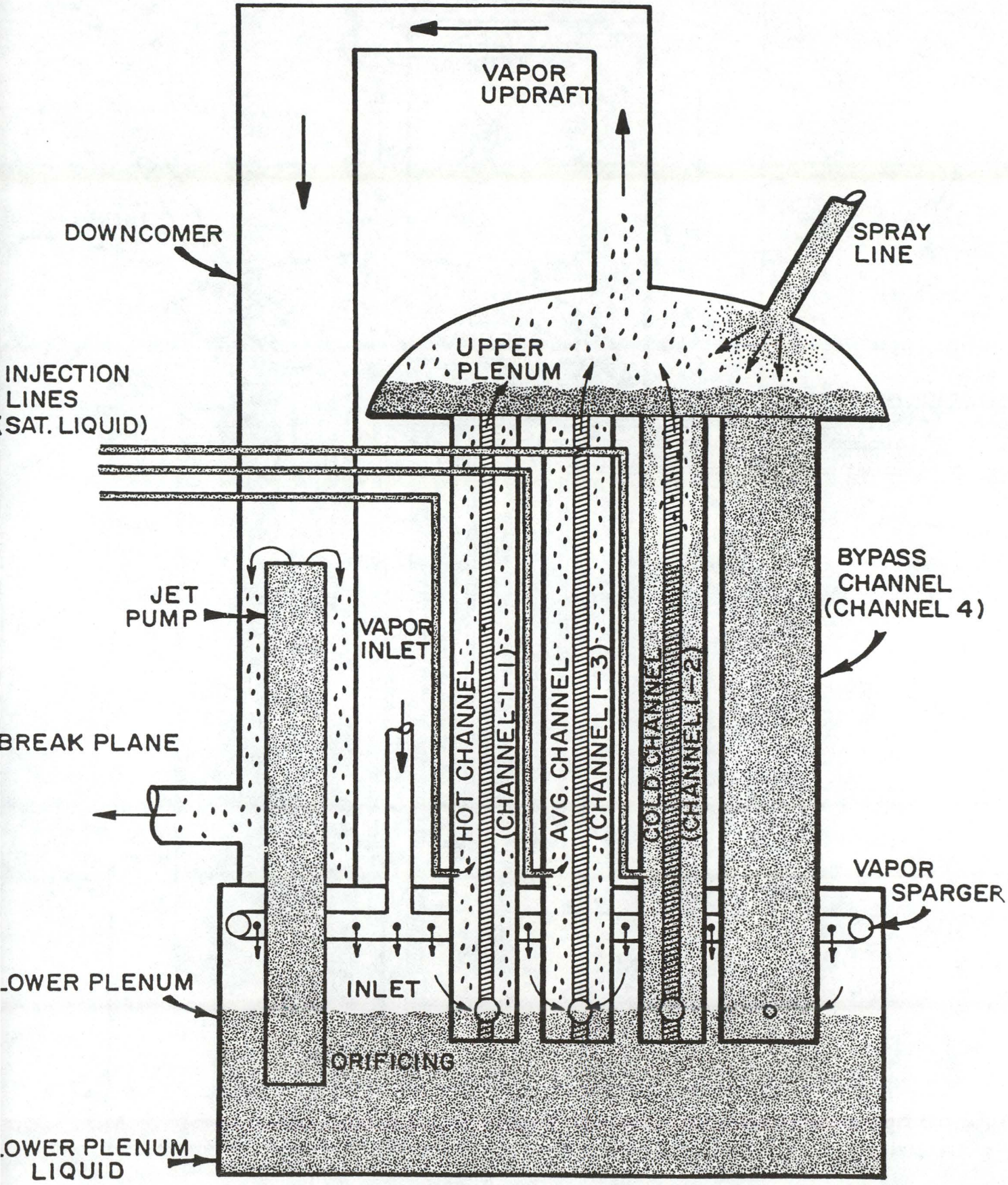

Figure 14d. Test C.011 (t=2 min)

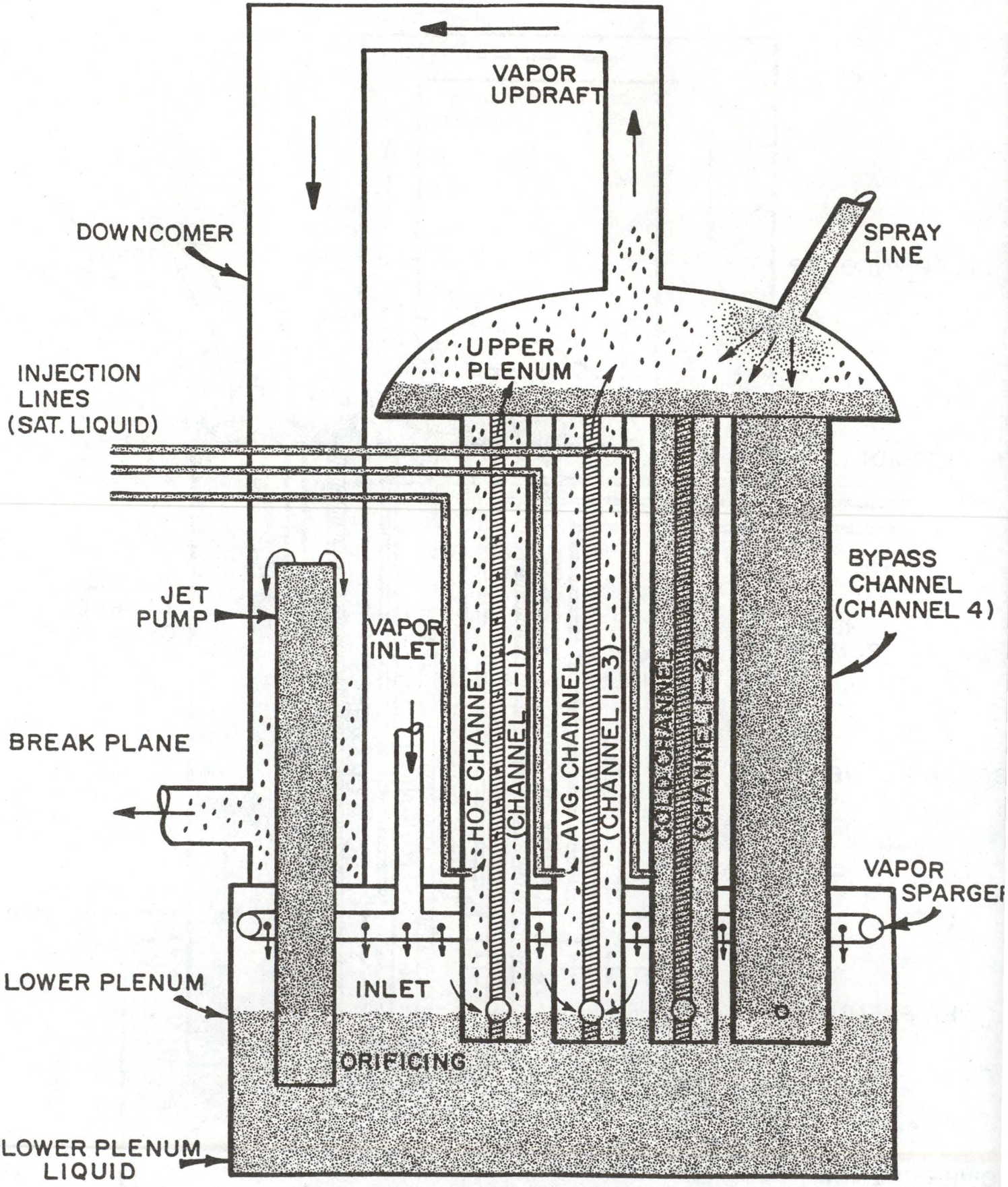

Figure 14e. Test C.011 (t=3 min)

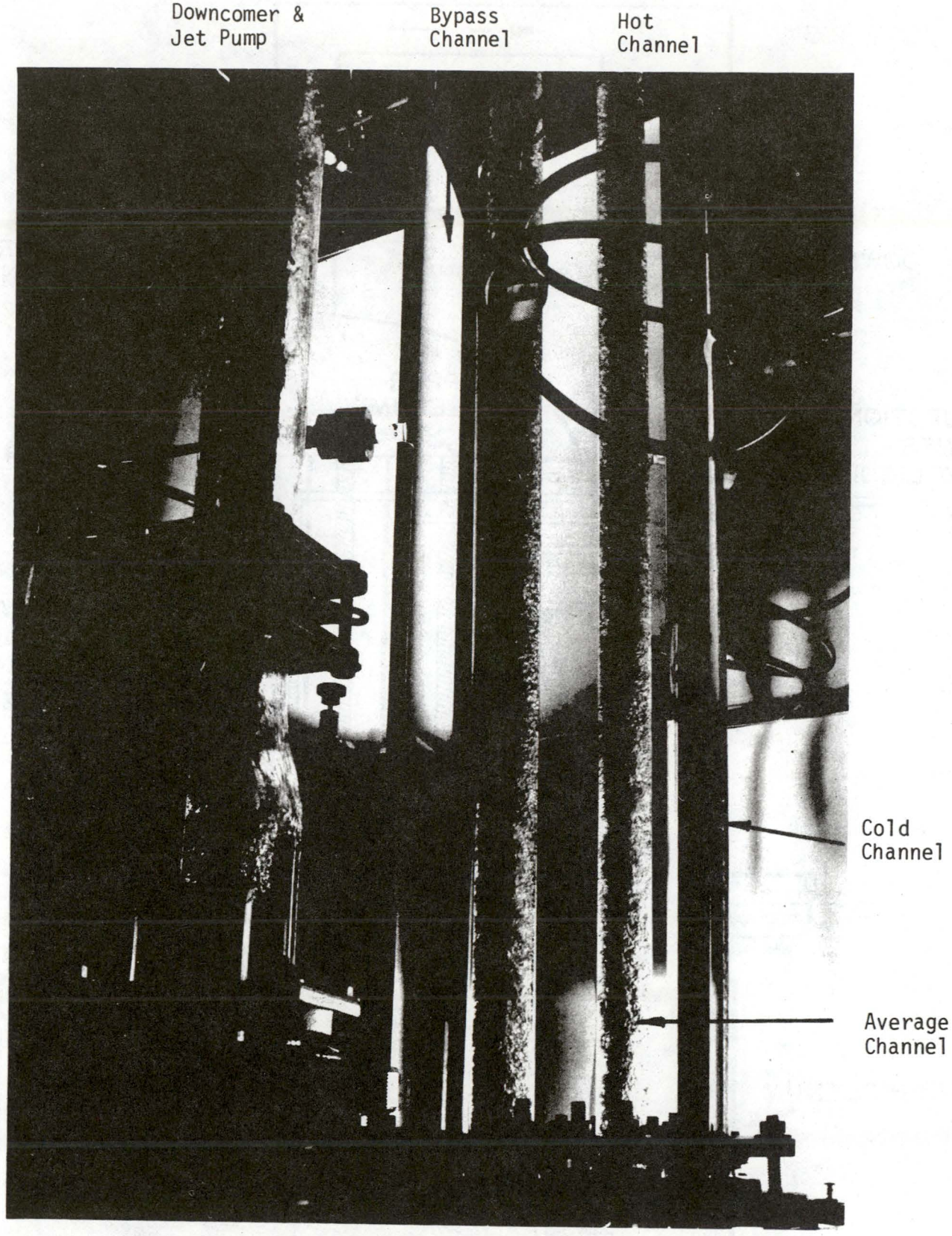

Figure-14f

Liquid Ingestion into Hot and Average Channels (Cold Channel and Bypass Filled, Jet Pump Spilling Over)

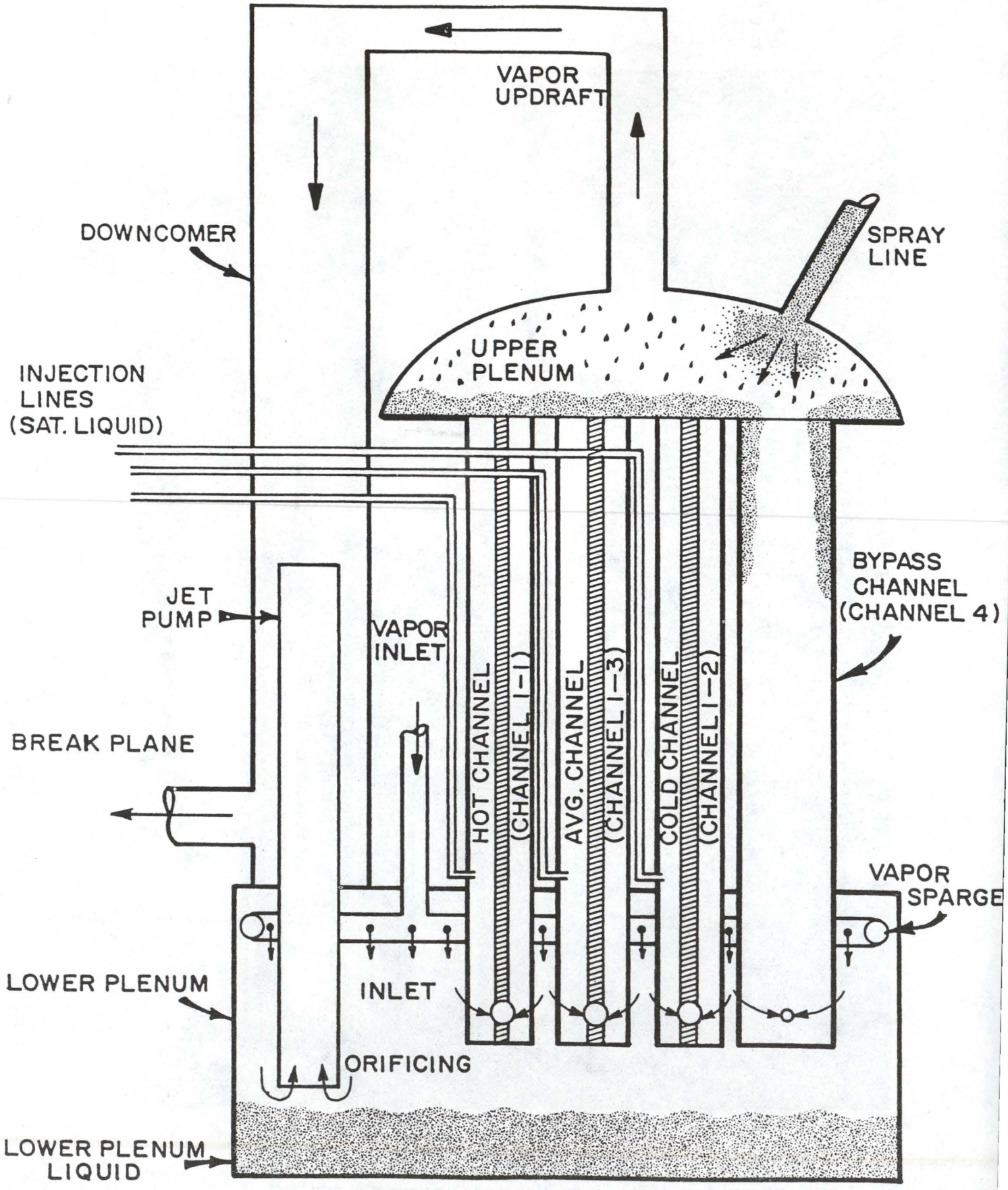

Figure 15a. Test C.013 (t≈5 sec)

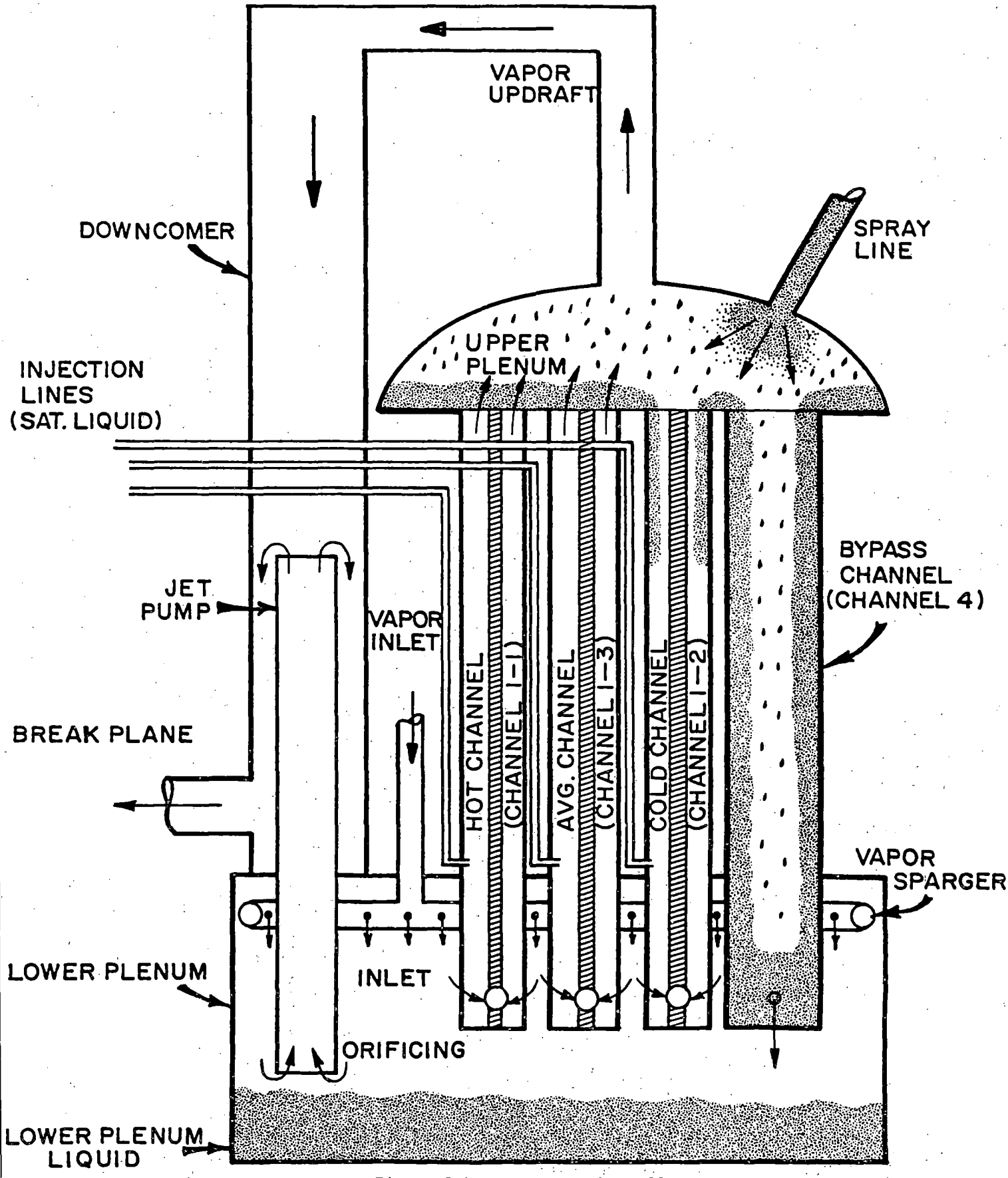

Figure 15b. Test C.013 (t≈20 sec)

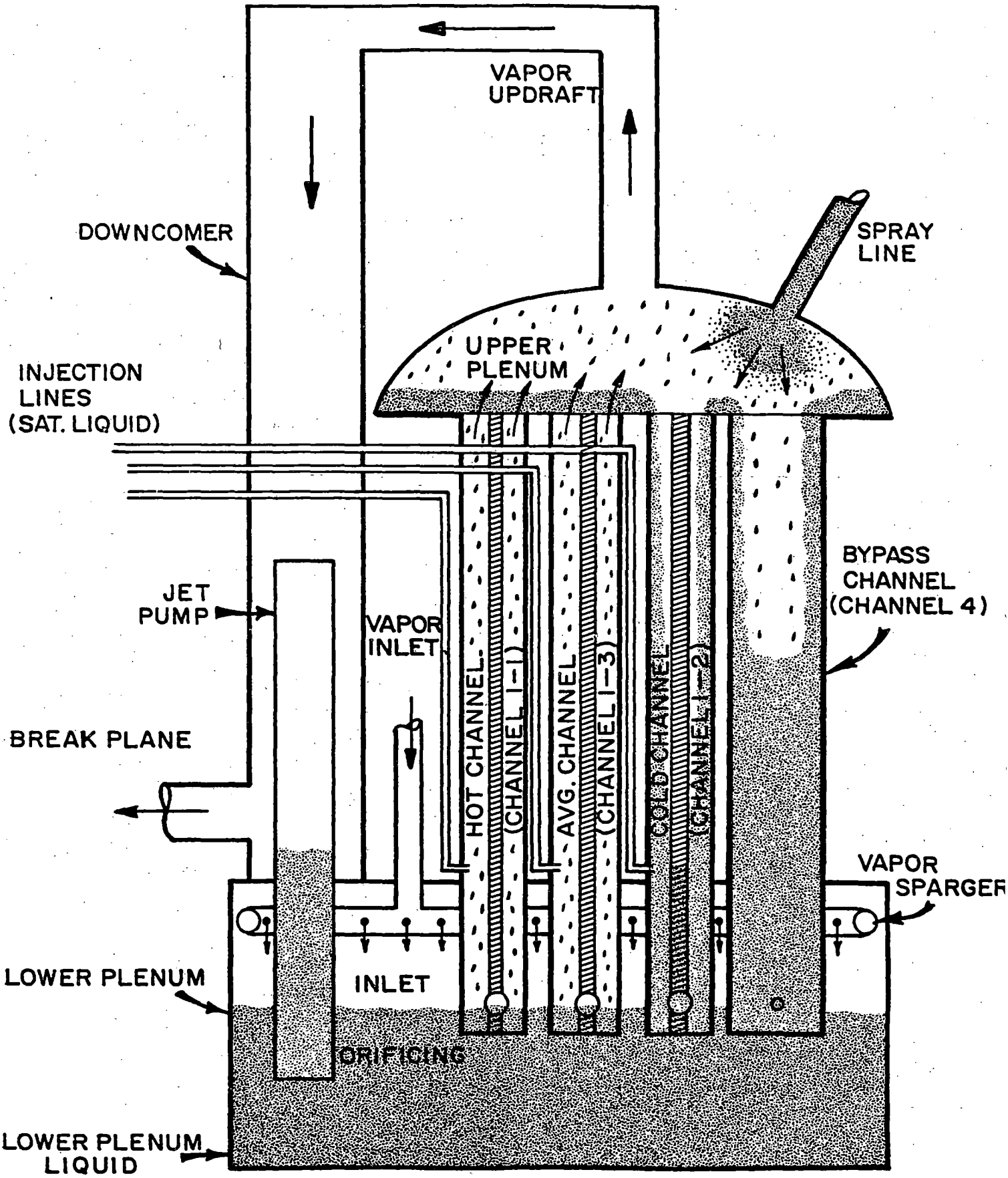

Figure 15c. Test C.013 (t≈2 min)

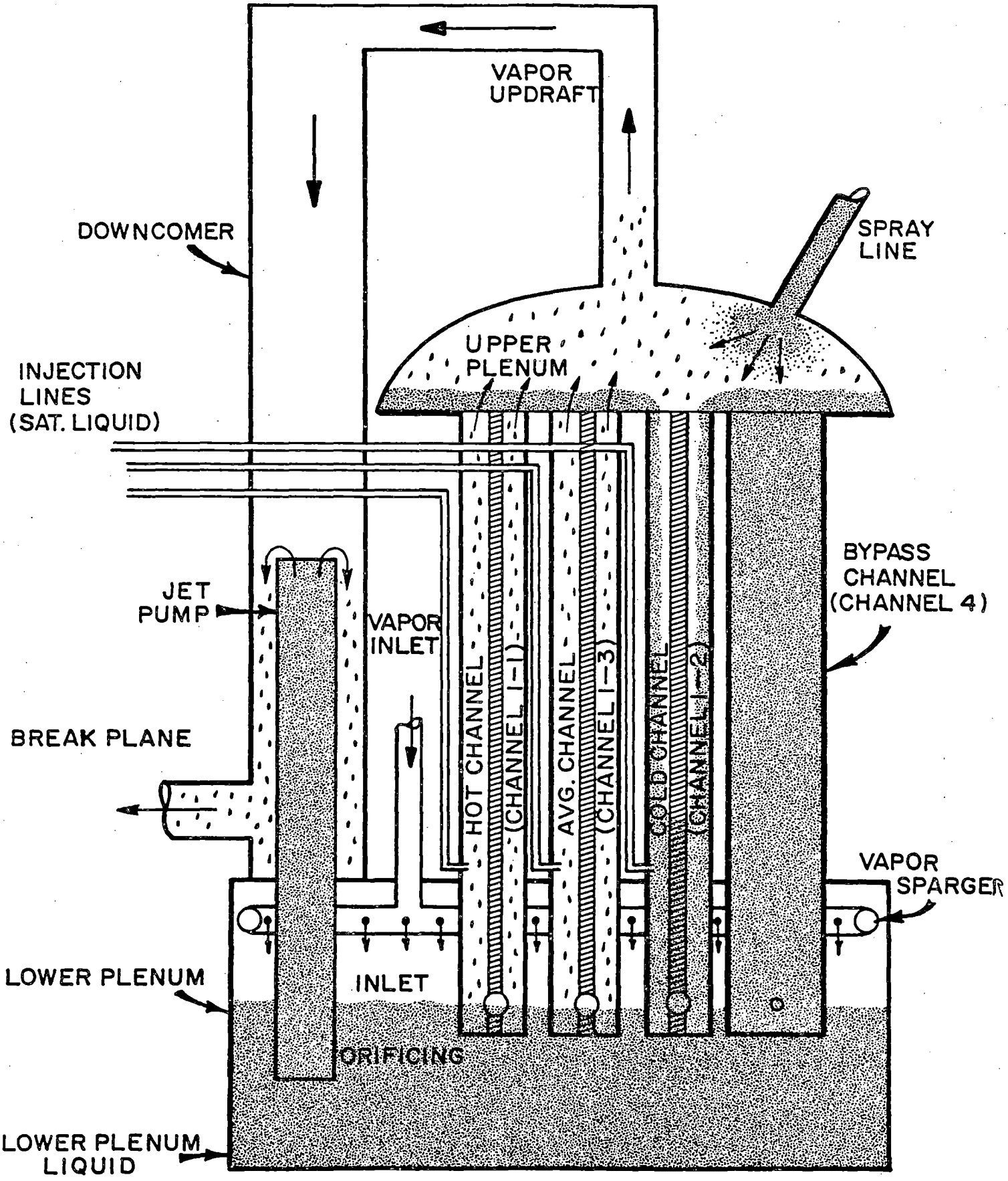

Figure 15d. Test C.013 (t≈5 min)

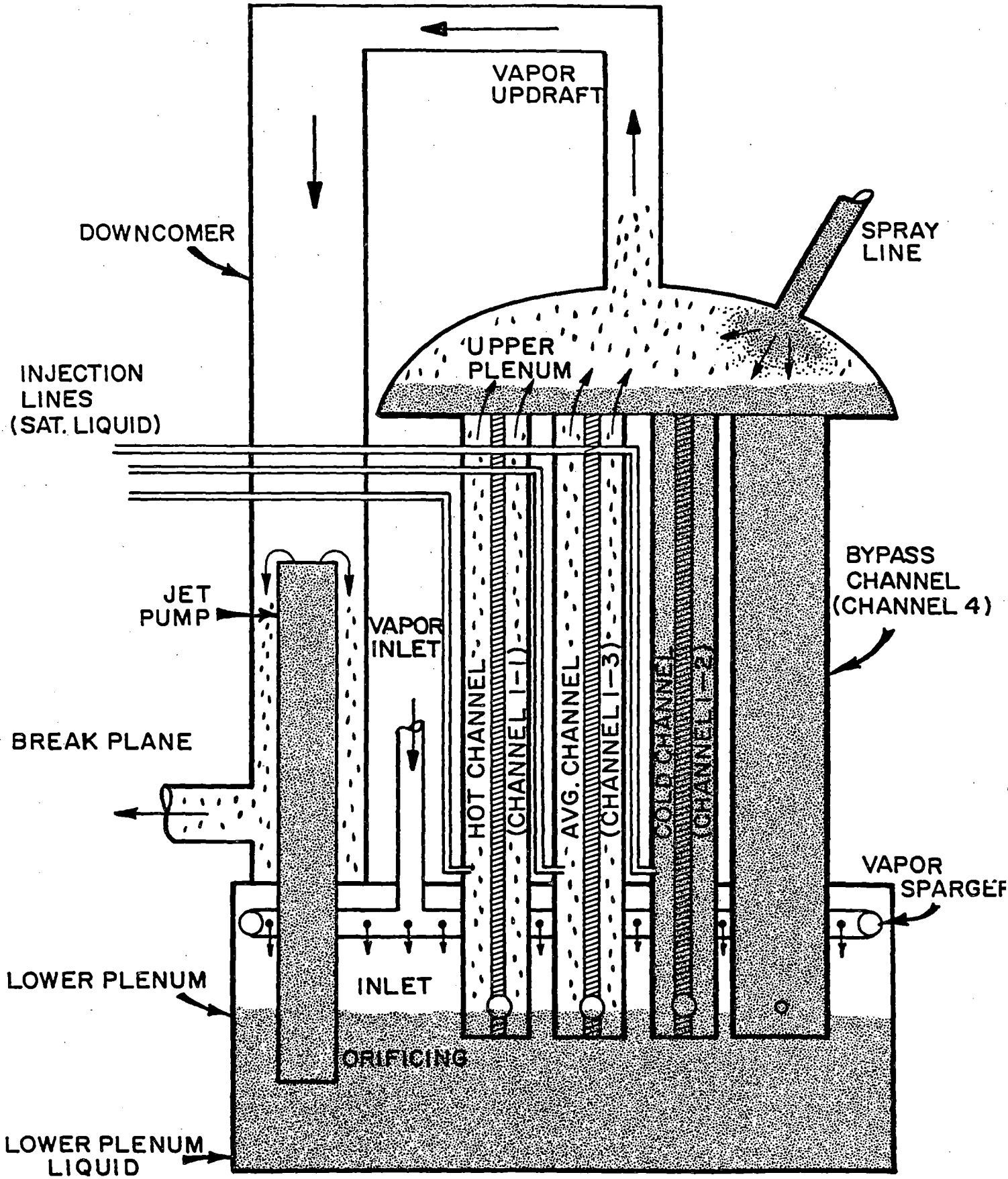

Figure 15e. Test C.013 ($t \geq 12$ min)

TECHNICAL PAPERS AND REPORTS RESULTING FROM USNRC SPONSORED RPI RESEARCH PROGRAMS

Topical Reports

(1) Cheng, L. Y., Drew, D. A., Lahey, Jr., R. T., "Virtual Mass Effects in Two-Phase Flow," NUREG/CR-0020, 1978.

(2) Honan, T. J. and Lahey, Jr., R. T., "The Measurement of Phase Separation in Wyes and Tees," NUREG/CR-0557, 1978.

(3) Schell, Susanne L., Gay, R. R., Lahey, Jr., R. T., "The Development of a Side-Scatter Gamma Ray System for the Measurement of Local Void Fraction," NUREG/CR-0677, 1978.

(4) Lahey, Jr., R. T. and Drew, D. A., "An Assessment of the Literature Related to LWR Instability Modes," NUREG/CR-1414, 1980.

(5) Vince, M. A. and Lahey, Jr., R. T., "Flow Regime Identification and Void Fraction Measurement Techniques in Two-Phase Flow," NUREG/CR-1692, 1980.

(6) Achard, J. L., Drew, D. A. and Lahey, Jr., R. T., "The Analysis of Linear and Non-Linear Stability Phenomena in Heated Channels," NUREG/CR-1718, 1980.

(7) Barasch, M. and Lahey, Jr., R. T., "The Measurement of Two-Dimensional Phase Separation Phenomena," NUREG/CR-1936, 1981.

(8) Perez-Griffo, M. L., Block, R. C. and Lahey, Jr., R. T., "Analysis of the Pulsed Neutron Activation Technique," NUREG in print, 1981.

RPI Theses (Not Published as Topical Reports)

(1) Saba, N., "An Experimental Technique for the Determination of Steam/Air Fraction," M.S. Thesis, November, 1977.

(2) Sim, S. K., "Analysis of Phase Distribution Mechanisms in Turbulent Two-Phase Pipe Flow," M.S Thesis, December, 1977.

(3) Shum, F. B., "The Development of a Four-Equation Drift-Flux Computer Code (DRIFT-4)," M.S. Thesis, May, 1978.

(4) Lombardo, N. J., "The Development of a Data Acquisition and Reduction System for the RPI BWR Parallel Channel Effects Experiment," M.E. Thesis, December, 1978.

(5) Drozd, A., "NUFREQ-S: A Frequency Domain Drift-Flux Technique for the Evaluation of the Thermal-Hydraulic Stability of Boiling Systems," M.S. Thesis, 1981.

Technical Papers

(1) Saba, N., Krycuk, G. and Lahey, Jr., R. T., "An Experimental Technique for the Determination of Steam/Air Fraction," ANS Transactions, Vol. 27, 1977.

(2) Block, R. C., Perez-Griffo, M., Singh, U. N. and Lahey, Jr., R. T., "N^{16} Tagging of Water for Transient Flow Measurements," ANS Transactions, Vol. 27, 1977.

(3) Perez-Griffo, M., Block, R. C. and Lahey, Jr., R. T., "N^{16} Tagging for Two-Phase Flow Measurements," ANS Transactions, Vol. 30, 1978.

(4) Lahey, Jr., R. T., Krycuk, G. and Malaviya, B. K., "A High Intensity X-ray System for Stochastic Measurements of Two-Phase Flows," ANS Transactions, Vol. 30, 1978.

(5) Vince, M. A., Breed, H. E. and Lahey, Jr., R. T., "The Development of a High Temperature Optical Void Probe," ANS Transactions, Vol. 30, 1978.

(6) Gay, R. R., Schell, S. and Lahey, Jr., R. T., "The Side-Scatter Gamma Technique for Local Density Measurements," ANS Transactions, Vol. 30, 1978.

(7) Moreira, S. H., Krycuk, G. and Lahey, Jr., R. T., "Development of a Radio Frequency Local Probe for Void Fraction Measurements," ANS Transactions, Vol. 30, 1978.

(8) Lahey, Jr., R. T., Cheng, L. Y., Drew, D. A. and Flaherty, J. E., "The Effect of Virtual Mass on the Numerical Stability of Accelerating Two-Phase Flow," Int. J. Multiphase Flow, Vol. 6, 1980.

(9) Drew, D. A., Sim, S. and Lahey, Jr., R. T., "Radial Phase Distribution Mechanisms in Two-Phase Flow," Proceedings of the CSNI Specialists Meeting on Transient Two-Phase Flow, Paris, 1977.

(10) Lahey, Jr., R. T., Vince, M. A., and Krycuk, G., "The Development of an Optical Digital Interferometer," Proceedings of the 2nd Multi-Phase Flow and Heat Transfer Symposium Workshop, April, 1979, Miami, Florida.

(11) Lahey, Jr., R. T. and Drew, D. A., "The Analysis of Phase Distribution in Fully Developed Two-Phase Flows," Proceedings of the 2nd Multi-Phase Flow and Heat Transfer Symposium Workshop, April, 1979.

(12) Honan, T. J. and Lahey, Jr., R. T., "The Analysis of Dynamic Bias in Gamma Densitometer Measurements," ANS Transactions, Vol. 32, 1979.

(13) Honan, T. J. and Lahey, Jr., R. T., "The Evaluation of Static Error in Gamma Densitometry," ANS Transactions, Vol. 32, 1979.

(14) Conlon, W. M. and Lahey, Jr., R. T., "Scaling of the RPI Parallel Channel Effects Experiment," ANS Transactions, Vol. 32, 1979.

Technical Papers (continued)

(15) Gay, R. R. and Lahey, Jr., R. T., "Dynamic Bias in Side-Scatter Gamma Density Measurements," ANS Transactions, Vol. 32, 1979.

(16) Lahey, Jr., R. T., Sim, S. and Drew, D. A., "An Evaluation of Interfacial Drag Models for Bubbly Two-Phase Flows," ASME Symposium Volume on Interfacial Transport Phenomena, 1979.

(17) Drew, D. A., Cheng, L. and Lahey, Jr., R. T., "The Analysis of Virtual Mass Effects in Two-Phase Flow," Int. J. Multiphase Flow," 5, 1979.

(18) Drew, D. A. and Lahey, Jr., R. T., "An Analytical Derivation of a Subchannel Void-Drift Model," ANS Transactions, 33, 1979.

(19) Honan, T. J. and Lahey, Jr., R. T., "The Measurement of Phase Separation in Wyes and Tees," J. of Nuclear Engineering and Design, 64, #1, 1981.

(20) Drew, D. A. and Lahey, Jr., R. T., "Phase Distribution Mechanisms in Turbulent Two-Phase Flow in Channels of Arbitrary Cross Section," accepted for publication in the J. of Fluids, 1981.

(21) Gay, R. R., Ohkawa, K. and Lahey, Jr., R. T., "The Measurement of Local Void Fraction with a Side-Scatter Gamma Technique," Proceedings of 26th International Symposium of Instrument Society of America, May 1980.

(22) Perez-Griffo, M., Block, R. C. and Lahey, Jr., R. T., "Basic Two-Phase Flow Measurements Using ^{16}N Tagging Techniques," Proceedings of ANS/ASME Meeting on Reactor Thermal-Hydraulics, October 1980.

(23) Drew, D. A., and Lahey, Jr., R. T., "Phase Distribution Mechanisms in Turbulent Low Quality Two-Phase Flow in a Circular Pipe," accepted for publication in J. of Fluid Mechanics, 1981.

(24) Saba, N., Lahey, Jr., R. T. and Corelli, J. C., "An Experimental Technique for Determination of Steam Fraction in Flowing Steam/Air Mixtures," Nuclear Technology, 1980.

(25) Malaviya, B. K. and Lahey, Jr., R. T., "Analysis of the Error in Instantaneous Void Fraction Measurements by a Dual-Beam X-ray Technique," ANS Transactions, Vol. 34, 1980.

(26) Vince, M. A. and Lahey, Jr., R. T., "Derivative Signal Thresholding for a Local Void Impedance Probe," ANS Transactions, Vol. 34, 1980.

(27) Vince, M. A. and Lahey, Jr., R. T., "Flow Regime Identification Using a High Intensity X-ray System," ANS Transactions, Vol. 34, 1980.

(28) Achard, J. L., Drew, D. A. and Lahey, Jr., R. T., "The Effect of Gravity and Friction on the Stability of Boiling Flow in a Channel," AIChE Symposium Series #199, Vol. 76, 1980; J. of Chem. Eng. Commun., 11, 1981.

Technical Papers (continued)

(29) Drew, D. A. and Lahey, Jr., R. T., "A Mixing Length Model for Fully-Developed Turbulent Two-Phase Flow," ANS Transactions, Vol. 35, 1980.

(30) Park, G., Becker, M. and Lahey, Jr., R. T., "The Effect of Radial Non-uniformity on BWR Stability Margins," ANS Transactions, Vol. 35, 1980.

(31) Lahey, Jr., R. T., Cheng, L., Drew, D. A. and Flaherty, J. E., "The Effect of Virtual Mass on the Numerical Stability of Accelerating Two-Phase Flows," Int. J. Multiphase Flow, 6, 1980.

(32) Perez-Griffo, M., Block, R. C. and Lahey, Jr., R. T., "Non-uniform Tagging and Flow Structure Effects in PNA Measurements," ANS Transactions 35, 1980.

(33) Drew, D. A. and Lahey, Jr., R. T., "Interfacial Dissipation in Two-Phase Flow," ASME Symposium Volume, Basic Mechanisms in Two-Phase Flow and Heat Transfer, 1980.

(34) Cheng, L., Lahey, Jr., R. T. and Drew, D. A., "The Effect of Virtual Mass on the Prediction of Critical Flow," Proceedings of CSNI Specialists Meeting on Transient Two-Phase Flow, Pasadena, 1981.

(35) Taleyarkhan, R., Podowski, M. and Lahey, Jr., R. T., "Stability Analysis for a Nonuniformly Heated Boiling Channel," ANS Transactions, 38, 1981.

(36) Shen, C. N., Balaram, J. and Lahey, Jr., R. T., "A State Variable Model and Stability Criterion for Density Wave Oscillations in Boiling Water Reactors," Proceedings of the 12th Annual Pittsburgh Conference on Modeling and Simulation, University of Pittsburgh, 1981.

(37) Shen, C. N., Balaram, J. and Lahey, Jr., R. T., "A State Variable Formulation of Density-Wave Oscillation in Boiling Water Reactors," ANS Transactions, 38, 1981.

(38) Perez-Griffo, M., Block, R. C. and Lahey, Jr., R. T., "A Mechanistic Analysis of LOFT Pulsed Neutron Activation Data," ANS Transactions, 38, 1981.

(39) Vince, M. A. and Lahey, Jr., R. T., "On the Development of a Radio-Frequency Excited Local Impedance Probe," accepted for publication, Nucl. Eng. and Design, 1981.

(40) Vince, M. A. and Lahey, Jr., R. T., "On the Development of an Objective Flow Regime Indicator," accepted for publication in Int. J. Multiphase Flow, 1981.

(41) Park, G. C., Park, J. K., Becker, M., Podowski, M. and Lahey, Jr., R. T., "An Improved Model for the Stability Analysis of BWRs," ANS Transactions, 39, 1981.

Technical Papers (continued)

(42) Lahey, Jr., R. T., "The Use of Microprocessors for the Evaluation of the Thermal-Hydraulic Stability of Boiling Systems," ANS Transactions, 39, 1981.

(43) Lahey, Jr., R. T., "A Review of Some Selected Nonintrusive Nuclear and Optical Techniques for the Determination of Void Fraction, Flow Regime and Two-Phase Flow Rates," ANS Transactions, 39, 1981.

(44) Taleyarkhan, R., Podowski, M. and Lahey, Jr., R. T., "Thermal-Hydraulic Stability of Interconnected Boiling Channels," ANS Transactions, 39, 1981.

Countercurrent Flow of Steam and Cold Water in an Inclined Rectangular Channel

S. G. Bankoff, H. J. Kim and S. C. Lee
Northwestern University, Evanston, Il. 60201

Experimental work on condensation rates and instability of a countercurrent flow of steam and water was carried out at atmospheric pressure in an inclined rectangular channel with an aspect ratio of 10.

A. Condensation Rate Measurements

Condensation heat transfer coefficients were determined as functions of local steam and water flow rates and the degree of subcooling. Steam flow rates were measured at six stations: 0.22m, 0.4m, 0.76m, 0.93m and 1.27m from the steam entrance along the channel centerline. This was accomplished by integrating the measured steam velocity profile at each station assuming two-dimensional flow. The steam velocity profile was measured using pitot tubes, which are electrically heated to prevent steam from condensing inside the tubes. The six pitot tubes were attached to a traversing table, allowing them to be positioned at selected elevations in the test section. To investigate the interfacial structure conductivity probes were used at the same five locations as the pitot tubes along the test section. Using these probes, the mean water layer thickness, wave height(range from 0-100% local void fraction) and wave frequency were measured. Typical data are shown in the figures. The data were separated according to wave structure and correlated by a least-square fit as shown in Fig. 11.

$$Nu = .173\ Re_g^{.027}\ Re_l^{.49}\ Pr^{.42} \qquad \text{for smooth regime}$$

$$= .34 \times 10^{-9}\ Re_g^{2.1}\ Re_l^{.56}\ Pr^{1.16} \qquad \text{for rough regime}$$

where $Nu = \frac{h \cdot t}{k}$, $Re_g = \frac{W_g}{b \cdot \mu_g}$, $Re_l = \frac{W_l}{b \cdot \mu_l}$

t = water layer thickness
b = channel width

Since the range of variation of Pr is small, this shows that $Nu \sim Re_l^{1/2}$, approximately, in the smooth regime(station 5), independent of Re_g, but in the rough regime the effect of Re_g is very strong. The dimensionless wave height, η/H, is likewise strongly affected by Re_g, but nearly independent of Re_l in this range (Fig. 12).

Comparisons are shown with a turbulence-centered equation (Thomas 1979, Bankoff 1980) in Fig. 13. Improved agreement is obtained by choosing the turbulent velocity scale to be the liquid interfacial friction velocity and the length scale to be the wave height, defined as the maximum wave height (Fig. 14). With these definitions an improved correlation is shown in Fig. 15.

B. Instability of Steam-Water Countercurrent Flow in an Inclined Channel

Two important events were observed to obstruct the normal condensation process during the test. The first one is the generation of dangerous pressure pulses which may lead to waterhammer. The occurrence of these pressure waves may be attributed to combined thermal and hydrodynamic instability of the stratified steam-water flow.

The other is "flooding", or the reversal of liquid flow by the upward steam flow, which may result from the hydrodynamic instability of the stratified flow.

Both instabilities were detected by the measurement of pressure drop together with visual observations. The static pressure measured during waterhammer shows that its fluctuation becomes very strong and frequent with accompanying periodic noises inside the test section. It is also found that the pressure drop in the steam phase increases sharply near the flooding point.

For a nearly horizontal channel, a slug with height approximately 4 times the mean film thickness appeared at the water exit, and then propagated upward to the middle of the test section, where rupture of the interface and bridging took place simultaneously. On the other hand, the slug formation was not seen at an inclination angle of 33.5°.

Liquid droplets started to entrain in the steam phase before flooding took place at both angles.

A simple analysis was performed to predict the dimensionless flooding flux in the inclined rectangular channel. The envelope model suggested originally by Wallis (1969) was modified to account for the effect of inclination angle in the stratified flow.

The effect of condensation rate on the flooding could be also predicted by this model as long as stratified flow was maintained. The envelope theory tells that the solution for the onset of flow reversal in an inclined rectangular channel can be obtained from the following simultaneous non-linear equations.

$$F(\alpha) = f_i\left[(1-\alpha)J_s^* + \alpha\left(\frac{\rho_s}{\rho_l}\right)^{\frac{1}{2}} J_l^*\right]^2 + f_s(1-\alpha)^3 J_s^{*2} + f_l\alpha^3 J_l^{*2}$$
$$-4\left(\frac{H}{L}\right)\left[\alpha(1-\alpha)^3 J_s^* - \left(\frac{\rho_s}{\rho_l}\right)^{\frac{1}{2}}\alpha^3(1-\alpha)J_l^*\right]\frac{dJ_s^*}{dx^*} - 2\alpha^3(1-\alpha)^3 = 0$$

$$G(\alpha) = \frac{dF}{d\alpha} = 0$$

In these equations, the interfacial friction factor was obtained from the correlation suggested by Bharathan,et al (1979) for the vertical angle and Linehan,et al (1970) for the nearly horizontal angle. The dimensionless condensation rate also was obtained from the heat transfer analysis and the empirical correlation suggested by Bankoff,et al (1980).

The results show that this analysis predicts successfully the vapor flooding flux and accounts for the condensation effect. It turns out that condensation decreases slightly the vapor flooding flux because it increases the interfacial shear stress.

It should be noted that condensation increases the vapor flux for zero penetration of liquid where the pattern of stratified flow is no longer maintained. It is also notable that the dimensionless vapor flooding flux decreases as the inclination angle increases while the superficial flooding flux at the angle of 33.5° is larger than that at the angle of 4.5°. Comparisons between the present analysis and other theories are also given.

Reference

Bankoff,S.G., Int.J.Multiphase Flow, Vol.6, No.1/2, pp 51-67, 1980

Bankoff,S.G.,et al, NUREG/CR-1898, 1980

Bharathan,D.,et al, NP-1165, 1979

Linehan,J.H.,et al, Ch.Eng.Prog.Symp.Ser., Vol.66, No.102, pp 11-20, 1970

Thomas,R.M., Int.J.Multiphase Flow, Vol.5, pp 1-15, 1979

Wallis,G.B., One Dimensional Two-Phase Flow, Chap. 11, McGraw-Hill, New York, 1969

1981 LWR SAFETY MEETING

DIRECT-CONTACT STEAM-WATER CONDENSING FLOWS

NORTHWESTERN UNIV.

EVANSTON, ILL. 60201

FLOW GEOMETRIES

1. COUNTERCURRENT STRATIFIED FLOW IN INCLINED FLAT-PLATE GEOMETRY-H.J. KIM, S.C. LEE, S.G. BANKOFF
2. COCURRENT STRATIFIED FLOW IN HORIZONTAL FLAT-PLATE GEOMETRY-I.S. LIM, R. JENSEN, M.C. YUEN
3. COUNTERCURRENT VERTICAL FLOW THROUGH PERFORATED PLATE-R. CHEN, I. DILBERS, S.G. BANKOFF
4. HOLOGRAPHIC STUDY OF WATER SPRAY IN STEAM OR AIR ATMOSPHERE-S.Y. LEE, R.S. TANKIN

INCLINED COUNTERCURRENT FLOW

RECTANGULAR SECTION 1.27 m long, 38 cm wide, variable height and inclination

Ranges:		
	Water flow	0.3-3.0 kg/s
	Steam flow	0.01-1.8 kg/s
	Water temp	5-90 °C
	Steam temp	110-130 °C
	Press	1 atm
	Aspect ratio	Variable, max. 10
	Inclination angle	0-90

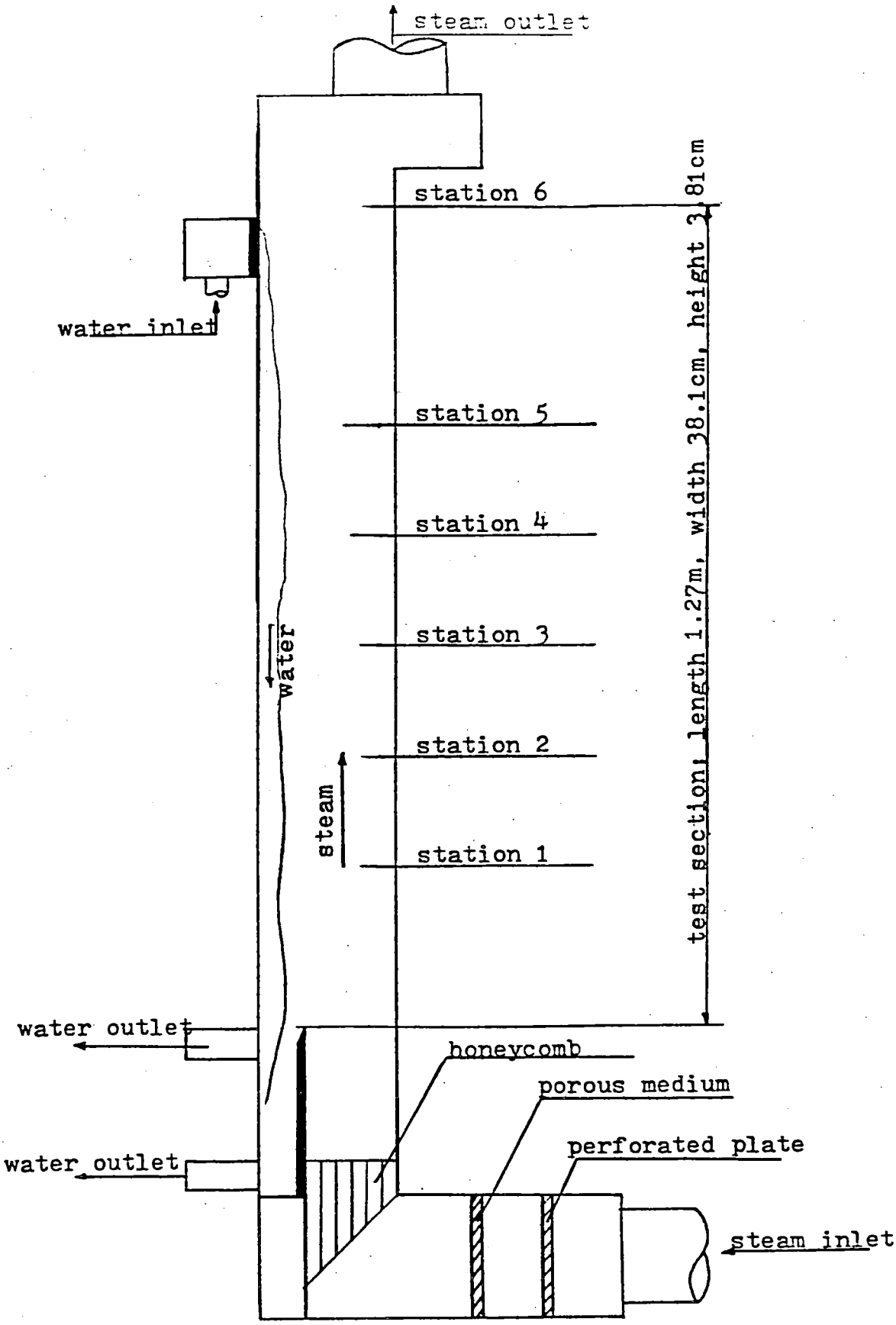

Fig. Sketch of test section

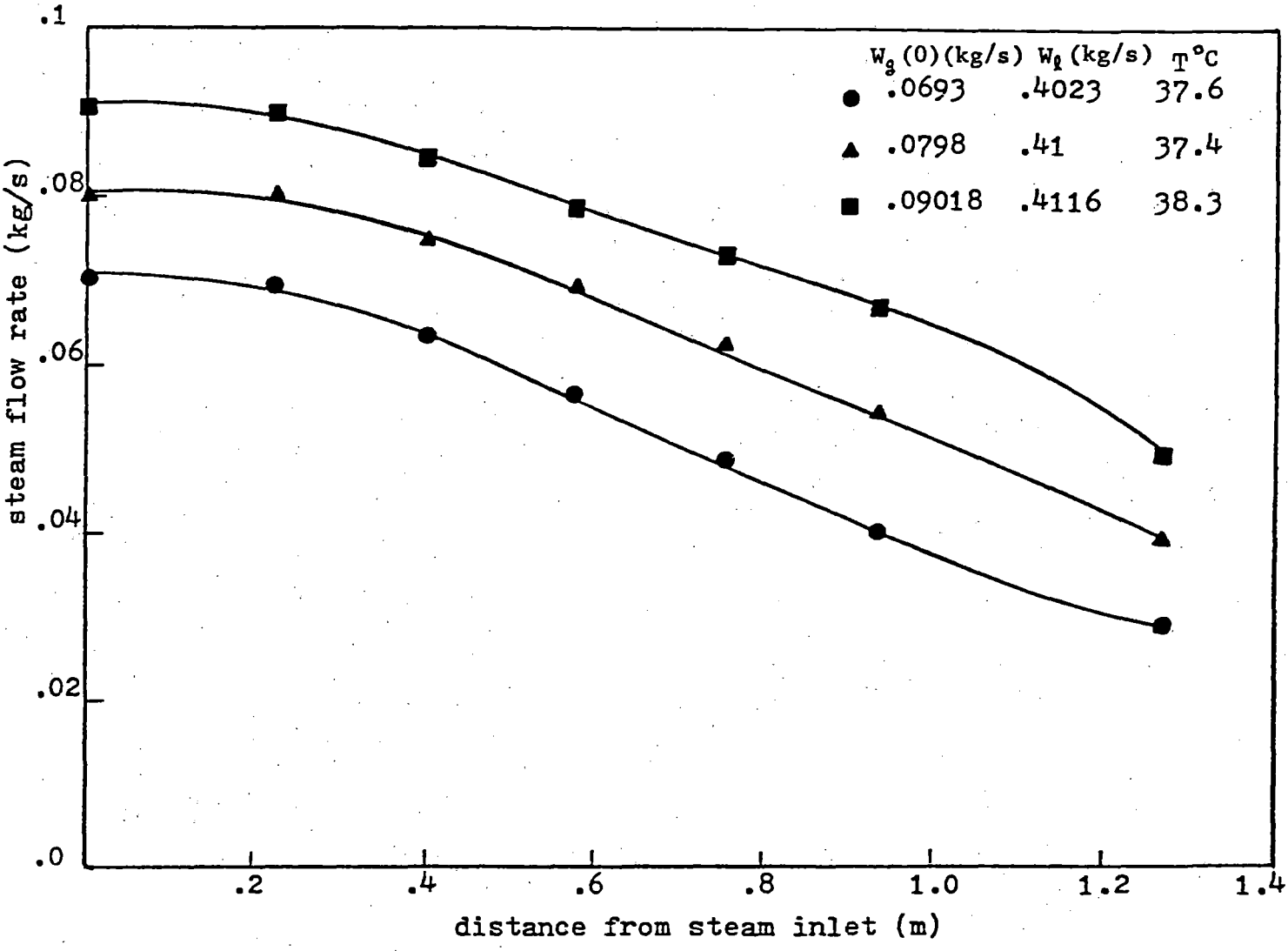

Fig. Axial steam flow rate profile as a function of inlet steam flow rate-inlet water temperature approximately 37°C, inlet water flow rate 0.41 kg/s.

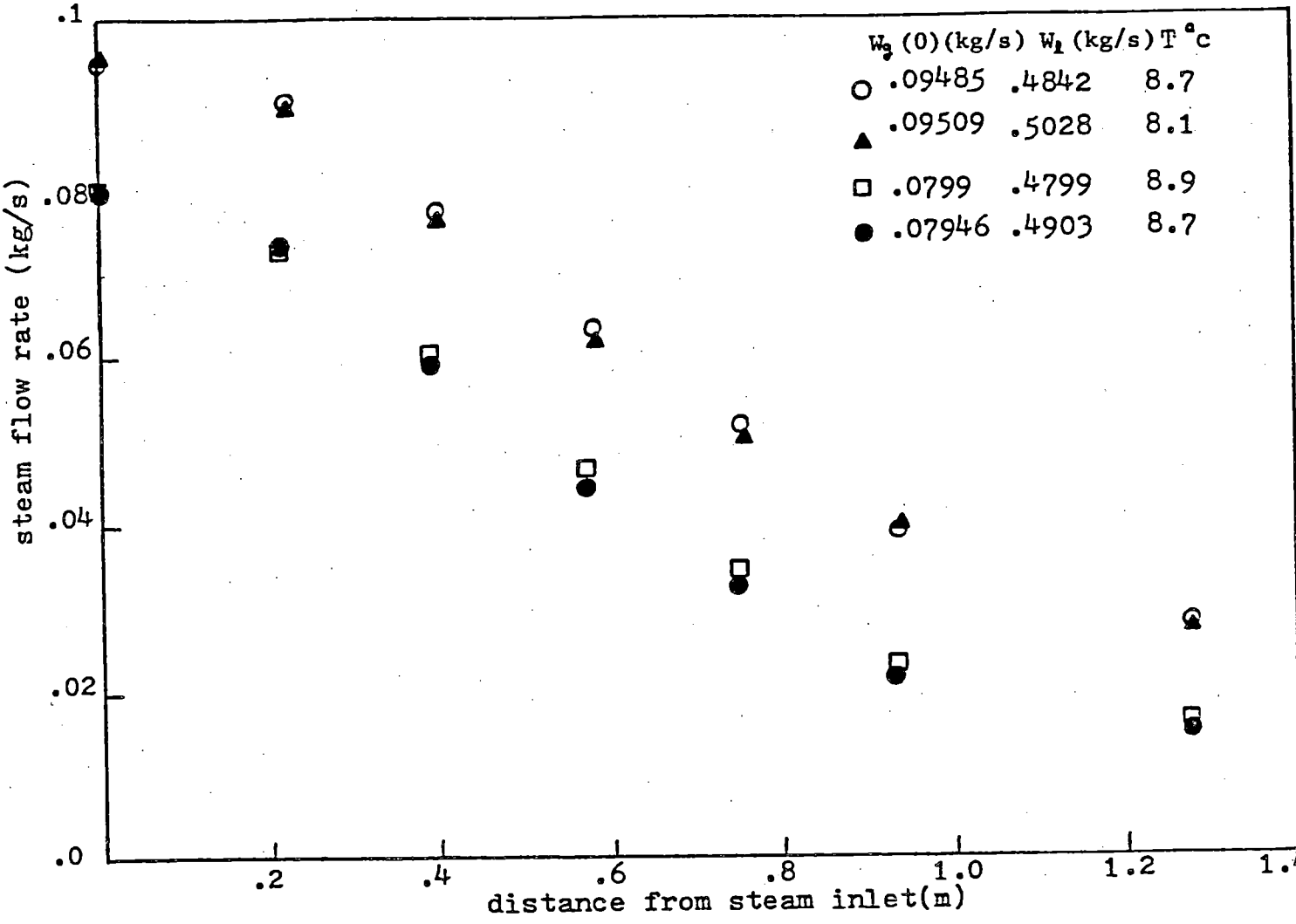

Fig. Repeat of experiment to show reproducibility of data

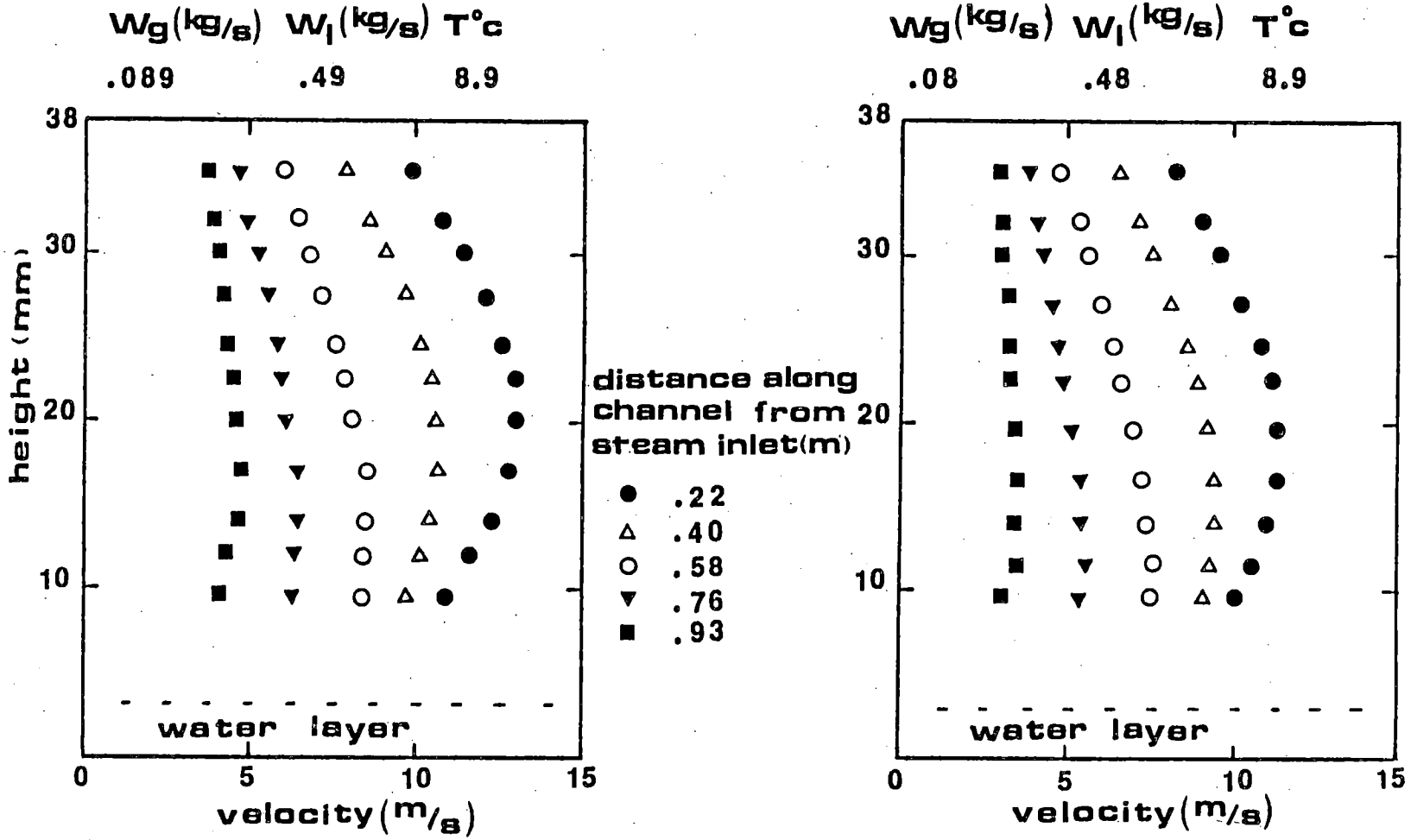

Fig. Steam Velocity Profiles

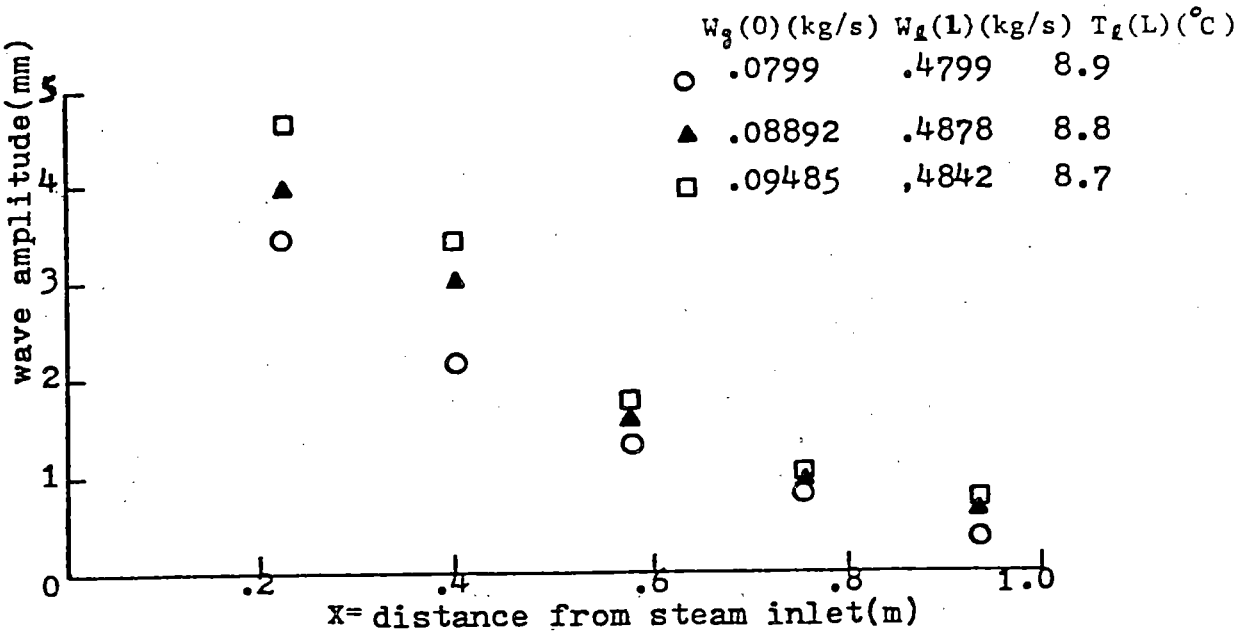

Fig. Wave height measurements for different steam flow rates.

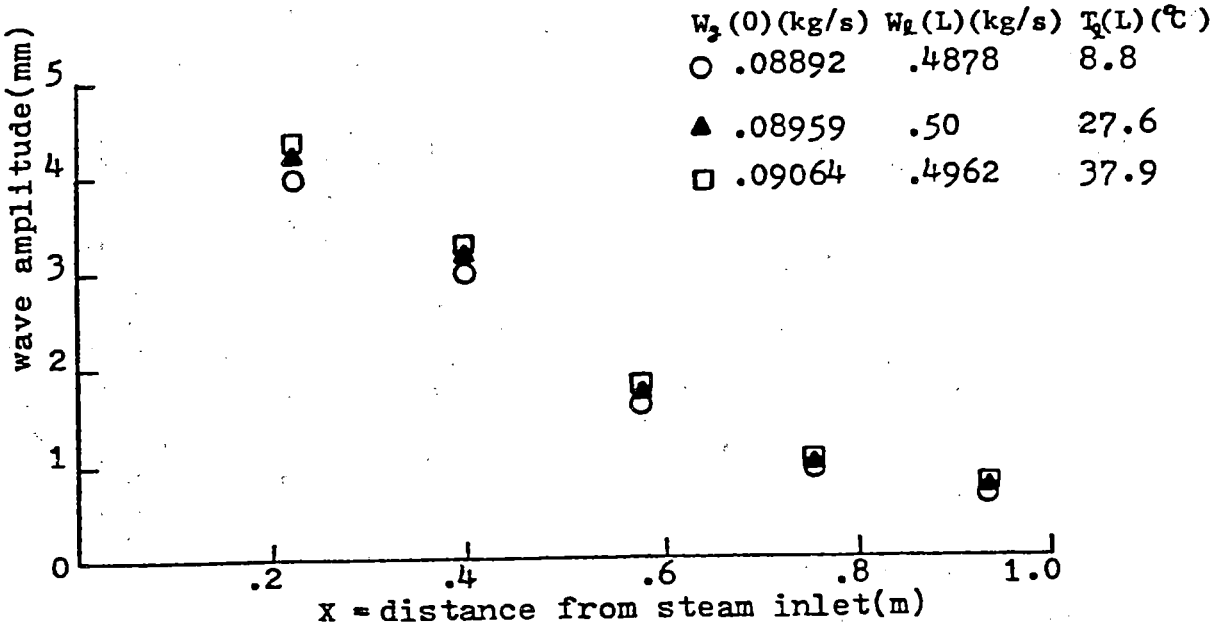

Fig. Wave height measurements for different inlet water temperatures.

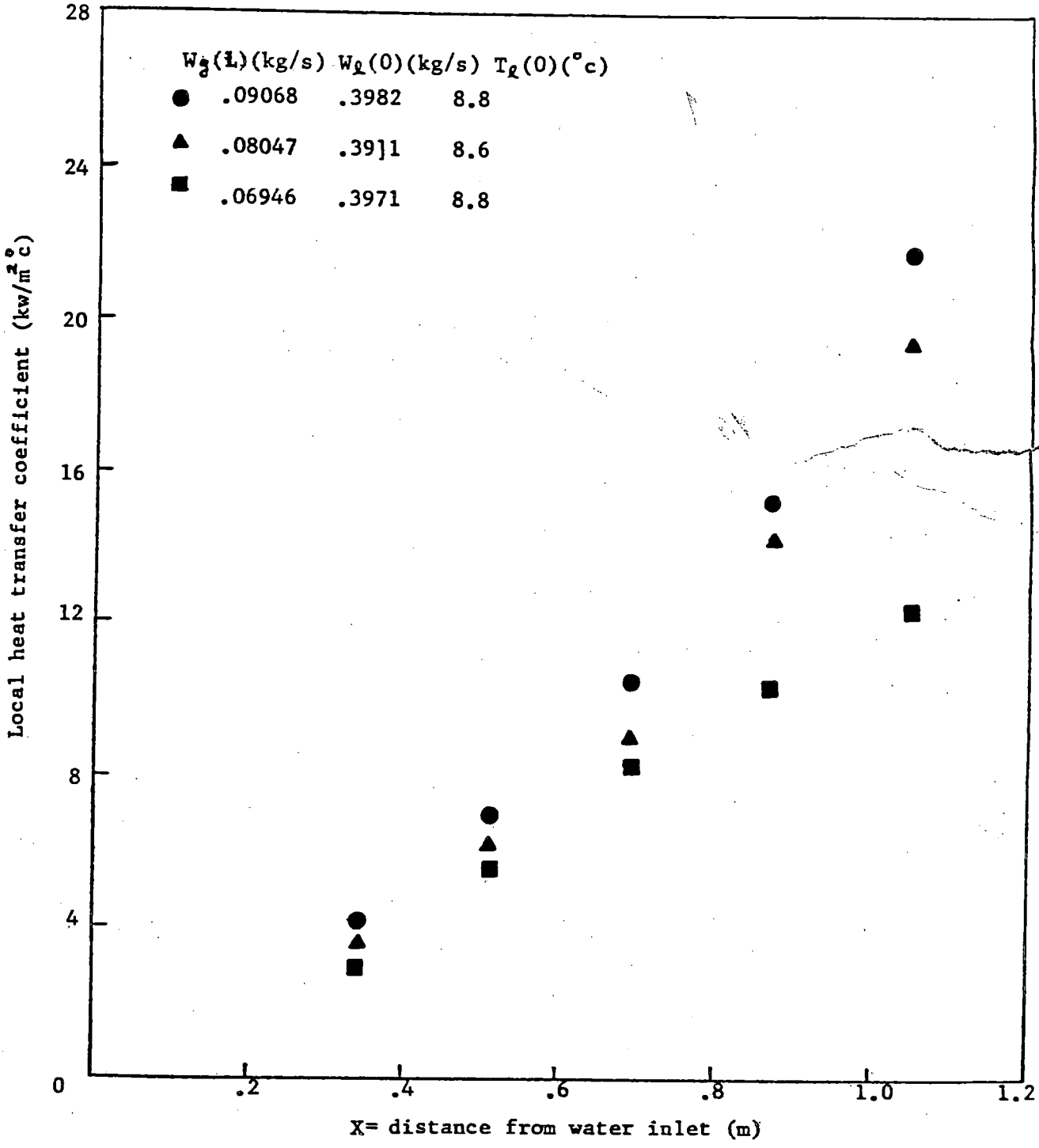

Fig. Axial heat transfer coefficient profile as a function of inlet steam flow rate.

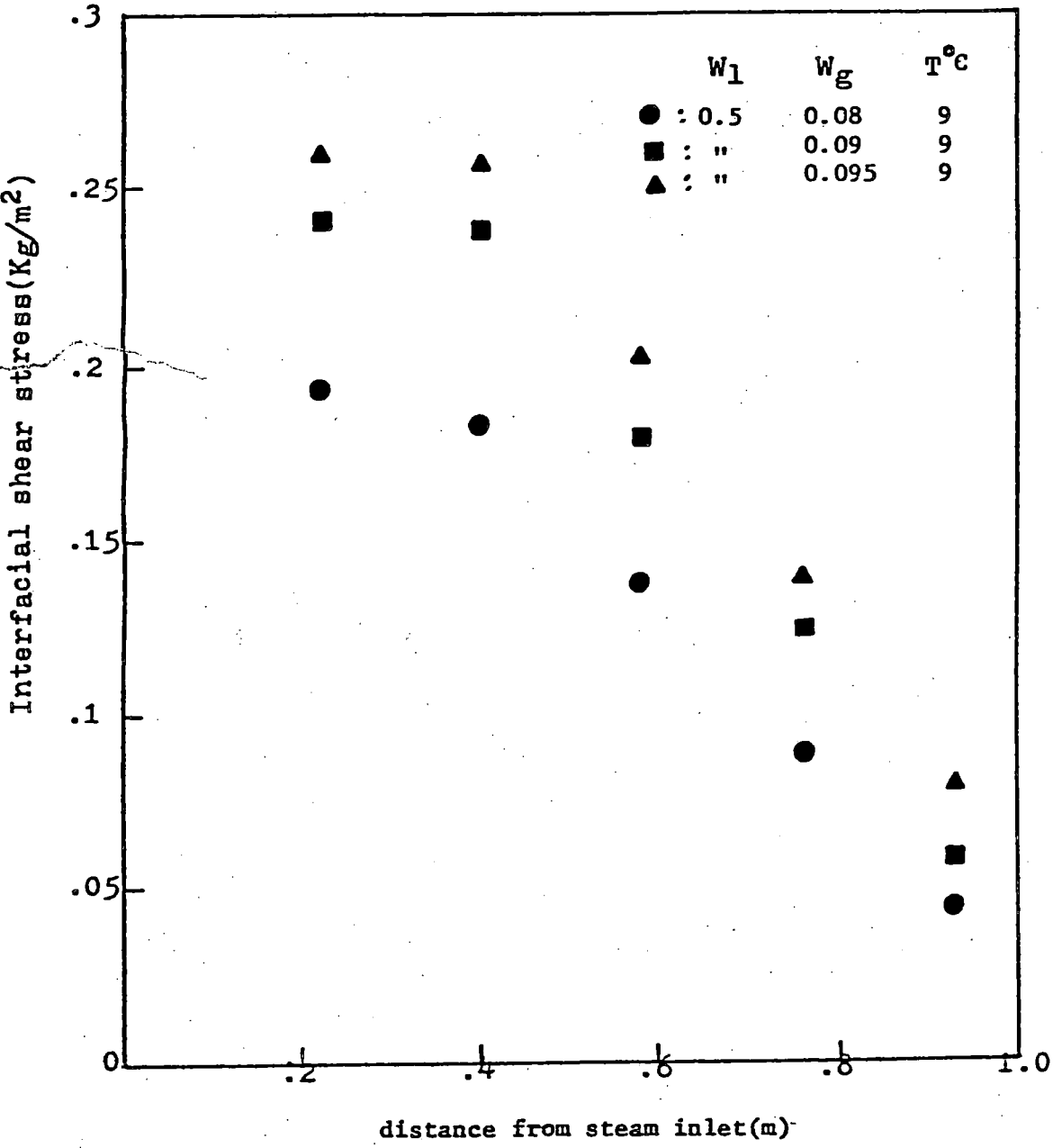

Fig. Interfacial shear stress comparison for different steam inlet flow rates

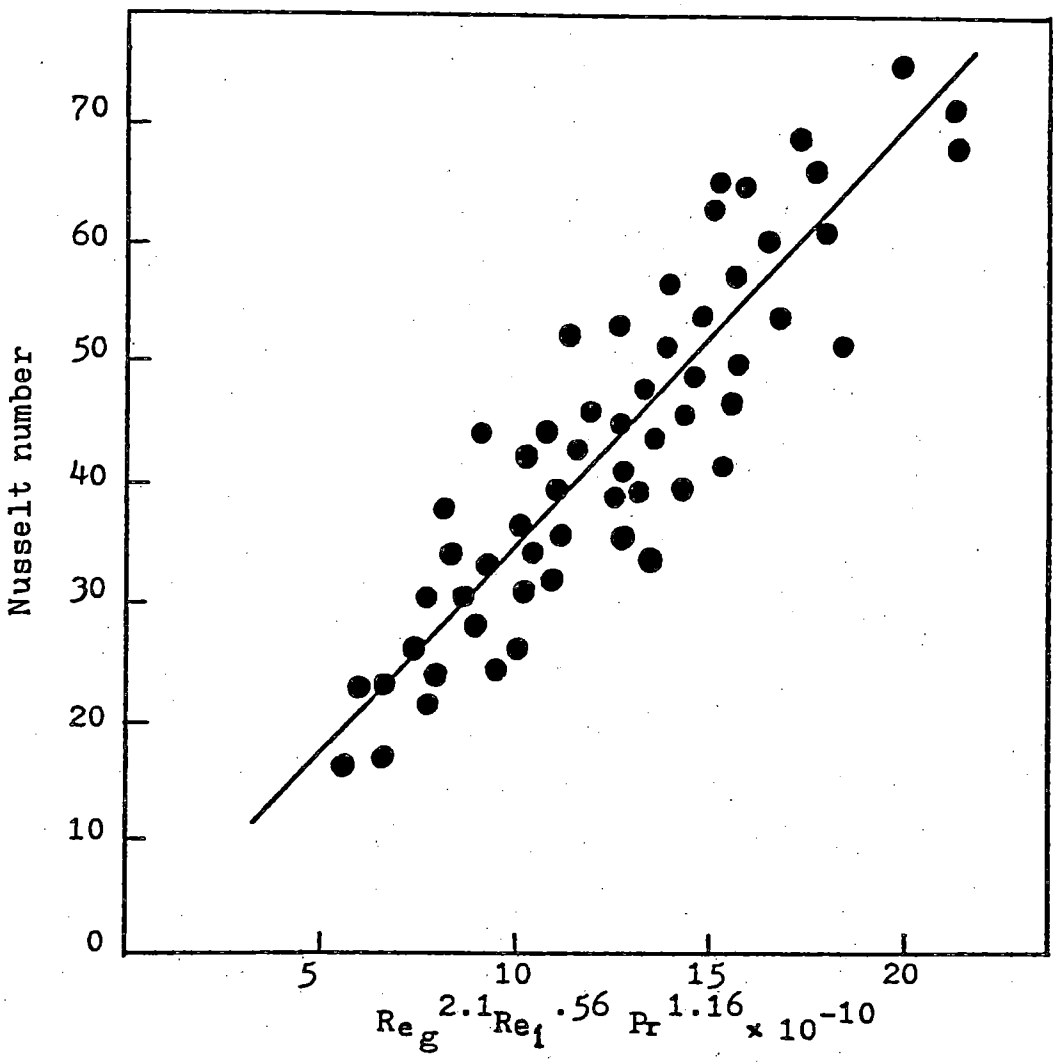

Fig. Experimental correlation for the rough regime

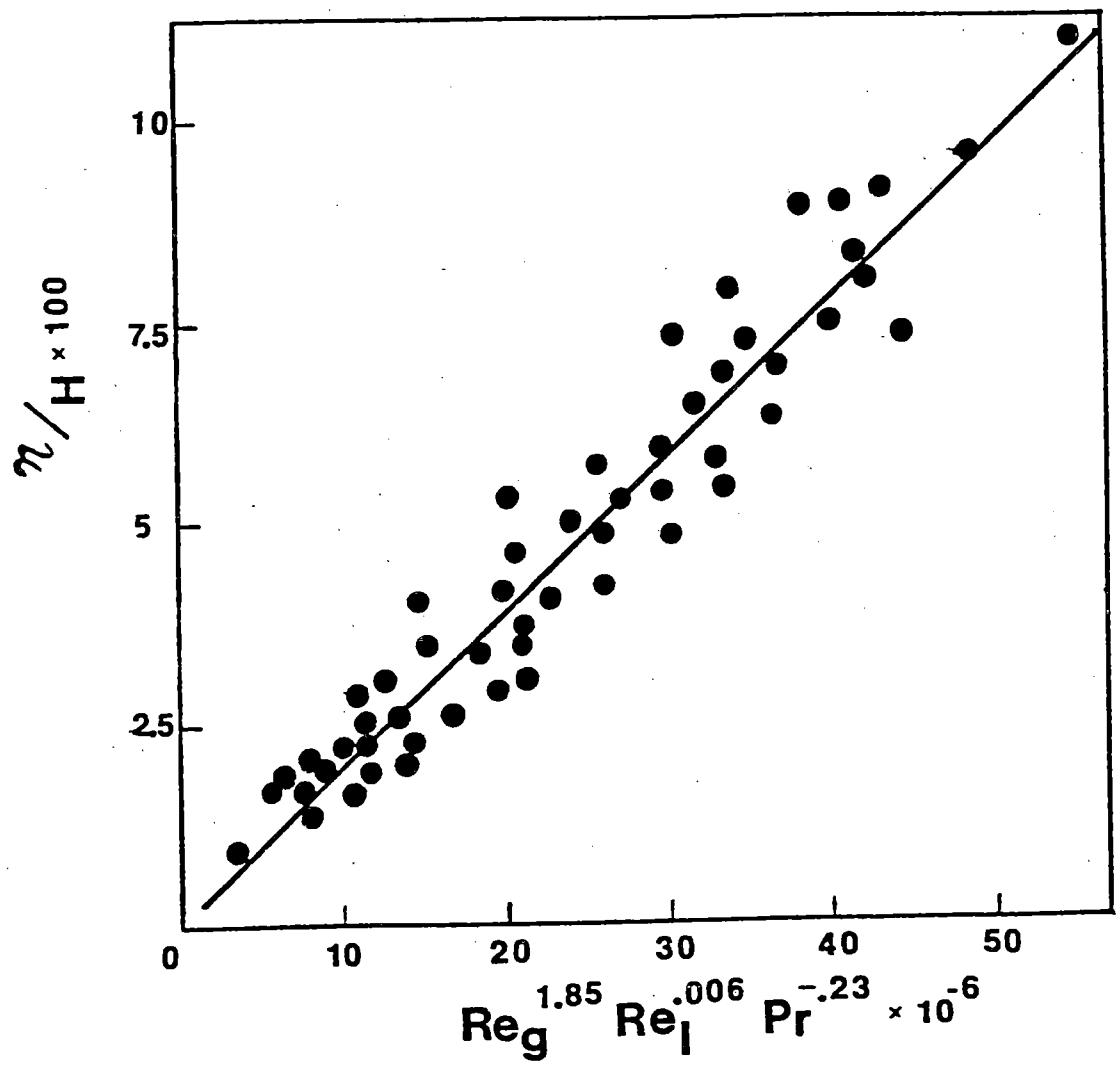

Fig. Experimental Correlation for wave amplitude

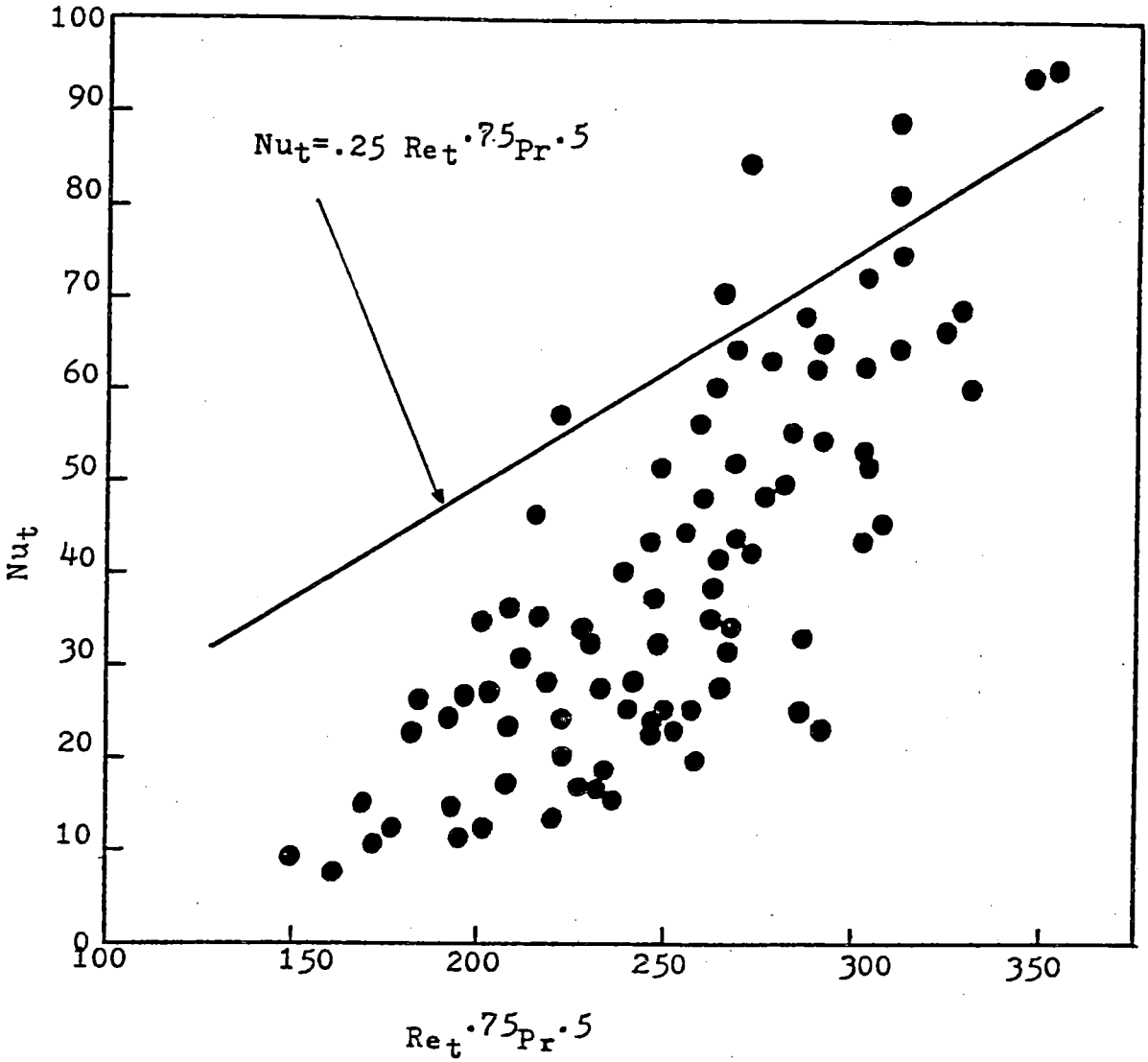

Fig. Comparison with turbulence equation using $U_t=.3\bar{U}_l$, λ_t=water layer thickness

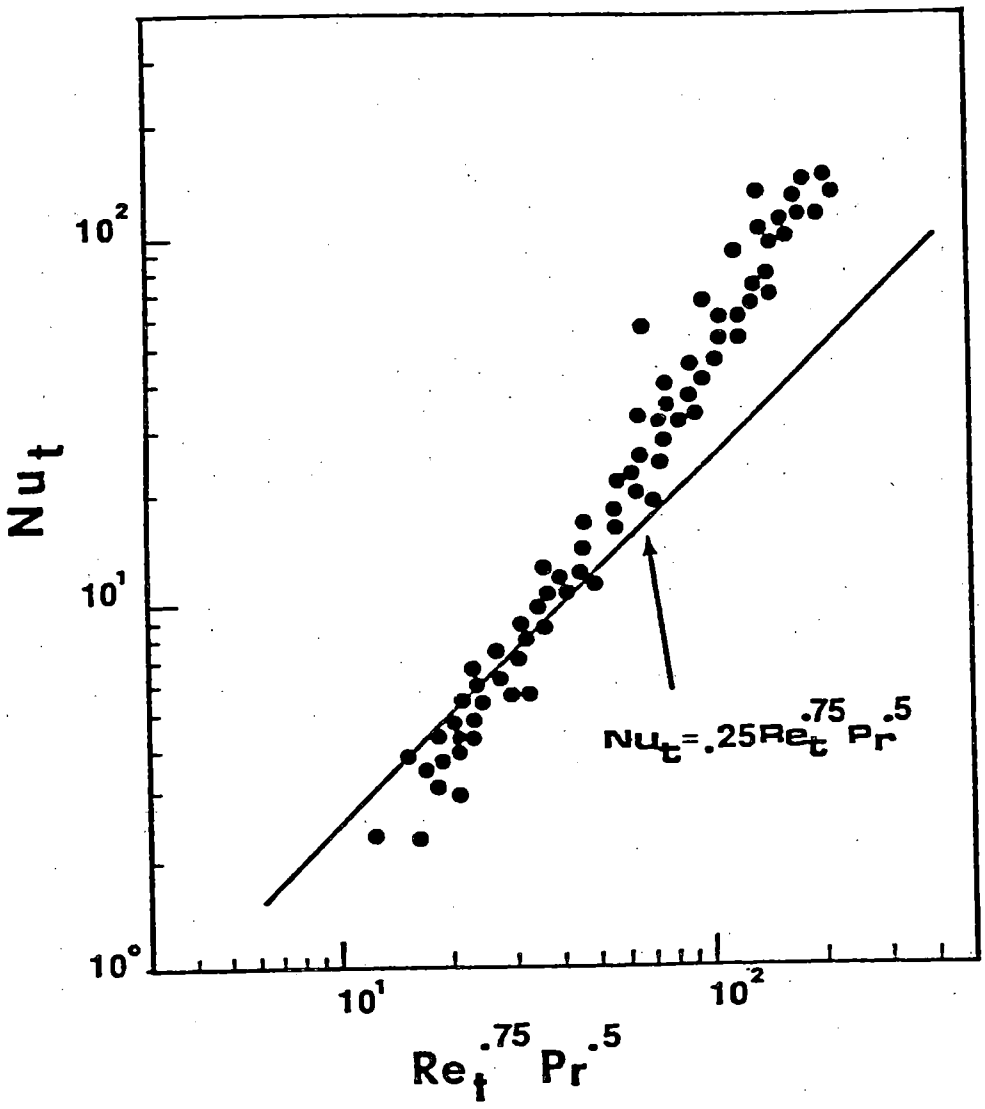

Fig. Comparison with turbulence eqn.

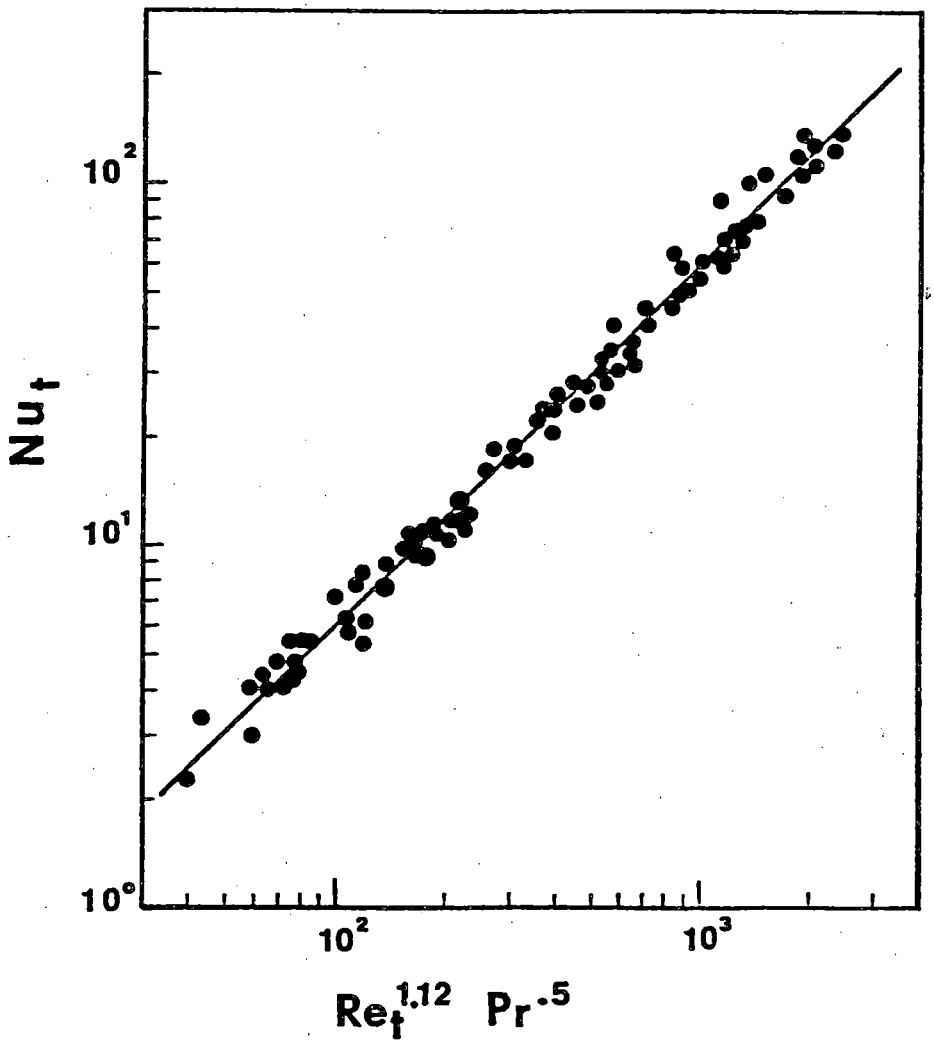

Fig. Experimental Correlation

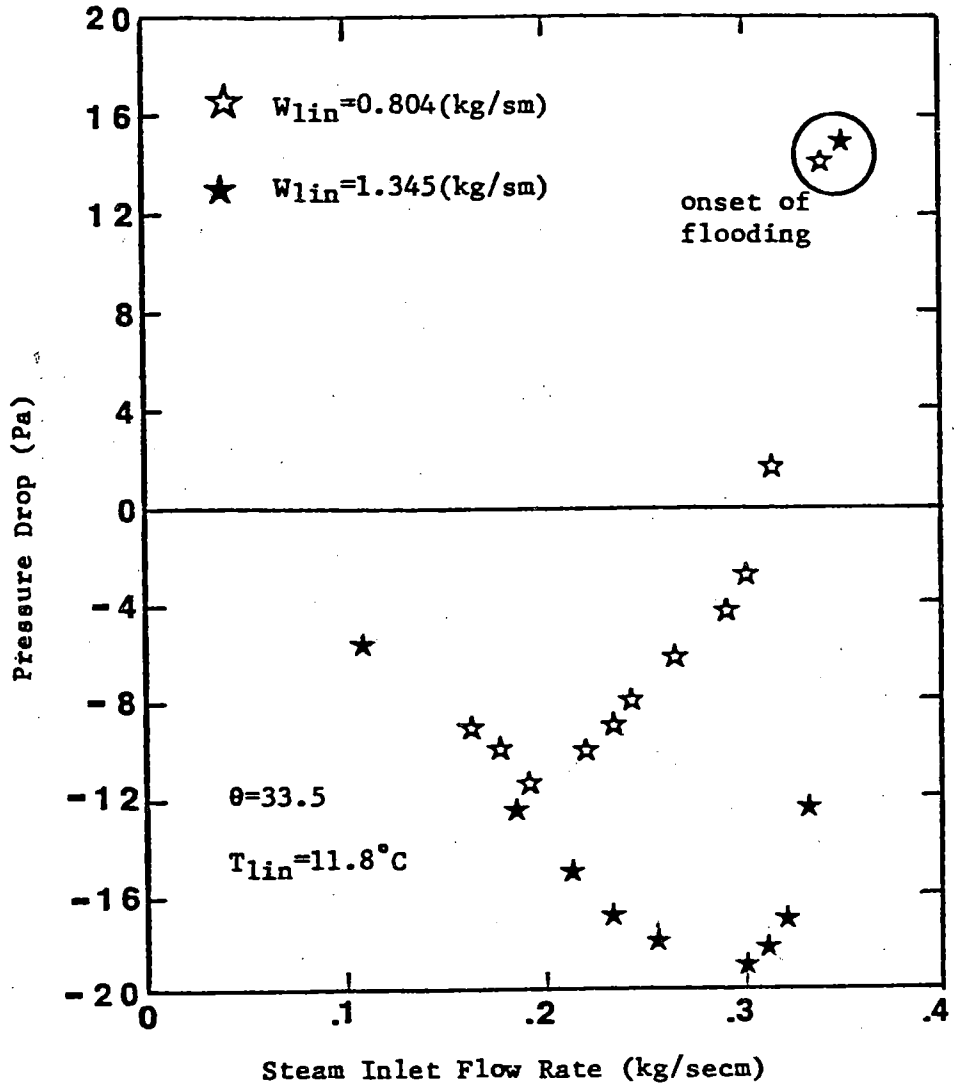

Typical pressure drop for onset of flooding

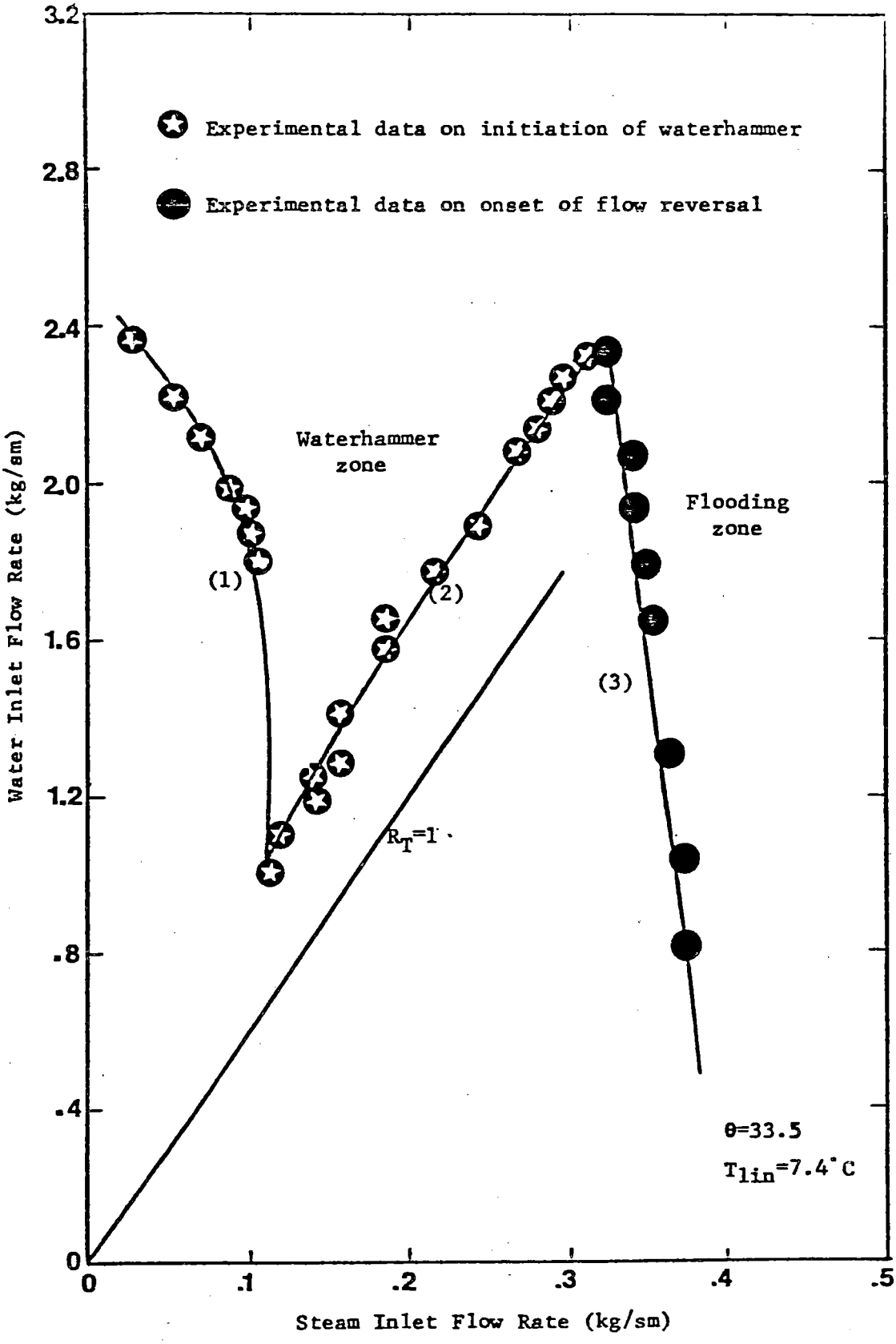

Typical flow map on the instability of the steam-water flow

Hydrodynamic Analysis

$$-\tau_1 - \tau_i - h\frac{dP}{dx} + \rho_1 g h \sin\theta = \frac{d}{dx}(W_1 V_1) - V_i \frac{dW_1}{dx}$$

$$\tau_s + \tau_i - (H-h)\frac{dP}{dx} + \rho_s g (H-h)\sin\theta = \frac{d}{dx}(W_s V_s) + V_i \frac{dW_1}{dx}$$

$$dW_1 = dW_s$$

where $W_1 = \rho_1 h V_1$

$W_s = \rho_s (H-h) V_s$

Define the friction factor as follows

$$\tau_s = \frac{1}{2} f_s \rho_s V_s^2$$

$$\tau_l = \frac{1}{2} f_l \rho_l V_l^2$$

$$\tau_i = \frac{1}{2} f_i \rho_s (V_s + V_l)^2 + V_i \frac{dW_s}{dx}$$

Define the dimensionless parameters

$$J_i^* = j_i \left[\frac{\rho_i}{gH\sin\theta(\rho_l - \rho_s)} \right]^{\frac{1}{2}} \qquad \text{for } i=s \text{ steam}, \; i=l \text{ water}$$

$$\alpha = \frac{H-h}{H}$$

$$x^* = \frac{x}{L}$$

For vertical flow, (Bharathan, D.,et al.,1979)

$$f_i = .005 + A(D^*/2)^B(1-\sqrt{\alpha})^B$$

where $\log_{10}A = -.56 + 9.07/D^*$

$$B = 1.63 + 4.74/D^*$$

$$D^* = \frac{2H}{\sqrt{\frac{\sigma}{(\rho_1-\rho_s)g}}}$$

For nearly horizontal flow, (Linehan,J.H.,et al.,1970)

$$f_i = .0188\ Re_1/1000 + .0068 \qquad Re_1 < 340$$

$$f_i = .0023\ Re_1/1000 + .0131 \qquad Re_1 \geq 340$$

where $$Re_1 = \frac{22.36}{\nu_1}\left[\frac{gH^3\sin\theta(\rho_1-\rho_s)}{\rho_1}\right]^{\frac{1}{2}}(1-\sqrt{\alpha})^{1.5}$$

For turbulent flow,

$$f_1 = .005$$

$$f_s = .079\ Re_s^{-\frac{1}{4}}$$

Heat transfer Analysis

$$d(W_l h_l) = h_s dW_s$$

$$h_s = h_{fg} + C_{pl}(T_s - T_r)$$

$$h_l = C_{pl}(T_l - T_r)$$

$$W_l(x) = W_{lin} \frac{h_{fg} + C_{pl}(T_s - T_{lin})}{h_{fg} + C_{pl}(T_s - T_l(x))}$$

Define the heat transfer coefficient

$$h \equiv \frac{h_{fg}}{T_s - T_l(x)} \left(\frac{dW_l}{dx}\right)$$

Then, $$h = \frac{h_{fg}}{\left[1 + \frac{C_{pl}(T_s - T_{lin})}{h_{fg}}\right] W_{lin} - W_l(x)} \left(\frac{dW_s}{dx}\right)$$

Define dimensionless parameter

$$K = \frac{C_{pl}(T_s - T_{lin})}{h_{fg}}$$

$$Nu = \frac{h\ x}{k_l}$$

$$Pr = \frac{\nu_l}{a_l}$$

$$Re_{lin} = \frac{W_{lin}}{\mu_l}$$

$$Re_s = \frac{W_s}{\mu_s}$$

Then, $$\frac{dJ_s^*}{dx^*} = \frac{1}{x^*}\left[(1 + K)\frac{J_l^*}{J_{lin}^*} - 1\right]\left(\frac{\rho_l}{\rho_s}\right)^{\frac{1}{2}} J_l^* \frac{Nu}{PrRe_{lin}}$$

Empirical correlation for condensation rate
(Bankoff,S.G.,et al.,1980)

$$J^*_{lin} = J^*_l/(1 + .0185x^{*.5}Re_s^{.5}K^{1.5}) \qquad \text{for } x^{*.5}Re_s^{.5} < 54.1K^{-.5}$$

$$J^*_{lin} = J^*_l/(1 + K) \qquad \text{for } x^{*.5}Re_s^{.5} \geq 54.1K^{-.5}$$

$$\frac{\overline{Nu}}{Pr\ Re_{lin}} = (1 + K)\ \ln \frac{1}{1-.0185x^{*.5}Re_s^{.5}K^{.5}} - .0185x^{*.5}Re_s^{.5}K^{1.5}$$

From the definition of avg. heat transfer coefficient

$$Nu = x^* \frac{d}{dx^*}(\overline{Nu})$$

Then, $$\frac{Nu}{Pr\ Re_{lin}} = .0093x^{*.5}Re_s^{.5}K^{.5}\left[\frac{1 + K}{1-.0185x^{*.5}Re_s^{.5}K^{.5}} - K\right]$$

Flooding Equation

$$F(\alpha) = f_i\left[(1-\alpha)J_s^* + \alpha\left(\frac{\rho_s}{\rho_1}\right)^{\frac{1}{2}} J_1^*\right]^2 + f_s(1-\alpha)^3 J_s^{*2} + f_1\alpha^3 J_1^{*2}$$
$$-4\left(\frac{H}{L}\right)\left[\alpha(1-\alpha)^3 J_s^* - \left(\frac{\rho_s}{\rho_1}\right)^{\frac{1}{2}}\alpha^3(1-\alpha)J_1^*\right]\frac{dJ_s^*}{dx^*} - 2\alpha^3(1-\alpha)^3 = 0$$

$$G(\alpha) = \frac{dF}{d\alpha}$$
$$= 2f_i\left[-J_s^* + \left(\frac{\rho_s}{\rho_1}\right)^{\frac{1}{2}} J_1^*\right]\left[(1-\alpha)J_s^* + \alpha\left(\frac{\rho_s}{\rho_1}\right)^{\frac{1}{2}} J_1^*\right]$$
$$+ \frac{df_i}{d\alpha}\left[(1-\alpha)J_s^* + \alpha\left(\frac{\rho_s}{\rho_1}\right)^{\frac{1}{2}} J_1^*\right]^2 - 3f_s(1-\alpha)^2 J_s^{*2}$$
$$+ 3f_1\alpha^2 J_1^{*2} - 4\left(\frac{H}{L}\right)\left[(1-\alpha)^3 J_s^* - 3\alpha(1-\alpha)^2 J_s^* - \right.$$
$$\left. 3\left(\frac{\rho_s}{\rho_1}\right)^{\frac{1}{2}}\alpha^2(1-\alpha)J_1^* + \left(\frac{\rho_s}{\rho_1}\right)^{\frac{1}{2}}\alpha^3 J_1^*\right]\frac{dJ_s^*}{dx^*} -$$
$$6\alpha^2(1-\alpha)^3 + 6\alpha^3(1-\alpha)^2 = 0$$

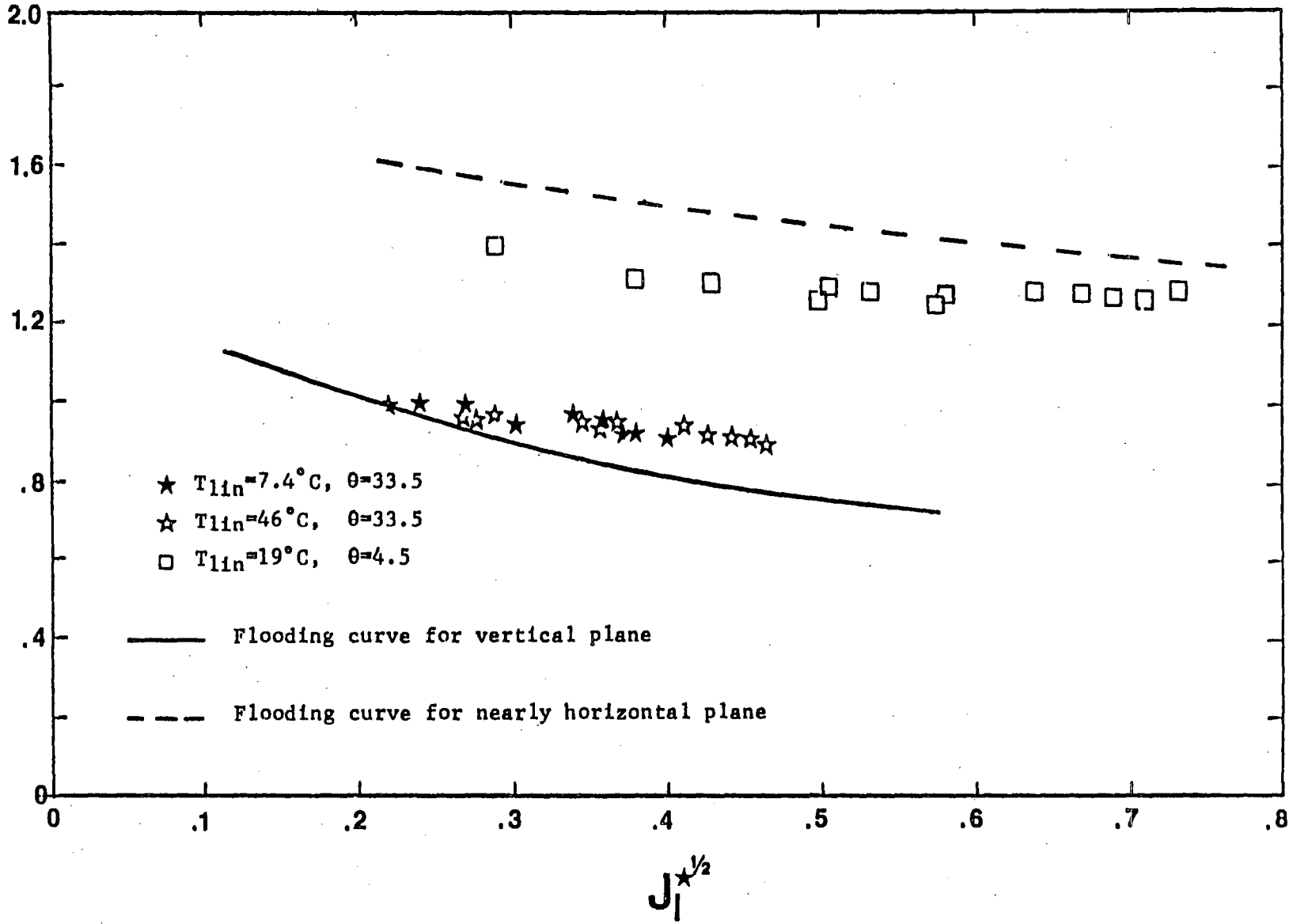

Effect of the inclination angle on the flooding flux

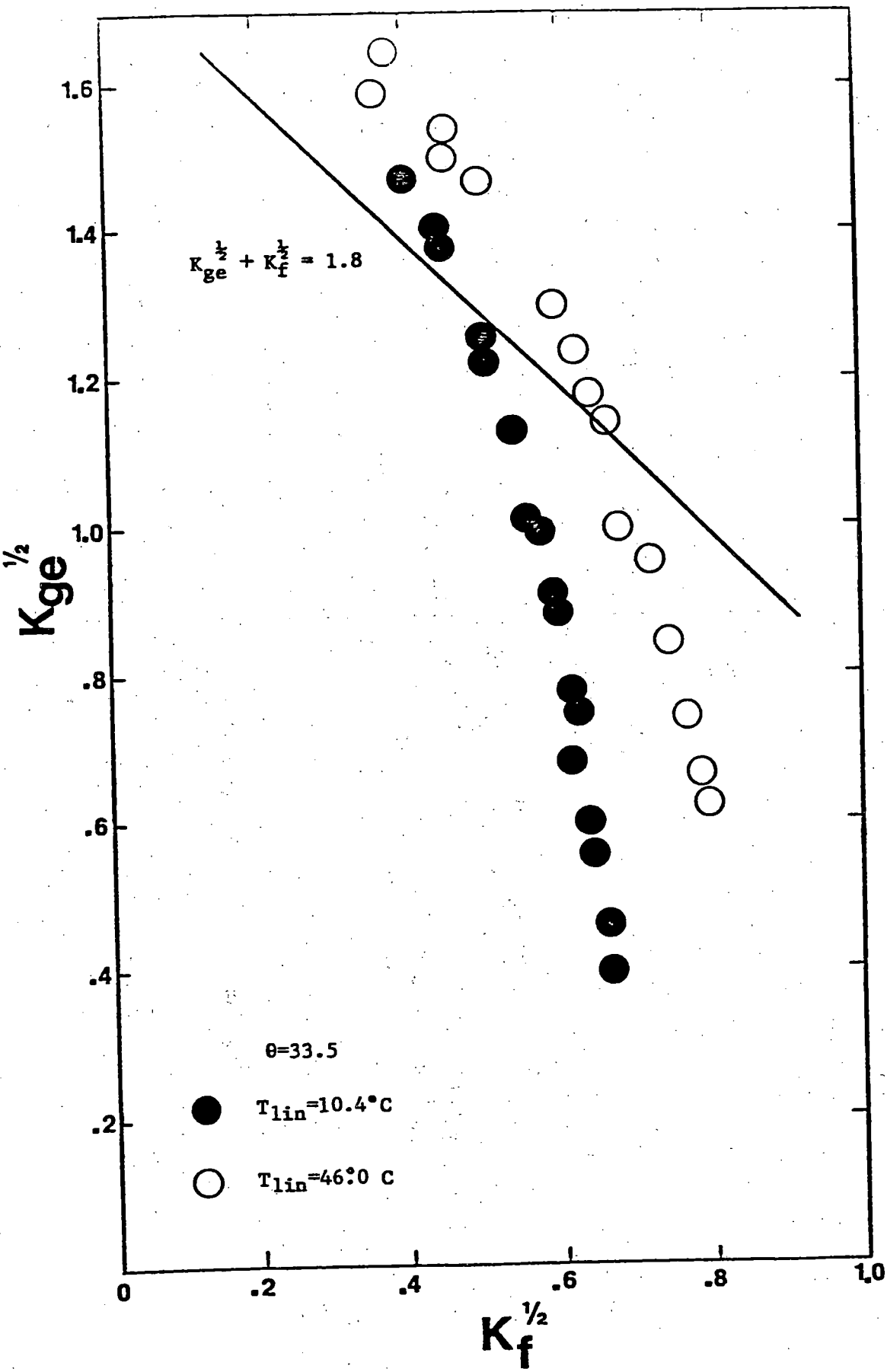

Comparison of the flooding data with Tien's suggestion

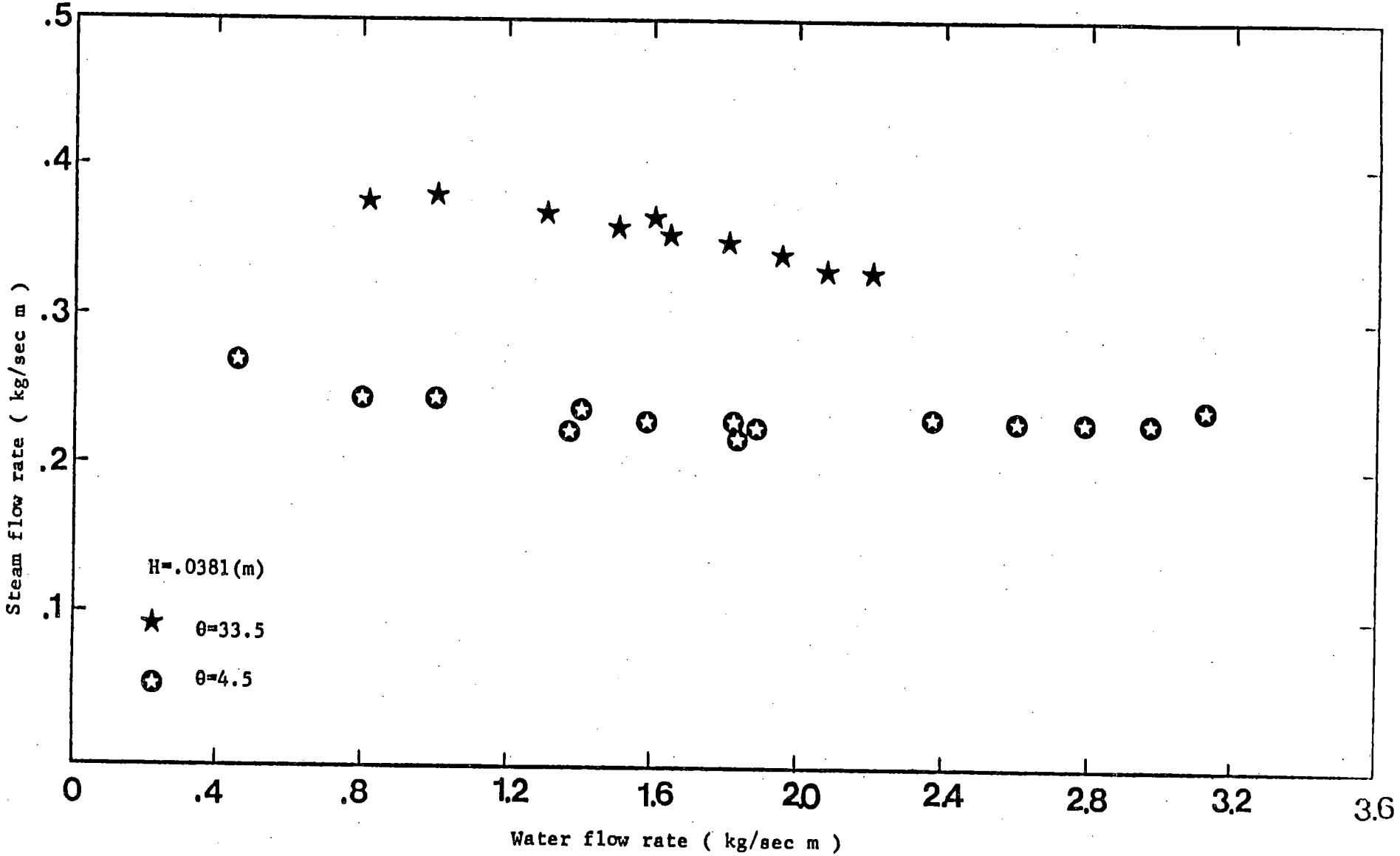

Flooding flux at the different angles in a rectangular channel

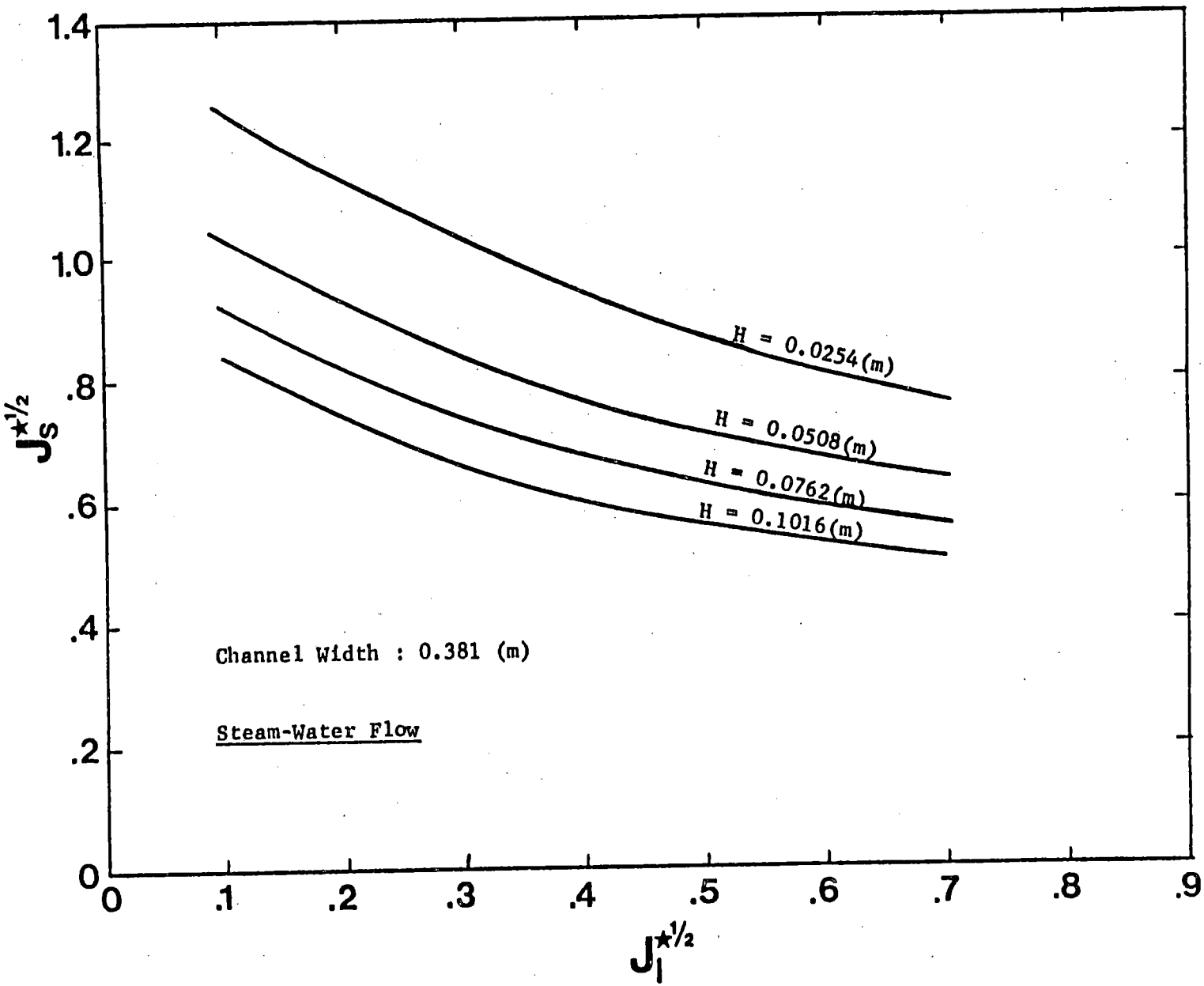

Dependence of channel depth on flooding flux in a vertical rectangular channel

Comparison with other models

For a vertical channel

Zvirin et al (1979)

$$\frac{J_s^*}{\alpha} + \left(\frac{\rho_s}{\rho_1}\right)^{\frac{1}{2}} \frac{J_1^*}{1-\alpha} = V_{cr}\left[\frac{\rho_s}{gH(\rho_1-\rho_s)}\right]^{\frac{1}{2}}$$

Momentum equation $F(\alpha) = 0$

where
$$V_{cr}^2 = \frac{4\mu_1}{\beta\rho_s}\left(\frac{\sigma}{\rho_1}\right)^{\frac{1}{2}} \frac{(2\pi/\lambda_{cr})^{1.5}}{\left[\tanh(2\pi h/\lambda_{cr})\right]^{\frac{1}{2}}}$$

and
$$\lambda_{cr} = \frac{h^2}{16\pi\nu_1}\left[\frac{2\pi\sigma}{\rho_1\lambda_{cr}} \tanh(2\pi h/\lambda_{cr})\right]^{\frac{1}{2}}$$

For a nearly horizontal channel

Taitel and Dukler (1976)

$$\frac{J_s^*}{\alpha} + \left(\frac{\rho_s}{\rho_1}\right)^{\frac{1}{2}} \frac{J_1^*}{1-\alpha} = \frac{h_G'}{h_G}(\alpha \cot\theta)^{\frac{1}{2}}$$

Mishima and Ishii (1979)

$$\frac{J_s^*}{\alpha} + \left(\frac{\rho_s}{\rho_1}\right)^{\frac{1}{2}} \frac{J_1^*}{1-\alpha} = 0.487\ (\alpha \csc\theta)^{\frac{1}{2}}$$

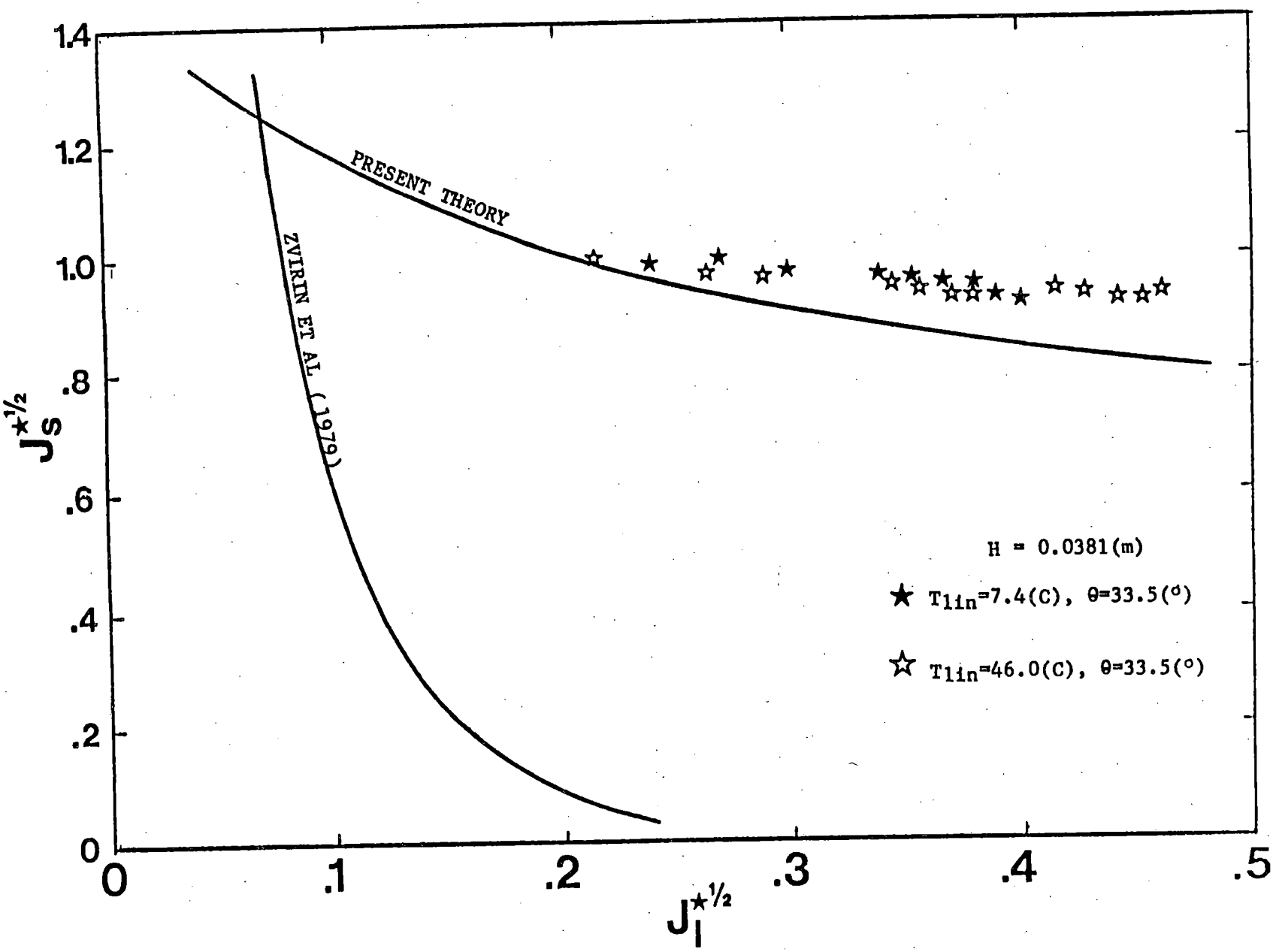

Comparison with other model at onset of interface growth in a vertical rectangular channel

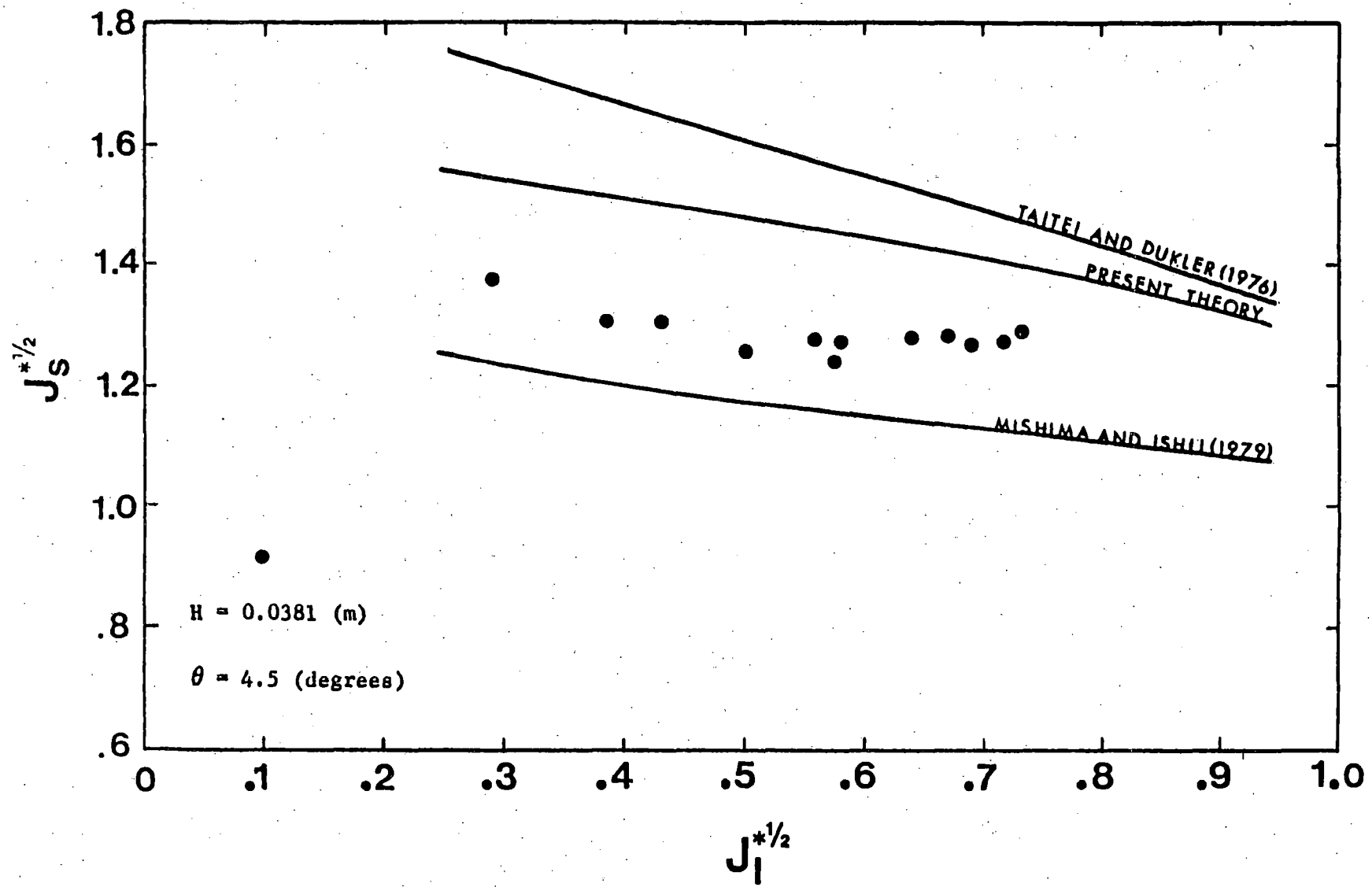

Comparison with other models at onset of interface growth in a nearly horizontal channel

IMPROVED MEASUREMENTS OF CLADDING TEMPERATURE AND FLUID VELOCITY FOR LOFT

D. J. Hanson

Presented at

The Ninth Water Reactor Safety Research Information Meeting

October 26 - 30, 1981

Gaithersburg, Maryland

Idaho National Engineering Laboratory

Idaho Falls, Idaho 83415

EG&G Idaho

Idaho Falls, Idaho 83415

IMPROVED MEASUREMENTS OF CLADDING TEMPERATURE AND FLUID VELOCITY FOR LOFT

D. J. Hanson
EG&G Idaho, Inc.

Knowledge of the fuel rod cladding temperature and system mass flow rates is important for understanding the behavior of reactor systems over the complete spectrum of possible accident conditions. However, measuring these parameters is difficult in the Loss-of-Fluid Test (LOFT) Facility due to the complex phenomena that occur and the harsh environment in which instruments must survive and function. Improvements have been made in thermocouple design and the method of installing them for more accurate fuel rod cladding temperature measurements. Improvements have also been made in the turbine flow meters to provide more reliable loop velocity measurements with smaller uncertainties. These improvements provide an increased understanding of the phenomena that occur under simulated accident conditions, which aids in assessment of computer code capabilities and planned plant operator response.

The improved method of measuring cladding temperature was developed because the currently used thermocouples may have large uncertainties under certain conditions of fluid flow and quality. Requirements established for the improved measurement method were to: (a) provide a direct measurement of cladding temperature, (b) minimize perturbation of fluid on the fuel rod surface and heat conduction within the fuel rod, and (c) maximize reliability. These requirements were met through development of a miniaturized zircaloy sheathed Type K thermocouple and a method of embedding this thermocouple near the inside surface of the cladding.

Use of zircaloy as the sheath material made miniaturization difficult, but was necessary to minimize material compatibility problems with the cladding, thereby increasing reliability. A process combining drawing, swaging, and flattening steps together with appropriate annealing was developed to provide a thermocouple junction 0.25 mm thick and 0.69 mm wide. Installation of the miniaturized thermocouple inside the fuel rod

is accomplished by first cutting an oblong patch from the cladding. A replacement patch is then prepared with a longitudinal slot cut on the inside surface. The thermocouple junction is laser-welded into the slot and, with the aid of special tooling, the patch is laser-welded back into the cladding. The thermocouple cable is routed to the top of the rod where a hermetic seal prevents the escape of fission gases and provides a transition from the zircaloy cable sheath to a stainless steel sheath. The cable exits the rod through a special fixture. Specially grooved fuel pellets are loaded up to the point the thermocouple enters the cladding and standard fuel pellets are used in the remainder of the rod, eliminating atypical fuel behavior in the vicinity of the thermocouple junction.

Cladding embedded thermocouples have been fabricated and installed in nuclear fuel rods used in the Power Burst Facility (PBF) TC-4 Test series.[1] These thermocouples were tested repeatedly under conditions expected during a loss-of-coolant accident. Peak temperatures ranged from about 900 to 1200 K and were generally followed by very rapid quenches of the cladding. Of the four embedded thermocouples installed, two survived five tests and two survived the full seven-test program. The results were excellent.

An improved method of measuring fluid velocities in LOFT was developed to provide an instrument capable of surviving long periods of time at operational flow rates (about 11 to 15 m/s) while still providing a natural circulation measurement of about 0.25 m/s. Requirements for this measurement included: (a) an extended range capability (b) long-term survivability, and (c) compatibility of materials within a reactor environment. A turbine meter using advanced materials was developed to fulfill these requirements. The basic turbine design includes two end posts which support a turbine shaft. The radial and thrust bearings are a special carbon compound and are pressed into the turbine hub. The shaft is highly polished tungsten carbide and is designed to allow relative movement of the end posts without fracturing the shaft. The relative movement feature allows the unit to withstand severe thermal gradients which may occur during emergency core cooling injection.

The improved turbine was incorporated into the standard LOFT drag-disc turbine rake and used in the intact loop hot leg during LOFT Test L6-7/L9-2.[2] These turbines survived for over 100 hours under conditions where the velocity exceeded 11 m/s yet were able to measure natural circulation velocities during Test L9-2 in the range of 0.25-0.45 m/s. The effect of velocity profile within the hot leg piping was evidenced by velocity differences measured by the turbines at the center and near the bottom of the pipe. These velocity data were similar to data obtained using pulse neutron activation and were within the measurement uncertainties of the two methods.

REFERENCES

1. R. W. Garner, PBF Thermocouple Effects Tests Test Series TC-4 Quick Look Report, EGG-TFBP-5465, August 1981.

2. J. P. Adams, Quick Look Report on LOFT Nuclear Experiment L6-7/L9-2, EGG-LOFT-5526, August 1981.

Development of Improved Measurements for LOFT

D.J. Hanson

EG&G Idaho, Inc.

IDAHO NATIONAL ENGINEERING LABORATORY

Requirements for Improved Cladding Temperature Measurement

- Direct measure of cladding temperature
- Minimize perturbation of fluid and heat transfer phenomena
- Maximize reliability

INEL-S-34 982

New Measurements Developed to Provide Improved LOFT Data

- Reliable cladding temperature
- Extended range fluid velocity

INEL-S-34 988

Cladding Embedded Thermocouple Installation

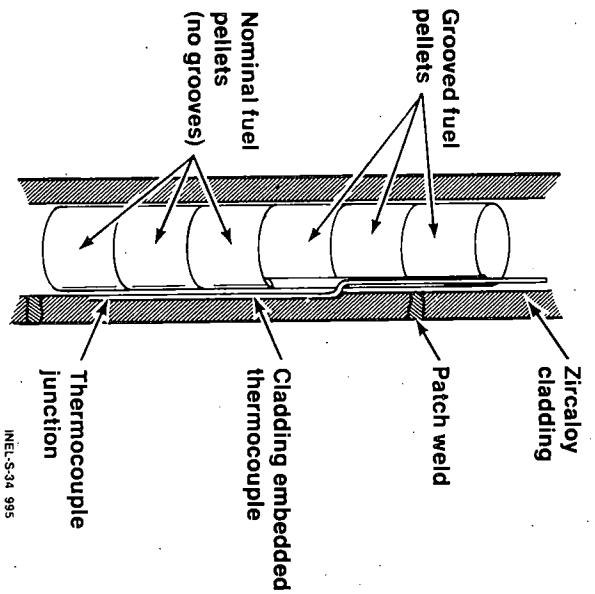

INEL-S-34 995

Embedded Zircaloy-Sheated Thermocouple on Inner Fuel Rod Cladding Surface

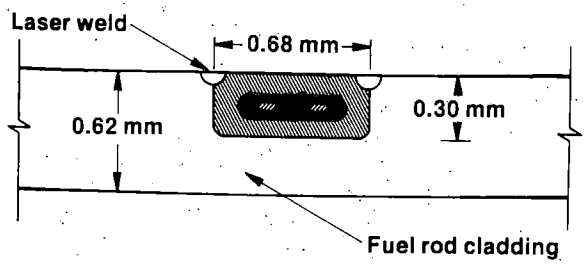

INEL-S-34 994

Cladding Embedded Thermocouple Patch

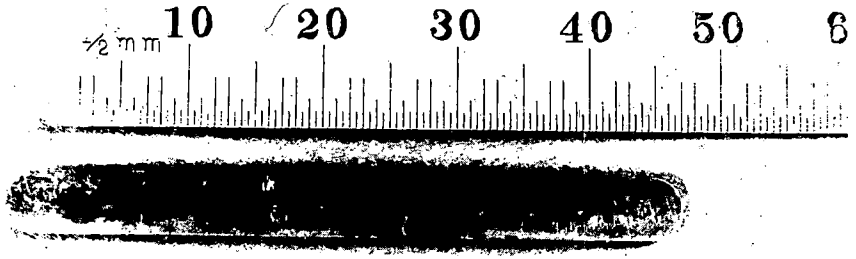

PBF Cladding Quench - Effects of LOFT Surface Thermocouples

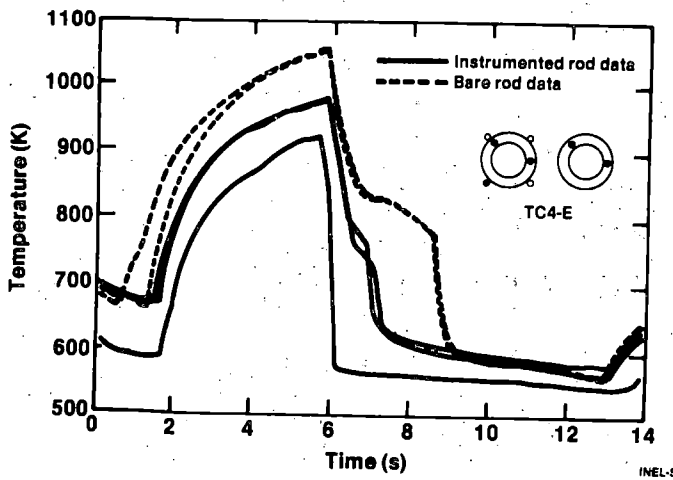

INEL-S-34 993

Requirements for Improved Turbine Flow Meter Design

- Extended range capabilities
- Long-term survivability
- Compatibility with reactor environment

INEL-S-34 981

DJH-5

Design Features for Improved Turbine Flow Meter Design

- Carbon bearing housed in rotor hub
- Silicon carbide shaft
- Shaft realignment capability

INEL-S-34 989

Improved Turbine Flowmeter Module

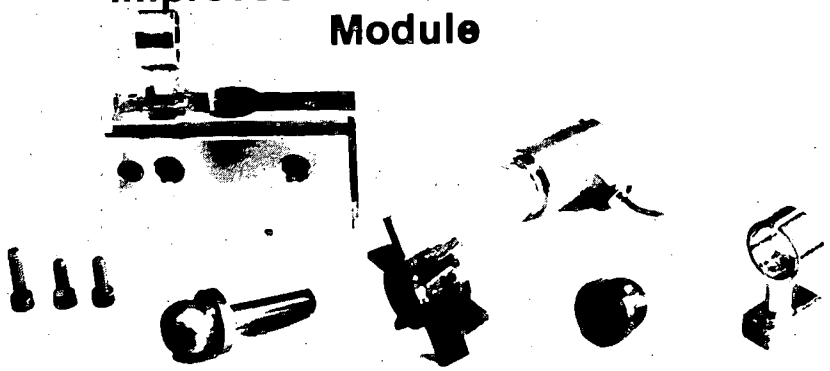

INEL-S-34 984

Improved Turbine Flowmeter Module

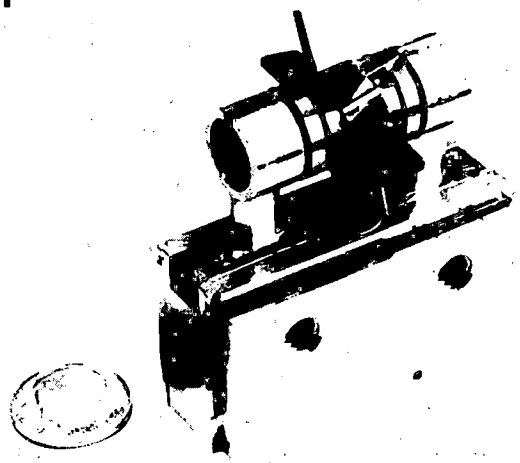

INEL-S-34 993

Intact Loop Flow Measurement Technique

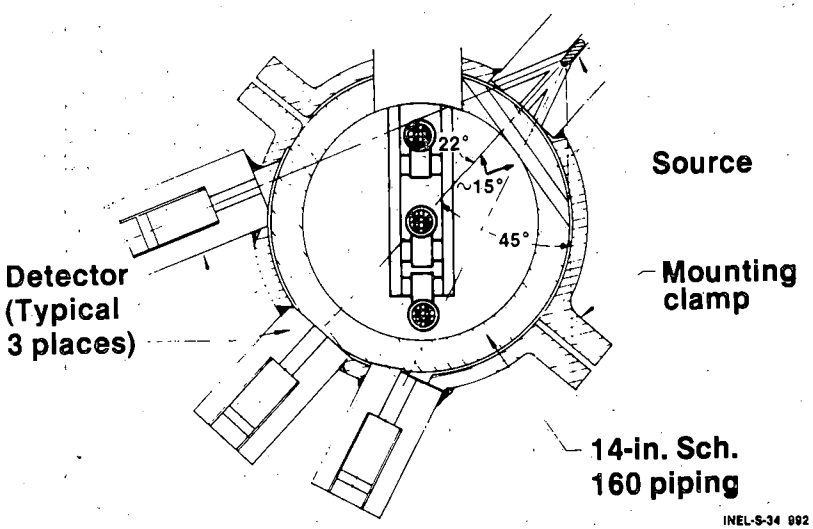

INEL-S-34 992

Hot Leg Fluid Velocity Spans Wide Range for Test L6-7/L9-2

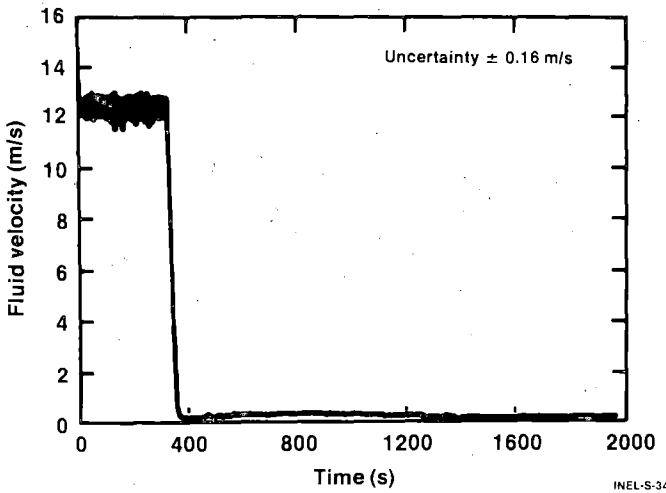

INEL-S-34 990

Natural Circulation Velocities Measured in Hot Leg for Test L9-2

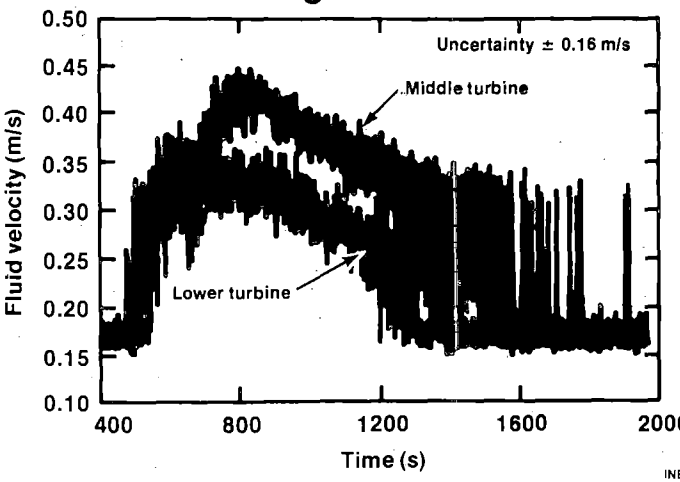

INEL-S-34 985

Comparison of Turbine Meter and PNA Velocities for Test L9-2

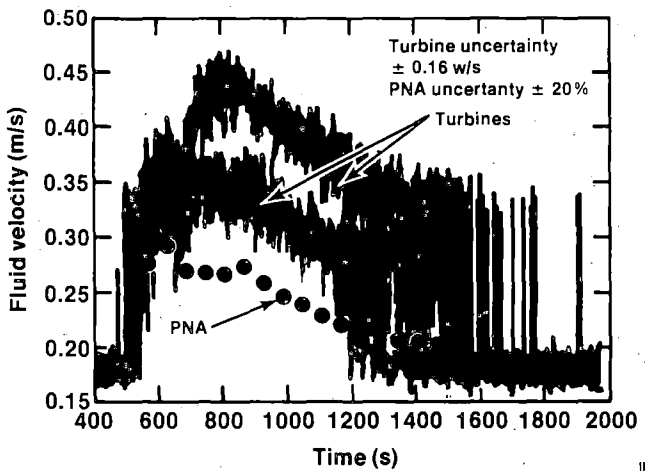

INEL-S-34 991

Conclusions

- Development of new measurements successful
- Excellent experimental results obtained
- Understanding of LOFT data will be enhanced

INEL-S-34 986

DJH-7

DETERMINING NON CONDENSIBLE GAS CONCENTRATIONS USING WET BULB & DRY BULB TEMPERATURE MEASUREMENTS

Peter Griffith
Massachusetts Institute of Technology

A means of determining the mass fraction of non-condensible gas present in a closed system has been investigated. The method involves measuring the wet bulb and dry bulb temperatures along with the system pressure, then relating these to the mass fraction of the non-condensible gas.

This instrument would have application in closed systems where sampling techniques could not be implemented. A specific application would be in PWR steam generator tests under simulated LOCA conditions, where an array of these instruments could be used to determine the concentration and distribution of non-condensible gases in the steam generator.

Analysis

The analysis consists of performing an energy balance on the wet bulb sock. Energy is convected towards the sock proportional to the temperature difference between the wet bulb sock and the surrounding gas/vapor mixture. Enthalpy is convected away from the sock proportional to the vapor concentration difference between the sock and the surrounding mixture. The equations are summarized on Figure 1.

Experiment

A test was set up to verify the analysis and to provide calibration. A schematic of the test apparatus is shown in Figure 2. With this apparatus the mass fractions of vapor and non-condensible gas (nitrogen) could be determined to within 2% using a sampling technique (not shown). Tests could be performed in either a forced convection mode (fan on; V = 6 ft/sec) or a natural convection mode (fan off). The wet bulb thermometer was kept moist with water from a small condenser. The dry bulb temperatures were obtained outside of the central duct and far removed from the influence of the wet bulb sock.

Results

A comparison between the measured vapor mass fraction (using the sampling technique) and the calculated vapor mass fraction (using wet bulb & dry bulb temperatures) is shown in Figure 3. For vapor mass fractions lower than 0.65; the calculated vapor mass fraction compares favorably with the measured mass fraction. At the higher vapor mass fractions, the correlation breaks down, due in part, to the shallow slope of the wet bulb temperature vs mass fraction curve. This is shown in Figure 4.

Forced Convection, Natural Convection and Stationary Systems

In a closed system, there will be no control over the flow conditions over the wet-bulb thermometer. The analysis described above, that is used for data reduction, assumes a forced convection case where the heat and mass transfer coefficients are related by:

$$\frac{h}{h_D} = \frac{k}{D} \left(\frac{Pr}{Sc}\right)^{1/3}$$

In the natural convection mode, the relation is identical in form save for the exponent which becomes 1/2. In the natural convection mode, circulation occurs as a result of density gradients. For combined thermal and species diffusion, the density gradients are a function of both phenomenon. One form of the Grashof number, which includes both phenomenon is shown in Figure 1.

For the wet bulb thermometer operating in a system where the non-condensible gas is nitrogen, the density gradients due to the thermal and concentration effects are opposite in sign thus there are regions where the Grashof number vanishes. This is shown in Figure 5. It would be expected that, in some region on either side of this line, there might be some idiosyncrocies associated with the wet bulb temperature data. In order to obtain an understanding of the instruments behavior in this region, the case of simultaneous thermal and species diffusion in a stationary system is being examined.

John K. Bowman
Massachusetts Institute of Technology
Cambridge, MA
Room 7-040
Telephone (617) 253-7489

WET BULB / DRY BULB THERMOMETER

ANALYSIS SUMMARY

Energy Balance Applied to Wet Bulb Sock

$$\underline{\text{heat flux in}} = \underline{\text{enthalpy flux out}}$$

$$h(T_{db} - T_{wb}) = h_d\,(C_{wb} - c_\infty)\,h_{fg}$$

Forced Convection

Chilton-Colburn j factors $\qquad j_H = j_D$

$$j_H = \frac{h}{\rho\, C_p\, V}\,(Pr)^{2/3}; \qquad j_D = \frac{h_D}{V}\,(Sc)^{2/3}$$

$$\frac{h_D}{h} = \frac{D}{k}\,\left(\frac{Sc}{Pr}\right)^{1/3}$$

Natural Convection

$$Gr^* = \frac{gx^3}{\nu^2}\left\langle\left(\frac{T_{wb} - T_{db}}{T_{db}}\right) - \frac{T_{wb}}{T_{db}}\left(\frac{M_v - M_g}{M_g}\right)\frac{P_{sat,wb}}{P}\right\rangle$$

$$Nu = 0.475\,(Gr^*\,\frac{Pr}{Sc})^{1/4}$$

$$Sh = 0.475\,(Gr^*\,\frac{Sc}{Pr})^{1/4}$$

$$\therefore \frac{h_D}{h} = \frac{D}{k}\,\left(\frac{Sc}{Pr}\right)^{1/2}$$

FIGURE 1.

WET BULB / DRY BULB THERMOMETER

TEST SET-UP

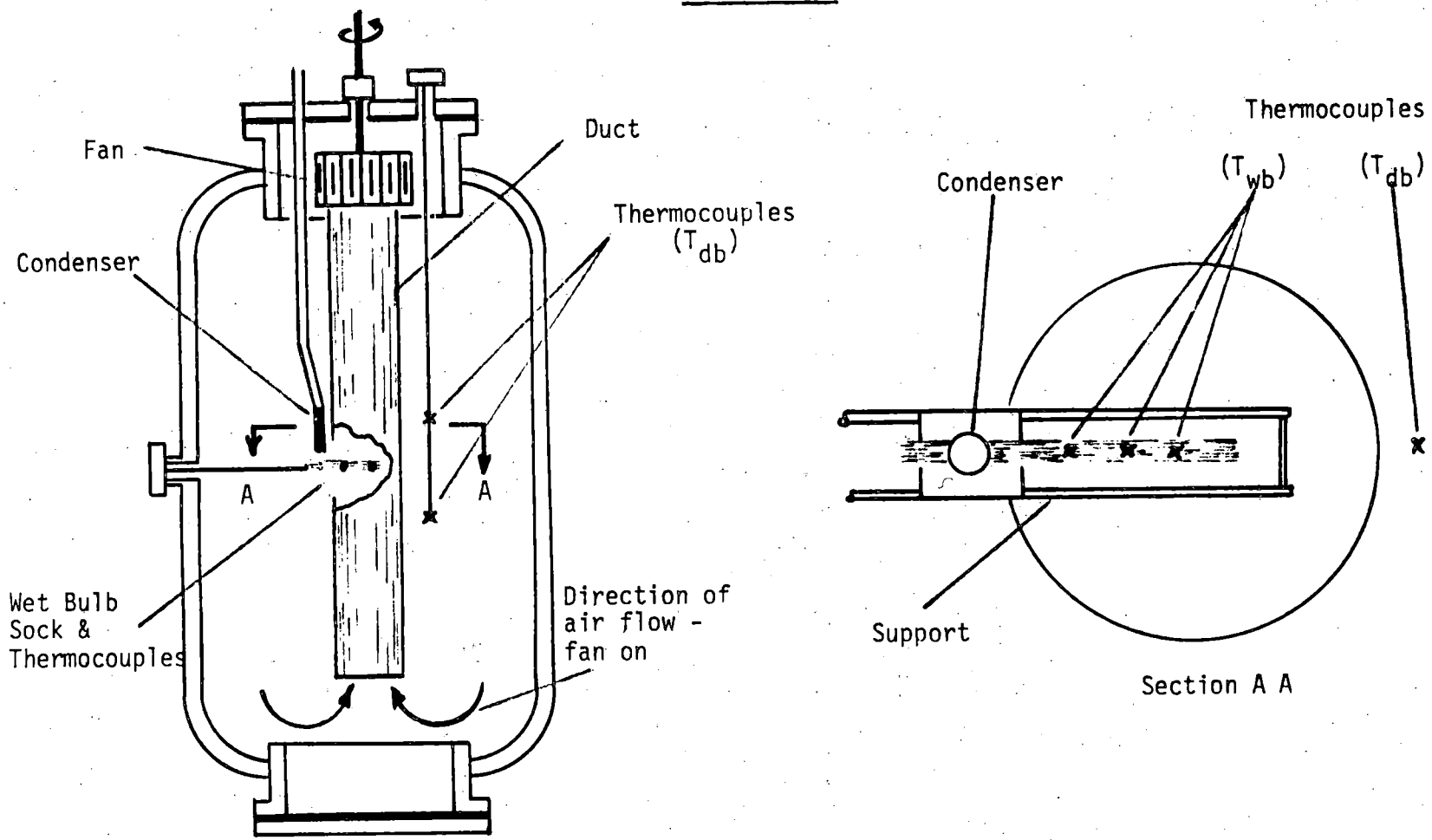

FIGURE 2.

COMPARISON
MEASURED VS CALCULATED*
VAPOR MASS FRACTION

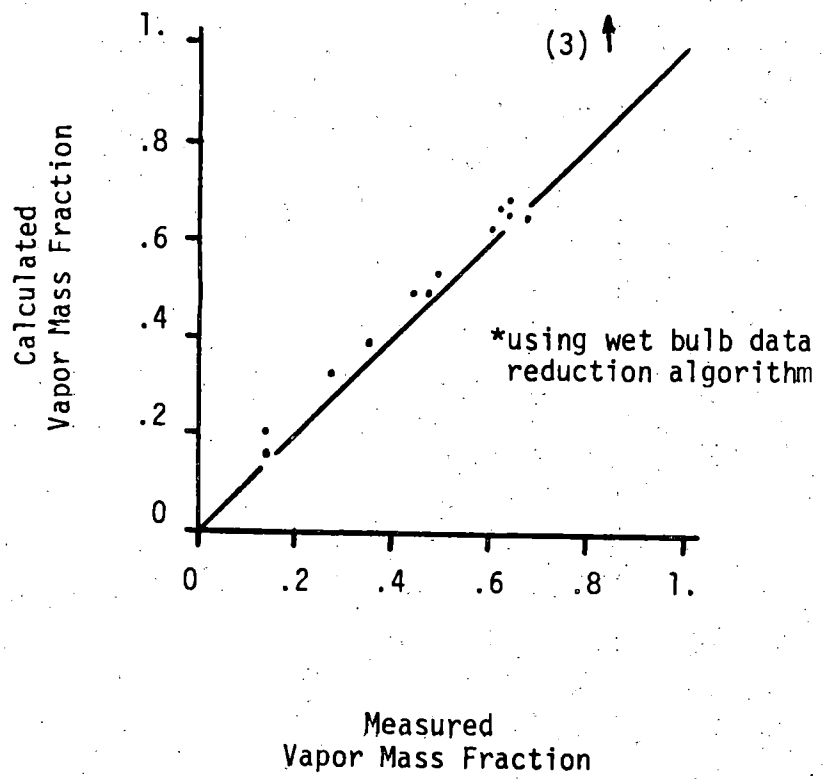

FIGURE 3.

WET BULB TEMPERATURE
VS
VAPOR MASS FRACTION

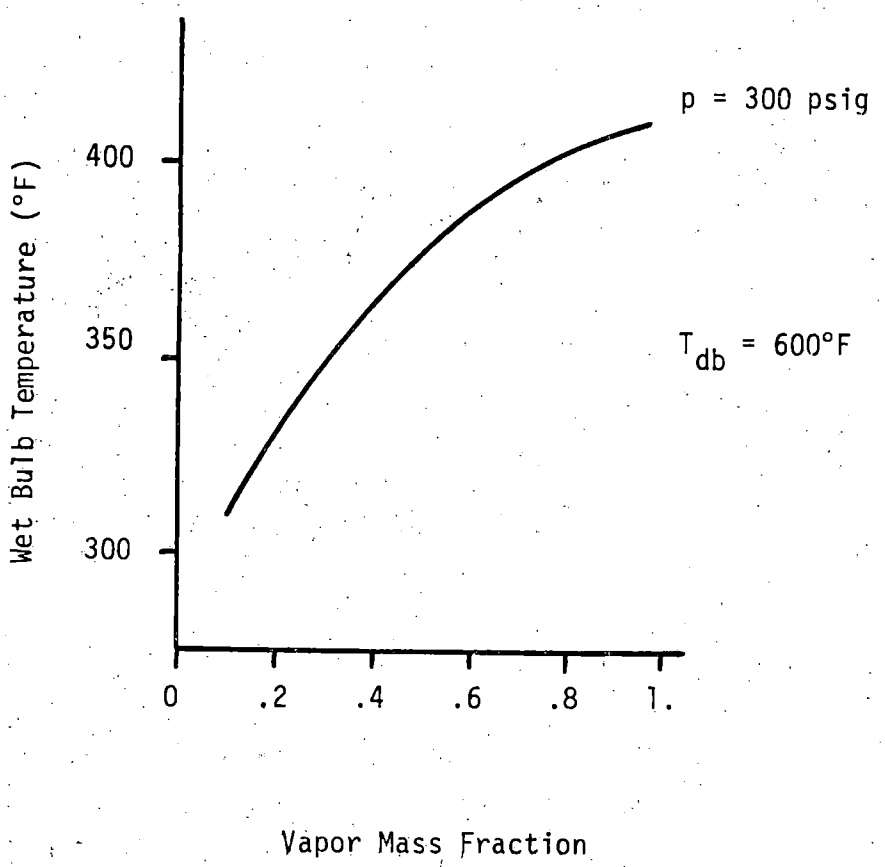

FIGURE 4.

WET BULB TEMPERATURE

VAPOR MASS FRACTION & SYSTEM PRESSURE

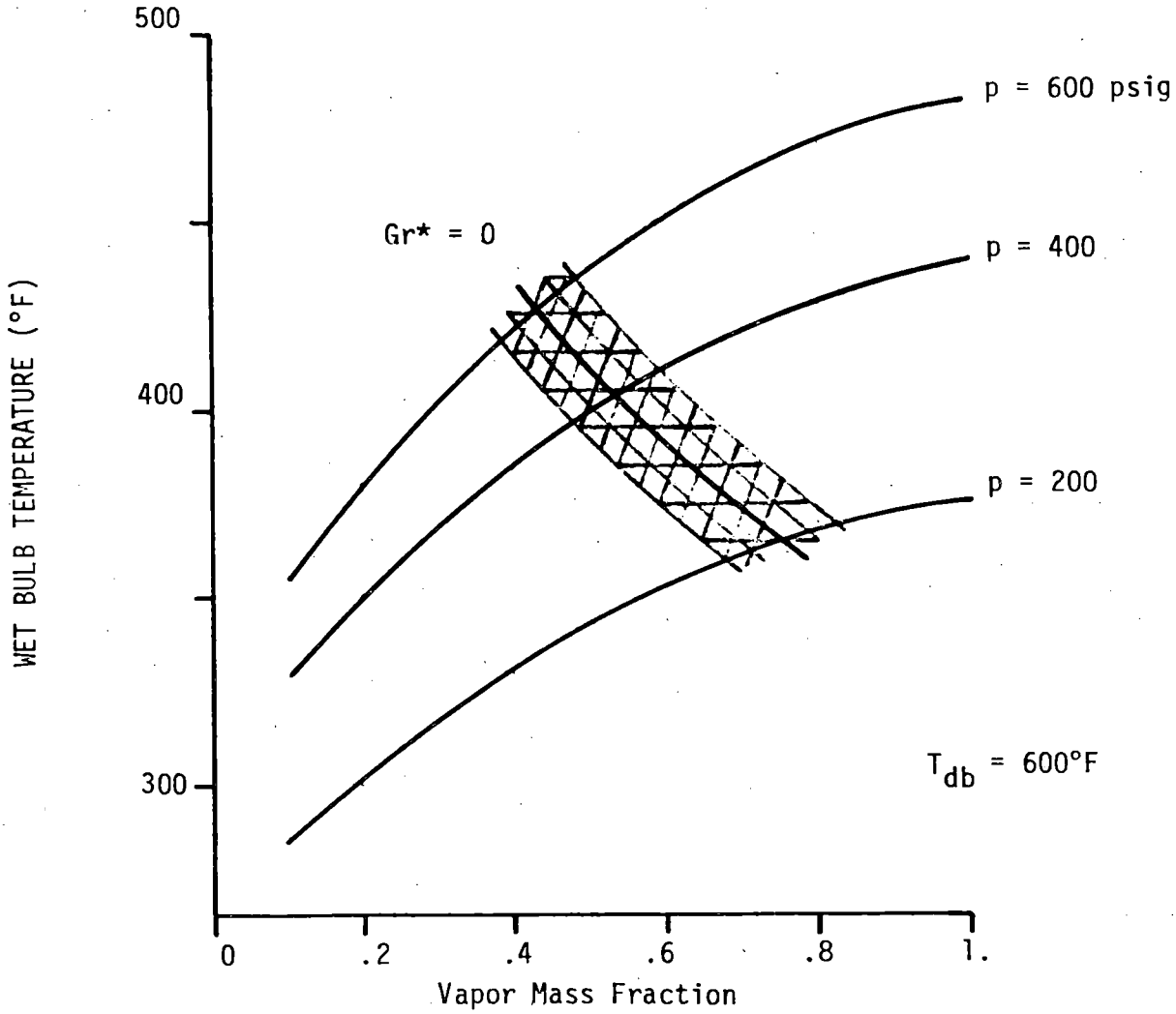

FIGURE 5.

TWO-PHASE FLOW MEASUREMENTS BY PULSED NEUTRON ACTIVATION TECHNIQUES.

COMPONENTS TECHNOLOGY DIVISION

PRESENTED BY PAUL KEHLER
AT THE NINTH WATER REACTOR SAFETY
RESEARCH INFORMATION MEETING.
GAITHERSBURG, MARYLAND, 26-30 OCTOBER 1981.

THE REPORTED WORK IS SPONSORED BY THE USNRC.
PROGRAM MANAGERS: A.L.HON / Y.Y.HSU.

TWO-PHASE FLOW MEASUREMENTS BY PULSED NEUTRON ACTIVATION TECHNIQUES.

Paul Kehler
Components Technology Division

Argonne National Laboratory
9700 South Cass Avenue
Argonne, Illinois 60439

In small-diameter pipes, the mass flow velocity and the density of two-phase flows can be measured accurately, applying basic principles of PNA testing, by using the uncorrected, fundamental velocity and density equations (Reference 1). In large-diameter pipes, conditions for which the basic velocity- and density equations were derived, are not met; i.e., neither the source nor the detectors are narrowly collimated, the neutron fluence across the diameter of the pipe is not constant, and the detector sensitivity across the diameter of the pipe is not constant either. In the past twelve months we have, therefore, concentrated our effort on the development of data reduction techniques for PNA data taken in large-diameter pipes (See Fig. 1). In the course of this work it was recognized that an accurate modeling of the PNA process is necessary for correction of large-diameter data. Once good analytical models of the process are developed, however, PNA techniques can be used for the characterization of regimes of two-phase flow. Work in this area was also done during the past twelve months. Finally, we have advanced the development of a circular densitometer, using common PNA detectors, which can be used for additional, independent density measurements in support of PNA derived density measurements.

Publications issued since last year's Safety Research Information meeting are listed in Figure 2.

In last year's Information meeting, a method was presented for adaptation of the basic PNA velocity equation for measurements in large-diameter pipes. This method consists of replacing the time exponent n in the basic velocity equation by another value. In the basic equation, n=2. For the particular experimental conditions existing at the downcomer of the PKL (at Erlangen, Germany), a time exponent of n=.5 was derived (Ref.2). At the last small-break test series at the PKL, the PNA system was the only one capable of measuring flow velocities over the whole range of velocities of interest. For some of the experimental conditions, velocities were measured by venturi meters or were calculated from thermal balace considerations across the electrically heated core (Ref.3). These two alternate flow measurements compared well with the PNA-derived data (See Fig. 3) and, therefore, increase the confidence that can be placed in the PNA data reduction technique proposed for large-diameter pipes.

At the PKL, only single phase flow had to be measured, and only one time exponent n had to be derived. PNA techniques may also be used at the Upper Plenum Test Facility (UPTF), on very large pipes (ID=75 cm) and over a wide range of densities (Ref.4). The attenuation of neutrons and gamma rays in such large-diameter pipes depends strongly on the density

of the fluid. Thus, for the UPTF, where the density is expected to range between .001 and 1.0 g/cm^3, different time exponents n have to be derived for each density (See Fig. 4). Unfortunately, PNA density readings have themselves to be corrected for the reasons mentioned above. The correction to be applied to 20 cm diameter pipes is shown in Ref.5, and the correction to be applied to 75 cm diameter pipes is shown in Fig. 5 (from Ref.4).

Both the Figures 4 and 5 were derived analytically and can be included into the computer software used for on-line, automatic data evaluation. The sequence of steps to be taken in an automatic data reduction program is shown in Fig.6. Using this procedure, the expected error of the mass-flow reading at the UPTF is shown in Fig.7. Most of this error is due to the uncertainty of the density reading, particularly at high densities (See Figs. 5 and 8). Thus, the overall accuracy of PNA massflow readings could be significantly improved if a better density reading were available, particularly at high densiies.

Gamma ray transmission techniques are known to be able to measure density accurately in high density regions, which happens to be the one where PNA derived densities are least accurate (See Fig.7). The largest uncertainty in gamma ray transmission density readings is caused by the need to know the flow regime, for proper modeling and interpretation of common three-beam densitometers (Ref.6). There are reasons to believe that a ring-type densitometer, consisting of a ring detector and a ring source that completely surround the pipe, will furnish gamma ray transmission density readings that are independent of the various flow regimes, and, therefore, will not need any analytical flow regime modeling for data interpretaion. Such ring type densitometers can be built around ring type detectors already used for PNA measurements. A mockup of such a ring type densitometer, utilizing the detectors previously used at the PKL, is shown in Figure 9.

Fig. 10 shows the dimensions of this mockup, and Fig. 11 is a summary of preliminary density measurements. The density readings of Fig. 11 were taken on lucite rods of various diameters, positioned at the center of the pipe or at its wall, as implied in Figure 10. Presently used single- or multi-beam densitometers could not at all be used for such measurements. Still, the difference of density readings for center- and off-center positions is considered to be too large. This difference will most likely be reduced when line sources will be used instead of the eight individual sources presently arranged in 'ring' geometry around the pipe, and when the spacing between the sources and the pipe will be increased to reduce the contribution of the scattered components presently interfering with the transmission measurements. Improvement of the design of ring densitometers is one of our present study objectives.

The need to model velocity distributions and flow regimes for the derivation of correction curves such as shown in Figures 4 and 5, has led to the recognition that PNA experimental techniques, when supported by proper analytical models, can be used for characterization of two-phase flow regimes and for the mesurement of flow velocity distributions in large-diameter pipes. Figure 12, for example, shows data taken by two detectors taken on opposite sides of a 20 cm pipe, with both detectors located downstream of a 90 degree turn of the pipe (on the FAST loop, Reference 5). If any one of PNA velocity equations is applied separately to these two distributions, the difference of the velocity reading will be about 5%. Obviously, the error is reduced significantly when these two distributions are lumped into only one, and when only the sum of all PNA data is used for velocity calculations. This is one of the reasons why ring detectors should be used for PNA tests.

In two-phase flow, the shape of the PNA counts distribution can be used for identifiation of flow regimes. An attempt to do this was undertaken by using test data taken at the air-water loop located at the Semiscale facility at the INEL (Reference 7). Using PNA data taken on a 7.5 cm horizontal pipe, it was shown that the variance of the counts vs. time distribution is significantly larger for slug flow than for any other flow regime. This difference holds for the whole density range (Fig. 13) and the whole velocity range (Fig. 14) of this particular test. Since stratified flow can also be recognized by PNA techniques (using a pair of detectors on opposide sides of the pipe), a flow regime chart similar to the one proposed by Mandhane and Aziz (Ref.8) was designed from the very limited number of data available from this test. This flow regime map is shown in Figure 15 (from Reference 9).

It is planned to eventually include a flow regime recognition routine into the automatic data reduction software presntly used (See Fig.6) to derive the proper timeexponents n for use in the PNA velocity equation.

References:

1.) Paul Kehler: Accuracy of Two-Phase Flow Measurements by Pulsed-Neutron Activation Techniques, in Multiphase Transport, Fundamentals, Reactor Safety, Applications, Vol. 5, p. 2483, Hemisphere Publishing Corp., Washington, DC, May 1980.

2.) Paul Kehler: Measurement of Slow Flow Velocities by the Pulsed Neutron Activation Technique, Proc. of the USNRC Review Group Conference on Advanced Instrumentation for Reactor Safety Research, NUREG/CP-0015, July 1980.

3.) H. Gaul: Measurement of Massflow Velocities in the Downcomer of the PKL Test Facility, using PNA (Pulsed Neutron Activation) Techniques (in German), Kraftwerk Union Report R 513/2/81, January 1981.

4.) Paul Kehler: Feasibility of Using PNA Techniques for In-Situ Calibration of UPTF Two-Phase Flow Instrumentaion, NUREG/CR-1971, ANL-CT-81-18, August 1981.

5.) T.H. Chen, Paul Kehler, N.N. Kondic, C.W. Solbrig: Two-Phase Velocity and Density in Finite Length Pipes, by Intrusive and Non-Intrusive Instrumentation, Paper presented at the 27th ISA International Instrumentation Symposium, Indianapolis, IN., April 1981.

6.) G.D. Lassahn: LOFT Experimental Measurements Uncertainties Analyses, Vol. 16, LOFT Three-Beam Densitometer System, TREE-NUREG-1089, Feb. 1987.

7.) Paul Kehler: Two-Phase Flow Mesurement by Pulsed Neutron Activation Techniques, ANL-NUREG-CT-78-17, January 1978.

8.) J.D. Mandhane et al.: A Flow Pattern Map for Gas-Liquid Flow in Horizontal Pipes, International Journal of Multiphase Flow 1, 537 (1974).

9.) Paul Kehler: Use of PNA Techniques for Tw0-Phase Flow Characterization. CSNI Report No. 61, Proc. OECD (NEA) CSNI Third Specialists Meeting on Transient Two-Phase Flow, Pasadena, CA., March 1981.

FIG. 1:

AREAS OF WORK IN THE PAST YEAR:

* DEVELOPMENT OF PNA DATA REDUCTION TECHNIQUES FOR LARGE-DIAMETER PIPES.

* DEVELOPMENT OF PNA TECHNIQUES FOR TWO-PHASE FLOW CHARACTERIZATION.

* DEVELOPMENT OF CIRCULAR DENSITOMETER.

FIG. 2:

PUBLICATIONS ISSUED AFTER 1980 RSR MEETING:

1.) Paul Kehler: Use of PNA Techniques for Two-Phase Flow Characterization. Proc. OECD (NEA) CSNI Third Specialists Meeting on Transient Two-Phase Flow, Pasadena,CA.,March 1981. CSNI Report No. 61.

2.) T.H. Chen, Paul Kehler, N.N. Kondic, C.W. Solbrig: Two-Phase Velocity and Density in Finite Length Pipes, by Intrusive and Non-Intrusive Instrumentation, Paper presented at the 27th ISA International Instrumentation Symposium, Indianapolis, IN., April 1981.

3.) Paul Kehler: Feasibility of using PNA Techniques for In-Situ Calibration of UPTF Two-Phase Flow Instrumentation, NUREG/CR-1971, ANL-CT-81-18, August 1981.

FIG. 3:
COMPARISON OF PNA TEST DATA
WITH OTHER READINGS AT THE PKL.

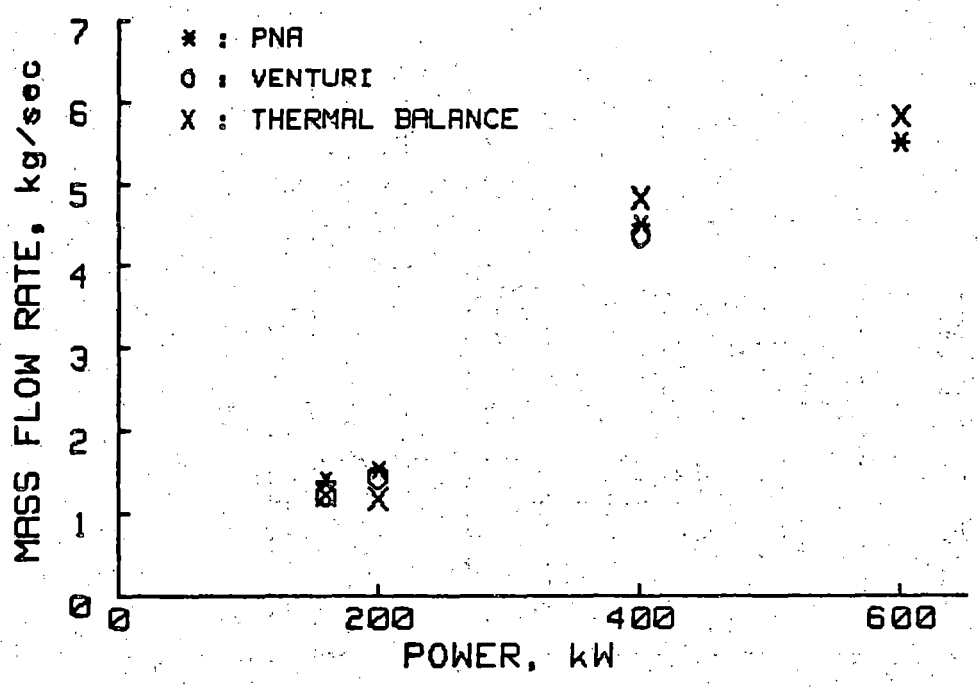

FIG. 4:
TIME EXPONENT N
OPTIMIZED FOR THE UPTF.

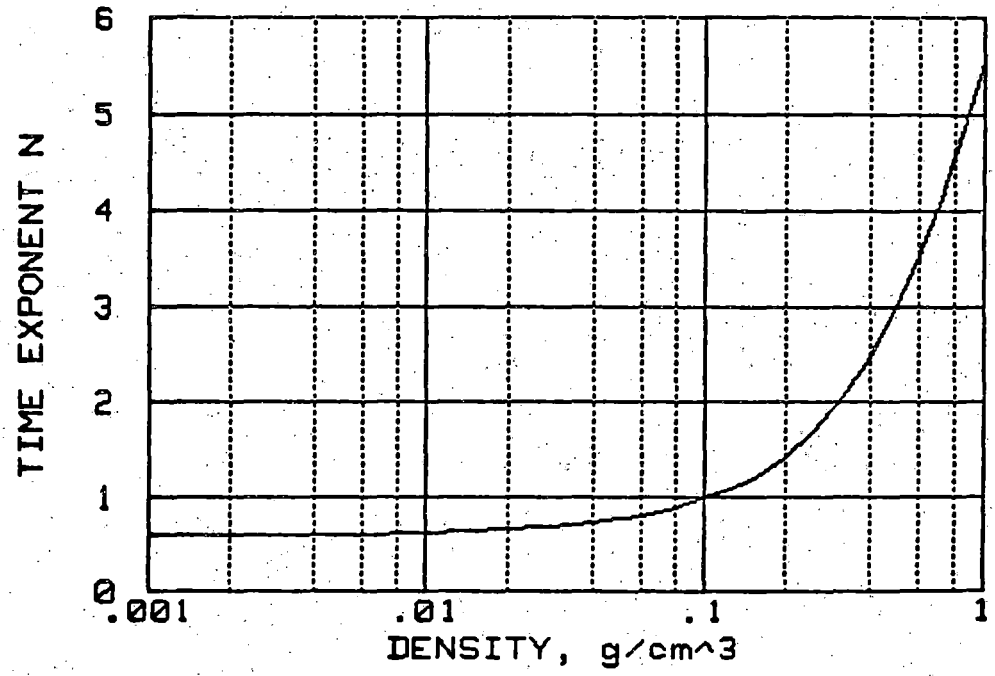

PK-29307.01

FIG. 5:
PNA DENSITY MEASUREMENT
AT THE UPTF

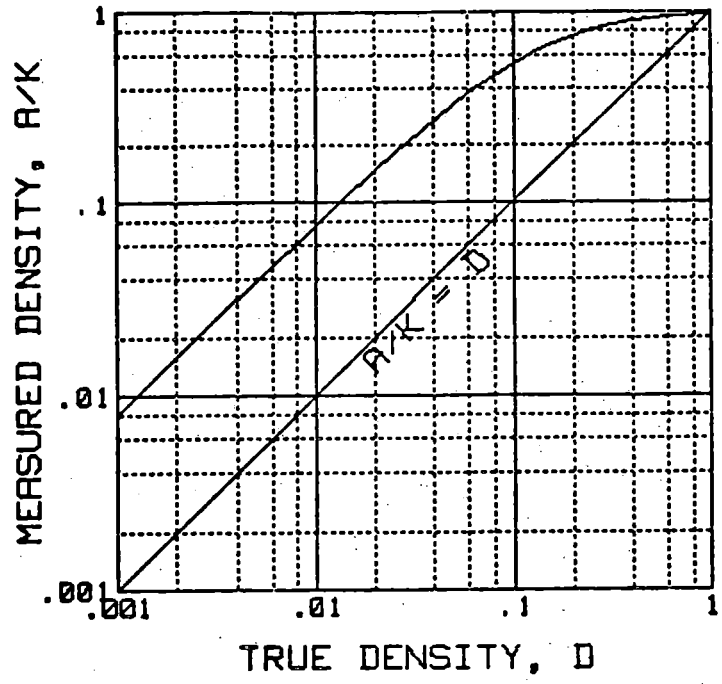

PK-25302.02

FIG. 6:

DATA EVALUATION TECHNIQUE FOR THE UPTF

* EVALUATE DENSITY
* SELECT TIME-EXPONENT N
* EVALUATE VELOCITY
* CALCULATE MASSFLOW

FIG. 7:
ACCURACY OF MASSFLOW READING
AT THE UPTF.

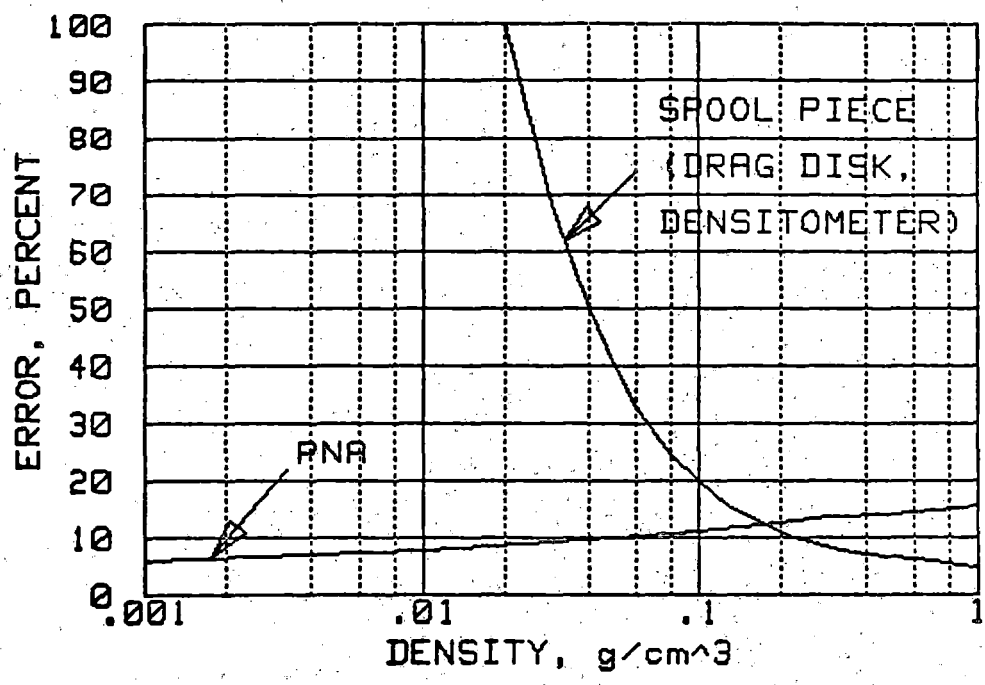

PK-28310.01

FIG. 8:
ACCURACY OF DENSITY READING
AT THE UPTF.

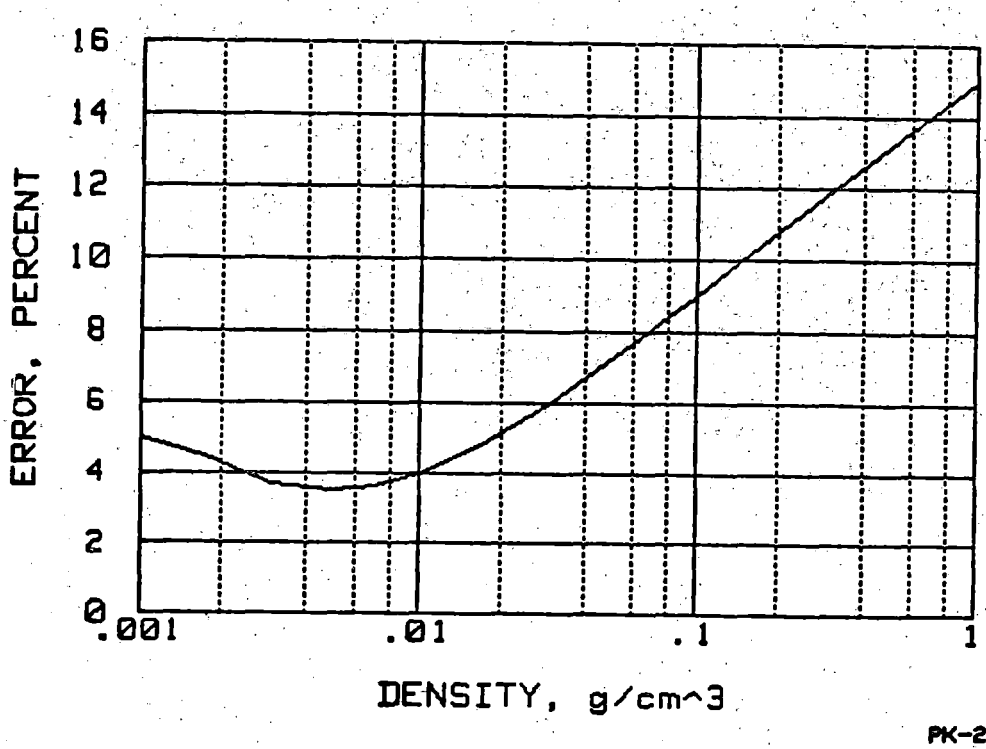

PK-28311.01

FIG. 9:

MOCKUP, CIRCULAR DENSITOMETER.

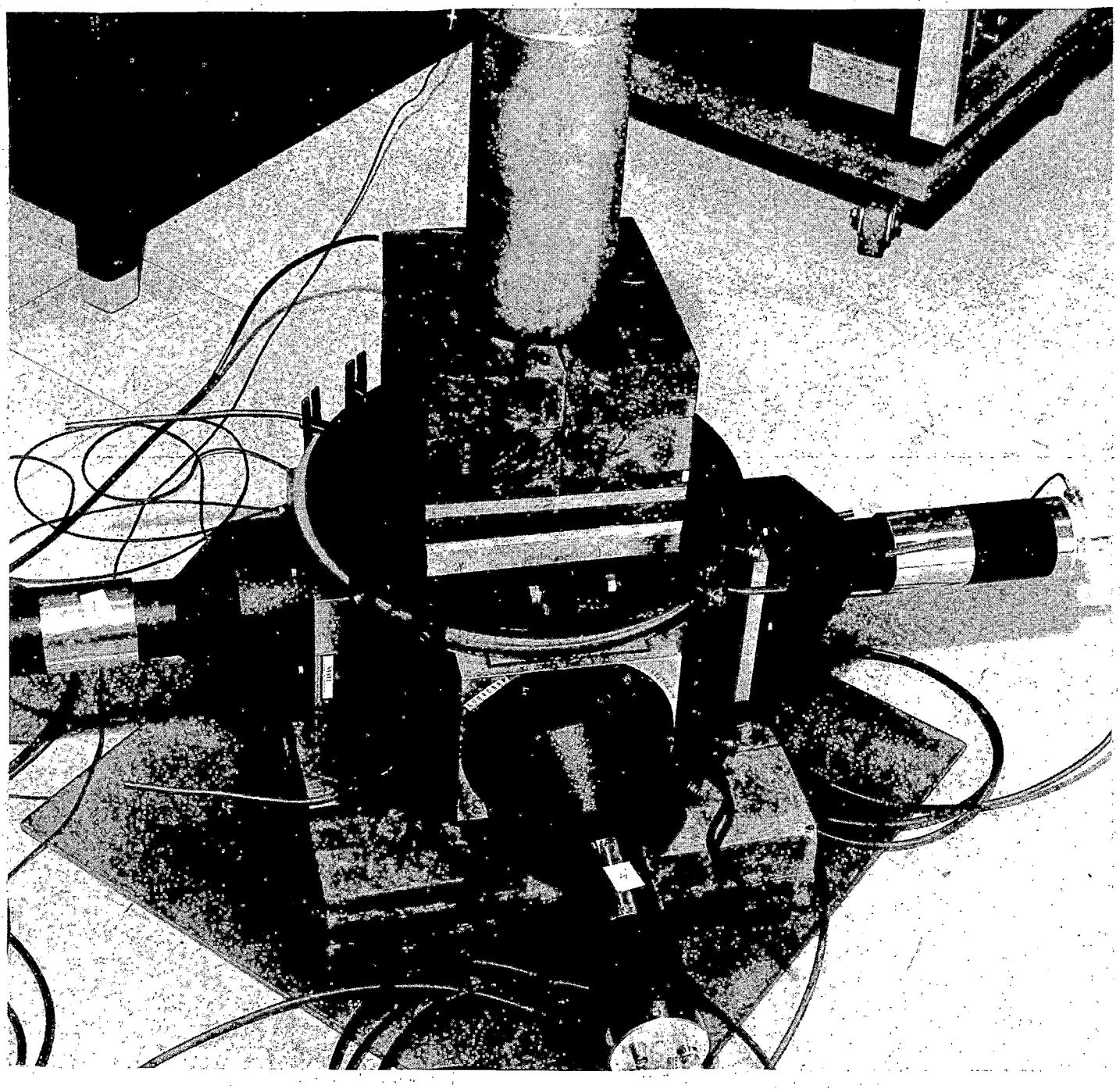

FIG. 10:
CIRCULAR DENSITOMETER
DIMENSIONS

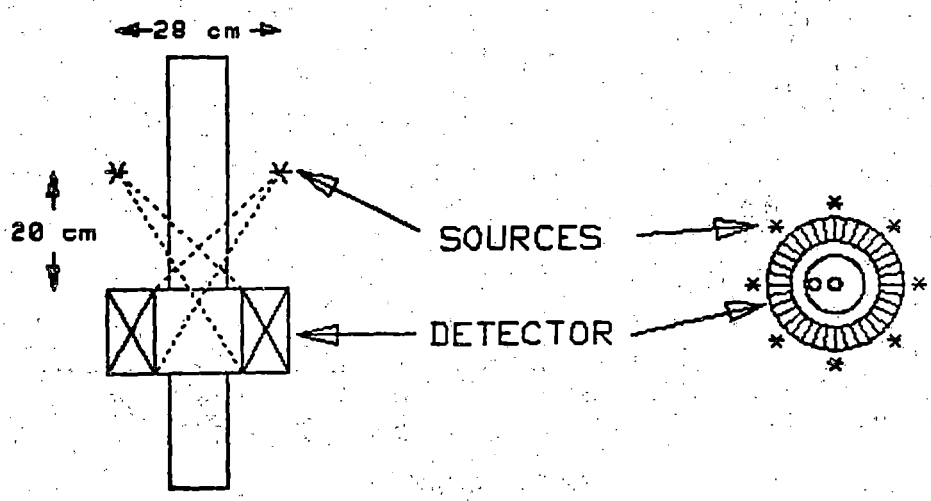

FIG. 11:
CIRCULAR DENSITOMETER
PRELIMINARY TEST DATA

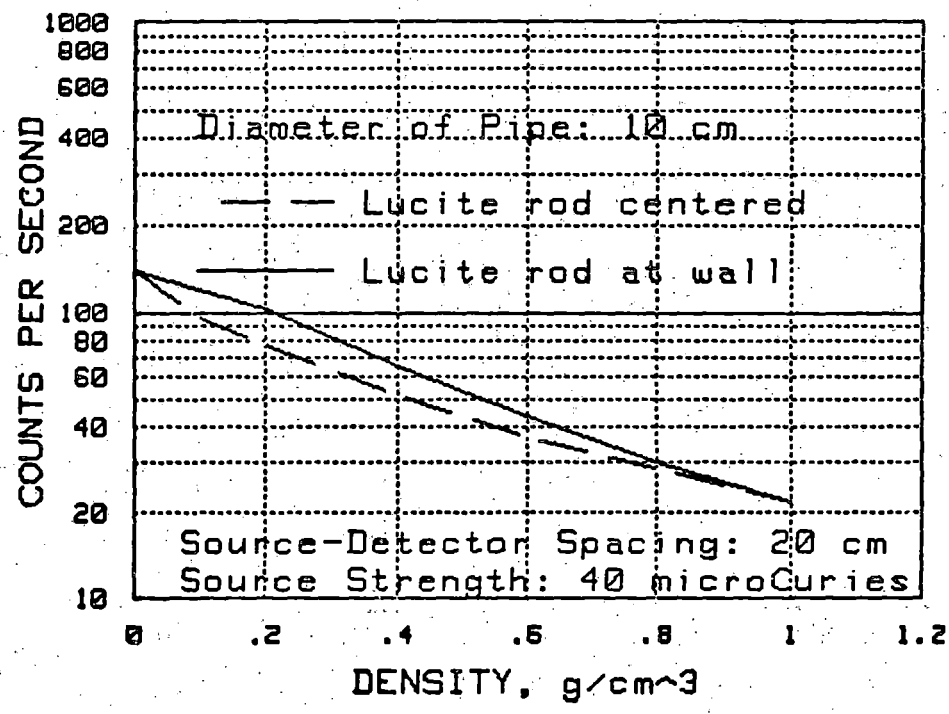

PK-22103.03

FIG. 12:
READINGS BY TWO OPPOSITE DETECTORS DOWNSTREAM OF A U-BEND.

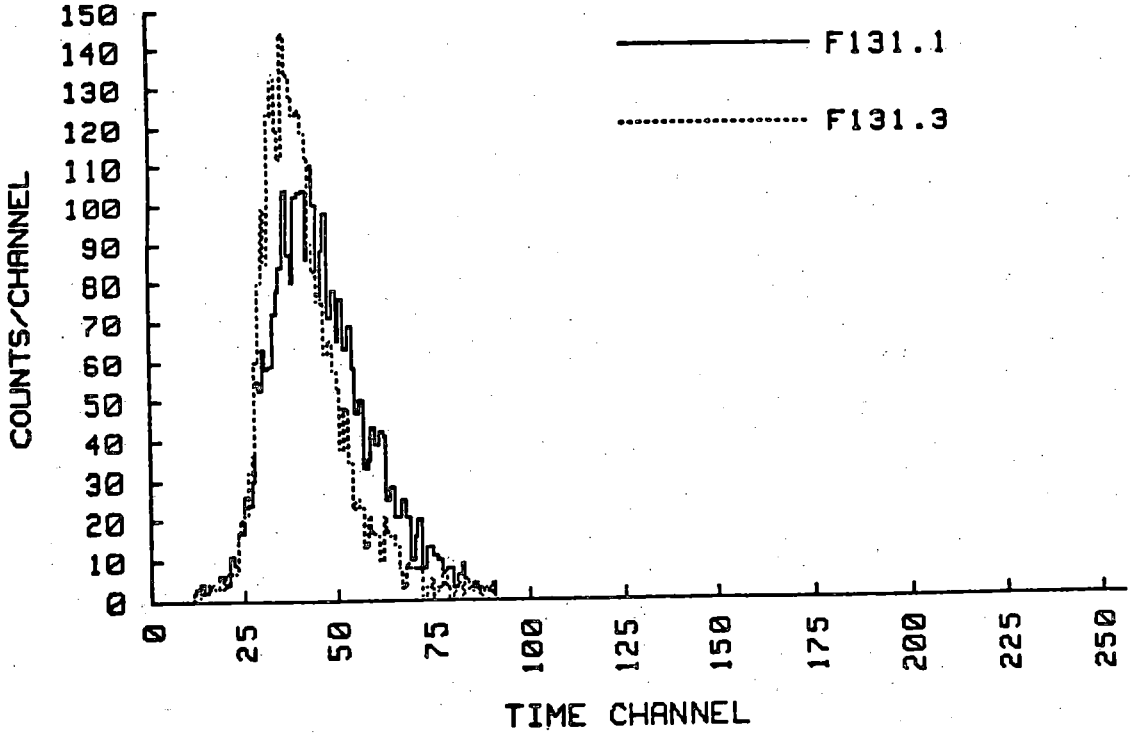

FIG. 13:
VARIANCE-DENSITY PLOT,
7.5 cm HORIZONTAL PIPE.

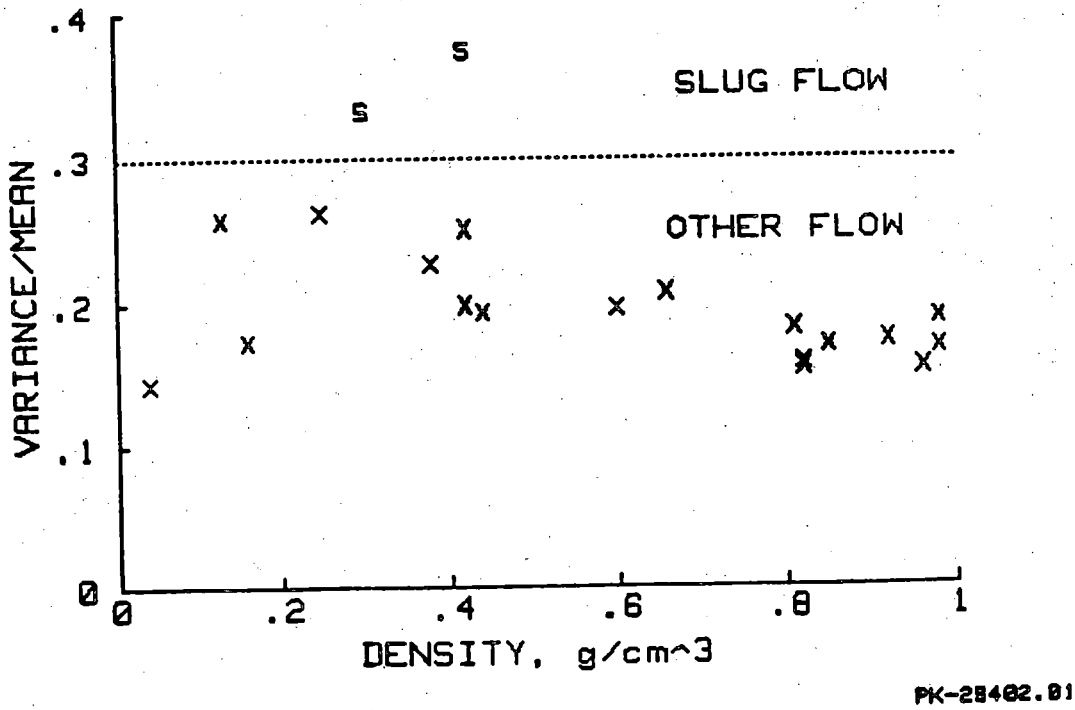

FIG. 14:
VARIANCE-VELOCITY PLOT,
7.5 cm HORIZONTAL PIPE.

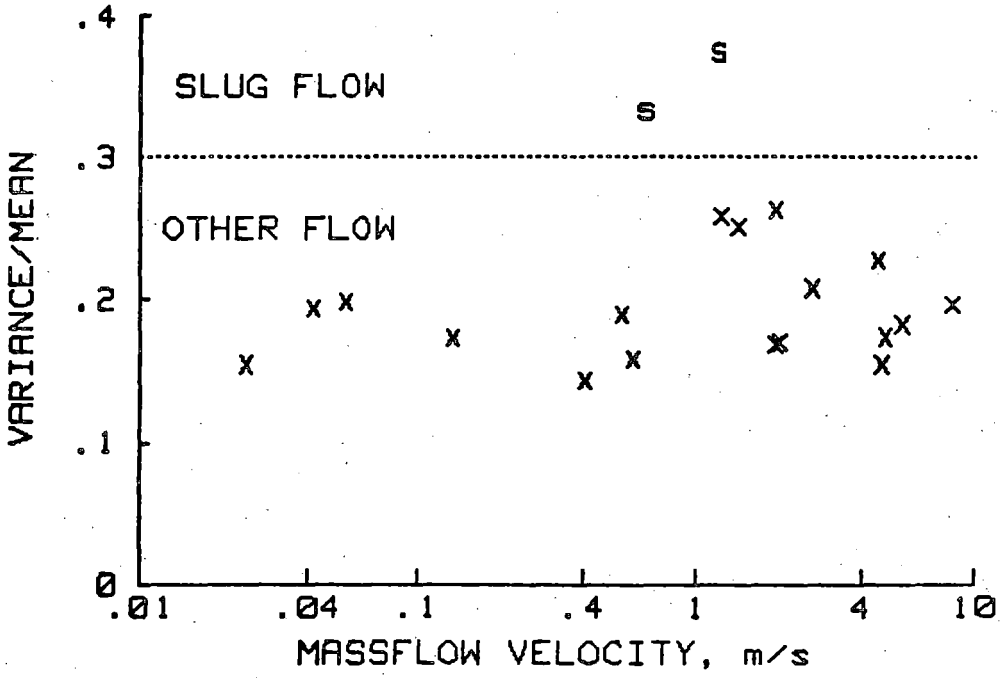

PK-28403.01

FIG. 15:
FLOW REGIME MAP
7.5 cm HORIZONTAL PIPE

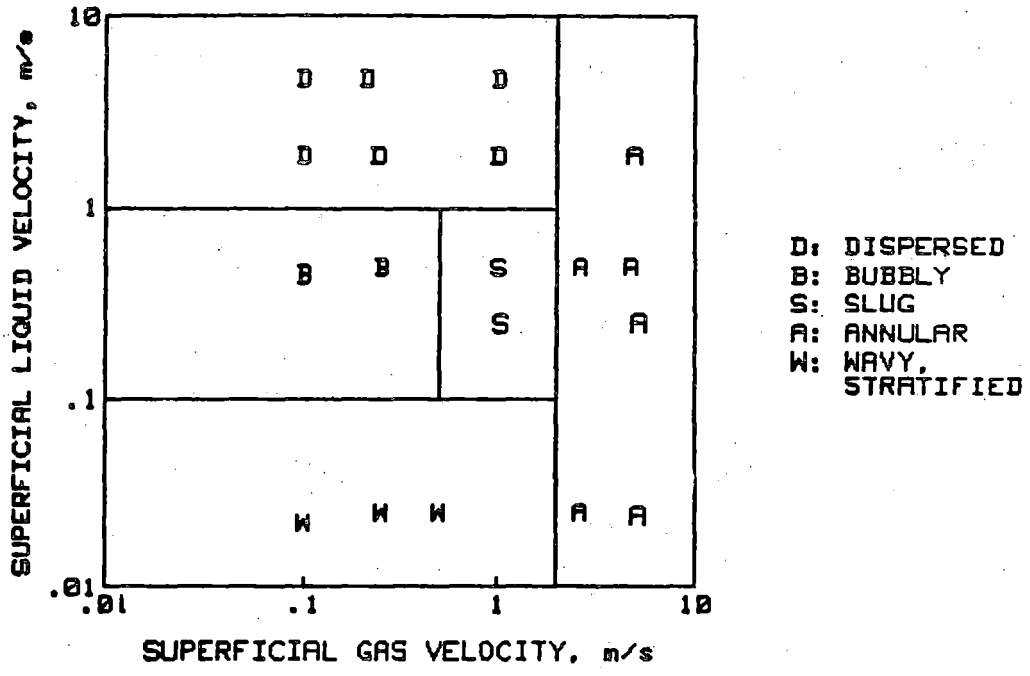

PK-28401.01

DEVELOPMENT AND EVALUATION OF LIQUID LEVEL SENSORS FOR USE IN PWRs

J. E. HARDY

G. N. MILLER

S. C. ROGERS

NINTH WATER REACTOR SAFETY RESEARCH
INFORMATION MEETING
OCTOBER 27, 1981
GAITHERSBURG, MARYLAND

DEVELOPMENT AND EVALUATION OF LIQUID LEVEL SENSORS FOR USE IN PWRs*

J. E. Hardy
G. N. Miller
S. C. Rogers

Oak Ridge National Laboratory
Oak Ridge, TN 37830

Presented at the Ninth Water Reactor Safety Research
Information Meeting, October 27, 1981
Gaithersburg, Maryland

An inadequate core cooling condition existed and was not detected in the reactor at Three Mile Island for a long period of time. The extensive damage that resulted highlighted the need for more reliable means for detecting inadequate core cooling (ICC) conditions in PWRs. Thermal, acoustic, and differential pressure techniques are being evaluated and/or developed at Oak Ridge National Laboratory. The goals are to evaluate the design of coolant level sensors and to determine whether there are conditions under which ambigous indications of coolant level exist.

Thermal sensors have been studied in a test facility that operated at PWR conditions for numerous film boiling experiments as well as uncovery and reflood tests. Data showed that the heated thermocouples (HTCs) remained operable after 40 hours at loss-of-coolant conditions and indicated poor cooling prior to rod bundle DNB at low outlet velocities. The HTCs, however, failed to show ICC at some higher outlet velocities and bundle powers. Splash shields designed to protect HTC from entrained droplets and spurious readings were tested under conditions that simulate the thermal-hydraulic conditions of a postulated PWR LOCA. Results indicated a surprising amount of cooling of a shielded HTC under high void conditions. The collapsed liquid level in a splash shield, or standpipe, was compared to surrounding two-phase media. Good agreement was noted between the collapsed level and flowing voids.

A sensor has been developed to measure simultaneously the level, temperature profile, and density profile of the fluid in which it is immersed. The sensor is a thin, rectangular stainless steel waveguide housed in a perforated tube. The waveguide is coupled to a section of magnetostrictive material which is excited by a pair of magnetic-coil transducers. These transducers are multiplexed in an alternating sequence to excite the sensor with both torsional ultrasonic waves and extensional ultrasonic waves. The measured torsional transit time is a function of density, level, and temperature of the fluid surrounding the waveguide. The measured extensional transit time is a function of the temperature of the waveguide only. Developments in acoustic wave dampener and pressure seal designs enhance the compatibility of the probe with high-temperature, high-pressure water-steam environments found in PWRs.

---

*Research sponsored by Division of Reactor Safety Research, U.S. Nuclear Regulatory Commission Under Interagency Agreements DOE 40-551-72 and 40-552-75 with the U.S. Department of Energy under contract W-7405-eng-26 with the Union Carbide Corporation.

Utilization of a microcomputer to automate data sampling and processing has resulted in improved resolution of the sensor.

The ultrasonic level sensor is one of the most promising long-term solutions for monitoring core cooling adequacy because it can display temperature and density profiles in addition to the collapsed liquid level and froth level. As a result of its profiling nature, the sensor can also detect voids which may exist along its length such as those found in the Semiscale S-UT-3 test.

Differential pressure sensors were monitored in several uncovery and reflood tests. Comparison of the dP-cells measurements were made with an HTC and the froth level in the rod bundle of the test facility. The HTC and dP sensors gave comparable results as to core cooling detection. In low flow conditions, the dP cell level measurement was conservative when compared to the froth height (coolant level) in the vessel. At higher flow rates, however, the dP level indication was higher than the two-phase froth level as determined by rod thermocouples. Thus, a nonconservative prediction of ICC was given by the differential pressure sensors.

The performance of the Westinghouse Reactor Vessel Level Instrumentation System (RVLIS) in the S-UT-3 test [a 2 1/2% communicative break in the cold leg of Semiscale] has been analyzed. The Westinghouse RVLIS, which employs dP cells, gave similar indications to Semiscale dP instrumentation measuring the same phenomena over equal spans. The Westinghouse measurement is conservative when compared to two-phase froth (coolant) level. These dP measurements result in nonconservative estimates of liquid level, however, when the measurement system spans the upper core support plate. Level measurement errors of up to 150 cm (60 in.) were observed during S-UT-3. Westinghouse claims these discrepancies are due to differences between Semiscale and Westinghouse PWR designs.

PUBLICATIONS

1. R. L. Anderson, G. N. Miller, S. C. Rogers, et al., "High Temperature, High Pressure Water Level Sensor," IEEE Ultrasonics Symposium Proc., Vol. 2, Cat. #80CH1602-2, pp. 877-881 (October 1980).
2. K. G. Turnage, et al., Preliminary Report on Heated Thermocouple Response During Thermal Hydraulic Test Facility Test 3.07.9 (December 1980).
3. K. G. Turnage, et al., Advanced Two-Phase Flow Instrumentation Program Quarterly Progress Report for October-December 1980, NUREG/CR-2007 (ORNL/NUREG/TM-443) (May 1981).
4. J. E. Hardy, et al., Advanced Two-Phase Flow Instrumentation Program Quarterly Progress Report for January-March 1981, NUREG/CR-2204 (ORNL/TM-7877) (July 1981).
5. J. E. Hardy, et al., Advanced Two-Phase Flow Instrumentation Program Quarterly Progress Report for April-June 1981, NUREG/CR-2204, Vol. 2 (ORNL/TM-8010) (October 1981).
6. G. N. Miller, et al., "Analysis of the Performance of the Westinghouse Reactor Vessel Level Instrumentation System (RVLIS) in the S-UT-3 Test at Semiscale," October 1981.
7. S. C. Rogers and G. N. Miller, "Ultrasonic Level, Temperature, and Density Sensor," IEEE Nuclear Science Symposium Proc. (October 1981).

PRESENTATION OUTLINE

- OVERVIEW ORNL LIQUID LEVEL DETECTOR PROGRAM
- DEVELOPMENT/EVALUATION OF THERMAL SENSORS
- EVALUATION OF DIFFERENTIAL PRESSURE TECHNIQUES
- DEVELOPMENT/EVALUATION OF ULTRASONIC SENSORS
- SUMMARY

ORNL PWR LIQUID LEVEL INSTRUMENT DEVELOPMENT AND EVALUATION

OBJECTIVES:

- IDENTIFY PRACTICAL TECHNIQUES THAT CONFORM TO NRC REQUIREMENTS FOR MAKING IN-VESSEL LIQUID LEVEL MEASUREMENTS
  [LLTF REPORT (NUREG-0578), TMI ACTION PLAN REQUIREMENTS (NUREG-0737)]
- PERFORM AND ANALYZE PROOF-OF-PRINCIPLE TESTING OF SENSORS UNDER "LOCA" THERMAL HYDRAULIC CONDITIONS
- IMPROVE SENSOR DESIGN WHERE APPROPRIATE
- COMMUNICATE WITH INDUSTRY AND NRC/RSR
- IDENTIFY POTENTIAL PROBLEM AREAS

PWR LIQUID LEVEL INSTRUTMENTATION: DETECT THE APPROACH TO OR EXTENT OF INADEQUATE CORE COOLING

REQUIREMENTS:

- UNAMBIGUOUS – LITTLE OPERATOR INTERPRETATION REQUIRED NO SPURIOUS INDICATIONS
- ADVANCE WARNING OF ICC
- RELIABLE – LONG LIFE, SURVIVE LOCA
- COVER VOIDING IN UPPER HEAD TO BOTTOM OF THE CORE
- TIME RESPONSE ~ SECONDS
- USEFUL RESPONSE UNDER STAGNANT BOILOFF OR HIGH VOID FRACTION FLOW

THREE TYPES OF LIQUID LEVEL SENSORS HAVE BEEN EVALUATED AT ORNL

- THERMAL (HEATED TCs OR RTDs)
- ACOUSTIC (WAVEGUIDE/TRANSIT TIME)
- DIFFERENTIAL PRESSURE

ORNL ATPI – LIQUID LEVEL SENSORS ACCOMPLISHMENTS

THERMAL SENSORS

- STUDIED OPERATION OF HJTCs IN THERMAL HYDRAULIC TEST FACILITY (THTF) DURING NUMEROUS FILM BOILING EXPERIMENTS (USED A CE PROBE)
- EVALUATED VARIOUS SPLASH SHIELDS IN NATURAL AND FORCED CONVECTION
- BUILT INEL HTC ELECTRONICS AND COMPLETED SCOPING TESTS
- INITIAL EVALUATION OF A STANDPIPE'S RELATIONSHIP BETWEEN ITS COLLAPSED LIQUID LEVEL TO FLOWING VOIDS

ORNL ATPI ACCOMPLISHMENTS (CON'T)

ULTRASONIC SENSORS

- VERIFIED PRINCIPLE OF OPERATION OF RIBBON-TYPE TORSIONAL-EXTENSIONAL PROBE AT HIGH TEMPERATURES AND PRESSURES
- IMPROVED ACCURACY AND SURVIVABILITY
- DEVELOPED PRESSURE SEAL DESIGNS FOR USE IN A PWR
- DEVELOPED PWR COMPATIBLE BACK REFLECTION DAMPENER
- MICRO PROCESSOR INTERFACED TO MEASUREMENT SYSTEM FOR FASTER TESTING AND COMPENSATION

ORNL ATPI ACCOMPLISHMENTS (CON'T)

DIFFERENTIAL PRESSURE

- PERFORMED SCOPING TESTS OF ΔP RESPONSE TO REPEATED BOILOFF AND REFLOOD IN THTF
- EVALUATED WESTINGHOUSE ΔP - LEVEL SYSTEM FOR TESTS AT SEMISCALE

TESTING OF LIQUID LEVEL DEVICES CAN BE ACCOMPLISHED AT ORNL AT A VARIETY OF FACILITES AND FLOW CONDITIONS

FACILITIES

- PRESSURIZER
- HIGH FLOW-HIGH VOID S/W TEST STAND
- S/W FLOW VISUALIZATION LOOP
- A/W TEST FACILITY
- 3-MODULE A/W INSTRUMENT DEVELOPMENT LOOP (IDL)
- 1-MODULE S/W IDL
- LIQUID LEVEL TEST STAND

TEST VARIABLES

NATURAL CONVECTION TESTS

- MEDIUM
- PRESSURE/TEMPERATURE
- ORIENTATION
- VARIABLE DENSITY FLUIDS
- PROBE DESIGN

FORCED CONVECTION TESTS

- VOID FRACTION
- VELOCITY
- PRESSURE/TEMPERATURE
- GEOMETRY

THERMAL SENSORS: ADVANTAGES

- CAN MEASURE COOLING CONDITIONS DIRECTLY
- RELATIVELY SMALL
- USE REACTOR-COMPATIBLE MATERIALS
- SIMPLE
- INEXPENSIVE

SOME DISADVANTAGES OF THERMAL TYPE SENSORS ARE

- DISCRETE INDICATION – ARRAYS NEEDED
- CAN BE AFFECTED BY ENTRAINED LIQUID ABOVE LIQUID-VAPOR INTERFACE
- MAY NOT BE USEFUL DURING NORMAL CONDITIONS (DIFFERENTIAL TC)
- HEATER CAN FAIL

A STANDPIPE ARRANGEMENT MAY PROTECT SENSOR FROM SPLASHING AND ALLOW ADEQUATE TIME RESPONSE

CHARACTERISTICS REQUIRE INVESTIGATION

- DOES IT INDICATE COLLAPSED LIQUID LEVEL?
- WHAT ARE EFFECTS OF VELOCITY?
- HOW LARGE SHOULD DRAIN AND VENT HOLES BE?

RESPONSE OF SHELDED HJTC WAS STUDIES IN THE AIR/WATER INSTRUMENT DEVELOPMENT LOOP (IDL)

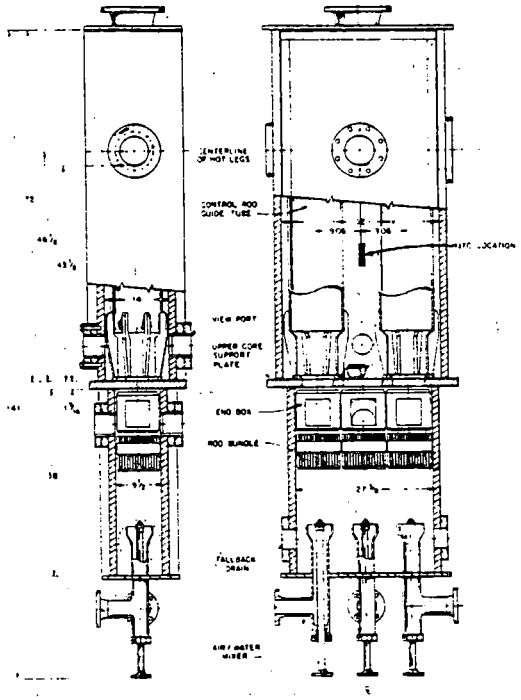

WITH MODERATE AIR FLOW RATES, MINIMAL AMOUNTS OF LIQUID WERE REQUIRED TO COOL SHIELDED HTC IN AIR-WATER IDL

VOID FRACTION	HTC OUTPUT (mV)
0.998	9
0.979	2.5
0.967	1.0

COOLING EFFECT OF A MIST FLOW ON A SHELDED HJTC WAS MONITORED

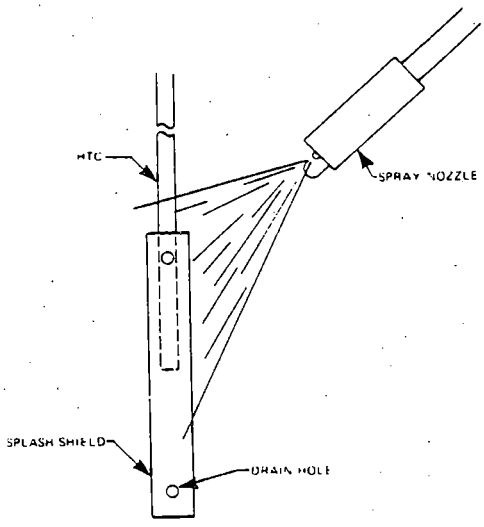

MIST FLOW CAUSED DETECTABLE COOLING OF SHIELDED HJTC

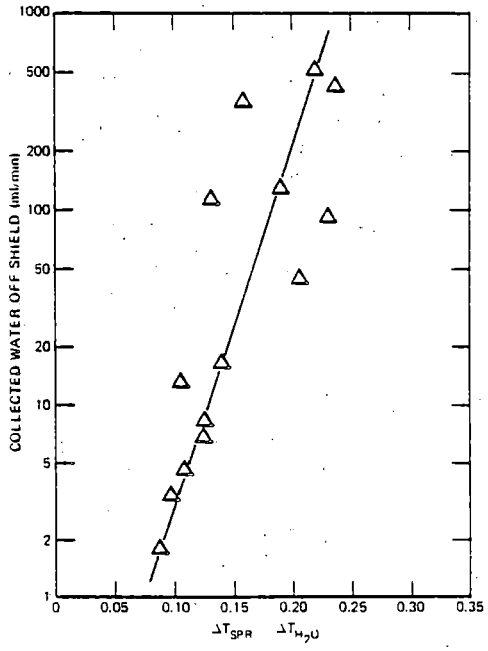

UNION CARBIDE ORNL

TEST ARRANGEMENT FOR A STANDPIPE

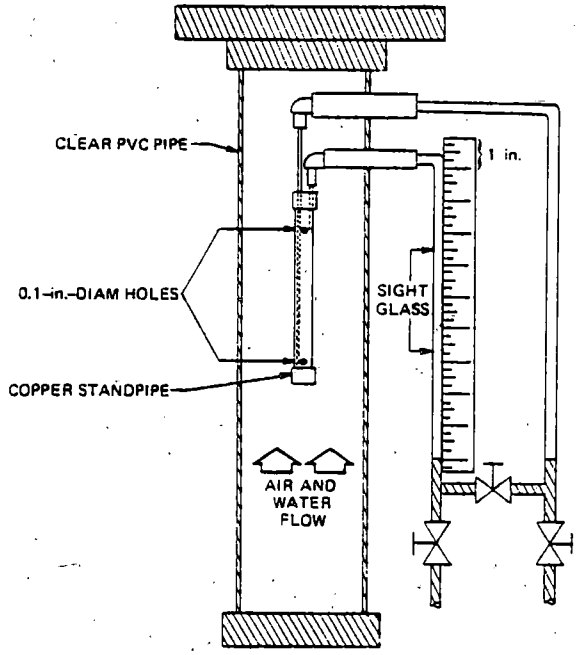

UNION CARBIDE ORNL

COMPARISON OF STANDPIPE LIQUID FRACTION TO LIQUID FRACTION OF SURROUNDING FLOW

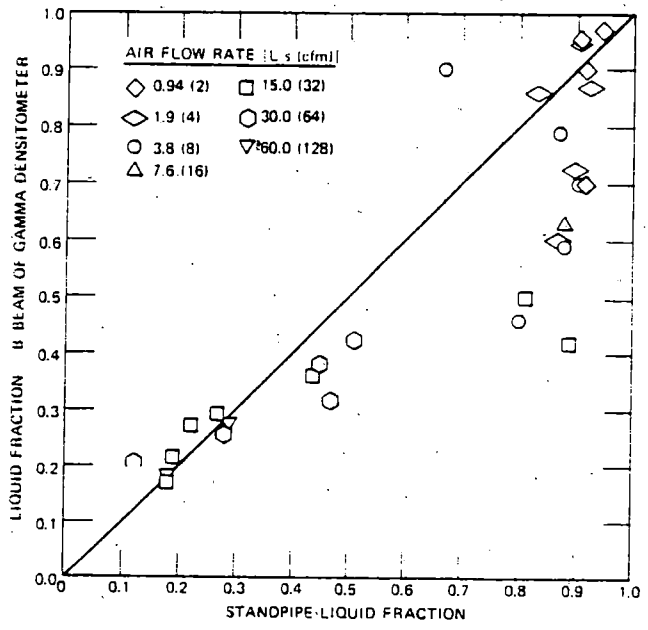

UNION CARBIDE ORNL

AN EXPERIMENTAL HTC SENSOR WAS EVALUATED DURING THTF STEADY STATE FILM BOILING EXPERIMENTS

- FLOW RATES AND CORE POWERS SIMULATED SMALL BREAK LOCA
- SINGLE HTCs LOCATED IN UPPER PLENUM, NEAR TEST SECTION OUTLET
- OUTPUT ΔT MONITORED BEFORE, DURING, AND AFTER PERIODS OF FILM BOILING IN ROD BUNDLE
- RESPONSE OF TEST SENSOR RELATED TO FRS TEMPERATURES AND FLUID CONDITIONS AT TEST SECTION OUTLET

UNION CARBIDE ORNL

HEATED THERMOCOUPLE RESPONSE IN THTF UPPER PLENUM WAS RELATED TO RESPONSE OF TEST SECTION AND OUTLET PIPING INSTRUMENTATION

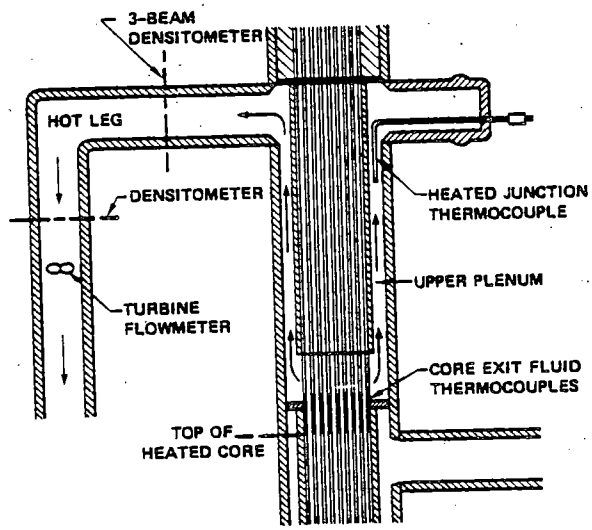

UNION CARBIDE ORNL

LOCATION OF HTCs IN THTF – PLAN VIEW

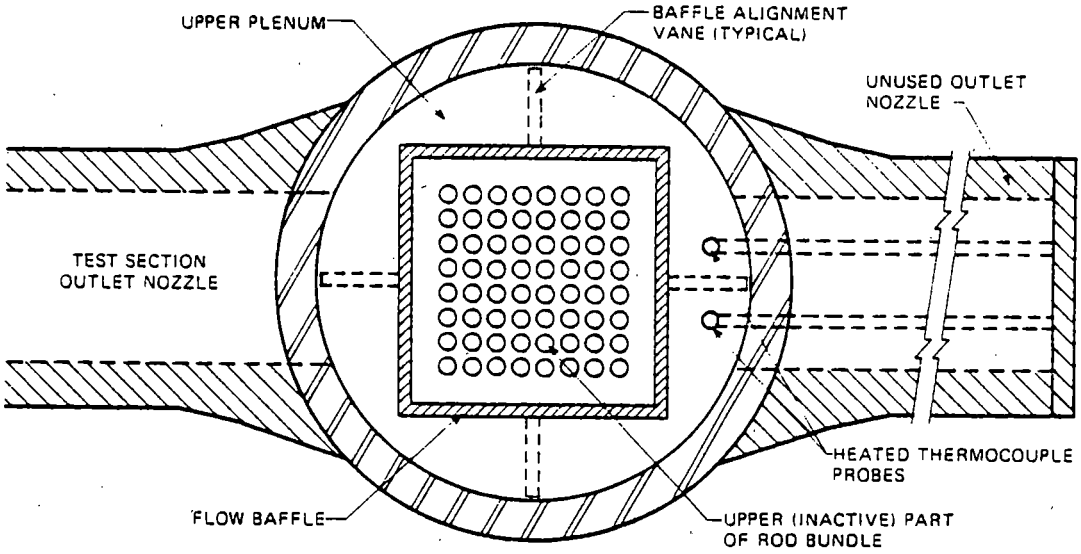

UNION CARBIDE ORNL

TYPICAL INSTRUMENT RESPONSE DURING THTF FILM BOILING TEST

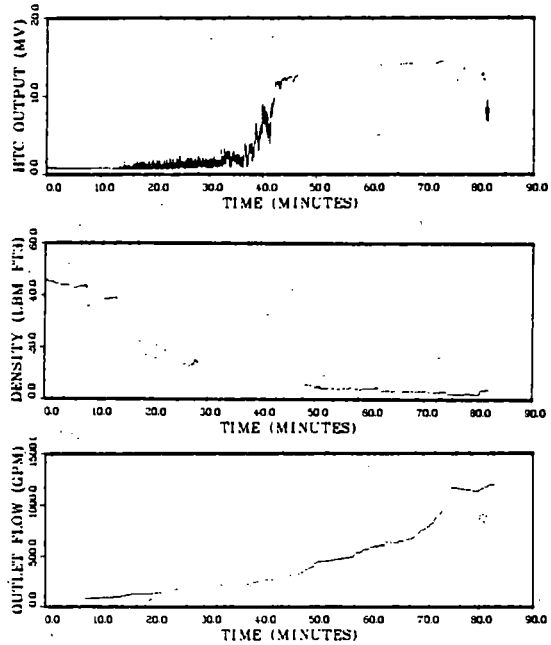

UNION CARBIDE ORNL

HTC OUTPUT DURING HIGH-FLOW FILM BOILING TEST INCORRECTLY SHOWED NO DNB

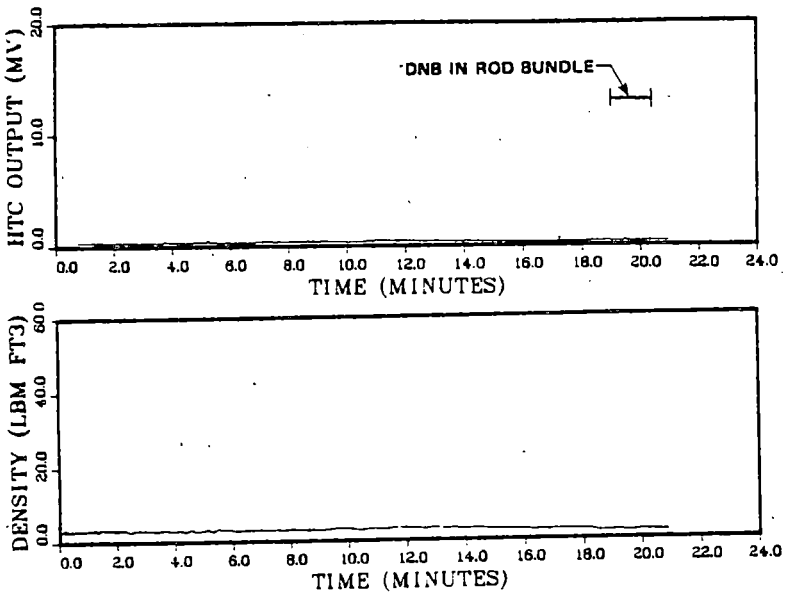

UNION CARBIDE ORNL

AS-TESTED HJTC RESPONDED INCORRECTLY AT HIGH BUNDLE FLOW RATES WITH HIGH POWERS

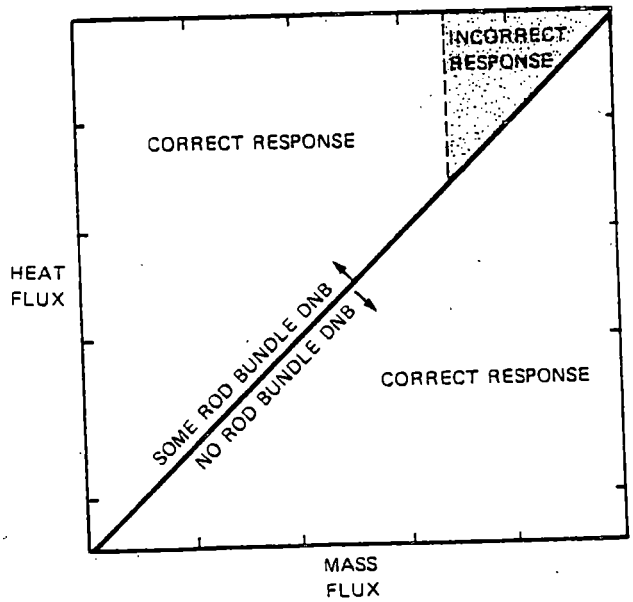

TEST RESULTS FROM THTF FILM BOILING EXPERIMENTS WITH HJTC PROBE

- SENSOR OPERABLE AFTER >40 h AT LOCA CONDITIONS
- INDICATED POOR COOLING PRIOR TO AND DURING ROD BUNDLE DNB AT 600, 900, 1200 AND 1800 psi WITH OUTLET VELOCITIES UP TO ~ 10 fps
- FAILED TO SHOW INADEQUATE COOLING WHILE PARTS OF ROD BUNDLE WERE IN DNB AT SOME HIGHER OUTLET VELOCITIES AND POWERS

COMPARISON OF HTC, dP AND ROD THERMOCOUPLE DATA FOR BOILOFF AND REFLOOD TESTS

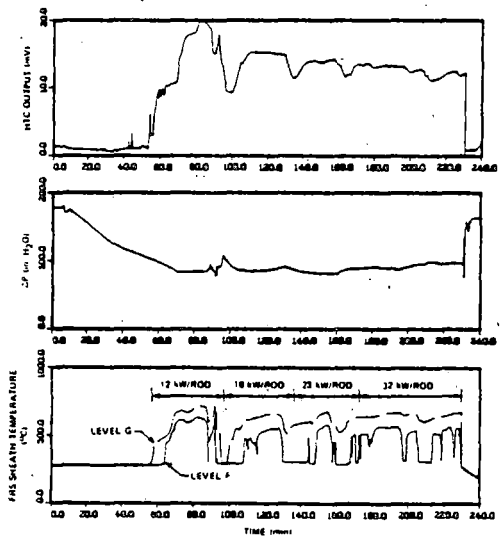

COMPARISONS OF HTC AND PRESSURE DIFFERENCE MEASUREMENTS DURING THTF TESTS SUGGEST THAT FOR A SLOW TRANSIENT,

- BOTH GIVE ADVANCE WARNING AND RELIABLY DETECT LOW LIQUID LEVEL
- DP PROVIDES EARLIER INDICATION OF VOIDING
- AFTER INITIAL DNB, HTC MAY BE MORE SENSITIVE TO CHANGES IN CORE FROTH LEVEL

DIFFERENTIAL PRESSURE CELL LOCATIONS IN THE THTF

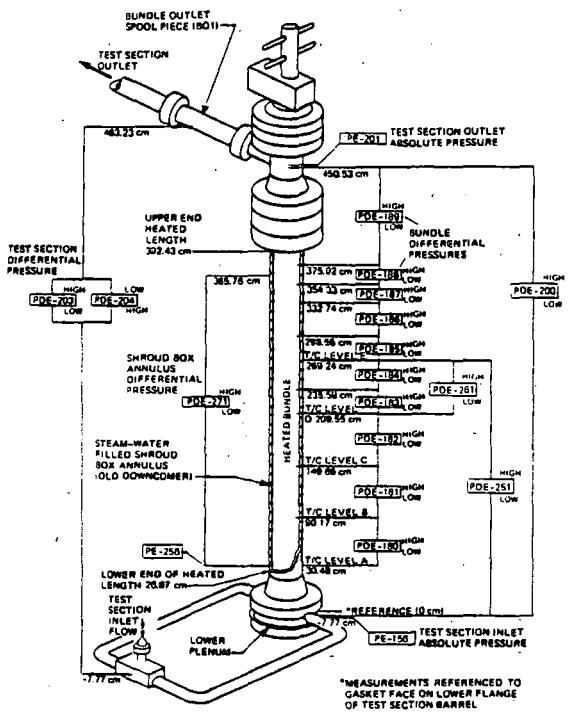

UNION CARBIDE ORNL

COMPARISON OF COLLAPSED LIQUID LEVEL AND QUENCH FRONT LOCATION FOR LOW FLOW TESTS IN THE THTF

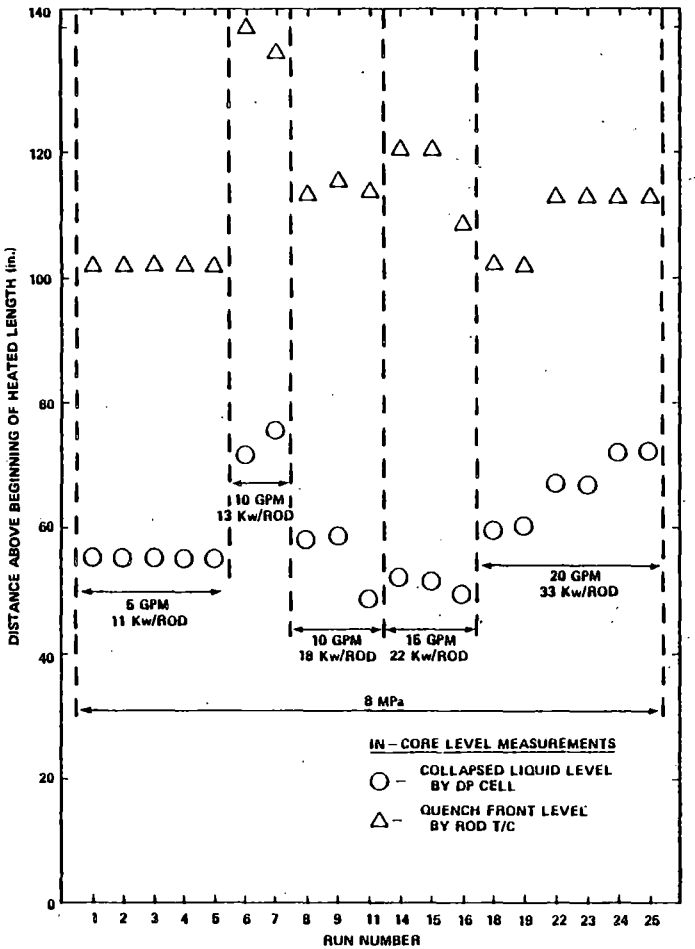

UNION CARBIDE ORNL

COMPARISON OF COLLAPSED LIQUID LEVEL AND QUENCH FRONT LOCATION FOR INTERMEDIATE FLOW TESTS IN THE THTF

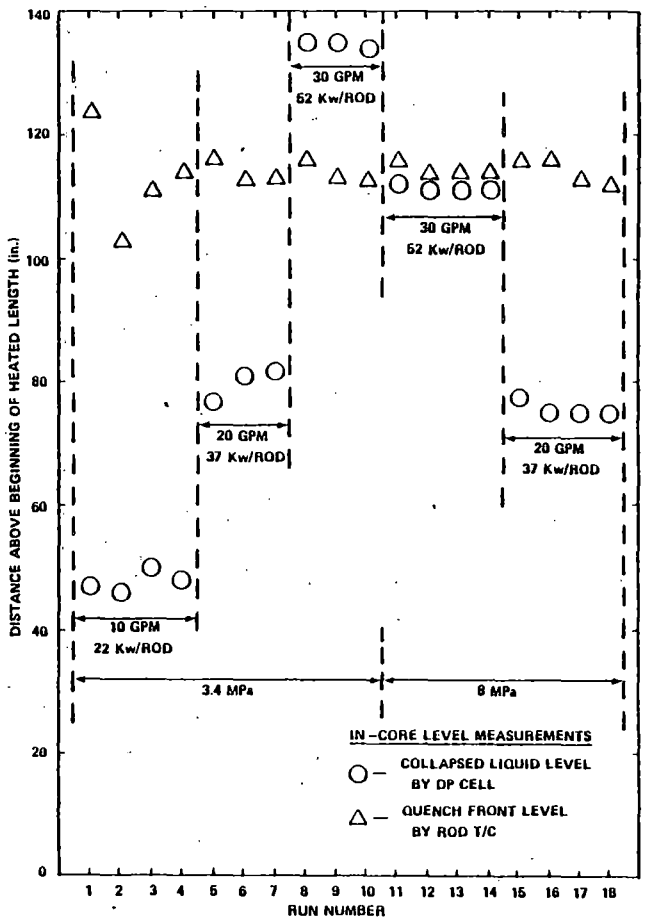

ORNL

INSTRUMENTATION LOCATION ON SEMISCALE INCLUDING WESTINGHOUSE dP - LEVEL SYSTEM

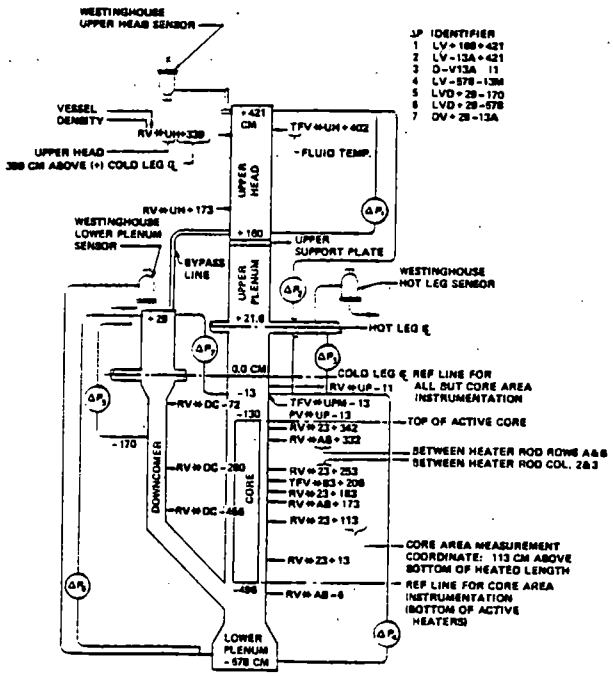

ORNL

COMPARISON OF WESTINGHOUSE UPPER HEAD LEVEL AND A SEMISCALE dP-LEVEL FOR S-UT-3

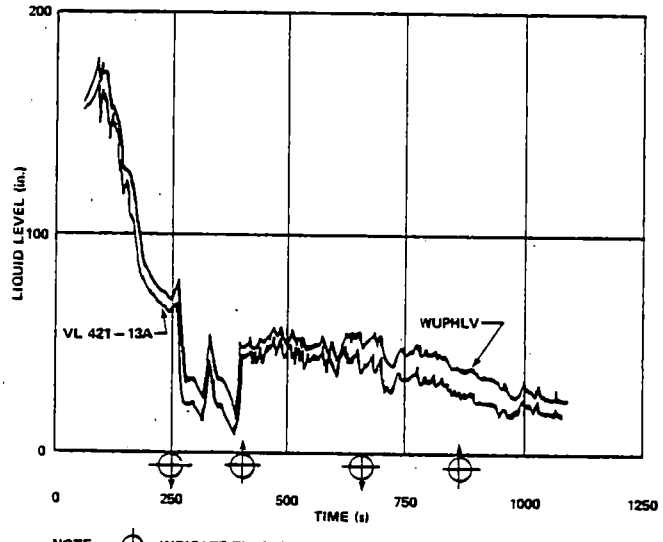

NOTE: ⊕ INDICATE TIME, ELEVATION AND PASSAGE DIRECTION OF TWO-PHASE MIXTURE LEVEL

UNION CARBIDE ORNL

WESTINGHOUSE COLLAPSED LIQUID LEVEL (UPPER HEAD TO LOWER PLENUM) COMPARED WITH SEMISCALE COLLAPSED LIQUID LEVEL (−13 cm TO LOWER PLENUM)

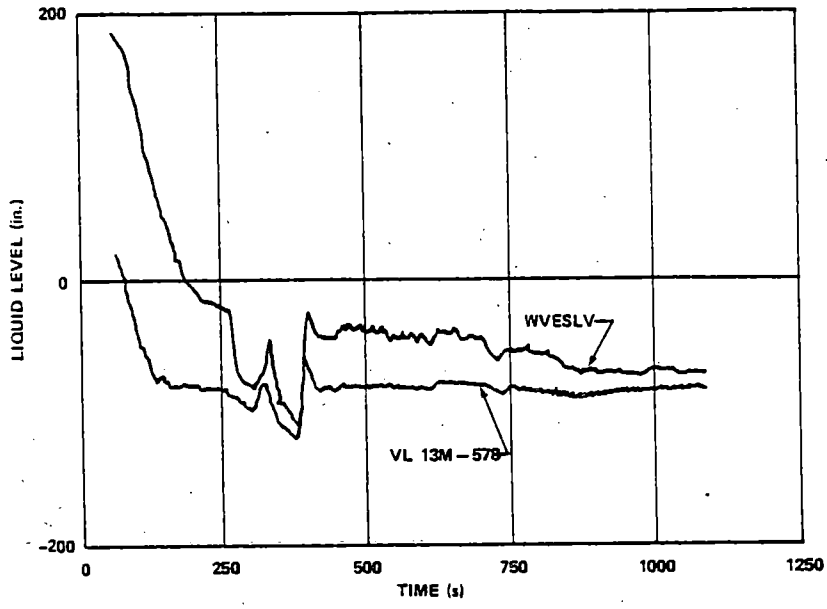

UNION CARBIDE ORNL

DIFFERENCE BETWEEN WESTINGHOUSE VESSEL LEVEL AND SEMISCALE LEVEL FROM −13 TO THE LOWER PLENUM

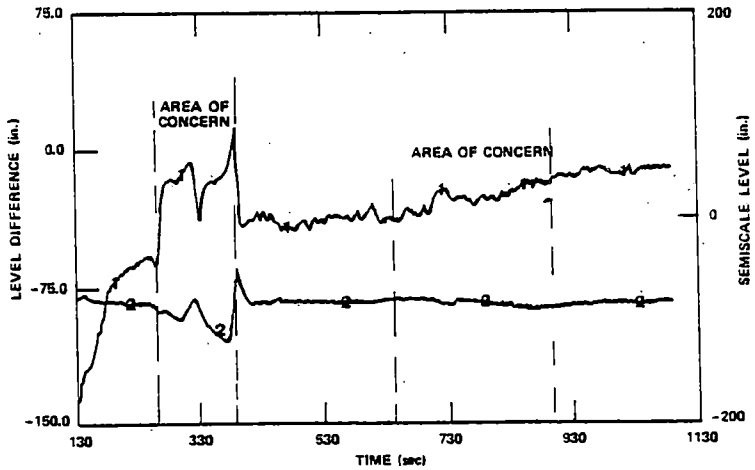

NOTE: CURVE 1 − | (VL 13 M−578) − WVESLV | = DIFFERENCE
CURVE 2 − VL 13 M−578

UNION CARBIDE ORNL

DIFFERENCE BETWEEN WESTINGHOUSE DYNAMIC MEASUREMENT AND SEMISCALE MEASUREMENTS FOR THE ENTIRE VESSEL

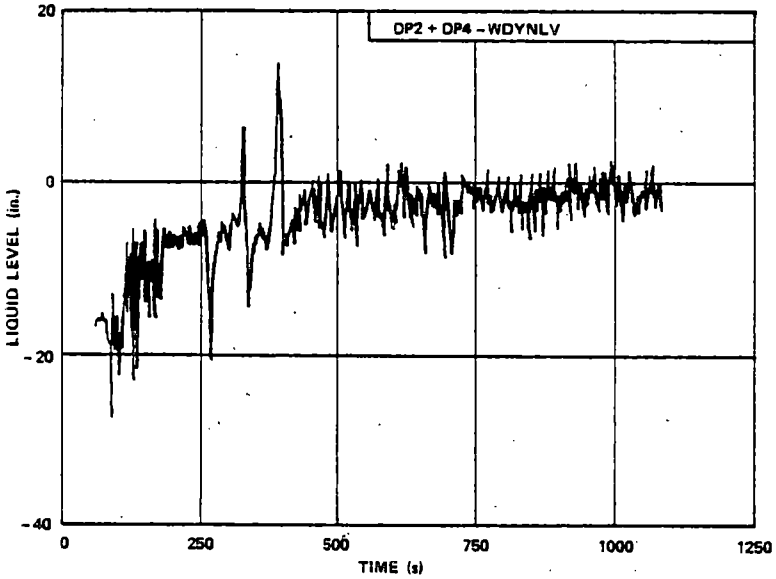

UNION CARBIDE ORNL

DIFFERENCE BETWEEN WESTINGHOUSE AND SEMISCALE LEVEL MEASUREMENTS FOR THE ENTRIE VESSEL

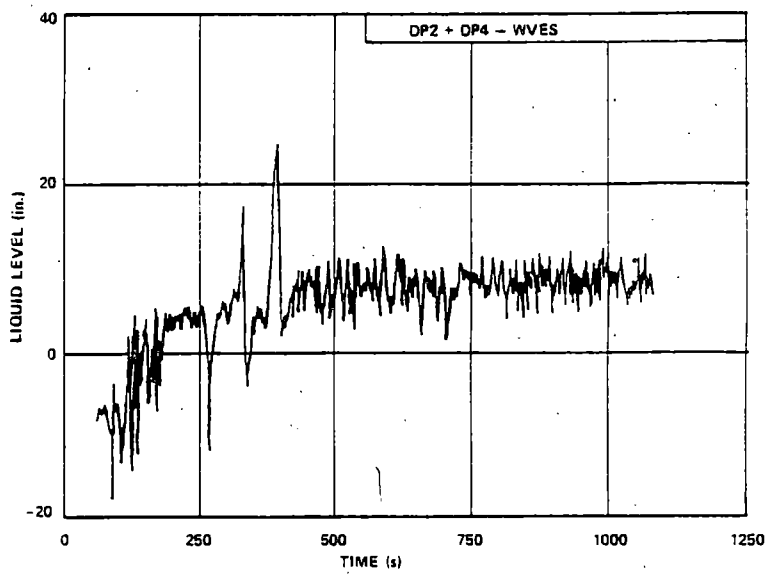

UNION CARBIDE ORNL

WESTINGHOUSE LEVEL MEASUREMENT APPEARS TO BE CONSERVATIVE TO TWO-PHASE MIXTURE LEVEL

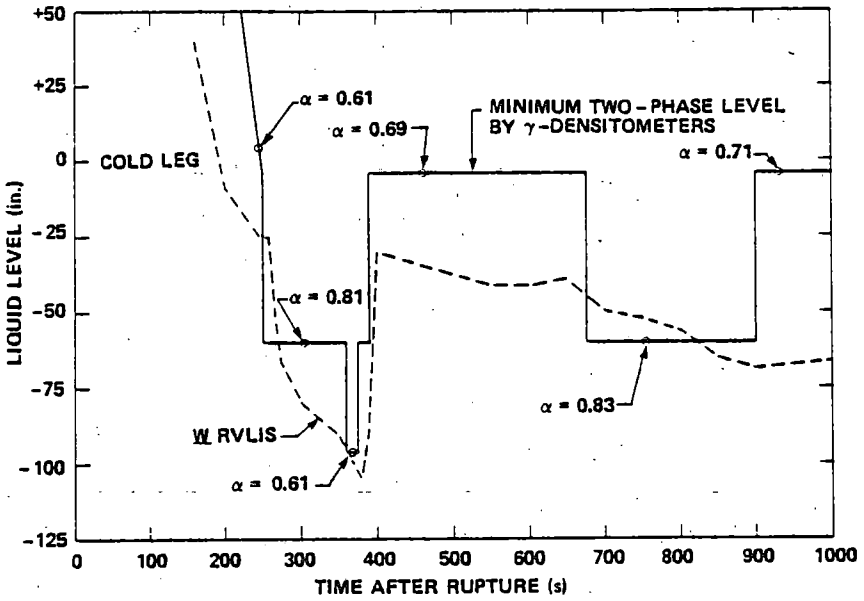

UNION CARBIDE ORNL

SEMISCALE SIMULATION OF A PWR

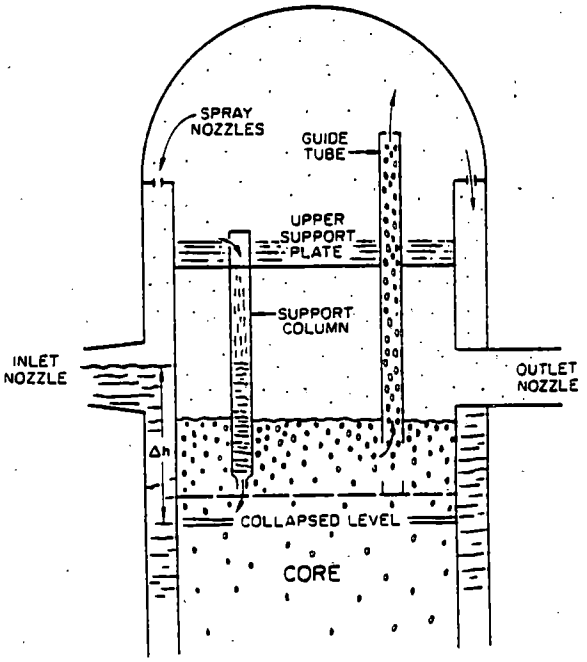

SCHEMATIC DIAGRAM OF A WESTINGHOUSE PWR

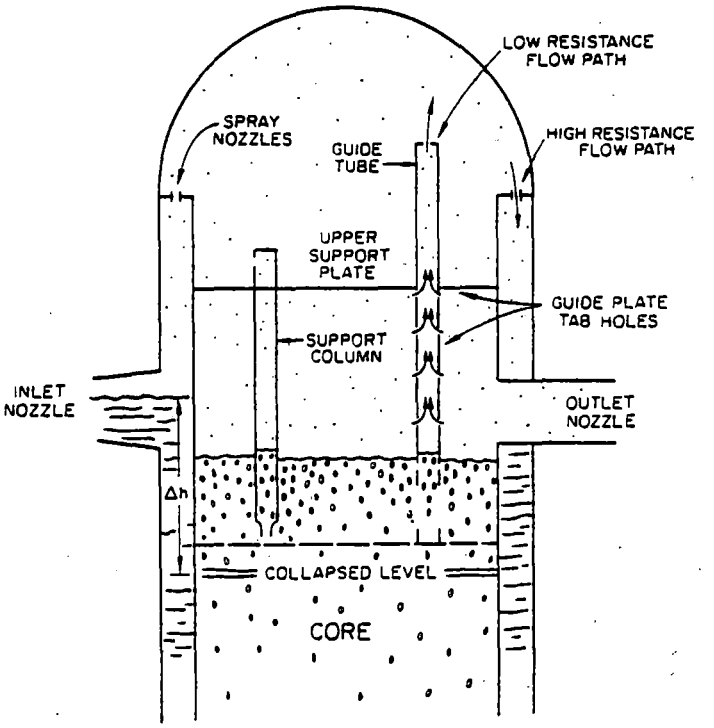

LEVEL DIFFERENCES IN SEMISCALE FOR TEST S-UT-3

TIME AFTER RUPTURE	APPARENT GUIDE TUBE LEVEL		DIFFERENCE IN WESTINGHOUSE AND SEMISCALE LEVELS	
(s)	(cm)	(in.)	(cm)	(in.)
220	100–165	40–65	150	60[a]
250–390	17–60	5–25	40–50	15–20[a]
250–390	17–60	5–25	25–115	10–45[b]
500	85–130	35–50	100	40[a]
675–910	10–50	5–20	25–50	10–20[a]

[a]DIFFERENCE BETWEEN WESTINGHOUSE AND SEMISCALE dP VALUES

[b]DIFFERENCE BETWEEN WESTINGHOUSE UPPER HEAD VALUE AND SEMISCALE DENSITOMETER

TMI—2 ANALYSIS MOTIVATES U. S. NRC TO ISSUE REQUIREMENTS FOR INSTRUMENTATION TO MEASURE REACTOR COOLANT LEVEL IN PWR's

- Provide unambiguous indication of core cooling adequacy
- Function properly under both natural and forced convection flow conditions
- Operate under normal operating conditions
- Survive loss-of-coolant-accident (LOCA)
- Provide indications useful for post-accident analysis

ULTRASONIC SENSOR IS ONE OF THE MOST PROMISING LONG TERM SOLUTIONS:

- Output temperature and density profiles
- Self checking capabilities
- Continuous mode information in engineering units
- Reactor compatibility
- Perform under normal and accident conditions
- Highly reliable, minimum maintenance
- Accurate

TORSIONAL PULSE ON FLATTENED WIRE IS DELAYED
BY DENSE MEDIUM MUCH LIKE A BOAT PADDLE IN WATER.

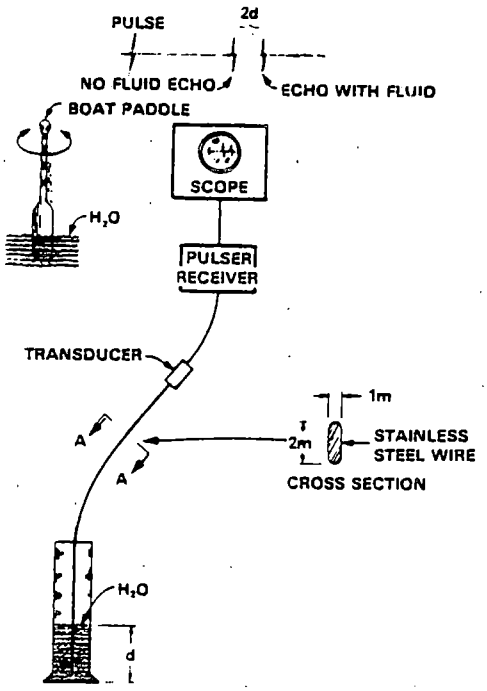

Comparison of Extensional and Torsional Pulse Reflection Times for the Various Zones.

Fluid Level Changes the Propagation Velocity of the Torsional Wave

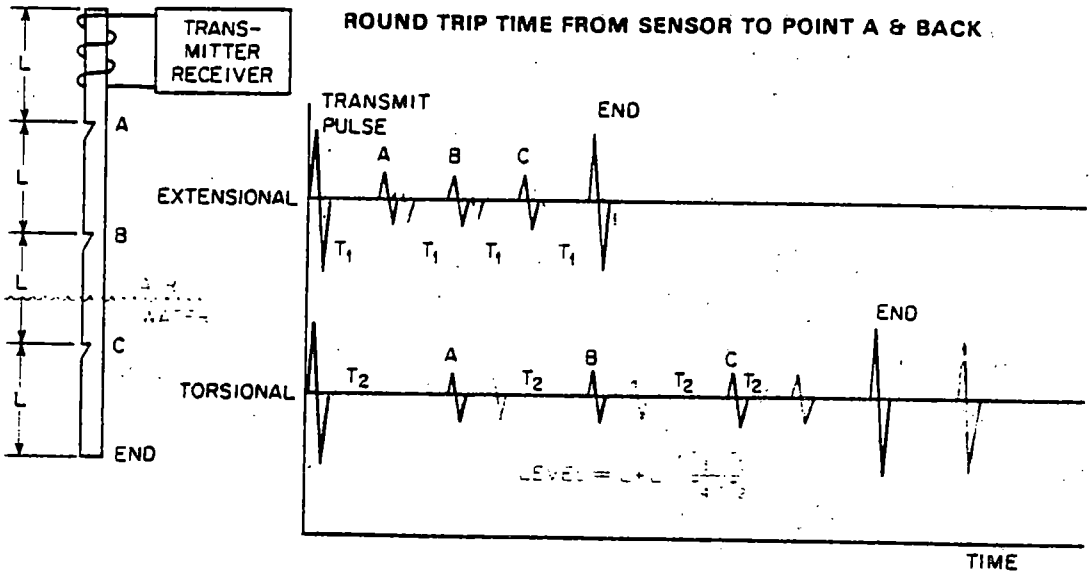

PRINCIPLE OF OPERATION BASED ON DEPENDENCY OF TORSIONAL AND EXTENSIONAL WAVE VELOCITY ON DENSITY AND TEMPERATURE:

$$v_e = \sqrt{\frac{Y}{\rho_s}}$$

$$v_t = K\sqrt{\frac{G}{\rho_s}}\left[1 + \frac{\rho}{\rho_s}\left(1 - \frac{1}{K}\right)\right]$$

WHERE Y = YOUNGS MODULUS
ρ_s = WAVEGUIDE DENSITY
G = SHEAR STRESS MODULUS
ρ = DENSITY OF FLUID
K = SHAPE FACTOR

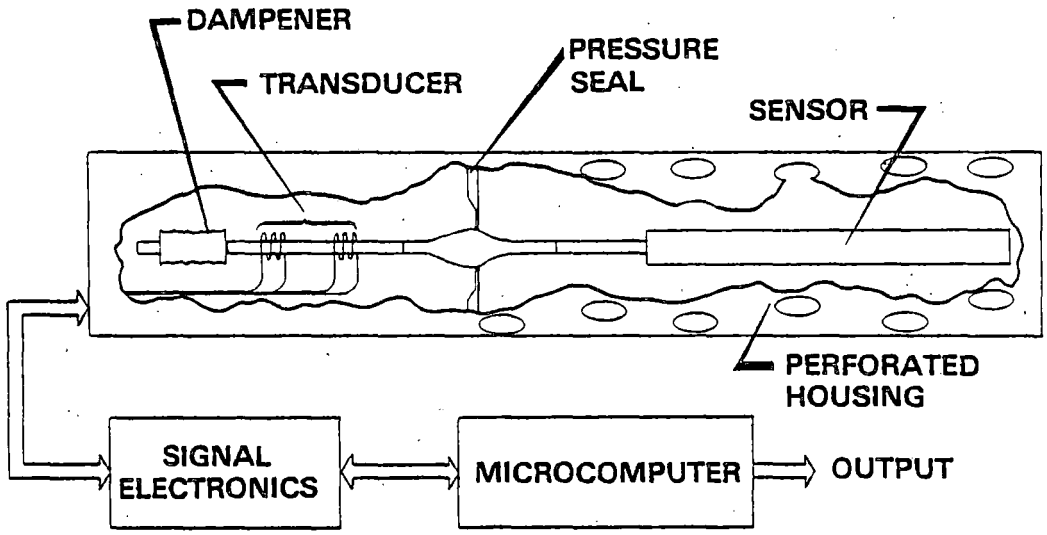

THE REMOTE LOCATION OF ELECTRONICS AND ABSENCE OF MOVING PARTS IN THE REACTOR VESSEL MAKES THE PROBE HIGHLY RELIABLE AND MINIMIZES MAINTENANCE REQUIREMENTS.

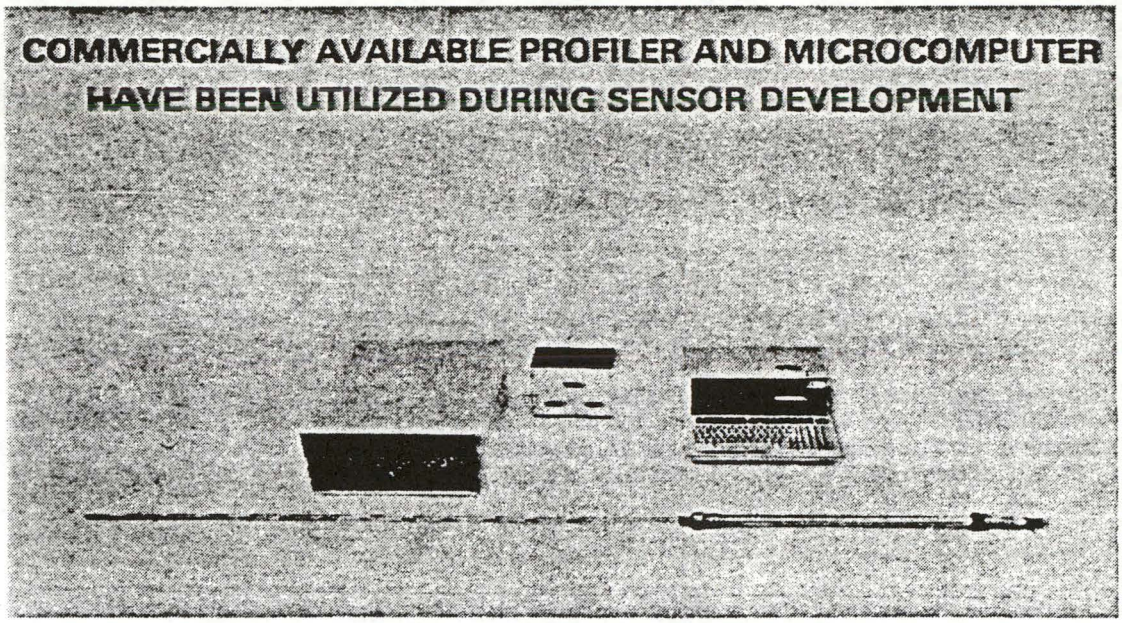

A NUCLEAR GRADE ACOUSTIC WAVE DAMPENER
ELIMINATES UNDESIRABLE END REFLECTIONS OF TORSIONAL
AND EXTENSIONAL WAVES FROM THE WAVEGUIDE

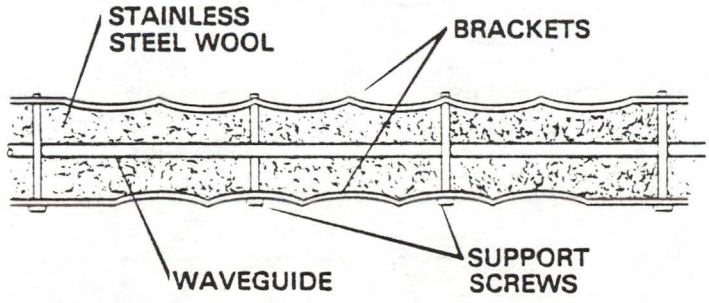

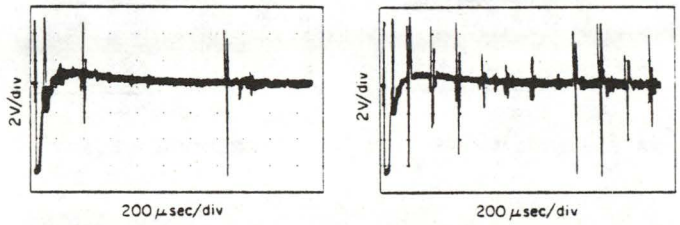

PROBE WITH DAMPENER

PROBE WITHOUT DAMPENER

LAVA COIL FORMS AND STAINLESS STEEL DAMPENER ENHANCE THE COMPATIBILITY OF THE TRANSDUCER WITH HIGH TEMPERATURE, HIGH RADIATION ENVIRONMENTS

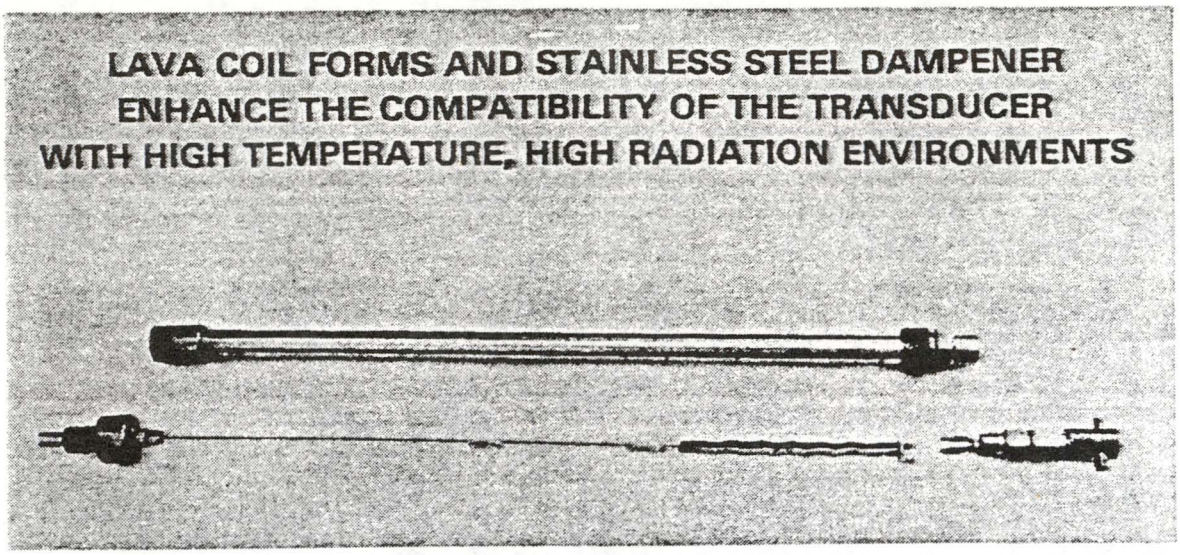

THE PRESSURE SEAL ALLOWS BOTH MODES OF ACOUSTIC WAVES TO PASS BETWEEN THE TRANSDUCER AND THE SENSOR

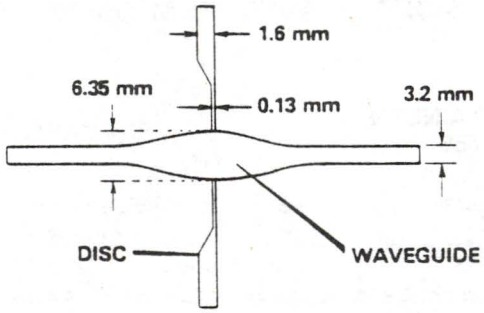

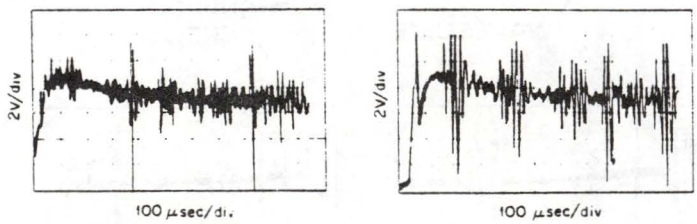

EXTENSIONAL WAVES

TORSIONAL WAVES

SENSOR/TRANSDUCER PRESSURE SEAL IS MACHINED FROM A SOLID PIECE OF STAINLESS STEEL

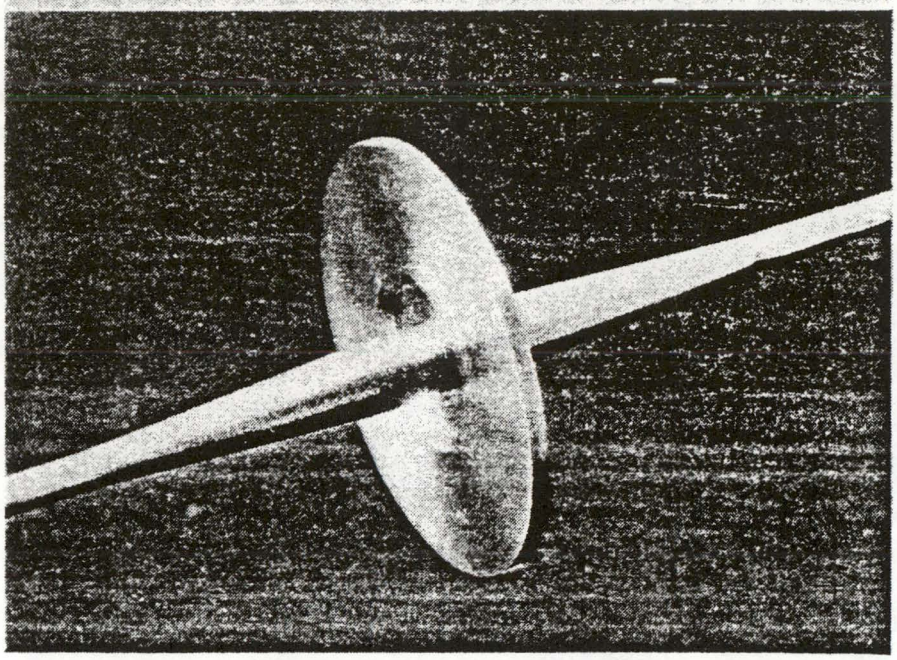

AUTOMATION OF SAMPLING AND PROCESSING OF THE DATA RESULTS IN IMPROVED RESOLUTION AND ACCURACY

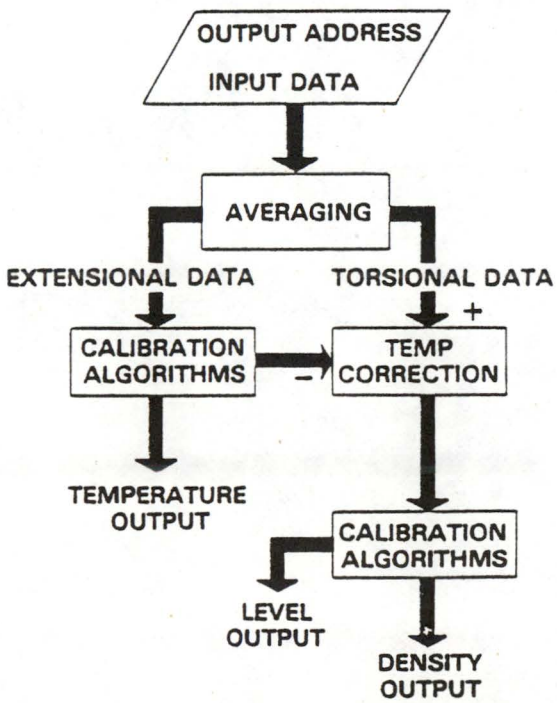

A CONCEPT FOR A FAST NEUTRON, NON-INVASIVE, LIQUID LEVEL AND DENSITY GAUGE FOR NUCLEAR POWER REACTORS

by

W. A. Jester
A. J. Baratta
J. Edwards
E. W. Okyere
D. Love
I. B. McMaster

Nuclear Engineering Department
The Pennsylvania State University
University Park, PA 16802

Presented at the
U.S. Nuclear Regulatory Commission's
9th Water Reactor Safety Research Meeting
Held at National Bureau of Standards
Gaithersburg, Maryland
Afternoon Session
October 27, 1981

INTRODUCTION

The accident at the Three Mile Island Nuclear Generating Station Unit-2 (TMI-2) has shown that it is important for pressurized water nuclear power reactors to have some means to determine reactor vessel liquid level when the reactor is shut down and the primary coolant pumps turned off. Also needed is a means to determine in-core coolant density when the pumps are running with the reactor in either an operational or shutdown mode. This latter requirement is needed to detect homogeneous voiding of the coolant in the pressure vessel, an early indication of primary coolant loss. Finally, the system should be able to distinguish between voiding of the core region and voiding of the downcomer region.

This paper briefly describes a concept for a non-invasive density and level gauge which would utilize the fast neutrons leaking through the reactor vessel wall into the air gap surrounding the vessel. This concept employs a series of fission detectors placed in existing instrument wells external to the pressure vessel. A demonstration of the concept is presented using data collected by the BF_3 Source Range Detector (SRD) during the first few hours after the start of the TMI-2 accident. Finally, this paper describes the results of a series of experiments conducted by the authors at The Pennsylvania State University's Breazeale Nuclear Reactor in which downcomer voiding with no corresponding core voiding was simulated.

BASIC GAUGING CONCEPT

Because of the approximately ten and one-half inches of steel which exists between the reactor core and the annulus which surrounds the TMI-2 reactor vessel, no significant amount of thermal neutrons would penetrate the annulus. (See Figure 1)

Fast neutrons reaching the concrete primary shield wall can be thermalized and scattered back into the annulus region to provide a neutron background not directly related to coolant density or level. The presence of steel and lead lining the primary shield wall and the three inches of lead surrounding the SRD will reduce the intensity of this source of neutrons reaching the detector.

Most of the neutrons, which reach the SRD, would be unscattered fast neutrons coming directly from the core region directly adjacent to the detector and moderated by the polyethylene surrounding the detector and then detected by the BF_3 counter. When the reactor was operating, these fast neutrons would come primarily from the fissioning of uranium fuel in the critical core. Once the reactor has been shutdown more than a few minutes, the fast neutrons reaching the SRD would be from photoneutrons and neutrons from the ABC start-up source which have been multiplied by the fuel in the subcritical core adjacent to the detector.

The amount of water in and above the core would affect both photoneutron production and core multiplication. Thus, the number of fast neutrons reaching the SRD would be a function of the source strength and the amount of water moderator in the primary containment and its associated downcomer adjacent to the detector.

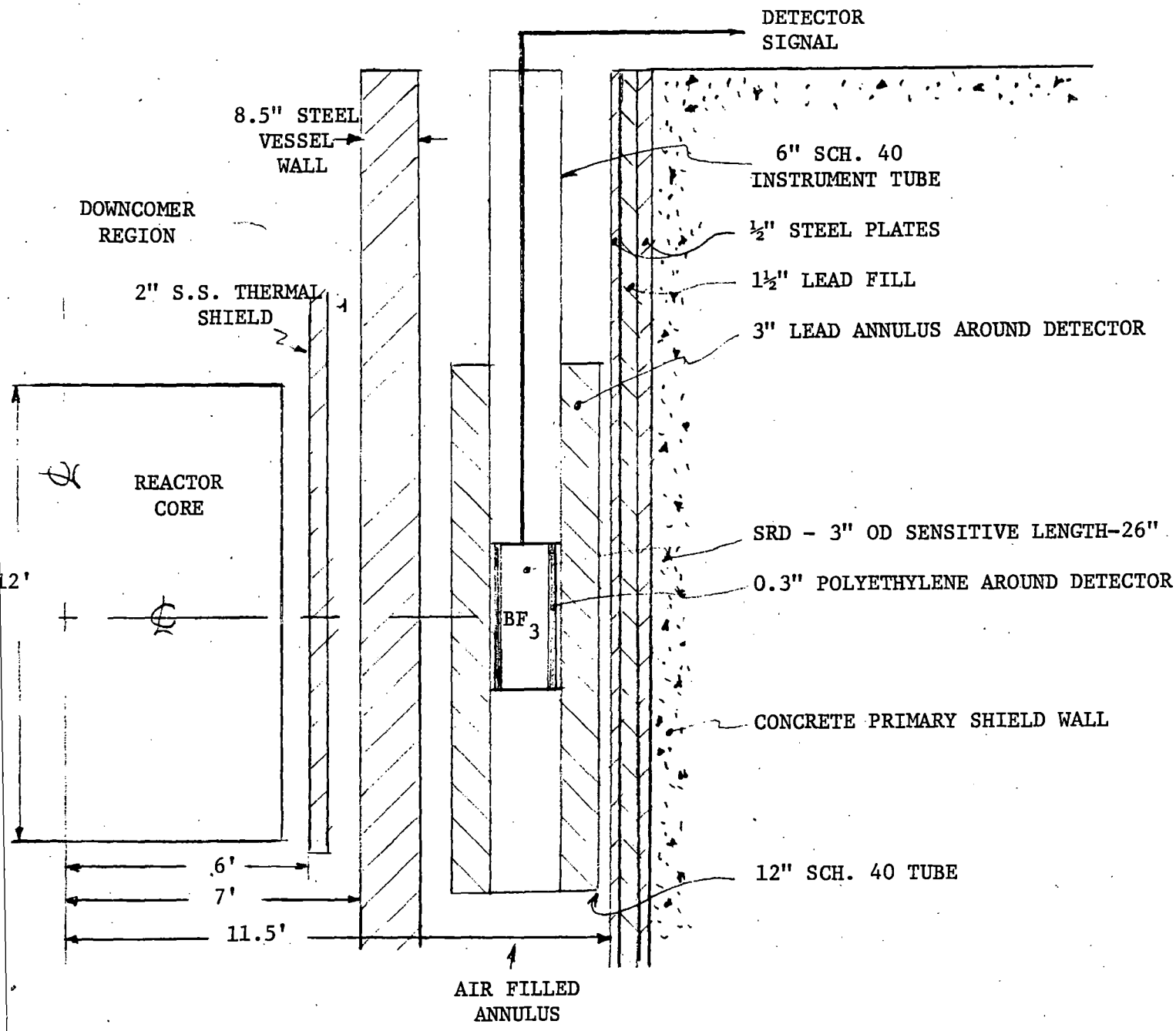

Figure 1. Layout of TMI-2 Source Range Detector Relative to the Reactor Core (not to scale)

In the proposed concept, the density or level of water in these regions would be determined by a series of fission chambers located in one or more existing vertical instrument tubes in the annulus region outside the pressure vessel. Fission detectors were chosen for this concept since they can be operated in a current mode when the reactor is operating and the neutron level is high and in the more sensitive pulse mode when the reactor is shutdown and the neutron level is considerably lower.

The bottommost of these detectors would be located adjacent to the bottom of the reactor core. There it would be least affected by changes in water density or level changes which would initially occur in the upper regions of the pressure vessel. By normalizing the outputs of the other detectors to the output of this bottommost detector, one should be able to compensate for changes in signals not related to level or density changes. This would include changes in core power level, temperature-caused coolant density changes, and changes in coolant water boron content.

RELEVANT INFORMATION FROM THE TMI-2 ACCIDENT AND THE NSAC ANALYSIS OF ACCIDENT CONDITIONS

The data collected by the TMI-2 SRD during the accident illustrates the type of data which could be obtained from one of the detectors in the proposed gauge under loss of coolant conditions. Figure 2 shows the SRD readings as a function of time after the turbine trip (1). During the first 20 minutes; the SRD indicated a normal decay curve, and thus was seeing no affect from the loss of coolant to this point.

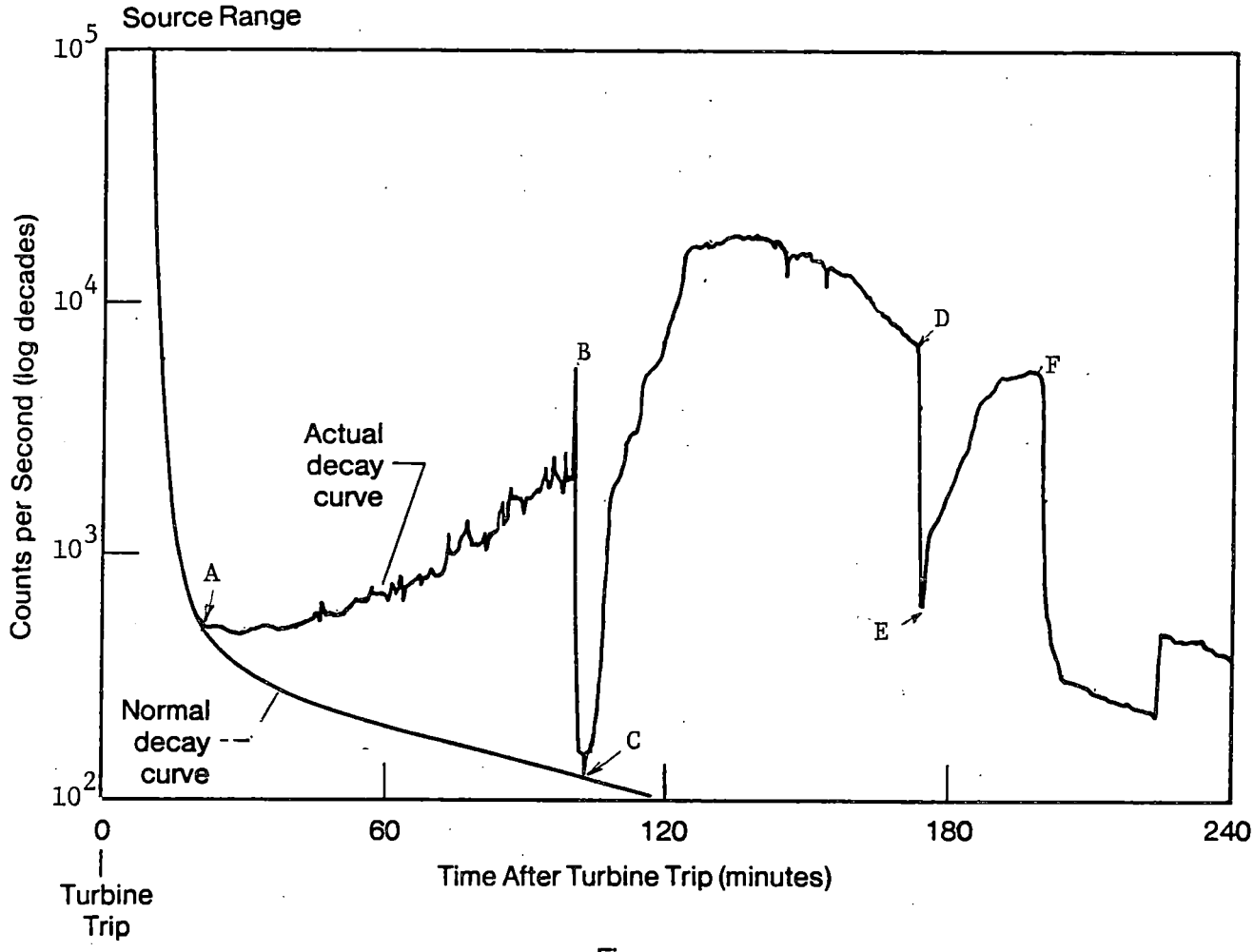

Figure

Figure 2. Source Range Detector Reading as a Function of Time after Turbine Trip (1)

Starting at approximately the 20 minute point, point A in Figure 2, the signal began to depart from the normal decay curve by the initiation of steam voids in the system, thereby increasing the fast neutron leakage. (See Figure 3 (1)). From this point (A) until the time (B) when the reactor coolant pumps were turned off about 100 minutes after the trip, the SRD acted as a density gauge. Figure 4 shows the relationship between the SRD response and the percent voids in the core and downcomer region as computed by the Nuclear Safety Analysis Center (NSAC)(2). This figure shows the type of response characteristic of a transmission-type density gauge. It should be noted that above 80% voiding, fast neutrons from the ABC start-up source rather than the photoneutrons, would make up the source of most of the monitored neutrons.

When the last of the operating coolant pumps was shutdown at 100 minutes into the turbine trip, there was a rapid drop in the SRD reading (B and C in Figure 2). This SRD reading momentarily returned to that of the normal shutdown curve. At this point, the voids rose to the top and coolant flowed into the core from the hot legs, producing a solid water condition as seen by the SRD.

During the next 75 minutes (C and D), the water level in the core region and downcomer was steadily being lowered as the water was being boiled off (see Figure 5(1)). During this period, the water in the downcomer, being cooler and thus more dense, would be somewhat lower than that in the core region. Figure 6 (3) shows the best estimate of the actual core water level as computed by NSAC from thermal-hydraulic consideration from 112 to 205 minutes after turbine trip. In Figure 7, (3) this estimate is compared with the results that NSAC obtained from

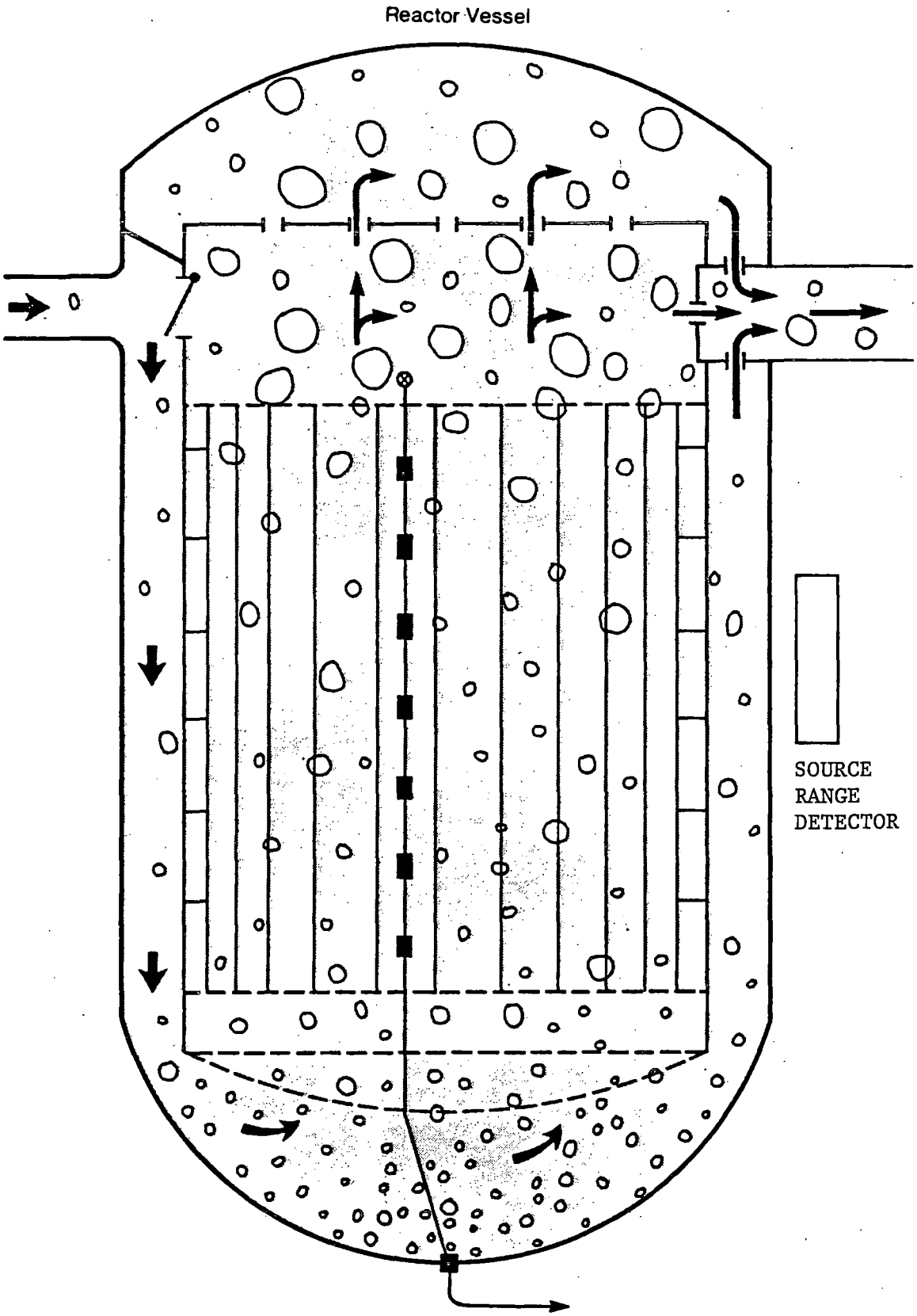

Figure 2. Forced core cooling; homogeneous void distribution.(1)

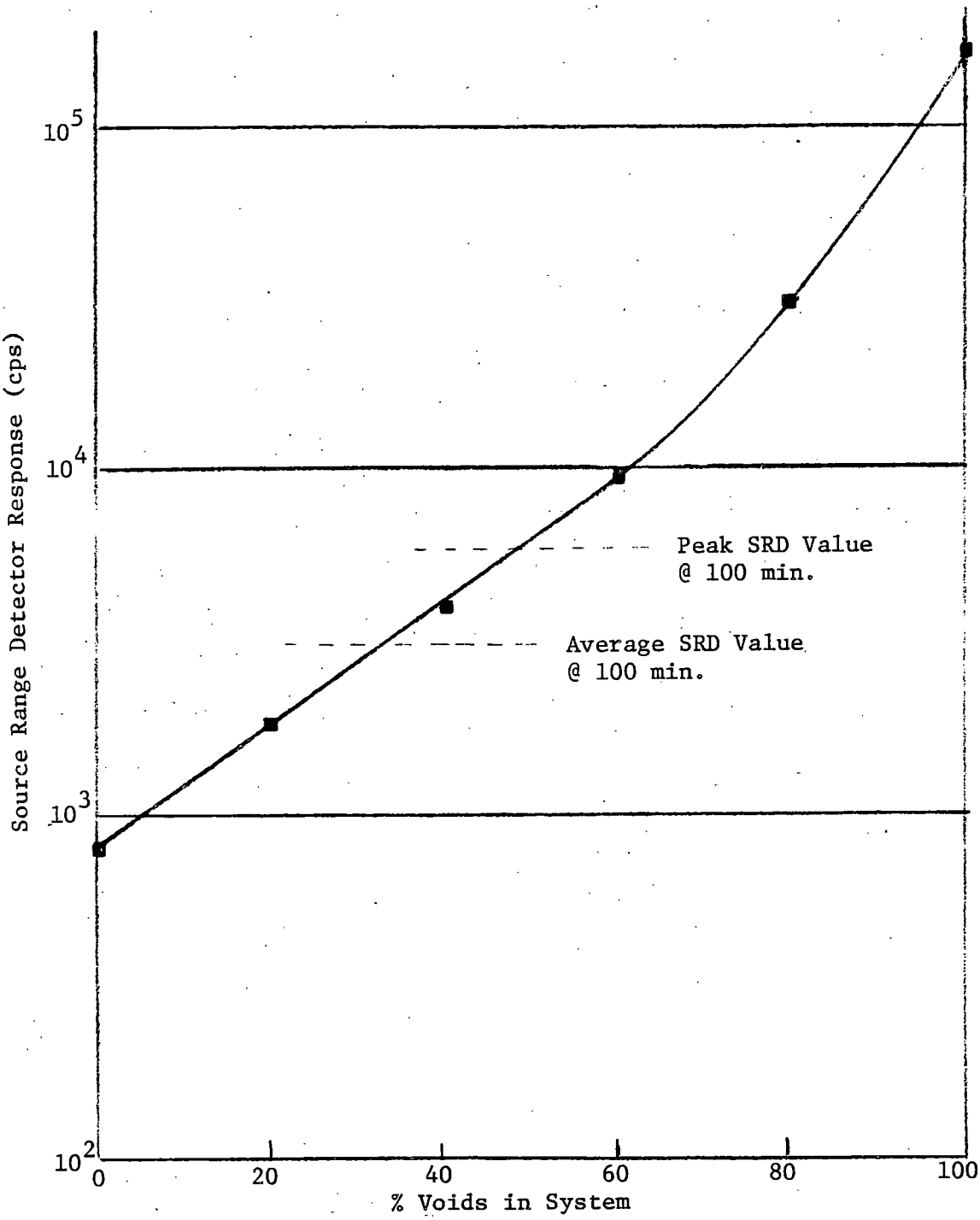

Figure 4. Source Range Detector Response to Homogeneous Voiding (2)

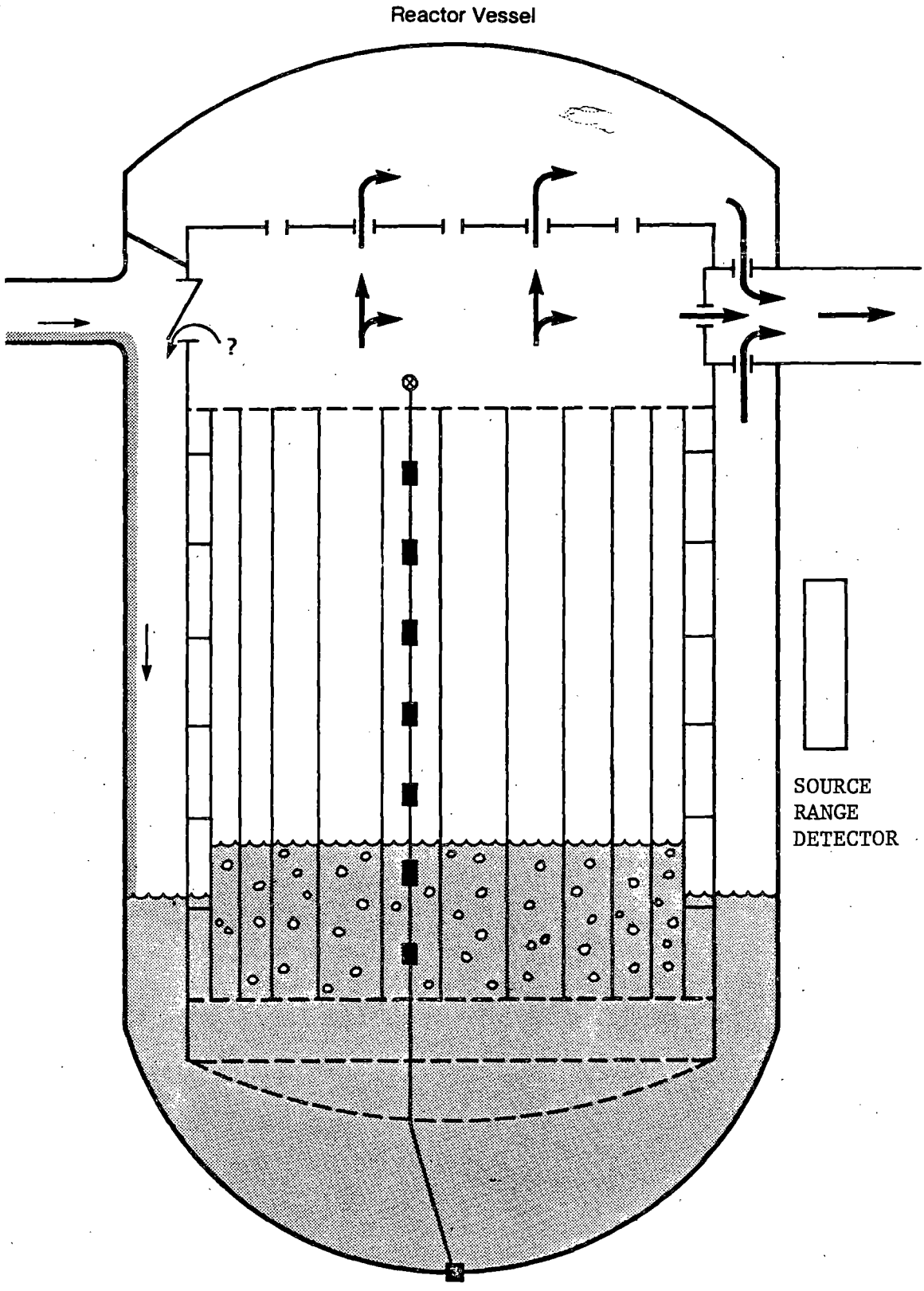

Figure 5. Core water level — time approximately 160–174 minutes after turbine trip. (1)

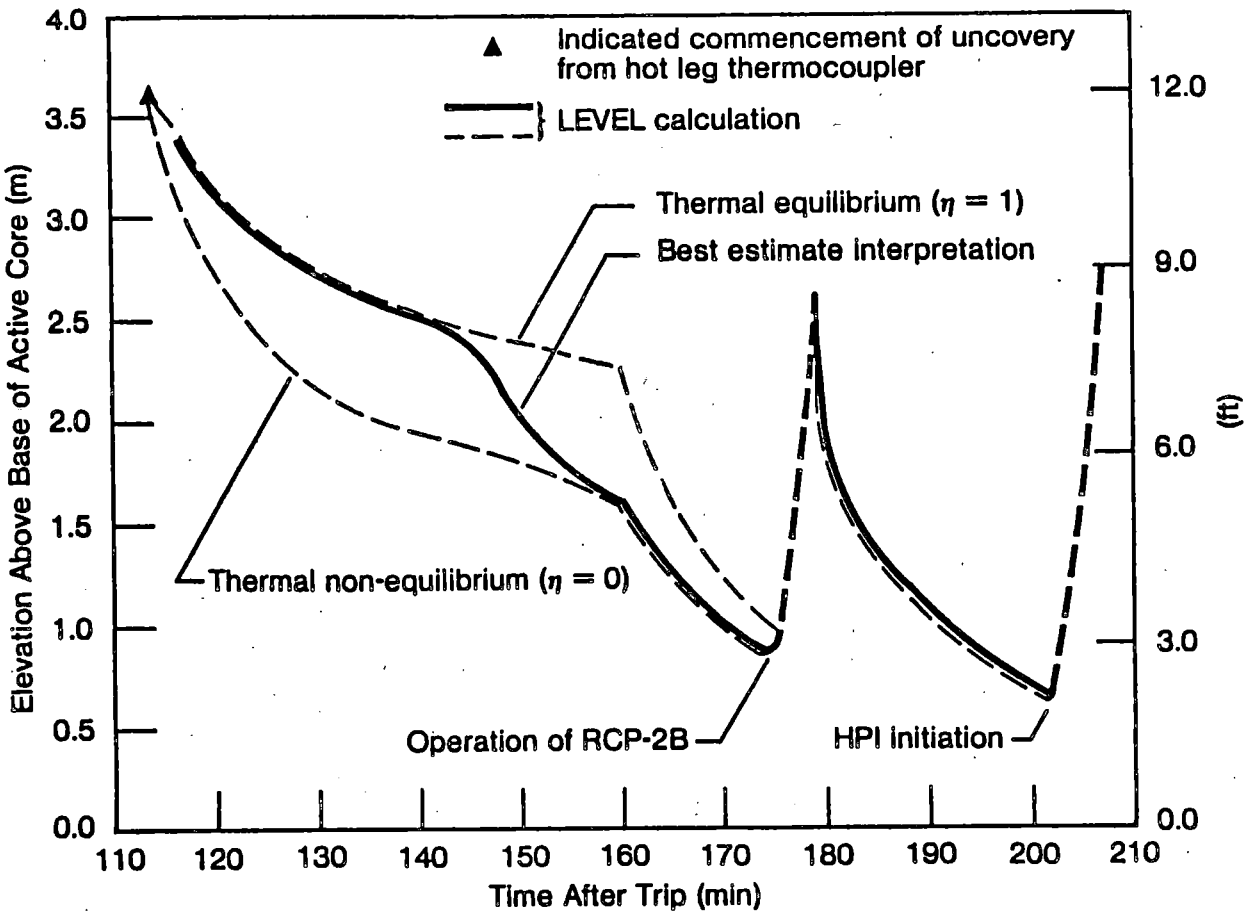

Figure 6. Calculated level path during uncovery of TMI-2 core. Solid curve is best estimate calculation. (3)

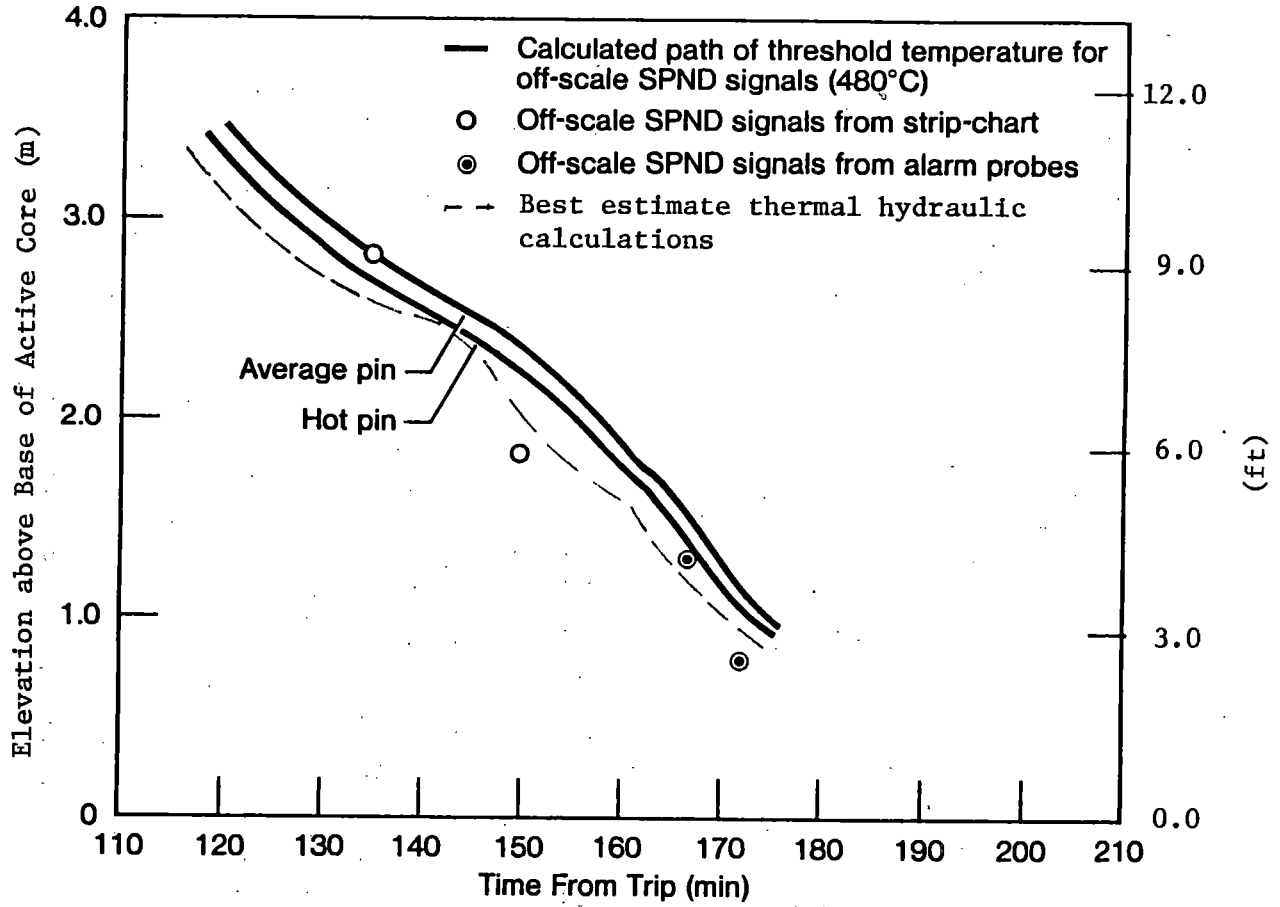

Figure 7. Comparison between calculated rate of core heat-up and indications from SPND behavior. (3)

the in-core self-powered neutron detectors (SPN) during the period of 120 to about 175 minutes after the trip. They found reasonable agreement from these two independent data sources. NSAC also got similar results from their neutron transport calculations simulating the accident conditions (3).

If one takes NSAC's best estimated coolant level between 112 and 175 minutes after the trip and plots this versus the source range detector response during this same period, one obtains the curve shown in Figure 8.

This curve indicates that the number of fast neutrons reaching the SRD increases rapidly until the water falls to a level near the upper level of the sensitive region of the detector. It remains about constant as the water level passes the detector, and then rapidly falls off again as the water level drops below the SRD.

It is believed by the authors of this paper that the initial rise in measured activity was caused by the removal of the water moderator from between the primary sources of fast neutrons and the SRD. The fall-off of the signal as the water falls below the detector is believed to be due to the movement of the fast neutron fission and photoneutron sources away from the detector. Thus, the output of a single detector such as the SRD would produce an ambiguous signal since one might not know which side of the response curve one was on and could not tell whether or not the coolant level was rising or falling. This ambiguity would be resolved in the proposed gauging concept by the use of a series of detectors positioned along the vertical axis. By interpreting the combined response curves of two or more detectors, the in-core coolant level under equilibrium conditions could be determined.

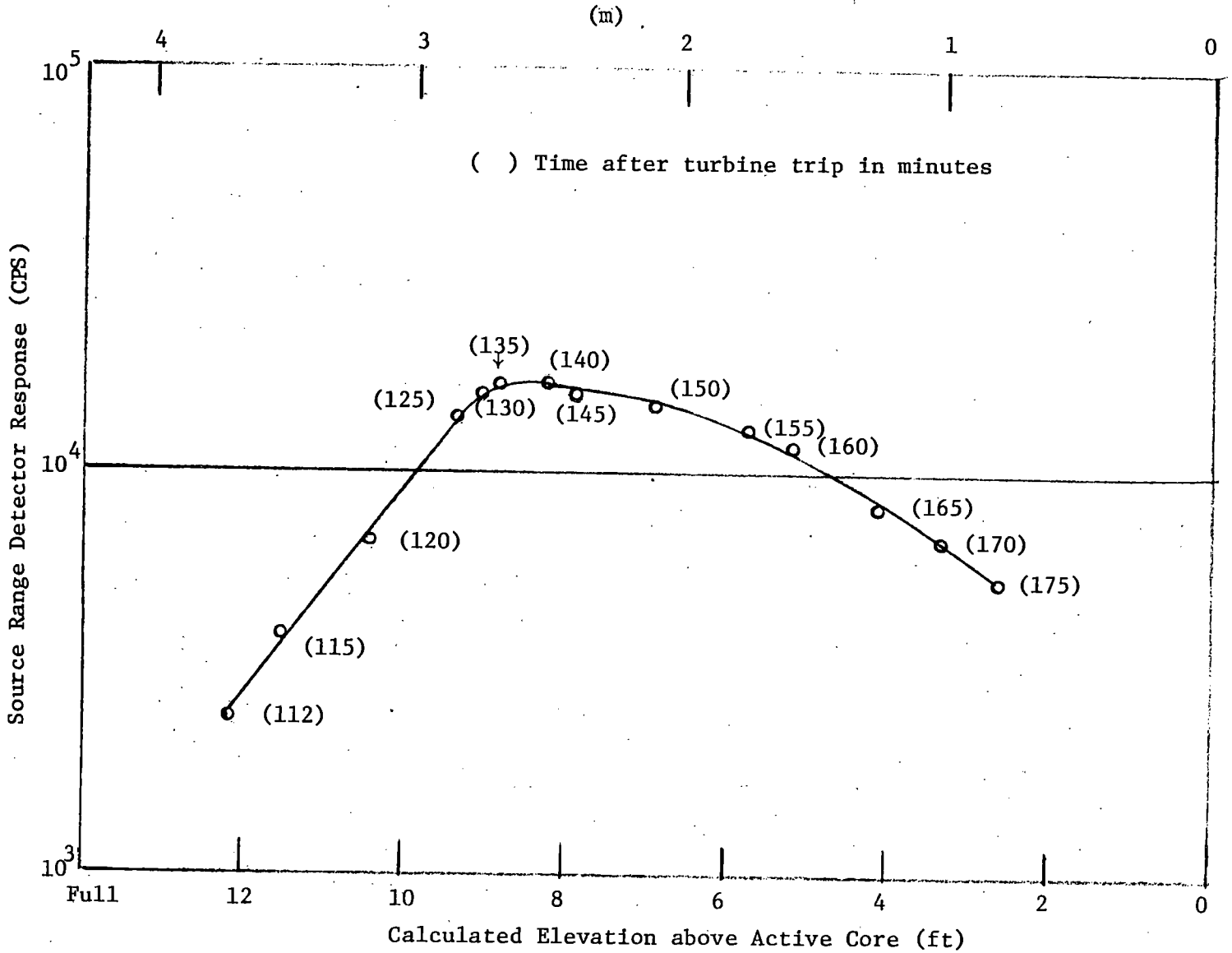

Figure 8. SRD Response as a Function of Thermal Hydraulic Calculated Level Path During Uncovering of TMI-2 Core

At about 175 minutes after the trip, the operators, for a brief period, started a reactor coolant pump, sending a slug of cold water into the downcomer and essentially filling it. This caused a rapid drop in the SRD reading with the return of a moderator to the downcomer (D-E) in Figure 2. During the period of time between 173 minutes after turbine trip and the 200 minute point, (E-F) at which time the high pressure injection flow was initiated, the water level in the downcomer was not in equilibrium with the water level in the reactor vessel and the SRD response did not follow that indicated by Figure 8. This situation poses the question of how to interpret the output of the proposed gauging system when the downcomer water level is not in hydraulic equilibrium with that in the core.

RECENT WORK BY THE AUTHORS

In order to better understand the response of a detector when the water level in the downcomer is not in hydraulic equilibrium with that of the core, the following experiment was conducted by the author using the reactor facilities of the Breazeale Nuclear Reactor.

A nominal 24-foot long 1.5 in. O.D. aluminum tube with a 0.049-inch wall thickness was placed inside and centered on a 24-foot long 6½ in. O.D. aluminum tube having a 5/32-inch wall thickness producing a 2.42-inch wide annulus. This annulus was used to mock up a downcomer region. This arrangement of tubes was placed in front of the Penn State Breazeale Reactor (PSBR) such that it passed 14 inches from the front row of fuel elements. (Figure 9) The reactor was operated at a power level of

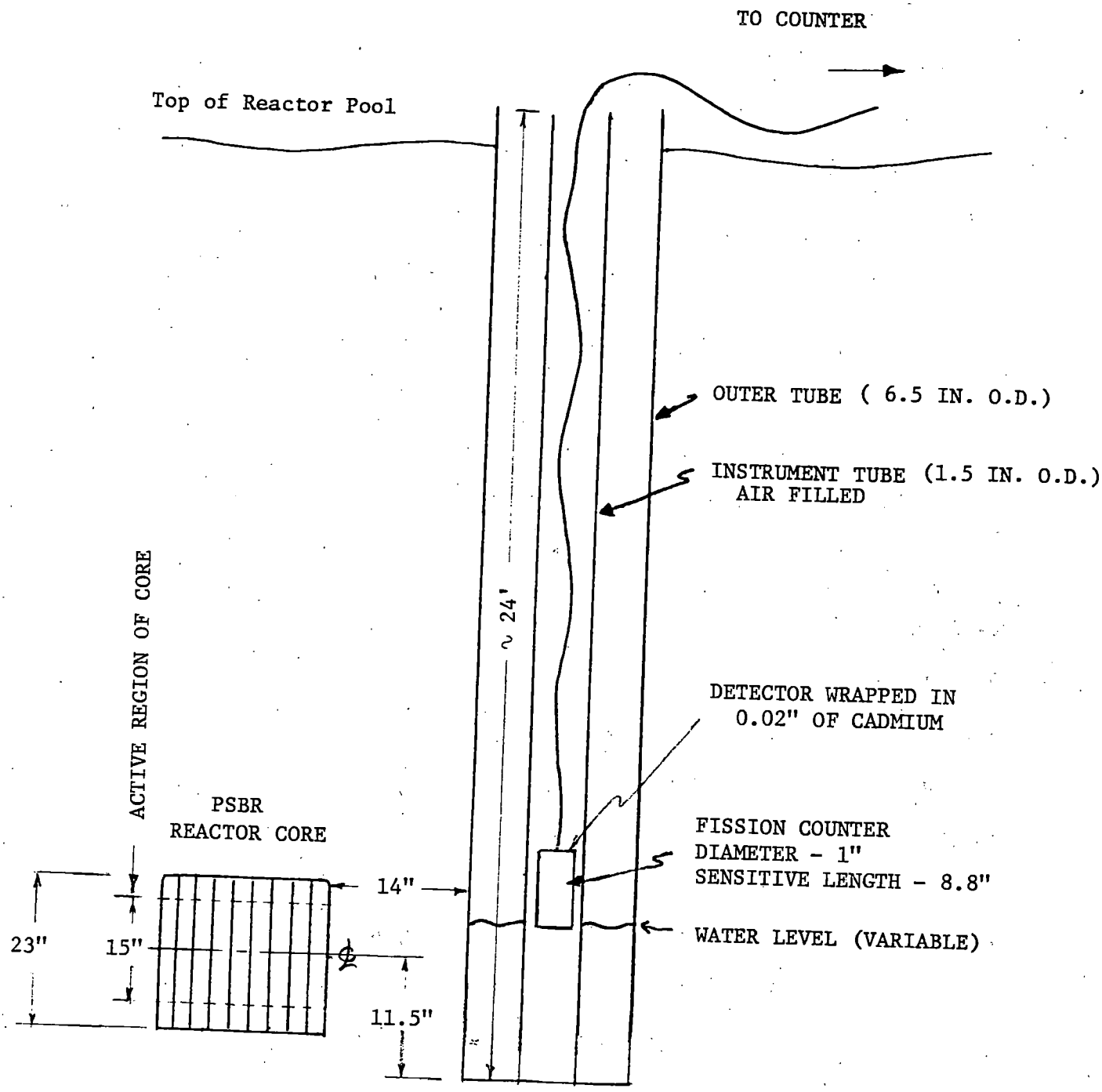

Figure 9. Equipment Arrangement for Downcomer Voiding Experiment
(not to scale)

1 kilowatt to simulate the photoneutron and fission neutron output of a recently shutdown power reactor core. A Westinghouse fission chamber, Model WL-23110, having a sensitive length of approximately 8.8 inches was moved to various vertical positions inside the air-filled inner tube for the five different water level conditions shown in Table 1.

The detector was surrounded by 0.02 inches of cadmium sheeting to screen out thermal neutrons. Thus only epicadmium neutrons were detected by epithermal fissioning of the uranium in the detector.

Figure 10 shows the detector response as a function of vertical distance between the bottom of the detector and the bottom of the inner tube for the five different water level conditions. This curve shows that for a full tube, the count rate drops off exponentially once the bottom of the detector is above the core region. A similar exponential fall-off occurs with an empty tube, but the measured fast neutron intensity is higher since the annulus moderator is missing. The fall-off is not as dramatic, indicating some epicadmium neutron streaming up the tube. For the water levels between these two extreme conditions, it can be seen that as the detector is raised for a given fixed water level, the neutron flux equals approximately that of the full tube until the top of the detector's sensitive region becomes adjacent to the water level. Then there is a slowing down in the drop-off of fast neutron intensity, approaching but not reaching that of the empty tube.

An even more interesting correlation of this data is given in Figure 11, where the detector position is fixed and the water level is varied. In this figure, the data for each detector position is normalized against data for the full tube condition. Again it is seen

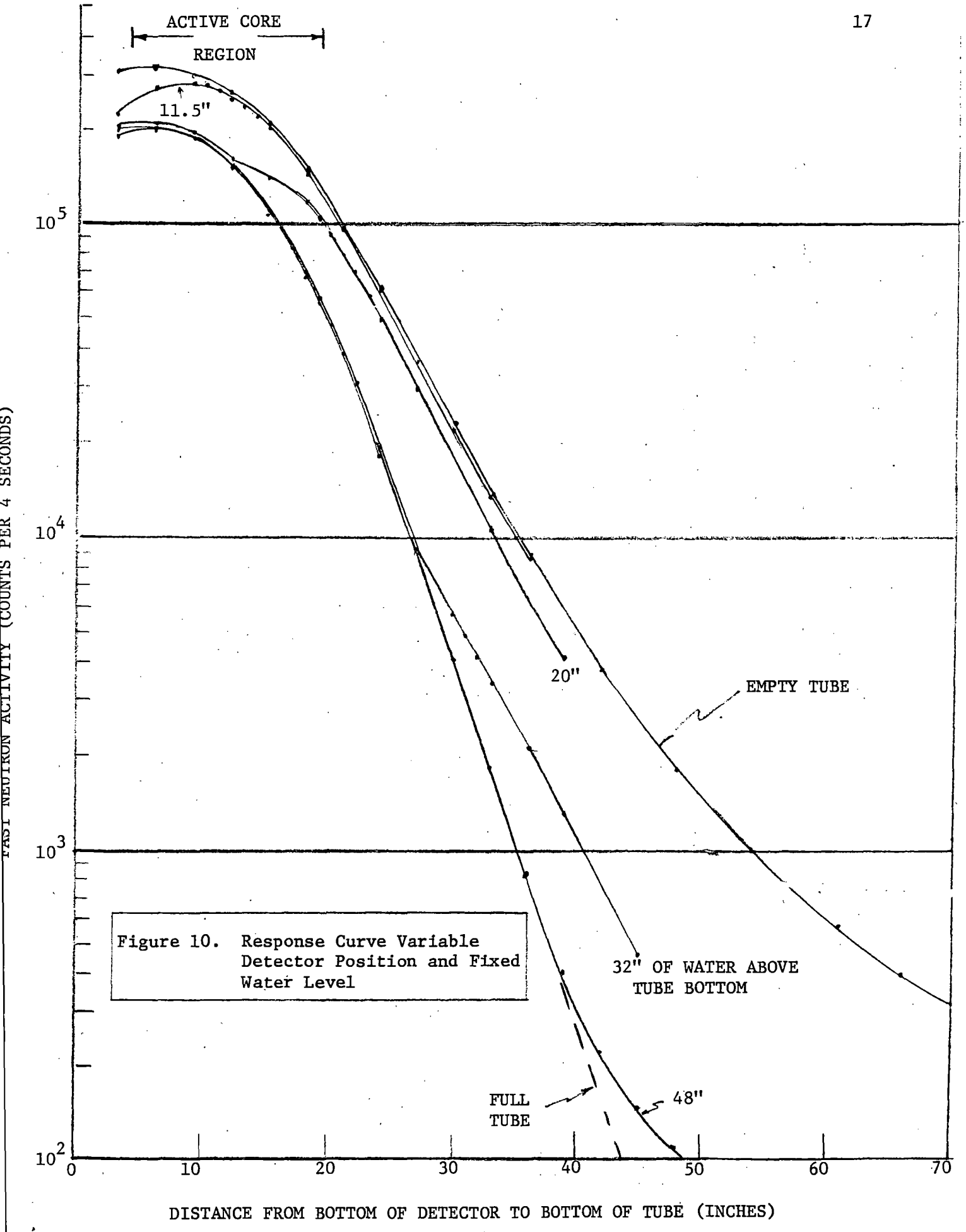

Figure 10. Response Curve Variable Detector Position and Fixed Water Level

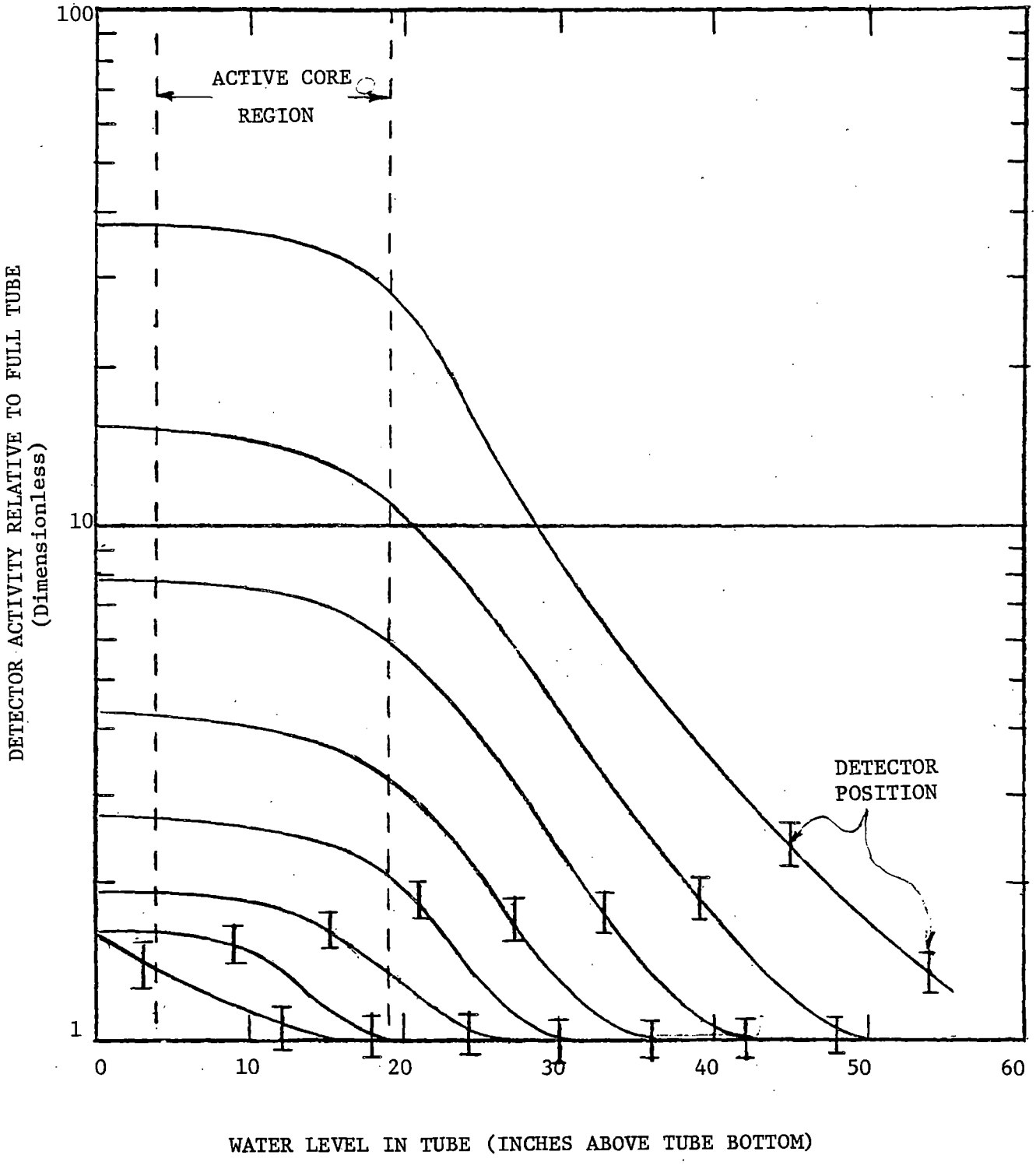

Figure 11. Relative Response Curve for Variable Water Level and Fixed Detector Position

Table 1

Water Level Conditions in Annulus Tested
in Downcomer Voiding Mockup

Run #	Inches of Water in Annulus	Water Level Condition
1	0	No water in annulus
2	11.5	Adjacent to core centerline
3	20	Adjacent to top of core
4	32	12 inches above top of core
5	48	28 inches above top of core

that the detector starts seeing a change in fast neutron intensity as the water level drops to a point adjacent to the top of the sensitive volume of the detector. There is an exponential increase in fast neutron intensity until the water level reaches the top of the active core region then it begins to level off reaching the maximum value with complete voiding of the annulus. It can be seen that the higher the detector is above the core, the greater is the change in signal between the full and empty tube conditions.

CONCLUSIONS

These test results demonstrate to the authors that voiding of only the downcomer region of a reactor will produce a distinctly different fast neutron detector response than that demonstrated by the SRD under hydraulic equilibrium during TMI-2 core voiding. In downcomer voiding, the neutron source strength and source-detector geometry will remain essentially constant. Thus there will be a significant rise in the measured fast neutron intensity once the water level falls below the top of the sensitive region of the detector. This occurs because moderator is starting to be removed from between the detector and the sources of fast neutrons. As the water level falls below the detector, there is an exponential rise in the fast neutron intensity as more moderator is being removed. This rise slows as the water level drops to the core region, reaching a maximum value at the point at which the downcomer is completely voided. This detector response is different from the case illustrated from TMI-2, Figure 8. In this latter case, there is a similar initial exponential rise in the fast neutron intensity as moderator is being removed from the core region, but this effect is observed starting when the water level is still well above the detector. In addition, as the water level drops below the detector, the fast neutron intensity began to drop off as the sources of fast neutrons began to move away from the detector with decreasing water level. This drop-off was caused by the removal of sources of photoneutrons formed in the water adjacent to the detector as well as a drop in core multiplication. Thus under conditions of hydraulic equilibrium, for at least those detectors located adjacent to the core, one should obtain a peak in the

fast neutron intensity response as the water level deops past each of the vertical detectors. No such peak should occur from the voiding or flooding of the downcomer alone. The computer processing of signals from a vertical series of detectors should be able to use these differences to determine changes in liquid level in both the downcomer region and the core region.

FUTURE WORK

An experimental apparatus designed to more closely simulate the core, downcomer, and annulus regions of an actual power reactor is now under construction for testing at the Breazeale Nuclear Reactor. This apparatus will allow for the voiding or partial voiding of one or both of two different regions and for the formation of varying amounts of homogeneous voids in these regions. This apparatus will contain a vertical instrument tube containing several fission detectors mounted at various positions relative to the core. Various detector packages will be tested to optimize the screening out of low energy neutrons.

Methods of on-line data processing will be developed to synthesize the output signals of the detectors to determine level or density changes. A computer model of the test apparatus, coupled with the reactor core, is being developed to guide the experimental program.

ACKNOWLEDGMENTS

This paper was prepared in part with the support of the U.S. Nuclear Regulatory Commission (NRC) under grant No. NRC-G-04-81-024. The opinions, findings, conclusions, and recommendations expressed herein are those of the authors and do not necessarily reflect the views of the NRC.

REFERENCES

1. "Analysis of Three Mile Island - Unit 2 Accident," NSAC-80-1, NSAC-1 Revised, March 1981.

2. "Neutron Transport Calculations," a NSAC Draft Report, Undated.

3. "Calculations of the Core Temperature Transient during the Early Phase of Core Uncovering at TMI-2," a NSAC Draft Report, December 1980.

Water Spray Studies

S.Y.Lee, S.G.Bankoff, R.S.Tankin, M.C.Yuen

Northwestern University

Water spray injected into steam environment

Scope of the study :

1. Object : Study the behaviour of water spray in steam.
2. Parameters : a) Ambient pressure
   b) Injection pressure (water flow rate)
   c) Subcooling temperature
   d) Compare with the case of air environment
3. Experiment : Holographic method is used to study
   a) Effect on the drop size distribution
   b) Effect on the spray angle
4. Model study

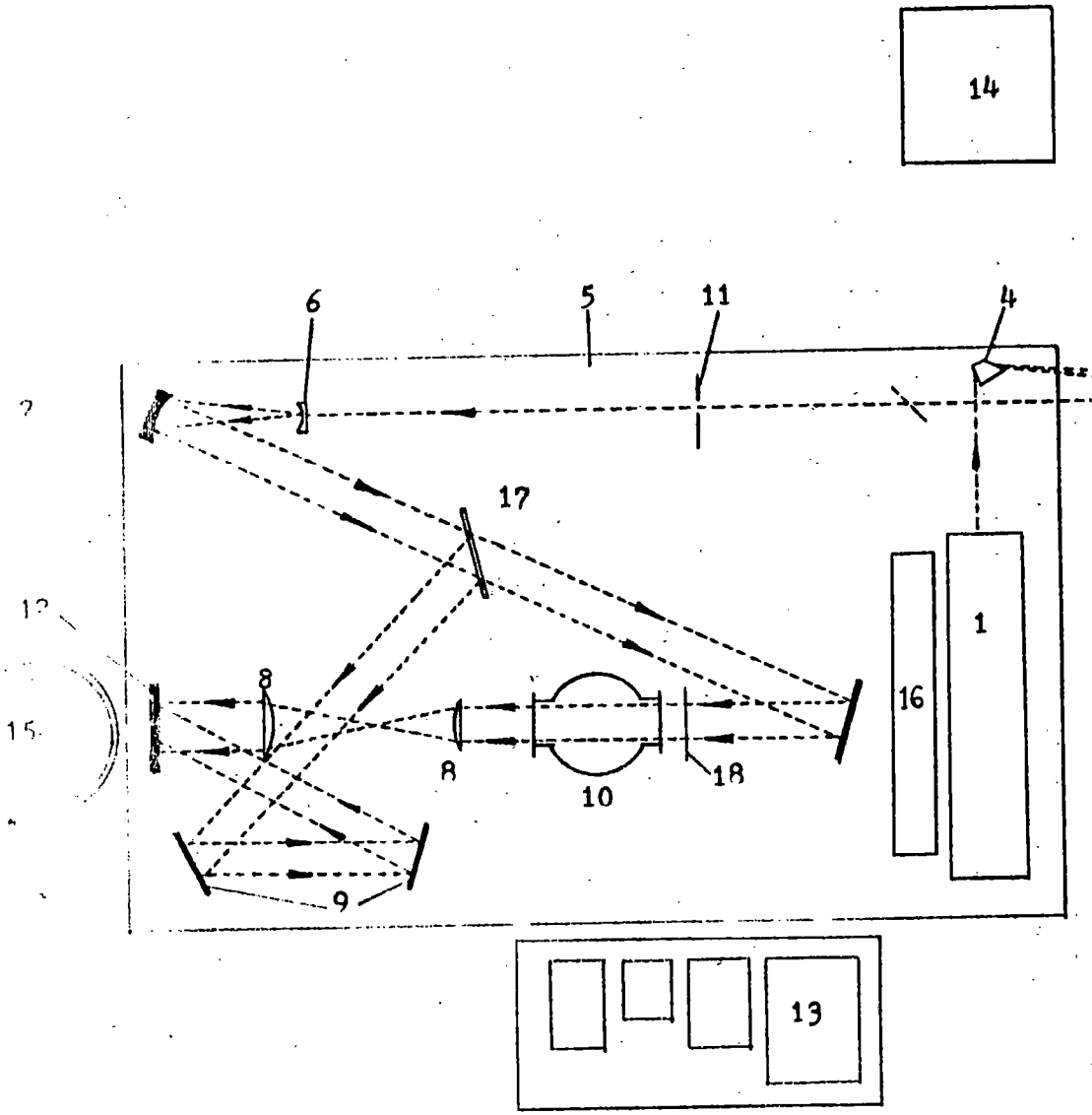

1. Nd:YAG laser
2. Folding mirror
3. Infrared trap(1.06μ)
4. Prism
5. Vibration isolated table
6. Plano-concave lense
7. Off-axis paraboloid mirror
8. Focusing lenses
9. Plane folding mirrors
10. Test section
11. Variable iris stop
12. Holographic plate
13. ELN line-width narrower
14. Laser power supply
15. Turn table
16. He-Ne laser(for reconstruction)
17. Beam Splitter
18. Ground glass diffuser

Fig.Ⅲ-3 Schematic diagram of OFF-AXIS hologram

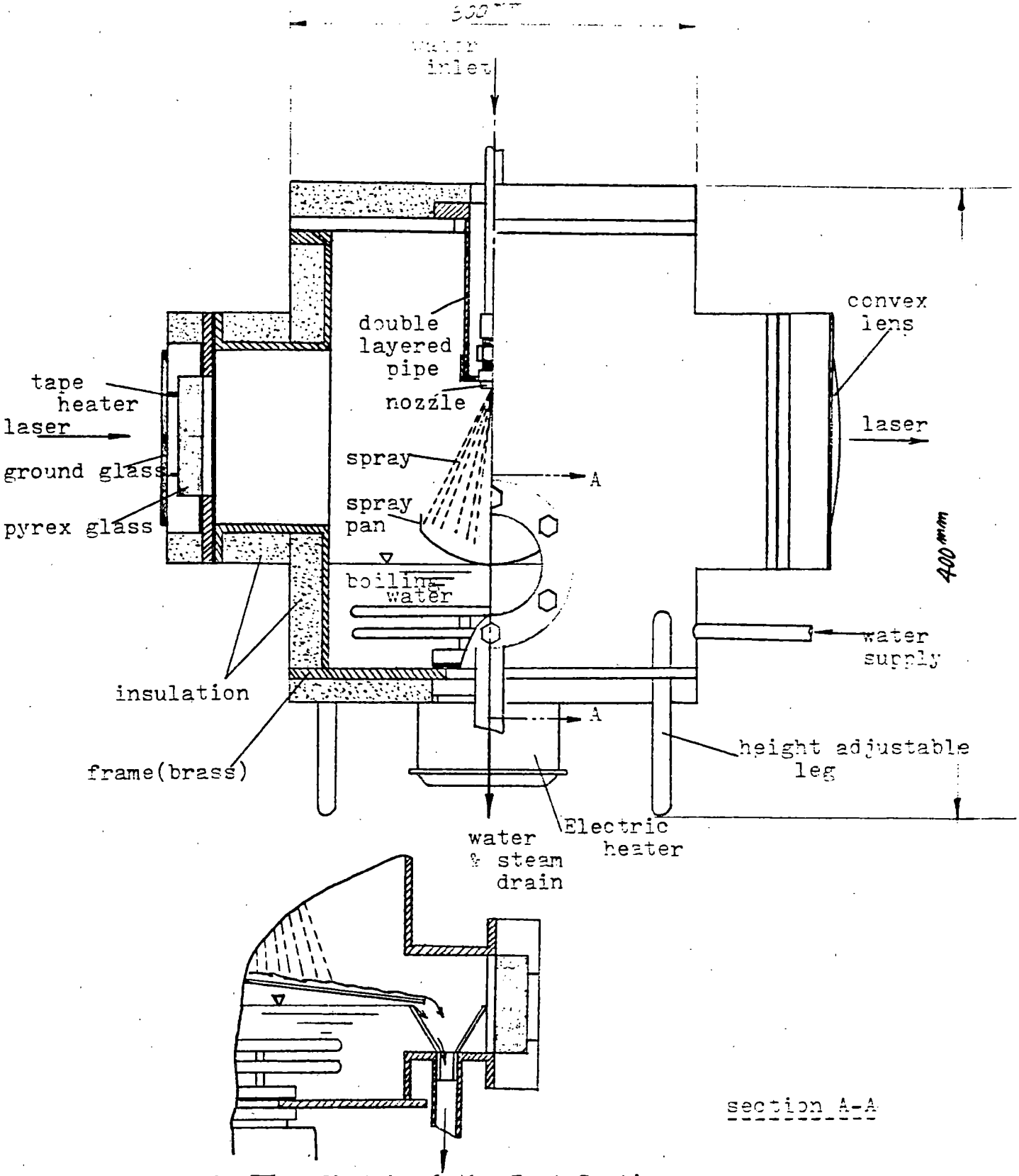

Fig.Ⅲ-2 Sketch of the Test Section

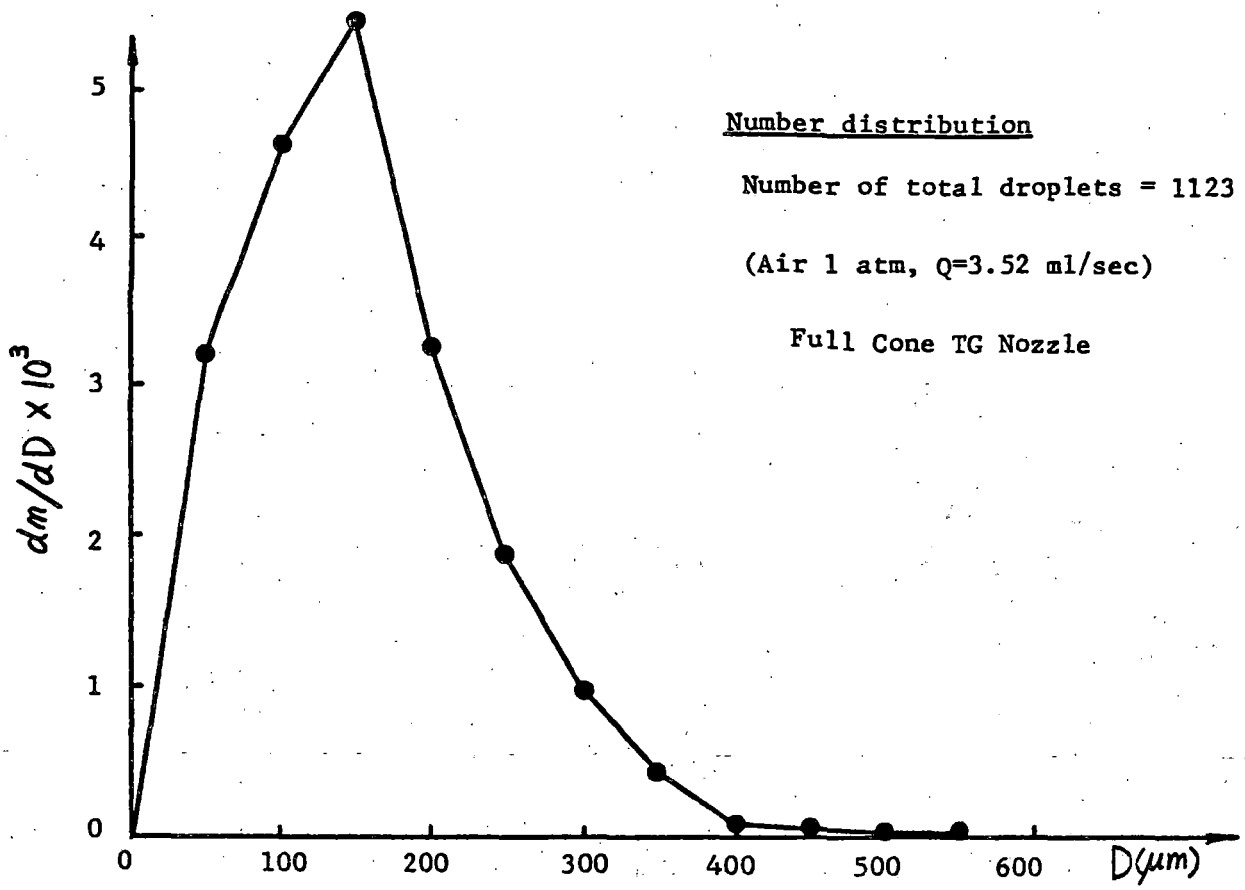

Number distribution

Number of total droplets = 1123

(Air 1 atm, Q=3.52 ml/sec)

Full Cone TG Nozzle

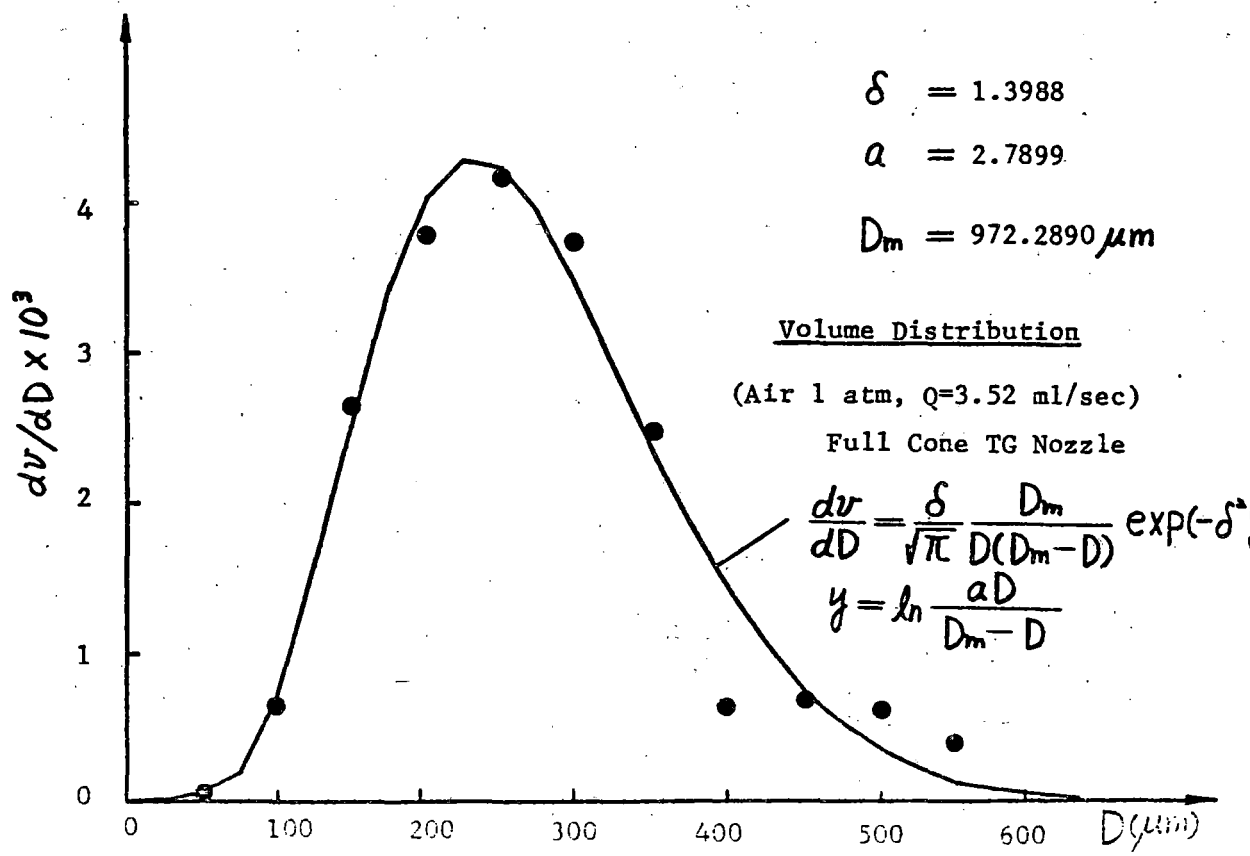

$\delta = 1.3988$

$a = 2.7899$

$D_m = 972.2890\,\mu m$

Volume Distribution

(Air 1 atm, Q=3.52 ml/sec)

Full Cone TG Nozzle

$$\frac{dv}{dD} = \frac{\delta}{\sqrt{\pi}} \frac{D_m}{D(D_m - D)} \exp(-\delta^2 y^2)$$

$$y = \ln \frac{aD}{D_m - D}$$

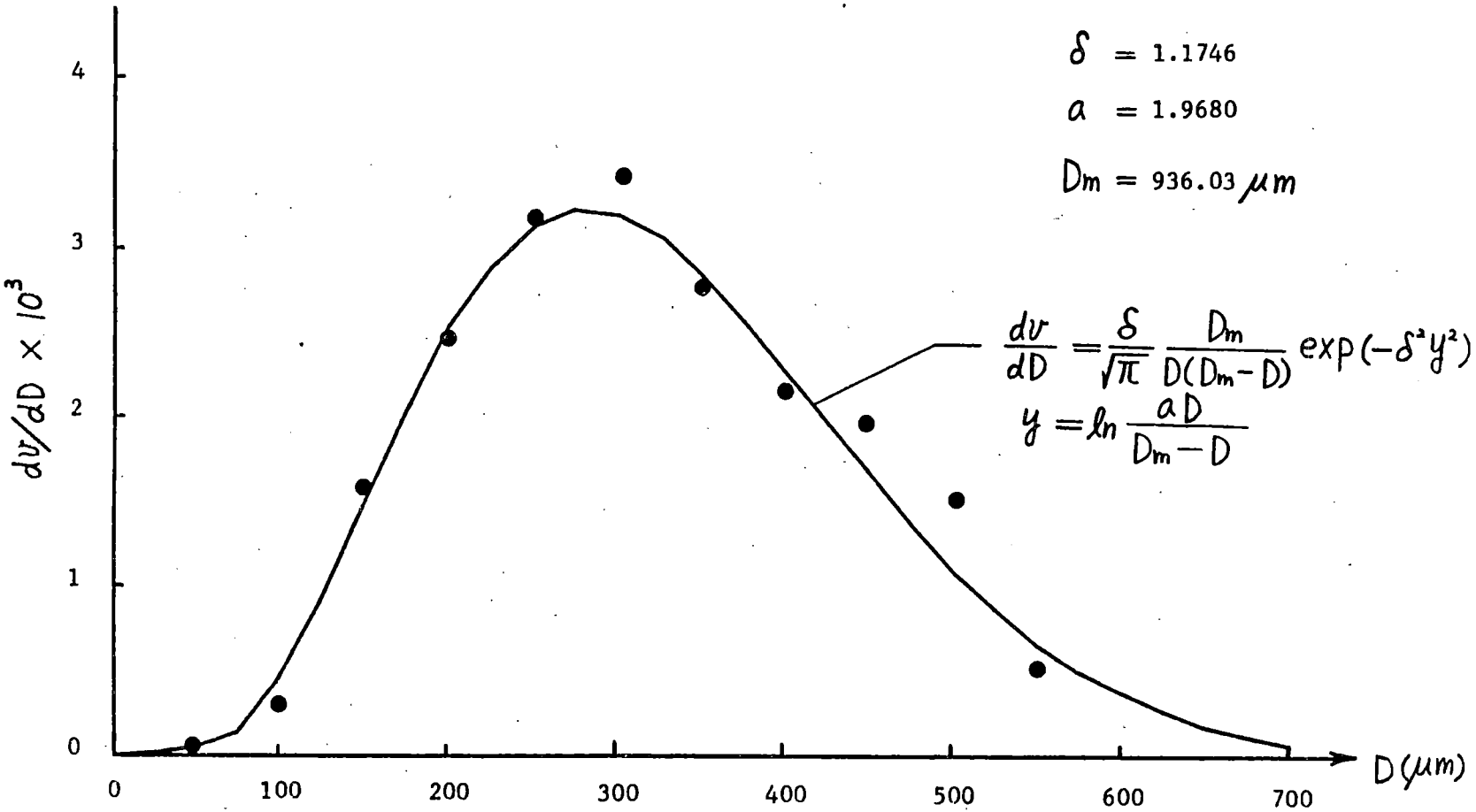

Volume distribution (Air 1 atm, Q=2.23 ml/sec) Full Cone TG Nozzle

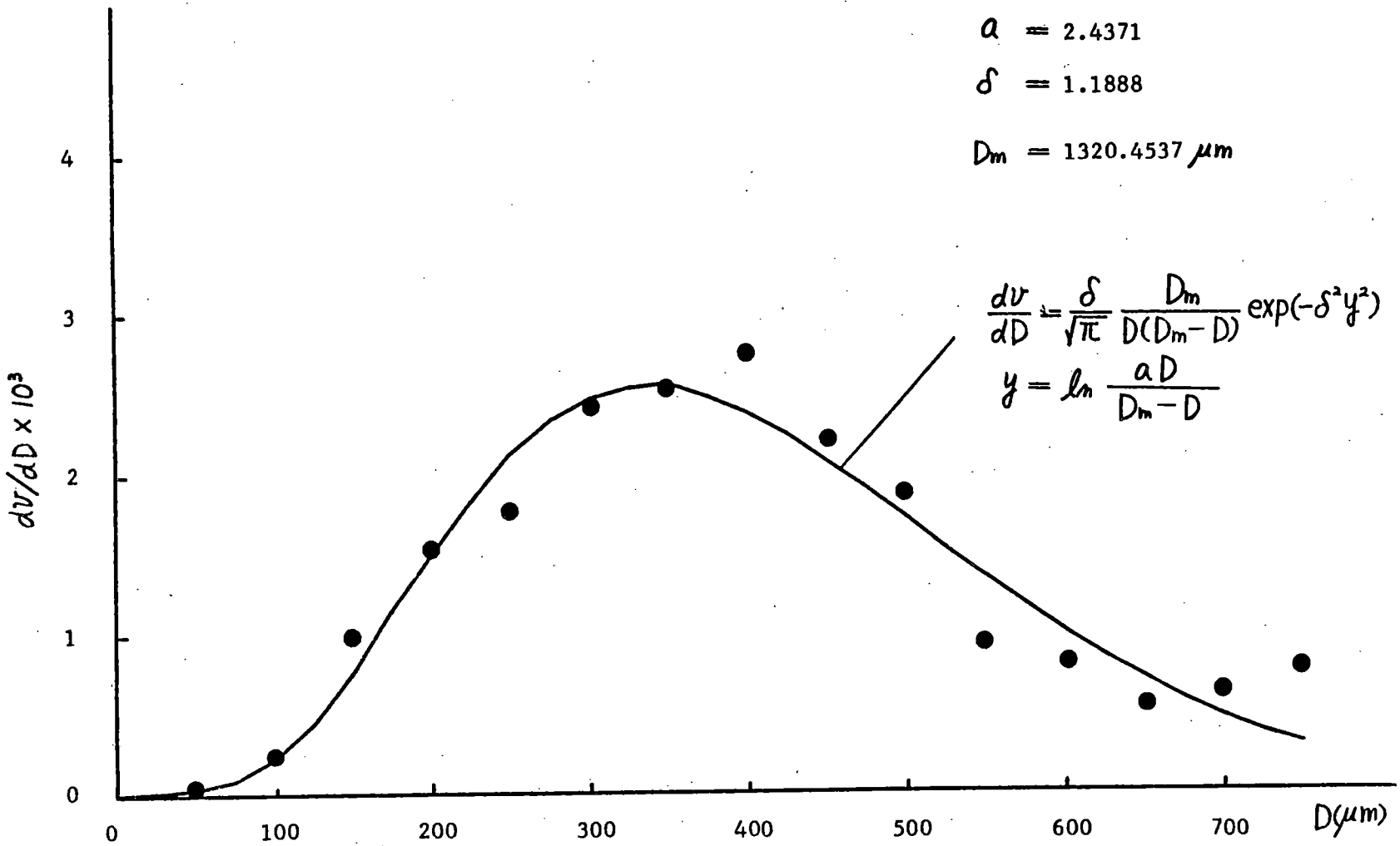

Volume distribution (Saturated steam 1 atm, Ts=100 C, Ti=24.5 C, Q=2.23 ml/sec)

Full Cone TG Nozzle

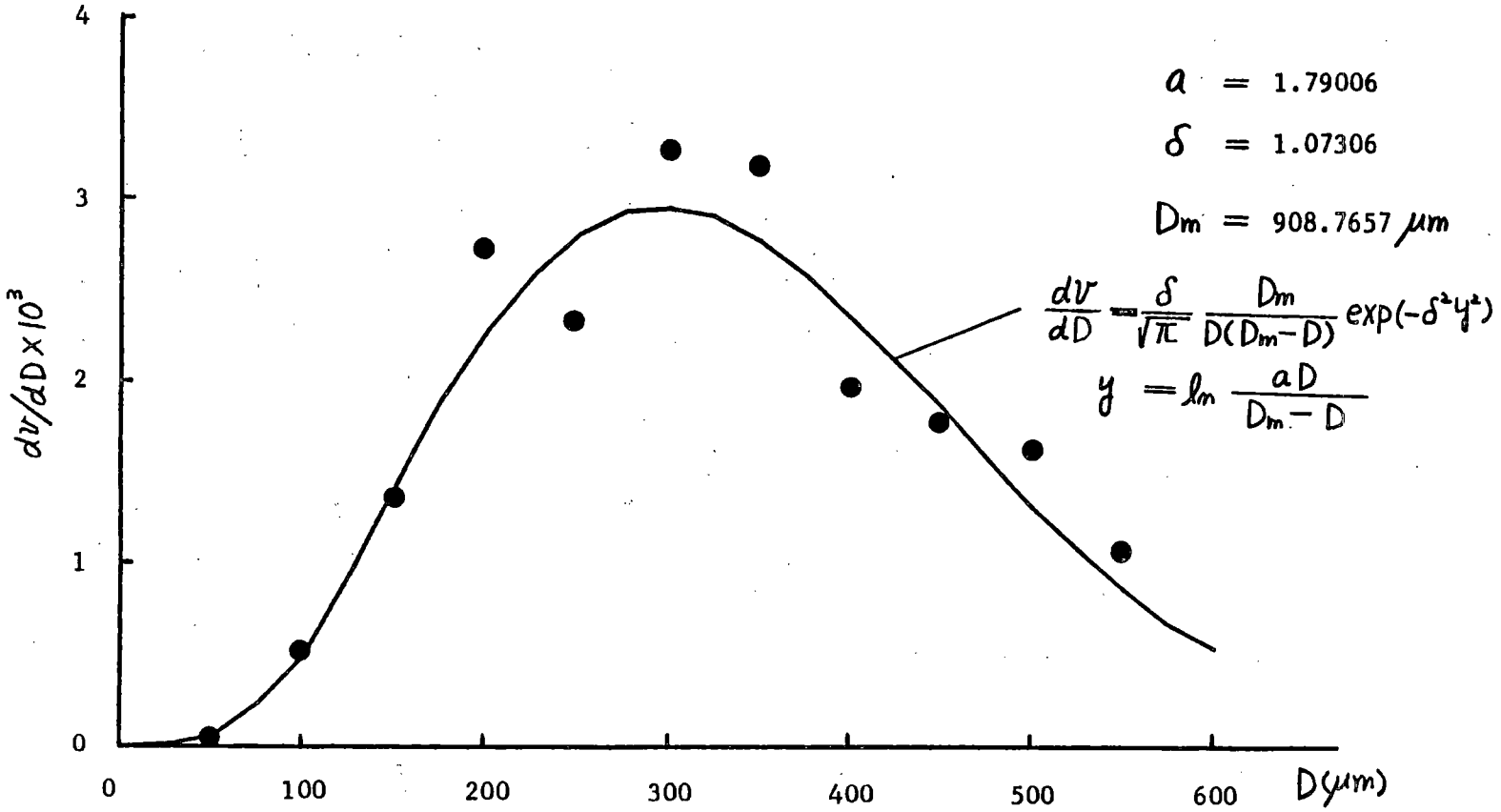

Volume distribution (Saturated steam 1 atm, Ts=100 C, Ti=24.5 C, Q=3.52 ml/sec)

Full Cone TG Nozzle

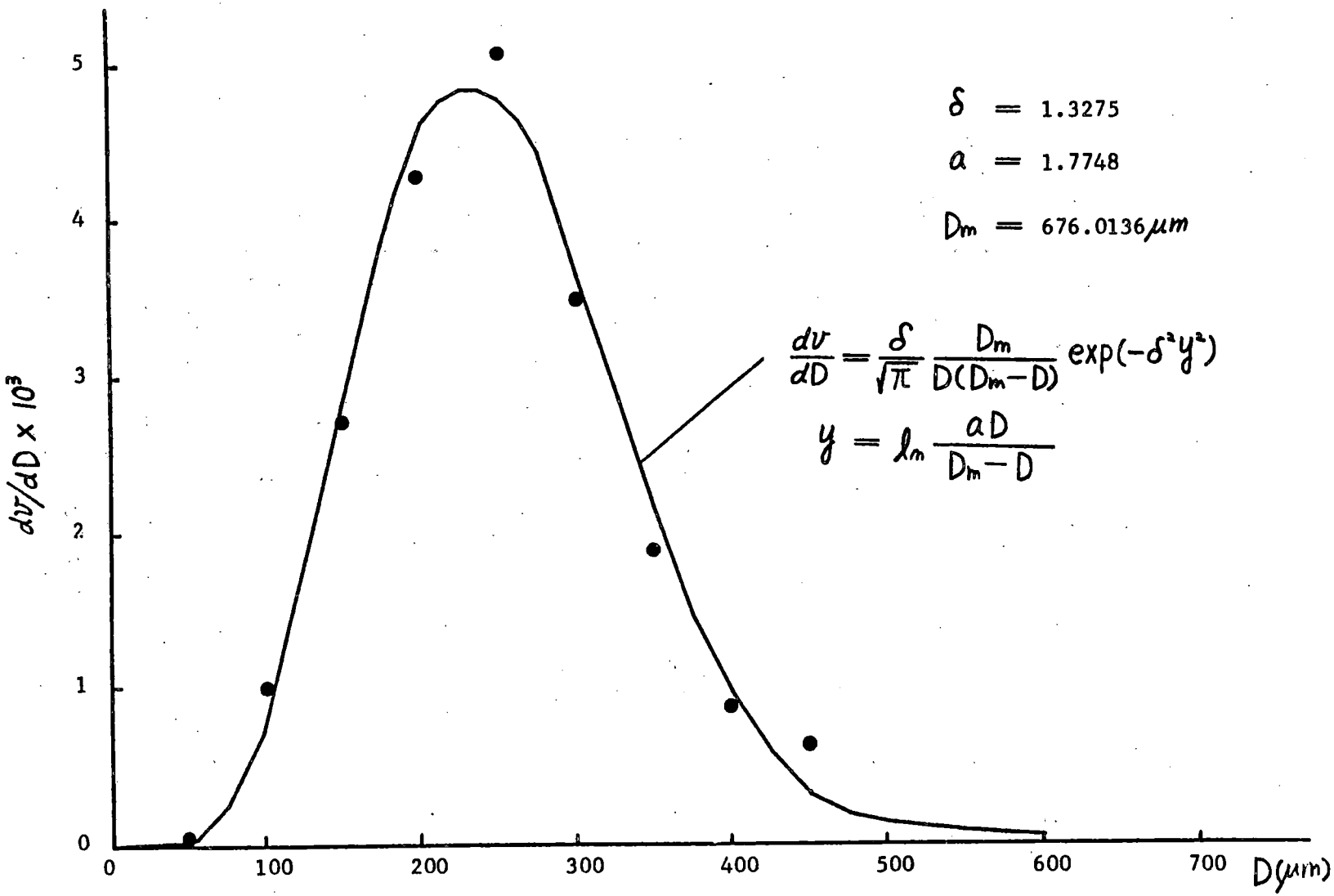

Volume distribution (Saturated steam 1 atm, Ts=100 C, Ti=61.1 C, Q=3.52 ml/sec)

Full Cone TG Nozzle

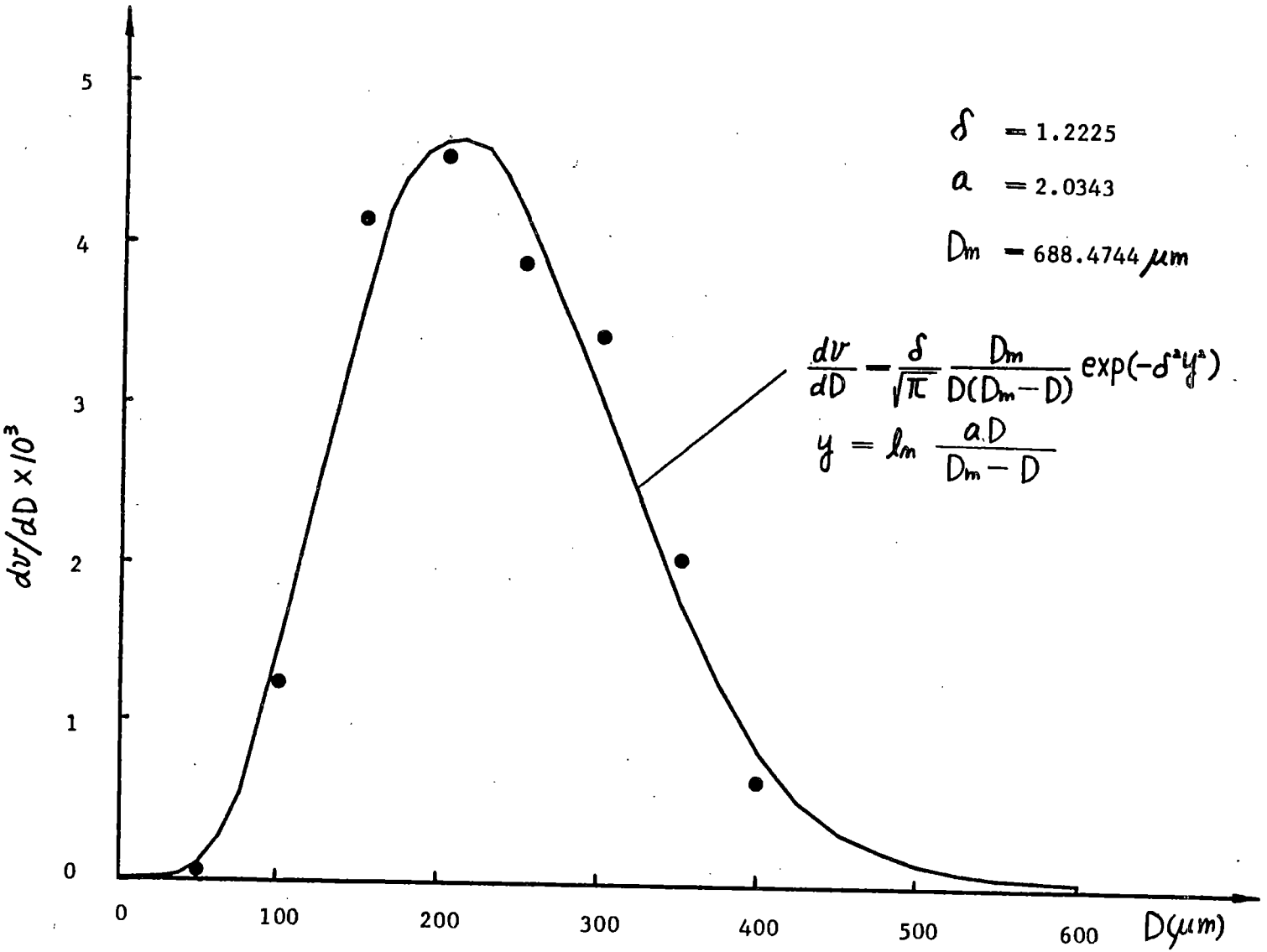

Volume distribution (Air 3 atm, Q=3.52 ml/sec) Full Cone TG Nozzle

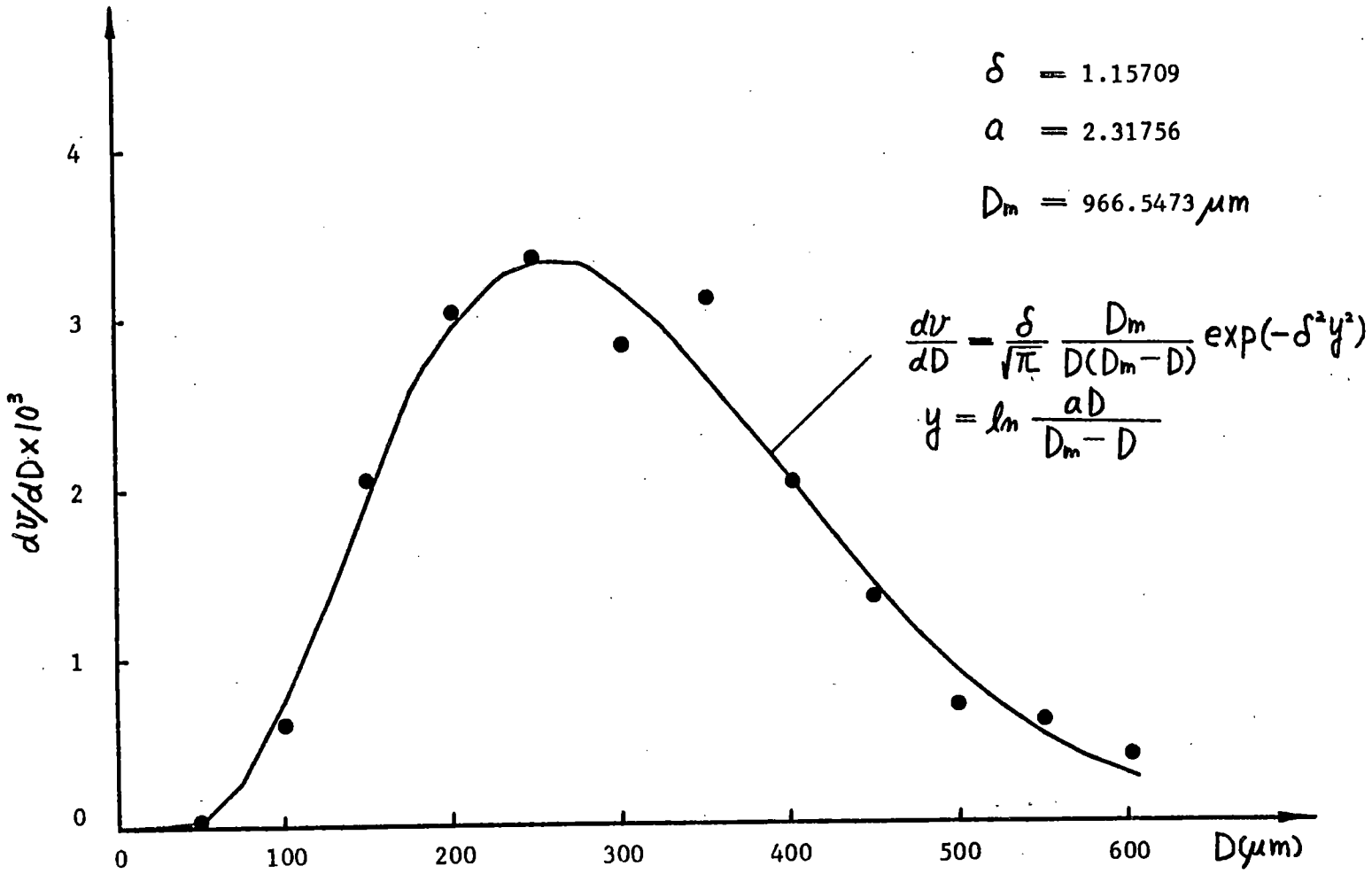

Volume distribution (Saturated steam 3 atm, Ts=133.98 C, Ti=24.5 C, Q=3.52 ml/sec)

Full Cone TG Nozzle

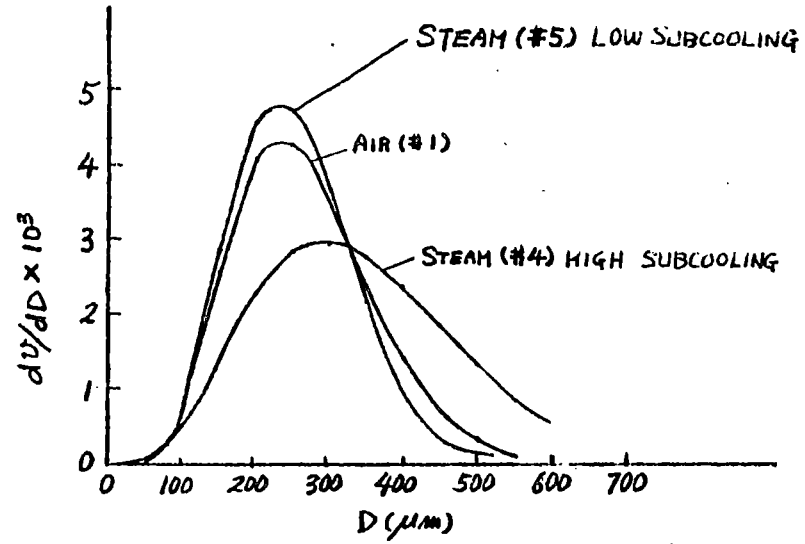

(a) COMPARISON BETWEEN STEAM & AIR ENVIRONMENT ($\dot{Q} = 3.52 ml/s$), 1 ATM

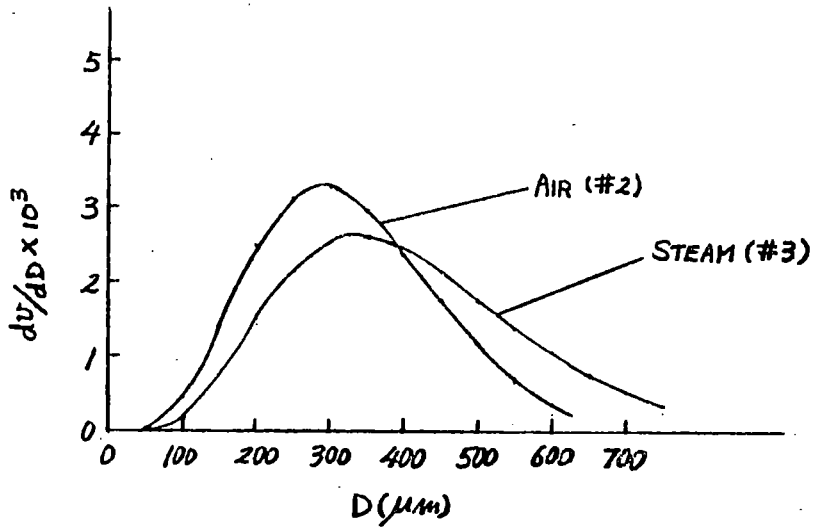

(b) COMPARISON BETWEEN STEAM & AIR ENVIRONMENT ($\dot{Q} = 2.23 ml/s$), 1 ATM

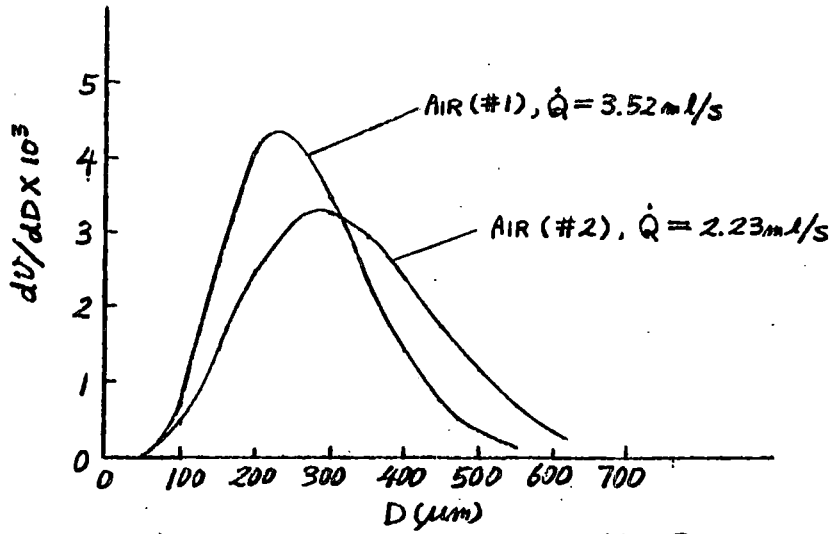

(c) EFFECT OF FLOW RATE (AIR ENVIRONMENT)

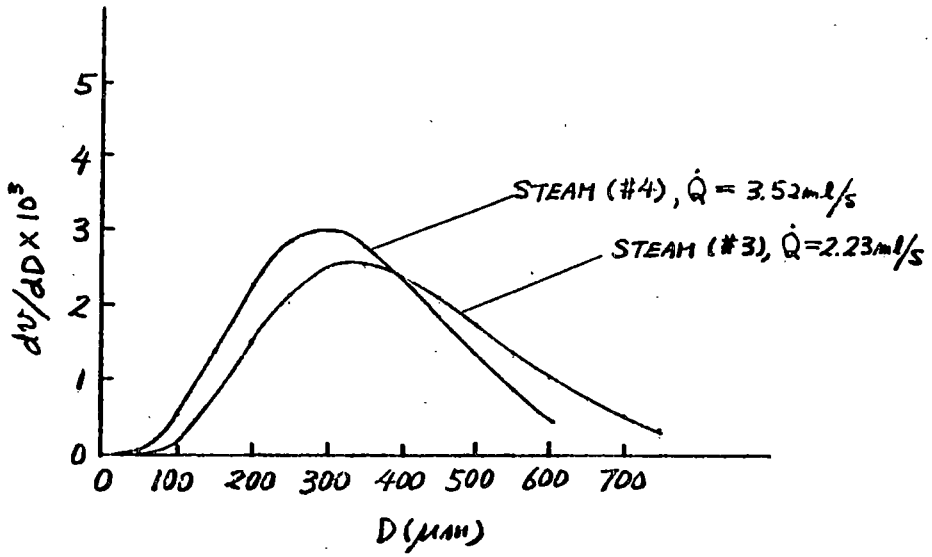

(d) EFFECT OF FLOW RATE (STEAM ENVIRONMENT)

FIG. 13

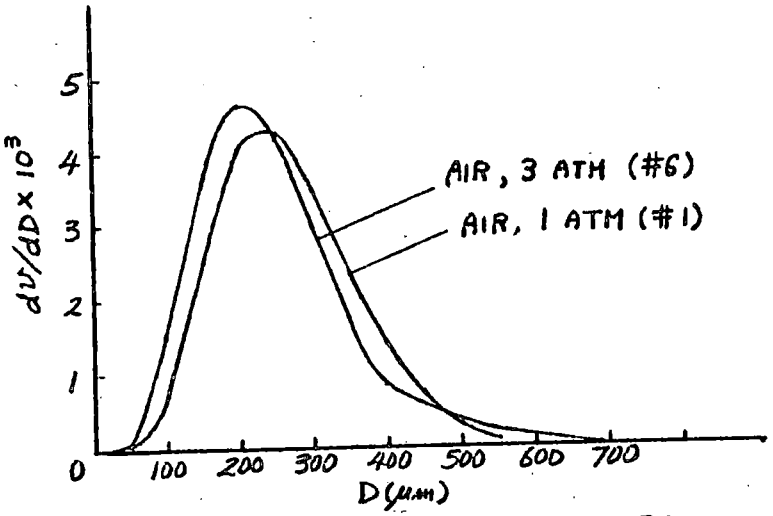

(e) EFFECT OF AMBIENT PRESSURE (AIR ENVIRONMENT, $\dot{Q} = 3.52$ ml/s)

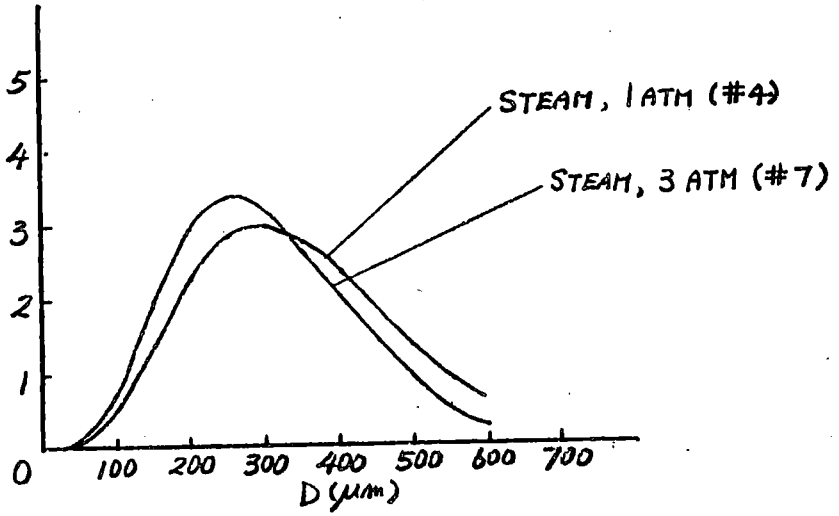

(f) EFFECT OF AMBIENT PRESSURE (STEAM ENVIRONMENT, $\dot{Q} = 3.52$ ml/s)

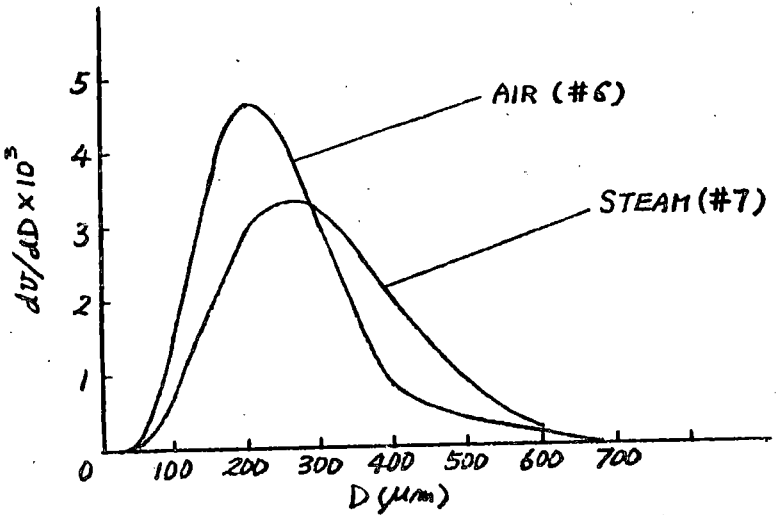

(g) COMPARISON BETWEEN STEAM & AIR ENVIRONMENT ($\dot{Q} = 3.52$ ml/s), 3 ATM

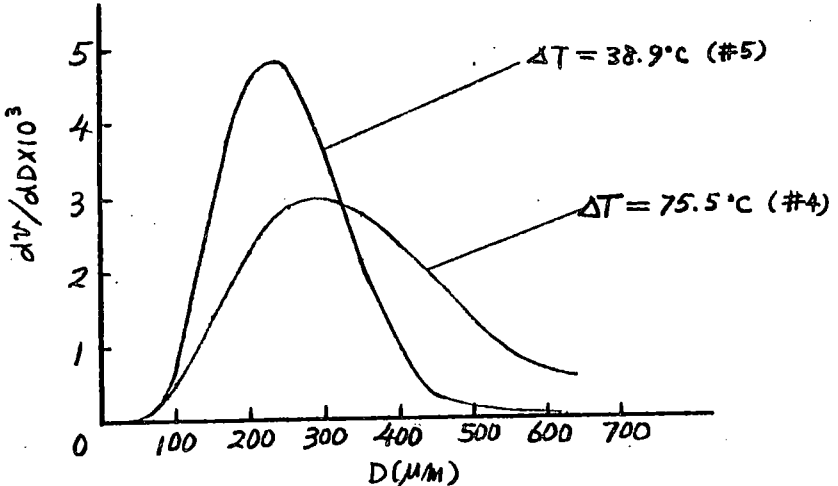

(h) EFFECT OF SUBCOOLING TEMPERATURE (STEAM ENVIRONMENT, 1 ATM, $\dot{Q} = 3.52$ ml/s)

FIG. 13 (CONT'D)

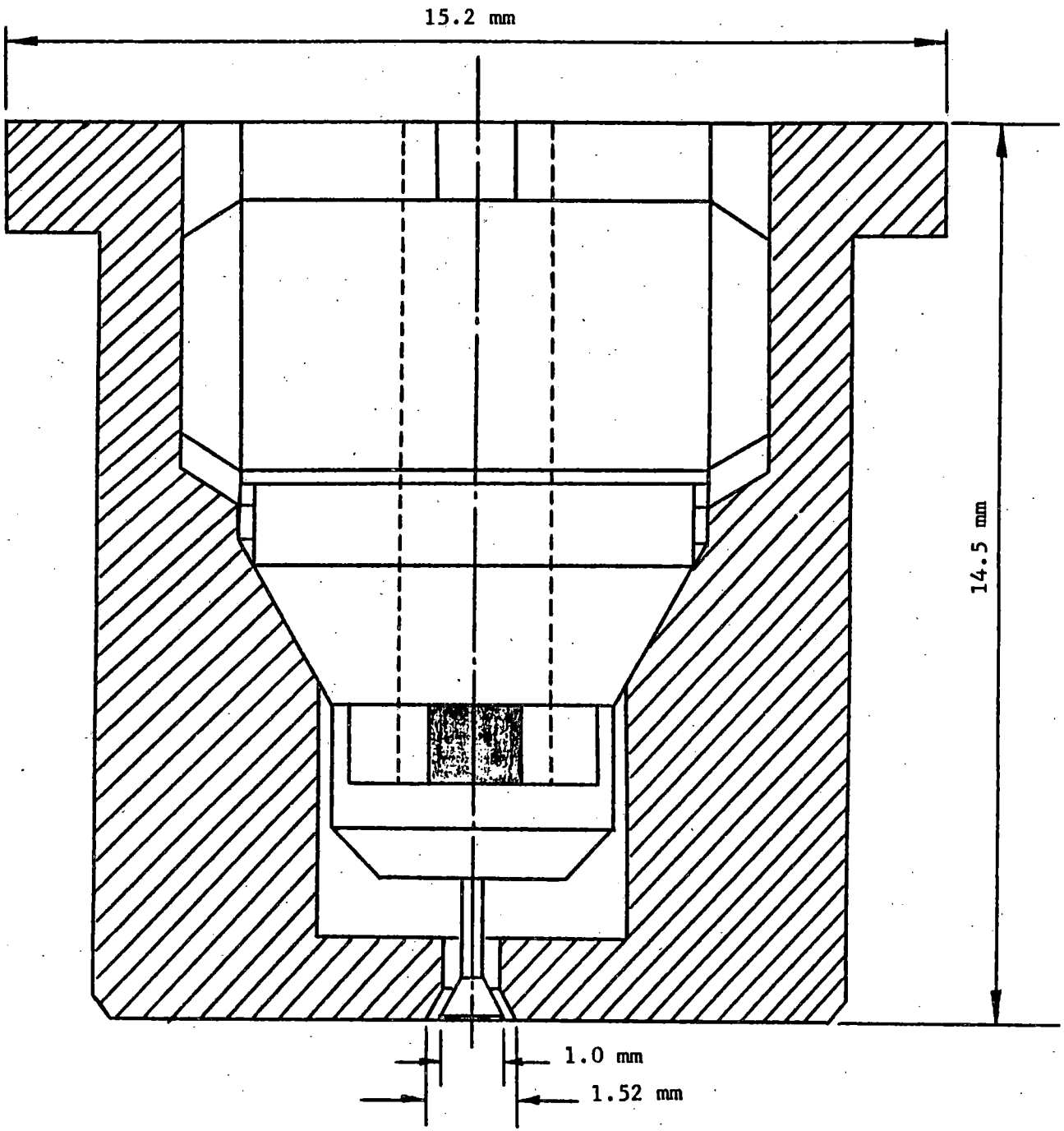
15.2 mm
14.5 mm
1.0 mm
1.52 mm

Conclusion

1. Most of the heat transfer occurs at sheet portion.
   (Before breakup occurs)
2. Breakup is important for the spray angle.
   (Breakup is earlier in case of steam environment)
3. The small droplets tend to deflect inwards.
4. Drop sizes : a) More uniform and smaller when ambient and injection pressure increases.
   b) Larger and less uniform in steam environment.
5. Shape of the spray :
   a) Spray angle reduces in case of condensation for full cone nozzle.
   b) When subcooling is small, the spray outline shape in steam is similar to the case of air environment.

Two-Phase Performance Characteristics of the LOBI Pump

L. Piplies, W. Kolar

Commission of the European Communities
EURATOM Joint Research Centre - Ispra Establishment
LOBI Project, Heat Transfer Division
I 21020 ISPRA/Varese (I)

Abstract

A comprehensive test programme has been carried out to determine the two-phase pump performance characteristics of the LOBI pump which has a specific speed of $n_q = 29.2\ min^{-1}$ (DIN 24260) or $N_s = 1509\ min^{-1}$ (american units). Two pumps of this type serve as primary pumps in the LOBI test facility.

Results for the pump head are presented in nondimensional and homologous form for pressures of 75 and 70 bars and for different void fractions.

Paper presented at the 9th Water Reactor Safety Research Information Meeting, October 26-30, 1981, Gaithersburg MD/USA.

1. Introduction

A comprehensive test programme has been carried out to determine the two-phase pump performance characteristics of the LOBI pump. The tests were executed at Westinghouse Canada Limited (WCL) under contract to the Commission of the European Communities (CEC). The evaluation was performed at the Joint Research Centre of the CEC, Ispra Establishment.

The LOBI[1)] test facility is the only high pressure integral system test facility within the European Communities, built and operated in the Joint Research Centre Ispra, Italy, in the framework of an R&D contract between the Bundesminister für Forschung und Technologie (BMFT), Bonn, Federal Republic of Germany, and the Commission of the European Communities.

In the experiments the thermal-hydraulic behaviour of the facility during a transient, resulting from a simulated loss-of-coolant accident (LOCA) is investigated to provide an experimental basis for analytical model development and code verification.

A view of the facility is given in Fig. 1. It is a 1/700 scale model of a four-loop 1300 MWe PWR and has two primary loops, the intact loop representing three loops, and the broken loop representing one loop of a PWR. The reactor pressure vessel model contains an electrically heated rod bundle with 64 rods and a heated length of 3.9 m. The nominal heating power is 5.3 MW. Each of the two primary loops contains a steam generator and a pump. These two pumps are identical and the different

---

1) LOBI = Loop Blowdown Investigations

mass flows are established by different pump speeds. The test pump with which the two-phase pump tests were performed is identical to these two units.

2. Rated Values and Specific Speed

The LOBI pump is especially designed for severe blowdown conditions, consequently the mechanical efficiency η_m is considerably lower than that for normal pumps. This means that the overall efficiency

$$\eta = \eta_m \cdot \eta_i$$

differs significantly from the hydraulic efficiency η_i. Hence the rated values of the pump were taken at the point of maximum hydraulic efficiency η_i and not at the point of maximum overall efficiency η, see Fig. 2.

The definitions used here are

$\eta_m = P_H/P$

$\eta_i = P_Q/P_H$ with

P_H ... Hydraulic Power,

P ... Shaft Power,

P_Q ... Power corresponding to pump head.

For a volume flow of $Q_R = 0.02788\ m^3/s$[1] the rated value

---

1) $Q = 0.02788\ m^3/s$ is the volume flow of the pump in the intact loop of the LOBI facility at nominal conditions ($\rho = 747\ kg/m^3$). Note that the rated values H_R and N_R are not the operating values at nominal conditions in the LOBI facility.

for the head is H_R = 139.9 m and the rated value for the speed is N_R = 7120 min^{-1}.

Using these values the specific speed is

$$n_q = 29.2\ min^{-1}$$ (according to DIN 24260).

Using the units $[\ Q_R\ ]$ = US gallons/min and $[\ H\ ]$ = feet the specific speed is

$$N_S = 1509\ min^{-1}.$$

3. Evaluation of the Experimental Results

The experimental programme comprised besides some specific experiments on the influence of pressure and void fraction a thorough investigation of five pump characteristics charts, called here full flow maps (FFM) at different pressures and void fractions, see Fig. 3. It is believed that this covers the full range of conditions of pressure and void fraction to be expected during a loss-of-coolant accident.

In performing experiments where the void fraction has to be kept constant the homogeneous void fraction is often used. This is due to the fact that the homogeneous void fraction (or the homogeneous density) can be relatively easily achieved in an experiment, by controlling for example, the liquid mass flow and the heating power. Furthermore, this quantity can be measured reasonably accurately. The LOBI pump tests were performed in this manner, see Fig. 3.

In performing the evaluation of two-phase pump experiments the question arose upon what void fraction or density (for calcula-

ting pump head and volumetric flow) this evaluation should be based. The calculated homogeneous or the actual measured density at inlet or outlet, or alternatively an average of these, can be chosen.

For the evaluation of the LOBI pump tests, pump inlet[1)] conditions were selected. To determine what density should be used plots like Figures 4 and 5 (which are valid for FFM 3) were prepared. In Fig. 4 the homogeneous void fraction VOIDH and the actual void fraction VOIDD (calculated from measured density) are plotted as a function of pressure. It can be seen that in the VOIDH plot all measurement points are close together, whereas the VOIDD plot shows considerably more spread in the VOIDD distribution due to the different flow patterns at pump inlet[2)], see also Fig. 5. It was decided to use the measured density for calculating pump head and volumetric flow. As a consequence all measurement points have been sorted using a range of VOIDD as sorting parameter.

4. Results

In the following, results for the two-phase pump head characteristics for pressures of 75 and 70 bars are presented.

For comparison the single-phase homologous head curves are shown in Fig. 6.

---

1) The meaning of "suction" and "discharge" does not change. For positive flow: suction is "inlet". For negative flow: discharge is "inlet".

2) The suction pipe is vertical, the discharge pipe is horizontal.

FFM 2

Figures 7 and 8 show the results for FFM 2. This is the flow map with the lowest void fraction, where the sort range of VOIDD is 0.0/0.2. Fig. 7 shows the curves for the locked rotor and for positive speeds. The same measurement points appear in Fig. 8 in dimensionless form. The symbols A, B ... refer to the definition given by Stepanoff [1] for the different zones of pump operation with the exception that in all plots (in this paper) the points of regions C and D are marked as C and those of regions G and H are marked as H.

In the homologous curves small letters signify $h/\alpha^2 = f(v/\alpha)$, whereas capital letters mean $h/v^2 = f(\alpha/v)$.

In Fig. 8 for comparison the single-phase curve is added and it can be seen that for VOIDD = 0.2 the head degradation in the pump region is small.

FFM 1

Figures 9 ... 12 describe FFM 1 where the void fraction range is VOIDD = 0.3/0.4 with additional points for VOIDD = 0.2/0.3.

Fig. 10 shows that a substantial head degradation occurs for VOIDD between 0.3 and 0.4. Here in region "a" the difference between points with VOIDD = 0.30/0.35 and those with VOIDD = 0.35/0.40 is made evident. It can be clearly seen that the points for VOIDD = 0.35/0.40 show the stronger degradation, thus demonstrating the consistency of the measurements.

For the same flow map the curves for negative speeds are plotted in Figures 11 and 12. The region "f" would not be necessary as input data in performing code calculations for LOCA analysis. However, the measurement points in the region "f", which, provided the volume flows are not too small, can be obtained relatively easily, can help in fitting a curve through the measurement points in the region "c/d". This is particularly useful when the number of measurement points at small v/α values seems to be insufficient. A suitable example for this is also Fig. 17.

FFM 3

The strongest head degradation was observed in FFM 3, for which examples are given in Figures 13 to 17. The nominal value of VOIDD here is 0.75. The head versus volume flow curves for locked rotor and a positive speed of 3250 min^{-1} are shown in Fig. 13, whereas Fig. 14 shows the measurement points for positive speeds of 6500 and 8450 min^{-1}. In the pump region a particularly large head degradation occurs. Fig. 15 shows the corresponding homologous curves. The results for negative speeds are presented in Figures 16 and 17.

The map FFM 3 was chosen for the determination of the fully degraded head $H_{2\varnothing max}$ according to the equation

$$H_{2\varnothing} = H_{1\varnothing} - M\,(H_{1\varnothing} - H_{2\varnothing max}),$$

$$\text{FFM 3}$$

see [2].

FFM 4

The homologous curves for FFM 4 with a nominal VOIDD = 0.88 (and a void fraction range of VOIDD = 0.78/0.98) are given in Figures 18 and 19. These curves are valid for positive speeds

and locked rotor. Compared to FFM 3 with a nominal VOIDD = 0.75 the pump head degradation is less, indicating a recovery of head as VOIDD approaches unity.

Fig. 18 shows the different zones of operation, Fig. 19 the different speeds for the measurement points of FFM4.

The scatter in the data for the locked rotor has still to be investigated. It may be caused for example by the weakness of the simple model used for calculating the mean density from the three-beam γ-densitometer readings (especially at lower mass flow densities). In addition, the homologous pump model may need some improvements for its application in the case of a locked rotor and two-phase flow.

The positive speeds used for FFM4 are n = 3250, 6000, 6500 and 8450 min^{-1}, see Fig. 19. It can be seen that there is a remarkably low scatter between measurement points belonging to different speeds. This again supports the fact that the application of the concept of the homologous curves is also a valid approach under two-phase flow conditions.

References

[1] A. J. Stepanoff: Radial- und Axialpumpen
Springer Berlin/Göttingen/Heidelberg, 1959

[2] RELAP4/MOD 6 - A Computer Code for Transient Thermal-Hydraulic Analysis of Nuclear Reactors and Related Systems
CDAP - TR003, January 1978

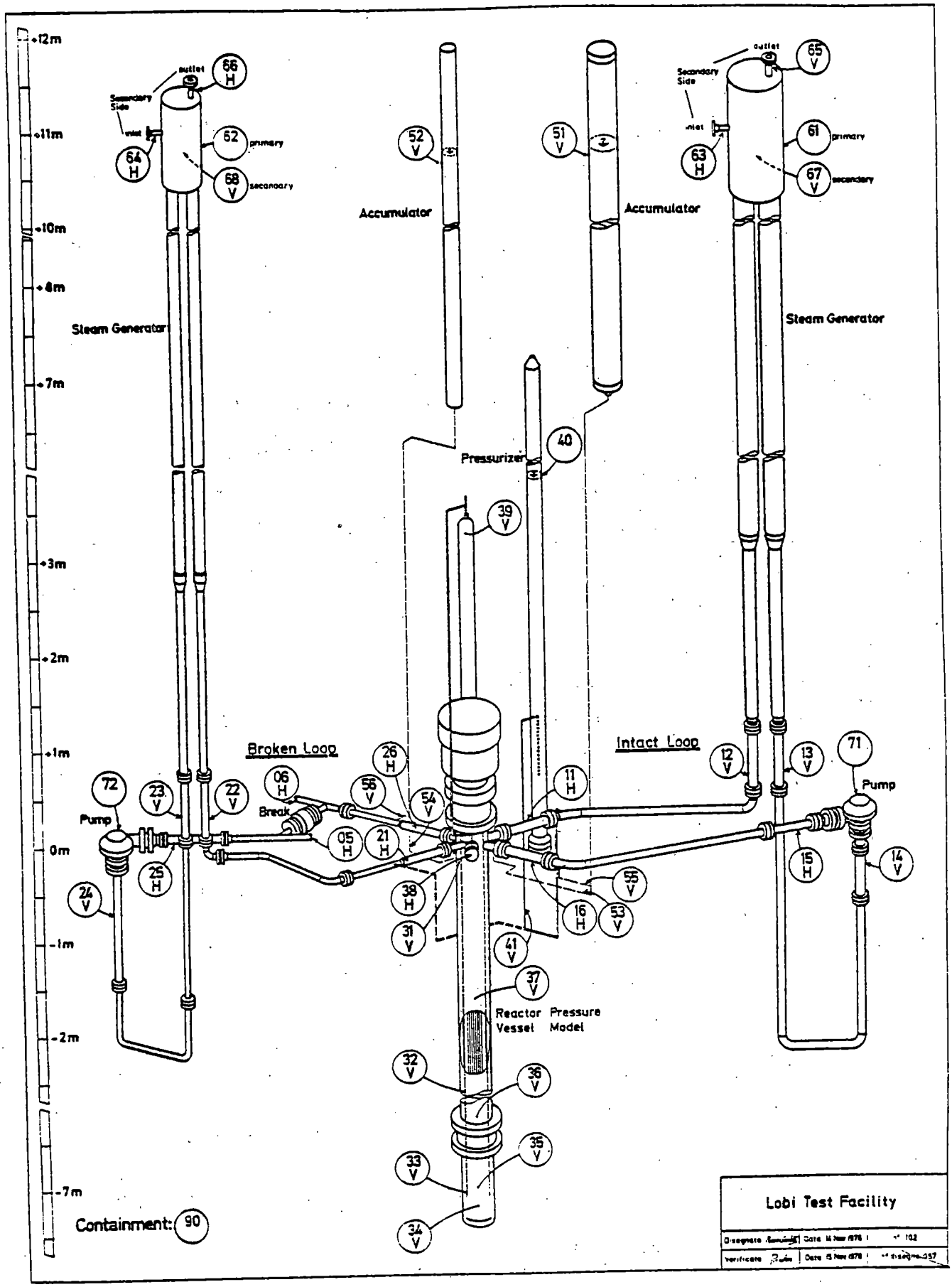

Fig. 1: LOBI Test Facility

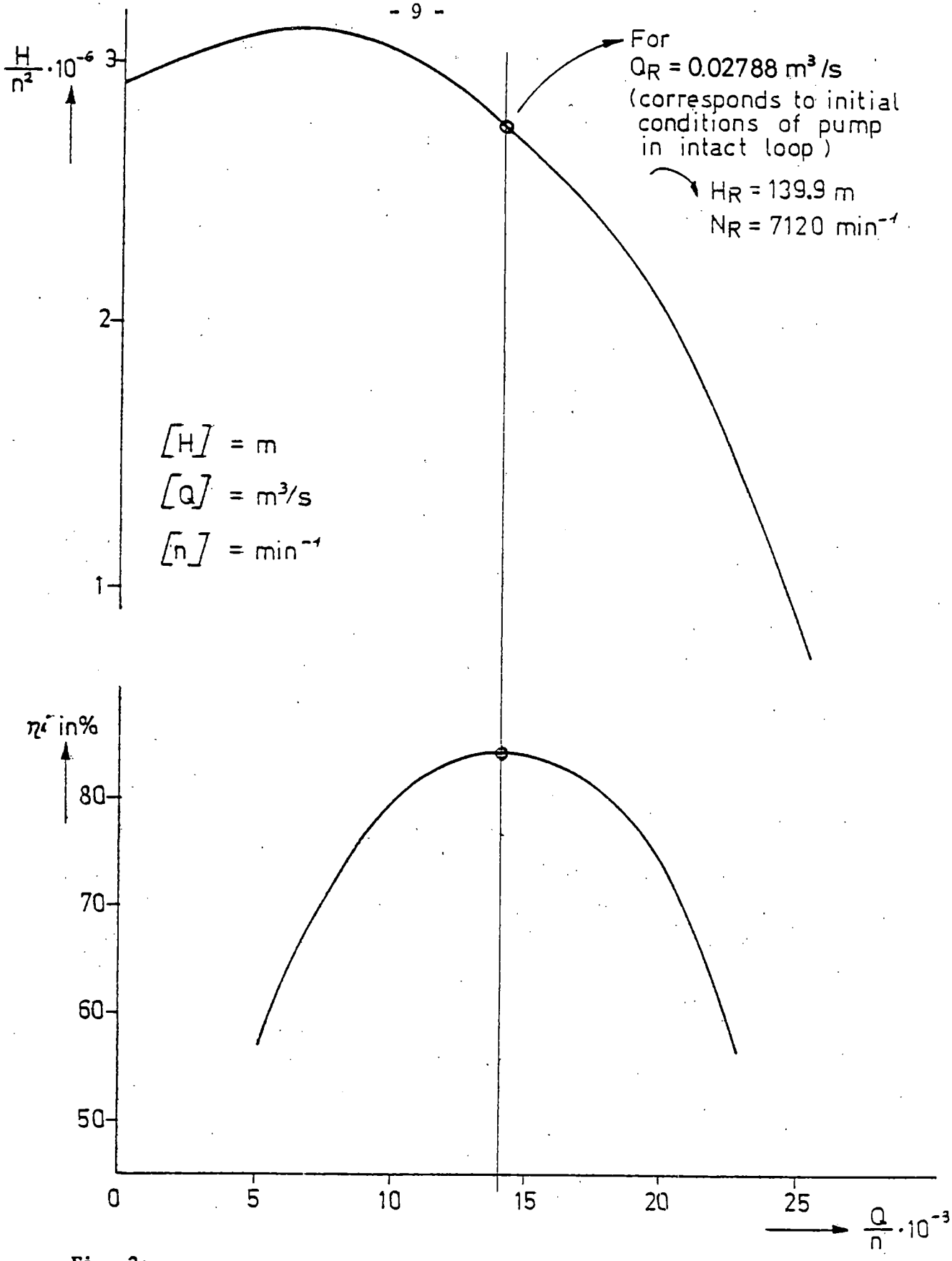

Fig. 2:
Homologous Head Curve and Hydraulic Efficiency for the LOBI Pump under Single Phase Flow Conditions

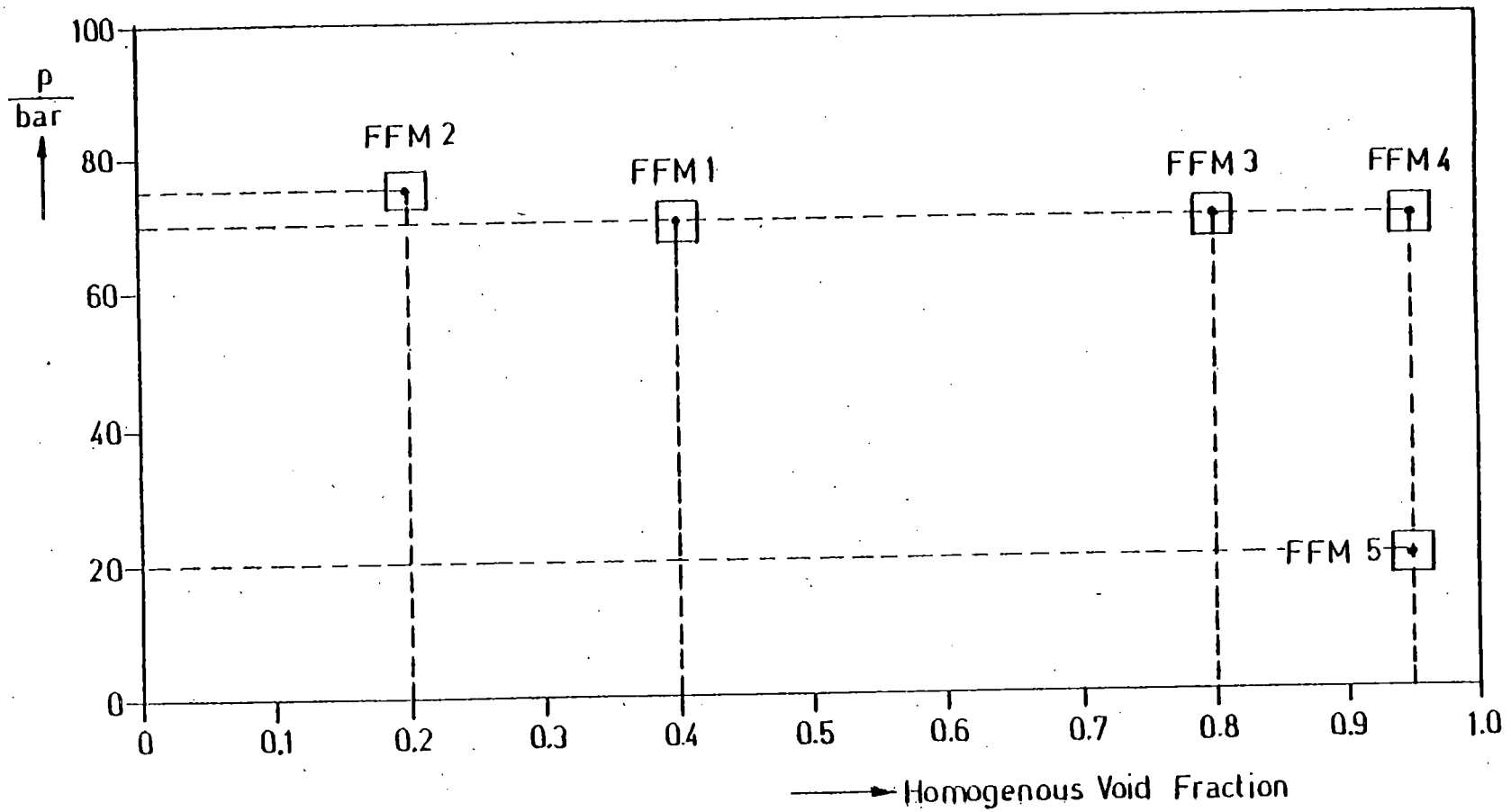

Fig. 3: Full Flow Maps in LOBI Pump 2ø – Tests

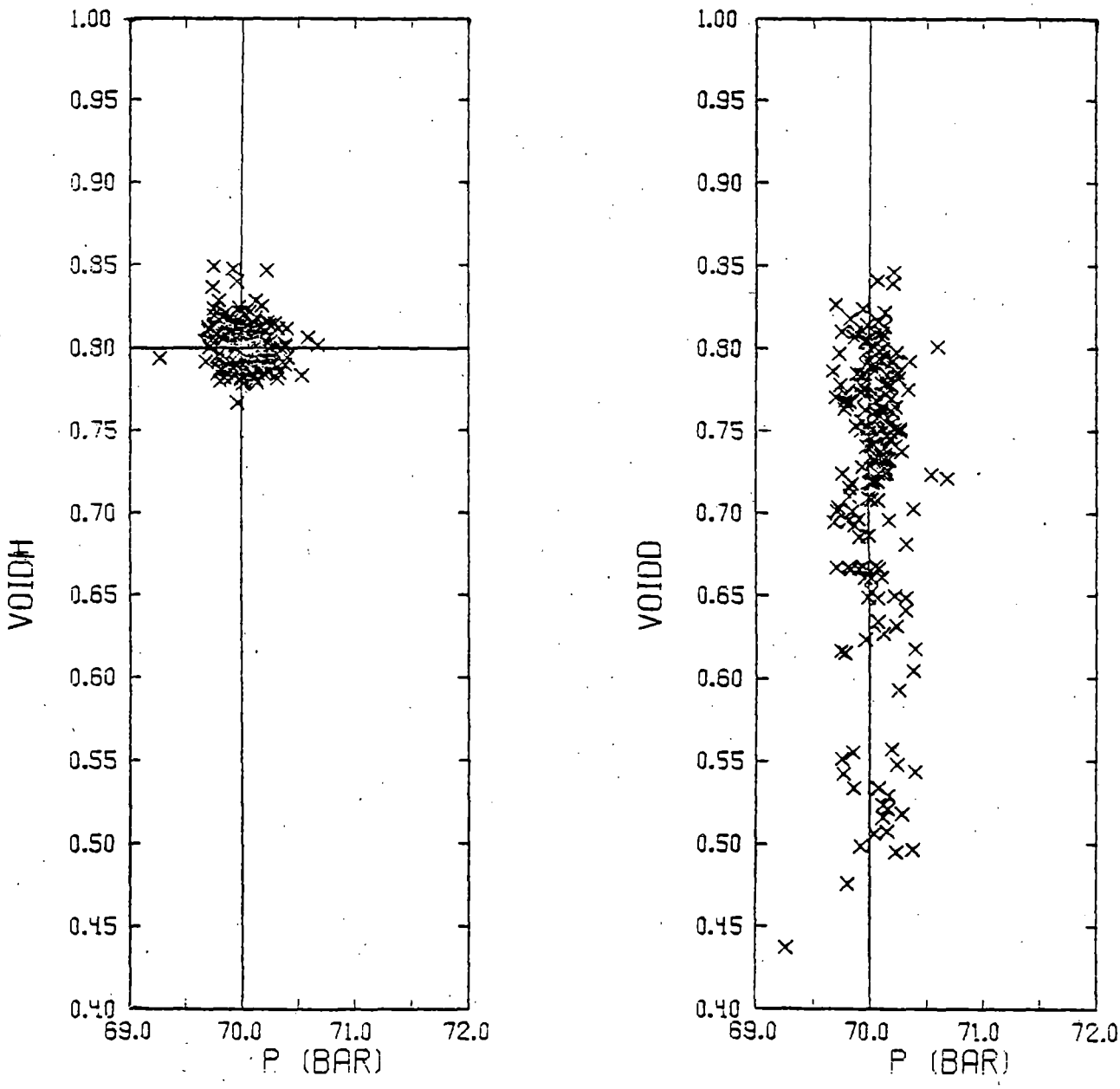

Fig. 4:

INLET VOID FRACTIONS AS FUNCTION OF INLET PRESSURE FOR FFM 3
NOMINAL VALUES AT PUMP INLET FOR FFM 3 : P=70 BAR AND VOIDH=0.8
SORT : P=69/71, VOIDH=0.75/0.85, VOIDD=0.40/1.00, N=ALL

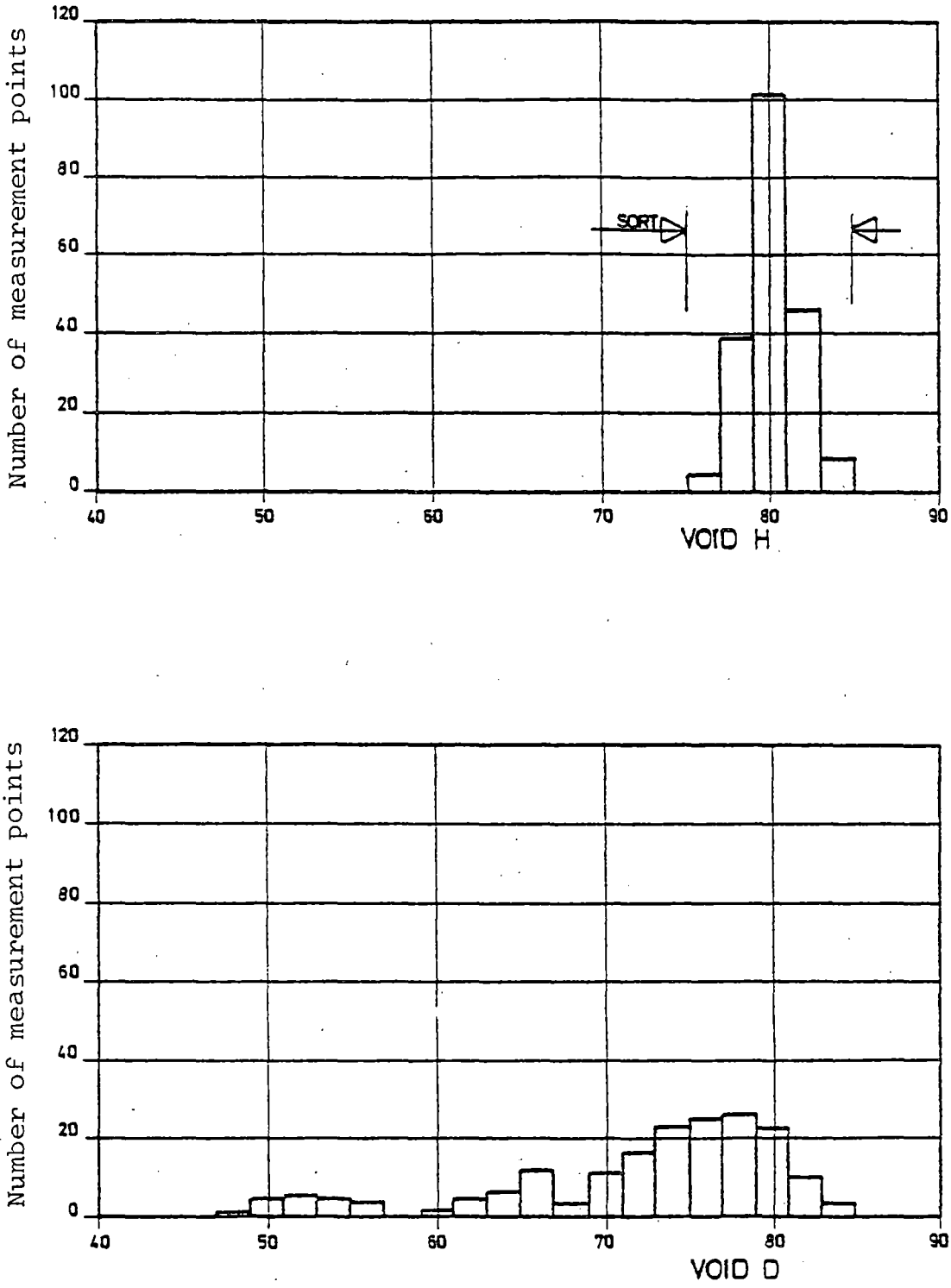

Figure 5:

Distribution of Void Fractions VOIDH and VOIDD for FFM 3

Nominal Values at Pump Inlet for FFM3: P=70 bar and VOIDH=0.8
SORT: P=69/71, VOIDH=0.75/0.85

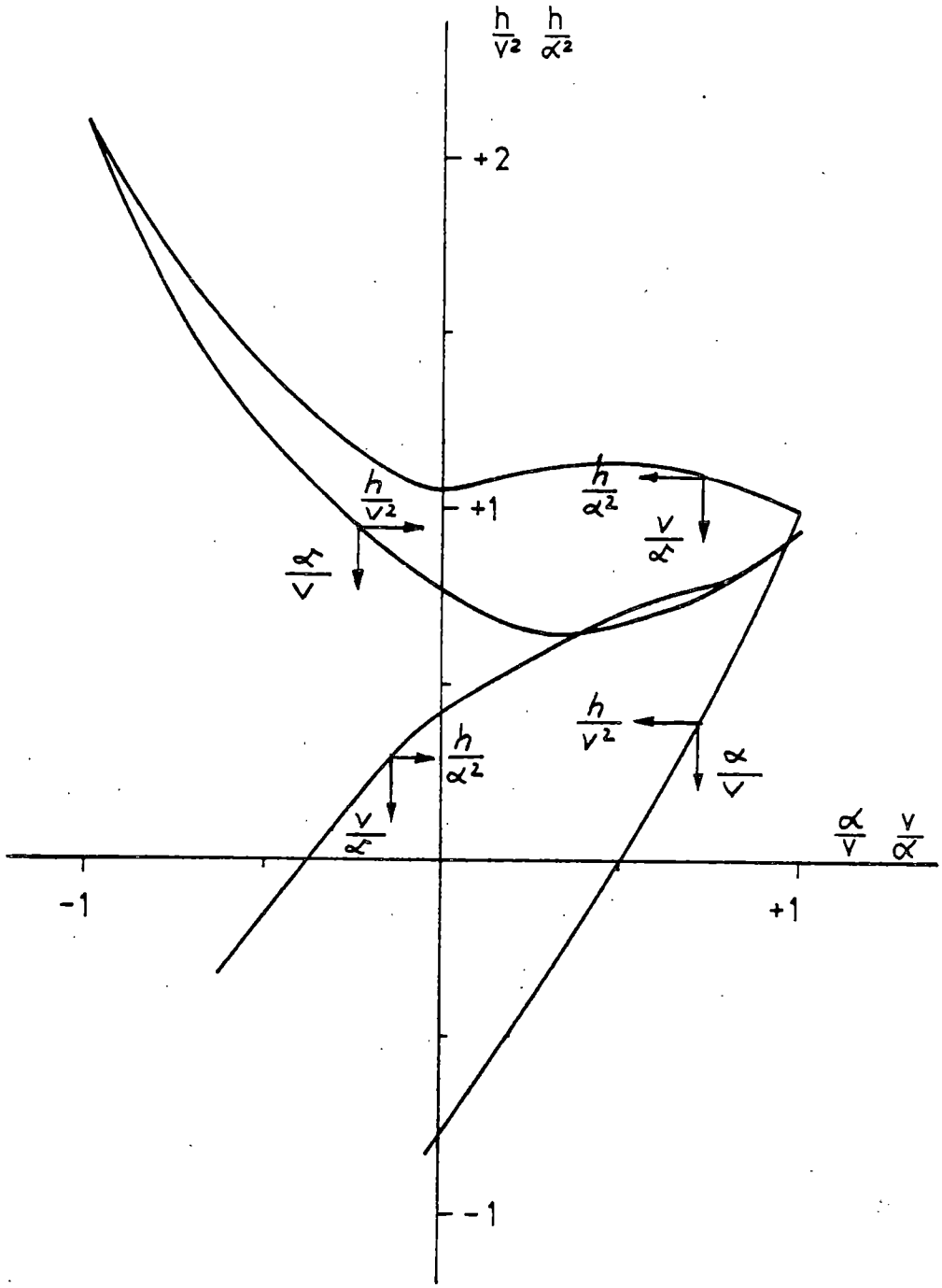

Rated Values:

Q_R = 0.02788 m^3/s

H_R = 139.9 m

N_R = 7120 min^{-1}

Fig. 6: Single-Phase Homologous Head Curve for the LOBI Pump

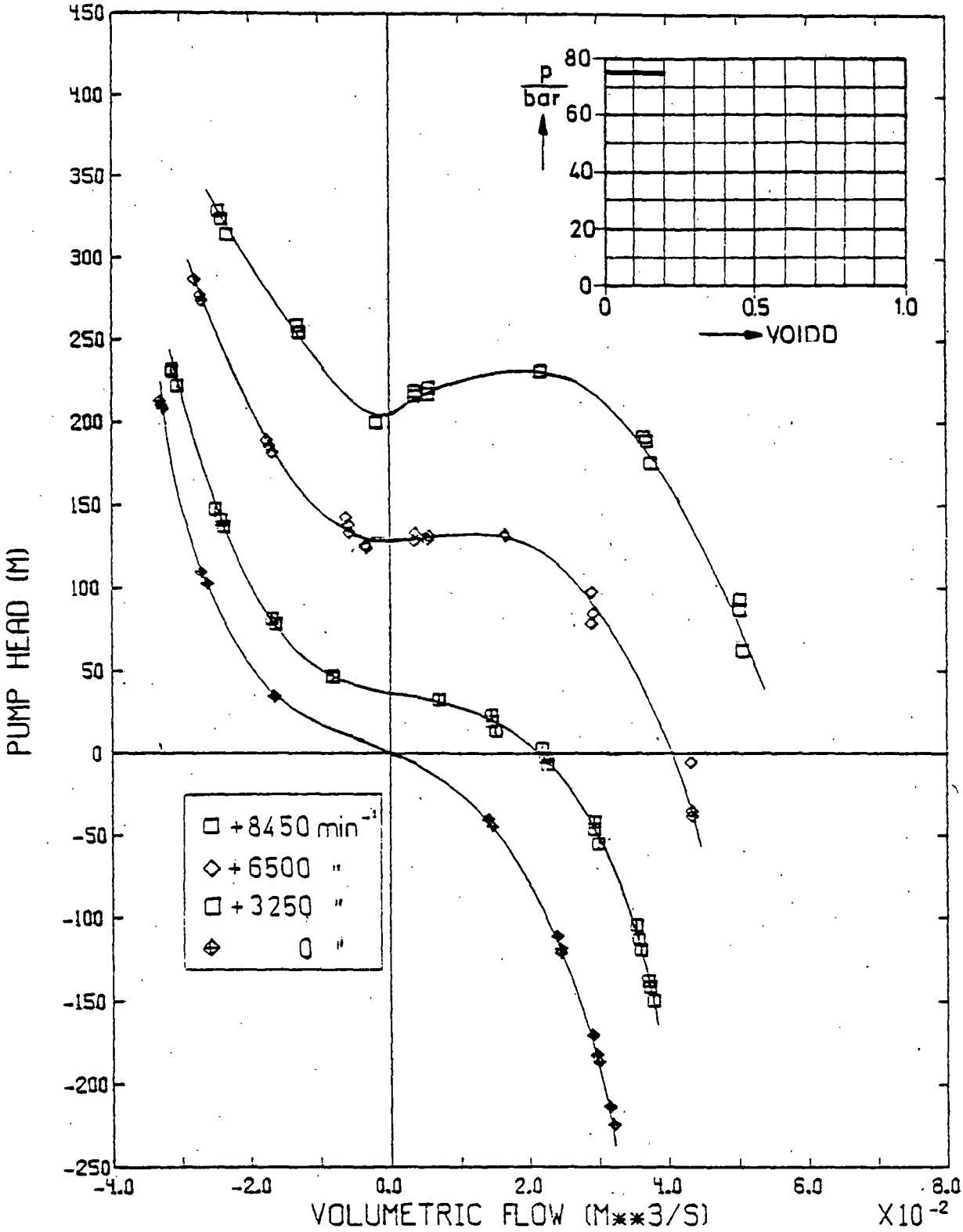

Fig. 7:
FULL FLOW MAP 2/2 SPEED: 0,3250, 6500,8450 RPM
NOMINAL VALUES AT PUMP INLET FOR FPM 2/2 : P=75 BAR AND VOIDD=0.10
SORT : P=74/76, VOIDD=0.00/0.20, SPEED=-50/8500

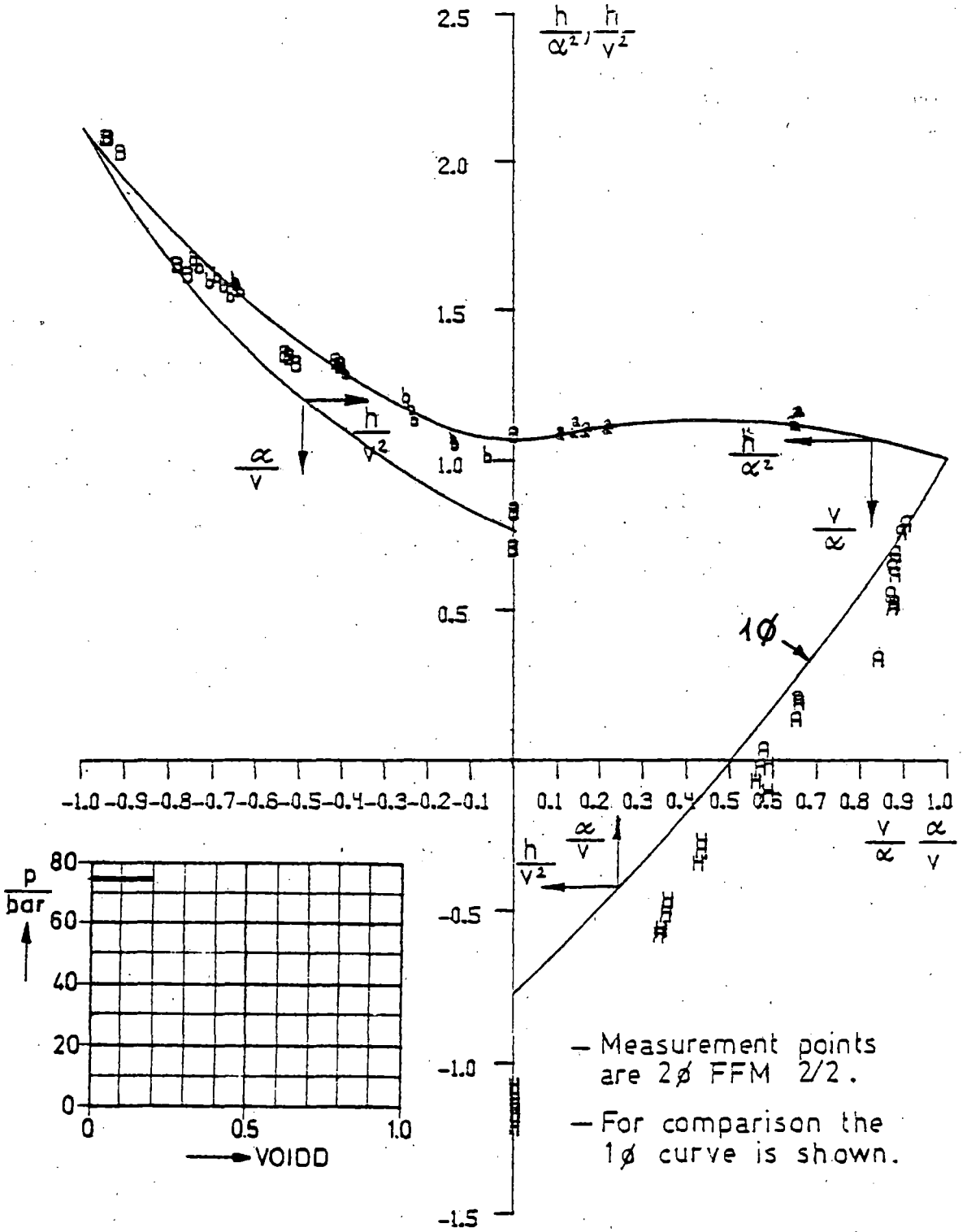

Fig. 8:

HOMOLOGOUS HEAD OF FFM 2/2 SPEED : 0,3250,6000,6500,8450 RPM
NOMINAL VALUES AT PUMP INLET FOR FFM 2/2 : P=75 BAR AND VOIDD=0.10
SORT : P=74/76, VOIDD=0.00/0.20, SPEED=-50/8500

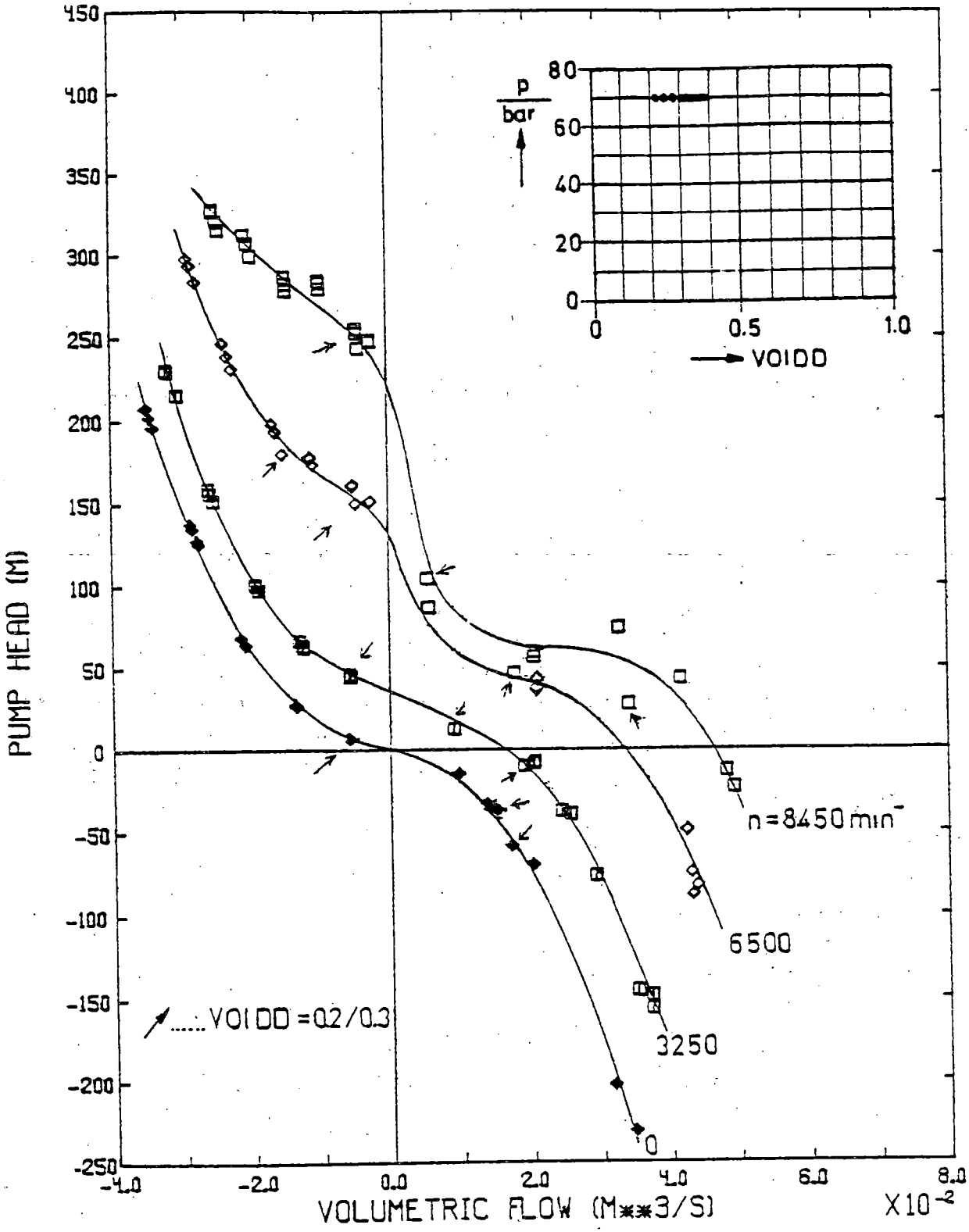

Fig. 9:
FULL FLOW MAP 1/2 SPEED: 0,3250, 6500,8450 RPM
NOMINAL VALUES AT PUMP INLET FOR FFM 1/2 : P=70 BAR AND VOIDD=0.30
SORT : P=69/71, VOIDD=0.20/0.40, SPEED=-50/8500

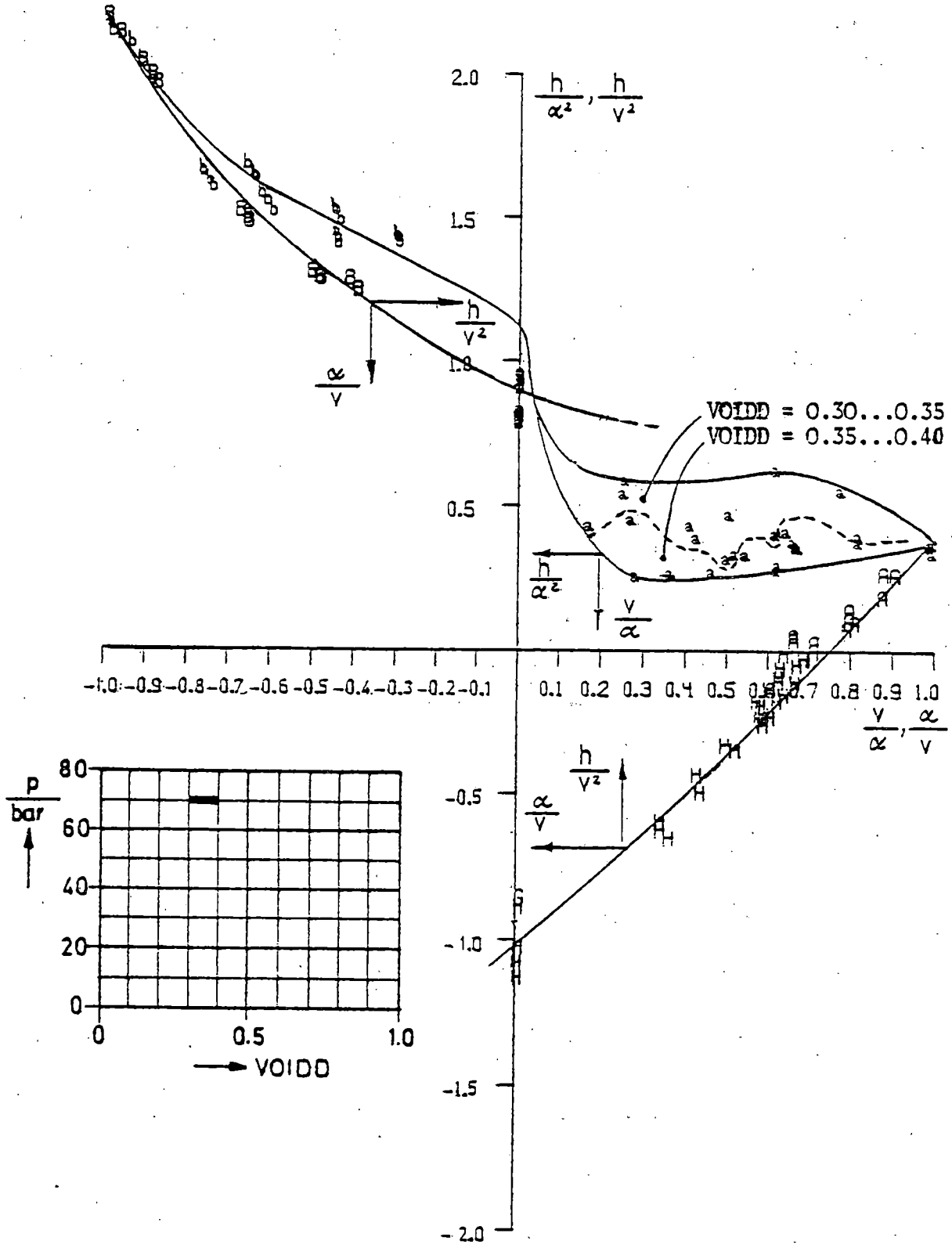

Fig. 10:

HOMOLOGOUS HEAD OF FFM 1/1 SPEED : 0,3250,6000,6500,8450 RPM
NOMINAL VALUES AT PUMP INLET FOR FFM 1/1 : P=70 BAR AND VOIDD=0.35
SORT : P=69/71, VOIDD=0.30/0.40, SPEED=-50/8500

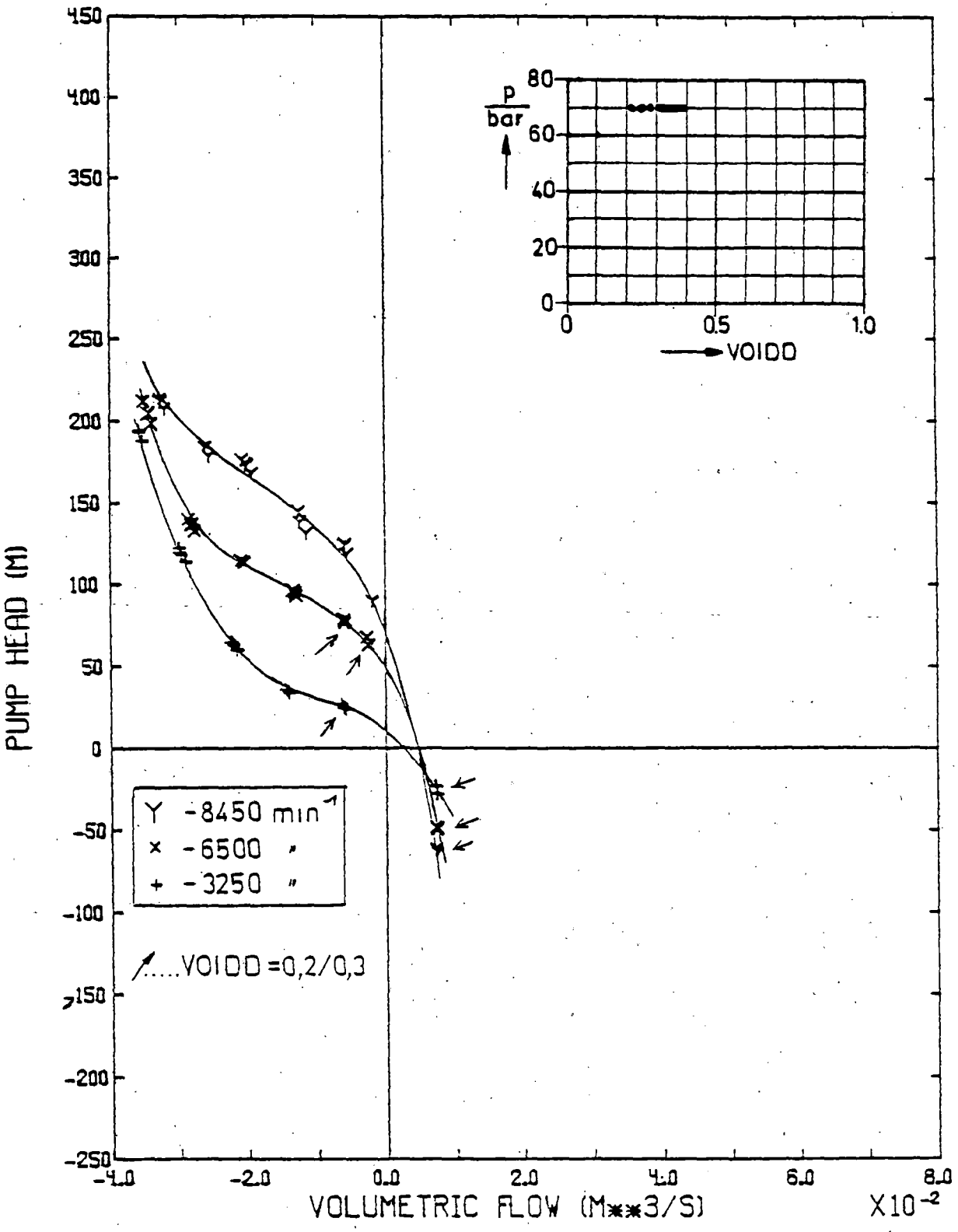

Fig. 11:
FULL FLOW MAP 1/2 SPEED : -3250,-6500,-8450 RPM
NOMINAL VALUES AT PUMP INLET FOR FFM 1/2 : P=70 BAR AND VOIDD=0.30
SORT : P=69/71, VOIDD=0.20/0.40, SPEED=-3200/-8500

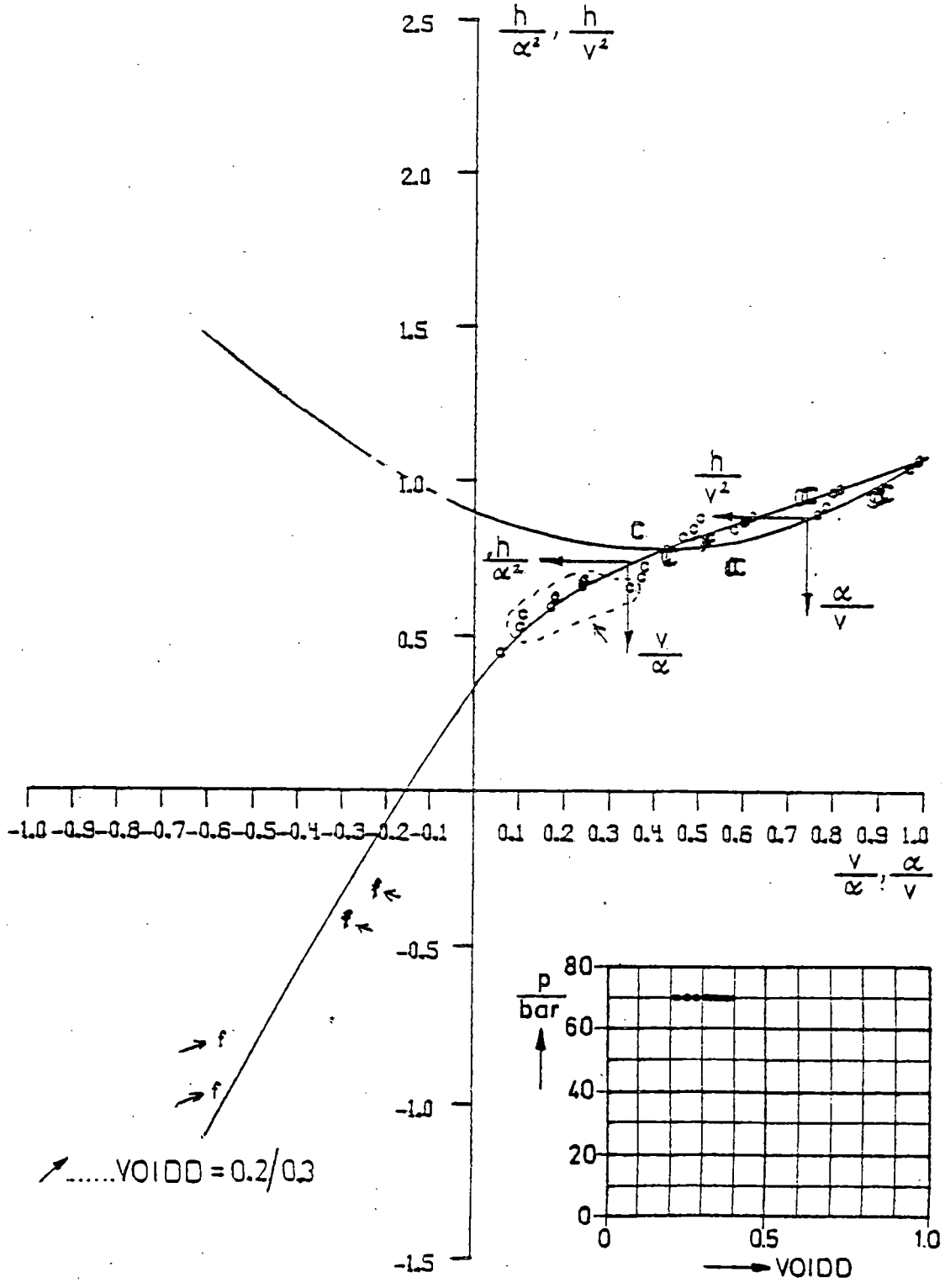

Fig. 12:

HOMOLOGOUS HEAD OF FFM 1/2 SPEED : -3250,-6500,-8450 RPM
NOMINAL VALUES AT PUMP INLET FOR FFM 1/2 : P=70 BAR AND VOIDD=0.30
SORT : P=69/71, VOIDD=0.20/0.40, SPEED=-3200/-8500

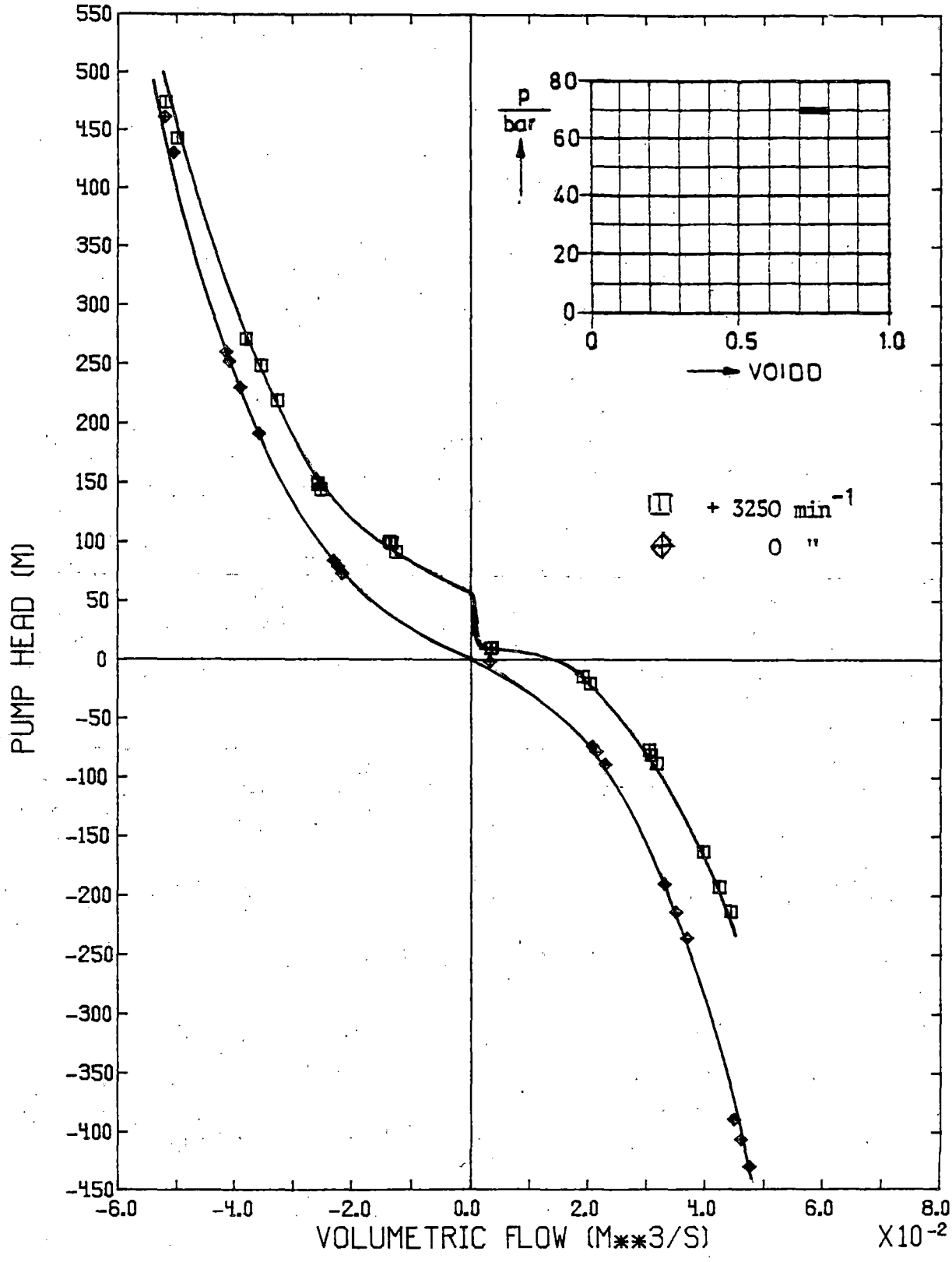

Fig. 13:
FULL FLOW MAP 3/1 SPEED: 0,3250 RPM
NOMINAL VALUES AT PUMP INLET FOR FFM 3/1 : P=70 BAR AND VOIDD=0.75
SORT : P=69/71, VOIDD=0.70/0.80, SPEED=-50/3300

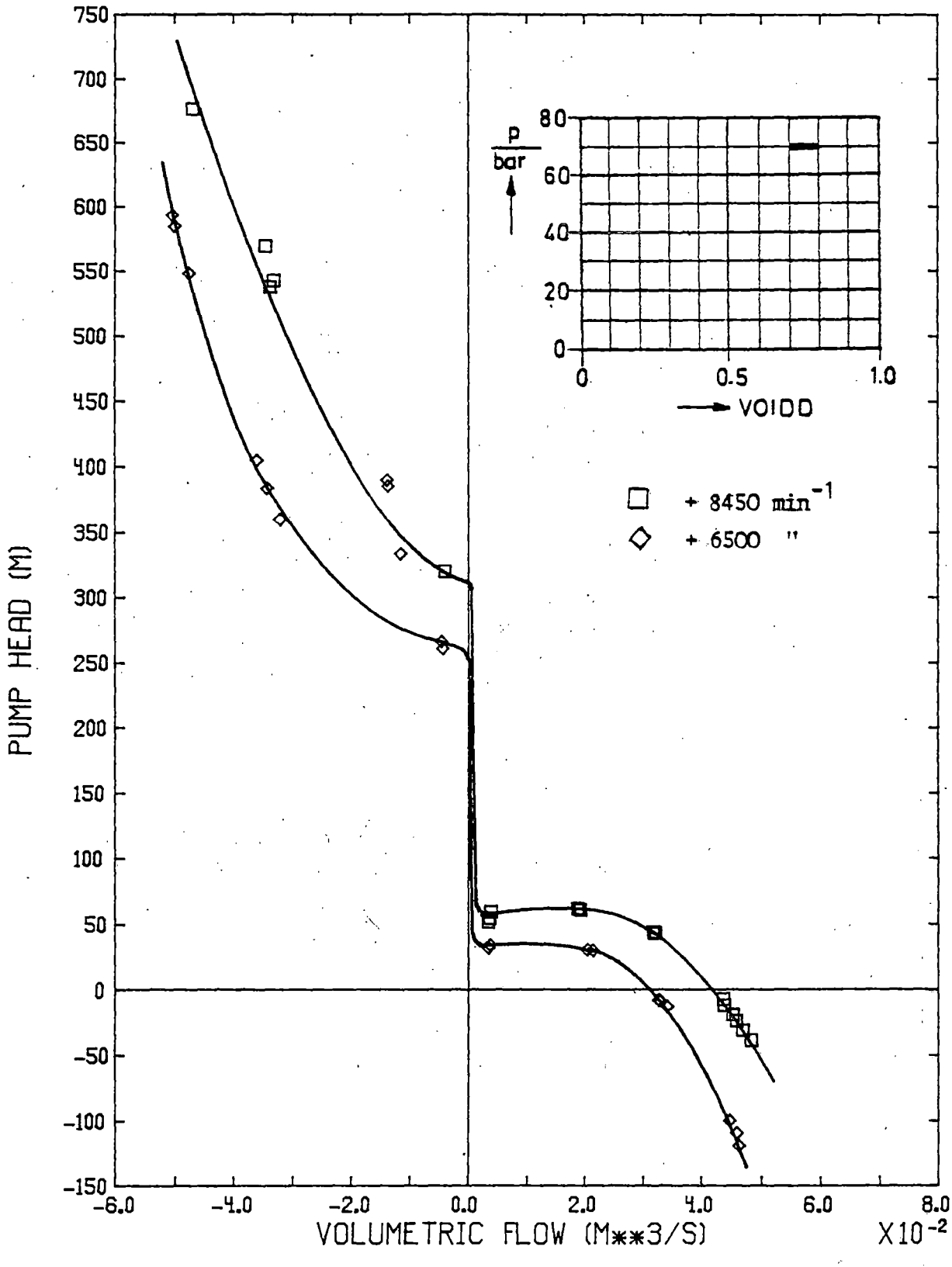

Fig. 14:

FULL FLOW MAP 3/1 SPEED: 6500,8450 RPM
NOMINAL VALUES AT PUMP INLET FOR FFM 3/1 : P=70 BAR AND VOIDD=0.75
SORT : P=69/71, VOIDD=0.70/0.80, SPEED=6450/8500

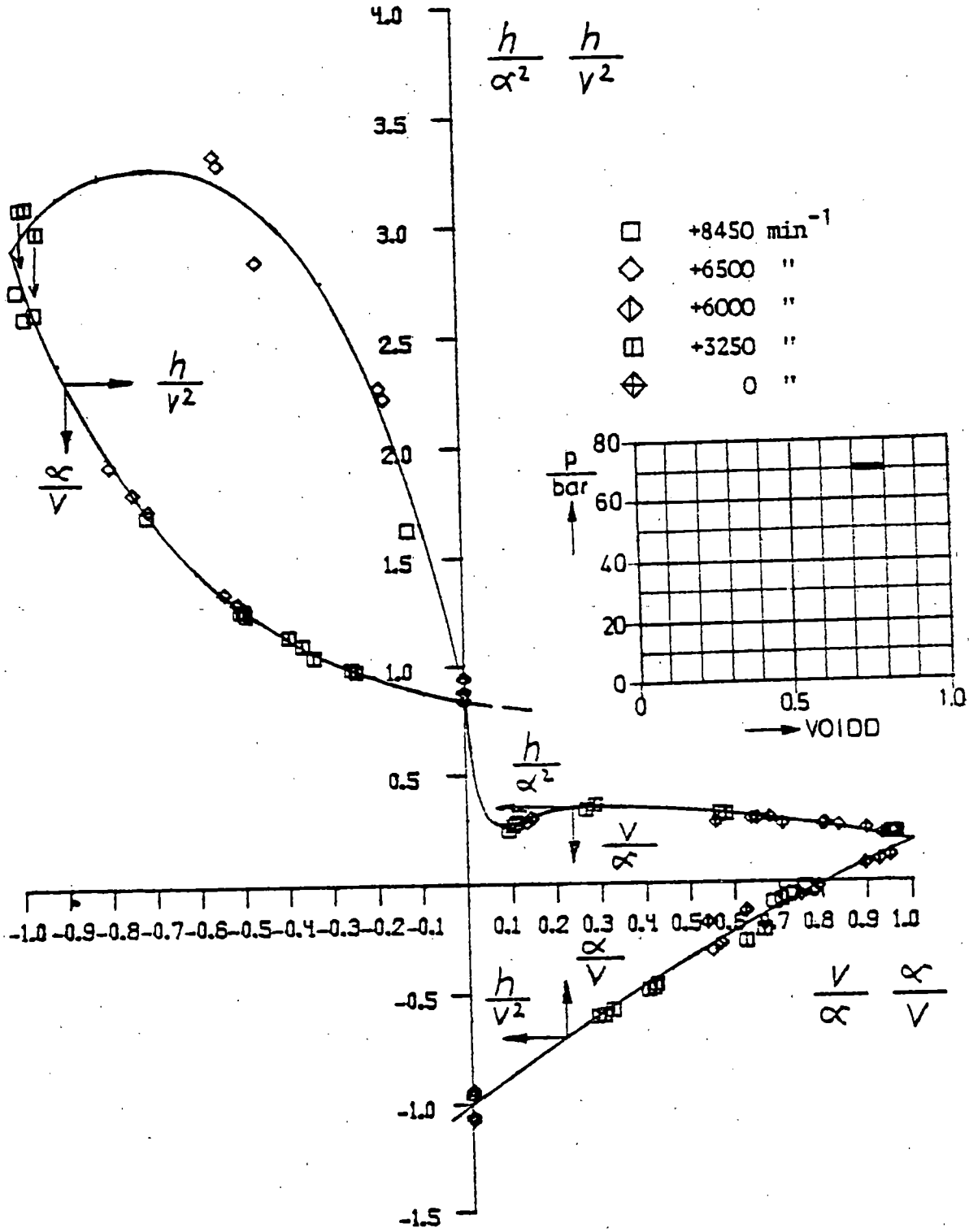

Fig. 15:
HOMOLOGOUS HEAD OF FFM 3/1 SPEED : 0,3250,6000,6500,8450 RPM
NOMINAL VALUES AT PUMP INLET FOR FFM 3/1 : P=70 BAR AND VOIDD=0.75
SORT : P=69/71, VOIDD=0.70/0.80, SPEED=-50/8500

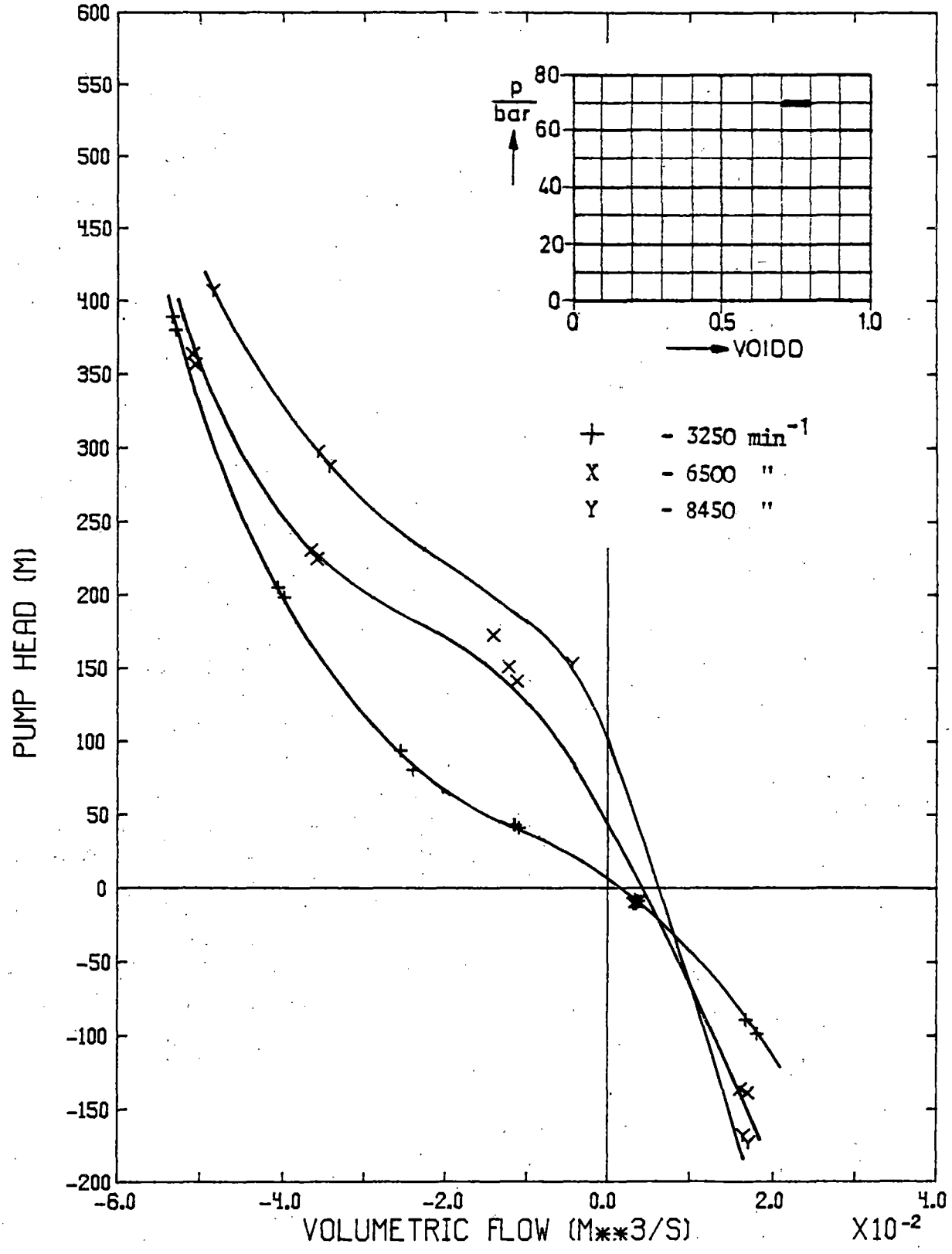

Fig. 16:

FULL FLOW MAP 3/1 SPEED : -3250,-6500,-8450 RPM
NOMINAL VALUES AT PUMP INLET FOR FFM 3/1 : P=70 BAR AND VOIDD=0.75
SORT : P=69/71, VOIDD=0.70/0.80, SPEED=-3200/-8500

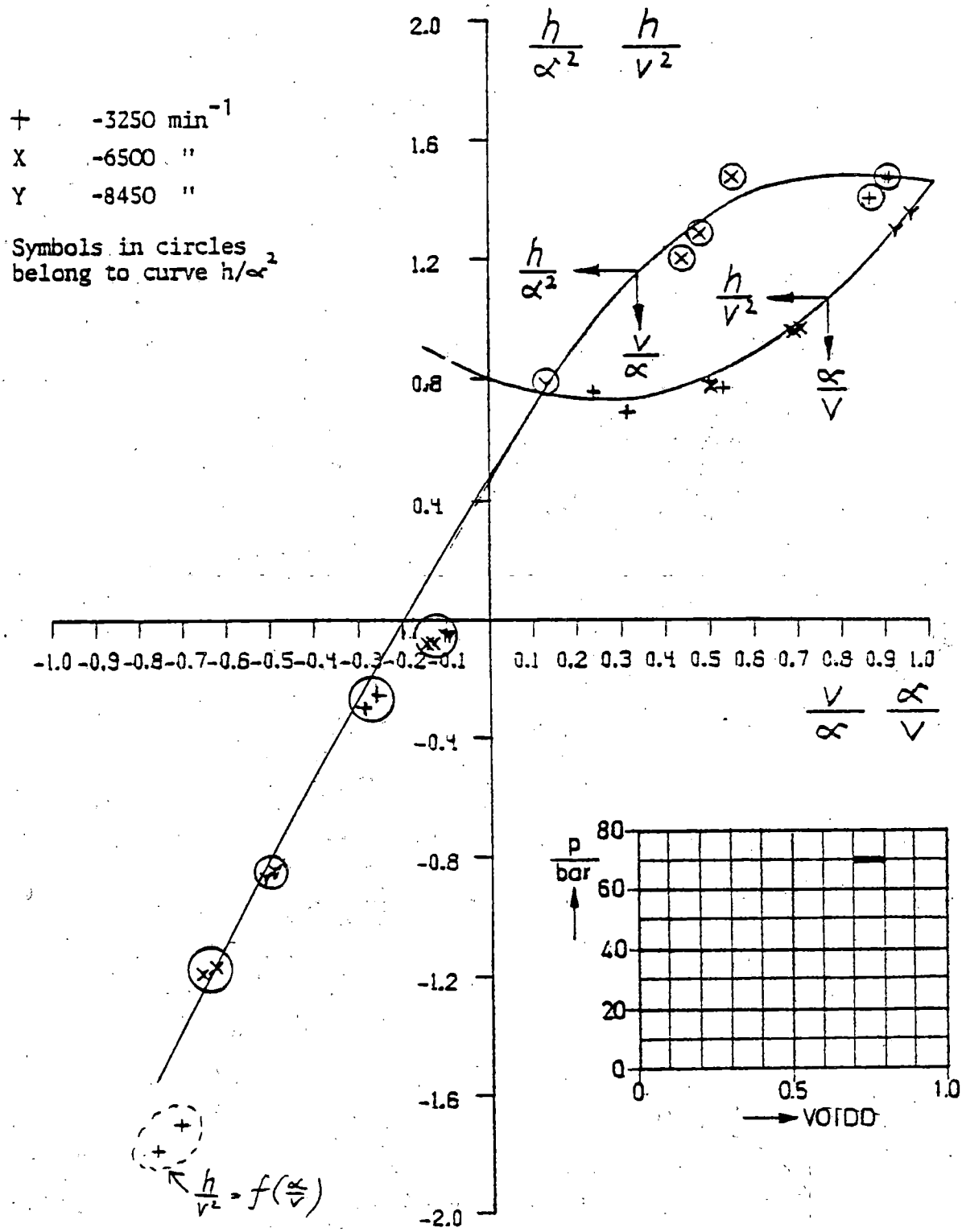

Fig. 17:

HOMOLOGOUS HEAD OF FFM 3/1 SPEED : -3250,-6500,-8450 RPM
NOMINAL VALUES AT PUMP INLET FOR FFM 3/1 : P=70 BAR AND VOIDD=0.75
SORT : P=69/71, VOIDD=0.70/0.80, SPEED=-3200/-8500

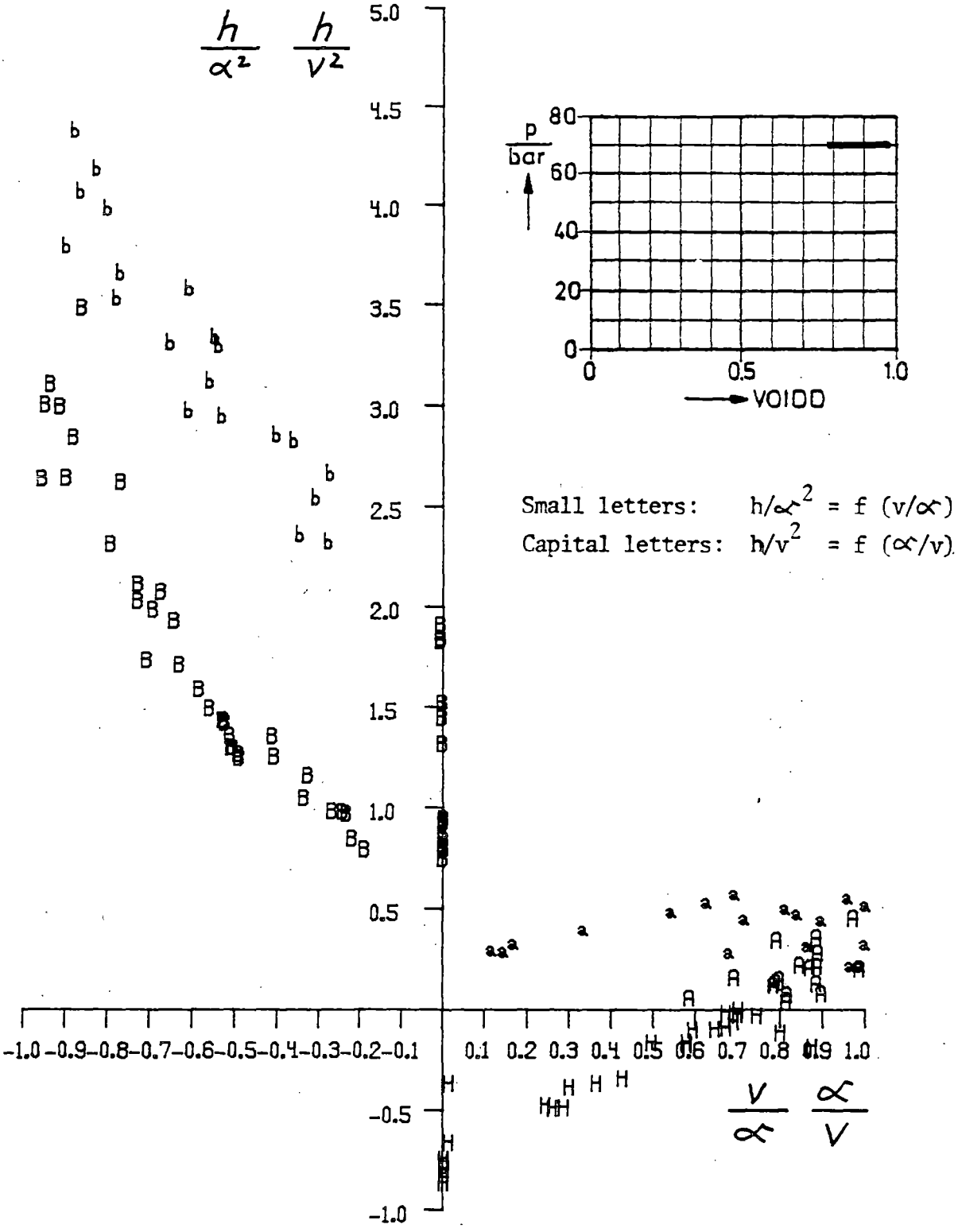

Fig. 18:
HOMOLOGOUS HEAD OF FFM 4/2 SPEED : 0,3250,6000,6500,8450 RPM
NOMINAL VALUES AT PUMP INLET FOR FFM 4/2 : P=70 BAR AND VOIDD=0.88
SORT : P=69/71, VOIDD=0.78/0.98, SPEED=-50/8500

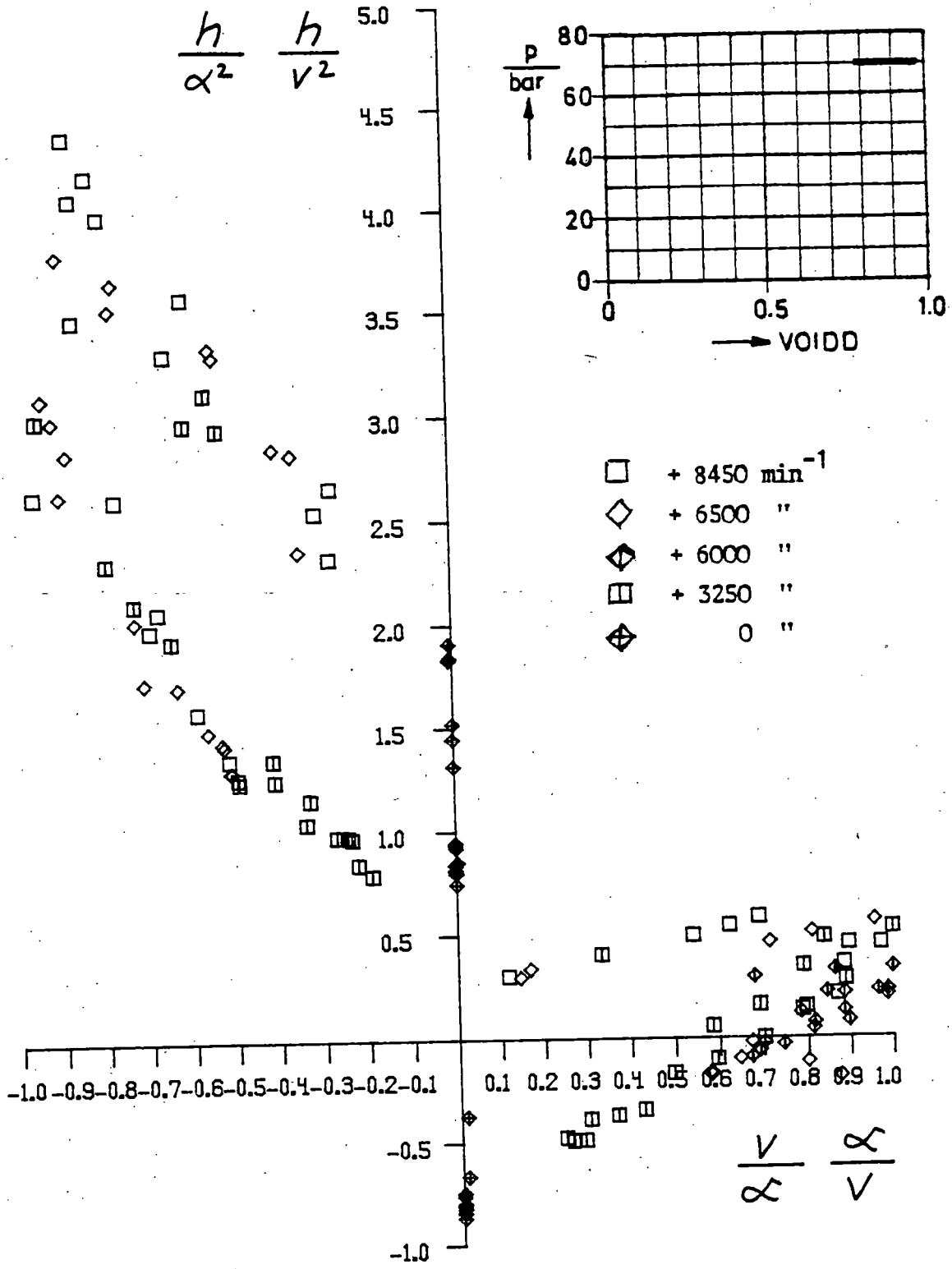

Fig. 19:
HOMOLOGOUS HEAD OF FFM 4/2 SPEED : 0,3250,6000,6500,8450 RPM
NOMINAL VALUES AT PUMP INLET FOR FFM 4/2 : P=70 BAR AND VOIDD=0.88
SORT : P=69/71, VOIDD=0.78/0.98, SPEED=-50/8500

Two-Phase Performance Characteristics of the LOBI Pump

L. Piplies, W. Kolar

Commission of the European Communities
EURATOM Joint Research Centre - Ispra Establishment
LOBI Project, Heat Transfer Division
I 21020 ISPRA/Varese (I)

Errata

Fig. 2: $[\,Q\,] = m^3/h$

Cover page and page 3:

Complete the units for the specific speeds n_q and N_s.

n_q : $min^{-1} \cdot (m^3/s)^{1/2} \cdot m^{-3/4}$

N_s : $min^{-1} \cdot (gall/min)^{1/2} \cdot ft^{-3/4}$

CONTAINMENT EMERGENCY SUMP STUDIES TO INVESTIGATE UNRESOLVED SAFETY ISSUE A-43

BY

G. G. WEIGAND, SANDIA NATIONAL LABORATORIES
M. PADMANABHAN, ALDEN RESEARCH LABORATORIES OF WPI
A. W. SERKIZ, U. S. NUCLEAR REGULATORY COMMISSION

PRESENTATION BY
G. G. WEIGAND

SANDIA NATIONAL LABORATORIES
ALBUQUERQUE, NEW MEXICO

NINTH WATER REACTOR SAFETY RESEARCH INFORMATION MEETING

GAITHERSBURG, MARYLAND

OCTOBER 27, 1981

CONTAINMENT EMERGENCY SUMP STUDIES TO INVESTIGATE UNRESOLVED SAFETY ISSUE A-43

by

G. G. Weigand, Sandia National Laboratories
M. Padmanabhan, Alden Research Laboratories WPI
A. W. Serkiz, U. S. Nuclear Regulatory Commission

This paper presents the results of a parametric study of hydraulic parameters; the study was conducted to aid in the resolution of Unresolved Safety Issue A-43 (USI-43), Containment Emergency Sump Performance. USI-43 addresses the issue of a long-term cooling capability; in particular, we are addressing the question of the sump, during the recirculation mode, providing the necessary flow of coolant following a LOCA. A disruption of long term cooling to the reactor core could lead to core damage.

The initiation of this program was motivated by the need for additional ECCS guidelines. Results from recent scale model studies have shown that sumps, not unlike ECCS sumps in current use, may suffer serious performance losses due to air ingestion, vortices, elevated swirl, and excessive pressure losses [1,2,3]. Another reason was that clear scaling laws were not established for sump testing. Because of the large number of variables present in a sump configuration, the regulation, industrial, and university communities could not agree upon the adequacy or utility of small-scale results. Clearly, there was a need for a full-scale parametric study of containment ECCS sumps.

Two important objectives of this research were (1) provide guidance and performance data for ECCS sump design, and (2) determine the utility of scale model testing. In this report, we will only discuss our results to date (first phase of tests, about 30 sump configurations) for objective (1). Conclusions concerning objective (2) await data from the second phase of testing.

Alden Research Laboratories, under contract to the DOE is performing the sump experiments. The test plan considers fourteen different flow and geometric variables, and it considers most flow issues concerning unusual flow conditions in containment sumps. The test plan is divided into four parts: (1) factorial testing, (2) secondary variable sensitivity tests, (3) severe perturbation tests, and (4) vortex suppression tests. In (1), primary sump flow and geometric variables are studied using a fractional factorial matrix of tests. The factorial matrix developed by Sandia National Laboratories was used since it is the most effective way to test a large number of variables, it provides a wide range of parameter variations, and the interdependency of different variables can be

determined. In (2), the effect on sump performance of secondary variables is tested by holding all sump variables but one, constant and testing several values of this one variable. In (1) and (2), the approach flow to the sump was reasonably uniform and unperturbed (low circulation). Parts 3 and 4 are tests where the approach flow was severely perturbed. In (3), we considered screen blockage (up to 75% blockage), nonuniform approach flow patterns including streaming, impinging break and drain flows, flow obstructions, and flow transients. Finally, in (4), we evaluate the effectiveness of several types of vortex suppressors. The several parts of the test plan are not performed sequentially, but are performed, as required, as each configuration is constructed. Consequently, intermediate results contain data analysis from all parts of the test program.

Our results are formed from two different approaches for analyzing the sump performance data: parameter and response correlations where we look for specific functional behavior, and an envelope analysis where we can prescribe bounded regions of the independent variables where we are confident of the maximum value of the dependent variables (vortex type, void fraction, swirl, and loss coefficient). The results we are presenting here are principally a result of the envelope analysis. The complex time varying three dimensional nature of the surface vortex has resulted in a wide scatter in the experimental data. This scatter is of the same order of magnitude as many of the weak responses resulting from changes in the independent flow and geometric variables. Although specific trends can be identified and are consistent with other published findings, the specific functional correlation to describe the behavior can only be found with a low degree of confidence and in many cases is simply the mean of the data.

Since the experimental data cover a wide range of ECCS sump geometries, flow parameters, and flow perturbations, the data provide a means of defining an envelope of maximum values for the dependent performance parameters. In other words the data display distinct boundaries. This envelope (or boundary) is valid for any sump and flow conditions provided there is a similiarity of characteristics between the sump being considered and the data base. Several attached figures illustrate this envelope analysis, and show the envelope curves for void fraction (% air) as functions of the Froude Number, average pipe velocity, u, and submergence, s. Using these types of curves, we can confidently predict under what conditions the void fraction, vortex type, or swirl should not exceed some prescribed value. As long as the sump under consideration is within the experimental data base, we can provide these predicted dependent variable levels irrespective of how extreme the flow perturbations may be. Thus, this envelope analysis can form the basis for establishing certain design guidelines.

General Conclusions

Vortices. In general, for submergences greater than 8 ft, only weak air-core (less than 1% air void), or more often non-air-core vortices, were observed. The vortices were, in general, unsteady and spatially unstable. Vortex type is not a sufficient indicator of sump performance, because the vortex type alone (i.e., an air-core vortex) does not reliably indicate swirl or air void fraction levels.

Void Fraction. Most of the air-core vortices (especially for the unperturbed tests) had small air ingestions--voids of 1% or less. Under highly perturbed flow conditions along with low submergence and high flow rate the maximum 30-minute-sample air void was about 7%. Air voids of 3% or more and strong surface vortices were observed for some, but not all, of the worst perturbed flows such as 75% screen blockage and streaming flow. Reliably predicting *a priori* whether sump conditions will result in air-voids exceeding 2% is not presently possible. For submergences greater than 8 ft and for all levels of swirl, blockage, etc., the measured air voids were less than 1%.

Swirl. Swirl measurements were recorded 14.5 diameters downstream of the pipe inlet. In almost all cases, the swirl level was less than four degrees. Some larger levels of swirl--maximum value observed was about eight degrees-- were measured when testing severely perturbed flows, but these larger levels occurred at low submergences and large flows. Submergence has a strong influence on swirl.

Loss Coefficient. The loss coefficient was found to be mostly independent of the overall sump geometry and sump flow conditions. In particular, the loss coefficient is independent of any surface vortex phenomena. We found that the loss coefficient had a weak dependence on the swirl (note that the range of swirl is typically 0 to 3 degrees). The value for the loss coefficient is dominated by the inlet pipe shape, and, for most cases, $C_p \approx 1.0$ can be considered as an upper bound loss coefficient value.

Vortex Suppression. The vortex suppression tests were performed using the cage-type suppressor (see attached figure) and using the perturbed flow configuration having the poorest performance (highest void fraction and swirl). In each test conducted to date the cage-type suppressor resulted in (1) the surface vortexing reduced from a full air core vortex to a surface swirl, (2) an air void fraction of zero, (3) measured swirl in the outlet pipe of less than 5 degrees, and (4) no significant change in the loss coefficient.

1. M. Padmanabhan, "Assessment of Flow Characteristics Within a Reactor Containment Recirculation Sump Using a Scale Model -- McGuire Nuclear Power Station," Alden Research Laboratory WPI, May 1978.

2. T. G. Fain, "Model Study of the Sequoyah RHR Sump," Report No. WM28-1-45-102, Tennessee Valley Authority, Division of Water Management, October 1978.

3. USNRC Docket No. 50-368, Trip Report - Western Canada Hydraulics Laboratory, ANO-2 Model Tests, 1978.

BACKGROUND

- EXCESSIVE PRESSURE LOSSES, INGESTION OF AIR FROM FREE SURFACE VORTICES OR BREAK JETS IMPINGING NEAR THE SUMP, AND CONSIDERABLE SWIRLING FLOW IN THE PUMP SUCTION LINES COULD LEAD TO A DEGRADATION OF PUMP PERFORMANCE

- HYDRAULIC MODEL STUDIES OF ECCS SUMPS SHOWED THAT AIR INGESTION, SURFACE VORTICES, AND ELEVATED SWIRL EXISTED AND THAT REMEDIAL MEASURES (REDESIGN, SUPPRESSORS, ETC.) WERE NEEDED TO INSURE SATISFACTORY SUMP OPERATION FOR LONG TERM COOLING

- THE HYDRAULIC PERFORMANCE OF ECCS SUMPS, AS AN INGREDIENT OF PUMP SUCTION PERFORMANCE, WAS CONSIDERED AS PART OF USI A-43 --CONTAINMENT EMERGENCY SUMP PERFORMANCE

OBJECTIVES OF THE RESEARCH

PRIMARY OBJECTIVES

- DEVELOP GENERAL ENGINEERING AND NUMERICAL GUIDELINES FOR ECCS SUMPS, CONSISTENT WITH THE NRC REGULATORY GUIDE CONTROL PROCEDURES, WHICH WOULD ALLOW AN EVALUATION OF SUMPS TO DETERMINE THE ADEQUACY OF THEIR HYDRAULIC PERFORMANCE

- PROVIDE A DATA BASE OF SUMP PERFORMANCE TO THE NRC AND INDUSTRY

SECONDARY OBJECTIVES

- DETERMINE THE ADEQUACY AND UTILITY OF SCALE MODEL TESTING

- DETERMINE THE EFFECTS OF TESTING AT TEMPERATURES BELOW THE WATER TEMPERATURE IN CONTAINMENT AFTER A LOCA (I.E., COLD WATER)

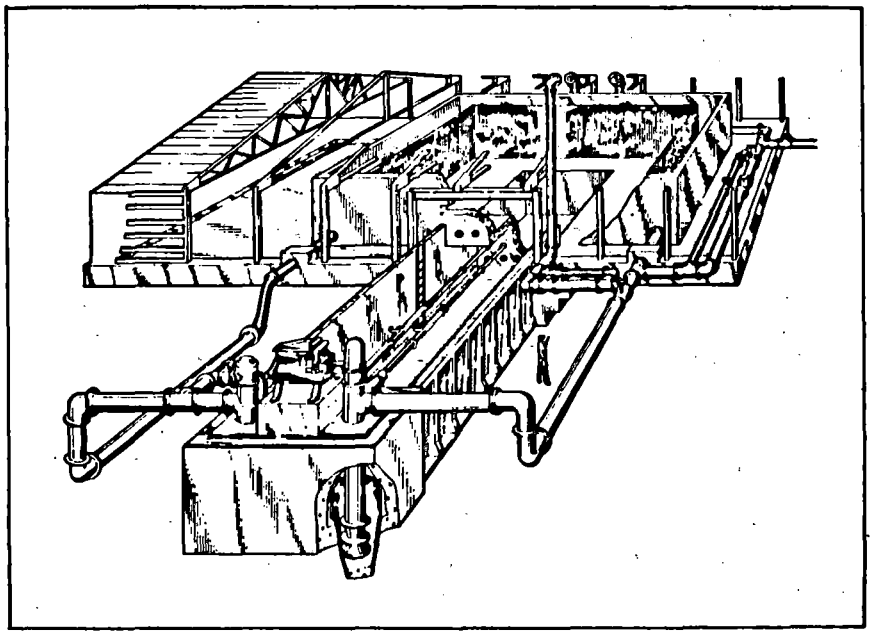

PERSPECTIVE VIEW OF THE FACILITY

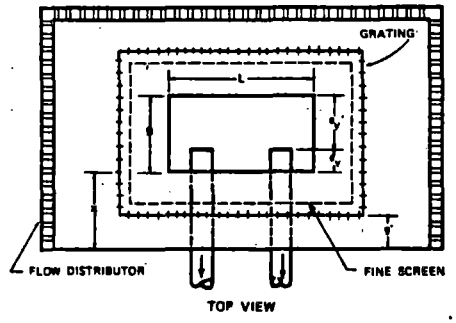

TOP VIEW

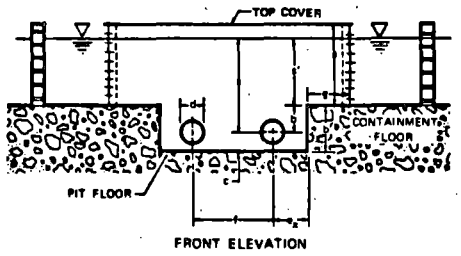

FRONT ELEVATION

GEOMETRIC PARAMETERS	TEST RANGE	GEOMETRIC PARAMETERS	TEST RANGE
a	0.5 TO 20 FT	e	0 TO 10 FT
a	1 TO 6 FT	f	4 TO 12 FT
b	1 TO 15 FT	g	0 TO 6 FT
c	0 TO 2 FT	g	4 TO 15 FT
d	6, 12, 18, 24 INCHES	L	6 TO 20 FT

GEOMETRIC PARAMETERS

TEST PLAN

FACTORIAL TESTING

- PRIMARY GEOMETRIC AND FLOW VARIABLES STUDIED PARAMETRICALLY USING A FRACTIONAL FACTORIAL TEST MATRIX
- EFFICIENT TECHNIQUE FOR STUDYING A LARGE NUMBER OF VARIABLES OVER A LARGE RANGE OF VALUES

SECONDARY VARIABLE, SENSITIVITY TESTS

- NONSYMMETRICAL PIPE EFFECTS
- PIPE DIAMETER
- REYNOLDS NUMBER EFFECTS
- COVER PLATE
- SCALE EFFECTS
- VARIABLE e_y
- VARIABLE e^y
- VARIABLE c^x
- VARIABLE b (SUMP DEPTH)
- OUTLET PIPE SHAPE
- VERTICAL PIPE ORIENTATION
- SINGLE SUCTION PIPE

TEST PLAN (CONT.)

SEVERE PERTURBATION TESTS

- NONUNIFORM APPROACH FLOW AND STREAMING
  - SWIRL
  - COUPLE
  - STREAMING
  - DOUBLE SWIRL
- BREAK FLOW
- CONDENSER DRAIN FLOW
- OBSTRUCTIONS
- TRANSIENTS (SWITCHOVER AND STARTUP)
- SCREEN BLOCKAGES (UP TO 75% BLOCKED)
- PIPE INLET SHAPES
- TYPICAL CAGE TYPE VORTEX SUPPRESSOR

VORTEX SUPPRESSORS

- CAGE TYPE
- HORIZONTAL GRATES
- GUIDE VANES IN THE INLET

NON-UNIFORM FLOW AND SCREEN BLOCKAGE SCHEMES

NON-UNIFORM FLOW
(FLOW DISTRIBUTOR BLOCKAGE)

W = 30 FT
L = 60 FT

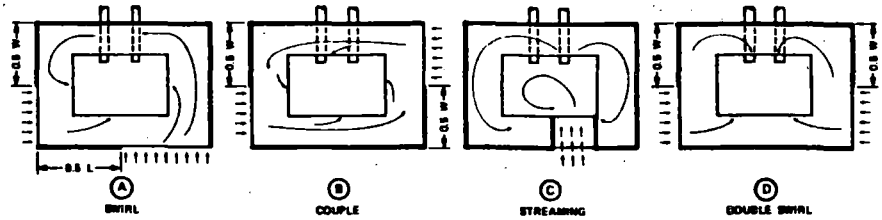

SCREEN BLOCKAGE

W = SUMP WIDTH
L = SUMP LENGTH

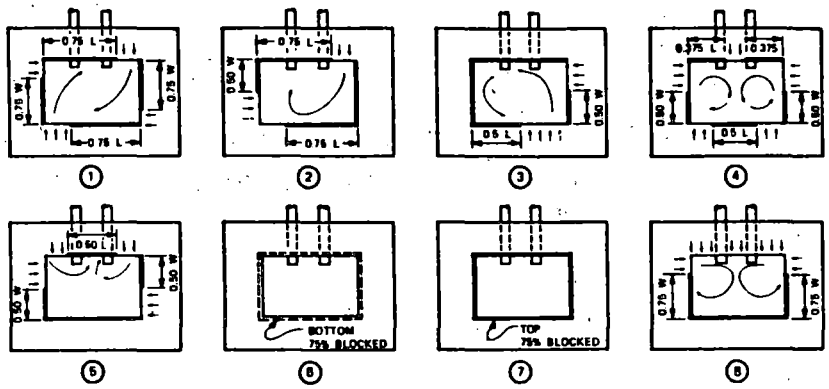

NON-UNIFORM FLOW AND SCREEN BLOCKAGE SCHEMES

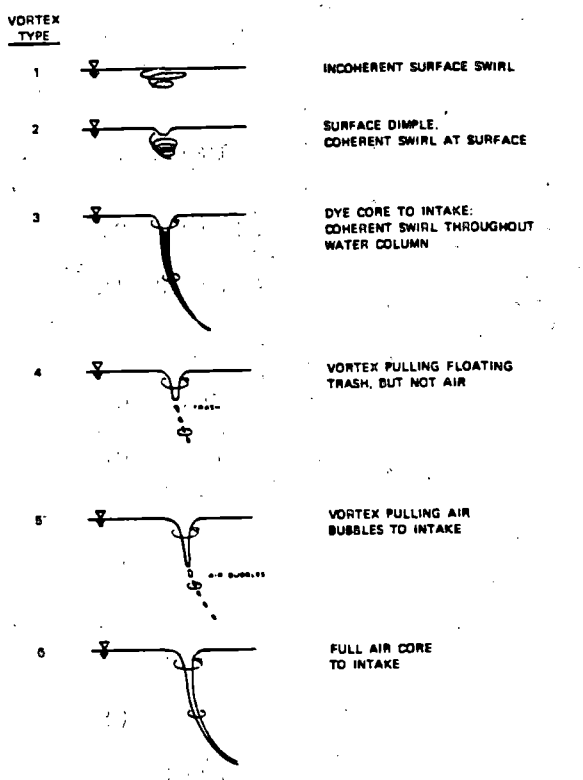

VORTEX TYPE CLASSIFICATION

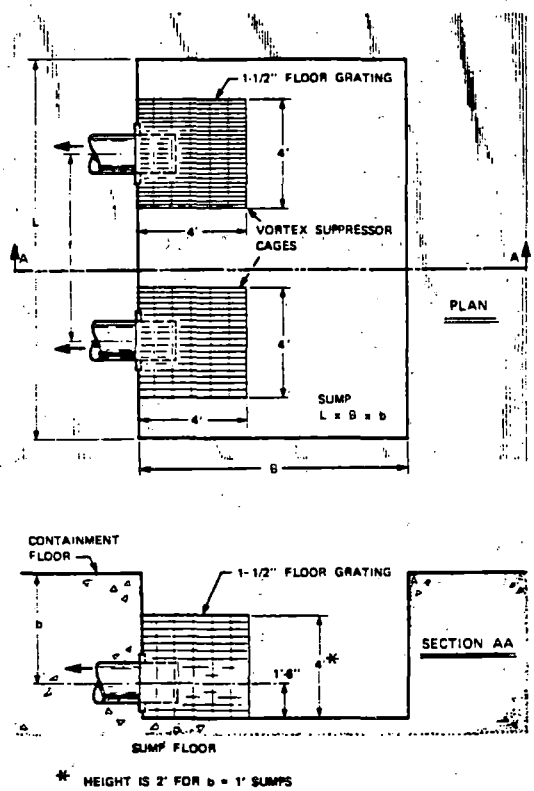

* HEIGHT IS 2' FOR b = 1' SUMPS

VORTEX SUPPRESSOR DEVICE FOR X-TESTS

RESULTS (BRIEF)

PARAMETER AND RESPONSE CORRELATIONS

- TIME VARYING, THREE-DIMENSIONAL NATURE OF VORTICES HAS RESULTED IN A STOCHASTIC DATA RESPONSE
- FUNCTIONALLY DESCRIBED TRENDS HAVE A LARGE UNCERTAINTY

ENVELOPE ANALYSIS

- ECCS SUMP DATA BASE COVERS A WIDE RANGE OF GEOMETRIC AND FLOW VARIABLES AND COVERS A WIDE RANGE OF PERTURBED FLOW CONDITIONS, THEREFORE, THE DATA FORMS AN ENVELOPE (OR BOUNDARY) OF MAXIMUM VALUES FOR THE DEPENDENT PERFORMANCE PARAMETERS
- USE ENVELOPE ANALYSIS TO CONFIDENTLY PREDICT UNDER WHAT CONDITIONS THE VOID FRACTION, SURFACE VORTEX TYPE, OR SWIRL SHOULD NOT EXCEED SOME PRESCRIBED VALUE IRRESPECTIVE OF HOW EXTREME THE FLOW PERTURBATIONS MAY BE
- THIS ENVELOPE ANALYSIS CAN FORM THE BASIS FOR ESTABLISHING SUMP DESIGN GUIDELINES

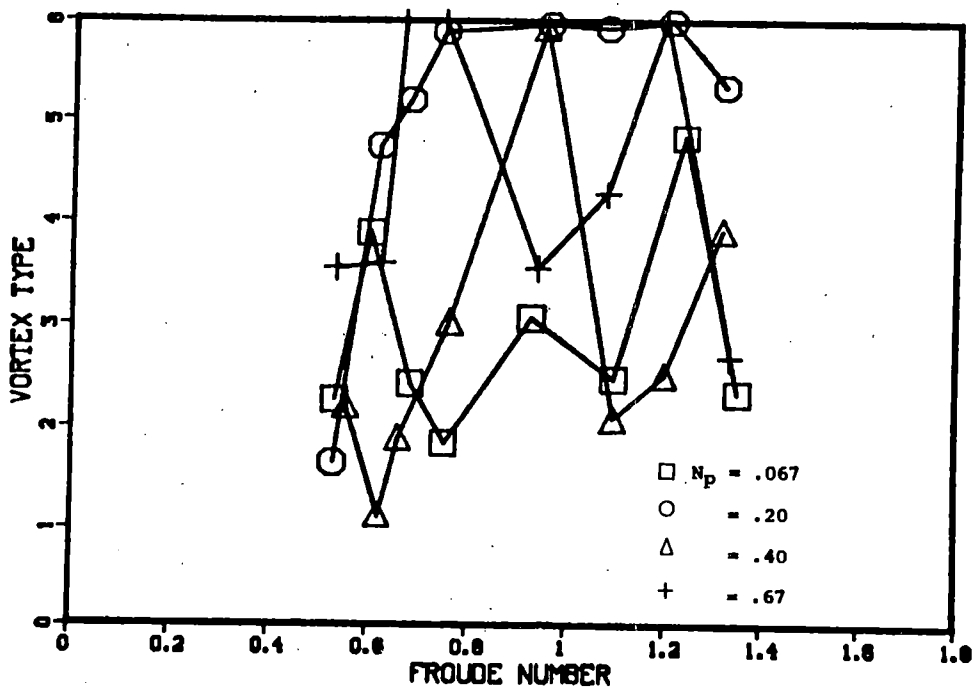

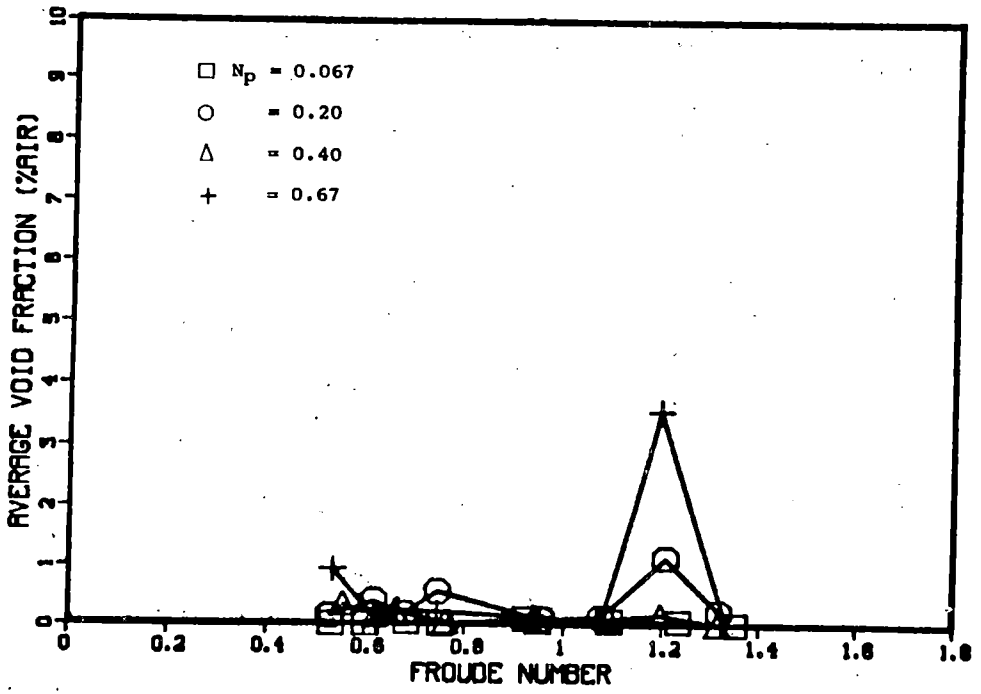

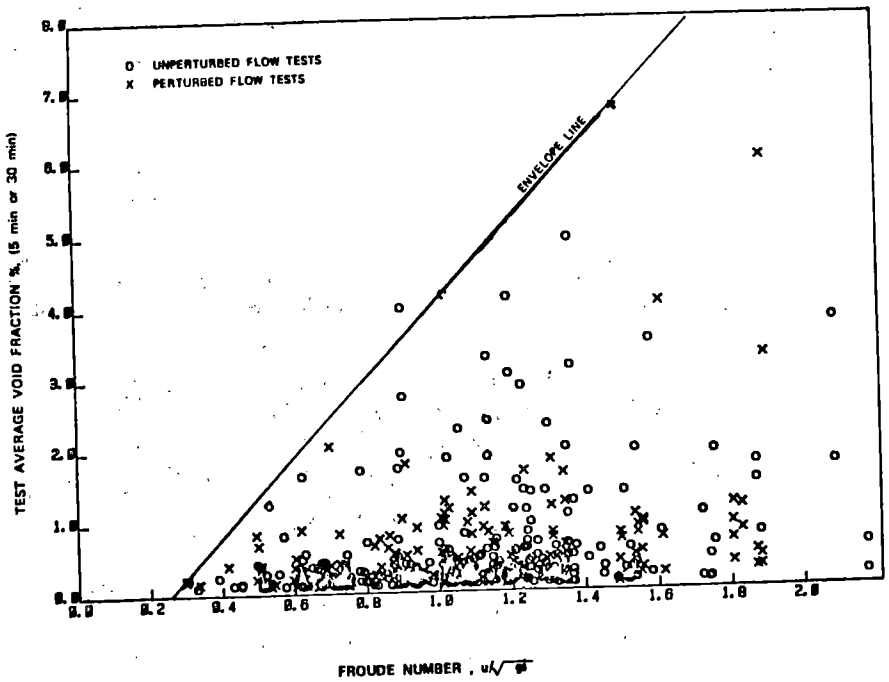

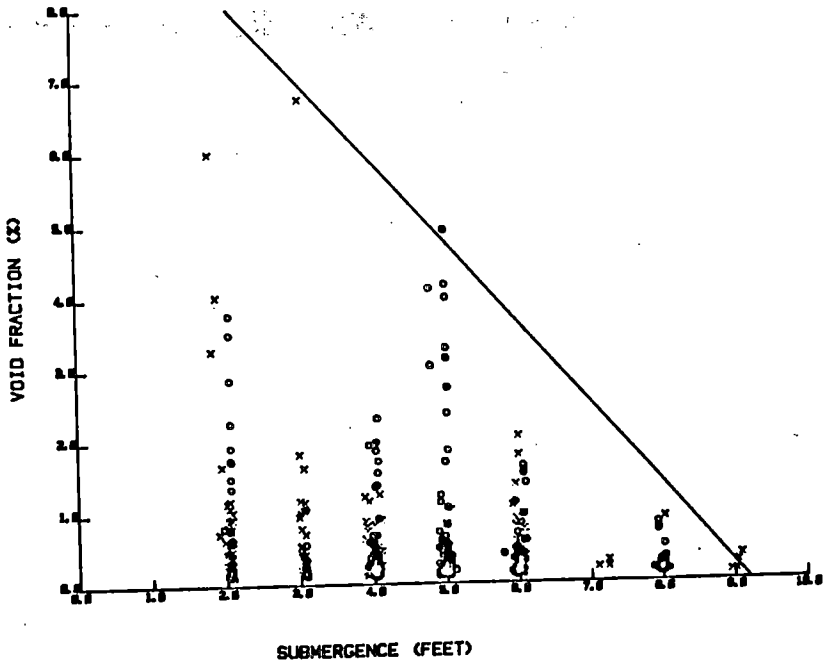

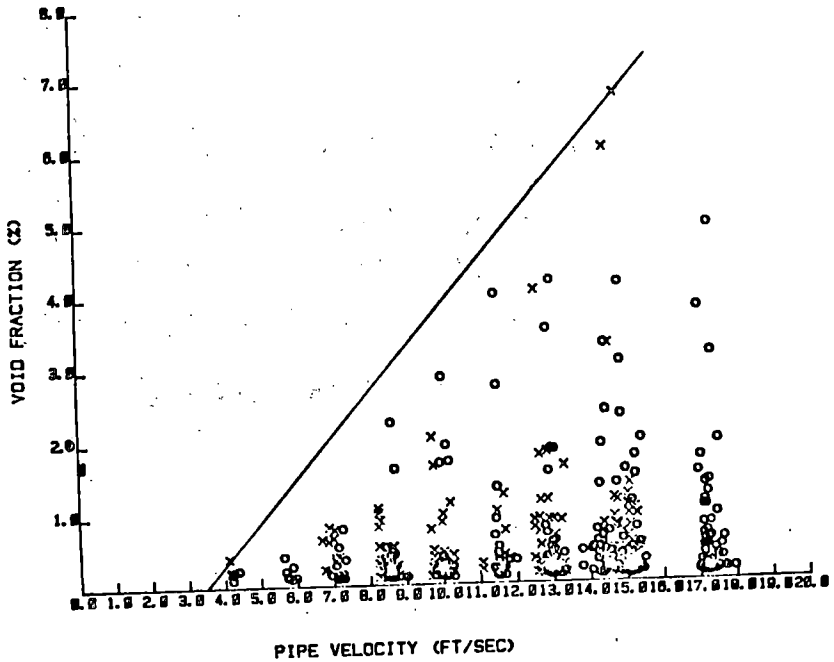

GENERAL CONCLUSIONS

VORTICES

- WEAK VORTICES (LESS THAN 1% AIR VOID) FOR SUBMERGENCES GREATER THAN 8 FT
- VORTICES, IN GENERAL, ARE UNSTEADY AND SPATIALLY UNSTABLE
- VORTICES (VORTEX TYPE) POOR INDICATOR OF SUMP PERFORMANCE
- VORTICES (VORTEX TYPE) POOR INDICATOR OF PIPE SWIRL OR AIR VOID FRACTION

GENERAL CONCLUSIONS (CONT.)

VOID FRACTION

- MOST AIR CORE VORTICES (ESPECIALLY UNPERTURBED TESTS) HAD VOID FRACTIONS OF LESS THAN 1%
- MAXIMUM VOID FRACTION MEASURED (30 MINUTE SAMPLE) WAS 7%; IT OCCURRED AT HIGH FLOW AND LOW SUBMERGENCE.
- VOID FRACTIONS GREATER THAN 3% WERE OBSERVED FOR SOME BUT NOT ALL OF THE BADLY PERTURBED FLOWS
- FOR SUBMERGENCES GREATER THAN 8 FT AND FOR ALL FLOW CONDITIONS (PERTURBED AND UNPERTURBED) MEASURED AIR VOIDS WERE LESS THAN 1%

PIPE SWIRL (14.5 DIAMETERS AWAY FROM INLET)

- IN MOST CASES SWIRL LEVEL WAS LESS THAN 4 DEGREES (30 MINUTE SAMPLE)
- SOME LARGER LEVELS OF SWIRL (MAXIMUM WAS 8 DEGREES) WERE MEASURED FOR PERTURBED FLOWS WITH HIGH FLOW AND LOW SUBMERGENCE
- SUBMERGENCE HAS A STRONG INFLUENCE ON THE SWIRL LEVEL

GENERAL CONCLUSIONS (CONT.)

LOSS COEFFICIENT

- LOSS COEFFICIENT NEARLY INDEPENDENT OF THE OVERALL SUMP GEOMETRY AND SUMP FLOW CONDITIONS
- THE LOSS COEFFICIENT IS INDEPENDENT OF ANY SURFACE VORTEX PHENOMENA
- THE LOSS COEFFICIENT IS A WEAK FUNCTION OF THE PIPE SWIRL
- THE LOSS COEFFICIENT IS PRINCIPALLY A FUNCTION OF THE SUCTION PIPE INLET GEOMETRY
- FOR MOST CASES A LOSS COEFFICIENT OF ABOUT $C_L = 1.0$ IS A REPRESENTATIVE UPPER BOUND LOSS VALUE

VORTEX SUPPRESSION

- CAGE TYPE SUPPRESSOR
- SUPPRESSION TESTS ALWAYS PERFORMED USING THE WORST POSSIBLE PERTURBED CONFIGURATION
- FULL AIR-CORE VORTICES WERE REDUCED TO SURFACE SWIRLS: SUPPRESSOR "KILLED" THE AIR-CORE VORTICES
- AIR VOID FRACTION WAS REDUCED TO ZERO
- MEASURED SUCTION PIPE SWIRL WAS LESS THAN 5 DEGREES
- THERE WAS NO SIGNIFICANT CHANGE IN THE LOSS COEFFICIENT DUE TO THE VORTEX SUPPRESSOR

SAND81-2398C

Ninth Water Reactor Research Information Meeting
October 26-30, 1981
Gaithersburg, Maryland

Structural Safety Margins of Containments*

Walter A. Von Riesemann, Thomas E. Blejwas,
Albert W. Dennis and Ronald L. Woodfin

Systems Safety Technology Division
Sandia National Laboratories
Albuquerque, New Mexico

The objectives of the Structural Safety Margins for Containments program are: 1) the generation of the data base needed to assess methods for predicting the behavior of LWR containments under accident conditions and severe environments beyond current design requirements; 2) the assessment of selected predictive numerical methods and 3) the improvement of predictive analytical techniques, as necessary. The structural behavior of containments up to their ultimate capacity and the failure modes of these containments are being determined. Static and dynamic internal overpressurization loads and loadings due to earthquakes are being considered.

The containment building is the final barrier to any fission products accidently released from within the reactor pressure boundary; hence, knowledge of its behavior is required for 1) risk studies, 2) design of accident mitigation equipment, 3) severe accident mitigation strategies, and 4) emergency preparedness planning.

Elaborate computer methods and simplified procedures which utilize many approximations and assumptions can be used to estimate the ultimate containment behavior. However, little test data is presently available to assess the validity of the estimates.

To achieve the objectives of the program both experimental and analytical efforts are being pursued. The experiments will consist of tests of scale models of complete containment structures. The analytical effort is presently providing preliminary data for planning and conducting the experiments. Extensive analyses and comparisons with experimental data will be conducted to assess existing numerical methods. Modifications of existing computer codes may be required.

*This work is being performed by Sandia National Laboratories for the Mechanical/Structural Engineering Branch, Division of Engineering Technology, Office of Nuclear Regulatory Research, U.S. Nuclear Regulatory Commission, under Memorandum of Understanding DOE 40-550-75.

The first phase of the program was a background study which resulted in a program plan which was completed in FY81. This background study included the identification of U.S. LWR containments according to reactor type, structural design and geometry; a review of the pertinent ASME, ASME/ACI design codes; a literature search of previous model tests and of tests performed on actual containments (dynamic tests at very low input); a preliminary evaluation of computer codes which could be used in assessing containment capacity; an examination of the scaling laws; the identification of critical structural elements and the relationship of these with various scales; and methods of simulating the dynamic internal pressurization and earthquake loadings.

The background study served two purposes. First, it confirmed the necessity of conducting the program. Second, it provided the basis for the program plan. In addition, a peer advisory group, consisting of nationally recognized experts in containment design, was formed to review and comment on the program. It was decided that the containments and loadings should be examined in the following sequence: static loadings on hybrid steel containments (typical of many MK III's and PWR ice-condensers), reinforced concrete containments and prestressed concrete containments; dynamic loadings on the same sequence and earthquake loadings on reinforced concrete, prestressed concrete, and hybrid steel containments. Several iterations of the program plan were performed. Only the final result for the static loading of the hybrid steel and reinforced concrete containments will be presented. The present plan reflects several modifications, such as use of prototypical models rather than replica models, which were necessitated by budget restrictions. Details are given in the figures.

In summary, the containment program combines both experimental and analytical efforts in a manner which will provide a substantially improved capability to evaluate predictions of the ultimate capacity of LWR containments when subjected to pressurization and earthquake loadings.

STRUCTURAL SAFETY MARGINS OF CONTAINMENTS

OBJECTIVES

- GENERATE THE DATA BASE NEEDED TO ASSESS METHODS FOR PREDICTING
  ULTIMATE LOAD CAPACITY AND
  FAILURE MODES OF LWR CONTAINMENTS
  UNDER
    ACCIDENT CONDITIONS AND SEVERE ENVIRONMENTS
- ASSESS SELECTED PREDICTIVE COMPUTER CODES
- IMPROVE ANALYSIS TECHNIQUES, AS NECESSARY

CONTAINMENT TYPES

STEEL

REINFORCED CONCRETE

PRESTRESSED CONCRETE

LOADINGS

INTERNAL PRESSURIZATION

STATIC

DYNAMIC

EARTHQUAKES

- WORK BEING PERFORMED BY SANDIA NATIONAL LABS FOR THE STRUCTURAL ENGINEERING SECTION OF THE MECHANICAL/STRUCTURAL ENGINEERING BRANCH, DIVISION OF ENGINEERING TECHNOLOGY, RESEARCH

LICENSING AND SAFETY ISSUE

- PROVIDE BASIS FOR STAFF DECISION FOR RELIABLE PREDICTION OF CONTAINMENT STRUCTURE CAPACITIES, WHICH WILL LEAD TO MORE REALISTIC ESTIMATES OF RISK TO PUBLIC HEALTH AND SAFETY

KNOWING THE STRUCTURAL BEHAVIOR OF THE CONTAINMENT BEYOND ITS DESIGN REQUIREMENTS AND KNOWLEDGE OF FAILURE MODES IS REQUIRED FOR:

- RISK STUDIES
- DESIGN OF ACCIDENT MITIGATION EQUIPMENT
- SEVERE ACCIDENT MITIGATION STRATEGIES
- EMERGENCY PREPAREDNESS PLANNING

NUREG-0772

TECHNICAL BASES FOR ESTIMATING FISSION PRODUCT BEHAVIOR DURING LWR ACCIDENTS

PAGE iii

"ONE OF THE LARGEST UNCERTAINTIES ASSOCIATED WITH PREDICTING THE AMOUNT OF RADIONUCLIDES RELEASED . . . RESULTS FROM LIMITATIONS IN THE ABILITY TO PREDICT THE TIMING, MODE AND LOCATION OF CONTAINMENT FAILURE."

STRUCTURAL SAFETY MARGINS OF CONTAINMENTS

APPROACH

- EXPERIMENTAL PROGRAM (UTILIZING STRUCTURAL MODELS)
  SUPPORTED BY A STRONG ANALYTICAL EFFORT

END PRODUCTS

- BENCH MARK DATA BASE
- ASSESSED ANALYTICAL METHODS
- SUBSTANTIALLY IMPROVED ABILITY TO EVALUATE
  PREDICTIONS OF ULTIMATE LOAD CARRYING CAPABILITY

BACKGROUND STUDY

TYPES OF CONTAINMENTS

CODE (ASME/ACI) REQUIREMENTS

PREVIOUS TESTS

ANALYSIS METHODS

SCALE MODELING (SIMILITUDE)

LOAD SIMULATION
- STATIC
- DYNAMIC
- SEISMIC

CONTAINMENT TYPES

- SINGLE VS. DOUBLE BARRIER
- SUPPRESSION TECHNIQUE (DRY, SUB-ATMOSPHERIC, WATER, ICE)
- PWR, BWR
- STEEL, HYBRID STEEL
  REINFORCED CONCRETE
  PRESTRESSED CONCRETE

SUMMARY OF OPERATING & FUTURE UNITED STATES POWER REACTOR CONTAINMENT STRUCTURES

JUNE30, 1980
DATA BASE

Sandia National Laboratories

			CONTAINMENT STRUCTURES										
			CONCRETE			STEEL							
			PRE-STRESSED VERTICAL CYL & DOME WITH FLAT BASE	DEFORMED BAR HEMISPHERICAL DOME VERT CYL BODY AND FLAT BASE	OTHER CONCRETE	LIGHT BULB TORUS CONTAINMENT	STEEL SPHERE	HEMISPHERICAL DOME CYL BODY AND ELLIPSOIDAL BASE	HYBRID STEEL-STEEL DOME AND BODY REINFORCED CONCRETE BASE	SUB-TOTAL	SUB-TOTAL	TOTAL
COMMERCIAL U.S. POWER REACTORS	PWR'S	ATMOSPHERIC CONTAINMENT STRUCTURES WITHOUT PRESSURE SUPPRESSION SYSTEMS	55	20	2		11	11		99	120	180
		SUB-ATMOSPHERIC CONTAINMENTS		11						11		
		ICE-CONDENSER CONTAINMENTS		2					8	10		
	BWR'S	MARK I			2	23				25	60	
		MARK II			10					10		
		MARK III		6					15	21		
		PRE MARK			2		2			4		
		SUB-TOTAL	55	39	16	23	13	11	23			
		SUB-TOTAL	110			70						
		TOTAL	180									

WASHINGTON 2 IS NOT INCLUDED IN THE ABOVE TABLE

CONTAINMENT STRUCTURE DESIGN PRESSURE RANGES
PRESSURE IN psi gage

JUNE 30, 1980
DATA BASE

Sandia National Laboratories

			CONTAINMENT STRUCTURES						
			CONCRETE			STEEL			
			PRE-STRESSED VERTICAL CYL & DOME WITH FLAT BASE	DEFORMED BAR HEMISPHERICAL DOME VERT CYL BODY AND FLAT BASE	OTHER CONCRETE	LIGHT BULB TORUS CONTAINMENT	STEEL SPHERE	HEMISPHERICAL DOME CYL BODY AND ELLIPSOIDAL BASE	HYBRID STEEL STEEL DOME AND BODY REINFORCED CONCRETE BASE
COMMERCIAL U.S. POWER REACTORS	PWR'S	ATMOSPHERIC CONTAINMENT STRUCTURES WITHOUT PRESSURE SUPPRESSION SYSTEMS	47–60	42–55	42–60		25–46 *	34–44 *	
		SUB ATMOSPHERIC CONTAINMENTS		45					
		ICE-CONDENSER CONTAINMENTS		12					11–15 *
	BWR'S	MARK I			56	56–62			
		MARK II			45–56				
		MARK III		15					15
		PRE-MARK			52		27–30 *		

* DESIGN PRESSURE ROUNDED TO WHOLE NUMBERS.

PREVIOUS TESTS

SCALE MODELS

- CANADA
- JAPAN
- INDIA
- POLAND
- UK, ITALY (REACTOR VESSELS)

ACTUAL CONTAINMENTS

DYNAMIC TESTS (LOW INPUT)

- GERMANY (HDR)
- JAPAN
- USA

ADVISORY GROUP

TOM AHL - CHICAGO BRIDGE & IRON

BILL BAKER - SOUTHWEST RESEARCH INSTITUTE

ASA HADJIAN - BECHTEL

GEORGE HOWARD - ANCO

METE SOZEN - UNIVERSITY OF ILLINOIS

JOHN STEVENSON - STRUCTURAL MECHANICS ASSOCIATES

JOE UCCIFERRO - UNITED ENGINEERS

DICK WHITE - CORNELL UNIVERSITY

IAN WALL - EPRI

RICH DENNING - BATELLE COLUMBUS LABS

BACKGROUND STUDY

TYPES OF CONTAINMENTS

CODE (ASME/ACI) REQUIREMENTS

PREVIOUS TESTS

ANALYSIS METHODS

SCALE MODELING (SIMILITUDE)

LOAD SIMULATION
- STATIC
- DYNAMIC
- SEISMIC

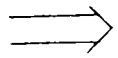

PROGRAM PLAN

ADVISORY GROUP

OVERALL PROGRAM PLAN

STATIC INTERNAL OVERPRESSURIZATION
- HYBRID STEEL
- REINFORCED CONCRETE
- PRESTRESSED CONCRETE

DYNAMIC INTERNAL OVERPRESSURIZATION
- SAME SEQUENCE

EARTHQUAKE LOADING
- REINFORCED CONCRETE
- PRESTRESSED CONCRETE
- HYBRID STEEL

PROGRAM SCHEDULE

FOR HYBRID STEEL AND REINFORCED CONCRETE MODELS SUBJECTED TO STATIC PRESSURIZATION LOADINGS

COMPLETION OF	STEEL	REINFORCED CONCRETE
EXPERIMENTAL PROGRAM	FY 83	FY 84
EVALUATION OF NUMERICAL METHODS	FY 84	FY 85

PROGRAM STATUS

- 1/32 SIZE HYBRID STEEL MODELS ARE BEING FABRICATED
- EXPERIMENTAL FACILITY IS IN PREPARATION
- ANALYSES ARE UNDER WAY
- TESTING TO BEGIN IN FIRST QUARTER OF CY'82

STATIC LOADING EXPERIMENTS FOR HYBRID STEEL CONTAINMENTS

EXPERIMENT	SIZE	DESCRIPTION
SC-1 & SC-2	~ 1/32	CLEAN SHELL EXPERIMENT TO SERVE AS THE "CONTROL" AND TO PROVIDE DATA FOR BASIC 2-D POST-YIELD METHOD EVALUATION
SC-3 & SC-4	~ 1/32	RING STIFFENED SHELL EXPERIMENT TO PROVIDE ADDITIONAL POST-YIELD METHOD EVALUATION DATA AND STRUCTURAL EFFECTS DATA
SC-5 & SC-6	~1/32	RING STIFFENED SHELL WITH PRIMARY PENETRATIONS TO PROVIDE DATA FOR 3-D POST-YIELD METHOD EVALUATION
SC-7	~1/10	RING STIFFENED SHELL WITH PENETRATIONS WHICH UTILIZES CONVENTIONAL CONSTRUCTION METHODS

STATIC LOADING EXPERIMENTS FOR REINFORCED CONCRETE CONTAINMENTS WITH STEEL LINER

EXPERIMENT	SIZE	DESCRIPTION
RCC-1 & RCC-2	~ 1/10	NO SEISMIC STEEL, NO PENETRATIONS. THESE EXPERIMENTS WILL SERVE AS THE "CONTROL" AND WILL PROVIDE DATA FOR BASIC 2-D POST-YIELD METHOD EVALUATION.
RCC-3 & RCC-4	~ 1/10	SEISMIC STEEL, BUT NO PENETRATIONS. THESE EXPERIMENTS WILL PROVIDE ADDITIONAL 2-D DATA AND STRUCTURAL EFFECTS DATA.
RCC-5 & RCC-6	~ 1/10	SEISMIC STEEL AND PRIMARY PENETRATIONS. THESE EXPERIMENTS WILL PROVIDE DATA FOR 3-D METHOD EVALUATION.

HYBRID STEEL EXPERIMENTS

1/32 SIZE

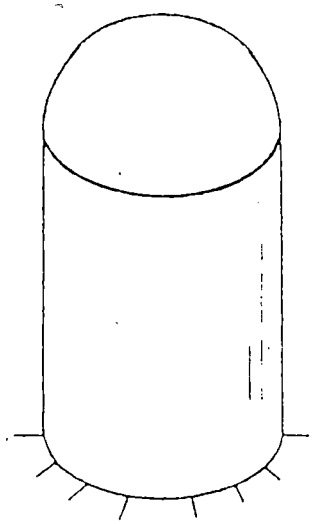

SC-1, -2

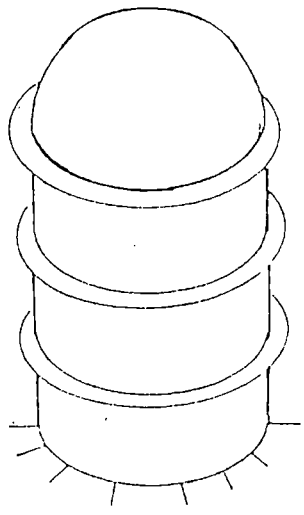

SC-3, -4

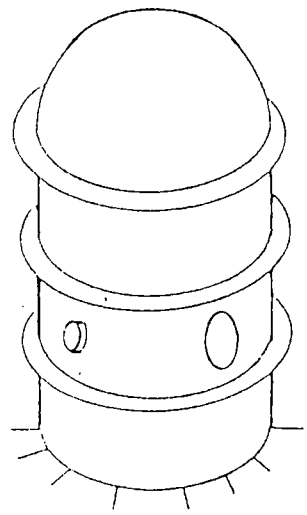

SC-5, -6

SUMMARY

STRUCTURAL SAFETY MARGINS OF CONTAINMENTS PROGRAM WILL PROVIDE,
THROUGH A COMBINED EXPERIMENTAL AND ANALYTICAL EFFORT,
A RELIABLE CAPABILITY
TO EVALUATE PREDICTIONS OF THE ULTIMATE CAPACITY OF LWR CONTAINMENTS
WHEN SUBJECTED TO STATIC AND DYNAMIC INTERNAL OVERPRESSURIZATION
LOADS AND TO EARTHQUAKE LOADINGS

DESIGN RECOMMENDATIONS BASED ON LARGE SCALE TESTING OF CONTAINMENT ELEMENTS

by

H. G. Russell*

ABSTRACT

Reinforced concrete containment vessels at nuclear power plants are designed to resist forces caused by internal pressure, gravity, severe earthquakes, and other severe natural phenomena. Reinforcement is generally placed in vertical and horizontal directions to resist internal pressure. Other bars are placed at 45° to resist horizontal tangential shear forces from earthquakes. This diagonal reinforcement is expensive, difficult to fabricate, and may cause significant congestion inhibiting concrete placement.

The primary reason for diagonal steel is that internal pressure acting in the containment vessel causes membrane tensile forces that in turn produce horizontal and vertical cracking of the wall. Cracking occurs from pressurization during acceptance tests. The ability of a cracked containment vessel to resist tangential shear forces without diagonal reinforcement has not been verified experimentally.

To investigate behavior of containment vessels without diagonal reinforcement, some large scale tests have been made. The experimental test set up was designed and constructed to simulate boundary conditions of an element in a containment wall. Specimens are 2-ft thick, 5-ft square, and reinforced orthogonally with No. 18 and No. 14 bars. Each specimen is subjected to biaxial tension and shear loading.

Test variables considered to date are level of biaxial tension and monotonic versus reversing load. The objective of the test program is to determine strength and deformation characteristics of a membrane element. Ability of a cracked containment to resist shear through dowel action and aggregate interlock will be determined.

The presentation describes the experimental program and discusses results obtained to date. Results are being used to evaluate current code requirements. Design criteria for combined tension and tangential shear are discussed.

*Director, Structural Development Department, Construction Technology Laboratories, a Division of the Portland Cement Association, Skokie, Illinois, U.S.A.

NUCLEAR CONTAINMENT

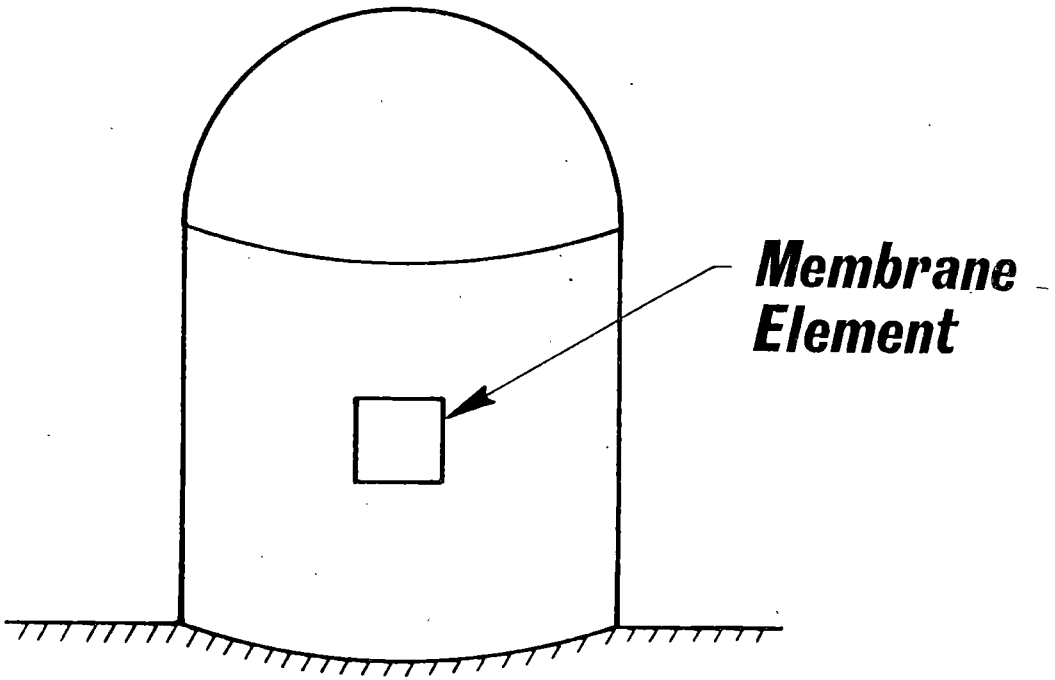

OBJECTIVES

TO DETERMINE:

1. LOAD DEFORMATION CHARACTERISTICS
2. SHEAR STRENGTH
3. EFFECT OF REVERSING SHEAR LOAD

TO DEVELOP:

4. DESIGN CRITERIA

TEST SPECIMEN

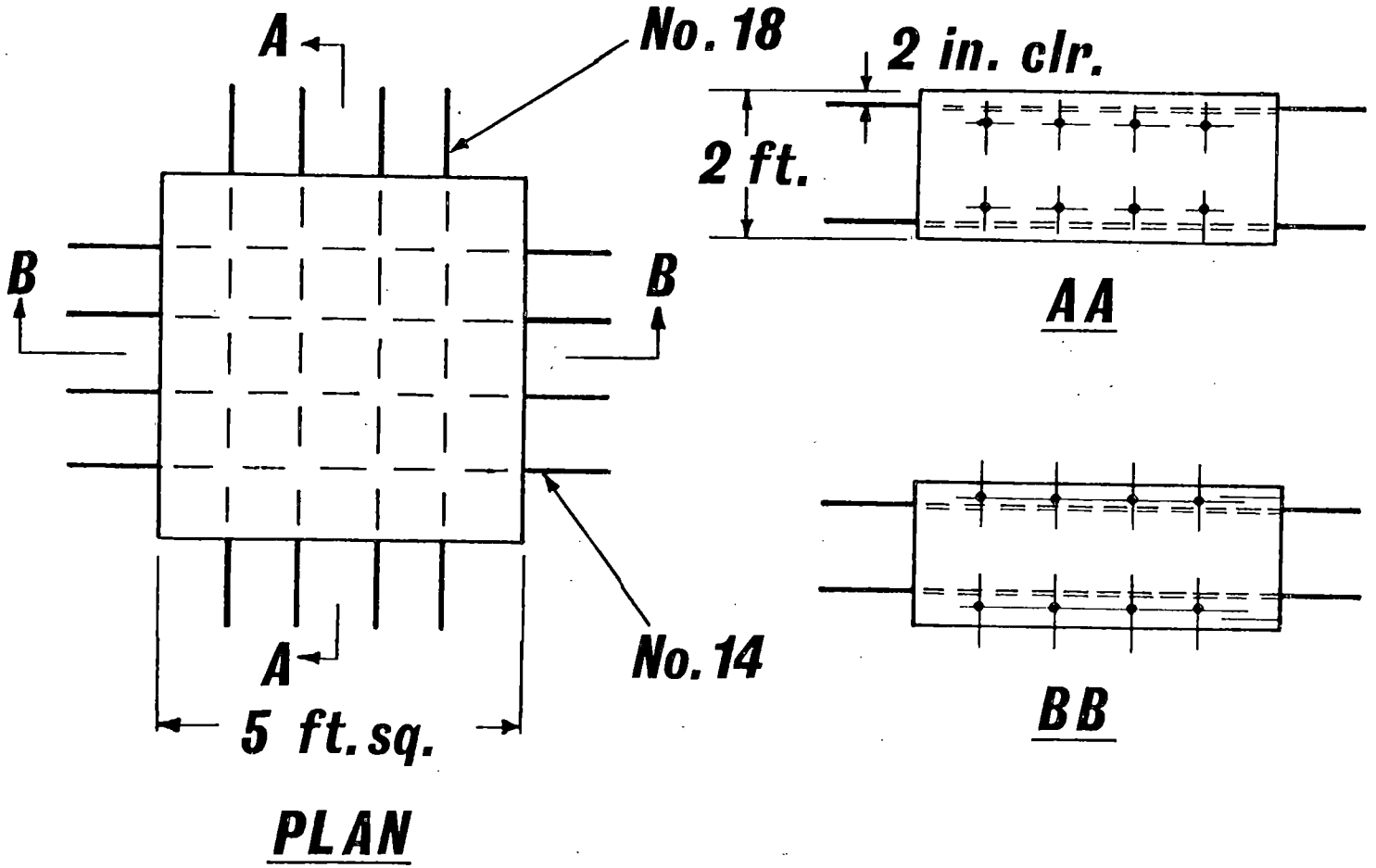

LOADING SYSTEM

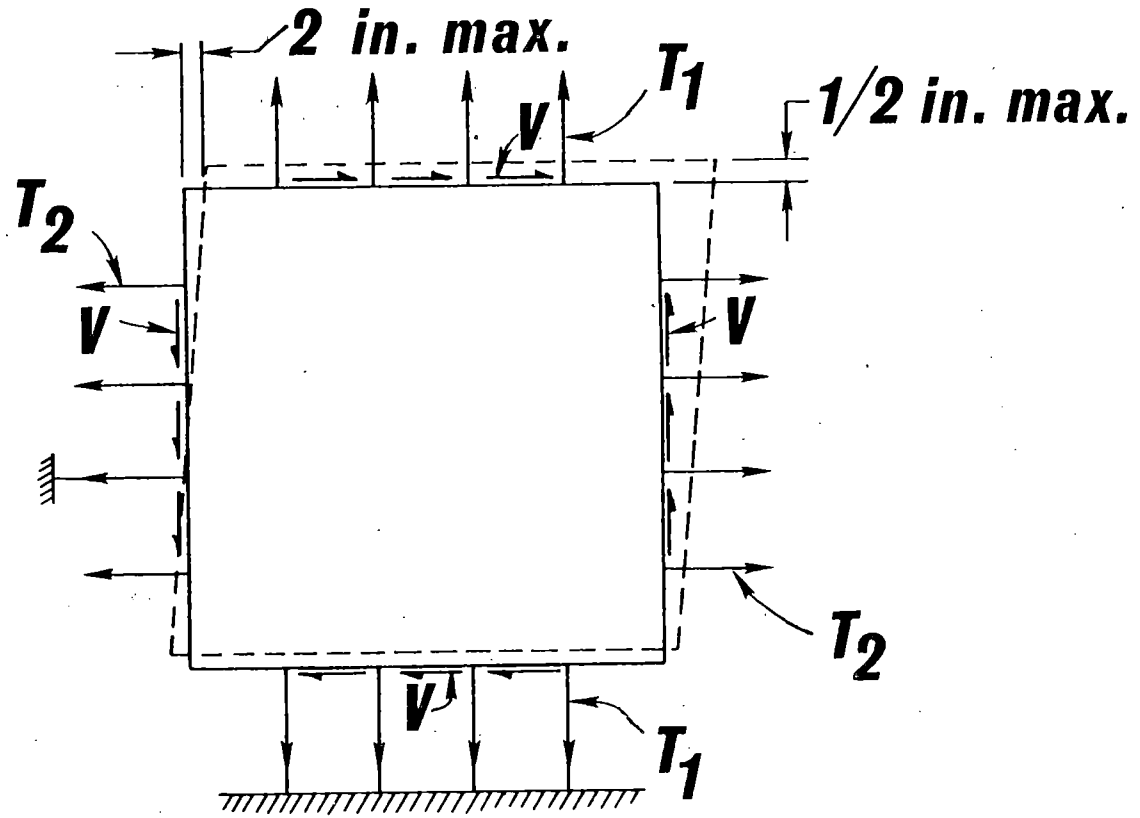

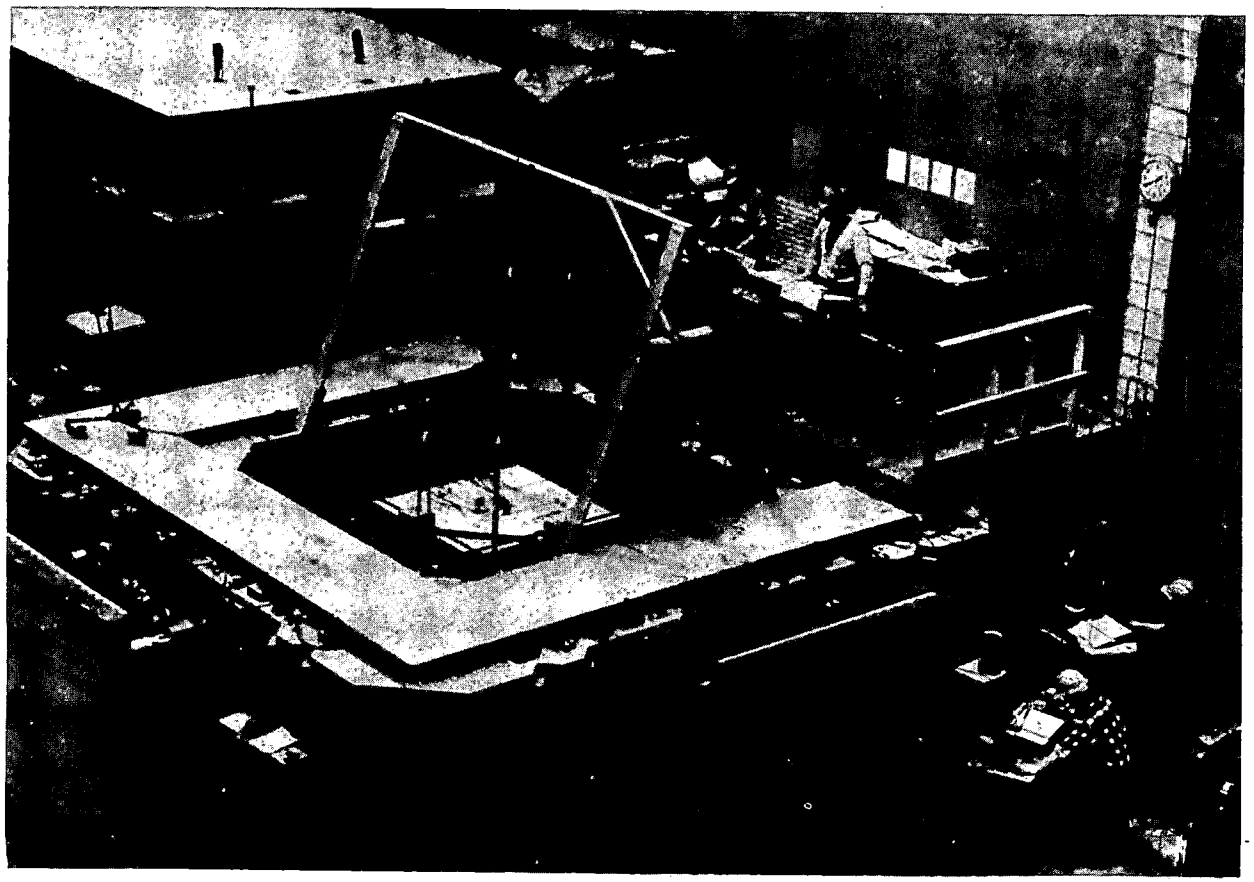

INSTRUMENTATION

1. LOADS
2. RIGID BODY MOVEMENT
3. SHEAR DISTORTIONS
4. ELONGATIONS
5. SLIP AT CRACKS
6. STEEL STRAINS

VARIABLES

1. LEVEL OF BIAXIAL TENSION

2. MONOTONIC VERSUS REVERSING SHEAR LOAD

LOAD HISTORY

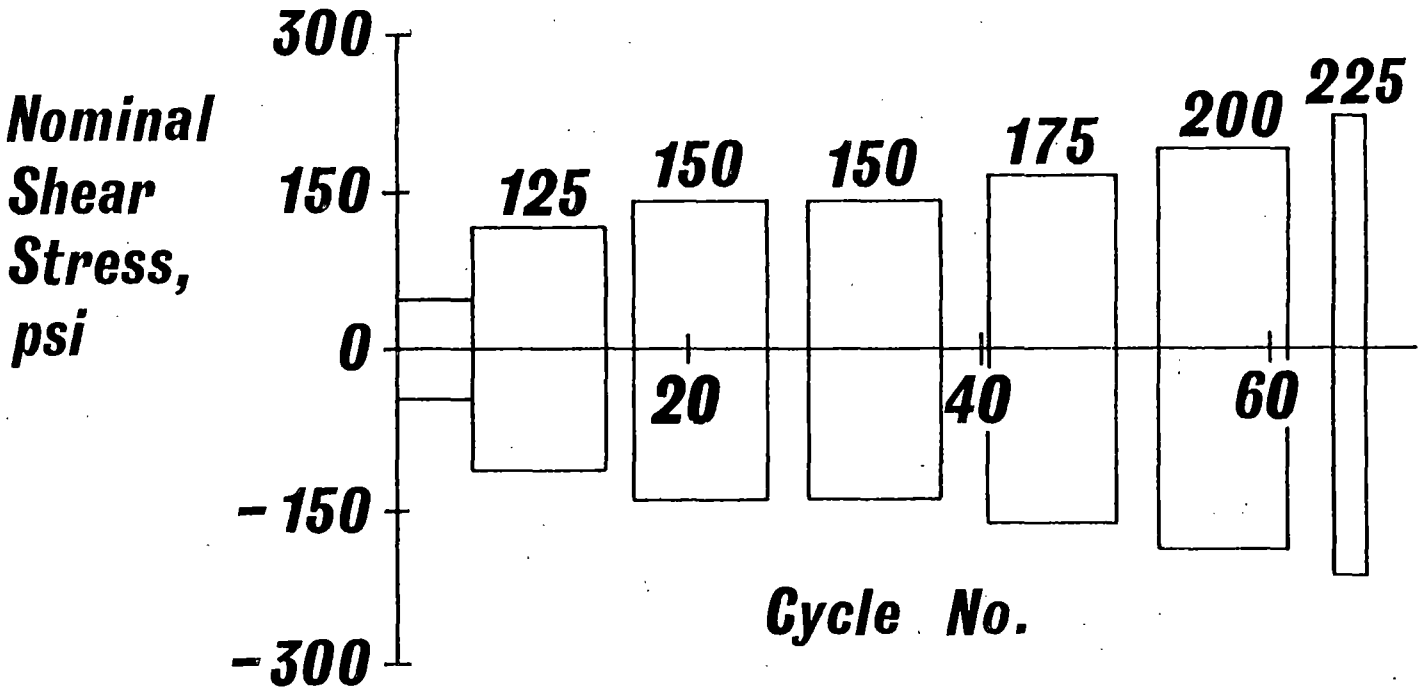

SHEAR STRESS VS. DISTORTIONS

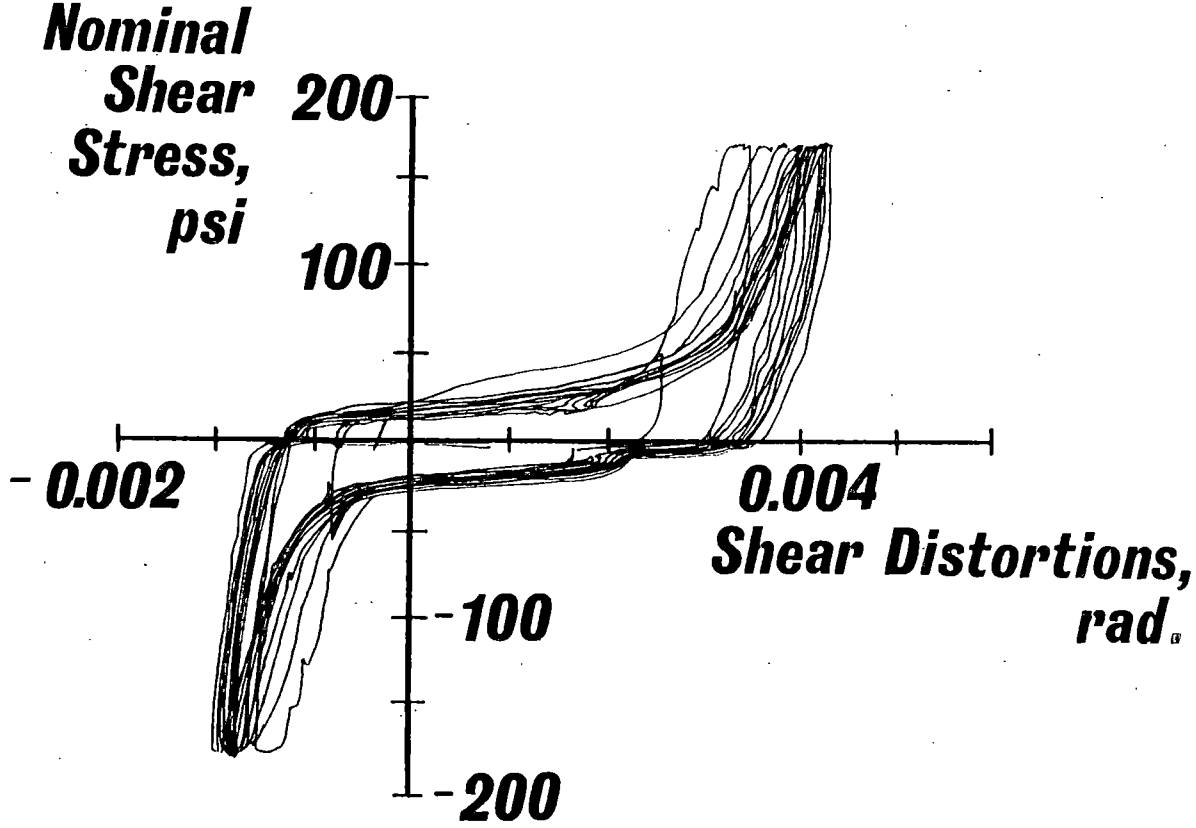

BIAXIAL TENSION 36 ksi

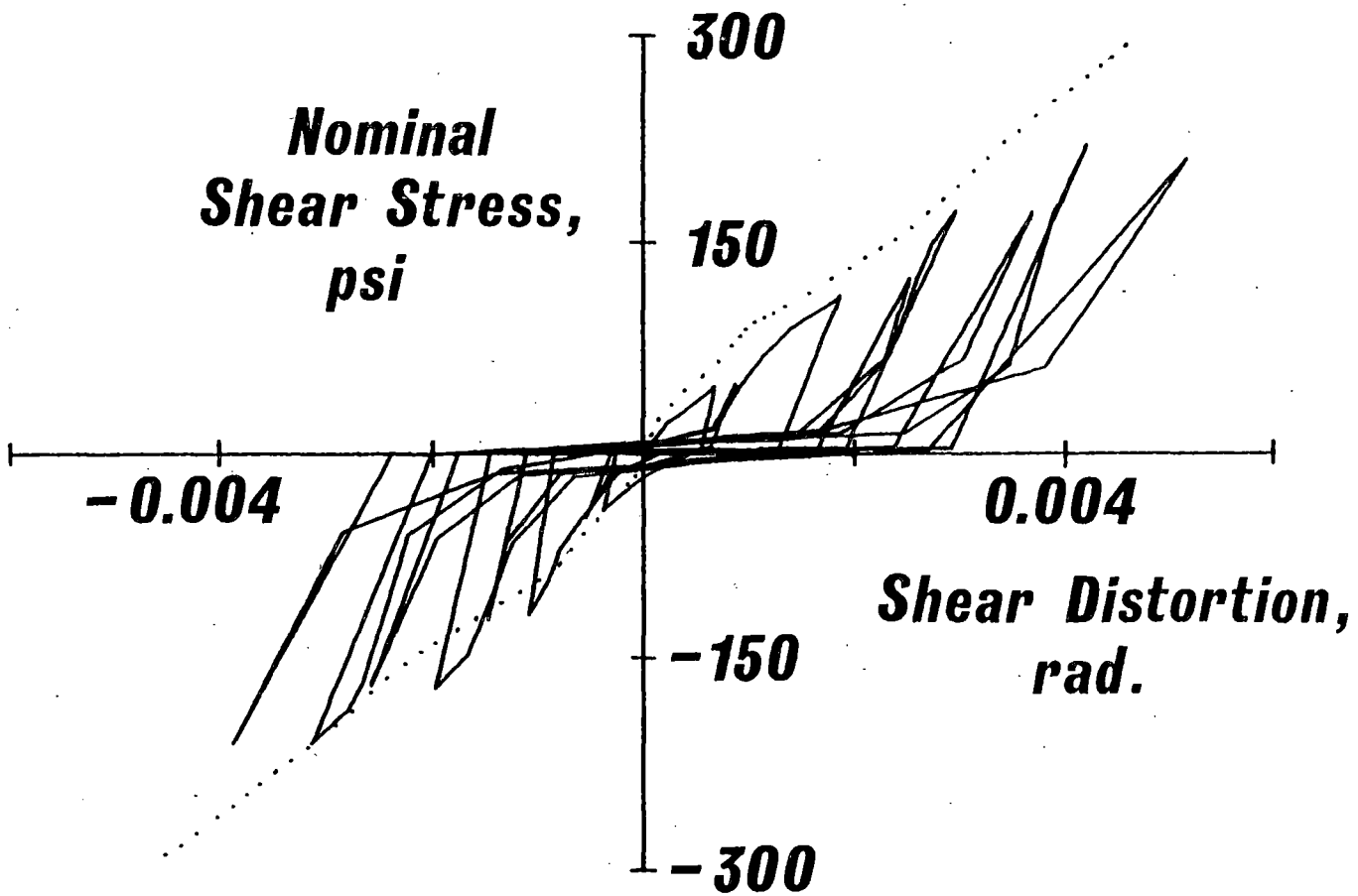

SHEAR STRENGTH

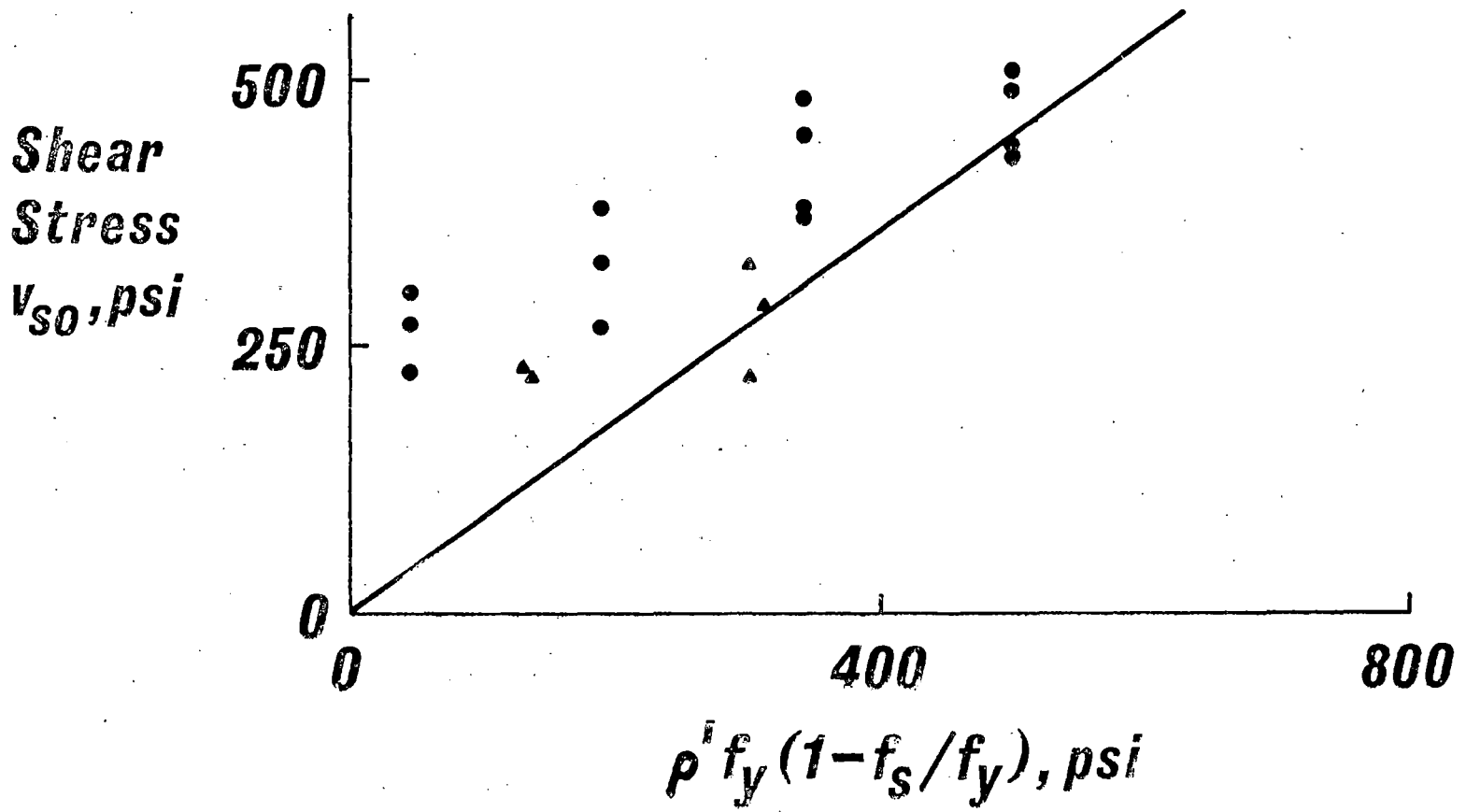

SHEAR STRENGTH

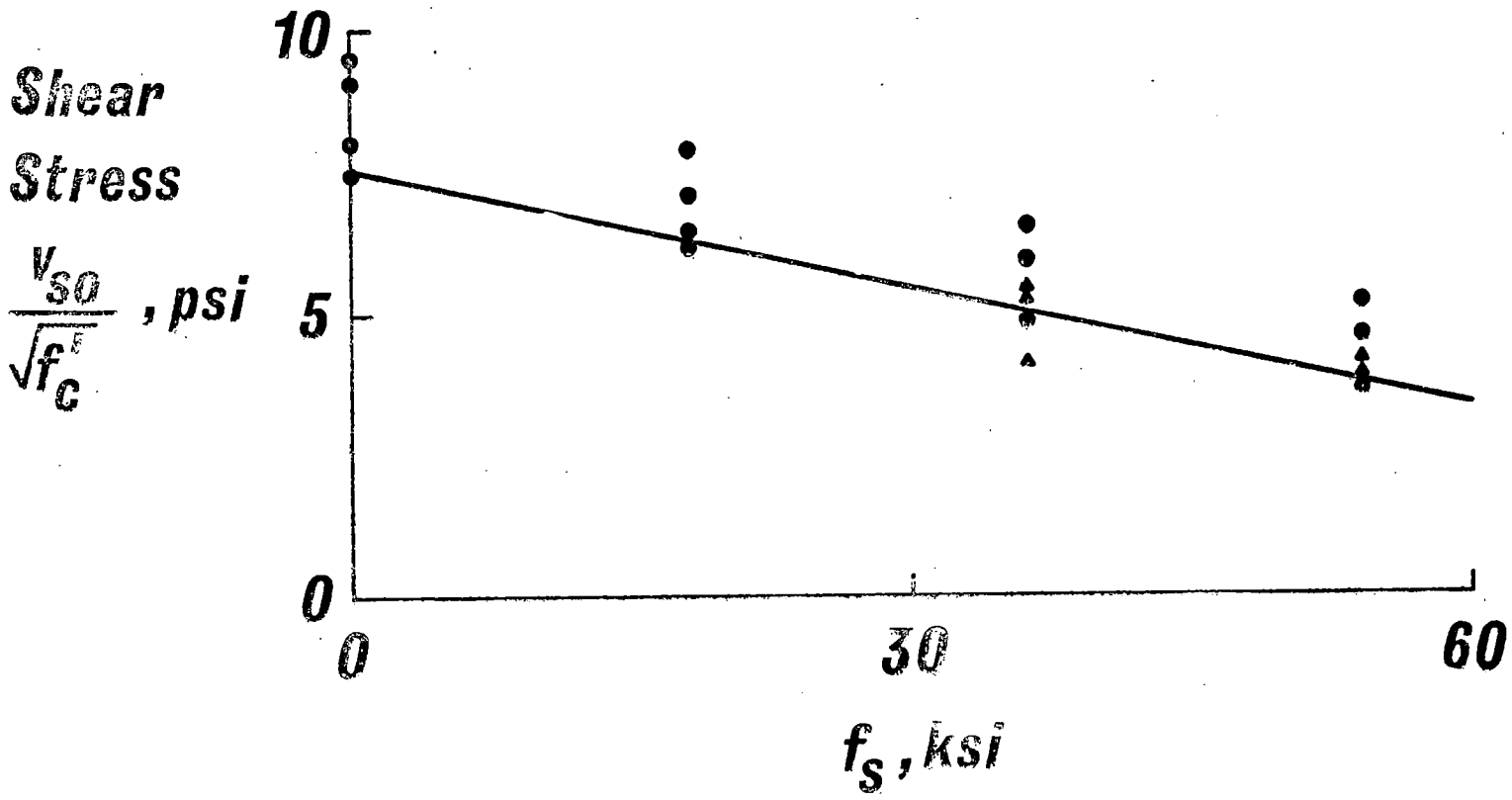

STRENGTH EQUATIONS

$$v_{so} = 0.9\rho' f_y (1 - f_s/f_y)$$

$$v_{so} < (7.5 - f_s/14{,}300)\sqrt{f'_c}$$

LIMITING DEFORMATIONS

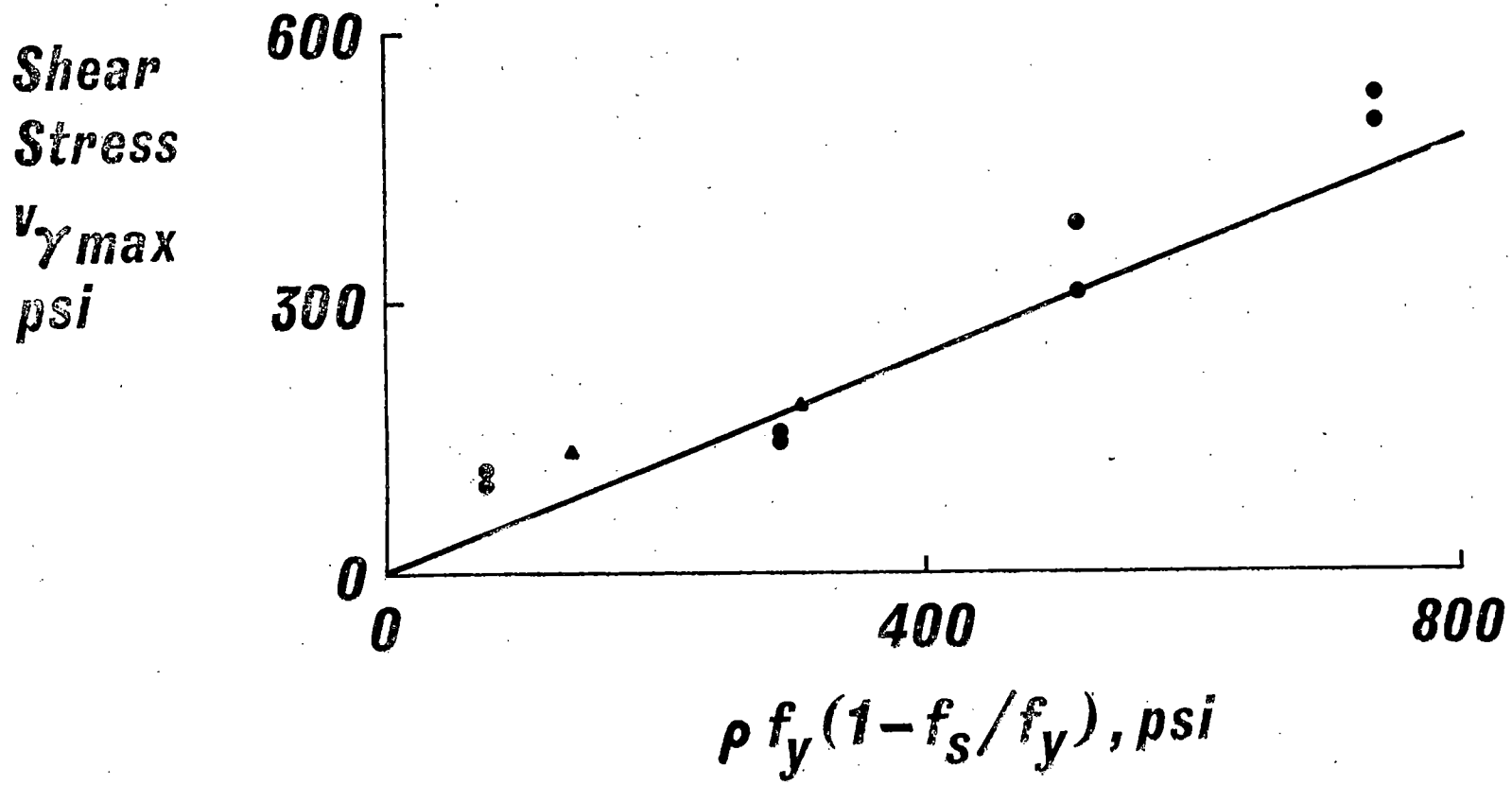

STRAIN LIMITATION

$$v_{\gamma max} = 0.6 \rho f_y (1 - f_s / f_y)$$

(Presented at the Ninth Water Reactor Safety Research Information Meeting
Gaithersburg, MD October 27, 1981)

SAFETY MARGIN IN SHEAR DESIGN CRITERIA FOR REINFORCED CONCRETE CONTAINMENTS

by Richard N. White and Peter Gergely, Cornell University

Current safety margins for shear design approaches for reinforced concrete containments are discussed from the perspective of test results achieved primarily through experiments at Cornell University under the sponsorship of the Nuclear Regulatory Commission. Conclusions drawn from the study include: (a) Punching shear strength is only slightly affected by high levels of biaxial tension in the containment wall, and current provisions are extremely conservative, (b) Concrete elements reinforced only with circumferential and meridional steel (no diagonal steel) can carry substantial amounts of in-plane tangential shear, even in the presence of biaxial tension levels up to $0.9f_y$ in the reinforcement. Current provisions could be relaxed to permit higher levels of shear to be carried by orthogonal reinforcement alone, (c) The same experiments on combined membrane shear and biaxial tension revealed that the effective shearing stiffness of the flat elements was very low, with typical values of about 5% of that for uncracked concrete. Implications for corresponding deformations in the steel liner of the containment need further assessment, and (d) Lessons learned from the experiments on punching and tangential shear indicate that radial shear needs a thorough study. Strength provisions may well be conservative, but potential redistribution of tangential shear away from highly stressed, "soft" regions into the stiffer regions will tend to accentuate radial shear problems. Directions of radial shear cracking must also be better assessed.

General observations include the fact that principal tension stress calculations may be nearly meaningless for concrete that is subject to cracking prior to shear loadings, and that containments subjected to combined pressurization and seismic loading will have large sections of the containment wall behaving in a highly nonlinear fashion. Experiments on complete containment models along with analytical studies that incorporate the true nonlinear behavior are needed to fully clarify containment response and safety for this load combination. This same research should include the extremely complex interaction between radial and tangential shear.

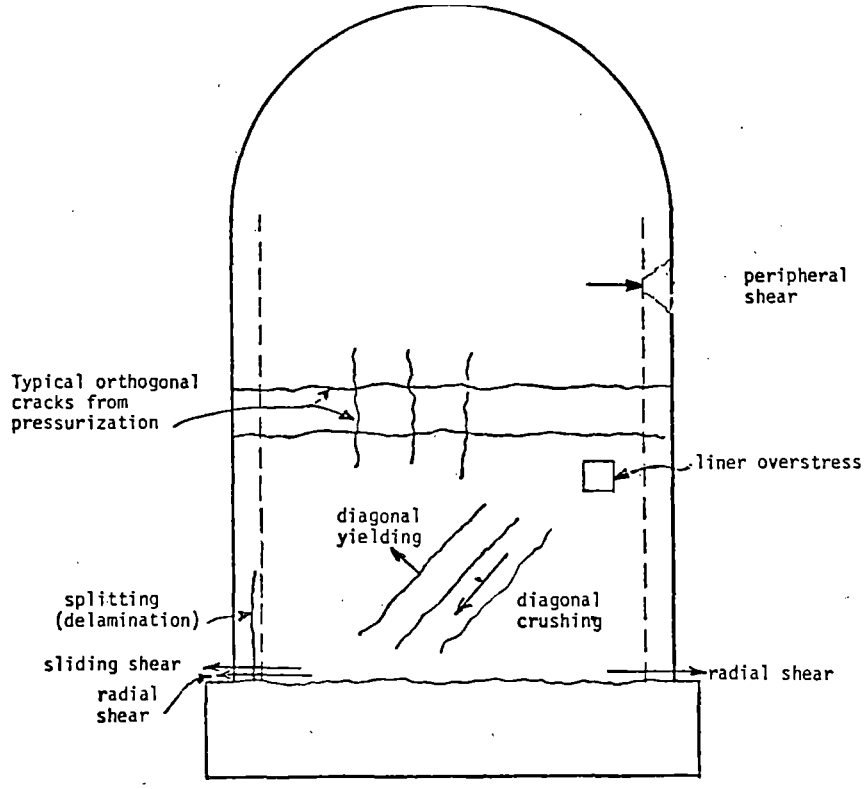

Potential Failure Modes - Containment

PUNCHING STRENGTH

OF

BIAXIALLY TENSIONED CONCRETE

RESEARCH OBJECTIVE:

TO DETERMINE THE DEPENDENCE OF SLAB PUNCHING STRENGTH ON THE LEVEL OF TENSION APPLIED TO ORTHOGONAL REINFORCING BARS IN THE SLAB, AND TO APPLY TO THE DESIGN OF CONTAINMENTS SUBJECTED TO PUNCHING LOADS.

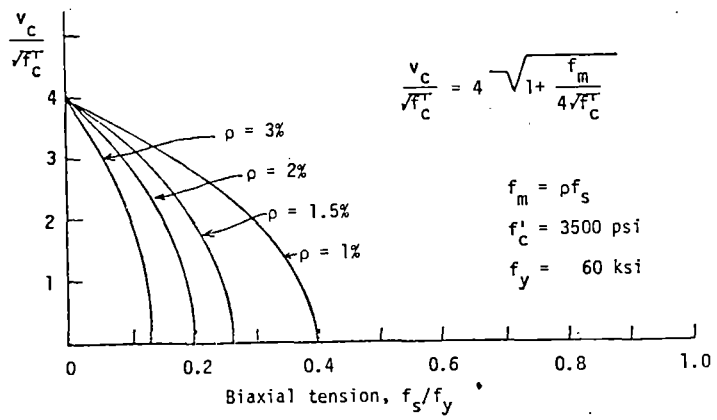

Current ASME-ACI Design Criteria

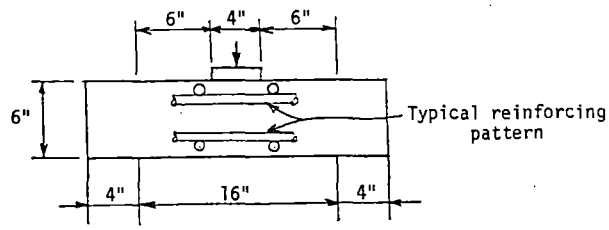

(a) Series A Specimens

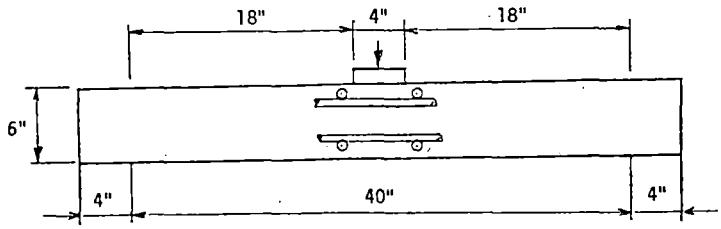

(b) Series B Specimens

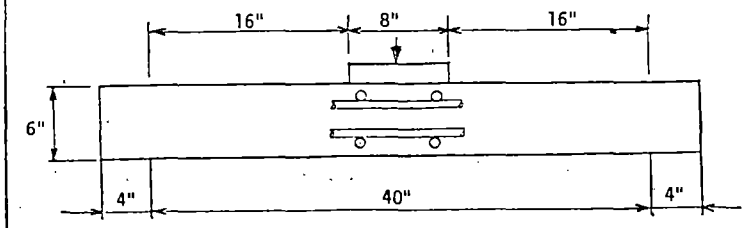

(c) Series C Specimens

Specimen geometry -- all specimens are square slabs

(34 Specimens)

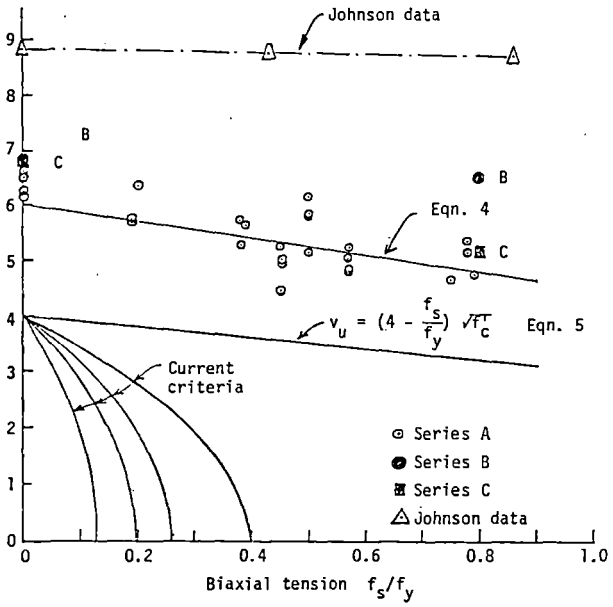

Test Results, Johnson results (England), Current Criteria, and Proposed Design Relationship for Concrete Shear Strength

CONCLUSIONS:

1. STATIC PUNCHING (PERIPHERAL) SHEAR STRENGTH OF ORTHOGONALLY REINFORCED CONCRETE SUBJECTED TO BIAXIAL TENSION IS ONLY MODERATELY SENSITIVE TO TENSION LEVEL.
2. CURRENT DESIGN RULES (ASME/ACI) ARE HIGHLY CONSERVATIVE, LEADING TO EXCESSIVE REINFORCING STEEL AND UNNECESSARY CONGESTION PROBLEMS, AND HENCE DIFFICULTIES IN OBTAINING HIGH QUALITY CONCRETE.
3. COMPARISONS ARE NEEDED WITH EXPERIMENTAL RESULTS FROM THICK SLABS, AND FROM EXPERIMENTS WITH PUNCHING LOADS APPLIED TO PENETRATIONS THROUGH THE SLAB.
4. BETTER ANALYTICAL MODELS ARE NEEDED TO HELP GENERALIZE THE RESULTS --- FRACTURE MECHANICS
   --- PLASTICITY

TANGENTIAL SHEAR DESIGN CONSIDERATIONS

RESEARCH OBJECTIVES:

TO DETERMINE THE STRENGTH AND DEFORMATIONAL BEHAVIOR OF REINFORCED CONCRETE CONTAINMENT STRUCTURES SUBJECTED TO SIMULTANEOUS PRESSURIZATION AND SEISMIC LOADS, WITH PARTICULAR EMPHASIS ON CONTAINMENTS WITH TWO-WAY REINFORCEMENT.

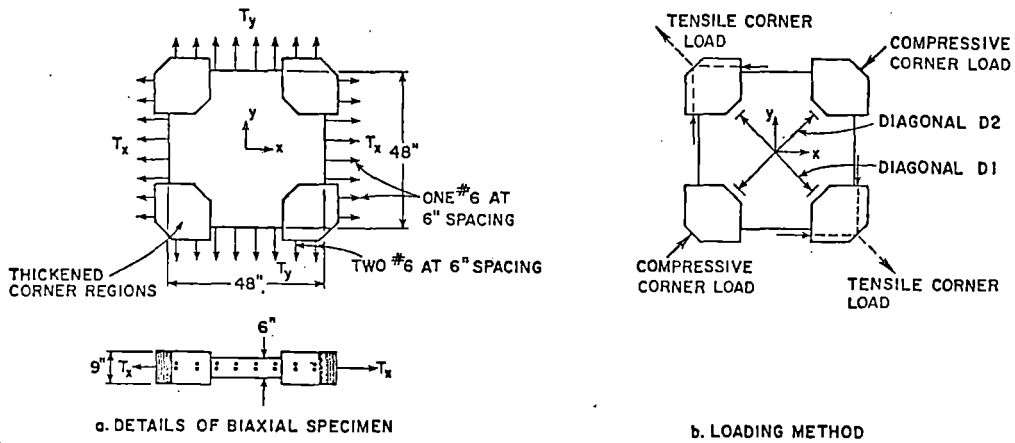

Specimen Geometry and Loading Method for Shear

VARIABLES:

1. REINFORCEMENT PATTERNS - 2 & 4 WAY
2. BIAXIAL AND UNIAXIAL TENSION IN REBARS
3. REINFORCEMENT RATIOS
4. LEVEL OF BIAXIAL TENSION
5. MONOTONIC AND CYCLIC SHEARS
6. SEQUENCE OF TENSION AND SHEAR LOADS

50 SPECIMENS TOTAL

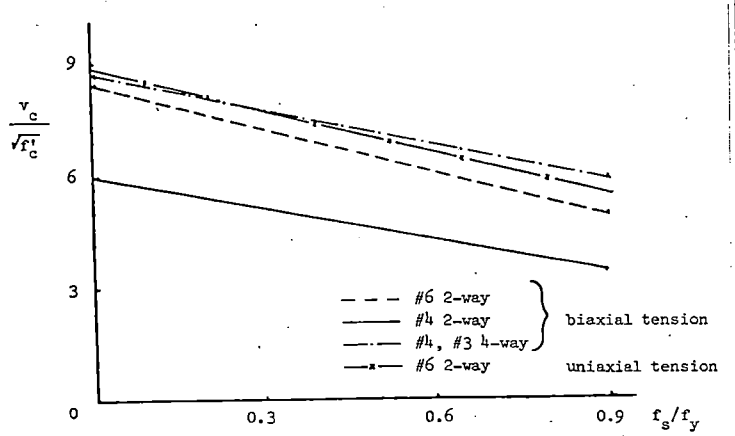

a) monotonic shear

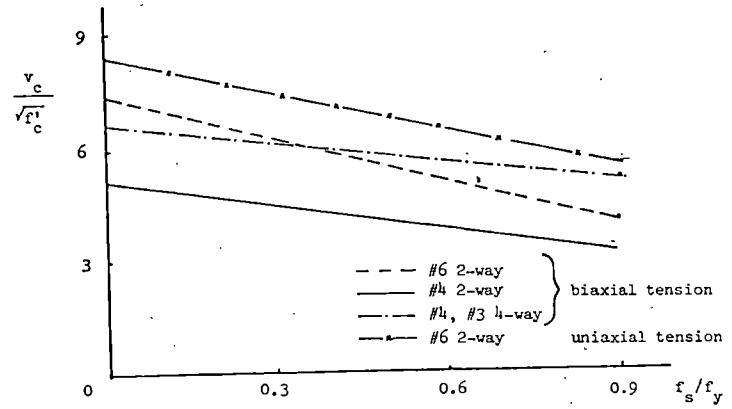

b) cyclic shear

Ultimate shear strength versus biaxial tension level

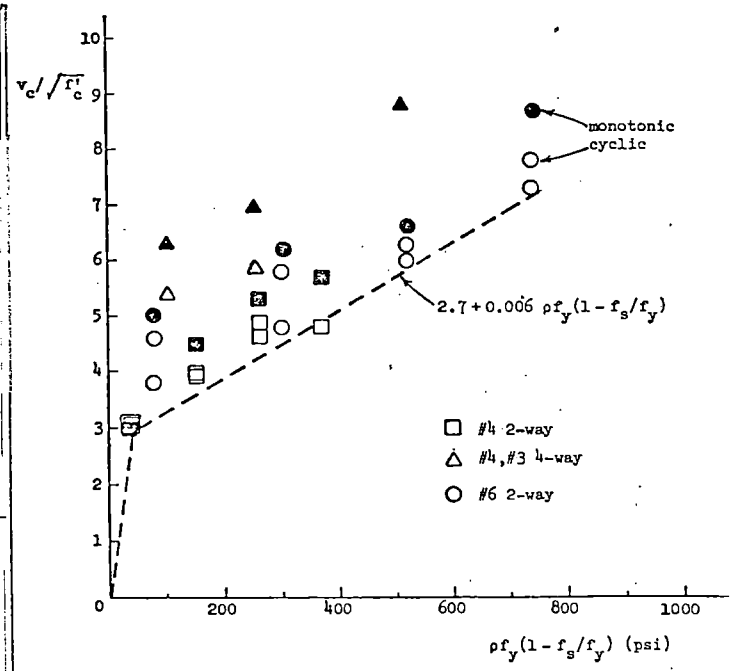

Ultimate strength versus stress parameter

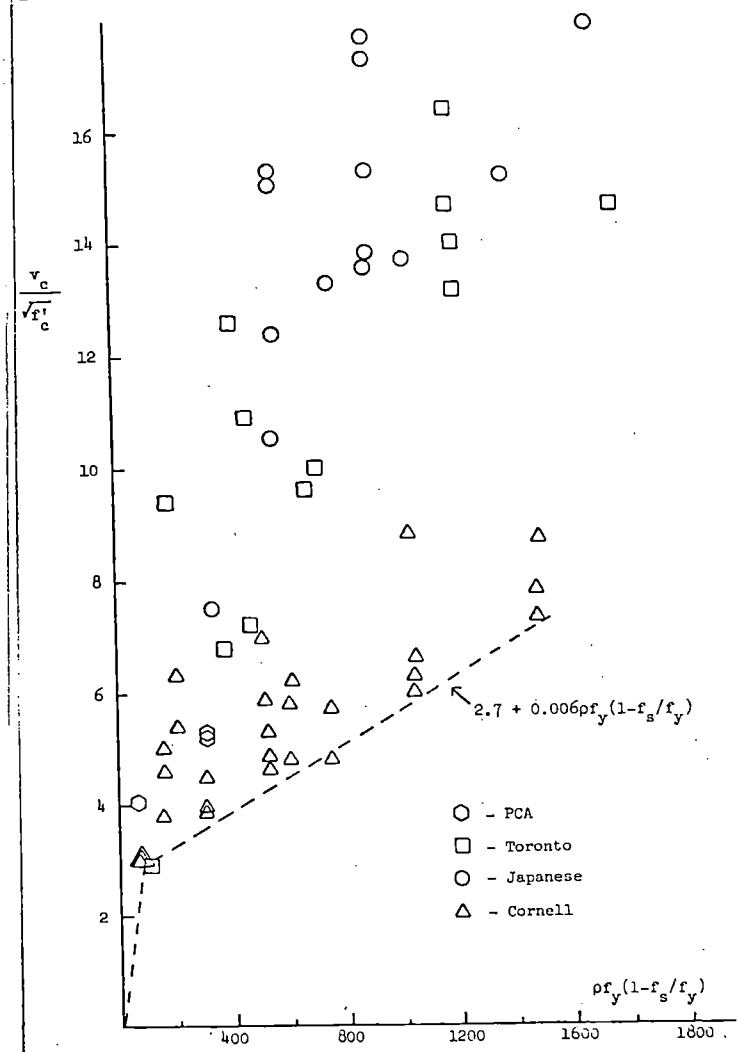

Cornell, PCA, Japanese, and Toronto experimental results

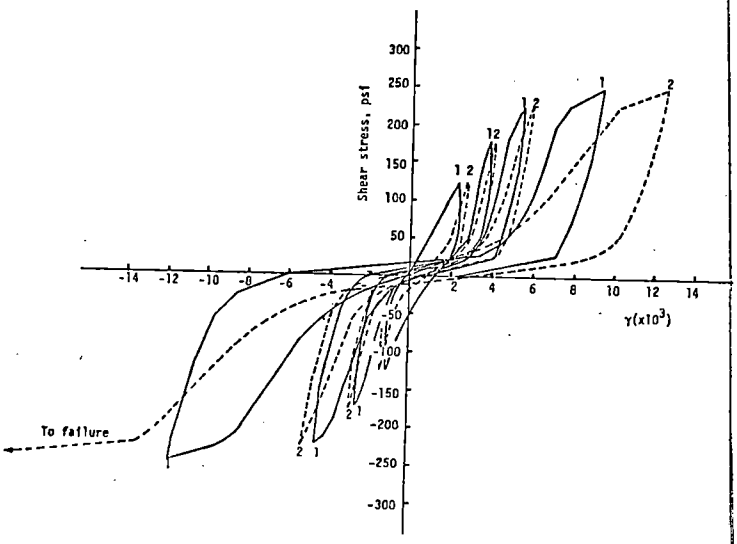

Typical shear stress-shear strain plot for cyclic shear test

CONCLUSIONS:

1. SHEAR STRENGTH OF CONCRETE IN FULL CONTAINMENT MAY BE SUBSTANTIALLY HIGHER THAN IN ISOLATED TEST SPECIMENS.
2. FOR CYCLIC SHEAR, WITH ORTHOGONAL STEEL UNDER BIAXIAL TENSION f_s, THE LOWER BOUND SHEAR STRENGTH IS
$$v_c = [2.7 + 0.006 \rho f_y (1 - f_s/f_y)] \sqrt{f'_c}$$
3. FOR A SIMILAR SITUATION, BUT WITH UNIAXIAL TENSION ONLY ON THE STEEL, STRENGTH IS 10% to 15% HIGHER.
4. ADDITION OF DIAGONAL STEEL ENHANCES STRENGTH APPRECIABLY: MORE THAN EXPECTED.
5. DOWEL ACTION CONTRIBUTES SUBSTANTIALLY TO SHEAR STRENGTH.
6. UPPER LIMIT ON SHEAR STRENGTH NOT YET ESTABLISHED; 8 to 10 $\sqrt{f'_c}$ APPEARS REASONABLE.
7. REVISED SHEAR STRENGTH DESIGN PROVISIONS UNDER DEVELOPMENT

Tension	Tangent Stiffness G/G_o		
	Phase 1	Phase 2	
	#6 - 2-way	#4 - 2-way	4-way
0.0	0.056	0.286	0.144
0.3	0.051	0.043	---
0.6	0.038	0.039	0.042
0.9	0.042	0.008	0.040

Average tangent stiffness values for monotonic shear tests

CONCLUSIONS:

1. EFFECTIVE SHEAR STIFFNESS G OF CRACKED CONCRETE IS ABOUT $0.05G_o$ FOR BIAXIALLY TENSIONED SPECIMENS.
2. JAPANESE TESTS ON FULL CONTAINMENT MODELS HAVE STIFFNESSES RANGING FROM $0.05G_o$ TO $0.15G_o$.
3. UNIAXIALLY TENSIONED SPECIMENS ARE ONLY SLIGHTLY STIFFER THAN BIAXIALLY TENSIONED SPECIMENS.
4. LINER PLATE WILL TEND TO ATTRACT HIGH STRESSES AND HIGH STRAINS; SHEAR DISPLACEMENT LIMITATIONS NEED TO BE GIVEN MORE RATIONAL ATTENTION.
5. BEHAVIOR OF "SOFT" WALL REGIONS IN A FULL CONTAINMENT VESSEL NEEDS STUDY TO DETERMINE OVERALL CONTAINMENT DISPLACEMENT BEHAVIOR.
6. INFLUENCE OF LOCAL SOFTNESS ON DYNAMIC RESPONSE NEEDS ATTENTION, AS DOES THE FACT THAT SHEAR CYCLICING LEADS TO A DECREASE IN EFFECTIVE HYSTERETIC DAMPING.

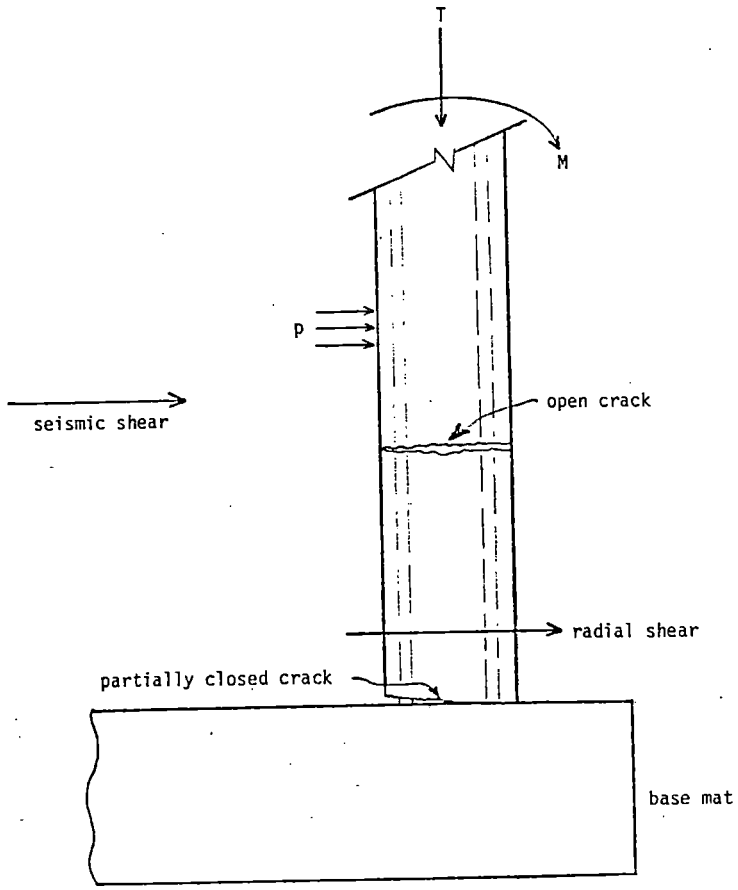

Forces near base mat; radial shear action

ISSUES TO BE RESOLVED:

1. DEVELOPMENT OF A HIERARCHY OF POTENTIAL FAILURE MODES FOR CONTAINMENTS.
2. DISTRIBUTION OF TANGENTIAL AND RADIAL SHEAR AROUND A CYLINDRICAL CONTAINMENT VESSEL, AND THE INTERACTION OF THE TWO SHEARING MODES.
3. TANGENTIAL SHEAR STRENGTH OF A COMPLETE CONTAINMENT.
4. MAXIMUM STRAIN LEVELS IN STEEL LINERS IN CONTAINMENTS.
5. RADIAL SHEAR STRENGTH IN THE PRESENCE OF TENSION.
6. PUNCHING SHEAR STRENGTH AROUND PENETRATIONS AND IN VERY THICK SLABS (CONTAINMENT WALL THICKNESSES).
7. INFLUENCE OF SEVERE NON-LINEARITIES (PRODUCED BY CRACKING OF CONCRETE) ON DYNAMIC RESPONSE OF CONTAINMENTS.

9th Water Reactor Safety Research Information Meeting

Gaithersburg, Maryland, October 1981

Hydrogen Detonation Loading on Reinforced Concrete Containments

by

Michael N. Fardis, M.I.T.

A hydrogen detonation inside the containment building generates a shock wave which propagates at very high speed within the containment atmosphere. Determination of the containment response to the associated dynamic loading requires quantification of the wall pressure time history.

Shock wave calculations were performed, assuming uniform concentration of hydrogen within the containment volume, ignition at a point on the axis and absence of obstacles. Under these conditions the detonation wave prior to first reflection at the wall is a spherical one, given by Taylor's analytical solution. Following reflection, a complex pattern of reflected and interacting waves is created, and wave calculations can be performed only numerically. An axisymmetric computer program was developed for the calculation of pressure, temperature and density time histories inside the containment volume and at the wall, using the random-choice technique, (proposed originally by Glimm & Chorin for shock wave problems without chemical reactions) modified appropriately for hydrogen detonations. The method is capable of producing infinitely sharp shock fronts, and avoids the artificial damping introduced by the Finite Difference technique. In the method both space and time are discretized,

and the solution at time t (assumed constant within each space cell) is propagated to t + Δt, by solving "exactly" a sequence of Riemann problems, then sampling pseudorandomly the resulting "exact" solution within each space cell and assigning the sampled values to the cell nodes.

The main result of interest is the time-history of wall pressure (normalized to the initial containment pressure), as a function of location. These normalized pressure time-histories depend on: 1) the point of initiation along the axis; and 2) the ratio of energy release rate (which depends on hydrogen concentration) to the initial absolute temperature. Considering initiation at an elevation below the springline, the peak pressure at the point of normal incidence on the wall is approximately 40 times higher than the initial pressure and is followed by a series of peaks with decreasing amplitude and increasing interarrival times. At points of oblique incidence on the cylindrical wall, the peak pressure is lower. At the dome, waves are reinforced by multiple reflections at the walls and along the axis of the containment, and generate extremely high wall pressures. Waves reflected at the dome generate, in turn, extremely high pressures at the lower portion of the cylinder.

In the wave calculations, containment walls were considered rigid, because parametric studies for a spherical geometry have shown the minor effect of wall deformability on pressures.

The containment response to the wall pressure time histories will be determined by dynamic nonlinear Finite Element analyses . In the F.E. model, the concrete is modeled by axisymmetric 4-node isoparametric elements, and the layers of steel by special axisymmetric thin shell elements (separately for the hoop, meridional, and ±45° seismic reinforcement and

for the liner), located at the external and internal faces of the concrete elements. The material model for the liner is elastic-perfectly plastic with classical von-Mises plasticity and elastic unloading-reloading. Thermal strains are considered as initial strains. The stress-strain model for the rebars is uniaxial, with a yield plateau and nonlinear strain hardening in monotonic loading, and nonlinear with the Bauschinger effect in reversed (cyclic) loading. The concrete is considered linear-elastic-orthotropic with a very small modulus in the directions of positive normal strain, to simulate cracking. The shear rigidity of cracked concrete takes into account the aggregate interlock and the dowel action of the reinforcement, and is a function of the stress in the meridional steel.

As preliminary steps to the dynamic analysis, the static response under uniform internal pressure and temperature, and the natural mode shapes and periods (the latter for linear-elastic materials and cracked concrete) were determined. Under static loading, the critical region of the containment is the dome and the upper half of the cylinder in the hoop direction. The first few natural periods (0.38, 0.22, 0.205, 0.20, 0.195, 0.19, 0.175 sec.) are well above the predominant periods of the dynamic load. Due to their shapes, higher modes are expected to have low participation in the response.

Containment integrity depends on the ductility of reinforcing bars. Data on ultimate strengths of mechanically spliced No. 18S bars have been used to fit an extreme-value type I distribution, smallest values, to the strength of a single "unit" consisting of one bar and one splice. Assuming independence of strengths of different "units", the distribution of the strength of a string of such "units" in series can be computed. It

was found by F.E. analyses that failure of such a string will not increase appreciably the stresses in neighboring strings, so that for given stress field failures of different strings of spliced bars can be considered independent. Therefore, a simple nonhomogeneous Poisson process model can be constructed for the failures of strings of bars, conditionally on given maximum stress field in the steel bars, as determined from the containment response analysis. This probabilistic procedure was used in conjunction with the static results, to derive the distribution of the number of broken bars, as a function of internal pressure.

CONTAINMENT SAFETY UNDER HYDROGEN LOADING

I. DETERMINATION OF PRESSURE LOADING ON CONTAINMENT WALL, DUE TO HYDROGEN DETONATION.

Conditions:
1. Uniform Concentration of hydrogen within containment volume.
2. Initiation at a point along the axis.
3. No obstacles

II. DETERMINATION OF CONTAINMENT DYNAMIC RESPONSE TO PRESSURE LOADING.

HYDROGEN DETONATION COMPUTATIONS

APPROACH: Random choice technique:
Discretize in space and time.
Find solution at time $t + \Delta t$ from that at t, by solving exactly a sequence of Riemann problems, sampling solution pseudorandomly within each space cell and assigning sampled valued to the nodes. Method can produce infinitely sharp discontinuities (shock fronts) and introduces no artificial damping.

RESULTS: In 1-D ("slab", sphere or cylinder): Peak wall pressure at 1st reflection, then decay to constant value; at 2nd reflection peak is lower, etc.
In axisymmetric (r-z) geometry (Indian Point, cylinder with hemispherical dome):
At cylinder, initially as in 1-D case with normal or oblique incidence, later on waves reflected at the dome cause extremely high pressures. At the dome, complex pattern of pressures, due to focussing of reflected waves.

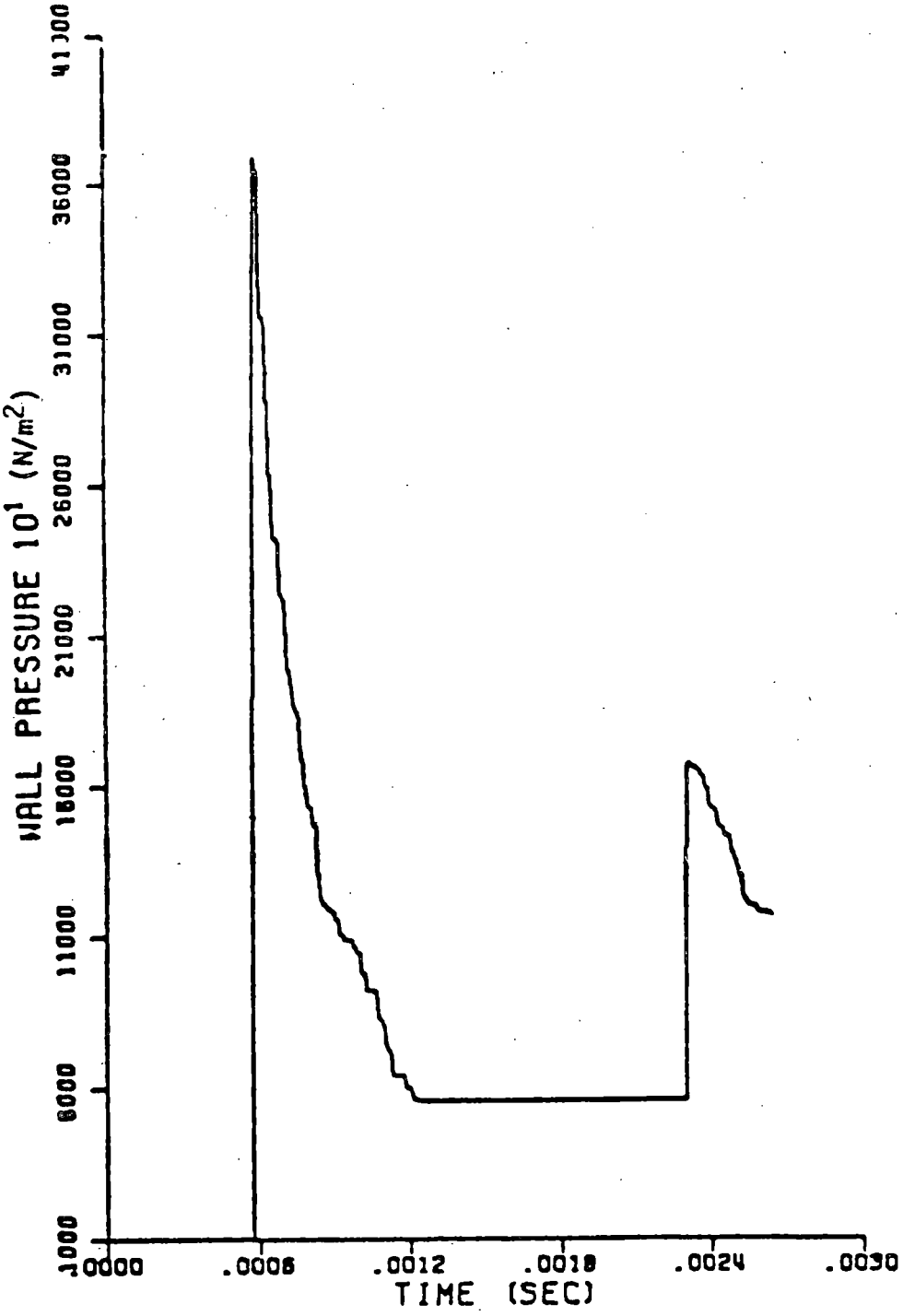

WALL PRESSURE HISTORY FOR A 1m RADIUS (planar geometry) 2 INITIAL GRID POINTS, SIGMA=0.8, Δx=0.01.

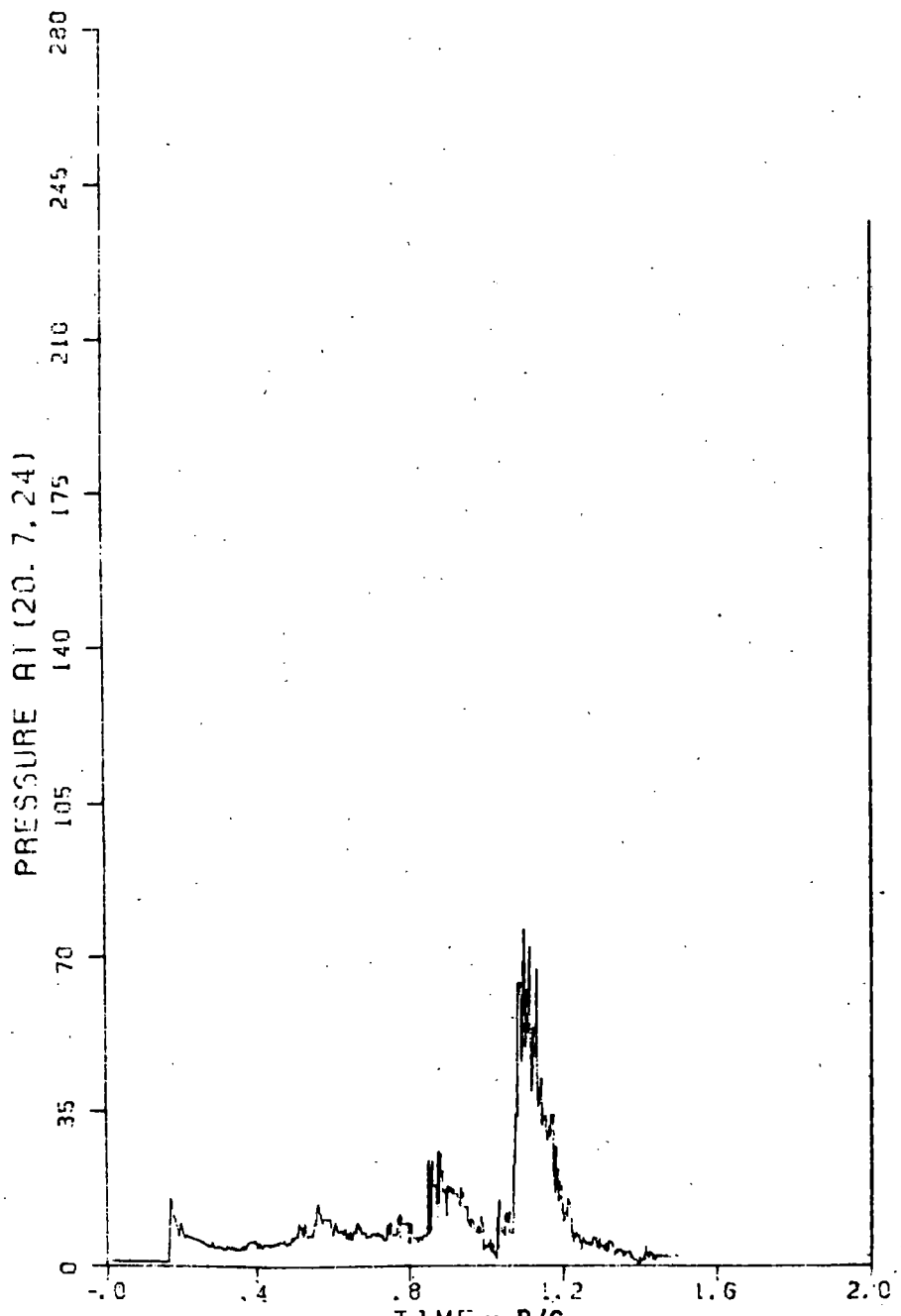

Cylinder, at midheight

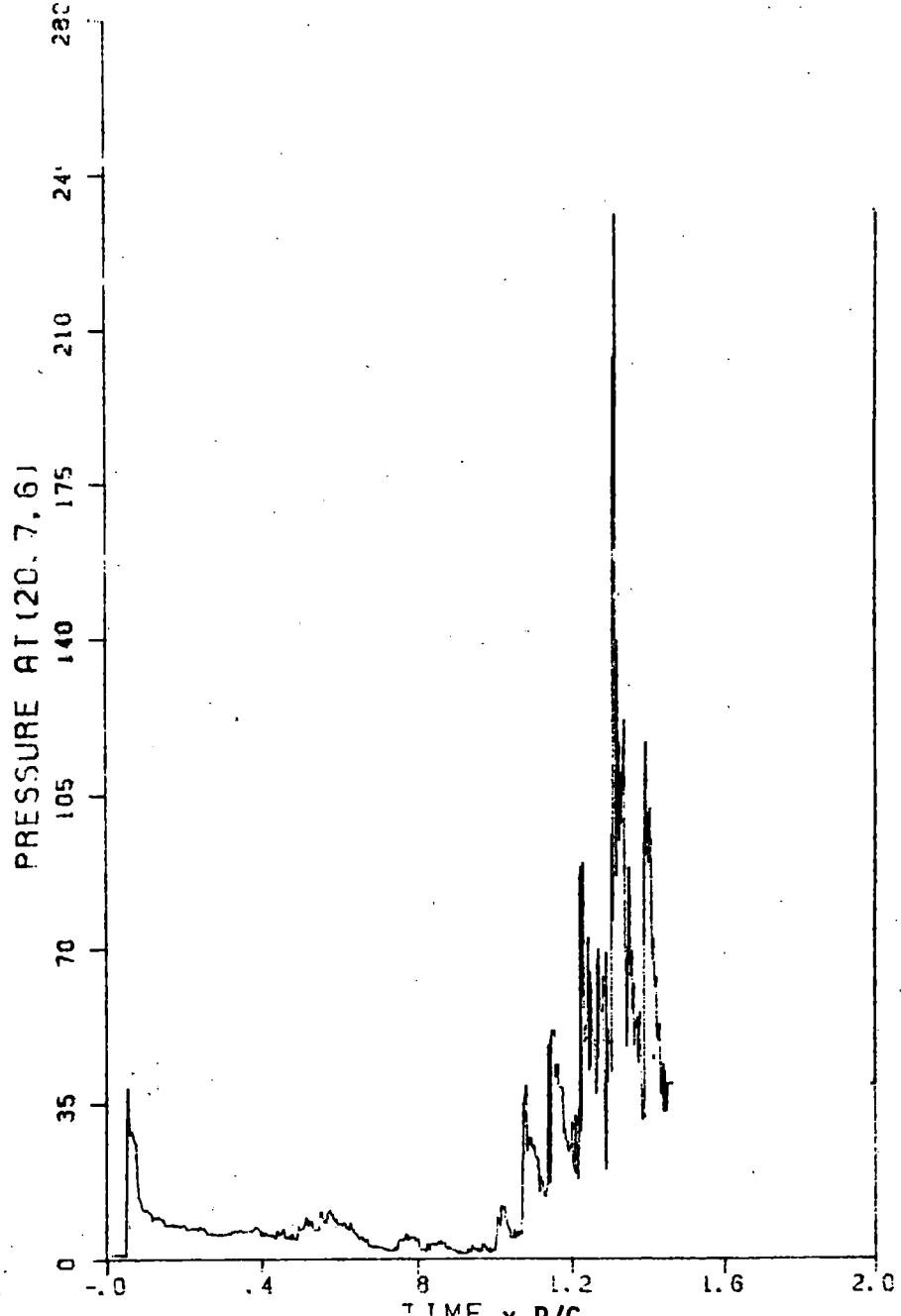

Cylinder, 6 m. from the base

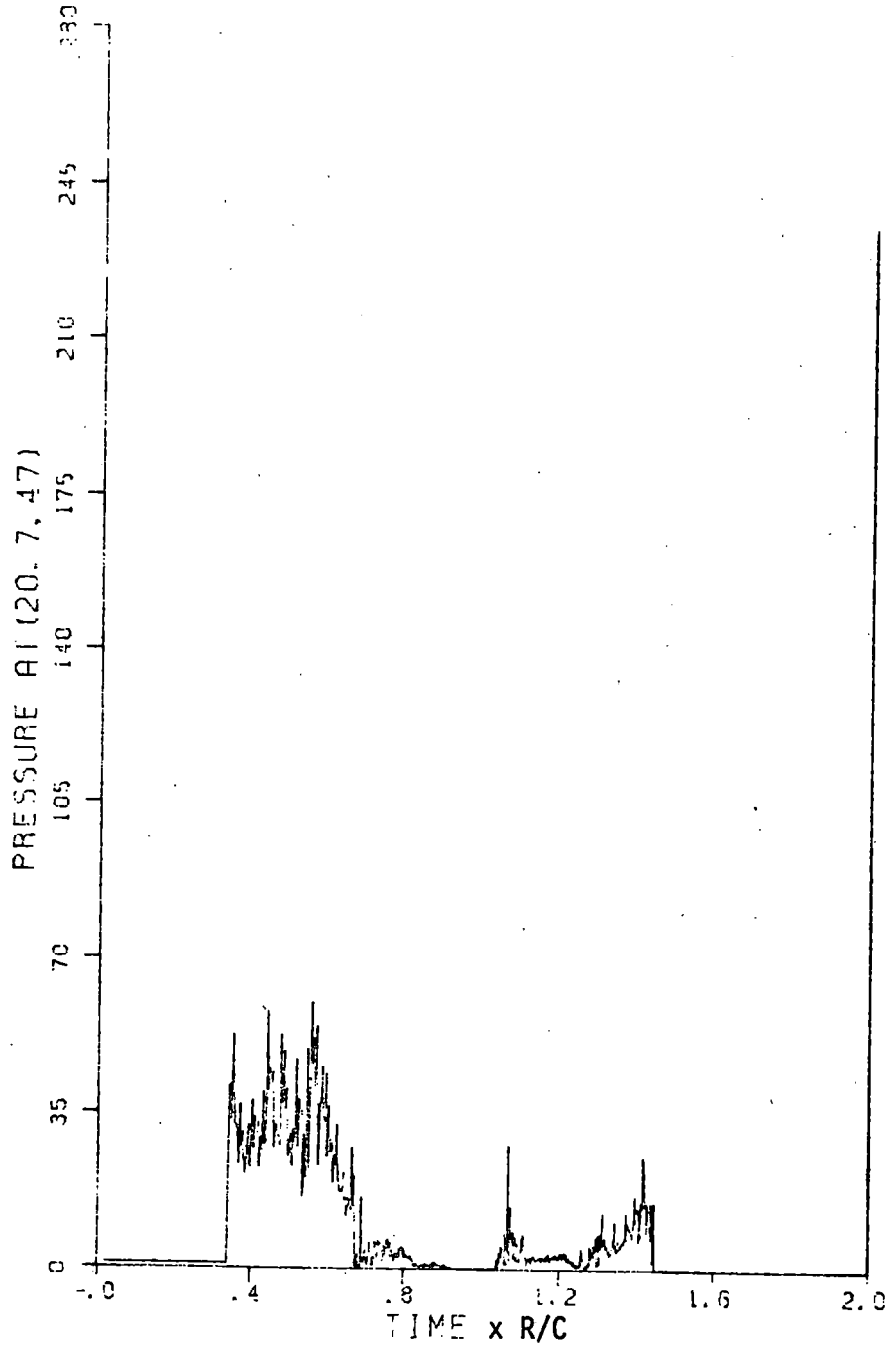

Dome, 5° from springline

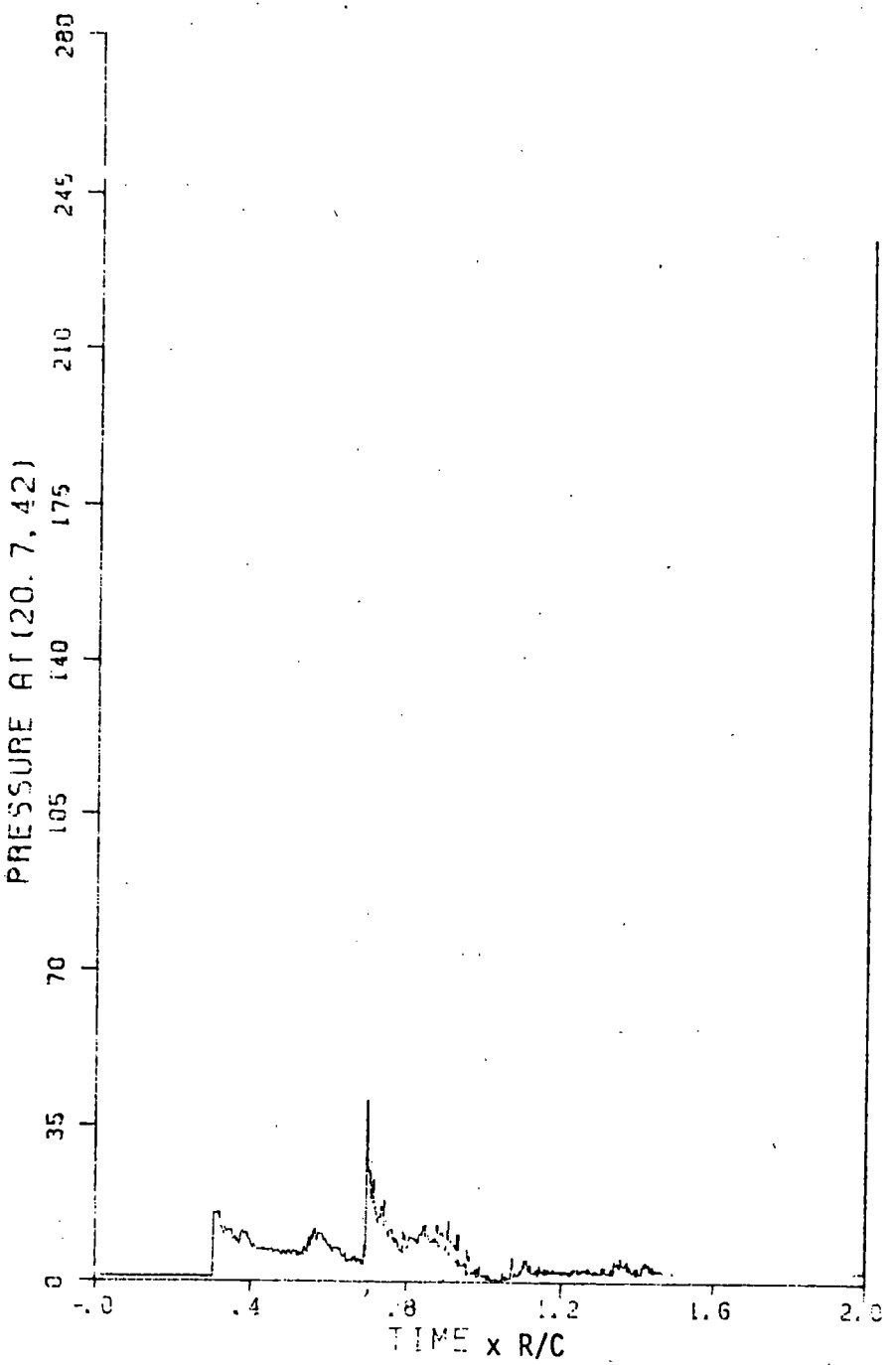

Cylinder, 3 m. below springline

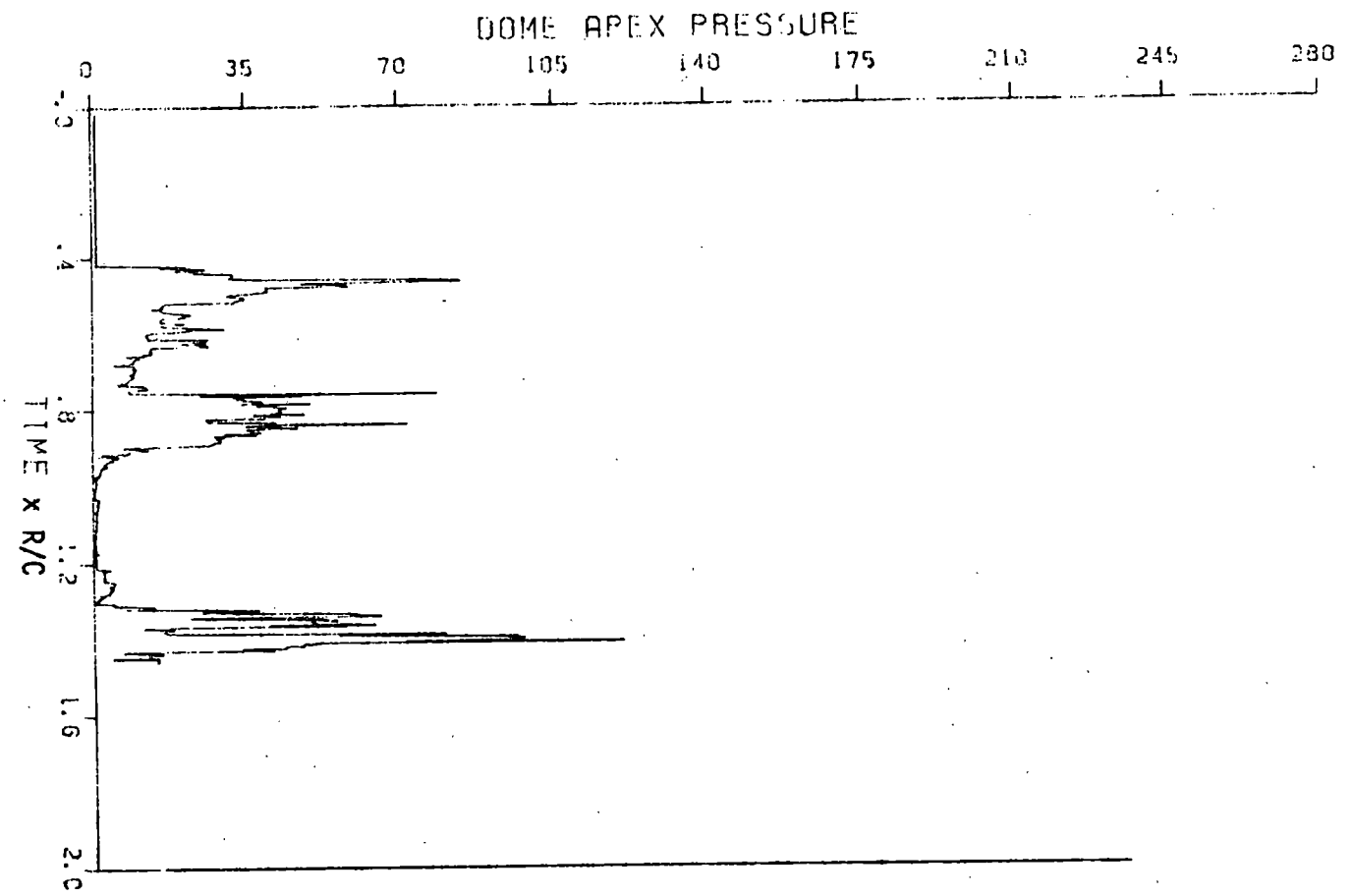

Apex

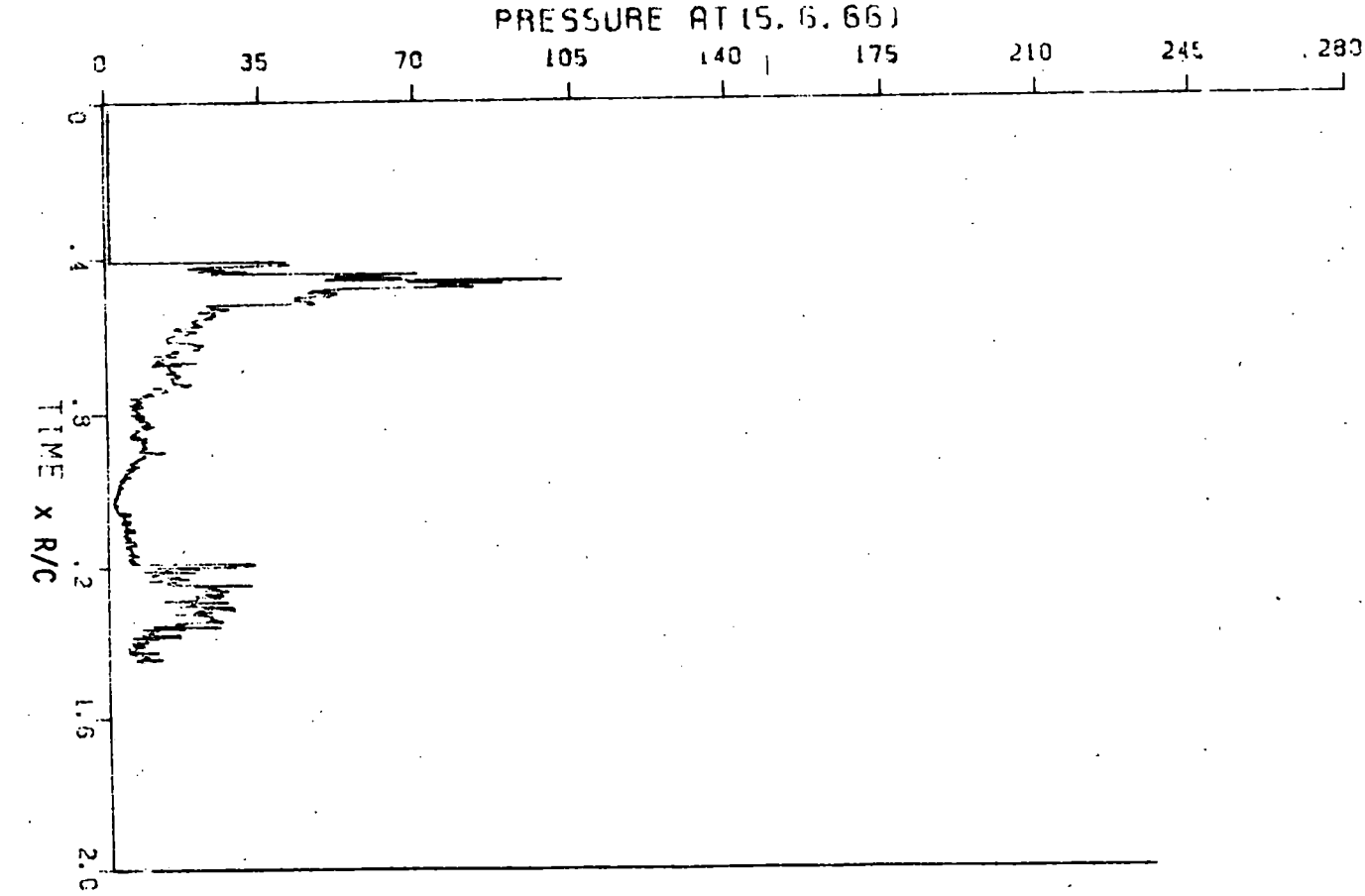

Dome, 75° from Springline

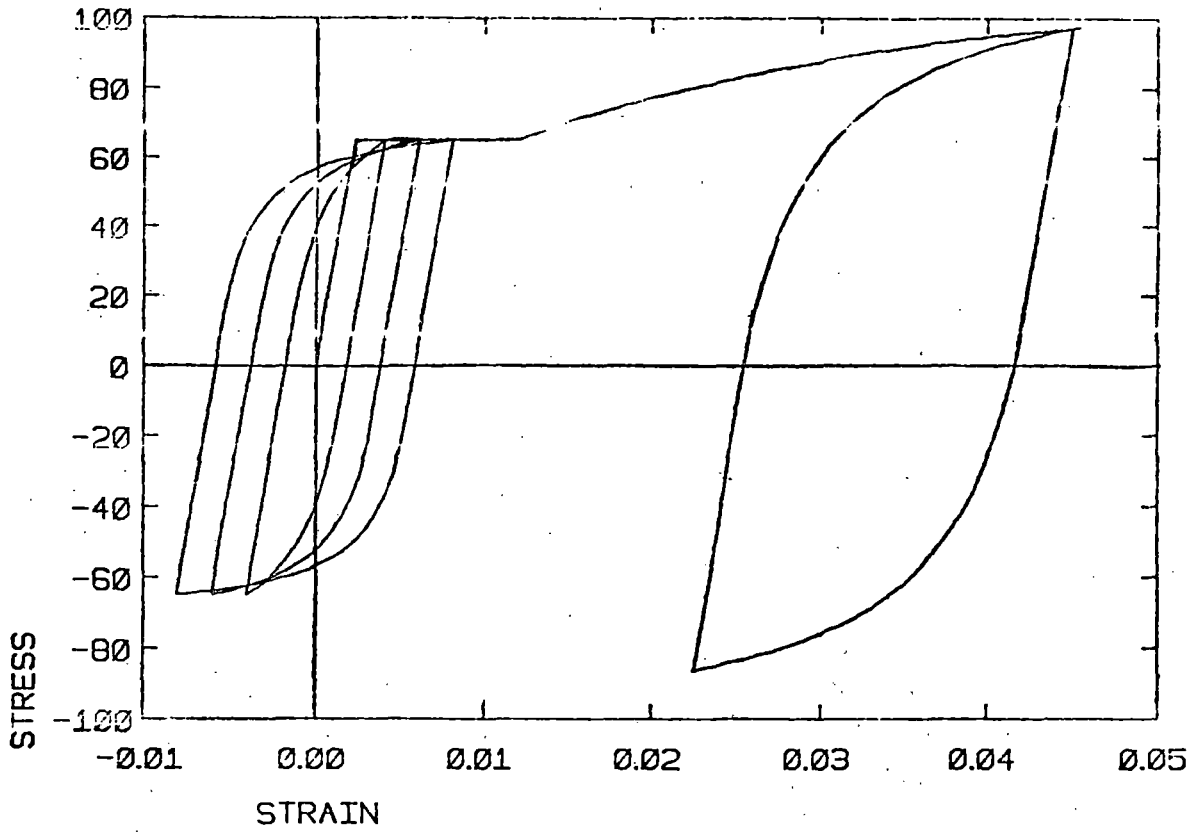

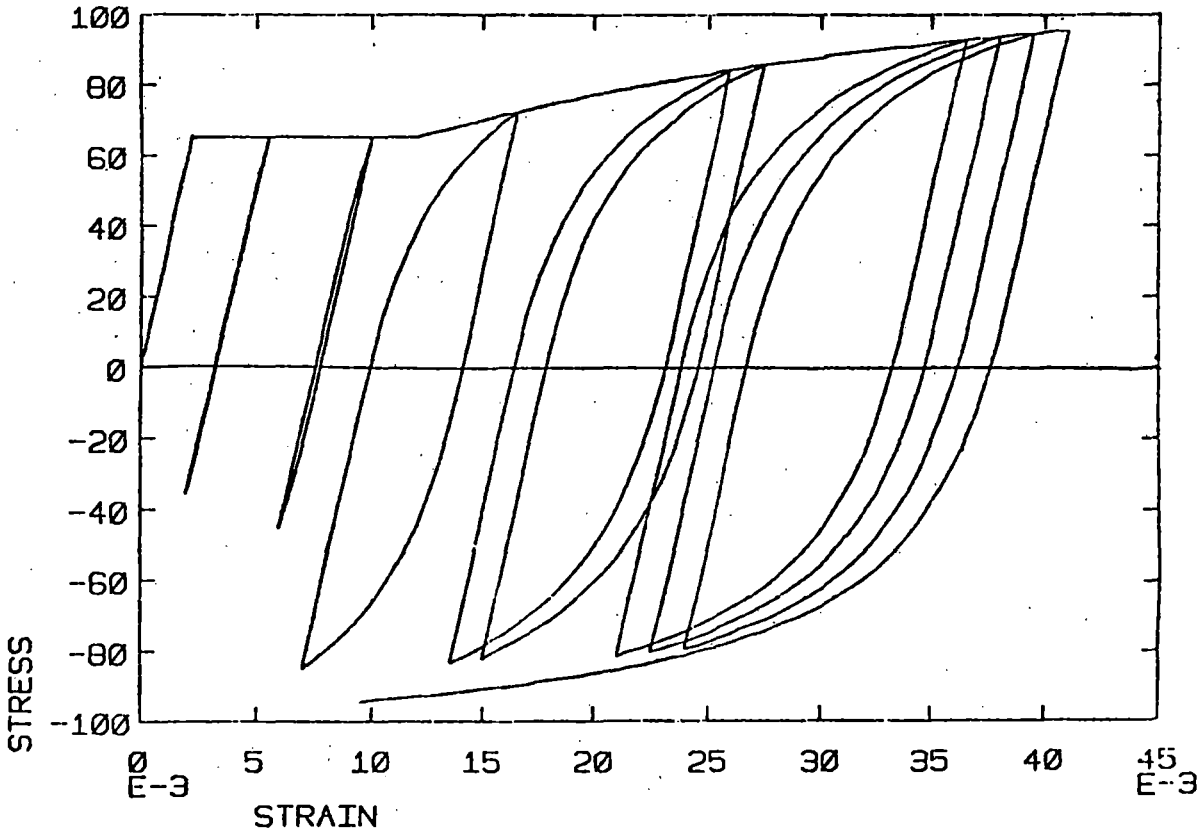

Typical results of σ-ε model for reinforcing steel.

CONTAINMENT RESPONSE

AXISYMMETRIC NONLINEAR DYNAMIC ANALYSIS WITH FINITE ELEMENTS

Separate concrete and steel elements, with 100% bond.

STEEL: Special axisymmetric thin shell elements, for the liner, the hoop and meridional reinforcement, the ±45° seismic bars and the radial ("dowel") bars near the base.

σ-ε laws: For the liner, elastic-perfectly plastic, with von-Mises classical plasticity and initial (thermal) strains.

For the rebars (uniaxial): Simple model with yield plateau and strain hardening in monotonic loading, and with the Bauschinger effect and closed hysteresis loops (Masing's rule) in cyclic.

CONCRETE: Axisymmetric ring elements (4-node isoparametric, with 2x2 integration scheme found best). Elastic-orthotropic material, with almost-zero stiffness (E/1000) normal to open cracks. Shear rigidity takes into account aggregate interlock and dowel action across cracks, as function of the amount, diameter and stress of the rebars normal to the cracks.

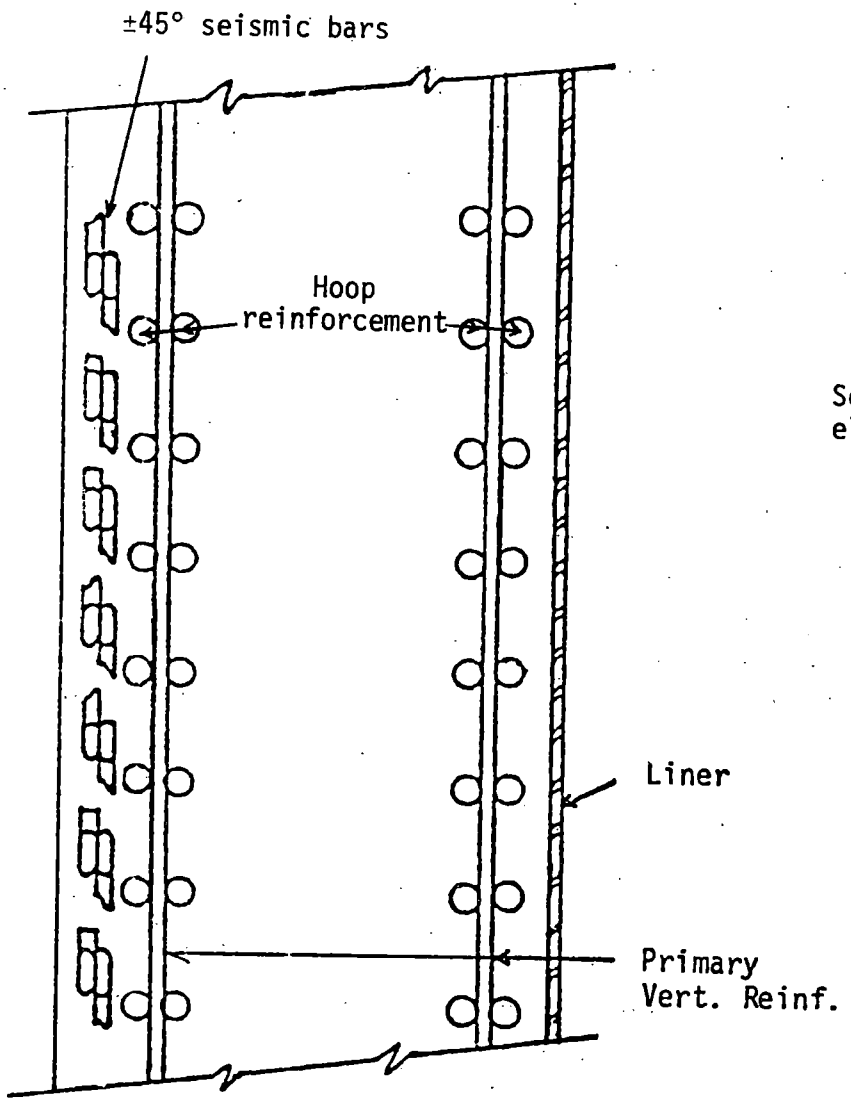

Section of Cylindrical Wall

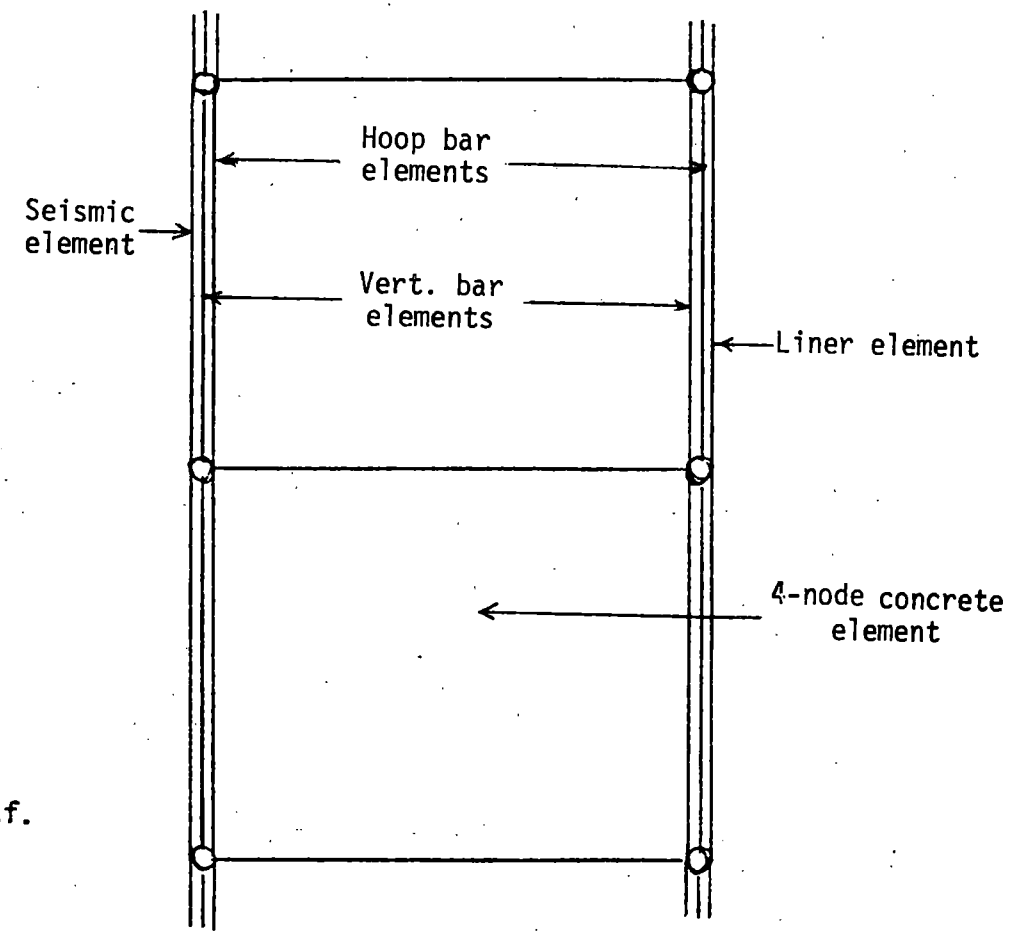

Finite Element Model

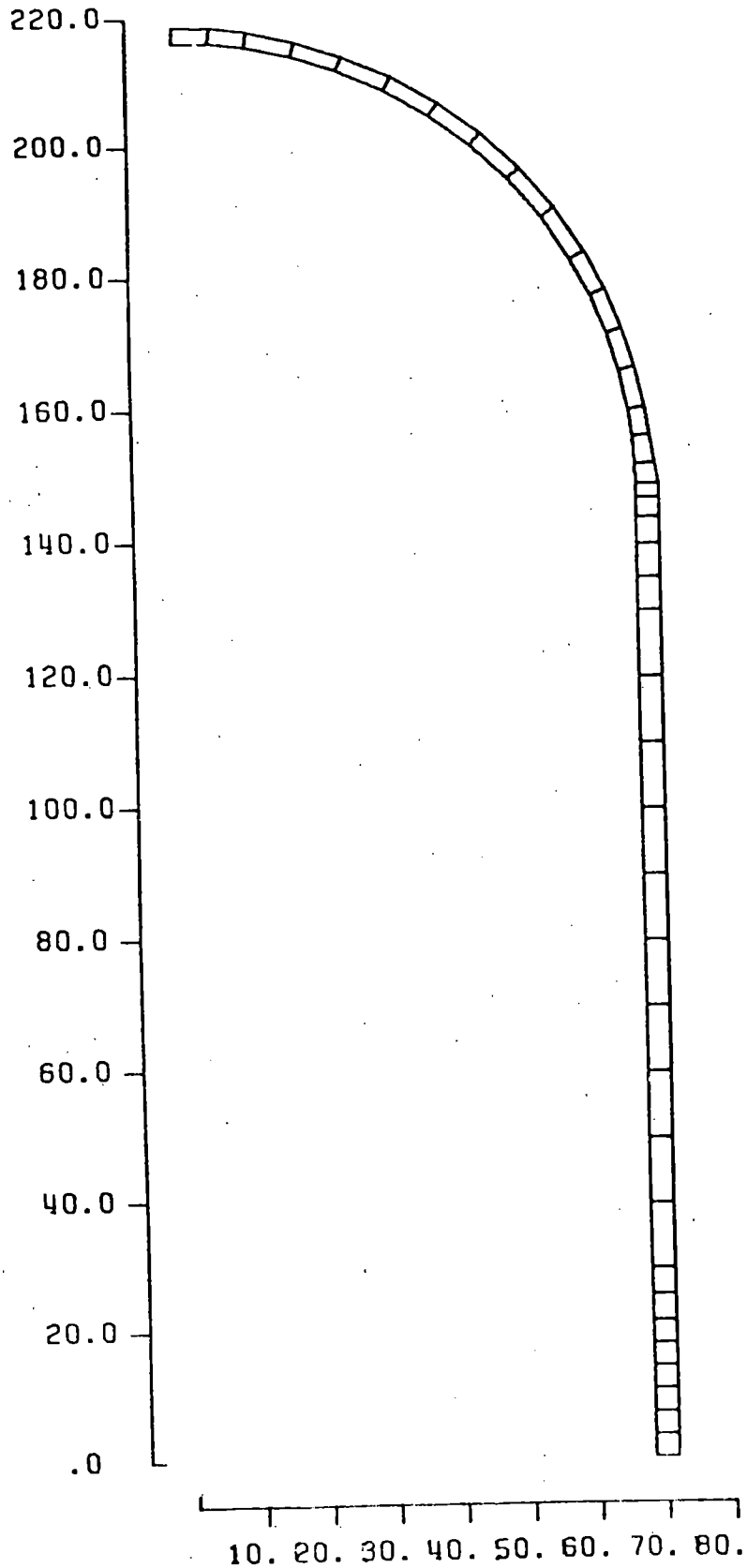

Finite Element Mesh

CONTAINMENT INTEGRITY

LINER: Very ductile material. Cracks not expected from brittle points (welds, shear connectors) due to elevated temperature during accident.

SPLICED BARS: Rupture at post-strain hardening strains, due to low strength of the splice or the bar. Probability distribution of strength of single spliced bars (:"unit") ∿ Extreme Type I, of smallest values.

Probabiliistc model of failures of a system of strings of spliced bars for given stress and strain field (obtained from containment response analysis).

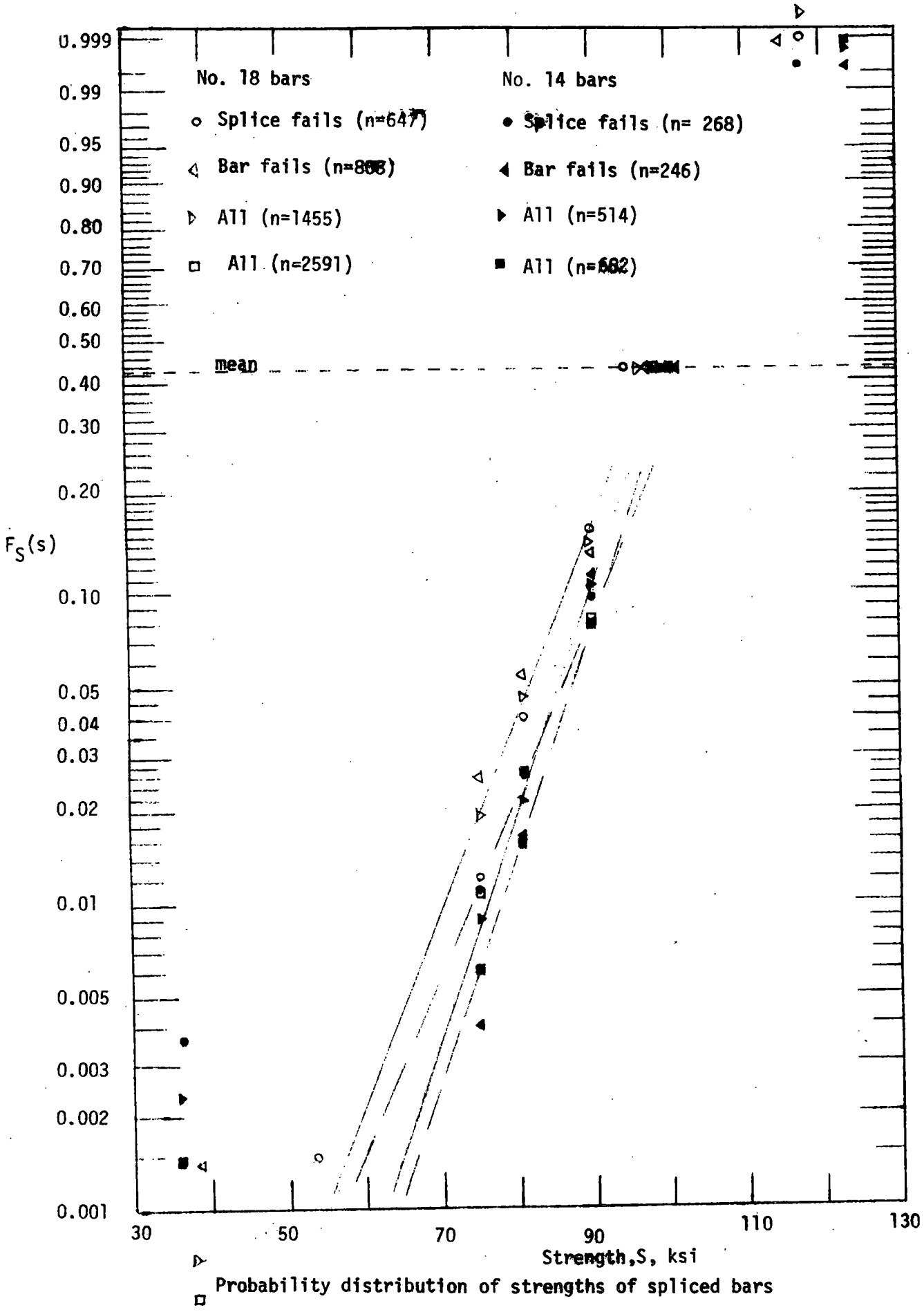

Probability distribution of strengths of spliced bars

FINITE ELEMENT RESULTS TO DATE:

CONTAINMENT: REINFORCED CONCRETE (INDIAN POINT)

I. Natural frequencies and mode shapes, for linear elastic materials but with concrete cracked in the hoop and meridional directions.

II. Static analysis to ultimate capacity, neglecting variability of spliced bar strengths.

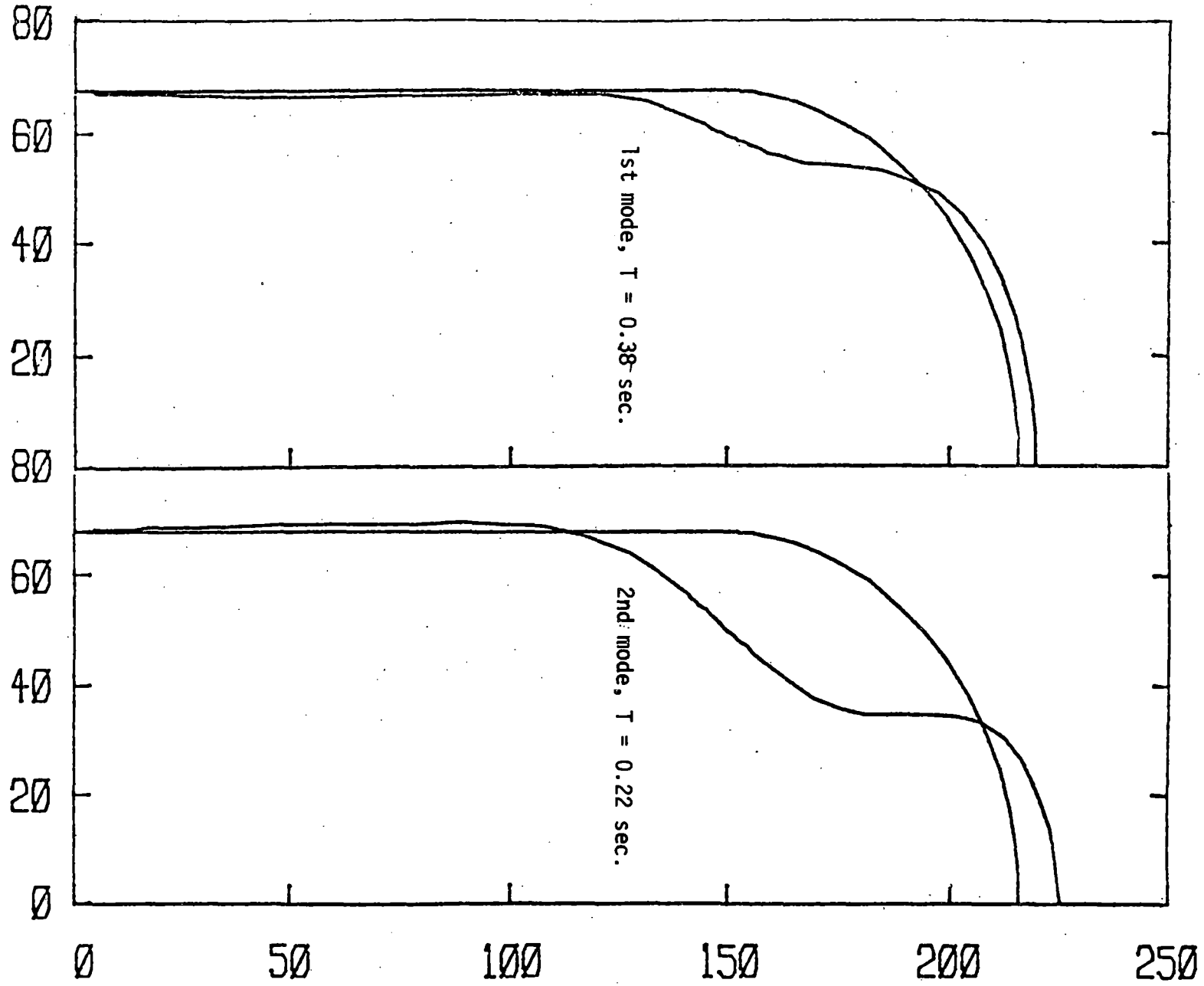
80
60
40
20
80
1st mode, T = 0.38 sec.
60
40
20
0
2nd mode, T = 0.22 sec.
0
50
100
150
200
250
Z (FEET) - ELEVATION -

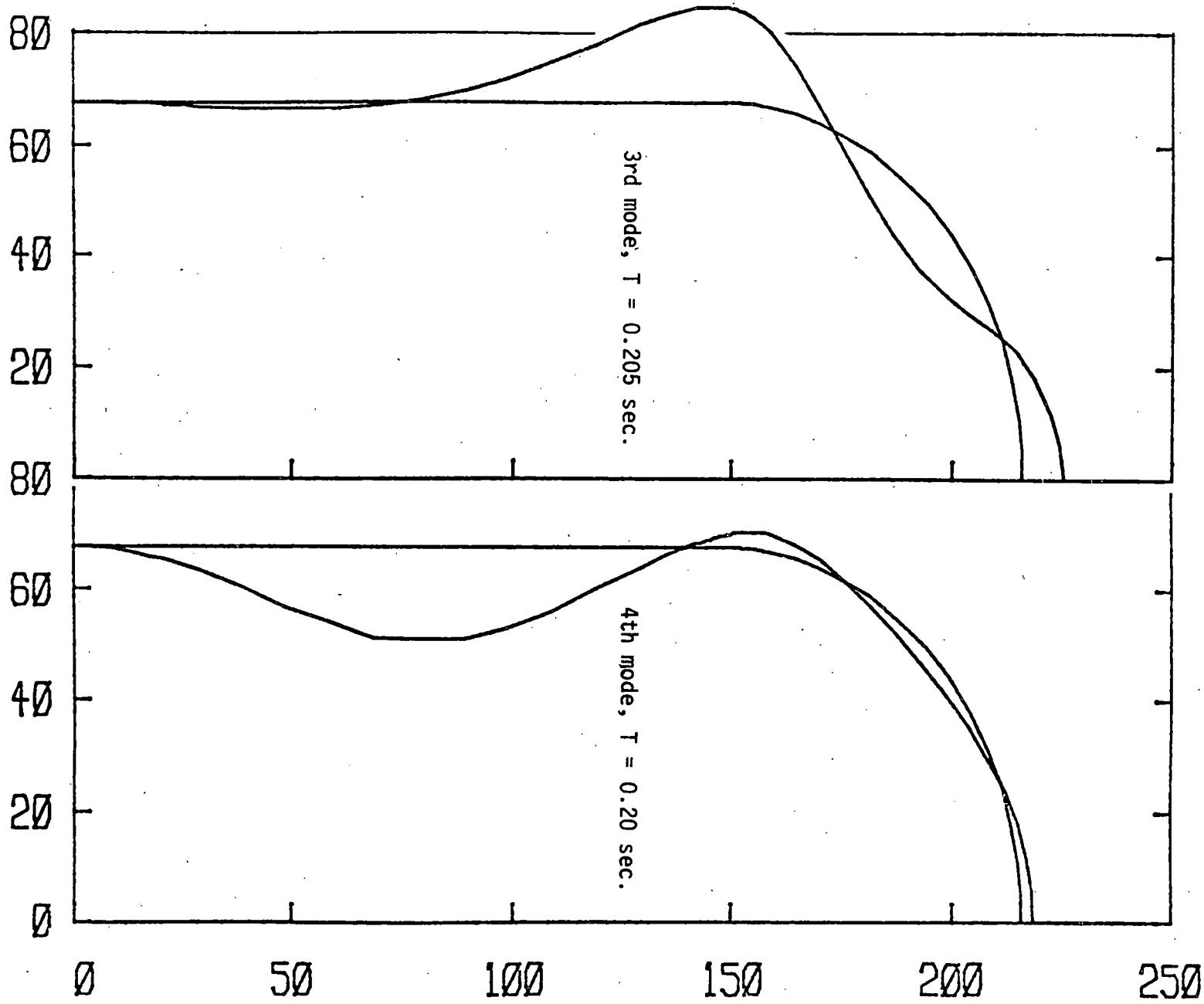
80
60
40
20
80
3rd mode, T = 0.205 sec.
60
40
20
0
4th mode, T = 0.20 sec.
0
50
100
150
200
250
Z (FEET) - ELEVATION -

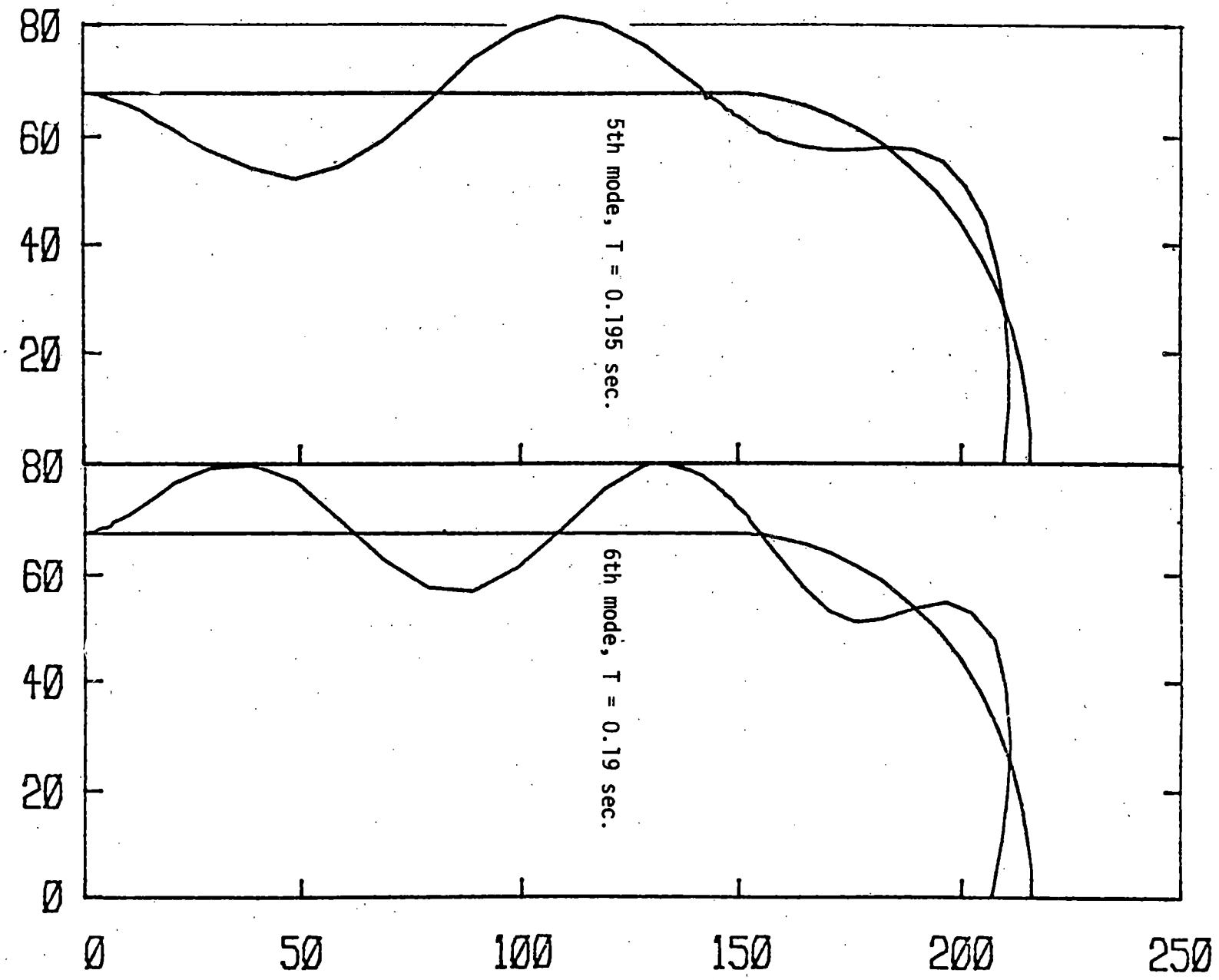
80
60
40
20
80
60
40
20
0
5th mode, T = 0.195 sec.
6th mode, T = 0.19 sec.
0
50
100
150
200
250
Z (FEET) - ELEVATION -

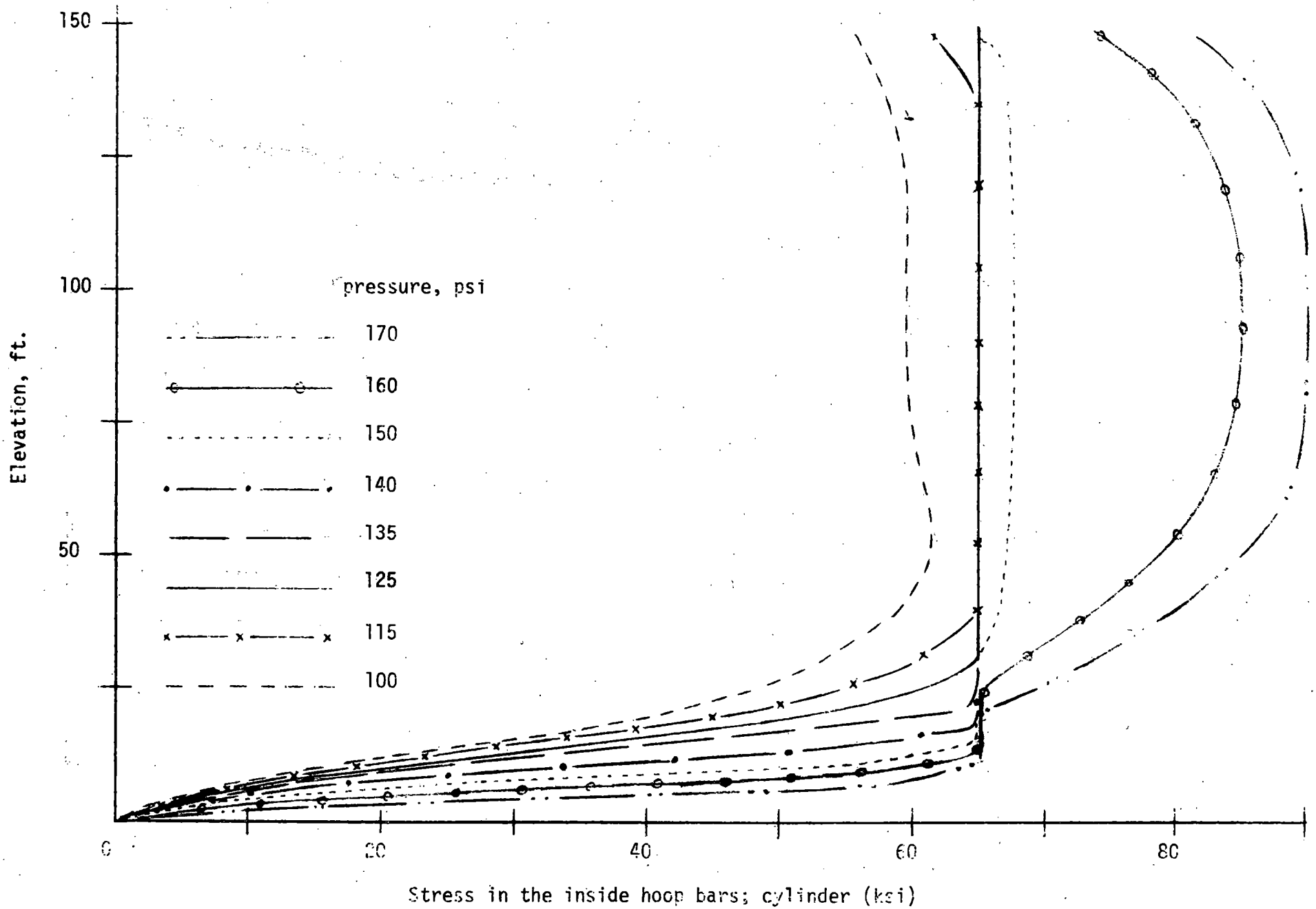
150
100
50
Elevation, ft.
pressure, psi
170
160
150
140
135
125
115
100
0
20
40
60
80
Stress in the inside hoop bars; cylinder (ksi)

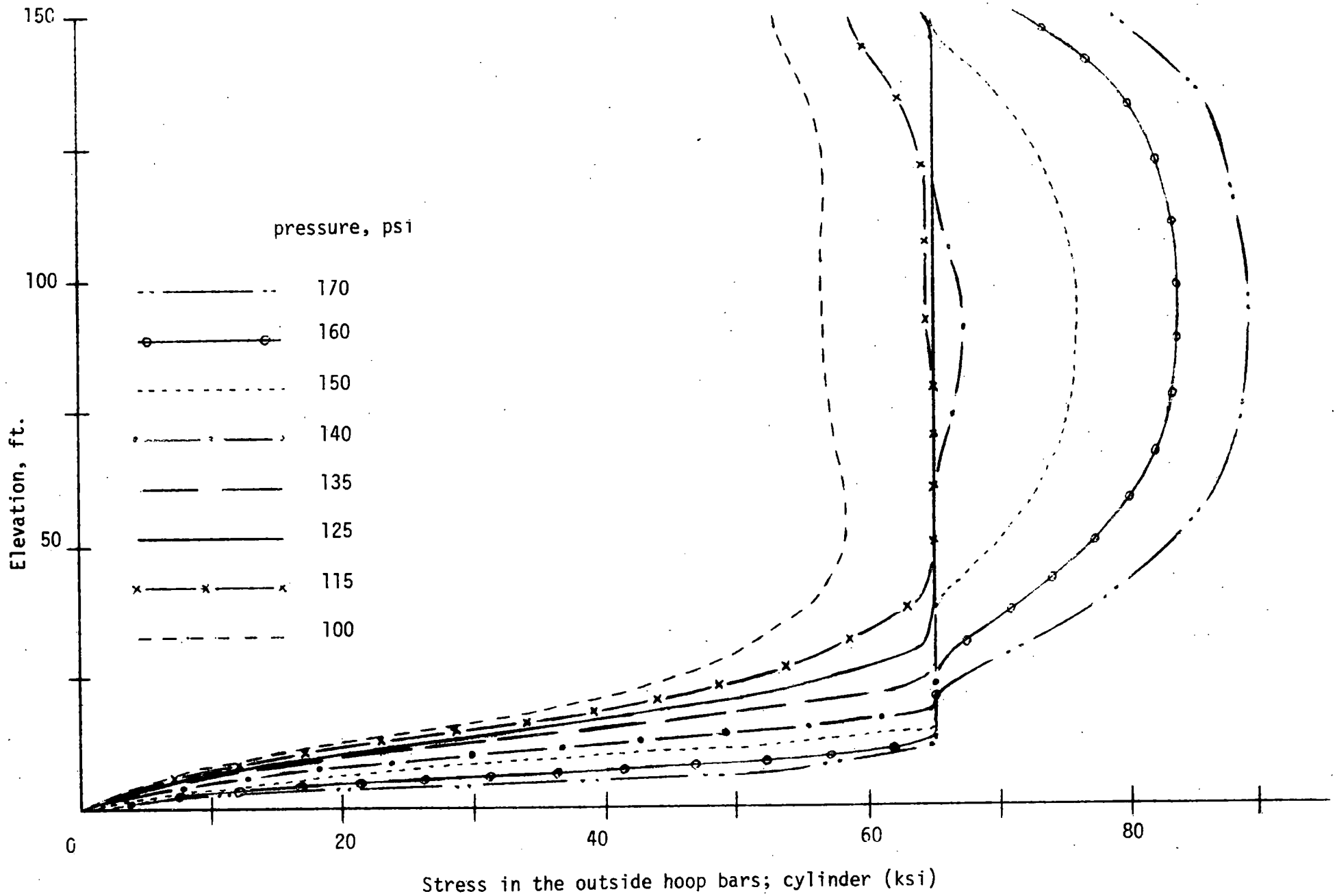
150
100
50
0
20
40
60
80
Elevation, ft.
Stress in the outside hoop bars; cylinder (ksi)
pressure, psi
170
160
150
140
135
125
115
100

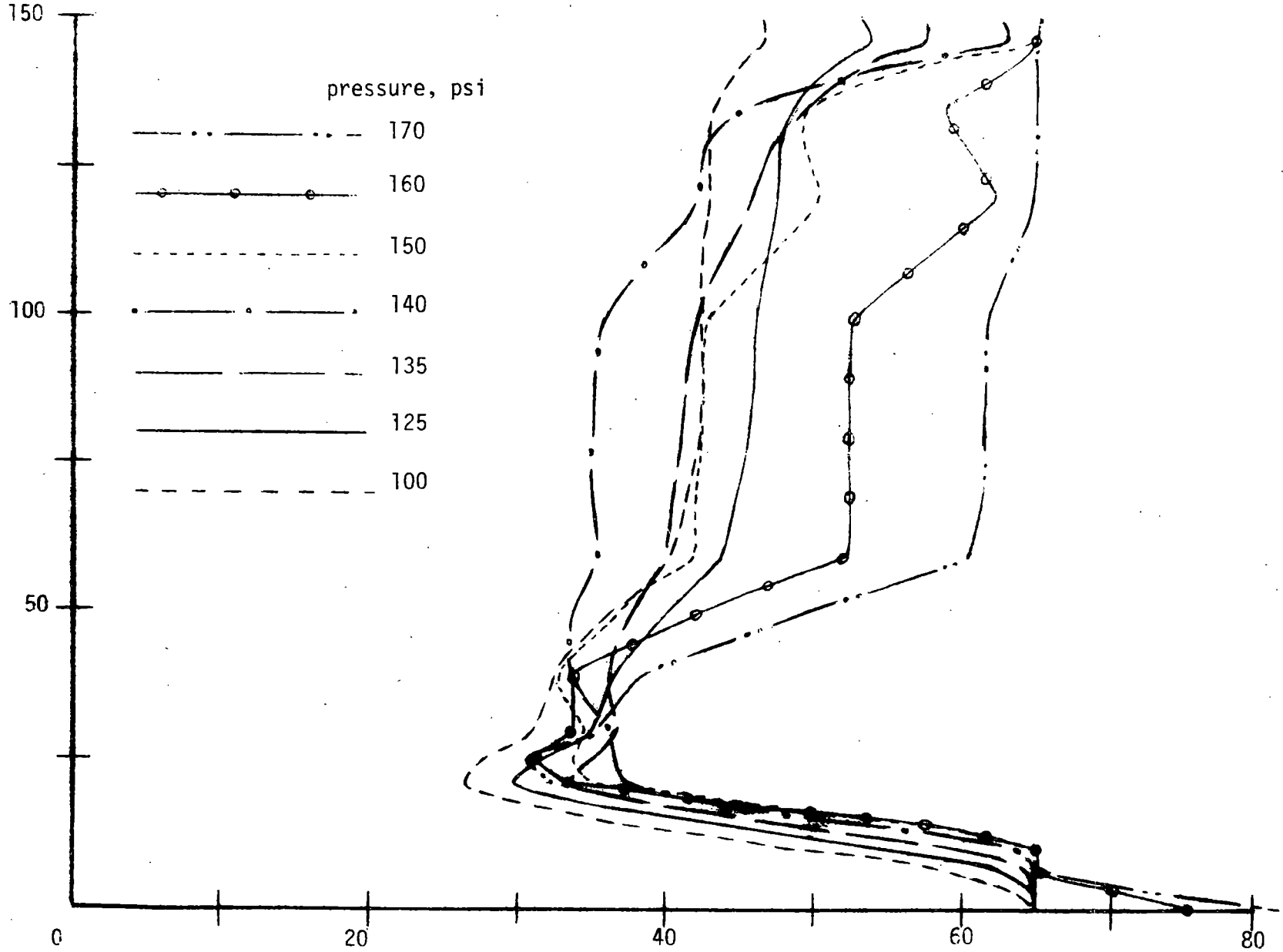

Stress in inside vertical bars; cylinder (ksi).

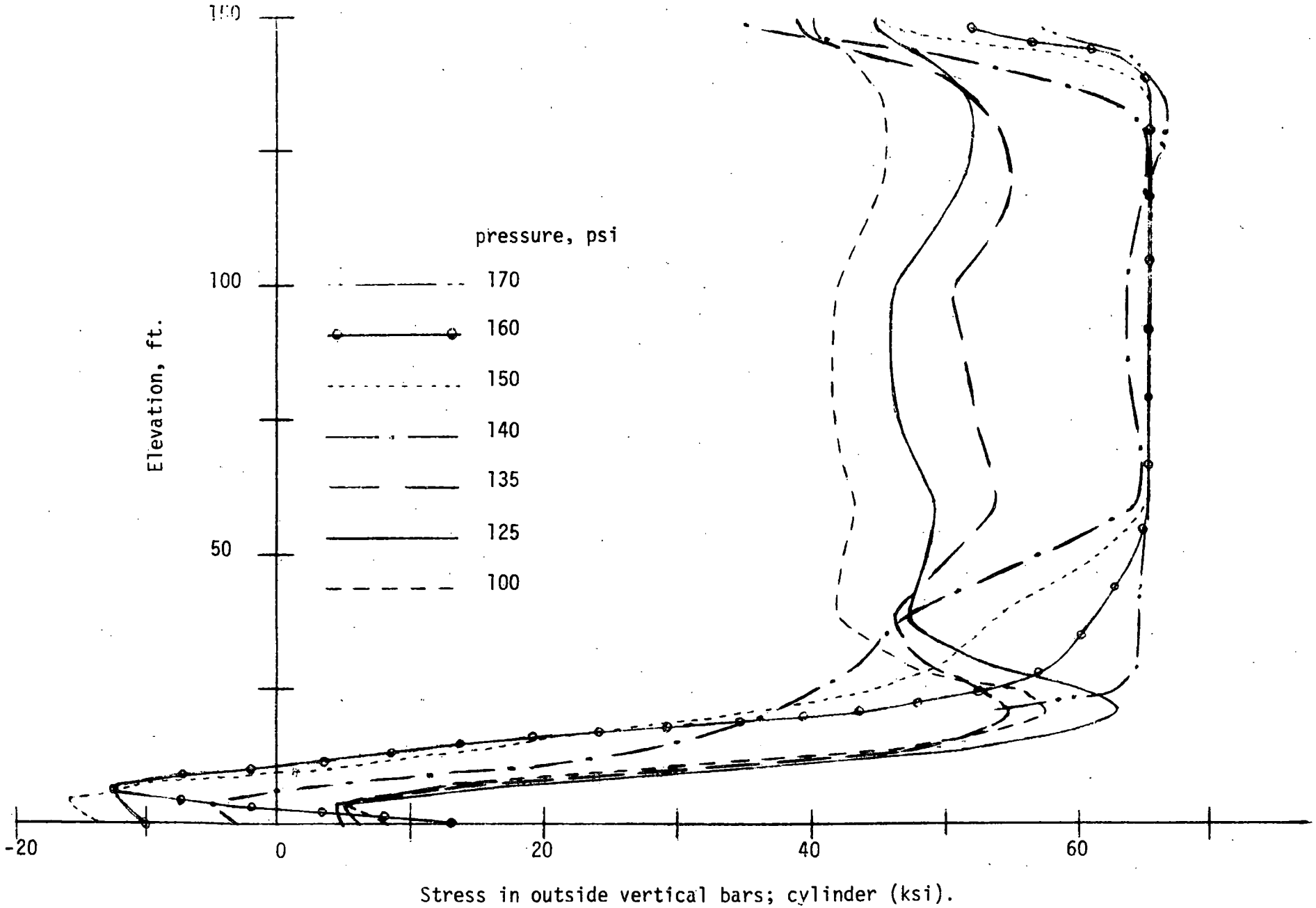
150
100
50
Elevation, ft.
pressure, psi
170
160
150
140
135
125
100
-20
0
20
40
60
Stress in outside vertical bars; cylinder (ksi).

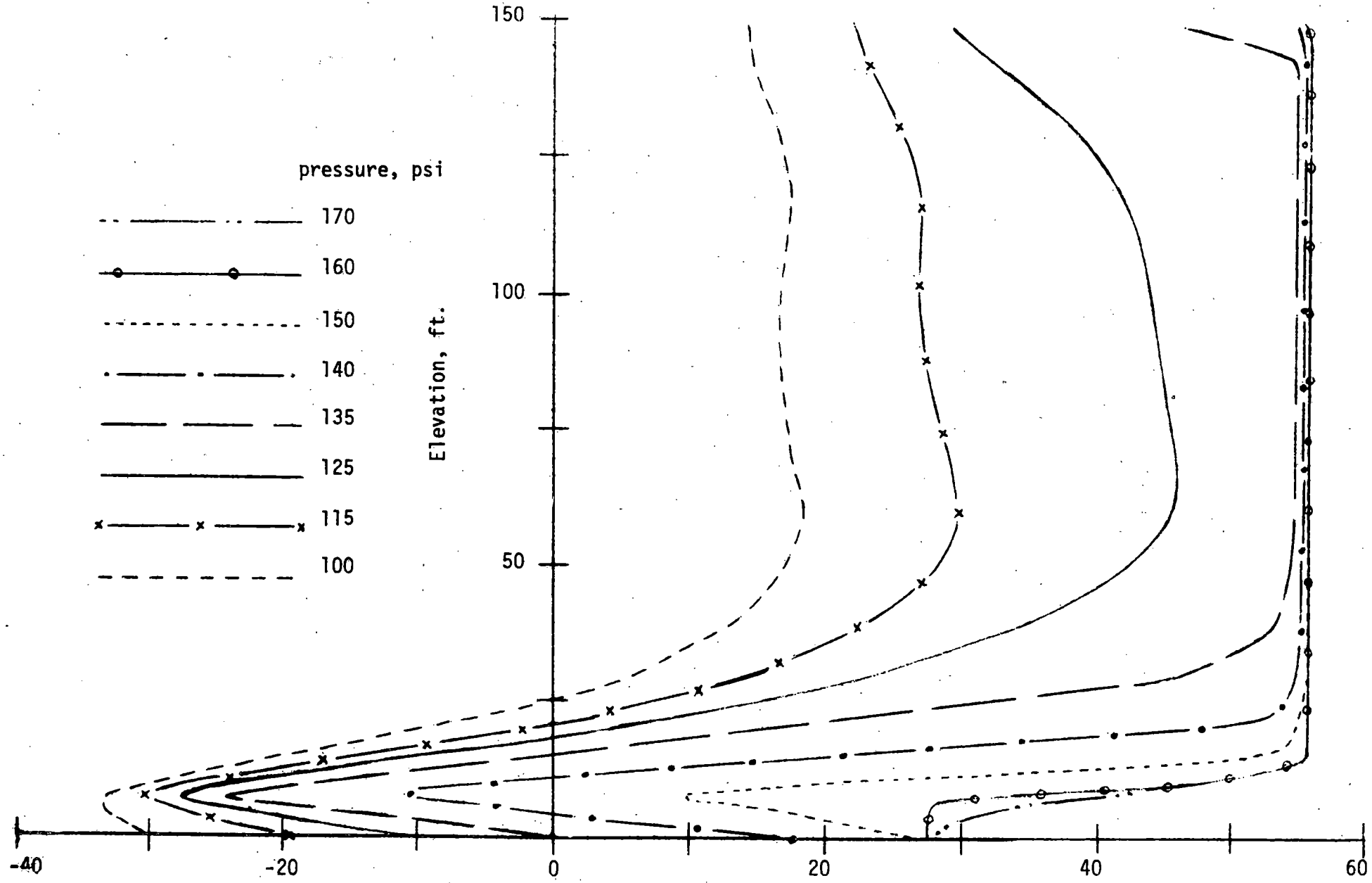
pressure, psi
170
160
150
140
135
125
115
100
Elevation, ft.
150
100
50
-40
-20
0
20
40
60
Liner stress in the hoop direction; cylinder (ksi)

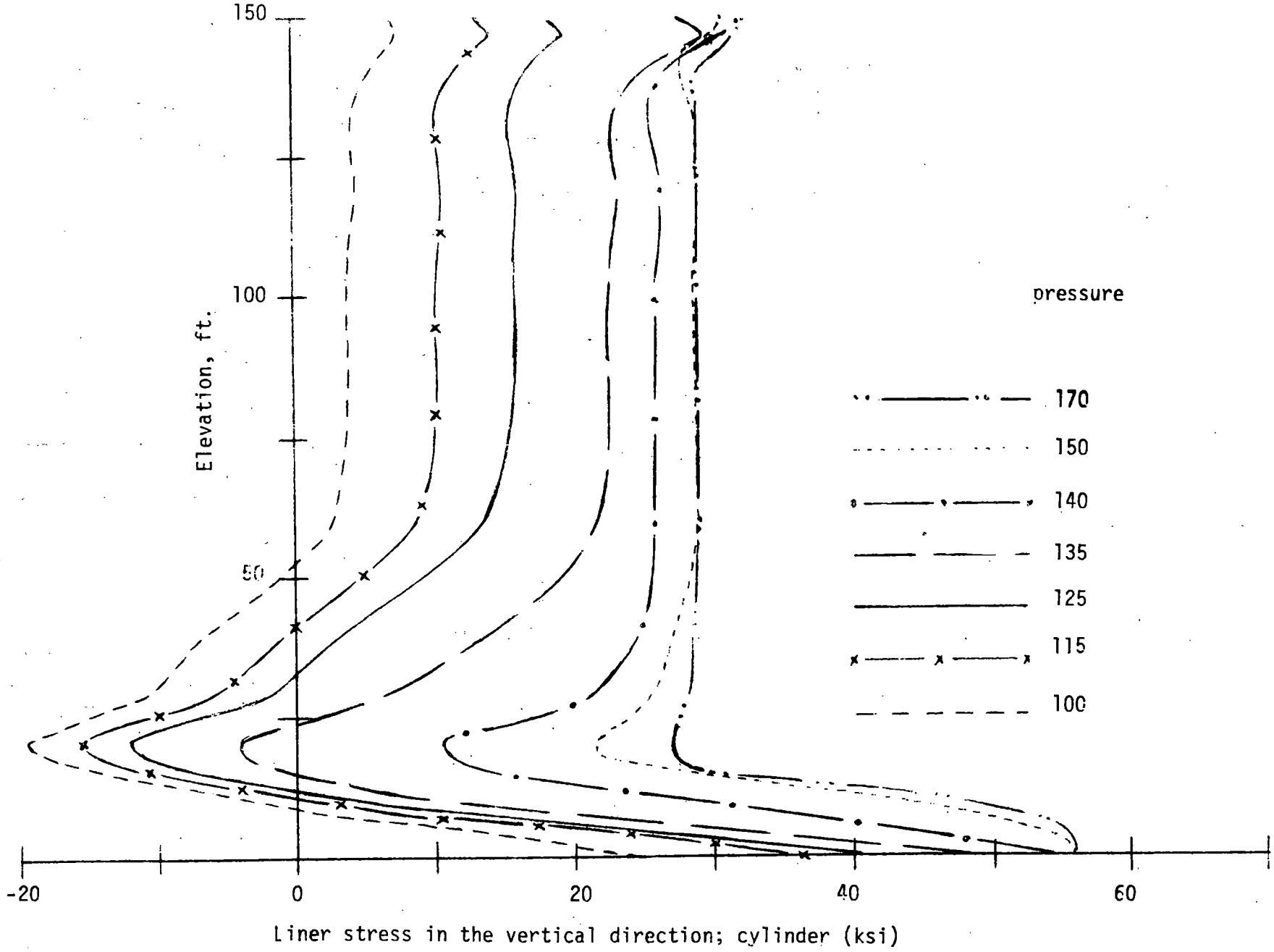
150
100
50
Elevation, ft.
pressure
170
150
140
135
125
115
100
-20
0
20
40
60
Liner stress in the vertical direction; cylinder (ksi)

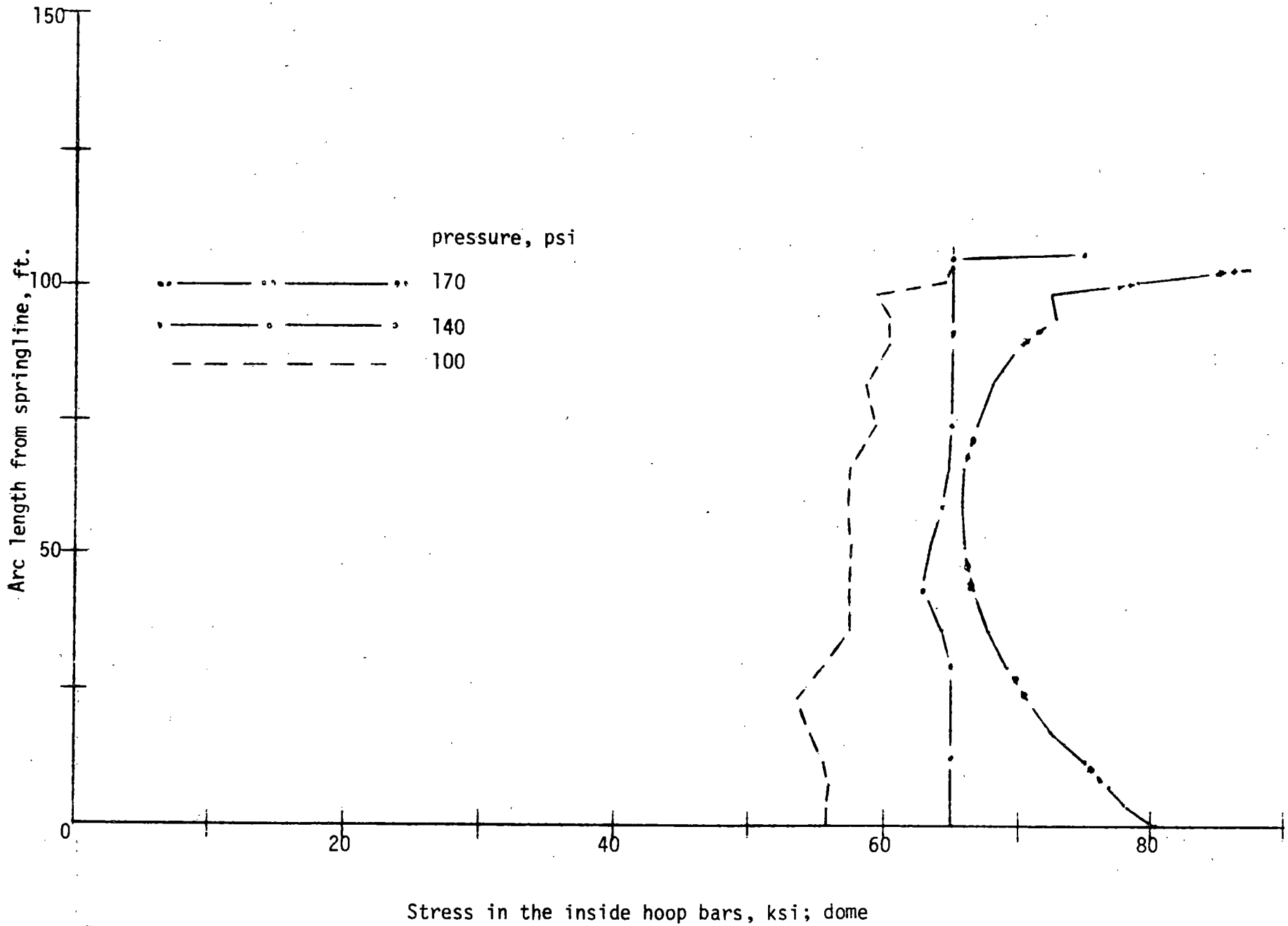
150
100
50
0
Arc length from springline, ft.
pressure, psi
170
140
100
20
40
60
80
Stress in the inside hoop bars, ksi; dome

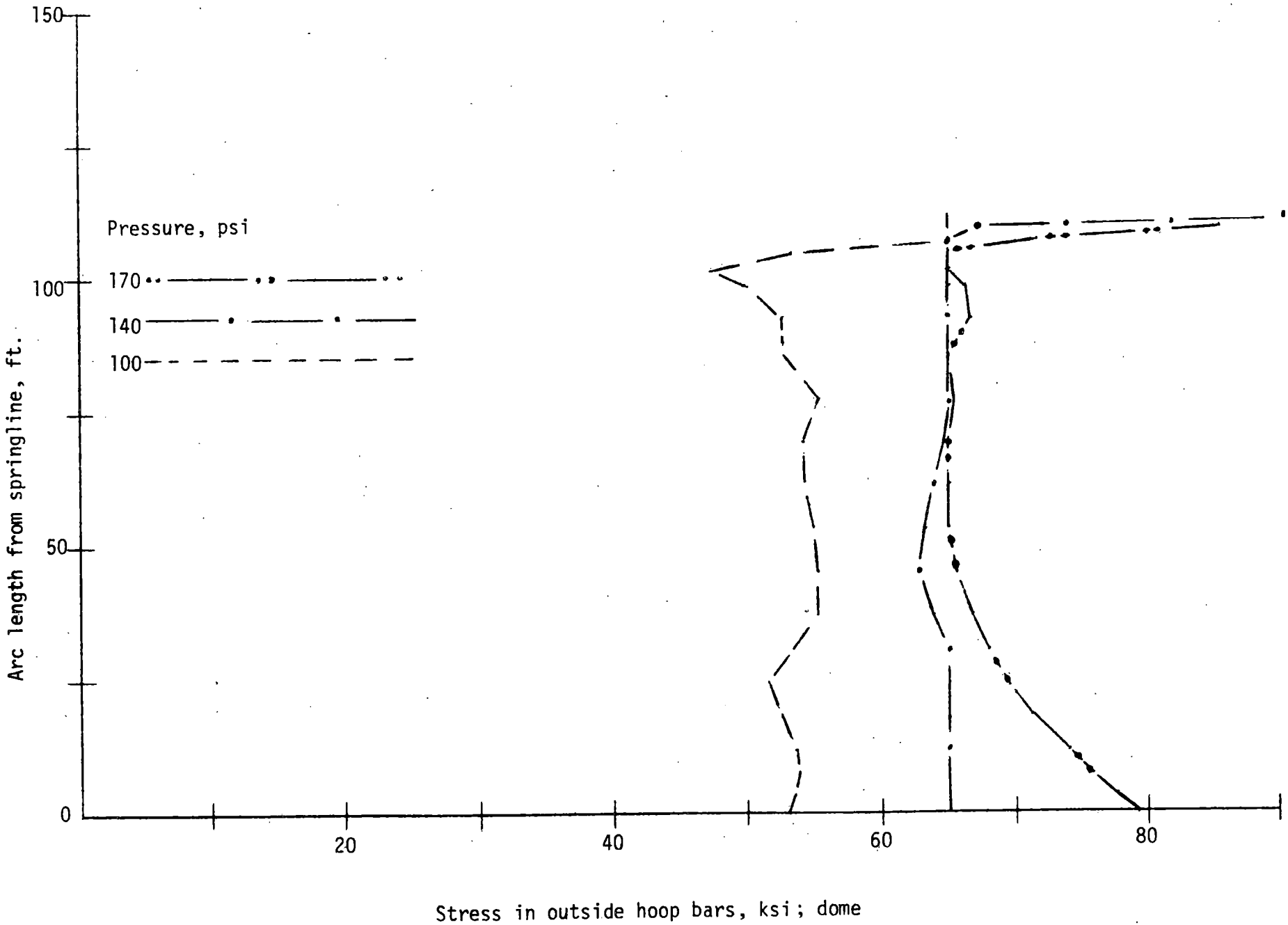
150
100
50
0
Arc length from springline, ft.
Pressure, psi
170
140
100
20
40
60
80
Stress in outside hoop bars, ksi; dome

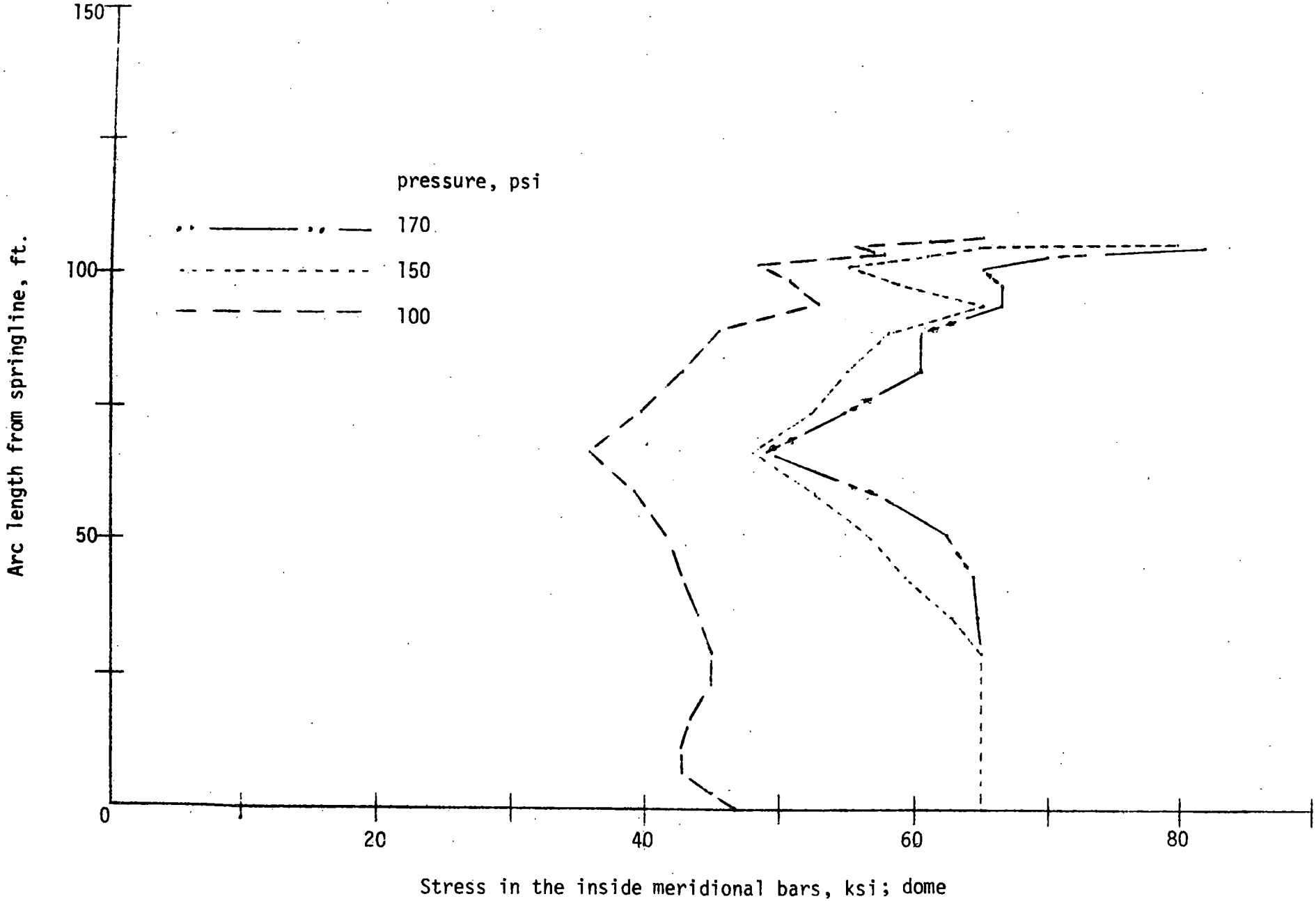
150
100
50
0
20
40
60
80
pressure, psi
170
150
100
Arc length from springline, ft.
Stress in the inside meridional bars, ksi; dome

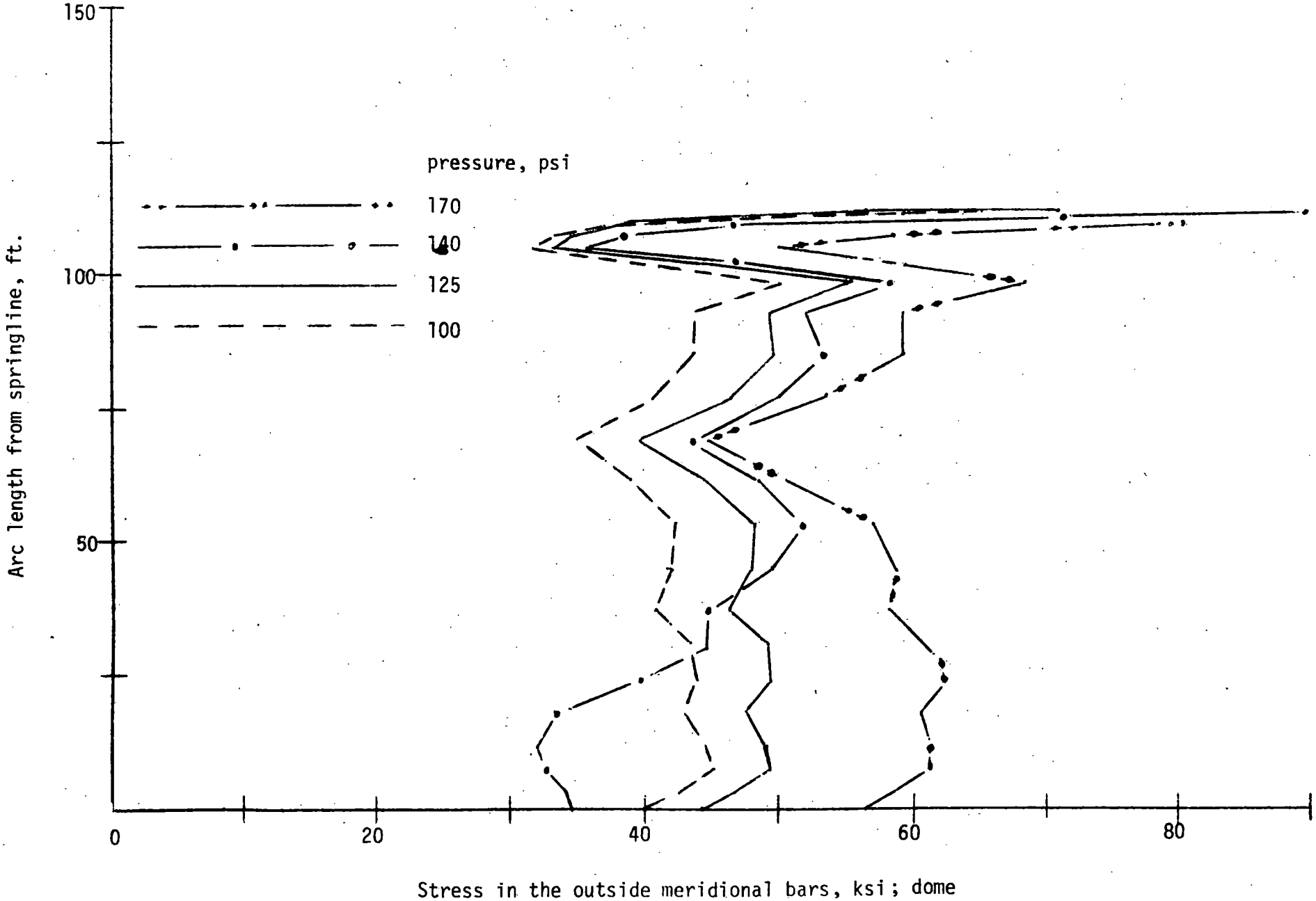
150
100
50
pressure, psi
170
140
125
100
Arc length from springline, ft.
0
20
40
60
80
Stress in the outside meridional bars, ksi; dome

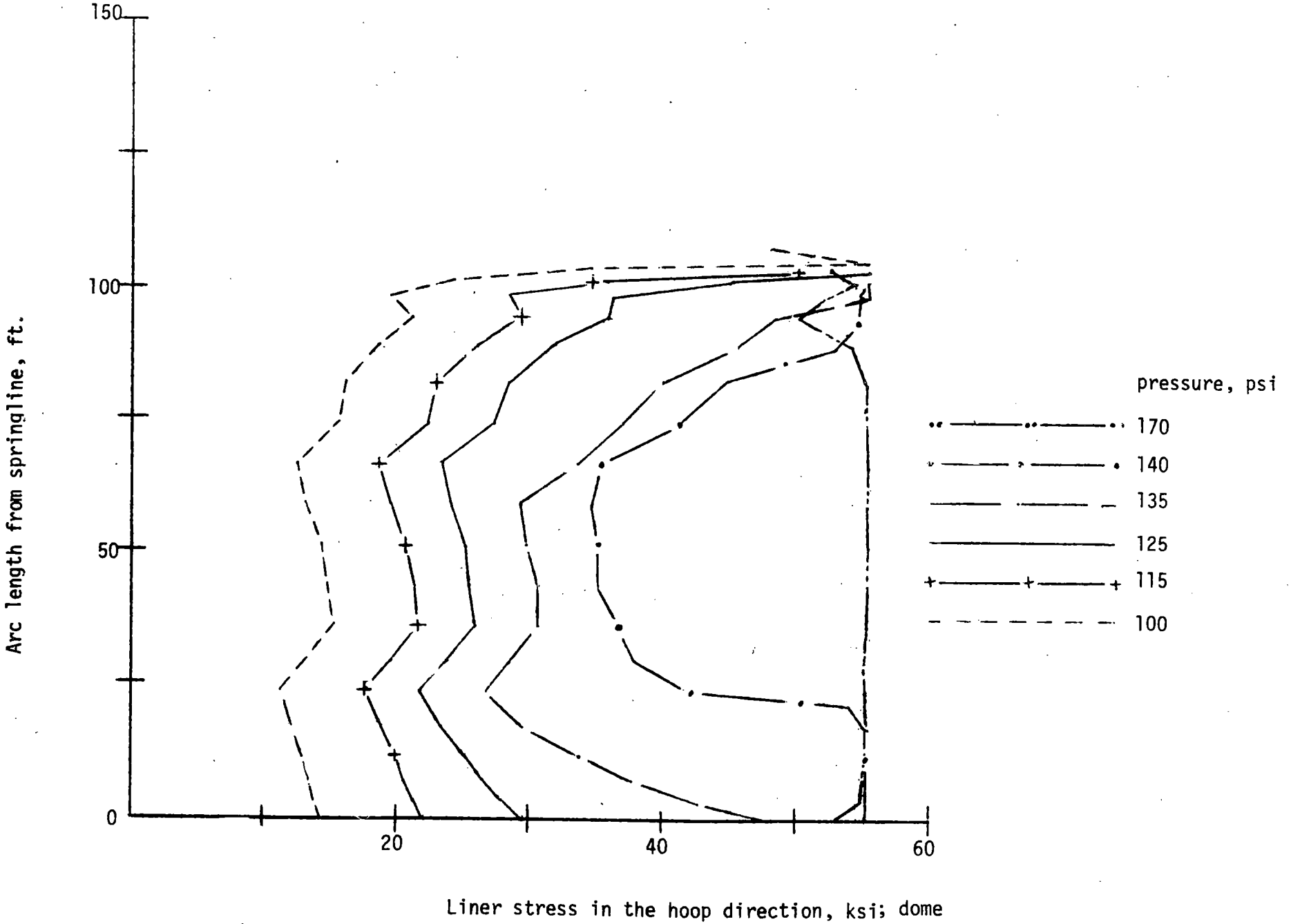
150
100
50
0
20
40
60
Arc length from springline, ft.
Liner stress in the hoop direction, ksi; dome
pressure, psi
170
140
135
125
115
100

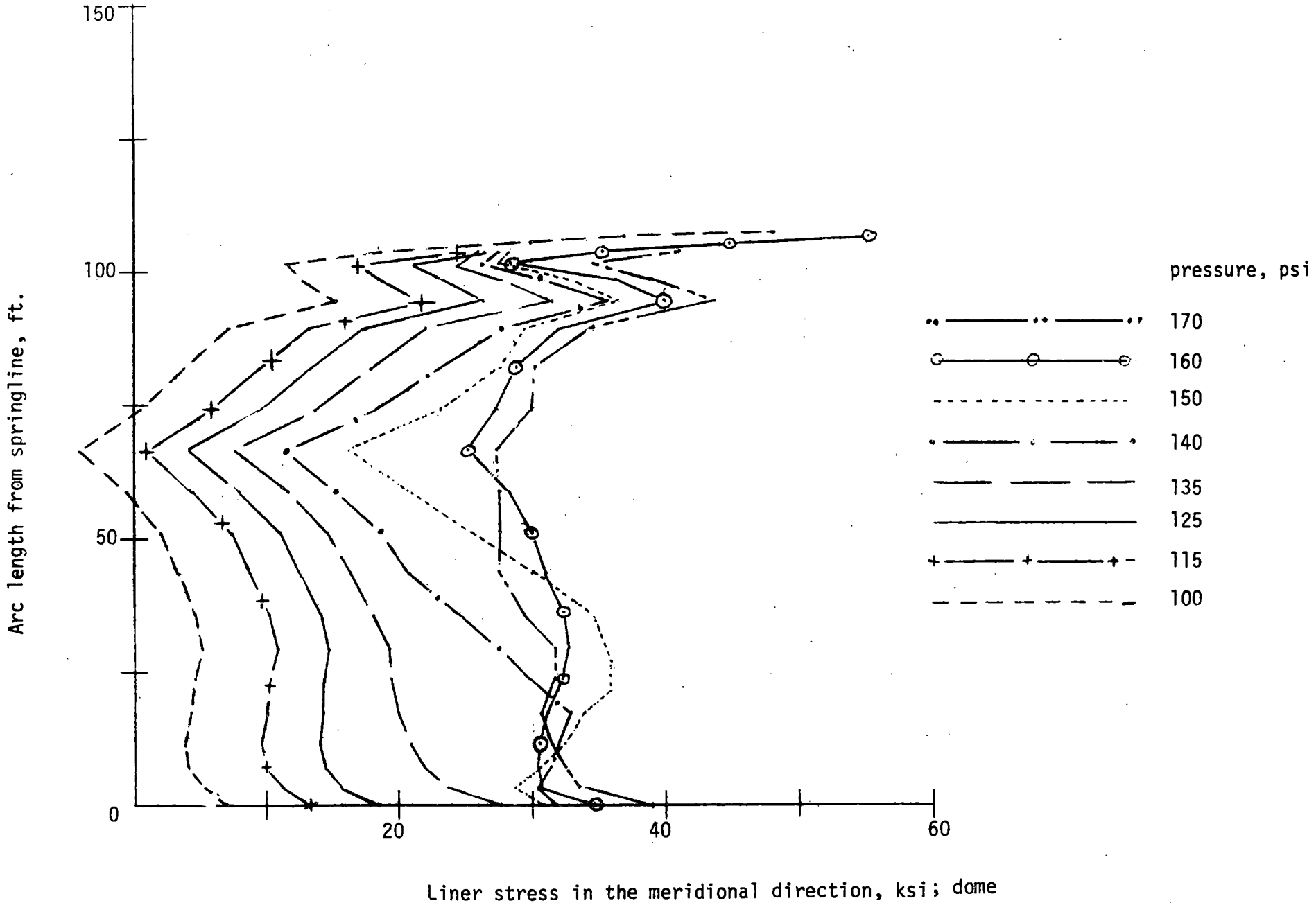
150
100
50
0
20
40
60
Arc length from springline, ft.
Liner stress in the meridional direction, ksi; dome
pressure, psi
170
160
150
140
135
125
115
100

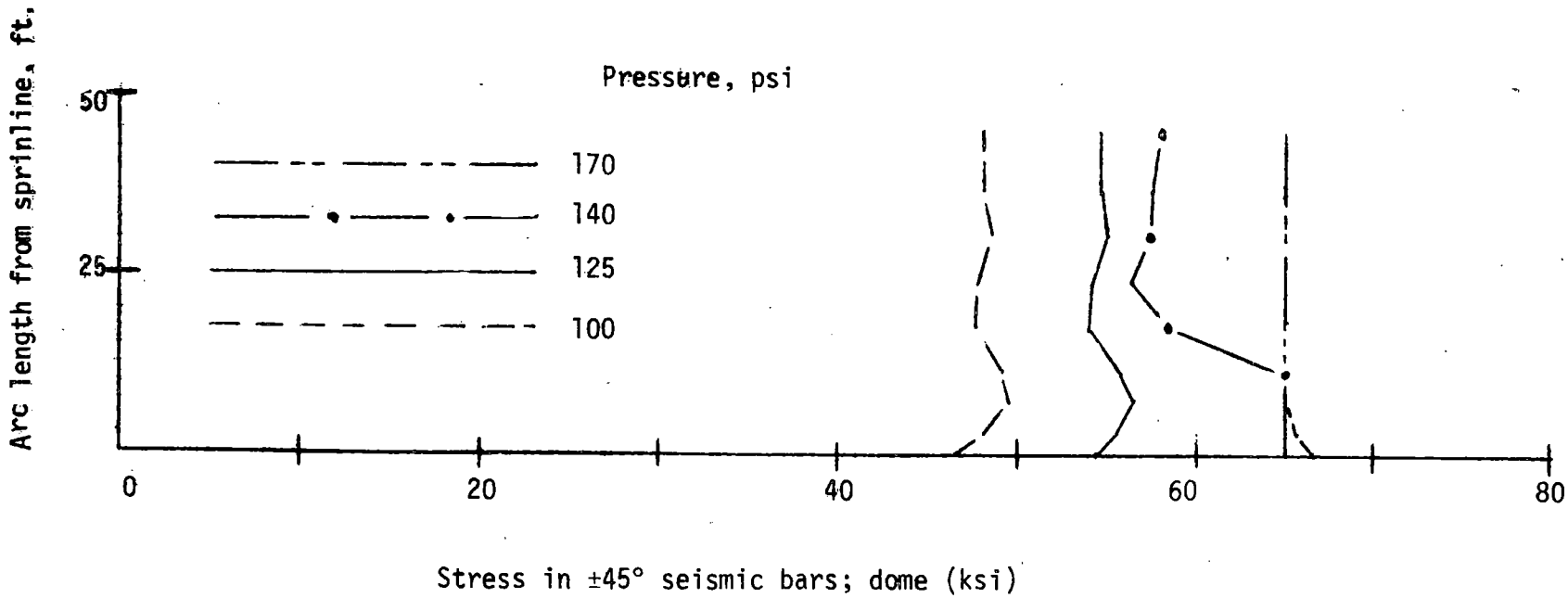
Arc length from sprinline, ft.
50
25
Pressure, psi
170
140
125
100
0
20
40
60
80
Stress in ±45° seismic bars; dome (ksi)

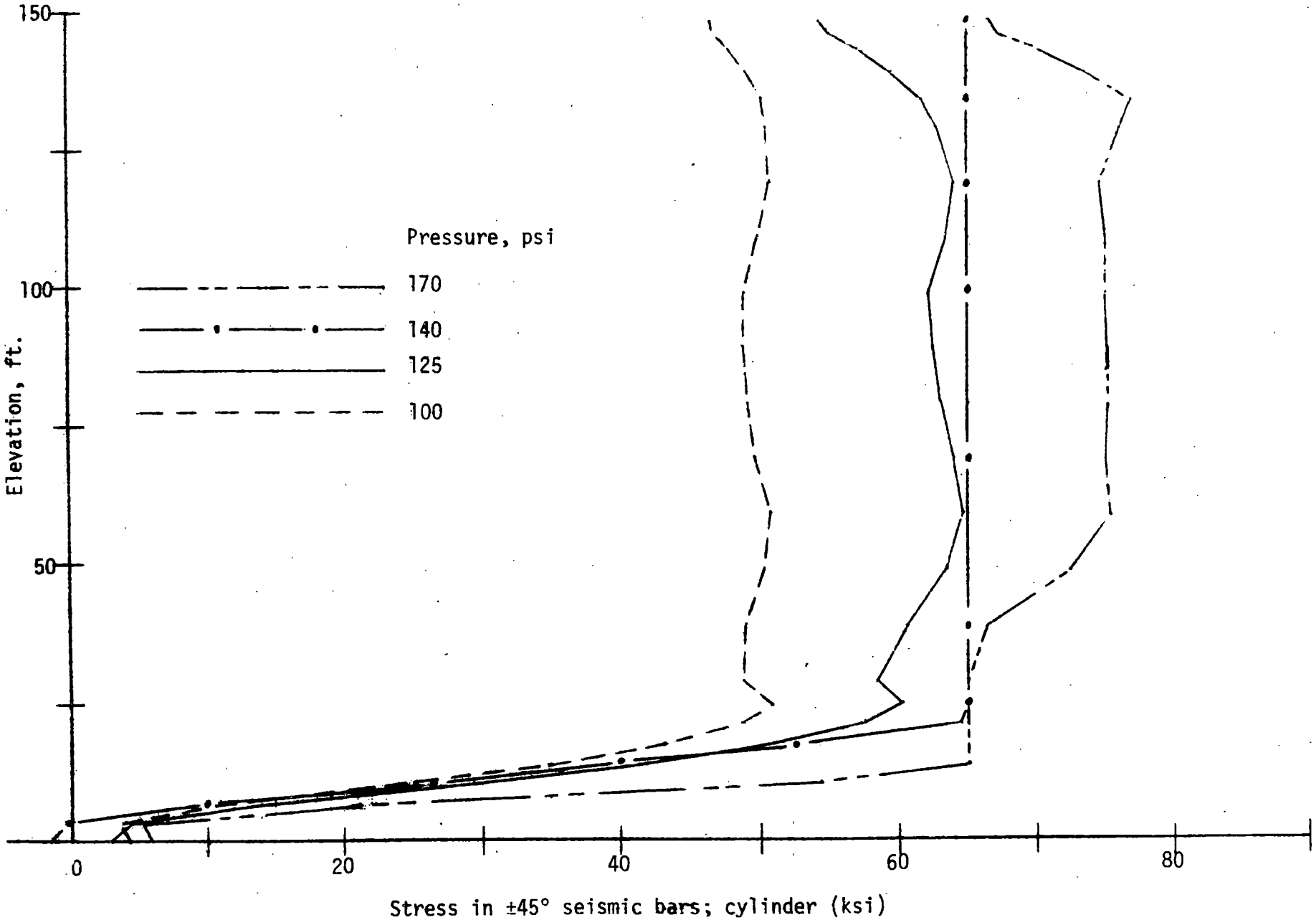
150
100
50
Elevation, ft.
Pressure, psi
170
140
125
100
0
20
40
60
80
Stress in ±45° seismic bars; cylinder (ksi)

TITLE: CATEGORY I STRUCTURES PROGRAM

AUTHOR(S): E. G. Endebrock, Q-13
R. C. Dove, Q-13

SUBMITTED TO: Ninth Water Reactor Safety Research Information Meeting
Oct. 26-28, 1981
Washington, DC

University of California

LOS ALAMOS SCIENTIFIC LABORATORY
Post Office Box 1663 Los Alamos, New Mexico 87545
An Affirmative Action/Equal Opportunity Employer

Form No. 836 R3
St. No. 2629
12/78

UNITED STATES
DEPARTMENT OF ENERGY
CONTRACT W-7405-ENG. 36

CATEGORY I STRUCTURES PROGRAM

E. G. Endebrock, and R. C. Dove, Q-13

Los Alamos National Laboratory

Ninth Water Reactor Safety Research Information

October 27, 1981

The objective of the Category I Structures Program is to supply experimental and analytical information needed to assess the structural capacity of Category I structures (excluding the reactor containment building). Because the shear wall is a principal structural element of a Category I structure, and because relatively little experimental information is available on the shear walls, it was selected as the test element for the experimental program. The large load capacities of shear walls in Category I structures dictates that the experimental tests be conducted on small size shear wall structures that incorporates the general construction details and characteristics of as-built shear walls (Figs. 1 and 2).

To assure the maximum utilization of the experimental information, analytical studies precede the experimental tests. Nonlinear finite element solutions were obtained to predict failure loads and modes, and these computer solutions are compared to the static experimental test results. Experimental information for computer code verification and/or development is a natural by-product of this program. Special computer programs for obtaining dynamic responses were developed. These programs use the typical softening and hysteretic restoring force relationships characteristic of reinforced concrete structures.

Quasi-static load cycling and monotonic loading tests on the shear wall structures precede the dynamic tests. This procedure is followed so that the results of static and dynamic tests on identical test structures can be compared. Results of several static tests are shown in Figs. 3-5.

The experimental program is divided into three phases. Phase I experiments are static and dynamic tests on small one- and two-story shear wall structures. Phase II experiments are similar to Phase I experiments except that there will be fewer tests on larger test structures. Phase III

experiments will be conducted on three-dimensional structures with simulated equipment loads. Phase I static tests on the one-story shear wall structure are near completion, and the dynamic tests are scheduled to start in September, 1981.

For a structure with a softening and hysteretic restoring force relationship and for a structure subjected to an earthquake motion, the analytical study that preceded the Phase I dynamic tests suggests the use of certain nondimensional parameters for describing the dynamic responses and the system inputs. The primary response parameter is the ratio of relative story displacement to the element yield displacement (ductility ratio). If the element failure ductility is known, the margin to failure can be directly determined from the analytical solution. The development and implications of this method are described in Ref. 1.

REFERENCES

1. E. G. Endebrock and R. C. Dove, "Seismic Response of Nonlinear Systems, "Los Alamos National Laboratory report NUREG/CR-2310 (LA-8981-MS) October 1981.

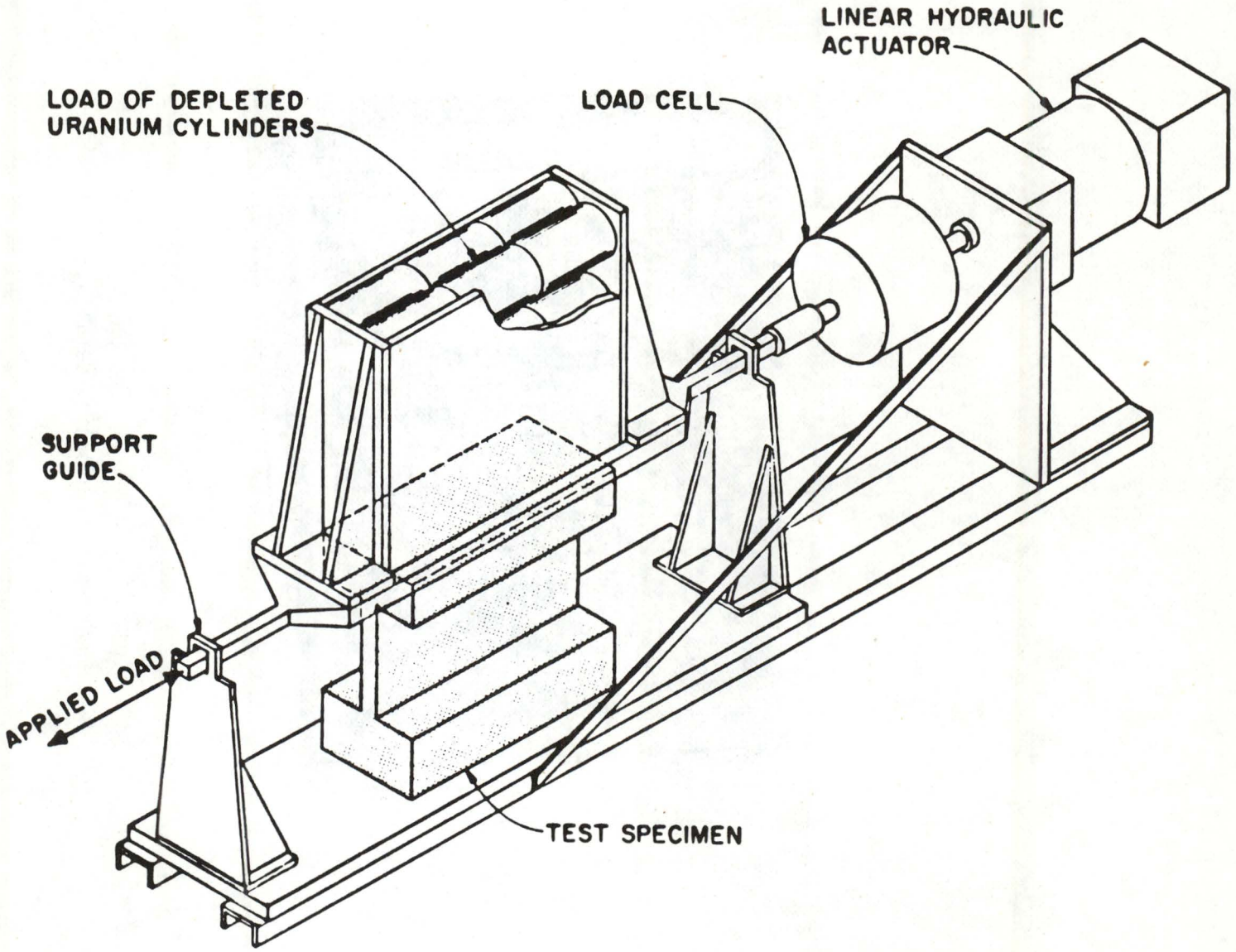

Fig. 1. Test structure and static test frame.

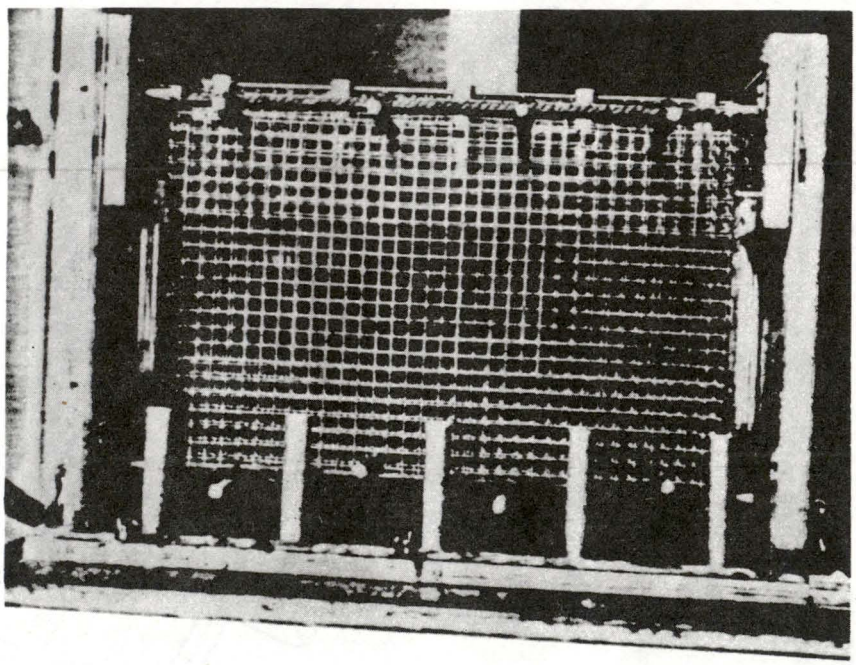

Fig. 2. Shear wall reinforcing details.

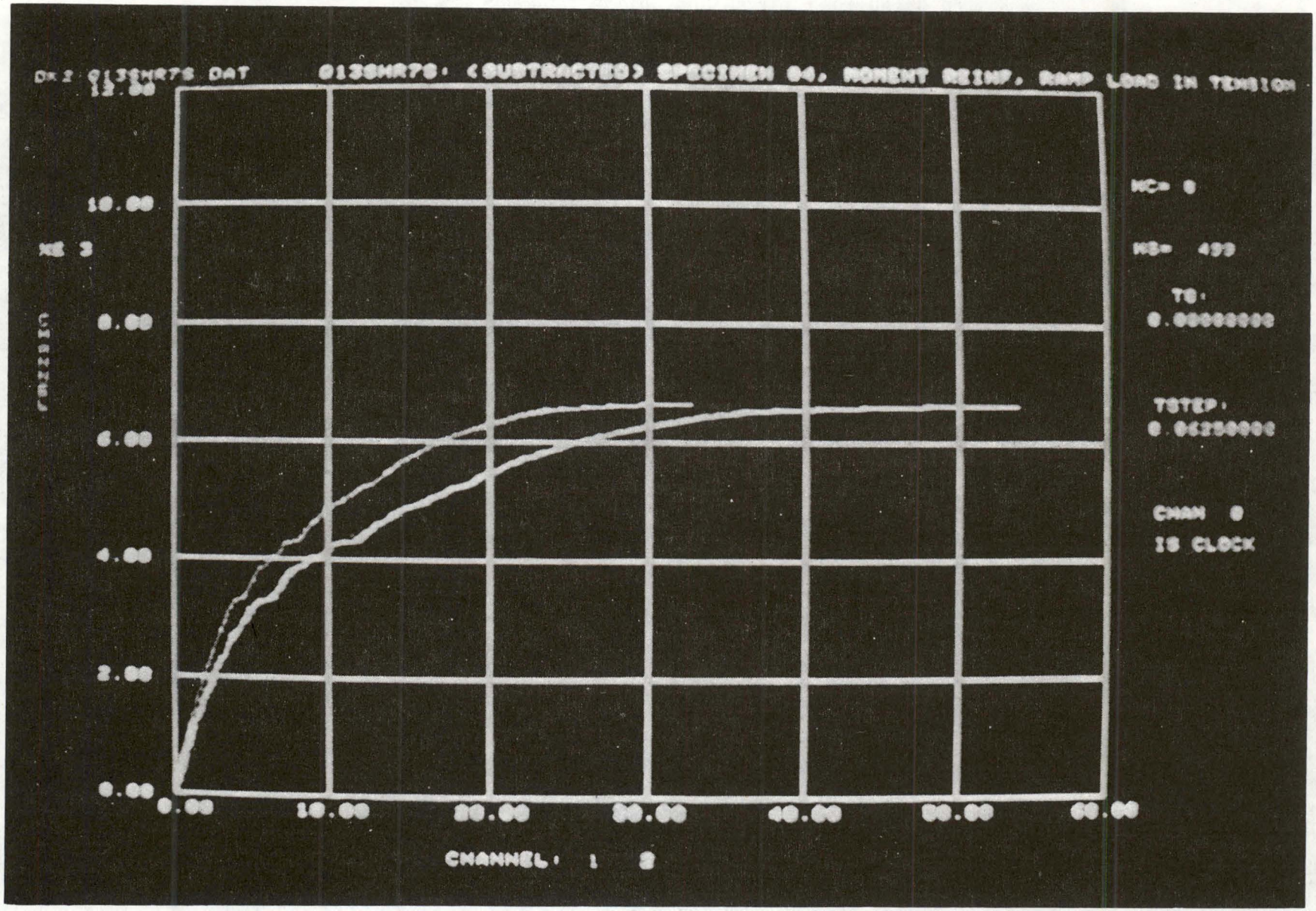

Fig. 3. Load-deflection curves for monotonic loading.

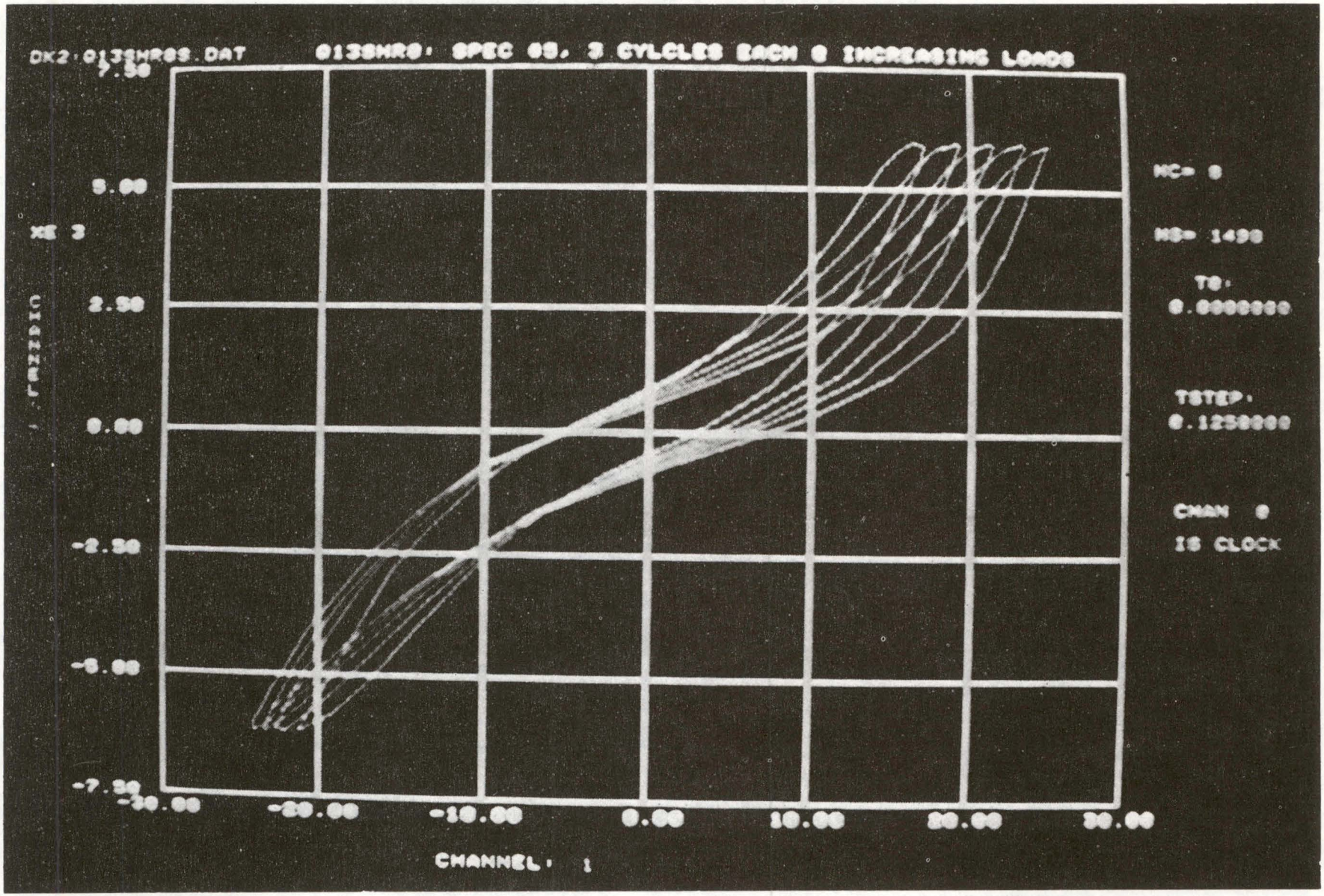

Fig. 4. Load-deflection curves for cycling load.

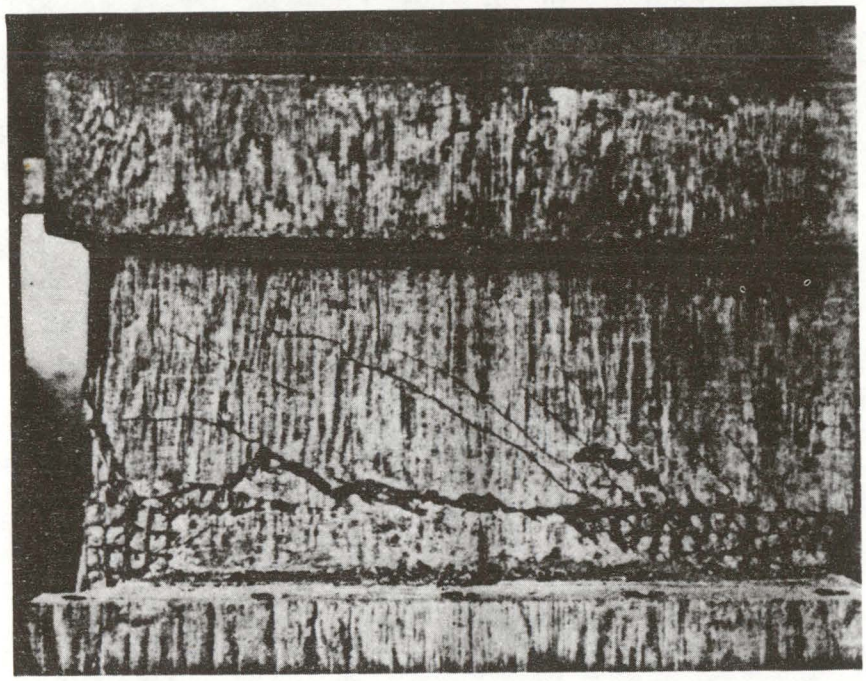

Fig. 5. Shear wall failure mode.

LA-UR - 81-2775

TITLE: CONTAINMENT BUCKLING PROGRAM

AUTHOR(S): C. A. Anderson, Q-13
J. G. Bennett, Q-13

SUBMITTED TO: Ninth Water Reactor Safety Research Information Meeting
Oct. 26-28, 1981
Washington, D.C.

University of California

LOS ALAMOS SCIENTIFIC LABORATORY
Post Office Box 1663 Los Alamos, New Mexico 87545
An Affirmative Action/Equal Opportunity Employer

Form No. 836 R3
St. No. 2629
12/78

UNITED STATES
DEPARTMENT OF ENERGY
CONTRACT W-7405-ENG. 36

CONTAINMENT BUCKLING PROGRAM

C. A. Anderson, Q-13
J. G. Bennett
Energy Division
Los Alamos National Laboratory
Ninth Water Reactor Safety Research Information
October 27, 1981

The Containment Buckling program at the Los Alamos National Laboratory is aimed at evaluating the adequacy of the current design procedures for free standing steel nuclear containment shells against static and dynamic structural instability. Such buckling behavior will typically produce large displacements in the shell wall that will potentially violate seals around hatches and penetrations, or even produce puncture or tearing of the shell wall resulting in a loss of containment function. The ultimate goal of the program is to provide NRC with a basis for evaluating the associated licensing issues and to recommend appropriate changes and additions to the NRC Review Criteria.

The program is proceeding in three basic phases. Phase I was an evaluation of the possibility of the ASME Area Replacement Method for Reinforcing around circular penetrations as also being a means to insure against buckling. This phase has been completed and is reported in detail in Ref. 1.

In Phase I steel cylinders simulating containment shells were fabricated to one-sixtieth actual size. A number of these cylinders were left unpenetrated; others were fabricated with a scaled penetration and then reinforced to various amounts according to the ASME code rules; none were stiffened by rings as is normal for containment vessels. The cylinders were checked for roundness, end parallelism, variation in wall thickness, and other imperfections, then were instrumented with strain gages. After careful shimming between the cylinder and testing machine to help approach uniform end loading, the cylinder was loaded to failure. Figure 1 shows one of the penetrated and reinforced cylinders after testing.

These experiments clearly showed that fabrication imperfections dominated the buckling failure of steel cylinders. For example, unpenetrated cylinders buckled at a load considerably lower than the value predicted for perfect cylinders. Cylinders with penetrations but no reinforcement failed at essentially

the same load as unpenetrated cylinders; that is, the effect of the hole was apparently too small to cause buckling before the shell failed from other imperfections. Imperfections are, thus, felt to be the main reason for the considerable scatter in the data for the steel cylinders shown in Fig. 2 (dots). For comparison, data (triangles) are also plotted from study of a reusable Mylar shell. Because the Mylar cylinder was of high enough qualtiy that the penetration lowered the buckling load, these data show little scatter as the buckling load increases with reinforcement. In this figure the amount of reinforcement is expressed as a percentage of that recommended in the ASME code for reinforced penetrations. The main conclusion from this study is that by reinforcing a circular penetration according to the ASME Area Replacement Method, the buckling load will be increased, but not necessarily back up to the unpenetrated value.

Phase II is a series of ring stiffened experiments that will be used to benchmark computer code buckling predictive capability. This phase is being carried out in coordination with Lockheed Palo Alto Research Laboratory's analytical studies of the same geometric configurations, and with the cooporation of Chicago Bridge and Iron who supplied typical penetration sizes and framing details in accordance with industry practice. Analytical predictions have been partially completed and experiments are now underway on these shells. Figure 3 shows a photograph of one of the "baseline" benchmark test cylinders that are currently undergoing imperfection measurements and instrumentation. The baseline benchmark test cylinders do not have penetrations.

Current plans call for loading the cylinder with a concentrated load applied at one-half the radius through a relatively rigid top loading plate and end ring, resulting in a nonaxisymmetric buckling mode. The present analytical predictions by Lockheed are that a nonsymmetric "elephants" foot local buckling pattern will develop in the 2.5 in. bay between the seventh and eighth ring from the top of the cylinder at a load of 17,840 lb.

Figure 4 shows plans for one of the typical follow-on test cylinders that are currently being fabricated that will have framed and reinforced penetrations. Penetrations fall into the category of interrupting no ring stiffeners, to interrupting up to three rings. Framing details can vary, but the basic philosophy is to frame the penetration in such a manner as to make the ring "look" continuous by replacing the area and bending stiffness of the interrupted rings. Reinforcing is in accordance with applicable ASME code requirements. Credit is also taken for the nozzle neck as part of the reinforcing up

to one shell wall thickness. Neck area greater than this appears to have an insignificant effect. Four of these cylinders, one for each type of penetration, are now under construction.

The third phase of the program is to study and develop recommendations on the dynamic buckling behavior of steel containments. Primary loads of interest are both earthquake and asymmetric accidental internal pressure transients.

There is no doubt that shell "buckling" or, at least a large displacement buckling type of failure that resembles those obtained statically, will occur at some value of dynamic loading (as evidenced in the numerous failed tanks in earthquake prone regions, for example). Beyond this, a dynamic buckling load is difficult to define. The generally accepted definition is the dynamic loading that will cause a large increase in displacement with little or no increase in acceleration magnitude. From experimental data on Lexan or Mylar shells that can "snap through" and recover, such displacement patterns can be observed to occur at a given magnitude of acceleration during sinusoidal forcing tests. For a steel shell, only one will occur before failure and a "different" shell is obtained. For this reason, studying this phenomena using Lexan or Mylar is attractive.

The currently accepted design practice for these loadings as they influence buckling is the "freezing in time" analysis method. The transient stresses in the containment shells are first calculated and then a static bifurcation analysis is performed using the stress field from the (usually linear) transient analysis. The "freezing in time" technique has not been subjected to rigorous evaluation except for a few isolated cases.

The details of the technique vary from investigation to investigation. The simplest method is to choose an appropriate time, based on engineering judgement and locate the largest compressive membrane stresses. These stresses are assumed to act uniformally over the complete shell as a prebuckling stress field and the buckling stress is then found from either a closed form solution, or an empirical formula, or a numerical analysis.

Other variations are to use the complete spatial distribution of the membrane stresses from the transient analysis and then perform a bifurcation analysis at various "snapshots" in time. Still another variation is to include the prebuckling bending stresses in the bifurcation analysis, although they usually have little effect on buckling.

The transient analysis can be both materially and geometrically nonlinear, although geometric nonlinearities probably have little effect. Shallow spherical caps under transient pressure are an exception. Plasticity has not been investigated to any extent in this type of problem. Realistic end conditions, discrete stiffeners, penetrations, attached masses, etc. probably should be but are not always included in the transient analysis.

Our program is proceeding along the line of a joint analytical/experimental effort, using Lexan as a model material in an effort to study the "freezing in time" technique. We are studying generic containment-like models, ultimately including ring stiffeners, penetrations, and significant attached masses. It is surprising that this method of analysis has gained acceptance without evidence being presented to verify its accuracy and assessing the limits of its applicability. We believe that this phase of the program may be the most important contribution to both NRC licensing criteria and the buckling literature in general.

REFERENCES

1. J. G. Bennett, R. C. Dove and T. A. Butler, "An Investigation of Buckling of Steel Cylinders with Circular Cutouts Reinforced in Accordance with ASME Rules," Los Alamos National Laboratory report NUREG/CR-2165 (LA-8853-MS) June 1981

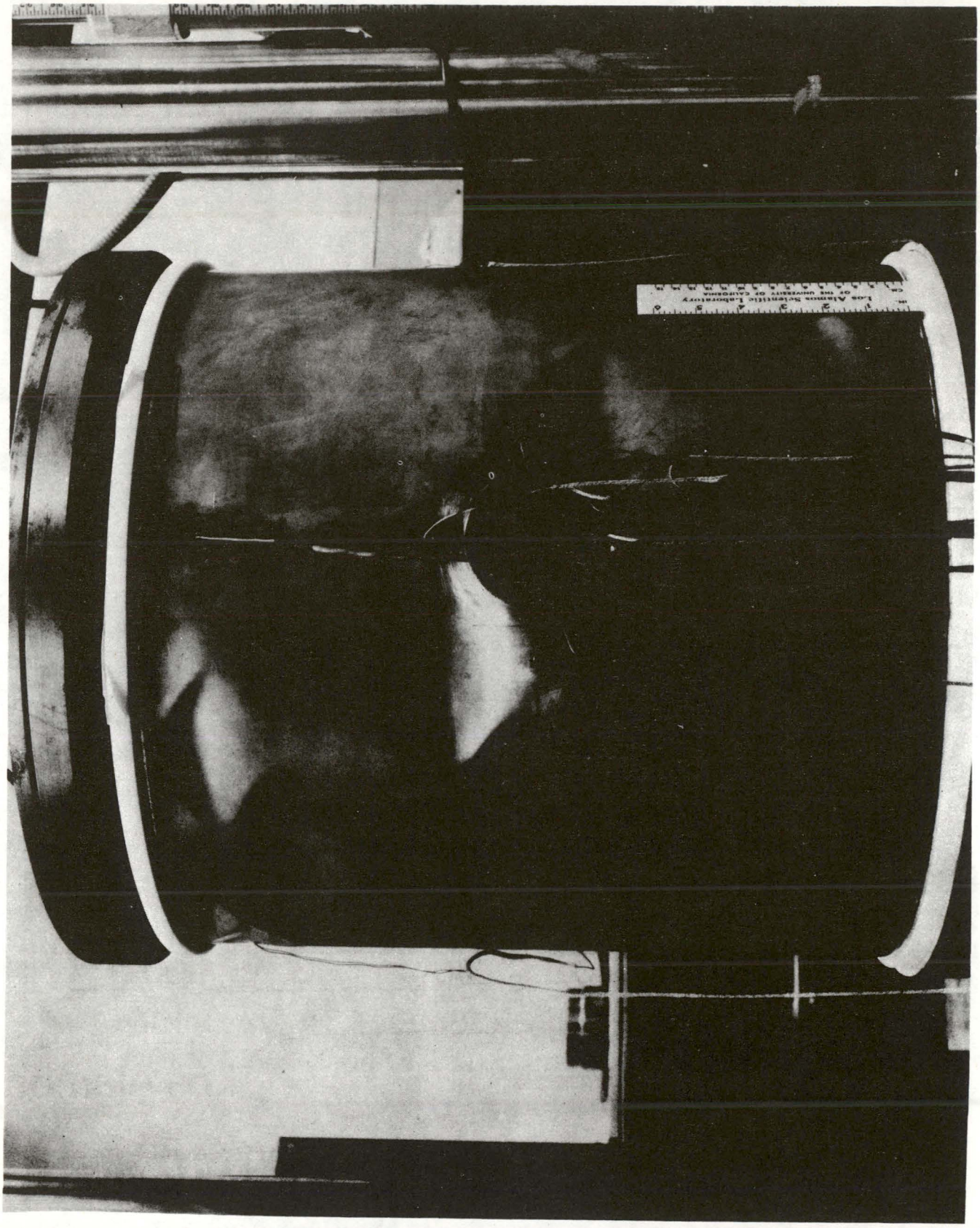

Fig. 1. Buckling mode for a penetrated and reinforced cylinder with 25% required reinforcement.

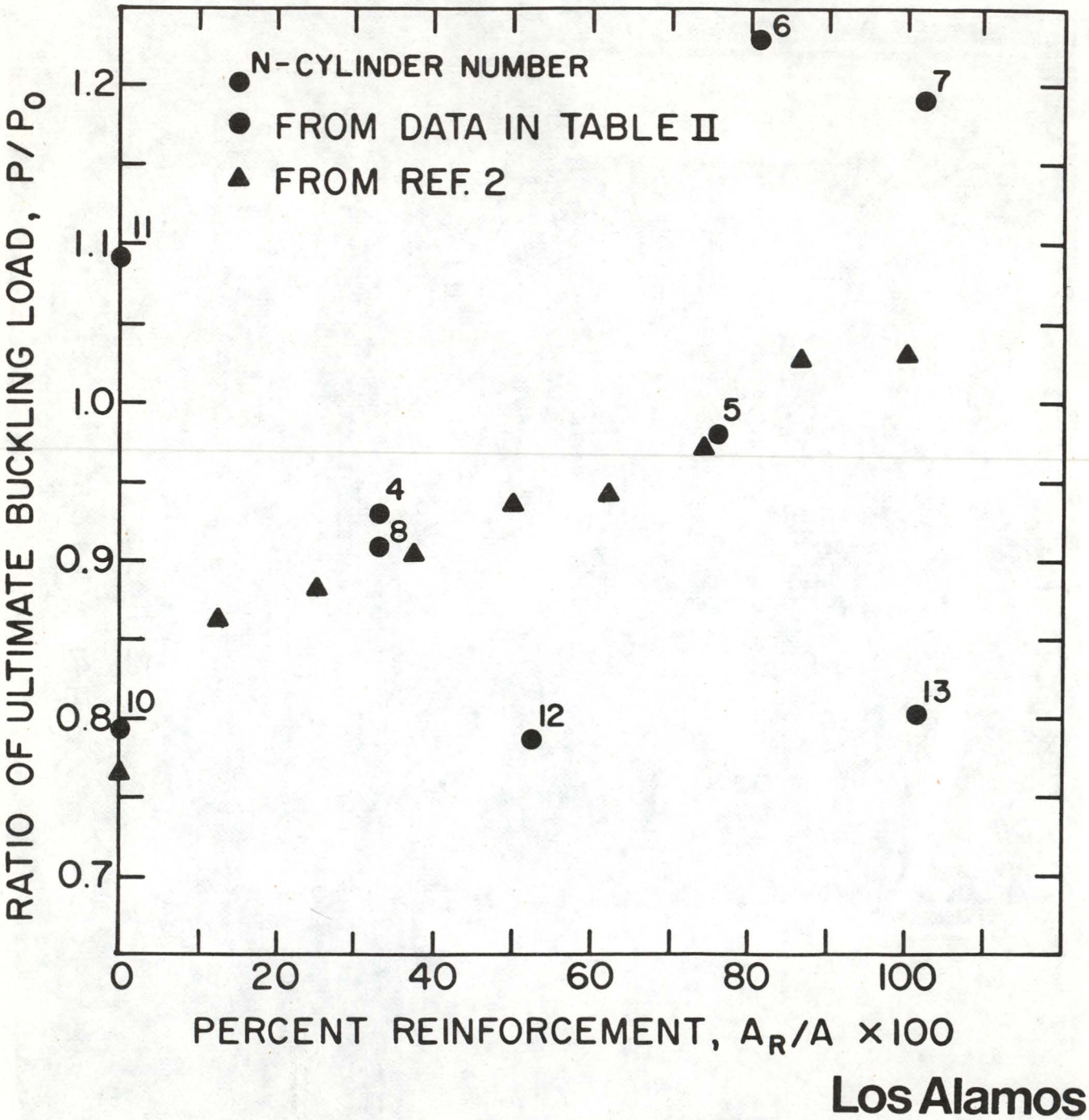

Fig. 2. Experimental data showing the effort of reinforcement on the buckling load.

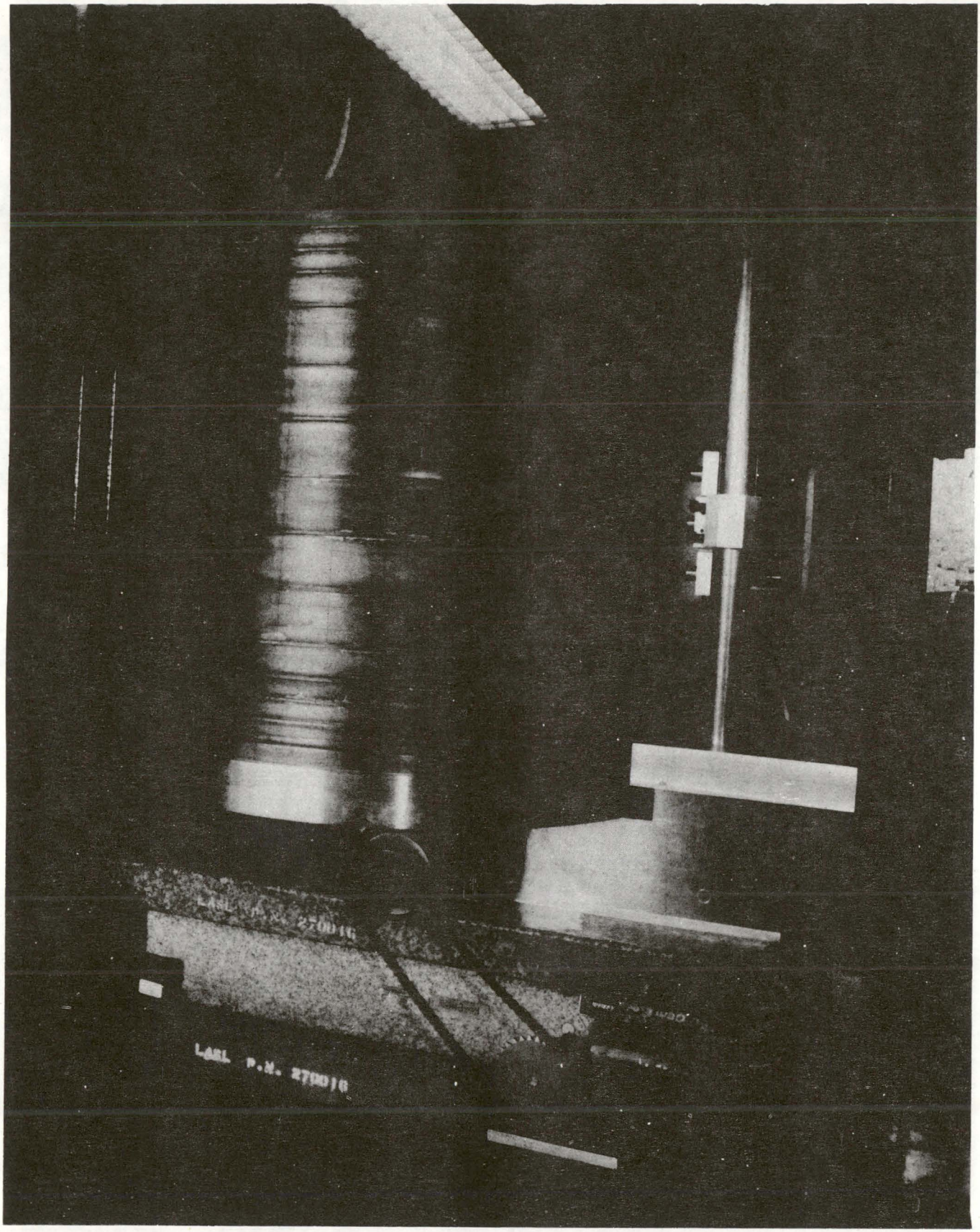

Fig. 3. Baseline benchmark test cylinder undergoing imperfection measurements.

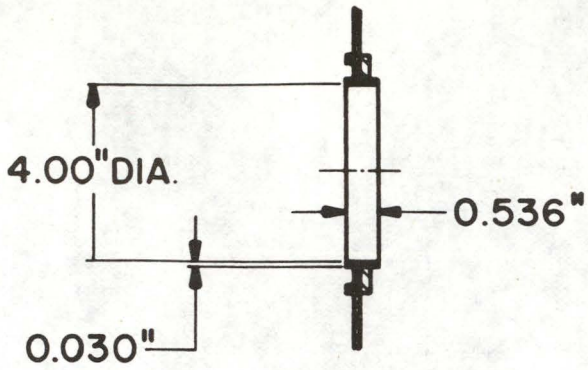

SECTION A-A
ENLARGED

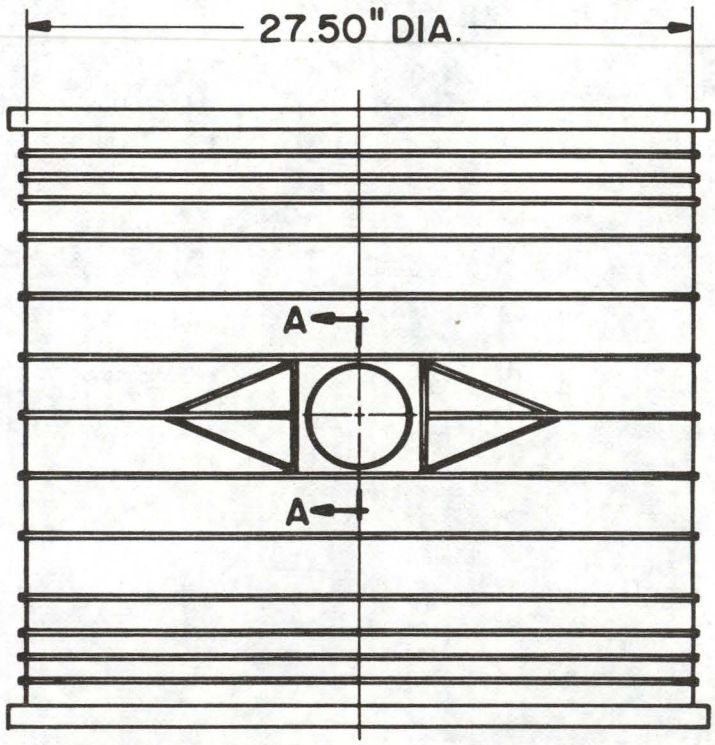

Fig. 4. Framing and construction plans for a test cylinder that has two interrupted rings.

Load Combinations for Design of Category I Structures

M. Shinozuka, H. Hwang, M. Reich and P. C. Wang

Structural Analysis Group
Brookhaven National Laboratory
Upton, New York 11973

The program entitled "Load Combinations for Design of Category I Structures" is supported by the U. S. Nuclear Regulatory Commission (NRC), Mechanical Structural Engineering Branch, Division of Reactor Safety Research (RSR). The program was initiated in mid 1980.

The objective of this program is to develop a rational approach, based on the probabilistic consideration, for the safety evaluation of reactor containment and other seismic category I structures subjected to multiple static and dynamic loadings.

The rational approach thus developed is expected to (1) establish probability based load factors, load combinations and quantitative measures of structural safety, (2) ensure consistent safety levels against various limit state modes and (3) establish a tool for rationally updating design standards.

In FY 1981, four major tasks have been carried out for this program. To be specific, these tasks were carried out to establish data bases for loads and structural resistance and to develop reliability analysis methods applicable to seismic category I structures. Some of the major accomplishments in this fiscal year are presented here.

PROGRAM: LOAD COMBINATIONS FOR DESIGN OF CATEGORY I STRUCTURES

OBJECTIVE: DEVELOP A RATIONAL APPROACH, BASED ON THE PROBABILISTIC CONSIDERATION, FOR THE SAFETY EVALUATION OF REACTOR CONTAINMENT AND OTHER SEISMIC CATEGORY I STRUCTURES SUBJECTED TO MULTIPLE STATIC AND DYNAMIC LOADINGS.

BENEFITS FROM THIS PROGRAM:

THE RATIONAL APPROACH THUS DEVELOPED IS EXPECTED TO:

(1) ESTABLISH PROBABILITY BASED LOAD FACTORS, LOAD COMBINATIONS AND QUANTITATIVE MEASURES OF STRUCTURAL SAFETY;

(2) INSURE CONSISTENT SAFETY LEVELS AGAINST VARIOUS LIMIT STATE MODES;

(3) ESTABLISH A TOOL FOR RATIONALLY UPDATING DESIGN STANDARDS.

GENERAL PROCEDURES

(1) ESTABLISH DATA BASES AND DEVELOP STATISTICAL MODELS FOR LOADS AND STRUCTURAL RESISTANCE.

(2) DEVELOP APPROPRIATE STRUCTURAL SYSTEM MODELS AND IDENTIFY LIMIT STATE MODES.

(3) ESTABLISH RELIABILITY ANALYSIS PROCEDURE.

(4) DEVELOP THE METHODOLOGY FOR LOAD COMBINATIONS.

(5) RECOMMEND DESIGN PROCEDURES BASED ON THE METHODOLOGY DEVELOPED ABOVE (E.G., SPECIFY LOAD FACTORS AND LOAD COMBINATIONS FOR PERTINENT SEISMIC CATEGORY I STRUCTURES).

SKS CARRIED OUT IN FY 1980

(1) REVIEWED THE STATE-OF-THE-ART PERTAINING TO THE RELIABILITY-BASED ANALYSIS AND DESIGN PROCEDURES FOR CIVIL ENGINEERING STRUCTURES. IN PARTICULAR, THEIR APPLICATIONS TO CATEGORY I NUCLEAR STRUCTURES WERE CAREFULLY EXAMINED.

(2) INITIATED DEVELOPMENT OF DATA BASE FOR LOADS AND STRUCTURAL RESISTANCE.

(3) INITIATED DEVELOPMENT OF STATISTICAL DATA BASE FOR SEVERE AND EXTREME ENVIRONMNETAL LOADS (WIND, SNOW, ETC.)

CCOMPLISHMENTS IN FY 1980

TECHNICAL REPORT ENTITLED "PROBABILITY BASED LOAD RITERIA FOR DESIGN OF NUCLEAR STRUCTURES: A CRITICAL EVIEW OF THE STATE-OF-THE-ART", (NUREG-CR-1979, NL-NUREG-/CR-51356).

TASKS UNDERTAKEN IN FY 1981

TASK 1 - ESTABLISHMENT OF DATA BASE FOR LOADS AND STRUCTURAL ANALYSIS OF CATEGORY I STRUCTURES

TASK 2 - ESTABLISHMENT OF STATISTICAL DATA BASE FOR ENVIRONMENTAL LOADING CONDITIONS

TASK 3 - DEVELOPMENT OF RELIABILITY ANALYSIS METHODS SPECIFICALLY APPLICABLE TO SEISMIC CATEGORY I STRUCTURES.

TASK 4 - INVESTIGATION OF RELIABILITY LEVEL IMPLIED IN EXISTING NON-PROBABILISTIC METHODS

BROOKHAVEN NATIONAL LABORATORY
ASSOCIATED UNIVERSITIES, INC.

TASK 1 - ESTABLISHMENT OF DATA BASE FOR LOADS AND STRUCTURAL ANALYSIS OF CATEGORY I STRUCTURES

1.1 ESTABLISHMENT OF DATA BASE FOR OPERATIONAL AND ACCIDENTAL LOADS

(A) REVIEW AVAILABLE DOCUMENTS SUCH AS FSAR, PSAR, ETC.

(B) PREPARE AND OBTAIN CONSENSUS ESTIMATIONS FROM EXPERTS

(C) PROCESS THE DATA OBTAINED IN (A) AND (B) ABOVE IN A FORM THAT IS USEFUL FOR THE RELIABILITY ANALYSIS

1.2 STRUCTURAL MODELING, LIMIT STATE IDENTIFICATION AND DEVELOPMENT OF DATA BASE FOR STRUCTURAL RESISTANCE

(A) PERFORM STRUCTURAL ANALYSIS ON SIMPLIFIED MODELS AND EVENTUALLY ON MORE REALISTIC MODELS

(B) IDENTIFY LIMIT STATE MODES

(C) DEVELOP STRUCTURAL RESISTANCE DATA BASE FOR RELIABILITY ANALYSIS UTILIZING THE RESULTS OBTAINED FROM (A) AND (B) ABOVE

TASK 2 - ESTABLISHMENT OF STATISTICAL DATA BASE FOR ENVIRONMENTAL LOADING CONDITIONS

THE LOADS TO BE INVESTIGATED INCLUDE WIND, EARTHQUAKE, TORNADO, SNOW, ETC. THE DATA ARE TO BE PRESENTED IN TERMS OF MEAN AND STANDARD DEVIATION, DISTRIBUTION FUNCTION, TIME HISTORY OR SPECTRAL DENSITY AS APPROPRIATE TO THE RELIABILITY ANALYSIS.

TASK 3 - DEVELOPMENT OF RELIABILITY ANALYSIS METHODS SPECIFICALLY APPLICABLE TO SEISMIC CATEGORY I STRUCTURES.

3.1 DEVELOP RELIABILITY ANALYSIS METHODOLOGY PERTINENT TO CATEGORY I STRUCTURES

3.2 DEVELOP TECHNIQUES FOR DETERMINING THE RELIABILITY LEVEL TO BE ASSIGNED TO EACH LOAD COMBINATION

3.3 INVESTIGATE SOME PARTICULAR TECHNIQUES FOR SUPPORT OF TASKS MENTIONED ABOVE: E.G., DEVELOP PRACTICAL TECHNIQUES FOR DEALING WITH DEPENDENT NON-GAUSSIAN VARIABLES.

TASK 4 - INVESTIGATION OF RELIABILITY LEVEL IMPLIED IN EXISTING NON-PROBABILISTIC METHODS

INITIATE STUDY TO COMPARE CURRENTLY USED AND/OR RECOMMENDED NON-PROBABILISTIC PROCEDURES WITH PROBABILISTIC METHODS DEVELOPED ABOVE.

(A) USING THE SPECIFIED SRP LOAD FACTORS 3.8.1 - 3.8.4 FOR THE DESIGN OF THE SIMPLIFIED STRUCTURE MENTIONED IN 1.2(A), COMPUTE ITS RELIABILITY AS IMPLIED BY THE LOAD FACTORS.

(B) ON THE BASIS OF THIS ANALYSIS, EVALUATE THE CONSISTENCY OF THE CURRENTLY USED NON-PROBABILISTIC PROCEDURE FROM A RELIABILITY VIEWPOINT.

MAJOR ACCOMPLISHMENTS

- USE OF LAGRANGE MULTIPLIER METHODS FOR EVALUATING RELIABILITY INDEX
- INTERPRETATION OF DESIGN POINT AS POINT OF MAXIMUM LIKELIHOOD
- DEVELOPMENT OF PRACTICAL TECHNIQUES FOR DEALING WITH NON-GAUSSIAN VARIABLES
- DERIVATION OF PROBABILITIES OF SIMULTANEOUS LOAD OCCURRENCES UNDER POISSON ARRIVAL, AND ERLANG DISTRIBUTION FOR DURATIONS
- DEVELOPMENT OF A COMPUTER CODE THAT EFFICIENTLY EVALUATES OUT-CROSSING RATES
- USE OF MORE REALISTIC FAILURE CRITERIA IN RELIABILITY ANALYSIS
- INCORPORATION OF FINITE ELEMENT METHODS INTO RELIABILITY ANALYSIS
- APPLICATION OF RELIABILITY ANALYSIS TO SIMPLIFIED CONTAINMENT AND SHEAR WALL STRUCTURES

ERRORS RESULTING FROM DYNAMIC REDUCTION *

By Charles A.Miller [1], M.ASCE

ABSTRACT

The errors associated with the reduction of structural static degrees of freedom before performing a dynamic analysis are considered. Guyan Reduction and a Modified Guyan Reduction are investigated. Numerical results are obtained for four sample problems : a ten story frame; a braced ten story frame; a piping system; and a reactor containment.

INTRODUCTION

The development of discrete models for structural frameworks requires that compromises be made when deciding on the total number of degrees of freedom to be retained. A precise description of the structure may require many more degrees of freedom than are acceptable from a computational viewpoint. Limitations of the degrees of freedom arise from both restrictions in the available software and economic considerations of the cost of generating a solution.

Such limitations are usually more serious for dynamic problems than for static problems. Most of the large structural software packages provide the user with the option of describing the structure with more degrees of freedom than are retained for dynamic response computations. Degrees of freedom to be retained in the dynamic analysis are specified by the user and a transformation to reduce the order of the system is employed.

This dynamic reduction is often (Refs. 1,2,3) performed based upon a transformation which neglects inertial effects for the degrees of freedom to be eliminated. The transformaationis then used to generate mass and stiffness matricies which approximate the kinetic and potential energies of the complete system. There are few data to asses the extent to which this dynamic reduction introduces errors.

The errors introduced in three small problems were studied and results reported in Ref.4. It was shown that Guyan Reduction may result in significant errors for member loads (20-40 %) while frequencies appeared to be quite good. A relatively simple modification was shown to give much better results.

1.Prof, Dept. of Civil Engineering, City College of New York

* Work carried out under contract for Brookhaven National Laboratory.

The purpose of the work reported here is to extend the studies in Ref.4 to include larger structural systems. To achieve this objective both Guyan Reduction and the Modified Guyan Reduction are added to the SAP V (Ref.5) computer program.Four sample problems are then considered and the errors resulting from each of the two reduction schemes studied.

ANALYSIS

The forced response of an elastic system to a seismic disturbance is treated by modal methods. The disturbance is represented with its response spectrum. Most of the analysis is standard and is not discussed here. The reduction of the complete system to the reduced system and the susequent expansion of the reduced to full mode shapes are discussed.

Reduction Methods- The problem of solving for the eigenvectors of a linear structural system described in terms of its mass and stiffness matricies is considered. In particular it is of interest to consider those problems where some reduction in the total number of degrees of freedom is attempted.

Consider the eigenvalue problem for a discrete system where it is desired to eliminate secondary degrees of freedom (X_s) and retain only primary degrees of freedom (X_p). The partitioned equations of motion describing free vibration of the system may be written as:

$$\begin{bmatrix} M_{pp} & M_{ps} \\ M_{sp} & M_{ss} \end{bmatrix} \begin{Bmatrix} \ddot{X}_p \\ \ddot{X}_s \end{Bmatrix} + \begin{bmatrix} K_{pp} & K_{ps} \\ K_{sp} & K_{ss} \end{bmatrix} \begin{Bmatrix} X_p \\ X_s \end{Bmatrix} = 0 \qquad (1)$$

where (M) is the mass matrix and (K) is the stiffness matrix. For each mode of the eigenvalue problem :

$$X = \begin{Bmatrix} \ddot{X}_p \\ \ddot{X}_s \end{Bmatrix} = -\lambda^2 \begin{Bmatrix} X_p \\ X_s \end{Bmatrix} \qquad (2)$$

where (λ) is the eigenvalue. Substituting (2) into (1) :

$$-\lambda^2 \begin{bmatrix} M_{pp} & M_{ps} \\ M_{sp} & M_{ss} \end{bmatrix} \begin{Bmatrix} X_p \\ X_s \end{Bmatrix} + \begin{bmatrix} K_{pp} & K_{ps} \\ K_{sp} & K_{ss} \end{bmatrix} \begin{Bmatrix} X_p \\ X_s \end{Bmatrix} = 0 \qquad (3)$$

Elimination of the secondary degrees of freedom may be accomplished from the second of the above equations to give:

$$X_s = -T\ X_p \qquad (4)$$

where, $T = (\lambda^2 M_{ss} - K_{ss})^{-1} (\lambda^2 M_{sp} - K_{sp})$

Substituting Eq (4) into the first of Eq (3) yields the eigenvalue problem in the reduced degrees of freedom (X_p) :

$$(M_{pp} - M_{ps}\, T\,)\, X_p = (K_{pp} - K_{ps}\, T\,)\, X_p \qquad (5)$$

Unfortunately the transformation matrix (T) involves the eigenvalue which is not known. If $(\lambda^2 M_{ss} - K_{ss})$ inverse is expanded about $(K_{ss})^{-1}$ and terms associated with (λ^4) are neglected as compared with terms associated with (λ^2):

$$T = K_{ss}^{-1} K_{sp} + \lambda^2 (-K_{ss}^{-1} M_{sp} + K_{ss}^{-1} M_{ss} K_{ss}^{-1} K_{sp}) \qquad (6)$$

This definition of (T) has an advantage over (4) in that an inverse need not be recalculated at each step in the iteration on (λ). The requirement for an iterative solution is eliminated if Eq (6) is substituted into the first of Eq (3) and again the (λ^4) terms neglected as compared to the (λ^2) terms to give :

$$\lambda^2 (M_{pp} - M_{ps} K_{ss}^{-1} K_{sp} - K_{ps} K_{ss}^{-1} M_{sp} + K_{ps} K_{ss}^{-1} M_{ss} K_{ss}^{-1} K_{sp})\, X_p = (K_{pp} - K_{ps} K_{ss}^{-1} Ksp)\, X_p \qquad (7)$$

Eigenvalues may be determined directly from Eq (7) without an iterative solution. This is the eigenvalue problem solved using both Guyan and Modified Guyan Reduction. Since the mass matrix in SAP V is diagonal the reduced mass matrix is:

$$M^* = M_{pp} + K_{ps} K_{ss}^{-1} M_{ss} K_{ss}^{-1} K_{sp} \qquad (8)$$

The reduced stiffness matrix is :

$$K^* = K_{pp} - K_{ps} K_{ss}^{-1} K_{sp} \qquad (9)$$

Expansion of Reduced Eigenvectors- The eigenvectors found above are of a length equal to the number of reduced degrees of freedom. If member loads are to be calculated these eigenvectors must be expanded to include all degrees of freedom. Guyan Reduction calculates the secondary degree of freedom from:

$$X_s = - K_{ss}^{-1} K_{sp} X_p \qquad (10)$$

The Modified Guyan Reduction calculates the secondary degrees of freedom from Eq (6) or :

$$X_s = \left[- K_{ss}^{-1} K_{sp} + \lambda^2 (K_{ss}^{-1} M_{ss} K_{ss}^{-1} K_{sp}) \right] X_p \qquad (11)$$

It should be noted that Eq (11) represents the displacement field assumed in Guyan Reduction for the eigenproblem solution. In the sense (Rayleigh-Ritz) that this field can represent the modes of interest one would expect reasonable

results. Guyan Reduction uses a different displacement field (Eq 10) to expand the reduced mode shapes. This inconsistency probably gives rise to the errors discussed in Ref.4 and below.

NUMERICAL RESULTS

Guyan and Modified Guyan Reduction methods are incorporated into the SAP V computer program and four sample problems are consideered. An exact solution (no reduction) is obtained and compared with results found when different primary degrees of freedom are retained.

Ten Story Building- The first problem considered is the ten story frame shown in Fig.1. The node numbers are shown by each of the nodes with element numbers underlined. All of the columns have a cross sectional area of 60 square inches and a moment of inertia of 1500 inches fourth. The beams have a cross sectional area of 40 square inches and a moment of inertia of 1000 inches fourth. The material of all members has a modulus of elasticity of 30,000 ksi and a density of 490 pounds per cubic foot.

The columns are fixed at the base and the response spectrum shown solid in Fig.2 is input in the horizontal direction. The frame is solved with no reduction and then with both Guyan and Modified Guyan Reduction. Four each reduction method four solutions are obtained retaining 3,4,6,and 10 degrees of freedom. In all cases the degreed of freedom retained are in the horizontal direction at nodes shown in Table 1.

Table 1
Master Degrees of Freedom Ten Story Frame

Case	Number of Degrees of Freedom	Degrees of Freedom-Horizontal Displacement at Nodes
1	3	11, 26, 41
2	4	12, 23, 34, 41
3	6	10, 17, 28, 35, 38, 41
4	10	6, 9, 16, 19, 22, 25, 32, 35, 38, 41

Three modes are included in the solution and the maximum errors in frequencies are 1% ,8% ,and 10% respectively showing little sensitivity to the number of degrees of freedom retained.

S o that the errors in the member bending moments may be evaluated , the percentage errors in four of the columns and four of the beams are shown in Table 2. The Modified Guyan Reduction gives excellent results (less than 2% errors) for all reductions. Guyan Reduction gives equally good results

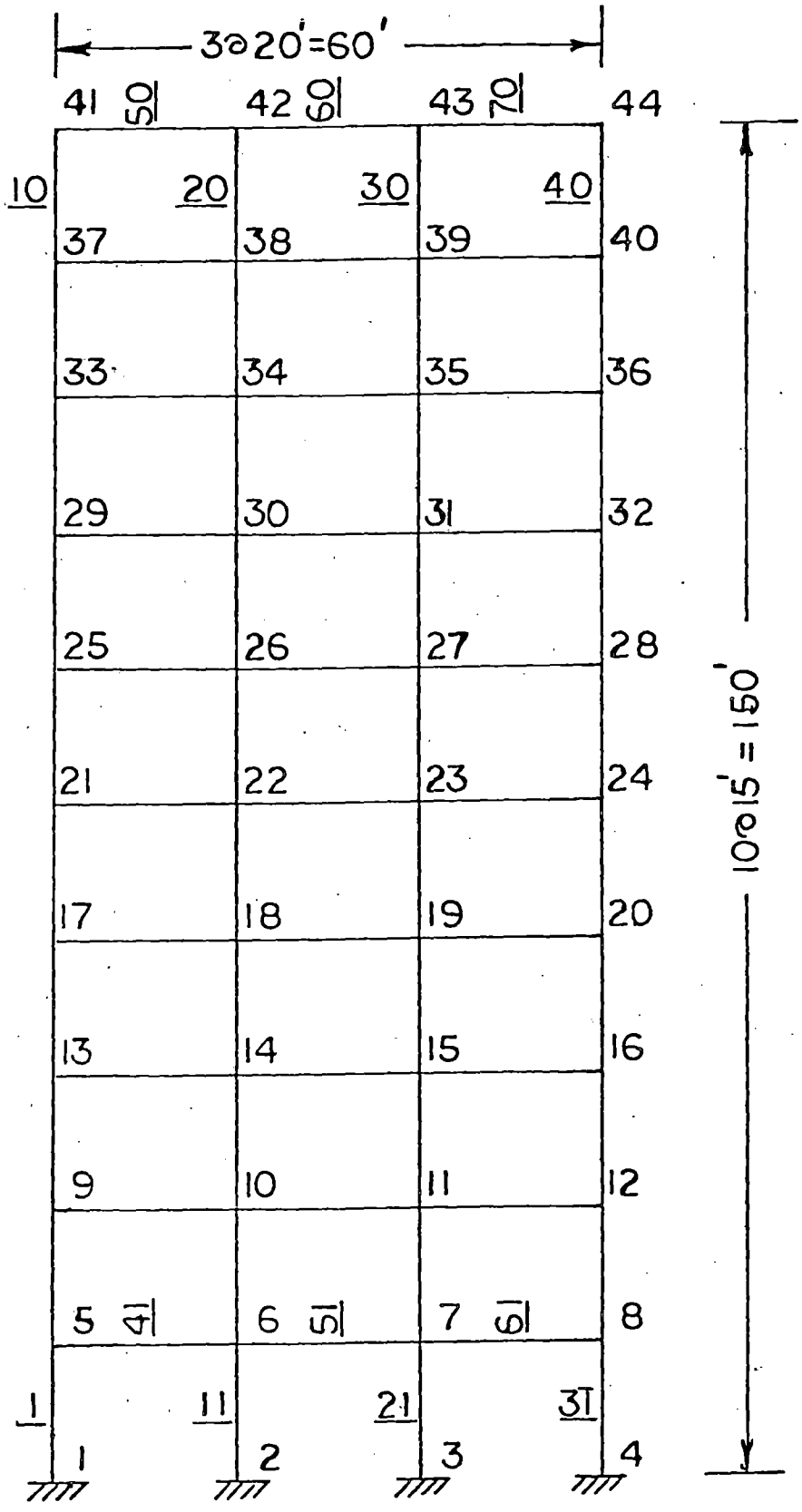

Fig. 1 TEN STORY BUILDING

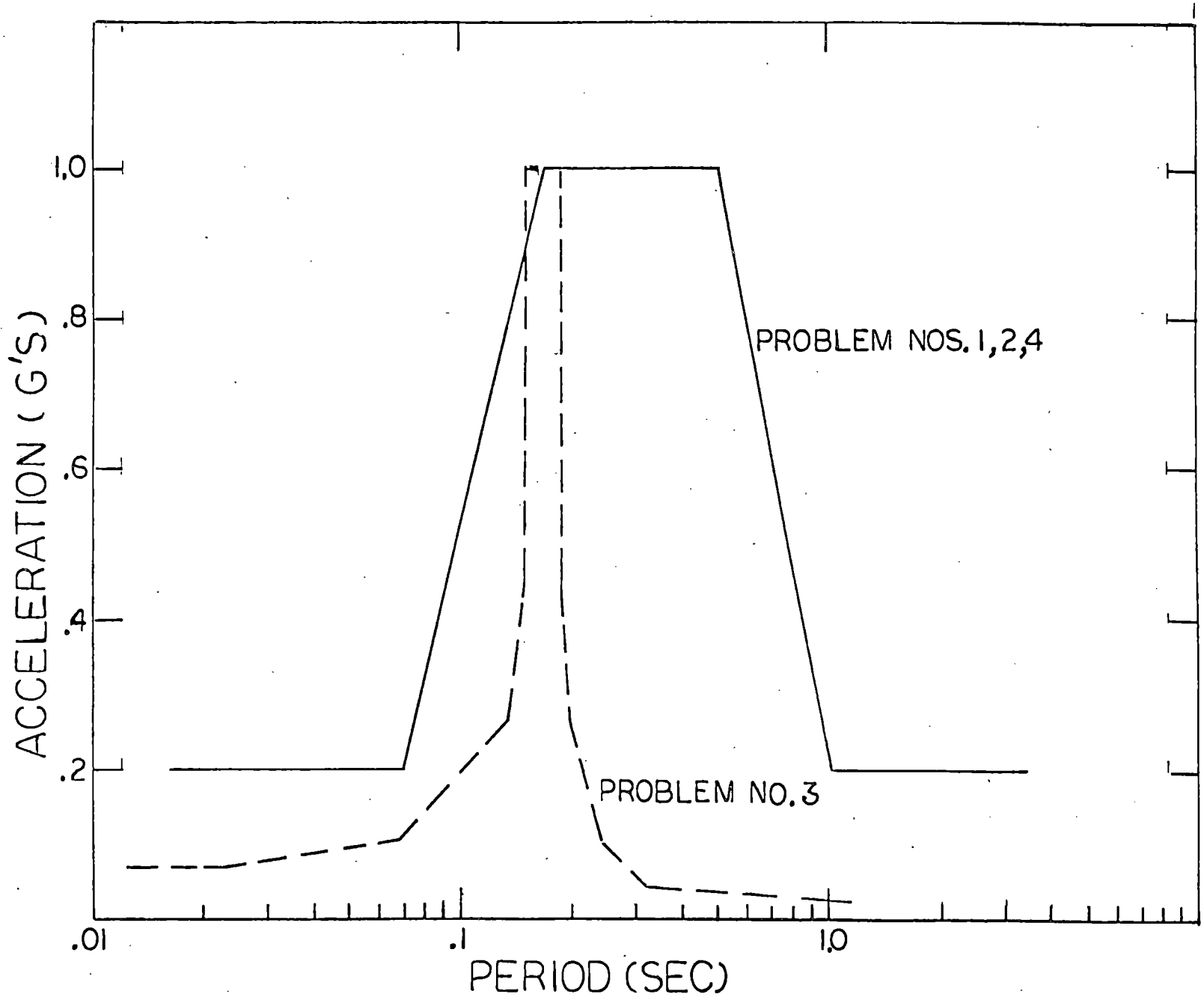

Fig. 2 RESPONSE SPECTRA

for the lower story members but very poor results for the upper story members unless 6 or more degrees of freedom are retained. This variation in accuracy would make it very difficult to review data for a Guyan Reduction run to determine the reliability of the results. It also appears that the Modified Guyan Reduction gives errors of one sign while Guyan Reduction gives errors of both signs.

Table 2
Percent Errors in Member Moments

Case	Guyan Reduction Member No.				Mod. Guyan Reduction Member No.			
	11	41	20	60	11	41	20	60
1	1.0	0.9	100.0	76.4	-1.6	-1.6	-1.3	-1.3
2	0.1	0.2	23.0	16.7	-0.5	-0.5	-0.4	-0.3
3	-0.3	0.1	-0.3	-0.2	-0.1	-0.1	-0.3	-0.1
4	0.0	0.0	-0.8	-0.5	0.0	0.0	-0.2	0.0

Braced Ten Story Frame- The frame shown in Fig. 1 is modified by adding "X" bracing to the middle bay throughout the entire ten stories. The bracing members have a cross sectional area of 6 square inches. The four cases defined in Table 1 are again used to obtain solutions with both Guyan and Modified Guyan Reduction methods. The percentage errors in the beams and column bending moments and in the bracing loads are shown in Table 3.

Table 3
Percent Errors In Member Forces

	Case	Moments in Member 11	41	20	60	Brace Forces Lower	Upper
GUYAN	1	-0.4	0.2	33.4	-18.1	0.0	295.0
	2	-1.1	-0.3	12.9	- 7.1	-0.8	72.3
	3	-0.2	-0.2	-0.2	- 0.2	-0.4	- 2.8
	4	0.0	0.0	-0.8	0.0	0.0	4.3
M. GUYAN	1	-1.4	-1.5	-1.3	-1.6	-1.7	- 2.1
	2	-0.6	-0.6	-0.4	-0.5	-0.8	- 2.1
	3	0.0	0.0	-0.8	0.6	-0.8	11.3
	4	0.0	0.0	-0.1	-0.4	-0.4	- 1.4

Once again the errors are small for members located near the base of the structure while large errors are found in all members near the top of the structure when Guyan Reduction is used.

Piping System- The piping system shown in Fig. 3 is considered. Elements 1 through 19 are 14 inch diameter pipes with a wall thickness of 0.438 inches. Elements 20 through 32 are 12 inch diameter pipes with a wall thickness of 1.312 inches. Weights of 3864 pounds are placed at nodes 19, 22, and 27 to simulate valve weights. The pipe supports are modeled with boundary elements having stiffnesses of 10^7, 10^7; 10^7; 450; 800; and 600 pounds per inch for elements between nodes : 7-37; 18-38; 18-39; 13-34; 25-35; and 31-36 respectively.

The piping system is subjected to the dashed response spectrum shown on Fig. 2. The spectrum is input in the two horizontal directions (X,Z) and 0.67 of the spectrum is input in the vertical (Y) direction. An exact solution is obtained and solutions are found using 7 sets of reduced degrees of freedom as shown on Table 4.

Table 4
Reduction Schemes for Piping System

Case	Number of Degrees of Freedom	Degrees of Freedom Retained
A	3	9-X; 9-Y; 9-Z
B	3	9-X; 15-Y; 22-Z
C	5	9-X; 15-Y; 18-X; 22-X; 27-Z
D	10	5-Y; 9-X; 9-Z; 13-Z; 15-Y; 18-X; 22-X; 22-Y; 27-Z; 31-Z
E	15	5-X; 5-Y; 7-Z; 9-X; 9-Z; 13-Z; 15-X; 15-Y; 18-X; 22-X; 22-Y; 27-X; 27-Z; 31-X; 31-Z
F	21	5-X; 5-Y; 7-X; 7-Z; 9-X; 9-Y; 9-Z; 13-X; 13-Z; 15-X; 15-Y; 15-Z; 18-X; 22-X; 22-Y; 22-Z; 27-X; 27-Y; 27-Z; 31-X; 31-Z
G	26	5-X; 5-Y; 5-Z; 7-X; 7-Z; 9-X; 9-Y; 9-Z; 11-X; 11-Y; 11-Z; 13-X; 13-Z; 15-X; 15-Y; 15-Z; 18-X; 22-X; 22-Y; 22-Z; 27-X; 27-Y; 27-Z; 31-X; 31-Z; 32-Y

Five modes are included in the solution with the resulting frequencies shown in Table 5. The same frequencies are found with both reduction methods. The frequency results may be seen to be quite different than for the frame structures. Ten percent errors are found in the first mode frequency

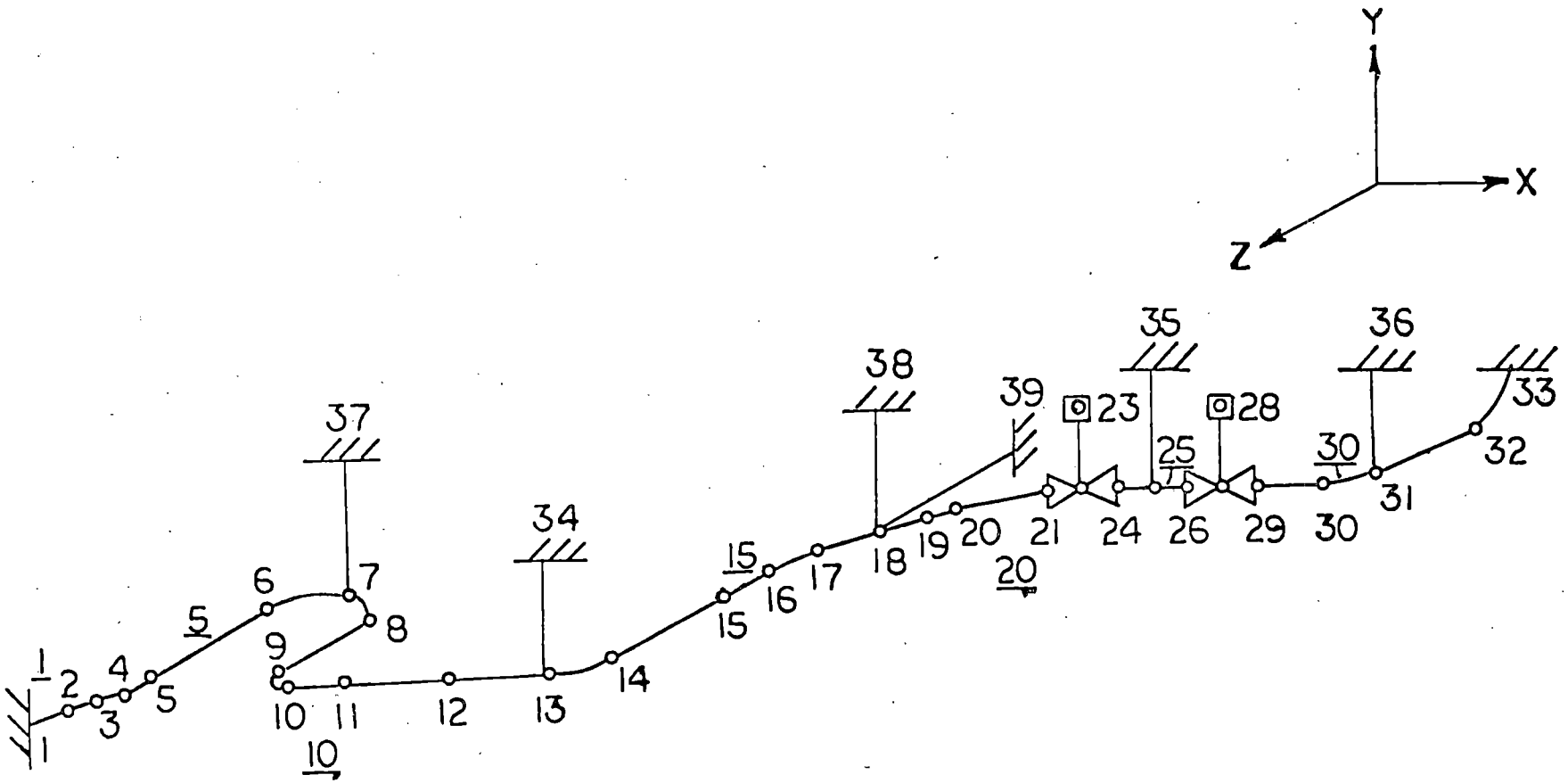

Fig. 3 PIPING SYSTEM

until 21 dynamic degrees of freedom are retained.

Table 5

Piping System Frequencies

Reduction Type (Table 4)	Frequencies (cps) Mode 1	Mode 2	Mode 3	Mode 4	Mode 5
Exact	5.71	6.14	12.85	13.32	14.90
A	6.21	7.11	14.70		
B	6.30	6.32	16.40		
C	6.28	6.32	14.30	20.2	42.1
D	6.18	6.22	13.90	14.20	15.70
E	6.15	6.20	13.70	14.00	15.60
F	5.86	6.14	13.00	13.30	15.00
G	5.75	6.14	12.90	13.30	14.90

Errors in the pipe axial force (P) and bending moments (M) are shown on Table 6. The following conclusions may be drawn from the data on Table 6:

(i) When reduction schemes are used the bending moment data appears to be more reliable than the thrust or pipe support data.

(ii) The Modified Guyan Reduction gives significantly better results than the Guyan Reduction. For example scheme G gives good results (errors less than 8.1%) when Modified Guyan Reduction is used but there are still 39% errors in pipe thrust when Guyan Reduction is used.

(iii) The good results are obtained for scheme G because degrees of freedom normal to the restraints provided by the pipe supports are retained. All degrees of freedom at the ends of the pipe supports should probably be retained to achieve good results with Guyan Reduction.

Reactor Containment Building- The reactor containment building shown in Fug. 4 is subjected to the solid response spectrum shown in Fig. 2 in the X direction. Plate elements 1 through 24 are used to model the exterior containment. The reactor floor is modeled with plate elements 25 through 32. A wall supporting the floor is modeled with plate elements 33 through 40. All plate elements are taken as concrete with a thickness of 36 inches. Beam elements 41 through 43 are used to model the reactor. Symmetric boundary conditions are specified for all nodes at Y = 0.

An exact solution is obtained and solutions using both Guyan and Modified Guyan Reductions are developed for the reduction schemes shown on Table 7.

Table 6
Percentage Errors in Piping Elements

Case		Pipe Element Nos. 1 P	1 M	5 P	5 M	12 P	12 M	18 P	18 M	Pipe Supports 7-37	18-38	13-34
	A	-18.0	12.7	55.2	2.9	545.2	20.3	31.8	3.8	14.4	-94.1	-79.7
G	B	- 3.4	-25.5	-48.8	-18.2	505.4	22.0	5.8	-3.7	-17.1	70.0	22.2
U	C	- 4.1	-26.0	-49.2	-18.8	479.5	20.0	148.6	16.2	- 3.7	99.3	43.3
Y	D	-31.4	- 7.6	32.5	-16.9	217.5	1.8	51.2	65.3	214.8	242.1	91.3
A	E	26.2	- 7.7	- 1.1	-27.3	183.7	5.5	40.8	64.0	211.1	254.5	90.4
N	F	13.9	- 0.1	- 5.5	- 0.4	170.5	6.1	23.5	1.7	91.3	42.6	-5.1
	G	3.5	1.6	-15.6	1.1	-39.2	2.7	22.8	1.9	-15.8	7.9	3.6
M.	A	- 0.4	0.2	0.4	0.0	6.0	0.4	-18.0	0.4	-43.9	-92.6	-78.8
	B	- 4.6	- 7.9	-12.0	-6.7	13.3	0.5	- 8.0	-2.0	- 5.6	-71.6	34.3
G	C	- 6.6	- 9.7	-13.7	-8.5	10.2	- 1.3	- 1.1	-3.2	7.7	-61.4	54.4
U	D	-16.8	-18.0	-17.7	-16.9	-13.9	- 4.5	-17.8	6.0	73.3	2.9	103.1
Y	E	-16.8	-17.5	-17.4	-17.4	-13.9	- 5.2	-17.2	5.6	73.1	14.7	101.7
A	F	1.0	1.2	1.5	1.2	6.0	1.3	2.7	1.4	2.3	- 8.1	0.4
N	G	1.2	1.5	1.8	1.5	4.8	1.6	2.9	1.8	3.1	- 7.8	6.5

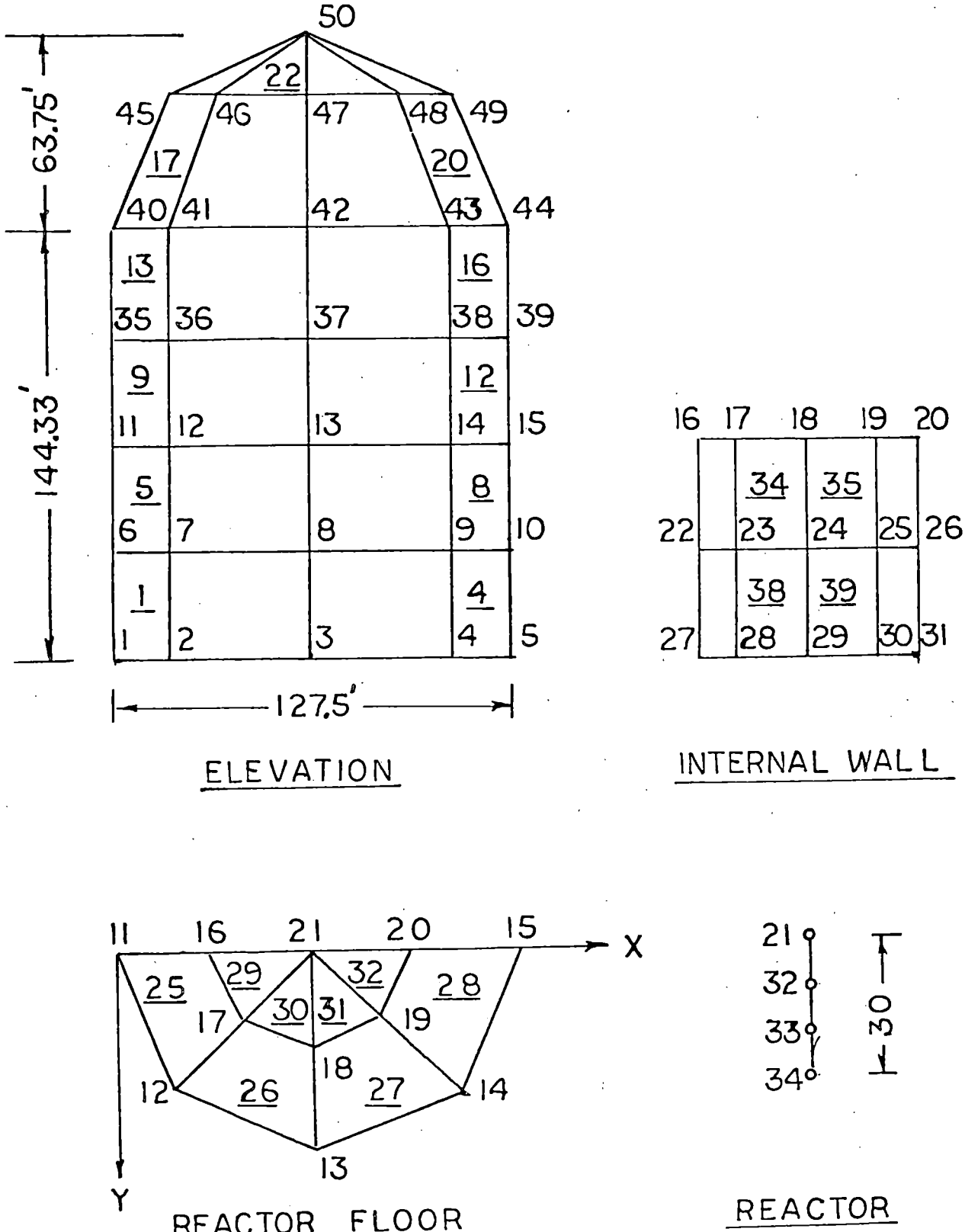

Fig. 4 REACTOR CONTAINMENT BUILDING

Table 7
Reduction Schemes for Containment Building

Case	Number of Degrees of Freedom	Degrees of Freedom Retained
A	3	21-X; 34-X; 50-X
B	6	13-X: 21-X; 34-X; 40-Z; 44-Z; 50-X
C	13	11-X; 11-Z; 15-X; 15-Z; 21-X; 21-Z; 34-X; 40-X; 40-Z; 42-Y; 44-X; 44-Z; 50-X
D	23	11-X; 11-Z; 13-X; 13-Y; 15-X; 15-Z; 16-X; 16-Z; 18-X; 18-Y; 20-X; 20-Z; 21-X; 21-Z; 33-X; 34-X; 40-X; 40-Z; 42-X; 42-Y; 44-X; 44-Z; 50-X
E	46	11-X; 11-Z; 13-X; 13-Y; 15-X; 15-Z; 16-X; 16-Z; 16-Y; 17-X; 17-Y; 17-Z; 17-YY; 17-ZZ; 18-X; 18-Y; 18-Z; 18-XX; 18-YY; 18-ZZ; 19-X; 19-Y; 19-XX; 19-YY; 19-ZZ; 20-X; 20-Z; 20-YY; 21-X; 21-Z; 21-YY; 33-X; 33-Z; 33-XX; 34-X; 34-Z; 34-YY; 40-X; 40-Z; 42-X; 42-Y; 44-X; 44-Z; 50-X

Stresses in typical plate elements and the peak bending moment in the reactor beam model are shown in Table 8.

Table 8
Stresses and Moments in Containment Building

Case		Peak Stress in Plate Element 1	5	13	25	29	33	Peak Moment in Reactor Beam
Exact		649	481	186	72	83	138	47,740
GUYAN	A	545	419	225	65	175	109	2,527,000
	B	548	426	244	63	180	109	2,738,000
	C	600	465	222	87	149	122	2,148,000
	D	635	475	192	46	104	140	350,900
	E	635	475	192	56	89	141	45,640
M. GUYAN	A	569	420	166	60	24	219	103,300
	B	570	422	167	60	29	117	56,450
	C	601	444	173	68	82	127	45,170
	D	632	466	178	71	93	135	46,410

The plate stresses appear to be quite good for all of the elements. Modified Guyan Reduction seems to be a little better than Guyan Reduction but not to the same degree as for the first three problems. The very significant difference shows up with the peak moment in the beam model of the reactor. Guyan Reduction yields totally unreliable results until 46 degrees of freedom are retained. Modified Guyan Reduction gives good results except for scheme A. The floor provides a very stiff support for the beam and results in the poor predictions. Reliable results are obtained only when all degrees of freedom around this connection between a stiff and soft element are retained. Note that degrees of freedom must be retained even though there is no mass associated with that degree of freedom (e.g.,the rotations).

CONCLUSIONS

Based upon the four sample problems the following conclusions may be drawn:

(i) The errors resulting from Guyan Reduction are significantly larger than those which result from Modified Guyan Reduction. For example the errors in member bending moments in the ten story frame are always less than 2% with Modified Guyan Reduction. The same errors are as large as 100% with Guyan Reduction and only become acceptable when 6 or more degrees of freedom are retained.

(ii)For a given reduction scheme the errors resulting from Modified Guyan Reduction are much more uniform throughout the structure than the errors resulting from Guyan Reduction.

(iii)Frequencies calculated with Guyan Reduction appear to be quite good as long as the degrees of freedom retained can adequately represent the mode shapes of interest.

(iv)The errors found in piping systems when reductions are used are much larger than the errors found for frame structures. The pipe bending moments are the most reliable with the pipe thrusts and support loads most unreliable. Modified Guyan Reduction again gives much more reliable results than does Guyan Reduction.

(v) Much larger errors result with the reduction schemes when there are both stiff and soft elements. This occurs in the piping problem(supports relative to pipe and axial thrust relative to flexure) and in the containment problem (in plane stiffness of floor relative to flexure of beam). In either case Guyan Reduction gives totally unreliable results unless care is taken to isolate the stiff element by containing it within primary degrees of freedom.

Acknowledgement- The work reported in this paper was supported by the Nuclear Regulatory Commission Through Brookhaven National Laboratory.

REFERENCES

1. Guyan,R.J.,"Reduction of Stiffness and Mass Matricies", American Institute of Aeronautics and Astronautics Journal,Vol.3,No.2,Feb.1965.
2. Irons,B.M.,"Structural Eigenvalue Problems:Elimination of Unwanted Variables",American Institute of Aeronautics and Astronautics,Vol.3,No.5,May 1965.
3. Kaufman,S.,and Hall,D.B.,"Reduction of Mass and Loading Matricies",American Institute of Aeronautics and Astronautics,Vol.6,No.3,Mar.1968.
4. Miller,C.A.,"Dynamic Reduction of Structural Models", Proceedings American Society of Civil Engineers, Structural Division,Vol.106,No.ST10,Oct.1980.
5. Bathe,K.J.,Wilson,E.L.,Peterson,F.E.,"A Structural Analysis Program for Static and Dynamic Response of Linear Systems",Earthquake Engineering Research Center, Univ. of California,June 1976.

EVALUATION OF DYNAMIC TESTING OF NUCLEAR POWER PLANT STRUCTURES

B. J. Hsieh, M. G. Srinivasan, and C. A. Kot

Components Technology Division
Argonne National Laboratory
Argonne, Illinois 60439

Presented at the
U.S. NRC
9th Water Reactor Safety Research Information Meeting
Gaithersburg, Maryland
October 26-30, 1981

EVALUATION OF DYNAMIC TESTING OF NUCLEAR POWER PLANT (NPP) STRUCTURES

SUMMARY

Current practice both for design and licensing of NPP structures relies entirely on estimating structural response by means of analytical models. The objective of the current program is to provide a rational basis for decisions concerning the inclusion of dynamic testing of NPP structures as part of the licensing process. This is to be accomplished through an integrated evaluation of dynamic-testing methods and associated analytical procedures.

One such procedure is the so-called system or parameter identification method. When applied to structural systems, which are governed by second-order differential equations, the goal of parameter identification techniques is to obtain from test data the number of degrees of freedom, the mass distribution, and the restoring force (the stiffness and damping distributions). The test data are composed of the locations and histories of the excitation (input) and response (output). Obviously, the number of data measurements are finite due to both the physical and economical constraints; however, since the systems are continuous,data at a sufficient number of locations may not have been measured so as to uniquely identify the physical parameters of the system, i.e., mass, stiffness and damping distributions. One approach used to circumvent this difficulty is to identify only the modal parameters, i.e., modal frequencies, damping ratios, and shapes for the first few modes. In fact, almost all past tests on NPP structures were performed to obtain the modal rather than physical parameters. In most cases the so-called transfer function or frequency-response function method was employed, i.e., the frequency and damping ratios were obtained by (visually sometimes) fitting the transfer function of a single-degree-of-freedom (SDOF) system to the corresponding part of the test data.

This transfer-function approach is aceptable for simple structures in which the modal frequencies are widely spaced. On the other hand, the SDOF transfer-function approach cannot yield accurate results when used for complicated structures in which closely spaced modal frequencies are excited. To obtain accurate parameters for complicated structures, two approaches are possible: one is to improve the experimental data through "mode tuning," and the other is to improve the identification methodology by use of the "multi-degree-of-freedom (MDOF) transfer function." The former is to appropriately excite the structure in such a way that only one mode is excited at a time; therefore, the use of SDOF transfer function for that mode is justified. The latter is to use a more realistic mathematical model rather than a linear, SDOF, damped spring-mass model to represent the structure being tested. In both approaches, the knowledge of the structure is of paramount importance. It is needed to formulate the mathematical model and to derive the appropriate forcing distribution to tune or isolate the modes. Considering the purposes of testing the NPP structure (any testing but proof testing), is to gain knowledge of the structure, one must conclude that the testing and system/parameter identification are interrelated.

Even though the term MDOF transfer function is used, implying that the identification is performed in the frequency domain, the time-series solution of the corresponding mathematical model can also be used to approximate the response histories, thus leading to identification in the time domain. If there were no computational errors in the transformation between the time and

frequency domains, these two approaches should yield identical results.

System/parameter identification is concerned with finding the number of degrees of freedom and the coefficients of the differential equations of the system from the input and output. This leads to such questions as identifiabililty (whether the parameters can be identified), sensitivity (whether and how much the parameters are sensitive to the input/output), and uniqueness of identified parameters. Only limited answers to these questions have been provided by the literature on system/parameter identification.

If the data are error-free, and if the number of degrees of freedom, the specific form of the differential equations, etc. are known, then one might be able to find a set of parameters that matches the model predictions and data exactly. This is the case where the "error function" is identically zero regardless of its specific definition. In such cases, it is then only necessary to find the set of parameters. Generally, an exact match is not expected; therefore an error function or criterion must also be defined. the set of parameters that minimizes this function are considered the parameters of the system. This approach leads to questions such as the definition of error functions, the systematic techniques to minimize these function, the convergence tolerance for accepting a minimum, and the standard for rejecting the error function as an appropriately defined one. The most popular approaches are least-square fitting of the model response either in the frequency or time domain.

All the above deterministic approaches are valid for noise-free data. When the data is mixed with noise, which is a random phenomenon, special techniques are required. Noisy data can be treated as composed of two components, the deterministic signal part and the random (stochastic) noise part. Once one of the components is known, the other one can be computed by a simple subtraction. However, since there is no unique definition of noise and signal, one can treat the signal as the deterministic response of a deterministic system and treat the noise as the part of response that does not correspond to the system response. Therefore, one can assume that the given data is composed entirely of the response of a complicated system of high order or alternatively the same data may be assumed to be all noise. Since it is reasonable to expect that noise should be white Gaussian and zero mean, this noise property can be used to help identify the system parameters.

A variety of methods is available in processing noisy data; e.g., weighted least-square method, in which the statistical distributions of data measurements are known and are used as weighting factors in defining the error function. Also available are methods such as autoregression, moving average, etc. In all these methods only the input/output, but not the parameters, are considered random. If one also considers the parameters as random, then another variety of methods, i.e. filtering techniques (Kalman filtering, etc.), Bayesian techniques, maximum liklihood method, etc. is available for processing data.

In summary, the study of system/parameter identification techniques is still a growing subject. Many techniques are proposed in the literature and tested against artificially generated (noisy) data. These methods appear logical. But the results are not very consistent particularly when the signal-to-noise ratio is not very high. Hence, it is certainly worthwhile to improve the signal-to-noise ratio in the experiments. Most of the parameter identification efforts on NPP structures were limited to using the SDOF transfer-function method. Therefore, one of the goals of this program is to use a set of real data, such as that of the HDR (Heissdampfreaktor), to test and validate the various methods.

EVALUATION OF DYNAMIC TESTING METHODS FOR SAFETY ASSESSMENT OF NUCLEAR POWER PLANT (NPP) STRUCTURES

PROGRAM STARTING DATE - MARCH 1980

BACKGROUND

- CURRENT DESIGN AND LICENSING OF NPP STRUCTURES IN GENERAL BASED ON LINEAR ANALYSIS PROCEDURES

- DIVERSE OPINIONS EXIST CONCERNING PROPER METHODS FOR SPECIFIC CASES, RANGE OF VALIDITY OF PARTICULAR METHODS, AND RELATIONSHIPS OF ANALYSES TO EXPERIMENTAL OBSERVATIONS

- UNCERTAINTY LEADS TO CONSERVATISM WHENEVER QUESTIONS OF APPLICABILITY ARE RAISED

MOTIVATION FOR EVALUATING DYNAMIC TESTING OF NPP STRUCTURES

- ESTABLISH RATIONAL CONNECTION BETWEEN RESPONSE PREDICTED BY ANALYSIS AND ACTUAL RESPONSE OF AS-BUILT STRUCTURES PARTICULARLY UNDER SEVERE LOADING CONDITIONS
- REDUCE UNNEEDED CONSERVATISM IN DESIGN METHODS USED IN LICENSING PROCESS
- VERIFY AND VALIDATE DESIGN METHODOLOGIES AND PREDICTION PROCEDURES
- PRECEDENT - QUALIFICATION AND OTHER TESTING OF NPP EQUIPMENT AS PART OF LICENSING PROCESS

OBJECTIVE

- Provide a Rational Basis for Possible Inclusion of Dynamic Testing of NPP Structures as Part of the Licencing Process
- Evaluate Dynamic Testing Methods
- Evaluate Analytical Models which use Experimental Results
- Verify and Validate Combined Methodologies As-built undamaged structures

TASK STRUCTURE

TASK 1: FEASIBILITY, EVALUATION AND UTILIZATION OF DYNAMIC TESTS ON AS-BUILT STRUCTURES

TASK 2: EVALUATION AND VERIFICATION OF ANALYTICAL METHODS UTILIZING DYNAMIC TEST DATA

TASK 1

EVALUATION AND UTILIZATION OF DYNAMIC TESTS ON EXISTING STRUCTURES

- PARTICIPATION IN HDR TEST PROGRAM
- EVALUATION OF NPP STRUCTURAL EXPERIMENTAL DATA
- REVIEW AND EVALUATION OF NON POWER PLANT STRUCTURAL TESTING
- INTERIM EVALUATION OF DYNAMIC TESTING FEASIBILITY

TASK 2

EVALUATION AND VERIFICATION OF ANALYTICAL METHODS UTILIZING DYNAMIC TEST DATA

- EVALUATION OF SYSTEMS IDENTIFICATION AND OTHER PERTINENT METHODOLOGIES
- VALIDATION OF SPECIFIC METHODOLOGIES
- RELATIONSHIP OF METHODOLOGIES TO DESIGN PRACTICE

PROGRAM ACTIVITIES IN PROGRESS

- CRITICAL REVIEW OF DYNAMIC TESTS ON NPP AND ASSOCIATED ANALYSIS
- PARTICIPATION IN PAST AND CURRENT HDR TESTS - EVALUATION OF HDR DATA
  - TRANAL ANALYSIS OF 5 KG BLAST TEST
  - INSTALLATION OF DATA ON NESC
- THE ASSESSMENT OF EXPERIMENTS ON STRUCTURES OTHER THAN NUCLEAR POWER PLANTS
- EVALUATION OF SYSTEM IDENTIFICATION METHODS

SYSTEM IDENTIFICATION FLOW-CHART

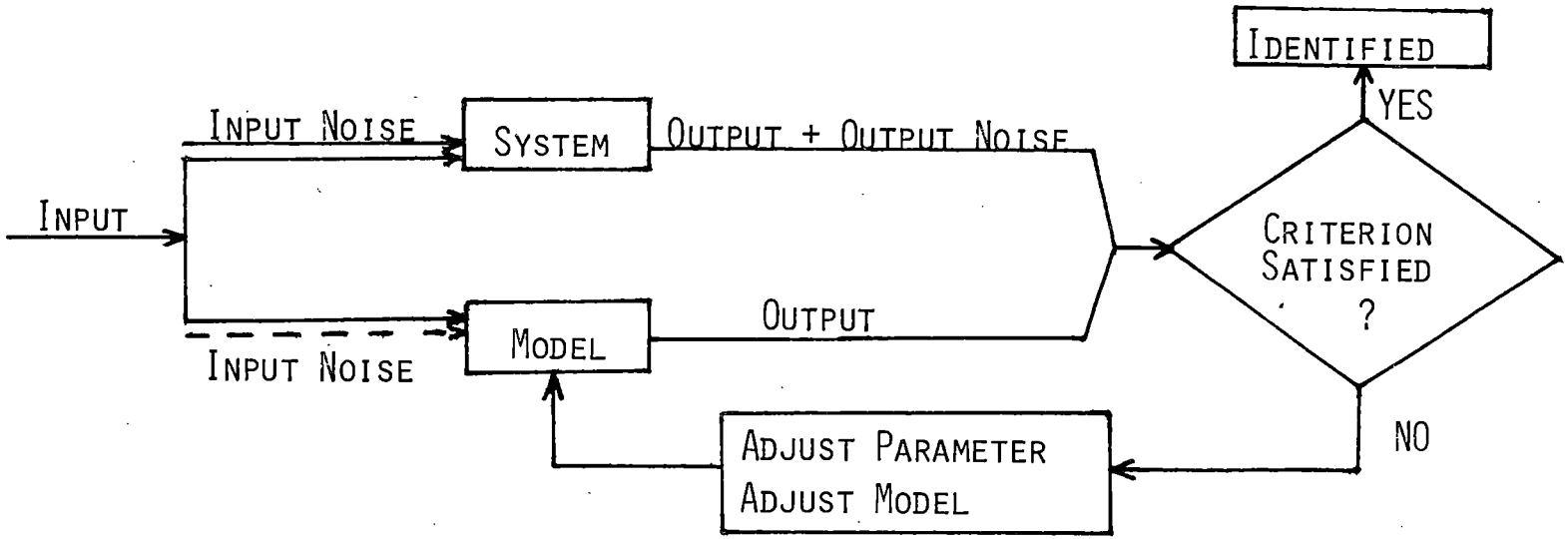

PARAMETER ESTIMATION

METHODS

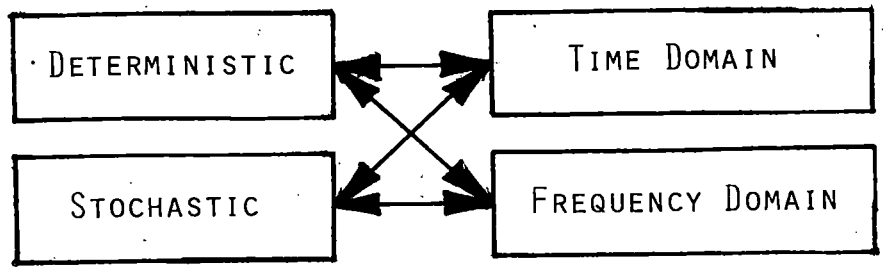

- BEST FIT OF MODEL RESPONSE TO TEST RESPONSE IN TIME OR FREQUENCY DOMAIN BY MINIMIZING A CRITERION EITHER DETERMINISTICALLY OR STOCHASTICALLY

KEY PROBLEMS

- IDENTIFIABILITY

  WHETHER THE SYSTEM/PARAMETERS CAN BE IDENTIFIED?

- SENSITIVITY

  WHETHER AND HOW MUCH THE PARAMETERS ARE SENSITIVE TO THE INPUT/OUTPUT?

- UNIQUENESS

  IS A SYSTEM/PARAMETER SET THE SYSTEM/PARAMETER SET?

ANALYTICAL MODELS

- NON PARAMETRIC; E.G., $M\ddot{x} + F_R(x, \dot{x}, T) = F(T)$
- PARAMETRIC; E.G., $M\ddot{x} + C\dot{x} + Kx = F(T)$

$$\ddot{Y} + 2\xi\omega\dot{Y} + \omega^2 Y = F(T)$$

- PHYSICAL PARAMETERS; E.G. M, C, K, ETC.
- MODAL PARAMETERS ω, ξ, MODE SHAPE, ETC.

PROBLEM ISSUES

- DEFINITION OF BEST FIT; DEFINITION OF OPTIMUM
- ERROR-FUNCTION EXTREMIZATION TECHNIQUE
- NUMBER OF DEGREE OF FREEDOM VS. NOISE
- DETERMINISTIC VS. STOCHASTIC APPROACH
- TIME VS. FREQUENCY DOMAIN

LIST OF SYSTEM/PARAMETER METHODS

- DETERMINISTIC
  - TIME DOMAIN
    - SDOF LEAST-SQUARE FIT - LOG DECREMENT METHOD, ETC.
    - MDOF LEAST-SQUARE FIT - PRONY'S METHOD, ETC.
  - FREQUENCY DOMAIN: (TRANSFER-FUNCTION METHOD)
    - SDOF LEAST-SQUARE FIT: HALF-POWER METHOD, ETC.
    - MDOF LEAST-SQUARE FIT

- STOCHASTIC
  - TIME DOMAIN
    - SDOF AND MDOF WEIGHTED LEAST-SQUARE FIT
    - AUTOREGRESSION, MOVING AVERAGE, ETC.
    - KALMAN FILTERING, BAYESIAN METHOD, ETC.
  - FREQUENCY DOMAIN
    - SDOF AND MDOF WEIGHTED LEAST-SQUARE FIT
    - FILTERING

DETERMINISTIC METHODS

- APPROXIMATE FREQUENCIES AND DAMPING RATIOS OBTAINED DIRECTLY FROM RESONANCE TEST
- MODAL COUPLING MATRIX IS ASSUMED KNOWN
- SIMPLE COMPLETE MODEL THEN CONSTRUCTED
- TRIAL AND ERROR METHOD IS USED TO FIND BEST VALUES
- NEED KNOWLEDGE OF SYSTEM AND SOUND JUDGMENT
- FREQUENCIES MUST BE WIDELY SPACED FOR SDOF OR UNCOUPLED MDOF

STOCHASTIC METHODS

- MAY CONSIDER BOTH MODEL PARAMETER AND TEST DATA RANDOM
- NEED PRIOR KNOWLEDGE ON PROBABILITY DISTRIBUTION
- MORE RATIONAL THAN DETERMINISTIC APPROACH
- SYSTEMATIC PROCEDURES FOR IMPROVING PARAMETERS EXIST
- RESULTS DEPEND ON PROBABILITY DISTRIBUTION

CONCLUSIONS

- ANALYTICAL SYSTEM/PARAMETER IDENTIFICATION ABILITY AND TESTING ABILITY ARE CLOSELY RELATED
- METHODS EXIST TO IDENTIFY PARAMETERS FOR A SYSTEM WITH KNOWN GOVERNING EQUATION FORM FROM NOISY DATA
- MOST TESTS ON NPP AND NON-NPP STRUCTURES ARE PERFORMED USING UNCOUPLED MDOF MODELS TO OBTAIN MODAL PARAMETERS
- TESTING CAN BE USED TO VALIDATE AND MODIFY ANALYTICAL MODELS USED IN DESIGN OF THE NPP STRUCTURES
- MOST ADVANCED IDENTIFICATION METHODS ARE TESTED AGAINST ARTIFICIALLY GENERATED NOISY DATA ONLY

FUTURE PLANS

HDR DATA AND/OR OTHER TEST DATA WILL BE USED TO VALIDATE AND COMPARE THE VARIOUS SYSTEM/PARAMETER IDENTIFICATION METHODS.

Projekt HDR-Sicherheitsprogramm
Dr. Wolf

Kernforschungszentrum Karlsruhe
05.10.1981 - sz

EXPERIMENTAL AND ANALYTICAL RESULTS OF COUPLED FLUID-STRUCTURE INTERACTIONS DURING BLOWDOWN OF THE HDR VESSEL

L. Wolf

Projekt HDR, Kernforschungszentrum Karlsruhe
Battelle-Institut e.V., Frankfurt, Germany

9th Water Reactor Safety Research Information Meeting
Gaithersburg, Maryland, USA
October 1981

This paper summarizes and compares the experimental as well as pre- and post-test analytical results of the first three preliminary blowdown tests, V29.2, V31.0, V31.1, with reactor pressure vessel internals (RPV-I) at the HDR-facility.

These experiments were performed with long ($\sim$ 4.6 m) and short ($\sim$ 1.5 m) discharge pipes with inside diameters of 0.2 m. The blowdowns were initiated with the subcooled fluid in the vessel at rest from system pressures of 90 and 110 bar, subcoolings of the downcomer fluid of 30 °C and 50 °C, respectively, as well as axial core enthalpy distributions representative of typical PWR conditions. The core barrel was specifically designed for these tests to resemble as close as possible the dynamic characteristics (e.g., eigenfrequencies, maximum stresses) of a typical PWR core barrel. In order to simplify the verification of computer codes accounting for fluid-structure interactions, no core internals were introduced but were simulated instead by a lower mass ring. The core barrel has been rigidly clamped at the top to provide clean, yet somewhat unrealistic, structural boundary conditions. The blowdowns were initiated within 2 ms by a double break disk arrangement, thereby inducing a steep depressurization transient. The thermodynamic and structural instrumentation for the three tests verified and qualified measurement principles, sensors, and procedures, as well as provided that important phenomena can be followed within their characteristic time frames. The complete blowdown histories (170 - 210 sec) were sampled together with the short and long term transient behaviors of the compartments and the inner steel shell of the containment.

The most important conclusions from the experimental data are:

- the HDR reactor pressure vessel can be safely operated in a way which results in unique and reproducible thermo-fluiddynamic and structural data

- the maximum core barrel displacements occur during the subcooled blowdown phase for the given initial and boundary conditions
- substantial fluid-structure interactions occur
- substantial pressure-wave damping exists
- core barrel displacements are small even at higher loadings for the chosen conditions

The experimental data were compared against pre- and post-test predictions by various American and German institutions. The computer codes used, cover a broad range of diverse numerical schemes and physical models to simulate the fluiddynamic and structural phenomena.

The comparisons between the data and the predictions yield the following general conclusions:

- only by consideration of coupled fluid-structure interactions can the local data be matched both in amplitude and frequency
- simplifications in fluid modeling, such as compressible single-phase flow assumption may be justified in a gross manner for limited periods of time into the blowdown
- for the problem at hand, a one-dimensional model for the core region deems to be appropriate and sufficient
- the assumption of linear elastic material behavior for the core barrel is appropriate
- the correct modeling of the pressure-wave damping phenomenon in the discharge pipe as well as in the transition region from the pipe into the three-dimensional downcomer is crucial to best-estimate simulation of local coupled fluid-structure interactions
- consistent two-fluid non-equilibrium formulation for two-phase flow and heat transfer together with advanced numerical schemes is able to simulate the relevant phenomena correctly

- other simplifications such as acoustic approximation and homogeneous equilibrium models generate non-realistic high frequency pressure wave amplitudes in the discharge nozzle leading to overall nonconservative smaller pressure differences and core barrel displacements
- codes which patch different methodologies and models of different dimensionalities together have difficulties producing reliable results at the interfaces

The comparisons between data and pre-test calculations resulted in the following:

- consistent multi-dimensional modeling schemes, especially for the downcomer, agree better with the data than equivalent network models which had some difficulties providing consistent results
- coupling a simplified flow model (compressible single-phase) with an advanced treatment of the discharge pipe phenomena results in better agreement than applying the acoustic approximation throughout

In general, the following conclusions can be drawn from the post-test calculations in comparison with the experimental data:

- adjustments for the experimentally determined initial- and boundary conditions in the codes did not result in any substantial improvements in local quantities thereby indicating a much lower sensitivity of the data upon thermodynamic conditions as previously anticipated
- overall, the multi-dimensional codes result in better agreement with the data than the equivalent network codes, although the disagreement as observed in the pre-test calculations has been remarkably reduced, thereby indicating a substantial learning effect by the users of the latter.

- a second post-test calculation over 200 ms by K-FIX (3D, FLX) resulted in good agreement with the data after eliminating some minor errors and readjustment of parameters
- results of MULTIFLEX are of about the some quality in the time span from 100 to 200 ms

Finally, the paper gives a brief overview over the four forthcoming blowdown tests with reactor pressure vessel internals and with a greatly extended instrumentation. Special emphasis will be given to the German Standard Problem No. 5.

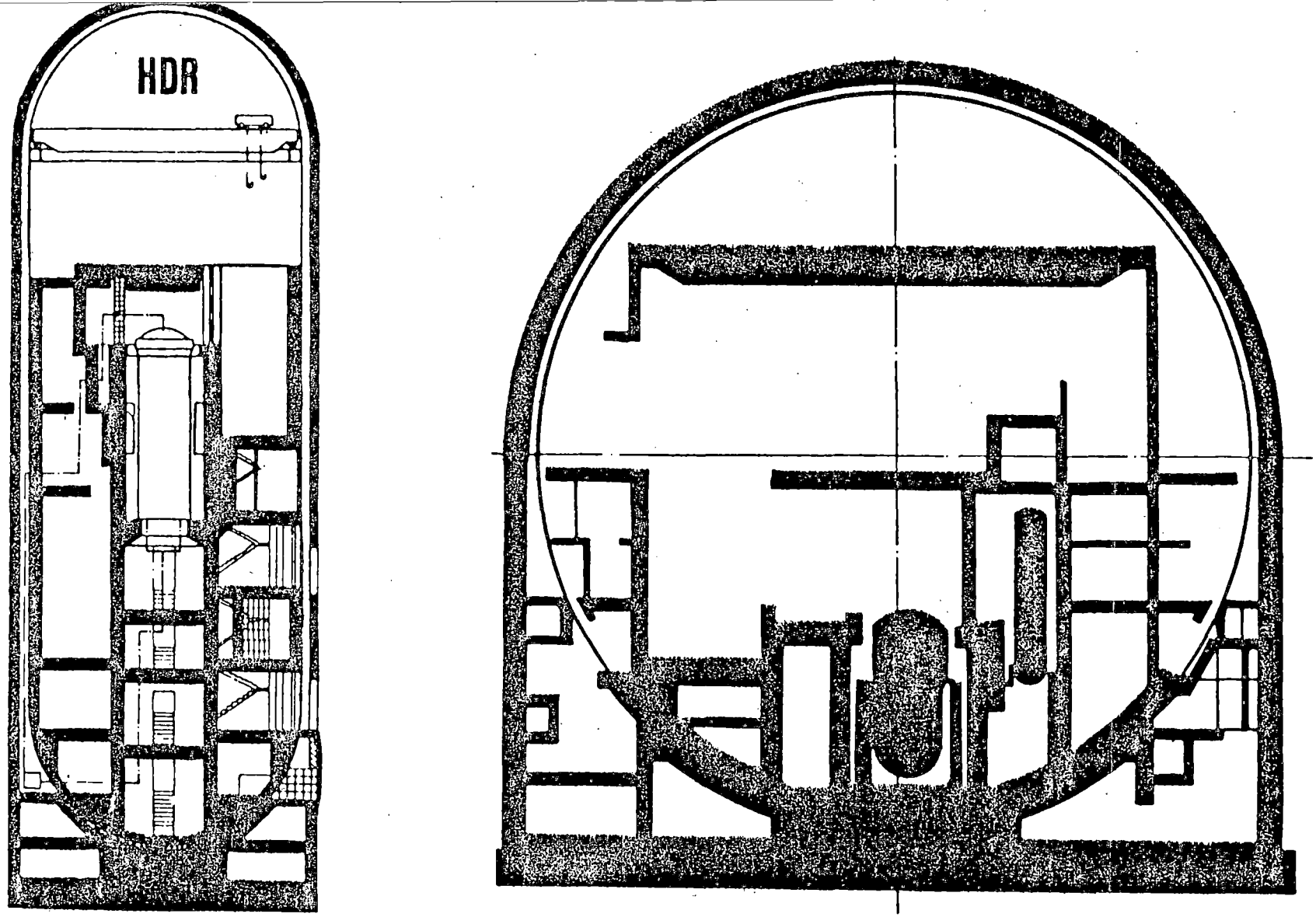

COMPARISON BETWEEN HDR-FACILITY AND BIBLIS-PWR

QUANTITY	HDR	PWR
Pressure, MPa	11	16
P_0 - P_{sat}, MPa	5.5	9
T_{core} - T_{downc}: °C	0-50	50
Break diameter, m	0.2	0.8
Break area	100 %	100 %
Break opening time, ms	1-2	15
Core barrel length, m	7.6	7.6
Core barrel thickness, mm	23	80
Core barrel diameter, m	2.66	4.3
Core representation	sim. by mass ring	bundles
Max. stress, MPA	100	250
Max. displacement, mm	2	3
Eff. pressure wave damping	0.52	0.71
Add. stiffness of CB due to water inside CB	0.52	0.21
Eigenfrequencies f_i of j-th mode, water/air, s^{-1}	f_0 18/600 f_1 7/71 f_2 17/69 f_3 14/15 f_4 20/53	29/353 16/19 36/80 32/58 44/68

KfK

COMPARISON BETWEEN MAJOR CHARACTERISTICS
OF THE HDR-FACILITY AND A GERMAN PWR

- **MODELS FOR DYNAMIC FLUID FLOWS**
  - single phase → three-dimensional (downcomer)
one-(two) dimensional (break nozzle)
  - two-phase → one-(two) dimensional (break nozzle)
three-dimensional (downcomer)

— Effects of

  - system pressure
  - break nozzle lengths
  - initial axial and radial temperature distributions

- **MODELS FOR DYNAMIC STRUCTURAL BEHAVIOR**
  - CORE BARREL
  - REACTOR PRESSURE VESSEL
- **MODELS FOR COUPLED FLUID STRUCTURE INTERACTIONS**
  - WITHOUT FLUID FLOW-SNAPBACK
  - WITH FLUID FLOW

KfK

MODELS OF PHENOMENA TO BE TESTED
ON THE BASIS OF HDR-RPV-I DATA

Test No	Pressure bar	Upper Core Temp. °C	Downcomer Temperature °C	Subcooling Downcomer Degrees	Length of break nozzle m
V29.2	90	293	273	30	4.524
V31	110	308	268	50	1.369
V31.1	110	308	268	50	1.369

KfK

Test Matrix for Preliminary Blowdown Tests

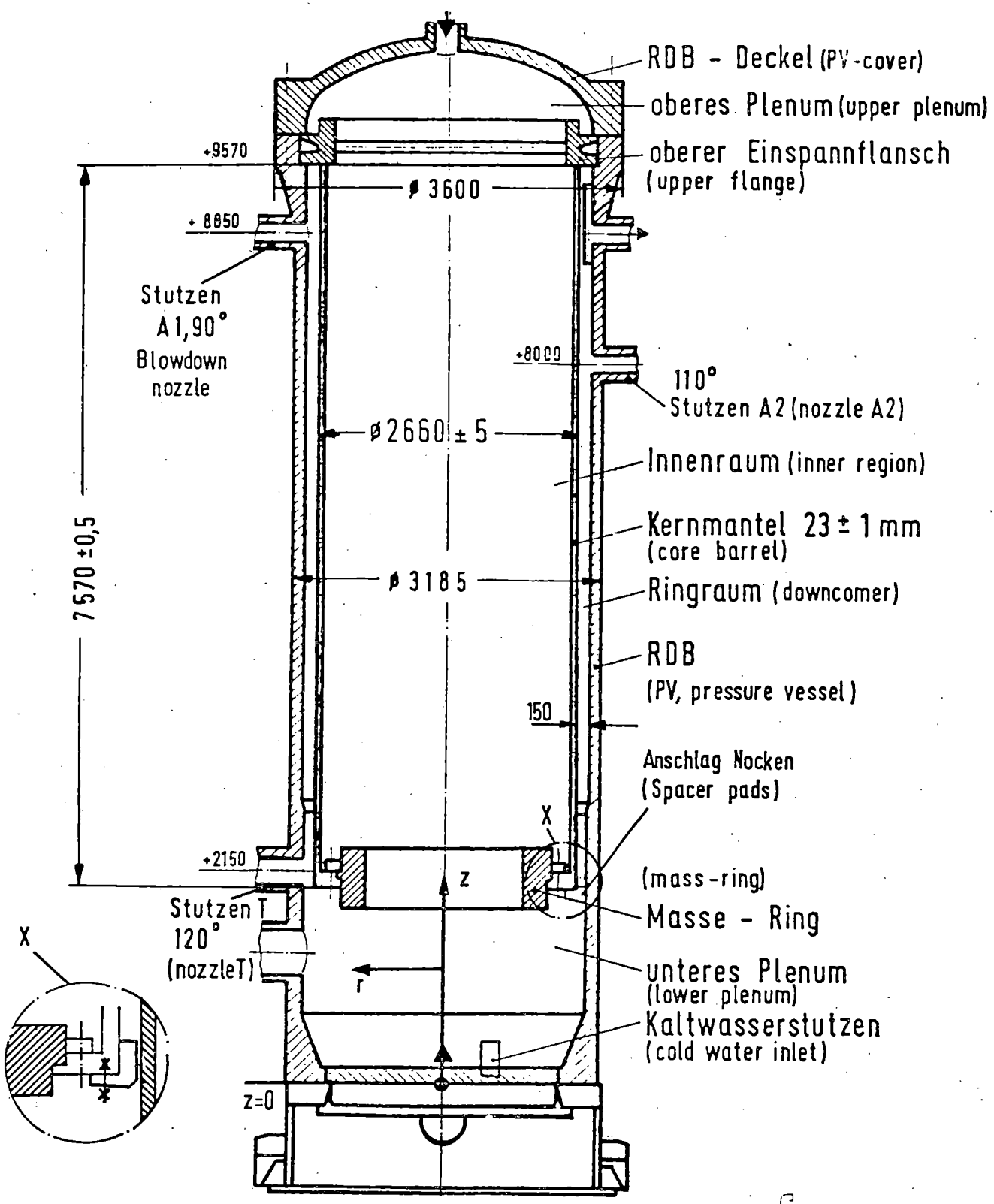

RDB und Kernmantelgeometrie für Blowdown Exp.

RPV and Core Barrel Geometries for Blowdown Experiments

Fig. 2.3

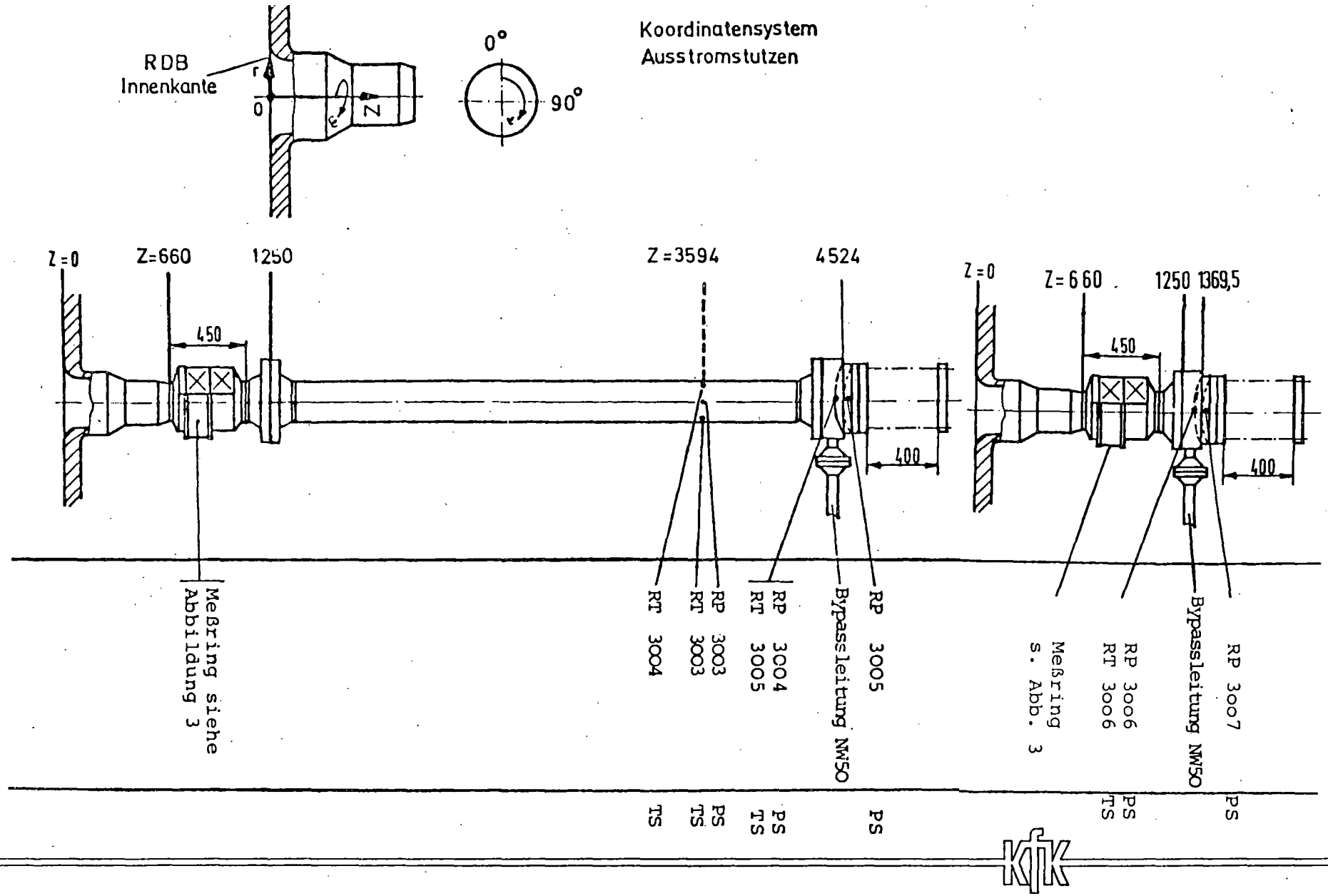

Identification of Measurement Sensors for Fluid Dynamic Quantities in the Long and Short Break Nozzles

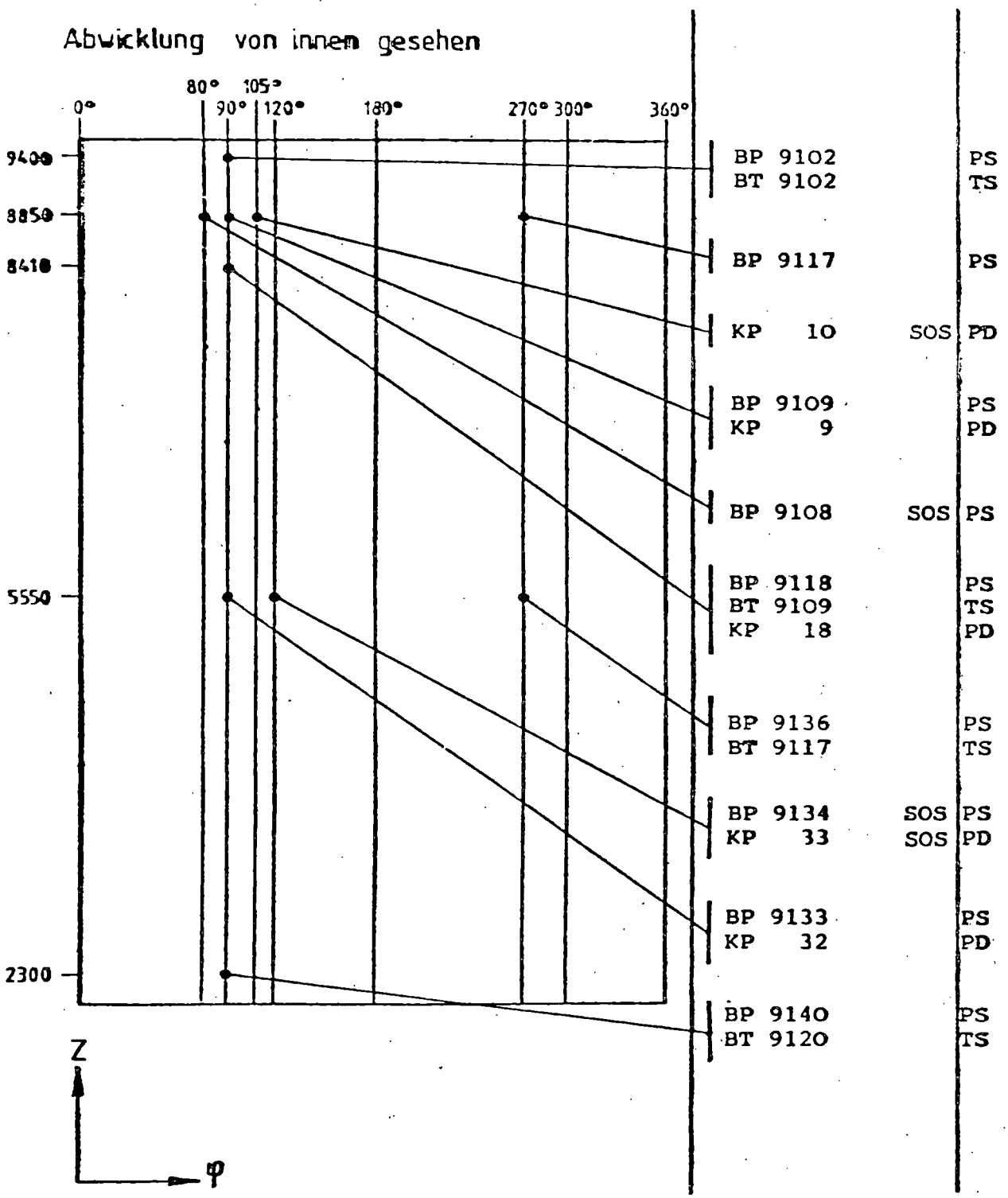

KfK

Wrap-Up of Core Barrel and Identification of Measurement Sensors for Fluiddynamic Quantities

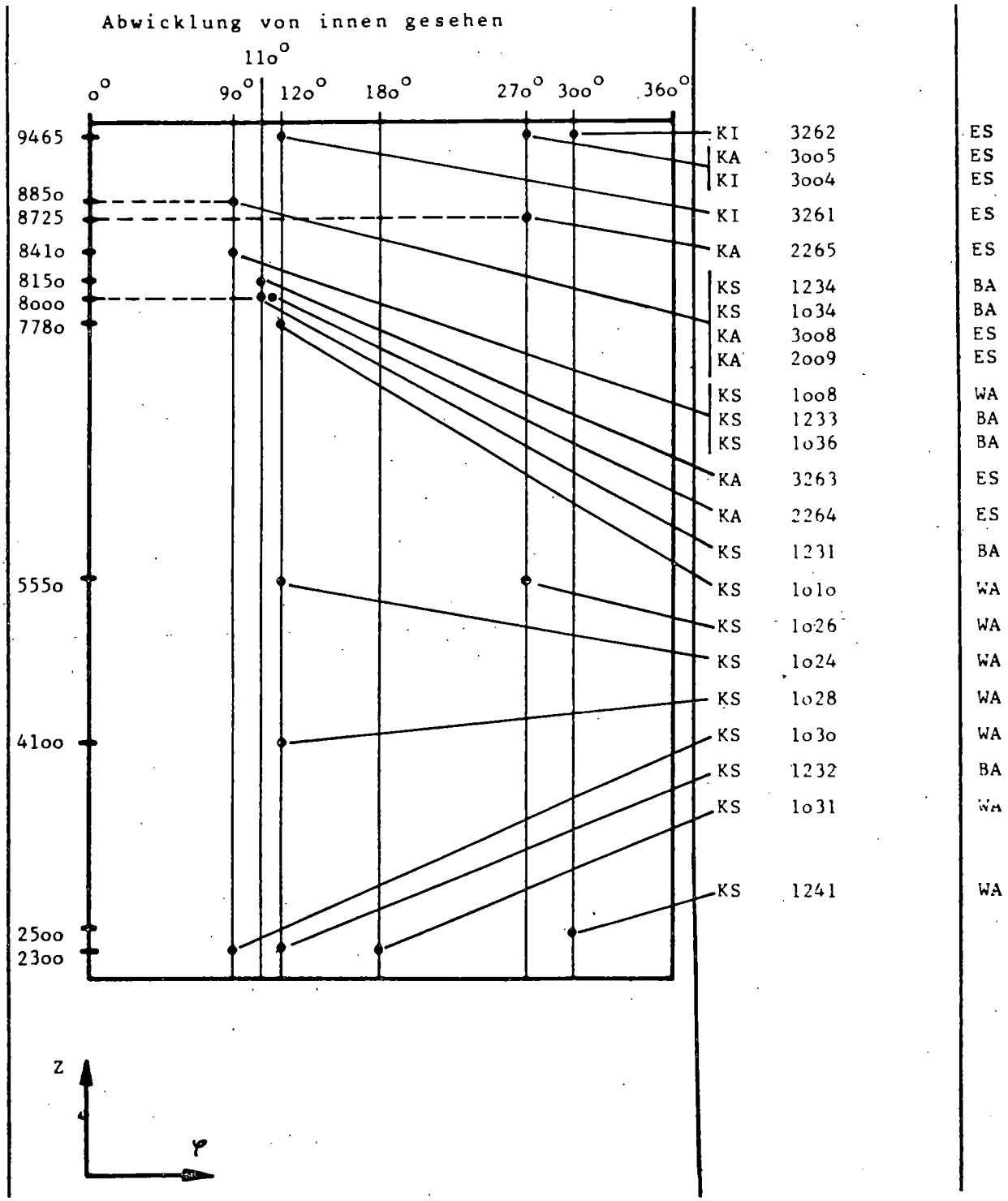

KfK

Wrap-Up of Core Barrel and Identification of Measurement Sensors for Structural Quantities

TEMPERATURE

Deviation: Measurement - Nominal °K

	Nozzle	Core Region
V 29.2	+ 4	+ 6
V 31	+ 1	+ 5
V 31.1	— 1	+ 5

PRESSURE

Deviation: Measurement - Nominal bar

	RPV
V 29.2	+ 1
V 31	— 2
V 31.1	— 2

BREAK OPENING TIME

Estimation: 2 ms

	Measurement
V 29.2	0.3
V 31	0.4
V 31.1	0.4

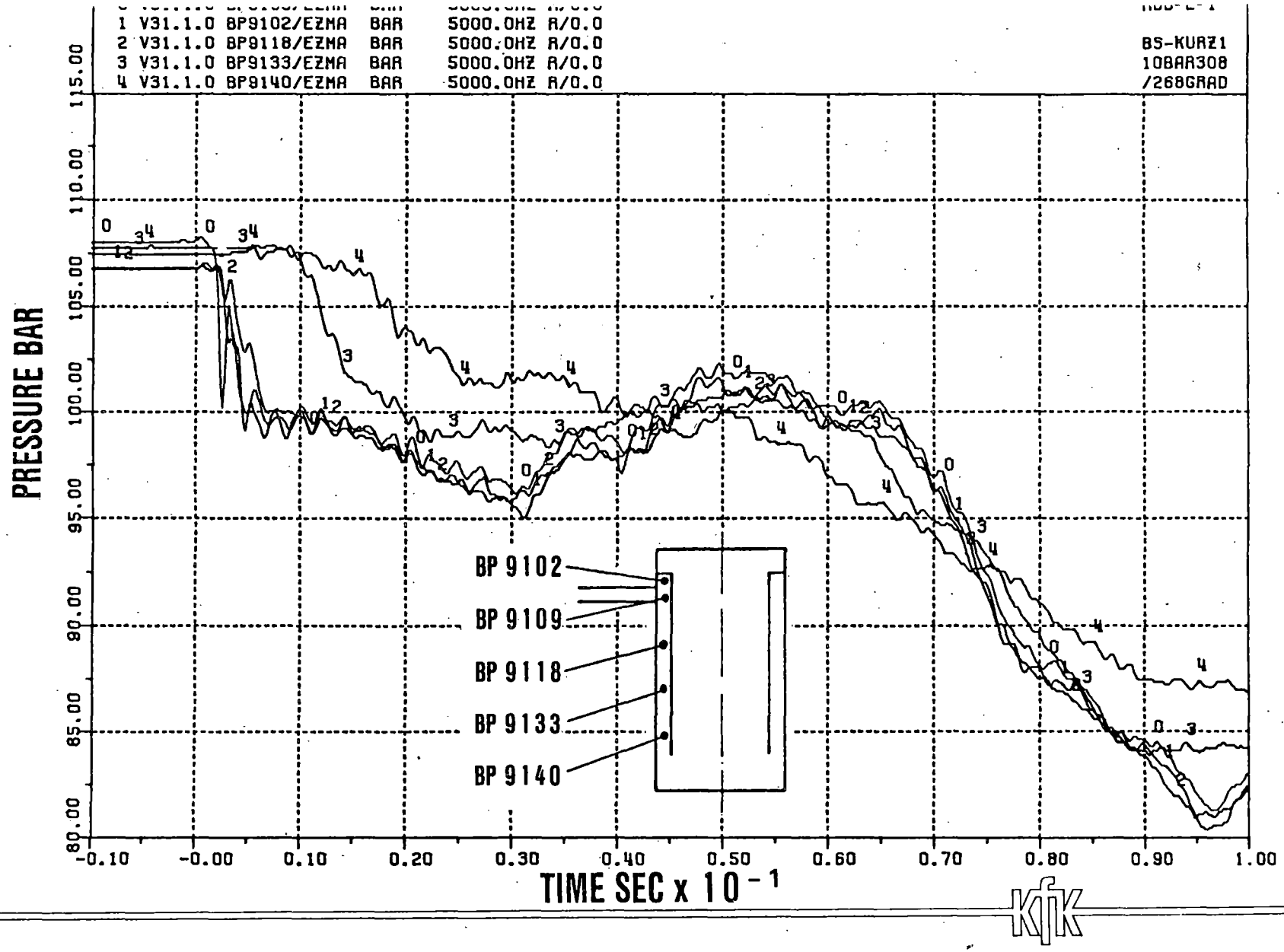

V31.1 / PRESSURE-TIME HISTORIES ALONG DOWNCOMER

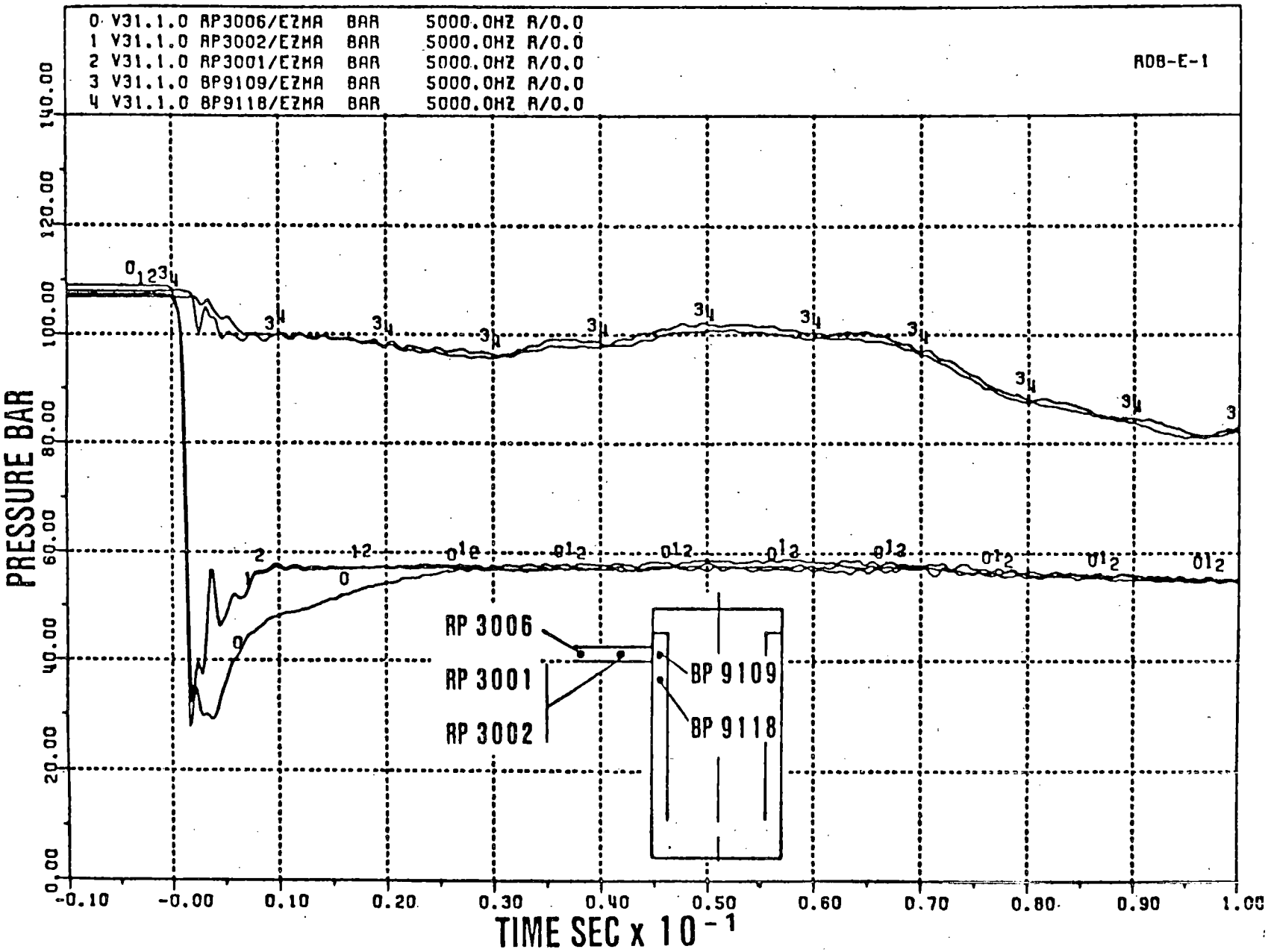

PRESSURES AT VARIOUS LOCATIONS IN THE DISCHARGE PIPE AND DOWNCOMER

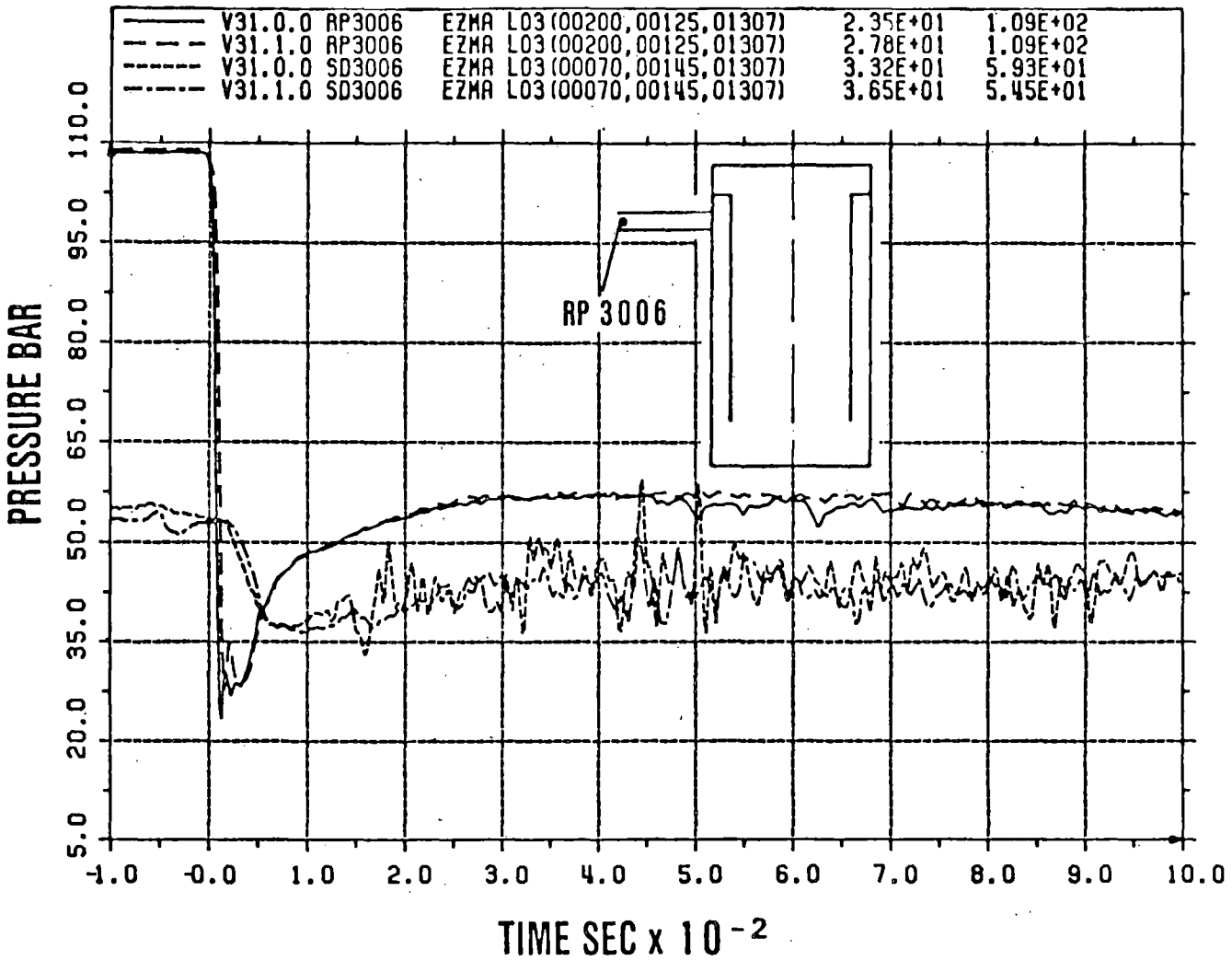

PRESSURES AND LOCAL SATURATION PRESSURES AT BREAK LOCATION

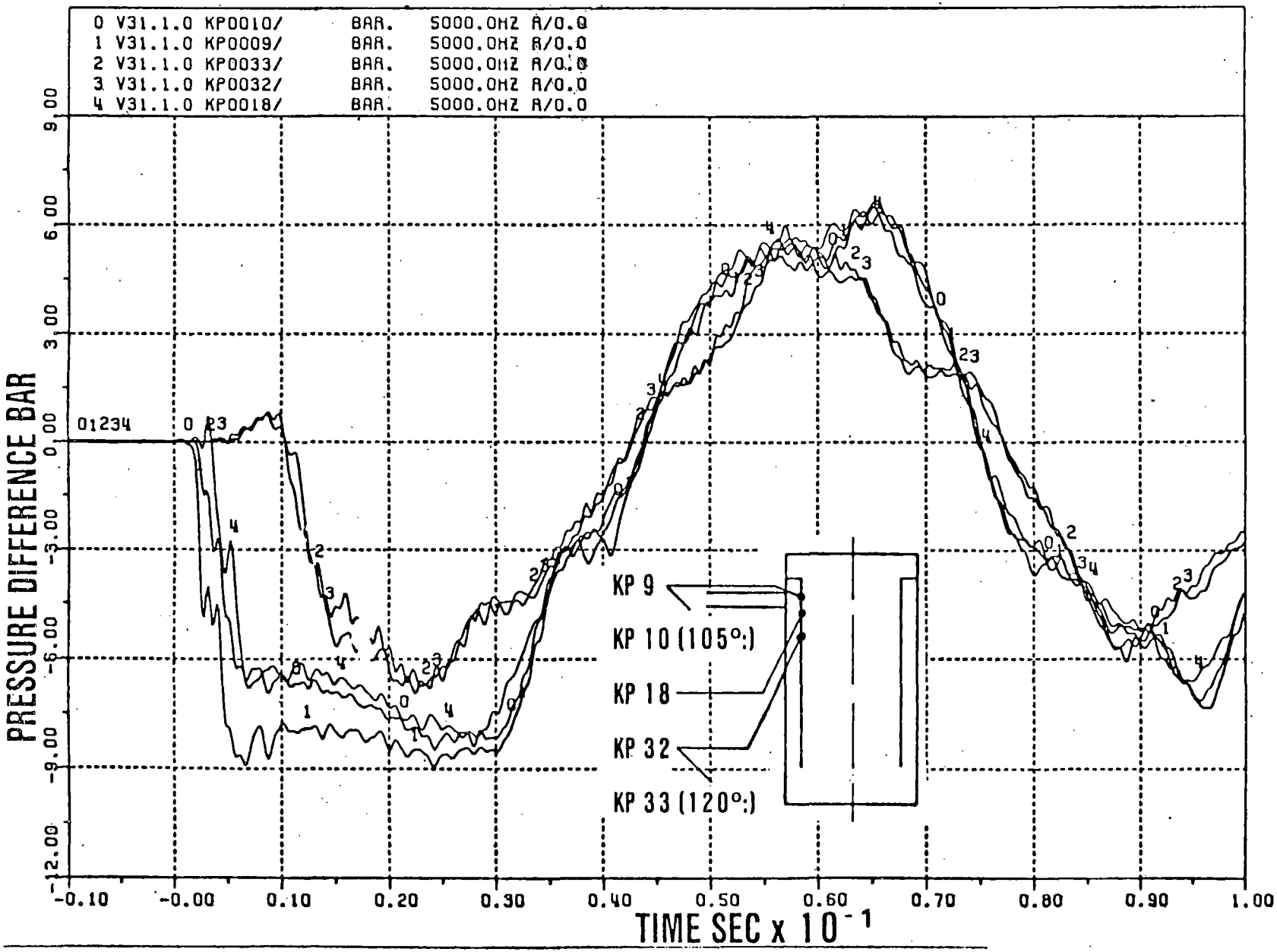

PRESSURE DIFFERENCES AT DIFFERENT POSITIONS ALONG THE CORE BARREL

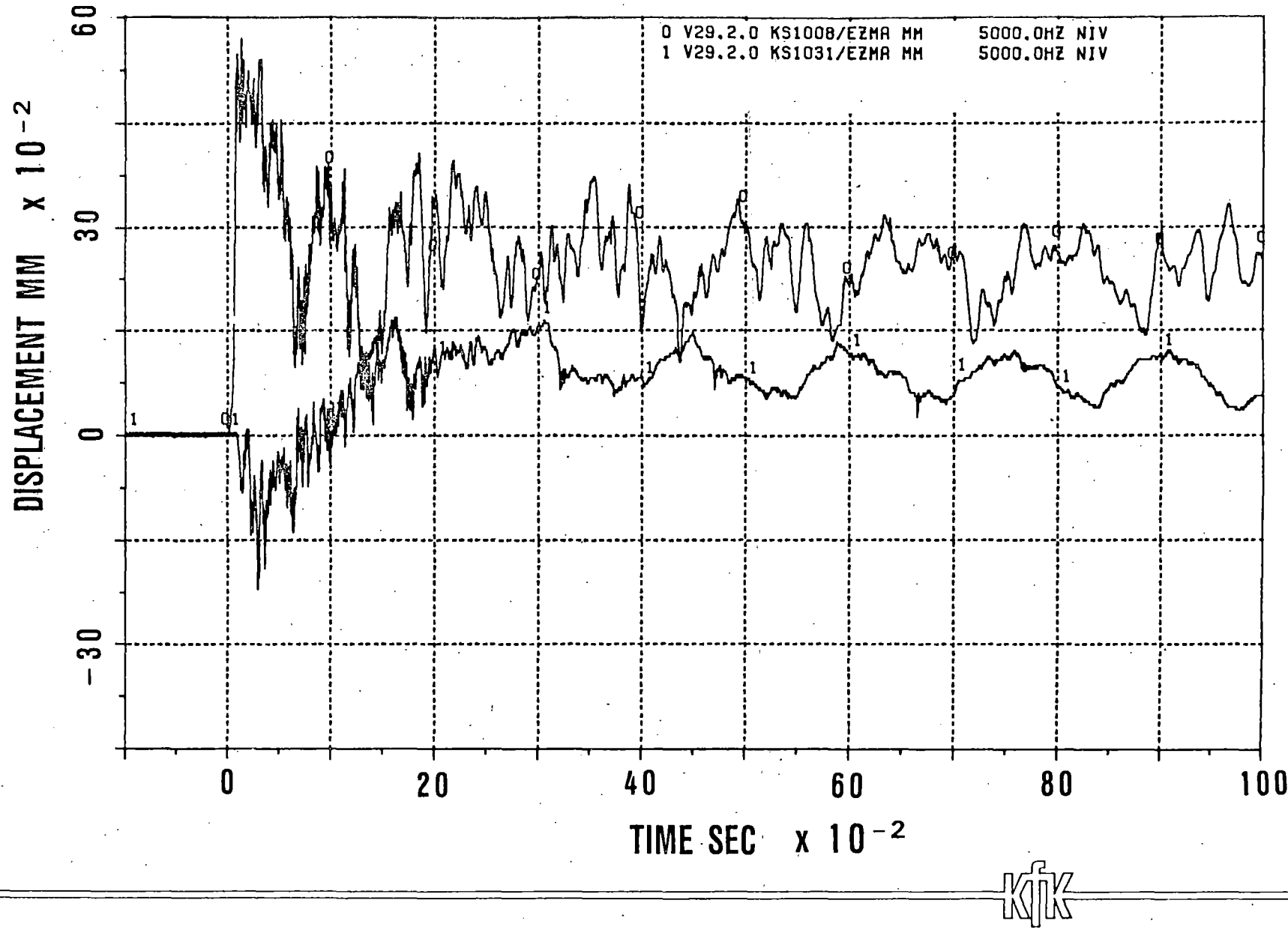

KfK

Displacements at Upper and Lower Parts of the Core Barrel for V29.2

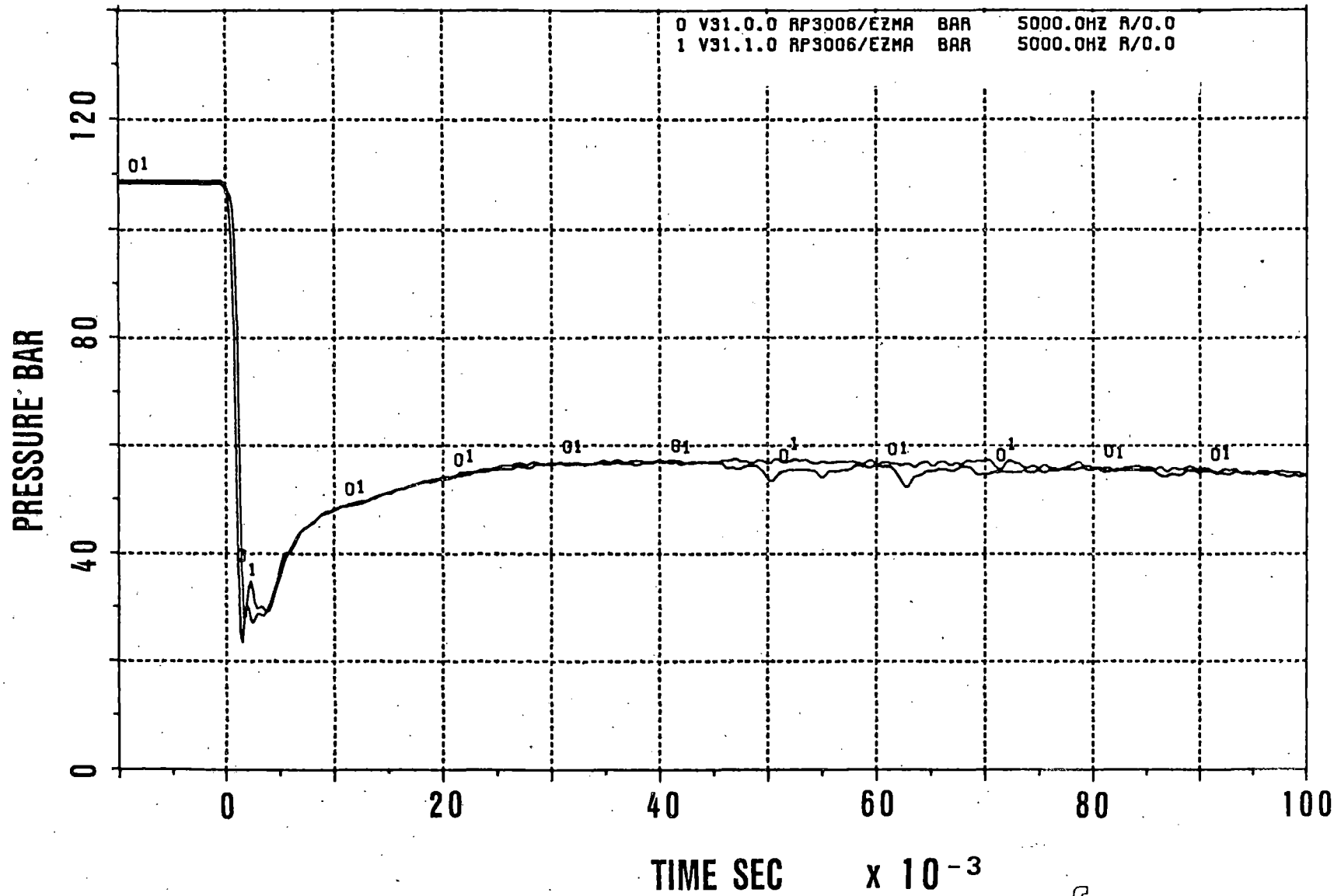

Comparison of Measured Pressure on Break Nozzle of Replicated Tests V31 and V31.1

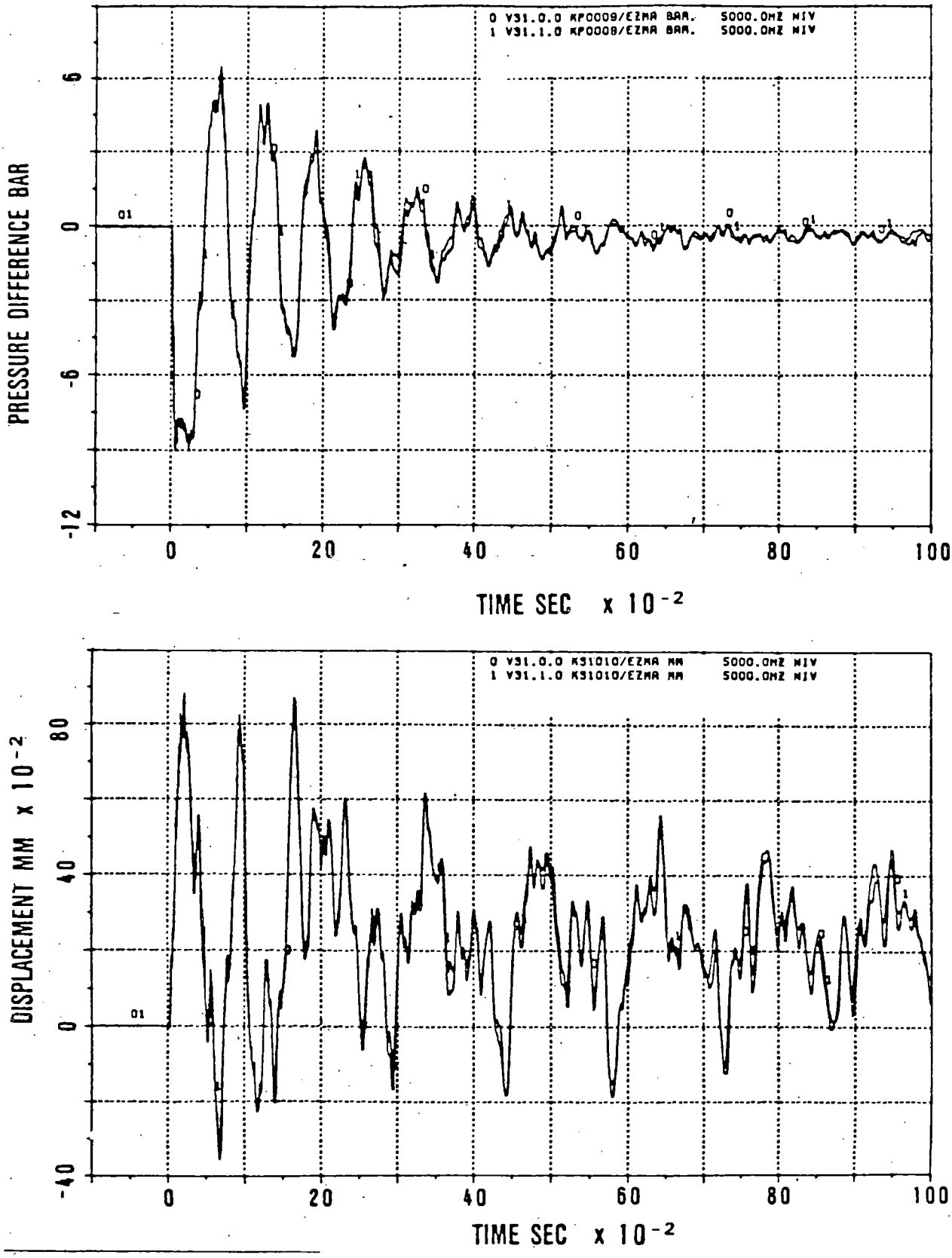

COMPARISONS OF PRESSURE DIFFERENCES AND CORE BARREL DISPLACEMENTS AS MEASURED FOR TESTS V 31.0 AND V 31.1

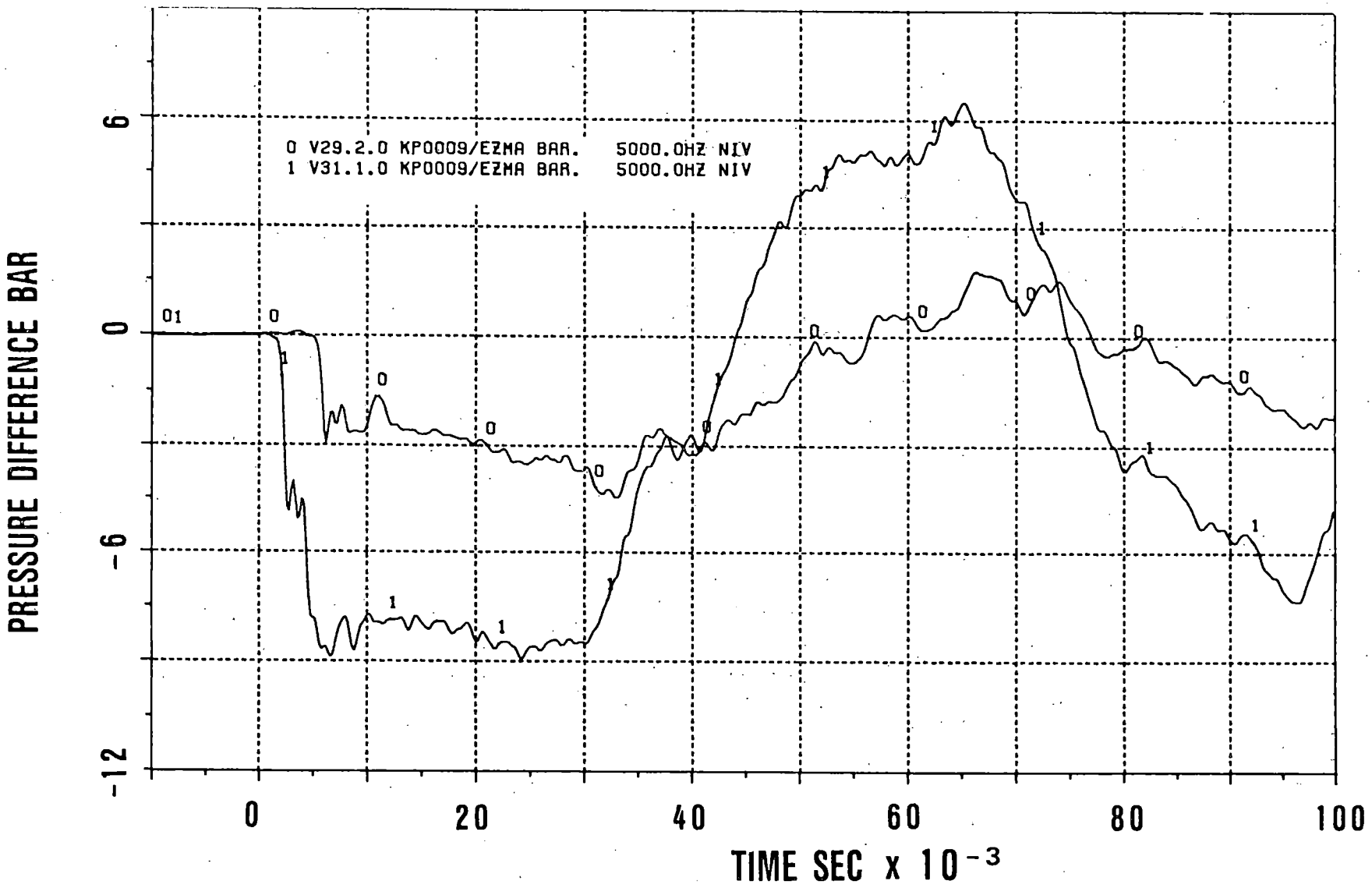

KfK

Comparison of Pressure Differences Across the Core Barrel at Break Nozzle Location for V29.2 and V31.1

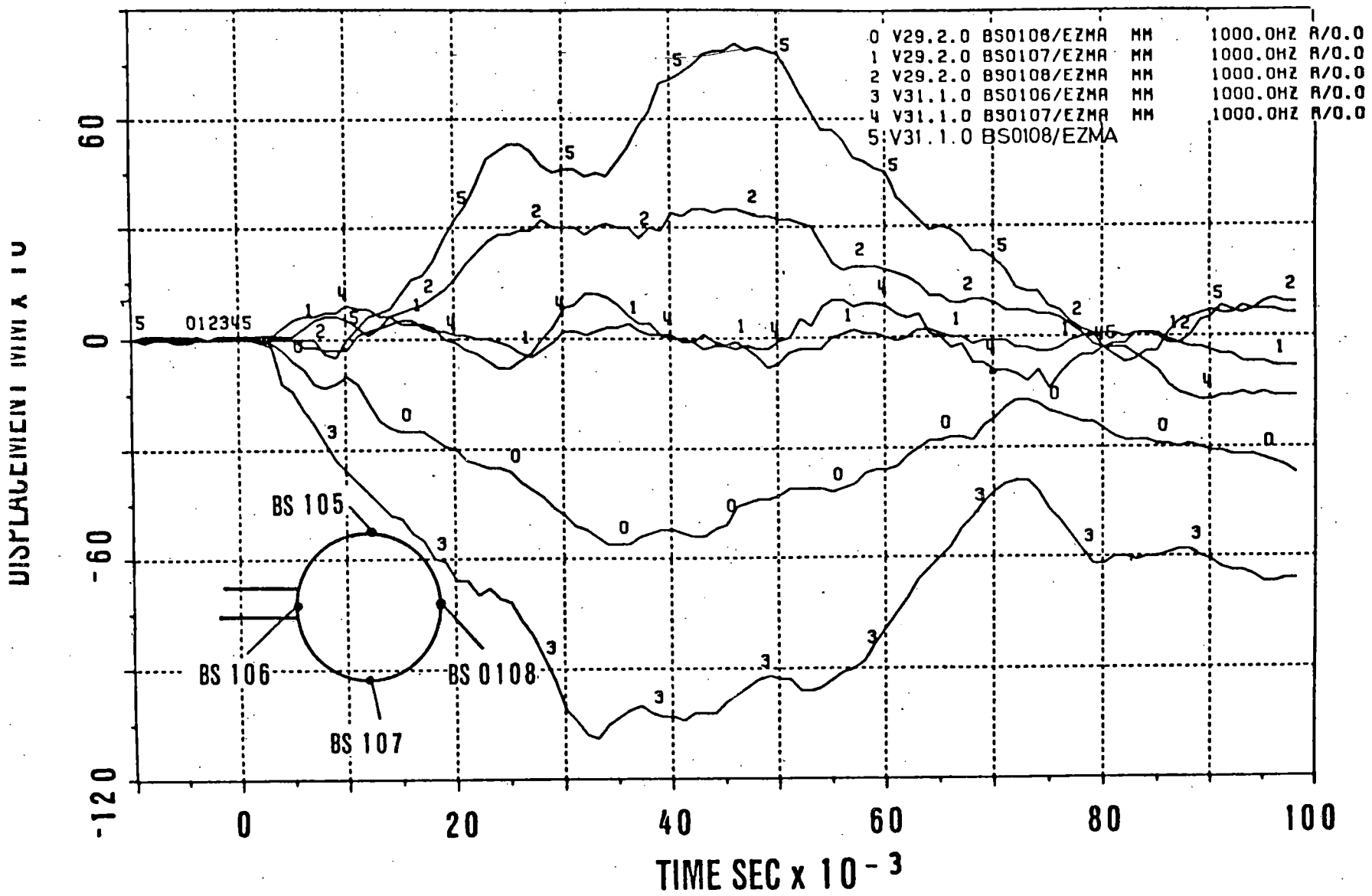

OUTSIDE PRESSURE VESSEL DISPLACEMENTS AT THREE AZIMUTHAL POSITIONS FOR TESTS V 29.2 AND V 31.1

QUANTITY	DIMENSION	EXPERIMENT	
		V29.2	V31.1
DEPRESSURIZATION	bar	12	30
PRESSURE DIFFERENCE	bar	6.1	15.2
MASS FLOW	kg/s	1350	2320
DISPLACEMENT	mm	0.7	1.3
ACCELERATION	m/s^2	410	441
STRAIN	10^{-3}	0.15	0.4
DISPLACEMENT OF RPV	mm	0.55	1.05

KfK

Comparison of the Maximum Variations in the Fluiddynamic and structural Quantities of Tests V29.2 and V31.1 During the First 100 ms

- SUBSTANTIAL REDUCTION OF PRESSURE WAVE PROPAGATION VELOCITY BY VIRTUE OF FSI
- SUBSTANTIAL REDUCTION OF CORE BARREL LOADS AND DEFORMATIONS BY EFFECTIVE FSI
- MAXIMUM CORE BARREL LOADS DURING SUBCOOLED PHASE OF BLOWDOWN
- 3-D, ASYMMETRIC T-H AND STRUCTURAL EFFECTS IN DOWNCOMER
- CONSISTANCY, FEASIBILITY AND REPRODUCIBILITY FOR THE MAJORITY OF DATA GUARANTEED
- HIGHER SUBCOOLING AND SHORTER BREAK NOZZLE RESULT IN HIGHER CORE BARREL LOADS
- CORE BARREL DISPLACEMENTS ARE COMPARATIVELY SMALL EVEN AT HIGHER FLUIDDYNAMIC LOADS
- SUBSTANTIAL REACTOR PRESSURE VESSEL DEFORMATIONS DETECTED
- DEVIATIONS FROM NOMINAL INITIAL CONDITIONS HAVE MINIMAL IMPACT ON MAJOR QUANTITIES; MUCH LESS THAN ANTICIPATED

CONCLUSIONS FROM EXPERIMENTAL RESULTS FOR t = 100 ms

CODE	INSTITUTION	REMARKS
2D / 3D FLUID-STRUCTURE-MODELS		
FLEXWALL	KWU	FLUID-STRUCTURE COUPLED
K-FIX (3D, FLX)	LASL (NRC)	
STEALTH-WHAMSE (3D)	EPRI	
FLUX	KfK-IRE	COUPLED / DECOUPLED
NETWORK FLUID-STRUCTURE-MODELS		
DAISY	GRS	FLUID-STRUCTURE COUPLED
MULTIFLEX	WESTINGHOUSE	
FLUID-MODELS ONLY		
DRIX-2D	KfK-IRE	FLUID-NOZZLE
DAPSY	GRS	FLUID DECOUPLED
FLUST-2D	KfK-IRE	
LECK	KWU	

KfK

CODES INCLUDED IN THE HDR VERIFICATION PROCESS

Fig. 3

Code Name	K-FIX	FLEX-WALL	FLUX-2	FLUST	MULTI-FLEX	DAISY	DAPSY	DRIX	STEALTH/WHAMSE
Dimensionality	3-D	2 1/2-D	3-D	2-D	equiv. network	equiv. network	equiv. network	2-D	3D
2-Model No. of Eqs.	2-Fluid 6-Eqs.	HEM 3-Eqs.	compress. Pot. Flow	HEM 3-Eqs.	HEM 3-Eqs.	Drift 4-Eqs.	Drift 4-Eqs.	Drift 5-Eqs.	equation of state Subcooled water
Nodalization of discharge pipe	16	40	15	28 of which 18 external	7	6	6	155 of which 60 external	60 grid points 14 zones
Nodalization in vessel	3774	downcomer: 2016 core+plena: 59 nodes 58 pipe sect.	5754	280	downcomer 120 legs 56 knots	downcomer 65 pipe sect 35 knots core+plena 135 pipe sect 54 knots	same as DAISY	91	downcomer: 720 grids points core+plena: 2025 grids points RPV-piping: 44 grids points each
Nodalization of core barrel	612	2016	423 degrees o. freedom	-	8x7=56 nodes	35 degrees o. freedom	-	-	504 elements (+56 dummies) 287 nodes (+30 dummies)
Time step, ms	0.04	0.02087	0.2	0.06	0.2	0.1	0.1	0.02	0.0042
Computation time, sec	3960	6182 CPA	5040	7620	780	~2000	~1500	9900	?
Computer	CDC-7600	CYBER 176	IBM 3033	IBM 3033	CDC-7600	Amdahl	Amdahl	IBM 3033	?
Geometry considered	0.5	1	0.5	0.5	1	0.5	0.5	0.5	0.5
Remarks			comp. time reduc. 3600		Beam vessel motion includ.				
Description avail.	yes	publ. yes prop. rep. no	yes	yes	publ. yes prop. rep. no	yes	yes	yes	yes

GEGENUBERSTELLUNG EINIGER HAUPTMERKMALE DER FUR V 31.1 EINGESETZTEN RECHEN-PROGRAMME

ANLAGE 5.2.11

SUMMARY OF IMPORTANT CHARACTERISTICS OF CODES USED IN PRE-TEST PREDICTIONS FOR V 31.1

2. Abbreviations Used for Plotting Pretest Prediction and Experimental Results into One Plot

Code Abbreviation	Code Name	Institution Country	Remarks
DRX	DRIX-2D	IRE, Germany	fluid, decoupled, nozzle only
DAI	DAISY	GRS, Germany	coupled
DAP	DAPSY	GRS, Germany	fluid, decoupled
EZMA	Experimental Data	PHDR, Germany	measurement
FLE	FLEXWALL	KWU, Germany	coupled, decoupled
FL 2	FLUST 2	IRE, Germany	fluid, decoupled
FX 2	FLUX 2	IRE, Germany	coupled, decoupled
FXD	FLUX 2 - DRIX-2D	IRE, Germany	coupled with pressur boundary condition calculated at nozzle inlet by DRIX-2D; calculation has been done after publishin experimental results of test V 29.2
KFX	KFX (3D, FLX)	LASL, USA	coupled
MFX	MULTIFLEX	W , USA	coupled
STE	STEALTH/WHAMSE	SAI, ITI (EPRI), USA	coupled calculations performed after release of experimental data and updated thereafter
KF2	KFX (3D,FLX)	LASL, USA	2.post-test calculat.

B...: pre-test prediction

D...: post-test prediction

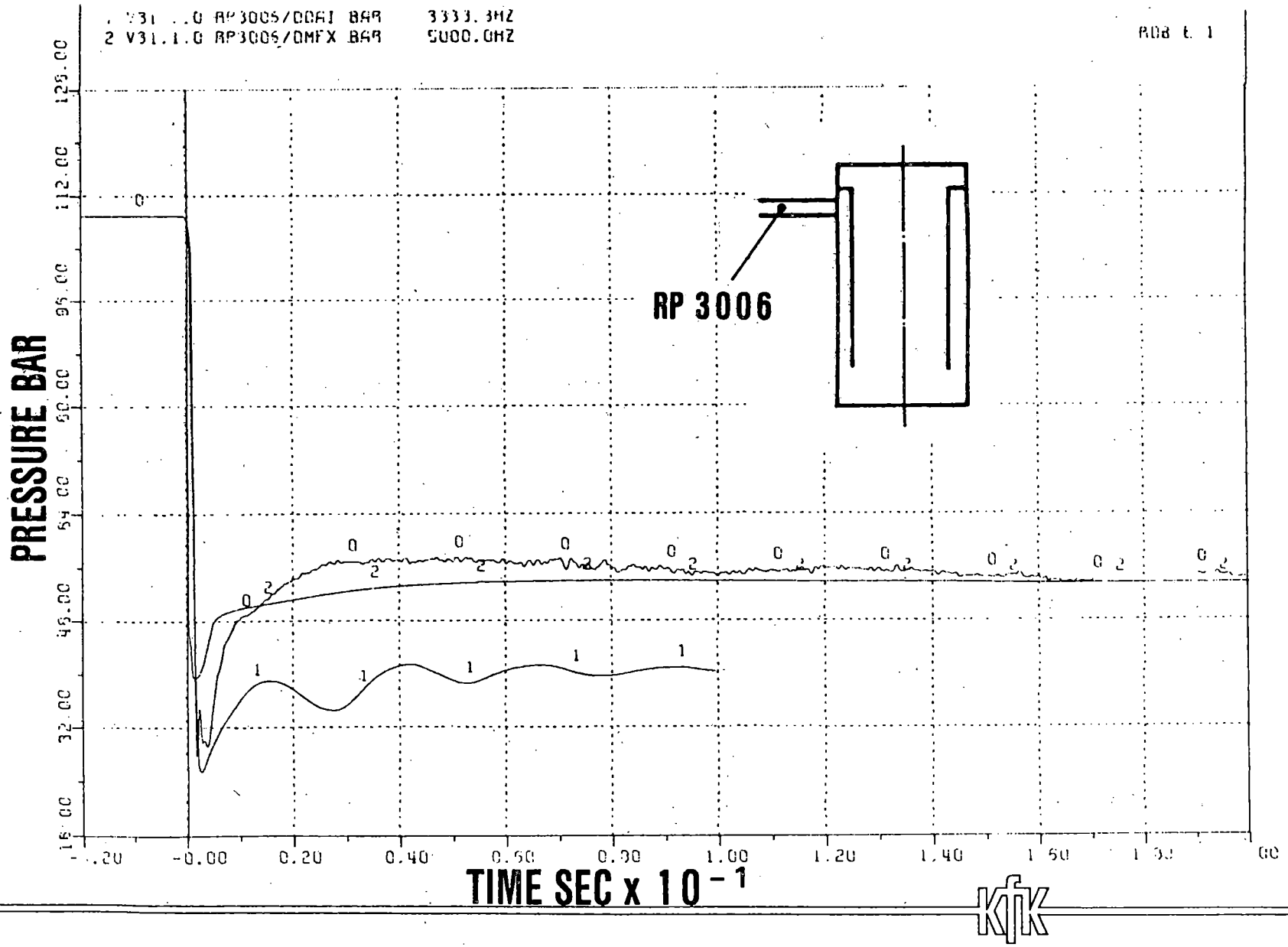

COMPARISON BETWEEN EXPERIMENTAL DATA AND POST-TEST PREDICTIONS OF EQUIVALENT NETWORK-CODES FOR PRESSURE AT BREAK

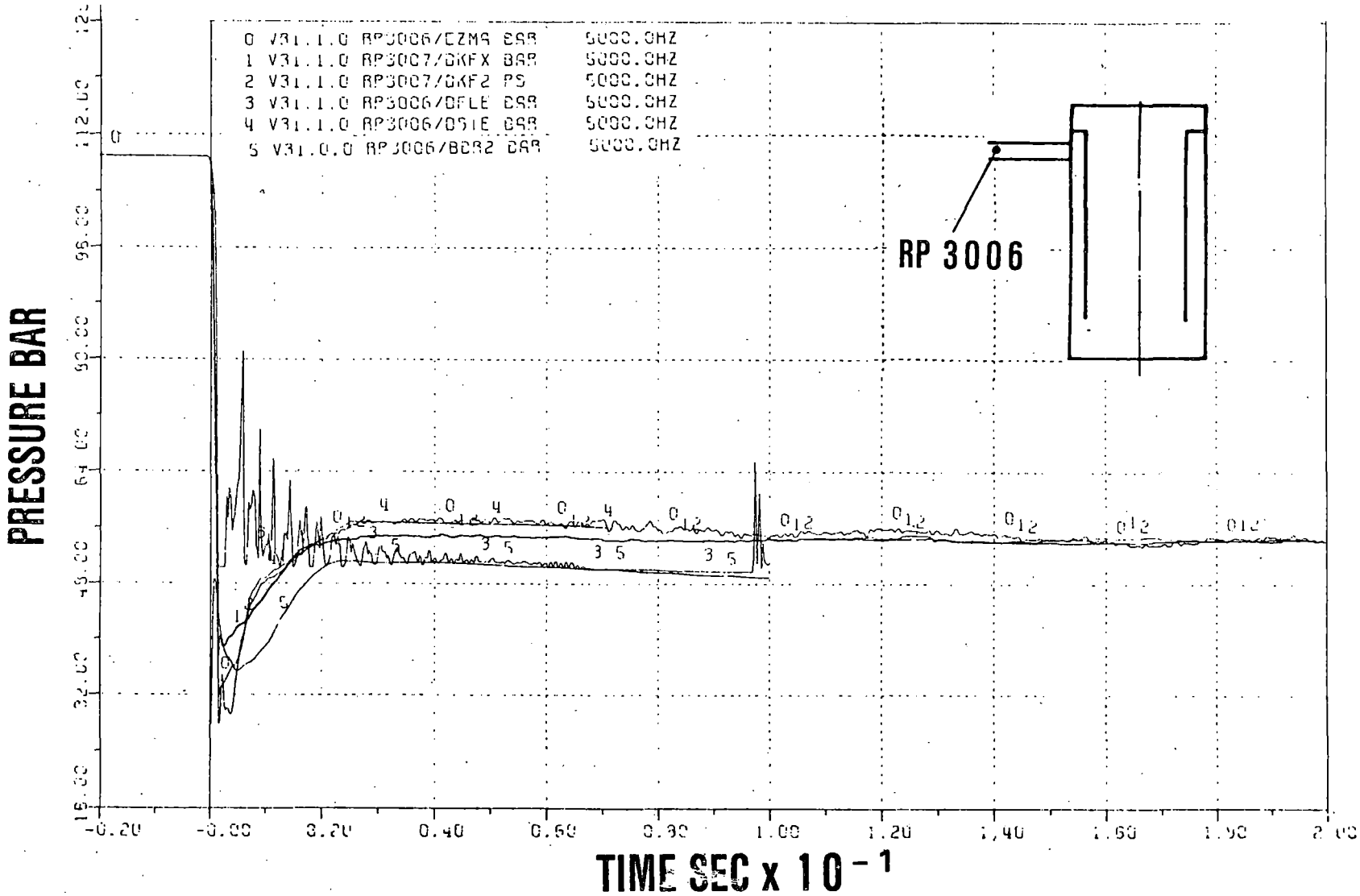

COMPARISON BETWEEN EXPERIMENTAL DATA AND POST-TEST PREDICTIONS OF MULTIDIMENSIONAL CODES FOR THE PRESSURE NEAREST TO THE BREAK

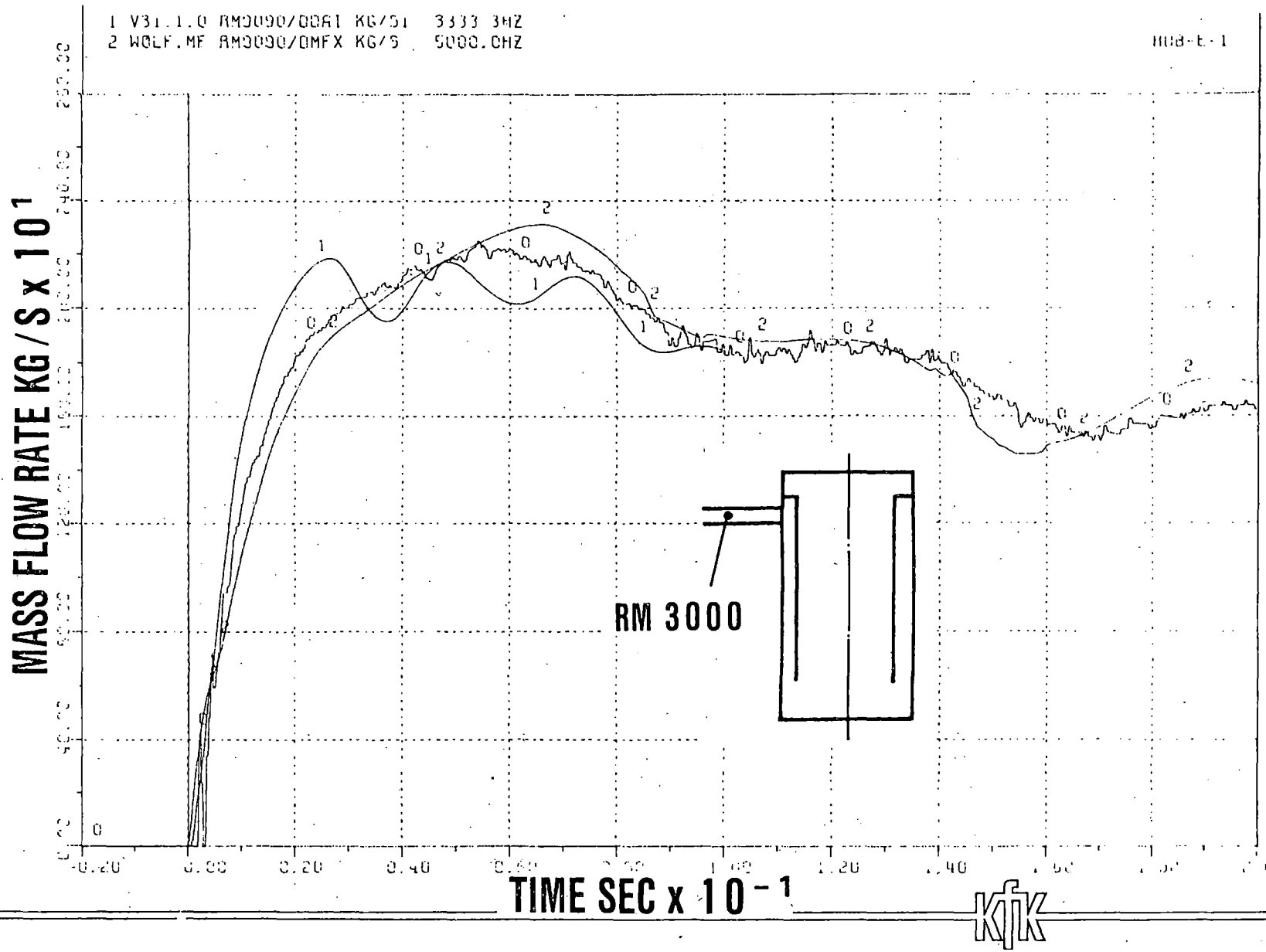

COMPARISON BETWEEN EXPERIMENTAL DATA AND POST-TEST PREDICTIONS OF EQUIVALENT NETWORK CODES FOR MASS FLOW RATE IN MEASUREMENT RING

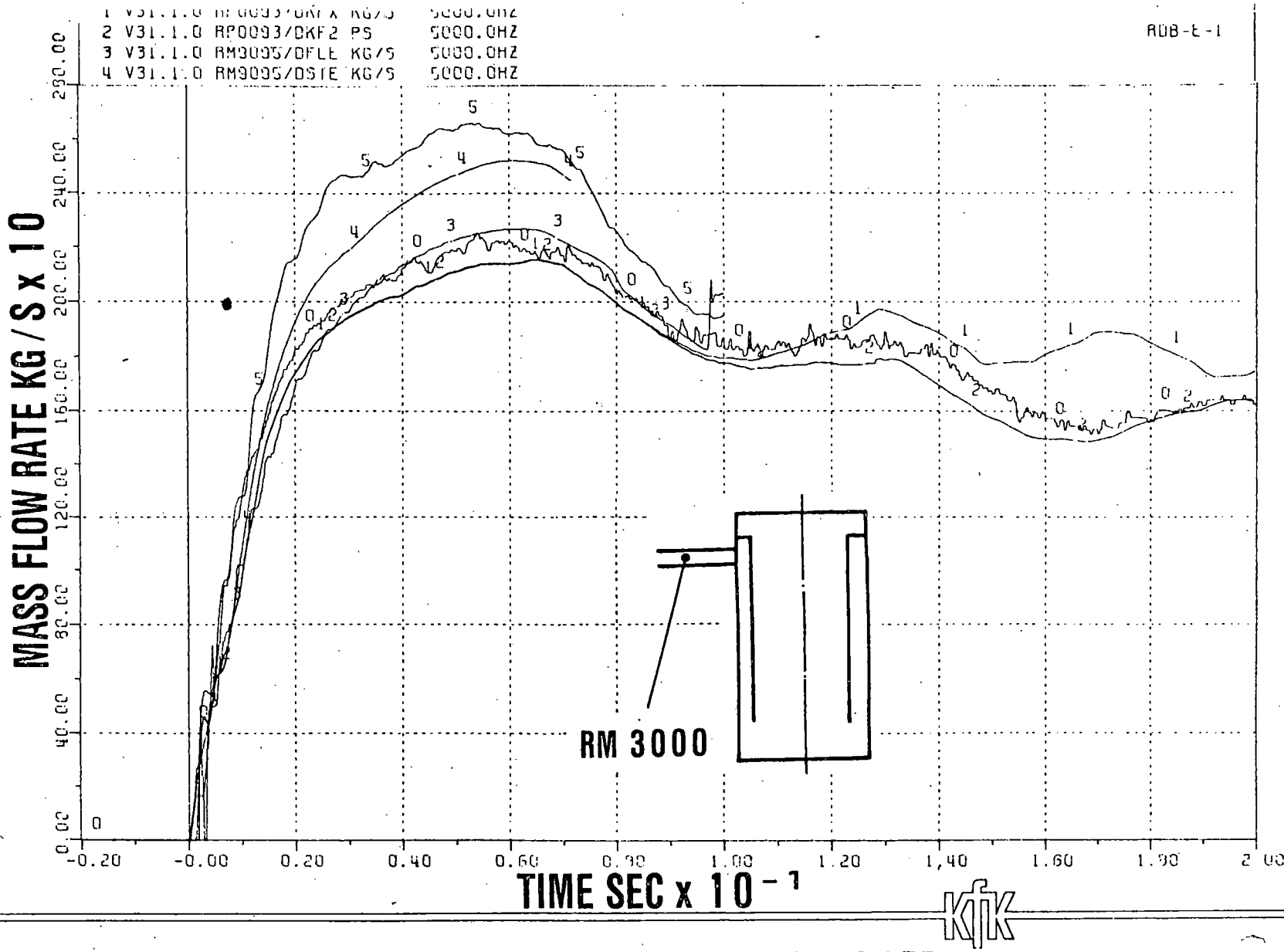

KfK

COMPARISON BETWEEN EXPERIMENTAL DATA AND POST-TEST PREDICTIONS OF MULTIDIMENSIONAL CODES FOR THE MASS FLOW RATE IN THE MEASUREMENT RING

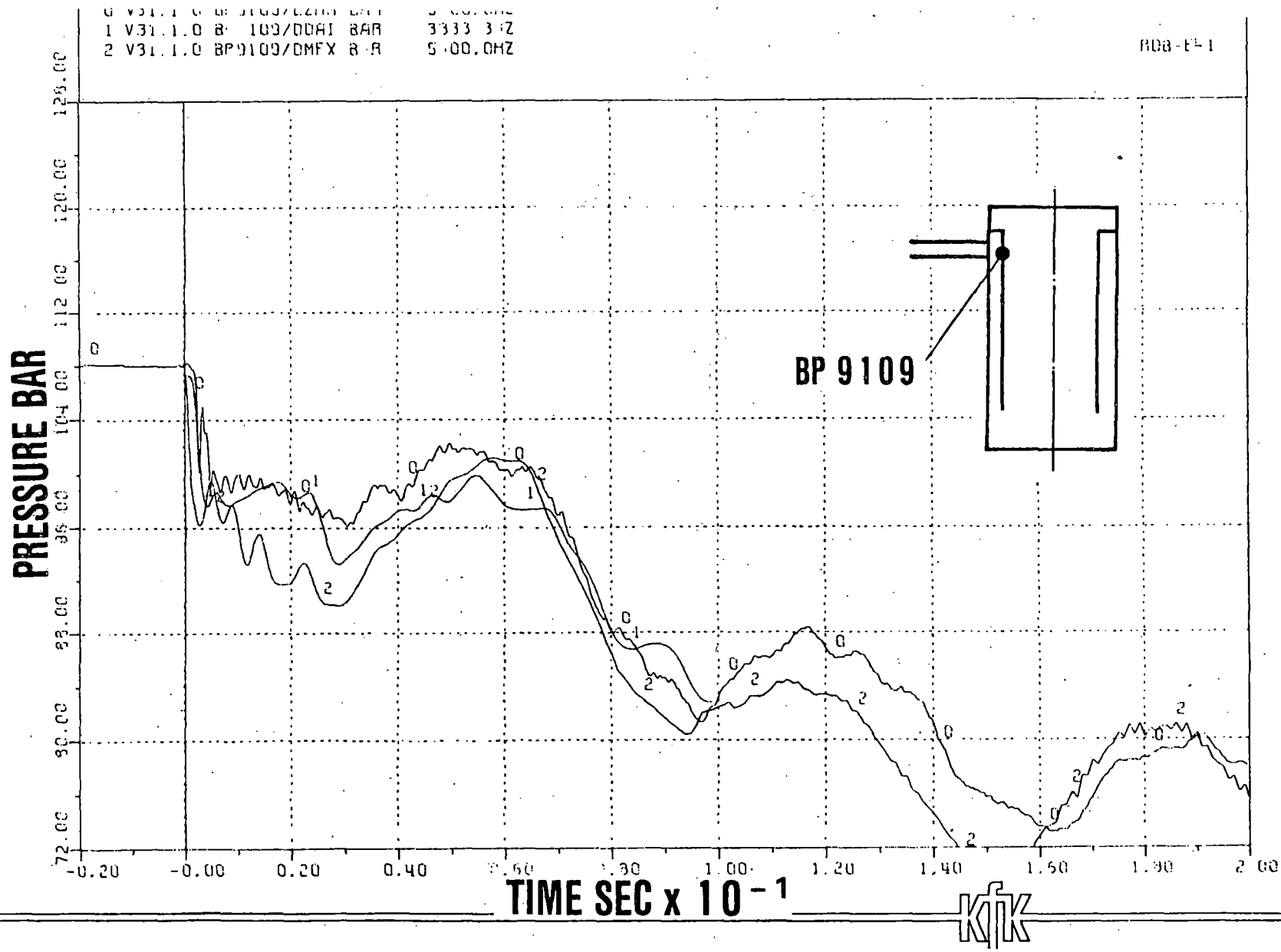

COMPARISON BETWEEN EXPERIMENTAL DATA AND POST-TEST PREDICTIONS OF EQUIVALENT NETWORK CODES FOR PRESSURE IN DOWNCOMER

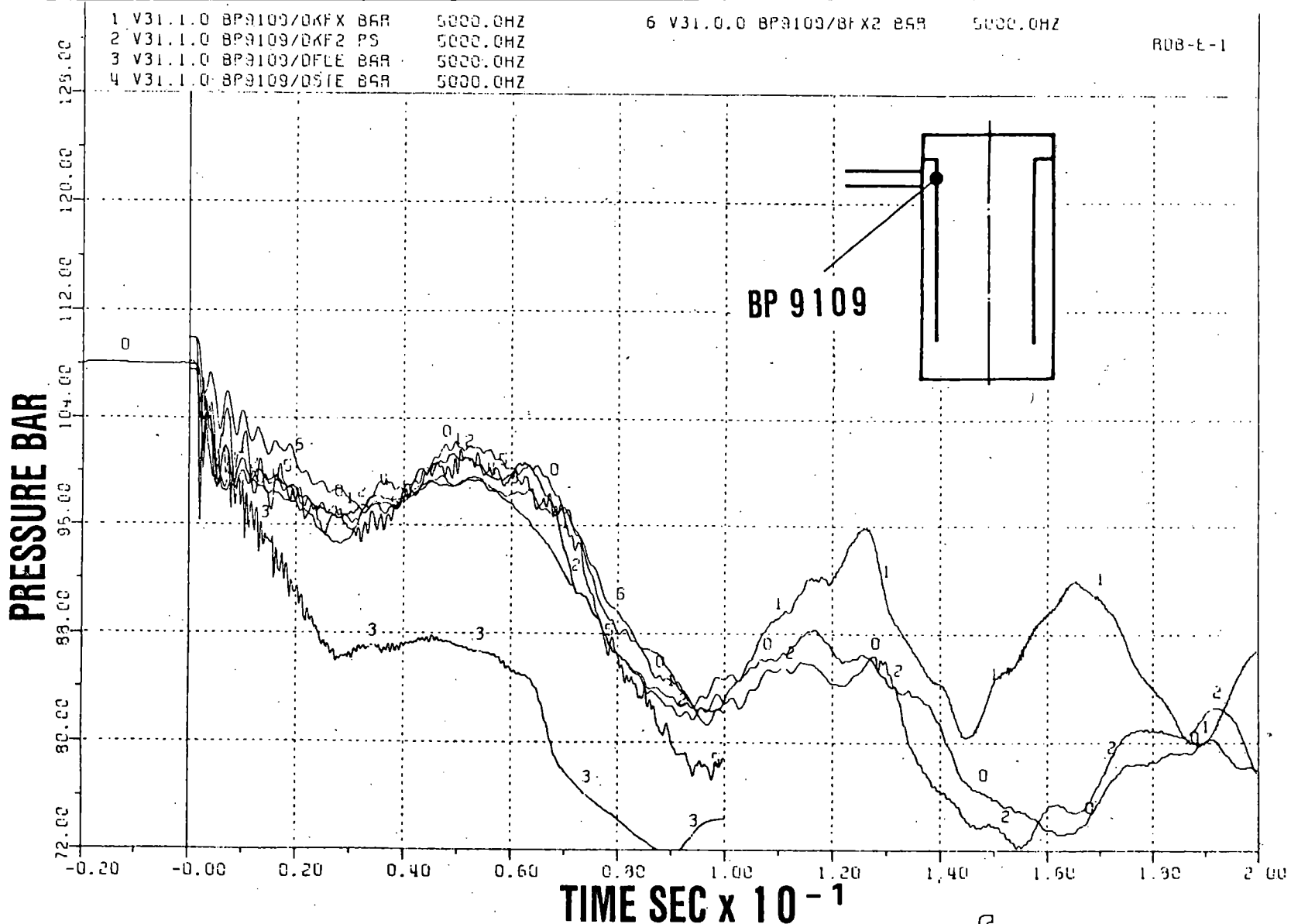

KfK

COMPARISON BETWEEN EXPERIMENTAL DATA AND POST-TEST PREDICTIONS OF MULTI DIMENSIONAL CODES FOR THE PRESSURE IN THE DOWNCOMER AT BREAK NOZZLE AXIS

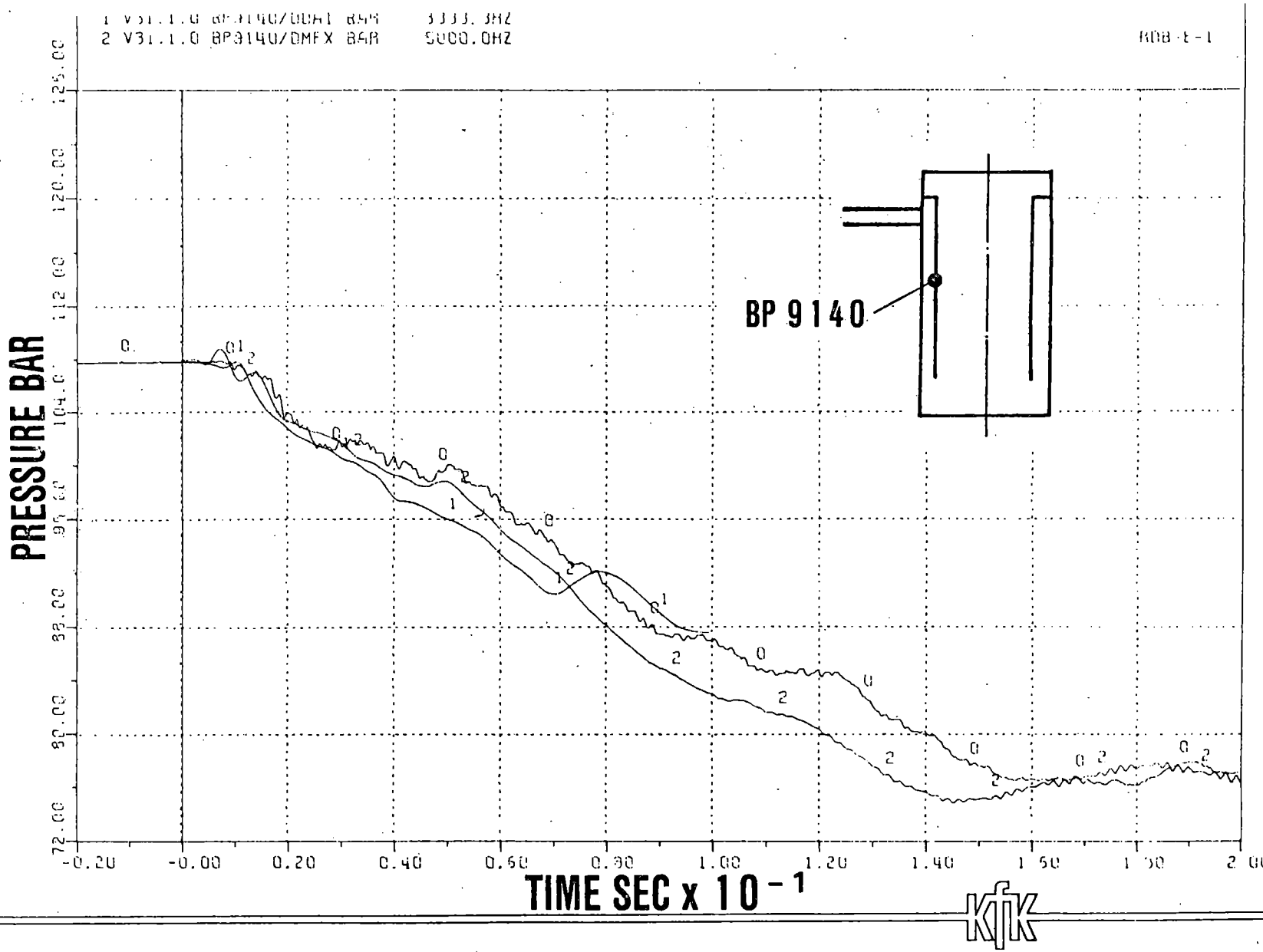

COMPARISON BETWEEN EXPERIMENTAL DATA AND POST-TEST PREDICTIONS OF EQUIVALENT NETWORK CODES FOR PRESSURE IN DOWNCOMER

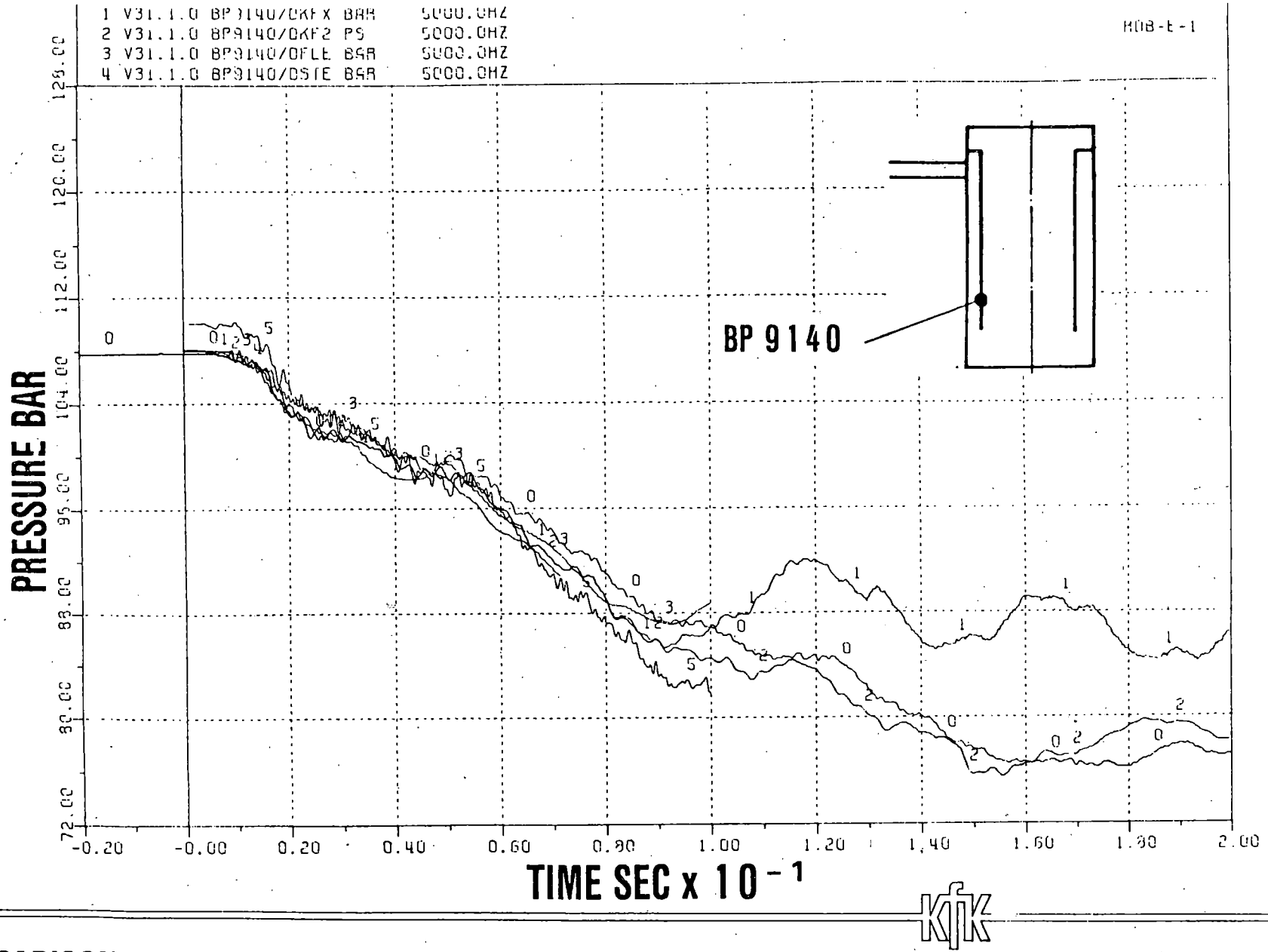

KfK

COMPARISON BETWEEN EXPERIMENTAL DATA AND POST-TEST PREDICTIONS OF MULTIDIMENSIONAL CODES FOR THE PRESSURE IN THE DOWNCOMER

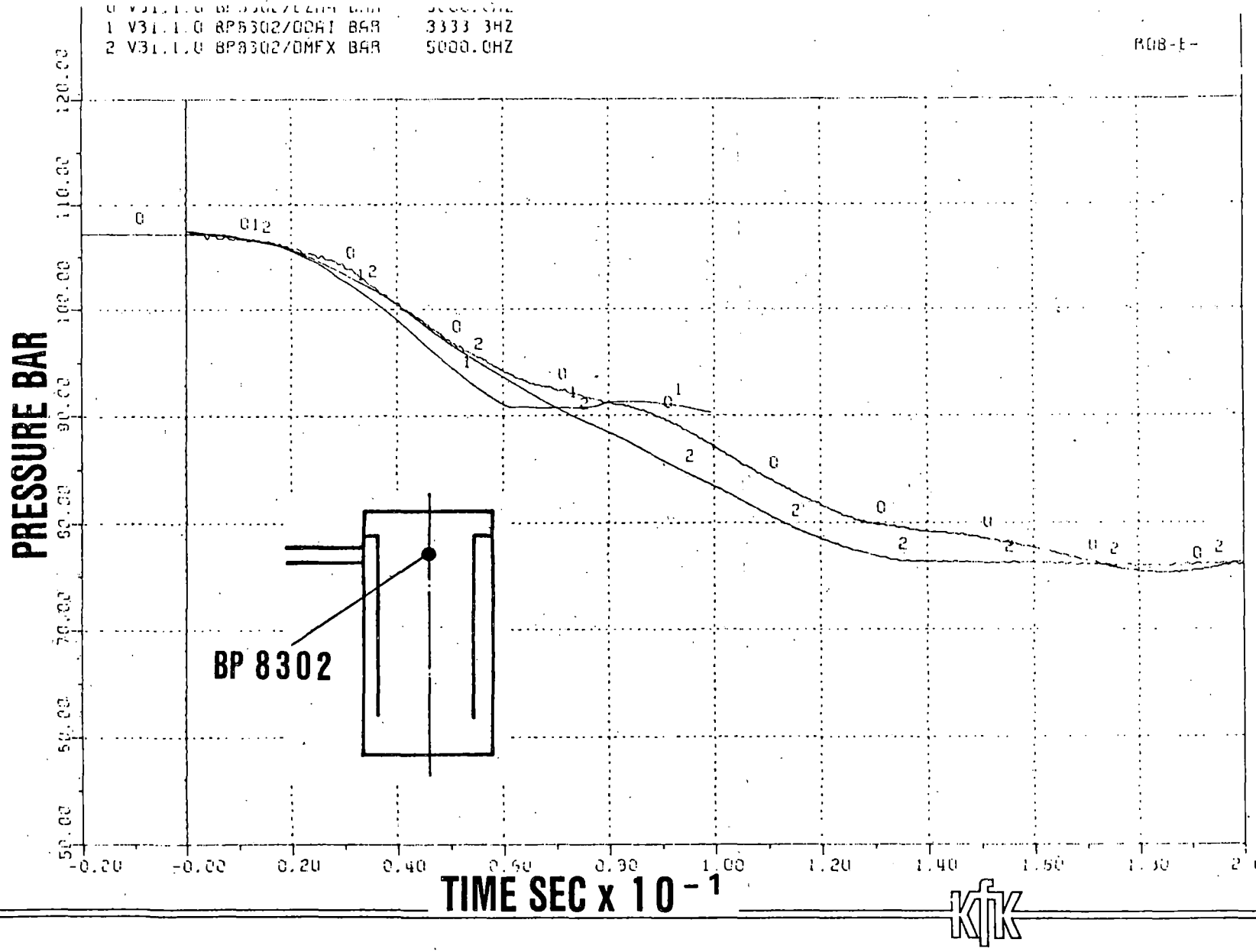

COMPARISON BETWEEN EXPERIMENTAL DATA AND POST-TEST PREDICTIONS OF EQUIVALENT NETWORK CODES FOR PRESSURE INSIDE CORE BARREL

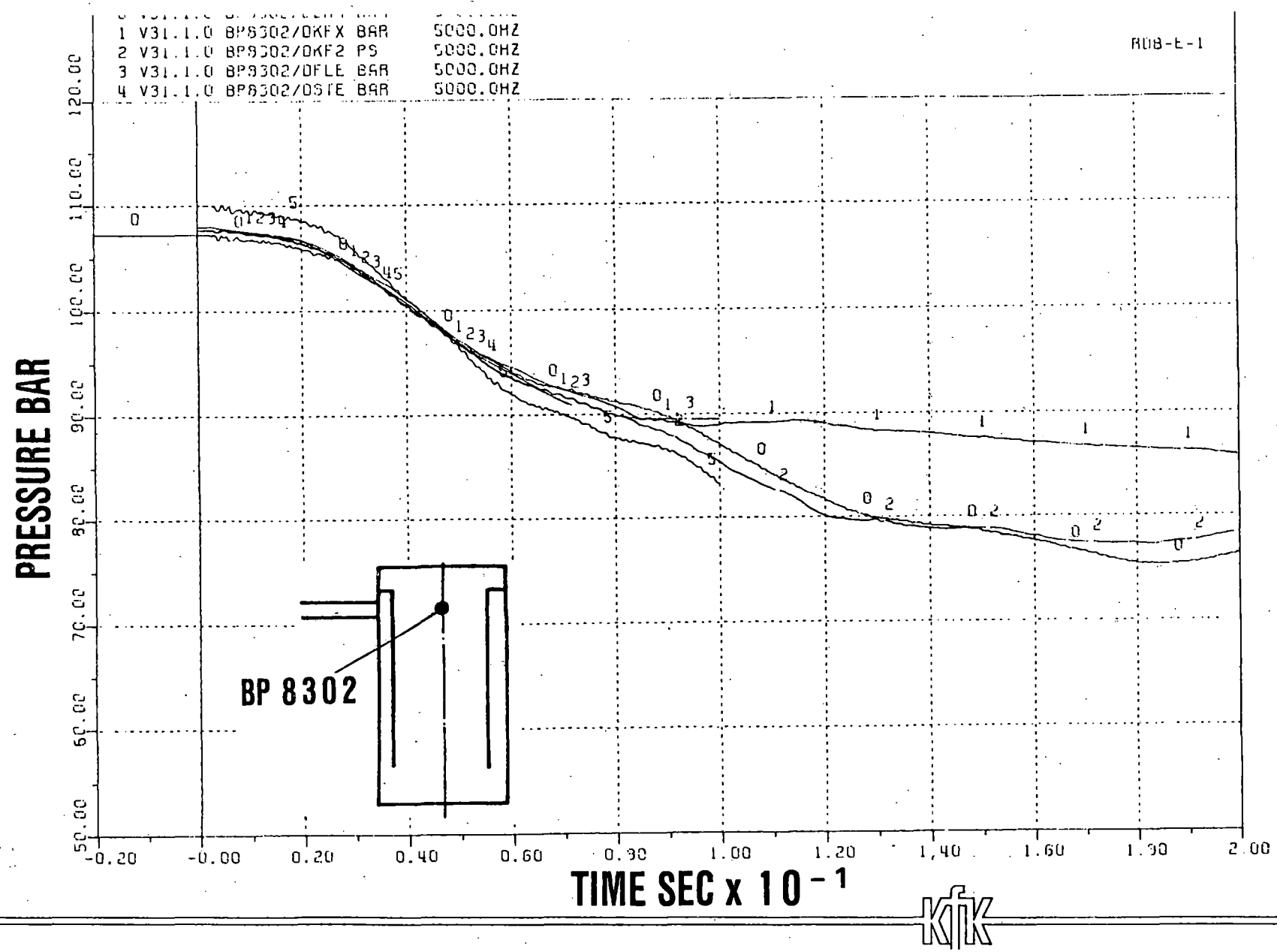

COMPARISON BETWEEN EXPERIMENTAL DATA AND POST-TEST PREDICTIONS OF MULTIDIMENSIONAL CODES FOR THE PRESSURE INSIDE THE CORE BARREL UPPER REGION

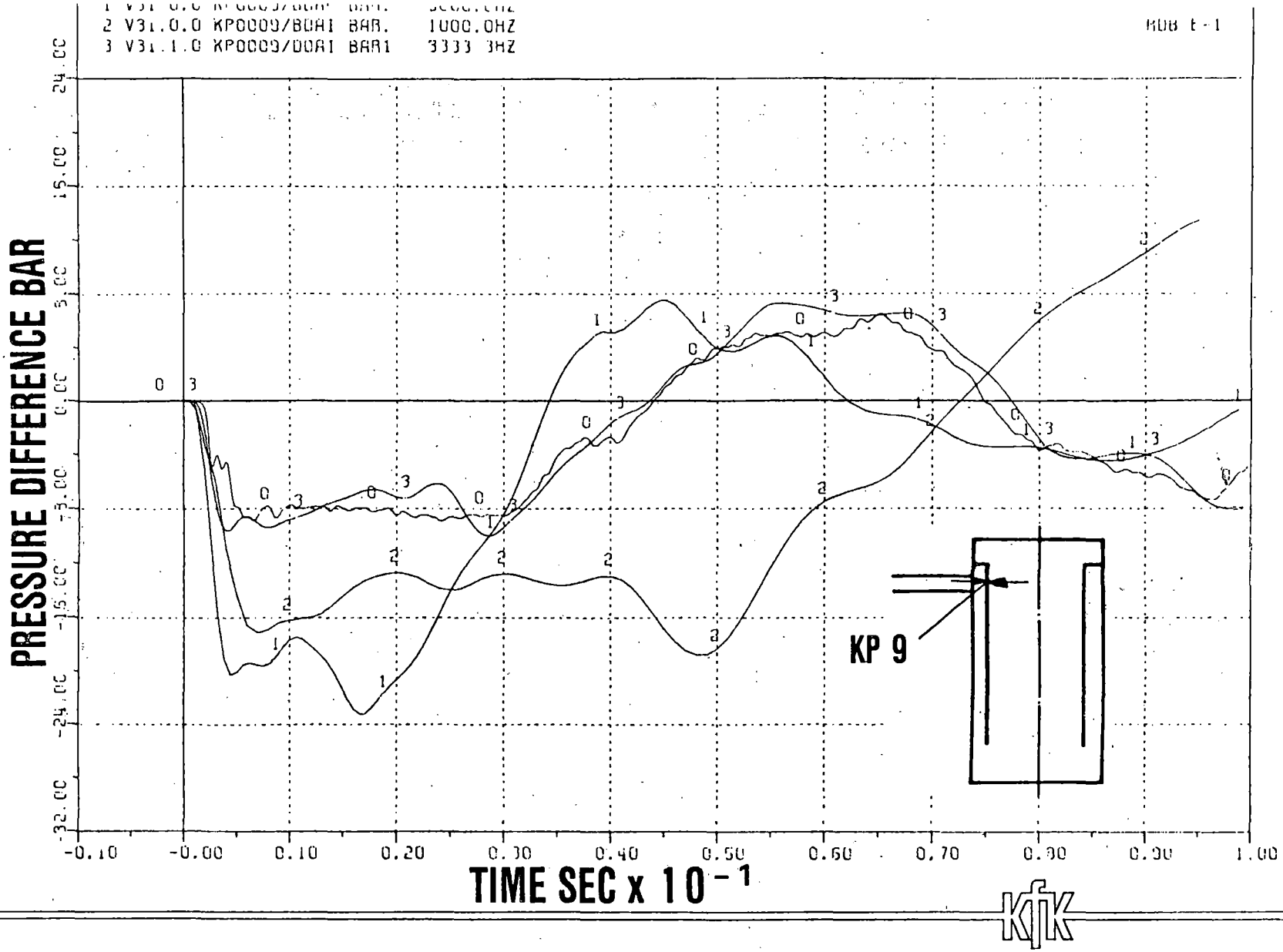

COMPARISON BETWEEN EXPERIMENTAL DATA AND PRE- AND POST-TEST PREDICTIONS FOR DECOUPLED AND COUPLED ANALYSES BY DAPSY AND DAISY

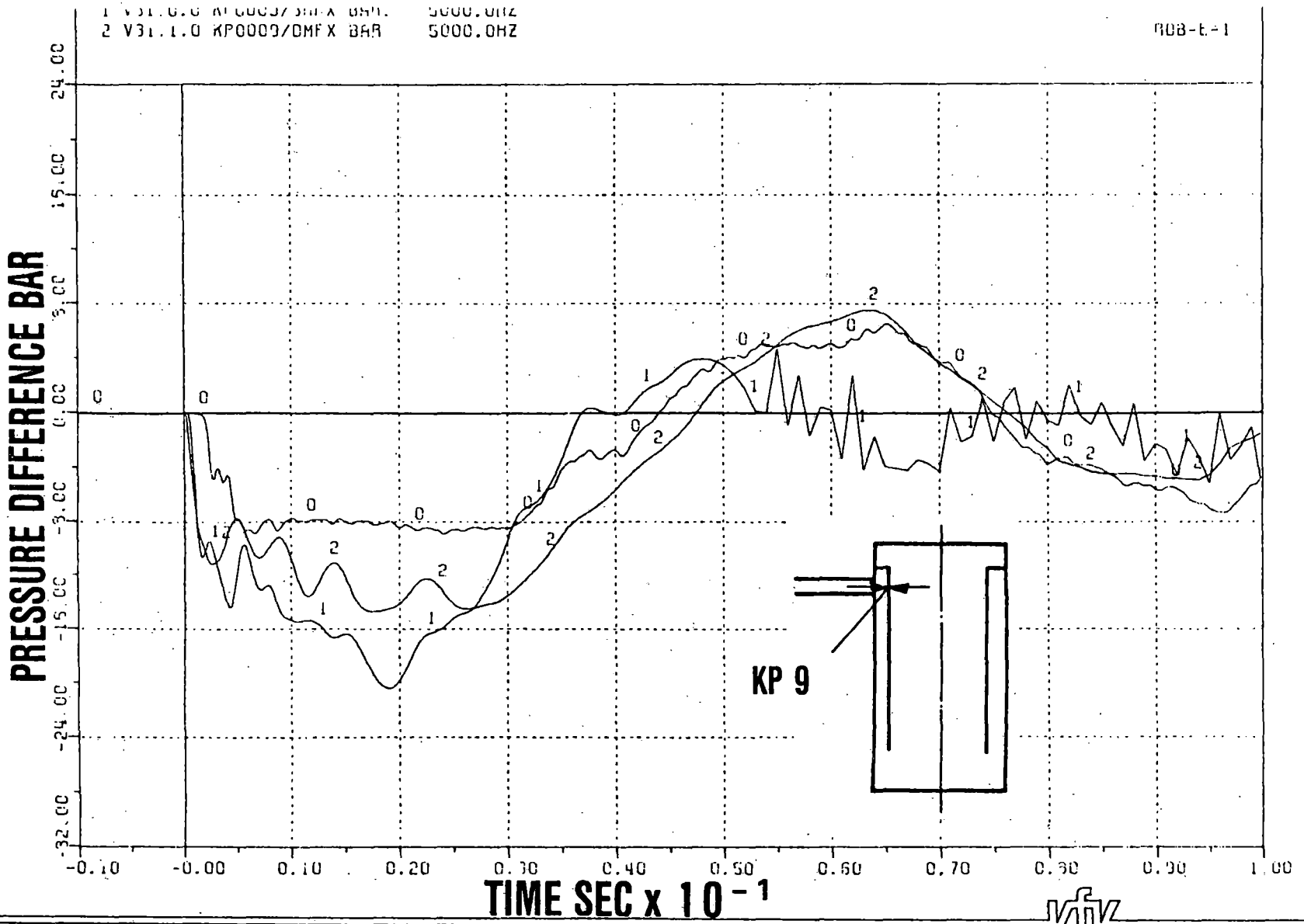

COMPARISON BETWEEN EXPERIMENTAL DATA AND PRE- AND POST-TEST PREDICTIONS BY MULTIFLEX

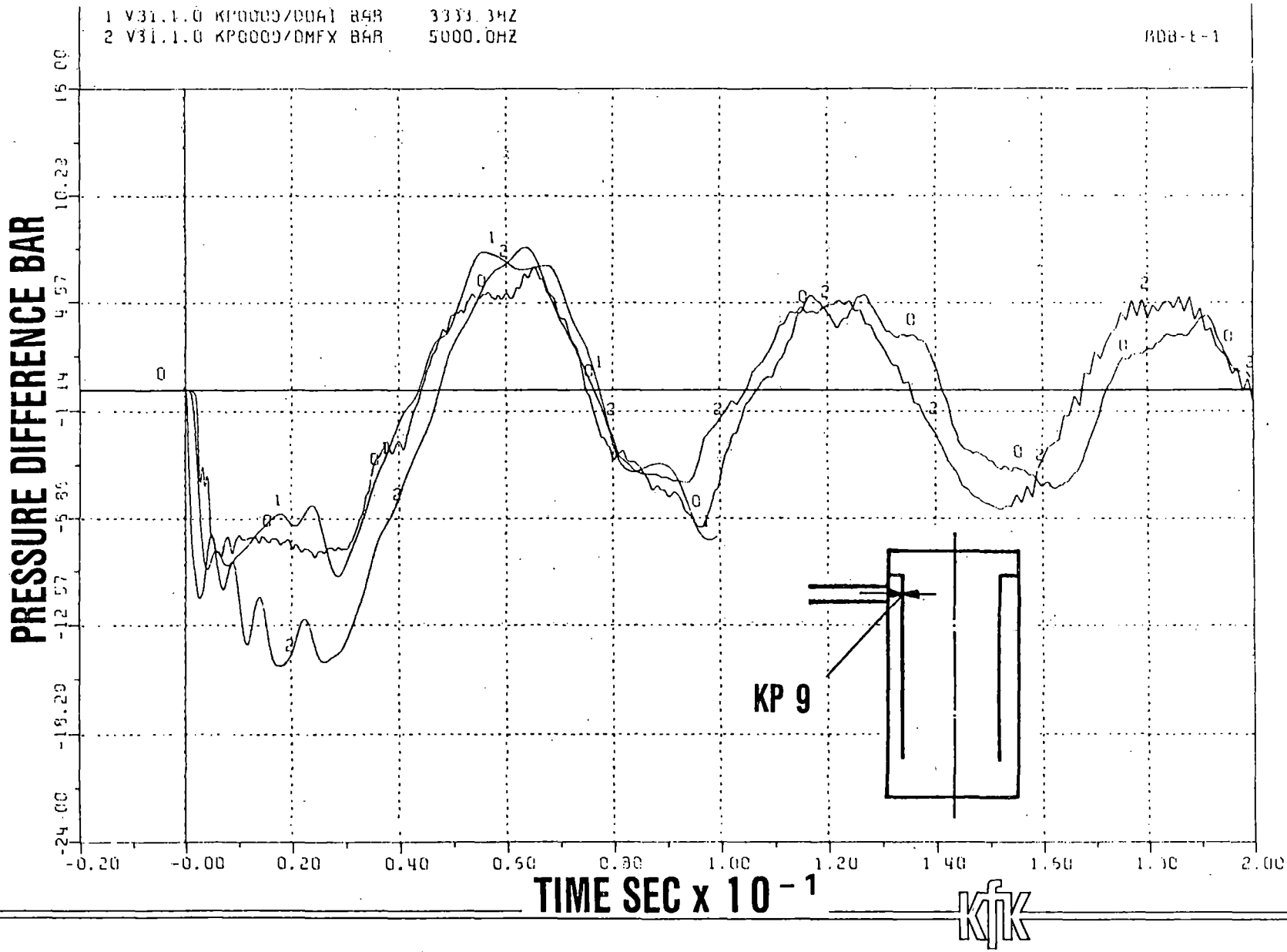

COMPARISON BETWEEN EXPERIMENTAL DATA AND POST-TEST PREDICTIONS OF EQUIVALENT NETWORK CODES FOR PRESSURE DIFFERENCE AT BREAK AXIS

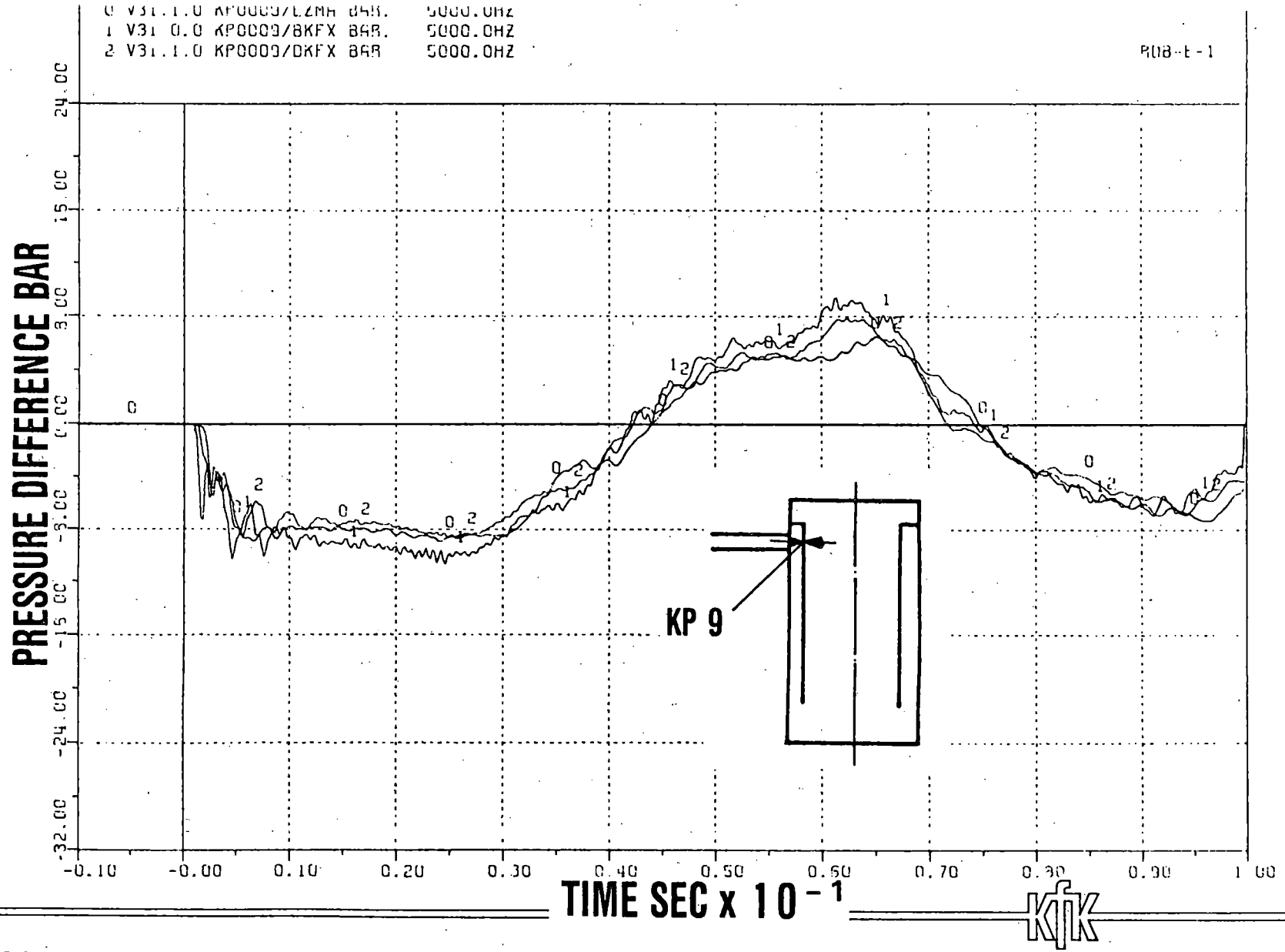

COMPARISON BETWEEN EXPERIMENTAL DATA AND PRE- AND POST-TEST PREDICTIONS BY KFIX (3D, FLX)

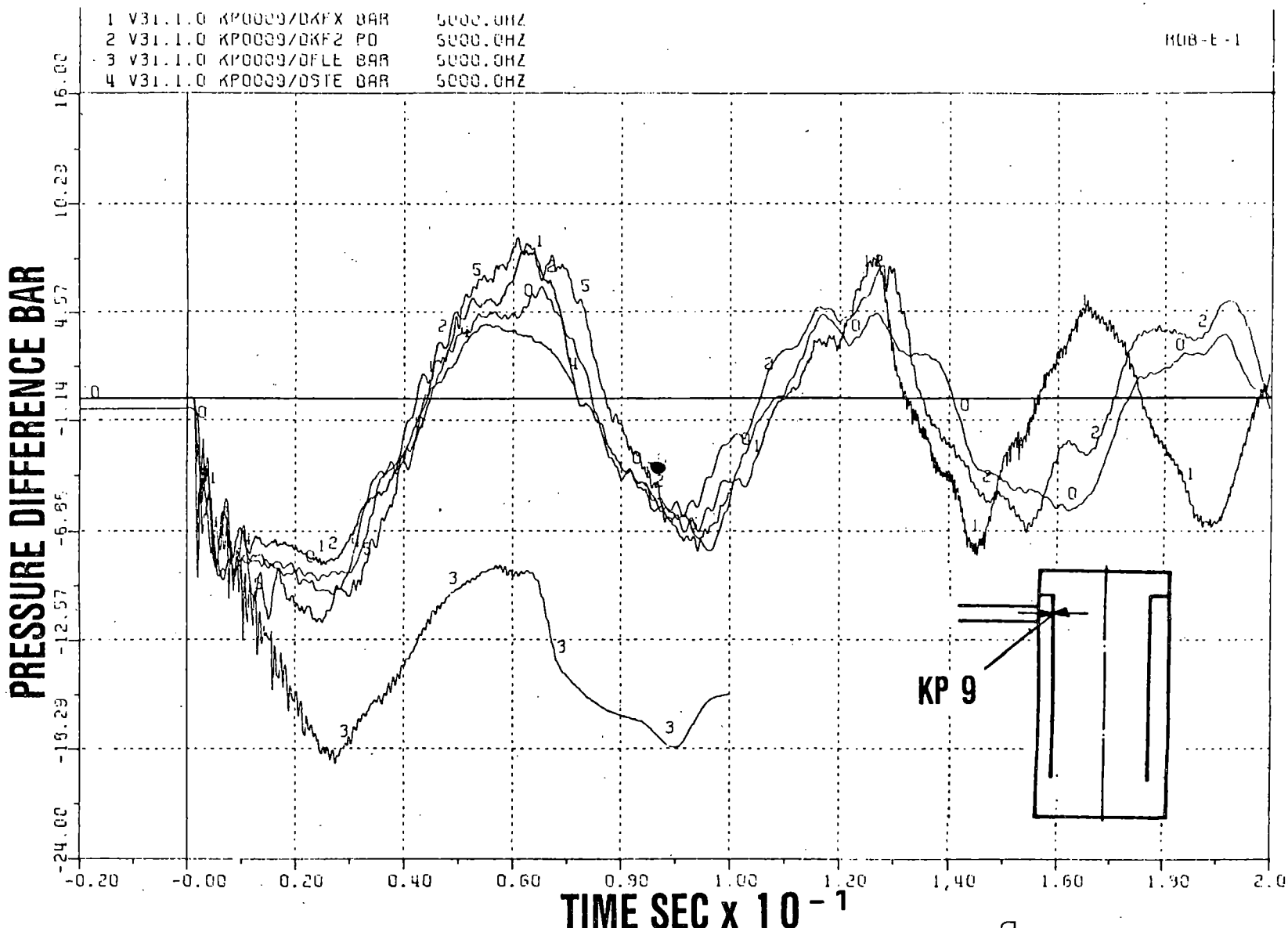

COMPARISON BETWEEN EXPERIMENTAL DATA AND POST-TEST PREDICTIONS OF MULTIDIMENSIONAL CODES FOR THE PRESSURE DIFFERENCE AT BREAK NOZZLE AXIS

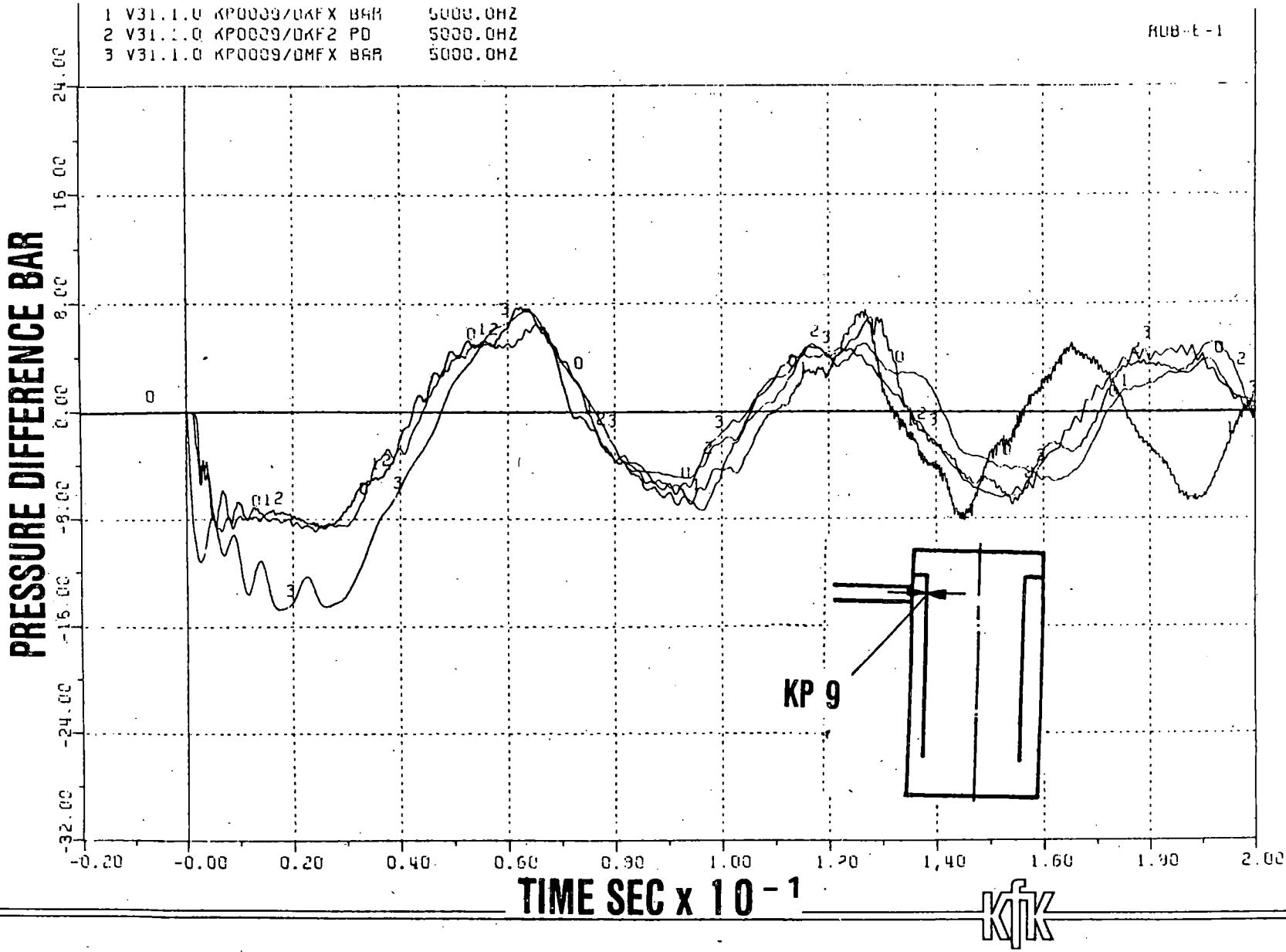

COMPARISON BETWEEN EXPERIMENTAL DATA AND POST-TEST PREDICTIONS BY EQUIVALENT NETWORK- AND MULTIDIMENSIONAL CODES

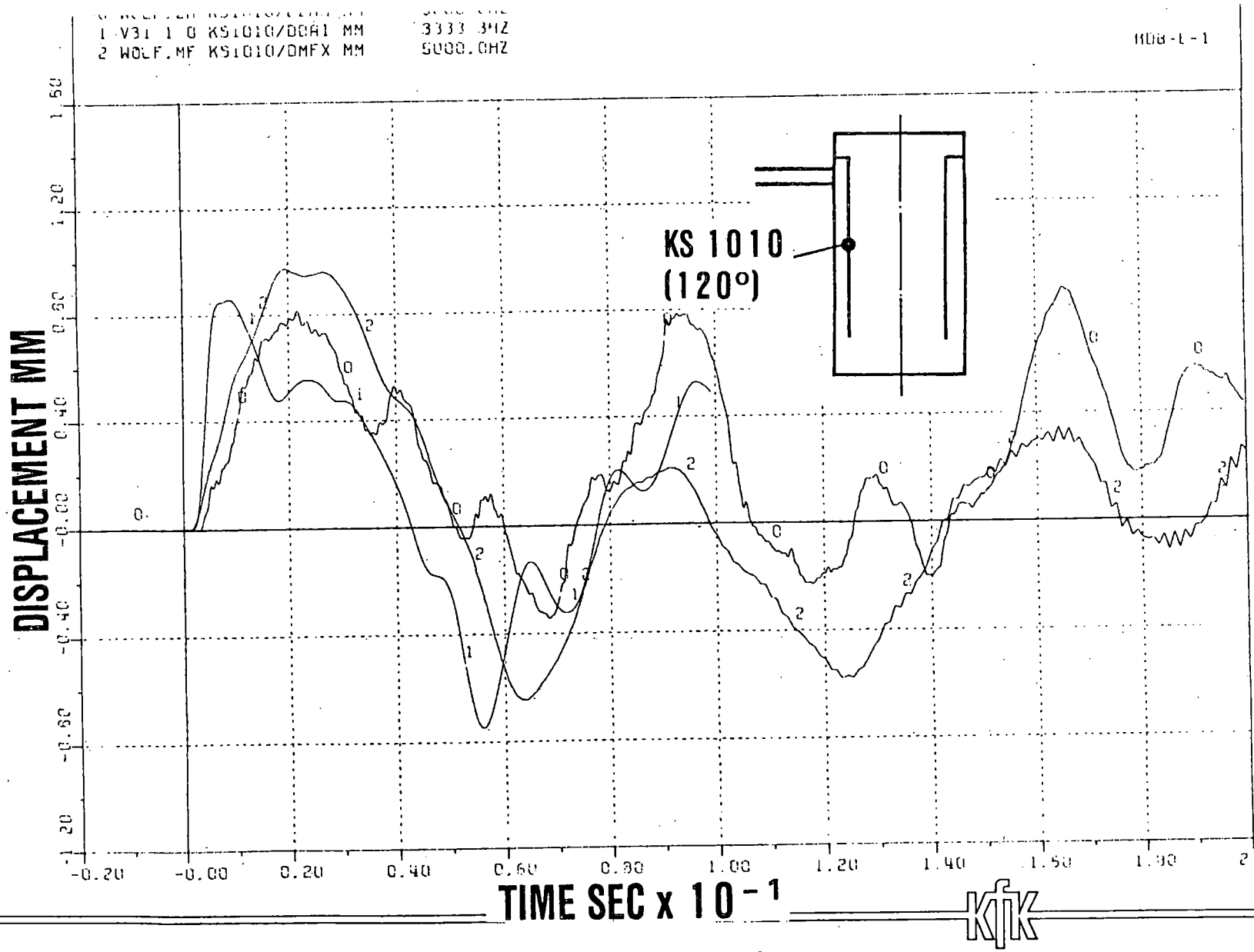

COMPARISON BETWEEN EXPERIMENTAL DATA AND POST-TEST PREDICTIONS OF EQUIVALENT NETWORK CODES FOR DISPLACEMENT

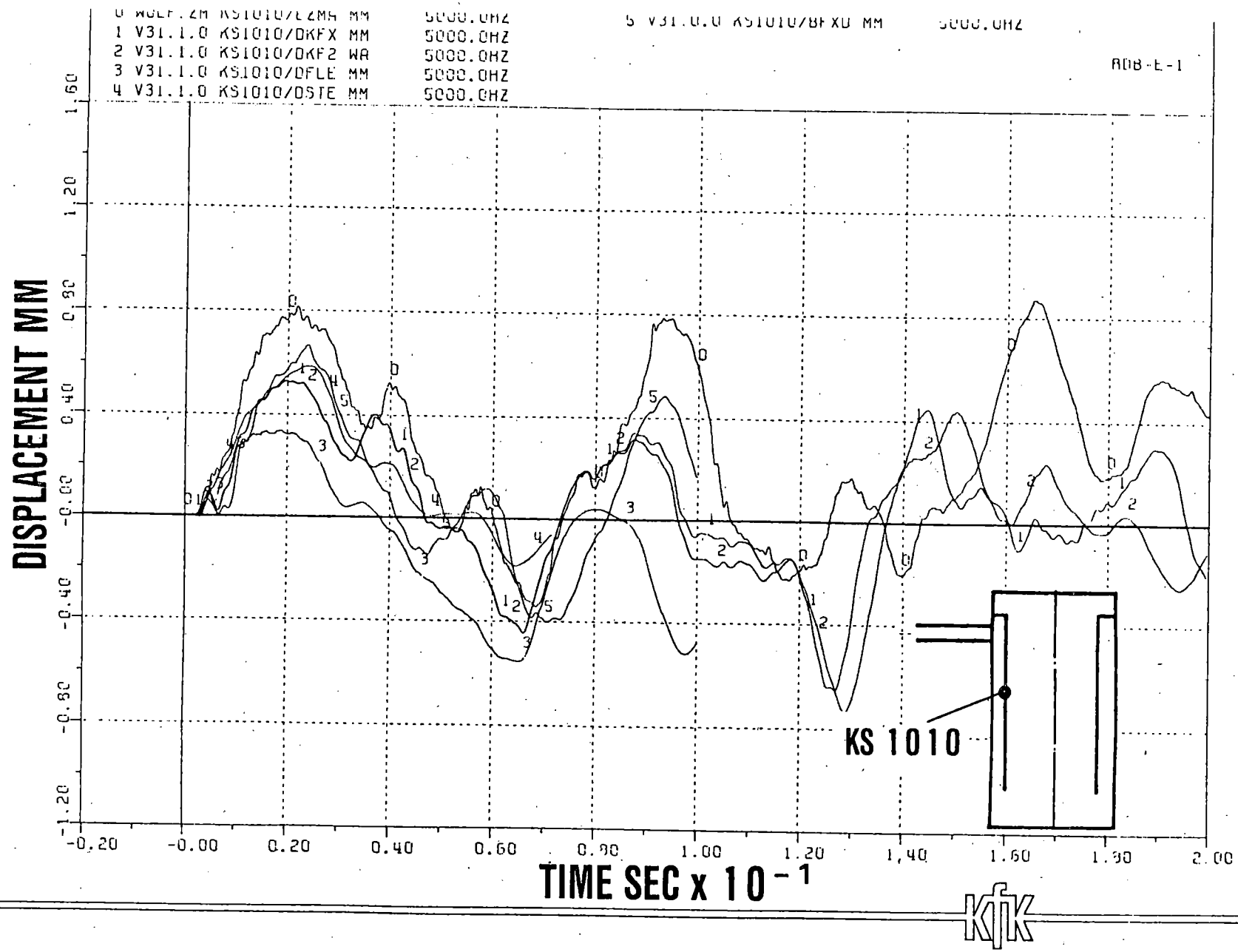

COMPARISON BETWEEN EXPERIMENTAL DATA AND POST-TEST PREDICTIONS OF MULTIDIMENSIONAL CODES FOR THE DISPLACEMENT OF THE CORE BARREL

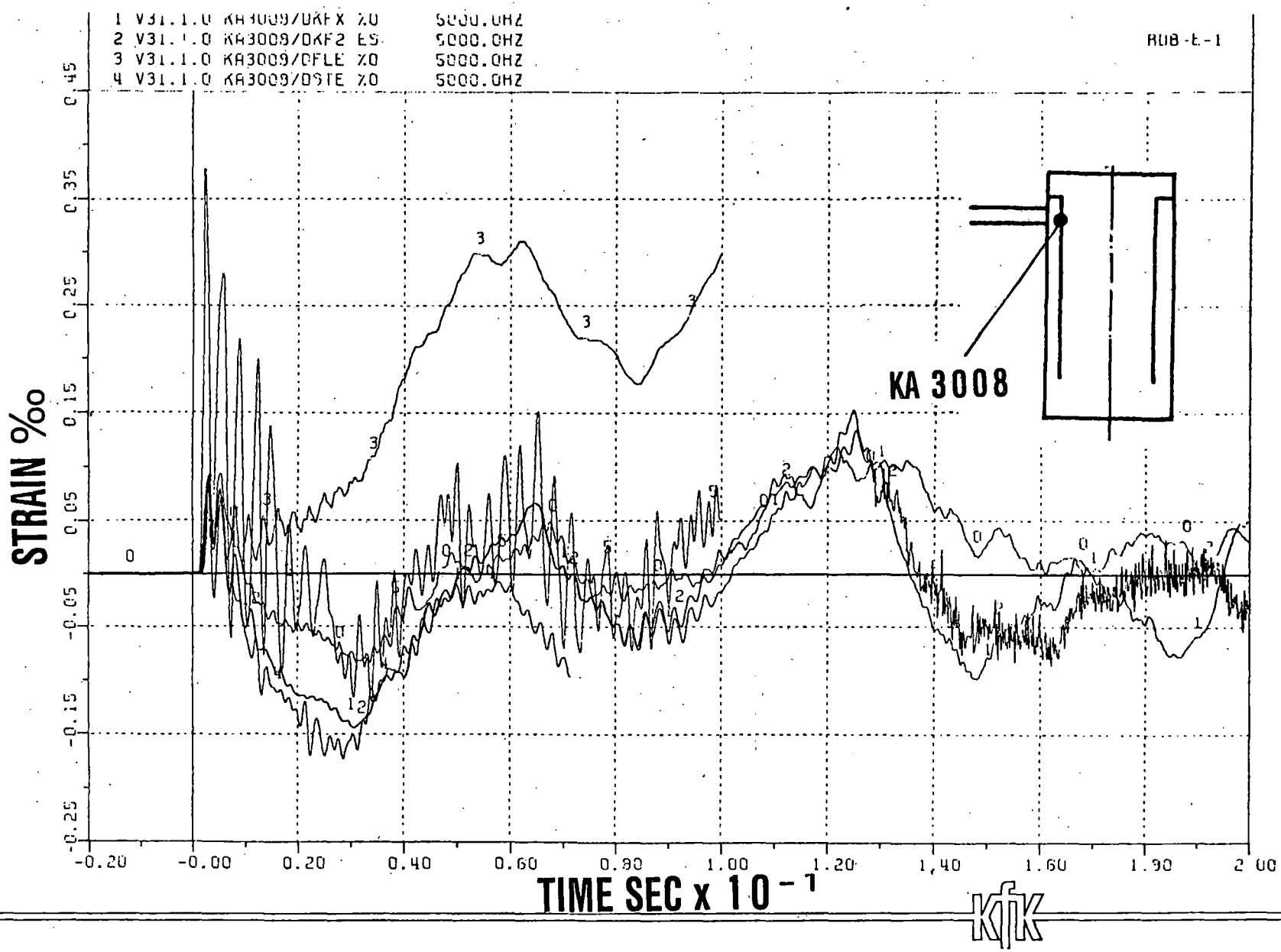

COMPARISON BETWEEN EXPERIMENTAL DATA AND POST-TEST PREDICTIONS OF MULTIDIMENSIONAL CODES FOR AXIAL, OUTSIDE CORE BARREL STRAIN

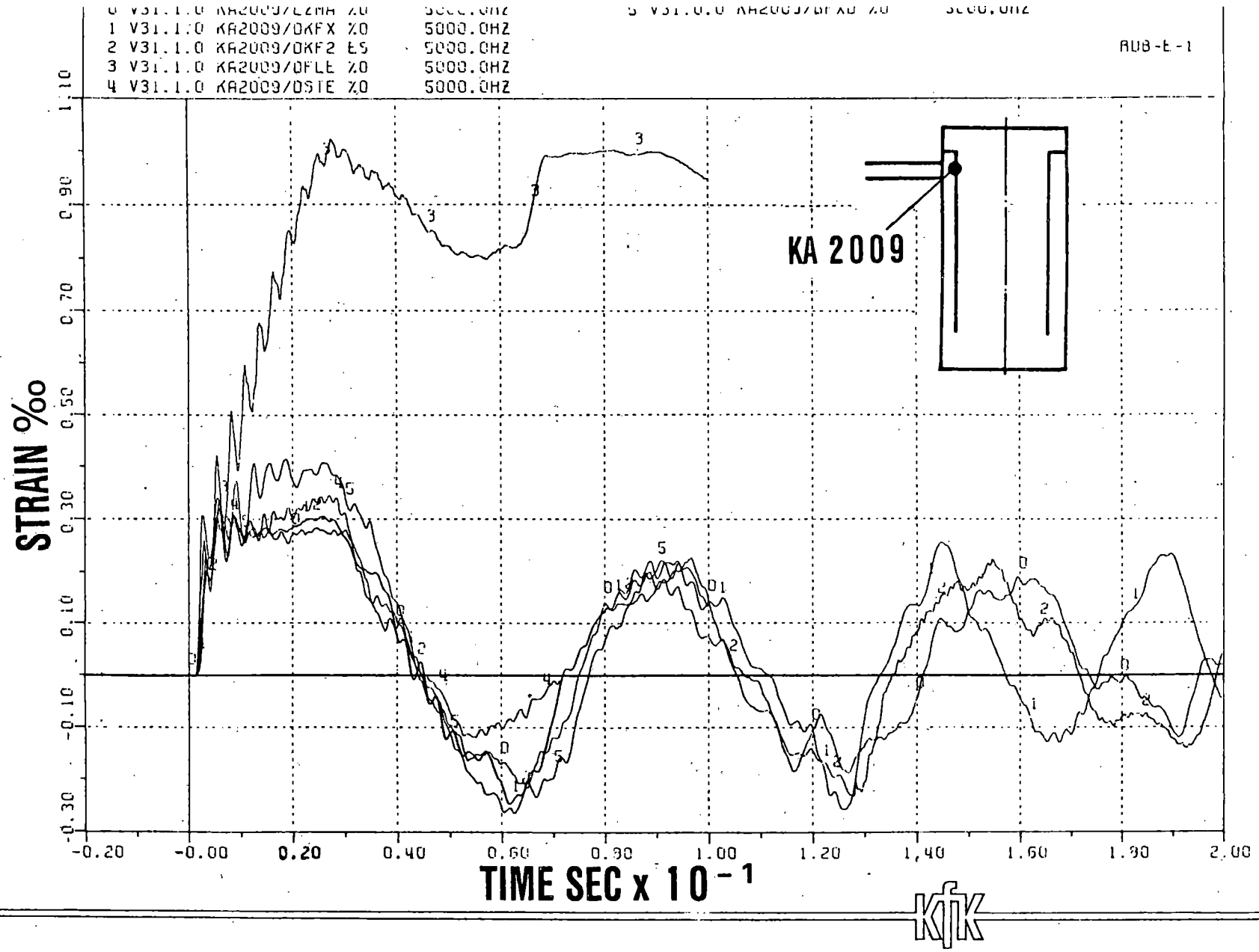

KfK

COMPARISON BETWEEN EXPERIMENTAL DATA AND POST-TEST PREDICTIONS OF MULTIDIMENSIONAL CODES FOR CIRCUMFERENTIAL, OUTSIDE CORE BARREL STRAIN

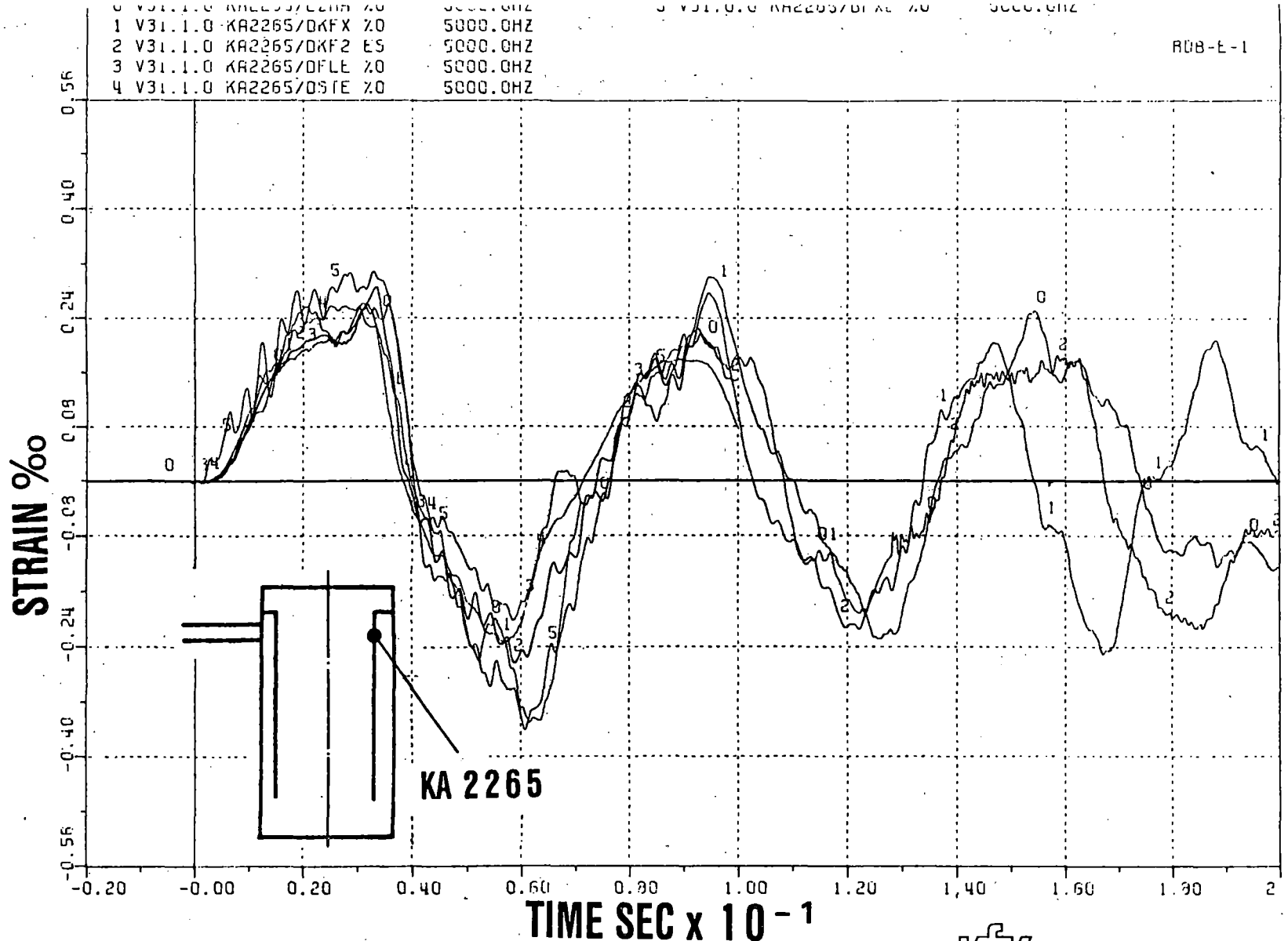

COMPARISON BETWEEN EXPERIMENTAL DATA AND POST-TEST PREDICTIONS OF MULTIDIMENSIONAL CODES FOR CIRCUMFERENTIAL, OUTSIDE CORE BARREL STRAIN

- INCORPORATION OF FSI INTO COMPUTER CODES IS ABSOLUTELY NECESSARY TO SATISFACTORILY INTERPRETING THE DATA

- MULTIDIMENSIONAL CODES GAVE BETTER AND MORE CONSISTENT RESULTS THAN EQUIVALENT NETWORK CODES FOR PRE-TEST CALCULATIONS

- LEARNING EFFECT FOR EQUIVALENT NETWORK CODES HIGHER THAN FOR MULTIDIMENSIONAL CODES

- DIFFERENCES IN RESULTS OF THESE TWO CODE METHODOLOGIES DECREASED MARKEDLY FOR POST-TEST CALCULATIONS

- NON-EQUILIBRIUM MODELS FOR TWO-PHASE FLOWS GIVE BETTER AGREEMENT WITH DATA OF BREAK NOZZLE PHENOMENA (FLASHING, PRESSURE WAVE DAMPING)

- COMPARISON WITH DATA INDICATE THAT THE FOLLOWING ASSUMPTIONS ARE SEEMINGLY APPROPRIATE
  - 2 1/2 D MODEL FOR DOWNCOMER
  - SINGLE-PHASE, FRICTIONLESS FLOW WITH CONSTANT WAVE SPEED FOR HIGHLY SUBCOOLED PHASE OF BLOWDOWN

CONCLUSIONS CONCERNING PRE- AND POST-TEST CALCULATIONS

- LINEARIZATION OF FLUID-STRUCTURE COUPLING FOR SMALL DISPLACEMENTS
- 1-D MODEL INSIDE CORE BARREL

— ADDITIONAL CONSIDERATION OF RPV SEEMS APPROPRIATE

— THE QUALITY OF MASS FLOW DETERMINATION IN BREAK NOZZLE DOES NOT GUARANTY THE QUALITY OF OTHER MAJOR QUANTITIES OF INTEREST IN THE VESSEL

— CORRECTIONS FOR INITIAL- AND BOUNDARY CONDITIONS AS MEASURED DID NOT RESULT IN MAJOR IMPROVEMENTS OF POST-TEST CALCULATIONS

— ALTHOUGH EXCELLENT AGREEMENT WITH DATA HAS BEEN REACHED OVER THE FIRST 100 ms, BLIND PRE-TEST PREDICTIONS FOR THE PERIOD 100 ms - 200 ms DO NOT AGREE WELL WITH THE DATA (KFIX-PHASE SHIFT)

— KFIX AND MULTIFLUX SHOW NUMERICAL NOISE BETWEEN 100 ms AND 200 ms

CONT'D

— DATA BASE FOR VERIFICATION AND QUALIFICATION OF COMPUTER CODES FOR

- DESIGN
- LICENSING
- BEST-ESTIMATE

— DIRECT IMPLICATIONS AND FEEDBACK OF TEST RESULTS ON ANALYTICAL RESULTS ALREADY OBSERVED IN

- INSIGHT OF PHENOMENA
- CODE APPLICATION
- MODELLING OF GEOMETRY
- CODE ADDITIONS AND ADJUSTMENTS
- CODE EXTENSIONS
- IDENTIFICATION OF WEAK POINTS (PATCHING OF MODELS, GEOMETRIES ETC.)

— IMPROVED RATIONALE FOR TEST MATRIX DEFINITION OF MAIN TEST PHASE

KfK

IMPACT OF HDR-RPV-I EXPERIMENTS UPON FSI-CODE DEVELOPMENTS AND APPLICATIONS

- EFFECT OF NUMERICAL DIFFUSION UPON PRESSURE WAVE DAMPING CANNOT BE SEPARATED
- MULTIDIMENSIONAL MODELING INSIDE CORE BARREL
- INCORPORATION OF RPV, COST / BENEFIT? WHAT KIND OF MODELING IS NEEDED?
- VALIDITY OF SINGLE-PHASE FLOW ASSUMPTION
- VALIDITY OF HOMOGENEOUS VS NONEQUILIBRIUM MODELS
- QUALIFICATION OF TUNED CODES FOR LONGER PERIODS OF REAL TIME
- EFFECT OF RADIAL TEMPERATURE DISTRIBUTIONS UPON LOCAL PHENOMENA
- VALIDITY OF INPUT DATA FOR OTHER INITIAL- AND BOUNDARY CONDITIONS

NEED FOR SENSITIVITY STUDY WITH BEST-ESTIMATE CODE

UNSOLVED PROBLEMS WITH RESPECT TO FSI-COMPUTER CODES AND THEIR MODELS

V31.2: REPLICATION OF V31.0/V31.1 WITH EXTENDED AND IMPROVED INSTRUMENTATION

- POSTERIOR EVALUATION OF REDUCED INSTRUMENTATION

V32: GERMAN STANDARD PROBLEM NO. 5

- HIGHER SUBCOOLING IN DOWNCOMER
- HENCE HIGHER CORE BARREL LOADS - UPPER LIMIT
- APPLICATION OF CODES BEYON REGION OF TUNING
- 2. MEASUREMENT POINT FOR SHORT NOZZLE TEST MATRIX

V33: ISOTHERMAL TEST, HENCE ELIMINATION OF PROBABLE TEMPERATURE DISTRIBUTION EFFECTS

- HIGHES SUBCOOLING THROUGHOUT VESSEL
- 3. MEASUREMENT POINT FOR SHORT NOZZLE TEST MATRIX

V34 (tentative):

AS V33, HOWEVER ISOTHERMAL CONDITIONS CLOSE TO SATURATION

- LOWEST SUBCOOLING THROUGHOUT VESSEL
- LOWEST CORE BARREL LOADS
- TEST OF VALIDITY OF TWO-PHASE FLOW MODELING

RATIONALE FOR TEST MATRIX OF BLOCK I OF MAIN TEST PHASE

TEST No	Pressure bar	Upper Core Temp. °C	Downcomer Temperature °C	Subcooling Downcomer Degrees	Length of break nozzle m
V 31.2	110	308	268	50	1.369
V 32	110	308	240	78	1.369
V 33	110	240	240	78	1.369
V 34	110	300	300	18	1.369

KfK

TEST MATRIX OF BLOCK I OF MAIN TEST PHASE

NRC FORM 335 (11-81)

U.S. NUCLEAR REGULATORY COMMISSION

BIBLIOGRAPHIC DATA SHEET

1. REPORT NUMBER *(Assigned by DDC)*
NUREG/CP-0024, Vol. 1

4. TITLE AND SUBTITLE *(Add Volume No., if appropriate)*
Ninth Water Reactor Safety Research Information Meeting

2. *(Leave blank)*

3. RECIPIENT'S ACCESSION NO.

7. AUTHOR(S)

5. DATE REPORT COMPLETED
MONTH | YEAR

9. PERFORMING ORGANIZATION NAME AND MAILING ADDRESS *(Include Zip Code)*
U.S. Nuclear Regulatory Commission
Office of Nuclear Regulatory Research
Washington, DC 20555

DATE REPORT ISSUED
MONTH: March | YEAR: 1982

6. *(Leave blank)*

8. *(Leave blank)*

12. SPONSORING ORGANIZATION NAME AND MAILING ADDRESS *(Include Zip Code)*
Same as 9, above.

10. PROJECT/TASK/WORK UNIT NO.

11. FIN NO.

13. TYPE OF REPORT

PERIOD COVERED *(Inclusive dates)*

15. SUPPLEMENTARY NOTES

14. *(Leave blank)*

16. ABSTRACT *(200 words or less)*

This is a compilation of papers which were presented at the Ninth Water Reactor Safety Research Information Meeting. It consists of three volumes.

17. KEY WORDS AND DOCUMENT ANALYSIS

17a. DESCRIPTORS

17b. IDENTIFIERS/OPEN-ENDED TERMS

18. AVAILABILITY STATEMENT
Unlimited

19. SECURITY CLASS *(This report)*
Unclassified

21. NO. OF PAGES

20. SECURITY CLASS *(This page)*
Unclassified

22. PRICE
S

UNITED STATES
NUCLEAR REGULATORY COMMISSION
WASHINGTON, D. C. 20555

OFFICIAL BUSINESS
PENALTY FOR PRIVATE USE, $300

POSTAGE AND FEES PAID
U.S. NUCLEAR REGULATORY
COMMISSION

Name Mail Stop Due Date

Return to: 823 LIBRARY/SNL, MS 0731